NUNC COGNOSCO EX PARTE

TRENT UNIVERSITY
LIBRARY

Digitized by the Internet Archive
in 2019 with funding from
Kahle/Austin Foundation

https://archive.org/details/advancesinchemic0012unse

INTERMOLECULAR FORCES

ADVANCES IN CHEMICAL PHYSICS

VOLUME 12

ADVANCES IN CHEMICAL PHYSICS

EDITORS
I. Prigogine
Faculté des Sciences, Université Libre de Bruxelles, Brussels, Belgium

S. Rice
James Franck Institute, University of Chicago, Chicago, Illinois

---

EDITORIAL BOARD

THOR A. BAK, Universitetets Fysik Kemiske Institut, Copenhagen, Denmark

J. DUCHESNE, University of Liège, Liège, Belgium

H. C. LONGUETT-HIGGINS, The University Chemical Laboratory, Cambridge, England

M. MANDEL, University of Leiden, Leiden, Holland

V. MATHOT, Université Libre de Bruxelles, Brussels, Belgium

P. MAZUR, Institut Lorentz, Leiden, Holland

A. MÜNSTER, Laboratoire de Chimie Physique, Université de Paris, Paris, France

S. ONO, Institute of Physics, College of General Education, Tokyo, Japan

B. PULLMAN, Laboratoire de Chimie Théorique, Université de Paris, Paris, France

J. W. STOUT, James Franck Institute, University of Chicago, Chicago, Illinois

G. SZASZ, General Electric Company, Zürich, Switzerland

M. V. VOLKENSTEIN, Institute of Macromolecular Chemistry, Leningrad, U.S.S.R.

B. H. ZIMM, School of Science and Engineering, University of California at San Diego, La Jolla, California

INTERMOLECULAR FORCES

Edited by JOSEPH O. HIRSCHFELDER

The University of Wisconsin,
Madison, Wisconsin

INTERSCIENCE PUBLISHERS
a division of John Wiley & Sons, New York - London - Sydney

Copyright © 1967 by John Wiley & Sons, Inc.

All Rights Reserved

Library of Congress Catalog Card Number 58-9935

PRINTED IN THE UNITED STATES OF AMERICA

AUTHORS

Richard B. Bernstein, Theoretical Chemistry Institute and Department of Chemistry, University of Wisconsin, Madison, Wisconsin

George Birnbaum, North American Aviation Science Center, Thousand Oaks, California

Myer Bloom, Department of Physics, The University of British Columbia, Vancouver, Canada

A. D. Buckingham, Department of Theoretical Chemistry, University of Bristol, Bristol, England

A. Dalgarno, Department of Astronomy, Harvard University, Cambridge, Massachusetts

J. O. Hirschfelder, The University of Wisconsin, Theoretical Chemistry Institute, Madison, Wisconsin

B. Linder, Department of Chemistry, Florida State University, Tallahassee, Florida

E. A. Mason, Institute for Molecular Physics, University of Maryland, College Park, Maryland

William J. Meath, University of Western Ontario, Department of Chemistry, London, Ontario, Canada

L. Monchick, Applied Physics Laboratory, The Johns Hopkins University, Silver Spring, Maryland

James T. Muckerman, Theoretical Chemistry Institute and Department of Chemistry, University of Wisconsin, Madison, Wisconsin

Irwin Oppenheim, Department of Chemistry, Massachusetts Institute of Technology, Cambridge, Massachusetts

E. A. Power, Mathematics Department, University College, London, England

O. Sinanoğlu, Sterling Chemical Laboratory, Yale University, New Haven, Connecticut

PREFACE

This book is intended to delve deeply and technically into the recent advances in both the theory of intermolecular forces and the experimental methods of determining intermolecular forces. A few years ago, the parametrized potential energy functions of Morse, Lennard-Jones, Buckingham, Stockmayer, and Kihara were satisfactory for representing the available experimental data. With the development of a variety of ingenious experimental techniques which provide detailed information regarding individual molecular collisions, it has become necessary to provide a more realistic basis for describing the energy of interaction.

A few years ago, we limited our discussions of intermolecular forces to the interactions of two noble gas atoms in their ground states. Now we are trying to understand the collisions between other kinds of atoms, in both excited and ground states. Corresponding to a particular type of collision, there are usually a considerable number of possible sets of electronic quantum numbers for the "diatomic molecule." For each of these electronic quantum states, we seek the potential energy curves which determine the forces on the atoms as a function of their separation R. It is clear that the problems of both interatomic and intermolecular forces are inseparably linked with molecular spectroscopy. It is also clear that the detailed fine structure and hyperfine structure which play an important role in spectroscopy correspond to whole families of closely spaced potential energy curves. Thus, the determination of intermolecular forces is inherently complex.

Very little detailed information is now available regarding the interaction of diatomic or polyatomic molecules with either atoms or molecules. Such interactions must be described in terms of many-dimensional potential energy surfaces which describe the energy as a function of the configurations of the separate molecules, the relative orientations of the molecules, and the separation between the molecules. These energy surfaces would serve as the input information required in the statistical mechanical calculation of a wide variety of macroscopic properties of materials, as well as the calculation of the rates of chemical reactions.

Theory and experiments must work together in order to unravel the complexities of intermolecular forces. Thus, the first six chapters in this book deal with the present status of the theory, and the next four chapters deal with the experimental determinations. The reader will be impressed with the rapid progress which is being made. However, he will be disappointed that there is so very much work left to be done before we can provide practical answers to many of his questions.

The first chapter by Hirschfelder and Meath is intended to be a survey of the nature of the intermolecular forces. It includes an intensive study of the interaction of two ground-state hydrogen atoms. Other examples could not be considered in such detail because of the lack of accurate theoretical calculations.

Buckingham (in Chapter 2) shows that the long-range forces between two polyatomic molecules can be explained in terms of the permanent and induced electric moments of the isolated molecules. He discusses these moments and their measurements in considerable detail. The formulas for asymmetric molecules are exceedingly complicated for human comprehension but they may be programmed on computing machines.

Thanks to the availability of high-speed computing machines and new types of variation and perturbation procedures, the theory of intermolecular forces is developing rapidly. As Dalgarno explains in Chapter 3, the long-range forces between atoms can be determined quite accurately with the use of perturbation theory and a number of new mathematical techniques. Instead of expressing the perturbed wave functions as a sum over all of the discrete energy states plus an integral over the continuum, the perturbed wave functions are determined explicitly by solving partial differential equations. Unfortunately, it is still difficult to calculate the forces between atoms at intermediate separations where the atomic wave functions overlap and exchange forces become important. Currently, a new type of perturbation procedure is being developed to cope with this problem.

It has been experimentally demonstrated that the force of attraction between the molecules in two separated sheets of mica in a vacuum agrees with the long-range (relativistically retarded) Casimir and Polder forces which Power discusses in Chapter 4. The same type of quantum electrodynamical considerations are used to explain the "excitons" which produce the energy of interaction of aromatic molecules in a crystal. It is likely that these same techniques will prove useful in considering the forces between biologically active molecules.

The reaction-field technique, which Linder presents in Chapter 5 treats intermolecular forces from a strictly phenomenological standpoint. For example, dispersion forces are related to frequency-dependent polarizabilities by averaging over the fluctuating instantaneous dipole–induced-dipole interactions. In this approach, both quantum mechanical and statistical mechanical fluctuations are simultaneously averaged. Reaction-field techniques are especially suited to the determination of forces in liquids, thermally averaged energies of interactions, and susceptibilities of gases and liquids. The method which has been developed up to now, in common with other field-theoretic approaches, is restricted to sufficiently weak interactions so that the response function is linear. This approximation neglects the effects of the molecular distortions on the response function. However, the many-body forces, including the fourth and higher-order nonadditive terms, can be included in the reaction-field formulation.

For many practical problems, it is necessary to understand the forces between molecules in a liquid. This is a very difficult problem since it involves the detailed packing of the molecules in a liquid as well as the many-body forces between neighboring molecules. For asymmetric and polar molecules there are additional complications, especially in the vicinity of the surface of the liquid. In Chapter 6, Sinanoğlu sets up the problem in a truly elegant fashion and obtains numerical solutions for some nonpolar liquids.

It is indeed a sad commentary that up to the present time, except for the interaction of two hydrogen atoms, the *best* potential energy curves are not obtained from *a priori* theoretical calculations. In Chapter 7 Mason and Monchick explain that the Rydberg-Klein-Rees method of analyzing band spectra provides an excellent direct determination of the intermolecular potential. Good potential energy curves are also obtained by adjusting the parameters in an idealized potential function so as to fit a set of experimental observations. There are many different types of experimental data which can be used for this sort of semiempiricism. Of these, molecular beam scattering provides the most direct and sensitive means for estimating the intermolecular forces.

Bernstein and Muckerman (Chapter 8) show that molecular beam techniques are now sufficiently advanced to allow the determination of at least the principal quantitative features characterizing atom–atom potential energy curves. First they outline the methodology, which takes advantage of various nonclassical effects such as the *glory extrema* and

rainbow effects. Then they review the present status of the results in considerable detail. It would appear that the greatest limitation to the molecular beam technique is in the development of detectors with sufficient sensitivity.

The pressure broadening of spectral lines in the microwave and infrared regions provides an intriguing way of determining anisotropic intermolecular forces, which change the rotational states of molecules. As Birnbaum explains in Chapter 9, this technique leads to good values for the quadrupole moments of molecules. However, theory does not account for several features of pressure broadening. Advances in the theory are necessary if progress is to continue in the application of pressure broadening to the study of intermolecular forces.

Only very recently has the usefulness of nuclear magnetic resonance measurements in gases been recognized as a means for obtaining precise information about intermolecular forces, especially the anisotropy of the potential energy which results in changes in the molecular rotations. This method is discussed by Bloom and Oppenheim in Chapter 10.

Thus, we hope that this volume will serve as a status report and explain the recent advances which have taken place in the field of intermolecular forces.

JOSEPH O. HIRSCHFELDER, EDITOR

CONTENTS

PART I. THEORY

1. **The Nature of Intermolecular Forces**
   By J. O. Hirschfelder and W. J. Meath 3
2. **Permanent and Induced Molecular Moments and Long-Range Intermolecular Forces**
   By A. D. Buckingham 107
3. **New Methods for Calculating Long-Range Intermolecular Forces**
   By A. Dalgarno 143
4. **Very Long-Range (Retardation Effect) Intermolecular Forces**
   By E. A. Power 167
5. **Reaction Field Techniques and Their Applications to Intermolecular Forces**
   By B. Linder 225
6. **Intermolecular Forces in Liquids**
   By O. Sinanoğlu 283

PART II. EXPERIMENTAL DETERMINATIONS

7. **Methods for the Determination of Intermolecular Forces**
   By E. A. Mason and L. Monchick 329
8. **Determination of Intermolecular Forces via Low-Energy Molecular Beam Scattering**
   By R. B. Bernstein and J. T. Muckerman 389
9. **Microwave Pressure Broadening and Its Application to Intermolecular Forces**
   By G. Birnbaum 487
10. **Intermolecular Forces Determined by Nuclear Magnetic Resonance**
    By M. Bloom and I. Oppenheim 549

Author Index 601

Subject Index 619

Cumulative Indexes to Volumes 1–13 631

PART I

THEORY

1. The Nature of Intermolecular Forces*

JOSEPH O. HIRSCHFELDER

The University of Wisconsin Theoretical Chemistry Institute
Madison, Wisconsin

and

WILLIAM J. MEATH

The University of Western Ontario Department of Chemistry
London, Ontario, Canada

CONTENTS

I. Introduction 5
A. Interaction of Two 1*s* Hydrogen Atoms 5
II. Concept of an Intermolecular Potential 8
A. The Born-Oppenheimer Approximation 12
B. The Adiabatic Approximation 12
C. The Nonadiabatic Approximation 13
D. Coupling between the Electronic and Rotational Angular Momenta 14
E. Discussion 15
III. The Effective Potential 17
IV. Electrostatic Variational Calculations 21
A. Small and Intermediate Separations 22
1. The Ground $X^1\Sigma_g^+$ State of the Hydrogen Molecule 22
2. The Lowest Excited Bound State, $B^1\Sigma_u^+$, of Hydrogen . . . 24
3. The Lowest Excited $^1\Sigma_g^+$ State of Hydrogen 25
B. Large Separations 25
V. Electrostatic Perturbation Calculations 29
A. Rayleigh-Schrödinger Perturbation Theory 29

* This research was supported in part by National Aeronautics and Space Administration Grant NsG-275-62 at the University of Wisconsin Theoretical Chemistry Institute. One of the authors (W.J.M.) wishes to thank the National Research Council of Canada for their grant which assisted him in this work. The other author (J.O.H.) wishes to thank the University of Florida Quantum Theory Project, Gainesville, Florida for their assistance.

B. Large Separations 31
1. The Multipole Expansion of V_e 31
2. The Perturbation Problem 33
3. Nonresonant Intermolecular Forces 34
a. First-Order Energy 34
b. Second-Order Energy 36
4. Resonant Intermolecular Forces 39
a. Resonance between Like Atoms 39
b. First-Order Dipole Resonance 40
c. First-Order Quadrupole Resonance 41
d. The Second-Order Energy 41
e. Resonance within One Molecule 42
5. Almost Degeneracy Due to the Effects of Atomic Fine Structure 42
a. (Λ,S) Coupling 43
b. (J_a,J_b) Coupling 43
c. Intermediate Coupling 43
C. Intermediate Separations 45
1. Charge-Transfer Interactions 49
D. Very Small Separations 51
VI. The Hellmann-Feynman Theorem 51
A. The Generalized Hellmann-Feynman Theorem 52
B. The Electrostatic Hellmann-Feynman Theorem 54
C. Application of the Electrostatic Hellmann-Feynman Theorem to the Long-Range Interaction of Two Hydrogen Atoms 55
D. Other Applications of the Hellmann-Feynman Theorem to the Long-Range Interaction of Two Atoms 60
1. Cartesian Coordinates with Laboratory-Fixed Origin 60
2. Electronic Coordinates Relative to the Associated Nucleus . . 60
3. Confocal Elliptic Coordinates 61
E. The Integral Hellmann-Feynman Theorem 62
VII. The Role of Electron Correlations in Intermolecular Forces 63
A. Large Separations 63
B. Intermediate Separations 67
C. Small Separations 69
D. Discussion of Davidson's Double Minimum Excited H_2 Potential Energy Curve 70
VIII. Magnetic or Relativistic Intermolecular Forces 71
A. The Breit-Pauli Hamiltonian 71
B. Small and Intermediate Separations 74
C. Large Separations 75
1. Calculation of the Interaction Energy 75
a. The Multipole Expansion of H_{rel} 75
2. Dispersion Energies 78
a. Comparison with the Exact Retarded Dipole–Dipole Interaction Energy 79
b. "Small R" Expansion 80
c. "Large R" Expansion 82

3. First-Order Energies 86
a. Retarded First-Order Interaction Energies 86
b. Comparison with the Exact Retarded Dipole Resonance Energy 87
c. Nonretarded First-Order Interaction Energies 90
d. Example: The Interaction of Two Hydrogen Atoms . . . 92
References 98

I. INTRODUCTION

Intermolecular forces are responsible for most of the physical and chemical properties of matter. Although the exact nature of these forces is very complicated, there are no conceptual difficulties. Most of the theory as we know it today was developed during the very early days of quantum mechanics.[4] Very few advances have been made during the past thirty years, and our present knowledge of the subject remains semi-quantitative. A lack of available precise experimental data led to a lack of interest in the development of the theory in the past. Now the situation is changing rapidly. As can be seen from Chapters 7–10, many new types of experiments have been devised for making very precise determinations of intermolecular forces. And, as can be seen from Chapters 2–6, there has been a renaissance in the theory. With the use of new types of quantum mechanical techniques and the availability of high-speed computing machines, it is now becoming possible to make accurate calculations of intermolecular forces.

Since each of the other chapters considers some specialized aspect, it seems appropriate to start with a survey of the general types of intermolecular forces and to discuss some of the conceptual and practical problems associated with the theory. In the interest of simplicity, we restrict our discussion to the interaction of two atoms. This avoids much of the complexity concerned with the orientations of the colliding molecules which Buckingham treats masterfully in Chapter 2. It also avoids the complexities of three- and four-body forces which Linder and Sinanoğlu consider in Chapters 5 and 6. However, if we are concerned with high accuracy, then the forces between even the simplest atoms require a very detailed explanation.

A. Interaction of Two 1*s* Hydrogen Atoms

In order to illustrate the complexity of intermolecular forces, let us consider the interaction of two hydrogen atoms in their ground states.

At small internuclear separations from $R = 0$ to $R = 0.8\,a_0$, Davidson and Jones[170] (see Sec. VII-C) have shown that the wave function for

the ground state of the hydrogen molecule is similar to the wave function for the He united atom.

In the small to intermediate range of separations, $0.4\,a_0 < R < 10.0\,a_0$, Kolos and Wolniewicz[49] (see Sec. IV-A and VII-A; note Table V) have made very accurate variational calculations of the energy for both the ground state, $X^1\Sigma_g^+$, and the first excited state, $b^3\Sigma_u^+$, of the hydrogen molecule. They include both the corrections for deviations from the Born-Oppenheimer approximation (discussed in Sec. II) and the relativistic corrections (discussed in Sec. VIII). The most accurate energy of dissociation which Kolos and Wolniewicz calculate for the lowest vibrational and rotational level of the ground state[22,25] is 1.1 cm^{-1} larger than the best experimental value.[50] The reason for this small discrepancy is not understood at the present time. For separations less than around $10\,a_0$, the atomic orbitals overlap and exchange energy is very important.

For large separations in the range $8\,a_0 < R < 200\,a_0$, the atomic orbitals do not overlap very much and the interaction energy can be expanded in an asymptotically converging series (see Sec. IV-B, V-B, VII-A, and VIII-C),

$$\begin{aligned} E_{\mathrm{H-H}} = \cdots &- 3986(1 + 0.0054)R^{-11} - (1135 + 2150)(1 + 0.0049)R^{-10} \\ &- 124.4(1 + 0.0038)R^{-8} - 6.499027(1 + 0.002723)R^{-6} \\ &+ 0.4628\,\alpha^2 R^{-4} + (W_3\,\alpha^2 - 0.3714\,\alpha^3)R^{-3} + \cdots \\ &\mp 0.818\,R^{5/2}\exp(-2R) \mp \ldots \end{aligned} \tag{1a}$$

Here, and throughout this chapter, all distances are given in Bohr radii and all energies (unless otherwise stated) are given in atomic units (e^2/a_0). The term in R^{-11} (see Sec. IX-A of Chapter 3) is the third-order dipole–quadrupole–dipole dispersion energy. Other third-order dispersion energy terms vary as higher powers of R^{-1}. The terms $-1135\ R^{-10}$, $-2150\ R^{-10}$, $-124.4\ R^{-8}$, and $-6.499027\ R^{-6}$ are the quadrupole–quadrupole, dipole–octopole, dipole–quadrupole, and dipole–dipole dispersion energies.[67] The factors 0.0054, 0.0049, 0.0038, and 0.002723 are due to the mass polarization correction to the Born-Oppenheimer approximation[16] discussed in Section II. The R^{-4} term is derived in Section VIII in two ways: first, as a mixed second-order energy—first-order with respect to the usual (electric dipole)–(electric dipole) perturbation and first order with respect to the Breit-Pauli relativistic correction term for the coupling of the orbital

angular momenta of the two electrons; secondly, it appears in the Casimir and Polder[199] "small R" expansion of the exact quantum electrodynamical (electric dipole)–(electric dipole) energy. The $-0.3714\,\alpha^3 R^{-3}$ also occurs in this "small R" expansion but its physical significance is questionable. The exponential term is the asymptotically correct form of the exchange energy [165c] (see Sec. VII-A). The minus sign applies to the electronic singlet state and the plus sign applies to the triplet states.

The $W_3\alpha^2 R^{-3}$ term results from the spin–spin interactions. For R less than around $9a_0$, only the electron spins need to be considered and $W_3 = 0$ for the $^1\Sigma_g^+$ state of the molecule; $W_3 = 1$ for the $^3\Sigma_u^+$ state with $M_s = 0$; and $W_3 = -\frac{1}{2}$ for the $^3\Sigma_u^+$ state with $M_s = \pm 1$. At larger separations, the interaction between the spin of an electron and the spin of its associated nucleus becomes larger than the interactions between the spins of the two electrons.[225] This means that 16 spin states for the system of two electrons and two protons must be considered (resulting in 11 potential curves). For values of R greater than $12a_0$, (see Table XI), $W_3 = -\frac{1}{2}$ for 3 of the states; $W_3 = -\frac{1}{4}$ for 4 states; $W_3 = (1 - 3^{1/2})/4$ for 1 state; $W_3 = 0$ for 1 state; $W_3 = \frac{1}{4}$ for 4 states; $W_3 = \frac{1}{2}$ for 2 states; and $W_3 = (1 + 3^{1/2})/4$ for 1 state.

At separations greater than $9a_0$ the electron spins of the 4 singlet states and 5 of the triplet states are partially decoupled and, for these, one can no longer speak of the molecular state as being an electron spin singlet or electron spin triplet. The other 7 states remain electron spin triplets at all separations. The other complication is that the atoms separate into hyperfine singlets and hyperfine triplets with (electron spin)–(nuclear spin) energies of $-\frac{3}{4}$ and $+\frac{1}{4}$ times 0.047384 cm^{-1}, respectively. One molecular state corresponds to both atoms being hyperfine singlets; six states correspond to one atom being a hyperfine singlet and the other a hyperfine triplet; and nine states correspond to both atoms being hyperfine triplets. The energies of the separated atoms, of course, do not appear in the interaction energy but they do effect the *a priori* statistical probabilities of the various states occurring in a collision. The hyperfine energies of the separated atoms have the other important effect of producing an apparent "doubling" or "natural line width" of 0.047 cm^{-1} in the potential energy curves for the interaction of two hydrogen atoms. Other causes of natural line width of the potential energy curves are the deviations from the adiabatic approximation (corresponding to the assumption of separability

of the electronic and nuclear coordinates) discussed in Section II (see also Sec. IV) and the other fine and hyperfine structural corrections discussed in Sections V and VIII.

At extremely large separations, $R > 1800\,a_0$, the energy of interaction has the form

$$E_{H-H} = W_3\alpha^2 R^{-3} - 37\alpha^{-1}R^{-7} + 1228\,\alpha^{-3}R^{-9} \ldots \qquad (1b)$$

Here the W_3 have the same values as discussed above and the $W_3\alpha^2R^{-3}$ term is dominant. The remaining terms arise from the "large R" expansion of the Casimir-Polder (electric dipole)–(electric dipole) dispersion energy taking retardation into account. In between $R = 200\,a_0$ and $R = 1800\,a_0$, it is necessary either to use the exact Casimir-Polder formulas for the dispersion energy in terms of sine and cosine integrals, or else Table IX given in Section VIII.

Before beginning our review, we should call attention to the wealth of articles and books which have already been written on the subject. The basis for much of our chapter is the last three chapters in the *Molecular Theory of Gases and Liquids* by Hirschfelder, Curtiss, and Bird.[1] The *Theory of Intermolecular Forces* by Margenau and Kestner[2] has very complete coverage of all aspects of intermolecular forces. The 1965 Symposium of the Faraday Society[3] has many interesting papers. However, the two general papers which we find most useful are Margenau's review article of *Van der Waals Forces*[4] (which is still authoritative after 28 years!); and Mulliken's brilliant treatment of the *Interaction of Differently Excited Like Atoms.*[5c] And finally, we should mention the new *Polyatomic Molecules* book of Herzberg[6] which contains a number of potential energy surfaces determined from experimental spectroscopic data which offer a challenge to the theoreticians.

II. CONCEPT OF AN INTERMOLECULAR POTENTIAL

The concept of intermolecular forces and potential energy surfaces is closely related to the Born-Oppenheimer[7–9] separation beween electronic and nuclear motions. For *most* practical applications, the approximations implicit in this separation do not lead to appreciable errors. In general, the separation requires the velocity of the electrons to be large compared to that of the nuclei. In addition, the nuclear motion is semiclassical if the rate of change of its de Broglie wavelength with the change of relative nuclear separations is small compared to unity.[10]

The concept of intermolecular forces also implies that the nuclear motion or the collision process is *adiabatic in the Ehrenfest sense.*[31] That is, the molecular aggregate or the collision complex can be characterized by a set of electronic quantum numbers (in addition to the quantum numbers for the rotation and the translation of the system as a whole); and these quantum numbers do not change during the course of the collision. Corresponding to each set of these quantum numbers, there is a potential energy surface which determines the motion of the nuclei.

For high precision, the Born-Oppenheimer energy has to be corrected for the coupling of the electronic and nuclear motions. The coupling is important if:

1. The nuclear velocities are large, as in "hot atom" collisions or in high-energy molecular beam collisions.

2. The potential energy surfaces of two electronic quantum states of the same symmetry cross in the Born-Oppenheimer approximation. (The correction terms prevent such crossings.)

3. The electronic state of a polyatomic molecule is degenerate and the nuclei approach a symmetric nonlinear configuration. The coupling produces the Jahn-Teller or Renner effects.[35]

4. The molecule is rotating rapidly and has a nonvanishing electronic angular momentum.

There are two causes for the deviations from the Born-Oppenheimer separation. First, coupling terms appear in the kinetic energy when the coordinates are transformed from the laboratory-fixed axes to the molecular axes. And second, the Breit-Pauli relativistic corrections to the electrostatic Hamiltonian lead to spin–spin, spin–orbit, and other magnetic coupling terms which are discussed in Section VIII and in Chapter 4.

There are two kinds of correction terms for the coupling of the electronic and nuclear motions. The *diagonal* corrections shift the energy levels. The *nondiagonal* corrections produce and broaden a natural line width to the energy and lead to transitions between quantum states. The energy corrected for the diagonal coupling terms is called the *adiabatic* approximation. The adiabatic approximation gives the best possible potential energy curves and surfaces. For specific electronic–vibrational–rotational states, the energy of the molecular system can be calculated by considering the nondiagonal as well as the diagonal corrections. This is called the *nonadiabatic* treatment.

In the present section, let us consider those coupling terms which arise

from a transformation of the coordinates from the laboratory-fixed axes to the molecular axes. For this purpose we neglect the relativistic corrections to the Hamiltonian. We treat an isolated molecular system composed of n electrons (designated by Roman subscripts) and γ nuclei (designated by Greek subscripts). The Hamiltonian for the molecule in a laboratory-fixed reference system (where the laboratory-fixed coordinates are designated by primes) and in atomic units[11] is

$$H' = -\frac{1}{2}\sum_i \nabla_i'^2 - \frac{1}{2}\sum_\alpha \frac{1}{m_\alpha}\nabla_\alpha'^2 + U$$

Here m_α is the ratio of the mass of the αth nucleus to the mass of an electron; and U is the coulombic energy of interaction of all of the particles (including the nuclear–nuclear repulsion terms).

Since U is a function of only the relative distances between the particles, the three coordinates of the center of mass of the molecular system can be separated from the $3(n + \gamma) - 3$ relative coordinates.[12–15] The optimum choice of the relative coordinates is not easy; the merits of several possible choices have been discussed by Jepsen and Hirschfelder,[13] Fröman,[12] and Pack.[16] A discussion of the diatomic molecule is given below. For triatomic and polyatomic molecular systems, it is desirable to use relative coordinates for the nuclei which diagonalize the kinetic energy for the relative nuclear motion. For triatomic molecules[17–19] this leads to the familiar Wigner-Eyring-Polanyi skewed coordinate systems.[20] For more complex molecules, the relative nuclear coordinates are obtained by constructing "mobiles" with vectors which either join together two nuclei or one nucleus with the center of mass of a group of other nuclei. These vectors then comprise the set of relative nuclear coordinates.[19] The electronic coordinates are chosen in any convenient manner relative to the nuclear framework.

In order to simplify further discussion, consider the interaction of two atoms to form a diatomic molecule with nuclei a and b. The coordinates of the nuclei and electrons in a laboratory-fixed coordinate system are denoted by $\mathbf{r}_a'$, $\mathbf{r}_b'$, and $\mathbf{r}_i'$, respectively. A convenient set of relative coordinates is[12,14,16,26]

$$\mathbf{R} = \mathbf{r}_b' - \mathbf{r}_a'; \qquad \mathbf{r}_i = \mathbf{r}_i' - [1/(m_a + m_b)](m_a\mathbf{r}_a' + m_b\mathbf{r}_b') \tag{2}$$

After separating off the motion of the center of mass, the Hamiltonian has the form

$$H = H_e - \frac{1}{2\mu}\nabla_R^2 - \frac{1}{2(m_a + m_b)}\left[\sum_i \nabla_i^2 + 2\sum_{i<j}\nabla_i \cdot \nabla_j\right] \tag{3}$$

where $\mu = m_a m_b/(m_a + m_b)$. Furthermore, H_e is the electrostatic Hamiltonian in the clamped nuclei approximation

$$H_e = -\frac{1}{2}\sum_i \nabla_i^2 - \sum_i \left[\frac{Z_a}{r_{ai}} + \frac{Z_b}{r_{bi}}\right] + \sum_{i<j}\frac{1}{r_{ij}} + \frac{Z_a Z_b}{R} \tag{4}$$

where Z_a and Z_b are the nuclear charges. The third term in H is due to mass polarization and might be considered a part of the electronic Hamiltonian.

The form of H depends upon the choice of the relative coordinates. For example, in their very accurate calculations of the diatomic molecular energy (see Sec. IV), Kolos and Wolniewicz[15,21–25] use the set, Eq. (2), for considering homonuclear molecules but for heteronuclear molecules they define

$$\mathbf{r}_i = \mathbf{r}_i' - \frac{1}{2}(\mathbf{r}_a' + \mathbf{r}_b') \tag{5}$$

This leads to a mass polarization term in the Hamiltonian which is proportional to $\nabla_R \cdot \sum_i \nabla_i$ and couples the electronic and nuclear motions.

In order to develop the concept of intermolecular potentials, let us assume that at each internuclear separation R the electronic Schrödinger equation

$$H_e\psi_k(\mathbf{r},\mathbf{R}) = E_k(R)\psi_k(\mathbf{r},\mathbf{R}) \tag{6}$$

can be solved exactly for the complete set of eigenfunctions $\psi_k(\mathbf{r},\mathbf{R})$ and eigenvalues $E_k(R)$. Here $\mathbf{r}$ represents the coordinates of all the electrons in the molecule and k is a set of electronic quantum numbers. Then the Schrödinger equation for the combined nuclear and electronic motions

$$H\Psi(\mathbf{r},\mathbf{R}) = E\Psi(\mathbf{r},\mathbf{R}) \tag{7}$$

can be solved by expanding Ψ in the form

$$\Psi(\mathbf{r},\mathbf{R}) = \sum_k \chi_k(\mathbf{R})\psi_k(\mathbf{r},\mathbf{R}) \tag{8}$$

This leads to a set of equations for the functions $\chi_k(\mathbf{R})$ which determine the nuclear motion of the system,

$$\left[-\frac{1}{2\mu} \nabla_R^2 + E_l(R) + E'_{ll}(R) + \mathbf{E}''_{ll}(R) \cdot \nabla_R - E \right] \chi_l(\mathbf{R})$$
$$= -\sum_{k \neq l} [E'_{lk}(R) + \mathbf{E}''_{lk}(R) \cdot \nabla_R] \chi_k(\mathbf{R}) \quad (9)$$

Here

$$E'_{lk}(R) = E'_{lk}(\nabla_R^2) + E'_{lk}(\nabla_i \cdot \nabla_j) + E'_{lk}(\nabla_i^2) \quad (10)$$

where

$$E'_{lk}(\nabla_R^2) = -\frac{1}{2\mu} \int \psi_l^*(\mathbf{r},\mathbf{R}) \nabla_R^2 \psi_k(\mathbf{r},\mathbf{R}) \, d\mathbf{r} \quad (11)$$

$$E'_{lk}(\nabla_i^2) = -\frac{1}{2(m_a + m_b)} \sum_i \int \psi_l^*(\mathbf{r},\mathbf{R}) \nabla_i^2 \psi_k(\mathbf{r},\mathbf{R}) \, d\mathbf{r} \quad (12)$$

$$E'_{lk}(\nabla_i \cdot \nabla_j) = -\frac{1}{(m_a + m_b)} \sum_{i<j} \int \psi_l^*(\mathbf{r},\mathbf{R}) \nabla_i \cdot \nabla_j \psi_k(\mathbf{r},\mathbf{R}) \, d\mathbf{r} \quad (13)$$

and

$$\mathbf{E}''_{lk}(R) = -\frac{1}{\mu} \int \psi_l^*(\mathbf{r},\mathbf{R}) \nabla_R \psi_k(\mathbf{r},\mathbf{R}) \, d\mathbf{r}$$

The $\mathbf{E}''_{lk}(R)$ give rise to velocity-dependent forces on the nuclei. However, if ψ_l is taken to be real,[14] the *diagonal* term $E''_{ll}(R) = 0$. In practice, Eq. (9) is extremely difficult to solve and various approximations must be used.

A. The Born-Oppenheimer Approximation

The Born-Oppenheimer approximation corresponds to neglecting *all* of the coupling terms $E'_{lk}(R)$. Equation (9) becomes a Schrödinger-type equation for the nuclear motion

$$\left[-\frac{1}{2\mu} \nabla_R^2 + E_l(R) - E \right] \chi_l(\mathbf{R}) = 0 \quad (14)$$

In this approximation, the $E_l(R)$ [determined from Eq. (6)] serve as the potential energy for the nuclear motion.

B. The Adiabatic Approximation

The adiabatic approximation corresponds to neglecting all nondiagonal coupling terms. Equation (9) becomes a Schrödinger-type equation for

the nuclear motion

$$\left[-\frac{1}{2\mu} \nabla_R^2 + V_l(R) - E \right] \chi_l(\mathbf{R}) = 0 \tag{15}$$

where the potential energy for the nuclear motion is

$$V_l(R) = E_l(R) + E'_{ll}(R) \tag{16}$$

The diagonal elements $E'_{ll}(R)$ can be interpreted as a correction to the potential energy due to the coupling between the electronic and nuclear motions. The adiabatic (or Born) approximation gives the "best" definition of the potential energy function.

As we have defined it, the adiabatic approximation to the energy is an *upper bound* to the true energy since it can be expressed as the expectation value to the correct Hamiltonian for the molecule evaluated with an approximate wave function.[26a] However, as discussed in Sec. IV, the recent calculations of Kolos and Wolniewicz[24] give values for the adiabatic energy for the equilibrium separation of the ground state of H_2 which are too low by 4.4 cm^{-1}. The reason for this is not understood at the present time[67] and is not explained by the recent work of Epstein[27] and Brattsev,[28] who give proofs that what they call the "adiabatic approximation" (which is different from the definition of Kolos and Wolniewicz which we use) accurately calculated should give a lower bound to the energy. In their definitions of the adiabatic potential, they do not include the term $E'_{ll}(\nabla_R^2)$ which is positive. It is indeed interesting to note that if we subtract $\int \chi_l(R)^* E'_{ll}(\nabla_R^2) \chi_l(R)\, d\mathbf{R}$ from *our* adiabatic energy, we obtain a lower bound to the true energy provided that our adiabatic energy is accurately calculated.

C. The Nonadiabatic Approximation

The nonadiabatic approximation corresponds to the consideration of the nondiagonal as well as the diagonal elements of $E'_{lk}(R)$. This is extremely difficult to carry out and, up to the present time, it has only been carried out in the case of the ground electronic state of H_2 by Kolos and Wolniewicz.[15] They avoided the separation of electronic and nuclear coordinates and solved the exact Schrödinger equation for all *four* of the particles (including the nuclei). They claim that the computational effort involved in this nonadiabatic treatment is of the same order as the computations necessary for the corresponding adiabatic

treatment. Their nonadiabatic method involves a direct calculation of the electronic-vibrational-rotational wave function for a molecule and is particularly useful in the determination of the expectation values of operators which depend explicitly on the nuclear coordinates. Using this procedure, the experimentally observable dissociation energy of the molecule can be calculated directly without requiring the determination of a potential energy curve. The application of the method by Kolos and Wolniewicz to two-electron diatomic molecules is discussed in Section IV. Similar applications have been made to "light" three-particle systems.[37]

D. Coupling between the Electronic and Rotational Angular Momenta

Coupling between the electronic and rotational angular momenta can cause deviations from the Born-Oppenheimer or adiabatic approximation if neither the electronic nor the rotational angular momentum quantum numbers are zero. This is not apparent from the previous equations in which the orientations of the electronic as well as the nuclear coordinates are referred to axes whose *directions* are space fixed. By the use of group theory, it is possible to separate off the rotational motion of a molecular system. (For polyatomic molecules, see Hirschfelder and Wigner,[38] Curtiss, Hirschfelder, and Adler,[39] and Curtiss;[40] for diatomic molecules see Pack[16] and Kolos and Wolniewicz.[15]) The total wave function is expressed as a sum of the products of rotational representation coefficients (which depend upon the Eulerian angles) and functions which depend upon the relative configuration of the particles (and not upon the orientation of this configuration). The energy of the system is determined by solving a set of coupled differential equations.

For diatomic molecules, after separating off the rotational coordinates, the Hamiltonian has the form[16]

$$H = \frac{-1}{2\mu R^2}\frac{\partial}{\partial R}\left[R^2\frac{\partial}{\partial R}\right] + H_e + \frac{\mathscr{L}^2}{2\mu R^2} + \frac{1}{\mu R}\left[\mathscr{P}_x\mathscr{L}_y - \mathscr{P}_y\mathscr{L}_x - i\mathscr{P}_z\frac{\partial}{\partial R}(R\quad)\right] \tag{17}$$

Here $\mathscr{L}$ is the operator for the orbital angular momentum of the nuclei

and $\mathscr{P}$ is the operator

$$\mathscr{P} = -i\left[\frac{\mu}{m_a}\sum_i \nabla_i - \frac{\mu}{m_b}\sum_j \nabla_j\right] \tag{18}$$

where the electrons i are associated with atom a and the electrons j are associated with atom b. The total angular momentum of the nuclei is equal to the difference between $\mathbf{J}$, the total angular momentum of the molecule, and $\mathscr{J}$, the total angular momentum of the electrons,

$$\mathscr{L} = \mathbf{J} - \mathscr{J} \tag{19}$$

If the molecule is not in an external field, J^2 is a constant of the motion. In terms of $\mathbf{J}$ and $\mathscr{J}$, the Hamiltonian involves raising and lowering operators of both the $\mathbf{J}$ and $\mathscr{J}$ varieties. The Schrödinger equation can then be written in the form

$$\begin{aligned} E\Psi(\mathbf{r},R;J,\Omega) &= H\Psi(\mathbf{r},R;J,\Omega) \\ &= H_0\Psi(\mathbf{r},R;J,\Omega) + H_+\Psi(\mathbf{r},R;J,\Omega+1) \\ &\quad + H_-\Psi(\mathbf{r},R;J,\Omega-1) \end{aligned} \tag{20}$$

Here the Ω is the component of $\mathbf{J}$ along the internuclear axis. The H_0, H_+, and H_- operators involve $\mathscr{J}$ and its raising and lowering operators. The determination of E and Ψ involve the solution of a set of coupled equations of the form of Eq. (20). The coupling of the electronic and nuclear angular momenta can be classified into Hund's cases[36] a, b, c, and d and treated accordingly by perturbation procedures (see Sec. V-B-5 and VIII-C). This "Ω-coupling" gives rise to the familiar Λ-doubling in molecular spectra. Usually this coupling is very small and unimportant in bound-state diatomic molecules, which helps to explain the success of the Born-Oppenheimer separation. In the special case of $J = 0$, the quantum number Ω can only have the value of zero and hence Eq. (20) reduces to the uncoupled relation

$$E\Psi(\mathbf{r},R;0,0) = H_0\Psi(\mathbf{r},R;0,0) \tag{21}$$

This greatly simplifies the determination of the intermolecular forces for $J = 0$ states.

E. Discussion

To summarize, the corrections to the Born-Oppenheimer approximation can be written as the sum of terms due to different causes,[16]

$$\Delta E_{BO} = \Delta E_M + \Delta E_\alpha + \Delta E_R + \Delta E_C + \Delta E_{EN} \tag{22}$$

Here ΔE_M is the correction due to mass polarization, ΔE_α is due to the relativistic corrections (see Sec. VIII and Chapter 4), ΔE_R corresponds to the radial motion, ΔE_C to the centrifugal forces, and ΔE_{EN} to the electronic and nuclear coupling. It should be emphasized that ΔE_{BO} is the correction to the effective intermolecular potential[75] (discussed in Sec. III). The $\Delta E_M + \Delta E_\alpha$ is the correction to the usual (static) intermolecular potential. These correction terms can be calculated by the use of perturbation theory. For ΔE_α, the perturbation parameter is $\alpha = 1/137$; for all of the other ΔE, the parameter is $1/\mu$. Generally, sufficient accuracy is obtained by calculating the energy through the first order. Problems involving electronic degeneracy or resonance require special consideration. The corrections for long-range energy of interaction are considered in Sec. IV, V, and VII. However, perhaps it should be mentioned here that for the interaction of one-electron atoms, the polarization corrections to energy terms C_n/R^n which vary as R^{-n} are given by[16] $\Delta E_M = [(n-1)/(2\mu)]C_n R^{-n}$. For H_2 this correction is 0.4% and for other isotopic molecules it is even smaller. Whereas corrections to the Born-Oppenheimer approximation are usually negligible, they are sometimes important.

The accuracy of the Born-Oppenheimer and the adiabatic approximations have been carefully tested by the calculations of Kolos and Wolniewicz,[15,21–25] Hunter,[26a] and Cashion,[29a] on two-electron diatomic molecules (see also Van Vleck,[30] Dalgarno and McCarroll,[14] Jepsen and Hirschfelder,[13] and Pack[16]). These calculations are discussed in Section IV. For many applications the approximations implicit in these approximations do not lead to serious error.

Spin–spin, spin–orbit, and other magnetic coupling terms contained in the Breit-Pauli relativistic correction to the electrostatic Hamiltonian (see Sec. VIII) can cause "forbidden transitions" from one potential energy curve to another.[32] Also the off-diagonal elements $E'_{lk}(R)$ appearing in Eq. (9) can induce transitions since they provide coupling between the various potential energy curves of the molecule. The probability of these transitions is greatest at "almost crossings" of two potential energy curves.[10,33,34] If the transition probabilities during the course of the collision are small compared to unity, the concept of potential energy surfaces is still useful and perturbation techniques can be used to provide corrections for the nonadiabatic behavior.[10] If, on

the other hand, the transition probability becomes large, the concept of potential energy surfaces and intermolecular forces loses its significance.

The probability P_{12} of an electronic jump from a potential energy curve *1* to a curve *2* depends upon whether the molecular states before and after the transition are discrete or continuous. Coulson and Zalewski[10] have examined this difficult problem and conclude that under a wide range of conditions P_{12} may be approximated by

$$P_{12} = \exp\left\{-(2/(\hbar^2 v_1 v_2)\left|\int_0^\infty E'_{12}(R)\, dR\right|^2\right\}$$

where v_1 and v_2 are some average values of the classical relative velocity of the nuclei in the initial and final states. Here

$$E'_{12}(R) = \int \psi_1(\mathbf{r},R)^* V(\mathbf{r},R)\psi_2(\mathbf{r},R)\, d\mathbf{r}$$

where $V(\mathbf{r},R)$ is the perturbation (a differential operator) which couples the electronic and nuclear motions. The older formula of Zener, Landau, and Stueckelberg[34] has been criticized by Bates[33] and seems to be applicable only under much more restrictive and unrealistic conditions. The problem of determining P_{12} accurately is one of the interesting problems in the theory of molecular beam scattering.

III. THE EFFECTIVE POTENTIAL

The *effective potential*, V_{eff}, is the apparent potential energy (curve or surface) which governs the relative motion of the nuclei after the rotational coordinates for the molecule have been separated off. Except for the small corrections to the Born-Oppenheimer separation discussed in Section II, the effective potential is the usual (static) potential energy, V, plus the centrifugal energy of the molecule.

Consider a diatomic molecule rotating with the quantum number K (and having the corresponding projection quantum number M_K). The wave function for the relative nuclear motion can be written as

$$\chi_l(\mathbf{R}) = R^{-1}\Phi_K(R)Y_K^{M_K}(\theta,\phi) \tag{23}$$

where $Y_K^{M_K}(\theta,\phi)$ is a normalized spherical harmonic. Substituting $\chi_l(\mathbf{R})$ into Eq. (14), we obtain the equation for the radial motion

$$-\frac{1}{2\mu}\frac{d^2\Phi_K}{dR^2} + V_{\text{eff}}(R)\Phi_K = E\Phi_K \tag{24}$$

The effective potential is given by

$$V_{\text{eff}} = V + K(K+1)/(2\mu R^2) \tag{25}$$

The term $K(K+1)/(2\mu R^2)$ is called the centrifugal potential. In the Born-Oppenheimer approximation, the potential energy V is given by $E_l(R)$. In the adiabatic approximation, according to Eq. (22), $V = E_l(R) + \Delta E_{BO}$. In order to make the corrections to the Born-Oppenheimer approximation as small as possible, the quantum number K should be chosen (Pack, unpublished work) as the integer which makes the best approximation to

$$K(K+1) \approx J(J+1) - 2\Omega^2 + \langle \mathcal{J}^2 \rangle \tag{26}$$

For example, if two hydrogen atoms in their ground states collide, then the correct centrifugal potential corresponds to[16]

$$K(K+1) = J(J+1)$$

if the molecular system is in the ${}^1\Sigma_g^+$ or the ${}^3\Sigma_u^+(M_s = \pm 1)$ states. If the system is in the ${}^3\Sigma_u^+(M_s = 0)$ state, then

$$K(K+1) = J(J+1) + 2$$

Equation (24) is then the starting point for the calculation of the vibrational and rotational energy levels of the molecular state.[24,26,29] The explicit calculation of the potential energy is discussed in Sections IV, V, and VIII.

Figure 1 shows that if the potential energy $V(R)$ has a minimum, then the effective potential has a hump or maximum for values of K in the range $K_{\text{crit}} > K > 0$. The hump in the effective potential has a number of interesting consequences. First of all, as explained in Chapter 8 and in reference 1, p. 553, it can lead to "orbiting" and to very large scattering angles for collisions between atoms in which the energy of the system is equal to, or almost equal to, the maximum value of V_{eff} for the angular momentum K which characterizes the collision. Secondly, it leads to metastable vibrational energy states (as shown in Fig. 1). From the standpoint of classical mechanics, diatomic molecules in these states are stable until they suffer collisions with other atoms or molecules. However, from the standpoint of quantum mechanics, the metastable diatomic molecules can break apart by tunneling through the energy hump and, therefore, each metastable state has a characteristic lifetime, τ. At extremely low pressures where

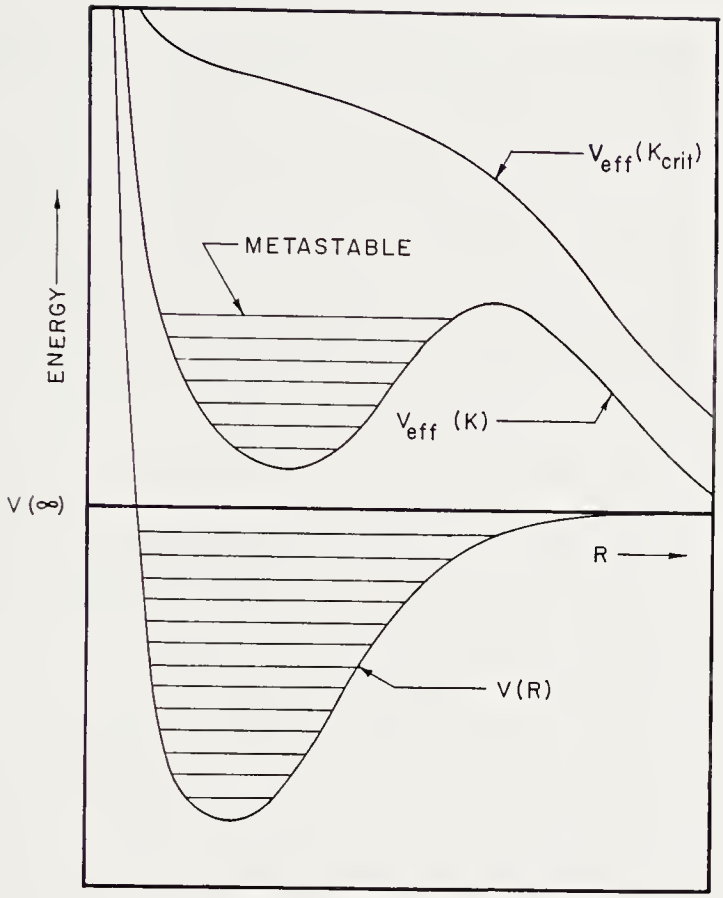

Fig. 1. The effective energy of interaction, V_{eff}, of two atoms. This figure shows the metastable vibrational energy levels which occur when the rotational quantum number K is less than K_{crit}.

the time between collisions is longer than τ, the metastable molecules dissociate by tunneling; whereas, at somewhat higher pressures (which still can be small compared to one atmosphere), the metastable molecules do not often dissociate between collisions. Quantum mechanical calculations of collision cross sections take the metastable states into consideration (in the determination of the phase shifts), but classical calculations have ignored them.[41] Metastable double molecules or atoms can lead to unexpected shifts in molecular spectra at high pressures.[42] Metastable double molecules also determine the pressure dependence of the thermal conductivity of a gas at low to medium density since the energy-rich metastable molecules, formed by a

three-body collision, diffuse to another place where they dissociate and release their energy.[43,44] The anomalous heat conductivity of NO_2 is a specially good example.

When the vibronic energy of a diatomic molecule equals the energy of the hump in V_{eff}, dissociation of the molecule is possible. Figure 1 shows that the more strongly the molecule vibrates, the smaller the K value at which a dissociation can occur. Since the hump in the effective potential often occurs at fairly large values of R, where the long-range interactions appear to be dominant, $V(R)$ can be approximated[45] (see Sec. V) by[46]

$$V(R) - V(\infty) = -\bar{C}_n/R^n \tag{27}$$

Here $\bar{C}_n$ is a positive constant and n is an effective power which best serves to represent the potential in the vicinity of the hump.

Substituting Eq. (27) into Eq. (25) and differentiating V_{eff} with respect to R, Bernstein[45] shows that for a given value of K:

1. The hump occurs at a separation

$$R_m(K) = \{n\mu\bar{C}_n/[K(K+1)]\}^{1/(n-2)} \tag{28}$$

2. The energy of the hump is

$$[V_{\text{eff}}(K)]_{\max} = S_n[K(K+1)]^{n/(n-2)} \tag{29}$$

where

$$S_n = \frac{1}{2}(n-2)(n\mu)^{-n/(n-2)}\bar{C}_n^{-2/(n-2)}$$

3. The value of n is determined by

$$d \log [V_{\text{eff}}(K)]_{\max}/d[K(K+1)] = n/(n-2) \tag{30}$$

For a particular vibrational state, v, it is likely that the rotational state with the largest observed quantum number (before predissociation), $K_m(v)$, should have an energy lying close to the maximum (or hump) of V_{eff}. Thus, for a set (corresponding to different values of v) of rotational quantum numbers $K_m(v)$, the experimental energy of the vibronic state can be equated[45] to $\{V_{\text{eff}}[K_m(v)]\}_{\max}$. In this way, Bernstein found it possible to experimentally determine the power n to within plus or minus 0.2 or 0.3.

Bernstein[45] cites two examples. For the $X^2\Sigma^+$ state of HgH and of HgD, he found (with an uncertainty of 10%) that $n = 6$ and $\bar{C}_6 = (3.07$

and 2.99) $\times 10^{-59}$ erg cm^6, respectively. For comparison, the Slater-Kirkwood[47] approximation leads to $\bar{C}_6 = 3.5 \times 10^{-59}$ erg cm^6. The other example is the controversial $C\,^3\Pi_u$ state of N_2. Here he found that $n = 6$ (instead of the $n = 5$ which would be characteristic of quadrupole–quadrupole interaction) and $\bar{C}_6 = 5.2 \times 10^{-59}$ erg cm^6. Thus, it is probable that this state dissociates into $N(^4S) + N(^2D)$.

This method of using predissociation data to determine long-range interatomic forces was applied by Byrne, Richards, and Horsely[228] to HF (and DF), for which the Rydberg-Klein-Rees potential curve was known. Results for the $\bar{C}_6$ constant obtained from the two methods agreed within 5%. In addition, these authors made use of predissociation data (obtained from emission) for Se_2, which showed good straight-line behavior in a Bernstein plot showing $V(R) \approx -\bar{C}_5 R^{-5}$, as expected for P-state atoms. Their investigation also revealed anomalous long-range behavior for the halogens.

IV. ELECTROSTATIC VARIATIONAL CALCULATIONS

With the use of the Rayleigh-Ritz variation principle and high-speed computing machines, it is now becoming practical to calculate intermolecular forces at all separations with an accuracy comparable to the best experimental data. The excellent variational calculations for the energy of interaction of two hydrogen atoms in various states[48] provides a sample of the kind of *ab initio* theoretical potential energy curves and surfaces which will be obtained during the next few years for the interaction of more complex atoms and molecules.

In the variational method, the total energy, E, of the interacting atoms a and b, is calculated directly and not the interaction energy E_{ab};

$$E_{ab} = E - E^{(0)} \tag{31}$$

where $E^{(0)}$ is the energy of the isolated atoms $[E^{(0)} = E(\infty)]$. For large values of R, where E_{ab} is much smaller than E, it is very difficult to obtain accurate values for the interaction energy using the variational method.[49] Instead, the interaction energy can be calculated directly by using perturbation theory (see Sec. V). At intermediate and small values of R, where E_{ab} is relatively large and where it is very difficult to use perturbation theory, the variational principle usually gives the most accurate results.

A. Small and Intermediate Separations

In the small and intermediate range of separations, the separated atoms have lost their identity and the system can be treated as a diatomic molecule. First, the interaction energy is calculated in the Born-Oppenheimer or fixed nuclei approximation. For high precision, this result can be corrected for the "diagonal" nuclear–electronic coupling terms (giving the adiabatic approximation) and for relativistic effects (Sec. VIII), both of which can be calculated using the wave function obtained in the fixed-nuclei approximation. The "diagonal" coupling terms do not take into account all of the interactions of the electronic, vibrational, and rotational motions. For highest accuracy, the energy of specific electronic–vibronic–rotational states can be calculated nonadiabatically as discussed in Section II.

1. *The Ground $X^1\Sigma_g^+$ State of the Hydrogen Molecule*

Table I contains some of the very excellent results which Kolos and Wolniewicz obtained for the ground state of the hydrogen molecule. They carried out their calculations with utmost precision and appear to have made every correction which is indicated by the most sophisticated quantum mechanical theory including relativistic corrections (see Sec. VIII and Table VI).

Thus, Kolos and Wolniewicz[22,25] treated H_2, D_2, T_2, and HD as four-particle problems in a nonadiabatic calculation of the vibronic energy levels of the electronic ground state using a 147-term wave function. Recently, Wolniewicz[24] has made a very careful vibrational–rotational study of the ground states of H_2, HD, and D_2 using accurate Born-Oppenheimer[49] and adiabatic[21] potentials. As Table I shows, the theoretical dissociation energies agree with the experimental values[50] to within one part in ten thousand and it is difficult to explain[24,26] why the agreement is not one part in one hundred thousand in accordance with the estimated accuracy of the experimental values. The discrepancy is not due to relativistic corrections since both the Breit-Pauli corrections of $O(\alpha^2)$ and the radiative corrections[24] of $O(\alpha^3)$ (where α is the fine structure constant) have been computed and cannot decrease the theoretical dissociation energy by more than 0.5 and 0.4 cm^{-1}, respectively (see Sec. VIII). The computed[24] vibrational quanta are larger than observed by about 1 cm^{-1} while the theoretical rotational quanta are in very good agreement with experiment.

It is interesting to note that the Born-Oppenheimer result for the dissociation energy agrees more closely with experiment than the theoretically better adiabatic approximation. As pointed out by Wolniewicz[24] and Hunter,[26a] the nonadiabatic calculation may not be

TABLE I

Kolos and Wolniewicz Variational Calculations for the $X^1\Sigma_g^+$ Ground State of The Hydrogen Molecule

All energies are given in cm^{-1}. Here $e^2/a_0 = 219{,}474.62\ cm^{-1}$.

A. The Energy of Dissociation from the Lowest Vibrational and Lowest Rotational State

	H_2	HD	D_2
Experimental[50]	36113.6	36400.5	36744.2
Born-Oppenheimer approximation[24]	36112.2[a]	36401.5	36745.6
Adiabatic approximation[24]	36118.0	36405.7	36748.3
Nonadiabatic calculation[22,25]	36114.7	36402.4	36746.2

B. Diagonal Deviations from the Separation of Electronic and Nuclear Coordinates[21] *(see Sec. II). Equilibrium Separation,* $R_e = 1.40108\ a_0$

$R/a_0 =$	0.60	1.4011	2.40	3.60	∞
$E'(\nabla_R^2)$	36.084	38.367	44.140	56.588	59.766
$E'(\nabla_l^2)$	113.994	70.193	53.496	53.575	59.766
$E'(\nabla_l \cdot \nabla_j)$	8.026	6.025	4.123	1.948	0.000
Total $E'(R)$	158.104	114.585	101.759	112.111	119.532

[a] Other values in the literature which appear equally reliable are: 36113.0 (ref. 26b), 36112.7 (ref. 29a), and 36111.2 (ref. 29b).

fully minimized and hence the close agreement between the nonadiabatic and experimental dissociation energies may be fortuitous. These calculations show that the Born-Oppenheimer approximation is excellent and the deviations from it are small even for H_2 (at least for the ground state, see subsection 2 below). For molecules with nuclei of greater mass, the Born-Oppenheimer approximation should be even more accurate.

2. *The Lowest Excited Bound State, $B^1\Sigma_u^+$, of Hydrogen*

Kolos and Wolniewicz[23] have also calculated the energy of dissociation (from the bottom of the potential energy curve) for the lowest excited *bound* state, $B\,^1\Sigma_u^+$, of hydrogen using a 54-term wave function. Their results are given in Table II. They obtained excellent agreement

TABLE II

Kolos and Wolniewicz Variational Calculations for the $B^1\Sigma_u^+$ First Bound Excited State of Hydrogen

All energies are given in cm^{-1}. Here $e^2/a_0 = 219{,}474.62\ cm^{-1}$.

A. The Energy of Dissociation from the Bottom of Potential Energy Curve

Experimental value[51]	$D_e = 28852.8$
Adiabatic calculation[23]	$D_e = 28850.2$
Born-Oppenheimer approximation[23]	$D_e = 28896.3$

B. Equilibrium Separation

Experimental value	$R_e = 2.443\ a_0$
Calculated value	$R_e = 2.43\ a_0$

C. Diagonal Deviations from the Separation of Electronic and Nuclear Coordinates[23] (*See Sec. II*)

R/a_0	1.5	2.43	3.0	5.0	∞
$E'(\nabla_R^2)$	131.890	65.800	50.987	35.291	37.354
$E'(\nabla_i^2)$	54.058	45.218	42.710	36.317	37.354
$E'(\nabla_i \cdot \nabla_j)$	7.452	9.825	9.407	5.369	0.000
Total $E'(R)$	193.400	120.843	103.104	76.977	74.707

with Namioka's experimental results.[51] The "diagonal" corrections for electronic–nuclear coupling are quite different from those for the ground-state calculation. For the equilibrium internuclear distance, the correction to the binding energy due to nuclear motion, $E_l'(\infty) - E_l'(R_e)$, amounts to $-46.1\ cm^{-1}$ which is larger by an order of magnitude than the corresponding correction for the ground state and has the opposite sign. For this excited state of H_2, the agreement of the Born-Oppenheimer results for the dissociation energy with experiment is not nearly as good as for the ground state; the adiabatic approximation gives an excellent result.

3. *The Lowest Excited* $^1\Sigma_g^+$ *State of Hydrogen*

Davidson[52,53] has calculated the potential energy curve for the lowest excited $^1\Sigma_g^+$ state of the hydrogen molecule (designated $E\,^1\Sigma_g^+$). His results are given in Table III (see also Gerhauser and Taylor[54];

TABLE III

Davidson's[53] Variational Calculations for the Lowest Excited $^1\Sigma_g^+$ State of the Hydrogen Molecule

Energy	e^2/a_0	cm^{-1}
For $R = \infty$, $E(\infty)$	−0.6250	−137,172
At outer minimum where $R = 4.3\ a_0$		
$E(4.3) - E(\infty)$, calculated	−0.0757	−16,610
$E(4.3) - E(\infty)$, experimental	−0.0685	−15,030
At the maximum where $R = 3.3\ a_0$		
$E(3.3) - E(\infty)$, calculated	−0.0634	−13,910
At inner minimum where $R = 1.9\ a_0$		
$E(1.9) - E(\infty)$, calculated	−0.0912	−20,020
$E(1.9) - E(\infty)$, experimental	−0.0931	−20,430

Kolos and Roothaan[55]). The special feature of this potential is its double minimum. At large separation this state dissociates into a $1s$ hydrogen atom and a $2s$ hydrogen atom. Around $R = 10\,a_0$, there is an almost crossing of potential curves with the second excited $^1\Sigma_g^+$ state (which also has a double minimum). From $R = 10$ to $4.4\,a_0$, the state behaves like the interaction of H^+ with the $(1s)^2$ state of H^-. An open shell wave function including nine ionic terms and nine atomic terms was used for the calculation at the outer minimum. On the other hand, at smaller separations the state corresponds to a $(1s\sigma)(2s\sigma)$ configuration. A 20-term open-shell covalent-type wave function was used for the calculation at the inner minimum. These results are discussed in terms of electron correlation in Section VII.

B. Large Separations

One of the principal difficulties with Rayleigh-Ritz variational calculations of the interaction energy at large separations is that one cannot calculate the interaction energy directly using this method. Rather, one obtains the interaction energy, Eq. (31), as the difference

of two large numbers, which for large R have approximately the same value.

Another difficulty appears, namely the evaluation of the two- or many-centered integrals which occur in the calculation. For example, the zeta-function expansions[56,57] of a Slater orbital about another center do not converge rapidly at intermediate to large separations.[58] Thus, most variational calculations of potential energy curves become inaccurate at intermolecular separations of greatest interest with respect to intermolecular forces. Now, with the use of Gaussian transforms developed by Shavitt and Karplus[59] and Karplus and Kern[60] (see also Foster and Boys,[61] and Kikuchi[62]), the many-centered integrals can be evaluated at all separations with high accuracy. Another approach, suggested by Boys,[63] is to make use of Gaussian-type orbitals[64] which lead to a fundamental simplification of the evaluation of the multicenter integrals. Clementi and Davis[65a] and Veillard and Clementi[65b] have shown that it is possible to obtain high accuracy using multiconfigurational wave functions composed of *large* numbers of Gaussian orbitals. Even though the convergence is relatively slow, the method is attractive because large basis sets can be used since the resulting multicenter integrals can be evaluated on an IBM 7094 computer at the rate of five million per hour!

Recently, Kolos and Wolniewicz[49] have obtained excellent values for the energy of both the ground state, $X\,^1\Sigma_g^+$, and the first excited state, $b\,^3\Sigma_u^+$, of the hydrogen molecule at separations ranging from $R = 0.4$ to 10.0 a_0. From $R = 0.4$ to 4.7 a_0, they used a 53-term wave function. For larger values of R, the number of terms in the wave function was reduced to avoid rounding errors. The van der Waals minimum for the $b\,^3\Sigma_g^+$ state occurs at $R = 7.85\ a_0$ and is 4.3 cm^{-1} deep. These results are discussed in more detail in Section VII.

For large separations, instead of calculating the values of the interaction energy, E_{ab}, at tabular values of R by the variational method, perturbation theory (see Sec. V for details) can be used to express the interaction energy in the form

$$E_{ab} = \sum_n C_n/R^n \tag{32}$$

and the individual coefficients C_n can be calculated by variational techniques. This perturbation-variation method enables the interaction energy to be calculated directly and, therefore, avoids many of

the difficulties inherent in the usual variational calculation for large separations.

Hirschfelder and Löwdin[66] considered the interaction of two hydrogen atoms in their ground state using this technique. They expanded the normalized wave function for the molecule in the form of a power series

$$\Psi_0 = \psi_0 + \sum_{n=1}^{\infty} \Psi_n R^{-n} \tag{33}$$

where ψ_0 corresponds to the wave function for the separated atoms. Then by writing $E_{ab} = \sum_n C_n R^{-n} = \langle \Psi_0 | H_e | \Psi_0 \rangle - E^{(0)}$, expanding H_e in powers of R^{-1} and equating like powers of R^{-1}, they obtained variational principles for each of the C_n (here R^{-1} is being treated as a perturbation parameter). Recently, Kolos[67] has used this same procedure, employing a very large number of basis functions, to obtain high accuracy for the C_n for a number of hydrogen molecular states. His results are given in Table IV (see also refs. 158–160). The series, as given in this table, gives the electrostatic interaction energy with less than 4% error for $R > 10\ a_0$ for the $1s$–$1s$ hydrogen interaction and for $R > 18\ a_0$ for the $1s$–$2s$ or $1s$–$2p$ interactions. There is a further discussion of the R^{-1} power series expansion of E_{ab} in Sections V and VII.

For very high precision, as explained in Section II, the C_n (including all of the values given in Table IV) should be correeted for deviations from the Born-Oppenheimer approximation. For example, as Dalgarno and McCarroll[14] and Pack[16] have shown, if C_n^0 is the value of the coefficient calculated in the Born-Oppenheimer approximation, then C_n corrected for mass polarization is given by $C_n = C_n^0[1 + (n-1)/(2\mu)]$. Thus, for the ground state, $X\,^1\Sigma_g^+$, of the hydrogen molecule using the values given in Table IV, the coefficients for the hydrogen isotopes corrected for mass polarization are:

Isotope	$-C_6$	$-C_8$	$-C_{10}$
H_2	6.516725	124.8734	3301.934
HD	6.512303	124.7549	3297.910
D_2	6.507881	124.6363	3293.885
T_2	6.504940	124.5575	3291.208

In this section we have briefly discussed variational calculations of

TABLE IV

Kolos[67] Values of the Coefficients C_n for the Long-Range Energy of Interaction of 1*s*, 2*s*, and 2*p* Hydrogen Atoms
(These coefficients are expressed in atomic units and *not* corrected for mass polarization)

		C_3	C_6	C_8	C_{10}			
Atomic configuration	Molecular states	Dip.–dip. resonance	Dip.–dip. dispersion	Dip.–quad. dispersion	Quad.–quad. dispersion	+ Dip.–octo. dispersion	=	Total
$1s1s$	$X^1\Sigma_g^+, b^3\Sigma_u^+$		−6.499027	−124.3991	−1135.214	−2150.614	=	−3285.828
$1s2s$	$B'^1\Sigma_u^+, {}^3\Sigma_g^+$		−148.769	−16607.2				
$1s2s$	$^1\Sigma_g^+, {}^3\Sigma_u^+$		−204.736	−19588.6				
$1s2p\sigma$	$B^1\Sigma_u^+, {}^3\Sigma_g^+$	−1.1098579	−174.166	−15780.9				
$1s2p\sigma$	$^1\Sigma_g^+, {}^3\Sigma_u^+$	+1.1098579	−174.166	−18309.8				
$1s2p\pi$	$^1\Pi_g, {}^3\Pi_u$	−0.5549290	−94.457	−7971.2				
$1s2p\pi$	$C^1\Pi_u, {}^3\Pi_g$	+0.5549290	−94.457	−9207.9				

molecular interaction energies. For energy calculations for the larger molecules, the Hartree-Fock and related methods are particularly useful. Also these self-consistent field potential energy curves need not agree with the exact curves to give useful information. They often provide a good account of the shapes[68,69] of the potential curves for diatomic molecules and therefore can give good vibrational and rotational constants and may be useful in establishing good semi-empirical estimates of the actual potential energy curves as well.

V. ELECTROSTATIC PERTURBATION CALCULATIONS

Whereas variational techniques are especially suited for the calculation of short- and intermediate-range intermolecular forces, perturbation techniques are suited for the calculation of long-range forces. Rayleigh-Schrödinger perturbation theory is used in part B of this section to classify the different types of long-range electrostatic intermolecular forces[70] and again in Section VIII to discuss relativistic intermolecular forces. Except where otherwise stated, only the Born-Oppenheimer approximation is considered in the present section.

A. Rayleigh-Schrödinger Perturbation Theory

In Rayleigh-Schrödinger perturbation theory,[71] the Hamiltonian of the system is expressed in the form $H = H_0 + V$, where H_0 is the unperturbed Hamiltonian and V is the perturbation potential. The eigenfunctions and eigenvalues for the jth state of the unperturbed system are ψ_j and ε_j so that $H_0\psi_j = \varepsilon_j\psi_j$. The exact wave function, Ψ_0, and the exact energy, E_0, for the state under consideration, labeled the 0th state, are expanded in the series

$$\Psi_0 = \psi_0 + \Psi_0^{(1)} + \Psi_0^{(2)} + \cdots \tag{34}$$

$$E_0 = \varepsilon_0 + E_0^{(1)} + E_0^{(2)} + E_0^{(3)} + \cdots \tag{35}$$

In order that both Ψ_0 and ψ_0 be normalized to unity through any given order n in the perturbation, we require

$$\sum_{k=0}^{n} \langle \Psi_0^{(k)} | \Psi_0^{(n-k)} \rangle = \delta_{no} \tag{36}$$

where $\Psi_0^{(0)} = \psi_0$. The perturbation differential equations have the form

$$(H_0 - \varepsilon_0)\psi_0 = 0 \tag{37}$$

$$(H_0 - \varepsilon_0)\Psi_0^{(1)} + (V - E_0^{(1)})\psi_0 = 0 \tag{38}$$

$$(H_0 - \varepsilon_0)\Psi_0^{(2)} + (V - E_0^{(1)})\Psi_0^{(1)} = E_0^{(2)}\psi_0 \tag{39}$$

. . .

from which it can be shown that

$$E_0^{(1)} = \langle\psi_0|\, V\,|\psi_0\rangle \tag{40}$$

$$E_0^{(2)} = \langle\psi_0|\, V\,|\Psi_0^{(1)}\rangle \tag{41}$$

$$E_0^{(3)} = \langle\Psi_0^{(1)}|\, V\,|\Psi_0^{(1)}\rangle - E_0^{(1)}\langle\Psi_0^{(1)}\,|\,\Psi_0^{(1)}\rangle \tag{42}$$

If the wave function is known through order n, the energy can be calculated through the $(2n + 1)$st order. Expanding the perturbed wave functions, $\Psi_0^{(n)}$, in the complete set of unperturbed wave functions, ψ_j, one can show that

$$\Psi_0^{(1)} = -\sum_j{}' \frac{\psi_j V_{j0}}{\varepsilon_j - \varepsilon_0} \tag{43}$$

$$\Psi_0^{(2)} = \sum_j{}' \sum_k{}' \frac{\psi_j V'_{jk} V_{k0}}{(\varepsilon_j - \varepsilon_0)(\varepsilon_k - \varepsilon_0)} - \frac{1}{2}\psi_0 \sum_k{}' \frac{V_{0k}V_{k0}}{(\varepsilon_k - \varepsilon_0)^2} \tag{44}$$

$$\begin{aligned} E_0^{(2)} &= -\sum_j{}' \frac{V_{0j}V_{j0}}{\varepsilon_j - \varepsilon_0} \\ E_0^{(3)} &= \sum_j{}' \sum_k{}' \frac{V_{0j}V_{jk}V_{k0}}{(\varepsilon_j - \varepsilon_0)(\varepsilon_k - \varepsilon_0)} - E_0^{(1)} \sum_j{}' \frac{V_{0j}V_{j0}}{(\varepsilon_j - \varepsilon_0)^2} \end{aligned} \tag{45}$$

Here $V_{j0} = \langle\psi_j|\, V|\psi_0\rangle$ and the primed sigmas indicate a sum over all the discrete states plus an integral over the continuum states of the unperturbed problem, *omitting* the states with energy ε_0. It is interesting to note that if the state 0 is the ground state, $E_0^{(2)}$ is *negative* irrespective of the nature of the perturbation potential.

If there is a set of unperturbed states k, all of which have the unperturbed energy ε_0, then ψ_0 must be taken as a linear combination of the degenerate wave functions such that for all $k \neq 0$ the $V_{0k} = 0$. With this choice of ψ_0, the equation for $E_0^{(2)}$ remains unaffected by the degeneracy. However, the equations for $\Psi_0^{(1)}$ and for the higher-order energies are changed as a result of the degeneracy and the changes depend upon the order of perturbation in which the degeneracy is removed.[71a]

B. Large Separations

Let us apply the Rayleigh-Schrödinger perturbation theory (see for example ref. 1, p. 916) to the long-range interaction of atom a in state q with atom b in state q'. At large separations, the wave functions for the two interacting atoms do not overlap appreciably. Thus the wave function for the molecular system does not have to be antisymmetrized with respect to exchange of electrons between the two atoms.[73] One set of electrons (designated by i) may be associated with atom a and another set of electrons (designated by j) may be associated with atom b. Electron exchange which is very important at intermediate separations, gives rise to exchange energies which decrease exponentially with R, and are negligible for sufficiently large R.

Choosing the zeroth-order Hamiltonian to be the sum of the electrostatic Hamiltonians for the two separated atoms

$$H_0 = H_a(i) + H_b(j) \tag{46}$$

the electrostatic approximation to the perturbation potential is given by

$$V_e = H_e - H_0 = -\sum_j \frac{Z_a}{r_{aj}} - \sum_i \frac{Z_b}{r_{bi}} + \sum_{i,j} \frac{1}{r_{ij}} + \frac{Z_a Z_b}{R} \tag{47}$$

Here H_e is the total electrostatic Hamiltonian for the diatomic molecule a–b, in the fixed-nuclei approximation. For long-range interactions, it is frequently desirable to express the perturbation or interaction potential V_e in terms of a multipole expansion.

1. *The Multipole Expansion of* V_e

For those electronic configurations where the separation is sufficiently large that $R > (r_{ai} + r_{bj})$ for all i and j, the r_{aj}^{-1} and r_{bi}^{-1} can be expanded in Neumann series and the r_{ij}^{-1} can be expanded in a bipolar series[76] to give the interaction potential in the form

$$V_e = \sum_{n=1}^{\infty} V_n / R^n \tag{48}$$

where

$$V_n = \sum_{l_a=0}^{n-1} \sum_{m=-l_<}^{l_<} \frac{(-1)^{l_b}(n-1)!\, Q_{l_a}^m(i) Q_{l_b}^{-m}(j)}{[(l_a-m)!(l_a+m)!(l_b-m)!(l_b+m)!]^{1/2}} \tag{49}$$

Here $l_<$ is the lesser of l_a and $l_b = n - l_a - 1$. Also, if the polar axis

is taken in the direction from nucleus a towards nucleus b and right-handed coordinate axes are used to describe the position of the electrons in both atoms a and b, then

$$Q_{l_a}^m(i) = Z_a\delta_{l_a0} - \sum_i [4\pi/(2l_a+1)]^{1/2} r_{ai}^{l_a} Y_{l_a}^m(\theta_{ai},\phi_{ai}) \tag{50}$$

where the $Y_l^m(\theta,\phi)$ are spherical harmonic functions; similar relations hold for $Q_{l_b}^m(j)$. The Q_l^m are the irreducible tensorial components of the electrostatic multipole operators for the interacting atoms: Q_0^0 is the charge on the given atom; the Q_1^m are the instantaneous dipole moment operators; the Q_2^m are the instantaneous quadrupole moment operators, etc. Note that the Q_l^m defined by Eq. (50) are equal to $[(l-|m|)!/(l+|m|)!]^{1/2}$ times the Q_l^m defined in reference 1, p. 840. This change of definition is required in order to make the Q_l^m conform to irreducible tensorial notation. As discussed in reference 1, the coefficients V_n represent the instantaneous interaction of the various electrostatic multipoles of atoms a and b: V_1 is the charge–charge interaction, V_2 the charge–dipole interaction, V_3 the sum of the dipole–dipole and charge–quadrupole interactions, etc.

Expressing the V_n in terms of the irreducible tensorial operators, Q_l^m, is very convenient[72a,77,78] for the actual calculation of long-range interatomic forces. Using this form for V_n permits this calculation to be carried out making the fullest possible use of group theory. For our purposes, however, it is more useful to write the V_n in the more familiar cartesian component representation. For example, for the interaction of neutral atoms, $V_1 = V_2 = 0$. Thus V_3R^{-3}, the lead term in the multipole expansion of the interaction potential for neutral atoms, can be written in either of the forms

$$\begin{aligned} V_3 &= -\sum_i \sum_j [2z_{ai}z_{bj} - x_{ai}x_{bj} - y_{ai}y_{bj}] \\ &= \boldsymbol{\mu}_a \cdot \boldsymbol{\mu}_b - 3(\boldsymbol{\mu}_a \cdot \hat{\mathbf{R}})(\boldsymbol{\mu}_b \cdot \hat{\mathbf{R}}) \end{aligned} \tag{51}$$

where $\hat{\mathbf{R}}$ is the unit vector in the direction of the polar axis and $\boldsymbol{\mu}_a = -\sum_i \mathbf{r}_{ai}$ and $\boldsymbol{\mu}_b = -\sum_j \mathbf{r}_{bj}$ are, respectively, the instantaneous electrostatic dipole moments of the atoms a and b. The coefficient V_3 clearly represents the electrostatic dipole–dipole interaction.

The multipole expansion of the interaction potential is very convenient for a conceptual understanding of long-range intermolecular forces. Combined with the perturbation theory outlined above, it

leads to a formal series expansion of both E_{ab} and of Ψ_0 in powers of $1/R$ [see Eqs. (32) and (33)]. However, the multipole expansion of V_e neglects those regions of electron configuration space for which some of the electrons do not satisfy the requirement that $R > (r_{ai} + r_{bj})$. It has been shown[73] that such electronic configurations lead to contributions to the molecular energy which decrease exponentially with separation and become negligible at sufficiently large separations. However, for some problems, the $1/R$ expansion of the energy may converge very slowly, asymptotically, or not at all.[72b,78–80]

2. *The Perturbation Problem*

Now let us return to the perturbation problem of atom a in state q and having electrons i interacting with atom b in state q' and having electrons j. Atom a has a complete set of states r with eigenfunctions $A_r(i)$ and energies a_r so that $H_a(i)A_r(i) = a_r A_r(i)$ and similarly for atom b, $H_b(j)B_u(j) = b_u B_u(j)$. Thus the complete set of wave functions for the zeroth-order Hamiltonian, H_0, is given by $\psi_{ru} = A_r(i)B_u(j)$, and the corresponding eigenvalues are $\varepsilon_{ru} = a_r + b_u$. The zeroth-order energy is

$$\varepsilon_0 = \varepsilon_{qq'} = a_q + b_{q'} \tag{52}$$

corresponding to the energy of the isolated atoms a and b, while the interaction energy is given by

$$E_{ab} = E_0 - \varepsilon_0 = E_0^{(1)} + E_0^{(2)} + E_0^{(3)} + \cdots \tag{53}$$

with $V = V_e$ in Eqs. (40)–(45).

There are three types of interactions: nonresonant, resonant, and almost degenerate which are considered in subsections 3, 4, and 5, respectively. The special feature of resonance interactions is that the initial state qq' is degenerate and at least part of the degeneracy is broken up in the first order of perturbation. There are two types of resonance. In subsections 4-a to 4-d, atoms a and b are taken to be the *same species* and resonance occurs when q and q' correspond to different states such that

$$\langle A_q(i)B_{q'}(j)|\, V_e \,|A_{q'}(i)B_q(j)\rangle \neq 0$$

In subsection 4-e, one-molecule resonance is considered where a and b need not be the same species but the state q or q' is degenerate and the degeneracy is removed by the interaction perturbation. In subsection 5, the difficult problems are considered, corresponding to atomic states

which are degenerate in the electrostatic approximation but which become almost degenerate as the result of the relativistic perturbations. If we ignore the relativistic effects and treat these states as degenerate, our results would be strictly valid for internuclear separations sufficiently small that the electrostatic interaction energy is larger than the fine-structure splitting in the interacting atoms.[77c,78,81] At larger internuclear separations, the spin–orbit interaction within the atoms becomes large compared to the electrostatic interaction and the atomic energy levels should be treated as being nondegenerate.

The results discussed in this section are valid for moderately large intermolecular separations.[72] By moderately long range, we mean an intermolecular separation R which is sufficiently large that the charge distributions of the interacting molecules do not overlap appreciably, and yet not large enough to involve strong retardation effects, $R \ll \lambda\!\!\!^{-}$, where $\lambda\!\!\!^{-}$ is the reduced wavelength characteristic of allowed electrostatic transitions in the interacting atoms. (It should be mentioned that charge overlap or exchange effects can be significant at fairly large values of R, for example[49,73,74] at $R \sim 9\ a_0$ for the H–H ground-state interaction; see Sec. VII.) By including relativistic effects obtainable from the Breit-Pauli approximation (see Sec. VIII) the region of validity of these results can be extended to larger values of R. However for very large values of the internuclear separation, $R > \lambda\!\!\!^{-}$, quantum electrodynamics must usually be used to calculate accurate interaction energies, as discussed by Power in Chapter 4.

3. *Nonresonant Intermolecular Forces*

a. **First-Order Energy.** For nonresonant interactions of two atoms, the zeroth-order wave function has the form

$$\psi_0 = \psi_{qq'} = A_q(\mathrm{i})B_{q'}(\mathrm{j}) \tag{54}$$

The corresponding first-order energy is

$$E_0^{(1)}(\text{nonres}) = \langle A_q(\mathrm{i})B_{q'}(\mathrm{j})|\, V_e \,|A_q(\mathrm{i})B_{q'}(\mathrm{j})\rangle \tag{55}$$

For sufficiently large separations,[73] Eqs. (48) and (49) can be used to express V_e in a series in powers of $1/R$. Thus, we obtain

$$E_0^{(1)}(\text{nonres}) = \sum_{n=1}^{\infty} \sum_{l_a=0}^{n-1} \sum_{m=-l_<}^{l_<} \frac{(-1)^{l_b}(n-1)!(Q_{l_a}^{m})_{qq}(Q_{l_b}^{-m})_{q'q'}R^{-n}}{[(l_a-m)!(l_a+m)!(l_b-m)!(l_b+m)!]^{1/2}} \tag{56}$$

Here $l_<$ is the lesser of l_a and $l_b = n - 1 - l_a$. Also, $(Q^m_{l_a})_{qq}$ and $(Q^m_{l_b})_{q'q'}$ are the expectation values of the multipole moments of the isolated atoms. Equation (56) would apply equally well to the first-order nonresonant energy of interaction between two *molecules* where the Q's are to be reinterpreted as the multipole moments of the isolated molcules.[100] Thus, $E_0^{(1)}$(nonres) corresponds to the interaction energy between the permanent moments of the atoms or molecules. For

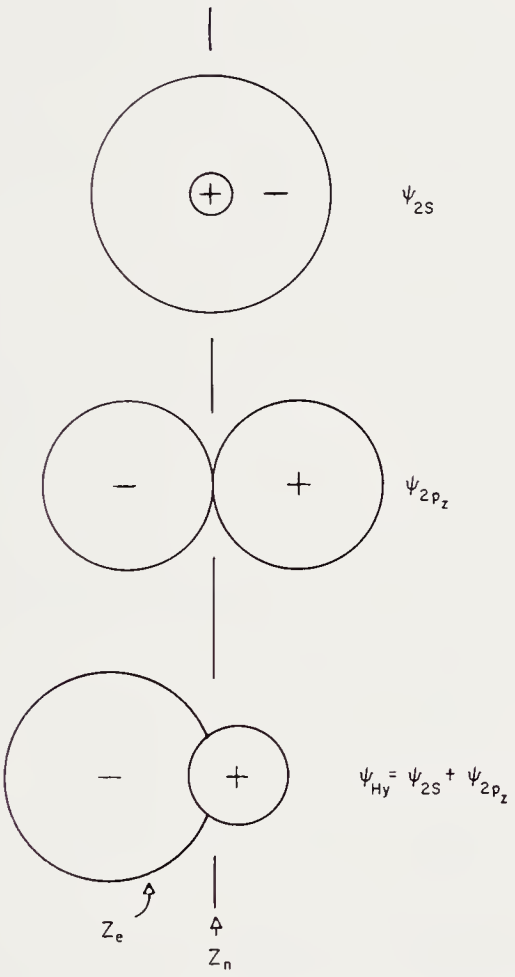

Fig. 2. Schematic diagram showing how hybridization of orbitals with different parity can produce a dipole moment in an atom. Consider a hydrogen $2s$ orbital, ψ_{2s}, and a hydrogen $2p_z$ orbital, ψ_{2p_z}, both centered on the nucleus n. The hybrid orbital, ψ_{Hy}, formed by adding ψ_{2s} and ψ_{2p_z}, has an electronic charge density $\rho_e = \psi^*_{Hy}\psi_{Hy} / \int \psi^*_{Hy}\psi_{Hy}\, d\tau$. The z coordinate of the center of the electronic charge density is $z_e = \int z\rho_e\, d\tau$. It is clear from the figure that z_e lies to the left of z_n, the z coordinate of the nucleus.

neutral atoms or molecules, the net charge, $(Q_0^0)_{qq}$, is zero. Thus, the leading term for the electrostatic interaction of two neutral polar molecules (corresponding to the perturbation V_3) is given by

$$E_0^{(1)}(\text{dipole–dipole}) = R^{-3}[(\boldsymbol{\mu}_a)_{qq} \cdot (\boldsymbol{\mu}_b)_{q'q} - 3\{(\boldsymbol{\mu}_a)_{qq} \cdot \hat{\mathbf{R}}\}\{(\boldsymbol{\mu}_b)_{q'q'} \cdot \hat{\mathbf{R}}\}] \tag{57}$$

Isolated atoms in pure quantum states cannot have a permanent dipole moment. In order to have a dipole moment, an atom must be hybridized with a wave function which is a mixture of quantum states of different parities (as illustrated in Fig. 2). Except for the hydrogen atom (where, for example, the $2s$ and $2p$ states have different parity), atomic states having the same energy have the same parity. Thus, insofar as nonresonant atomic collisions are concerned, the dipole–dipole interactions can be ignored.

However, atoms which are not in an S state can have a quadrupole moment. For these atoms, Knipp[81] and Chang[78] (see ref. 1, p. 1013) have calculated the first-order quadrupole–quadrupole interaction energy, corresponding to V_5 as the perturbing potential (V_4 as well as V_3 give zero contributions to $E_0^{(1)}$ as the result of parity considerations). However, the quadrupole moments result from the coupling of the electronic spin and orbital angular momenta. The nature of this coupling changes and the values of the quadrupoles change with R. Thus, the discussion of these quadrupole–quadrupole interactions is deferred to subsection 5 where problems of almost degeneracy due to fine-structure effects are considered.

b. **Second-Order Energy.** The second-order energy is a sum of terms corresponding to the transitions from the state qq' to each of the *other* states ru. There are three kinds of these transitions:

1. $r = q$, $u \neq q'$. Such transitions correspond to the permanent moments in a polarizing b. The induced moments in b then react with the permanent moments in a.

2. $r \neq q$, $u = q'$. These transitions correspond to the permanent moment in b polarizing a.

3. $r \neq q$, $u \neq q'$. These transitions lead to the second-order dispersion energy.

Thus, the second-order perturbation energy can be expressed as the sum of three terms:

$$E_0^{(2)} = E_0^{(2)}(a \text{ polarizes } b) + E_0^{(2)}(b \text{ polarizes } a) + E_0^{(2)}(\text{dispersion})$$

The second-order induction energy terms have the form

$$E_0^{(2)}(a \text{ polarizes } b) = -\sum_{u \neq q'} \frac{|\langle A_q(i)B_{q'}(j)|\, V_e\, |A_q(i)B_u(j)\rangle|^2}{b_u - b_{q'}} \qquad (58)$$

If q' is the ground state of b, then $E_0^{(2)}$ (a polarizes b) is negative corresponding to an attraction between the two molecules. However, the second-order induction energy involving excited-state molecules can be either positive or negative.

If V_e is expanded in the series [Eq. (48)] in powers of $1/R$, then $E_0^{(2)}$ can also be expressed in a series in powers of $1/R$. The individual coefficients correspond to the interaction of the dipole–polarizability, quadrupole-polarizability, ... of b with the permanent multipole moments of a (see Chapter 2). Thus, for example, the induction energy between an ion having the net charge C_a and a neutral molecule having the dipole-polarizability α_b (in the direction of a) is $-C_a^2\alpha_b/(2R^4)$. The induction energy between a polar molecule with a dipole moment $\boldsymbol{\mu}_a$ and a nonpolar molecule[89] is $-\mu_a^2\alpha_b(3\cos^2\theta_a + 1)/(2R^6)$ where θ_a is the angle between $\boldsymbol{\mu}_a$ and the internuclear axis. The induction energy between a quadrupolar molecule and an induced dipole[90] varies as R^{-8}. Induction forces are treated in considerable detail in reference 1, pages 29 and 985. The ion-molecule induction forces are very important. However, the induction forces between neutral molecules are usually small except for the interaction of large zwitterions or large conjugate double-bonded molecules where the induced dipoles may become very large. Indeed, induction forces may have considerable importance in interactions between molecules of biological interest.

The second-order dispersion energy has the form

$$E_0^{(2)}(\text{dispersion}) = -\sum_{r \neq q} \sum_{u \neq q'} \frac{|\langle A_q(i)B_{q'}(j)|\, V_e\, |A_r(i)B_u(j)\rangle|^2}{(a_r - a_q) + (b_u - b_{q'})} \qquad (59)$$

If the states q and q' are the ground states of their respective molecules, then $E_0^{(2)}$(dispersion) is negative corresponding to an attraction between the molecules. Otherwise, the contribution to the second-order dispersion energy from a particular transition is either negative or positive depending on whether $(a_r - a_q) + (b_u - b_{q'})$ is positive or negative.

If V_e is expanded in a power series in R^{-1}, then

$$E_0^{(2)}(\text{dispersion}) = \sum_{n=6}^{\infty} C_n(\text{dis})/R^n \qquad (60)$$

The leading term (corresponding to V_3) is

$$C_6(\text{dis}) = -\sum_{r\neq q}\sum_{u\neq q'} \frac{|2(\mu_{az})_{qr}(\mu_{bz})_{q'u} - (\mu_{ax})_{qr}(\mu_{bx})_{q'u} - (\mu_{ay})_{qr}(\mu_{by})_{q'u}|^2}{(a_r - a_q) + (b_u - b_{q'})} \quad (61)$$

and the corresponding interaction energy, $C_6(\text{dis})/R^6$, is the well-known London dispersion energy.[91] The term $C_8(\text{dis})\ R^{-8}$ results from the dipole–quadrupole perturbation, V_4. The term $C_{10}(\text{dis})\ R^{-10}$ is the result of contributions from both the quadrupole–quadrupole and the dipole–octopole interactions. The importance of the dipole–octopole contribution to the R^{-10} interaction energy should be emphasized[77a,92,93] and, in the case of two hydrogen atoms, can be seen in Table IV. Selection rules usually prevent the occurrence of contributions to the $E_0^{(2)}$(dispersion) from mixed terms such as

$$-\sum_{r\neq q}\sum_{u\neq q'} \frac{\langle A_q(i)B_{q'}(j)|\, V_k\, |A_r(i)B_u(j)\rangle\langle A_r(i)B_u(j)|\, V_l\, |A_q(i)B_{q'}(j)\rangle}{[(a_r - a_q) + (b_u - b_{q'})]R^{k+l}}$$

where V_k and V_l are different operators. However, such mixed terms may be important in molecular interactions. For atom–atom interactions, the third-order dispersion energy has a leading term that varies as R^{-11}.

The older approach (harmonic oscillator and hydrogenic approximations) to the calculation of the dispersion energies has been thoroughly treated by Margenau[94] and presented in reference 1, p. 955 (a more recent presentation is given by Fontana[77a]). The newer techniques, which are capable of giving very accurate results, are discussed by Dalgarno in Chapter 3.

In Eqs. (59) and (61), it is necessary to use the exact wave functions and exact energies of the isolated atoms. If approximate wave functions and approximate energies of the isolated atoms are used, then an additional perturbation procedure[71] must be used to correct for the badness of the zeroth-order wave function. Thus, it is no surprise that Hartree-Fock calculations (which lead to poor values of polarizabilities) can lead to poor values of the London dispersion energies. The importance of electron correlations is explained in Section VII. Recent research[95–97] confirms the supposition of early workers that the intra-atomic correlation effects (which are important in determining the polarizabilities of the atoms) have a substantial effect on the dispersion energy. Thus, the Hartree-Fock calculations for C_6 should be corrected

for correlation effects. Without such a correction, C_6 is in error by 13% for the He–He interaction[98] and about 50% for the Be–Be interaction.[99]

4. *Resonant Intermolecular Forces*

Perhaps the most characteristic feature of resonant interactions is that the wave function for a resonant state corresponds to an electric moment when classically such a moment would not occur. The zeroth-order wave functions are those linear combinations of the degenerate set which diagonalize the perturbation potential matrix. The first-order perturbation energies vanish[4,73] when summed (or averaged) over all the original degenerate states of the system. Thus if the perturbation, V_e, leads to an abnormally large energy of attraction in one state, it will produce an abnormally large energy of repulsion in another state of the degenerate set. After averaging over the original degeneracy, the interaction energy is comprised of second- (or higher) order energies which do not vanish. Resonant interactions (between like atoms in different energy states), unlike the nonresonant collisions, have retarded first-order interaction energies in the range of separations $\hat{\lambda} < R < 10^3\hat{\lambda}$.

There are two kinds of resonant interactions: resonance between like atoms or molecules (considered in subsections a–d) and resonance within one molecule (considered in subsection e).

a. **Resonance between Like Atoms.**[5c,77b] This type of force occurs in the interaction of two *like* atoms in *different* energy states. Thus, atom a is the same species as atom b, but $q \neq q'$. Then $\varepsilon_{qq'} = \varepsilon_{q'q}$ and there are two types of zeroth-order wave functions, both corresponding to the same zeroth-order energy. Since we are neglecting electron exchange, these can be written in the form

$$\psi_g = (2)^{-1/2}[A_q(i)B_{q'}(j) - wA_{q'}(i)B_q(j)]$$
$$\psi_u = (2)^{-1/2}[A_q(i)B_{q'}(j) + wA_{q'}(i)B_q(j)] \qquad (62)$$

The functions ψ_g and ψ_u themselves do not necessarily have gerade or ungerade symmetry. Rather what is meant is that if ψ_g or ψ_u is properly antisymmetrized with respect to the exchange of electrons between the atoms a and b, then the resulting function has gerade or ungerade symmetry, respectively. The number w has the values ± 1 depending upon the parity of the states q and q', as well as on the number of

electrons in the atoms and the spin of the molecular state.[5c,83] Mulliken[5c] remarks that it is extremely easy to make mistakes in the sign of w.

One can classify resonances according to the order of perturbation and the type of perturbation which destroys the resonant degeneracy. Thus, we start by considering first-order dipole resonance which concerns interactions where the degeneracy is destroyed by the first-order perturbation with respect to the electric dipole–electric dipole interaction potential, V_3.

b. **First-Order Dipole Resonance.** If $(\boldsymbol{\mu})_{qq'} \neq 0$ then the lead term in the first-order perturbation energy is given by the matrix components of V_3,

$$E_g^{(1)} = -E_u^{(1)} = +wR^{-3}[2\,|(\mu_z)_{qq'}|^2 - |(\mu_x)_{qq'}|^2 - |(\mu_y)_{qq'}|^2] \qquad (63)$$

This interaction energy will be nonzero for S–P, P–D, etc. like-atom interactions.

One of the best examples of this type of resonance is the interaction of two doublet atoms or of two singlet atoms, one in an S state and the other in a P state. In such a collision there is an *a priori* probability of 2/3 that the component of orbital angular momentum along **R** is ± 1, in which case the resulting diatomic molecule has Π symmetry and $\langle S|\mu_z|P(\pm 1)\rangle = 0$. There is also an *a priori* probability of 1/3 that the component along **R** is zero so that the resulting diatomic molecule has Σ symmetry and $\langle S|\mu_x|P(0)\rangle = \langle S|\mu_y|P(0)\rangle = 0$. Thus the first-order resonance energy has the form

$$E_0^{(1)}(\text{res}) = w\gamma R^{-3}|\langle S|\mu_z|P(0)\rangle| \qquad (64)$$

where $w = +1$ for singlet states and $w = -1$ for triplet states and γ has the values

State of diatomic molecule	Value of γ
Σ_g	$+2$
Π_u	$+1$
Π_g	-1
Σ_u	-2

The square of the dipole moment matrix element, $\langle S|\mu_z|P(0)\rangle$, for the hydrogen atom $1s$–$2p$ transition[67] is $2^{15}/3^{10} = 0.5549290$ and sub-

stitution of this value into Eq. (64) leads to the results given in Table IV.

For H_2, Li_2, Na_2, K_2, Rb_2, Cd_2, and Hg_2 there is experimental[85] evidence that one of the states $^1\Sigma_g$, $^1\Pi_u$, $^3\Sigma_u$, or $^3\Pi_g$ corresponds to a stable molecule at small separations in spite of the fact that their resonance energy is positive for large values of R. This means that their potential energy curves have a maximum at some intermediate value of R. For example, in the lowest $^1\Pi_u$ state of Na_2 there is a pronounced minimum at 6.45 a_0 and a resonance maximum near $12a_0$.[5c,84]

There is considerable interest at the present time in the resonance interaction of two helium atoms where one atom is in the 1^1S, state and the other is in the 2^1P state and in the two helium-atom resonance where one atom is 2^1P and the other is 3^1D. Both of these cases have been observed experimentally[86] by the temperature variation of the pressure-induced line broadening in helium gas. This is discussed in Chapter 9 by Birnbaum and Maryott.

The interaction of two hydrogen atoms, both of which are in the $(2s,2p)$ degenerate energy states, is another example of a first-order dipole resonance where there is a $1/R^3$ contribution to the interaction energy. This interaction leads to 16 different molecular states and a complicated pattern of interaction energies.[73] However, as Fontana[77b] and Kim and Hirschfelder[79] have shown, some of these states interact as a result of V_4, V_5, . . ., so that the energy of a particular state can have a very complicated dependency on R even at moderately large separations. The correct zeroth-order wave functions for this problem are actually hybrid states of mixed parity which can therefore give rise to a nonzero matrix element for V_3 and V_4.

c. **First-Order Quadrupole Resonance.** If $(\mu)_{qq'} = 0$, but $(Q_2^m)_{qq'} \neq 0$, then the lead term in the first-order perturbation energy is given by the matrix components of V_5 and the resonance energy varies as $1/R^5$. This quadrupole-type resonance should be much weaker than the dipole but, nevertheless, it should be recognized and expected in S–D, P–F, etc. collisions between like atoms.

d. **The Second-Order Energy.** The second-order energy for resonant interactions of two like atoms has the same form as for nonresonant interactions (since the cross terms vanish because of selection rules). However, the induction energy is given by

$$E_0^{(2)}(a \text{ polarizes } b) = -\sum_{\substack{u \\ u \neq q \text{ or } q'}} \frac{|\langle A_q(i)B_{q'}(j)|\, V_e\, |A_{q'}(i)B_u(j)\rangle|^2}{b_u - b_{q'}}$$

and the dispersion energy is given by

$$E_0^{(2)}(\text{dispersion}) = -\sum_{\substack{r \\ r \neq q \text{ or } q' \\ u \neq q \text{ or } q'}} \sum_{u} \frac{|\langle A_q(i)B_{q'}(j)|\, V_e\, |A_r(i)B_u(j)\rangle|^2}{(a_r - a_q) + (b_u - b_{q'})}$$

e. **Resonance within One Molecule.** Some atoms or molecules have degenerate states which are separated by the perturbation produced by a second different molecule. In such cases, there is a possiblity of resonance. In reference 1, p. 994, an example is given of an excited hydrogen atom in either the $2s$ or $2p$ state colliding with a proton. Under the influence of the proton's electric field, the azimuthal quantum number of the hydrogen atom is no longer a good quantum number, while the magnetic quantum number remains a good quantum number. Thus, the zeroth-order wave function for the interaction can be written as

$$\psi_0 = C_1\phi_{2s} + C_2\phi_{2p_z} \tag{65}$$

where C_1 and C_2 are determined by diagonalizing the lead nonzero term in the $1/R$ expansion of V_e, namely the charge–dipole interaction Hamiltonian V_2/R^2. The resulting interaction energy varies as $1/R^2$ instead of $1/R^4$ as one would expect of a charge-induced dipole energy.

This type of resonance should also occur whenever a hydrogen atom excited to the $2s$ or $2p$ state collides with a molecule having a permanent dipole or quadrupole moment. Atoms with quadrupoles include the ground states of B, Al, Ga, C, Si, O, S, F, Cl, Br, I, etc. For a resonance collision between the excited hydrogen atom and the dipolar molecule, the first-order perturbation energy should vary as $1/R^3$; in collisions with a quadrupolar molecule, the energy should vary as $1/R^4$.

5. *Almost Degeneracy Due to the Effects of Atomic Fine Structure*

In many cases, the first-order interaction energies discussed previously become even more complicated at moderately large values of R, since the states of the isolated atoms are often almost degenerate due to fine-structure splittings.[77c,78,81] Let us consider the Hamiltonian for the system which includes the atomic spin–orbit Hamiltonians, $H_{SL}(a)$ and $H_{SL}(b)$, of the interacting atoms,

$$H' = H_0 + V_e + H_{SL}(a) + H_{SL}(b) \tag{66}$$

For the calculation of the electrostatic interaction energy based on Eq. (66), it is convenient to consider three cases.[87]

a. (Λ,S) **Coupling.** For interatomic separations for which the electrostatic interaction energy is greater than the atomic fine structure splittings, the $(S_a,L_a,M_{S_a},M_{L_a})$ coupling scheme[88] is applicable for the atomic states and the spin–orbit coupling is neglected. The molecular states of the interacting atoms can usually be characterized by the quantum numbers Λ and S, respectively, for the absolute value of the projection of the total orbital angular momentum along **R** and for the total spin of the system.

b. (J_a,J_b) **Coupling.** For values of R for which the electrostatic interaction energy is less than the atomic fine structure splitting the (S_a,L_a,J_a,M_{J_a}) coupling scheme[88] is most suitable for the atomic states and the zeroth-order Hamiltonian is taken to be $H_0' = H_0 + H_{SL}(a) + H_{SL}(b)$. The molecular states are now characterized by the quantum number Ω for the absolute value of the total angular momentum along **R**. This coupling scheme is often referred to as Hund's case *c* coupling.[5a,5b]

c. **Intermediate Coupling.**[77c] For regions of space where the interaction energy and the fine structure atomic splitting are approximately equal, a transition region between (Λ,S) and (J_a,J_b) couplings may exist. Here, instead of successively diagonalizing perturbations of different sizes, as in (*a*) and (*b*), essentially one must simultaneously diagonalize the perturbations $(H'-H_0)$. The potential energy curves that are calculated by this method merge into the (Λ,S) results at small R and asymptotically approach the (J_a,J_b) results at large R.[77c]

These atomic fine-structure effects produce splittings in potential energy curves that are degenerate for smaller values of R [(Λ,S) coupling] and the multiplet components of a *given* molecular state at small separations must often be correlated with components of *different* multiplets of the separated atoms [ref. 36a, p. 320; an example is given below]. At large separations [(J_a,J_b) coupling], the interaction energy (now defined as the molecular energy less the energy of the isolated atoms, including relativistic terms) often either has basically the same R dependence as in (Λ,S) coupling or else vanishes from symmetry considerations. Retardation or magnetic effects which introduce new powers of R^{-1} in the interaction energy, even for (Λ,S) coupling, are discussed in Section VIII and in Chapter 4.

The quadrupole–quadrupole interaction energy for atoms in their ground states has been studied by Knipp[81] for both the (Λ,S) and (J_a,J_b)

coupling schemes. Recently, a more extensive study of the problem has been made by Chang[78] who considered the intermediate coupling scheme and the effect of higher multipole interactions.

As an example, consider the effect of fine-structure splitting on the quadrupole–quadrupole energy between two ground-state boron atoms. A probable correlation diagram[78] for the transition from (Λ,S) to (J_a,J_b) coupling is given in Figure 3. For very large separations, where

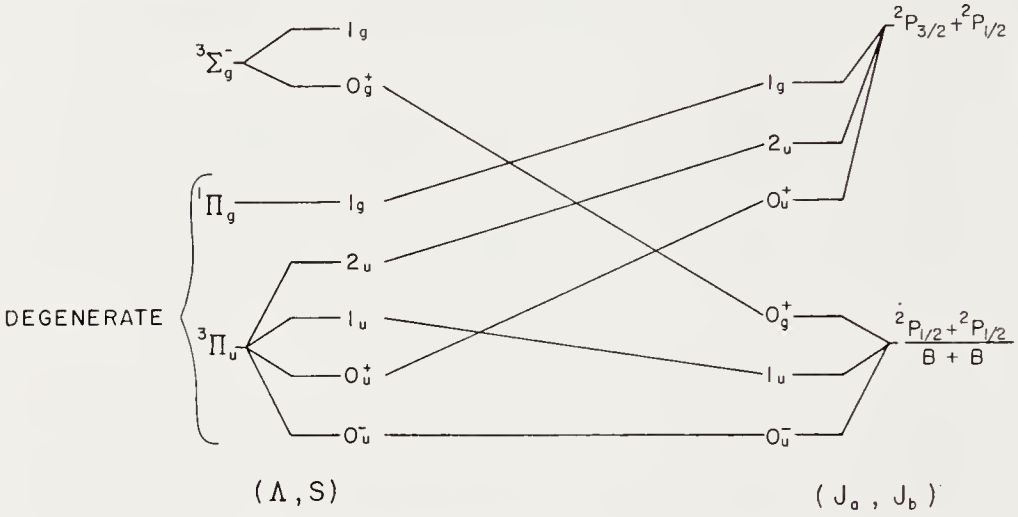

Fig. 3. A probable schematic diagram[78] for the transition from (Λ,S) to (J_a,J_b) coupling for the $^1\Pi_g$ and the $^3\Pi_u$ states which arise from the interaction of two ground-state boron atoms.

$R > 18\ a_0$, the (J_a,J_b) coupling is applicable and the interaction energies of the states that are correlated to the Π states of lowest energy are[78]

$$E_0^{(1)}(0_u^+) = -36.21\ R^{-5} \tag{67}$$

$$E_0^{(1)}(1_g) = -24.14\ R^{-5} \tag{68}$$

$$E_0^{(1)}(2_u) = -\ 6.05\ R^{-5} \tag{69}$$

$$E_0^{(1)}(0_u^-) = E_0^{(1)}(1_u) = 0 \tag{70}$$

At separations between $10\ a_0 < R < 18\ a_0$, the coupling is intermediate. For separations where $R < 10\ a_0$, the (Λ,S) is applicable and the states of the lowest energy ($^1\Pi_g$ and $^3\Pi_u$) have $E_0^{(1)} = -36.21R^{-5}$. The first-order energy is to be compared with the second-order dispersion energy,[78] $C_6R^{-6} = -140.5R^{-6}$ which is smaller in magnitude than $-36.21R^{-5}$ by the factor $3.88/R$.

The interaction of the two boron atoms is a good example of the very complicated splittings and crossings of the potential energy curves that can be caused by atomic fine structural effects. For the interaction of atoms with larger atomic number, the (J_a,J_b) coupling remains valid down to smaller values of R. Thus, for the CO molecule the (J_a,J_b) coupling applies to $R > 10\ a_0$ in contrast to the B_2 example where it applies to $R > 18\ a_0$. In some cases, the fine-structure coupling leads to maxima (or humps) in the potential energy curves of stable diatomic molecules.

Some very interesting examples of the effect of fine structure splitting on interaction energies have been worked out by Fontana[77c] for the resonance interaction of ground and excited alkali atoms and for the interaction of alkali atoms in excited states. The results are quite complicated and it suffices to note that for large internuclear distances ($R \sim 20\ a_0$ for the H–H resonance interaction) the degeneracy in the singlet and triplet curves is removed and the number of potential energy curves is increased by a factor of four.

C. Intermediate Separations

The region of intermediate separations is characterized by the overlapping of atomic orbitals and it is no longer possible to associate particular electrons with particular atoms. The wave functions for the molecular system must be properly antisymmetrized with respect to the exchange of the electrons between the two atoms.[229] Thus, it is very difficult to choose a *natural* unperturbed Hamiltonian to begin a Rayleigh-Schrödinger perturbation calculation of the interaction energy. However, the Rayleigh-Schrödinger theory can be applied to one- and two-electron diatomic molecules by using Sternheimer[71] techniques. Here, one chooses a "good" zeroth-order wave function which allows for electron exchange and then one calculates the corresponding zeroth-order Hamiltonian and perturbation potential. For the ground state of H_2^+ and HeH^{++}, one can solve the first-order perturbation differential equation exactly and obtain excellent results[101,102] for the interaction energy and the wave functions (for all R). For the ground state of H_2, Matcha[103] has used variation–perturbation techniques to solve the perturbation equations. The results are very good; for example, the perturbation energy, through fifth order at the equilibrium separation, is comparable in accuracy to the most accurate variational calculations. For molecules involving more than two

electrons, the space and spin portions of the wave function do not separate. Because of this, Sternheimer techniques are not very useful[104] since (*1*) the corresponding H_0 will contain nonlocal potentials[105] or (*2*) if H_0 is local, it will be very complex and involve N-body forces and a complicated spin dependence.[106]

There are many people who are currently trying to develop a more satisfactory form of perturbation theory that can be used for the calculation of intermediate-range intermolecular forces. Each of the proposed methods[70,107–110] is subject to criticism and, therefore, we confine ourselves to those statements which we can make with confidence. The eventual goal is to express the first-order wave function in closed form and to obtain the second- and third-order energies (including exchange terms) by quadrature.

Because of the difficulty in choosing an "H_0" for the intermediate range problem, it is convenient to use a perturbation theory which does not require a zeroth order Hamiltonian. One of the simplest of these is the Brillouin perturbation theory[111] and here we use a modification of the Brillouin treatment as proposed by Löwdin.[112] For simplicity, we treat a state whose energy level is nondegenerate when the atoms are separated at $R = \infty$. With the use of partition techniques,[113] the treatment can be extended to degenerate states.[112]

Let ψ_0 be the wave function for the separated atoms, properly antisymmetrized so that it corresponds to the molecular state under consideration; let Ψ_0 be the exact wave function for the system at the separation R; and let ψ_0 plus the set of functions ψ_j form a complete set which spans that part of many-electron space which has the same symmetry as Ψ_0. Then,

$$\Psi_0 = \psi_0 + \sum_{j\neq 0}{}' c_j \psi_j \tag{71}$$

There is great freedom in the choice of the ψ_j and the rate of convergence of the perturbation series depends upon making a favorable choice. The Ψ_0 satisfies the Schrödinger equation,

$$0 = (H_e - E_0)\Psi_0 = (H_e - E_0)\psi_0 + \sum_{j\neq 0}{}' c_j (H_e - E_0)\psi_j \tag{72}$$

Let

$$H_{ij} = \langle \psi_i | H_e | \psi_j \rangle \quad \text{and} \quad S_{ij} = \langle \psi_i | \psi_j \rangle \tag{73}$$

Then, multiplying Eq. (72) by ψ_0^* and integrating over electron space,

one obtains

$$E_0 S_{00} = H_{00} + \sum_j{}' c_j (H_{0j} - E_0 S_{0j}) \tag{74}$$

Also, multiplying Eq. (72) by ψ_j^*, integrating over electron space, and rearranging the terms, gives

$$c_j = -\frac{H_{j0} - E_0 S_{j0}}{H_{jj} - E_0 S_{jj}} - \sum_{\substack{j' \\ j' \neq 0 \text{ or } j}}{}'' \frac{c_{j'}(H_{jj'} - E_0 S_{jj'})}{H_{jj} - E_0 S_{jj}} \tag{75}$$

Now substituting Eq. (75) into Eq. (74), we obtain

$$E_0 = (H_{00}/S_{00}) - \sum_{\substack{j \\ j \neq 0}}{}' \frac{|H_{0j} - E_0 S_{0j}|^2}{(H_{jj} - E_0 S_{jj}) S_{00}} + Re_2 \tag{76}$$

where the remainder, in order to make Eq. (76) exact, is

$$Re_2 = - \sum_{\substack{j \\ j \neq 0,\ j' \neq 0 \text{ or } j}}{}' \sum_{j'}{}'' \frac{c_{j'}(H_{jj'} - E_0 S_{jj'})(H_{0j} - E_0 S_{0j})}{(H_{jj} - E_0 S_{jj}) S_{00}} \tag{77}$$

In Eq. (76), H_{00}/S_{00} is the usual Heitler-London zeroth plus first-order energy[114] and the summation is the "second-order" term in Brillouin perturbation theory. By substituting $c_{j'}$ from Eq. (75) into Re_2, a "third-order" term plus a new remainder is obtained. The usual Brillouin[111] series results from the continued repetition of this substitution of c_j into the remainder.

The convergence of the Brillouin series depends upon the nondiagonal matrix components being small compared to the diagonal terms. Thus for example in Eq. (75), the first term in the expression for c_j is "first order in smallness" and the summation is therefore "second order in smallness." If the states 0 and k were degenerate, then c_k would be of zeroth order and a separate treatment would be required for a degenerate problem. In practical calculations, the ψ_j would be taken as a finite truncated set; the larger the set, the smaller the truncation errors. As Murrell, Randić, and Williams[70] point out, in such a truncated set it is frequently advisable to include ionic terms in the set of ψ_j since the wave function in the intermediate region is likely to have a substantial ionic character, as will be discussed in Section VII and in the following treatment of charge transfer interactions.

The problem now is to approximate the "second-order" term, $\mathscr{E}^{(2)}$,

in Eq. (76). The Re_2 involves higher-order terms which we neglect in our treatment. Margenau[115] and Dalgarno and Lynn[116] suggest one method, namely to normalize the functions ψ_0 and ψ_j (so as to make $S_{00} = S_{jj} = 1$) and to apply Unsöld's approximation[117] to the denominator (letting $H_{jj} - E_0 = \varepsilon$, a constant, for all values of j). Then,

$$\mathscr{E}^{(2)} \approx -\frac{1}{\varepsilon} \sum_{j\neq 0}{}' \langle\psi_0| H_e - E_0 |\psi_j\rangle\langle\psi_j| H_e - E_0 |\psi_0\rangle$$

$$\approx -\frac{1}{\varepsilon} [\langle\psi_0| (H_e - E_0)^2 |\psi_0\rangle - (\langle\psi_0| H_e - E_0 |\psi_0\rangle)^2] \quad (78)$$

Keeping terms only through the "second order" we obtain

$$E_0 \approx \langle\psi_0| H_e |\psi_0\rangle - \frac{1}{\varepsilon} [\langle\psi_0| H_e^2 |\psi_0\rangle - (\langle\psi_0| H_e |\psi_0\rangle)^2] \quad (79)$$

The next problem is to evaluate the Unsöld constant ε. To do this we require Eq. (79) to agree with the Rayleigh-Schrödinger energy through second order for large separations, where the atomic wave functions no longer overlap.

For intermediate separations, we write ψ_0 as the antisymmetrized function

$$\psi_0 = N_0 \sum_{P_{ij}} (-1)^p P_{ij}\{A_q(i)B_{q'}(j)\} \quad (80)$$

where the summation is to be taken over all permutations which exchange electrons between the two atoms. Then letting $H_e = H_0 + V_e$, where $H_0 = H_a(i) + H_b(j)$ as before, Eq. (79) can be expressed in the form

$$E_0 \approx \varepsilon_0 + \frac{\sum(-1)^p P_{i'j'}\langle A_q(i')B_{q'}(j')| V_e |A_q(i)B_{q'}(j)\rangle}{\sum(-1)^p P_{i'j'}\langle A_q(i')B_{q'}(j') | A_q(i)B_{q'}(j)\rangle}$$

$$-\frac{1}{\varepsilon}\left[\begin{array}{l} +\dfrac{\sum(-1)^p P_{i'j'}\langle A_q(i')B_{q'}(j')| V_e^2 |A_q(i)B_{q'}(j)\rangle}{\sum(-1)^p P_{i'j'}\langle A_q(i')B_{q'}(j') | A_q(i)B_{q'}(j)\rangle} \\ -\left\{\dfrac{\sum(-1)^p P_{i'j'}\langle A_q(i')B_{q'}(j')| V_e |A_q(i)B_{q'}(j)\rangle}{\sum(-1)^p P_{i'j'}\langle A_q(i')B_{q'}(j') | A_q(i)B_{q'}(j)\rangle}\right\}^2 \end{array}\right] \quad (81)$$

In the limit of large separations where the overlaps become negligible, the only permutation which gives contributions to the integrals is the identity. Thus E_0 becomes

$$E_0 \approx \varepsilon_0 + \langle A_q(i)B_{q'}(j)|\, V_e\, |A_q(i)B_{q'}(j)\rangle - \frac{1}{\varepsilon}\begin{bmatrix}\langle A_q(i)B_{q'}(j)|\, V_e^2\, |A_q(i)B_{q'}(j)\rangle \\ -[\langle A_q(i)B_{q'}(j)|\, V_e\, |A_q(i)B_{q'}(j)\rangle]^2\end{bmatrix} \tag{82}$$

Equation (82) is then exactly the same formula that we would obtain from the Rayleigh-Schrödinger perturbation theory using the Unsöld approximation for the second-order energy. At large separations, V_e may also be approximated by its leading term V_3/R^3, in which case the second-order energy is equal to C_6/R^6. In order for the second-order term in Eq. (82) to lead to the same asymptotic form for large separations, it is necessary that

$$\varepsilon = -\frac{1}{C_6}\begin{bmatrix}\langle A_q(i)B_{q'}(j)|\, V_3^2 |A_q(i)B_{q'}(j)\rangle \\ -[\langle A_q(i)B_{q'}(j)|\, V_3\, |A_q(i)B_{q'}(j)\rangle]^2\end{bmatrix} \tag{83}$$

This relation is particularly simple when a and b do not have permanent dipole moments in their initial states.

Our derivations are quite different from the ones used by Margenau[115] and by Dalgarno and Lynn,[116] but the final results are the same. Dalgarno and Lynn used this technique to obtain good results for the energy of interaction of two ground-state hydrogen atoms at intermediate separations ($R > 4a_0$).

Recently, Kestner and Sinanoğlu[95] have applied the many-electron theory of atoms and molecules (Sinanoğlu[118]) to the He–He interaction with encouraging results. Since this theory yields equations that are valid for all separations and involves some of the best features of both perturbation and variational techniques, it is capable of treating intermediate-range intermolecular forces.

1. *Charge-Transfer Interactions*

Charge transfer (charge exchange) between two molecules may take place at intermediate separations and greatly increase the energy of interaction. Charge transfer is characterized by the (almost) crossing of two potential energy curves, one corresponding to $a + b$, the other corresponding to $a^+ + b^-$ as shown in Figure 4.

Whenever charge transfer may be important, the wave function for the two-molecule system should be written in the form

$$\Psi = c_1\Psi(ab) + c_2\Psi(a^+b^-) \tag{84}$$

Equation (84) results from the fact that in the charge-transfer zone, the energies corresponding to $\Psi(ab)$ and $\Psi(a^+ b^-)$ are degenerate and, therefore, the proper linear combination of these degenerate wave functions must be used in the calculation of the interaction energy. The

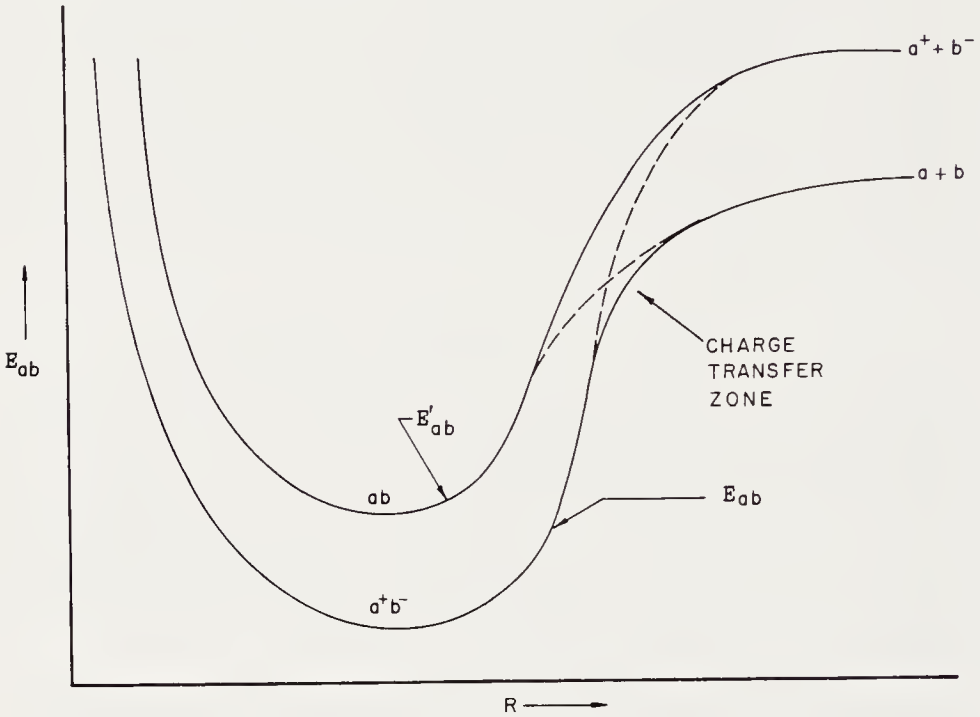

Fig. 4. Schematic diagram showing an "almost crossing" of two potential energy curves: E_{ab} which at large separations corresponds to the interaction of atom a in state "a" and atom b in state "b" and E'_{ab} which at large separations corresponds to the interaction of the ion a^+ with the ion b^-. The dashed lines (----) correspond to the zeroth-order approximation in which the two potential curves cross.

contribution of the ionic state can be varied by adjusting the parameters c_1 and c_2 ($c_1^2 + c_2^2 = 1$). For the interaction of two molecules a and b, without charge transfer ($c_2 = 0$), one would expect the interaction energy to be E'_{ab} at intermediate separations (see Fig. 4). With charge transfer ($c_2 \neq 0$) one obtains a considerably lower interaction energy, E_{ab}, at intermediate separations. There are many examples of donor–acceptor charge-transfer complexes, such as benzene–iodine which behave in this manner.[119] Aono[120] suggests that charge transfers are very important in the interactions between conjugate double-bond molecules.

The probability of transitions from one potential energy curve to another[10,34] has been discussed in Section II.

D. Very Small Separations

In the region of very small separations, perturbation techniques can again be used to good advantage. However, the zeroth-order wave function corresponds to the *united atom* and the resulting treatment does not properly belong in the realm of intermolecular forces. Thus, the reader is referred to the excellent work of Byers Brown and Steiner.[121,122] They find that the *united atom* expansion of the interaction energy of two atoms has the form

$$E_{ab} = Z_a Z_b / R + C_0 + C_2 R^2 + C_3 R^3 + C_4 R^4 + C_5 R^5 + C_5' R^5 \ln(R) + \cdots \quad (85)$$

The presence of the $R^5 \ln(R)$ term indicates that R is not a *natural* perturbation parameter. We believe that the presence of this term is in some way associated with the transition from the *in–out* to the *left–right* types of electron correlation as R is increased. This transition is discussed in Section VII.

VI. THE HELLMANN-FEYNMAN THEOREM

Hellmann[123] and Feynman[124] have shown that (except for the small forces which arise from the deviations from the Born-Oppenheimer separation and magnetic or relativistic effects) the quantum mechanical forces on the nuclei of a molecule are just exactly the classical electrostatic coulombic forces which result from the charges on the nuclei interacting with the charge density of the electron cloud. Berlin[125] dramatized this result by making a diagram showing the regions in which an increment of the electron cloud helps to draw the nuclei of a diatomic molecule together, in contrast to other regions where it would tend to pull the nuclei apart. Thus, the Hellmann-Feynman theorem is very interesting and illuminating from the conceptual standpoint. However, the theorem is only valid if the charge density is determined from a wave function which is an *exact* solution to the Schrödinger equation. Small errors in the wave function can result in large errors in the calculated forces on the nuclei.

A. The Generalized Hellmann-Feynman Theorem

Let Ψ and E be the exact normalized eigenfunction and exact eigenvalue of the Hamiltonian H_e and let γ be *any* parameter on which Ψ or H_e may depend. Then the *generalized* Hellmann-Feynman theorem states that

$$\frac{\partial E}{\partial \gamma} = \langle \Psi | \frac{\partial H_e}{\partial \gamma} | \Psi \rangle / \langle \Psi | \Psi \rangle \tag{86}$$

The proof of the generalized Hellmann-Feynman theorem is easy.[124,126] Differentiating the equation

$$\langle \Psi | H_e - E | \Psi \rangle = 0 \tag{87}$$

with respect to γ gives

$$\langle \Psi | \frac{\partial H_e}{\partial \gamma} - \frac{\partial E}{\partial \gamma} | \Psi \rangle + \langle \frac{\partial \Psi}{\partial \gamma} | H_e - E | \Psi \rangle + \langle \Psi | H_e - E | \frac{\partial \Psi}{\partial \gamma} \rangle = 0 \tag{88}$$

The integrals involving $\partial\Psi/\partial\gamma$ vanish since $(H_e - E)\Psi = 0$ and H_e is Hermitian. Thus, Eq. (88) becomes the generalized Hellmann-Feynman theorem. Exactly what this theorem means depends to a large extent on what coordinates are used to describe the electronic configuration[132] (see subsection D). The electronic coordinate system usually determines what properties are held constant when the parameter γ is varied.[127–132] Thus, for one parameter γ, there can be a number of generalized Hellmann-Feynman theorems. This point should be emphasized because it has been a source of considerable confusion.

The validity of the generalized Hellmann-Feynman theorem is sensitively dependent on the wave function. For an approximate wave function, $\tilde{\psi}$, the approximate energy is

$$\tilde{E} = \langle \tilde{\psi} | H_e | \tilde{\psi} \rangle / \langle \tilde{\psi} | \tilde{\psi} \rangle$$

For *most* approximate wave functions, $\partial\tilde{E}/\partial\gamma$ deviates a great deal from the Hellmann-Feynman expectation

$$\left(\frac{\partial \tilde{E}}{\partial \gamma}\right)_{HF} = \langle \tilde{\psi} | \frac{\partial H_e}{\partial \gamma} | \tilde{\psi} \rangle / \langle \tilde{\psi} | \tilde{\psi} \rangle$$

Furthermore, $(\partial\tilde{E}/\partial\gamma)_{HF}$ is usually a poor approximation to the *exact* $\partial E/\partial\gamma$. However, there is a class of approximate wave functions, $\tilde{\psi}_f(\mathbf{r};\beta_1, \ldots, \beta_k)$, for which the generalized Hellmann-Feynman theorem

is satisfied in the sense that $\partial\tilde{E}/\partial\gamma = (\partial\tilde{E}/\partial\gamma)_{HF}$ (but of course $(\partial\tilde{E}/\partial\gamma)_{HF} \neq \partial E/\partial\gamma$). The $\tilde{\psi}_f$ do not contain the parameter γ *explicitly*. Instead, they contain a set of parameters $\beta_1, \ldots, \beta_k$ (which may be functions of γ) whose values have been determined by optimizing the approximate energy $\tilde{E}$ so that, for each β_j, the relation $\partial\tilde{E}/\partial\beta_j = 0$ is satisfied. Thus,

$$\frac{\partial\tilde{E}}{\partial\gamma} = \left(\frac{\partial\tilde{E}}{\partial\gamma}\right)_\beta + \sum_j \left(\frac{\partial\beta_j}{\partial\gamma}\right)\left(\frac{\partial\tilde{E}}{\partial\beta_j}\right) = \left(\frac{\partial\tilde{E}}{\partial\gamma}\right)_\beta$$

where $(\partial\tilde{E}/\partial\gamma)_\beta$ means taking the derivative with respect to γ of $\tilde{E} = \langle\tilde{\psi}_f | H_e | \tilde{\psi}_f\rangle / \langle\tilde{\psi}_f | \tilde{\psi}_f\rangle$ while holding each of the β's constant. Thus, since the $\tilde{\psi}_f$ do not contain the γ explicitly, it follows that $\partial\tilde{E}/\partial\gamma = \langle\tilde{\psi}_f | \partial H_e/\partial\gamma | \tilde{\psi}_f\rangle / \langle\tilde{\psi}_f | \tilde{\psi}_f\rangle$. Hurley[136] calls the $\tilde{\psi}_f$ "floating" wave functions. He has shown[137] that they are equivalent to Hall's "stable" wave functions[138] which also satisfy the generalized Hellmann-Feynman condition. Hurley's recent review article[129] has an excellent discussion of the types of approximate wave functions that satisfy this theorem.

In order to answer the question, how well can we approximate $\partial E/\partial\gamma$ by using an approximate wave function, let us apply[133–135] the Rayleigh-Schrödinger perturbation theory to the generalized Hellmann-Feynman theorem. The Hamiltonian is written in the form $H_e = H_0 + V$ and Ψ and E are expressed in the perturbation series, Eqs. (34) and (35). Then substitute these equations into Eq. (88) and use Eqs. (36)–(37) to simplify the result. Grouping terms according to their order in the perturbation V, one obtains a family of generalized Hellmann-Feynman-type relations;

$$\begin{aligned}
\frac{\partial\varepsilon_0}{\partial\gamma} &= \langle\psi_0| \frac{\partial H_0}{\partial\gamma} |\psi_0\rangle \\
\frac{\partial E^{(n)}}{\partial\gamma} &= \sum_{j=0}^{n} \langle\Psi^{(j)}| \frac{\partial H_0}{\partial\gamma} |\Psi^{(n-j)}\rangle \\
&\quad + \sum_{j=0}^{n-1} \langle\Psi^{(j)}| \frac{\partial V}{\partial\gamma} |\Psi^{(n-1-j)}\rangle
\end{aligned} \tag{89}$$

Thus we see that:

1. If H_0 is a function of γ, then the calculation of $\partial E/\partial\gamma$ through the nth order of perturbation requires a knowledge of the wave function through the nth order.[135]

2. If H_0 is not a function of γ, then the calculation of $\partial E/\partial\gamma$ through nth order may require a knowledge of the wave function through the $(n-1)$st order.[133] However, if $\partial V/\partial\gamma$ is proportional to V, then Eq. (89) can be further simplified with the use of the hierarchy of perturbation equations of different orders and, in this special case, Yaris[133] showed that the wave function through the nth order suffices to calculate $\partial E/\partial\gamma$ through the $(2n+1)$st order.

B. The Electrostatic Hellmann-Feynman Theorem

The electrostatic Hellmann-Feynman theorem[123,124] provides a conceptually interesting way of determining the forces on the nuclei of an arbitrary molecular configuration. In this application of the generalized Hellmann-Feynman theorem, H_e and Ψ are expressed in terms of space-fixed Cartesian coordinates and γ is taken to be z_a, the z coordinate of nucleus a. In the electrostatic Hamiltonian H_e, only the distances r_{ai} and $R_{a\beta}$ are functions of z_a [for diatomic molecules, this can be seen from Eq. (14)]. Thus,

$$\frac{\partial H_e}{\partial z_a} = Z_a\left[\sum_\beta \frac{Z_\beta z_{a\beta}}{R_{a\beta}^3} - \sum_i \frac{z_{ai}}{r_{ai}^3}\right] \tag{90}$$

Here $R_{a\beta}$ is the distance from nucleus a to nucleus β; the capital Z's are atomic numbers (not to be confused with the lower case z's which are the particle coordinates); and $z_{ai} = z_i - z_a$, whereas $z_{a\beta} = z_\beta - z_a$. Substituting this expression for $\partial H_e/\partial z_a$ into Eq. (86), we obtain the *electrostatic Hellmann-Feynman theorem*

$$F_{az} = -\frac{\partial E}{\partial z_a} = -Z_a\left[\sum_\beta \frac{Z_\beta z_{a\beta}}{R_{a\beta}^3} - \int\left(\frac{z_{a1}}{r_{a1}^3}\right)\rho_1\, d\tau_1\right] \tag{91}$$

Here F_{az} is the force on nucleus a in the z direction and ρ_1 is the total electronic charge density,

$$\rho_1 = n_e \int\cdots\int \Psi^*\Psi\, d\tau_2 \ldots d\tau_{n_e} \tag{92}$$

where n_e is the number of electrons in the system. For diatomic molecules, $\beta = b$ and $z_{a\beta} = R_{a\beta} = R$. According to the electrostatic Hellmann-Feynman theorem, once the electronic charge density ρ_1 has been determined by solving the Schrödinger equation for the appropriate nuclear configuration, the forces on the nuclei are the coulombic forces which would be expected on the basis of classical electrostatics.

It is reasonable that the electrostatic Hellmann-Feynman theorem should be valid only if the wave function used in the calculation of the electronic charge density satisfies the virial theorem. Both the exact wave function and the Hurley "floating" approximate wave functions satisfy this condition. The electrostatic Hellmann-Feynman theorem expresses the nuclear forces in terms of the electronic charge density or the first-order density matrix. The nuclear forces could then be integrated to give the energy of a molecular configuration (relative to the separated atoms) again in terms of the first-order density matrix. The kinetic energy of the system (which can be expressed as the expectation value of a one-electron operator) should involve only the first-order density matrix. However, the potential energy involves electron correlations and, hence, the second-order density matrix. The virial theorem provides a simple relationship between the kinetic and the potential energies. Thus, for wave functions which satisfy the virial theorem, the energy can be expressed in terms of the kinetic energy and therefore a knowledge of only the first-order density matrix is required.

For approximate wave functions which do not satisfy the virial theorem, the use of the electrostatic Hellmann-Feynman theorem leads to serious errors (see refs. 130,133,135,139,140). Indeed, a first-order error in the wave function (according to our perturbation analysis) leads to a first-order error in the nuclear forces. The same first-order error in the wave function would produce only a second-order error in the expectation value of the energy.

C. Application of the Electrostatic Hellmann-Feynman Theorem to the Long-Range Interaction of Two Hydrogen Atoms

In order to better understand the electrostatic Hellmann-Feynman theorem, let us apply it to the calculation of the long-range interaction of two ground-state hydrogen atoms. According to Sections IV-B and V-B, the interaction energy is

$$E_{ab} = C_6 R^{-6} + C_8 R^{-8} + \cdots$$

The force on nucleus a in the z direction (towards nucleus b) is therefore

$$F_{az} = \partial E_{ab}/\partial R = -6C_6 R^{-7} - 8C_8 R^{-9} - \cdots$$

Let us answer the following questions[143]: (*1*) How accurately do we need to know the wave function in order to calculate the leading term,

$-6C_6R^{-7}$? (*2*) What is the explanation of the attractive force between the two hydrogen atoms in terms of the electronic charge distribution?

The exact wave function for the hydrogen molecule can be written in the form

$$\Psi = (1/\sqrt{2})[\Phi(a1,b2) \pm \Phi(b1,a2)] \tag{93}$$

The plus sign pertains to the singlet and the minus sign to the triplet states of the H_2 molecule. In the function $\Phi(a1,b2)$, electron 1 is associated with atom a and electron 2 is associated with atom b. At large separations, the overlap integral

$$\int \Phi^*(a1,b2)\Phi(b1,a2)\, d\tau_2$$

varies as $\exp(-2R)$ and becomes negligible with respect to terms which vary as powers of $1/R$. Thus, the total electronic charge density of Eq. (92) can be written in the form

$$\rho_1 = \rho_1(a) + \rho_1(b)$$

Here

$$\rho_1(a) = \int \Phi^*(a1,b2)\Phi(a1,b2)\, d\tau_2$$

$$\rho_1(b) = \int \Phi^*(b1,a2)\Phi(b1,a2)\, d\tau_2$$

The function $\Phi(a1,b2)$ can be expanded in powers of $1/R$

$$\Phi(a1,b2) = N\begin{bmatrix} \psi_0 + R^{-3}\psi_3^{(1)} + R^{-4}\psi_4^{(1)} \\ \quad + R^{-5}\psi_5^{(1)} + R^{-6}\{\psi_6^{(1)} + \psi_3^{(2)}\} \\ \quad + R^{-7}\{\psi_7^{(1)} + \psi_{3,4}^{(1,1)}\} + \cdots \end{bmatrix} \tag{94}$$

Here the normalization constant N is equal to 1 plus terms of the order of R^{-6} which shall not concern us. The zeroth-order function ψ_0 is equal to $A_0(1)B_0(2)$ where A_0 is the $1s$ hydrogen orbital on atom a. The functions $\psi_n^{(1)}$ are the first-order perturbed wave functions corresponding to the perturbation potential V_n. The $\psi_3^{(2)}$ is the second-order perturbed function corresponding to V_3; and $\psi_{3,4}^{(1,1)}$ is the mixed second-order function, first order with respect to V_3 and first order with respect to V_4.

The zeroth-order function ψ_0 varies as $Y_0^0(\theta_{a1},\phi_{a1})\, Y_0^0(\theta_{b2},\phi_{b2})$. Thus,

from Eqs. (43) and (49), it follows that $\psi_n^{(1)}$ has the same angular dependence as the perturbation potential V_n. As a result, the $\psi_n^{(1)}$ vary as $Y_k^m(\theta_{a1},\phi_{a1})\,Y_j^{-m}(\theta_{b2},\phi_{b2})$ where neither k nor j is equal to zero. Because of the orthonormality of the spherical harmonics it follows that

$$\int \psi_0^* \psi_n^{(1)}\, d\tau_2 = 0$$

Furthermore, $\psi_{3,4}^{(1,1)}$ can be expressed as the sum of two terms

$$\psi_{3,4}^{(1,1)} = \chi(a1)B_0(2) + \Lambda(a1,b2)$$

Here $\Lambda(a1,b2)$ contains all of those parts of $\psi_{3,4}^{(1,1)}$ which correspond to the excitation of electron 2. It follows that

$$\int \psi_0^* \Lambda(a1,b2)\, d\tau_2 = 0$$

Thus, through terms of the order of $1/R^7$,

$$\rho_1(a) = N^2 A_0^*(1)A_0(1) + R^{-6}[\rho_{33}^{(1)}(a) + \rho_{03}^{(2)}(a)] + R^{-7}[\rho_{34}^{(1)}(a) + \rho_{34}^{(2)}(a)]$$

where

$$\rho_{33}^{(1)}(a) = \int \psi_3^{(1)*}\psi_3^{(1)}\, d\tau_2$$

$$\rho_{03}^{(2)}(a) = \int [\psi_0^*\psi_3^{(2)} + \psi_3^{(2)*}\psi_0]\, d\tau_2$$

$$\rho_{34}^{(1)}(a) = \int [\psi_3^{(1)*}\psi_4^{(1)} + \psi_4^{(1)*}\psi_3^{(1)}]\, d\tau_2$$

$$\rho_{34}^{(2)}(a) = A_0^*(1)\chi(a1) + \chi^*(a1)A_0(1)$$

Since $\psi_3^{(1)}$ has the same angular dependence as V_3 [see Eq. (51)] it is easy to show that $\rho_{33}^{(1)}(a)$ is an *even* function of z_{a1}. We can also show that $\rho_{03}^{(2)}(a)$ is an *even* function of z_{a1}. The argument goes as follows: We use Eq. (44) to consider the nature of $\psi_3^{(2)}$. Since ψ_0 varies as $Y_0^0(\theta_{a1},\phi_{a1})$ $Y_0^0(\theta_{b2},\phi_{b2})$ and since the V_3 varies as the $Y_1^m(\theta_{a1},\phi_{a1})$ $Y_1^{-m}(\theta_{b2},\phi_{b2})$, it follows that the only nonvanishing matrix components V_{k0} in Eq. (44) correspond to ψ_k which vary as the products $Y_1^m(\theta_{a1},\phi_{a1})$ $Y_1^{-m}(\theta_{b2},\phi_{b2})$. Thus, in order that the matrix elements V_{jk} be nonvanishing, the ψ_j must vary as $Y_s^m(\theta_{a1},\phi_{a1})$ $Y_t^{-m}(\theta_{b2},\phi_{b2})$ where s and t can be either 0 or 2. The angular dependence of $\psi_3^{(2)}$ must be the same as the ψ_j. Thus

$\rho_{03}^{(2)}(a)$ must vary as a spherical harmonic of even order and hence must be an even function of $\cos\theta_{a1} = z_{a1}/r_{a1}$.

Since $\rho_{33}^{(1)}(a)$ and $\rho_{03}^{(2)}(a)$ are *even* functions of z_{a1} they cannot contribute to the integral $\int (z_{a1}/r_{a1}^3)\rho_1 d\tau_1$ where the limits of integration over z_{a1} extend from $-\infty$ to ∞.

Next, let us investigate the contributions of $\rho_1(b)$ to F_{az}. It is clear that $\rho_1(b) = B_0^*(1)B_0(1)$ plus terms of the order of R^{-6}. However, without making approximations,

$$\int (z_{a1}/r_{a1}^3)B_0^*(1)B_0(1)\, d\tau_1 = R^{-2} - (2 + 2R^{-1} + R^{-2}) \exp(-2R)$$

At the large separations which we are considering, the exponential term can be neglected with respect to the R^{-2}. The terms of the order R^{-6} in $\rho_1(b)$ contribute terms of the order of R^{-8} to the integral $\int (z_{a1}/r_{a1}^3)\rho_1 d\tau_1$ (and hence may be neglected), since z_{a1}/r_{a1}^3 expanded about the center b is a series in powers of $1/R$ with a leading term R^{-2},

$$(z_{a1}/r_{a1}^3) = R^{-2} - 2R^{-3}z_{b1} + \cdots$$

Thus, Hirschfelder and Eliason[143] showed that the leading term in F_{az} varies as R^{-7}, since the contribution to the force from the lower powers of $1/R$ vanishes. Equation (91) becomes

$$\begin{aligned} F_{az} = \partial E_{ab}/\partial R &= R^{-7}\left[\int (z_{a1}/r_{a1}^3)\rho_{34}^{(1)}(a)\, d\tau_1 \right. \\ &\quad \left. + \int (z_{a1}/r_{a1}^3)\rho_{34}^{(2)}(a)\, d\tau_1\right] \\ &\quad + \cdots \\ &= -6C_6R^{-7} - \cdots \end{aligned} \tag{95}$$

The integral involving $\rho_{34}^{(1)}(a)$ is easy to evaluate in terms of the $\psi_3^{(1)}$ and $\psi_4^{(1)}$ which were very accurately determined by Hirschfelder and Löwdin[66] (and, more recently, with even greater accuracy by Kolos[67]). The integral involving $\rho_{34}^{(2)}$ requires a determination of $\chi(a1)$.

If one multiplies the appropriate double perturbation equation[71b] for $\psi_{34}^{(1,1)}$ by $B_0^*(2)$ and integrates over the coordinates of electron 2, one obtains the following equation for $\chi(a1)$,[143]

$$\left(H_a(1) + \frac{1}{2}\right)\chi(a1) = \int B_0^*(2)[\varepsilon_{3,4}^{(1,1)}\psi_0 - V_3\psi_4^{(1)} - V_4\psi_3^{(1)}]\, d\tau_2$$

where

$$\varepsilon_{3,4}^{(1,1)} = \langle \psi_0 | V_3 | \psi_4^{(1)} \rangle + \langle \psi_0 | V_4 | \psi_3^{(1)} \rangle$$

It is quite surprising that this equation is easy to integrate. Thus $\chi(a1)$ was obtained explicitly in terms of the basis sets used in the $\psi_3^{(1)}$ and $\psi_4^{(1)}$. The final integration to obtain the contribution to the force was not difficult.

Thus, Hirschfelder and Eliason obtained[143]:

$$\int R^{-7} \ (z_{a1}/r_{a1}^3)\rho_{34}(a)\, d\tau_1 = 2.717\, R^{-7} \quad \text{a.u.}$$

$$R^{-7} \int (z_{a1}/r_{a1}^3)\rho_{34}^{(2)}(a)\, d\tau_1 = 36.284\, R^{-7} \quad \text{a.u.}$$

Adding these numbers gives the force as calculated by the electrostatic Hellmann-Feynman theorem,

$$\mathbf{F}_{az}(\text{calculated}) = 39.001\, R^{-7} \quad \text{a.u.}$$

This is to be compared with the *exact* force, $-6C_6R^{-7}$ (see Table IV),

$$\mathbf{F}_{az}(\text{exact}) = 38.994\, R^{-7} \quad \text{a.u.}$$

As can be seen from the results above, the leading term in F_{az} has been determined to a precision of one part in 5000 with the use of the electrostatic Hellmann-Feynman theorem.

Now we can answer the two questions which were posed at the beginning of this section.

Question 1: How accurately do we need to know an approximate wave function in order to use the electrostatic Hellmann-Feynman theorem to calculate the leading term in F_{az} [140]? *Answer*: In order to determine the R^{-7} contribution to F_{az} accurately, it is necessary to know accurately the R^{-3}, R^{-4}, and R^{-7} parts of the approximate wave function. If the approximate wave function were accurate through terms of the order of R^{-4}, one would only obtain 7% of the R^{-7} component of F_{az}. As Frost has shown,[140] a wave function (such as the Hirschfelder-Linnett[141]) which has essentially the correct R^{-3} behavior and therefore gives a good value for C_6R^{-6} as part of the expectation value of the Hamiltonian, is still not sufficiently accurate to use with the electrostatic Hellmann-Feynman theorem. Indeed, with such a function, one would obtain the leading term in F_{az} varying as R^{-10} instead of R^{-7}. Frost[140] considers a number of types of approximate wave

functions (including floating orbitals) for H_2^+ and concludes that none of the functions which he tried were accurate enough to give good forces, as calculated by the electrostatic Hellmann-Feynman theorem.

Question 2: What is the explanation of the attractive force in terms of the electronic charge distribution? *Answer*[140,143]: The R^{-6} component of $\rho_1(a)$ (which results from the R^{-3} component of the wave function) forms a quadrupolar charge distribution around the nucleus a, and being symmetric with respect to the coordinate z_{a1} does not lead to an attraction between the two nuclei [except for the R^{-10} attraction between the quadrupoles from $\rho_1(a)$ and from $\rho_1(b)$; the moment of each varies as R^{-6}]. The R^{-7} component of $\rho_1(a)$, that is $\rho_{34}^{(1)}(a)$ and $\rho_{34}^{(2)}(a)$, in the vicinity of nucleus a is slightly larger in the direction of nucleus b than away from it. The negatively charged $\rho_1(a)$, together with the positively charged nucleus a, then forms an electric dipole whose moment varies as R^{-7}. Thus, just as Feynman had conjectured in his original paper,[124] the force on the nucleus results from its attraction to the centroid of the charge density corresponding to its associated electrons.

D. Other Applications of the Hellmann-Feynman Theorem to the Long-Range Interaction of Two Atoms

In subsection A, it was stated that exactly what the generalized Hellmann-Feynman theorem means depends to a large extent upon the coordinates which are used to describe the electronic configuration. Let us consider the force on a nucleus when two atoms interact at large separation. Using three types of electronic coordinates, the generalized Hellmann-Feynman theorem gives three types of results.

1. *Cartesian Coordinates with Laboratory-Fixed Origin*

The use of Cartesian coordinates with laboratory-fixed origin leads to the *electrostatic Hellmann-Feynman* method for determining the force on a nucleus, as discussed in subsection B. Here the zeroth-order Hamiltonian, $H_a(1) + H_b(2)$, is a function of the parameter z_a so that it is necessary to calculate the wave function accurate through the nth order in order to determine the force F_{az} accurate through the nth order.

2. *Electronic Coordinates Relative to the Associated Nucleus*

Let us take an approximate wave function having the form $\tilde{\Psi} = \sum_n R^{-n}\tilde{\psi}_n$ where each of the $\tilde{\psi}_n$ is an explicit function of the electronic

coordinates: $r_{ai},\theta_{ai},\phi_{ai}$ and $r_{bj},\theta_{bj},\phi_{bj}$, but not an explicit function of R. Here we have associated the electrons designated by i with atom a, and the electrons j with atom b. The Hamiltonian for the molecule can be written in the form

$$H_e = H_a(i) + H_b(j) + \sum_n R^{-n} V_n$$

where (in terms of these electronic coordinates) the $H_a(i),H_b(j)$, and the V_n are unaffected by changes in R. The approximate energy of the molecule is then $\tilde{E} = \langle \tilde{\Psi} \mid H_e \mid \tilde{\Psi} \rangle / \langle \tilde{\Psi} \mid \tilde{\Psi} \rangle$. It is easy to show that taking $\gamma = R$ and substituting $\tilde{\Psi}$ for the exact wave function in the generalized Hellmann-Feynman theorem, Eq. (86), leads to the same expression[133] for the change of energy with R as is obtained by differentiating $\tilde{E}$ with respect to R. Thus, with this choice of electronic coordinates, the generalized Hellmann-Feynman theorem does not lead to any new way of determining the force on the nuclei.

3. *Confocal Elliptic Coordinates*

A more interesting result is obtained if the positions of the electrons are specified by confocal elliptic coordinates and γ is taken to be R. Here H_e is taken to be the sum of the electronic kinetic energy operator K and the potential energy U of the system. In confocal elliptic coordinates $K = R^{-2}K_0$, where K_0 does not involve R explicitly. Similarly, if U is electrostatic in origin, then $U = R^{-1}U_0$ where U_0 does not involve R explicitly. Thus, $\partial H_e/\partial R = -R^{-1}(2K + U)$. As a result, Hirschfelder and Coulson[144] showed that the generalized Hellmann-Feynman theorem, Eq. (86), becomes

$$-R \frac{\partial E}{\partial R} = 2\langle \Psi | K | \Psi \rangle + \langle \Psi | U | \Psi \rangle \tag{96}$$

Coulson and Hurley[127] have reduced the confusion which existed regarding the distinction between Eq. (96) and the quantum mechanical virial theorem which, for the same electrostatic Hamiltonian H_e, has the form[145]

$$-\langle \Psi | R \frac{\partial U}{\partial R} | \Psi \rangle = 2\langle \Psi | K | \Psi \rangle + \langle \Psi | U | \Psi \rangle \tag{97}$$

Here the meaning of $\partial U/\partial R$ is clarified by expressing the $\mathbf{r}$ in $\Psi(\mathbf{r},R)$ in laboratory-fixed Cartesian coordinates. According to subsection A, the

Hellmann-Feynman theorem gives, for exact wave functions, $\partial E/\partial R = \langle \Psi | \partial U/\partial R | \Psi \rangle$. Therefore, Eq. (96) is frequently called the virial theorem. However, an approximate wave function $\tilde{\Psi}$ substituted for the exact wave function may not satisfy the *true* virial theorem, Eq. (97); whereas, in the Hellmann-Feynman theorem of Eq. (96), it gives some sort of approximation to $\partial E/\partial R$. This distinction need not be made for those approximate wave functions which satisfy the virial theorem. Hirschfelder and Kincaid[148] (and later Löwdin[149]) showed that *any* approximate wave function satisfies the virial theorem provided that one or more[150] parameters which control the scale of all of the coordinates (including the separation R) are energy optimized. Thus,[144,147] both Hurley's "floating" and Hall's "stable" wave functions[136–138] satisfy the virial theorem.

The virial theorem, Eq. (97), is easily derived from the hypervirial relation[126,146]

$$\langle \Psi | H_e W - W H_e | \Psi \rangle = 0$$

where $W = \sum_i \mathbf{r}_i \cdot \mathbf{p}_i$ and $\mathbf{r}_i$ and $\mathbf{p}_i$ are the coordinates and momenta of the ith electron. The derivation of the hypervirial relation is trivial provided that H_e is Hermitian with respect to $W\Psi$ and Ψ is an eigenfunction of H_e.

E. The Integral Hellmann-Feynman Theorem

Mention should also be made of the *integral Hellmann-Feynman theorem* stated by Kim and Parr[151]: If A and B correspond to two configurations of the nuclei, then

$$\langle \Psi_B | (H_B - H_A) - (E_B - E_A) | \Psi_A \rangle = 0 \tag{98}$$

Here H,E and Ψ correspond to the Schrödinger equations, $(H_A - E_A)\Psi_A = 0$ and $(H_B - E_B)\Psi_B = 0$, for the two configurations. Wyatt and Parr[152] have used the *integral* Hellmann-Feynman theorem to determine the energy of hindered rotation in ethane. It is therefore reasonable to suppose that this theorem might also be used to determine intermolecular forces. The integral Hellmann-Feynman theorem, like the other forms of the theorem, is apt to give a bad estimate of $(E_B - E_A)$ if approximate wave functions are used in Eq. (98). However, Epstein, Hurley, Wyatt, and Parr[153] have shown that if $\tilde{\Psi}_A$ and $\tilde{\Psi}_B$ are approximate wave functions expanded in linear combinations of the same basis

functions, and if these linear combinations are adjusted to minimize the approximate energies, $\tilde{E}_A = \langle \tilde{\Psi}_A | H_A | \tilde{\Psi}_A \rangle$ and $\tilde{E}_B = \langle \tilde{\Psi}_B | H_B | \tilde{\Psi}_B \rangle$, then

$$\langle \tilde{\Psi}_B | (H_B - H_A) - (\tilde{E}_B - \tilde{E}_A) | \tilde{\Psi}_A \rangle = 0$$

VII. THE ROLE OF ELECTRON CORRELATIONS IN INTERMOLECULAR FORCES

Electron correlations play a major role in determining the nature of intermolecular forces. This fact is obscured by the electrostatic Hellmann-Feynman theorem where the forces are determined by the electronic charge density ρ_1 which contains no information regarding electron correlations. However, the Hellmann-Feynman theorem is only valid if ρ_1 is derived from the exact wave function, Ψ, or from some approximate wave function which satisfies auxiliary conditions (such as the virial theorem), which involve electron correlations. In this section we sketch the role of electron correlations in large, intermediate, and short-ranged intermolecular forces.

A. Large Separations

At large separations, the London dispersion energy can be explained in the following manner. At any given instant, the electronic configuration of atom a corresponds to an instantaneous dipole moment, $\boldsymbol{\mu}(a;\text{inst})$. The electric field corresponding to $\boldsymbol{\mu}(a;\text{inst})$ polarizes atom b and induces a dipole moment $\boldsymbol{\mu}(b;\text{ind})$ in atom b. If $\boldsymbol{\mu}(a;\text{inst})$ lies in the xz plane where the z axis is pointed along the internuclear axis $a \rightarrow b$, then $\mu(b;\text{ind})_z = 2\alpha_b' \mu(a;\text{inst})_z R^{-3}$ and $\mu(b;\text{ind})_x = -\alpha_b' \mu(a;\text{inst})_x R^{-3}$. Here α_b' is the polarizability of atom b [not the static polarizability, but more closely related to the frequency-dependent polarizability with a frequency corresponding to the rate of change of $\boldsymbol{\mu}(a;\text{inst})$]. The instantaneous energy of interaction,[154] $E(\text{inst})$, is then the dipole–dipole energy corresponding to $\boldsymbol{\mu}(a;\text{inst})$ and $\boldsymbol{\mu}(b;\text{ind})$,

$$E(\text{inst}) = -R^{-6}\alpha_b'\{[\mu(a;\text{inst})_x]^2 + 4[\mu(a;\text{inst})_z]^2\} \tag{99}$$

and there is a similar term for the induction of a dipole moment in atom a by the instantaneous dipole moment of atom b. In Chapter 5, Linder uses reaction-field techniques to obtain the London dispersion energy as the time average of $E(\text{inst})$ over all instantaneous configurations of the electrons in atom a. For the interaction of two ground-state

atoms, the dispersion energy is always negative, corresponding to an attraction between the two atoms.

This simple explanation of the dispersion energy has some interesting implications regarding electron correlations. To be specific, let us consider the long-range interaction of two ground-state hydrogen atoms with electron 1 associated with atom a and electron 2 associated with atom b. Statistically, the positions of electrons 1 and 2 must be coordinated in accordance with the relationship between $\boldsymbol{\mu}(a;\text{inst})$ and $\boldsymbol{\mu}(b;\text{ind})$. Hence, the expectation value $\langle z_{a1}z_{b2}\rangle$ is positive and $\langle x_{a1}x_{b2}\rangle$ is negative.[141] Figure 5 shows a typical instantaneous charge distribution which would correspond to this type of polarization.

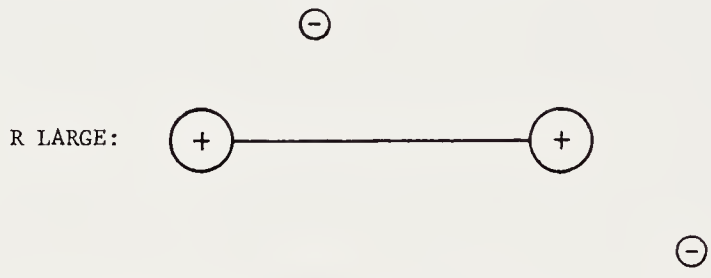

Fig. 5. Typical instantaneous charge distribution corresponding to the relationship between $\boldsymbol{\mu}(a;\text{inst})$ and $\boldsymbol{\mu}(b;\text{ind})$.

The London dispersion energy may also be considered as the expectation value of the perturbation V_3R^{-3}; for two hydrogen atoms

$$E(\text{dis}) = R^{-3}[\langle x_{a1}x_{b2}\rangle + \langle y_{a1}y_{b2}\rangle - 2\langle z_{a1}z_{b2}\rangle] \tag{100}$$

Thus the dispersion energy can be calculated by using an approximate wave function with sufficient flexibility to represent the required type of polarization or electron correlation. Indeed, Hirschfelder and Linnett[141,155] obtained fairly good values for the expectation value of the total Hamiltonian, H_e, for all separations, using the simple variational wave function,

$$\begin{aligned}\tilde{\Psi} = {} & a_{1s}(1)b_{1s}(2)[1 + \alpha(x_{a1}x_{b2} + y_{a1}y_{b2}) + \beta z_{a1}z_{b2}] \\ & + a_{1s}(2)b_{1s}(1)[1 + \alpha(x_{a2}x_{b1} + y_{a2}y_{b1}) + \beta z_{a2}z_{b1}] \\ & + \gamma[a_{1s}(1)a_{1s}(2) + b_{1s}(1)b_{1s}(2)]\end{aligned} \tag{101}$$

Here a_{1s} and b_{1s} are $1s$ hydrogenic wave functions with a variational

screening constant; α,β, and γ are variational constants.[142] At large separations, $\alpha = -\frac{1}{2}$ $\beta = -R^{-3}$ and $\gamma = 0$. The $\tilde{\Psi}$ gives a good value for the London energy, $C_6/R^6 = -6/R^6$. The electron-exchange terms in $\tilde{\psi}$ give a vanishingly small contribution to the energy at large separations.

Recently, Kolos and Wolniewicz[49] have obtained excellent values for the energy of both the $X^1\Sigma_g^+$ and $b^3\Sigma_u^+$ states of the hydrogen molecule from $R = 0.4$ a_0 to $R = 10.0$ a_0. The interaction energy of the two ground-state hydrogen atoms (at all separations) can be resolved into a coulombic and an exchange component,[156,157,165] E(coul) and E(exch), where

$$E(\text{coul}) = \frac{1}{2}\left[E(^1\Sigma_g^+) + E(^3\Sigma_u^+)\right]$$

$$E(\text{exch}) = \frac{1}{2}\left[E(^1\Sigma_g^+) - E(^3\Sigma_u^+)\right] \tag{102}$$

At large separations, since ground-state hydrogen atoms have no electrostatic dipole, the coulombic energy becomes equal to the dispersion energy, $E(\text{dis}) = C_6R^{-6} + C_8R^{-8} + C_{10}R^{-10}$, where the coefficients C_n are given in Table IV (see also refs. 66,97,158,159). In addition, Bell[160] has calculated the contribution of the second-order energy through R^{-20}. However, as he points out, the leading term of the third-order energy varies as R^{-11} and, therefore, the additional terms have limited interest. Table V shows that there is good agreement between the Kolos and Wolniewicz variational calculations of E(coul) and the series calculation of E(dis). It is clear from Table V that even at $R = 10$ a_0, E(exch) is not negligible.[49,73,74]

In Table V the Kolos and Wolniewicz calculations for E(exch) are compared with the asymptotic formula of Herring and Flicker[165c] (who followed the work of Gor'kov and Pitaevski[162]). Herring and Flicker obtained for the leading term in the exchange energy,

$$E(\text{exch})_{\text{HF}} = -0.818\ R^{5/2} \exp(-2R) + O(R^2 \exp(-2R)) \tag{103}$$

The derivation of this result required some very clever perturbatoin theory in which the relative size of each term in the perturbation plays a key role.[165c]

Since the unknown correction term $O(R^2 \exp(-2R))$ might be comparable in magnitude to the first term, the accuracy of the asymptotic

values of the exchange energy is not known. The very excellent agreement with the Kolos and Wolniewicz calculations might be fortuitous.

TABLE V

Comparison of Kolos and Wolniewicz[49] Variational Calculations for the Interaction of Two Ground-State Hydrogen Atoms with the Series Calculations for the Dispersion Energy (See Table IV) and with the Asymptotic Form[161] of the Exchange Energy. All energies are given in cm^{-1}. The underlined figures are uncertain.

	Kolos and Wolniewicz						Asymptotic
R/a_0	$-E$(exch)	$-E$(coul)	$-E$(dis)	$= -C_6R^{-6}$	$-C_8R^{-8}$	$-C_{10}R^{-10}$	$-E$(exch)
10.0	0.26	1.73	1.77	1.43	0.27	0.07	0.12
9.5	0.29	2.37	2.47	1.94	0.41	0.12	0.28
9.0	0.64	3.42	3.53	2.68	0.63	0.21	0.67
8.5	1.65	5.25	5.15	3.78	1.00	0.37	1.56
8.0	3.64	7.95	7.74	5.44	1.63	0.67	3.65

It is quite surprising that the Heitler-London[114,163] (HL) wave functions $\Psi_{HL} = a_{1s}(1)b_{1s}(2) \pm b_{1s}(1)a_{1s}(2)$, which lead to the exact wave function for the atoms in the limit that $R \to \infty$, do not even give the correct sign to E(exch) at large separations,

$$E(\text{exch})_{HL} = \{-(28/45) + (2/15)[C + \ln(R)]\}R^3 \exp(-2R) + \{-(5/2) + (4/5)[C + \ln(R)]\}R^2 \exp(-2R) + O(R \exp(-2R)) \quad (104)$$

where $C = 0.5772$ is the Euler constant. At separations greater than $R = 49.5\ a_0$ the Heitler-London energy for the $^3\Sigma_u^+$ is lower than for the ground state, $^1\Sigma_g^+$. It should be mentioned[162,164–166] that the serious errors in the Heitler-London treatment occur at large values of R (greater than 20 a_0) where dispersion and magnetic effects dominate the exchange energy (see Sec. VIII).

The reasons for the error in the Heitler-London exchange energy have recently been analyzed by Alexander and Salem.[161] They used a multiconfigurational wave function and considered the contributions

of each term to the exchange energy. The principal contributions come from ionic terms. It is interesting to note that a truncated expansion of the wave functions in powers of $1/R$ [see Eqs. (93) and (94)], which gives exact values of the dispersion energy, gives corrections to the Heitler-London exchange energy which vary as $R^{-n}\exp(-2R)$ where n is positive. Thus, the van der Waals type of polarization of the wave function plays only a minor role in determining the exchange energy.

In contrast to the very accurate wave function of Kolos and Wolniewicz,[49] *most* approximate wave functions do not give reasonable correlations between the coordinates of electrons 1 and 2 and therefore cannot give the dispersion energy in terms of the expectation value of the Hamiltonian. For example, if the approximate wave function is taken as the product of the wave functions of the separated atoms (such as the Heitler-London functions), there is no correlation between the electrons in the different atoms. It is because of the deficiencies of *most* approximate wave functions that it is customary to express the van der Waals energy in terms of second-order perturbation theory. Also, as discussed in Sections IV and V, the dispersion energies can be calculated *directly* by using perturbation theory.

B. Intermediate Separations

The region of *intermediate separation* is characterized by the overlapping of atomic orbitals. In this region, it is no longer possible to associate particular electrons with particular atoms. Indeed, as Nesbet has pointed out,[167] at intermediate separations the molecular system should be described in terms of molecular orbitals, whereas at large separations the molecular system can best be expressed in terms of atomic orbitals.

Numerical calculations for H_2, N_2, and other diatomic molecules[167–169] show that for each orbital there is a critical separation, R_c, at which it changes from an atomic orbital to a molecular orbital as the internuclear separation decreases. For the Coulson-Fischer[169] orbital $\psi_a + \lambda\psi_b$, where ψ_a and ψ_b are one-electron functions centered on the nuclei a and b, respectively, R_c corresponds to the separation where the energy-optimized parameter λ changes rapidly from the value zero (corresponding to the atomic orbital) to unity (corresponding to the molecular orbital) as R decreases. Thus, for each orbital, there is a ciritical separation R_c at which it changes from a pure atomic orbital to a pure molecular orbital. The value of R_c for the valence orbitals is

much larger than for the inner shells. Corresponding to these changes in the character of the orbitals, the optimum extended Hartree-Fock approximation shifts from the Hartree-Fock for the atoms at large separations to the molecular Hartree-Fock at intermediate separations. Wahl[168] has constructed some very beautiful and accurate computer-drawn pictures of the orbital for H_2 as a function of R and pictures of the orbitals of the other homonuclear diatomic molecules in the first row of the periodic table at their equilibrium separations.

The wave function for the $^1\Sigma_g^+$ state of the hydrogen molecule utilizing the Coulson-Fischer orbitals is

$$\begin{aligned}\Psi_{CF} &= [\psi_a(1) + \lambda\psi_b(1)][\psi_b(2) + \lambda\psi_a(2)] \\ &\quad + [\psi_b(1) + \lambda\psi_a(1)][\psi_a(2) + \lambda\psi_b(2)] \\ &= (1 + \lambda^2)[\psi_a(1)\psi_b(2) + \psi_b(1)\psi_a(2)] + 2\lambda[\psi_a(1)\psi_a(2) + \psi_b(1)\psi_b(2)]\end{aligned}$$

Thus, at large separations where λ is zero, Ψ_{CF} is a valence-bond function; whereas, at intermediate separations when λ is unity, Ψ_{CF} has equal contributions from the ionic and the valence-bond functions. The point of this remark is to emphasize that, from the point of view of atomic orbitals, the molecular orbitals lead to large ionic contributions to the wave functions. Thus, the actual molecular wave functions in the intermediate-separation range are mixtures of valence-bond and ionic functions and charge-exchange forces are very important (see Sec. V-C and VII-A).

For bound-state molecules at intermediate separations, there is a piling up of the electrons between the nuclei. This is evident from an examination of the expectation value of the square of the z component of the distance between two electrons. Thus, from the calculations of Kolos and Wolniewicz,[49,141]

$$\langle (z_2 - z_1)^2 \rangle < R^2$$

for the ground state of the hydrogen molecule in the range of separations from $R = 3.8\ a_0$ to $R = 1.8\ a_0$. Figure 6 shows a typical instantaneous charge distribution corresponding to this type of polarization. The electrons dodge each other in the x and y directions but tend to come towards each other in the region between the nuclei. The binding in a bound-state molecule is due to this buildup of negative charge between the two positive nuclei.[125]

C. Small Separations

At small separations, the electronic structure becomes closely related to the *united atom*. Indeed, there comes a critical separation where an abrupt change in the orbital structure takes place. At small separations, the correlation of the valence electrons is predominantly of the *in–out* type; at larger separations their correlation is of the *left–right* type.

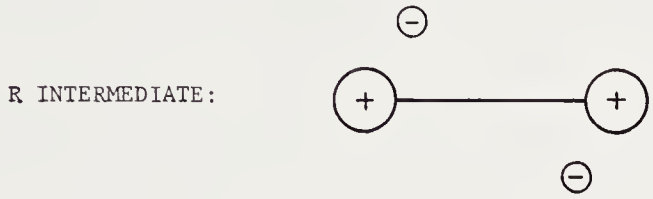

Fig. 6. Typical instantaneous charge distribution corresponding to a bound-state molecule at intermediate separations.

Consider the following examples.

a. Davidson and Jones[170] used an *open shell* representation of the approximate wave function for the ground state of the hydrogen molecule, $\tilde{\Psi} = u(1)v(2) + u(2)v(1)$. For $R = 0$, one of the orbitals, u for example, tends to become the inner orbital which is approximately $\exp(-2.15r)$ while v tends to become the outer orbital given approximately by $\exp(-1.19r)$. The *open shell* wave function for the helium atom has this well-known form.[171] Clearly, this form for the wave function represents *in–out* correlation between the electrons. At large separations, the u and v tend to become the $1s$ orbitals centered on nucleus a and nucleus b, respectively. The *open-shell* wave function then becomes the Wang or Heitler-London function with left–right correlation. Davidson and Jones find that the orbitals u and v have *in–out* correlations for R less than $0.8\ a_0$ and left–right correlation for R greater than $0.8\ a_0$. This value of R can be interpreted[170] as the internuclear distance at which the hydrogen molecule changes from a united atom into two separate but strongly interacting atoms. The change takes place so abruptly that it appears to be in the nature of an almost crossing of potential energy functions.

b. Buckingham and Duparc,[172] Miller and Present,[173] and Matsumoto, Bender, and Davidson[230] have considered the interaction of two ground-state helium atoms.[174] The wave function at large separations, with its *left–right* electron correlation corresponding to two separated

ground-state He atoms, correlates with the $(1s)^2(2p)^2$ excited configuration of the Be atom as $R \rightarrow 0$. On the other hand, the $(1s)^2(2s)^2$ ground-state configuration of Be, which has *in–out* electron correlation between the $1s$ and $2s$ electrons, correlates with the $(1s)(2s)$ excited configuration for each of the separated atoms. Thus, there is a crossing of these two correlation curves and a corresponding almost crossing of potential energy curves (cf. *a* above). Miller and Present conclude that there is a rapid change in the two types of orbital structure around $R = 0.75\ a_0$, which agrees roughly with Buckingham and Duparc's result. Matsumoto, Bender, and Davidson[230] find that the change occurs around $R = 0.60\ a_0$. Failure to take account of this change of orbital structure as R approaches zero would give calculated energies that are much too high for small values of R. However as Phillipson[175] has shown, this effect is not appreciable[176] at values of R greater than $1\ a_0$. Indeed, even around $1\ a_0$, the ground state of He_2 is still far from the united atom.[175]

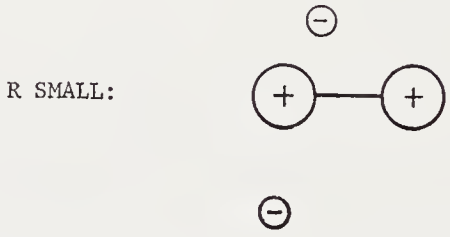

Fig. 7. Typical instantaneous charge distribution corresponding to atoms at small separations.

Corresponding to the *in–out* correlations, Figure 7 shows a typical instantaneous charge distribution for small R, which gives rise to the strong repulsive forces expected at small internuclear separations.

D. Discussion of Davidson's Double Minimum Excited H_2 Potential Energy Curve

Davidson[52,53] has made some interesting calculations of the potential energy curve for the lowest excited $^1\Sigma_g^+$ state ($E\,^1\Sigma_g^+$) of the hydrogen molecule (discussed in Sec. IV and the results summarized in Table III). The surprising feature of his potential energy curve is that it has two deep minima. At smaller separations (including the inner potential minimum at $R = 1.9\ a_0$), the wave function is essentially $(1s\sigma)(2s\sigma)$ and the electrons are *in–out* correlated. At large separations (including the outer minimum at $R = 4.3\ a_0$), the wave function corresponds to a

symmetrized $H^+ + H^-$ system and the electrons are *left–right* correlated. Moser[177] suggests that this sort of double-minimum potential should be expected for some of the excited states of many diatomic molecules. The inner minimum is to be associated with Rydberg excitation of the valence electrons; the outer minimum with the valence-bond forces.

VIII. MAGNETIC OR RELATIVISTIC INTERMOLECULAR FORCES

In this section, the relativistic or magnetic corrections to the electrostatic intermolecular forces are considered. In general, degenerate energy levels are split into a set of energy levels as a result of the magnetic interactions (see Sec. VIII-C-3 and V-B-5). Most of our discussion is based on the corrections obtained from the Breit-Pauli approximation to the exact relativistic Hamiltonian. For short, intermediate, and moderately large intermolecular separations the Breit-Pauli approximation represents the interaction accurately. For larger values of R, higher-order relativistic corrections are required for the accurate calculation of intermolecular forces. To simplify the discussion, only atom–atom interactions are considered in detail, but similar results apply for the interaction of molecules as well.

A. The Breit-Pauli Hamiltonian

Corrections to the electrostatic (nonrelativistic) static interaction energy through $O(\alpha^2)$, where $\alpha = e^2/\hbar c \doteq 1/137$ is the fine-structure constant, can be obtained by using the generalized Breit-Pauli[178] Hamiltonian, H,

$$H = H_e + \alpha^2 H_{\text{rel}} \tag{105}$$

The perturbation $\alpha^2 H_{\text{rel}}$ contains terms which couple the magnetic moments of the electrons in the system. If the electronic nonrelativistic wave function, Ψ, is known exactly, then the energy of the system, through $O(\alpha^2)$, is given by

$$\mathscr{E} = E + \alpha^2 \mathscr{E}^{(1)} = E + \alpha^2 \langle \Psi | H_{\text{rel}} | \Psi \rangle \tag{106}$$

where E is the usual electrostatic energy. For a diatomic molecule, the corresponding interaction energy is given by

$$\mathscr{E}_{ab} = \mathscr{E} - \mathscr{E}(\infty) = E_{ab} + \alpha^2 \mathscr{E}^{(1)}_{ab} \tag{107}$$

where $\mathscr{E}(\infty) = E(\infty) + \alpha^2\mathscr{E}^{(1)}(\infty)$ is the energy of the isolated atoms including relativistic terms.

The Breit-Pauli Hamiltonian is derived for a two-electron atom in the book by Bethe and Salpeter;[179,180] the generalization to a molecular system is given in reference 1, p. 1044 (see also Itoh[181]). Let the operators for the spin and linear momentum of the kth electron be denoted by $\mathbf{s}_k$ and $\mathbf{p}_k = (1/i)\nabla_k$, respectively. Then

$$H_{\text{rel}} = H_{LL} + H_{SS} + H_{SL} + H_p + H_D \tag{108}$$

$$H_{LL} = -\frac{1}{2}\sum_{k>j}(1/r_{jk}^3)[r_{jk}^2\mathbf{p}_j\cdot\mathbf{p}_k + \mathbf{r}_{jk}\cdot(\mathbf{r}_{jk}\cdot\mathbf{p}_j)\mathbf{p}_k] \tag{109}$$

$$H_{SS} = \sum_{k>j}\{-(8\pi/3)(\mathbf{s}_j\cdot\mathbf{s}_k)\delta^{(3)}(\mathbf{r}_{jk}) + (1/r_{jk}^5)[\mathbf{r}_{jk}^2\mathbf{s}_j\cdot\mathbf{s}_k - 3(\mathbf{s}_j\cdot\mathbf{r}_{jk})(\mathbf{s}_k\cdot\mathbf{r}_{jk})]\} \tag{110}$$

$$H_{SL} = \frac{1}{2}\sum_{\beta,j}(Z_\beta/r_{j\beta}^3)(\mathbf{r}_{j\beta}\times\mathbf{p}_j)\cdot\mathbf{s}_j - \frac{1}{2}\sum_{\substack{j,k\\k\neq j}}(1/r_{jk}^3)[(\mathbf{r}_{jk}\times\mathbf{p}_j)\cdot\mathbf{s}_j - 2(\mathbf{r}_{jk}\times\mathbf{p}_k)\cdot\mathbf{s}_j] \tag{111}$$

$$H_p = -\frac{1}{8}\sum_j p_j^4 \tag{112}$$

$$H_D = \frac{1}{2}\pi\{\sum_{\beta,j}Z_\beta\delta^{(3)}(\mathbf{r}_{j\beta}) - 2\sum_{k>j}\delta^{(3)}(\mathbf{r}_{jk})\} \tag{113}$$

In these equations, the nuclei are considered fixed (Born-Oppenheimer); errors introduced by this approximation are of $O(\alpha^2/M)$, where M is a nuclear mass.[16] In the generalized Breit-Pauli Hamiltonian we have omitted terms[182] which take account of the effects of nuclear spin [they are of $O(\alpha^2/M)$] and we have also assumed that no external magnetic or electric fields are present. These effects can be very important in discussing many types of phenomena: electron spin resonance (ESR) and nuclear magnetic resonance (NMR) spectroscopy,[182] collision problems such as spin-flip or spin-exchange processes,[183] etc. The nuclear spin terms can also be important in the calculation of long-range intermolecular forces, see Section VIII-C-3.

The various terms in H_{rel} have the following significance:

H_{LL} corresponds to the classical[184] electromagnetic coupling of the

electrons through the interaction of the magnetic fields created by their motion. It contains[185] terms which couple the orbital magnetic moments of the electrons.

H_{SS} gives the interaction between the spin magnetic moments of the electrons. The electron–electron Fermi-type contact term, involving the delta function, gives the behavior when $r_{jk} = 0$. The second term, corresponding to the usual magnetic dipole–magnetic dipole interaction, is only applicable when $r_{jk} \neq 0$.[179,182a]

H_{SL} represents the spin–orbit magnetic coupling between electrons. The first term gives the interaction between the spin of an electron and the magnetic moment associated with its motion. The remainder of H_{SL} gives the spin–other orbit coupling between the spin of one electron and the orbital magnetic moment of another.

H_p is the relativistic correction due to the variation of mass with velocity.

H_D is a term characteristic of the Dirac theory,[179] which appears to have no simple interpretation.

The generalized Breit-Pauli Hamiltonian gives the $O(\alpha^2)$ leading term of a perturbation expansion of the exact relativistic Hamiltonian in powers of $(Z\alpha)$. As emphasized by Bethe and Salpeter[179] the treatment cannot be used consistently to evaluate higher-order corrections (see also ref. 72). Also, the energy which is accurate through $O(\alpha^2)$ does *not* imply that the Breit-Pauli formalism is correct through $O(\alpha^2)$ in the sense of photon exchanges. The photon exchange terms missing in the Breit-Pauli formalism are discussed by Power and Zienau[186] and appear to give energy corrections of higher order in α.

Strictly speaking, the use of the Breit-Pauli approximation implies that $Z \ll 137$ (so that αZ is small). For large atoms or ions, the behavior of the inner shell electrons is appreciably affected by the higher-order relativistic effects. Such effects may be important in nuclear magnetic resonance and also make the calculations[187] of relativistic corrections to the energy of atoms (and hence for molecules) very difficult for $Z > 30$. Unfortunately, it is very difficult to write down the exact relativistic Hamiltonian in closed form, although many of the correction terms through $O(\alpha^3)$ and $O(\alpha^4)$ have been obtained explicitly (see, for example, the recent work of Kim[188]). However, for many problems of chemical interest, the higher-order corrections are probably not too important since the valence electrons are shielded by the inner-shell electrons and are not appreciably affected by the bare nuclear charges.

B. Small and Intermediate Separations

In order to calculate the relativistic corrections to the electrostatic energy, it is necessary to obtain an accurate representation of the exact nonrelativistic wave function Ψ. The expectation values of the operators in H_{rel} are very sensitive[179,187,189] to the choice of the wave function and, therefore, accurate values for the matrix elements of H_{rel} are very difficult to obtain in the charge overlap region, especially for large systems. Usually, in the calculation of relativistic interaction energies at small and intermediate separations, the electrostatic wave function obtained by the Raleigh-Ritz variational procedure (see Sec. IV) is used in Eq. (107).

Kolos and Wolniewicz[21] have calculated the relativistic corrections to the electrostatic energy for the ground-state hydrogen molecule through $O(\alpha^2)$ for $0.6\, a_0 \leqslant R \leqslant 3.6\, a_0$. Their results are given in Table VI and were obtained by using a 54-term representation of the exact

TABLE VI

Relativistic Corrections for the Ground State of the Hydrogen Molecule Calculated by Kolos and Wolniewicz.[21] Energies are given in cm^{-1}.

Type of energy	$R/a_0 =$ 0.60	1.40	2.40	3.60	∞
E_P	−45.983	−19.355	−13.243	−13.160	−14.609
E_{LL}	−1.074	−0.559	−0.270	−0.092	−0.000
E_D	+37.379	+16.273	+11.082	+10.668	+11.687
E_{SS}	+3.765	+1.244	+0.383	+0.083	+0.000
E_{SL}	0.000	0.000	0.000	0.000	0.000
Total E_{rel}	−5.913	−2.398	−2.048	−2.502	−2.922

wave function. Also, the radiative corrections of $O(\alpha^3)$ and $O(\alpha^3 \log \alpha)$ for the ground-state hydrogen molecule have been calculated by Ladik,[190] Wolniewicz,[24] and Garcia.[191] The Breit-Pauli corrections give a relativistic correction to the dissociation energy of H_2 of $-0.524\ cm^{-1}$, while the radiative corrections amount to[191] only $-0.22 \pm 0.03\ cm^{-1}$. As discussed in Section IV, these effects are not large enough to account for the discrepancy between the theoretical and experimental dissociation energies of the hydrogen molecule.

For atoms with nuclei of high atomic number, the relativistic corrections to the energy can be quite large (Clementi,[187a] and Hartman and Clementi[187b]) and any appreciable deviation from additivity of the relativistic energy shifts in the colliding molecules could change the intermolecular potential significantly. These effects are important in the calculation of molecular properties other than the interaction energy for small and intermediate separations, for example: "forbidden" transition probabilities,[32,192] diamagnetic susceptibilities of aromatic compounds,[193] fine structure of rotational energy levels,[36,194] and chemical shifts.[182]

C. Large Separations

Relativistic or retardation effects appreciably modify the interaction between atoms and molecules for large intermolecular separations and, in general, the corresponding interaction energies for large R cannot be calculated accurately from the Coulomb potential energy V_e. These effects begin to become important for $R > \lambda\!\!\!^{-}/3$ where $\lambda\!\!\!^{-} = (\alpha\Delta\varepsilon)^{-1}$ is the reduced wavelength characteristic of allowed electrostatic transitions in the interacting atoms or molecules ($\Delta\varepsilon$ is the corresponding excitation energy).

A complete review of very long-range retarded or relativistic interaction energies is given in Chapter 4. Here, the Breit-Pauli Hamiltonian is used to discuss the relativistic corrections, through $O(\alpha^2)$, for some of the electrostatic energies discussed in Section V. In general, the Breit-Pauli approximation is accurate for moderately large values of $R < \lambda\!\!\!^{-}$, but the range of validity (as determined by comparison with the exact quantum electrodynamic results) depends markedly upon the type of interaction, as discussed below.

1. *Calculation of the Interaction Energy*

For large separations, where the wave functions of the interacting atoms a and b do not overlap appreciably, the electrostatic problem can be solved by the use of perturbation theory as discussed in Section V. Using the result for the electrostatic wave function and the multipole expansion[72a,185,195,196] of H_{rel}, it is possible to obtain an expansion in powers of R^{-1} for the relativistic interaction energy which is analogous to the corresponding expansion for the electrostatic interaction energy E_{ab} (for notation, see Sec. V).

a. **The Multipole Expansion of H_{rel}.** Assuming $R > (r_{ai} + r_{bj})$ for all

electrons i associated with atom a and electrons j associated with atom b, it can be shown that[72a]

$$H_\sigma = H_{\sigma,0} + H_\sigma^{\text{int}} \qquad \sigma = LL,SL,SS,p,D \tag{114}$$

where

$$H_{\sigma,0} = H_{\sigma,0}(a) + H_{\sigma,0}(b) \tag{115}$$

and

$$H_\sigma^{\text{int}} = \sum_{m=1}^{\infty} H_{\sigma,m} R^{-m} \qquad \sigma = LL,SS,SL$$

$$= 0 \qquad \sigma = p,D \tag{116}$$

$$H_{SL,1} = H_{SS,1} = H_{SS,2} = 0 \tag{117}$$

Here the $H_{\sigma,0}(a)$ are the relativistic Hamiltonians for the isolated atom a and H_σ^{int} is the relativistic interaction potential corresponding to the relativistic correction σ. General expressions for the $H_{\sigma,m}$, for all m greater than zero, have been derived[197] and explicit expressions for the most important of these coefficients (for $m = 1$, 2, and 3) are given by Meath and Hirschfelder.[72a] The $H_{\sigma,m}$ of specific interest in this paper are given below. These relativistic multipole interaction coefficients for m greater than zero represent the interaction of the various orbital and spin magnetic multipoles of molecule a with those of molecule b. For example:

$H_{LL,1}$ can be written as

$$H_{LL,1} = -\frac{1}{2}[\mathbf{P}_a \cdot \mathbf{P}_b + (\mathbf{P}_a \cdot \hat{\mathbf{R}})(\mathbf{P}_b \cdot \hat{\mathbf{R}})] \tag{118}$$

where $\mathbf{P}_a = +\sum_i \mathbf{p}_{ai}$ and $\mathbf{P}_b = +\sum_j \mathbf{p}_{bj}$ are, respectively, the linear momentum (or current) operators for molecules a and b. Thus, $H_{LL,1}$ gives the (orbital-current)–(orbital-current) interaction between the two interacting molecules.

$H_{LL,2}$ represents the (orbital-current)–(orbital-dipole) interaction and $H_{SL,2}$ gives the (orbital-current)–(spin-dipole) interaction.

$H_{\sigma,3}$ for $\sigma = LL,SL,SS$ can be written in the form

$$H_{\sigma,3} = \Gamma_{\sigma,3} + \chi_{\sigma,3}; \qquad \chi_{SS,3} = 0 \tag{119}$$

where

$$\Gamma_{LL,3} = \frac{1}{4}[\mathbf{L}_a \cdot \mathbf{L}_b - 3(\mathbf{L}_a \cdot \hat{\mathbf{R}})(\mathbf{L}_b \cdot \hat{\mathbf{R}})] \tag{120}$$

$$\Gamma_{SL,3} = \frac{1}{2}[\mathbf{L}_a \cdot \mathbf{S}_b + \mathbf{S}_a \cdot \mathbf{L}_b - 3(\mathbf{L}_a \cdot \hat{\mathbf{R}})(\mathbf{S}_b \cdot \hat{\mathbf{R}}) - 3(\mathbf{S}_a \cdot \hat{\mathbf{R}})(\mathbf{L}_b \cdot \hat{\mathbf{R}})] \tag{121}$$

$$\Gamma_{SS,3} = \mathbf{S}_a \cdot \mathbf{S}_b - 3(\mathbf{S}_a \cdot \hat{\mathbf{R}})(\mathbf{S}_b \cdot \hat{\mathbf{R}}) \tag{122}$$

and $\mathbf{L}_a$ and $\mathbf{S}_a$ are, respectively, the orbital and spin angular momentum operators for molecule a. Thus the coefficients $\Gamma_{\sigma,3}$ for $\sigma = LL,SL$, and SS represent, respectively, the magnetic orbit–orbit, spin–orbit, and spin–spin dipole interactions between molecules a and b. The $\chi_{\sigma,3}$ represent other types of magnetic interactions; $\chi_{LL,3}$ represents the (orbital-current)–(orbital-quadrupole) interaction and $\chi_{SL,3}$ the (orbital-current)–(spin-quadrupole) interaction.

Substitution of the multipole expansion of H_{rel} and the $1/R$ expansions for the electrostatic wave function [Eq. (33)] and interaction energy [Eq. (32)] into Eq. (107) gives the $1/R$ expansion for the total interaction energy through $O(\alpha^2)$,

$$\mathscr{E}_{ab} = \sum_{m \neq 0}^{\infty} [C_m + \alpha^2 \sum_{\sigma} W_{\sigma,m}] R^{-m} \tag{123}$$

where (letting $\Psi_0 = \psi_0$)

$$W_{\sigma,m} = \sum_{l=0}^{m} \sum_{q=0}^{m-l} \langle \Psi_q | H_{\sigma,l} | \Psi_{m-l-q} \rangle \tag{124}$$

The $W_{\sigma,m}R^{-m}$ are the $O(\alpha^2)$ relativistic interaction energies arising from the relativistic multipole coefficients $H_{\sigma,l}$. The most important effect of the relativistic Hamiltonians for the isolated atoms, the $H_{\sigma,0}$, has been discussed in Section V. The $H_{\sigma,0}$ terms cause splittings in the nonrelativistic potential energy curves at moderately large R. On the other hand, the relativistic interaction Hamiltonians, H_{σ}^{int}, can give rise to relativistic interaction energies that are of lower order in R^{-1} than the electrostatic energies discussed in Section V. The interaction energies given by Eq. (123) are strictly valid only for separations R sufficiently small that $\mathscr{E}_{ab}$ is larger than the hyperfine structure splittings in the interacting atoms, as discussed in Section VIII-C-3.

2. *Dispersion Energies*

For the interaction of two ground-state nondegenerate atoms all first-order energies vanish and the interaction energy is given by a sum of dispersion energies. For these interactions, the attractive force is considerably smaller than that predicted by the London dispersion energy for large values of R. The reduction of the force of attraction is due to retardation effects which result from the finite velocity of the propagation of electromagnetic radiation *between* the molecules. The retardation effects may be described qualitatively as follows.[198] As discussed in Section VII, one molecule has an instantaneous dipole moment which produces an electromagnetic field. At a time R/c later (where c is the velocity of light) this field induces an electric moment in the second molecule and at a time $2R/c$ later, the instantaneous dipole-induced dipole interaction takes place. If the interacting molecules are sufficiently far apart, the instantaneous dipole in the first molecule can change both in direction and in magnitude during the time $2R/c$ so that the energy of interaction is less than would be expected from Coulomb's law.

Casimir and Polder[199] put these qualitative ideas on a quantitative basis by using quantum electrodynamics to calculate the retarded dispersion energy for the interaction of two ground-state nondegenerate atoms. They found that for very large $R > \hat{\lambda}$, the interaction energy varies as R^{-7} rather than as the R^{-6} which would be expected for the London dispersion energy. This effect gives an explanation[198] of the stability of suspensions involving lyophobic colloids, in which the long-range forces appear to be smaller than predicted by the London energy.

The zeroth-order wave function for the perturbation calculation of the interaction energy is given by $\psi_0 = A_q(i)B_{q'}(j)$. Using the perturbation method outlined above, the interaction energy, through $O(\alpha^2/R^6)$ and $O(1/R^8)$, has the form[72a,186,200]

$$\mathscr{E}_{ab} = C_6R^{-6} + C_8R^{-8} + \alpha^2[W_4R^{-4} + W_6R^{-6}] + \cdots \qquad (125)$$

Here C_6/R^6 is the well-known London dispersion energy, Eq. (61), and the C_6 can be considered as the sum of different two-electron excitation terms,

$$C_6 = \sum_{r \neq q} \sum_{u \neq q'} C_6(r,u) \qquad (126)$$

where

$$C_6(r,u) = -\frac{6\,|(\mu_{az})_{qr}|^2\,|(\mu_{bz})_{q'u}|^2}{(a_r - a_q) + (b_u - b_{q'})} \tag{127}$$

The leading term in the relativistic correction to the London energy is $\alpha^2 W_4 R^{-4}$ and $W_4 = W_{LL,4} = 2\langle \Psi_3 | H_{LL,1} | \psi_0 \rangle$ is given by

$$W_4 = \sum_{r \neq q} \sum_{u \neq q'} W_4(r,u) \tag{128}$$

where

$$W_4(r,u) = \frac{2(a_r - a_q)(b_u - b_{q'})\,|(\mu_{az})_{qr}|^2\,|(\mu_{bz})_{q'u}|^2}{(a_r - a_q) + (b_u - b_{q'})} \tag{129}$$

There is a strong similarity between the coefficient C_6 and W_4, but while C_6 is negative for the interaction of ground-state atoms, W_4 is positive, giving rise to a repulsive correction to the London energy which tends to reduce the force of attraction between the interacting atoms. The interaction energy $\alpha^2 W_4 R^{-4}$ was first discovered by Penfield and Zatzkis[200] in a one-dimensional relativistic harmonic oscillator calculation. It is the most important correction[72b] to the London dispersion energy in an expansion of the exact dipole–dipole retarded interaction energy valid for $R < \lambda\!\!\!^{-}$ (see below and see also Power and Zienau[186]).

The relativistic correction $\alpha^2 W_6/R^6$ is comprised of several terms.[72a] One of these[72b] appears to be the principal retardation or relativistic correction to the electrostatic dipole–quadrupole dispersion energy valid for $R < \lambda\!\!\!^{-}$. Estimates for all the coefficients in Eq. (125) have been made for some rare gas interactions using Unsöld's approximation and the energy $\alpha^2 W_6 R^{-6}$ is negligible for most interactions. It is of $O(10\alpha^2) \approx 5 \times 10^{-4}$ times smaller than the London dispersion energy.

a. **Comparison with the Exact Retarded Dipole–Dipole Interaction Energy.** Casimir and Polder[199] obtained an expression for the exact retarded dipole–dipole interaction energy between two ground-state atoms. Their result has been reaffirmed by a number of authors[201] using many different techniques (see Chapter 4, Sec. II). The Hamiltonian for the system consists of contributions from the isolated atoms, the free radiation field, and the interaction between the atoms and the radiation field. The fields are then expanded in a multipole series keeping only electrostatic dipole terms [in this approximation, C_8 and W_6 are zero in Eq. (125)]. The interaction energy in the electric dipole approximation

is calculated using quantum electrodynamics and the result may be written in the form

$$\mathscr{E}_{ab} = \sum_{r \neq q} \sum_{u \neq q'} U(r,u) \tag{130}$$

The interaction energy, $\mathscr{E}_{ab}$, is a sum of terms, $U(r,u)$, corresponding to the atomic dipolar transitions $q \leftrightarrow r$ and $q' \leftrightarrow u$ with reduced wavelengths $\lambda\!\!\!^{-}_a = [\alpha(a_r - a_q)]^{-1}$ and $\lambda\!\!\!^{-}_b = [\alpha(b_u - b_{q'})]^{-1}$, respectively. The $U(r,u)$ are given in terms of sine and cosine integrals [Eq. (33) of Chapter 4], which can be expanded in powers of $(R/\lambda\!\!\!^{-})$ for small values of $R < \lambda\!\!\!^{-}$ or in powers of $(\lambda\!\!\!^{-}/R)$ for large values of $R > \lambda\!\!\!^{-}$, where $\lambda\!\!\!^{-}$ can be $\lambda\!\!\!^{-}_a$ or $\lambda\!\!\!^{-}_b$.

b. **"Small R" Expansion,**[72b,186,201] $R < \lambda\!\!\!^{-}$. For "small" values of R [but note, $R > (r_{ai} + r_{bj})$], the expansion of $U(r,u)$ has the form

$$\begin{aligned} U(r,u) &= \sum_{n=6,4,3,2,\ldots} U_n(r,u) R^{-n} \\ &= C_6(r,u)R^{-6} + \alpha^2 W_4(r,u)R^{-4} + \alpha^3 D_3(r,u)R^{-3} \\ &\qquad + \alpha^4 D_2(r,u)R^{-2} + \cdots \end{aligned} \tag{131}$$

This expansion, through $O(\alpha^2)$, agrees with the result of Eq. (125) in the electric dipole approximation. The other terms[72b] in Eq. (131) give rise to corrections to the London dispersion energy of higher order than α^2 and are not obtainable in the Breit-Pauli approximation.

In order to simplify our discussion of the accuracy of the "small R" expansion, let us consider $U(r,r)$ which depends upon a single reduced wavelength $\lambda\!\!\!^{-}$ rather than the more general function $U(r,u)$ which depends upon the two reduced wavelengths $\lambda\!\!\!^{-}_a$ and $\lambda\!\!\!^{-}_b$. The variation of $U(r,r)$ with the separation R is typical of the $U(r,u)$. The term $U(r,r)$ is the contribution to the interaction energy between two like atoms corresponding to the dipolar transitions $q \leftrightarrow r$ with reduced wavelengths $\lambda\!\!\!^{-} = \lambda\!\!\!^{-}_a = \lambda\!\!\!^{-}_b = [\alpha(a_r - a_q)]^{-1}$. Detailed calculations of the ratios $\sum_n U_n(r,r)R^{-n}/U(r,r)$ as functions of $(R/\lambda\!\!\!^{-})$ have been carried out by Meath and Hirschfelder[72b] and are given in Figure 8. The values of $(R/\lambda\!\!\!^{-})$ which correspond to 1, 2, 5, and 10% error in using expansions of the form $\sum_n U_n(r,r)R^{-n}$ are given in Table VII. The Breit-Pauli values [the first two terms of Eq. (131)] give results accurate to 5% for $R < 0.6\lambda\!\!\!^{-}$. For larger values of R, the Breit-Pauli Hamiltonian becomes a poor representation of the interaction. Including the $O(\alpha^3)$ correction improves the situation a little but including the $O(\alpha^4)$ correction gives

poorer results for $R > 0.4\lambda\!\!\!^{-}$. It appears that the $O(\alpha^2)$ energy is the most important correction to the London energy for $R < \lambda\!\!\!^{-}$.

The regions of validity of the "small R" expansion of the $U(r,u)$ are unambiguous. However, since the $\lambda\!\!\!^{-}$ have a maximum value $\lambda\!\!\!^{-}_0$ corresponding to the transition from the ground state to the first excited state

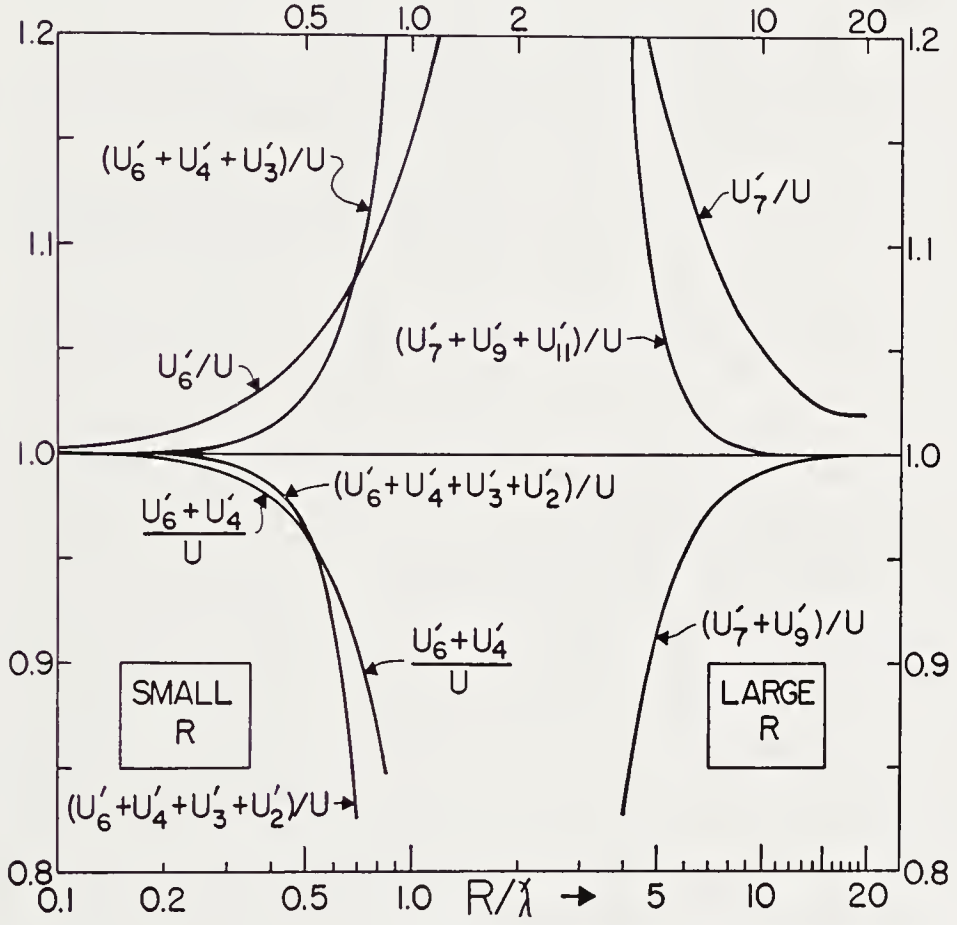

Fig. 8. Comparison of the "small R" and the "large R" expansions with the exact Casimir and Polder energy U. Here $U'_n = U_n R^{-n}$. This figure is taken from Meath and Hirschfelder, ref. 72b.

of one of the atoms and the $\lambda\!\!\!^{-}$ become smaller for transitions to excited states, the region of validity of the corresponding expansion for $\mathscr{E}_{ab}$ is not as clear. For some interactions, it may be possible to define an "average" reduced wavelength, $\lambda\!\!\!^{-}_{av}$, such that the expansion of $\mathscr{E}_{ab}$ is valid for $R < \lambda\!\!\!^{-}_{av}$. Since transitions to highly excited states and the

TABLE VII

"Small R" Expansion of the Dispersion Energy. Values of $R/\lambda\!\!\!^{-}$ for the Following Cases. This Table is Taken from Meath and Hirschfelder, Ref. 72b.

X =	1	2	5	10
A. $U_6(r,r)R^{-6}$ Differs from the Exact $U(r,r)$ by $X\%$				
$R/\lambda\!\!\!^{-}$ =	0.20	0.30	0.50	0.76
B. $U_6(r,r)R^{-6} + U_4(r,r)R^{-4}$ Differs from the Exact $U(r,r)$ by $X\%$				
$R/\lambda\!\!\!^{-}$ =	0.30	0.40	0.56	0.72
C. $U_6(r,r)R^{-6} + U_4(r,r)R^{-4} + U_3(r,r)R^{-3}$ Differs from the Exact $U(r,r)$ by $X\%$				
$R/\lambda\!\!\!^{-}$ =	0.37	0.45	0.58	0.71
D. $U_6(r,r)R^{-6} + U_4(r,r)R^{-4} + U_3(r,r)R^{-3} + U_2(r,r)R^{-2}$ Differs from the Exact $U(r,r)$ by $X\%$				
$R/\lambda\!\!\!^{-}$ =	0.37	0.43	0.53	0.62

continuum can give an appreciable contribution[202] to $\mathscr{E}_{ab}$, the value of $\lambda\!\!\!^{-}_{av}$ can be *much* smaller than $\lambda\!\!\!^{-}_0$.

c. **"Large R" Expansion,**[72b,186,201] $R > \lambda\!\!\!^{-}$. For very large values of R, the expansion of $U(r,u)$ has the form

$$U(r,u) = \sum_{n=7,9,11,\ldots} U_n(r,u)R^{-n} \tag{132}$$

$$= D_7(r,u)\alpha^{-1}R^{-7} + D_9(r,u)\alpha^{-3}R^{-9} + D_{11}(r,u)\alpha^{-5}R^{-11} + \cdots \tag{133}$$

where

$$D_7(r,u) = -\left(\frac{23}{\pi}\right)\frac{|(\mu_{az})_{qr}|^2\,|(\mu_{bz})_{q'u}|^2}{(a_r - a_q) + (b_u - b_{q'})} \tag{134}$$

The corresponding expansion for the interaction energy, $\mathscr{E}_{ab}$, is obtained from Eq. (130) and cannot be obtained from the Breit-Pauli approximation. The lead term in the "large" R expansion of $\mathscr{E}_{ab}$ is $\sum_{r,u} U_7(r,u)R^{-7} = -(23/4\pi\alpha R^7)\alpha_d(a)\alpha_d(b)$, where $\alpha_d(a)$ is the dipole polarizability of atom a. This is the well-known result of Casimir and Polder.[199] The interaction energies[72b] arising from $U_9(r,u)R^{-9}$ and $U_{11}(r,u)R^{-11}$ are correction terms. Since $\lambda\!\!\!^{-} \leq \lambda\!\!\!^{-}_0$ for all r and u, the "large R" expansion of $\mathscr{E}_{ab}$ is clearly valid for $R > \lambda\!\!\!^{-}_0$.

Ratios of the form $\sum_n U_n(r,r)R^{-n}/U(r,r)$ for the "large R" expansion of $U(r,r)$ are plotted as functions of $(R/\lambda\!\!\!^{-})$ in Figure 8 and the values of $(R/\lambda\!\!\!^{-})$ which correspond to 1, 2, 5, and 10% error in using these expansions are given in Table VIII. It is clear that $U_7(r,r)R^{-7}$ is not a

TABLE VIII

"Large R" Expansion of the Dispersion Energy. Values of $R/\lambda\!\!\!^{-}$ for the Following Cases. This Table is Taken from Meath and Hirschfelder, Ref. 72b.

X =	1	2	5	10
A. $U_7(r,r)R^{-7}$ Differs from the Exact $U(r,r)$ by $X\%$				
$R/\lambda\!\!\!^{-}$ =		17.0	10.2	7.0
B. $U_7(r,r)R^{-7} + U_9(r,r)R^{-9}$ Differs from the Exact $U(r,r)$ by $X\%$				
$R/\lambda\!\!\!^{-}$ =	9.1	7.5	5.9	4.8
C. $U_7(r,r)R^{-7} + U_9(r,r)R^{-9} + U_{11}(r,r)R^{-11}$ Differs from the Exact $U(r,r)$ by $X\%$				
$R/\lambda\!\!\!^{-}$ =	7.4	6.4	5.5	4.7

particularly good approximation to $U(r,r)$. One obtains a considerable improvement by including the next term in the expansion and the three-term approximation is accurate to 5% for $R > 5.5\lambda\!\!\!^{-}$.

Both the "large R" and the "small R" expansions for $U(r,u)$ (and hence $\mathscr{E}_{ab}$) are asymptotic in nature. For values of R outside the region of validity of the expansions, including more terms in the series can yield a poorer approximation to $U(r,u)$. For the region $0.6\lambda\!\!\!^{-} < R < 5.0\lambda\!\!\!^{-}$, it is necessary to use the exact or integral form for the interaction energy if accurate results are required. Table IX gives the exact values of $U(r,r)$ for a wide range of separations.[72b]

The $1/R$ expansion of the interaction energy is very convenient for applications involving intermolecular forces. Also, the coefficients involved in these expansions can be calculated accurately by using variational techniques or oscillator-strength sum rules for the London dispersion energies as discussed by Dalgarno in Chapter 3 (see, for example, Mavroyannis and Stephen,[201d] Karplus and Kolker,[203] and Chan and Dalgarno[158]). Recently Johnson, Epstein, and Meath[204] have extended the techniques to the other coefficients involved in the

TABLE IX

Exact Values of $U(r,r)$ for a Wide Range of $R/\lambda\!\!\!^{-}$. Here $\kappa = (\alpha/\lambda\!\!\!^{-5})|(\mu_{az})_{qr}|^4$. The Numbers in Parentheses Indicate a Power of 10. Thus, $2.9(18) = 2.9 \times 10^{18}$. This Table is Taken from Meath and Hirschfelder, Ref. 72b.

$R/\lambda\!\!\!^{-}$	$-\kappa^{-1}U(r,r)$	$R/\lambda\!\!\!^{-}$	$-\kappa^{-1}U(r,r)$	$R/\lambda\!\!\!^{-}$	$-\kappa^{-1}U(r,r)$
0.001	2.9999(18)	0.420	5.2652(2)	4.000	3.5542(−4)
0.005	1.9200(14)	0.440	3.9712(2)	4.500	1.6161(−4)
0.010	2.9999(12)	0.460	3.0323(2)	5.000	7.9538(−5)
0.040	7.3205(8)	0.480	2.3417(2)	5.500	4.1758(−5)
0.060	6.4229(7)	0.500	1.8272(2)	6.000	2.3135(−5)
0.080	1.1422(7)	0.520	1.4395(2)	6.500	1.3413(−5)
0.100	2.9913(6)	0.550	1.0231(2)	7.000	8.0855(−6)
0.120	1.0006(6)	0.580	7.4019(1)	7.500	5.0414(−6)
0.140	3.9626(5)	0.600	6.0190(1)	8.000	3.2377(−6)
0.160	1.7757(5)	0.620	4.9270(1)	8.500	2.1342(−6)
0.180	8.7447(4)	0.650	3.6913(1)	9.000	1.4398(−6)
0.200	4.6389(4)	0.680	2.8008(1)	9.500	9.9177(−7)
0.220	2.6135(4)	0.700	2.3452(1)	10.000	6.9604(−7)
0.240	1.5474(4)	0.750	1.5361(1)	11.000	3.6007(−7)
0.260	9.5520(3)	0.800	1.0332(1)	12.000	1.9707(−7)
0.280	6.1094(3)	0.850	7.1133(0)	13.000	1.1310(−7)
0.300	4.0289(3)	0.900	4.9995(0)	14.000	6.7598(−8)
0.320	2.7286(3)	0.950	3.5792(0)	15.000	4.1844(−8)
0.340	1.8917(3)	1.000	2.6051(0)	16.000	2.6707(−8)
0.360	1.3389(3)	2.000	3.3107(−2)	17.000	1.7512(−8)
0.380	9.6536(2)	3.000	2.3856(−3)	18.000	1.1760(−8)
0.400	7.0764(2)	3.500	8.6337(−4)		

"large" and "small" R expansions of $\mathscr{E}_{ab}$. For the ground-state He–He interaction, the results are

$$\mathscr{E}_{\text{He–He}}(R < \lambda\!\!\!^{-}_{\text{av}}) = -1.4577\, R^{-6} + 0.6643\, \alpha^2 R^{-4} - 1.485\, \alpha^3 R^{-3} + 6.4\, \alpha^4 R^{-2} + \cdots$$

$$\mathscr{E}_{\text{He–He}}(R > \lambda\!\!\!^{-}_{\text{av}}) = -3.4786\, \alpha^{-1} R^{-7} + 21.51\, \alpha^{-3} R^{-9} - 395.3\, \alpha^{-5} R^{-11} + \cdots \quad (135)$$

In order to obtain an estimate for the values of R where retardation effects may be important, let us consider the He–He interaction. By using Unsöld's approximation on C_6, one can obtain[72a] an estimate for

the mean excitation energy, Δ_{He}, for the helium atom: $\Delta_{He} = 1.14$. The corresponding average characteristic wavelength is $\lambda\!\!\!^{-}_{av} = [\alpha\Delta_{He}]^{-1} = 120\,a_0$. Thus, from Table VII, using this approximation, it can be seen that the London energy is in error by 2% at $R = 36\,a_0$ and by 5% at $R = 60\,a_0$ when compared to the exact retarded dipole interaction energy. At the present time, experimental data on the interaction energy can be obtained from low-energy atom beam scattering experiments for interatomic separations of the order of $R \approx 35\,a_0$. As discussed by Bernstein and Muckerman in Chapter 8, the coefficient C_6 can be estimated in some cases to within 10–15% using these methods. Hence, at the present time, it appears that the retardation effects discussed above are too small to be observed by atomic beam techniques (see also Fontana and Bernstein[205]).

The calculation of Casimir and Polder[199] involved the interaction, in the electrostatic dipole approximation, of atoms in nondegenerate ground states. By considering excited-state interactions and by including magnetic dipoles in the calculation, many other types of interesting retarded dispersion energies can be obtained. The following are examples.

1. For the nonresonant interaction between nonidentical molecules, McLone and Power[206] (see also Philpott[207]) used quantum electrodynamics to calculate the interaction energy (in the electrostatic dipole approximation) when one atom is in an excited state and the other in the ground state. For $R < \lambda\!\!\!^{-}$, the leading term in the expansion of the interaction energy is the usual R^{-6} London result. On the other hand, for $R > \lambda\!\!\!^{-}$, the energy has a leading term which varies as $R^{-2}\cos^2(R/\lambda\!\!\!^{-})$ and is quite different from the Casimir and Polder result for ground-state atoms. Since this interaction involves an excited atom, the interaction energy has a line width caused by the finite life-time of the excited state. This effect is discussed in detail in Chapter 4 and by Philpott[207] (see also Stephen[208]).

2. By including orbital magnetic dipoles in the quantum electrodynamic calculation of the retarded interaction energy, Mavroyannis and Stephen[201d] found some interesting magnetic dipolar dispersion energies of $O(\alpha^2)$ and $O(\alpha^4)$. One of these,

$$\mathscr{E}_{ab}^{(\text{opt act})} = -\frac{\alpha^2}{3R^6}\sum_{r,u}\frac{[(\boldsymbol{\mu}_a)_{qr}\cdot(\mathbf{L}_a)_{rq}][(\boldsymbol{\mu}_b)_{q'u}\cdot(\mathbf{L}_b)_{uq'}]}{(a_r - a_q) + (b_u - b_{q'})} \tag{136}$$

is nonzero only for molecules without centers of inversion (optically

active molecules) and, since it becomes relatively more important as the molecule becomes larger, it may be of interest in biological problems. Equation (136) was obtained on the assumptions that the interacting molecules are rapidly rotating and that $R < \lambda\!\!\!^{-}$. The corresponding energy[201d] for $R > \lambda\!\!\!^{-}$ goes as R^{-9}. Recently Condiff[209] has derived expressions for retarded dispersion energies in the magnetic dipole approximation (including spin dipoles) valid for all values of R.

3. *First-Order Energies*

The general treatment of interactions between atoms in excited (or degenerate ground) states is very complicated due to the original degeneracy in the separated atoms. In these problems, one of the main difficulties is in the construction of the proper zeroth-order wave functions which must be chosen to diagonalize the perturbation Hamiltonian. Often, a simultaneous diagonalization of more than one perturbation is required. As discussed by Kim and Hirschfelder[79] and Chang,[78] this can often lead to convergence difficulties in the resulting $1/R$ expansion of the interaction energy, Eq. (123) (indeed, in some problems, such a $1/R$ expansion may not be feasible[71b]).

For these interactions, which correspond to at least one of the atoms having a nonzero angular momentum, the first-order interaction energies do not vanish, in general. Here, first order denotes energies that are first order in V_e and zeroth order in H_{rel} (terms of the form $\langle\psi_0| V_e |\psi_0\rangle$) or first order in H_{rel} and zeroth order in V_e (terms of the form $\langle\psi_0| H_{\text{rel}} |\psi_0\rangle$). Both of these first-order interaction energies vanish[4,73,210] when summed or averaged over all the original degenerate states of the system, leaving an averaged interaction energy comprised of the electrostatic and relativistic (or magnetic) dispersion energies.

In discussing relativistic or retarded corrections to the first-order electrostatic interaction energies, it is convenient to divide the interactions into two types: those that are *retarded* in the usual retardation zone, $\lambda\!\!\!^{-} < R < 10^3 \lambda\!\!\!^{-}$, and those that are *not retarded* in the usual retardation zone.

a. **Retarded First-Order Interaction Energies.** The resonant interaction energies[82] between two like atoms in *different* energy states are retarded in first order.[195,208,211,212] These interactions are responsible for the transfer[213] of energy between well-separated like atoms or molecules

($R \lesssim 200\ a_0$) and are necessary, for example, in the interpretation of such phenomena as sensitized fluorescence[196,214] in gases, fluorescence of aromatic or dye molecules,[215,216] and in the resonance transfer of energy between impurity atoms in crystals (see also Chapter 4).

As a specific example, let us consider the interaction of two *singlet* atoms, one in an S state and the other in a P state, which was discussed in Section V (the corresponding interaction for *doublet* atoms is more complicated, and is discussed briefly later in this section). It can be shown that the interaction energy through $O(\alpha^2/R^3)$ and $O(1/R^3)$ has the form $\mathscr{E}_{ab} = \langle\psi_0|\, V_3 R^{-3} + H_{LL,1} R^{-1}\, |\psi_0\rangle$, where the proper zeroth-order wave functions have the form of Eqs. (62) with $w = +1$. The resulting Breit-Pauli interaction energies are given by[217]

$$\mathscr{E}_{\substack{u\\g}}(\Sigma) = \mp w\mathscr{E}(\Sigma) \qquad \mathscr{E}_{\substack{u\\g}}(\Pi) = \pm w\mathscr{E}(\Pi) \tag{137}$$

where

$$\mathscr{E}(\Sigma) = |\langle S|\, \mu_z\, |P(0)\rangle|^2 [2R^{-3} + \alpha^2(\Delta\varepsilon)^2 R^{-1} + \cdots] \tag{138}$$

$$\mathscr{E}(\Pi) = |\langle S|\, \mu_z\, |P(0)\rangle|^2 \left[R^{-3} - \frac{1}{2}\alpha^2(\Delta\varepsilon)^2 R^{-1} + \cdots \right] \tag{139}$$

In Eq. (137) the upper sign corresponds to the u state and the lower sign to the g state and in Eqs. (138) and (139) the $\Delta\varepsilon$ is the excitation energy corresponding to the $S \leftrightarrow P$ transition. Here the $O(1/R^3)$ term is the usual electrostatic resonant interaction energy of Eq. (64) and the term varying as $O(\alpha^2/R^3)$ is a relativistic correction arising from the Breit-Pauli approximation.

b. **Comparison with the Exact Retarded Dipole Resonance Energy.** McLone and Power[211] (see also Stephen[208]) obtained an expression for the exact retarded dipole resonance energy, by using quantum electrodynamics in the electrostatic dipole approximation, which is valid for all $R > (r_{ai} + r_{bj})$. The resulting expressions for $\mathscr{E}(\Sigma)$ and $\mathscr{E}(\Pi)$ are given by[217]

$$\mathscr{E}(\Sigma) = \frac{2|\langle S|\, \mu_z\, |P(0)\rangle|^2}{R^3} [\cos(R/\lambda\!\!\!^{-}) + (R/\lambda\!\!\!^{-}) \sin(R/\lambda\!\!\!^{-})] \tag{140}$$

$$\mathscr{E}(\Pi) = \frac{|\langle S|\, \mu_z\, |P(0)\rangle|^2}{R^3} \left[\begin{array}{r} \cos(R/\lambda\!\!\!^{-}) + (R/\lambda\!\!\!^{-}) \sin(R/\lambda\!\!\!^{-}) \\ -(R/\lambda\!\!\!^{-})^2 \cos(R/\lambda\!\!\!^{-}) \end{array} \right] \tag{141}$$

where $\lambda\!\!\!^{-} = (\alpha\Delta\varepsilon)^{-1}$. These exact results can be expanded in powers of

$(R/\lambda\!\!\!^{-})$ and have the form[195,208,211,217]

$$\mathscr{E}(\Sigma) = U_3(\Sigma)R^{-3} + U_1(\Sigma)R^{-1} + U_{-1}(\Sigma)R + \cdots \tag{142}$$

$$\mathscr{E}(\Pi) = U_3(\Pi)R^{-3} + U_1(\Pi)R^{-1} + U_{-1}(\Pi)R + \cdots \tag{143}$$

Through $O(\alpha^2)$ these expansions of the exact result agree precisely with the results of the Breit-Pauli approximation. In Eqs. (142) and (143),

$$U_{-1}(\Sigma) = -\frac{\alpha^4(\Delta\varepsilon)^4}{4}\,|\langle S|\,\mu_z\,|P(0)\rangle|^2 \tag{144}$$

and

$$U_{-1}(\Pi) = +\frac{3\alpha^4(\Delta\varepsilon)^4}{8}\,|\langle S|\,\mu_z\,|P(0)\rangle|^2 \tag{145}$$

are higher-order correction terms that are not obtainable in the Breit-Pauli approximation.

TABLE X

Expansion of the Exact S–P Resonance Interaction Energy. Values of $R/\lambda\!\!\!^{-}$ for the Following Cases. This Table is Taken from Meath, Ref. 217.

X =	1	2	5	10
A. $U_3(\Sigma)R^{-3}$ Differs from the Exact $\mathscr{E}(\Sigma)$ by $X\%$				
$R/\lambda\!\!\!^{-}$ =	0.14	0.20	0.35	0.50
B. $U_3(\Sigma)R^{-3} + U_1(\Sigma)R^{-1}$ Differs from the Exact $\mathscr{E}(\Sigma)$ by $X\%$				
$R/\lambda\!\!\!^{-}$ =	0.56	0.70	0.90	1.05
C. $U_3(\Sigma)R^{-3} + U_1(\Sigma)R^{-1} + U_{-1}(\Sigma)R$ Differs from the Exact $\mathscr{E}(\Sigma)$ by $X\%$				
$R/\lambda\!\!\!^{-}$ =	1.10	1.25	1.50	1.70
D. $U_3(\Pi)R^{-3}$ Differs from the Exact $\mathscr{E}(\Pi)$ by $X\%$				
$R/\lambda\!\!\!^{-}$ =	0.14	0.20	0.32	0.48
E. $U_3(\Pi)R^{-3} + U_1(\Pi)R^{-1}$ Differs from the Exact $\mathscr{E}(\Pi)$ by $X\%$				
$R/\lambda\!\!\!^{-}$ =	0.39	0.45	0.60	0.70
F. $U_3(\Pi)R^{-3} + U_1(\Pi)R^{-1} + U_{-1}(\Pi)R$ Differs from the Exact $\mathscr{E}(\Pi)$ by $X\%$				
$R/\lambda\!\!\!^{-}$ =	0.80	0.90	1.05	1.20

Values of $(R/\lambda\!\!\!^{-})$ which correspond to 1, 2, 5, and 10% error in using the first few terms of Eqs. (142) and (143) are given in Table X. It is clear that the $O(\alpha^2/R^3)$ interaction energy is a very important correction to the electrostatic term, even for $R \sim \lambda\!\!\!^{-}$. For example $U_3(\Sigma)R^{-3}$ is accurate to within 5% for $R < 0.35\lambda\!\!\!^{-}$, whereas $[U_3(\Sigma)R^{-3} + U_1(\Sigma)R^{-1}]$, the Breit-Pauli result, is accurate to 5% for $R < 0.9\lambda\!\!\!^{-}$. Similarly, $U_3(\Pi)R^{-3}$ is accurate to 5% for $R < 0.35\lambda\!\!\!^{-}$, while $[U_3(\Pi)R^{-3} + U_1(\Pi)R^{-}]^1$ is accurate to 5% for $R < 0.6\lambda\!\!\!^{-}$. For the He–He resonant ^1S–^1P interaction, $\lambda\!\!\!^{-} = 175\ a_0$; and for the Π molecular state, the electrostatic interaction energy U_3R^{-3} is in error by 5% at $R \sim 56\ a_0$ and by 2% at $R \sim 35\ a_0$.

It should be emphasized that the expansions for the first-order resonant interaction energies, Eqs. (137)–(139) as well as Eqs. (142) and (143), are valid for both "large $R > \lambda\!\!\!^{-}$" and "small $R < \lambda\!\!\!^{-}$." This is quite different from the case of the dispersion energy, where completely different expansions are needed for $R < \lambda\!\!\!^{-}$ and $R > \lambda\!\!\!^{-}$ [see Eqs. (131) and (132), respectively]. The accuracy of the expansion for the first-order resonant energy for large R can be *improved*, however, by including more terms in the series for $\mathscr{E}(\Sigma)$ and $\mathscr{E}(\Pi)$. For example $[U_3(\Sigma)R^{-3} + U_1(\Sigma)R^{-1} + U_{-1}(\Sigma)R]$ is accurate to 5% for $R < 1.5\lambda\!\!\!^{-}$ while the corresponding two term expansion is accurate to 5% for $R < 0.9\lambda\!\!\!^{-}$.

For the interaction of ^1S and ^1P like atoms, $J_a = L_a$ and $J_b = L_b$ (since atomic spin is zero), and hence (Λ,S) coupling and (J_a,J_b) coupling are equivalent. Thus, for this interaction, the results given by Eqs. (137)–(145) are valid for large, as well as small, values of R. On the other hand, for the interaction of ^2S and ^2P atoms, the coupling schemes are not equivalent and the zeroth-order wave functions of the form of Eqs. (62) are valid only for (Λ,S) coupling. The corresponding interaction energies are given by the above results, with $w = 1$ for the resulting singlet molecular states and $w = -1$ for the triplet states. These energies are strictly valid for values of R such that the interaction energy is less than the fine-structure splittings within the isolated atoms. For larger values of R, the calculation should be performed either in intermediate coupling or in (J_a,J_b) coupling as discussed in Section V-B-5. The (Λ,S) interaction energies are split due to the atomic fine-structure effects.

The resonant interaction of two identical atoms involves an excited atom with a finite lifetime and, hence, the interaction energy has a natural linewidth corresponding to the lifetime of the molecular state

formed in the collision process. Stephen,[208] Hutchinson and Hameka,[218] and Power[219] have calculated the lifetime of the molecular state as a function of R. As pointed out by Dicke[220] the g and u molecular states have markedly different lifetimes for separations $R \lesssim \hat{\lambda}$. For example, in the collisions forming singlet molecular states, the u states have half the lifetime, τ, of the isolated excited atom, while the g states are stabilized [they have a lifetime of order $(\hat{\lambda}^2/R^2)\tau$]. Numerical calculations[217] indicate that at $R = 0.5\hat{\lambda}$, the lifetimes of the $^1\Pi_g$ and $^1\Sigma_g$ states are 20τ and 42τ, respectively; while at $R = 2\hat{\lambda}$, the lifetimes are 1.5τ and 2.8τ, respectively. On the other hand, at larger values of R, the $^1\Sigma_g$ state can have a shorter lifetime than the $^1\Pi_g$ state (as discussed by Hutchinson and Hameka[218]). At very large values of $R \gg \hat{\lambda}$, the lifetimes of both the u and g states are equal to τ, as expected, since the interacting atoms are "well" separated.

c. **Nonretarded First-Order Interaction Energies.** The interactions between two *unlike* atoms in arbitrary degenerate quantum states or the interactions of two *like* atoms in degenerate quantum states of the *same* energy are not retarded[195,221] in the usual electrostatic retardation zone. This is easy to see from Eqs. (140) and (141) since $\hat{\lambda} = (\alpha\Delta\varepsilon)^{-1} = \infty$ for these interactions, leaving an unretarded dipole-interaction energy (a more rigorous proof is given by Gomberoff and Power[195]).

For these interactions,[210] the interaction energy, through $O(1/R^3)$ and $O(\alpha^2/R^3)$, has the form

$$\mathscr{E}_{ab} = C_3 R^{-3} + \alpha^2 W_3 R^{-3} + \cdots \tag{146}$$

where

$$C_3 = \langle \psi_0 | V_3 | \psi_0 \rangle \tag{147}$$

and

$$W_3 = \langle \psi_0 | \Gamma_{LL,3} + \Gamma_{SL,3} + \Gamma_{SS,3} | \psi_0 \rangle \tag{148}$$

Here, $C_3 R^{-3}$ is the permanent[222] electrostatic dipole–dipole interaction energy and $\alpha^2 W_3 R^{-3}$ is the permanent[222] magnetic dipole–dipole interaction energy.[4] For the interactions considered here, the electrostatic coefficients C_3 and C_4 usually vanish from parity considerations[223] (see Sec. V). Hence, the lead term in the expansion of the nonrelativistic interaction energy is often the $O(1/R^5)$ electrostatic quadrupole–quadrupole energy and, therefore, the magnetic dipole energy can be important for sufficiently large R. In this case,

$$\mathcal{E}_{ab} = C_5 R^{-5} + \alpha^2 W_3 R^{-3} + \cdots \tag{149}$$

Chang[78] has calculated $\alpha^2 W_3 R^{-3}$ for the 0_g^+ states of O_2 and Cu_2. He finds that the magnetic interaction energy is 10–20% of the quadrupole–quadrupole interaction energy at $R = 30\ a_0$, and 30–50% at $R = 50\ a_0$. The magnetic effects can be of more importance for interactions where the quadrupole–quadrupole energy vanishes, leaving a nonvanishing magnetic dipole energy together with the London dispersion energy. In this case,

$$\mathcal{E}_{ab} = C_6 R^{-6} + \alpha^2 W_3 R^{-3} + \cdots \tag{150}$$

If either of the total orbital angular momentum quantum numbers for the interacting atoms is zero, then $C_5 = 0$ and (from the selection rules for the magnetic multipole coefficients $\Gamma_{\sigma,3}$) one can determine a number of interactions[210] for which Eq. (150) applies.

Since the permanent multipole (both magnetic and electrostatic) interactions are not retarded in the usual retardation zone, they can sometimes dominate the very long-range interactions between atoms and molecules. However, it should be pointed out that retardation effects can occur in these interactions for $R \gg \lambda\!\!\!^{-}$. For example, in the interaction of two like atoms with fine structure, there is a retardation of the long-range first-order energies for values of $R \sim \lambda\!\!\!^{-}_f$, where $\lambda\!\!\!^{-}_f$ (which is of the order $10^3 \lambda\!\!\!^{-}$) is the reduced wavelength characteristic of the fine-structure energy splittings within the interacting atoms.[224] Also, even if there is no fine structure in the energy levels of the interacting atoms, the hyperfine splitting of the atomic energy levels can retard the interaction for $R \sim \lambda\!\!\!^{-}_{hf}$, where $\lambda\!\!\!^{-}_{hf}$ (which is of the order of $10^6 \lambda\!\!\!^{-}$) is the reduced wavelength characteristic of the hyperfine energy splittings within the interacting atoms.[224]

A more important effect[225] of the hyperfine structure in the interacting atoms is that it can produce a splitting in the potential energy curves calculated using the Breit-Pauli approximation (or quantum electrodynamics) for relatively small values of $R \ll \lambda\!\!\!^{-}_{hf}$. This effect is completely analogous to the transition from (Λ,S) to (J_a,J_b) coupling discussed in Section V-B-5 and applies to all types of interactions (both retarded and nonretarded). It can be important for values of R for which the interaction energy (neglecting nuclear spin effects) is approximately equal to or less than the atomic hyperfine splittings within the interacting atoms (for example, $R \sim 10\,a_0$ for the interaction of two

ground-state hydrogen atoms). For these values of R one must essentially diagonalize the perturbation Hamiltonian

$$(H' - H_0) = V_e + H_{\text{rel}} + H_{hf}(a) + H_{hf}(b) \tag{151}$$

where $H_{hf}(a)$ is the hyperfine Hamiltonian for atom a which couples the nuclear spin with the electronic angular momenta of the atom.

d. **Example: The Interaction of Two Hydrogen Atoms.** The interaction of two hydrogen atoms in their ground states, which was discussed in the introduction to this chapter, provides an excellent example of the energy splittings due to both the (electron spin)–(electron spin) and the hyperfine structural (electron spin)–(nuclear spin) interactions. The hyperfine splitting constant for hydrogen is[179,182,227] $A = 0.047384$ cm^{-1} so that $\lambda\!\!\!^{-}_{hf} = (2\pi A)^{-1} = 3.359$ cm. Let us associate electron 1 with atom a and electron 2 with atom b. The spins of the nuclei are $\mathbf{I}_a$ and $\mathbf{I}_b$. As usual, we take the z axis to point from a toward b. Then, the effective Hamiltonian for the spin states of the electrons and protons can be written in the form,[225]

$$H_{\text{eff}} = E(\text{coul}) - \left[\frac{1}{2} + 2\mathbf{s}_1 \cdot \mathbf{s}_2\right] E(\text{exch})$$

$$+ [\mathbf{s}_1 \cdot \mathbf{s}_2 - 3s_{z1}s_{z2}](\alpha^2/R^3) + A[\mathbf{s}_1 \cdot \mathbf{I}_a + \mathbf{s}_2 \cdot \mathbf{I}_b] \tag{152}$$

The spin space of the electrons and protons is spanned by 16 functions of the form $|m_{s1},m_{Ia};m_{s2},m_{Ib}\rangle = \phi_i$. The actual spin functions χ_j corresponding to stationary states of the molecular system (in the Born-Oppenheimer approximation) are linear combinations of the ϕ_i, that is, $\chi_j = \sum_i c_{ji}\phi_i$. The χ_j are eigenfunctions of H_{eff} and the energies of these spin states are the corresponding eigenvalues of H_{eff}.

Thus, at separations less than $R = 9\ a_0$, Harriman, Twerdochlib, Milleur, and Hirschfelder[225] (see also ref. 183d) found that the hyperfine structure term in H_{eff} is unimportant and four of the spin eigenfunctions, ${}^1a, \ldots, {}^1d$, correspond to the ${}^1\Sigma_g^+$ symmetry and have $W_3 = 0$. Eight of the spin functions, ${}^3a, \ldots, {}^3h$, correspond to the ${}^3\Sigma_u^+$ symmetry with $M_s = \pm 1$ and have $W_3 = -\frac{1}{2}$. The remaining four spin functions, ${}^3i, \ldots, {}^3l$, have the ${}^3\Sigma_u^+$ symmetry with $M_s = 0$ and, for them, $W_3 = 1$.

Between $R = 9\ a_0$ where $E(\text{exch}) = 14A$ and $R = 12\,a_0$ where $E(\text{exch}) = \frac{1}{12}A$, all three terms in H_{eff} must be considered. The hyperfine structure term tends to decouple the electron spins and neither the

TABLE XI

Hyperfine Structural States for the Interaction of Two Ground-State Hydrogen Atoms (The Fraction of Triplet Character of a State is Given by $\langle \mathcal{S}^2 \rangle/2$. In this Table $y = A^{-1}\alpha^2 R^{-3}$) This Table is Taken from Harriman, Twerdochlib, Milleur, and Hirschfelder.[225]

State	$\mathcal{E}_{ab}$, cm^{-1} (including coulombic and exchange)				For $R > 12\,a_0$		
	$R/a_0 = 9$	10	11	12	W_0	W_3	$\langle \mathcal{S}^2 \rangle/2$
^1a	−4.092	−1.860	−0.935	−0.622	−3/2	0	3/4
$^1b,^1c$	−4.091	−1.854	−0.902	−0.578	−1/2	−1/4	$(2+y)/4$
^1d	−4.091	−1.853	−0.899	−0.574	−1/2	+1/2	$(1-y)/2$
^3a	−2.789	−1.646	−0.878	−0.577	−1/2	−1/2	1
$^3b,^3c$	−2.780	−1.639	−0.872	−0.572	−1/2	+1/4	1
$^3d,^3e$	−2.741	−1.599	−0.830	−0.529	+1/2	−1/2	1
$^3f,^3g$	−2.765	−1.620	−0.842	−0.531	+1/2	−1/4	$(2-y)/4$
^3h	−2.805	−1.656	−0.853	−0.531	+1/2	$+(1-3^{1/2})/4$	$[20-3y-(4+y)3^{1/2}]/32$
$^3i,^3j$	−2.727	−1.588	−0.823	−0.524	+1/2	+1/4	1
^3k	−2.741	−1.603	−0.831	−0.525	+1/2	+1/2	$(1+y)/2$
^3l	−2.724	−1.586	−0.821	−0.522	+1/2	$+(1+3^{1/2})/4$	$[20-3y+(4+y)3^{1/2}]/32$

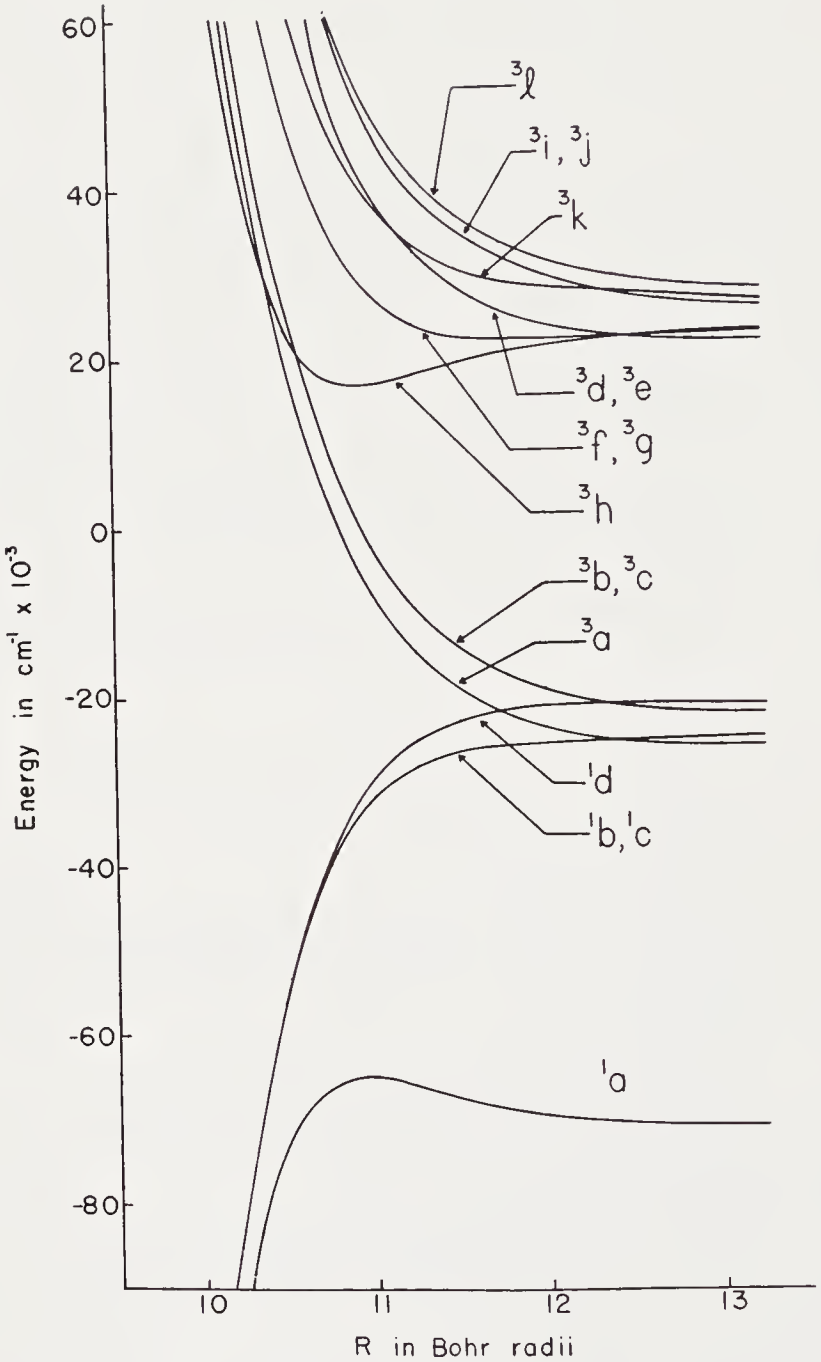

Fig. 9. $\mathscr{E}_{ab} - E(\text{coul})$, the spin dependent part of the energy of the hyperfine states. This figure is taken from Harriman, Twerdochlib, Milleur, and Hirschfelder, ref. 225.

square of the total electron spin, $\mathscr{S}^2$, nor M_s needs to be a good quantum number for a particular state. Figure 9 shows $\mathscr{E}_{ab} - E(\text{coul})$, the spin-dependent part of the energy of the hyperfine states. The total energy $\mathscr{E}_{ab}$ (including the coulombic and exchange) for these states is given in Table XI. Note that the states ^1b and ^1c, ^3b and ^3c, ^3d and ^3e,

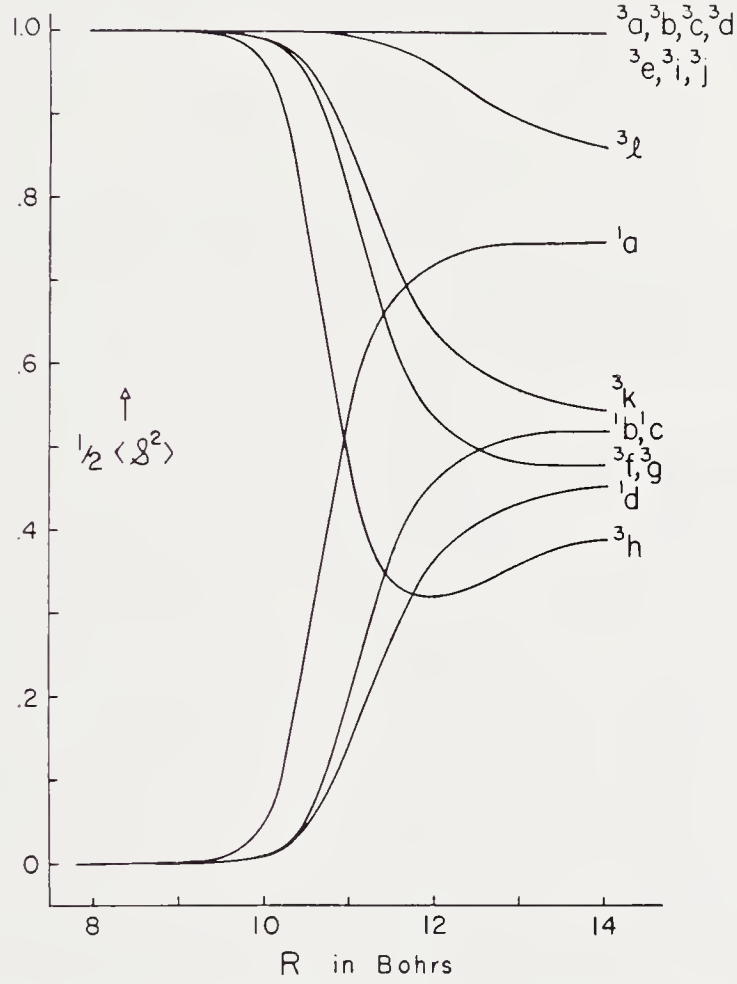

Fig. 10. Fractional triplet character for the hyperfine states as a function of internuclear separations. A pure electronic triplet corresponds to $(\frac{1}{2})\langle\mathscr{S}^2\rangle = 1$ and a pure singlet corresponds to $(\frac{1}{2})\langle\mathscr{S}^2\rangle = 0$. This figure is taken from Harriman, Twerdochlib, Milleur, and Hirschfelder, ref. 225.

^3f and ^3g, and ^3i and ^3j are doubly degenerate, so that there are 11 potential energy curves. Figure 10 shows how the electronic spin of the hyperfine states varies with R. For *all* separations, seven states

(^3a,^3b,^3c,^3d,^3e,^3i, and ^3j) remain *electronic triplets*. The remaining states, four of which are electronic singlets at small separations and five of which are electronic triplets at small separations, become mixed electronic spin states at separation greater than 9 a_0.

For values of R greater than 12 a_0, the exchange energy is so small relative to the hyperfine splitting constant A that it can be neglected. The energy of the hyperfine structural states is then given by

$$\mathscr{E}_{ab} = E(\text{coul}) \begin{matrix} \cdots\cdots\cdots \\ \vdots \\ \cdots\cdots\cdots \end{matrix} + AW_0 \begin{matrix} \cdots\cdots\cdots \\ \vdots \\ \cdots\cdots\cdots \end{matrix} + W_3\alpha^2R^{-3} + \cdots \tag{153}$$

where the constant W_0 and W_3 and given in Table XI. It is questionable whether the term AW_0 should appear in the interaction energy since it corresponds to the hyperfine structural energy of the separated atoms [$-\frac{3}{4}A$ for the hyperfine singlet hydrogen atom and $+\frac{1}{4}A$ for the hyperfine triplet]. However, if AW_0 is subtracted from $\mathscr{E}_{ab}$ in Eq. (153) as *it should be*, then AW_0 should be subtracted from the interaction energy $E_{\text{H-H}}$ at *all* separations. Thus, at separations of $R < 9\,a_0$, there are two $^1\Sigma_g^+$ potential curves separated by an energy of 0.047 cm^{-1}. One potential energy curve corresponds to the ^1a state; the other corresponds to the ^1b,^1c and ^1d states. Similarly for $R < 9\,a_0$, there are two $^3\Sigma_u^+$ potential energy curves separated by an energy of 0.047 cm^{-1}. One potential energy curve corresponds to the ^3a,^3b, and ^3c states; the other corresponds to the remaining nine states ^3d, ..., ^3l. Thus, if the hyperfine structural states are not labeled explicitly, both the $^1\Sigma_g^+$ and the $^3\Sigma_u^+$ potential energy curves, depending on the experiment, would appear to be either double or else to have natural line widths of 0.047 cm^{-1} as the result of hyperfine structural effects. The other effect of the AW_0 is on the *a priori* probability of the various hyperfine structural states occurring in a collision. Note that one hyperfine structural state (^1a) corresponds to the two atoms separating into hyperfine singlets; six states (^1b, ..., ^3c) correspond to one of the separated atoms being a singlet and the other a triplet; and the other nine states (^3d, ..., ^3l) correspond to both atoms being triplets.

Since the spin–spin magnetic dipole energy $\alpha^2W_3R^{-3}$ is not retarded, it does not change its functional form when $R > \lambda\!\!\!^{-}$. Thus, at very large separations, $R > 1800\,a_0 \approx 6\lambda\!\!\!^{-}$, the energy of interaction (not including the hyperfine energies of the separated atoms) has the form[221]

$$\mathscr{E}_{ab} = \alpha^2W_3R^{-3} - 37\alpha^{-1}R^{-7} + \cdots \tag{154}$$

Except for the state ^1a, for which $W_3 = 0$, the spin–spin interaction energy becomes equal to the dispersion energy at a separation between $50\,a_0$ and $100\,a_0$. Thus, for larger separations the spin–spin interaction energy is dominant.

The practical importance of this hyperfine interaction is in connection with *spin exchange scattering.*[183] This affects the intensity of the 21-cm line in radio astronomy, the line broadening of the hyperfine structure of atomic hydrogen, the optical pumping in a hydrogen maser, and the polarization in electron spin resonance. The same sort of hyperfine splittings occur in the interactions of other atoms. Indeed there has been considerable interest in the polarization of the spin-exchange scattering of alkali atoms.

Since the exchange energy decreases exponentially with the separation (decreasing by a factor of ten when the separation is increased between one and two a_0), it seems reasonable to expect that, for *most* atomic interactions, the hyperfine effect will start to uncouple the electron spin states at separations less than $20\,a_0$.

At small separations, $R < 9\,a_0$, the four electronic singlet states are further classified by the nuclear spin quantum number I. The state ^1a with $I = 0$ is called *para hydrogen*; the states ^1b,^1c, and ^1d with $I = 1$ are called *ortho hydrogen.* At larger separations, I is no longer a good quantum number and for these states the fractional triplet (or ortho) character $(\frac{1}{2})\langle I^2 \rangle$ varies with the separation.

The rotational quantum numbers of the hyperfine states,[225] however, remain invariant with separation. This can be seen in the following way: At small separations, there are six hyperfine states which (according to the Pauli exclusion principle) must have *odd* rotational quantum numbers. These are the states ^1b,^1c, and ^1d with $S = 0$ and $I = 1$ and the states ^3f,^3g, and ^3k with $S = 1$ and $I = 0$. The other ten hyperfine states have *even* rotational quantum numbers. These restrictions are a consequence of the fact that the wave function describing the "electronic" spatial motion is symmetric or antisymmetric (for electronic singlet or triplet states, respectively) on the interchange of the *nuclei* as well as of the electrons. Note that the spin functions for the states with *even* rotational quantum numbers are symmetric with respect to the interchange of the two atoms and the other states are antisymmetric. Since H_{eff} is symmetric with respect to the interchange of the two atoms, there is no coupling between the symmetric and antisymmetric spin functions. Thus, for example, at large separations

the wave function for the ^1b state contains a linear combination of the six antisymmetric spin functions and requires an odd rotational quantum number. The classification of *ortho* and *para* hydrogen therefore remains meaningful only if it is based upon the rotational quantum number rather than the nuclear spin quantum number.

Acknowledgments

This chapter was the logical outgrowth of a series of lectures which one of the authors (J.O.H.) presented in 1965 at a symposium on molecular biophysics.[226] This author's interest in intermolecular forces was further stimulated by a *Study Week of the Pontifical Academy* in 1966 which was arranged by Peter Debye. The authors wish to express their gratitude to R. B. Bernstein, M. A. Eliason, S. T. Epstein, J. E. Harriman, R. T. Pack, and E. A. Power for many helpful discussions during the course of this work. We are also grateful to Mrs. E. S. Hirschfelder for her careful proofreading of the manuscript and to Mrs. G. Lawton for her preparation of the manuscript.

References

1. J. O. Hirschfelder, C. F. Curtiss, and R. B. Bird, *Molecular Theory of Gases and Liquids*, Wiley, New York, 1964.
2. H. Margenau and N. Kestner, *Theory of Intermolecular Forces*, Pergamon Press, London, 1967.
3. *Intermolecular Forces*, Discussions Faraday Soc., No. 40 (1965).
4. H. Margenau, "Van der Waals Forces", *Rev. Mod. Phys.*, **11**, 1 (1939).
5. See for example: (a) R. S. Mulliken, *Rev. Mod. Phys.*, **3**, 89 (1931); (b) R. S. Mulliken, *Phys. Rev.*, **57**, 500 (1940); (c) R. S. Mulliken, *Phys. Rev.*, **120**, 1674 (1960).
6. G. Herzberg, *Electronic Spectra of Polyatomic Molecules*, Van Nostrand, New York, 1966, Chap. 4.
7. M. Born and J. R. Oppenheimer, *Ann. Phys.* (*Germany*), **84**, 457 (1927).
8. M. Born and K. Huang, *Dynamical Theory of Crystal Lattices*, Oxford University Press, London, 1954, pp. 166 and 402.
9. M. Born, *Nachr. Akad. Wiss. Göttingen*, **1951**, p. 1.
10. C. A. Coulson and K. Zalewski, *Proc. Roy. Soc.* (*London*), **A268**, 437 (1962).
11. In this chapter, unless otherwise specified, all quantities are expressed in atomic units; length in units of the Bohr radii $a_0 = 0.529172$ Å; energy in units of $e^2/a_0 = 219474.62$ cm^{-1}; mass in units of the electronic mass.
12. A. Fröman, *J. Chem. Phys.*, **36**, 1490 (1962).
13. D. W. Jepsen and J. O. Hirschfelder, *J. Chem. Phys.*, **32**, 1323 (1960).
14. A. Dalgarno and R. McCarroll, *Proc. Roy. Soc.* (*London*), **A237**, 383 (1956); **A239**, 413 (1957).
15. W. Kolos and L. Wolniewicz, *Rev. Mod. Phys.*, **35**, 473 (1963).
16. R. T. Pack, Ph.D. Dissertation, University of Wisconsin Theoretical Chemistry Institute Report, No. WIS-TCI-197, 1966.
17. J. O. Hirschfelder and J. S. Dahler, *Proc. Nat. Acad. Sci. U.S.*, **42**, 363 (1956).

18. D. W. Jepsen and J. O. Hirschfelder, *J. Chem. Phys.*, **30**, 1032 (1959).
19. D. W. Jepsen and J. O. Hirschfelder, *Proc. Nat. Acad. Sci. U.S.*, **45**, 249 (1959).
20. H. Eyring and M. Polanyi, *Z. Phys. Chem.* (*Germany*), **B12**, 279 (1931). The kinematics in this paper was carried out by E. Wigner. Unfortunately, these authors took the angle between the relative nuclear coordinates to be 120° instead of 60° for a collision of three atoms of equal mass moving in a line.
21. W. Kolos and L. Wolniewicz, *J. Chem. Phys.*, **41**, 3663 (1964).
22. W. Kolos and L. Wolniewicz, *J. Chem. Phys.*, **41**, 3674 (1964).
23. W. Kolos and L. Wolniewicz, *J. Chem. Phys.*, **45**, 509 (1966).
24. L. Wolniewicz, *J. Chem. Phys.*, **45**, 515 (1966).
25. W. Kolos and L. Wolniewicz, *J. Chem. Phys.*, **45**, 944 (1966).
26. (a) G. Hunter, *J. Chem. Phys.*, **45**, 3022 (1966); (b) T. G. Waech and R. B. Bernstein, *J. Chem. Phys.*, **46**, 4905 (1967); (c) G. Hunter and H. O. Pritchard, *J. Chem. Phys.*, **46**, 2146 and 2153 (1967).
27. S. T. Epstein, *J. Chem. Phys.*, **44**, 836, 4062 (1966).
28. V. F. Brattsev, *Dokl. Akad. Nauk SSSR*, **160**, 570 (1965).
29. See for example: (a) J. K. Cashion, *J. Chem. Phys.*, **45**, 1037 (1966); (b) J. D. Poll and G. Karl, *Can. J. Phys.*, **44**, 1467 (1966).
30. J. H. Van Vleck, *J. Chem. Phys.*, **4**, 327 (1936).
31. This is one of the principles enunciated by P. Ehrenfest in the early 1920's which served as a guide to N. Bohr and others in the development of modern quantum mechanics.
32. See for example: (a) M. Kasha, *Chem. Rev.*, **41**, 401 (1947); (b) D. S. McClure, *J. Chem. Phys.*, **17**, 665 (1949); (c) M. Mizushima and S. Koide, *J. Chem. Phys.*, **20**, 765 (1952); (d) H. F. Hameka and L. J. Oosterhoff, *Mol. Phys.*, **1**, 358 (1958); (e) M. Mizushima, *Phys. Rev.*, **134**, A883 (1964).
33. D. R. Bates, *Proc. Roy. Soc.* (*London*), **A257**, 22 (1960).
34. C. Zener, *Proc. Roy. Soc.* (*London*), **A137**, 696 (1932); L. Landau, *Soviet Phys. JETP Engl. Translation*, **1**, 89 (1932) and *Z. Phys. Sowj.*, **2**, 46 (1932); E. G. C. Stueckelberg, *Helv. Phys. Acta*, **5**, 369 (1932).
35. H. C. Longuet-Higgins, *Advances in Spectroscopy*, Vol. 2., Interscience, New York, 1961, p. 429.
36. See for example: (a) G. Herzberg, *Spectra of Diatomic Molecules*, Van Nostrand, New York, 1950, Chap. 5; (b) G. Herzberg, *Electronic Spectra of Polyatomic Molecules*, Van Nostrand, New York, 1966; (c) H. A. Kramers, *Z. Physik.*, **53**, 422 (1929); (d) P. R. Fontana, *Phys. Rev.*, **125**, 220 (1962).
37. (a) W. Kolos, C. C. J. Roothaan, and R. A. Sack, *Rev. Mod. Phys.*, **32**, 178 (1960); (b) H. Diehl, S. Flügge, U. Schröder, A. Völkel, and A. Weiguny, *Z. Physik.*, **162**, 1 (1961); (c) A. Fröman and J. L. Kinsey, *Phys. Rev.*, **123**, 2077 (1961).
38. J. O. Hirschfelder and E. Wigner, *Proc. Nat. Acad. Sci. U.S.*, **21**, 113 (1935).
39. C. F. Curtiss, J. O. Hirschfelder, and F. T. Adler, *J. Chem. Phys.*, **18**, 1638 (1950).
40. C. F. Curtiss, *J. Chem. Phys.*, **21**, 1199 (1953).
41. H. T. Wood and C. F. Curtiss, *J. Chem. Phys.*, **41**, 1167 (1964).
42. J. O. Hirschfelder, *Colloq. Intern. Centre Natl. Recherche Sci.* (*Paris*), No. 77, 557–568 (1959).

43. D. E. Stogryn and J. O. Hirschfelder, *J. Chem. Phys.*, **31**, 1531 and 1545 (1959).
44. S. K. Kim and J. Ross, *J. Chem. Phys.*, **42**, 263 (1965).
45. R. B. Bernstein, *Phys. Rev. Letters*, **16**, 385 (1966).
46. For some interactions, $V(R)$ itself may have a hump or $V(R)$ may vary exponentially in the vicinity of the maximum in V_{eff}. In either case, Eq. (27) would not apply.
47. J. C. Slater and J. G. Kirkwood, *Phys. Rev.*, **37**, 682 (1931); J. G. Kirkwood, *Physik. Z.*, **33**, 57 (1932).
48. The nomenclature of the various states of diatomic molecules is quite confusing. It is explained in ref. 36a, pages 245 and 501.
49. W. Kolos and L. Wolniewicz, *J. Chem. Phys.*, **43**, 2429 (1965).
50. G. Herzberg and A. Monfils, *J. Molecular Spectry.*, **5**, 482 (1960).
51. T. Namioka, *J. Chem. Phys.*, **40**, 3154 (1964).
52. E. R. Davidson, *J. Chem. Phys.*, **33**, 1577 (1960).
53. E. R. Davidson, *J. Chem. Phys.*, **35**, 1189 (1961).
54. J. Gerhauser and H. S. Taylor, *J. Chem. Phys.*, **42**, 3621 (1965).
55. W. Kolos and C. C. J. Roothaan, *Rev. Mod. Phys.*, **32**, 219 (1960).
56. M. P. Barnett and C. A. Coulson, *Phil. Trans. Roy. Soc.* (*London*), **A243**, 221 (1951).
57. M. P. Barnett, *Methods of Computational Physics*, Vol. 2, Academic Press, New York, 1963, p. 95.
58. P. O. Löwdin, *Adv. Phys.*, **5**, No. 17, 103 (1956).
59. I. Shavitt and M. Karplus, *J. Chem. Phys.*, **43**, 398 (1965).
60. C. W. Kern and M. Karplus, *J. Chem. Phys.*, **43**, 415 (1965).
61. J. M. Foster and S. F. Boys, *Rev. Mod. Phys.*, **32**, 303 and 305 (1960).
62. R. Kikuchi, *J. Chem. Phys.*, **22**, 148 (1954).
63. S. F. Boys, *Proc. Roy. Soc.* (*London*), **A200**, 542 (1950.
64. See also for example: (a) K. Singer, *Proc. Roy. Soc.* (*London*), **A258**, 412 (1960); J. V. L. Longstaff and K. Singer, *Proc. Roy. Soc.* (*London*), **A258**, 421 (1960); (b) M. Krauss, *J. Chem. Phys.*, **34**, 692 (1961); **38**, 564 (1963); (c) H. Preuss, *Mol. Phys.*, **8**, 157 (1964).
65. (a) E. Clementi and D. R. Davis, *J. Comput. Phys.*, **1**, 223 (1967); (b) A. Veillard and E. Clementi, *Theor. Chim. Acta*, **7**, 133 (1967).
66. J. O. Hirschfelder and P. O. Löwdin, *Mol. Phys.*, **2**, 229 (1959); 9, 491 (1965).
67. W. Kolos, *Int. J. Quantum Chem.*, **1**, 169 (1967).
68. S. Fraga and B. J. Ransil, *J. Chem. Phys.*, **35**, 669 (1961).
69. G. Das and A. C. Wahl, *J. Chem. Phys.*, **44**, 87 (1966).
70. (a) J. N. Murrell, M. Randić and D. R. Williams, *Proc. Roy. Soc.* (*London*), **A284**, 566 (1965); (b) J. N. Murrell and G. Shaw, *J. Chem. Phys.*, **46**, 1768 (1967).
71. See, for example, the review articles: (a) A. Dalgarno, in *Quantum Theory*, Vol. 1, D. R. Bates, Ed., Academic Press, New York, 1961, Chap. 5; (b) J. O. Hirschfelder, W. Byers Brown, and S. T. Epstein, in *Advances in Quantum Chemistry*, P. O. Löwdin, Ed., Academic Press, New York, 1964, p. 255.
72. (a) W. J. Meath and J. O. Hirschfelder, *J. Chem. Phys.*, **44**, 3197 (1966); (b) W. J. Meath and J. O. Hirschfelder, *J. Chem. Phys.*, **44**, 3210 (1966).
73. J. S. Dahler and J. O. Hirschfelder, *J. Chem. Phys.*, **25**, 986 (1956).

74. F. O. Ellison, *J. Chem. Phys.*, **34**, 2100 (1961).
75. H. Laue, *Bull. Am. Phys. Soc.*, **12**, 478 (1967).
76. (a) Reference 1, p. 839–846; (b) R. J. Buehler and J. O. Hirschfelder, *Phys. Rev.*, **83**, 628 (1951); **85**, 149 (1952); (c) B. C. Carlson and G. S. Rushbrooke, *Proc. Cambridge Phil. Soc.*, **46**, 626 (1950); (d) M. E. Rose, *J. Math. Phys.*, **37**, 215 (1958).
77. (a) P. R. Fontana, *Phys. Rev.*, **123**, 1865 (1961); (b) P. R. Fontana, *Phys. Rev.*, **123**, 1871 (1961); (c) P. R. Fontana, *Phys. Rev.*, **125**, 1597 (1962).
78. T. Y. Chang, Ph.D. Dissertation, University of Wisconsin (1966); *Rev. Mod. Phys.*, Oct. (1967).
79. H. J. Kim and J. O. Hirschfelder, *J. Chem. Phys.*, **46**, 4553 (1967).
80. (a) A. Dalgarno and J. T. Lewis, *Proc. Phys. Soc.* (*London*), **A69**, 57 (1956); (b) L. C. Cusachs, *Phys. Rev.*, **125**, 561 (1962).
81. J. K. Knipp, *Phys. Rev.*, **53**, 734 (1938).
82. This is the usual definition of resonant interactions used when discussing retardation effects. See for example, Chapter IV and Refs. 195, 206–8, and 221.
83. E. Wigner and E. E. Witmer, *Z. Physik.*, **51**, 859 (1928).
84. C. W. King and J. H. Van Vleck, *Phys. Rev.*, **55**, 1165 (1939). The results for the triplet interaction energies given in this paper have the wrong sign. [Mulliken, ref. 5c.]
85. See for example: ref. 36a, p. 380, and refs. 5c and 84.
86. H. G. Kuhn and J. M. Vaughan, *Proc. Roy. Soc.* (*London*), **A277**, 297 (1964).
87. See for example the excellent discussions of refs. 5a; 5b; 36a, pp. 315–322; 77c; 78; and 81.
88. See for example E. U. Condon and G. H. Shortley, *The Theory of Atomic Spectra*, Cambridge University Press, 1963, Chaps. 7 and 8.
89. H. Falkenhagen, *Physik. Z.*, **23**, 87 (1922).
90. P. Debye, *Physik. Z.*, **21**, 178 (1920).
91. F. London, *Z. Phys. Chem.* (*Germany*), **B11**, 222 (1930); *Trans. Faraday Soc.* **33**, 8 (1937).
92. F. Berencz, *Acta Phys. Acad. Sci. Hungary*, **20**, 1 (1960).
93. J. F. Hornig and J. O. Hirschfelder, *J. Chem. Phys.*, **20**, 1812 (1952).
94. H. Margenau, *J. Chem. Phys.*, **6**, 896 (1938).
95. N. R. Kestner, *J. Chem. Phys.*, **45**, 208 (1966).
96. N. R. Kestner and O. Sinanoğlu, *J. Chem. Phys.*, **45**, 194 (1966).
97. W. D. Davison, *Proc. Phys. Soc.* (*London*), **87**, 133 (1966).
98. W. J. Deal, Jr. and N. R. Kestner, *J. Chem. Phys.*, **45**, 4014 (1966).
99. N. R. Kestner, *J. Chem. Phys.*, **45**, 3121 (1966).
100. D. E. Stogryn and A. P. Stogryn, *Mol. Phys.*, **11**, 371 (1966), give an excellent review and a summary of everything which is currently known about molecular multipole moments.
101. W D. Lyon, R. L. Matcha, W. A. Sanders, W. J. Meath, and J. O. Hirschfelder, *J. Chem. Phys.*, **43**, 1095 (1965).
102. R. L. Matcha, W. D. Lyon, and J. O. Hirschfelder, *J. Chem. Phys.*, **43**, 1101 (1965).
103. R. L. Matcha, University of Wisconsin Theoretical Chemistry Institute Report No. WIS-TCI-129, 1965.

104. S. T. Epstein, in *Perturbation Theory and its Applications in Quantum Mechanics*, C. H. Wilcox, Ed., Wiley, New York, 1966, p. 49.
105. S. T. Epstein, *J. Chem. Phys.*, **41**, 1045 (1964); G. C. Ghirardi and A. Rimini, *J. Math. Phys.*, **5**, 722 (1964).
106. S. T. Epstein and J. H. Karl, *J. Chem. Phys.*, **44**, 4347 (1966).
107. J. N. Murrell and G. Shaw, *J. Chem. Phys.*, **46**, 1768 (1967).
108. L. Salem, *Discussions Faraday Soc.*, No. 40, 150 (1965).
109. J. I. Musher and L. Salem, *J. Chem. Phys.*, **44**, 2943 (1966).
110. J. O. Hirschfelder and R. Silbey, *J. Chem. Phys.*, **45**, 2188 (1966).
111. L. Brillouin, *J. Phys. Radium*, **3**, (*Sec. 7*), 373 (1932). See also: J. E. Lennard-Jones, *Proc. Roy. Soc.* (*London*), **A129**, 598 (1930); E. P. Wigner, *Math. Naturwiss. Anz. Ungar Akad. Wiss.*, **53**, 475 (1935).
112. P. O. Löwdin, *J. Chem. Phys.*, **19**, 1396 (1951).
113. P. O. Löwdin, in *Perturbation Theory and its Applications in Quantum Mechanics*, C. H. Wilcox, Ed., Wiley, New York, 1966, p. 255.
114. H. Eyring, J. Walter, and G. E. Kimball, *Quantum Chemistry*, Wiley, New York, 1958.
115. H. Margenau, *Phys. Rev.*, **56**, 1000 (1939).
116. A. Dalgarno and N. Lynn, *Proc. Phys. Soc.* (*London*), **A69**, 821 (1956).
117. A. Unsöld, *Z. Physik.*, **43**, 563 (1927).
118. See for example: O. Sinanoğlu, in *Advances in Chemical Physics*, Vol. 6, I. Prigogine, Ed., Interscience, New York, 1964; *J. Chem. Phys.*, **37**, 191 (1962); *J. Phys. Chem.*, **66**, 2283 (1962).
119. (a) R. S. Mulliken, *J. Am. Chem. Soc.*, **72**, 600 (1950); **74**, 811 (1952); *J. Phys. Chem.*, **56**, 801 (1952); (b) J. L. Magee, *J. Phys. Chem.*, **56**, 555 (1952).
120. S. Aono, *Progr. Theoret. Phys.* (*Kyoto*), **20**, 133 (1958); **21**, 217 (1959); **22**, 313 (1959).
121. W. Byers Brown, *Discussions Faraday Soc.*, No. 40, 140 (1965).
122. W. Byers Brown and E. Steiner, *J. Chem. Phys.*, **44**, 3934 (1966).
123. H. Hellmann, *Einfuhrung in die Quantenchemie*, Deuticke, Leipzig, 1937, p. 285.
124. R. P. Feynman, *Phys. Rev.*, **56**, 340 (1939). This was Feynman's senior (undergraduate) thesis under the direction of J. C. Slater at Massachusetts Institute of Technology. He did not know about ref. 123.
125. T. Berlin, *J. Chem. Phys.*, **19**, 208 (1951). See also ref. 1, p. 935.
126. S. T. Epstein and J. O. Hirschfelder, *Phys. Rev.*, **123**, 1495 (1961).
127. C. A. Coulson and A. C. Hurley, *J. Chem. Phys.*, **37**, 448 (1962).
128. P. Phillipson, *J. Chem. Phys.*, **39**, 3010 (1963).
129. A. C. Hurley, in *Molecular Orbitals in Chemistry, Physics and Biology*, P. O. Löwdin and B. Pullman, Eds., Academic Press, New York, 1964, p. 161.
130. M. L. Benston and B. Kirtman, *J. Chem. Phys.*, **44**, 119 (1966).
131. M. L. Benston, *J. Chem. Phys.*, **44**, 1300 (1966).
132. S. T. Epstein, *J. Chem. Phys.*, **42**, 3813 (1965); **46**, 571 (1967).
133. R. Yaris, *J. Chem. Phys.*, **39**, 863 (1963).
134. See also ref. 71.
135. L. Salem and E. B. Wilson, Jr., *J. Chem. Phys.*, **36**, 3421 (1962).
136. A. C. Hurley, *Proc. Roy. Soc.* (*London*), **A226**, 170 and 179 (1954).

137. A. C. Hurley, *J. Chem. Phys.*, **37**, 449 (1962).
138. G. G. Hall, *Phil. Mag.* (*London*), **6** (Series 8), 249 and 256 (1961).
139. R. F. W. Bader, *Can. J. Chem.*, **41**, 2303 (1963).
140. A. A. Frost, University of Wisconsin Theoretical Chemistry Institute Rept. No. WIS-TCI-204, 1966.
141. J. O. Hirschfelder and J. W. Linnett, *J. Chem. Phys.*, **18**, 130 (1950).
142. H. R. Hassé, *Proc. Cambridge Phil. Soc.*, **27**, 66 (1931).
143. J. O. Hirschfelder and M. A. Eliason, *J. Chem. Phys.*, **47**, 1164 (1967).
144. J. O. Hirschfelder and C. A. Coulson, *J. Chem. Phys.*, **36**, 941 (1962).
145. J. C. Slater, *J. Chem. Phys.*, **1**, 687 (1933); V. Fock, *Z. Physik.*, **63**, 855 (1930).
146. J. O. Hirschfelder, *J. Chem. Phys.*, **33**, 1462 (1960).
147. T. L. Cottrell and S. Paterson, *Trans. Faraday Soc.*, **47**, 233 (1951).
148. J. O. Hirschfelder and J. F. Kincaid, *Phys. Rev.*, **52**, 658 (1937).
149. P. O. Löwdin, *J. Mol. Spectry.*, **3**, 46 (1959).
150. W. J. Meath and J. O. Hirschfelder, *J. Chem. Phys.*, **39**, 1135 (1963); **39**, 3534 (1963).
151. H. J. Kim and R. G. Parr, *J. Chem. Phys.*, **41**, 2892 (1964).
152. R. E. Wyatt and R. G. Parr, *J. Chem. Phys.*, **43**, S217 (1965); **44**, 1529 (1966).
153. S. T. Epstein, A. C. Hurley, R. E. Wyatt, and R. G. Parr, *J. Chem. Phys.*, **47**, Aug. (1967).
154. If a molecule a possesses a permanent dipole moment, $\mu(a)$, in a direction θ_a with respect to **R**, this dipole can induce a dipole moment in molecule b. The corresponding dipole-induced dipole interaction energy[89] is $E(\text{ind}) = -\mu(a)^2\alpha_b(3\cos^2\theta_a + 1)/2R^6$, where α_b is the polarizability of molecule b. Eq. (99) is analogous to this result; $\alpha_b \rightarrow \alpha_b'$ and $\mu(a) \rightarrow \mu(a;\text{inst})$.
155. For a calculation of the He–He interaction using a Hirschfelder-Linnett type function, see N. Moore, *J. Chem. Phys.* **33**, 471 (1960).
156. P. O. Löwdin, *Rev. Mod. Phys.*, **34**, 80 (1962).
157. See also for example: P. A. M. Dirac, *Quantum Mechanics*, Oxford University Press, London, 1935; J. H. Van Vleck, *The Theory of Electric and Magnetic Susceptibilities*, Oxford University Press, London, 1932.
158. Y. M. Chan and A. Dalgarno, *Mol. Phys.*, **9**, 349 (1965).
159. R. J. Bell, *Proc. Phys. Soc.* (*London*), **86**, 239 (1965).
160. R. J. Bell, *Proc. Phys. Soc.* (*London*), **87**, 594 (1966).
161. M. H. Alexander and L. Salem, *J. Chem. Phys.*, **46**, 430 (1967).
162. L. P. Gor'kov and L. P. Pitaevskii, *Dokl. Akad. Nauk SSSR*, **151**, 822 (1963).
163. W. Heitler and F. London, *Z. Physik.*, **44**, 455 (1927).
164. W. A. Bingel, H. Preuss, and H. H. Schmidtke, *Z. Naturforsch.*, **16a**, 434 (1961).
165. (a) C. Herring, in *Magnetism*, Vol. 2-B, G. T. Rado and H. Suhl, Eds., Academic Press, New York, 1966. This is a very complete survey of the exchange between well-separated atoms; (b) C. Herring, *Rev. Mod. Phys.*, **34**, 631 (1962), a less recent review of exchange energy; (c) C. Herring and M. Flicker, *Phys. Rev.*, **134**, A362 (1964), exchange energy between two hydrogen atoms.
166. W. J. Carr, Jr., and M. Ashkin, *J. Chem. Phys.*, **42**, 2796 (1965).
167. (a) R. K. Nesbet, *Phys. Rev.*, **122**, 1497 (1961); (b) R. K. Nesbet, "Electronic Correlations in Atoms and Molecules," *Advances in Chemical Physics*, Vol. 9, I. Prigogine, Ed. Interscience, New York, 1965, p. 321.

168. (a) A. C. Wahl, Argonne National Laboratory, Report No. 7076 (1966). Here the molecular orbitals are shown for the homonuclear diatomic molecules in the first row of the periodic table. The orbital for H_2 is given as a function of R. (b) A. C. Wahl, *Science*, **151**, 961 (1966). (c) A. C. Wahl, *Quantum Theory of Atoms, Molecules, and the Solid State* (*Tribute to Slater*), P. O. Löwdin, Ed., Academic Press, New York, 1966, p. 243. (d) J. O. Hirschfelder, *ibid.*, p. 217.
169. C. A. Coulson and I. Fischer, *Phil. Mag.*, **40**, 386 (1949).
170. E. R. Davidson and L. L. Jones, *J. Chem. Phys.*, **37**, 1918 (1962).
171. L. Pauling and E. B. Wilson, *Introduction to Quantum Mechanics*, McGraw-Hill, New York, 1935, p. 223.
172. R. A. Buckingham and D. M. Duparc, American Society of Mechanical Engineers Symposium, *Thermophysical Properties*, Academic Press, New York, 1962, p. 378.
173. R. V. Miller and R. D. Present, *J. Chem. Phys.*, **38**, 1179 (1963).
174. For a review on the He–He interaction up to 1958, see S. Huzinaga, *Progr. Theoret. Phys.* (*Kyoto*), **18**, 139 (1957).
175. P. E. Phillipson, *Phys. Rev.*, **125**, 1981 (1962).
176. See also the discussion of H. S. Taylor and F. E. Harris, *Mol. Phys.*, **7**, 287 (1964).
177. C. Moser, private communication, 1966.
178. The starting point for this Hamiltonian is the Breit Hamiltonian: G. Breit, *Phys. Rev.*, **34**, 553 (1929); **36**, 383 (1930); **39**, 616 (1932).
179. H. A. Bethe and E. E. Salpeter, *Quantum Mechanics of One- and Two-Electron Atoms*, Academic Press, New York, 1957.
180. For a derivation based on classical considerations, see J. C. Slater, *Quantum Theory of Atomic Structure*, Vol 2, McGraw-Hill, New York, 1960.
181. T. Itoh, *Rev. Mod. Phys.*, **37**, 159 (1965).
182. See for example: (a) the review article by G. G. Hall and A. T. Amos, "Molecular Orbital Theory of the Spin Properties of Conjugated Molecules," in *Advances in Atomic and Molecular Physics*, D. R. Bates and I. Estermann, Eds., Academic Press, New York, 1965, Vol. 1, p. 2; (b) C. P. Slichter, *Principles of Magnetic Resonance*, Harper and Row, New York, 1963; (c) R. McWeeny, *J. Chem. Phys.*, **42**, 1717 (1965).
183. (a) O. von Roos, *Phys. Rev.*, **115**, 911 (1959); (b) A. Dalgarno, *Proc. Roy. Soc.* (*London*), **A262**, 132 (1961); (c) A. E. Glassgold, *Phys. Rev.*, **132**, 2144 (1963); (d) P. L. Bender, *Phys. Rev.*, **132**, 2154 (1963); (e) R. M. Herman, *Phys. Rev.*, **137**, A1062 (1965); (f) A. Dalgarno and M. R. H. Rudge, *Proc. Roy. Soc.* (*London*), **A286**, 519 (1965).
184. The classical analog of H_{LL} was first obtained by C. G. Darwin, *Phil. Mag.*, **39**, (Series 6) 537 (1920).
185. P. R. Fontana and W. J. Meath, University of Wisconsin, Theoretical Chemistry Institute Report No. WIS-TCI-125, 1965.
186. E. A. Power and S. Zienau, *J. Franklin Inst.*, **264**, 403 (1957).
187. See, for example, (a) E. Clementi, *J. Chem. Phys.*, **38**, 2248 (1963); (b) H. Hartman and E. Clementi, *Phys. Rev.*, **133**, A1295 (1964).
188. K. Y. Kim, *Phys. Rev.*, **140**, A1498 (1965) and references cited therein.

189. See also for example: (a) C. W. Ufford and H. B. Callen, *Phys. Rev.*, **110**, 1352 (1958); (b) R. E. Christoffersen, *J. Chem. Phys.*, **42**, 2616 (1965).
190. J. Ladik, *J. Chem. Phys.*, **42**, 3340 (1965).
191. J. D. Garcia, *Phys. Rev.*, **147**, 66 (1966).
192. H. F. Hameka, *Advanced Quantum Chemistry*, Addison-Wesley, Reading, Massachusetts, 1965.
193. R. E. Christoffersen and G. G. Hall, *Theoret. Chim. Acta*, **4**, 250 (1966).
194. L. C. Chiu, *Phys. Rev.*, **145**, 1 (1966).
195. L. Gomberoff and E. A. Power, *Proc. Roy. Soc.* (*London*), **A295**, 476 (1966).
196. J. S. Avery, *Proc. Phys. Soc.*, **88**, 1 (1966).
197. W. J. Meath, Ph.D. Dissertation, University of Wisconsin, Theoretical Chemistry Institute, Report No. WIS-TCI-75, 1965.
198. E. J. W. Verwey, J. T. G. Overbeck, and K. van Nes, *Theory of Stability of Lyophobic Colloids*, Elsevier, Amsterdam, 1948; see also Ref. 1, p. 967.
199. H. B. G. Casimir and P. Polder, *Phys. Rev.*, **73**, 360 (1948).
200. R. H. Penfield and H. Zatzkis, *J. Franklin Inst.*, **263**, 331 (1957).
201. See for example: (a) I. E. Dzialoshinskii, *Soviet Phys. JETP Engl. Translation*, **3**, 977 (1957); (b) E. A. Power and S. Zienau, *Nuovo Cimento*, **6**, 7 (1957); (c) M. R. Aub, E. A. Power and S. Zienau, *Phil. Mag.*, **2** (Series 8), 571 (1957); (d) C. Mavroyannis and M. J. Stephen, *Mol. Phys.*, **5**, 629 (1962); (e) A. D. McLachlan, *Proc. Roy. Soc.* (*London*), **A271**, 387 (1963); (f) G. Feinberg and J. Sucher, *Phys. Rev.*, **139**, B 1619 (1965).
202. For example, the continuum states account for 18.6% of the dipolar polarizability of the hydrogen atom. See M. Inokuti, Argonne National Laboratory Report No. ANL-6769 (1964).
203. M. Karplus and H. J. Kolker, *J. Chem. Phys.*, **41**, 3955 (1964).
204. R. E. Johnson, S. T. Epstein, and W. J. Meath, *J. Chem. Phys.*, **47**, Aug. (1967).
205. P. R. Fontana and R. B. Bernstein, *J. Chem. Phys.*, **41**, 1431 (1964).
206. R. R. McLone and E. A. Power, *Proc. Roy. Soc.* (*London*), **A286**, 573 (1965).
207. M. R. Philpott, *Proc. Phys. Soc.*, **87**, 619 (1966).
208. M. J. Stephen, *J. Chem. Phys.*, **40**, 669 (1964).
209. D. W. Condiff, University of Wisconsin Theoretical Chemistry Institute Report No. WIS-TCI-155, 1966.
210. W. J. Meath, *J. Chem. Phys.*, **45**, 4519 (1966).
211. R. R. McLone and E. A. Power, *Mathematika*, **11**, 91 (1964).
212. W. T. Simpson, *Radiation Res.*, **20**, 87 (1963).
213. A. D. McLachlan, *Mol. Phys.*, **8**, 409 (1964).
214. T. Förster, *Discussions Faraday Soc.*, No. 27, 7 (1959).
215. T. Förster, *Ann. Phys.* (*Germany*), **2**, 55 (1948); *Naturwiss.*, **33**, 166 (1946).
216. S. Singh, W. J. Jones, W. Siebrand, B. P. Stoicheff, and W. G. Schneider, *J. Chem. Phys.*, **42**, 330 (1965).
217. W. J. Meath, *J. Chem. Phys.*, to be published.
218. D. A. Hutchinson and H. F. Hameka, *J. Chem. Phys.*, **41**, 2006 (1964).
219. E. A. Power, *J. Chem. Phys.*, **46**, 4297 (1967).
220. R. H. Dicke, *Phys. Rev.*, 93, 99 (1954).
221. E. A. Power, W. J. Meath, and J. O. Hirschfelder, *Phys. Rev. Letters*, **17**, 799 (1966).

222. These multipole moments of the atom are not necessarily permanent in the sense of having an infinite lifetime; i.e., excited states of an atom have a finite lifetime. Also, the lifetimes may be affected by the interaction itself.
223. An exception, for example, is the interaction of $2s$ and $2p$ hydrogen atoms.
224. The resulting expression for the retarded interaction energies should be analogous to Eqs. (140) and (141) with λ replaced by λ_f (or λ_{hf}).
225. J. E. Harriman, M. Twerdochlib, M. B. Milleur, and J. O. Hirschfelder, *Proc. Nat. Acad. Sci. U.S.*, **57**, June (1967).
226. J. O. Hirschfelder, *Molecular Biophysics*, B. Pullman and M. Weissbluth, Eds., Academic Press, New York, 1965, p. 325.
227. J. P. Wittke and R. H. Dicke, *Phys. Rev.*, **103**, 620 (1956).
228. M. A. Byrne, W. G. Richards, and J. A. Horsely, *Mol. Phys.*, **12**, 273 (1967).
229. H. Primas, *Modern Quantum Chemistry, Part II*, O. Sinanoğlu, Ed., Academic Press, New York, 1965, p. 45.
230. G. H. Matsumoto, C. F. Bender, and E. R. Davidson, *J. Chem. Phys.*, **46**, 402 (1967).

2. Permanent and Induced Molecular Moments and Long-Range Intermolecular Forces

A. D. BUCKINGHAM

School of Chemistry, The University of Bristol
Bristol, England

CONTENTS

I. Introduction 107
II. A Molecule in a Static Electric Field 108
III. A Molecule in a Periodic Field 115
IV. Interaction of Two Molecules 122
V. Some Particular Molecular Interactions 128
A. A Point Charge and a Linear Molecule 129
B. A Point Charge and a Tetrahedral Molecule 130
C. A Spherical and a Tetrahedral Molecule 131
D. Two Linear Molecules 132
VI. Measurements of Molecular Moments and Polarizabilities 134
VII. Long-Range Dipolar Interactions 138
References 140

I. INTRODUCTION

There is now general agreement that the significant forces between atoms and molecules have an electric origin. It is true that other sources exist, such as magnetic and gravitational interactions, but these can normally be neglected. When the molecules are far apart and the separation is large compared to the dimensions of the molecules, the interaction energy is determined by the permanent electric moments, and their interactions comprise the *electrostatic energy*. The permanent moments produce a field that distorts the electronic structures of neighboring molecules leading to an additional interaction, the *induction energy*. Since the distortions of molecules in their ground electronic states always lower the total energy, the induction energy is associated

with an attractive intermolecular force. Both the electrostatic and induction energies are determined by the properties of the free molecules; also the *dispersion energy* of Fritz London may be approximately related to the polarizabilities describing the distortion of the free molecules by external fields.[1] Therefore, detailed knowledge of molecular charge distributions and polarizabilities is essential for an understanding of intermolecular forces.

In the study of molecular interactions, we are normally concerned with the question: What is the difference between the energy of a group of molecules (preferably a pair, although larger clusters are often of interest) and the energy of separate molecules *for fixed molecular positions and orientations*? This interaction energy is usually small compared to molecular-electronic and vibrational energies, so there is no difficulty in assigning the molecules to particular internal states; the energy is averaged over the nuclear vibrational motion. However, the interaction energy may be much larger than the difference between rotational energy levels; the rotational and translational motions of the interacting molecules can, therefore, be very different from those of the free molecules. The basic problem is the evaluation of the energy as a function of relative molecular position and orientation. When this has been solved, the effects of the interaction can be determined by considering the translational and rotational motion; in some cases this is a formidable task, but often the occupied states have energy separations that are small compared to kT, and a classical treatment suffices.

This chapter is concerned with the interaction energies of simple molecules at distances from one another that are large compared to molecular dimensions (but small compared to the separations at which retardation effects are important). The aim is to describe the dependence of the energy on the separations and orientations of the molecules. The relevant molecular moments and polarizabilities are those for the nonrotating states of the free molecules. New methods of determining these molecular constants are briefly described after the presentation of the theory of the interaction of a molecule with an external field and with another molecule.

II. A MOLECULE IN A STATIC ELECTRIC FIELD

The Hamiltonian describing a molecule in weak interaction with fixed external charges is

$$\mathscr{H} = \mathscr{H}^{(0)} - \mu_\alpha F_\alpha - \frac{1}{3}\Theta_{\alpha\beta}F_{\alpha\beta} - \cdots \tag{1}$$

where $\mathscr{H}^{(0)}$ is that for the free molecule and $\mu_\alpha = \sum_i e_i r_{i_\alpha}$ and $\Theta_{\alpha\beta} = \Theta_{\beta\alpha} = \frac{1}{2}\sum_i e_i(3r_{i_\alpha}r_{i_\beta} - r_i^2\delta_{\alpha\beta})$ are the dipole and quadrupole moment operators; e_i is the ith element of charge at the point $\mathbf{r}_i$ relative to an origin fixed at some point in the molecule. The Greek subscripts α, β denote vector or tensor components and can be equal to x, y, z; a repeated Greek subscript denotes a summation over all three Cartesian components, so that $\frac{1}{3}\Theta_{\alpha\beta}F_{\alpha\beta} = \frac{1}{3}\sum_{\alpha,\beta=x,y,z}\Theta_{\alpha\beta}F_{\alpha\beta}$ = a scalar quantity (the quadrupolar interaction with the field gradient). F_α and $F_{\alpha\beta}$ are the electric field and the field gradient at the origin due to the external charges. If the molecule is in the internal quantum state Ψ, its energy for a fixed position and orientation is

$$\begin{aligned} W &= \langle\Psi|\mathscr{H}|\Psi\rangle \\ &= W^{(0)} - \mu_\alpha^{(0)}F_\alpha - \frac{1}{2}\alpha_{\alpha\beta}F_\alpha F_\beta - \frac{1}{6}\beta_{\alpha\beta\gamma}F_\alpha F_\beta F_\gamma - \frac{1}{24}\gamma_{\alpha\beta\gamma\delta}F_\alpha F_\beta F_\gamma F_\delta \\ &\quad - \frac{1}{3}\Theta_{\alpha\beta}^{(0)}F_{\alpha\beta} - \frac{1}{3}A_{\gamma,\alpha\beta}F_\gamma F_{\alpha\beta} - \frac{1}{6}B_{\alpha\beta,\gamma\delta}F_\alpha F_\beta F_{\gamma\delta} \\ &\quad - \frac{1}{6}C_{\alpha\beta,\gamma\delta}F_{\alpha\beta}F_{\gamma\delta} - \cdots \end{aligned} \tag{2}$$

where $\mu_\alpha^{(0)} = \langle\Psi^{(0)}|\mu_\alpha|\Psi^{(0)}\rangle$ and $\Theta_{\alpha\beta}^{(0)} = \langle\Psi^{(0)}|\Theta_{\alpha\beta}|\Psi^{(0)}\rangle$ are the permanent dipole and quadrupole moments of the molecule, $\Psi^{(0)}$ being the unperturbed wave function (i.e., $\mathscr{H}^{(0)}\Psi^{(0)} = W^{(0)}\Psi^{(0)}$); $\alpha_{\alpha\beta}$, $\beta_{\alpha\beta\gamma}$, $\gamma_{\alpha\beta\gamma\delta}$ and $A_{\alpha,\beta\gamma}$, $B_{\alpha\beta,\gamma\delta}$, $C_{\alpha\beta,\gamma\delta}$ are molecular polarizabilities describing the distortion of the molecule by the external electric field and field gradient. $\boldsymbol{\alpha}$, $\boldsymbol{\beta}$, and $\boldsymbol{\gamma}$ are symmetric in all suffixes, $A_{\alpha,\beta\gamma}$ in $\beta\gamma$, $B_{\alpha\beta,\gamma\delta}$ in $\alpha\beta$ and $\gamma\delta$, and $C_{\alpha\beta,\gamma\delta}$ in $\alpha\beta$ and $\gamma\delta$ and in the pairs $(\alpha\beta)$, $(\gamma\delta)$.

The total dipole and quadrupole moments of the molecule in the state Ψ are the expectation values of the operators and are

$$\begin{aligned} \mu_\alpha &= -\frac{\partial W}{\partial F_\alpha} = \mu_\alpha^{(0)} + \alpha_{\alpha\beta}F_\beta + \frac{1}{2}\beta_{\alpha\beta\gamma}F_\beta F_\gamma + \frac{1}{6}\gamma_{\alpha\beta\gamma\delta}F_\beta F_\gamma F_\delta \\ &\quad + \frac{1}{3}A_{\alpha,\beta\gamma}F_{\beta\gamma} + \frac{1}{3}B_{\alpha\beta,\gamma\delta}F_\beta F_{\gamma\delta} + \cdots \end{aligned} \tag{3}$$

$$\Theta_{\alpha\beta} = -3\frac{\partial W}{\partial F_{\alpha\beta}} = \Theta^{(0)} + A_{\gamma,\alpha\beta}F_\gamma + \frac{1}{2}B_{\gamma\delta,\alpha\beta}F_\gamma F_\delta + C_{\alpha\beta,\gamma\delta}F_{\gamma\delta} + \cdots \tag{4}$$

The second-rank tensor $\boldsymbol{\alpha}$ is the familiar static polarizability, and $\boldsymbol{\beta}$ and $\boldsymbol{\gamma}$ are hyperpolarizabilities describing deviations from a linear polarization law. The tensor $\mathbf{A}$ determines both the dipole induced by a field gradient and the quadrupole induced by a uniform field. If the molecular origin is a center of symmetry, as it would be if it were at the carbon atom in CO_2, $\boldsymbol{\mu}$, $\boldsymbol{\beta}$, and $\mathbf{A}$ are zero.

Only the first, nonvanishing moment is independent of the choice of origin. Thus for an ion like OH^-, the dipole and quadrupole moments vary with the origin, and $\boldsymbol{\mu} = 0$ at the "center of charge." Similarly, in HF, $\boldsymbol{\Theta}$ depends on origin and is zero at the "center of dipole." In an uncharged molecule, $\boldsymbol{\mu}$ is independent of the origin, and the dipole $\boldsymbol{\mu}'$ relative to a new origin O' at the point $\mathbf{r}'$ from the old origin O is equal to $\boldsymbol{\mu}$, and $F'_\alpha = F_\alpha + F_{\beta\alpha} r'_\beta + \cdots$, whence, from Eqs. (3) and (4)

$$\mu'_\alpha = \mu_\alpha \tag{5a}$$

$$\Theta'_{\alpha\beta} = \Theta_{\alpha\beta} - \left(\frac{3}{2} r'_\alpha \mu_\beta + \frac{3}{2} r'_\beta \mu_\alpha - r'_\gamma \mu_\gamma \delta_{\alpha\beta}\right) \tag{5b}$$

$$\alpha'_{\alpha\beta} = \alpha_{\alpha\beta} \tag{5c}$$

$$\beta'_{\alpha\beta\gamma} = \beta_{\alpha\beta\gamma} \tag{5d}$$

$$\gamma'_{\alpha\beta\gamma\delta} = \gamma_{\alpha\beta\gamma\delta} \tag{5e}$$

$$A'_{\alpha,\beta\gamma} = A_{\alpha,\beta\gamma} - \left(\frac{3}{2} r'_\beta \alpha_{\gamma\alpha} + \frac{3}{2} r'_\gamma \alpha_{\alpha\beta} - r'_\delta \alpha_{\delta\alpha} \delta_{\beta\gamma}\right) \tag{5f}$$

$$B'_{\alpha\beta,\gamma\delta} = B_{\alpha\beta,\gamma\delta} - \left(\frac{3}{2} r'_\gamma \beta_{\delta\alpha\beta} + \frac{3}{2} r'_\delta \beta_{\gamma\alpha\beta} - r'_\varepsilon \beta_{\varepsilon\alpha\beta} \delta_{\gamma\delta}\right) \tag{5g}$$

$$\begin{aligned} C'_{\alpha\beta,\gamma\delta} = C_{\alpha\beta,\gamma\delta} &- \frac{1}{3}\left(\frac{3}{2} r'_\alpha A_{\beta,\gamma\delta} + \frac{3}{2} r'_\beta A_{\alpha,\gamma\delta} - r'_\varepsilon A_{\varepsilon,\gamma\delta}\delta_{\alpha\beta}\right) \\ &- \frac{1}{3}\left(\frac{3}{2} r'_\gamma A_{\delta,\alpha\beta} + \frac{3}{2} r'_\delta A_{\gamma,\alpha\beta} - r'_\varepsilon A_{\varepsilon,\alpha\beta}\delta_{\gamma\delta}\right) \\ &+ \frac{r'_\alpha}{2}\left(\frac{3}{2} r'_\gamma \alpha_{\beta\delta} + \frac{3}{2} r'_\delta \alpha_{\beta\gamma} - r'_\varepsilon \delta_{\gamma\delta}\alpha_{\varepsilon\beta}\right) \\ &+ \frac{r'_\beta}{2}\left(\frac{3}{2} r'_\gamma \alpha_{\delta\alpha} + \frac{3}{2} r'_\delta \alpha_{\alpha\gamma} - r'_\varepsilon \delta_{\gamma\delta}\alpha_{\varepsilon\alpha}\right) \\ &- \frac{r'_\varepsilon}{3}\left(\frac{3}{2} r'_\gamma \delta_{\alpha\beta}\alpha_{\varepsilon\delta} + \frac{3}{2} r'_\delta \delta_{\alpha\beta}\alpha_{\varepsilon\gamma} - r'_\phi \delta_{\alpha\beta}\delta_{\gamma\delta}\alpha_{\varepsilon\phi}\right) \end{aligned} \tag{5h}$$

The number of independent constants needed to describe the interaction energy with the external field [Eq. (2)] is determined by the symmetry of the molecule. The number of constants required to specify

TABLE I

Number of Constants

Group symbol	μ_α	$\Theta_{\alpha\beta}$	$\alpha_{\alpha\beta}$	$\beta_{\alpha\beta\gamma}$	$\gamma_{\alpha\beta\gamma\delta}$	$A_{\alpha,\beta\gamma}$	$B_{\alpha\beta,\gamma\delta}$	$C_{\alpha\beta,\gamma\delta}$	$G'_{\alpha\beta}$	$D'_{\alpha,\beta\gamma}$
C_1	3	5	6	10	15	15	30	15	9	15
C_i	0	5	6	0	15	0	30	15	0	15
C_s	2	3	4	6	9	8	16	9	4	7
C_2	1	3	4	4	9	7	16	9	5	7
C_{2h}	0	3	4	0	9	0	16	9	0	7
C_{2v}	1	2	3	3	6	4	9	6	2	3
D_2	0	2	3	1	6	3	9	6	3	3
D_{2h}	0	2	3	0	6	0	9	6	0	3
C_4	1	1	2	2	5	3	8	5	3	3
S_4	0	1	2	2	5	4	8	5	2	3
C_{4h}	0	1	2	0	5	0	8	5	0	3
C_{4v}	1	1	2	2	4	2	5	4	1	1
D_{2d}	0	1	2	1	4	2	5	4	1	1
D_4	0	1	2	0	4	1	5	4	2	1
D_{4h}	0	1	2	0	4	0	5	4	0	1
C_3	1	1	2	4	5	5	10	5	3	5
S_6	0	1	2	0	5	0	10	5	0	5
C_{3v}	1	1	2	3	4	3	6	4	1	2
D_3	0	1	2	1	4	2	6	4	2	2
D_{3d}	0	1	2	0	4	0	6	4	0	2
C_{3h}	0	1	2	2	3	2	6	3	0	3
C_6	1	1	2	2	3	3	6	3	3	3
C_{6h}	0	1	2	0	3	0	6	3	0	3
D_{3h}	0	1	2	1	3	1	4	3	0	1
C_{6v}	1	1	2	2	3	2	4	3	1	1
D_6	0	1	2	0	3	1	4	3	2	1
D_{6h}	0	1	2	0	3	0	4	3	0	1
T	0	0	1	1	2	1	3	2	1	1
T_h	0	0	1	0	2	0	3	2	0	1
T_d	0	0	1	1	2	1	2	2	0	0
O	0	0	1	0	2	0	2	2	1	0
O_h	0	0	1	0	2	0	2	2	0	0
$C_{\infty v}$	1	1	2	2	3	2	4	3	1	1
$D_{\infty h}$	0	1	2	0	3	0	4	3	0	1
Sphere	0	0	1	0	1	0	1	1	0	0

the tensors $\boldsymbol{\mu}$, $\boldsymbol{\Theta}$, $\boldsymbol{\alpha}$, $\boldsymbol{\beta}$, $\boldsymbol{\gamma}$, **A**, **B**, and **C** for various molecular symmetry types is given in Table I; the Schoenflies notation has been used for the groups. The numbers have been evaluated by a group theoretical method [Bhagavantam and Suryanarayana,[2] Jahn[3]], and extend an earlier table [Buckingham and Stephen[4]]. It can be shown that the maximum number of constants specifying a multipole moment of order n is $2n + 1$—thus one charge, three dipoles, five quadrupoles, seven octopoles, . . . , are needed for the general molecule; the three dipoles could be given as μ_1, μ_2, μ_3 with respect to mutually perpendicular axes fixed in the molecule, or as a total dipole μ and two numbers specifying the orientation of this dipole with respect to the bonds of the molecule. The number of quadrupoles is one fewer than the number of polarizabilities $\alpha_{\alpha\beta}$, because the trace $\Theta_{\alpha\alpha} = 0$. Similarly, the number of octopoles is the difference between the number of polarizabilities $\beta_{\alpha\beta\gamma}$ and the number of dipoles μ_α.

If the molecule is axially symmetric ($C_{\infty v}$), then it is possible to specify the tensors in terms of the orientation l_α of this axis:

$$\mu_\alpha = \mu l_\alpha \tag{6a}$$

$$\Theta_{\alpha\beta} = \frac{1}{2}\Theta(3l_\alpha l_\beta - \delta_{\alpha\beta}) \tag{6b}$$

$$\begin{aligned}\alpha_{\alpha\beta} &= \alpha_\perp \delta_{\alpha\beta} + (\alpha_\parallel - \alpha_\perp) l_\alpha l_\beta \\ &= \frac{1}{3}(\alpha_\parallel + 2\alpha_\perp)\delta_{\alpha\beta} + \frac{1}{3}(\alpha_\parallel - \alpha_\perp)(3l_\alpha l_\beta - \delta_{\alpha\beta})\end{aligned} \tag{6c}$$

$$\beta_{\alpha\beta\gamma} = \beta_\perp(l_\alpha\delta_{\beta\gamma} + l_\beta\delta_{\gamma\alpha} + l_\gamma\delta_{\alpha\beta}) + (\beta_\parallel - 3\beta_\perp) l_\alpha l_\beta l_\gamma \tag{6d}$$

$$\begin{aligned}\gamma_{\alpha\beta\gamma\delta} = {} & \frac{1}{45}(3\gamma_{3333} + 12\gamma_{3311} + 8\gamma_{1111})(\delta_{\alpha\beta}\delta_{\gamma\delta} + \delta_{\alpha\gamma}\delta_{\beta\delta} + \delta_{\alpha\delta}\delta_{\beta\gamma}) \\ & + \frac{1}{63}(3\gamma_{3333} + 3\gamma_{3311} - 4\gamma_{1111})[(3l_\alpha l_\beta - \delta_{\alpha\beta})\delta_{\gamma\delta} \\ & + (3l_\alpha l_\gamma - \delta_{\alpha\gamma})\delta_{\beta\delta} + (3l_\alpha l_\delta - \delta_{\alpha\delta})\delta_{\beta\gamma} + (3l_\beta l_\gamma - \delta_{\beta\gamma})\delta_{\alpha\delta} \\ & + (3l_\beta l_\delta - \delta_{\beta\delta})\delta_{\alpha\gamma} + (3l_\gamma l_\delta - \delta_{\gamma\delta})\delta_{\alpha\beta}] + \frac{1}{35}(\gamma_{3333} - 6\gamma_{3311} \\ & + \gamma_{1111})[35l_\alpha l_\beta l_\gamma l_\delta - 5(l_\alpha l_\beta\delta_{\gamma\delta} + l_\alpha l_\gamma\delta_{\beta\delta} + l_\alpha l_\delta\delta_{\beta\gamma} + l_\beta l_\gamma\delta_{\alpha\delta} \\ & + l_\beta l_\delta\delta_{\alpha\gamma} + l_\gamma l_\delta\delta_{\alpha\beta}) + \delta_{\alpha\beta}\delta_{\gamma\delta} + \delta_{\alpha\gamma}\delta_{\beta\delta} + \delta_{\alpha\delta}\delta_{\beta\gamma}]\end{aligned} \tag{6e}$$

$$A_{\alpha,\beta\gamma} = \frac{1}{2} A_{\|} l_\alpha (3 l_\beta l_\gamma - \delta_{\beta\gamma}) + A_\perp (l_\beta \delta_{\alpha\gamma} + l_\gamma \delta_{\alpha\beta} - 2 l_\alpha l_\beta l_\gamma) \tag{6f}$$

$$\begin{aligned} B_{\alpha\beta,\gamma\delta} = {} & \frac{2}{15}(B_{33,33} + 4B_{13,13} + B_{11,33} + 4B_{11,11})\left[\frac{3}{4}(\delta_{\alpha\gamma}\delta_{\beta\delta} + \delta_{\alpha\delta}\delta_{\beta\gamma})\right. \\ & \left. - \frac{1}{2}\delta_{\alpha\beta}\delta_{\gamma\delta}\right] - \frac{2}{21}(B_{33,33} + 2B_{13,13} - 3B_{11,33} - 4B_{11,11}) \\ & \times (3 l_\alpha l_\beta - \delta_{\alpha\beta})\delta_{\gamma\delta} + \frac{1}{42}(3B_{33,33} - 8B_{13,13} + 26B_{11,33} \\ & + 16B_{11,11})(3 l_\gamma l_\delta - \delta_{\gamma\delta})\delta_{\alpha\beta} + \frac{1}{14}(B_{33,33} + 2B_{13,13} - 3B_{11,33} \\ & - 4B_{11,11})[(3 l_\alpha l_\gamma - \delta_{\alpha\gamma})\delta_{\beta\delta} + (3 l_\alpha l_\delta - \delta_{\alpha\delta})\delta_{\beta\gamma} + (3 l_\beta l_\gamma - \delta_{\beta\gamma})\delta_{\alpha\delta} \\ & + (3 l_\beta l_\delta - \delta_{\beta\delta})\delta_{\alpha\gamma}] + \frac{1}{70}(3B_{33,33} - 8B_{13,13} - 2B_{11,33} \\ & + 2B_{11,11})[35 l_\alpha l_\beta l_\gamma l_\delta - 5(l_\alpha l_\beta \delta_{\gamma\delta} + \cdots) + \delta_{\alpha\beta}\delta_{\gamma\delta} + \delta_{\alpha\gamma}\delta_{\beta\delta} \\ & + \delta_{\alpha\delta}\delta_{\beta\gamma}] \end{aligned} \tag{6g}$$

$$\begin{aligned} C_{\alpha\beta,\gamma\delta} = {} & \frac{1}{10}(C_{33,33} + 8C_{13,13} + 8C_{11,11})\left[\frac{1}{2}(\delta_{\alpha\gamma}\delta_{\beta\delta} + \delta_{\alpha\delta}\delta_{\beta\gamma}) - \frac{1}{3}\delta_{\alpha\beta}\delta_{\gamma\delta}\right] \\ & + \frac{1}{28}(5C_{33,33} + 4C_{13,13} - 8C_{11,11})\left[(3 l_\alpha l_\gamma - \delta_{\alpha\gamma})\delta_{\beta\delta}\right. \\ & + (3 l_\alpha l_\delta - \delta_{\alpha\delta})\delta_{\beta\gamma} + (3 l_\beta l_\gamma - \delta_{\beta\gamma})\delta_{\alpha\delta} + (3 l_\beta l_\delta - \delta_{\beta\delta})\delta_{\alpha\gamma} \\ & \left. - \frac{4}{3}(3 l_\alpha l_\beta - \delta_{\alpha\beta})\delta_{\gamma\delta} - \frac{4}{3}(3 l_\gamma l_\delta - \delta_{\gamma\delta})\delta_{\alpha\beta}\right] \\ & + \frac{1}{35}(2C_{33,33} - 4C_{13,13} + C_{11,11}) \\ & \times [35 l_\alpha l_\beta l_\gamma l_\delta - 5(l_\alpha l_\beta \delta_{\gamma\delta} + \cdots) + \delta_{\alpha\beta}\delta_{\gamma\delta} + \delta_{\alpha\gamma}\delta_{\beta\delta} + \delta_{\alpha\delta}\delta_{\beta\gamma}] \end{aligned} \tag{6h}$$

where $\mu = \mu_3$, $\Theta = \Theta_{33} = -2\Theta_{11} = -2\Theta_{22}$, and the subscripts $\|$ and $\perp$ denote components along and at right angles to the axis of symmetry (the 3-axis). There is just one permanent multipole moment of any order for an axially symmetric molecule.[5]

If the species is spherically symmetric,

$$\mu = \Theta = \beta_{\parallel} = \beta_{\perp} = A_{\parallel} = A_{\perp} = 0$$

and all the polarizability tensors are isotropic, and

$$\alpha_{\alpha\beta} = \alpha\delta_{\alpha\beta} \tag{7a}$$

$$\gamma_{\alpha\beta\gamma\delta} = \frac{1}{3}\gamma(\delta_{\alpha\beta}\delta_{\gamma\delta} + \delta_{\alpha\gamma}\delta_{\beta\delta} + \delta_{\alpha\delta}\delta_{\beta\gamma}) \tag{7b}$$

$$B_{\alpha\beta,\gamma\delta} = B\left[\frac{3}{4}(\delta_{\alpha\gamma}\delta_{\beta\delta} + \delta_{\alpha\delta}\delta_{\beta\gamma}) - \frac{1}{2}\delta_{\alpha\beta}\delta_{\gamma\delta}\right] \tag{7c}$$

$$C_{\alpha\beta,\gamma\delta} = C\left[\frac{1}{2}(\delta_{\alpha\gamma}\delta_{\beta\delta} + \delta_{\alpha\delta}\delta_{\beta\gamma}) - \frac{1}{3}\delta_{\alpha\beta}\delta_{\gamma\delta}\right] \tag{7d}$$

The polarizabilities

$$\alpha = \frac{1}{3}\alpha_{\beta\beta}, \quad \gamma = \frac{1}{5}\gamma_{\alpha\beta,\alpha\beta}, \quad B = \frac{2}{15}B_{\alpha\beta,\alpha\beta}, \quad \text{and} \quad C = \frac{1}{5}C_{\alpha\beta,\alpha\beta}$$

have been chosen so that in a field F_3, $F_{33} = -2F_{11} = -2F_{22}$,

$$W = W^{(0)} - \frac{1}{2}\alpha F_3^2 - \frac{1}{24}\gamma F_3^4 - \frac{1}{4}BF_3^2F_{33} - \frac{1}{4}CF_{33}^2 - \cdots \tag{8a}$$

$$\mu_3 = \alpha F_3 + \frac{1}{6}\gamma F_3^3 + \frac{1}{2}BF_3F_{33} + \cdots \tag{8b}$$

$$\Theta_{33} = \frac{1}{2}BF_3^2 + CF_{33} + \cdots \tag{8c}$$

Quantum mechanical perturbation theory[6] may be used to express the perturbed energy W_n of the nth state of the molecule as a power series in F_α, $F_{\beta\gamma}$, and by comparison with Eq. (2) to give

$$\alpha_{\alpha\beta}^{(n)} = S(\alpha, \beta)\sum_{i\neq n}\frac{\langle n|\mu_\alpha|i\rangle\langle i|\mu_\beta|n\rangle}{W_i^{(0)} - W_n^{(0)}} \tag{9}$$

$$\beta_{\alpha\beta\gamma}^{(n)} = S(\alpha, \beta, \gamma)\sum_{i\neq n}\left[\sum_{j\neq n}\frac{\langle n|\mu_\alpha|i\rangle\langle i|\mu_\beta|j\rangle\langle j|\mu_\gamma|n\rangle}{(W_i^{(0)} - W_n^{(0)})(W_j^{(0)} - W_n^{(0)})} - \frac{\langle n|\mu_\alpha|n\rangle\langle n|\mu_\beta|i\rangle\langle i|\mu_\gamma|n\rangle}{(W_i^{(0)} - W_n^{(0)})^2}\right] \tag{10}$$

$$\gamma^{(n)}_{\alpha\beta\gamma\delta} = S(\alpha, \beta, \gamma, \delta)$$

$$\times \sum_{i\neq n}\left\{\sum_{j\neq n}\left[\sum_{k\neq n}\frac{\langle n|\mu_\alpha|i\rangle\langle i|\mu_\beta|j\rangle\langle j|\mu_\gamma|k\rangle\langle k|\mu_\delta|n\rangle}{(W_i^{(0)}-W_n^{(0)})(W_j^{(0)}-W_n^{(0)})(W_k^{(0)}-W_n^{(0)})}\right.\right.$$

$$\left.\left.-\frac{\langle n|\mu_\alpha|i\rangle\langle i|\mu_\beta|n\rangle\langle n|\mu_\gamma|j\rangle\langle j|\mu_\delta|n\rangle + 2\langle n|\mu_\alpha|n\rangle\langle n|\mu_\beta|i\rangle\langle i|\mu_\gamma|j\rangle\langle j|\mu_\delta|n\rangle}{(W_i^{(0)}-W_n^{(0)})^2(W_j^{(0)}-W_n^{(0)})}\right]\right.$$

$$\left.+\frac{\langle n|\mu_\alpha|n\rangle\langle n|\mu_\beta|n\rangle\langle n|\mu_\gamma|i\rangle\langle i|\mu_\delta|n\rangle}{(W_i^{(0)}-W_n^{(0)})^3}\right\} \tag{11}$$

$$A^{(n)}_{\alpha,\beta\gamma} = 2\sum_{i\neq n}\frac{\langle n|\mu_\alpha|i\rangle\langle i|\Theta_{\beta\gamma}|n\rangle}{W_i^{(0)}-W_n^{(0)}} \tag{12}$$

$$B^{(n)}_{\alpha\beta,\gamma\delta} = S(\alpha,\beta)\sum_{i\neq n}$$

$$\times\left[\sum_{j\neq n}\frac{2\langle n|\mu_\alpha|i\rangle\langle i|\mu_\beta|j\rangle\langle j|\Theta_{\gamma\delta}|n\rangle + \langle n|\mu_\alpha|i\rangle\langle i|\Theta_{\gamma\delta}|j\rangle\langle j|\mu_\beta|n\rangle}{(W_i^{(0)}-W_n^{(0)})(W_j^{(0)}-W_n^{(0)})}\right.$$

$$\left.-\frac{2\langle n|\mu_\alpha|n\rangle\langle n|\mu_\beta|i\rangle\langle i|\Theta_{\gamma\delta}|n\rangle + \langle n|\Theta_{\gamma\delta}|n\rangle\langle n|\mu_\alpha|i\rangle\langle i|\mu_\beta|n\rangle}{(W_i^{(0)}-W_n^{(0)})^2}\right] \tag{13}$$

$$C_{\alpha\beta,\gamma\delta} = \frac{2}{3}\sum_{i\neq n}\frac{\langle n|\Theta_{\alpha\beta}|i\rangle\langle i|\Theta_{\gamma\delta}|n\rangle}{(W_i^{(0)}-W_n^{(0)})} \tag{14}$$

where the symbol $S(\alpha, \beta, \gamma, \ldots)$ implies a summation of all the following tensor components in which $\alpha, \beta, \gamma, \ldots$ are permuted. Thus $S(\alpha, \beta, \gamma)$ $X_{\alpha\beta\gamma} = X_{\alpha\beta\gamma} + X_{\alpha\gamma\beta} + X_{\beta\alpha\gamma} + X_{\beta\gamma\alpha} + X_{\gamma\alpha\beta} + X_{\gamma\beta\alpha}$; S is therefore a symmetrizing operator. These formulas for the polarizabilities are valid provided $W_i^{(0)} - W_n^{(0)}$ is large compared to $W_n - W_n^{(0)}$, as given by Eq. (2), for all states i that are mixed with n by the particular perturbation.

III. A MOLECULE IN A PERIODIC FIELD

In Section II, the interaction of a molecule with an electrostatic field was described in terms of permanent moments and a variety of polarizabilities. If the electric field is periodic and of angular frequency ω, the

interaction is modified and the polarizabilities are functions of ω. Their evaluation may be carried out by quantum mechanical time-dependent perturbation theory.[7,8] Some of the most accurate methods of measuring molecular polarizabilities involve optical fields, so before the results can be applied in the elucidation of intermolecular forces, it is important to know their frequency dependence.

Maxwell's equations for an electromagnetic field require that there be a magnetic field **H** associated with a time-dependent electric field. The Maxwell relationships in a vacuum are

$$\varepsilon_{\alpha\beta\gamma}F_{\beta\gamma} = -\frac{1}{c}\dot{H}_\alpha \tag{15a}$$

$$\varepsilon_{\alpha\beta\gamma}H_{\beta\gamma} = \frac{1}{c}\dot{F}_\alpha \tag{15b}$$

$$F_{\alpha\alpha} = 0 = H_{\alpha\alpha} \tag{15c}$$

where $\varepsilon_{\alpha\beta\gamma}$ is the unit skew-symmetric tensor and is equal to $+1$ or -1 if α, β, γ is an even or odd permutation of x, y, z, and is zero if any two of the subscripts α, β, γ are the same.

For a linearly polarized plane wave, of angular frequency ω traveling in the direction of the unit vector **k** with a velocity c,

$$F_\alpha = F_\alpha^{(0)} \cos\omega\left(t - \frac{k_\gamma r_\gamma}{c}\right) \tag{16a}$$

$$F_{\alpha\beta} = F_\beta^{(0)} \frac{\omega k_\alpha}{c} \sin\omega\left(t - \frac{k_\gamma r_\gamma}{c}\right) \tag{16b}$$

$$H_\alpha = \varepsilon_{\alpha\beta\gamma}k_\beta F_\gamma \tag{16c}$$

The magnetic moment operator in a uniform magnetic field is

$$m'_\alpha = \sum_i \frac{e_i}{2c}(\varepsilon_{\alpha\beta\gamma}r_{i_\beta}\dot{r}_{i_\gamma} + 2m_i^{-1}s_{i_\alpha})$$

$$= \sum_i \frac{e_i}{2m_i c}(\varepsilon_{\alpha\beta\gamma}r_{i_\beta}p_{i_\gamma} + 2s_{i_\alpha}) + \sum_i \frac{e_i^2}{4m_i c^2}(r_{i_\alpha}r_{i_\beta} - r_i^2\delta_{\alpha\beta})H_\beta$$

$$= m_\alpha + \chi_{d_{\alpha\beta}}H_\beta \tag{17}$$

where **m** is the moment in the absence of the field and e_i, m_i, and $\mathbf{s}_i$ are the charge, mass, and spin of particle i at $\mathbf{r}_i$ and $p_{i_\alpha} = -i\hbar\,\partial/\partial r_{i_\alpha}$ is

its momentum operator; $\chi_d \cdot \mathbf{H}$ is the diamagnetic contribution to $\mathbf{m}'$. The Hamiltonian describing a molecule in a field has frequently been considered[9,10] and for an uncharged system in any external field may conveniently be written in the form

$$\mathscr{H} = \mathscr{H}^{(0)} - \mu_\alpha F_\alpha - \frac{1}{3}\Theta_{\alpha\beta}F_{\alpha\beta} - m_\alpha H_\alpha - \frac{1}{2}\chi_{d_{\alpha\beta}}H_\alpha H_\beta - \cdots \quad (18)$$

The molecular multipoles may be evaluated by time-dependent perturbation theory, and the terms depending linearly on the field strengths are

$$\mu_\alpha = \mu_\alpha^{(0)} + \alpha_{\alpha\beta}F_\beta + \alpha'_{\alpha\beta}\dot{F}_\beta\omega^{-1} + \frac{1}{3}A_{\alpha,\beta\gamma}F_{\beta\gamma} + \frac{1}{3}A'_{\alpha,\beta\gamma}\dot{F}_{\beta\gamma}\omega^{-1} + G_{\alpha\beta}H_\beta + G'_{\alpha\beta}\dot{H}_\beta\omega^{-1} + \cdots \quad (19a)$$

$$\Theta_{\alpha\beta} = \Theta_{\alpha\beta}^{(0)} + A_{\gamma,\alpha\beta}F_\gamma - A'_{\gamma,\alpha\beta}\dot{F}_\gamma\omega^{-1} + C_{\alpha\beta,\gamma\delta}F_{\gamma\delta} + C'_{\alpha\beta,\gamma\delta}\dot{F}_{\gamma\delta}\omega^{-1} + D_{\gamma,\alpha\beta}H_\gamma - D'_{\gamma,\alpha\beta}\dot{H}_\gamma\omega^{-1} + \cdots \quad (19b)$$

$$m'_\alpha = m_\alpha^{(0)} + \chi_{\alpha\beta}H_\beta + \chi'_{\alpha\beta}\dot{H}_\beta\omega^{-1} + \frac{1}{3}D_{\alpha,\beta\gamma}F_{\beta\gamma} + \frac{1}{3}D'_{\alpha,\beta\gamma}\dot{F}_{\beta\gamma}\omega^{-1} + G_{\beta\alpha}F_\beta - G'_{\beta\alpha}\dot{F}_\beta\omega^{-1} + \cdots \quad (19c)$$

where, for the nth nondegenerate state,

$$\alpha_{\alpha\beta}^{(n)} = \sum_j \frac{\omega_{jn}}{\hbar(\omega_{jn}^2 - \omega^2)}(\langle n|\mu_\alpha|j\rangle\langle j|\mu_\beta|n\rangle + \langle n|\mu_\beta|j\rangle\langle j|\mu_\alpha|n\rangle) = \alpha_{\beta\alpha}^{(n)} \quad (20a)$$

$$\alpha_{\alpha\beta}^{\prime(n)} = \sum_j \frac{i\omega}{\hbar(\omega_{jn}^2 - \omega^2)}(\langle n|\mu_\alpha|j\rangle\langle j|\mu_\beta|n\rangle - \langle n|\mu_\beta|j\rangle\langle j|\mu_\alpha|n\rangle) = -\alpha_{\beta\alpha}^{\prime(n)} \quad (20b)$$

$$A_{\alpha,\beta\gamma}^{(n)} = \sum_j \frac{\omega_{jn}}{\hbar(\omega_{jn}^2 - \omega^2)}(\langle n|\mu_\alpha|j\rangle\langle j|\Theta_{\beta\gamma}|n\rangle + \langle n|\Theta_{\beta\gamma}|j\rangle\langle j|\mu_\alpha|n\rangle) = A_{\alpha,\gamma\beta}^{(n)} \quad (20c)$$

$$A_{\alpha,\beta\gamma}^{\prime(n)} = \sum_j \frac{i\omega}{\hbar(\omega_{jn}^2 - \omega^2)}(\langle n|\mu_\alpha|j\rangle\langle j|\Theta_{\beta\gamma}|n\rangle - \langle n|\Theta_{\beta\gamma}|j\rangle\langle j|\mu_\alpha|n\rangle) = A_{\alpha,\gamma\beta}^{\prime(n)} \quad (20d)$$

$$G^{(n)}_{\alpha\beta} = \sum_j \frac{\omega_{jn}}{\hbar(\omega^2_{jn} - \omega^2)} (\langle n|\mu_\alpha|j\rangle\langle j|m_\beta|n\rangle + \langle n|m_\beta|j\rangle\langle j|\mu_\alpha|n\rangle) \quad (20e)$$

$$G'^{(n)}_{\alpha\beta} = \sum_j \frac{i\omega}{\hbar(\omega^2_{jn} - \omega^2)} (\langle n|\mu_\alpha|j\rangle\langle j|m_\beta|n\rangle - \langle n|m_\beta|j\rangle\langle j|\mu_\alpha|n\rangle) \quad (20f)$$

$$C^{(n)}_{\alpha\beta,\gamma\delta} = \sum_j \frac{\omega_{jn}}{3\hbar(\omega^2_{jn} - \omega^2)} (\langle n|\Theta_{\alpha\beta}|j\rangle\langle j|\Theta_{\gamma\delta}|n\rangle + \langle n|\Theta_{\gamma\delta}|j\rangle\langle j|\Theta_{\alpha\beta}|n\rangle) = C^{(n)}_{\gamma\delta,\alpha\beta} \quad (20g)$$

$$C'^{(n)}_{\alpha\beta,\gamma\delta} = \sum_j \frac{i\omega}{3\hbar(\omega^2_{jn} - \omega^2)} (\langle n|\Theta_{\alpha\beta}|j\rangle\langle j|\Theta_{\gamma\delta}|n\rangle - \langle n|\Theta_{\gamma\delta}|j\rangle\langle j|\Theta_{\alpha\beta}|n\rangle) = -C'^{(n)}_{\gamma\delta,\alpha\beta} \quad (20h)$$

$$D^{(n)}_{\alpha,\beta\gamma} = \sum_j \frac{\omega_{jn}}{\hbar(\omega^2_{jn} - \omega^2)} (\langle n|m_\alpha|j\rangle\langle j|\Theta_{\beta\gamma}|n\rangle + \langle n|\Theta_{\beta\gamma}|j\rangle\langle j|m_\alpha|n\rangle) = D^{(n)}_{\alpha,\gamma\beta} \quad (20i)$$

$$D'^{(n)}_{\alpha,\beta\gamma} = \sum_j \frac{i\omega}{\hbar(\omega^2_{jn} - \omega^2)} (\langle n|m_\alpha|j\rangle\langle j|\Theta_{\beta\gamma}|n\rangle - \langle n|\Theta_{\beta\gamma}|j\rangle\langle j|m_\alpha|n\rangle) = D'^{(n)}_{\alpha,\gamma\beta} \quad (20j)$$

$$\chi^{(n)}_{\alpha\beta} = \sum_i \frac{e_i^2}{4m_i c^2} \langle n|r_{i_\alpha} r_{i_\beta} - r_i^2 \delta_{\alpha\beta}|n\rangle + \sum_j \frac{\omega_{jn}}{\hbar(\omega^2_{jn} - \omega^2)} \times (\langle n|m_\alpha|j\rangle\langle j|m_\beta|n\rangle + \langle n|m_\beta|j\rangle\langle j|m_\alpha|n\rangle) = \chi^{(n)}_{\beta\alpha} \quad (20k)$$

$$\chi'^{(n)}_{\alpha\beta} = \sum_j \frac{i\omega}{\hbar(\omega^2_{jn} - \omega^2)} (\langle n|m_\alpha|j\rangle\langle j|m_\beta|n\rangle - \langle n|m_\beta|j\rangle\langle j|m_\alpha|n\rangle) = -\chi'^{(n)}_{\beta\alpha} \quad (20l)$$

In the absence of an external magnetic field, the wave functions n, j, etc. may be chosen to be real (if n is degenerate), and then

$$\boldsymbol{\alpha}' = 0 = \mathbf{A}' = \mathbf{G} = \mathbf{C}' = \mathbf{D} = \boldsymbol{\chi}'$$

since the operators $\boldsymbol{\mu}$, $\boldsymbol{\Theta}$ are real and $\mathbf{m}$ is entirely imaginary. The numbers of independent constants needed to specify $\boldsymbol{\alpha}$, $\mathbf{A}$, $\mathbf{G}'$, $\mathbf{C}$, and $\mathbf{D}'$ for various symmetries are shown in Table I and the number for $\boldsymbol{\chi}$ is the same as for $\boldsymbol{\alpha}$.

There are two types of contribution to the magnetic susceptibility tensor $\chi^{(n)}_{\alpha\beta}$, the diamagnetic $\chi^{(n)}_{d_{\alpha\beta}}$, and the temperature-independent paramagnetic $\chi^{(n)}_{p_{\alpha\beta}}$, where the former arises from the fact that the

magnetic moment operator in the presence of the magnetic field is $m'_\alpha = m_\alpha + \chi_{d_{\alpha\beta}} H_\beta$ [see Eq. (17)]. The diamagnetic susceptibility is independent of the frequency ω but the temperature-independent paramagnetism varies as ω^{-2} for very large ω. If $\omega = 0$, the external field is electrostatic and/or magnetostatic, and all the primed polarizabilities in Eqs. (19) are equal to zero, and the unprimed ones then correspond to the static values of Eqs. (9)–(14). Some of the polarizabilities are already well known—thus $\boldsymbol{\alpha}$ is the normal frequency-dependent polarizability of Kramers and Heisenberg[11] and is the dominant contributor to the index of refraction. Natural optical activity is proportional to $\mathbf{G}'$,[12] and $\mathbf{C}$ is the quadrupole polarizability;[13] the variation of $\boldsymbol{\alpha}'$ and $\boldsymbol{\chi}'$ with a static magnetic field determines the Faraday effect (rotation of the plane of polarization of a light beam by a magnetic field along the direction of propagation).[14]

If the moments of the molecule change by $d\boldsymbol{\mu}$, $d\boldsymbol{\Theta}$, $d\mathbf{m}$, the corresponding change in interaction energy is

$$dW = -F_\alpha d\mu_\alpha - \frac{1}{3} F_{\alpha\beta}\, d\Theta_{\alpha\beta} - H_\alpha dm_\alpha - \cdots \tag{21}$$

and the power absorbed by the molecule from the field is

$$\dot{W} = -\dot{\mu}_\alpha F_\alpha - \frac{1}{3} \dot{\Theta}_{\alpha\beta} F_{\alpha\beta} - \dot{m}_\alpha H_\alpha - \cdots \tag{22}$$

This is equal to zero when averaged over a full period of the oscillation, as can be shown by substituting Eqs. (19) into Eq. (22). The medium therefore has no loss or gain. The cases of absorption and stimulated emission can be included easily in a complex representation. The periodic fields of Eqs. (16) are the real parts of

$$F_\alpha = F_\alpha^{(0)} e^{i\omega(t - k_\gamma r_\gamma/c)} \tag{23a}$$

$$F_{\alpha\beta} = -\frac{i\omega k_\alpha}{c} F_\beta^{(0)} e^{i\omega(t - k_\gamma r_\gamma/c)} \tag{23b}$$

$$H_\alpha = H_\alpha^{(0)} e^{i\omega(t - k_\gamma r_\gamma/c)} = \varepsilon_{\alpha\beta\gamma} k_\beta F_\gamma^{(0)} e^{i\omega(t - k_\gamma r_\gamma/c)} \tag{23c}$$

The complex moments are

$$\mu_\alpha = \mu_\alpha^{(0)} + \alpha_{\alpha\beta} F_\beta + \frac{1}{3} A_{\alpha,\beta\gamma} F_{\beta\gamma} + G_{\alpha\beta} H_\beta + \cdots \tag{24a}$$

$$\Theta_{\alpha\beta} = \Theta_{\alpha\beta}^{(0)} + C_{\alpha\beta,\gamma\delta}F_{\gamma\delta} + A_{\gamma,\alpha\beta}^{*}F_{\gamma} + D_{\gamma,\alpha\beta}^{*}H_{\gamma} + \cdots \tag{24b}$$

$$m_{\alpha}' = m_{\alpha}^{(0)} + \chi_{\alpha\beta}H_{\beta} + \frac{1}{3}D_{\alpha,\beta\gamma}F_{\beta\gamma} + G_{\beta\alpha}^{*}F_{\beta} + \cdots \tag{24c}$$

where the complex polarizabilities for the nth nondegenerate state are

$$\alpha_{\alpha\beta}^{(n)} = \sum_{j} \frac{2\hbar^{-1}}{(\omega_{jn}^{2} - \omega^{2})} [\omega_{jn}\mathrm{Re}\{\langle n|\mu_{\alpha}|j\rangle\langle j|\mu_{\beta}|n\rangle\} - i\omega\mathrm{Im}\{\langle n|\mu_{\alpha}|j\rangle\langle j|\mu_{\beta}|n\rangle\}] = \alpha_{\beta\alpha}^{(n)*} \tag{25a}$$

$$A_{\alpha,\beta\gamma}^{(n)} = \sum_{j} \frac{2\hbar^{-1}}{(\omega_{jn}^{2} - \omega^{2})} [\omega_{jn}\mathrm{Re}\{\langle n|\mu_{\alpha}|j\rangle\langle j|\Theta_{\beta\gamma}|n\rangle\} - i\omega\mathrm{Im}\{\langle n|\mu_{\alpha}|j\rangle\langle j|\Theta_{\beta\gamma}|n\rangle\}] \tag{25b}$$

$$G_{\alpha\beta}^{(n)} = \sum_{j} \frac{2\hbar^{-1}}{(\omega_{jn}^{2} - \omega^{2})} [\omega_{jn}\mathrm{Re}\{\langle n|\mu_{\alpha}|j\rangle\langle j|m_{\beta}|n\rangle\} - i\omega\mathrm{Im}\{\langle n|\mu_{\alpha}|j\rangle\langle j|m_{\beta}|n\rangle\}] \tag{25c}$$

$$C_{\alpha\beta,\gamma\delta}^{(n)} = \sum_{j} \frac{2\hbar^{-1}}{3(\omega_{jn}^{2} - \omega^{2})} [\omega_{jn}\mathrm{Re}\{\langle n|\Theta_{\alpha\beta}|j\rangle\langle j|\Theta_{\gamma\delta}|n\rangle\} - i\omega\mathrm{Im}\{\langle n|\Theta_{\alpha\beta}|j\rangle\langle j|\Theta_{\gamma\delta}|n\rangle\}] = C_{\gamma\delta,\alpha\beta}^{(n)*} \tag{25d}$$

$$D_{\alpha,\beta\gamma}^{(n)} = \sum_{j} \frac{2\hbar^{-1}}{(\omega_{jn}^{2} - \omega^{2})} [\omega_{jn}\mathrm{Re}\{\langle n|m_{\alpha}|j\rangle\langle j|\Theta_{\beta\gamma}|n\rangle\} - i\omega\mathrm{Im}\{\langle n|m_{\alpha}|j\rangle\langle j|\Theta_{\beta\gamma}|n\rangle\}] \tag{25e}$$

$$\chi_{\alpha\beta}^{(n)} = \chi_{d_{\alpha\beta}}^{(n)} + \sum_{j} \frac{2\hbar^{-1}}{(\omega_{jn}^{2} - \omega^{2})} [\omega_{jn}\mathrm{Re}\{\langle n|m_{\alpha}|j\rangle\langle j|m_{\beta}|n\rangle\} - i\omega\mathrm{Im}\{\langle n|m_{\alpha}|j\rangle\langle j|m_{\beta}|n\rangle\}] = \chi_{\beta\alpha}^{(n)*} \tag{25f}$$

These complex polarizability tensors $\mathbf{X}^{(n)}$ are equal to $\mathbf{X}^{(n)} + i\mathbf{X}'^{(n)}$, where the unprimed and primed tensors are those in Eqs. (20); since $\omega^{-1}\dot{F}_{\alpha} = iF_{\alpha}$, $\omega^{-1}\dot{F}_{\alpha\beta} = iF_{\alpha\beta}$, and $\omega^{-1}\dot{H}_{\alpha} = iH_{\alpha}$, Eqs. (19) and (24) are equivalent. The actual moments are the real parts of Eqs. (24). Near regions of absorption, $(\omega_{jn}^{2} - \omega^{2})^{-1}$ in Eqs. (25) must be replaced by $Z(\omega, \omega_{jn})$ where[15,16]

$$Z(\omega, \omega_{jn}) = f(\omega, \omega_{jn}) - ig(\omega, \omega_{jn}) \tag{26}$$

where f and g have the general forms illustrated in Figure 1. The Weisskopf-Wigner treatment of absorption leads to $Z = (\omega_{jn}^{2} - \omega^{2} + i\omega\Gamma_{jn})^{-1}$ [17] and hence to

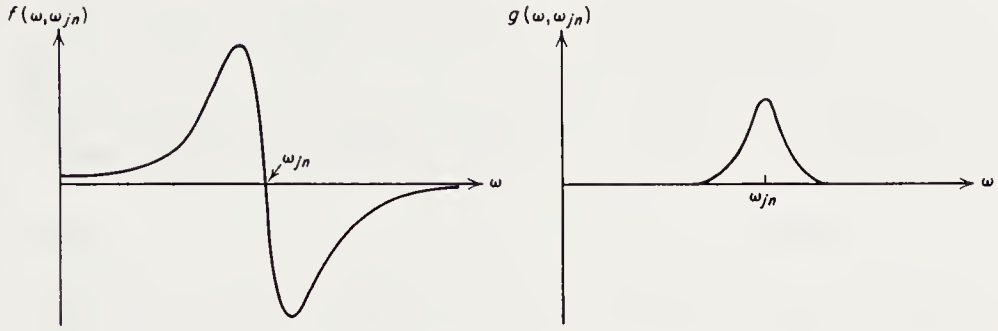

Fig. 1. Curves showing the general forms of the functions $f(\omega, \omega_{jn})$ and $g(\omega, \omega_{jn})$ in Eq. (26); f approximately describes the frequency dependence of the real part of the refractive index, and g describes that of the absorption coefficient.

$$f(\omega, \omega_{jn}) = (\omega_{jn}^2 - \omega^2)/[(\omega_{jn}^2 - \omega^2)^2 + \omega^2\Gamma_{jn}^2] \tag{27a}$$

$$g(\omega, \omega_{jn}) = \omega\Gamma_{jn}/[(\omega_{jn}^2 - \omega^2)^2 + \omega^2\Gamma_{jn}^2] \tag{27b}$$

where Γ_{jn} is approximately the width at half the maximum height of the $j \leftarrow n$ absorption spectral line. The mean value of $\dot{W}$ is no longer zero, and from Eq. (22), the mean energy absorbed from the radiation field in one second is

$$\begin{aligned}\overline{\dot{W}} = &-\frac{1}{4}\overline{(\dot{\mu}_\alpha + \dot{\mu}_\alpha^*)(F_\alpha + F_\alpha^*)} - \frac{1}{12}\overline{(\dot{\Theta}_{\alpha\beta} + \dot{\Theta}_{\alpha\beta}^*)(F_{\alpha\beta} + F_{\alpha\beta}^*)} \\ &- \frac{1}{4}\overline{(\dot{m}_\alpha + \dot{m}_\alpha^*)(H_\alpha + H_\alpha^*)} - \cdots \\ = &\frac{1}{2}\omega\mathrm{Im}\{\alpha_{\alpha\beta}\}F_\alpha^{(0)}F_\beta^{(0)} + \frac{1}{6}\frac{\omega^3}{c^2}\mathrm{Im}\{C_{\alpha\beta,\gamma\delta}\}k_\alpha k_\gamma F_\beta^{(0)}F_\delta^{(0)} \\ &+ \frac{1}{2}\omega\mathrm{Im}\{\chi_{\alpha\beta}\}H_\alpha^{(0)}H_\beta^{(0)} + \cdots\end{aligned} \tag{28}$$

If there are N_n molecules per unit volume initially in state n, and they are isotropically oriented, Eq. (28) leads to the result

$$-\frac{dI}{I} = \frac{2\omega k}{c}\,dz \tag{29}$$

where $-dI$ is the loss in the intensity I of the radiation field over a distance of propagation dz, and the "absorption coefficient" (minus the imaginary part of the refractive index of the gas) is

$$k = -2\pi N_n\left[\mathrm{Im}\{\alpha\} + \frac{1}{6}\frac{\omega^2}{c^2}\,\mathrm{Im}\{C\} + \mathrm{Im}\{\chi\} + \cdots\right] \tag{30}$$

The mean polarizabilities $\alpha = \frac{1}{3}\alpha_{\beta\beta}$ and $C = \frac{1}{5}C_{\alpha\beta,\alpha\beta}$ are those of Eqs. (7) and $\chi = \frac{1}{3}\chi_{\alpha\alpha}$. The imaginary parts of α, C, and χ are [see Eqs. (25)]

$$\mathrm{Im}\{\alpha\} = -\frac{2}{3\hbar}\sum_j \omega_{jn} g(\omega, \omega_{jn})\langle n|\mu_\alpha|j\rangle\langle j|\mu_\alpha|n\rangle \tag{31a}$$

$$\mathrm{Im}\{C\} = -\frac{2}{15\hbar}\sum_j \omega_{jn} g(\omega, \omega_{jn})\langle n|\Theta_{\alpha\beta}|j\rangle\langle j|\Theta_{\alpha\beta}|n\rangle \tag{31b}$$

$$\mathrm{Im}\{\chi\} = -\frac{2}{3\hbar}\sum_j \omega_{jn} g(\omega, \omega_{jn})\langle n|m_\alpha|j\rangle\langle j|m_\alpha|n\rangle \tag{31c}$$

so α, C, and χ are entirely real outside absorption bands (for g is then zero). In an isotropic medium Eqs. (24) reduce to

$$\mu_\alpha = \alpha F_\alpha + GH_\alpha + \cdots \tag{32a}$$

$$\Theta_{\alpha\beta} = \frac{1}{2}C(F_{\alpha\beta} + F_{\beta\alpha}) + \cdots \tag{32b}$$

$$m'_\alpha = \chi H_\alpha + G^* F_\alpha + \cdots \tag{32c}$$

where α and C are defined in Eqs. (7a) and (7d), and $\chi = \frac{1}{3}\chi_{\alpha\alpha}$, $G = \frac{1}{3}G_{\alpha\alpha}$. α, C, and χ determine the refractive index of the medium, and G determines its optical rotation and circular dichroism.

IV. INTERACTION OF TWO MOLECULES

When a pair of molecules, 1 and 2, are far apart, electron exchange can be neglected and the interaction Hamiltonian treated as a perturbation to the Hamiltonian $\mathscr{H}_1^{(0)} + \mathscr{H}_2^{(0)}$ of the free molecules.[18,19] The eigenvalues and eigenfunctions of the unperturbed system are $W_{j_1}^{(0)} + W_{j_2}^{(0)}$ and $\psi_{j_1}^{(0)}\psi_{j_2}^{(0)}$, and the perturbation is

$$\mathscr{H}' = \sum_{i_1,i_2} e_{i_1}e_{i_2}R_{i_1i_2}^{-1} = q_2\phi_2 - \mu_{2_\alpha}F_{2_\alpha} - \frac{1}{3}\Theta_{2_{\alpha\beta}}F_{2_{\alpha\beta}} - \cdots \tag{33}$$

$$= q_1\phi_1 - \mu_{1_\alpha}F_{1_\alpha} - \frac{1}{3}\Theta_{1_{\alpha\beta}}F_{1_{\alpha\beta}} - \cdots \tag{34}$$

where $R_{i_1i_2}$ is the distance from the element of charge e_{i_1} in molecule 1

to e_{i_2} in molecule 2 and where q_2, $\boldsymbol{\mu}_2$, and $\boldsymbol{\Theta}_2$ are the charge ($q_2 = \sum_{i_2} e_{i_2}$), dipole, and quadrupole moment operators for molecule 2; ϕ_2 is the electric potential at the origin of molecule 2 due to the instantaneous charge distribution of molecule 1, and

$$F_{2_\alpha} = -\nabla_\alpha \phi_2 \qquad \text{and} \qquad F_{2_{\alpha\beta}} = \nabla_\alpha F_{2_\beta} = -\nabla_\alpha \nabla_\beta \phi_2$$

are the field and field-gradient operators.

The interaction Hamiltonian can be written as a multipole series[20,21]:

$$\begin{aligned}\mathscr{H}' = {} & T_2 q_1 q_2 + T_{2_\alpha}(q_1 \mu_{2_\alpha} - q_2 \mu_{1_\alpha}) \\ & + T_{2_{\alpha\beta}}\left(\frac{1}{3} q_1 \Theta_{2_{\alpha\beta}} + \frac{1}{3} q_2 \Theta_{1_{\alpha\beta}} - \mu_{1_\alpha}\mu_{2_\beta}\right) \\ & + T_{2_{\alpha\beta\gamma}}\left(\frac{1}{15} q_1 \Omega_{2_{\alpha\beta\gamma}} - \frac{1}{15} q_2 \Omega_{1_{\alpha\beta\gamma}} - \frac{1}{3} \mu_{1_\alpha}\Theta_{2_{\beta\gamma}} + \frac{1}{3} \mu_{2_\alpha}\Theta_{1_{\beta\gamma}}\right) \\ & + T_{2_{\alpha\beta\gamma\delta}}\left(\frac{1}{9} \Theta_{1_{\alpha\beta}}\Theta_{2_{\gamma\delta}} + \cdots\right) + \cdots \end{aligned} \tag{35}$$

where, if $\mathbf{R}$ is the vector from the origin of 1 to 2,

$$T_2 = R^{-1} \tag{36a}$$

$$T_{2_\alpha} = \nabla_\alpha R^{-1} = -R_\alpha R^{-3} \tag{36b}$$

$$T_{2_{\alpha\beta}} = T_{2_{\beta\alpha}} = \nabla_\alpha \nabla_\beta R^{-1} = (3R_\alpha R_\beta - R^2\delta_{\alpha\beta})R^{-5} \tag{36c}$$

$$T_{2_{\alpha\beta\gamma}} = \nabla_\alpha \nabla_\beta \nabla_\gamma R^{-1} = -3[5R_\alpha R_\beta R_\gamma - R^2(R_\alpha \delta_{\beta\gamma} + R_\beta \delta_{\gamma\alpha} + R_\gamma \delta_{\alpha\beta})]R^{-7} \tag{36d}$$

$$T_{2_{\alpha\beta\gamma\delta\cdots}} = \nabla_\alpha \nabla_\beta \nabla_\gamma \nabla_\delta \cdots R^{-1} \tag{36e}$$

The $\mathbf{T}$ tensors are symmetric in all suffixes, and since

$$\nabla_\alpha \nabla_\alpha R^{-1} = \nabla^2 R^{-1} = 0$$

a repeated Greek suffix reduces any $\mathbf{T}$ to zero. Because the vector from 1 to 2 is minus the vector from 2 to 1, $\mathbf{T}_1 = (-1)^n \mathbf{T}_2$, where n is the order of the tensor. The $\mathbf{T}$ tensor of order n is proportional to $R^{-(n+1)}$,

so Eq. (35) is a series in inverse powers of the molecular separation, and this is rapidly convergent when R is large compared to molecular dimensions.

The energy of the pair when the free molecules were in states $\psi_{n_1}^{(0)}$ and $\psi_{n_2}^{(0)}$ may be obtained from perturbation theory and is

$$W_{n_1,n_2} = W_{n_1}^{(0)} + W_{n_2}^{(0)} + \langle \psi_{n_1}^{(0)}\psi_{n_2}^{(0)}|\mathscr{H}'|\psi_{n_1}^{(0)}\psi_{n_2}^{(0)}\rangle - \sum{}' \frac{|\langle \psi_{n_1}^{(0)}\psi_{n_2}^{(0)}|\mathscr{H}'|\psi_{j_1}^{(0)}\psi_{j_2}^{(0)}\rangle|^2}{(W_{j_1}^{(0)} - W_{n_1}^{(0)}) + (W_{j_2}^{(0)} - W_{n_2}^{(0)})} + \cdots \quad (37)$$

where $\sum'$ is a summation over all unperturbed states $\psi_{j_1}^{(0)}\psi_{j_2}^{(0)}$ except $\psi_{n_1}^{(0)}\psi_{n_2}^{(0)}$. The first-order perturbed energy is called the *electrostatic energy* u_{elec}, and for nondegenerate unperturbed states $\psi_{n_1}^{(0)}$ and $\psi_{n_2}^{(0)}$,

$$\begin{aligned} u_{\text{elec}}^{(n_1,n_2)} &= \langle \psi_{n_1}^{(0)}\psi_{n_2}^{(0)}|\mathscr{H}'|\psi_{n_1}^{(0)}\psi_{n_2}^{(0)}\rangle \\ &= T_2 q_1 q_2 + T_{2_\alpha}(q_1\mu_{2_\alpha}^{(n_2)} - q_2\mu_{1_\alpha}^{(n_1)}) \\ &\quad + T_{2_{\alpha\beta}}\left(\frac{1}{3}q_1\Theta_{2_{\alpha\beta}}^{(n_2)} + \frac{1}{3}q_2\Theta_{1_{\alpha\beta}}^{(n_1)} - \mu_{1_\alpha}^{(n_1)}\mu_{2_\beta}^{(n_2)}\right) \\ &\quad + T_{2_{\alpha\beta\gamma}}\left(\frac{1}{15}q_1\Omega_{2_{\alpha\beta\gamma}}^{(n_2)} - \frac{1}{15}q_2\Omega_{1_{\alpha\beta\gamma}}^{(n_1)} - \frac{1}{3}\mu_{1_\alpha}^{(n_1)}\Theta_{2_{\beta\gamma}}^{(n_2)} + \frac{1}{3}\mu_{2_\alpha}^{(n_2)}\Theta_{1_{\beta\gamma}}^{(n_1)}\right) \\ &\quad + T_{2_{\alpha\beta\gamma\delta}}\left(\frac{1}{9}\Theta_{1_{\alpha\beta}}^{(n_1)}\Theta_{2_{\gamma\delta}}^{(n_2)} + \cdots\right) + \cdots \end{aligned} \quad (38)$$

where q_1, $\boldsymbol{\mu}_1^{(n_1)}$, $\boldsymbol{\Theta}_1^{(n_1)}$, $\boldsymbol{\Omega}_1^{(n_1)}$, etc. are the "permanent" moments (charge, dipole, quadrupole, octopole) of molecule 1 when it is in the unperturbed internal state $\psi_{n_1}^{(0)}$, e.g., $\mu_{1_\alpha}^{(n_1)} = \langle \psi_{n_1}^{(0)}|\mu_{1_\alpha}|\psi_{n_1}^{(0)}\rangle$.

The second-order perturbed energy in Eq. (37) includes both the induction energy and the dispersion energy. The sets of excited unperturbed states $\psi_{j_1}^{(0)}\psi_{n_2}^{(0)}$ and $\psi_{n_1}^{(0)}\psi_{j_2}^{(0)}$, in which the matrix elements of $\mathscr{H}'$ are diagonal in n_2 and n_1, produce the *induction energy* u_{ind}, and the remaining excited states constitute the *dispersion energy* u_{disp}. Thus

$$u_{\text{ind}}^{(n_1,n_2)} = -\sum_{j_1 \neq n_1} \frac{|\langle \psi_{n_1}^{(0)}\psi_{n_2}^{(0)}|\mathscr{H}'|\psi_{j_1}^{(0)}\psi_{n_2}^{(0)}\rangle|^2}{W_{j_1}^{(0)} - W_{n_1}^{(0)}} - \sum_{j_2 \neq n_2} \frac{|\langle \psi_{n_1}^{(0)}\psi_{n_2}^{(0)}|\mathscr{H}'|\psi_{n_1}^{(0)}\psi_{j_2}^{(0)}\rangle|^2}{W_{j_2}^{(0)} - W_{n_2}^{(0)}} = u_{\text{ind}}^{(n_1)} + u_{\text{ind}}^{(n_2)} \quad (39)$$

where, from Eqs. (9), (12), (14), and (34),

$$u_{\text{ind}}^{(n_1)} = -\frac{1}{2}\alpha_{1_{\alpha\beta}}^{(n_1)} F_{1_\alpha}^{(n_2)} F_{1_\beta}^{(n_2)} - \frac{1}{3} A_{1_{\alpha,\beta\gamma}}^{(n_1)} F_{1_\alpha}^{(n_2)} F_{1_{\beta\gamma}}^{(n_2)} - \frac{1}{6} C_{1_{\alpha\beta,\gamma\delta}}^{(n_1)} F_{1_{\alpha\beta}}^{(n_2)} F_{1_{\gamma\delta}}^{(n_2)} - \cdots \tag{40}$$

$F_{1_\alpha}^{(n_2)}$ and $F_{1_{\alpha\beta}}^{(n_2)}$ are the electric field and field gradient at the origin of molecule 1 arising from the "permanent" moments of molecule 2 in its unperturbed state $\psi_{n_2}^{(0)}$. Hence

$$F_{1_\alpha}^{(n_2)} = -T_{1_\alpha} q_2 + T_{1_{\alpha\beta}} \mu_{2_\beta}^{(n_2)} - \frac{1}{3} T_{1_{\alpha\beta\gamma}} \Theta_{2_{\beta\gamma}}^{(n_2)} + \cdots \tag{41a}$$

$$F_{1_{\alpha\beta}}^{(n_2)} = -T_{1_{\alpha\beta}} q_2 + T_{1_{\alpha\beta\gamma}} \mu_{2_\gamma}^{(n_2)} - \frac{1}{3} T_{1_{\alpha\beta\gamma\delta}} \Theta_{2_{\gamma\delta}}^{(n_2)} + \cdots \tag{41b}$$

The remainder of the second-order perturbed energy in Eq. (37) is the dispersion energy, and

$$u_{\text{disp}}^{(n_1,n_2)} = -\sum_{\substack{j_1 \neq n_1 \\ j_2 \neq n_2}} \frac{|\langle \psi_{n_1}^{(0)} \psi_{n_2}^{(0)} | \mathscr{H}' | \psi_{j_1}^{(0)} \psi_{j_2}^{(0)} \rangle|^2}{(W_{j_1}^{(0)} - W_{n_1}^{(0)}) + (W_{j_2}^{(0)} - W_{n_2}^{(0)})} \tag{42}$$

$$\begin{aligned}
= -\sum_{\substack{j_1 \neq n_1 \\ j_2 \neq n_2}} \Bigg[& T_{2_{\alpha\beta}} T_{2_{\gamma\delta}} \frac{\langle \psi_{n_1}^{(0)} \psi_{n_2}^{(0)} | \mu_{1_\alpha} \mu_{2_\beta} | \psi_{j_1}^{(0)} \psi_{j_2}^{(0)} \rangle \langle \psi_{j_1}^{(0)} \psi_{j_2}^{(0)} | \mu_{1_\gamma} \mu_{2_\delta} | \psi_{n_1}^{(0)} \psi_{n_2}^{(0)} \rangle}{(W_{j_1}^{(0)} - W_{n_1}^{(0)}) + (W_{j_2}^{(0)} - W_{n_2}^{(0)})} \\
& + \frac{2}{3} T_{2_{\alpha\beta}} T_{2_{\gamma\delta\varepsilon}} \frac{\langle \psi_{n_1}^{(0)} \psi_{n_2}^{(0)} | \mu_{1_\alpha} \mu_{2_\beta} | \psi_{j_1}^{(0)} \psi_{j_2}^{(0)} \rangle \langle \psi_{j_1}^{(0)} \psi_{j_2}^{(0)} | \mu_{1_\gamma} \Theta_{2_{\delta\varepsilon}} - \mu_{2_\gamma} \Theta_{1_{\delta\varepsilon}} | \psi_{n_1}^{(0)} \psi_{n_2}^{(0)} \rangle}{(W_{j_1}^{(0)} - W_{n_1}^{(0)}) + (W_{j_2}^{(0)} - W_{n_2}^{(0)})} \\
& + \frac{1}{9} T_{2_{\alpha\beta\gamma}} T_{2_{\delta\varepsilon\phi}} \frac{\langle \psi_{n_1}^{(0)} \psi_{n_2}^{(0)} | \mu_{1_\alpha} \Theta_{2_{\beta\gamma}} - \mu_{2_\alpha} \Theta_{1_{\beta\gamma}} | \psi_{j_1}^{(0)} \psi_{j_2}^{(0)} \rangle \langle \psi_{j_1}^{(0)} \psi_{j_2}^{(0)} | \mu_{1_\delta} \Theta_{2_{\varepsilon\phi}} - \mu_{2_\delta} \Theta_{1_{\varepsilon\phi}} | \psi_{n_1}^{(0)} \psi_{n_2}^{(0)} \rangle}{(W_{j_1}^{(0)} - W_{n_1}^{(0)}) + (W_{j_2}^{(0)} - W_{n_2}^{(0)})} \\
& - \frac{2}{9} T_{2_{\alpha\beta}} T_{2_{\gamma\delta\varepsilon\phi}} \frac{\langle \psi_{n_1}^{(0)} \psi_{n_2}^{(0)} | \mu_{1_\alpha} \mu_{2_\beta} | \psi_{j_1}^{(0)} \psi_{j_2}^{(0)} \rangle \langle \psi_{j_1}^{(0)} \psi_{j_2}^{(0)} | \Theta_{1_{\gamma\delta}} \Theta_{2_{\varepsilon\phi}} | \psi_{n_1}^{(0)} \psi_{n_2}^{(0)} \rangle}{(W_{j_1}^{(0)} - W_{n_1}^{(0)}) + (W_{j_2}^{(0)} - W_{n_2}^{(0)})} + \cdots \Bigg]
\end{aligned} \tag{43}$$

The dispersion energy therefore varies as R^{-6} for large R, with additional contributions in R^{-7}, R^{-8}, etc.

Simplification of this expression for $u_{\text{disp}}^{(n_1,n_2)}$ can only be achieved by introducing approximations. Following to some extent Unsöld[22] and London,[1] the energy denominators of Eq. (43) are replaced as follows:

$$\frac{1}{(W_{j_1}^{(0)} - W_{n_1}^{(0)}) + (W_{j_2}^{(0)} - W_{n_2}^{(0)})} = \frac{U_1^{(n_1)} U_2^{(n_2)}(1 + \Delta)}{(U_1^{(n_1)} + U_2^{(n_2)})(W_{j_1}^{(0)} - W_{n_1}^{(0)})(W_{j_2}^{(0)} - W_{n_2}^{(0)})} \tag{44}$$

where

$$\Delta = \frac{[U_1^{(n_1)^{-1}} + U_2^{(n_2)^{-1}}] - [(W_{j_1}^{(0)} - W_{n_1}^{(0)})^{-1} + (W_{j_2}^{(0)} - W_{n_2}^{(0)})^{-1}]}{(W_{j_1}^{(0)} - W_{n_1}^{(0)})^{-1} + (W_{j_2}^{(0)} - W_{n_2}^{(0)})^{-1}} \tag{45}$$

The approximation is made by neglecting Δ and setting $U_1^{(n_1)}$ and $U_2^{(n_2)}$ equal to fixed energies associated with the states $\psi_{n_1}^{(0)}$ and $\psi_{n_2}^{(0)}$. Then Eq. (43) simplifies to

$$\begin{aligned} u_{\text{disp}}^{(n_1,n_2)} = -\frac{U_1^{(n_1)} U_2^{(n_2)}}{4(U_1^{(n_1)} + U_2^{(n_2)})} \Big[& T_{2_{\alpha\beta}} T_{2_{\gamma\delta}} \alpha_{1_{\alpha\gamma}}^{(n_1)} \alpha_{2_{\beta\delta}}^{(n_2)} \\ & + \frac{2}{3} T_{2_{\alpha\beta}} T_{2_{\gamma\delta\varepsilon}} (\alpha_{1_{\alpha\gamma}}^{(n_1)} A_{2_{\beta,\delta\varepsilon}}^{(n_2)} - \alpha_{2_{\alpha\gamma}}^{(n_2)} A_{1_{\beta,\delta\varepsilon}}^{(n_1)}) \\ & + T_{2_{\alpha\beta\gamma}} T_{2_{\delta\varepsilon\phi}} \left(\frac{1}{3} \alpha_{1_{\alpha\delta}}^{(n_1)} C_{2_{\beta\gamma,\varepsilon\phi}}^{(n_2)} + \frac{1}{3} \alpha_{2_{\alpha\delta}}^{(n_2)} C_{1_{\beta\gamma,\varepsilon\phi}}^{(n_1)} - \frac{2}{9} A_{1_{\alpha,\varepsilon\phi}}^{(n_1)} A_{2_{\delta,\beta\gamma}}^{(n_2)} \right) \\ & - \frac{2}{9} T_{2_{\alpha\beta}} T_{2_{\gamma\delta\varepsilon\phi}} A_{1_{\alpha,\gamma\delta}}^{(n_1)} A_{2_{\beta,\varepsilon\phi}}^{(n_2)} + \cdots \Big] \end{aligned} \tag{46}$$

where $\boldsymbol{\alpha}^{(n_1)}$, $\mathbf{A}^{(n_1)}$, and $\mathbf{C}^{(n_1)}$ are the polarizabilities of Eqs. (9), (12), and (14). If $\psi_{n_1}^{(0)}$ and $\psi_{n_2}^{(0)}$ are the internal ground states of molecules 1 and 2, $U_1^{(n_1)}$ and $U_2^{(n_2)}$ may conveniently be set equal to the first ionization potentials or to the lowest allowed excitation energies of 1 and 2; in the latter case, Eq. (46) gives a lower limit to the magnitude of the leading term (proportional to R^{-6}) of the dispersion energy.

If $\boldsymbol{\alpha}_1^{(n_1)}$ and $\boldsymbol{\alpha}_2^{(n_2)}$ are isotropic [see Eqs. (7)], Eq. (46) reduces to

$$u_{\text{disp}}^{(n_1,n_2)} = -\frac{3U_1^{(n_1)}U_2^{(n_2)}}{2(U_1^{(n_1)}+U_2^{(n_2)})}\Big[R^{-6}\alpha_1^{(n_1)}\alpha_2^{(n_2)}$$

$$+\frac{1}{9}T_{2_{\alpha\beta}}T_{2_{\alpha\gamma\delta}}(\alpha_1^{(n_1)}A_{2_{\beta,\gamma\delta}}^{(n_2)}-\alpha_2^{(n_2)}A_{1_{\beta,\gamma\delta}}^{(n_1)})$$

$$+\frac{1}{18}T_{2_{\alpha\beta\gamma}}T_{2_{\alpha\delta\varepsilon}}(\alpha_1^{(n_1)}C_{2_{\beta\gamma,\delta\varepsilon}}^{(n_2)}+\alpha_2^{(n_2)}C_{1_{\beta\gamma,\delta\varepsilon}}^{(n_1)})$$

$$-\frac{1}{27}(T_{2_{\alpha\delta}}T_{2_{\beta\gamma\varepsilon\phi}}+T_{2_{\alpha\varepsilon\phi}}T_{2_{\beta\gamma\delta}})A_{1_{\alpha,\beta\gamma}}^{(n_1)}A_{2_{\delta,\varepsilon\phi}}^{(n_2)}+\cdots\Big] \tag{47}$$

After averaging over all molecular orientations for fixed R, the polarizabilities in Eq. (47) must be replaced by their isotropic parts, yielding

$$u_{\text{disp}}^{(n_1,n_2)} = -\frac{3U_1^{(n_1)}U_2^{(n_2)}}{2(U_1^{(n_1)}+U_2^{(n_2)})}\Big[R^{-6}\alpha_1^{(n_1)}\alpha_2^{(n_2)}+5R^{-8}(\alpha_1^{(n_1)}C_2^{(n_2)}$$

$$+\alpha_2^{(n_2)}C_1^{(n_1)})+\cdots\Big] \tag{48}$$

For two like molecules in interaction in their ground states this simplifies to

$$u_{\text{disp}} = -(3U\alpha^2/4R^6)[1+(10C/\alpha R^2)+\cdots] \tag{49}$$

The ratio of the R^{-8} to R^{-6} terms is therefore equal to $10C/\alpha R^2$ in this approximation. For the hydrogen atom $\alpha = 9a^3/2$ and $C = 15a^5/2$, where a is the Bohr radius,[13,20] so that in the interaction of two hydrogen atoms this ratio is $\frac{50}{3}(a^2/R^2)$; the accurate value is $19.14(a^2/R^2)$.[23,24]

If one or both of the interacting molecules is in an excited state, the long-range interaction energy may be very different from its value for ground internal states. If the molecules are identical, then resonance may occur through the exchange of excitation energy; if the free molecules are in the states n_1 and j_2, the unperturbed states $n_1 j_2$ and $j_1 n_2$ are degenerate and the stationary states are those in which the Hamiltonian is diagonal. The first-order perturbed energy is then the sum of the *electrostatic* and *resonance* energies.[18,25] If there is an allowed dipole transition between the states n_1 and j_1, i.e., if $\langle n_1|\mu_\alpha|j_1\rangle \neq 0$, the leading term in the resonance energy varies as R^{-3} even when neither molecule 1 nor molecule 2 has a permanent dipole moment.

Similarly, if $\langle n_1|\mu_\alpha|j_1\rangle = 0$ but $\langle n_1|\Theta_{\alpha\beta}|j_1\rangle \neq 0$, there is a quadrupole resonance energy varying as R^{-5}. As an example, consider two identical interacting atoms: the stationary states are $\psi_g = (n_1 j_2 + j_1 n_2)/\sqrt{2}$ and $\psi_u = (n_1 j_2 - j_1 n_2)/\sqrt{2}$, and if the photon is exchanged by a dipole mechanism (as it would be between S and P states) the first-order energy of interaction varies as R^{-3}; if there is a quadrupole transition moment (as between S and D, or P and P states), the long-range energy is proportional to R^{-5}. In general,

$$W_{\substack{g\\u}} = \mp\left[T_{2_{\alpha\beta}}\langle n|\mu_\alpha|j\rangle\langle j|\mu_\beta|n\rangle - \frac{1}{9}T_{2_{\alpha\beta\gamma\delta}}\langle n|\Theta_{\alpha\beta}|j\rangle\langle j|\Theta_{\gamma\delta}|n\rangle + \cdots\right] \quad (50)$$

If state j is spatially degenerate (as for a P or D state), the interaction partly lifts the degeneracy, giving different intermolecular energy curves.

The polarizabilities of excited states may differ greatly from that of the ground internal state of a molecule. They may be very large or even negative, according to the magnitude and sign of the energy denominators in Eqs. (9)–(14), and, therefore, influence the induction energy of Eq. (40). Similarly, the energy denominator in Eq. (42) for the dispersion energy may be small and of either sign if the initial state $\psi_{n_1}^{(0)}\psi_{n_2}^{(0)}$ is not the ground state; this can produce a very powerful dispersion force to which a single unperturbed state $\psi_{j_1}^{(0)}\psi_{j_2}^{(0)}$ makes a predominant contribution.

The charges of two interacting molecules at long range are constants, so there are no "transition charges" or off-diagonal matrix elements of q. The first nonvanishing transition moment is the dipole and this leads to the R^{-6} dispersion energy in Eq. (43). This energy may be considered to arise approximately from fluctuations in the molecular dipoles. In the same way, the R^{-2} energy of interaction between dissolved polyelectrolyte molecules at their isoelectric point, discovered by Kirkwood and Shumaker,[26] can be considered to be due to fluctuations in the charges of the large molecules, although, in this case, the presence of the medium is essential, for it provides the source and the sink for the charges.

V. SOME PARTICULAR MOLECULAR INTERACTIONS

To determine the nature and importance of some of the higher terms in the general expressions for long-range interaction energies derived in the previous section, some special cases are now considered.

A. A Point Charge and a Linear Molecule

This is appropriate to a collision between a charged particle, such as a proton, and a diatomic molecule like HCl. If q_1 is the charge, Eq. (38) yields

$$u_{\text{elec}} = q_1 T_{2_\alpha} \mu_{2_\alpha} + \frac{1}{3} q_1 T_{2_{\alpha\beta}} \Theta_{2_{\alpha\beta}} + \frac{1}{15} q_1 T_{2_{\alpha\beta\gamma}} \Omega_{2_{\alpha\beta\gamma}} + \cdots$$

$$= q_1 \left[\mu R^{-2} \cos\theta + \Theta R^{-3} \left(\frac{3}{2} \cos^2\theta - \frac{1}{2} \right) + \Omega R^{-4} \left(\frac{5}{2} \cos^3\theta - \frac{3}{2} \cos\theta \right) + \cdots \right] \quad (51)$$

where μ, Θ, and Ω, which is equal to $\sum_i e_i r_i^3 P_3(\cos\theta_i)$, are the dipole, quadrupole, and octopole of the molecule, respectively, and θ is the angle between $\boldsymbol{\mu}$ and the vector from the center of the molecule to the point charge. Also, from Eqs. (6) and (40)

$$u_{\text{ind}} = -\frac{1}{2} q^2 R^{-4} \left[\alpha + \frac{1}{3} (\alpha_{\parallel} - \alpha_{\perp})(3\cos^2\theta - 1) + A_{\parallel} R^{-1} (3\cos^3\theta - \cos\theta) + 4A_{\perp} R^{-1} \cos\theta \sin^2\theta + 2CR^{-2} + \cdots \right] \quad (52)$$

u_{disp} is zero in this case.

The interaction energy must be independent of the choice of the origin in the linear molecule; a movement of this origin through a distance z' along its axis causes the following changes:

$$R^{-1} \to R'^{-1} = (R^2 - 2z'R\cos\theta + z'^2)^{-1/2} = R^{-1} + z'\cos\theta R^{-2} + z'^2 \left(\frac{3}{2} \cos^2\theta - \frac{1}{2} \right) R^{-3} + \cdots$$

$$\cos\theta \to \cos\theta' = R'^{-1}(R\cos\theta - z') = \cos\theta - z'R^{-1}\sin^2\theta - \frac{3}{2} z'^2 R^{-2} \cos\theta \sin^2\theta + \cdots$$

$$\mu \to \mu' = \mu$$

$$\Theta \to \Theta' = \Theta - 2z'\mu$$

$$\Omega \to \Omega' = \Omega - 3z'\Theta + 3z'^2\mu$$

$$\boldsymbol{\alpha} \to \boldsymbol{\alpha}' = \boldsymbol{\alpha}$$

$$A_{\parallel} \to A'_{\parallel} = A_{\parallel} - 2z'\alpha_{\parallel}$$

$$A_{\perp} \to A'_{\perp} = A_{\perp} - \frac{3}{2}z'\alpha_{\perp}$$

$$C \to C' = C - \frac{2}{5}z'(A_{\parallel} + 2A_{\perp}) + \frac{1}{5}z'^2(2\alpha_{\parallel} + 3\alpha_{\perp})$$

$$u_{\text{elec}} \to u'_{\text{elec}} = u_{\text{elec}}$$

$$u_{\text{ind}} \to u'_{\text{ind}} = u_{\text{ind}}$$

B. A Point Charge and a Tetrahedral Molecule

It is convenient to describe the orientation of a tetrahedron by associating with it a cube such that the tetrahedrally disposed atoms are at the corners (1, 1, 1), (1, −1, −1), (−1, 1, −1), and (−1, −1, 1); the cartesian axes are then the x, y, z axes of the cube. The first nonvanishing multipole moment of an uncharged tetrahedron is its octopole $\Omega = \Omega_{xyz} = \frac{5}{2}\sum_i e_i x_i y_i z_i$; its polarizability $\boldsymbol{\alpha}$ is isotropic, and there is one constant describing the **A** tensor [$A = A_{xyz}$, and A is independent of the origin—see Eq. (5f)], and two constants describing **C**[$C_{xx,xx}$ and $C_{xy,xy}$; $C = \frac{1}{5}C_{\alpha\beta,\alpha\beta} = \frac{3}{5}(C_{xx,xx} + 2C_{xy,xy})$]. There is also just one hyperpolarizability $\beta = \beta_{xyz}$. Hence

$$A_{\alpha,\beta\gamma} = A(i_\alpha j_\beta k_\gamma + i_\alpha j_\gamma k_\beta + i_\beta j_\gamma k_\alpha + i_\beta j_\alpha k_\gamma + i_\gamma j_\alpha k_\beta + i_\gamma j_\beta k_\alpha) \tag{53a}$$

$$C_{\alpha\beta,\gamma\delta} = C\left[\frac{1}{2}(\delta_{\alpha\gamma}\delta_{\beta\delta} + \delta_{\alpha\delta}\delta_{\beta\gamma}) - \frac{1}{3}\delta_{\alpha\beta}\delta_{\gamma\delta}\right]$$
$$+ \left[\frac{3}{10}C_{xx,xx} - \frac{2}{5}C_{xy,xy}\right][5(i_\alpha i_\beta i_\gamma i_\delta + j_\alpha j_\beta j_\gamma j_\delta + k_\alpha k_\beta k_\gamma k_\delta)$$
$$- (\delta_{\alpha\beta}\delta_{\gamma\delta} + \delta_{\alpha\gamma}\delta_{\beta\delta} + \delta_{\alpha\delta}\delta_{\beta\gamma})] \tag{53b}$$

$$\beta_{\alpha\beta\gamma} = \beta(i_\alpha j_\beta k_\gamma + i_\alpha j_\gamma k_\beta + i_\beta j_\gamma k_\alpha + i_\beta j_\alpha k_\gamma + i_\gamma j_\alpha k_\beta + i_\gamma j_\beta k_\alpha) \tag{53c}$$

and

$$u_{\text{elec}} = 6q_1\Omega R^{-4}\cos\theta_x\cos\theta_y\cos\theta_z + \cdots \tag{54a}$$

$$u_{\text{ind}} = -\frac{1}{2} q_1^2 R^{-4}\Big[\alpha + 12AR^{-1}\cos\theta_x\cos\theta_y\cos\theta_z + 2CR^{-2} + \left(\frac{9}{2}C_{xx,xx} - 6C_{xy,xy}\right)R^{-2}\left(\cos^4\theta_x + \cos^4\theta_y + \cos^4\theta_z - \frac{3}{5}\right) + 2q_1\beta R^{-2}\cos\theta_x\cos\theta_y\cos\theta_z + \cdots\Big] \quad (54b)$$

$$u_{\text{disp}} = 0 \quad (54c)$$

where θ_α is the angle between the α axis of the cube and the vector from the center of the tetrahedron to the point charge.

The order of magnitude of the constant A may be obtained from a molecular model in which the tetrahedron is comprised of four atoms at a distance R_0 from the center and having polarizabilities $\alpha_\parallel$ and $\alpha_\perp$ along and at right angles to their bonds to the central atom; in this case $A = 4(\alpha_\parallel - \alpha_\perp)R_0/\sqrt{3}$,[21] so that A may be of the order of 10^{-32} cm^4 for small tetrahedral molecules like CH_4.

C. A Spherical and a Tetrahedral Molecule

If both molecules are uncharged, $u_{\text{elec}} = 0$ and u_{ind} is proportional to R^{-10} and negligible. The dispersion energy may be large and angle dependent; the approximate Eq. (47) gives

$$u_{\text{disp}} = -\frac{3U_1U_2}{2(U_1+U_2)R^6}\left\{\alpha_1\alpha_2 + \frac{8\alpha_1A_2}{R}\cos\theta_x\cos\theta_y\cos\theta_z + \frac{5\alpha_2C_1}{R^2} + \frac{5\alpha_1C_2}{R^2} + \frac{\alpha_1(3C_{xx,xx} - 4C_{xy,xy})}{4R^2} \times [5(\cos^4\theta_x + \cos^4\theta_y + \cos^4\theta_z) - 3] + \cdots\right\} \quad (55)$$

The A_2 contribution to the dispersion energy is the longest range angle-dependent energy and it could be important in inelastic scattering or pressure broadening experiments involving collisions between molecules such as CH_4 and Ar. It could also be a significant contributor to the binding energy of solid tetrahedra, but since it vanishes on averaging over all orientations, it plays an insignificant role in determining equilibrium properties of gases, like virial coefficients.

D. Two Linear Molecules

In the case of two dipolar linear molecules in the configuration of Figure 2, Eqs. (38), (40), and (46) yield

$$u_{\text{elec}} = \mu_1\mu_2 R^{-3}(2\cos\theta_1\cos\theta_2 + \sin\theta_1\sin\theta_2\cos\phi)$$
$$+\frac{3}{2}\mu_1\Theta_2 R^{-4}[\cos\theta_1(3\cos^2\theta_2 - 1) + 2\sin\theta_1\sin\theta_2\cos\theta_2\cos\phi]$$
$$+\frac{3}{2}\mu_2\Theta_1 R^{-4}[\cos\theta_2(3\cos^2\theta_1 - 1) + 2\sin\theta_1\cos\theta_1\sin\theta_2\cos\phi]$$
$$+\frac{3}{4}\Theta_1\Theta_2 R^{-5}(1 - 5\cos^2\theta_1 - 5\cos^2\theta_2 + 17\cos^2\theta_1\cos^2\theta_2$$
$$+ 2\sin^2\theta_1\sin^2\theta_2\cos^2\phi + 16\sin\theta_1\cos\theta_1\sin\theta_2\cos\theta_2\cos\phi)$$
$$+\cdots \quad (56)$$

$$u_{\text{ind}}^{(2)} = -\frac{1}{2}\alpha_2[\mu_1^2 R^{-6}(3\cos^2\theta_1 + 1) + 12\mu_1\Theta_1 R^{-7}\cos^3\theta_1 + \cdots]$$
$$-\frac{1}{6}(\alpha_\parallel - \alpha_\perp)_2\mu_1^2 R^{-6}(12\cos^2\theta_1\cos^2\theta_2$$
$$+ 3\sin^2\theta_1\sin^2\theta_2\cos^2\phi - 3\cos^2\theta_1 - 1$$
$$+ 12\sin\theta_1\cos\theta_1\sin\theta_2\cos\theta_2\cos\phi)$$
$$-\frac{3}{2}A_{2_\parallel}\mu_1^2 R^{-7}(6\cos^2\theta_1\cos^3\theta_2 - 2\cos^2\theta_1\cos\theta_2$$
$$+ 7\sin\theta_1\cos\theta_1\sin\theta_2\cos^2\theta_2\cos\phi - \sin\theta_1\cos\theta_1\sin\theta_2\cos\phi$$
$$+ 2\sin^2\theta_1\sin^2\theta_2\cos\theta_2\cos^2\phi)$$
$$+ 2A_{2_\perp}\mu_1^2 R^{-7}(6\cos^2\theta_1\cos^3\theta_2 - 5\cos^2\theta_1\cos\theta_2$$
$$+ 7\sin\theta_1\cos\theta_1\sin\theta_2\cos^2\theta_2\cos\phi$$
$$-2\sin\theta_1\cos\theta_1\sin\theta_2\cos\phi + 2\sin^2\theta_1\sin^2\theta_2\cos\theta_2\cos^2\phi$$
$$-\cos\theta_2) + \cdots \quad (57)$$

$$u_{\text{disp}} = -[3U_1U_2/2(U_1+U_2)R^6]\Big[\alpha_1\alpha_2 + \frac{1}{3}\alpha_1(\alpha_{\parallel}-\alpha_{\perp})_2 \times \left(\frac{3}{2}\cos^2\theta_2 - \frac{1}{2}\right) + \frac{1}{3}\alpha_2(\alpha_{\parallel}-\alpha_{\perp})_1\left(\frac{3}{2}\cos^2\theta_1 - \frac{1}{2}\right) + 2\alpha_1 A_{2_{\parallel}} R^{-1}\cos^3\theta_2 + 2\alpha_2 A_{1_{\parallel}} R^{-1}\cos^3\theta_1 + \frac{4}{3}\alpha_1 A_{2_{\perp}} R^{-1} \times (3\cos\theta_2 - 2\cos^3\theta_2) + \frac{4}{3}\alpha_2 A_{1_{\perp}} R^{-1} \times (3\cos\theta_1 - 2\cos^3\theta_1) + \cdots\Big] \quad (58)$$

The interaction of a spherical atom, such as argon, with a dipolar molecule may be obtained from these formulas by setting

$$\mu_2 = 0 = \Theta_2 = (\alpha_{\parallel} - \alpha_{\perp})_2 = A_{2_{\parallel}} = A_{2_{\perp}}$$

and is

$$u = -\frac{1}{2}\alpha_2\mu_1^2 R^{-6}(3\cos^2\theta_1 + 1) - 6\alpha_2\mu_1\Theta_1 R^{-7}\cos^3\theta_1 + \cdots - [3U_1U_2\alpha_2/2(U_1+U_2)R^6]\Big[\alpha_1 + \frac{1}{3}(\alpha_{\parallel}-\alpha_{\perp})_1\left(\frac{3}{2}\cos^2\theta_1 - \frac{1}{2}\right) + 2A_{1_{\parallel}}R^{-1}\cos^3\theta_1 + \frac{4}{3}A_{1_{\perp}}R^{-1}(3\cos\theta_1 - 2\cos^3\theta_1) + \cdots\Big] \quad (59)$$

The dipole–quadrupole induction energy proportional to $R^{-7}\cos^3\theta$ was first added to the well-known dipole term by Anderson[27] to explain the pressure broadening of the ammonia inversion microwave spectrum by spherical atoms. The additional terms in Eq. (59) in $A_{\parallel}R^{-7}\cos^3\theta$ and $A_{\perp}R^{-7}(3\cos\theta - 2\cos^3\theta)$ are likely also to be important in these and other collisional experiments; the ratio of the $A_{\parallel}$ term to the $\mu\Theta$

Fig. 2. The coordinates **R**, θ_1,θ_2, and ϕ describing the configuration of two axially symmetric molecules.

induction term is approximately $\frac{1}{4}UA_{\parallel}/\mu\Theta$ which is generally not small. This ratio may be large for the alkali halide molecules because of their large polarizabilities and small quadrupole moments. Since $A_{\parallel}$ and $A_{\perp}$ depend on the choice of origin (see Eq. 5f), the R^{-7} contribution can be varied at will, although the total energy must be unaltered by this arbitrary choice. There is, in general, no unique "center of action" of the dispersion force relative to which the R^{-7} contribution to the energy is zero for all θ, but it is possible to define a point for which the term in $R^{-7}\ P_1(\cos\theta)$ vanishes. This point was termed the "center of the dispersion force" by Herman[28]; according to the approximate Eq. (59), this point is where $A_{\parallel} = -2A_{\perp}$ and is independent of the perturbing spherical molecule. However, there is still a term in $(3A_{\parallel} - 4A_{\perp})R^{-7}$ $P_3(\cos\theta)$; this is the leading term with $P_3(\cos\theta)$ angular dependence and is independent of the origin if $\alpha_{\parallel} = \alpha_{\perp}$ in the linear molecule. Herman[28] calculated that the center of the dispersion force in HCl is about 0.11 Å from the center of mass in the direction of the proton; however, his model did not embrace the two independent quantities $A_{\parallel}$ and $A_{\perp}$. Reliable values for $A_{\parallel}$ and $A_{\perp}$ are unfortunately not yet available for any molecule.

VI. MEASUREMENTS OF MOLECULAR MOMENTS AND POLARIZABILITIES

Accurate measurements of $\mu^{(0)}$ and α have been made over many years by a variety of methods, particularly as a result of the classical work of Debye.[29] The direction of the dipole with respect to molecular axes may be obtained through measurements of Stark splittings in the pure rotation spectra of isotopically substituted molecules, and its sign may be obtained through an ingenious experiment involving the determination of the effect of isotopic substitution on the rotational magnetic moment.[30] It is of interest to note that a measurement of the change in the quadrupole moment relative to the center of mass due to isotopic substitution would yield the sign of the dipole moment through Eq. (5b); the difference in the quadrupole moments of HCl and DCl relative to their centers of mass is $\pm 0.08 \times 10^{-26}$ esu, the plus sign being associated with a dipole in which hydrogen is positive.

An accurate method exists for the determination of all of the molecular constants in Eq. (2) with the exception of **A** and **C**. The technique consists of measuring the effect of a strong static electric field or field

gradient on the refractive index of a gas. The refractive index is determined primarily by the electric dipole induced in a molecule by the oscillating electric field $\mathscr{F}_\alpha$ associated with the light wave, that is, by the polarizability $\alpha_{\alpha\beta}$ in Eq. (24a). In the presence of other fields, it is convenient to call this parameter the differential polarizability $\pi_{\alpha\beta}$, which is defined as $\partial\mu_\alpha/\partial\mathscr{F}_\beta$, and may be written as a function of the static fields F_α and $F_{\alpha\beta}$ as follows:

$$\pi_{\alpha\beta} = \alpha_{\alpha\beta} + \beta_{\alpha\beta,\gamma}F_\gamma + \frac{1}{2}\gamma_{\alpha\beta,\gamma\delta}F_\gamma F_\delta + \frac{1}{3}B_{\alpha\beta,\gamma\delta}F_{\gamma\delta} + \cdots \tag{60}$$

where the polarizabilities $\boldsymbol{\alpha}$, $\boldsymbol{\beta}$, $\boldsymbol{\gamma}$, and $\mathbf{B}$ are the frequency-dependent variants of the static polarizabilities in Eq. (3). Hence, $\boldsymbol{\beta}$ and $\boldsymbol{\gamma}$ describe the effects of an electric field, and $\mathbf{B}$ describes those of a field gradient, on the polarizability tensor. The refractive-index tensor of a gas is

$$\mathbf{n} - \mathbf{1} = 2\pi N\bar{\boldsymbol{\pi}} \tag{61}$$

where N is the number of gas molecules in unit volume, and the bar denotes a statistical average. Thus

$$\bar{\boldsymbol{\pi}} = \sum_n \langle\psi_n|\boldsymbol{\pi}|\psi_n\rangle \exp(-W^{(n)}/kT)/\sum_m \exp(-W^{(m)}/kT) \tag{62}$$

where the summations extend over all the molecular states ψ_n appropriate to the molecule in the electric field or field gradient. It is usually sufficiently accurate to consider only the ground internal state and to treat the rotational degrees of freedom classically, so that $\boldsymbol{\pi}$ and $W^{(n)}$ are functions of the orientation $\boldsymbol{\omega}$, and the summation in Eq. (62) is replaced by an integral:

$$\bar{\boldsymbol{\pi}} = \int \boldsymbol{\pi} \exp(-W/kT)\, d\boldsymbol{\omega} / \int \exp(-W/kT)\, d\boldsymbol{\omega} \tag{63}$$

The anisotropy in the refractive index induced by a uniform electric field is known as the Kerr effect [for an early review, see Beams[31]]. There are three distinct contributions to the anisotropy: (*1*) The first is common to all substances and arises from $\boldsymbol{\gamma}$ in Eq. (60). It gives a temperature-independent Kerr constant and is the only nonvanishing term for isotropic molecules. (*2*) The second is only found in dipolar molecules and is due to the polarizability $\beta_{\alpha\beta,\gamma}F_\gamma$ in Eq. (60) contributing to the mean polarizability of a molecule which is partially oriented through the action of the electric field on the dipole moment.

(*3*) Thirdly, in a molecule with an anisotropic polarizability tensor $\alpha_{\alpha\beta}$, the partial alignment of the molecule through interaction of its permanent and induced dipole moments with the field leads to a change in the refractive index. These three effects combine to yield the following classical statistical mechanical formula for the refractive index difference, $n_{xx} - n_{yy}$, of a gas in a strong static electric field F_x:[32]

$$n_{xx} - n_{yy} = 2\pi N(\overline{\pi_{xx}} - \overline{\pi_{yy}})$$

$$= (2\pi N F_x^2/15)\left\{\left(\frac{3}{2}\gamma_{\alpha\beta,\alpha\beta} - \frac{1}{2}\gamma_{\alpha\alpha,\beta\beta}\right) + (1/kT)(3\beta_{\alpha\beta,\alpha}\mu_\beta - \beta_{\alpha\alpha,\beta}\mu_\beta)\right.$$

$$\left. + \frac{1}{kT}\left[\frac{3}{2}\alpha_{\alpha\beta}\left(\alpha_{\alpha\beta}^{(0)} + \frac{1}{kT}\mu_\alpha\mu_\beta\right) - \frac{1}{2}\alpha_{\alpha\alpha}\left(\alpha_{\beta\beta}^{(0)} + \frac{1}{kT}\mu_\beta\mu_\beta\right)\right]\right\} \quad (64)$$

where $\boldsymbol{\alpha}^{(0)}$ is the static polarizability tensor. For dipolar molecules, the final term, and principally that in $k^{-2}T^{-2}$, is dominant and forms the basis of the application of the Kerr effect to molecular structure determinations with the aid of "bond polarizabilities."[33] If the molecule is comprised of axially symmetric bonds at angles of approximately $\cos^{-1}(1/\sqrt{3})$ to the molecular dipole moment, the polarizability in this direction is nearly equal to the mean polarizability and the T^{-2} term in Eq. (64) is small; such a situation exists in the methylene dihalides,[34] and provides an excellent opportunity to measure the $\boldsymbol{\beta}$ contribution to $n_{xx} - n_{yy}$ and hence gain accurate information about this hyperpolarizability. Additional information about $\boldsymbol{\beta}$ may be obtained through intensity and polarization studies of second harmonic generation in the interaction of molecules with an intense flash of light from a pulsed laser.[35]

For isotropically polarizable molecules, only the temperature-independent term in Eq. (64) survives and

$$n_{xx} - n_{yy} = \pi N F_x^2(\overline{\gamma_{xx,xx}} - \overline{\gamma_{yy,xx}}) \quad (65)$$

Therefore, the Kerr constant of a gas of spherical molecules gives a direct measurement of $\gamma_{xx,xx} - \gamma_{yy,xx}$ appropriate to the frequency of the light beam used in the measurement of the refractive index. If this frequency is well below the lowest electronic absorption frequency of the molecule, γ is likely to be very little different from its static value, and $\gamma_{xx,yy} = \frac{1}{3}\gamma_{xx,xx} = \frac{1}{3}\gamma$ [see Eq. (7b)], thus

$$n_{xx} - n_{yy} = 2\pi N\gamma F_x^2/3 \quad (66)$$

TABLE II

The Hyperpolarizabilities γ of Spherical Atoms

	H	He	Ne	Ar	Kr	Xe
$10^{38}\gamma$(esu)	67.1	2.6	5	70	160	400

Some recent preliminary results[36,37] are shown in Table II. Except for the hydrogen atom (which is from an accurate quantum mechanical calculation,[38]) these results were obtained through Kerr effect measurements using a helium–neon gas laser operating at 6328 Å as a light source.

If the externally applied orienting field is the field gradient of a two-wire condenser ($F_{xx} = -F_{yy}$, $F_{zz} = 0$), the anisotropy in the refractive index has a first-order dependence on the applied voltage (unlike the Kerr effect, which is quadratic), and measurements of $n_{xx} - n_{yy}$ lead to the molecular quadrupole moment Θ and to the hyperpolarizability B. The equation analogous to Eq. (64) is

$$\begin{aligned} n_{xx} - n_{yy} &= 2\pi N(\overline{\pi_{xx}} - \overline{\pi_{yy}}) \\ &= (4\pi N F_{xx}/15)[B_{\alpha\beta,\alpha\beta} + (1/kT)\alpha_{\alpha\beta}\Theta_{\alpha\beta}] \end{aligned} \tag{67}$$

where the temperature-independent term arises from the effect of the field gradient on the polarizability π in Eq. (60), and the T^{-1} term is due to the partial orientation of a molecule through the interaction of its quadrupole moment with the field gradient. If the molecule is isotropically polarizable, the second term is zero. The scalar $B_{\alpha\beta,\alpha\beta} = 15B/2$ [see Eq. (7c)]. For molecules with just one quadrupole Θ (see Table I),

$$n_{xx} - n_{yy} = (4\pi N F_{xx}/15)\left[\frac{15}{2}B + (1/kT)(\alpha_{\parallel} - \alpha_{\perp})\Theta\right] \tag{68}$$

Values for the anisotropy in α are, therefore, needed before Θ can be obtained through measurements of the effect of a field gradient on the refractive index. Very accurate values of $(\alpha_{\parallel} - \alpha_{\perp})$ have recently been obtained from studies of the depolarization of the light scattered by gases from a helium–neon gas laser beam.[39] A similar light source has been used in the measurements of $n_{xx} - n_{yy}$. Some recently determined molecular quadrupole moments are listed in Table III.[37,40]

TABLE III

Quadrupole Moments of Molecules

	CO_2	N_2	O_2	C_2H_6	N_2O	CO	H_2
$10^{26}\Theta^{(0)}$(esu)	−4.2	−1.5	−0.4	−0.6	−3.0	−2.5	+0.651

The value for H_2 was obtained for the ground state by a very detailed quantum mechanical calculation.[41,42] Equation (68) would not apply accurately to H_2 at room temperature because in its derivation, the rotational motion was assumed to be classical, whereas the effect of the field-gradient on each rotational state should actually be considered, and an average should then be performed over all rotational states. This more accurate procedure leads to a reduction of the T^{-1} contribution to $n_{xx} - n_{yy}$ for H_2 at room temperature to three-fourths of its classical value. The quantum effect is much smaller for D_2 and is negligible for heavier molecules like CO_2;[43] it is larger at lower temperatures, and in *para* hydrogen at low temperatures ($J = 0$) $(n_{xx} - n_{yy})/N$ is independent of T, but in *ortho* hydrogen ($J = 1$) the lifting of the threefold rotational degeneracy by the field gradient leads to a T^{-1} dependence down to the lowest temperatures.

For molecules without a quadrupole moment, Eq. (68) simplifies to

$$n_{xx} - n_{yy} = 2\pi NBF_{xx} \tag{69}$$

Preliminary anisotropy measurements on CH_4 lead to $B = -0.3 \times 10^{-38}$ esu,[37] which compares with -0.487×10^{-38} calculated for H.[44]

The question of the appropriate origin of the quadrupole moment obtained through application of Eq. (67) to a dipolar gas is still unresolved. There seems little doubt that it is not the center of mass, for the angular distribution of classical molecules is determined by their potential energy in the field gradient, and this is the same for isotopically distinct species, although the quadrupole moments relative to the centers of mass are different [see Eq. (5b)].

VII. LONG-RANGE DIPOLAR INTERACTIONS

The dipolar coupling, $u_{\text{dipole}} = -T_{2_\alpha\beta}\mu_{1_\alpha}\mu_{2_\beta}$, between two molecules with permanent dipole moments, varies as R^{-3} and is angle dependent.

Although this electrostatic energy averages to zero if all orientations are equally probable, it produces a second-order temperature-dependent energy of the Keesom type:[45]

$$\bar{u} = \left[\iint u_{\text{dipole}} \exp\left(-u_{\text{dipole}}/kT\right) d\omega_1\, d\omega_2\right] \Big/ \left[\iint \exp\left(-u_{\text{dipole}}/kT\right) d\omega_1\, d\omega_2\right]$$
$$= -\langle u^2_{\text{dipole}}\rangle/kT + \cdots = -2\mu_1^2\mu_2^2/3kTR^6 + \cdots \quad (70)$$

where the brackets $\langle\ \rangle$ denote an unweighted average over all orientations ω_1 and ω_2. This long-range attraction is not subject to retardation effects of the type which Casimir and Polder[46] showed changed the R^{-6} dispersion energy into an R^{-7} interaction at separations large compared to the wavelength $\lambda^{(n)} = hc/U^{(n)}$ associated with the important excitation energies in the denominator of Eq. (42). Retardation effects reduce dispersion energies at separations $\sim 10^4$ Å, whereas the excitations associated with the energy $\bar{u}$ of Eq. (70) involve very long wavelength rotational transitions, so retardation effects do not set in until $R \sim 10^7$ Å; at this separation the energy is negligible.

Recently, there have been several attempts to measure the forces between macroscopic bodies,[47] and the thickness of films,[48] and to use the results to obtain information about retarded intermolecular forces. The purpose of this section is to evaluate the interaction between two macroscopic spheres of volume V_1 and V_2 separated by a distance R. If their instantaneous dipole moments are $\mathbf{M}_1$ and $\mathbf{M}_2$,

$$u = -\ T_{2_{\alpha\beta}} M_{1_\alpha} M_{2_\beta}$$

and

$$\bar{u} = -\langle u^2\rangle/kT = -(2/3kTR^6)\langle M_1^2\rangle\langle M_2^2\rangle \quad (71)$$

The mean square dipole moments of the spheres can be expressed in terms of their bulk dielectric constants,

$$\frac{4\pi\langle M_1^2\rangle}{9kTV_1} = \frac{\varepsilon_1 - 1}{\varepsilon_1 + 2} - \frac{\varepsilon_{\infty_1} - 1}{\varepsilon_{\infty_1} + 2} = \frac{3(\varepsilon_1 - \varepsilon_{\infty_1})}{(\varepsilon_1 + 2)(\varepsilon_{\infty_1} + 2)} \quad (72)$$

where ε_1 and ε_{∞_1} are the static and high-frequency dielectric constants of the material comprising sphere 1.[49,50] Hence

$$\frac{\bar{u}}{V_1V_2} = -\frac{243kT}{8\pi^2R^6}\frac{(\varepsilon_1 - \varepsilon_{\infty_1})(\varepsilon_2 - \varepsilon_{\infty_2})}{(\varepsilon_1 + 2)(\varepsilon_{\infty_1} + 2)(\varepsilon_2 + 2)(\varepsilon_{\infty_2} + 2)} \quad (73)$$

If the spheres contain highly polar molecules, $\varepsilon \gg \varepsilon_\infty$ and ε_∞ is normally approximately 2 in a condensed phase. So at room temperature, $\bar{u}/(V_1 V_2) \sim -10^{-14} R^{-6}$ erg cm^{-6}. The unretarded dispersion energy between the spheres is obtainable from Eq. (48), and since

$$(4\pi N\alpha/3) = (\varepsilon_\infty - 1)/(\varepsilon_\infty + 2) \tag{74}$$

it may be written in the form

$$\frac{u_{\text{disp}}}{V_1 V_2} = -\frac{27 U_1 U_2}{32\pi^2 (U_1 + U_2) R^6} \frac{\varepsilon_{\infty_1} - 1}{\varepsilon_{\infty_1} + 2} \frac{\varepsilon_{\infty_2} - 1}{\varepsilon_{\infty_2} + 2} \tag{75}$$

If $U_1 = U_2 = 10^{-11}$ erg, $\bar{u}/u_{\text{disp}} \sim 0.4$. However, at macroscopic separations, the dispersion energy is much reduced by retardation, and $\bar{u}$ may predominate.

If the macroscopic spheres are surrounded by a medium whose static dielectric constant is ε_0,

$$4\pi\langle M^2\rangle/9kTV = [(\varepsilon - \varepsilon_\infty)(2\varepsilon_0 + 1)^2]/[3(\varepsilon + 2\varepsilon_0)(\varepsilon_\infty + 2\varepsilon_0)] \tag{76}$$

where $\langle M^2\rangle$ is now the mean square dipole moment of the sphere in the medium.[51] If the dielectric absorption frequencies of the medium are much higher than those of the spheres, u has to be divided by ε_0 and if both spheres are comprised of the same material,

$$\bar{u}/V_1 V_2 = -[3kT/8\pi^2 \varepsilon_0^2 R^6][(\varepsilon - \varepsilon_\infty)^2 (2\varepsilon_0 + 1)^4]/[(\varepsilon + 2\varepsilon_0)^2 (\varepsilon_\infty + 2\varepsilon_0)^2] \tag{77}$$

For $\varepsilon \gg \varepsilon_\infty$ and $\varepsilon_0 = \varepsilon_\infty = 2$, this gives $\bar{u}/(V_1 V_2) \sim -0.6 \times 10^{-14}\ R^{-6}$ erg cm^{-6}.

These long-range dipole interactions may be of significance in the dynamics of interactions in emulsions as well as in experiments of the general type described in references 47 and 48.

References

1. F. London, *Trans. Faraday Soc.*, **33**, 8 (1937).
2. S. Bhagavantam and D. Suryanarayana, *Acta Cryst.*, **2**, 21 (1949).
3. H. A. Jahn, *Acta Cryst.*, **2**, 30 (1949).
4. A. D. Buckingham and M. J. Stephen, *Trans. Faraday Soc.*, **53**, 884 (1957).
5. L. Jansen, *Physica*, **23**, 599 (1957).
6. E. U. Condon and G. H. Shortley, *Theory of Atomic Spectra*, Cambridge University Press, 1935, Chap. 2.

7. H. Eyring, J. Walter, and G. E. Kimball, *Quantum Chemistry*, Wiley, New York, 1944, Chaps. 8, 17.
8. L. I. Schiff, *Quantum Mechanics*, 2nd ed., McGraw-Hill, New York, 1955, Chap. 8.
9. K. F. Herzfeld and M. Goeppert-Mayer, *Phys. Rev.*, **49**, 332 (1936).
10. J. Fiutak, *Can. J. Phys.*, **41**, 12 (1963).
11. H. A. Kramers and W. Heisenberg, *Z. Physik*, **31**, 681 (1925).
12. E. U. Condon, *Rev. Mod. Phys.*, **9**, 432 (1937).
13. A. Dalgarno, *Advan. Phys.*, **11**, 281 (1962).
14. A. D. Buckingham and P. J. Stephens, *Ann. Rev. Phys. Chem.*, **17**, 399 (1966).
15. M. Born and K. Huang, *Dynamical Theory of Crystal Lattices*, Clarendon Press, Oxford, 1954, p. 189.
16. W. Kauzmann, *Quantum Chemistry*, Academic Press, New York, 1957, Chaps. 15, 16.
17. W. Heitler, *The Quantum Theory of Radiation*, 3rd ed., Oxford University Press, London, 1954, p. 182.
18. H. Margenau, *Rev. Mod. Phys.*, **11**, 1 (1939).
19. H. C. Longuet-Higgins, *Proc. Roy. Soc.* (*London*), **235 A**, 537 (1956).
20. A. D. Buckingham, *Quart. Rev.* (*London*), **13**, 189 (1959).
21. A. D. Buckingham, *Discussions Faraday Soc.*, **40**, 232 (1965).
22. A. Unsöld, *Z. Physik*, **43**, 563 (1927).
23. L. Pauling and J. Y. Beach, *Phys. Rev.*, **47**, 686 (1935).
24. J. O. Hirschfelder and P. O. Löwdin, *Mol. Phys.*, **2**, 229 (1959); **9**, 491 (1965).
25. J. O. Hirschfelder, C. F. Curtiss, and R. B. Bird, *Molecular Theory of Gases and Liquids*, Wiley, New York, 1954, p. 991.
26. J. G. Kirkwood and J. B. Shumaker, *Proc. Nat. Acad. Sci.*, **38**, 863 (1952).
27. P. W. Anderson, *Phys. Rev.*, **80**, 511 (1950).
28. R. M. Herman, *J. Chem. Phys.*, **44**, 1346 (1966).
29. P. Debye, *Polar Molecules*, Chemical Catalog Co., 1929; see also R. J. W. Le Fèvre, *Dipole Moments*, Methuen, London, 1953.
30. C. H. Townes, G. C. Dousmanis, R. L. White, and R. F. Schwarz, *Discussions Faraday Soc.*, **19**, 56 (1955).
31. J. W. Beams, *Rev. Mod. Phys.*, **4**, 133 (1932).
32. A. D. Buckingham and J. A. Pople, *Proc. Phys. Soc.* (*London*), **68A**, 905 (1955); A. D. Buckingham, *Proc. Roy. Soc.* (*London*), **267A**, 271 (1962).
33. C. G. Le Fèvre and R. J. W. Le Fèvre, in *Physical Methods of Organic Chemistry* (*Technique of Organic Chemistry*, Vol. I), 3rd ed., Part III, A. Weissberger, Ed., Interscience, New York, 1960, p. 2459.
34. A. D. Buckingham and B. J. Orr, *Quart. Rev.* (*London*), **21**, 195 (1967).
35. R. W. Terhune, P. D. Maker, and C. M. Savage, *Phys. Rev. Letters*, **14**, 681 (1965).
36. L. L. Boyle, A. D. Buckingham, R. L. Disch, and D. A. Dunmur, *J. Chem. Phys.*, **45**, 1318 (1966).
37. D. A. Dunmur, *Induced Birefringence in Gases*, Oxford University, D. Phil. Thesis, 1965.
38. G. L. Sewell, *Proc. Cambridge Phil. Soc.*, **45**, 678 (1949).
39. N. J. Bridge and A. D. Buckingham, *Proc. Roy. Soc.* (*London*), **295A**, 334 (1966).

40. A. D. Buckingham and R. L. Disch, *Proc. Roy. Soc.* (*London*), **273A**, 275 (1963).
41. L. Wolniewicz, *J. Chem. Phys.*, **45**, 515 (1966).
42. D. E. Stogryn and A. P. Stogryn, *Mol. Phys.*, **11**, 371 (1966).
43. A. D. Buckingham and M. Pariseau, *Trans. Faraday Soc.*, **62**, 1 (1966).
44. A. D. Buckingham, C. A. Coulson, and J. T. Lewis, *Proc. Phys. Soc.* (*London*), **69 A**, 639 (1956).
45. W. H. Keesom, *Physik. Z.*, **22**, 129 (1921).
46. H. B. G. Casimir and D. Polder, *Phys. Rev.*, **73**, 360 (1948).
47. W. Black, J. G. V. de Jongh, J. Th. Overbeek, and M. J. Sparnaay, *Trans. Faraday Soc.*, **56**, 1597 (1960); J. Th. G. Overbeek, *Discussions Faraday Soc.*, **42**, 7 (1966).
48. K. J. Mysels and M. N. Jones, *Discussions Faraday Soc.*, **42**, 42 (1966).
49. F. E. Harris and B. J. Alder, *J. Chem. Phys.*, **21**, 1031 (1953).
50. A. D. Buckingham, *Proc. Roy. Soc.* (*London*), **238 A**, 235 (1956).
51. H. Fröhlich, *Theory of Dielectrics*, 2nd ed., Clarendon Press, Oxford, 1958, p. 181.

3. New Methods for Calculating Long-Range Intermolecular Forces

A. DALGARNO*

School of Physics and Applied Mathematics, The Queen's University of Belfast, Belfast, Northern Ireland

CONTENTS

I. Introduction 143
II. General Theory 144
III. Accurate Calculations 146
A. Atomic Hydrogen 146
B. Helium 148
C. Lithium 149
D. Molecular Hydrogen 150
IV. Semiempirical Methods 150
V. Hartree-Fock Theories 152
VI. Double Perturbation Theory 155
A. Sinanoğlu's Procedure 158
VII. Many-Body Perturbation Theory 160
VIII. Three-Body Forces 160
IX. Special Topics 162
A. Higher-Order Interactions 162
B. Long-Range Effects on Hyperfine Structure 162
X. Recommended Values 163
References 164

I. INTRODUCTION

Substantial advances have been made in recent years in improving the accuracy of the predicted magnitudes of the forces between atomic systems at large separations where exchange forces are negligible. Most of the advances have stemmed from the recognition that the original two-center molecular problem can be transformed into a one-center problem, the solution of which can be obtained using extensions of the various methods that have been developed for calculating the response of an atom to an external perturbation.

* Present address: Department of Astronomy, Harvard University, Cambridge, Massachusetts.

II. GENERAL THEORY

The general theory appropriate to the description of the forces between atomic systems at large separations where the overlap of their charge distributions can be neglected (but not so distant that retardation effects are significant) has been reviewed recently.[1] At large distances R_{ab}, the interaction potential between a neutral atomic system a with n_a electrons with position vectors $\mathbf{r}_i$ measured with respect to the center of charge of a and a second atomic system b with n_b electrons with position vectors $\boldsymbol{\rho}_j$ measured with respect to the center of charge of b may be written

$$V(\mathbf{R}) = \sum_{l_a=1}^{\infty} \sum_{l_b=1}^{\infty} V_{l_a l_b} / R_{ab}^{l_a+l_b+1} \tag{1}$$

where

$$V_{l_a l_b}(\mathbf{r},\boldsymbol{\rho}) = \sum_i \sum_j \sum_\mu \times \frac{(-)^{l_b} 4\pi (l_a + l_b)!\, r_i^{l_a} \rho_j^{l_b} Y_{l_a}^{\mu}(\hat{\mathbf{r}}_i) Y_{l_b}^{-\mu}(\hat{\boldsymbol{\rho}}_j)}{[(2l_a+1)(2l_b+1)(l_a-\mu)!(l_a+\mu)!(l_b-\mu)!(l_b+\mu)!]^{1/2}} \tag{2}$$

The first-order change in the total energy resulting from Eq. (2) is given by

$$E_1 = \langle \psi_0^a \psi_0^b |\, V \,| \psi_0^a \psi_0^b \rangle \tag{3}$$

where $\psi_0^a(\mathbf{r})$ is the eigenfunction of system a and $\psi_0^b(\boldsymbol{\rho})$ is the eigenfunction of system b at an infinite separation.

The evaluation of E_1 is essentially an algebraic problem involving the coupling of angular momenta and it can be solved by a straightforward application of Racah techniques for those systems which can be accurately described by the L–S or by the J–J coupling schemes.[2] Special considerations are necessary for intermediate coupling schemes and at those distances where internal spin–orbit and spin–spin interactions are comparable to the electrostatic interaction.[3] We restrict our attention to the higher-order effects of the electrostatic interaction $V(\mathbf{R})$ and to avoid algebraic complexities we assume that a and b are spherically symmetric. Then $V(\mathbf{R}) = V(R)$ and E_1 vanishes. The second-order energy can be written[1] in atomic units

$$E_2(a,b/R_{ab}) = -16\pi^2 \sum_{l_a=1}^{\infty} \sum_{l_b=1}^{\infty} \frac{(2l_a+2l_b)!}{(2l_a+1)!(2l_b+1)!} \frac{1}{R_{ab}^{2(l_a+l_b+1)}} \times \mathop{S'}_{s} \mathop{S'}_{t} \frac{|\langle\psi_0^a| \sum_i r_i^{l_a} Y_{l_a}^0(\hat{\mathbf{r}}_i) |\psi_s^a\rangle|^2 |\langle\psi_0^b| \sum_j \rho_j^{l_b} Y_{l_b}^0(\hat{\boldsymbol{\rho}}_j) |\psi_0^b\rangle|^2}{(E_s^a - E_0^a) + (E_t^b - E_0^b)} \quad (4)$$

where ψ_s is the eigenfunction of the sth state of the system (a or b according to the superscript), E_s is the associated eigenvalue and the primes indicate that the term $s = 0 = t$ is to be excluded. The leading term of Eq. (4) can be expressed in terms of the electric dipole oscillator strengths

$$f_s = \frac{2}{3}(E_s - E_0) |\langle\psi_0| \sum_i \mathbf{r}_i |\psi_s\rangle|^2 \quad (5)$$

in the form

$$\varepsilon_2(1,1) = -\frac{3}{2R_{ab}^6} \mathop{S'}_{s} \mathop{S'}_{t} f_s^a f_t^b \frac{[(E_s^a - E_0^a)(E_t^b - E_0^b)]^{-1}}{(E_s^a - E_0^a) + (E_t^b - E_0^b)} \quad (6)$$

In the forms of Eqs. (4) and (6), the problem of calculating E_2 is a two-center molecular problem. The single-center method makes use of the identity

$$\frac{1}{a+b} = \frac{2}{\pi} \int_0^{\infty} \frac{ab}{(a^2+u^2)(b^2+u^2)} du \quad \text{when} \quad a > 0, b > 0 \quad (7)$$

Then defining the multipole frequency-dependent polarizabilities

$$\alpha_l(\omega) = \frac{8\pi}{(2l+1)} \mathop{S'}_{s} \frac{(E_s - E_0) |\langle\psi_0| \sum_i r_i^l Y_l^0(\hat{\mathbf{r}}_i) |\psi_s\rangle|^2}{(E_s - E_0)^2 - \omega^2} \quad (8)$$

Eq. (4) can be written[1,4,5]

$$E_2(a,b/R_{ab}) = -\sum_{l_a=1}^{\infty} \sum_{l_b=1}^{\infty} \frac{(2l_a+2l_b)!}{4(2l_a)!(2l_b)!} \frac{1}{R_{ab}^{2(l_a+l_b+1)}} \times \frac{2}{\pi} \int_0^{\infty} \alpha_{l_a}(i\omega)\alpha_{l_b}(i\omega) d\omega \quad (9)$$

The leading term of Eq. (9) is the dipole–dipole interaction term

$$\varepsilon_2(1,1) = -\frac{3}{\pi R^6} \int_0^{\infty} \alpha_1^a(i\omega)\alpha_1^b(i\omega) d\omega \quad (10)$$

where

$$\alpha_1(\omega) = \sum_s{}' f_s/[(E_s - E_0)^2 - \omega^2] \tag{11}$$

The importance of Eq. (9) lies in its reduction of the two-center molecular problem to a one-center atomic problem. Special importance is attached to Eq. (10) because $\alpha_1(\omega)$ equals (apart from a constant factor) the departure from unity of the refractive index of a gas.

The frequency-dependent multipole polarizabilities [Eq. (8)] describe the response of the atomic system to a time-varying (frequency-dependent) external electric field. The problem of calculating the response of an atomic system to a static external field has been investigated in detail[6] and most of the recent developments in the calculation of high-order long-range interactions have been based (or can be based) on extensions of the static field techniques.

III. ACCURATE CALCULATIONS

The infinite summation [Eq. (8)] can be written[5,7]

$$\alpha_l(i\omega) = \frac{8\pi}{2l+1} \langle \psi_0 | \sum_i \nabla_i [r_i^l Y_l^0(\hat{\mathbf{r}}_i)] \cdot \sum_i \nabla_i | \Psi_l \rangle \tag{12}$$

where

$$[(H - E_0)^2 + \omega^2]\Psi_l(\mathbf{r} \mid \omega) + \sum_i r_i^l Y_l^0(\hat{\mathbf{r}}_i)\psi_0(\mathbf{r}) = 0 \tag{13}$$

or alternatively

$$\alpha_l(i\omega) = \frac{8\pi}{2l+1} \langle \psi_0 | \sum_i r_i^l Y_l^0(\hat{\mathbf{r}}_i) | \Phi_l \rangle \tag{14}$$

where

$$[(H - E_0)^2 + \omega^2]\Phi_l(\mathbf{r} \mid \omega) + \sum_i \nabla_i [r_i^l Y_l^0(\hat{\mathbf{r}}_i)] \cdot \sum_i \nabla_i \psi_0(\mathbf{r}) = 0 \tag{15}$$

A. Atomic Hydrogen

Chan and Dalgarno[5] solved Eq. (13) for the ground state of atomic hydrogen by minimizing the functional

$$J(\omega) = \langle \Psi_l | (H - E_0)^2 + \omega^2 | \Psi_l \rangle + 2\langle \Psi_l | r^l Y_l^0(\hat{\mathbf{r}}) | \psi_0 \rangle \tag{16}$$

with respect to the trial function

$$\Psi_l(\mathbf{r} \mid \omega) = \sum_{m=1}^{p} a_m r^m [r^l Y_l^0(\hat{\mathbf{r}})\psi_0(r)] \tag{17}$$

Convergence was very rapid and they obtained for a pair of hydrogen atoms

$$E_2(\text{H–H}) = -[(6.4990/R^6) + (124.4/R^8) + (3285/R^{10}) + O(R^{-12})] \tag{18}$$

With only four parameters, the accuracy is comparable to that of the elaborate two-center calculations of Pauling and Beach,[8] Hirschfelder and Lowdin,[9] and Davison.[10]

For more complex systems, an alternative method of evaluating Eq. (8) has considerable advantages.[1,7,11,12] We may write

$$\alpha_l(\omega) = -\frac{4\pi}{2l+1} \langle \psi_0 | \sum_i r_i^l Y_l^0(\hat{\mathbf{r}}_i) \, | \theta_l(\omega) + \theta_l(-\omega) \rangle \tag{19}$$

where

$$(H - E_0 \pm \omega)\theta_l(\pm\omega) + \sum_{r_i} r_i^l Y_l^0(\hat{\mathbf{r}}_i)\psi_0(\mathbf{r}) = 0 \tag{20}$$

Alternatively

$$\alpha_l(\omega) = -\frac{4\pi}{(2l+1)} \langle \psi_0 | \sum_i \nabla_i (r_i^l Y_l^0(\hat{\mathbf{r}}_i) \cdot \sum \nabla_i \, | \theta_l(\omega) - \theta_l(-\omega) \rangle \tag{21}$$

or

$$\alpha_l(\omega) = -\frac{4\pi}{(2l+1)} \frac{1}{\omega} \langle \psi_0 | \sum_i r_i^l Y_l^0(\hat{\mathbf{r}}_i) \, | \eta_l(\omega) - \eta_l(-\omega) \rangle \tag{22}$$

where

$$(H - E_0 \pm \omega)\eta_l(\pm\omega) + \sum_i \nabla_i [r_i^l Y_l^0(\hat{\mathbf{r}}_i)] \cdot \sum_i \nabla_i \psi_0(\mathbf{r}) = 0 \tag{23}$$

For atomic hydrogen, Eqs. (20) and (23) can be solved analytically and $\alpha_l(\omega)$ can be expressed in terms of the hypergeometric function ${}_2F_1$.[13] Accordingly, exact values of E_2(H–H) could be obtained (the calculation has not in fact been carried out). For other than one-electron systems, solutions cannot be obtained, but variational procedures are available, based on the functionals[14,15]

$$J_1(\omega) = \langle \theta_l | \, H - E_0 + \omega \, | \theta_l \rangle + 2 \langle \theta_l | \sum_i r_i Y_l^0(\hat{\mathbf{r}}_i) \, | \psi_0 \rangle \tag{24}$$

$$J_2(\omega) = \langle \eta_l |\, H - E_0 + \omega \,| \eta_l \rangle + 2 \langle \eta_l | \sum_i \nabla_i [r_i Y_l^0(\hat{\mathbf{r}}_i)] \cdot \sum_i \nabla_i \,| \psi_0 \rangle \quad (25)$$

The stationary values of J_1 and J_2 are actually minima for frequencies such that $E_1 - E_0 + \omega > 0$, E_1 being the eigenvalue of the first excited state for which the matrix element $\langle \psi_0 | \sum r_i^l Y_l^0(\hat{\mathbf{r}}_i) \,| \psi_1 \rangle$ is nonvanishing.[14] By a suitable choice of trial function, it is possible to minimize Eq. (24) or (25) for positive values of ω and to analytically continue the solution to negative and to imaginary values of ω.

Variational solutions of Eq. (20) have been obtained for the ground state of atomic hydrogen by minimizing Eq. (24) with respect to a trial function of the form in Eq. (17).[14,16,17] The procedure yields a representation of $\alpha_1^0(\omega)$ in the form

$$\alpha_1(\omega) = \sum_{m=1}^{p} g_m / (\omega_m^2 - \omega^2) \quad (26)$$

so that

$$\alpha_1(i\omega) = \sum_{m=1}^{p} g_m / (\omega_m^2 + \omega^2) \quad (27)$$

and

$$\varepsilon_2(1,1) = -\frac{3}{2R_{ab}^6} \sum_{m=1}^{p_a} \sum_{m'=1}^{p_b} \frac{g_m^a g_{m'}^b}{\omega_m^a \omega_{m'}^b (\omega_m^a + \omega_{m'}^b)} \quad (28)$$

Similar formulas can be written for the coefficients of higher powers of R_{ab}^{-1}. The calculations result in Eq. (18).

B. Helium

A similar procedure has been applied to the ground state of helium[17,18] based on a 20-parameter representation of the unperturbed eigenfunction $\psi_0(\mathbf{r}_1, \mathbf{r}_2)$ and using the trial function

$$\theta_l(\mathbf{r}_1, \mathbf{r}_2 \mid \pm\omega) = \left[\mathbf{r}_1 \sum_{m=1}^{p} a_m^{\pm}(\omega) r_1^m + \mathbf{r}_2 \sum_{m=1}^{p} a_m^{\pm}(\omega) r_2^m \right] \psi_0(\mathbf{r}_1, \mathbf{r}_2) \quad (29)$$

in Eq. (24). The resulting value of $\varepsilon_2(1,1)$ for a pair of helium atoms is $-1.458/R_{ab}^6$.[12] A comparison of Eq. (26) with experimental refractive-index data shows that the calculations uniformly underestimated the refractive index in the visible region by 0.47%.[18] The form of the trial function [Eq. (29)] is such that the oscillator-strength sum rule

$$\sum_{m=1}^{p} g_m = n \quad (30)$$

is automatically satisfied so that Eq. (26) is exact in the limit of infinite frequency. Thus the value $-1.471/R_{ab}^6$ obtained from scaling up the calculated value of $\varepsilon_2(1,1)$ by 0.94%, as Eq. (10) would suggest, is almost certainly an absolute upper limit to, and must be very near, the correct value. A value of $-1.47/R_{ab}^6$ has also been obtained by Davison[10] from a two-center calculation scaled according to the static polarizability.

An important advantage of the one-center formulation [Eq. (9)] is that having determined $\alpha_l(i\omega)$ for hydrogen and helium it is trivial to calculate E_2(H–He). The value of $\varepsilon_2(1,1)$ for H–He is $-2.830/R_{ab}^6$,[12] again in harmony with two-center calculations.[10]

Trial functions in the form of Eqs. (17) and (29) are inappropriate for systems for which $\psi_0(\mathbf{r})$ contains nodes, partly because they force nodes to occur in $\theta_l(\mathbf{r} \mid \pm\omega)$ at the same points. The trial functions may be made more flexible by writing θ_l as a linear combination of selected basis functions of the appropriate symmetry and performing the standard Rayleigh-Ritz variational procedure. The coefficients g_m may then be computed directly from the matrix elements connecting ψ_0 to each member of the variationally determined set of eigenfunctions and the ω_m is given directly from the variationally determined set of eigenvalues. The oscillator-strength sum rule [Eq. (30)] is not, in general, satisfied identically* and the closeness with which it is reproduced is a measure of the accuracy of the calculated dipole polarizability. Preliminary calculations on the metastable states of helium by the author and G. A. Victor indicate that limited basis sets suffice to yield highly accurate frequency-dependent polarizabilities.

C. Lithium

For systems for which $\alpha_l(\omega)$ is dominated by a single transition matrix element $\langle\psi_0|\sum_i r_i^l Y_l^0(\hat{\mathbf{r}}_i)|\psi_1\rangle$, say, a trial function of the form

$$\theta_l(\mathbf{r}) = \left[\sum_i \sum_{m=1}^{p} a_m r_i^m (r_i^l Y_l^0(\hat{\mathbf{r}}_i))\right]\psi_0(\mathbf{r}) + \lambda\psi_1(\mathbf{r}) \tag{31}$$

is particularly useful. If $\psi_1(\mathbf{r})$ were an exact representation of the eigenfunction, the sum rule in Eq. (30) would still be satisfied. The form of

* The procedure used for H and He corresponds to a special choice of a basis set such that Eq. (30) is satisfied identically.

Eq. (31) has been used by Dalgarno and Stacey[19] to calculate the frequency-dependent dipole polarizability of lithium using the representation of the eigenfunctions of the ground and first excited states obtained by Weiss.[20] The values of $\varepsilon_2(1,1)$ for lithium interacting with hydrogen, helium, and lithium are given in Table I.

TABLE I

Values of $-\varepsilon_2(1,1)R_{ab}^6$ for Mixtures of Atomic Hydrogen, Helium, and Lithium in Atomic Units

	H	He	Li
H	6.499	2.830	66.65
He	2.830	1.471	22.49
Li	66.65	22.49	1391

D. Molecular Hydrogen

The dipole polarizability of molecular hydrogen has also been calculated using trial functions essentially in the form of Eq. (29) (but distinguishing between parallel and perpendicular polarizabilities) and various assumed representations of $\psi_0\ (r_1,r_2)$.[21] The resulting values of $\varepsilon_2(1,1)$ are less accurate than those derived by semiempirical methods.

IV. SEMIEMPIRICAL METHODS

The use of semiempirical methods has been restricted to the dipole–dipole interaction term $\varepsilon_2(1,1)$. In its simplest form, the semiempirical method substitutes the available theoretical and experimental oscillator strengths into Eq. (6).[22] For few systems are all the oscillator strengths that contribute significantly to Eq. (6) reliably known. The lack of data can be partly remedied and the accuracy of the data partly controlled by the use of sum rules. Defining the dipole summations

$$S(k) = \sum_s{}' f_s/(E_s - E_0)^k \tag{32}$$

we have

$$S(0) = n \tag{33}$$

$$S(1) = \frac{2}{3} \langle \psi_0 | \left(\sum_i \mathbf{r}_i \right)^2 | \psi_0 \rangle \tag{34}$$

and

$$\alpha_1(\omega) = \sum_{k=1}^{\infty} S(2k)\omega^{2k} \qquad \omega < E_1 - E_0 \tag{35}$$

Thus values of $S(2k)$ for small values of k can be obtained from measurements of the refractive index (and also of the Verdet constant).[23] The available set of oscillator strengths is augmented and corrected to insure that the various summations are reproduced and then substituted into Eq. (6). This procedure was first applied systematically by Dalgarno and Lynn[24] who obtained a value of $-1.5/R_{ab}^6$ for He–He. In subsequent work, it has yielded values of high precision for a large number of gas mixtures including the inert gases.[25–28] Most of the experimental values are now consistent with the semiempirical predictions.[1]

An interesting modification of the procedure has been suggested by Bell,[26] who pointed out that Eq. (6) could be written

$$\varepsilon_2(1,1) = -\frac{3}{2E^3} \mathop{\mathbf{S}'}_{s} \mathop{\mathbf{S}'}_{t} f_s^a f_t^b \phi(x_s, y_t) \tag{36}$$

where

$$E = \min (E_1^a - E^a, E_1^b - E^b) \tag{37}$$

$$x_s = E/(E_s^a - E_0^a) \qquad y_t = E/(E_t^b - E_0^a) \tag{38}$$

and

$$\phi(x,y) = x^2y^2/(x + y) \tag{39}$$

The function $\phi(x,y)$ can be accurately represented by

$$\phi(x,y) \simeq \sum_i \sum_j C_{ij} x^i y^j \tag{40}$$

where C_{ij} are constants chosen to make Eq. (40) accurate in the range $0 \leq x \leq 1$, $0 \leq y \leq 1$. Then

$$\varepsilon_2(1,1) = -\frac{3}{2E^3} \sum_i \sum_j C_{ij} E^{i+j} S_a(i) S_b(j) \tag{41}$$

and no explicit oscillator strength distribution is required. The procedure has been extended to treat three-body long-range interactions.[27]

Bell's summation procedure is computationally more convenient than the procedure employing a selected oscillator-strength distribution and the loss of accuracy that it necessarily entails will usually be negligible within the uncertainties attendant on the refractive-index data.

Another modification has been suggested by Dalgarno, Morrison, and Pengelly,[28] who proceed directly from the refractive-index data without explicitly deriving either an oscillator-strength distribution or the summations. They use a numerical method to fit the refractive-index data into the form of Eq. (26). The procedure is readily extended to three-body long-range interactions.[28]

Semiempirical methods cannot be applied effectively to terms falling off more rapidly than R_{ab}^{-6}. The semiempirical dipole–dipole values provide a valuable check on the usefulness of the purely theoretical methods that are necessary for the higher terms of the series expansion for $E_2(R)$.

V. HARTREE-FOCK THEORIES

In seeking a method generally applicable to complex systems, it is natural to adopt as a description of the unperturbed system the Hartree-Fock approximations $\phi_0^a(\mathbf{r})$ and $\phi_0^b(\boldsymbol{\rho})$ for the eigenfunctions of the separated systems (the Hartree-Fock approximation applied directly without configuration interaction to the molecular system does not yield the long-range interactions). Hartree-Fock perturbation theories have been widely applied to atoms and molecules perturbed by static fields. If the orbitals are constrained to relax independently of each other, the *uncoupled* version results and if the restriction is removed the coupled version results.[6,30] The extension of the uncoupled version to time-dependent perturbations has been carried out by Karplus and Kolker[31] and the coupled version has been extended by Dalgarno and Victor.[32]*

In the uncoupled scheme, the Hamiltonian in Eq. (20) is replaced by the Hartree-Fock Hamiltonian H_F. Then, writing

$$\phi_0(\mathbf{r}) = \mathscr{A} \prod_{i=1}^{n} u_i^{(0)}(\mathbf{r}_i) \tag{42}$$

* The coupled version is what is customarily described as time-dependent Hartree-Fock theory (TDHF) and it is closely related to the random phase approximation (RPA).

and

$$\theta_i(\mathbf{r}) = \mathscr{A} \sum_{j=1}^{n} \prod_{i \neq j} u_i^{(0)}(\mathbf{r}_i) u_j^{(1)}(\mathbf{r}_j \mid \omega) \tag{43}$$

where $u_j^{(0)}$ is the unperturbed orbital satisfying the usual Hartree-Fock equation

$$(H_i - \varepsilon_i^{(0)}) u_i^{(0)}(\mathbf{r}_i) = 0 \tag{44}$$

it may be shown that

$$(H_i - \varepsilon_i^{(0)} \pm \omega) u_i^{(1)}(\mathbf{r} \mid \pm\omega) + r^l Y_l^0(\hat{\mathbf{r}}) u_i^{(0)}(\mathbf{r}) - \sum_{k \neq i} \{(\varepsilon_k^{(0)} - \varepsilon_i^{(0)} \pm \omega) \langle u_k^{(0)} \mid u_i^{(1)}(\pm\omega) \rangle + \langle u_k^{(0)} \mid r^l Y_l^0 \mid u_k^{(0)} \rangle\} u_k^{(0)}(\mathbf{r}) = 0 \tag{45}$$

The nonlocal Hamiltonian H_i contains a summation over the occupied orbitals $u_k^{(0)}$. It may either include or exclude the orbital $u_i^{(0)}$. For perturbations which distort the electron density at large distances from the nucleus, it appears more accurate to exclude the self-interaction term.[33] In proceeding to higher-order approximations, it may be more convenient to retain this term.

For the frequency-dependent dipole polarizability of helium, Eq. (45) reduces to

$$(h - \varepsilon^{(0)} \pm \omega) u^{(1)}(\mathbf{r} \mid \pm\omega) + r Y_l^0(\hat{\mathbf{r}}) u^{(0)}(r) = 0 \tag{46}$$

where

$$h = \left[-\frac{1}{2} \nabla^2 - \frac{2}{r} + \int_0^\infty \frac{|u_0(r')|^2}{|\mathbf{r} - \mathbf{r}'|} d\mathbf{r}' \right] \tag{47}$$

and

$$\alpha_1(\omega) = -8\pi \langle u^{(0)} \mid r Y_1^0(\hat{\mathbf{r}}) \mid u^{(1)}(+\omega) + u^{(1)}(-\omega) \rangle \tag{48}$$

Since only the sum $u^{(1)}(+\omega) + u^{(1)}(-\omega)$ enters into Eq. (47), Eq. (46) can be replaced as follows,

$$[(h - \varepsilon^{(0)})^2 + \omega^2][u^{(1)}(\mathbf{r} \mid i\omega) + u^{(1)}(\mathbf{r} \mid -i\omega)] + 2(h - \varepsilon^{(0)}) r Y_1^0(\hat{\mathbf{r}}) u^{(0)}(\mathbf{r}) = 0 \tag{49}$$

and $\alpha_1(i\omega)$ can be obtained directly.

Equation (46) has been solved variationally using a trial function

$$u^{(1)}(\mathbf{r} \mid \pm\omega) = \sum_{m=1}^{p} r^m (rY_1^{(0)}(\hat{\mathbf{r}}))u^{(0)}(r) \tag{50}$$

Various values of the dipole–dipole interaction term for a pair of helium atoms have been obtained, depending upon the representation adopted

TABLE II

$-\varepsilon_2(1,1)R_{ab}^6$ for He–He Using the Uncoupled Hartree-Fock Theory

Karplus and Kolker[31]	1.6551
Kestner[35]	1.6443
Deal and Kestner[36]	1.649
	1.655
Victor[37]	1.664[a]
Correct value	1.471

[a] This value is probably the most accurate.

for $u^{(0)}(r)$. They are listed in Table II. Because the uncoupled approximation ignores correlation between the electrons, it overestimates $\varepsilon_2(1,1)$.* For He–He, the error is about 12%.

An approximate form of the uncoupled approximation has been used[31] to calculate dipole–dipole interactions for heavier systems. The values are generally much too large but it is uncertain how much of the error can be attributed to the additional approximations that were invoked to simplify the computations.

Correlation effects can be incorporated into the uncoupled Hartree-Fock theory by the application of double perturbation theory or by proceeding to coupled Hartree-Fock theory. We shall not reproduce the general equations of the coupled theory.[32] For helium, they have the comparatively simple form

$$(h - \varepsilon^{(0)} \pm \omega)u^{(1)}(\mathbf{r} \mid \pm\omega) + \left[\int \frac{u^0(r)\{u^{(1)}(\mathbf{r} \mid +\omega) + u^{(1)}(\mathbf{r} \mid -\omega)\}}{|\mathbf{r} - \mathbf{r}'|}\, d\mathbf{r}' + rY_1^0(\hat{\mathbf{r}})\right]u^0(r) = 0 \tag{51}$$

* It overestimates essentially because in the Hartree-Fock approximation the matrix element $\langle\phi_0|\, \mathbf{r}_1 \cdot \mathbf{r}_2\, |\phi_0\rangle$ vanishes. The inclusion of correlation would make it negative. This argument can be made quantitative.

Thus, the positive and negative frequency solutions are coupled together.

Alternatively, Eq. (51) may be replaced by

$$[(h-\varepsilon^{(0)})^2+\omega^2][u^{(1)}(\mathbf{r}\mid i\omega)+u^{(1)}(\mathbf{r}\mid -i\omega)]$$
$$+2(h-\varepsilon^{(0)})rY_1^0(\mathbf{r})u^{(0)}(r)$$
$$+2(h-\varepsilon^{(0)})\int\frac{u^{(0)}(r')[u^{(1)}(\mathbf{r}'\mid i\omega)+u^{(1)}(\mathbf{r}'\mid -i\omega)]}{|\mathbf{r}-\mathbf{r}'|}\,d\mathbf{r}'$$
$$\times u^{(0)}(r)=0 \quad (52)$$

Equations (51) have been solved variationally[38] and the resulting value of $\varepsilon_2(1,1)R_{ab}^6$ for He–He is -1.376, i.e., about 7% too small in magnitude. Similar procedures have been applied to the higher terms of the series expansion of $E_2(R)$ with the result that[38] for He–He

$$E_2(R)=-\left[\frac{1.376}{R_{ab}^6}+\frac{13.18}{R_{ab}^8}+\frac{110.44+59.39}{R_{ab}^{10}}+O(R^{-12})\right] \quad (53)$$

the dipole–octupole term contributing 110.44 to the R_{ab}^{-10} coefficient and the quadrupole–quadrupole term contributing 59.39. Two-center calculations[10] give a value of -14.09 for the R^{-8} so that the coupled theory again overestimates by 7%. The best estimate of $E_2(R)$ for He–He is accordingly

$$E_2(R)=-\left[\frac{1.471}{R_{ab}^6}+\frac{14.1}{R_{ab}^8}+\frac{182}{R_{ab}^{10}}+O(R_{ab}^{-12})\right] \quad (54)$$

VI. DOUBLE PERTURBATION THEORY

Double perturbation theory[7,38,39] is an attractive procedure for including the first-order effects of correlation because of interchange theorems which render the determination of the correlated wave function unnecessary. The procedure was used by Dalgarno and Stewart[39] to calculate the static dipole polarizability of helium and by Dalgarno, Davison, and Stewart[40] to calculate the static quadrupole polarizability and shielding factor of helium. It was extended to time-dependent problems by Hirschfelder, Brown, and Epstein[7] and was used to calculate the refractive index of helium by Musulin and Epstein.[41] The first application to long-range forces has been made recently by Deal and Kestner.[35]

The Hamiltonian H of an atomic system is written as a sum of a Hamiltonian H_0 and a perturbation potential $v(r)$:

$$H = H_0 + v(r) \tag{55}$$

Then expanding

$$E_m = \sum_{h=0}^{\infty} E_m^{(n)} \qquad \psi_0 = \sum_{h=0}^{\infty} \psi_0^{(n)} \qquad \theta_l = \sum_{h=0}^{\infty} \theta_l^{(n)} \tag{56}$$

the superscript (n) denoting the order in the perturbation $v(r)$, Eq. (20) is replaced to first order in $v(r)$ by the equations

$$(H_0 - E_0^{(0)})\psi_0^{(0)} = 0 \qquad (H_0 - E_0^{(0)})\psi_0^{(1)} + (v - E_1^{(0)})\psi_0^{(0)} = 0 \tag{57}$$

$$(H_0 - E_0^{(0)} \pm \omega)\theta_l^{(0)}(\mathbf{r} \mid \pm\omega) + \sum_i r_i Y_l^0(\hat{\mathbf{r}}_i)\psi_0^{(0)} = 0 \tag{58}$$

$$(H_0 - E_0^{(0)} \pm \omega)\theta_l^{(1)}(\mathbf{r} \mid \pm\omega) + \sum_i r_i Y_l^0(\hat{\mathbf{r}}_i)\psi_0^{(1)} + (v - E_1^{(0)})\theta_l^{(0)}(\mathbf{r} \mid \pm\omega) = 0 \tag{59}$$

and Eq. (19) is replaced by

$$\alpha_l(\omega) = \alpha_l^{(0)}(\omega) + \alpha_l^{(1)}(\omega) \tag{60}$$

where

$$\alpha_l^{(0)}(\omega) = -[4\pi/(2l+1)]\langle\psi_0^{(0)}| \sum_i r_i Y_l^0(\hat{\mathbf{r}}_i)\,|\theta_l^{(0)}(+\omega) + \theta_l^{(0)}(-\omega)\rangle \tag{61}$$

$$\alpha_l^{(1)}(\omega) = -[4\pi/(2l+1)]\Big\{\langle\psi_0^{(0)}| \sum_i r_i Y_l^0(\hat{\mathbf{r}}_i)\,|\theta_l^{(1)}(\omega) + \theta_l^{(1)}(-\omega)\rangle + \langle\psi_0^{(1)}| \sum_i r_i Y_l^{(0)}(\hat{\mathbf{r}}_i)\,|\theta_l^{(0)}(\omega) + \theta_l^{(0)}(-\omega)\rangle\Big\} \tag{62}$$

We can avoid the determination of the first-order correlated wave function $\psi_0^{(1)}$ by using the interchange theorem[7,38,39]

$$\langle\psi_0^{(1)}| \sum_i r_i Y_l^{(0)}(\hat{\mathbf{r}}_i)\,|\theta_l^{(0)}(\pm\omega)\rangle = \langle X|\, v - E_0^{(1)}\,|\psi_0^{(0)}\rangle \tag{63}$$

where

$$(H_0 - E_0^{(0)})X + \sum_i r_i Y_l^0(\hat{\mathbf{r}}_i)\theta_l^{(0)}(\pm\omega) = \langle\psi_0^{(0)}| \sum_i r_i Y_l^0(\hat{\mathbf{r}}_i)\,|\theta_l^{(0)}(\pm\omega)\rangle\psi_0^{(0)} \tag{64}$$

Then

$$\alpha_l^{(1)}(\omega) = -[4\pi/(2l+1)]\{\langle\theta_l^{(0)}(+\omega)|\, v - E_0^{(1)}\,|\theta_l^{(0)}(-\omega)\rangle + \langle\theta_l^{(0)}(-\omega)|\, v - E_0^{(1)}\,|\theta_l^{(0)}(-\omega)\rangle + 2\langle X|\, v - E_0^{(1)}\,|\psi_0^{(0)}\rangle\} \tag{65}$$

We can proceed alternatively by replacing Eq. (58) by the equivalent equations

$$[(H_0 - E_0^{(0)})^2 - \omega^2][\theta_l(+\omega) + \theta_l(-\omega)] + 2(H_0 - E_0^{(0)}) \sum_i r_i^l Y_l^0(\hat{\mathbf{r}}_i)\psi_0^{(0)} = 0 \tag{66}$$

and

$$[(H - E_0^{(0)})^2 - \omega^2][\theta_l(+\omega) - \theta_l(-\omega)] + 2\omega \sum_i r_i^l Y_l^{(0)}(\hat{\mathbf{r}}_i)\psi_0^{(0)} = 0 \tag{67}$$

which have the advantage of being directly solvable for the imaginary values of ω required in Eq. (10). The equations can be obtained directly by substituting Eq. (56) into Eq. (15).

Deal and Kestner[35] in fact solved Eqs. (66) and (67) with ω^2 replaced by $-\omega^2$ by minimizing the appropriate functionals, [cf. Eqs. (13), (16), and (15)].* They carried out calculations for helium based upon a screened hydrogenic approximation[42] for ψ_0 and upon the Hartree-Fock approximation for ψ_0. The results in the screened hydrogenic approximation are, of course, comparable in accuracy to those obtained for the refractive index.[41] The accuracy will presumably decrease for heavier systems. The inclusion of first-order correlation in the Hartree-Fock theory changes $\varepsilon_2(1,1)R_{ab}^6$ from 1.649 to 1.375 or from 1.655 to 1.382, depending upon the representation adopted for the unperturbed orbital. Within the computational uncertainties, the effect of correlation is identical to that derived from coupled time-dependent perturbation theory.[37]

The main disadvantage of the approach using double perturbation theory is the fact that Eq. (64) involves the coordinates of two electrons whereas time-dependent Hartree-Fock theory reduces to single electron

* For more complex systems, it will usually be less laborious to solve Eq. (58), as suggested in Section III-A. Some simplification of the procedure of Deal and Kestner might be possible by using the perturbation expansion of Eqs. (12) and (13) rather than of Eqs. (14) and (15).

orbital equations. Double perturbation theory can of course be extended to higher order without formal difficulty.

Calculations have also been carried out for Li^+–Li^+. The inclusion of correlation changes $\varepsilon_2(1,1)R_{ab}^6$ from 0.0867 to 0.0774. Thus, as expected, the importance of correlation diminishes with increasing nuclear charge.

A. Sinanoğlu's Procedure

Sinanoğlu and Kestner[43] have described a procedure for the calculation of intermolecular forces which has been used for a detailed study of the He–He interaction potential.[43,44] We present a version of it, appropriate to long-range forces, within the framework of double perturbation theory. The theory is a two-center one and as such it is concerned with solving the equation

$$(H_a + H_b - E_0^a - E_0^b)\Psi^{(1)} + V(R)\Psi^{(0)} = 0 \tag{68}$$

where

$$\Psi^{(0)}(\mathbf{r}, \boldsymbol{\rho}) = \psi_0^a(\mathbf{r})\psi_0^b(\boldsymbol{\rho}) \tag{69}$$

and

$$(H_a - E_0^a)\psi_0^a = (H_b - E_0^b)\psi_0^b = 0 \tag{70}$$

The second-order interaction arising from $V(R)$ is given by

$$E_2(R) = \langle \Psi^{(0)} | \, V \, | \Psi^{(1)} \rangle \tag{71}$$

We write

$$H_a = H_{a0} + v_a(\mathbf{r}), \qquad H_b = H_{b0} + v_b(\boldsymbol{\rho})$$

where

$$(H_{a0} - E_{00}^a)\psi_{00}^a(\mathbf{r}) = (H_{b0} - E_{00}^b)\psi_{00}^b(\boldsymbol{\rho}) = 0 \tag{72}$$

Then expanding in powers of v_a and v_b

$$\Psi^{(0)} = \psi_{00}^a\psi_{00}^b + \psi_{00}^a\psi_{01}^b + \psi_{01}^a\psi_{00}^b + \cdots \tag{73}$$

$$\Psi^{(1)} = \Psi_0^{(1)} + \Psi_1^{(1)} + \cdots \tag{74}$$

$$E_2(R) = E_2^{(0)}(R) + E_2^{(1)}(R) + \cdots \tag{75}$$

we have that

$$E_2^{(0)}(R) = \langle \psi_{00}^a\psi_{00}^b | \, V \, | \Psi_0^{(1)} \rangle \tag{76}$$

and

$$E_2^{(1)}(R) = \langle(\psi_{00}^a\psi_{00}^b + \psi_{01}^a\psi_{00}^b)|\ V\ |\Phi_0^{(1)}\rangle + \langle\psi_{00}^a\psi_{00}^b|\ V\ |\Psi_1^{(1)}\rangle \quad (77)$$

where

$$(H_{a0} - E_{00}^a)\psi_{01}^a(\mathbf{r}) + (v_a - E_{01}^a)\psi_{00}^a(\mathbf{r}) = 0 \quad (78)$$

$$(H_{b0} - E_{00}^b)\psi_{01}^b(\boldsymbol{\rho}) + (v_b - E_{01}^b)\psi_{00}^b(\boldsymbol{\rho}) = 0 \quad (79)$$

$$(H_{a0} + H_{b0} - E_{00}^a - E_{00}^b)\Psi_0^{(1)} + V(R)\psi_{00}^a\psi_{00}^b = 0 \quad (80)$$

and

$$(H_{a0} + H_{b0} - E_{00}^a - E_{00}^b)\Psi_1^{(1)} + V(R)(\psi_{00}^a\psi_{01}^b + \psi_{01}^a\psi_{00}^b) + (v_a + v_b - E_{01}^a - E_{01}^b)\Psi_0^{(1)} = 0 \quad (81)$$

If we identify ψ_{00}^a and ψ_{00}^b as the Hartree-Fock approximations to the eigenfunctions of the separated systems, $E_1^{(0)}(R)$ is *identical* to the uncoupled Hartree-Fock value obtained from the single-center method.

With some slight manipulation,[39] the first-order correction for correlation $E_2^{(1)}(R)$ can be written in the form

$$E_2^{(1)}(R) = 2\langle(\psi_{00}^a\psi_{01}^b + \psi_{01}^a\psi_{00}^b)|\ V(R)\ |\Psi_0^{(1)}\rangle + \langle\Psi_0^{(1)}|\ v_a + v_b\ |\Psi_0^{(1)}\rangle \quad (82)$$

In the notation of Sinanoğlu and Kestner, the first term is IV(1,2,3) arising from inter- and intraatomic pairs (it involves the correlation corrections to the separated atomic system eigenfunctions and the uncorrelated molecular wave function perturbed by the mutual interaction) and the second term is III(1,3,2) arising from two interatomic pairs (it involves only the uncorrelated molecular wave function perturbed by the mutual interaction).

As employed by Sinanoğlu and Kestner, the procedure requires a knowledge of the first-order correlated-pair eigenfunctions of the individual atoms. For complex systems it may be more convenient to escape from this requirement by using an interchange theorem:

$$\langle(\psi_{00}^a\psi_{01}^b + \psi_{01}^a\psi_{00}^b)|\ V(R)\ |\Psi_0^{(1)}\rangle = \langle\Theta_1^{ab}|\ v_a + v_b\ |\Psi_0^{(0)}\rangle \quad (83)$$

where

$$(H_{a0} + H_{b0} - E_{a0} - E_{b0})\Theta_1^{ab} + V(R)\Psi_0^{(1)} = \langle\Psi_0^{(0)}|\ V(R)\ |\Psi_0^{(1)}\rangle\Psi_0^{(0)} \quad (84)$$

Equation (84) can be solved by variational procedures similar to those used for the determination of $\Psi_0^{(1)}$.

The separate terms of Eq. (82) can be identified with the products of the separate terms of Eq. (65) with those of the other atom. In the single-center method, there are additional cross terms and some second-order correlation effects not included in the two-center procedure. There are other second-order correlation effects which are probably larger than those included in the single-center method (when taken to only first order).[45]

Kestner[44] has evaluated Eqs. (81) and (82) for the helium–helium interaction, obtaining the following result

$$E_2(R_{ab}) = -\left(\frac{1.353}{R_{ab}^6} + \frac{13.25}{R_{ab}^8} + \frac{94.45 + 52.45}{R_{ab}^{10}} + O(R^{-12})\right) \quad (85)$$

There are numerical uncertainties in Eq. (85) arising from the lack of convergence of the variational procedures used to solve Eq. (80) and from the use of a simple approximate representation of the correlated-pair wave function ψ_{01}^a. Comparison with the value -1.375 of the R^{-6} coefficient derived from the first-order calculations in the single-center method and with the results [Eq. (53)] of time-dependent Hartree-Fock theory provides tentative support for the expectation that the single-center formulation is slightly more accurate but emphasizes that the second-order correlation effects that are included are less important than those that are not.

VII. MANY-BODY PERTURBATION THEORY

The many-body perturbation theory of Brueckner[46] and Goldstone[47] has been applied to the calculation of many atomic properties and in particular to the calculation of static atomic polarizabilities.[48] Because of Eq. (9) only a simple extension is required for the calculation of long-range interactions, especially since it represents the static polarizabilities in the zero frequency form of Eq. (11). No application to long-range interactions has been reported, though results have been obtained for the frequency-dependent dipole polarizability of beryllium[49] with a many-body procedure comparable in physical content to the uncoupled Hartree-Fock theory.

VIII. THREE-BODY FORCES

The leading term of the nonadditive contribution to the energy of interaction of three nonoverlapping systems a, b, and c at separations

R_{ab}, R_{bc}, and R_{ca} can be expressed as[4]

$$E_3(R_{ab},R_{bc},R_{ca}) = \nu(a,b,c)(1 + 3\cos\theta_a\cos\theta_b\cos\theta_c)/(R_{ab}R_{bc}R_{ca})^3 \quad (86)$$

where θ_a, θ_b, and θ_c are the internal angles of the triangle abc and

$$\nu(a,b,c) = \frac{3}{\pi}\int_0^\infty d\omega\alpha_1^a(i\omega)\alpha_1^b(i\omega)\alpha_1^c(i\omega) \quad (87)$$

Accurate values of $\nu(a,b,c)$ have been predicted from variational determinations of $\alpha_1(i\omega)$ for mixtures of hydrogen and helium atoms[37] and they are presented in Table III. They are in harmony with a previous

TABLE III

Accurate Values of $\nu(a,b,c)$ for H–He Mixtures in Atomic Units

a	b	c	Accurate	Uncoupled Hartree-Fock	Coupled Hartree-Fock
H	H	H	21.6425	—	—
H	H	He	8.12	8.70	7.78
H	He	He	3.28	3.76	3.03
He	He	He	1.49	1.82	1.33

TABLE IV

Values of $\nu(a,b,c)$ for $a \equiv b \equiv c$[27,28] in Atomic Units

a	$\nu(a,b,c)$
H	21.6
He	1.49
Ne	11.8
Ar	521
Kr	1560
Xe	5430
H_2^a	49.0
N_2^a	620

[a] The molecular values refer to the spherical average of the coefficients.

calculation using an alternative single-center version of Eq. (87)[50] and with values derived by Bell's summation technique.[27] Values have also

been obtained in the uncoupled and coupled time-dependent Hartree-Fock approximations[51] and they are included in Table III.

Dalgarno, Morrison, and Pengelly[28] have derived values from refractive index data for mixtures of a wide range of gases, most of which have been treated also by Bell and Kingston[27] by the summation procedure. Values of $\nu(a,b,c)$ for identical atoms $a \equiv b \equiv c$ are given in Table IV.

IX. SPECIAL TOPICS

A. Higher-Order Interactions

The reduction of the second-order two-center problem to a single-center problem can also be achieved for higher-order interactions.[52] The third-order energy $E_3(R_{ab})$ for a pair of atoms is given by

$$E_3(R_{ab}) = -\sum_{s}{}' \sum_{t}{}' \sum_{u}{}' \sum_{v}{}' \times \frac{\langle\psi_0^a\psi_0^b|\ V\ |\psi_s^a\psi\psi_t^b\rangle\langle\psi_s^a\psi_t^b|\ V\ |\psi_n^a\psi_v^b\rangle\langle\psi_n^a\psi_v^b|\ V\ |\psi_0^a\psi_0^b\rangle}{(E_s^a - E_0^a + E_t^b - E_0^b)(E_u^a - E_0^a + E_v^b - E_0^b)} \tag{88}$$

For spherically symmetric systems, the leading term is a dipole–quadrupole–dipole interaction varying as R^{-11}. Using Eq. (7), Eq. (88) can be reduced to a double integral of sums of products of terms

$$\langle\Phi_l^a(\omega)|\sum_i r_i^{l'} Y_{l'}^0(\hat{\mathbf{r}}_i)\,|\Phi_{l''}^a(\omega)\rangle \tag{89}$$

where $\Phi_l^a(\omega)$ is the solution of Eq. (15). Other formulas can be derived for $E_3(R_{ab})$ in terms of double integrals involving solutions of Eq. (23). For H–H, Chan and Dalgarno[52] solved Eq. (15) by variational methods and obtained

$$E_3(\text{H–H}\mid R_{ab}) = -3986^*/R_{ab}^{11} \tag{90}$$

B. Long-Range Effects on Hyperfine Structure

The single-center method can be used to simplify the study of the influence of long-range interactions on other perturbations, such as those responsible for hyperfine structure. Thus, the differences in the interactions between an atom in one hyperfine level and a perturbing molecule

* Earlier estimates by Dalgarno and Lewis[53] are in error by a factor of three.

and an atom in another hyperfine level are of importance to the understanding of the observed shifts in the collision broadening of spectral lines[54] and the differences are also significant for the interpretation of electron spin resonance spectra of atoms trapped in a solid matrix.[55] As an example, we demonstrate the application of the single-center method to the latter problem, which reduces to the evaluation[55] of

$$\begin{aligned}\Delta E = &-2 \sum_s{}' \sum_t{}' \sum_u{}' \langle\psi_0^a| h' |\psi_s^a\rangle\langle\psi_s^a| \sum_i r_i Y_1^0(\hat{\mathbf{r}}_i) |\psi_t^a\rangle \\ &\times \langle\psi_0^b| \sum_j \rho_j Y_1^0(\hat{\boldsymbol{\rho}}_j) |\psi_u^b\rangle\langle\psi_t^a| \sum_i r_i Y_1^0(\hat{\mathbf{r}}_i) |\psi_0^a\rangle \\ &\times \langle\psi_u^b| \sum_j \rho_j Y_1^0(\hat{\boldsymbol{\rho}}_j) |\psi_0^b\rangle / (E_s^a - E_0^a)(E_t^a - E_0^a + E_u^b - E_0^b) \\ &- \langle\psi_0^a| h' |\psi_0^a\rangle \sum_t{}' \sum_u{}' \frac{|\langle\psi_0^a| \sum_i r_i Y_1^0(\hat{\mathbf{r}}_i) |\psi_t^0\rangle|^2 |\langle\psi_0^l| \sum_j \rho_j Y_1^0(\hat{\boldsymbol{\rho}}_j) |\psi_u^b\rangle|^2}{(E_t^a - E_0^a + E_u^b - E_0^b)^2}\end{aligned} \tag{91}$$

where h' is the operator causing the hyperfine structure splitting.

Introduce X such that

$$(H_a - E_0^a)X + \{h' - \langle\psi_0^a| h' |\psi_0^a\rangle\}\psi_0^a = 0 \tag{92}$$

Then

$$\begin{aligned}\Delta E = \frac{3}{2\pi^2} \int_0^\infty d\omega \alpha_1^b(i\omega) \langle\Phi_1^a(\omega)| \sum_i r_i Y_1^{(0)}(\hat{\mathbf{r}}_i) |X\rangle \\ - \langle\psi_0^a| h' |\psi_0^a\rangle \frac{2}{\pi} \int_0^\infty d\omega \Phi_1^a(\omega)\Phi_1^b(\omega)\end{aligned} \tag{93}$$

where Φ_1 is the solution of Eq. (15).

In one of the cases of interest, $h' = \delta(\mathbf{r})$ and atom a is atomic hydrogen. Equation (92) may be solved analytically[56] and

$$X = \frac{1}{4}\{-(1/r) + 2lnr + 2r\}\psi_0 \tag{94}$$

For other systems, variational methods can be used.

X. RECOMMENDED VALUES

For the analysis of experimental data on transport phenomena, the equilibrium properties of gases, and on crystal structure, it may be

useful to present a collection of values of the dipole–dipole interaction term. The collection is given in Table V. With the possible exception

TABLE V

Recommended Values of the Dipole–Dipole Interaction Term $-\varepsilon_2(1,1)R_{ab}^6$ for Spherically Symmetric Systems in Atomic Units ($e^2a_0^5$)

	H	He	Ne	Ar	Kr	Xe	H_2	N_2	CH_4	Li	Na	K	Rb	Cs
H	6.50	2.83	5.6	20	29	42	8.7	21	30	67	73	100	110	140
He	2.83	1.47	3.0	9.6	13	19	4.1	10	14	22	25	34	37	45
Ne	5.6	3.0	6.3	20	27	38	8.2	21	29	42	48	66	72	87
Ar	20	9.6	20	65	91	130	28	69	98	180	190	270	290	350
Kr	29	13	27	91	130	190	40	96	140	260	280	400	430	520
Xe	42	19	38	130	190	270	58	140	200	410	450	630	690	830
H_2	8.7	4.1	8.2	28	40	58	13	30	43	83	91	130	140	170
N_2	21	10	21	69	96	140	30	73	100	180	200	280	310	370
CH_4	30	14	29	98	140	200	43	100	150	290	310	440	480	580
Li	67	22	42	180	260	410	83	180	290	1390	1470	2290	2510	3160
Na	73	25	48	190	280	450	91	200	310	1470	1580	2440	2670	3350
K	100	34	66	270	400	630	130	280	440	2290	2440	3820	4190	5300
Rb	110	37	72	290	430	690	140	310	480	2510	2670	4190	4600	5820
Cs	140	45	87	350	520	830	170	370	580	3160	3350	5300	5820	7380

of interactions involving Xe, in no case should the error exceed 10% and it is usually much smaller.

References

1. A. Dalgarno and W. D. Davison, *Advan. At. Mol. Phys.*, **2**, 1 (1966).
2. J. K. Knipp, *Phys. Rev.*, **53**, 734 (1938); P. G. Burke, A. Dalgarno, and J. H. Tait, in press, 1967.
3. P. R. Fontana, *Phys. Rev.*, **125**, 1597 (1962).
4. M. R. Aub and S. Zienau, *Proc. Roy. Soc.* (*London*), **A257**, 464 (1960); C. Mavroyannis and M. J. Stephen, *Mol. Phys.*, **5**, 629 (1962); B. Linder, *J. Chem. Phys.*, **37**, 963 (1962); A. D. McLachlan, *Proc. Roy. Soc.* (*London*), **A271**, 387 (1963); B. Linder and D. Hoernschmeyer, *J. Chem. Phys.*, **40**, 622 (1964).
5. Y. M. Chan and A. Dalgarno, *Mol. Phys.*, **9**, 349, (1965).
6. Cf. A. Dalgarno, *Advan. Phys.*, **11**, 281 (1962).
7. J. O. Hirschfelder, W. B. Brown, and S. T. Epstein, *Advan. Quantum Chem.*, **1**. 256 (1964).
8. L. Pauling and J. Y. Beach, *Phys. Rev.*, **47**, 686 (1935).

9. J. O. Hirschfelder and P. O. Löwdin, *Mol. Phys.*, **2**, 229 (1959); and **9**, 491 (1965).
10. W. D. Davison, *Proc. Phys. Soc.* (*London*), **87**, 133 (1966).
11. C. M. Mavroyannis and M. J. Stephen, *Mol. Phys.*, **5**, 629 (1962); M. Karplus and H. J. Kolker, *J. Chem. Phys.*, **41**, 880 (1964); H. J. Kolker and H. H. Michels, *J. Chem. Phys.*, **43**, 1027 (1965).
12. Y. M. Chan and A. Dalgarno, *Proc. Phys. Soc.* (*London*), **86**, 777 (1965).
13. M. Gavrila, *Acad. Soc. Rep. Romania Inst. At. Phys.* F.T.60, 1966.
14. M. Karplus and H. J. Kolker, *J. Chem. Phys.*, **38**, 1863 (1963) and **39**, 2997 (1963); S. T. Epstein, *ibid.*, **43**, 4398 (1965).
15. R. Yaris, *J. Chem. Phys.*, **39**, 2474 (1963); **40**, 664 (1964); and **43**, 3528 (1966).
16. H. J. Kolker and H. H. Michels, *J. Chem. Phys.*, **43**, 1027 (1965).
17. A. Dalgarno and G. A. Victor, *Mol. Phys.*, **10**, 333 (1966).
18. Y. M. Chan and A. Dalgarno, *Proc. Phys. Soc.* (*London*), **85**, 277 (1965).
19. A. Dalgarno and G. M. Stacey (in press) (1967).
20. A. Weiss, *Phys. Rev.*, **122**, 1826 (1961); *Astrophys. J.*, **138**, 1262 (1963).
21. M. Karplus, *J. Chem. Phys.*, **41**, 880 (1964); M. N. Adamov and R. A. Evarestov, *Opt. Spectry.* (*USSR*) (*Engl. Trans.*), **19**, 362 (1965); J. C. Browne, A. Dalgarno, and G. A. Victor (in press) (1967).
22. H. Margenau, *Phys. Rev.*, **64**, 131 (1943).
23. A Dalgarno and A. E. Kingston, *Proc. Roy. Soc.* (*London*), **A259**, 424 (1960).
24. A. Dalgarno and N. Lynn, *Proc. Phys. Soc.* (*London*), **A70**, 802 (1957).
25. A. Dalgarno and A. E. Kingston, *Proc. Phys. Soc.* (*London*), **73**, 455 (1959); A. Dalgarno and A. E. Kingston, *Proc. Phys. Soc.* (*London*), **78**, 607 (1961); J. A. Barker and P. J. Leonard, *Phys. Letters*, **13**, 127 (1964); A. E. Kingston, *Phys. Rev.*, **135**, A1018 (1964); A. Dalgarno and D. A. Williams, *Proc. Phys. Soc.* (*London*), **85**, 685 (1965).
26. R. J. Bell, *Proc. Phys. Soc.* (*London*), **86**, 17 (1965)
27. R. J. Bell and A. E. Kingston, *Proc. Phys. Soc.* (*London*), **88**, 901 (1966).
28. A. Dalgarno, I. H. Morrison, and R. M. Pengelly, *Intern. J. Quantum Chem.*, **1**, 161 (1967).
29. Cf. A. Dalgarno, *Advan. Phys.*, **11**, 281 (1962); M. Yoshamine and R. P. Hurst, *Phys. Rev.*, **35**, A612 (1964); A. Dalgarno and H. A. McIntyre, *Proc. Phys. Soc.* (*London*), **85**, 47 (1965); P. W. Langhoff and R. P. Hurst, *Phys. Rev.*, **139**, A1415 (1965); H. D. Cohen and C. C. J. Roothaan, *J. Chem. Phys.*, **43**, 534 (1966); P. W. Langhoff, M. Karplus, and R. P. Hurst, *J. Chem. Phys.*, **44**, 505 (1966); H. D. Cohen, *J. Chem. Phys.*, **45**, 10 (1966); J. Lahiri and A. Mukherji, *Phys. Rev.*, **121**, 228 (1966); *J. Phys. Soc.* (*Japan*), **21**, 178 (1966); P. W. Langhoff, J. D. Lyons, and R. P. Hurst, *Phys. Rev.*, **148**, 18 (1966).
30. A. Dalgarno, *Proc. Roy. Soc.* (*London*), **A251**, 282 (1959).
31. M. Karplus and H. J. Kolker, *J. Chem. Phys.*, **41**, 3955 (1964).
32. A. Dalgarno and G. A. Victor, *Proc. Roy. Soc.* (*London*), **A291**, 291 (1966).
33. P. W. Langhoff, M. Karplus, and R. P. Hurst, *J. Chem. Phys.*, **44**, 505 (1966).
34. N. R. Kestner, *J. Chem. Phys.*, **45**, 3121 (1966).
35. W. J. Deal and N. R. Kestner, *J. Chem. Phys.*, **45**, 4014 (1966).
36. G. A. Victor, unpublished results, 1965.
37. A. Dalgarno and G. A. Victor, *Proc. Phys. Soc.* (*London*), **90**, 605 (1967).

38. A. Dalgarno and A. L. Stewart, *Proc. Roy. Soc.* (*London*), **A238**, 269 (1956).
39. A. Dalgarno and A. L. Stewart, *Proc. Roy. Soc.* (*London*), **A247**, 245 (1958).
40. A. Dalgarno, W. D. Davison, and A. L. Stewart, *Proc. Roy. Soc.* (*London*), **A257**, 115 (1960).
41. B. Musulin and S. T. Epstein, *Phys. Rev.*, **136**, A966 (1964)
42. A. Dalgarno and A. L. Stewart, *Proc. Roy. Soc.* (*London*), **A257**, 115 (1960).
43. O. Sinanoğlu, *Advan. Chem. Phys.*, **6**, 315 (1964); N. R. Kestner and O. Sinanoğlu, *J. Chem. Phys.*, **45**, 194 (1966).
44. N. R. Kestner, *J. Chem. Phys.*, **45**, 208 (1966).
45. N. R. Kestner, *J. Chem. Phys.*, **45**, 213 (1966).
46. K. A. Brueckner, *Phys. Rev.*, **97**, 1353 (1955); **100**, 36 (1955).
47. J. Goldstone, *Proc. Roy. Soc.* (*London*), **A239**, 267 (1957).
48. H. P. Kelly, *Phys. Rev.*, 131, 684 (1963); **136**, B896 (1964); **144**, 39 (1966); **152**, 62 (1966); H. P. Kelly and H. S. Taylor, *J. Chem. Phys.*, **40**, 1478 (1964).
49. H. B. Levine and H. S. Taylor, *J. Chem. Phys.*, **41**, 1367 (1964).
50. Y. M. Chan and A. Dalgarno, *Mol. Phys.*, **9**, 525 (1965).
51. A. Dalgarno and G. A. Victor, unpublished results, 1965.
52. Y. M. Chan and A. Dalgarno, unpublished results, 1965.
53. A. Dalgarno and J. T. Lewis, *Proc. Phys. Soc.* (*London*), **A69**, 57 (1956).
54. Cf. R. Herman and H. Margenau, *Phys. Rev.*, **122**, 1204 (1961).
55. Cf. F. Adrian, *J. Chem. Phys.*, **32**, 972 (1960).
56. A. Dalgarno and A. L. Stewart, *Proc. Phys. Soc.* (*London*), **75**, 441 (1960).

4. Very Long-Range (Retardation Effect) Intermolecular Forces

EDWIN A. POWER

Mathematics Department
University College, London, England

CONTENTS

I. Introduction to Very Long-Range Forces 167
A. General Background. 168
B. Historical Survey and Summary 173
II. Calculation of Dispersion Interaction: the Casimir-Polder Potential . . 187
A. Noncovariant Method 187
B. Feynman Method 194
III. Interaction Energies Involving Excited States 199
A. Concept of Potential 200
B. Energy Shifts with Excited States: Resonance Interaction 202
C. Excitation Present but Nonresonant 206
IV. Nondispersive Forces in the Long-Range Limit 209
A. Breit Operator 209
B. Pauli Approximation 216
References 222

I. INTRODUCTION TO VERY LONG-RANGE FORCES

Theoretical chemistry can normally base its dynamics on the quantum mechanics of Schrödinger's equation with the Coulomb and spin interactions between the constituent charges forming the potential energy. In particular, this is true for the calculations of interatomic and intermolecular forces. Only when the interaction of light with atoms or molecules is under discussion does the radiation theory of Dirac[1] become important and then only in its semiclassical approximation as outlined in many textbooks. In this chapter, the complete theory of quantum electrodynamics is used to discuss intermolecular forces and this modifies the predictions of elementary quantum mechanics at very

large separations between the molecules. Section 1–B of this chapter gives an outline of the background to this situation. The most important landmark was the discovery by Casimir and Polder[2] that the London dispersion potential[3] for van der Waals forces is altered in its functional form at intermolecular separations of the order of the wavelength of optical energy transitions of the constituent molecules.

A. General Background

Intermolecular forces outside the overlap regions of electronic wave functions fall off with R, the separation distance between the nuclei, according to some high inverse power of R which, if the molecules are not both ionized, is higher than 2, the Coulombic inverse square law. The fundamental quantum mechanical calculation of London[3] gives, for two ground-state molecules whose induced dipole–induced dipole attraction dominates, the attractive potential

$$U_{G\text{-}G}(R) = -\tfrac{3}{4}\bar{E}[\alpha(1)\alpha(2)/R^6] \tag{1}$$

In Eq. (1), $\alpha(\xi)$ is the polarizability of molecule ξ and is given in the dipole approximation by

$$\alpha(\xi) = 2\sum_n \frac{e^2\,|\langle n|\,\mathbf{q}(\xi)\,|0\rangle|^2}{E_n - E_0} \tag{2}$$

where $\langle n|\,\mathbf{q}(\xi)\,|0\rangle$ is the transition moment for molecule ξ between the ground-state $|0\rangle$ with energy E_0 and optically allowed states $|n\rangle$ with energy E_n. $\bar{E}$ is some characteristic energy of the systems and is equal to E, the level separation between the ground state and the excited state if both molecules are identical and essentially two-level systems. This so-called dispersion force, Eq. (1), is the basis for the van der Waals attraction between molecular systems where valence forces have practically disappeared and its calculation by London was one of the early successes of quantum mechanics.

Energies of interactions with inverse powers of R less than 6 occur in several cases, for example the potential between an ion with charge Ze and a ground-state molecule of polarizability α is

$$U_{G\text{-}I}(R) = -\tfrac{1}{2}(Z^2e^2\alpha/R^4) \tag{3}$$

A further example is the potential energy between resonant systems with one molecule being excited and the other in its ground state is

$$U_{G\text{-}E(\text{res})}(R) = e^2\langle E|\, q_i(1)\,|0\rangle\langle 0|\, q_j(2)\,|E\rangle\beta_{ij}/R^3 \tag{4}$$

In Eq. (4), the excited state assumed optically coupled to $|0\rangle$ is labeled $|E\rangle$ and β_{ij} is the tensor familiar in dipole–dipole interactions,

$$\beta_{ij} = \delta_{ij} - 3\hat{R}_i\hat{R}_j \tag{5}$$

$\hat{\mathbf{R}}$ is the unit vector in the $\mathbf{R}$ direction with direction cosines $\hat{R}_i$. The energy $U_{G\text{-}E}(R)$, first computed by Eisenshitz and London,[4] is thus orientation dependent and may be repulsive or attractive unlike $U_{G\text{-}G}(R)$ and $U_{G\text{-}I}(R)$ which are always attractive. These latter forces are attractive because energy must be borrowed from the vacuum over short times, consistent with the uncertainty principle in the fluctuating processes involved. This physical picture from quantum electrodynamics has its counterpart in elementary quantum mechanics where the physical admixture of states due to the perturbation includes only those of higher energy than the unperturbed state. Where energy can be given from the system to the radiation field as is the case for $U_{G\text{-}E}(R)$, no such general argument is possible.

The ramifications and extensions to more complicated situations including higher multipolarities, many-body forces, realistic transition moments, the matching at the electronic boundaries with valence forces, and the applications of these intermolecular potentials to concrete situations form the content of most of the other contributions to this volume. In this chapter, a survey is made concerning what is known about the generalization of the basic van der Waals and resonance interaction energies at very large R. Here, very large R means of the order of $\lambda = hc/E$, the wavelength of light emitted in the transition $|E\rangle$ to $|0\rangle$. The unit of length used throughout this paper is $\lambda\!\!\!^{-} = \hbar c/E = \lambda/2\pi$. It is immediately clear that the distances involved are really quite large according to the scale of atomic size. For Lyman transitions in hydrogen, $\lambda\!\!\!^{-} \sim 1.3 \times 10^{-6}$ cm, but many applications will have a $\lambda\!\!\!^{-}$ up to an order of magnitude larger; for example, in anthracene $\lambda\!\!\!^{-} \sim 0.6 \times 10^{-5}$ cm and in quartz $\lambda\!\!\!^{-}_{\text{eff}} \sim 0.6 \times 10^{-5}$ cm. One consequence of this is that it is quite accurate to express the potential energies in terms of the physical properties of the isolated molecules.

Three different adjectives have been used to describe the effective change of the intermolecular forces at these separations, namely, radiative, relativistic, and retarded. All three are suggestive of some positive aspect of their character—the first, i.e., *radiative*, because the

exchange (albeit virtual) of radiation in the form of transverse photons is involved; the second, *relativistic*, mainly because the motion of photons cannot be considered otherwise, but also because the exact properties of the Dirac electron become important; the third, *retarded*, describes the situation in which the instantaneous Coulomb interactions between the constitutent charges of the atomic or molecular systems although giving rise to the potentials $U_{G\text{-}G}(R)$, $U_{G\text{-}I}(R)$, and $U_{G\text{-}E}(R)$ of Eqs. (1), (3), and (4), are not sufficient to give the required generalizations to very large R, but in this situation the interactions between the charges are propagated with the speed of light. However, radiative corrections to the potentials suggest corrections to the interactions of higher order in e that the basic lowest order (which is 4 for dispersion forces and 2 for resonance and spin forces) and this is not what is involved. Also, even at smaller separations than we have in mind, interactions of the spin–spin type or spin–orbit type are relativistic in the sense that they arise through the Dirac nature of the electrons. These occur even for two electrons in the same atom and are usually analyzed in terms of the Breit-Pauli interaction. We have thus decided to use the description *retarded* intermolecular forces for those discussed in this chapter.

The usual[5] starting point for quantum mechanical calculations of intermolecular forces is the Hamiltonian

$$H = \sum_{i=1}^{N} H_i + \sum_{i<j}^{N} U^{\text{Coulomb}}(r_{ij}) \tag{6}$$

where H_i is the free Hamiltonian of particle (i) and

$$U^{\text{Coulomb}}(r_{ij}) = e_i e_j / r_{ij} \tag{7}$$

For two-body intermolecular forces, it is convenient to divide H differently as follows

$$H = H(1) + H(2) + U_{\text{int}}^{\text{Coulomb}}(1,2) \tag{8}$$

where now

$$H(\xi) = \sum_{i=1}^{N(\xi)} H_i + \sum_{i<j}^{N(\xi)} U^{\text{Coulomb}}(r_{ij}) \tag{9}$$

is the Hamiltonian of the isolated molecule (ξ) the summation being over the $N(\xi)$ particles in system (ξ). $U_{\text{int}}^{\text{Coulomb}}$ (1,2) is the pairwise potential energy between electrons and protons of the different molecules (1) and (2). From the two-centered expansion of $1/r_{ij}$, $U_{\text{int}}^{\text{Coulomb}}$ (1,2) can[6] be expanded in powers of R^{-1} and if (1) and (2) are electrically

neutral, the leading term is proportional to R^{-3} and is

$$U_{\text{int;3}}^{\text{Coulomb}}(R) = \frac{\boldsymbol{\mu}(1)\cdot\boldsymbol{\mu}(2) - 3\boldsymbol{\mu}(1)\cdot\hat{\mathbf{R}}\boldsymbol{\mu}(2)\cdot\hat{\mathbf{R}}}{R^3} = \frac{\mu_i(1)\mu_j(2)\beta_{ij}}{R^3} \tag{10}$$

where

$$\boldsymbol{\mu}(\xi) = \sum_{i=1}^{N(\xi)} e_i \mathbf{r}_i \tag{11}$$

is the dipole moment of system (ξ). The expression for $U_{G\text{-}E(\text{res})}(R)$ of Eq. (4) follows immediately from Eq. (10) and the dipole approximation is clearly evident. The energy of interaction [Eq. (10)] also has a non-zero expectation value for systems with permanent moments; these are not considered further in this review but have properties analogous to the spin forces discussed in Section IV. Finally, from Eq. (10) the London-van der Waals interaction [Eq. (1)] is obtained in the standard manner by second-order perturbation theory, namely,

$$U_{G\text{-}G}(R) = -\sum_I \frac{\langle 0|\, U_{\text{int;3}}^{\text{Coulomb}}(R)\,|I\rangle\langle I|\, U_{\text{int;3}}^{\text{Coulomb}}(R)\,|0\rangle}{E_I(1) + E_I(2) - E_0(1) - E_0(2)} \tag{12}$$

It is very convenient to introduce a time-ordered diagram corresponding to matrix elements such as that occurring in Eq. (12). Such a diagram is given in Figure 1. The heavy line represents the propagation of an excited atom with energy $E_I(\xi)$. The horizontal dotted lines are representations of the instantaneous dipole–dipole interaction $U_{\text{int;3}}^{\text{Coulomb}}(R)$. The diagram which corresponds to the dipole resonance interaction $U_{G\text{-}E(\text{res})}(R)$ is shown in Figure 2.

It should be noted that $U_{G\text{-}E(\text{res})}(R)$ is not precisely the potential energy of the system of two identical atoms of which one is excited, because of the necessity to insure the correct symmetry of the total wave function. The wave function of the two-molecule system may be in either of the two states

$$\Psi_+ = (1/\sqrt{2})[|E\rangle_1|0\rangle_2 + |0\rangle_1|E\rangle_2] \tag{13}$$

or

$$\Psi_- = (1/\sqrt{2})[|E\rangle_1|0\rangle_2 - |0\rangle_1|E\rangle_2] \tag{14}$$

Then the potential of interaction is

$$+U_{G\text{-}E(\text{res})}(R) \quad \text{for} \quad \Psi_+$$

and is

$$-U_{G\text{-}E(\text{res})}(R) \quad \text{for} \quad \Psi_-$$

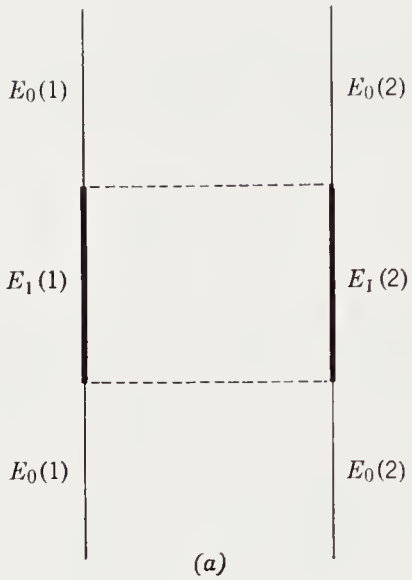

Fig. 1. The diagram corresponding to the matrix element for the London force between neutral atoms. The heavy line represents the propagation of an excited atom. The horizontal dotted line is a representation of the instantaneous Coulombic interaction between the atoms.

The essential fact concerning the retarded dispersion and resonance forces is that when $R \sim \hat{\lambda}$, in the radiation zone, the Coulomb potential energy is not sufficient to describe the interaction between charges and the complete interaction with the full Maxwell field, including transverse photons, is essential. Thus, the fundamental Hamiltonian [Eq. (8)] is replaced by the coupled systems, molecules, and the radiation field, so that the Hamiltonian under consideration is

$$H = H(1) + H(2) + H_{\text{rad}} + H_{\text{int}} \tag{15}$$

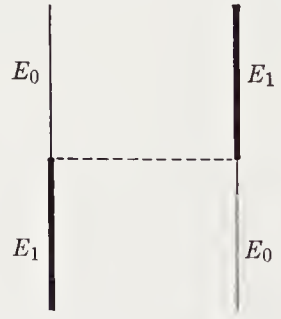

Fig. 2. The diagram corresponding to the matrix element for the dipole resonance interaction $U_{G\text{-}E(\text{res})}(R)$. The time direction is upward in this and subsequent time-ordered graphs.

In terms of the Thomson-Maxwell theory, assuming the space between the molecules does not involve any medium, **E** and **B** being the electric and magnetic field vectors,

$$H_{\text{rad}} = \frac{1}{8\pi}\int(\mathbf{E}^2 + \mathbf{B}^2)d\tau \tag{16}$$

Various forms for H_{int}, the coupling between the charges and the field, will be considered in later sections. Roughly speaking, the coupling is between the vector potential (three-vector **A** or four-vector A_μ) and the currents. In extreme nonrelativistic theory it is[7]

$$H_{\text{int}} = -\sum_i \frac{e_i\mathbf{p}_i \cdot \mathbf{A}(\mathbf{x}_i)}{m_i c} + \sum_i \frac{e_i^2\mathbf{A}^2(\mathbf{x}_i)}{2m_i c^2} + U_{\text{int}}^{\text{Coulomb}}(1,2) \tag{17}$$

while in quantum electrodynamics it is[8]

$$H_{\text{int}} = -\int j_\mu(x)A_\mu(x)\,d\tau \tag{18}$$

where

$$j_\mu(x) = e\bar{\psi}(x)\gamma^\mu\psi(x) \tag{19}$$

in terms of Dirac spinors $\psi(x)$ and Dirac matrices γ^μ. When working in various approximations, it is often convenient to reduce these. For example, in dipole approximation,[9] one may use

$$H_{\text{int}} = -\boldsymbol{\mu}(1) \cdot \mathbf{E}^\perp(1) - \boldsymbol{\mu}(2) \cdot \mathbf{E}^\perp(2) \tag{20}$$

where the radiation electric field $\mathbf{E}^\perp$ is taken to vary very little in amplitude over the molecules. Similarly, for spin interaction with the magnetic field, Eq. (18) reduces to

$$H_{\text{int}} = -(e/2m)\boldsymbol{\sigma}(1) \cdot \mathbf{B}(1) - (e/2m)\boldsymbol{\sigma}(2) \cdot \mathbf{B}(2) \tag{21}$$

B. Historical Survey and Summary

Once the interpretation of light as electromagnetic oscillations was understood, it was clear that a mechanical action of the waves on the sources and absorbers would be involved. In fact, Lebedeff in 1894 wrote,[10] "From the standpoint of the electromagnetic theory of light it must be admitted that between two light emitting molecules there exist mechanical forces, caused by the electrodynamic interaction of the alternating electric currents in the molecules (according to Ampere's law), and by the alternating charges in them (according to Coulomb's

law). We must therefore admit that in this case there exist intermolecular forces whose origin is intimately connected with radiation processes."

The first quantitative theories of molecular forces could be built only after the structure and the internal dynamics of atoms and molecules were understood. So, following the discovery of quantum mechanics, the London theory outlined in the previous section was soon formulated. The problem of considering the true radiation field as well as the Coulombic forces was partially solved for resonance interactions by the application of the Breit equation[11] to two electrons in *different* centers. For example, the Breit Hamiltonian contains the following spin-independent parts

$$H_1 = -(1/8m^3c^2)(p_1^4 + p_2^4) \tag{22}$$

$$H_2 = -(e^2/2(mc)^2)(1/r_{12})[\mathbf{p}_1 \cdot \mathbf{p}_2 + \widehat{\mathbf{r}_{12}} \cdot (\widehat{\mathbf{r}_{12}} \cdot \mathbf{p}_1)\mathbf{p}_2] \tag{23}$$

$$H_4 = +\frac{ie^2\hbar}{(2mc)^2}\frac{(\mathbf{p}_1 \cdot \widehat{\mathbf{r}_{12}})}{r_{12}^2} - \frac{ie^2\hbar}{(2mc)^2}\frac{\mathbf{p}_1 \cdot \widehat{(\mathbf{R} - \mathbf{r}_1)}}{|\mathbf{R} - \mathbf{r}_1|^2}$$

$$-\frac{ie^2\hbar}{(2mc)^2}\frac{(\mathbf{p}_2 \cdot \widehat{\mathbf{r}_{12}})}{r_{12}^2} + \frac{ie^2\hbar}{(2mc)^2}\frac{\mathbf{p}_2 \cdot \widehat{(\mathbf{R} + \mathbf{r}_2)}}{|\mathbf{R} + \mathbf{r}_2|^2} \tag{24}$$

The coordinate scheme is shown in Figure 3, and the notation is that of Bethe and Salpeter.[12]

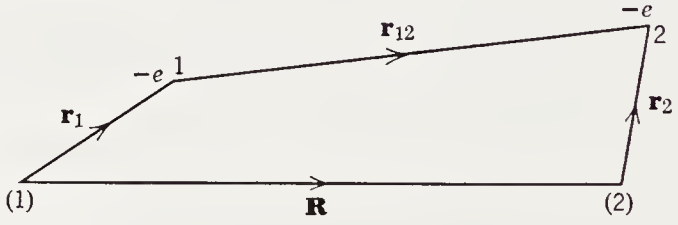

Fig. 3. Coordinate system for intermolecular forces.

H_1 is a free-particle correction due to relativity and is independent of the fine structure constant. H_2 is normally considered to be magnetic orbit interactions since it corresponds to the classical electromagnetic coupling of the electrons through the interaction of the magnetic fields created by their motion. However, for the electrons on different atoms (as in Fig. 3) when a *resonance* situation exists, H_2 has an electric

dipole–electric dipole component. To the first approximation in R^{-1},

$$\langle 0|_1\langle E|_2 H_2 |0\rangle_2|E\rangle_1 \doteq -(e^2/2\lambda\!\!\!^{-2}R)\langle 0| q_i(1) |E\rangle\langle E| q_j(2) |0\rangle(\delta_{ij} + \hat{R}_i\hat{R}_j) \tag{25}$$

This is the first-order retardation correction to the resonance potential $U_{G\text{-}E(\text{res})}(R)$ of Eq. (4).

The complete retarded dipole–dipole potential (discussed fully in Section III) is[13,14]

$$V_{G\text{-}E(\text{res})}(R) = -e^2\langle 0| q_i(1) |E\rangle\langle E| q_j(2) |0\rangle \times \left[\frac{\alpha_{ij}\cos R/\lambda\!\!\!^{-}}{\lambda\!\!\!^{-2}R} - \beta_{ij}\left(\frac{\sin R/\lambda\!\!\!^{-}}{\lambda\!\!\!^{-}R^2} + \frac{\cos R/\lambda\!\!\!^{-}}{R^3}\right)\right] \tag{26}$$

The tensors α_{ij} and β_{ij} are defined by

$$\alpha_{ij} = \delta_{ij} - \hat{R}_i\hat{R}_j$$
$$\beta_{ij} = \delta_{ij} - 3\hat{R}_i\hat{R}_j \tag{27}$$

For $R < \lambda\!\!\!^{-}$, the potential [Eq. (26)] can be expanded as

$$V_{G\text{-}E(\text{res})}(R) = e^2\langle 0| q_i(1) |E\rangle\langle E| q_j(2) |0\rangle\left\{\frac{\delta_{ij} - 3\hat{R}_i\hat{R}_j}{R^3} - \frac{1}{2}\frac{(\delta_{ij} + \hat{R}_i\hat{R}_j)}{\lambda\!\!\!^{-2}R} + \frac{R}{8\lambda\!\!\!^{-4}}(3\delta_{ij} - \hat{R}_i\hat{R}_j)\ldots\right\}$$
$$= U_{G\text{-}E(\text{res})}(R) + \langle 0|_1\langle E|_2 H_2 |0\rangle_2|E\rangle_1 + \ldots \tag{28}$$

for nondegenerate atoms[15] $\langle\Psi| H_2 |\Psi\rangle = 0$.

In the analysis of dispersion forces, the situation is quite different. As emphasized especially by Bethe and Salpeter,[12] the Breit additions to the nonrelativistic Hamiltonian can only be used in a limited context and certainly not in a fourth-order perturbation calculation which is required for the van der Waals potential. Several attempts[15,16] have been made to mix the $U_{\text{int}}^{\text{Coulomb}}(1,2)$ and H_2 [Eqs. (10) and (23)] to obtain some corrections, called relativistic corrections by their authors, to the London potential. The R dependence of these terms is $1/R^4$. Power and Zienau[17] have discussed the fact that this procedure is incomplete. Indeed, it is well known that the classical analog of the Breit Hamiltonian, namely, the Darwin Lagrangian,[18] is valid only for $R < \lambda\!\!\!^{-}$.

Those corrections to the London potential which are obtainable by this mixed method are given in full by Meath and Hirschfelder.[19]

In the wave zone, the electric field of a dipole falls off like a modulated $1/R$ law and, since it is the near-zone field which gives the β_{ij}/R^3 interaction $U_{\text{int};3}^{\text{Coulomb}}(R)$ of Eq. (10) which itself leads to the London potential [Eq. (11)], it was pointed out by Wheeler[20] in 1941 that modifications of the London interaction energy could be expected at distances of the order of $\lambda\!\!\!^{-}$. It is a plausible conjecture that some interaction energies falling as $1/R^2$ may be involved and indeed in the region $R \lesssim \lambda$ there are such corrections to the London potential arising from second-order perturbation theory through H_2 of Eq. (25) but these are *smaller* than the $1/R^4$ terms involving mixed H_2 and $U_{\text{int};3}^{\text{Coulomb}}$ mentioned in the previous paragraph. The important $1/R^2$ potentials in the wave zone $R \gtrsim \lambda$ appear not in the ground state–ground state interactions but in the off-resonance interaction energy between two dissimilar systems—one excited and one in its ground state.[21] Their general forms are, for $R \gg \lambda\!\!\!^{-}$

$$V_{G\text{-}E(\text{non-res})}(R) \simeq \frac{2e^4}{(\hbar c)^4} \frac{E_1^4 E_2}{E_1^2 - E_2^2} \frac{\alpha_{ij}\alpha_{kl} \cos^2(R/\lambda\!\!\!^{-}_1)}{R^2}$$

$$\times \langle E_1 | q_i(1) | 0 \rangle \langle 0 | q_k(1) | E_1 \rangle \langle 0 | q_j(2) | E_2 \rangle \langle E_2 | q_l(2) | 0 \rangle \quad (29)$$

Molecule (1) is excited with energy E_1, the state being optically coupled to its ground state; and molecule (2) is in its ground state but with its optically accessible level $|E_2\rangle$ with energy E_2 being involved in the virtual excitations which give rise to its polarizability through Eq. (2).

A completely new approach to dispersion forces, both retarded and in the London limit, was initiated by Casimir[2,22,23] in 1948. The problem was attacked through a perturbation approach to the Hamiltonian (15); according to this approach, the radiation field gives extra degrees of freedom to the system in addition to the degrees of freedom associated with the coordinates of the particles which make up the constituent atoms or molecules. It is interesting that the stimulus to such calculations came from the field of colloidal chemistry. It is surprising to many field theorists that one of the trickiest and the first nontrivial calculation of a complicated fourth-order process in quantum electrodynamics was initiated by investigations of the stability of lyophobic colloids (like quartz suspension or a gold sol). This stability problem has been the subject of considerable investigation by Overbeek in Holland and by

Deryagin in Russia. The stability is due to the competition between electrostatic forces of repulsion—mostly in the form of double layers on relatively "flat" molecules—and the van der Waals attraction. Some sols or gels are thixotropic and there is a very weak minimum in the potential-energy curve so that the stability of the gel can be broken fairly easily. Detailed investigation (see Verwey and Overbeek[24]) showed that the minimum was too large and that a *weaker* van der Waals attraction is required in the range ~ 200 Å or so. Overbeek suggested that the retardation of the basic interactions into electronic ones would cause a reduction in the potential energy between the two molecules. He states[24] "The London-forces being of an electrical nature need a certain time for their propagation. In the theory of London this time is completely neglected as it uses the nonrelativistic Schrödinger equation. If we picture the London-van der Waals forces as an attraction between the temporary dipole of one atom and the dipole induced by it on the second atom the finite velocity of propagation of electromagnetic actions causes the induced dipole to be retarded against the inducing one by a time equal to Rn/c (n is the refractive index of the medium at the frequency coupled with the temporary dipole). The reaction of the induced dipole on the first one again is retarded by the same time and if in this time lag of $2Rn/c$ the direction of the first dipole is altered by 90°, the force exerted is exactly nullified . . ."

One sees immediately that the time lag becomes of the order of the dipole rotation time when

$$R/c \sim 1/\nu \tag{30}$$

and so the distance involved is

$$R \sim c/\nu \sim \lambda \tag{31}$$

The calculation by Casimir and Polder[2] of the dispersion force to fourth order in the coupling constant e was made before the simplifying computational techniques of Feynman[8] were known. It rests on Heisenberg's method[25] which involves calculating the perturbation on the state of one system due to the radiation fields induced by the other. Since the coupling energy is given by Eq. (17) which has terms quadratic in e as well as linear terms, it is necessary to calculate second-order, third-order, and fourth-order perturbation matrix elements to obtain the complete e^4 interaction potential. The second-order contribution includes the London interaction potential, the diagram of

which appears in Figure 1; but in second order, there is also a term due to the $(e^2/2mc^2)\mathbf{A}^2$ interaction Hamiltonian which is pictured in Figure 4. The mixed $U_{\text{int};3}^{\text{Coulomb}}$ and single propagated transverse photon

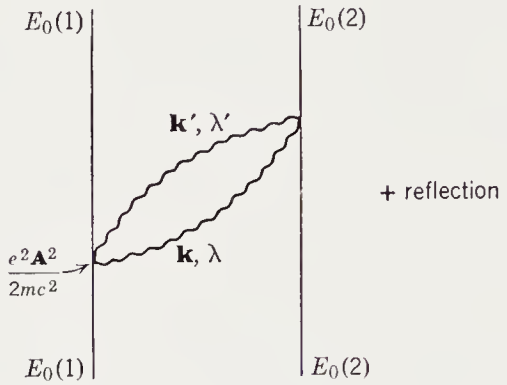

Fig. 4. Two-photon vertex contributions to the Casimir and Polder potential. The wavy lines represent the propagation of transverse photons.

terms occur in third order as shown in Figure 5, and also the mixed single- and double-vertex diagrams shown in Figure 6. The mixed Coulomb-Breit H_2 terms are contained in c and d of Figure 5. They lead to a potential proportional to R^{-4} in the $R < \lambda\!\!\!^{-}$ limit. However, the use of this formalism alone will ignore many important terms, for example those of order R^{-3} which arise from interference of a transverse photon and the Coulomb interaction while the former is actually being exchanged as in e of Figure 5. Such contributions to the energy cannot

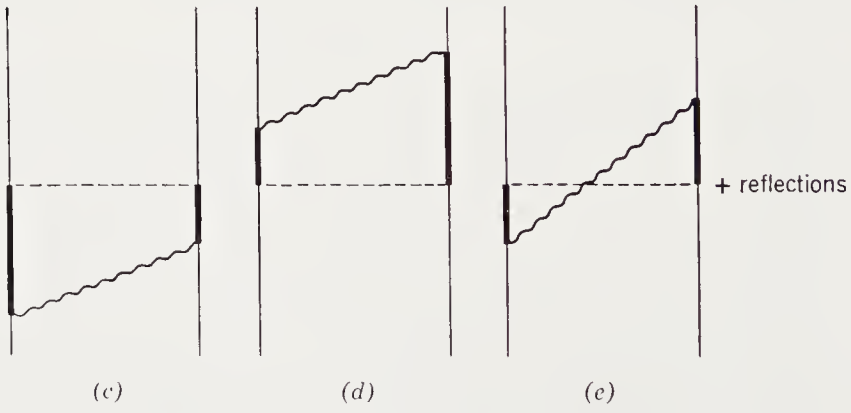

Fig. 5. Third-order perturbation terms contributing to the potential involving one transverse and one Coulombic photon.

be computed by simply taking the Breit interaction matrix element with the frequencies modified by the Coulomb energy as can be done for the R^{-4} terms and which also gives a simple model to compute the London energy as in Born's textbook.[26] All contributions which involve a two-photon vertex due to the $e^2\mathbf{A}^2/2mc^2$ interaction energy, such as in b (Fig. 4) and f, g, and h (Fig. 6), are even less accessible to this

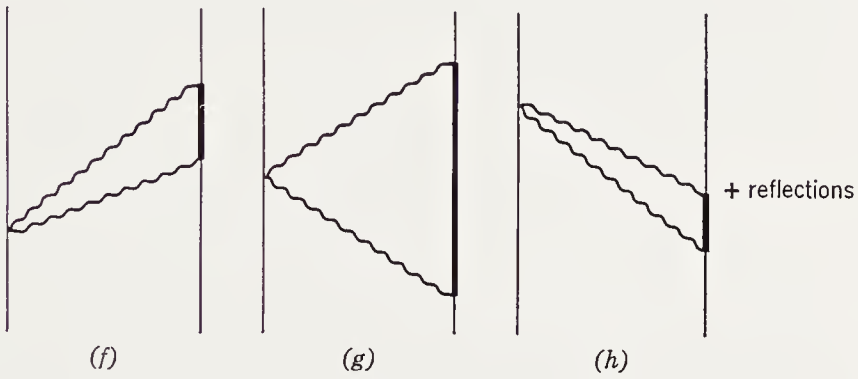

Fig. 6. Mixed single and double vertex diagrams in the third-order perturbation term.

formalism. From a strict point of view, these contributions arise from transitions via negative energy states of the Dirac electron or, more precisely, they involve positron theory. They are, of course, essential to obtain the complete interaction between neutral atoms correct to order e^4. Finally, the fourth-order perturbation matrix elements due to single transverse photon vertices are drawn in Figure 7. One should note that in the "old-fashioned" perturbation theory, when made diagrammatic in this way, the time orderings are important and, hence, one needs to consider six uncrossed and six crossed time-ordered diagrams in the single vertex case. There are 27 individual terms which when collected together give the potential in the form of an integral. If units are chosen such that $\hbar = c = 1$, so that energies are inverse lengths one obtains

$$V_{G\text{-}G}(R) = -\frac{4e^4}{\pi} \sum_{n,p} |\langle n|\,\mathbf{q}(1)\,|0\rangle|^2\,|\langle p|\,\mathbf{q}(2)\,|0\rangle|^2\,E_{no}(1)E_{po}(2)$$
$$\times \int_0^\infty \frac{du\; u^4 e^{-2uR}}{R^2(E_{no}^2(1)+u^2)(E_{po}^2(2)+u^2)} \left\{1 + \frac{2}{uR} + \frac{5}{u^2R^2} + \frac{6}{u^3R^3} + \frac{3}{u^4R^4}\right\} \tag{32}$$

This can be evaluated in closed form in terms of the sine and cosine integrals[21,27]

$$V_{G\text{-}G}(R) = -\frac{4e^4}{\pi} \sum_{n,p} |\langle n|\,\mathbf{q}(1)\,|0\rangle|^2\,|\langle p|\,\mathbf{q}(2)\,|0\rangle|^2\,\frac{E_{no}(1)E_{po}(2)}{E_{no}^2(1) - E_{po}^2(2)}$$

$$\times \left[\frac{1}{R^2}\{E_{po}^3(2)A_{po}(R) - E_{no}^3(1)A_{no}(R) + [E_{no}^2(1) - E_{po}^2(2)]/(2R)\}\right.$$

$$+ \frac{2}{R^3}\{E_{po}^2(2)B_{po}(R) - E_{no}^2(1)B_{no}(R) - [E_{po}(2)A_{po}(R) - E_{no}(1)A_{no}(R)]/R\}$$

$$\left.+ \frac{3}{R^4}\{E_{no}(1)A_{no}(R) - E_{po}(2)A_{po}(R) + 2[B_{no}(R) - B_{po}(R)]/R + [A_{po}(R)/E_{po}(2) - A_{no}(R)/E_{no}(1)]/R^2\}\right] \quad (33)$$

The functions $A_{\lambda\mu}(R)$ and $B_{\lambda\mu}(R)$ are defined as follows:

$$A_{\lambda\mu}(R) = \sin(2E_{\lambda\mu}R)\,\mathrm{Ci}(2E_{\lambda\mu}R) - \cos(2E_{\lambda\mu}R)\,\mathrm{si}(2E_{\lambda\mu}R) \quad (34)$$

$$B_{\lambda\mu}(R) = \cos(2E_{\lambda\mu}R)\,\mathrm{Ci}(2E_{\lambda\mu}R) + \sin(2E_{\lambda\mu}R)\,\mathrm{si}(2E_{\lambda\mu}R) \quad (35)$$

$E_{no}(1)$ and $E_{po}(2)$ are the energies of the optically accessible states $|n\rangle$ and $|p\rangle$ of molecules (1) and (2), respectively, relative to their ground states. The sine and cosine integrals are defined as

$$\mathrm{si}(x) = -\int_x^\infty \frac{\sin t}{t}\,dt \quad (36a)$$

$$\mathrm{Ci}(x) = -\int_x^\infty \frac{\cos t}{t}\,dt \quad (36b)$$

for small R compared with λ_1 and λ_2,

$$\mathrm{si}(x) \sim -\pi/2 \quad (37a)$$

and

$$\mathrm{Ci}(x) \sim \ln x \quad (37b)$$

and so $A \sim \pi/2$ and $B \sim R$. Thus, the leading term in Eq. (32) is the very last term giving

$$V_{G\text{-}G}(R) \underset{R\to 0}{\simeq} -6e^4 \sum_{n,p} \frac{|\langle n|\,\mathbf{q}(1)\,|0\rangle|^2\,|\langle p|\,\mathbf{q}(2)\,|0\rangle|^2}{E_{no}(1) + E_{po}(2)} \cdot \frac{1}{R^6} \quad (38)$$

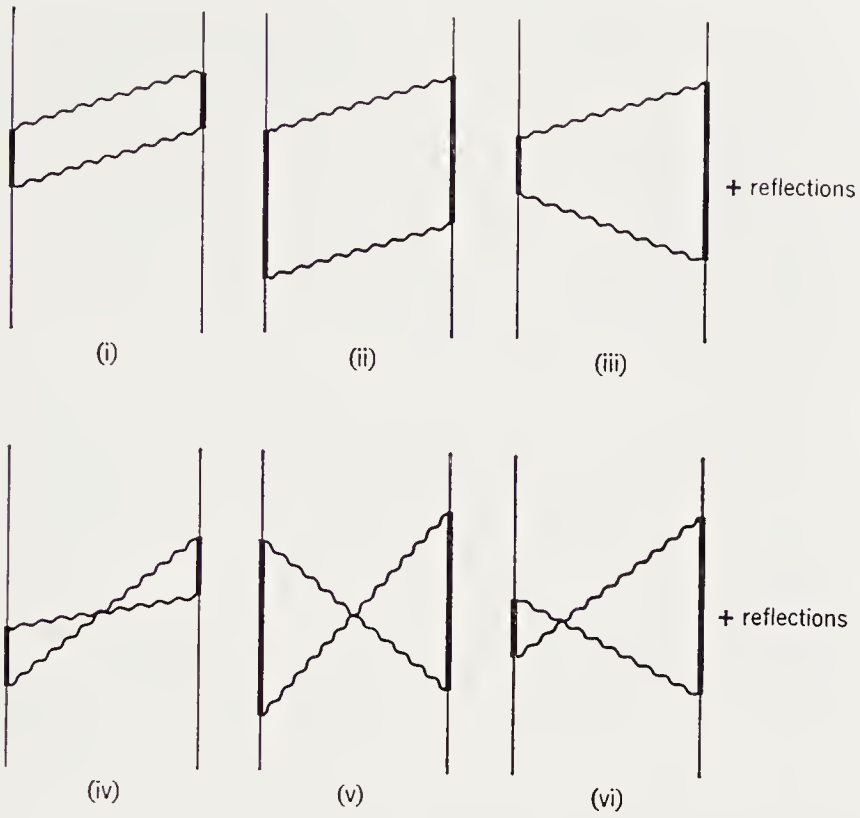

Fig. 7. Fourth-order perturbation terms involving transverse photons which contribute to the Casimir and Polder potential.

which using Eq. (2) is $U_{G\text{-}G}(R)$. So that

$$V_{G\text{-}G}(R) \underset{R\to 0}{\simeq} U_{G\text{-}G}(R) \tag{39}$$

On the other hand,[28] when R is large compared with $\hat{\lambda}$

$$A_{\lambda\mu}(R) \sim 1/2E_{\lambda\mu}R - 2/(2E_{\lambda\mu}R)^3 + 24/(2E_{\lambda\mu}R)^5 - \cdots \tag{40}$$

$$B_{\lambda\mu}(R) \sim -1/2E_{\lambda\mu}R + 3/(2E_{\lambda\mu}R)^4 - \cdots \tag{41}$$

and for Eq. (33) (replacing the $\hbar$ and c)

$$V_{G\text{-}G}(R) \underset{R\to\infty}{\simeq} -(23/4\pi)\hbar c[\alpha(1)\alpha(2)/R^7] \tag{42}$$

which we shall call the asymptotic Casimir-Polder potential $V_{C\text{-}P}(R)$.*

It is to be emphasized that $V_{C\text{-}P}(R)$, the R^{-7} potential, is *not* a correction to the London R^{-6} interaction potential (as higher multipoles would be) but the R^{-6} term has been completely cancelled by contributions from the transverse photons in the region $R > \lambda\!\!\!^{-}$ leaving, as predicted by Overbeek, a much weaker potential. The complete dispersion potential for all R outside any overlap regions, not only in the ground state but in important excited states,[29] is given by Eqs. (33). It can be expanded in powers of $(R/\lambda\!\!\!^{-})$ for $R < \lambda\!\!\!^{-}$ with leading term $\sim \hbar c\alpha^2/\lambda\!\!\!^{-}R^6$ (London) and retardation corrections $\sim \hbar c\alpha^2/(\lambda\!\!\!^{-3}R^4)$, $\sim \hbar c\alpha^2(\lambda\!\!\!^{-4}R^3)$, etc., and in powers of $(\lambda\!\!\!^{-}/R)$ for $R > \lambda\!\!\!^{-}$ with leading term $\sim \hbar c\alpha^2/R^7$ (Casimir-Polder) and corrections $\sim \hbar c\alpha^2\lambda\!\!\!^{-2}/R^9$, $\sim \hbar c\alpha^2\lambda\!\!\!^{-4}/R^{11}$, etc. An evaluation of these terms is given by Meath and Hirschfelder.[19] (See also these authors' contribution to this volume, page 3.) In the wave-zone region, the cancellations leading to the R^{-7} potential are considerably more than just that of the R^{-6} terms mentioned above. For example, the contribution given by the matrix element illustrated in diagram (i) of Figure 7 is, as will be seen in Section II-A, proportional to $\hbar c\alpha^2/(\lambda\!\!\!^{-4}R^3)$ and this cancels with other terms including the longitudinal interactions. This means that when using this method, specific evaluation of all terms is necessary and explains the error in the first[30] attempt at rederiving Casimir and Polder's potential. A numerical error in the two-photon vertex graph (Fig. 4) led to the erroneous suggestion that Casimir and Polder's result was not obtainable by symmetrical perturbation theory. During 1956, it was shown[31] that indeed the correct $V_{G\text{-}G}(R)$ is obtained from elementary Rayleigh-Schrödinger perturbation theory and also[32] that the same result follows by the use of Feynman's covariant method.

A description of Dzyaloshinskii's method[32] is given in Section II-B. Here, his expression for $V_{G\text{-}G}(R)$ is written down in terms of the four-vector currents, Eq. (19),

* $V_{C\text{-}P}(R)$ can be obtained directly from Eq. (32) without using the asymptotic form of the sine and cosine integrals, Eqs. (40) and (41) by noticing that for large R, the contribution to the integral arises from small u. Thus, when u^2 is neglected with respect to $E_{no}^2(1)$ and $E_{po}^2(2)$ in the denominator of the integrand, the fact that the polarizations $\alpha(\xi)$ arise as factors is automatic from the overall dependence on $E_{no}^{-1}(1)E_{po}^{-1}(2)$; the remaining factor $23/4\pi R^7$ comes from the now trivial integral

$$\frac{1}{\pi}\int_0^\infty e^{-2uR}\left\{\frac{3}{R^6}+\frac{6u}{R^5}+\frac{5u^2}{R^4}+\frac{2u^3}{R^3}+\frac{u^4}{R^2}\right\}du$$

$$j_\mu(\mathbf{r}) = e\bar{\psi}(\mathbf{r})\gamma^\mu\psi(\mathbf{r}) \qquad \mu = 1, 2, 3, 4$$

associated with the electronic motions.

$$V_{G\text{-}G}(R) = \frac{i}{16\pi^5}\int\cdots\int d\mathbf{r}_1\, d\mathbf{r}_2\, d\mathbf{r}_3\, d\mathbf{r}_4\, d\mathbf{p}\, d\mathbf{p}' \int_{-\infty}^{+\infty} d\omega e^{i\mathbf{p}\cdot(\mathbf{r}_1-\mathbf{r}_2)} e^{i\mathbf{p}'\cdot(\mathbf{r}_3-\mathbf{r}_4)}$$
$$\times \frac{1}{\mathbf{p}^2-\omega^2-i\varepsilon}\frac{1}{\mathbf{p}'^2-\omega^2-i\varepsilon}\sum_{n,p}\left[\frac{j_\mu^{on}(\mathbf{r}_1)j_\nu^{no}(\mathbf{r}_3)}{E_{no}-\omega-i\varepsilon}+\frac{j_\nu^{op}(\mathbf{r}_3)j_\mu^{po}(\mathbf{r}_1)}{E_{no}+\omega-i\varepsilon}\right]$$
$$\times\left[\frac{j_\mu^{op}(\mathbf{r}_2)j_\nu^{po}(\mathbf{r}_4)}{E_{po}+\omega-i\varepsilon}+\frac{j_\nu^{op}(\mathbf{r}_4)j_\mu^{po}(\mathbf{r}_2)}{E_{po}-\omega-i\varepsilon}\right] \tag{43}$$

Now if

$$B_{no}^{\mu\nu}(\mathbf{p},\mathbf{p}';\omega) = \iint d\mathbf{r}\, d\mathbf{r}' e^{i\mathbf{p}\cdot\mathbf{r}} e^{i\mathbf{p}\cdot\mathbf{r}'}\sum_n\left[\frac{j_\mu^{on}(\mathbf{r})j_\nu^{no}(\mathbf{r}')}{E_{no}-\omega-i\varepsilon}+\frac{j_\nu^{on}(\mathbf{r}')j_\mu^{no}(\mathbf{r})}{E_{no}+\omega-i\varepsilon}\right] \tag{44}$$

then

$$V_{G\text{-}G}(R) = \frac{i}{16\pi^5}\iint d\mathbf{p}\, d\mathbf{p}' \int_{-\infty}^{+\infty}\frac{B_{no}^{\mu\nu}(\mathbf{p},\mathbf{p}';\omega)B_{po}^{\nu\mu}(-\mathbf{p},-\mathbf{p}';\omega)}{(\mathbf{p}^2-\omega^2-i\varepsilon)(\mathbf{p}'^2-\omega^2-i\varepsilon)} e^{i(\mathbf{p}+\mathbf{p}')\cdot\mathbf{R}} \tag{45}$$

In nonrelativistic and dipole approximation,

$$B_{no}^{ij} = \frac{2E_{no}\omega^2}{(E_{no}-i\varepsilon)^2-\omega^2} q_{on}^i q_{no}^j \tag{46}$$

$$B_{no}^{4i} = \frac{-2iE_{no}\omega p^j}{(E_{no}-i\varepsilon)^2-\omega^2} q_{on}^j q_{no}^i \tag{47}$$

$$B_{no}^{44} = \frac{2E_{no}p^i p'^j}{(E_{no}-i\varepsilon)^2-\omega^2} q_{on}^i q_{no}^j \tag{48}$$

and so

$$V_{G\text{-}G}(R) = \frac{i}{4\pi^5}\sum_{n,p} E_{no}(1)E_{po}(2)q_{on}^i(1)q_{no}^j(1)q_{op}^k(2)q_{po}^l(2)\iint d\mathbf{p}\, d\mathbf{p}' e^{(\mathbf{p}+\mathbf{p}')\cdot\mathbf{R}}$$
$$\times\int_{-\infty}^{+\infty} d\omega\frac{(\omega^2\delta_{ik}-p_ip_k)(\omega^2\delta_{jl}-p'_jp'_l)}{(p^2-\omega^2-i\varepsilon)(p'^2-\omega^2-i\varepsilon)} \tag{49}$$
$$\times[(E_{no}(1)-i\varepsilon)^2-\omega^2][(E_{po}(2)-i\varepsilon)^2-\omega^2]$$

which by long algebraic manipulation with judicious integration gives Eq. (33) exactly.

At the same time, a very simplified version of the older method was found.[33] By coupling the dipoles directly with the transverse electric

field as in Eq. (20), the number of time-ordered graphs needed is reduced to six (plus reflections), since no two-photon vertices are involved at all. Also, surprisingly, no static Coulomb potential $U_{\text{int};3}^{\text{Coulomb}}(1,2)$ is present and the London graph (Fig. 1) is not required.* Now in the large R limit, no cancellations appear at all and the $V_{C\text{-}P}(R)$ asymptotic form arises entirely from graphs (i) and (iv) of Figure 7 when both photons are in the field at the same time as both atoms are in their ground states. However, more work is necessary with this method to extract the London limit to which all six graphs contribute. A detailed discussion is given in Section II-A.

In 1962, a recalculation of the Casimir and Polder potential by the method of Dzyaloshinskii was made[34] using nonrelativistic currents

$$\mathbf{j}(\mathbf{r}) = \frac{ie\hbar}{2m} \sum_j [\delta(\mathbf{r} - \mathbf{r}_j)\nabla_j + \nabla_j \delta(\mathbf{r} - \mathbf{r}_j)] \tag{50}$$

but Lorentz gauge four-potentials, A_μ. It was found that the $\sum_j e^2/2m\mathbf{A}^2(\mathbf{r}_j)$ term was also necessary to reduce the potential to that of Casimir and Polder. Besides a numerical discussion of the dipole terms, especially in the London limit $R \ll \lambda\!\!\!^{-}$ in terms of frequency–dependent polarizabilities, these authors obtained the fourth–order potentials involving magnetic dipole couplings as well as the electric dipole ones. The leading terms were given in both limits. Among these are mixed electric dipole–magnetic dipole terms

$$V_{\text{mix}}(R) = -\frac{16}{3\pi}\frac{(\hbar c)^3}{R^9} \times \sum_{n,p} \frac{\langle 0|\, e\mathbf{q}(1)\,|n\rangle \cdot \langle n|\, \mathbf{M}(1)\,|0\rangle}{E_{no}^2} \frac{\langle 0|\, e\mathbf{q}(2)\,|p\rangle \cdot \langle p|\, \mathbf{M}(2)\,|0\rangle}{E_{po}^2}$$

$$R \gg \lambda\!\!\!^{-} \tag{51}$$

$$= -\frac{4}{3}\frac{1}{R^6} \sum_{n,p} \frac{\langle 0|\, e\mathbf{q}(1)\,|n\rangle \cdot \langle n|\, \mathbf{M}(1)\,|0\rangle \langle 0|\, e\mathbf{q}(2)\,|p\rangle \cdot \langle p|\, \mathbf{M}(2)\,|0\rangle}{(E_{no} + E_{po})}$$

$$R \ll \lambda\!\!\!^{-} \tag{52}$$

* For a general discussion of the relation between the Coulomb gauge and the interaction Hamiltonian, see Power and Zienau.[9]

where

$$\mathbf{M} = \frac{e}{2mc} \sum_{i=1}^{N(\xi)} \mathbf{r}^{(i)} \times \mathbf{p}^{(i)} \tag{53}$$

is the orbital magnetic moment. Finally, they commented on the fact that this type of potential gives rise to differing dispersion energies for optically active molecules having the same or mirror-image configurations.

In a similar vein are the methods of McLachlan.[35] Here, the energy of interaction is calculated by use of the general susceptibility of both the molecules *and* the electromagnetic field. For the molecules, this susceptibility is[36]

$$\alpha_{ik}(\omega) = \sum_m \left\{ \frac{\langle n| eq_i |m\rangle\langle m| eq_k |n\rangle}{E_{mn} - \omega - i\varepsilon} + \frac{\langle n| eq_k |m\rangle\langle m| eq_i |n\rangle}{E_{mn} + \omega + i\varepsilon} \right\} \tag{54}$$

and for the field-vector potential, it is

$$A_{\mu\nu}(\mathbf{r},\mathbf{r}'; \omega) = \delta_{\mu\nu} \frac{\exp(\pm i\omega |\mathbf{r} - \mathbf{r}'|)}{|\mathbf{r} - \mathbf{r}'|} \tag{55}$$

The mutual polarization energy is then shown, by perturbation theory applied to the density matrix, to be

$$-\frac{1}{2\pi} \int_0^\infty \alpha_{\mu\nu}(\mathbf{r}_1,\mathbf{r}_2; i\xi)\alpha'_{\nu\mu}(\mathbf{r}'_1,\mathbf{r}'_2; i\xi) \frac{\exp[-\xi(R_1 + R_2)]}{R_1 R_2} d\xi \tag{56}$$

where the prime denotes the second molecule and $R_1 = |\mathbf{r}_1 - \mathbf{r}'_2|$, $R_2 = |\mathbf{r}_2 - \mathbf{r}'_1|$. In terms of *relativistic* currents, Eq. (56) is then

$$-\frac{1}{2\pi} \int_0^\infty d\xi \frac{\exp[-\xi(R_1 + R_2)]}{R_1 R_2} \left[\frac{j^\mu_{on}(\mathbf{r}_1) j^\nu_{no}(\mathbf{r}_2)}{E_{no} - i\xi} + \frac{j^\nu_{on}(\mathbf{r}_2) j^\mu_{no}(\mathbf{r}_1)}{E_{no} + i\xi} \right] \times \left[\frac{j^\nu_{op}(\mathbf{r}'_2) j^\mu_{po}(\mathbf{r}'_1)}{E_{po} - i\xi} + \frac{j^\mu_{op}(\mathbf{r}'_1) j^\nu_{po}(\mathbf{r}'_2)}{E_{po} + i\xi} \right] \tag{57}$$

which has the appearance of Dzyaloshinskii's energy [Eq. (43)] if the $\mathbf{p}$ and $\mathbf{p}'$ integrals are done first before the $\mathbf{r}$ integrals. The small R and large R limits, i.e., the London and $V_{C\text{-}P}$ potentials are then obtained by using the $e\mathbf{q} \cdot \mathbf{E}^\perp$ interaction energy. It is claimed that this method uses elementary quantum mechanics and almost no quantum field theory. However, to obtain Eq. (55), one uses the retarded propagators through the commutators of the electric field. If, on the other hand, it is to be assumed that what is meant is that no propagators of the electron

field are used, then it should be stated that to progress from Eq. (57) to the full interaction $V_{G\text{-}G}(R)$ of Eq. (33), it is necessary to use the currents that give rise to negative energy states in the summation over (n) and (p). By use of quantum field theory, Eq. (57) is almost immediate and "to pursue this formidable expression" requires considerable effort in relativistic wave equations. McLachlan has successfully pursued his methods in further work to examine many-body forces, temperature effect interaction with surfaces, etc.[37-39]

During the mid 1950's, there was a completely different approach to these problems by Lifshitz and his collaborators.[40,41] This was based on macroscopic electrodynamics and fluctuation analysis. Between two solids, the attractive forces arise from the fluctuating electromagnetic fields present and by use of the general theory of Matsubara, field theoretical techniques are applied to statistical physics. The reviewer does not feel qualified to discuss this work but, instead, refers the reader to the discussion in Landau and Lifshitz's books[36,42] and the review article by Dzyaloshinskii, Lifshitz, and Pitaevskii.[41] By considering the force between the two solids when they are very dilute, it is possible to extract the intermolecular force. For temperatures below $c\hbar/kL$, where L is the separation between the two solids, the forces are exactly the London force and the asymptotic Casimir and Polder force in the two limits $R \ll \lambda$, $R \gg \lambda$. The direct macroscopic measurement of these long-range intermolecular forces has been carried out with quartz by Deryagin and co-workers.[43] Experimental work has also been carried out by London[44] and Holland.[45] A particular case where the solids involved are metallic with the vacuum between them is of interest. The force of attraction is

$$F = (\pi^2/240)(\hbar c/L^4) \tag{58}$$

independent of the fine-structure constant. This beautiful result was first obtained by Casimir[23] by a simple appeal to the changes in the zero-point energy brought about by making a cavity of conducting walls. This proof has reached the textbooks.[46]

To complete this survey, several allied topics will be briefly mentioned. The retarded resonance interactions have been considered in problems of exciton chemistry. Initiated by Craig and Walsh[47] and by Simpson,[48] further applications of the long-range forces have been carried out by Rice,[49] Philpott,[50] and Dissado.[51] Due to the weak falloff of the radiative resonance potential compared with the static $1/R^3$ law,

considerable difficulty occurs with convergence problems. Corrections in the Davydov splitting terms of 20% can be found for crystals whose size is of the order of λ .These can occur where the near-zone dipole sum with β_{ij} angle dependence is small on account of cancellations through structural accidents. Care is needed since this is also the condition where higher multipoles can make large relative contributions. The radiative resonance energy is also involved in the resonance transfer of excitation between an excited atom and a distant similar atom in its ground state. This problem goes back to the beginning of the quantum theory of radiation[52] and is important in energy transfer in biological systems.[53-55] Two-body forces have been computed when both molecules are excited;[56,57] they are discussed in Section III-C. Three-body forces, first considered by Axilrod and Teller[58] for the static potential, have been calculated in the wave zone by Aub and Zienau,[59] McLachlan,[38] and (with excitation present) by Philpott.[50] Recent calculations[60,61] of radiative effects for spin–spin and spin–orbit-type interactions are summarized in Section IV.

II. CALCULATION OF DISPERSION INTERACTION: THE CASIMIR-POLDER POTENTIAL

In this section brief accounts are given of two of the methods available for computing the Casimir and Polder potential $V_{G\text{-}G}(R)$ of Eq. (33). The first method is based on the noncovariant Rayleigh-Schrödinger perturbation theory and should be the one more easily accessible to theoretical chemists. The second method starts from the S matrix of quantum field theory and requires some knowledge of relativistic quantum mechanics. This has been kept to a minimum in the short survey given here.

A. Noncovariant Method

The starting point for this method is the Hamiltonian [Eq. (15)] with the interaction energy

$$H_{\text{int}} = -\boldsymbol{\mu}(1) \cdot \mathbf{E}^{\perp} - \boldsymbol{\mu}(2) \cdot \mathbf{E}^{\perp} \tag{59}$$

of Eq. (20). The spectrum of the unperturbed Hamiltonian $H(1) + H(2) + H_{\text{rad}}$ is supposedly known and the first nonvanishing perturbation of the spectrum due to H_{int} is calculated by the Rayleigh-Schrödinger method. The only innovation from elementary quantum mechanics is

that the states of the complete system involve photons as well as the normal single atom or molecular terms. The quantization of the radiation field is carried out in the usual way.[1,62] The transverse electric field, in the Schrödinger representation, is expanded into the Fourier series

$$\mathbf{E}^{\perp}(\mathbf{r}) = \sum_{\substack{\mathbf{k} \\ \lambda=1,2}} \left(\frac{2\pi\hbar\omega}{V}\right)^{1/2} i\mathbf{e}^{(\lambda)}(\mathbf{k})[a^{(\lambda)}(\mathbf{k})e^{i\mathbf{k}\cdot\mathbf{r}} - a^{(\lambda)\dagger}e^{-i\mathbf{k}\cdot\mathbf{r}}] \tag{60}$$

V is the quantization volume, $\omega = kc$ is the circular frequency, and $\mathbf{k}$ the wave vector. $\mathbf{e}^{(\lambda)}(\mathbf{k})$ is a unit vector along the direction of polarization for the wave vector $\mathbf{k}$ and polarization $\lambda = 1, 2$. Due to the transverse nature of the photon

$$\mathbf{e}^{(\lambda)}(\mathbf{k}) \cdot \mathbf{k} = 0 \tag{61}$$

which gives the two possible values of λ. Finally, $a^{(\lambda)}(\mathbf{k})$ and $a^{(\lambda)\dagger}(\mathbf{k})$ are the annihilation and creation operators for photons of mode $\mathbf{k}$, λ and satisfy the commutation relations

$$[a^{(\lambda)}(\mathbf{k}), a^{(\lambda')\dagger}(\mathbf{k}')] = \delta_{\lambda\lambda'}\delta_{\mathbf{k}\mathbf{k}'} \tag{62}$$

By using the interaction Hamiltonian [Eq. (59)] which contains terms linear in the electric field and no others, only fourth-order perturbation matrix elements contribute to the energy shift.[33] They correspond to the diagrams of Figure 7. The fourth-order energy shift is for a state $|i\rangle$ given by[63,64]

$$\Delta E^{(4)} = \sum_{\mathrm{I,II,III} \neq i} \langle i| H_{\mathrm{int}} \frac{|\mathrm{III}\rangle\langle\mathrm{III}|}{E_i - E_{\mathrm{III}}} \Bigg[(H_{\mathrm{int}} - \langle i| H_{\mathrm{int}} |i\rangle) \frac{|\mathrm{II}\rangle\langle\mathrm{II}|}{E_i - E_{\mathrm{II}}}$$

$$\times (H_{\mathrm{int}} - \langle i| H_{\mathrm{int}} |i\rangle) - \langle i| H_{\mathrm{int}} \frac{|\mathrm{II}\rangle\langle\mathrm{II}|}{E_i - E_{\mathrm{II}}} H_{\mathrm{int}} |i\rangle \Bigg] \frac{|\mathrm{I}\rangle\langle\mathrm{I}|}{E_i - E_{\mathrm{I}}} H_{\mathrm{int}} |i\rangle \tag{63}$$

which, for the H_{int} of Eq. (59) with no diagonal term $\langle i| H_{\mathrm{int}} |i\rangle$ reduces to

$$\Delta E^{(4)} = \sum_{\mathrm{I,II,III} \neq i} \frac{\langle i| H_{\mathrm{int}} |\mathrm{III}\rangle\langle\mathrm{III}| H_{\mathrm{int}} |\mathrm{II}\rangle\langle\mathrm{II}| H_{\mathrm{int}} |\mathrm{I}\rangle\langle\mathrm{I}| H_{\mathrm{int}} |i\rangle}{(E_i - E_{\mathrm{III}})(E_i - E_{\mathrm{II}})(E_i - E_{\mathrm{I}})}$$

$$- \sum_{\mathrm{I} \neq i} \frac{\langle i| H_{\mathrm{int}} |\mathrm{I}\rangle\langle\mathrm{I}| H_{\mathrm{int}} |i\rangle}{(E_i - E_{\mathrm{I}})^2} \sum_{\mathrm{II} \neq i} \frac{\langle i| H_{\mathrm{int}} |\mathrm{II}\rangle\langle\mathrm{II}| H_{\mathrm{int}} |i\rangle}{E_i - E_{\mathrm{II}}} \tag{64}$$

The second term does not contribute to the problem under consideration, as the only nonvanishing term in either sum is independent of R.

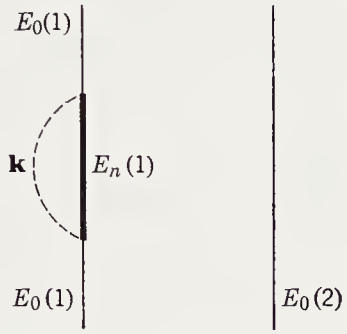

Fig. 8. Diagram corresponding to the matrix element involved in the evaluation of the second term of Eq. (64). Its contribution to ΔE is independent of R.

Figure 8 illustrates such a matrix element; it is a self-energy contribution to ΔE. Thus, one is left with

$$\Delta E^{(4)}(R) = \sum_{\mathrm{I,II,III} \neq i} \frac{\langle i|\, H_{\mathrm{int}}\, |\mathrm{III}\rangle\langle \mathrm{III}|\, H_{\mathrm{int}}\, |\mathrm{II}\rangle\langle \mathrm{II}|\, H_{\mathrm{int}}\, |\mathrm{I}\rangle\langle \mathrm{I}|\, H_{\mathrm{int}}\, |i\rangle}{(E_i - E_{\mathrm{III}})(E_i - E_{\mathrm{II}})(E_i - E_{\mathrm{I}})} \tag{65}$$

and the relationship of this sum to the structure of the diagrams in Figure 7 is apparent. In Figure 9, the two diagrams (i) and (iv) of Figure 7

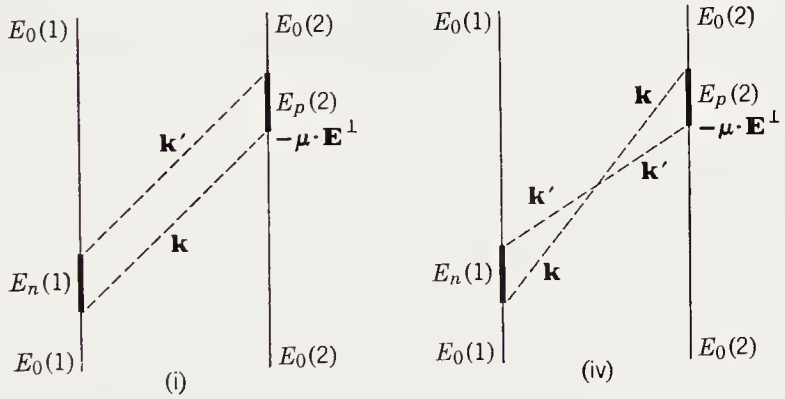

Fig. 9. The ordered diagrams which give the asymptotic Casimir-Polder potential.

are reproduced showing explicitly the vertex functions and the photon labels corresponding to the matrix elements involved. The contribution to $\Delta E(R)$ from (i) of Figure 7 is

$$\Delta E^{(4)}_{(\mathrm{i})}(R) = \langle E_o : 0|\ \boldsymbol{\mu}(2)\cdot\mathbf{E}^{\perp}(2)\,|E_p : \mathbf{k}',\ \lambda'\rangle$$
$$\times \langle E_p : \mathbf{k}', \lambda'|\ \boldsymbol{\mu}(2)\cdot\mathbf{E}^{\perp}(2)\,|E_o : \mathbf{k}', \lambda'; k, \lambda\rangle$$
$$\times \langle E_o : \mathbf{k}', \lambda'; \mathbf{k}, \lambda|\ \boldsymbol{\mu}(1)\cdot\mathbf{E}^{\perp}(1)\,|E_n : \mathbf{k}, \lambda\rangle$$
$$\times \langle E_n : \mathbf{k}, \lambda|\ \boldsymbol{\mu}(1)\cdot\mathbf{E}^{\perp}(1)\,|E_o : 0\rangle$$
$$\sum_{\substack{p,n\\ \mathbf{k},\mathbf{k}'}} \frac{}{[E_o(1)+E_o(2)-(E_o(1)+E_p(2)+\hbar ck')]}$$
$$\times [E_o(1)+E_o(2)-(E_o(1)+E_o(2)+\hbar ck'+\hbar ck)]$$
$$\times [E_o(1)+E_o(2)-(E_n(1)+E_o(2)+\hbar ck)] \tag{66}$$

The matrix elements over the electric field operator follow from the expansion [Eq. (60)] for $E^{\perp}$; a typical such element is

$$\langle 0|\ \mathbf{E}^{\perp}\,|\mathbf{k}, \lambda\rangle = i\left(\frac{2\pi\hbar ck}{V}\right)^{1/2}\mathbf{e}^{(\lambda)}(\mathbf{k})e^{i\mathbf{k}\cdot\mathbf{r}} \tag{67}$$

Thus, Eq. (66) reduces to

$$\Delta E^{(4)}_{(\mathrm{i})}(R) = -\sum_{\substack{p,n\\ \mathbf{k},\mathbf{k}'}} \frac{(2\pi\hbar ck)(2\pi\hbar ck')}{V^2}\, e^{i(\mathbf{k}+\mathbf{k}\cdot\mathbf{R})}$$
$$\langle E_o|\ \boldsymbol{\mu}(2)\cdot\mathbf{e}^{(\lambda')}\,|E_p\rangle\langle E_p|\ \boldsymbol{\mu}(2)\cdot\mathbf{e}^{(\lambda)}\,|E_o\rangle$$
$$\times \frac{\times \langle E_o|\ \boldsymbol{\mu}(1)\cdot\mathbf{e}^{(\lambda')}\,|E_n\rangle\langle E_n|\ \boldsymbol{\mu}(1)\cdot\mathbf{e}^{(\lambda)}\,|E_o\rangle}{(E_{po}(2)+\hbar ck')(\hbar ck+\hbar ck')(E_{no}(1)+\hbar ck)} \tag{68}$$

where $E_{po} = E_p - E_o$.

In a similar way

$$\Delta E^{(4)}_{(\mathrm{iv})}(R) = -\sum_{\substack{p,n\\ \mathbf{k},\mathbf{k}'}} \frac{(2\pi\hbar c)^2 kk'}{V^2}\, e^{i(\mathbf{k}+\mathbf{k}')\cdot\mathbf{R}}$$
$$\langle E_o|\ \boldsymbol{\mu}(2)\cdot\mathbf{e}^{(\lambda)}\,|E_p\rangle\langle E_p|\ \boldsymbol{\mu}(2)\cdot\mathbf{e}^{(\lambda')}\,|E_o\rangle$$
$$\times \frac{\times \langle E_o|\ \boldsymbol{\mu}(1)\cdot\mathbf{e}^{(\lambda')}\,|E_n\rangle\langle E_n|\ \boldsymbol{\mu}(1)\cdot\mathbf{e}^{(\lambda)}\,|E_o\rangle}{(E_{po}(2)+\hbar ck)(\hbar ck+\hbar ck')(E_{no}(1)+\hbar ck)} \tag{69}$$

The summations over the polarization indices (λ) and (λ') for the photons is carried out by means of the formula

$$\sum_{\lambda} e_i^{(\lambda)}(\mathbf{k}) e_j^{(\lambda)}(\mathbf{k}) = \delta_{ij} - \hat{k}_i \hat{k}_j \tag{70}$$

and thus

$$\Delta E_{(i)}^{(4)}(R) + \Delta E_{(iv)}^{(4)}(R) = -\frac{4\pi^2 \hbar^2 c^2}{V^2} \sum_{\substack{p,n \\ \mathbf{k},\mathbf{k}'}} \frac{kk'(1 + (\hat{k} \cdot \hat{k}')^2)}{(\hbar ck + \hbar ck')} \frac{e^{i(\mathbf{k}+\mathbf{k}')\cdot\mathbf{R}}}{(E_{no}(1) + \hbar ck)}$$

$$\times \left[\frac{1}{E_{po}(2) + \hbar ck} + \frac{1}{E_{po}(2) + \hbar ck'} \right] |\langle \boldsymbol{\mu}(1) \rangle|^2 |\langle \boldsymbol{\mu}(2) \rangle|^2 \tag{71}$$

In the limit $R \gg \lambda_1, \lambda_2$ the leading contributions to the sum over $\mathbf{k}$ and $\mathbf{k}'$ come from those terms with k and $k' \ll E/hc$ because of the exponential factor in the summand. Thus, for this limiting case the terms hck, hck' can be ignored compared with $E_{no}(1)$ and $E_{no}(2)$ in the summation and the result, adding the contributions from the reflected diagrams to (i) and (vi) (Fig. 7), is

$$\Delta E(R) \simeq -\frac{4\pi^2 \hbar c}{(2\pi)^6} \iint \frac{k^3 k'^3 (1 + (\hat{k} \cdot \hat{k}')^2) e^{i(\mathbf{k}+\mathbf{k}')\cdot\mathbf{R}}}{(k + k')} \, dk \, dk' \, d\Omega \, d\Omega'$$

$$\times \sum_{p,n} \frac{4 |\langle \boldsymbol{\mu}(1) \rangle|^2 |\langle \boldsymbol{\mu}(2) \rangle|^2}{E_{no}(1) E_{po}(2)} \tag{72}$$

The summation over $\mathbf{k}$ and $\mathbf{k}'$ having been replaced by an integration with the factor $V^2 k^2 \, dk \, d\Omega k'^2 \, dk' \, d\Omega'$. From the definition of polarization Eq. (2),

$$\Delta E(R) \simeq -\alpha(1)\alpha(2) \frac{\hbar c}{(2\pi)^4} \iint \frac{k^3 k'^3 (1 + (\hat{k} \cdot \hat{k}')^2)}{(k + k')} e^{i(\mathbf{k}+\mathbf{k}')\cdot\mathbf{R}} \, dk \, dk' \, d\Omega \, d\Omega' \tag{73}$$

It is easy to see from the dimensions of the integral that as a function of R it varies as R^{-7}. So

$$\Delta E(R) \simeq -\gamma \frac{\alpha(1)\alpha(2)\hbar c}{R^7} \tag{74}$$

where γ is a number whose value $23/4\pi$ can be found by carrying out the integration explicitly. Thus, as mentioned on page 184, the Casimir and Polder asymptotic potential arises from those matrix elements (i), (iv) and reflections where the two photons are in the field simultaneously with the ground-state molecules.

In the same way, it can be seen that the contributions of diagrams (ii),

(iii), (v), and (vi) (Fig. 7) are each of the order $\alpha(1)\alpha(2)E^{-1}R^{-8}$ for $R \gg \lambda\!\!\!^{-}$. This is so because no energy denominator contains hck and hck' alone and so three powers of E are in the denominator of the energy shift when expressed in terms of the dipole moments and one power is left when the energy shift is expressed in terms of the polarizabilities. In Table I are listed the energy denominators for the graphs (i)–(vi) and the reflections of Figure 7.

TABLE I

Graph	Energy denominator
(i)	$D_{\mathrm{i}} = -(\nu_{no} + k)(k + k')(\nu_{po} + k')$
(ii)	$D_{\mathrm{ii}} = -(\nu_{no} + k)(\nu_{no} + \nu_{po})(\nu_{po} + k')$
(iii)	$D_{\mathrm{iii}} = -(\nu_{no} + k)(\nu_{no} + \nu_{po})(\nu_{no} + k')$
(iv)	$D_{\mathrm{iv}} = -(\nu_{no} + k)(k + k')(\nu_{po} + k)$
(v)	$D_{\mathrm{v}} = -(\nu_{no} + k)(\nu_{no} + \nu_{po} + k + k')(\nu_{po} + k)$
(vi)	$D_{\mathrm{vi}} = -(\nu_{po} + k')(\nu_{no} + \nu_{po} + k + k')(\nu_{po} + k)$

At this stage, it is possible to see the great advantage of using the $-\boldsymbol{\mu} \cdot \mathbf{E}^{\perp}$ interaction. If similar arguments, namely counting powers of k and k' are made using $(e/mc)\mathbf{p} \cdot \mathbf{A}$, one can see* that the contribution of (i) is proportional to E^4R^{-3} and large cancellations with other terms, including the longitudinal interactions, must occur to give the final R^{-7} dependence.

To obtain the complete Casimir-Polder potential, $V_{G\text{-}G}(R)$, the contributions of (ii), (iii), (v), and (vi) must be added to Eq. (71). The essential variations in the matrix elements for the various orderings lie in the energy denominators when use is made of the symmetry of the multiplicand in $\mathbf{k}$ and $\mathbf{k}'$ and since $\boldsymbol{\mu}$ is Hermitian. So

$$V_{G\text{-}G}(R) = \frac{(2\pi\hbar c)^2}{V^2} \sum_{p,n;\mathbf{k},\mathbf{k}';\lambda,\lambda'} e^{i(\mathbf{k}+\mathbf{k}')\cdot\mathbf{R}} k k' e_i^{(\lambda)} e_j^{(\lambda)} e_\sigma^{(\lambda')} e_\tau^{(\lambda')} \times \mu_{on}^{i}(1)\mu_{no}^{\sigma}(1)\mu_{op}^{j}(2)\mu_{po}^{\tau}(2) \sum_{a=\mathrm{i}}^{\mathrm{xii}} D_a^{-1} \qquad (75)$$

the D's being given in Table I. The summation over the polarization directions λ, λ' follows Eq. (70) and the summation over $\mathbf{k}$ and $\mathbf{k}'$ are

* This is due to the matrix element of $(e/mc)\mathbf{p} \cdot \mathbf{A}$ having a factor $E/\sqrt{k}$ while that of $-\boldsymbol{\mu} \cdot \mathbf{E}^{\perp}$ has the factor $\sqrt{k}$.[46]

replaced by integrations. The angular integrations are standard using

$$\tau_{ij}(kR) \equiv \frac{1}{4\pi}\int e^{i\mathbf{k}\cdot\mathbf{R}}(\delta_{ij} - \hat{k}_i\hat{k}_j)\,d\Omega$$
$$= \alpha_{ij}\frac{\sin kR}{kR} + \beta_{ij}\left(\frac{\cos kR}{k^2R^2} - \frac{\sin kR}{k^3R^3}\right) \quad (76)$$

and thus

$$V_{G\text{-}G}(R) = -\frac{1}{\pi^2}\sum_{p,n}\mu^i_{on}(1)\mu^\sigma_{no}(1)\mu^j_{op}(2)\mu^\tau_{po}(2)$$
$$\times \int_0^\infty\int_0^\infty k^3k'^3\tau_{ij}(kR)\tau_{\sigma\tau}(k'R)\sum_a D_a^{-1}\,dk\,dk' \quad (77)$$

The summation over a can be carried out in various ways[21,27,50] leading to

$$V_{G\text{-}G}(R) = -\frac{4}{\pi^2}\sum_{n,p}\mu^i_{on}(1)\mu^\sigma_{no}(1)\mu^j_{op}(2)\mu^\tau_{po}(2)$$
$$\times \int_0^\infty\int_0^\infty k^3k'^3\tau_{ij}(kR)\tau_{\sigma\tau}(k'R)\frac{(\nu_{po}+\nu_{no}+k')}{(\nu_{po}+k')(\nu_{no}+k')}$$
$$\times\left(\frac{1}{k'+k} - \frac{1}{k'-k}\right)dk\,dk' \quad (78)$$

The integration over the pole at $k = k'$ is to be taken as a Cauchy principal value integral. On integrating over k

$$V_{G\text{-}G}(R) = -\frac{4}{\pi}\sum_{n,p}\frac{\mu^i_{on}(1)\mu^\sigma_{no}(1)\mu^j_{op}(2)\mu^\tau_{po}(2)}{(\nu_{no}+\nu_{po})(\nu_{no}-\nu_{po})}$$
$$\times\int_0^\infty\left(\frac{\nu_{no}}{\nu_{po}+k'} - \frac{\nu_{po}}{\nu_{no}+k'}\right)\left\{\frac{\alpha_{ij}\alpha_{\sigma\tau}}{R^2}k'^4\sin k'R\cos k'R\right.$$
$$+\frac{\alpha_{ij}\beta_{\sigma\tau}}{R^3}[k'^3\cos^2 k'R - (k'^2\sin k'R\cos k'R)/R]$$
$$-\frac{\alpha_{\sigma\tau}\beta_{ij}}{R^3}[k'^3\sin^2 k'R + (k'^2\sin k'R\cos k'R)/R]$$
$$+\frac{\beta_{ij}\beta_{\sigma\tau}}{R^4}[-k'^2\sin k'R\cos k'R$$
$$\left.-k'(\cos^2 k'R - \sin^2 k'R)/R + (\sin k'R\cos k'R)/R^2]\right\}dk' \quad (79)$$

Now making use of integrals such as

$$\int_0^\infty \frac{\sin 2\omega R}{\nu + \omega}\, d\omega = \sin(2\nu R)\,\mathrm{Ci}(2\nu R) - \cos(2\nu R)\,\mathrm{si}(2\nu R) \qquad \nu > 0, \quad R > 0 \tag{80}$$

$$\begin{aligned} V_{G\text{-}G}(R) = -\frac{2}{\pi}\sum_{n,p} \mu^i_{on}(1)\mu^\sigma_{no}(1)\mu^j_{op}(2)\mu^\tau_{po}(2)\,\frac{\nu_{no}\nu_{po}}{(\nu_{no}^2 - \nu_{po}^2)} \\ \times \left[\frac{\alpha_{ij}\alpha_{\sigma\tau}}{R^2}\left\{\nu_{po}^3 A_{po} - \nu_{no}^3 A_{no} + \frac{1}{2R}(\nu_{no}^2 - \nu_{po}^2)\right\}\right. \\ + \frac{2\alpha_{ij}\beta_{\sigma\tau}}{R^3}\left\{\nu_{po}^2 B_{po} - \nu_{no}^2 B_{no} - \frac{1}{R}(\nu_{po}A_{po} - \nu_{no}A_{no})\right\} \\ \left. + \frac{\beta_{ij}\beta_{\sigma\tau}}{R^4}\left\{\nu_{no}A_{no} - \nu_{po}A_{po} + \frac{2}{R}(B_{no} - B_{po}) + \frac{1}{R^2}\left(\frac{A_{po}}{\nu_{po}} - \frac{A_{no}}{\nu_{no}}\right)\right\}\right] \end{aligned} \tag{81}$$

Finally, if the summations over the magnetic quantum numbers of the n, p states are made

$$\sum \langle 0|\,\mu_i(1)\,|n\rangle\langle n|\,\mu_\sigma(1)\,|0\rangle = \delta_{i\sigma}\,|\langle \boldsymbol{\mu}(1)\rangle|^2 \tag{82}$$

Eq. (81) reduces to Eq. (33) and so

$$\begin{aligned} V_{G\text{-}G}(R) = -\frac{4}{\pi}\sum_{n,p} |\langle \boldsymbol{\mu}(1)\rangle|^2\,|\langle \boldsymbol{\mu}(2)\rangle|^2\,\frac{\nu_{no}\nu_{po}}{\nu_{no}^2 - \nu_{po}^2} \\ \times \left\{\frac{1}{R^2}\left[\nu_{po}^3 A_{po} - \nu_{no}^3 A_{no} + (\nu_{no}^2 - \nu_{po}^2)/(2R)\right]\right. \\ + \frac{2}{R^3}\left[\nu_{po}^2 B_{po} - \nu_{no}^2 B_{no} - (\nu_{po}A_{po} - \nu_{no}A_{no})/R\right] \\ \left. + \frac{3}{R^4}\left[\nu_{no}A_{no} - \nu_{po}A_{po} + 2(B_{no} - B_{po})/R + (A_{po}/\nu_{po} - A_{no}/\nu_{no})/R^2\right]\right\} \end{aligned} \tag{83}$$

B. Feynman Method

Feynman's formalism in quantum electrodynamics has not been used extensively to discuss intermolecular interactions. This is due

partially to the fact that the S matrix theory is primarily involved in computing scattering amplitudes—the ingoing and outgoing particles being free. A prominent exception is that the Casimir and Polder dispersion energy has been computed by Dzyaloshinskii[32] by field theoretical methods. More recently, the S matrix formalism has been used to obtain the resonance[13] and spin interactions.[60] These are discussed in Sections III and IV. The S matrix for quantum electrodynamics is

$$S = \sum_{n=0}^{\infty} \frac{(-i)^n}{n!} \int \cdots \int d^4x_1 \cdots d^4x_n P\{\mathscr{H}_I(x_1)\mathscr{H}_I(x_2) \cdots \mathscr{H}_I(x_n)\} \quad (84)$$

where the integral is over all the space–time volume of each local coordinate in the interaction Hamiltonian density $\mathscr{H}_I(x)$. P is the chronological operator which, when operating on a product of time-labeled operators, rearranges them in the same order as the time sequence of their label—the latest one occurring first in the product. So, as an example, for $n = 2$

$$\begin{aligned} P[\mathscr{H}_I(x_1)\mathscr{H}_I(x_2)] &= \mathscr{H}_I(x_1)\mathscr{H}_I(x_2) \qquad \text{if } t_1 > t_2 \\ &= \mathscr{H}_I(x_2)\mathscr{H}_I(x_1) \qquad \text{if } t_1 < t_2 \end{aligned} \quad (85)$$

For $n = 4$, there are 12 possible orderings. (Note the 12 diagrams in Figure 7 for the stationary-state perturbation theory.) $\mathscr{H}_I(x)$ is given in terms of the four-vector potential $A_\mu(x)$ and the four-current $j_\mu(x)$ as the integrand of Eq. (18)*

$$\mathscr{H}_I(x) = -j_\mu(x)A_\mu(x) \quad (86)$$

The current is defined in terms of the Dirac spinor $\psi(x)$ and its Hermitian conjugate $\psi^\dagger(x)$ as

$$j_\mu(x) = e\bar{\psi}(x)\gamma^\mu\psi(x) \quad (87)$$

where

$$\bar{\psi}(x) = \psi^\dagger(x)\gamma^4 \quad (88)$$

The system of units used is again such that $\hbar = c = 1$ and such that the

* The full theory of quantum electrodynamics requires the algorithm of renormalization as well as the coupled Maxwell-Dirac field equations obtained from Eq. (15). This involves, for example, a discussion of self interactions where light is emitted and reabsorbed by the same charge. The formal technique requires the addition of counter terms to the interaction energy density. For the purpose of this paper, all such low-order self-energy parts are easily identifiable and will be dropped. The masses and charges in the matrix elements are all observed masses and charges.

fourth components of four vectors are imaginary so that there is no need to distinguish between covariant and contravariant components of tensors. The gauge of the electromagnetic potentials is chosen to be the Lorentz gauge.

For the intermolecular potential problem, only the submatrix of S connecting no photon states is relevant, so taking the photon vacuum expectation value of S, a contraction of the photon operators $A_\mu(x)$ is possible. With the double dot notation for contraction,[65] one obtains

$$A_\mu^{\cdot}(x)A_\nu^{\cdot}(y) = \tfrac{1}{2}\delta_{\mu\nu}D_F(x-y) \tag{89}$$

Here D_F is the Feynman-Green function for the wave equation

$$D_F(x-y) = -\frac{2i}{(2\pi)^4}\int_{C_F}\frac{d^4p}{p^2}\exp\,(ip_\mu x_\mu) \tag{90}$$

C_F is the contour in the p_0 plane which bypasses the poles $\pm|\mathbf{p}|$ above and below the real axis, respectively. For the problem in hand, the first nontrivial nonvanshing term in the expansion, Eq. (84), is of the fourth order; in the photon vacuum subspace, it is

$$\begin{aligned} S^{(4)} = 2\pi^2 e^4 \iiiint & [(\bar\psi\gamma^\mu\underline{\psi})_{x_1}(\underline{\bar\psi}\gamma^\nu\psi)_{x_3} + (\bar\psi\gamma^\nu\underline{\psi})_{x_3}(\underline{\bar\psi}\gamma^\mu\psi)_{x_1}] \\ & \times [(\bar\psi\gamma^\mu\underline{\psi})_{x_2}(\underline{\bar\psi}\gamma^\nu\psi)_{x_4} + (\bar\psi\gamma^\nu\underline{\psi})_{x_4}(\underline{\bar\psi}\gamma^\mu\psi)_{x_2}] \\ & \times D_F(x_1-x_2)D_F(x_3-x_4)\,d^4x_1\,d^4x_2\,d^4x_3\,d^4x_4 \end{aligned} \tag{91}$$

where

$$\begin{aligned} \underline{\psi(x_1)}\bar\psi(x_2) &= \psi^{(+)}(x_1)\psi^{(+)}(x_2) \qquad t_1 > t_2 \\ &= -\psi^{(-)}(x_1)\psi^{(-)}(x_2) \qquad t_1 < t_2 \end{aligned} \tag{92}$$

The corresponding Feynman graphs are shown in Figure 10.

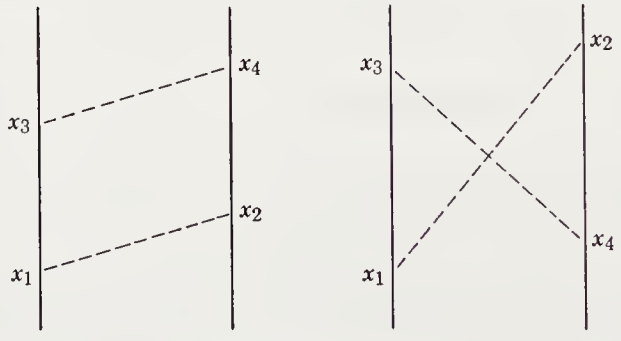

Fig. 10. Feynman graphs corresponding to $S^{(4)}$ of Eq. (91).

If the atomic states are labeled $|n\rangle$ and $|m\rangle$ with energies E_n and E_m, the current-density matrix elements are separable in space and time

$$\langle m|j^{\mu}(x)|n\rangle = j^{\mu}_{mn}(\mathbf{r}) \exp\left[i(E_m - E_n)t\right] \tag{93}$$

and the time dependence of the integrand is $S^{(4)}$ is then explicit. Carrying out the integration over the time variables gives

$$S^{(4)} = \frac{1}{8\pi^4}\,\delta(E_i - E_f) \int d\mathbf{p} \int d\mathbf{p}' \int_{C_F} d\omega \,\frac{1}{\mathbf{p}^2 - \omega^2}\,\frac{1}{\mathbf{p}'^2 - \omega^2}$$
$$\times B^{\mu\nu}_m(\mathbf{p},\mathbf{p}';\omega) B^{\nu\mu}_p(-\mathbf{p},-\mathbf{p}';-\omega) \tag{94}$$

where

$$B^{\mu\nu}_m(\mathbf{p},\mathbf{p}';\omega) = \int d^3\mathbf{r}\, d^3\mathbf{r}' \exp\left[i(\mathbf{p}\cdot\mathbf{r} + \mathbf{p}'\cdot\mathbf{r}')\right]$$
$$\times \sum_n \left\{ \frac{j^{\mu}_{mn}(\mathbf{r}) j^{\nu}_{nm}(\mathbf{r}')}{E_n - E_m - i\varepsilon + \omega} + \frac{j^{\nu}_{mn}(\mathbf{r}) j^{\mu}_{nm}(\mathbf{r}')}{E_n - E_m - i\varepsilon - \omega} \right\} \tag{95}$$

To extract the energy shift $E^{(4)}(R)$ from $S^{(4)}$, one makes use of the general theory of scattering[66,67]; a brief discussion is given in Section III-D. Specifically,

$$S^{(4)} = -2\pi i \delta(E_i - E_f)\Delta E^{(4)} \tag{96}$$

for the so-called "connected" contribution to the S matrix. Hence, for $m = p = 0$, the ground state for each system

$$V_{G\text{-}G}(R) = \Delta E^{(4)}(R) = \frac{ie^4}{16\pi^5} \int d^3\mathbf{p}\, d^3\mathbf{p}' \int_{C_F} d\omega \,\frac{1}{\mathbf{p}^2 - \omega^2}\,\frac{1}{\mathbf{p}'^2 - \omega^2}$$
$$\times B^{\mu\nu}_0(\mathbf{p},\mathbf{p}';\omega) B^{\nu\mu}_0(-\mathbf{p},-\mathbf{p}';-\omega) \tag{97}$$

With the nonrelativistic and dipole approximations for the currents, the B's are given by Eqs. (46)–(48) and hence,

$$V_{G\text{-}G}(R) = \frac{i}{16\pi^5} \int d^3\mathbf{p} \int d^3\mathbf{p}'\, e^{i(\mathbf{p}+\mathbf{p}')\cdot\mathbf{R}}$$
$$\times \int_{C_F} d\omega \,\frac{3\omega^4 - \omega^2(\mathbf{p}^2 + \mathbf{p}'^2) + (\mathbf{p}\cdot\mathbf{p}')^2}{(\mathbf{p}^2 - \omega^2)(\mathbf{p}'^2 - \omega^2)}\,\alpha^{(1)}(\omega)\alpha^{(2)}(\omega) \tag{98}$$

where

$$\alpha^{(\xi)}(\omega) = 2 \sum_n \frac{E_{on} |\langle \mu_{on}(\xi) \rangle|^2}{(E_{on} - i\varepsilon)^2 - \omega^2} \tag{99}$$

Now the integrals over the solid angles for $\mathbf{p}$ and $\mathbf{p}'$ are easily computed and

$$V_{G\text{-}G}(R) = \frac{-i}{4\pi^3} \int_{-\infty}^{+\infty} p\, dp\, p'\, dp' (p^2 \delta_{ij} + \nabla_i \nabla_j) \frac{e^{ipR}}{R} (p'^2 \delta_{ij} + \nabla_i \nabla_j) \frac{e^{ip'R}}{R}$$

$$\times \int_{C_F} d\omega\, \alpha^{(1)}(\omega) \alpha^{(2)}(\omega) \frac{1}{\mathbf{p}^2 - \omega^2} \frac{1}{\mathbf{p}'^2 - \omega^2} \tag{100}$$

This is essentially Eq. (49) from which the Casimir-Polder potential of Eqs. (32) and (33) follows.

Recently, Feinberg and Sucher[68] have shown that the asymptotic falloff $\sim R^{-7}$, in the interaction energy between any two neutral spinless centers due to two-photon exchange, is a consequence of the Mandelstam representation for the scattering amplitude and the Lorentz covariance of the vertex functions describing the coupling of the neutral systems to the electromagnetic field. By this method, one investigates the behavior of the scattering amplitude in a scattering between the two systems as a function of momentum transfer near zero. This is a reflection on the far-distant potential. In particular, if the spectral function

$$A(t) \sim t^N \qquad \text{as } t \to 0 \tag{101}$$

then

$$V(R) \sim 1/R^{2N+3} \qquad \text{as } R \to \infty \tag{102}$$

t is the square of the four-momentum transfer, in terms of the three-momentum $\mathbf{p}$ and the angle of scattering θ,

$$t = -2\mathbf{p}^2(1 - \cos\theta) \tag{103}$$

$A(t)$ is the spectral function which defines the direct-scattering amplitude $F(t)$ through the equation

$$F(t) = \frac{1}{\pi} \int_0^\infty \frac{A(t')}{t' - t}\, dt' \tag{104}$$

A detailed calculation shows that for two photons exchanged between

spinless particles, $N = 2$ and so $V \sim 1/R^7$. However, without adding considerable structures to the particles and reverting, in fact, to Dzyaloshinskii's calculation, it is not possible to obtain the general Casimir and Polder potential by this method.

III. INTERACTION ENERGIES INVOLVING EXCITED STATES

If an atom or a molecule is in an excited state, the interaction between it and a neighboring atom or molecule is not governed by the London potential (nor by the Casimir-Polder potential at long range). In order to bring the problem into perspective, the interaction energies in the near limit, where elementary quantum mechanics with basically Coulomb forces between the constituent charges is sufficient to obtain them, are now summarized. First, if the two atoms are identical, with the second of these in its ground state, the interaction is the resonance interaction [Eq. (41)]

$$\pm U_{G\text{-}E(\text{res})}(R) = \pm e^2(\mathbf{q}(1) \cdot \mathbf{q}(2) - 3\mathbf{q}(1) \cdot \hat{\mathbf{R}}\mathbf{q}(2) \cdot \hat{\mathbf{R}})/R^3 \qquad (105)$$

with + and − for the symmetric and antisymmetric states respectively. It is assumed that the excited state $|n\rangle$ is optically coupled to the ground state $|0\rangle$. In terms of the β tensor

$$U_{G\text{-}E(\text{res})}(R) = e^2 q^i_{no}(1) q^j_{on}(2) \beta_{ij}/R^3 \qquad (106)$$

Secondly, if the atoms do not resonate because the excitation is not transferable to the second system, the energy of interaction is

$$U_{G\text{-}E(\text{non-res})}(R) = \frac{e^4 q^i_{no}(1) q^j_{op}(2) q^\sigma_{on}(1) q^\tau_{po}(2) \beta_{ij}\beta_{\sigma\tau}}{(|E_{no}(1)| - |E_{po}(2)|)R^6} \qquad (107)$$

This is very similar to the London potential. However, it is not always attractive. It is attractive if $E_{po}(2) > E_{no}(1)$. Molecule (1) is excited to state $|n\rangle$ and $E_{po}(2)$ is the relevant transition energy of the second molecule. Finally, if both molecules are in excited states $|n\rangle$ and $|p\rangle$, the energy of interaction is given by

$$U_{E\text{-}E}(R) = \frac{e^4 q^i_{no}(1) q^j_{po}(2) q^\sigma_{on}(1) q^\tau_{op}(2) \beta_{ij}\beta_{\sigma\tau}}{(|E_{no}(1)| + |E_{po}(2)|)R^6} \qquad (108)$$

a repulsive potential. In Eqs. (107) and (108), only two-level systems are considered. For realistic systems, one must add the contributions to the energy from higher levels which are of the London type and attractive; the overall sign will depend on the relative magnitudes of the various contributions. The energies [Eqs. (106)–(108)] may be read from Figures 1 and 2 with the appropriate changes in the energy-level labels. The calculations summarized in Sections III-B and III-C are those needed to obtain the generalizations of these energies to the wave-zone separations $R \sim \lambda\!\!\!^{-}$. However, there is another very important question, as emphasized especially by Stephen,[13] namely, the validity of the concept of a potential energy of interaction at these distances. A discussion of this is given in Section A.

A. Concept of Potential

The calculations reported in Sections II, III-B, III-C, and IV are of energy shifts. In fact, they are all based on calculating the energy difference between the states where the two atoms or molecules are at infinite separation and where they are separated by a distance R. The general theory tells us that computing energy shifts by the use of the S-matrix formalism will give the same results as that of stationary-state perturbation theory. However, from the calculation of the S and T matrices, one sees that the energy shift is not necessarily the complete story. In any situation where other states are physically accessible (allowing conservation of energy) from the given state, the T matrix has an imaginary term. Now in the cases of interest in this section where either or both systems are excited, there will be such physically accessible states, namely those corresponding to the ground states of the molecules with appropriate free radiation. If we let

$$T = V + i\Gamma \tag{109}$$

then we shall see that for the resonance case

$$V_{G\text{-}E(\text{res})}(R) \to U_{G\text{-}E(\text{res})}(R) \tag{110}$$

as $R \ll \lambda\!\!\!^{-}$, and

$$\Gamma_{G\text{-}E(\text{res})}(R) \to \text{constant} = \tfrac{2}{3}k^3 |\boldsymbol{\mu}|^2 = \tfrac{1}{2}\omega \quad \text{(Einstein)} \tag{111}$$

where ω (Einstein) is the Einstein A coefficient for dipole radiation. However, in the range $R \sim \lambda\!\!\!^{-}$, $|\Gamma|$ is of the same order of magnitude as $|V|$. In the analysis of certain problems such as the rate of transfer of

excitation,[69] the potential energy V is not sufficient and the complete T matrix is needed. The imaginary part of the T matrix is related to the possible emission of real photons. Probability is not conserved in that subspace of the general quantum space spanned by the no photon part of the space. To some extent, there are several ways of bypassing this problem. The most common way is to associate widths to the energy levels of the system. It is sometimes claimed that to speak of an energy shift, it is necessary that the shift be larger than the width. This appears to the reviewer to be too restrictive. An extremely important example where energy shifts are measured and compared with theory even when the shifts are smaller than the line width occurs in the analysis of the Lamb shifts in hydrogen and helium. For the fundamental $2P_{1/2}$–$2S_{1/2}$ interval in hydrogen, the line width is about a tenth of the complete energy shift (which is about 1058 Mc/sec), but the measurements are accurate to about 0.1 Mc/sec so that shifts of 1 part in 10^4 of the width are discernable.[70] For Lamb shift splittings of lines with $j \geqslant 3/2$, the whole shift is smaller than the line width.[12]

In the problem of intermolecular forces, the extreme long-range interaction energies are very small individually—it remains to be seen whether there are any unambiguous methods of testing the two-body interactions. Even for two atoms in their ground states, the spin energies can be larger than the Casimir-Polder potential.[61] In this case, of course, there is no imaginary contribution to T. With excitation present, it could be that the emission of a photon is so fast relative to a collision time that the molecules no longer see the so-called potential. However, for a typical optical decay time of 10^{-8} sec, there is plenty of time for an excited atom to feel the perturbation of neighboring atoms out to 100 cm.

In some situations, the concept of potential is not so important as that of the T matrix. For example, in the aforementioned calculation of the transition rate for excitation to jump from an excited molecule to a similar atom in its ground state, the rate is[55] proportional to $|T_{G\text{-}E(\text{res})}|^2$ while in the nonrelativistic theory[69] is it proportional to $|U_{G\text{-}E(\text{res})}|^2$. In the close range, $R \ll \lambda\!\!\!^{-}$, where the nonrelativistic theory is applicable, the rate is proportional to R^{-6}. ($U_{G\text{-}E(\text{res})}$ is given by Eq. (106) in this instance.) For R large compared with $\lambda\!\!\!^{-}$, $|V_{G\text{-}E(\text{res})}|^2$ falls off like R^{-2} and so does $|T_{G\text{-}E(\text{res})}|^2$ so that the rate of transfer follows the classical inverse-square law.[52] $V_{G\text{-}E(\text{res})}$ is associated with virtual transfer of photons, $\Gamma_{G\text{-}E(\text{res})}$ with real photon exchange. In the near zone, the

excitation is dominated by virtual photons (in fact, this occurs just by longitudinal interactions in the Coulomb gauge), while in the wave zone, the transfer is due to true radiation photons satisfying the wave equation.

In this chapter, no attention has been paid to the difficulties in the concept of a potential associated with crossing of energy-level surfaces. These are discussed in Hirschfelder and Meath's chapter on page 8. However, it is of interest to point out that the same fundamental problem is encountered in the two cases, namely, that the system in the assumed given state is closely coupled to that of another state with which it is degenerate. In the quantum electrodynamic case the degeneracy is with radiation plus molecules, while in the crossing case it is within the two-molecule subspace alone.

B. Energy Shifts with Excited States: Resonance Interaction

The resonance-interaction energy is easily found from second-order perturbation theory applied to the $-\boldsymbol{\mu} \cdot \mathbf{E}^{\perp}$ interaction energy of Eq. (20). The corresponding time-ordered graphs are shown in Figure 11.

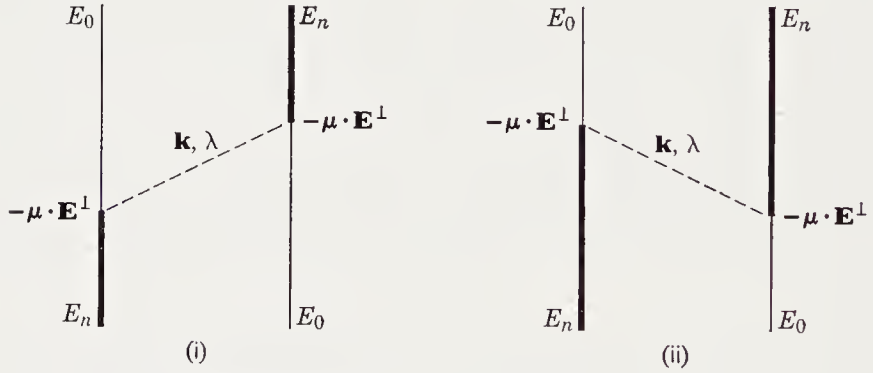

Fig. 11. Time-ordered diagram for dipole–dipole resonance potential.

The calculations[14] follow those in Sections I and II, but are considerably simpler. The second-order energy shift is

$$\Delta E^{(2)}(R) = \sum_{\mathrm{I}} \frac{\langle i|\, \boldsymbol{\mu}(1) \cdot \mathbf{E}^{\perp}(1)\, |\mathrm{I}\rangle\langle \mathrm{I}|\, \boldsymbol{\mu}(2) \cdot \mathbf{E}^{\perp}(2)\, |i\rangle}{E_i - E_{\mathrm{I}}} + \sum_{\mathrm{II}} \frac{\langle i|\, \boldsymbol{\mu}(2) \cdot \mathbf{E}^{\perp}(2)\, |\mathrm{II}\rangle\langle \mathrm{II}|\, \boldsymbol{\mu}(1) \cdot \mathbf{E}^{\perp}(1)\, |i\rangle}{E_i - E_{\mathrm{II}}} \quad (112)$$

where

$$|i\rangle = |E_n\rangle\,|0\rangle \tag{113}$$

For the Ψ_+ and Ψ_- states using symmetrized and antisymmetrized wave functions, Eqs. (13) and (14) replace Eqs. (113) and the energies are $\pm V_{G\text{-}E(\mathrm{res})}(R)$, respectively. The transverse electric-field vector operator $\mathbf{E}^{\perp}$ is expanded into annihilation and creation operators as in Eq. (60). The matrix elements over the photon occupation-number space are immediate and

$$\Delta E^{(2)}(R) = \frac{2\pi}{V}\sum_{\mathbf{k},\lambda=1,2}(\hbar ck)\left[\frac{\mu^i_{on}(1)\mu^j_{no}(2)e^{(\lambda)}_i e^{(\lambda)}_j e^{i\mathbf{k}\cdot\mathbf{R}}}{(E-(\hbar ck))} - \frac{\mu^i_{on}(1)\mu^j_{no}(2)e^{(\lambda)}_i e^{(\lambda)}_j e^{-i\mathbf{k}\cdot\mathbf{R}}}{(E+(\hbar ck))}\right] \tag{114}$$

The polarization sum is given in Eq. (70) and therefore,

$$\Delta E^{(2)}(R) = 4\pi\mu^i_{on}(1)\mu^j_{no}(2)\int\frac{(\delta_{ij}-\hat{k}_i\hat{k}_j)e^{i\mathbf{k}\cdot\mathbf{R}}(\hbar ck)^2}{E^2-(\hbar ck)^2}\frac{d^3\mathbf{k}}{(2\pi)^3} \tag{115}$$

The angular integral is the same as in that Eq. (76). Hence,

$$\Delta E^{(2)}(R) = \frac{2}{\pi}\mu^i_{on}(1)\mu^j_{no}(2)(\hbar c)^2\int_0^\infty\frac{\tau_{ij}(kR)k^4\,dk}{(E^2_{no}-(\hbar ck)^2)} \tag{116}$$

The pole explicitly shown in Eq. (116) which originates in Eq. (112) from Figure 11 (i) when the photon energy equals E_{no} is the manifestation (in this simple case) of the difficulties discussed in Section A. For an energy shift, the summation [Eq. (112)] excludes the vanishing denominator so that the integral [Eq. (116)] is a Cauchy principal value integral. Hence, computing the k integral

$$V^{(2)}_{G\text{-}E(\mathrm{res})}(R) = -\mu^i_{on}(1)\mu^j_{no}(2)\left[\frac{\alpha_{ij}\cos(R/\hat{\lambda})}{\hat{\lambda}^2R} - \beta_{ij}\left\{\frac{\sin(R/\hat{\lambda})}{\hat{\lambda}R^2}+\frac{\cos(R/\hat{\lambda})}{R^3}\right\}\right] \tag{117}$$

and the result, Eq. (26), is obtained. As mentioned previously,

$$V^{(2)}_{G\text{-}E(\mathrm{res})}(R) \to U_{G\text{-}E(\mathrm{res})}(R) \tag{118}$$

for $R \ll \hat{\lambda}$ but still greater than electronic overlap. Equation (117) is exactly the classical result

$$-\boldsymbol{\mu}(2)\cdot\mathbf{E}^{\perp}_{(1)}(2)\,(=-\boldsymbol{\mu}(1)\cdot\mathbf{E}^{\perp}_{(2)}(1)) \tag{119}$$

where $\mathbf{E}^{\perp}_{(1)}(2)$ is the transverse electric-field vector at position (2) due to dipole (1). A more complicated calculation starting from Eq. (17) leads to the same result. Care is needed in this case at a pole at $k = 0$.

If, on the other hand, the T matrix corresponding to Figure 11 is required, the prescription for the pole at $E = \hbar ck$ is not the principal value, but it bypasses the pole according to outgoing wave boundary conditions.[71] This is achieved by including a $-i\varepsilon$ in the energy denominator factor

$$1/(E - \hbar ck - i\varepsilon) \qquad (\varepsilon > 0) \tag{120}$$

The T matrix can be calculated[13] from the analog of Eq. (115), namely

$$T^{(2)}_{if} = 4\pi\mu^{i}_{on}(1)\mu^{j}_{no}(2)\int\frac{(\delta_{ij}-\hat{k}_i\hat{k}_j)e^{i\mathbf{k}\cdot\mathbf{R}}(\hbar ck)^2}{E^2-(\hbar ck)^2-i\varepsilon}\frac{d^3\mathbf{k}}{(2\pi)^3} \tag{121}$$

$$=-\mu^{i}_{on}(1)\mu^{j}_{no}(2)\left[\frac{\alpha_{ij}}{\lambda\!\!\!^{-2}R}-\beta_{ij}\left(\frac{i}{\lambda\!\!\!^{-}R^2}+\frac{1}{R^3}\right)\right]e^{-iR/\lambda\!\!\!^{-}} \tag{122}$$

or, more directly [after computing $V_{G\text{-}E(\mathrm{res})}(R)$] by using the distribution equality

$$1/(E - \hbar ck - i\varepsilon) = P/(E - \hbar ck) + i\pi\delta(E - \hbar ck) \tag{123}$$

so that

$$T^{(2)}_{G\text{-}E(\mathrm{res})} = V^{(2)}_{G\text{-}E(\mathrm{res})} + i\Gamma^{(2)}_{G\text{-}E(\mathrm{res})} \tag{124}$$

where

$$\Gamma^{(2)}_{G\text{-}E(\mathrm{res})} = \mu^{i}_{on}(1)\mu^{j}_{no}(2)\int_0^{\infty}\tau_{ij}(kR)\delta(E-\hbar ck)E^3\,dk$$

$$=\mu^{i}_{on}(1)\mu^{j}_{no}(2)\left[\frac{\alpha_{ij}\sin(R/\lambda\!\!\!^{-})}{\lambda\!\!\!^{-2}R}+\beta_{ij}\left\{\frac{\cos(R/\lambda\!\!\!^{-})}{\lambda\!\!\!^{-}R^2}-\frac{\sin(R/\lambda\!\!\!^{-})}{R^3}\right\}\right] \tag{125}$$

$$=k^3\mu^{i}_{on}(1)\mu^{j}_{no}(2)\tau_{ij}(kR) \tag{126}$$

It is clear that the imaginary contribution to $T^{(2)}_{G\text{-}E(\text{res})}$ comes from those photons which actually lie on the energy shell, $E = \hbar ck$. It can also be calculated by first-order perturbation theory and unitarity. If $T^{(1)}_{in}$ and $T^{(1)}_{nf}$ are the T matrices for emission and absorption of a photon by molecules (1) and (2), respectively, then

$$\Gamma^{(2)}_{G\text{-}E(\text{res})} = \pi \sum_n T^{(1)}_{in} T^{(1)}_{nf} \delta(E_i - E_n) \tag{127}$$

when $R \ll \lambda\!\!\!^{-}$

$$|\Gamma^{(2)}_{G\text{-}E(\text{res})}| \ll |V^{(2)}_{G\text{-}E(\text{res})}| \sim |U^{(2)}_{G\text{-}E(\text{res})}| \tag{128}$$

and the transition rate for excitation to pass from one system to another is determined essentially by the potential $U^{(2)}$. For $R \sim \lambda\!\!\!^{-}$ or $R > \lambda\!\!\!^{-}$, it is necessary to use the complete T matrix to calculate this transition rate.

As pointed out by Dicke,[72] the two states Ψ_+ and Ψ_- have different properties other than the difference in sign in their potential energy. This is in their transition rate for emission of a photon and dropping to their ground state. When the two atoms are separated by a distance $R < \lambda\!\!\!^{-}$, the two atoms see essentially the same amplitude of the electric field and dipole selection rules apply to the decay of the combined system. The antisymmetric state is stable (superradiant); the symmetric state has half the lifetime of an isolated atom. Stephen,[13] Hutchinson and Hameka,[73] and Power[74] have computed the lifetime as a function of R. In the notation of this chapter, the transition probabilities per unit time are

$$\omega^{\pm}_{if} = 2k^3 \mu_i \mu_j [\tau_{ij}(0) \pm \tau_{ij}(kR)] \tag{129}$$

where $\tau_{ij}(kR)$ is given by Eq. (76). For $R \ll \lambda\!\!\!^{-}$

$$\tau_{ij}(kR) \to \tfrac{2}{3}\delta_{ij} \tag{130}$$

and

$$\omega^{+}_{if} \to \tfrac{8}{3}k^3 |\boldsymbol{\mu}|^2 = 2\omega_{if} \quad \text{(Einstein)} \tag{131}$$

$$\omega^{-}_{if} \to 0 \tag{132}$$

where ω_{if} (Einstein) is the Einstein A coefficient for the transition

probability per unit time for an isolated atom. For $R \gg \lambda\!\!\!^{-}$

$$\omega_{if}^{+} = \omega_{if}^{-} = \omega_{if} \quad \text{(Einstein)} \tag{133}$$

Numerical discussion of the case of intermediate R is given by Meath.[75]

Clearly it will be easier to measure the interaction energy in the antisymmetric state for small R because it is relatively long lived. A discussion is given in Stephen's paper.[13] Although it is very important to discuss the stability and time constants of these quantum mechanical systems, this is not our primary task in this paper. As mentioned in Section III–A, the energies of the various states considered are computed even if the shifts are smaller than their widths.

C. Excitation Present but Nonresonant

Two dissimilar molecules with nonoverlapping spectra interact in a nonresonant manner. In the near-zone region, the interaction energy behaves as R^{-6} (London) with or without excitation present; however, when one or both molecules are excited the force can be repulsive. The very long-range potential has a strikingly different behavior from that of Casimir and Polder. This is because the photons can be real; i.e., they can be on the energy shell. The basic results are illustrated with the two mathematical formulas ($v > 0$, $R > 0$).

$$\int_0^\infty \frac{\sin 2\omega R}{v + \omega}\, d\omega = \sin(2vR)\,\mathrm{Ci}(2vR) - \cos(2vR)\,\mathrm{si}(2vR) \tag{134}$$

and

$$P\int_0^\infty \frac{\sin 2\omega R}{v - \omega}\, d\omega = \sin(2vR)\,\mathrm{Ci}(2vR) - \cos(2vR)\,\mathrm{si}(2vR) - \pi\cos(2vR) \tag{135}$$

For $R \gg \lambda\!\!\!^{-}$

$$\int_0^\infty \frac{\sin 2\omega R}{v + \omega}\, d\omega \sim \frac{1}{2}\left(\frac{\lambda\!\!\!^{-}}{R}\right) \tag{136}$$

and

$$P\int_0^\infty \frac{\sin 2\omega R}{v - \omega}\, d\omega \sim -\pi\cos(2R/\lambda\!\!\!^{-}) + \frac{1}{2}\left(\frac{\lambda\!\!\!^{-}}{R}\right) \tag{137}$$

and the oscillating form dominates in the second integral.

The calculations for the potentials in these cases are complicated and they are spelled out in detail in our papers.[21,57] In this chapter, a summary of the results are given. Let atom (1) be in state l and atom (2) in state s; label the states dipole-coupled to these atoms n for atom (1) and p for atom (2). Define

$$\Phi_{ln;sp}(R) = -\frac{2}{\pi}\mu^{i}_{ln}(1)\mu^{\sigma}_{nl}(1)\mu^{j}_{sp}(2)\mu^{\tau}_{ps}(2)\frac{|v_{nl}|\,|v_{ps}|}{|v_{nl}|^2 - |v_{ps}|^2}$$

$$\times\left[\frac{\alpha_{ij}\alpha_{\sigma\tau}}{R^2}\{|v_{ps}|^3 A_{ps} - |v_{nl}|^3 A_{nl} + \tfrac{1}{2}(|v_{nl}|^2 - |v_{ps}|^2)/R\}\right.$$

$$+\frac{2\alpha_{ij}\beta_{\sigma\tau}}{R^3}\{|v_{ps}|^2 B_{ps} - |v_{nl}|^2 B_{nl} - (|v_{ps}|\,A_{ps} - |v_{nl}|\,A_{nl})/R\}$$

$$+\frac{\beta_{ij}\beta_{\sigma\tau}}{R^4}\{|v_{nl}|\,A_{nl} - |v_{ps}|\,A_{ps} + 2(B_{nl} - B_{ps})/R$$

$$\left.+(A_{ps}/|v_{ps}| - A_{nl}/|v_{nl}|)/R^2\}\right] \quad (138)$$

As before

$$v_{nl} = E_n - E_l \qquad (\hbar = c = 1) \quad (139)$$

and A_{nl}, B_{nl} are defined by Eq. (34) and (35). Then, if both l and s are the ground states, from Eq. (81)

$$V_{G\text{-}G}(R) = \sum_{n,p}\Phi_{on;op}(R) \quad (140)$$

If atom (1) is excited and atom (2) is in its ground state

$$V_{G\text{-}E(\text{non-res})}(R) = \sum_{p}\left\{+\sum_{\substack{n\\E_n > E_l}}\Phi_{ln;op}(R)\right.$$

$$\left.+\sum_{\substack{n\\E_n < E_l}}[-\Phi_{ln;op}(R) + \Lambda^{(1)}_{ln;op}(R)]\right\} \quad (141)$$

where

$$\Lambda^{(1)}_{ln;sp}(R) = \mu^{i}_{ln}(1)\mu^{\sigma}_{nl}(1)\mu^{j}_{sp}(2)\mu^{\tau}_{ps}(2)\,\frac{2\,|v_{ps}(2)|}{|v_{nl}(1)|^2 - |v_{ps}(2)|^2}$$
$$\times [\alpha_{ij}\,|v_{nl}|^2\,R^{-1}\cos|v_{nl}|\,R - \beta_{ij}\,|v_{nl}|\,R^{-2}$$
$$\times (\sin|v_{nl}|\,R + |v_{nl}|^{-1}\,R^{-1}\cos|v_{nl}|\,R)]$$
$$\times [\alpha_{\sigma\tau}\,|v_{nl}|^2\,R^{-1}\cos|v_{nl}|\,R - \beta_{\sigma\tau}\,|v_{nl}|\,R^{-2}$$
$$\times (\sin|v_{nl}|\,R + |v_{nl}|^{-1}\,R^{-1}\cos|v_{nl}|\,R)] \quad (142)$$

$$= \frac{2\,|v_{ps}(2)|}{|v_{nl}(1)| + |v_{ps}(2)|}\,\frac{V^{(2)}_{G\text{-}E(\mathrm{res})}(R)V^{(2)}_{G\text{-}E(\mathrm{res})}(R)}{|v_{nl}| - |v_{ps}|} \quad (143)$$

Note from Eq. (143) the consistency as resonance is approached $|v_{nl}| \to |v_{ps}|$ when $\Lambda^{(1)}$ becomes the second-order perturbation result applied to $V^{(2)}_{G\text{-}E(\mathrm{res})}(R)$.

Finally, if both atoms are excited

$$V_{E\text{-}E}(R) = \left(\sum_{\substack{n,p\\E_n>E_l\\E_p>E_s}} - \sum_{\substack{n,p\\E_n<E_l\\E_p>E_s}} - \sum_{\substack{n,p\\E_n>E_l\\E_p<E_s}} + \sum_{\substack{n,p\\E_n<E_l\\E_p<E_s}}\right)\Phi_{ln;sp}(R)$$
$$+ \sum_{\substack{n,p\\E_n<E_l\\E_p>E_s}} \Lambda^{(1)}_{ln;sp}(R) + \sum_{\substack{n,p\\E_n>E_l\\E_p<E_s}} \Lambda^{(2)}_{ln;sp}(R)$$
$$- \sum_{\substack{n,p\\E_n<E_l\\E_p<E_s}} [\Lambda^{(1)}_{ln;sp}(R) + \Lambda^{(2)}_{ln;sp}(R)] \quad (144)$$

$\Lambda^{(2)}_{ln;sp}(R)$ is obtained from $\Lambda^{(1)}_{ln;sp}(R)$ by changing $v_{ps}(2) \rightleftharpoons v_{ln}(1)$.

The behavior [Eqs. (107) and (108)] for small R is easily checked using the asymptotic form for $\Phi(R)$ and $\Lambda(R)$ for small R. These are

$$\Phi_{ln;sp}(R) \to -\frac{\mu^{i}_{ln}(1)\mu^{\sigma}_{nl}(1)\mu^{j}_{sp}(2)\mu^{\tau}_{ps}(2)\beta_{ij}\beta_{\sigma\tau}}{R^6}\,\frac{1}{|v_{nl}| + |v_{ps}|} \quad (145)$$

and

$$\Lambda^{(1)}_{ln;sp}(R) \to +\frac{\mu^{i}_{ln}(1)\mu^{\sigma}_{nl}(1)\mu^{j}_{sp}(2)\mu^{\tau}_{ps}(2)\beta_{ij}\beta_{\sigma\tau}}{R^6}\,\frac{2\,|v_{ps}|}{|v_{nl}|^2 - |v_{ps}|^2} \quad (146)$$

So that, for example, the contribution to the second order in Eq. (141) has the value

$$U_{G\text{-}E(\text{non-res})}(R) = \frac{\mu^i_{ln}(1)\mu^\sigma_{nl}(1)\mu^j_{op}(2)\mu^\tau_{po}(2)\beta_{ij}\beta_{\sigma\tau}}{R^6}\frac{1}{|\nu_{nl}| - |\nu_{po}|} \quad (147)$$

which is in agreement with Eq. (107). Finally, we quote the asymptotic forms for the interaction energies for large R compared with $\lambda\!\!\!^{-}$. They are

$$V_{G\text{-}E(\text{non-res})}(R) = \mu^i_{ln}(1)\mu^\sigma_{nl}(1)\mu^j_{op}(2)\mu^\tau_{po}(2)\frac{\alpha_{ij}\alpha_{\sigma\tau}\cos^2(R/\lambda\!\!\!^{-})}{R^2}\frac{2|\nu_{ln}||\nu_{po}|}{(|\nu_{ln}|^2 - |\nu_{po}|^2)} \quad (148)$$

and

$$V_{E\text{-}E}(R) = -\mu^i_{ln}(1)\mu^\sigma_{nl}(1)\mu^j_{sp}(2)\mu^\tau_{ps}(2) \times \frac{\alpha_{ij}\alpha_{\sigma\tau}(|\nu_{nl}|^3\cos^2(R/\lambda\!\!\!^{-(1)}) - |\nu_{ps}|^3\cos^2(R/\lambda\!\!\!^{-(2)}))}{R^2}\frac{2|\nu_{ln}||\nu_{ps}|}{|\nu_{ln}|^2 - |\nu_{ps}|^2} \quad (149)$$

IV. NONDISPERSIVE FORCES IN THE LONG-RANGE LIMIT

Some relativistic corrections to nondispersive interatomic forces have been considered[76] by using the Breit-Pauli Hamiltonian[11,77,78] generalized to two-centered systems.[5] In this section, quantum electrodynamics is used to study the intermolecular forces in second order in the coupling constant between the charges and the electromagnetic field. In second order, one distinguishes between direct and exchange interactions. A prototype for the former are spin–spin forces while well-known examples of the latter are the resonance forces discussed in Section III–B. In Section A, below, the retarded Breit operator is calculated. It reduces to the standard Breit operator for $r_{12} \ll \lambda\!\!\!^{-}$ where r_{12} is the interelectronic distance. In Section B, the Pauli approximation is made to evaluate the interaction energy and the T matrix in several cases such as spin–spin, spin–orbit and mixed interactions. This section is based on the paper by Gomberoff and Power[60]; see also Gomberoff.[79]

A. Breit Operator

Theoretical chemists like to start calculating with a Hamiltonian that is a function of the coordinates of the particles. The interaction terms are functions of the particle separations at a given time. These chemists will write a Hamiltonian, which includes some relativistic corrections,

as [see Eq. (8)]

$$H = H(1) + H(2) + U_{\text{int}}^{\text{Coulomb}}(1,2) + H_{\text{rel}} \tag{150}$$

where H_{rel} is of the order of v^2/c^2. Relativistic corrections are then made by calculating the expectation value of H_{rel} for the appropriate state. A well-known contribution to H_{rel} is

$$H_5 = (e^2/m^2)(1/r_{12})[\mathbf{s}(1) \cdot \mathbf{s}(2) - 3\mathbf{s}(1) \cdot \hat{\mathbf{r}}_{12}\mathbf{s}(2) \cdot \hat{\mathbf{r}}_{12}] \tag{151}$$

This is the spin–spin interaction between electrons 1 and 2 which for our intermolecular calculations are supposedly located on different centers (Fig. 3). The other spin-dependent interaction Hamiltonian is

$$H_3 = \frac{e^2}{2m^2}\left\{\left[\frac{(\mathbf{R} + \mathbf{r}_1) \times \mathbf{p}(1)}{|\mathbf{R} + \mathbf{r}_1|^3} - \frac{\mathbf{r}_{12} \times \mathbf{p}(1)}{\mathbf{r}_{12}^3} + \frac{2[\mathbf{r}_{12} \times \mathbf{p}(2)]}{\mathbf{r}_{12}^3}\right] \cdot \mathbf{s}(1) + \text{term } 1 \rightleftharpoons 2\right\} \tag{152}$$

which is of the spin–orbit type. Equations (151) and (152) together with Eqs. (22)–(24) complete the relevant* Breit-Pauli Hamiltonian with no external field. The suffix notation is that of Bethe and Salpeter[12] and the correspondence with Hirschfelder and Meath (Chapter 1 of this volume) is

$$\left.\begin{aligned} H_1 &= H_{\text{P}} \\ H_2 &= H_{\text{LL}} \\ H_3 &= H_{\text{LS}} \\ H_4 &= H_{\text{D}} \\ H_5 &= H_{\text{SS}} \end{aligned}\right\} \tag{153}$$

Alternatively, if one is prepared to use Dirac wave functions, the Breit operator

$$B = -(e^2/2r_{12})[\boldsymbol{\alpha}(1) \cdot \boldsymbol{\alpha}(2) + \boldsymbol{\alpha}(1) \cdot \hat{\mathbf{r}}_{12}\boldsymbol{\alpha}(2) \cdot \hat{\mathbf{r}}_{12}] \tag{154}$$

may be used (at least for direct interactions, see below). $\boldsymbol{\alpha}$ is the 4×4 Dirac matrix vector and is given in terms of the γ matrices by

$$\alpha^i = \gamma^4\gamma^i \qquad (i = 1,2,3) \tag{155}$$

* Equation (152) does not contain the spin–orbit corrections to isolated atoms; these are independent of R and correspond to $H_{\text{SL},0}$ of Hirschfelder and Meath.

Theoretical physicists, on the other hand, prefer the interaction energies in the Hamiltonian to be contact terms between the particles and the boson fields. The latter now contribute to the dynamics of the overall system. In this section the connection between the two viewpoints is made and the Breit operator B, together with an extension to B_{ex} where retardation is important in exchange interactions is shown to follow from quantum electrodynamics.

From Eq. (84)

$$S^{(2)} = -\frac{1}{2}\iint d^4x_1 d^4x_2 P[\mathscr{H}_1(x_1)\mathscr{H}_1(x_2)] \tag{156}$$

and for the states considered there are no photons present so that, taking the Maxwell vacuum expectation value

$$\langle O|\, S^{(2)}\,|O\rangle = -\iint d^4x_1 d^4x_2 j_\mu(x_1) D_F(x_1 - x_2) j_\mu(x_2) \tag{157}$$

D_F is the Feynman-Green function defined by Eq. (90). The electronic wave functions of the two systems are taken to be the Dirac spinors

$$\psi_{(n)}(\mathbf{r}_1)e^{-iE_n t}$$

and

$$\psi_{(m)}(\mathbf{r}_2)e^{-iE_m t} \tag{158}$$

respectively. (n) and (m) are sets of quantum numbers sufficient to determine the atomic states at infinite separation of the centers. By convention, $(n) = 0$ will denote the ground state without specification of the spin. For an excited state, we set $(n) = p$. Then if both atoms are in their ground states, the total wave function, excluding internuclear motion, is

$$\psi_0(\mathbf{r}_1)\psi_0(\mathbf{r}_2) \equiv |\,0\rangle \tag{159}$$

On the other hand, if one atom is in an excited state, it is necessary to distinguish identical and nonidentical systems. In the former case, the wave function will be either Ψ_+ or Ψ_- of Eqs. (13) and (14). For nonidentical systems, the wave function will be

$$\psi_0(\mathbf{r}_1)\psi_p(\mathbf{r}_2) \equiv |\,0,p\rangle \tag{160}$$

if the excited system is atom (2). We calculate the expectation value of

$S^{(2)}$ for the state Ψ_- and later quote the corresponding values for the states Ψ_+, $|0\rangle$, and $|0,p\rangle$. For notation in Eq. (157), see Eqs. (87) and (88),

$$\langle u|S^{(2)}|u\rangle = \frac{ie^2}{(2\pi)^4}\iiint_{C_F} d^4x_1 d^4x_2 d^4k[\bar{\psi}_0(x_1)\gamma^\mu e^{ik\cdot x_1}\psi_0(x_1) \times \bar{\psi}_p(x_2)\gamma^\mu e^{-ik\cdot x_2}\psi_p(x_2) - \bar{\psi}_0(x_1)\gamma^\mu e^{ik\cdot x_1}\psi_p(x_1) \times \bar{\psi}_p(x_2)\gamma^\mu e^{-ik\cdot x_2}\psi_0(x_2)]/k^2 \quad (161)$$

This expression can be analyzed in terms of two Feynman diagrams as shown in Figure 12.

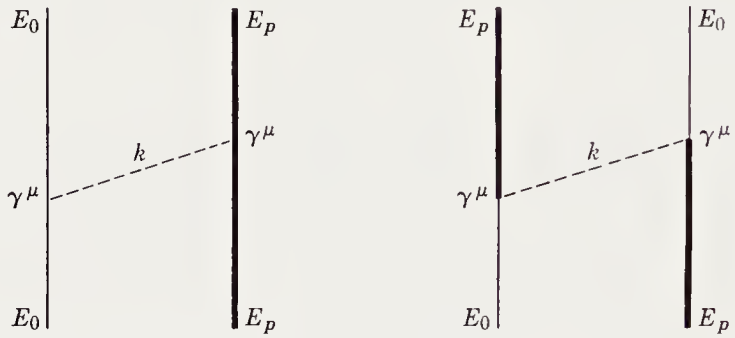

Fig. 12. Feynman graphs corresponding to $S^{(2)}$ of Eq. (161).

The contribution $S_D^{(2)}$ represented by the first diagram is called a direct matrix element and that by the second diagram is called an exchange interaction $S_{ex}^{(2)}$. In the case of the Ψ_+ state, a similar division is made and the exchange matrix element changes sign. For the ground state–ground state interaction $|0\rangle$ and for the nonresonant case $|0,p\rangle$ there are only direct contributions.

The time integrals involved in Eq. (161) can be performed on substituting the explicit time dependence of the wave functions as given in Eq. (158). Following this, the k_0-integration is immediate and the results are

$$S_D^{(2)} = \frac{ie^2}{(2\pi)^2}\delta(E_f - E_i)\iiint d\mathbf{r}_1 d\mathbf{r}_2 d\mathbf{k}\,\frac{e^{i\mathbf{k}\cdot\mathbf{R}}}{\mathbf{k}^2 - i\varepsilon}\,\bar{\psi}_0(\mathbf{r}_1)\gamma^\mu e^{i\mathbf{k}\cdot\mathbf{r}_1}\psi_0(\mathbf{r}_1) \times \bar{\psi}_p(\mathbf{r}_2)\gamma^\mu e^{-i\mathbf{k}\cdot\mathbf{r}_2}\psi_p(\mathbf{r}_2) \quad (162)$$

and

$$S_{ex}^{(2)} = \frac{-ie^2}{(2\pi)^2}\,\delta(E_f - E_i)\iiint d\mathbf{r}_1 d\mathbf{r}_2 d\mathbf{k}\,\frac{e^{i\mathbf{k}\cdot\mathbf{R}}}{\mathbf{k}^2 - E_{p0}^2 - i\varepsilon}\,\bar{\psi}_0(\mathbf{r}_1)\gamma^\mu e^{i\mathbf{k}\cdot\mathbf{r}_1}\psi_p(\mathbf{r}_1)$$

$$\times\,\bar{\psi}_p(\mathbf{r}_2)\gamma^\mu e^{-i\mathbf{k}\cdot\mathbf{r}_2}\psi_0(\mathbf{r}_2) \quad (163)$$

First, the direct term is considered further. On changing to Gaussian units for e and using the relation

$$\gamma_{(1)}^\mu\gamma_{(2)}^\mu = \gamma_{(1)}^4\gamma_{(2)}^4(\boldsymbol{\alpha}(1)\cdot\boldsymbol{\alpha}(2) - 1) \quad (164)$$

$$S_D^{(2)} = \frac{ie^2}{\pi}\,\delta(E_f - E_i)\iiint d\mathbf{r}_1 d\mathbf{r}_2\,\frac{d\mathbf{k}}{\mathbf{k}^2 - i\varepsilon}$$

$$\times\,\{\psi_0^\dagger(\mathbf{r}_1)\psi_p^\dagger(\mathbf{r}_2)[\boldsymbol{\alpha}(1)\cdot\boldsymbol{\alpha}(2) - 1]e^{i\mathbf{k}\cdot\mathbf{r}_{12}}\psi_0(\mathbf{r}_1)\psi_p(\mathbf{r}_2)\} \quad (165)$$

If the Feynman denominator is decomposed in the usual way

$$1/(\mathbf{k}^2 - i\varepsilon) = (P/\mathbf{k}^2) + i\pi\delta(\mathbf{k}^2) \quad (166)$$

there is no contribution to the *direct* term from the δ function. So, defining the T matrix by

$$S^{(2)} = -2\pi i\delta(E_f - E_i)T^{(2)} \quad (167)$$

one obtains

$$T_D^{(2)} = -\frac{e^2}{2\pi^2}\,P\iiint\frac{d\mathbf{r}_1 d\mathbf{r}_2 d\mathbf{k}}{\mathbf{k}^2}\,\{\psi_0^\dagger(\mathbf{r}_1)\psi_p^\dagger(\mathbf{r}_2)[\boldsymbol{\alpha}(1)\cdot\boldsymbol{\alpha}(2) - 1]$$

$$\times\,e^{i\mathbf{k}\cdot\mathbf{r}_{12}}\psi_0(\mathbf{r}_1)\psi_p(\mathbf{r}_2)\} \quad (168)$$

This method is equivalent to and gives the result of Brown[80] for electrons on a single center. $T_D^{(2)}$ is real and will be written $U_D^{(2)}$, an energy shift. It is easy to relate Eq. (168) to the Breit operator by subtracting the Coulomb interaction, whence

$$U_D^{(2)} - U^{\text{Coulomb}} = -\frac{e^2}{2\pi^2}\iiint\frac{d\mathbf{r}_1 d\mathbf{r}_2 d\mathbf{k}}{\mathbf{k}^2}$$

$$\times\,[\psi_0^\dagger(\mathbf{r}_1)\psi_p^\dagger(\mathbf{r}_2)\boldsymbol{\alpha}(1)\cdot\boldsymbol{\alpha}(2)e^{i\mathbf{k}\cdot\mathbf{r}_{12}}\psi_0(\mathbf{r}_1)\psi_p(\mathbf{r}_2)]$$

$$= \langle\psi_0(\mathbf{r}_1)\psi_p(\mathbf{r}_2)|\,B\,|\psi_0(\mathbf{r}_1)\psi_p(\mathbf{r}_2)\rangle \quad (169)$$

where

$$B = -\frac{e^2}{2\pi^2}\int\frac{d\mathbf{k}}{\mathbf{k}^2}[\boldsymbol{\alpha}(1)\cdot\boldsymbol{\alpha}(2) - \boldsymbol{\alpha}(1)\cdot\hat{\mathbf{k}}\boldsymbol{\alpha}(2)\cdot\hat{\mathbf{k}}]e^{i\mathbf{k}\cdot\mathbf{r}_{12}} \tag{170}$$

$$= -\frac{e^2}{2r_{12}}[\boldsymbol{\alpha}(1)\cdot\boldsymbol{\alpha}(2) + \boldsymbol{\alpha}(1)\cdot\hat{\mathbf{r}}_{12}\boldsymbol{\alpha}(2)\cdot\hat{\mathbf{r}}_{12}] \tag{171}$$

which is the Breit operator [Eq. (154)]. When both systems are in their ground state, Eq. (159), exactly the same B is found.

Secondly, the exchange term in Eq. (161) is simplified. It is

$$S_{\text{ex}}^{(2)} = -\frac{ie^2}{(2\pi)^2}\delta(E_f - E_i)\iiint\frac{d\mathbf{r}_1 d\mathbf{r}_2 d\mathbf{k}}{\mathbf{k}^2 - E_{p0}^2 - i\varepsilon}$$

$$\times\{\psi_0^\dagger(\mathbf{r}_1)\psi_p^\dagger(\mathbf{r}_2)[\boldsymbol{\alpha}(1)\cdot\boldsymbol{\alpha}(2) - 1]e^{i\mathbf{k}\cdot\mathbf{r}_{12}}\psi_p(\mathbf{r}_1)\psi_0(\mathbf{r}_2)\} \tag{172}$$

In this case there will be a contribution to the $\mathbf{k}$ integration from the imaginary term $-i\varepsilon$ as well as from the principal part. The former contribution is related to the possibility of real photon exchange and will contribute an imaginary term to the transition matrix. With T^2 defined by Eq. (167) we write

$$T_{\text{ex}}^{(2)} = V_{\text{ex}}^{(2)} + i\Gamma_{\text{ex}}^{(2)} \tag{173}$$

Hence

$$V_{\text{ex}}^{(2)} = \frac{e^2}{2\pi^2}P\iiint\frac{d\mathbf{r}_1 d\mathbf{r}_2 d\mathbf{k}}{\mathbf{k}^2 - E_{p0}^2}$$

$$\times\{\psi_0^\dagger(\mathbf{r}_1)\psi_p^\dagger(\mathbf{r}_2)[\boldsymbol{\alpha}(1)\cdot\boldsymbol{\alpha}(2) - 1]e^{i\mathbf{k}\cdot\mathbf{r}_{12}}\psi_p(\mathbf{r}_1)\psi_0(\mathbf{r}_2)\} \tag{174}$$

Proceeding as in Eq. (169), we subtract the exchange Coulomb interaction, namely

$$U_{\text{ex}}^{\text{Coulomb}} = -\frac{e^2}{2\pi^2}\iiint\psi_0^\dagger(\mathbf{r}_1)\psi_p^\dagger(\mathbf{r}_2)\frac{e^{i\mathbf{k}\cdot\mathbf{r}_{12}}}{\mathbf{k}^2}\psi_p(\mathbf{r}_1)\psi_0(\mathbf{r}_2)d\mathbf{r}_1 d\mathbf{r}_2 d\mathbf{k} \tag{175}$$

to obtain

$$V_{\text{ex}}^{(2)} - U_{\text{ex}}^{\text{Coulomb}} = \frac{e^2}{2\pi^2}P\iiint\frac{d\mathbf{r}_1 d\mathbf{r}_2 d\mathbf{k}}{\mathbf{k}^2 - E_{p0}^2}$$

$$\times\psi_0^\dagger(\mathbf{r}_1)\psi_p^\dagger(\mathbf{r}_2)[\boldsymbol{\alpha}(1)\cdot\boldsymbol{\alpha}(2) - E_{p0}^2/\mathbf{k}^2]e^{i\mathbf{k}\cdot\mathbf{r}_{12}}\psi_p(\mathbf{r}_1)\psi_0(\mathbf{r}_2)$$

$$= \langle\psi_0(\mathbf{r}_1)\psi_p(\mathbf{r}_2)|\, B_{\text{ex}}\,|\psi_p(\mathbf{r}_1)\psi_0(\mathbf{r}_2)\rangle \tag{176}$$

where

$$B_{ex} = \frac{e^2}{2\pi^2} P \int \frac{d\mathbf{k}}{\mathbf{k}^2 - E_{p0}^2} (\boldsymbol{\alpha}(1) \cdot \boldsymbol{\alpha}(2) - E_{p0}^2/\mathbf{k}^2) e^{i\mathbf{k} \cdot \mathbf{r}_{12}} \tag{177}$$

The Dirac equation can be used* to show that the matrix element of Eq. (177) is equivalent to that of

$$B_{ex} = \frac{e^2}{2\pi^2} P \int \frac{d\mathbf{k}}{\mathbf{k}^2 - E_{p0}^2} (\boldsymbol{\alpha}(1) \cdot \boldsymbol{\alpha}(2) - \boldsymbol{\alpha}(1) \cdot \hat{\mathbf{k}} \boldsymbol{\alpha}(2) \cdot \hat{\mathbf{k}}) e^{i\mathbf{k} \cdot \mathbf{r}_{12}} \tag{178}$$

If now the $\mathbf{k}$ integration is carried out, the exchange Breit operator is given as a function of r_{12} and $\lambda\!\!\!^{-} = \hbar c/E_{p0}$ by

$$B_{ex} = e^2 \frac{\alpha^i(1)\alpha^j(2)\lambda\!\!\!^{-2}\beta_{ij}}{r_{12}^3} + e^2\alpha^i(1)\alpha^j(2)\left\{\frac{\alpha_{ij} \cos(r_{12}/\lambda\!\!\!^{-})}{r_{12}} - \beta_{ij}\left[\frac{\lambda\!\!\!^{-} \sin(r_{12}/\lambda\!\!\!^{-})}{r_{12}^2} + \frac{\lambda\!\!\!^{-2} \cos(r_{12}/\lambda\!\!\!^{-})}{r_{12}^3}\right]\right\} \tag{179}$$

For the $|g\rangle$ state, the sign is changed. This exchange Breit operator B_{ex} takes care of *all* retardation effects in $U^{(2)}$. The first term does not contain any oscillating terms and corresponds to the instantaneous Coulomb interaction. The remaining term is the generalization to Dirac particles of the operator given previously, Eq. (26), for dipole sources. In the limit $r_{12} \ll \lambda\!\!\!^{-}$ which will be always true for a one-center problem and also in the near zone of the intermolecular two-center problem

$$B_{ex} \to \mp B \tag{180}$$

the two signs corresponding to Ψ_- and Ψ_+ states, respectively. Note that for large $\lambda\!\!\!^{-}$, the first term of Eq. (179) cancels with the last. All the r^{-2} terms also cancel and one is left with the terms varying as r_{12}^{-1}

* Use

$$\langle \psi_0(\mathbf{r}_1)\psi_p(\mathbf{r}_2)| (\boldsymbol{\alpha}(1) \cdot \hat{\mathbf{k}} \boldsymbol{\alpha}(2) \cdot \hat{\mathbf{k}} - E_{p0}^2/\mathbf{k}^2) e^{i\mathbf{k} \cdot \mathbf{r}_{12}} |\psi_p(\mathbf{r}_1)\psi_0(\mathbf{r}_2)\rangle = 0$$

This, and many other details of the reduction of the Breit operator are given by Akhiezer and Berestetskii.[81]

which add together to give B. If the Breit operator B is used for exchange interactions (it is exact for direct interactions) retardation is only partially taken into account. It is easy to see that for small $r_{12}/\lambda\!\!\!^{-}$ the limit B for B_{ex} arises directly from Eq. (174). If the **k** integral in Eq. (174) is carried out one obtains[12]

$$V_{ex}^{(2)} = \langle \psi_0(\mathbf{r}_1)\psi_p(\mathbf{r}_2) \left| \frac{e^2(\boldsymbol{\alpha}(1)\cdot\boldsymbol{\alpha}(2) - 1)\cos(r_{12}/\lambda\!\!\!^{-})}{r_{12}} \right| \psi_p(\mathbf{r}_1)\psi_0(\mathbf{r}_2)\rangle \quad (181)$$

If now the delay factor $\cos(r_{12}/\lambda\!\!\!^{-})$ is expanded to the first two terms and the substitution[81]

$$-E_{p0}^2 r_{12} \rightarrow \frac{\alpha^i(1)\alpha^j(2)\alpha_{ij}}{r_{12}} \quad (182)$$

is used, the Breit operator is obtained together with the exchange Coulomb operator. It is also immediately clear that putting $E_{p0} = 0$ in Eq. (177) leads to the same approximation.

The imaginary part of the T matrix is not zero for the exchange interaction. The result is closely analogous to the dipole case given in detail in Sections III-A and III-B. Following from Eq. (172) one finds for $\Gamma_{ex}^{(2)}$ the value

$$\Gamma_{ex}^{(2)} = \langle \psi_0(\mathbf{r}_1)\psi_p(\mathbf{r}_2) \left| \frac{e^2}{r_{12}} [\boldsymbol{\alpha}(1)\cdot\boldsymbol{\alpha}(2) - 1] \sin(r_{12}/\lambda\!\!\!^{-}) \right| \psi_p(\mathbf{r}_1)\psi_0(\mathbf{r}_2)\rangle \quad (183)$$

B. Pauli Approximation

The wave functions in Eqs. (168) and (174) for the direct and exchange interactions $U_D^{(2)}$ and $U_{ex}^{(2)}$ are four-component Dirac spinors. It is convenient to reduce them to Pauli spinors with the appropriate modification to the operators. However, first we wish to comment on the exponential factor $e^{i\mathbf{k}\cdot\mathbf{r}_{12}}$ and its relation to retardation. For the electrons on two centers,

$$e^{i\mathbf{k}\cdot\mathbf{r}_{12}} = e^{i\mathbf{k}\cdot\mathbf{R}} e^{-i\mathbf{k}\cdot\mathbf{r}_1} e^{i\mathbf{k}\cdot\mathbf{r}_2} \quad (184)$$

where $\mathbf{r}_1$ and $\mathbf{r}_2$ are vectors from the two centers to their electrons (Fig. 3). Thus

$$U_D^{(2)} = -\frac{e^2}{2\pi^2}\iiint d\mathbf{r}_1 d\mathbf{r}_2 d\mathbf{k}\,\frac{e^{i\mathbf{k}\cdot\mathbf{R}}}{\mathbf{k}^2}$$
$$\times [\psi_0^\dagger(\mathbf{r}_1)\alpha^i(1)e^{-i\mathbf{k}\cdot\mathbf{r}_1}\psi_0(\mathbf{r}_1)\psi_p^\dagger(\mathbf{r}_2)\alpha^i(2)e^{i\mathbf{k}\cdot\mathbf{r}_2}\psi_p(\mathbf{r}_2)$$
$$-\psi_0^\dagger(\mathbf{r}_1)e^{-i\mathbf{k}\cdot\mathbf{r}_1}\psi_0(\mathbf{r}_1)\psi_p^\dagger(\mathbf{r}_2)e^{i\mathbf{k}\cdot\mathbf{r}_2}\psi_p(\mathbf{r}_2)] \quad (185)$$

There is now an obvious distinction between expanding the localized exponentials $e^{-i\mathbf{k}\cdot\mathbf{r}_1}$ and $e^{+i\mathbf{k}\cdot\mathbf{r}_2}$ which contribute various moments to the electronic matrix elements and expanding $e^{i\mathbf{k}\cdot\mathbf{r}_{12}}$ which involves partial consideration of retardation. In this method the retardation factor between the nuclei, i.e., $e^{i\mathbf{k}\cdot\mathbf{R}}$, is considered with no approximation. It is clear that at the long range contemplated in this chapter, this retardation is the most important. It may well be possible to approximate the local factors $e^{-i\mathbf{k}\cdot\mathbf{r}_1}$ and $e^{i\mathbf{k}\cdot\mathbf{r}_2}$ when it is not accurate to approximate $e^{i\mathbf{k}\cdot\mathbf{r}_{12}}$. No similar division is possible for electrons on a single center.

To write Eq. (185) in terms of two-component spinors, let

$$\psi = \begin{pmatrix}\psi_A\\ \psi_B\end{pmatrix} \quad (186)$$

where

$$\psi_B = \frac{\boldsymbol{\sigma}\cdot\mathbf{p}}{(2m+E)}\psi_A \quad (187)$$

Using the properties of the $\boldsymbol{\alpha}$ matrices, and keeping terms to order $(E/2m)$, one has

$$\psi^\dagger\alpha^i e^{i\mathbf{k}\cdot\mathbf{r}}\psi = \psi_A^\dagger e^{i\mathbf{k}\cdot\mathbf{r}}\left[\frac{p^i}{m} + \frac{k^i}{2m} + \frac{i[\mathbf{k}\times\boldsymbol{\sigma}]^i}{2m}\frac{Ek^i}{(2m)^2} - \frac{2Ep^i}{(2m)^2}\right]\psi_A \quad (188)$$

and

$$\psi^\dagger e^{i\mathbf{k}\cdot\mathbf{r}}\psi = \psi_A^\dagger e^{i\mathbf{k}\cdot\mathbf{r}}\left\{1 + \frac{i[\mathbf{k}\times\mathbf{p}]\cdot\boldsymbol{\sigma}}{(2m)^2} + \frac{\mathbf{k}\cdot\mathbf{p}}{(2m)^2}\right\}\psi_A \quad (189)$$

When these matrix elements are substituted in Eq. (185) and the index A is dropped

$$U_D^{(2)} = -\frac{e^2}{2\pi^2}\iiint d\mathbf{r}_1 d\mathbf{r}_2 \frac{d\mathbf{k}}{\mathbf{k}^2} e^{i\mathbf{k}\cdot\mathbf{R}}$$

$$\times \left[\psi_0^\dagger(\mathbf{r}_1)e^{-i\mathbf{k}\cdot\mathbf{r}_1}\left(\frac{p^i(1)}{m} - \frac{k^i}{2m} - \frac{i[\mathbf{k}\times\boldsymbol{\sigma}(1)]^i}{2m}\right.\right.$$

$$\left.+ \frac{E_0 k^i}{(2m)^2} - \frac{2E_0 p^i(1)}{(2m)^2}\right)\psi_0(\mathbf{r}_1)\psi_p^\dagger(\mathbf{r}_2)e^{i\mathbf{k}\cdot\mathbf{r}_2}$$

$$\times \left(\frac{p^i(2)}{m} + \frac{k^i}{2m} + \frac{i[\mathbf{k}\times\boldsymbol{\sigma}(2)]^i}{2m} - \frac{E_p k^i}{(2m)^2} - \frac{2E_p p^i(2)}{(2m)^2}\right)\psi_p(\mathbf{r}_2)$$

$$- \psi_0^\dagger(\mathbf{r}_1)e^{-i\mathbf{k}\cdot\mathbf{r}_1}\left(1 - \frac{i[\mathbf{k}\times\mathbf{p}(1)]\cdot\boldsymbol{\sigma}(1)}{(2m)^2} - \frac{\mathbf{k}\cdot\mathbf{p}(1)}{(2m)^2}\right)\psi_0(\mathbf{r}_1)$$

$$\left.\times \psi_p^\dagger(\mathbf{r}_2)e^{i\mathbf{k}\cdot\mathbf{r}_2}\left(1 + \frac{i[\mathbf{k}\times\mathbf{p}(2)]\cdot\boldsymbol{\sigma}(2)}{(2m)^2} + \frac{\mathbf{k}\cdot\mathbf{p}(2)}{(2m)^2}\right)\psi_p(\mathbf{r}_2)\right] \quad (190)$$

In exactly the same way, the exchange interaction matrix $T_{ex}^{(2)}$ can be reduced to two-component spinors.

$$T_{ex}^{(2)} = \frac{e^2}{2\pi^2}\iiint d\mathbf{r}_1 d\mathbf{r}_2 \frac{d\mathbf{k}e^{i\mathbf{k}\cdot\mathbf{R}}}{\mathbf{k}^2 - E_{p0}^2 - i\varepsilon}$$

$$\times \left[\psi_0^\dagger(\mathbf{r}_1)e^{-i\mathbf{k}\cdot\mathbf{r}_1}\left(\frac{p^i(1)}{m} - \frac{k^i}{2m} - \frac{i[\mathbf{k}\times\boldsymbol{\sigma}(1)]^i}{2m}\right.\right.$$

$$\left.+ \frac{E_0 k^i}{(2m)^2} - \frac{(E_0+E_p)}{(2m)^2}p^i(1) + \frac{iE_{p0}[\mathbf{p}(1)\times\boldsymbol{\sigma}(1)]^i}{(2m)^2}\right)\psi_p(\mathbf{r}_1)$$

$$\times \psi_p^\dagger(\mathbf{r}_2)e^{i\mathbf{k}\cdot\mathbf{r}_2}\left(\frac{p^i(2)}{m} + \frac{k^i}{2m} + \frac{i[\mathbf{k}\times\boldsymbol{\sigma}(2)]^i}{2m}\right.$$

$$\left.- \frac{E_p k^i}{(2m)^2} - \frac{(E_0+E_p)}{(2m)^2}p^i(2) - \frac{iE_{p0}[\mathbf{p}(2)\times\boldsymbol{\sigma}(2)]^i}{(2m)^2}\right)\psi_0(\mathbf{r}_2)$$

$$- \psi_0^\dagger(\mathbf{r}_1)e^{-i\mathbf{k}\cdot\mathbf{r}_1}\left(1 - \frac{i[\mathbf{k}\times\mathbf{p}(1)]\cdot\boldsymbol{\sigma}(1)}{(2m)^2} - \frac{\mathbf{k}\cdot\mathbf{p}(1)}{(2m)^2}\right)\psi_p(\mathbf{r}_1)$$

$$\left.\times \psi_p^\dagger(\mathbf{r}_2)e^{i\mathbf{k}\cdot\mathbf{r}_2}\left(1 + \frac{i[\mathbf{k}\times\mathbf{p}(2)]\cdot\boldsymbol{\sigma}(2)}{(2m)^2} + \frac{\mathbf{k}\cdot\mathbf{p}(2)}{(2m)^2}\right)\psi_0(\mathbf{r}_2)\right] \quad (191)$$

For the total intermolecular potentials, one must add the Coulomb energies between the nuclei and between the nuclei and electrons to this interelectron energy.

It is from Eqs. (190) and (191) that the specific interaction energy terms are obtained. Some examples of these are given below. However, before making the separation of r_{12} implicit in Eq. (184), it is easy to obtain the Breit-Pauli Hamiltonian terms given by Eqs. (23), (24), (151), and (152) from $U_D^{(2)}$. This direct potential together with Coulomb energies can be expressed as the expectation value of the operator

$$H_{\text{effective}} = -\frac{e^2}{2\pi^2}\int\frac{d\mathbf{k}}{\mathbf{k}^2}\left[e^{i\mathbf{k}\cdot\mathbf{r}_{12}}\left(\frac{\mathbf{p}(1)\cdot\mathbf{p}(2)}{m^2} - \frac{[\mathbf{p}(1)-\mathbf{p}(2)]\cdot\mathbf{k}}{2m^2} - \frac{\mathbf{k}^2}{(2m)^2}\right.\right.$$

$$+\frac{[\mathbf{k}\times\boldsymbol{\sigma}(1)]\cdot[\mathbf{k}\times\boldsymbol{\sigma}(2)]}{(2m)^2} - \frac{i\mathbf{p}(1)\cdot[\mathbf{k}\times\boldsymbol{\sigma}(2)]}{2m^2}$$

$$+\frac{i\mathbf{p}(2)\cdot[\mathbf{k}\times\boldsymbol{\sigma}(1)]}{2m^2} - 1 - \frac{[\mathbf{p}(1)-\mathbf{p}(2)]\cdot\mathbf{k}}{(2m)^2}$$

$$\left.-\frac{i[\mathbf{k}\times\mathbf{p}(1)]\cdot\boldsymbol{\sigma}(1)}{(2m)^2} + \frac{i[\mathbf{k}\times\mathbf{p}(2)]\cdot\boldsymbol{\sigma}(2)}{(2m)^2}\right)$$

$$+e^{i\mathbf{k}\cdot(\mathbf{R}-\mathbf{r}_2)}\left(1 - \frac{i[\mathbf{k}\times\mathbf{p}(2)]\cdot\boldsymbol{\sigma}(2)}{(2m)^2} - \frac{\mathbf{k}\cdot\mathbf{p}(2)}{(2m)^2}\right)$$

$$\left.+e^{i\mathbf{k}\cdot(\mathbf{R}+\mathbf{r}_1)}\left(1 + \frac{i[\mathbf{k}\times\mathbf{p}(1)]\cdot\boldsymbol{\sigma}(1)}{(2m)^2} + \frac{\mathbf{k}\cdot\mathbf{p}(1)}{(2m)^2}\right)\right] \quad (192)$$

If the Pauli approximation of the identity of the footnote on page 215 is used namely

$$\langle i\left|e^{i\mathbf{k}\cdot\mathbf{r}_{12}}\left(\frac{\mathbf{p}(1)\cdot\hat{\mathbf{k}}\mathbf{p}(2)\cdot\hat{\mathbf{k}}}{m^2} - \frac{\mathbf{k}^2}{(2m)^2} - \frac{\mathbf{p}(1)\cdot\mathbf{k}-\mathbf{p}(2)\cdot\mathbf{k}}{2m^2}\right)\right|i\rangle = 0 \quad (193)$$

one may replace $-\{[\mathbf{p}(1)-\mathbf{p}(2)]\cdot\mathbf{k}/2m^2 - [\mathbf{k}^2/(2m)^2]\}$ by $-\mathbf{p}(1)\cdot\hat{\mathbf{k}}\mathbf{p}(2)\cdot\hat{\mathbf{k}}/m^2$. Then Eq. (194) reduces to

$$H_{\text{effective}} = -\frac{e^2}{2\pi^2}\int\frac{d\mathbf{k}}{\mathbf{k}^2}e^{i\mathbf{k}\cdot\mathbf{r}_{12}}\left\{\frac{\mathbf{p}(1)\cdot\mathbf{p}(2)}{m^2} - \frac{\mathbf{p}(1)\cdot\hat{\mathbf{k}}\mathbf{p}(2)\cdot\hat{\mathbf{k}}}{m^2}\right.$$
$$-\frac{i[\mathbf{k}\times\mathbf{p}(1)]\cdot\boldsymbol{\sigma}(1)}{(2m)^2} + \frac{i[\mathbf{k}\times\mathbf{p}(1)]\cdot\boldsymbol{\sigma}(2)}{2m^2}$$
$$+\frac{[\mathbf{k}\times\boldsymbol{\sigma}(1)]\cdot[\mathbf{k}\times\boldsymbol{\sigma}(2)]}{(2m)^2} + \frac{i[\mathbf{k}\times\mathbf{p}(2)]\cdot\boldsymbol{\sigma}(2)}{(2m)^2}$$
$$\left.-\frac{i[\mathbf{k}\times\mathbf{p}(2)]\cdot\boldsymbol{\sigma}(1)}{2m^2} - \frac{[\mathbf{p}(1)-\mathbf{p}(2)]\cdot\mathbf{k}}{(2m)^2}\right\}$$
$$+\frac{e^2}{2\pi^2}\int\frac{d\mathbf{k}}{\mathbf{k}^2}e^{i\mathbf{k}\cdot\mathbf{r}_{12}} + \frac{e^2}{2\pi^2}\int\frac{d\mathbf{k}}{\mathbf{k}^2}e^{i\mathbf{k}\cdot\mathbf{R}}$$
$$-\frac{e^2}{2\pi^2}\int\frac{d\mathbf{k}}{\mathbf{k}^2}e^{i\mathbf{k}\cdot(\mathbf{R}-\mathbf{r}_2)}\left(1 - \frac{i[\mathbf{k}\times\mathbf{p}(2)]\cdot\boldsymbol{\sigma}(2)}{(2m)^2} - \frac{\mathbf{k}\cdot\mathbf{p}(2)}{(2m)^2}\right)$$
$$-\frac{e^2}{2\pi^2}\int\frac{d\mathbf{k}}{\mathbf{k}^2}e^{i\mathbf{k}\cdot(\mathbf{R}+\mathbf{r}_1)}\left(1 + \frac{i[\mathbf{k}\times\mathbf{p}(1)]\cdot\boldsymbol{\sigma}(1)}{(2m)^2} - \frac{\mathbf{k}\cdot\mathbf{p}(1)}{(2m)^2}\right) \quad (194)$$

The integrals over $\mathbf{k}$ are elementary, for example

$$\frac{1}{2\pi^2}\int\frac{d\mathbf{k}}{\mathbf{k}^2}e^{i\mathbf{k}\cdot\mathbf{r}}\hat{k}_i\hat{k}_j = \frac{1}{2r}(\delta_{ij} - \hat{r}_i\hat{r}_j) \quad (195)$$

and the result is

$$H_{\text{effective}} = H_0 + H_2 + H_3 + H_4 + H_5 \quad (196)$$

where

$$H_0 = \frac{e^2}{r_{12}} - \frac{e^2}{|\mathbf{R}-\mathbf{r}_2|} - \frac{e^2}{|\mathbf{R}+\mathbf{r}_1|} + \frac{e^2}{R} \quad (197)$$

and H_2, H_3, H_4, and H_5 are given by Eqs. (23), (24), (151), and (152). The term H_1 is missing, as this is a relativistic correction to the free Hamiltonian and is independent of e. Also, in H_5 there is no contact term as the electrons are on separate systems. For another derivation from quantum electrodynamics, see Itoh[82] who discusses how H_4 can be replaced by a Hermitian operator. In a similar way, from Eq. (191) it is possible to extract a fully retarded Breit-Pauli Hamiltonian for exchange interactions. However, it is much more elegant to use the T matrix directly.

It is usual to divide the interaction energy into additive parts where the structure of each part has a direct physical significance. In the near-zone limit this division is into electric multipoles, magnetic or orbit multipoles, spin–spin, spin–orbit, and spin–other orbit. When the full retardation corrections are considered, these divisions are not so clear cut. As explained after Eq. (23), the so-called orbit–orbit Hamiltonian H_2 has, for electron and different atoms, an electric dipole–electric dipole component whose lead term is proportional to R^{-1} and is given by Eq. (25). Again, the spin–spin Hamiltonian H_5 has a leading term which is, of course, proportional to R^{-3} and is

$$(e^2/m^2)\{[\mathbf{s}(1)\cdot\mathbf{s}(2) - 3\mathbf{s}(1)\cdot\hat{\mathbf{R}}\mathbf{s}(2)\cdot\hat{\mathbf{R}}]/R^3\} \tag{198}$$

However, as is well known, H_5 contains other types of interactions including spin–spin dipole and spin dipole–spin dipole. When exchange interactions are considered, it is essential (for very large R) to use Eq. (181) and not the Breit-Pauli Hamiltonians to obtain the *complete* retardation corrections. Compare Eq. (25) with Eq. (26) for the electric dipole–electric dipole case. Several other examples are given in reference 60. For instance, the fully retarded T matrix for dipole–spin dipole is

$$\begin{aligned} T^{(2)}_{D\text{-}(S\text{-}D)} = {} & \frac{iE_{p0}}{m}\langle\psi_0(\mathbf{r}_1)\psi_p(\mathbf{r}_2)|\, q^i(1)q^j(2)\sigma^k(2)\,|\psi_p(\mathbf{r}_1)\psi_0(\mathbf{r}_2)\rangle \\ & \times\left\{\varepsilon_{ist}\left[\frac{\hat{\mathbf{R}}_s\hat{\mathbf{R}}_j e^{-i\mathbf{R}/\lambda}}{\lambda^2 R} + \beta_{sj}\left(\frac{ie^{-i\mathbf{R}/\lambda}}{\lambda R^2} + \frac{e^{-i\mathbf{R}/\lambda}}{R^3}\right)\right]\right. \\ & \left. - \tfrac{1}{2}\varepsilon_{sjt}\left[\frac{-\alpha_{si}e^{-i\mathbf{R}/\lambda}}{\lambda^2 R} + \beta_{si}\left(\frac{-ie^{-i\mathbf{R}/\lambda}}{\lambda R^2} + \frac{e^{-i\mathbf{R}/\lambda}}{R^3}\right)\right]\right\} \end{aligned} \tag{199}$$

On the other hand the spin–orbit energy is not retarded and has the value

$$\begin{aligned} U^{(2)}_{S\text{-}O} = {} & -\frac{e^2}{2m^2}\frac{1}{R^3}\langle\psi_n(\mathbf{r}_1)\psi_m(\mathbf{r}_2)|\, -[\mathbf{r}_1\times\mathbf{p}(1)]\cdot\boldsymbol{\sigma}(2) \\ & + 3\hat{\mathbf{R}}\cdot\mathbf{r}_1[\hat{\mathbf{R}}\times\mathbf{p}(1)]\cdot\boldsymbol{\sigma}(2) + \tfrac{1}{2}[\mathbf{r}_1\times\mathbf{p}(1)]\cdot\boldsymbol{\sigma}(1) \\ & - \tfrac{3}{2}\hat{\mathbf{R}}\cdot\mathbf{r}_1[\hat{\mathbf{R}}\times\mathbf{p}(1)]\cdot\boldsymbol{\sigma}(1) + \text{terms } 1\rightleftharpoons 2\;|\psi_n(\mathbf{r}_1)\psi_m(\mathbf{r}_2)\rangle \end{aligned} \tag{200}$$

exactly as obtained for the Breit-Pauli Hamiltonian.

Finally, the retarded resonance interaction is written down[79] for arbitrary electric multipoles. This follows from Eq. (191). If $Q_{i_1 i_2 \cdots i_n}(1)$ and $Q_{j_1 j_2 \cdots j_n}(2)$ are the $n$ple moments of atoms (1) and (2), respectively, the $T_{ex}^{(2)}$ matrix is

$$T_{ex}^{(2)} = \frac{(-1)^{n-1}}{(n!)^2} Q_{i_1 i_2 \cdots i_n}^{p0}(1) Q_{j_1 j_2 \cdots j_n}^{0p}(2) \nabla_{i_1} \nabla_{j_1} \nabla_{i_2} \nabla_{j_2} \cdots$$

$$\nabla_{i_{n-1}} \nabla_{j_{n-1}} [E_{p0}^2 \delta_{i_n j_n} + \nabla_{i_n} \nabla_{j_n}] \left(\frac{e^{-i\mathbf{R}/\lambda}}{R} \right) \quad (201)$$

Acknowledgments

It is a great pleasure to acknowledge the stimulation and help from many friends and colleagues including D. P. Craig, L. Dissado, L. Gomberoff, J. O. Hirschfelder, R. R. McLone, W. J. Meath, and S. Zienau. I am especially indebted to L. Gomberoff and S. Zienau for their collaboration in various stages of this work.

References

1. P. A. M. Dirac, *Proc. Roy. Soc.* (*London*), **114A**, 243 (1927).
2. H. B. G. Casimir and D. Polder, *Phys. Rev.*, **73**, 360 (1948).
3. F. London, *Z. Physik.*, **63**, 245 (1930).
4. R. Eisenshitz and F. London, *Z. Physik.*, **60**, 491 (1930).
5. J. O. Hirschfelder, C. F. Curtiss, and R. B. Bird, *Molecular Theory of Gases and Liquids*, Wiley, New York, 1954.
6. B. C. Carlson and G. S. Rushbrooke, *Proc. Cambridge Phil. Soc.*, **46**, 626, 1950.
7. H. A. Kramers, *Quantum Mechanics*, North-Holland, Amsterdam, 1958.
8. R. P. Feynman, *Phys. Rev.*, **76**, 749 (1949).
9. E. A. Power and S. Zienau, *Phil. Trans. Roy. Soc.* (*London*), **251A**, 427 (1959).
10. P. N. Lebedeff, *Wied. Ann.*, **52**, 621 (1894).
11. G. Breit, *Phys. Rev.*, **34**, 553 (1929).
12. H. A. Bethe and E. E. Salpeter, *Quantum Mechanics of One-and-Two Electron Atoms*, Academic Press, New York, 1957.
13. M. J. Stephen, *J. Chem. Phys.*, **40**, 669, 1964.
14. R. R. McLone and E. A. Power, *Mathematika*, **11**, 91 (1964).
15. W. J. Meath, Thesis, University of Wisconsin (1965).
16. R. H. Penfield and H. Zatskis, *J. Franklin Inst.*, **263**, 331 (1957).
17. E. A. Power and S. Zienau, *J. Franklin Inst.*, **264**, 403 (1957).
18. C. G. Darwin, *Proc. Cambridge Phil. Soc.*, **20**, 56 (1920).
19. W. J. Meath and J. O. Hirschfelder, *J. Chem. Phys.*, **44**, 3197 (1966).
20. J. A. Wheeler, *Phys. Rev.*, **59**, 928 (1941).
21. R. R. McLone and E. A. Power, *Proc. Roy. Soc.* (*London*) **286A**, 573 (1965).
22. H. B. G. Casimir, *Proc. Koninkl. Ned. Akad. Wetenschap.*, **60**, 793 (1948).
23. H. B. G. Casimir, *J. Chim. Phys.*, **46**, 407 (1949).

24. E. J. W. Verwey and J. Th. G. Overbeek, *Theory of the Stability of Lyophobic Colloids*, Elsevier, Amsterdam, 1948.
25. W. Heisenberg, *Ann. Phys. Lpz.*, **9**, 338 (1931).
26. M. Born, *Atomic Physics*, Blackie, London, 1957.
27. M. R. Aub, Thesis, University of London, 1960.
28. M. Abramowitz and I. A. Stegun, *Handbook of Mathematical Functions*, Dover, New York, 1964.
29. O. Sinanoğlu, *Advan. Chem. Phys.*, **6**, 315 (1964).
30. J. Leech, *Phil. Mag.*, **46**, 1328 (1955).
31. M. R. Aub, E. A. Power, and S. Zienau, *Phil. Mag.*, **2**, 571 (1957).
32. I. E. Dzyaloshinskii, *Soviet Phys. JETP* (*English Transl.*), **3**, 977 (1956).
33. E. A. Power and S. Zienau, *Nuovo Cimento*, **6**, 7 (1957).
34. C. Mavroyannis and M. J. Stephen, *Mol. Phys.*, **5**, 629 (1962).
35. A. D. McLachlan, *Proc. Roy. Soc.* (*London*), **271A**, 387 (1963).
36. L. D. Landau and E. M. Lifshitz, *Statistical Physics*, Pergamon, London, 1958.
37. A. D. McLachlan, *Proc. Roy. Soc.* (*London*), **274A**, 80 (1963).
38. A. D. McLachlan, *Mol. Phys.*, **6**, 423 (1963).
39. A. D. McLachlan, *Mol. Phys.*, **7**, 381 (1964).
40. E. M. Lifshitz, *Soviet Phys. JETP* (*English Transl.*), **2**, 73 (1956).
41. I. E. Dzyaloshinskii, E. M. Lifshitz, and L. P. Pitaevskii, *Advan. Phys.*, **10**, 165 (1961).
42. L. D. Landau and E. M. Lifshitz, *Electrodynamics of Continuous Media*, Pergamon, London, 1960.
43. B. V. Deryagin, I. I. Abrikosova, and E. M. Lifshitz, *Quart. Rev.*, **10**, 295 (1965).
44. J. A. Kitchener and A. P. Prosser, *Proc. Roy. Soc.* (*London*), **242A**, 403 (1957).
45. W. Black, J. G. V. De Jongh, J. Th. G. Overbeek, and M. J. Sparnaay, *Trans. Faraday Soc.*, **56**, 1597 (1960).
46. E. A. Power, *Introductory Quantum Electrodynamics*, Longmans, London, 1964.
47. D. P. Craig and J. P. Walsh, *J. Chem. Soc.*, **II**, 1613 (1958).
48. W. T. Simpson, *Radiation Res.*, **20**, 87 (1963).
49. S. A. Rice, *J. Chem. Phys.*, **42**, 1515 (1965).
50. M. R. Philpott, *Proc. Roy. Soc.* (*London*), **292A**, 78 (1966).
51. L. Dissado, Thesis, University of London, 1966.
52. E. Fermi, *Rev. Mod. Phys.*, **4**, 87 (1932).
53. J. S. Avery, Z. Bay, and A. Szent-Györgyi, *Proc. Natl. Acad. Sci. U.S.*, **47**, 1742 (1961).
54. J. S. Avery, *Proc. Phys. Soc.*, **88**, 1 (1966).
55. L. Gomberoff and E. A. Power, *Proc. Phys. Soc.*, **88**, 281 (1966).
56. M. R. Philpott, *Proc. Phys. Soc.*, **87**, 619 (1966).
57. L. Gomberoff, R. R. McLone, and E. A. Power, *J. Chem. Phys.*, **44**, 4148 (1966).
58. B. M. Axilrod and E. Teller, *J. Chem. Phys.*, **11**, 299 (1943).
59. M. R. Aub and S. Zienau, *Proc. Roy. Soc.* (*London*), **257A**, 464 (1960).
60. L. Gomberoff and E. A. Power, *Proc. Roy. Soc.* (*London*), **295A**, 476 (1966).
61. E. A. Power, W. J. Meath, and J. O. Hirschfelder, *Phys. Rev. Letters*, **17**, 799 (1966).
62. W. Heitler, *The Quantum Theory of Radiation*, Oxford University Press, Oxford, 1954.

63. K. A. Brueckner, *Phys. Rev.*, **100**, 36 (1955).
64. J. O. Hirschfelder, W. Byers-Brown, and S. T. Epstein, *Advan. Quantum Chem.*, **1**, 255 (1964).
65. S. S. Schweber, *Relativistic Quantum Field Theory*, Harper and Row, New York, 1964.
66. R. P. Feynman, *Phys. Rev.*, **76**, 769 (1949).
67. L. S. Rodberg, *Phys. Rev.*, **110**, 277 (1958).
68. G. Feinberg and J. Sucher, *Phys. Rev.*, **139B**, 1619 (1965).
69. Th. Förster, *Naturwiss.*, **33**, 166 (1946).
70. G. W. Series, *Spectrum of Atomic Hydrogen*, Oxford University Press, London, 1957.
71. A. Sommerfeld, *Jahresbericht der Deutschen Mathematiker Vereinigung (Stuttgart)*, **21**, 309 (1912).
72. R. H. Dicke, *Phys. Rev.*, **93**, 99 (1954).
73. D. A. Hutchinson and H. F. Hameka, *J. Chem. Phys.*, **41**, 2006 (1964).
74. E. A. Power, University of Wisconsin Tech. Rept. WIS TCI-186 (1966).
75. W. J. Meath, University of Wisconsin Tech. Rept. WIS TCI-174 (1966).
76. W. J. Meath, private communication.
77. G. Breit, *Phys. Rev.*, **36**, 383 (1930).
78. G. Breit, *Phys. Rev.*, **39**, 616 (1932).
79. L. Gomberoff, Thesis, University of London, 1967.
80. G. E. Brown, *Phil. Mag.*, **43**, 467 (1952).
81. A. I. Akhiezer and V. B. Berestetskii, *Quantum Electrodynamics*, Interscience, New York, 1965.
82. T. Itoh, *Rev. Mod. Phys.*, **37**, 159 (1965).

5. Reaction-Field Techniques and Their Applications to Intermolecular Forces*

BRUNO LINDER

Department of Chemistry, The Florida State University
Tallahassee, Florida

CONTENTS

I. Introduction 226
II. The Reaction Field of a Static Moment in a Continuous Medium . . 228
A. The Reaction Field of a Nonpolarizable Dipole 229
B. The Reaction Field of an Arbitrary System of Charges 233
C. Critique of the Method 235
III. The Reaction Field of a Fluctuating Moment in a Medium of Arbitrary Distribution 237
A. General Formulation 237
B. Dielectric Description 239
C. Molecular Description 239
IV. Generalized Potential 243
V. Additive and Nonadditive van der Waals Potentials 249
A. Pair and Triple Potentials 250
B. Molecular Susceptibilities 251
1. Harmonic Oscillator 255
2. Rigid Rotor 255
C. Dispersion-, Orientation-, and Induction Forces 257
1. Pair Potentials 257
2. Triple Potentials 259
VI. Forces in Dense Media 260
A. Molecular Formulation 261
B. Dielectric Formulation 266
1. The Continuum Model 266
2. The Cavity Concept 268
VII. Two-Temperature Potentials 275
VIII. Concluding Remarks 279
References 280

* Supported (in part) by a grant from the Petroleum Research Fund, administered by the American Chemical Society, and (in part) by the Institute of Molecular Biophysics under contract with the Division of Biology and Medicine, U.S. Atomic Energy Commission.

I. INTRODUCTION

The van der Waals forces can be thought of as arising from three different sources: orientation-, induction-, and dispersion interaction. The orientation interaction results from the correlation between the rotational motion of the permanent moments in different molecules; the induction interaction is due to the polarization of one molecule by the permanent moment of another. The dispersion interaction arises from the correlation of the motion of electrons in neighboring molecules. These three types of interactions have traditionally been treated by different methods: the orientation- and induction effects (the electrostatic forces) were first formulated by Keesom[1] and Falkenhagen,[2] respectively, on the basis of classical theory; the dispersion effect was first derived by London[3] on the basis of quantum mechanics. For general reviews of the earlier developments in this field, the reader is referred to the papers by Margenau[4] and Pitzer.[5]

The expressions for the potentials as formulated by Keesom, Falkenhagen, and London are only first approximations to the true potentials of interaction. Aside from the fact that all of these are based on the dipolar approximation, there are several other reasons why these potentials cannot adequately describe the cohesive properties of a many-body system. In the first place, intermolecular forces are not strictly additive. Thus, in a many-body system, the overall potential cannot be obtained by simply adding all pair potentials; nonadditive corrections have to be included and these are not related to the pair potential, at least not in a simple way. Nonadditivity corrections arising in the interaction between three bodies were first derived by Axilrod and Teller[6] and Muto[7] for a simplified model, and by Kihara[8] for a more general case. Higher-order corrections were obtained by Bade and Kirkwood[9] and by Bade[10]—for a harmonic oscillator model. An effective pair potential which, in an approximate way, takes account of three-body nonadditivity has been proposed by Kestner and Sinanoğlu.[11] Secondly, retardation effects are ignored in the quantum mechanical treatment of the London dispersion forces. These effects were first investigated by Casimir and Polder[12] who showed that when the internuclear separation is very large compared with the wavelength of the radiation that causes electronic transitions in the molecules, the dispersion energy drops off as the inverse seventh power with distance rather than as the inverse sixth power as in the London approxi-

mation. These results have been verified by a number of investigators[13–18] and are reviewed in Chapter 4 of this volume.[19] Thirdly, since the Keesom and Falkenhagen potentials are based on classical mechanics, they are inapplicable at low temperatures; the London formula, which ignores thermal effects, fails when the temperature is so high that electronically excited molecules are present.

In recent years, it has become possible to treat intermolecular forces by macroscopic theory. Lifshitz[13] has laid the foundation for a general theory of attraction between macroscopic bodies which automatically takes retardation effects into consideration. The theory is based on the idea that the interaction is caused by fluctuations of the electromagnetic field which is in the interior of the material and which extends beyond the boundaries. These fluctuations are always present; they may be purely quantum mechanical in character or they may be thermal in origin. The theory has been reformulated in terms of quantum-field theory[14,20,21] and extended to bodies separated by a liquid layer. From this, it is possible to deduce effective forces of attraction between two molecules immersed in a liquid at separations which are far enough apart to treat the intervening liquid as a continuum.

Other theories have been advanced to calculate the cohesive energy of a van der Waals crystal.[22] These theories are based on a formulation of the many-body problem which makes use of the concept of collective modes of motion and, like the macroscopic theories of Lifshitz and others, are formulated in terms of the dielectric properties of the material. Methods based on dynamic susceptibilities have also been devised to treat interactions between individual molecules[17,20,23] and have been adapted to studies of forces in biologically significant systems.[24,25]

The reaction-field approach to intermolecular forces is a technique which is also based on the susceptibility method. The reaction field of a molecule i is the field produced at i by the surrounding medium which was polarized by i. The concept has been employed in a wide variety of problems other than ones dealing explicitly with intermolecular forces.[26] In the treatment of intermolecular forces, two general approaches have been followed: one in which the molecules of the medium are treated individually[27–31] and one in which they are treated collectively as a continuous dielectric.[32,33]

Originally, the reaction field was formulated for a static moment in a continuous medium. In Section II, the early development of the theory is reviewed and the nature of the approximations inherent in the model

is discussed. In Section III, the reaction field is generalized to a fluctuating moment in a medium of arbitrary distribution. In Section IV a unified treatment of the long-range interaction between a single molecule and its surrounding neighbors for fixed internuclear separations is given. This generalized potential includes nonadditivity and retardation effects. From this potential, general expressions are abstracted in Section V for the pair-, triple-, and higher-order potentials and explicit formulas are given for the dispersion- , orientation- , and induction potentials. In Section VI, the potentials of interaction are linked to the thermodynamic properties of fluid systems. Two general approaches are followed—one based on a molecular description and one on the continuum model. The latter approach can be expected to have approximate validity when the dissolved molecule is so large that statistical fluctuations are negligible. An analysis of the cavity concept follows, which suggests ways of improving the continuum-model calculations in situations where translational fluctuations are important. Section VII contains a description of two-temperature potentials. These arise from the adiabatic interaction between molecules having distribution functions characteristic of different temperatures. These investigations were motivated by recent molecular beam studies in which the beam temperature and the temperature of the scattering substance are different.[34,35] These potentials have properties which differ considerably from the single-temperature pair potential and, under suitable conditions, can become repulsive. The quantum-statistical implications underlying the two-temperature as well as the single-temperature potentials are examined in this section and discussed. Finally, in Section VIII a brief assessment is given of the reaction-field technique in its present stage of development and attention is drawn to the direction for further work.

II. THE REACTION FIELD OF A STATIC MOMENT IN A CONTINUOUS MEDIUM

In this section, we discuss the reaction-field concept as commonly employed in dielectric theory and its relevance to electrostatic forces. The treatment is based on the continuum model and the relevant formulas are expressed in terms of the macroscopic dielectric constant. The objections to the model and the qualitative nature of the approximations are discussed in Section II-C; their quantitative importance is analyzed more fully in Section VI-B-2.

The great success of the Debye-Hückel theory[36] in accounting for the departure from ideal behavior of ionic solutions has prompted a number of investigators[37,38] to formulate similar theories for solutions of polar molecules. The first rigorous treatment was given by Kirkwood[39] whose formulation took account not only of dipolar interactions but also included interactions due to higher-order moments as well as ionic interactions. Kirkwood's theory was based on a continuum model in which the electrical contribution to the chemical potential was expressed in terms of the charge distributions and two dielectric constants—one for the dissolved molecule and another for the surrounding medium. The interpretation of the inner dielectric constant was not clear and Kirkwood later assigned to it the value unity. The notion of a reaction field had not yet been advanced. When the reaction-field concept was was later introduced by Onsager[40] (in another context, namely, in the theory of polarization of dielectrics), it became apparent that the dipolar part of the electrostatic interaction of the Kirkwood theory (and earlier theories) was expressible in terms of the reaction-field response function and, in fact, that the whole approach to the theory of dipolar interaction could be reformulated in terms of the reaction-field concept. A number of investigators have discussed the electrostatic interaction from this standpoint.[41–44] The reaction-field technique treats the polarization of the dissolved molecule in a different way and avoids the difficulty of assigning to it an internal dielectric constant which is different from that of the medium.

A. The Reaction Field of a Nonpolarizable Dipole

Consider an ideal dipole situated at the center of a spherical cavity of radius a in a uniform medium of dielectric constant ε. For the moment we assume the dipole to be rigid; the extension to a polarizable dipole will be considered in the next section. Let Φ_1 and Φ_0 represent the potentials inside and outside the spherical region, respectively. Each of the potential functions must satisfy Laplace's equation $\nabla^2\Phi = 0$. The general solution is

$$\Phi_1 = \sum_{l=0}^{\infty} \sum_{m=l}^{l} \left(\frac{A_l^{(m)}}{r^{l+1}} + B_l^{(m)} r^l \right) P_l^{(m)}(\cos\theta) e^{im\phi} \qquad r < a \qquad (1)$$

$$\Phi_0 = \sum_{l=0}^{\infty} \sum_{m=-l}^{l} \left(\frac{C_l^{(m)}}{r^{l+1}} + D_l^{(m)} \right) P_l^{(m)}(\cos\theta) e^{im\phi} \qquad r > a \qquad (2)$$

where $A_l^{(m)}$, $B_l^{(m)}$, $C_l^{(m)}$, and $D_l^{(m)}$ are constants to be determined by the boundary conditions of the problem and $P_l^{(m)}(\cos\theta)$ are the associated Legendre functions. For simplicity, we take the direction of the dipole moment, $\boldsymbol{\mu}$, to coincide with the z direction of the coordinate system in which case only $m = 0$ values contribute. The boundary conditions are as follows:

$$\Phi_0 = 0 \qquad \text{as } r \to \infty \tag{3a}$$

$$\Phi_1 = (\mu/r^2)\cos\theta \qquad \text{as } r \to 0 \tag{3b}$$

$$\Phi_1 = \Phi_0 \qquad \text{at } r = a \tag{3c}$$

$$\mathbf{D}_1 \cdot \mathbf{n} = \mathbf{D}_0 \cdot \mathbf{n} \qquad \text{at } r = a \tag{3d}$$

where $\mathbf{D}_1$ and $\mathbf{D}_0$ are the electric displacement vectors inside and outside the spherical region, respectively, and $\mathbf{n}$ is the unit normal (outward) to the surface. From the first boundary condition, it follows that $D_l^{(0)} = 0$. Boundary condition (3b) can be obtained by replacing the dielectric surrounding the spherical region by a vacuum in which case the potential due to to the true charges, i.e., the dipolar potential, must be recovered. In this regard, we mention that since there are no net charges the terms with $l = 0$ are eliminated. It follows from Eq. (3b) that

$$\begin{aligned} A_l^{(0)} &= \mu \qquad \text{for } l = 1 \\ &= 0 \qquad \text{for } l > 1 \end{aligned} \tag{4}$$

To proceed further, we set

$$\mathbf{D}_1 = \mathbf{E}_1 + 4\pi\mathbf{P} \quad \text{and} \quad \mathbf{D}_0 = \varepsilon\mathbf{E}_0 \tag{5}$$

where $\mathbf{E}_1 = -\nabla\Phi_1$ and $\mathbf{E}_0 = -\nabla\Phi_0$. $\mathbf{E}_1$ and $\mathbf{E}_0$ are the field intensities inside and outside the cavity, respectively. For our assumed model of a rigid dipole $\mathbf{P} = 0$ and condition (3d) reduces to

$$\frac{\partial\Phi_1}{\partial r} = \varepsilon\frac{\partial\Phi_0}{\partial r} \qquad \text{at } r = a \tag{3d'}$$

From the fact that the Legendre functions are linearly independent we obtain, on using Eqs. (3c) and (3d'), the coefficients

$$\begin{aligned} B_l^{(m)} &= -\{(\varepsilon - 1)(l + 1)/[l + (l + 1)\varepsilon]\}(A_l^{(m)}/a^{2l+1}) \\ \text{and} \\ C_l^{(m)} &= \{(2l + 1)/[l + (l + 1)\varepsilon]\}A_l^{(m)} \end{aligned} \tag{6}$$

which, in accordance with Eq. (4), vanish for all values of l except $l = 1$. On substituting these results in Eqs. (1) and (2), we get

$$\Phi_1 = (\mu/r^2)\cos\theta - [(2\varepsilon - 2)/(2\varepsilon + 1)](\mu/a^3)r\cos\theta \tag{7}$$

$$\Phi_0 = [3/(2\varepsilon + 1)](\mu/r^2)\cos\theta \tag{8}$$

It is seen that the potential inside the cavity consists of two parts. The first term is the potential due to the true charges and the second term represents the deviations from the purely dipolar potential and this is attributed to the interaction with the surroundings. We shall be concerned mainly with the latter potential which will be referred to as the reaction potential and denoted as

$$\Phi^{(R)} = -g\mu r\cos\theta \tag{9}$$

where

$$g = [(2\varepsilon - 2)/(2\varepsilon + 1)](1/a^3) \tag{10}$$

The field corresponding to this potential is the reaction field, i.e.,

$$\mathbf{R} = -\nabla\Phi^{(R)} = g\boldsymbol{\mu} \tag{11}$$

In order to determine the mutual interaction of the dipole and the medium, we imagine a hypothetical charging process whereby the dipole moment is changed reversibly from zero to its full value. Quite generally, if $e_1 \ldots e_\eta \ldots e_M$ are the true charges which constitute the center molecule and $\Phi(r_\eta\theta_\eta\phi_\eta; e'_\eta)$ is the average potential at $\mathbf{r}_\eta$, due to all charges of the center molecule (including the ηth charge) and of the surrounding, then the work of charging the molecule is

$$w = \sum_{\eta=1}^{M} \int_0^{e_\eta} de'_\eta \Phi(r_\eta\theta_\eta\phi_\eta; e'_\eta) \tag{12}$$

where e'_η is the fractional charge of η. If we apply this to the charges of a dipole, pointing in the positive Z direction and having a magnitude $\mu = |e|\, r_0$, we get, on using the reaction-field part of the internal potential,

$$w = \int_0^{|e|} \Phi^{(R)}(0;|e'|)d|e'| = -\int_0^{|e|} r_0 g|e'|r_0 d|e'| = \frac{1}{2}|e|\Phi^{(R)}(0;|e|) \tag{13a}$$

$\Phi^{(R)}(0;|e'|)$ is the reaction potential at the origin, where the dipole is

located. This expression can be written also as

$$w = -\int_0^{\mu} g\mu' d\mu' \tag{13b}$$

Equation (13a) or (13b) yields

$$w = -\frac{1}{2}\boldsymbol{\mu} \cdot \mathbf{R} \tag{14}$$

This is the mutual electrostatic interaction between the dipole and the surroundings. (The dipolar part of the internal potential gives rise to the self-energy of the charge distribution and is of no interest here.)

The charging process employed here is one in which the dipole carrying molecule inside the cavity is charged from zero to its full value while keeping the solvent molecules intact. The work so obtained corresponds to the work of transferring a molecule from empty space into a cavity in the dielectric medium (presumably at constant temperature and volume) and is, in fact, equal to the electrical part of the chemical potential, i.e., $w = \mu_{el}$. There is another charging process whereby all molecules (the central one as well as the surrounding molecules) are taken through an intermediate charging step. This charging process produces the total free energy of the solution from which the chemical potential can be obtained by the usual method of partial differentiation. These two different methods of charging produce the same results provided the potentials used in the calculation are correct or at least consistent with the integrability requirement of thermodynamic functions.[45,46] Thus, if $\Phi_i^{(R)}(|e'_1|, \ldots |e'_i| \ldots |e'_N|)$ is the reaction potential at the center of molecule i, written here implicitly as a function of the fractional charges $|e'_1|, \ldots |e'_i| \ldots$ etc. of the dipoles of all molecules of the system,* then the total electrical free energy can be obtained by integrating the expression

$$d\tilde{F}_{el} = \sum_{i=1}^{N} \Phi_i^{(R)}(|e'_1|, \ldots |e'_N|) d|e'_i| \tag{15}$$

It is immaterial whether the molecules are charged simultaneously or one at a time, provided $d\tilde{F}_{el}$ is an exact differential. The requirement

* Unlike the charges, e'_η, with Greek indices [Eq. (12)] which refer to charges comprising the center molecule, the charges, $|e'_i|$, with Latin indices refer to dipolar charges of different molecules.

that this be so is

$$\frac{\partial \Phi_i^{(R)}}{\partial |e_k'|} = \frac{\partial \Phi_k^{(R)}}{\partial |e_i'|} \tag{16}$$

Thus, to be thermodynamically consistent, the reaction potential must satisfy the reciprocity relation in Eq. (16). We show in Section II-C that the reaction potential based on the static approach does not, in general, satisfy this condition.

B. The Reaction Field of an Arbitrary System of Charges

The formalism presented in Part A can readily be extended to a polarizable charge distribution in a cavity in a continuous medium. As a model for the dissolved molecule, we consider an arbitrary set of charges e_η, such that $\sum e_\eta = 0$, enclosed by a sphere of radius a. The potential Φ_0 outside the spherical region is of the form given by Eq. (2) but the potential inside has to be modified to

$$\Phi_1 = \sum_\eta \frac{e_\eta}{|\mathbf{r} - \mathbf{r}_\eta|} + \sum_{l=0}^{\infty} \sum_{m=-l}^{l} B_l^{(m)} r^l P_l^{(m)}(\cos\theta) e^{im\phi} \tag{17}$$

The terms $\sum_\eta \frac{e_\eta}{|\mathbf{r} - \mathbf{r}_\eta|}$ arise from the true charges inside the spherical cavity. Near the boundary but for distances r larger than any r_η, this expression can be expanded to give

$$\sum_\eta \frac{e_\eta}{|\mathbf{r} - \mathbf{r}_\eta|} = \sum_{l=0}^{\infty} \sum_{m=-l}^{l} \frac{A_l^{(m)}}{r^{l+1}} P_l^{(m)}(\cos\theta) e^{im\phi} \tag{18}$$

and the coefficients $A_l^{(m)}$ can be calculated from the coordinates of the charges. In particular, if we take the direction of the resulting dipole μ of the charge distribution to coincide with the z axis we can immediately identify $A_1^{(0)}$ with μ.

The boundary conditions given by Eqs. (3a), (3c), and (3d) apply equally well to the present case; condition (3d′) requires the following modification:

$$\frac{\partial \Phi_1}{\partial r} + 4\pi \mathbf{P} \cdot \mathbf{n} = \varepsilon \frac{\partial \Phi_0}{\partial r} \qquad \text{at } r = a \tag{3d*}$$

where $\mathbf{P}$ is the polarization produced by surroundings and is assumed

to be constant throughout the spherical region. With these modifications, we obtain the following expression for $B_1^{(0)}$ [compare with Eq. (6)]:

$$B_1^{(0)} = -\frac{2\varepsilon - 2}{2\varepsilon + 1}\frac{\mu}{a^3} + \frac{4\pi P}{2\varepsilon + 1} \tag{19}$$

(The vector $\mathbf{P}$ has the same direction as $\boldsymbol{\mu}$, as will be discussed more fully below, and so $\mathbf{P}\cdot\mathbf{n} = P\cos\theta$.) The other coefficients $B_l^{(m)}$ for $l > 1$ are not affected by the presence of $4\pi\mathbf{P}\cdot\mathbf{n}$ in (3d*) and the general solutions given by Eq. (6) remain unaltered. Accordingly, we have

$$\Phi_1 = \sum_\eta \frac{e_\eta}{|\mathbf{r} - \mathbf{r}_\eta|} - g\mu r\cos\theta + \frac{4\pi}{2\varepsilon + 1} Pr\cos\theta - \sum_{l=2}^{\infty}\sum_{m=-l}^{l} B_l^{(m)} r^l P_l^{(m)}(\cos\theta) e^{im\phi} \tag{20}$$

The terms other than $\sum_\eta \frac{e_\eta}{|\mathbf{r} - \mathbf{r}_\eta|}$ are due to all sources except the true charges. However, not all of these terms arise from the reaction field—part represent the potential due to the self-field of the polarization. To obtain the reaction potential, we imagine a hypothetical process whereby the dielectric surrounding the polarized sphere is replaced by a vacuum while the charges are held fixed. The potential then drops to

$$\Phi_1' = \sum_\eta \frac{e_\eta}{|\mathbf{r} - \mathbf{r}_\eta|} + \frac{4\pi}{3} Pr\cos\theta \tag{21}$$

The difference $\Phi_1 - \Phi_1'$ is the reaction potential, i.e.,

$$\Phi^{(R')} = -g\mu r\cos\theta + \frac{4\pi}{3} Pr\left(\frac{3}{2\varepsilon + 1} - 1\right)\cos\theta - \sum_{l=2}^{\infty}\sum_{m=-l}^{l} B_l^{(m)} r^l P_l^{(m)}(\cos\theta) e^{im\phi} \tag{22}$$

It is obvious that the value of the reaction field obtained from this potential, i.e., $\mathbf{R}' = -\nabla\Phi^{(R')}$, will depend not only on the dipole moment of the charge distribution but also on the higher-order moments and the vector $\mathbf{r}$. However, because of the properties of spherical harmonics, all higher-order terms vanish when averaged over the whole spherical region,[42,44,47] i.e.,

$$\left\langle -\nabla \sum_{l=2}^{\infty} \sum_{m=-l}^{l} B_l^{(m)} r^l P_l^{(m)}(\cos\theta) e^{im\phi} \right\rangle = 0$$

and so

$$\bar{\mathbf{R}}' = g[\boldsymbol{\mu} + (4\pi/3)a^3\mathbf{P}] = g(\boldsymbol{\mu} + \mathbf{P}v) \tag{23}$$

where v is the volume of the sphere.

Since $\mathbf{P}$ is taken to be uniform throughout the spherical region, the quantity $(4\pi/3)a^3\mathbf{P}$ represents the total induced moment of the sphere and, in the absence of an applied field,

$$(4\pi/3)a^3\mathbf{P} = \alpha\bar{\mathbf{R}}' \tag{24}$$

where α is the polarizability. On combining Eqs. (23) and (24), we get

$$\bar{\mathbf{R}}' = g\boldsymbol{\mu}/(1 - \alpha g) \tag{25}$$

which leads to

$$\Phi^{(\bar{R}')} = -[g\mu/(1 - \alpha g)]r\cos\theta \tag{26}$$

and by the same arguments as before, we obtain

$$w = -\frac{1}{2} g\mu^2/(1 - \alpha g) \tag{27}$$

The same result can be derived in a much more elegant fashion[42,44] by direct integration of the expression $dw = (4\pi)^{-1}(\mathbf{E}\cdot d\mathbf{D})dv$ which explicitly avoids the arguments based on reversible charging. The present approach has merit in that it appeals more to physical intuition and shows more directly which criteria the potential functions, $\Phi^{(\bar{R}')}$ must satisfy to be thermodynamically consistent. If w is to be equated to the electrochemical potential, the potential functions $\Phi^{(\bar{R}')}$ at different molecules must obey the integrability condition mentioned in Section II-A. We shall see in the next section that for the polarizable charge distribution also, this is generally not the case.

C. Critique of the Method

The methods outlined in the previous sections for evaluating the reaction field and the work function can be objected to on several grounds.

In the first place, the continuum model is highly artificial when applied to the molecular scale. It is based on the assumption that the molecules

surrounding a specific molecule can be characterized as a uniform dielectric and, thus, this model ignores density, concentration, and other types of fluctuations. Such a model can be expected to describe reasonably well the situation where the "center sphere" is small but nevertheless of macroscopic dimensions in which case these fluctuations are of minor importance. The radius of the cavity containing the center sphere then has a well-defined meaning, namely, the radius of the sphere. The difficulties occur when the cavity shrinks to molecular size. In that case, the statistical fluctuations take on a role of major importance and the cavity concept—already a vague concept—loses its meaning as a well-defined quantity. It is shown in Section VI-B-2 that by properly choosing a value for a^3, the reaction field, based on the dielectric formulation, can be made consistent to a good approximation with statistically calculated fields but it is clear that no simple choice of a^3 can yield an expression which is exact to all orders.

A second objection to the present scheme is that it is based on a model which ignores the dynamic effects of the field-producing moment. For, it can be argued, since the dipole is rotatory rather than stationary, it cannot produce a reaction field which will instantaneously follow its motion. To take account of the time lag, the results may be expected to depend on time-varying response functions, of which the Fourier transforms are frequency-dependent susceptibilities. This argument, of course, does not take into consideration the statistical nature of the fluctuations which could give values for w that are independent of frequency. It is, however, not apparent that the results are expressible in terms of the static susceptibility and, in fact, it turns out that this is not generally the case except when the fluctuations are of thermal origin.

Finally, if w is to be related to a thermodynamic function, the potentials from which it is calculated must satisfy the reciprocity relations discussed in the previous sections. That this is generally not the case can be inferred from the following example. Suppose the dielectric material consists of polar and nonpolar molecules; let i denote a particular polar molecule and j a particular nonpolar one. If we take i to be the "center" molecule and calculate $\mu_{i;\mathrm{el}}$ by the preceding formalism, then $\mu_{i;\mathrm{el}}$ will contain contributions from the interaction with all molecules including the jth molecule which induces a moment in i. On the other hand, if we take the jth molecule to be the "center" molecule, the predicted $\mu_{j;\mathrm{el}}$ would be zero inasmuch as j has no permanent moment and, therefore, cannot create a reaction field. These results are, of course,

incompatible: $\mu_{j;\mathrm{el}}$ cannot be zero but must contain contributions arising from polarization of j by i (as well as all other polar molecules). (We are referring here only to the orientation and induction interactions and not to the dispersion interaction which would further complicate matters.)

Because of these and other conceptual difficulties, we shall henceforth discard the reaction-field formulation based on the present model, retaining only the reaction-field concept as useful. We define the reaction field of a molecule as *the field produced at the center of the molecule by the surrounding medium which was polarized by the molecule.* The medium is neither required to have a uniform distribution nor is the molecule required to have a static moment.

III. THE REACTION FIELD OF A FLUCTUATING MOMENT IN A MEDIUM OF ARBITRARY DISTRIBUTION

In this section, we consider the reaction field produced by a fluctuating moment. The fluctuations may be due to the random oscillations of the electrons about their equilibrium positions in a molecule, they may be caused by the rotational motion of the permanent dipole moment, or they may arise from a combination of these factors. The exact nature of these fluctuations is unimportant for the purpose of the present development; the only requirement is that they be electrical in origin. (Translational and other types of fluctuations are excluded.)

A. General Formulation

Consider a system of N nonoverlapping particles at a fixed internuclear distance from each other. We single out one particle, i, and consider the response of the surrounding molecules to the electrical fluctuations in i. Suppose that, as a result of these fluctuations, molecule i acquires a moment $\mathbf{m}_i(t)$ at any particular instant of time, t. This moment will polarize the surrounding medium which, in turn, produces the reaction field $\mathbf{R}_i(q,t)$ at molecule i. The symbol q has been introduced to indicate a particular molecular configuration characterized by a given set of position vectors $\mathbf{r}_{ij}$, $\mathbf{r}_{ik}$, etc. ($\mathbf{r}_{ij} = \mathbf{r}_i - \mathbf{r}_j$). Since, in general, the field produced by the fluctuating moment does not polarize the surrounding medium instantaneously, the reaction field $\mathbf{R}_i(q,t)$ at a given instant of time t will depend not only on $\mathbf{m}_i(t)$ at the same instant of time, but will depend on all preceding ones. If the relationship between $\mathbf{R}_i$ and $\mathbf{m}_i$ is

taken to be linear (the significance of this approximation will be discussed more fully in Section III-B), then this relationship may be expressed as

$$\mathbf{R}_i(q,t) = \int_0^\infty \mathbf{G}(q,\tau) \cdot \mathbf{m}_i(t-\tau)d\tau \tag{28a}$$

or equivalently as

$$\mathbf{R}_i(q,t) = \int_{-\infty}^t \mathbf{G}(q,t-t') \cdot \mathbf{m}_i(t')dt' \tag{28b}$$

where the tensor $\mathbf{G}(q,\tau)$ is the response function of the medium (for the particular configuration q) and $\tau = t - t'$. Equations (28) also define a complex susceptibility

$$\hat{\mathbf{g}}(q,\omega) = \int_0^\infty \mathbf{G}(q,\tau)e^{-i\omega\tau}d\tau \tag{29}$$

which linearly relates the Fourier component of $\mathbf{R}_i(q,t)$ and $\mathbf{m}_i(t)$, i.e.,

$$\mathbf{R}_{i,\omega}(q) = \hat{\mathbf{g}}(q,\omega) \cdot \mathbf{m}_{i,\omega}$$

as can be verified by decomposing the field quantities in Eq. (28a)

$$\int_{-\infty}^\infty \mathbf{R}_{i,\omega}(q)e^{i\omega t}d\omega = \int_0^\infty d\tau \mathbf{G}(q,\tau) \cdot \int_{-\infty}^\infty d\omega \mathbf{m}_{i,\omega}e^{i\omega(t-\tau)}$$

$$= \int_{-\infty}^\infty \hat{\mathbf{g}}(q,\omega) \cdot \mathbf{m}_{i,\omega}e^{i\omega t}d\omega \tag{30}$$

It is clear from the form of Eq. (29) that, if we write $\hat{\mathbf{g}}(q,\omega) = \mathbf{g}'(q,\omega) - i\mathbf{g}''(q,\omega)$ where $\mathbf{g}'(q,\omega)$ and $\mathbf{g}''(q,\omega)$ are, respectively, the real and imaginary parts of the complex susceptibility, the following symmetry relations must hold

$$\mathbf{g}'(q,\omega) = \mathbf{g}'(q,-\omega) \tag{31}$$

and

$$\mathbf{g}''(q,-\omega) = -\mathbf{g}''(q,\omega)$$

The development in Section IV of the general expression for the polarization free energy will depend only on these symmetry properties and not on the specific form for $\hat{\mathbf{g}}(q,\omega)$.

B. Dielectric Description

For an isotropic fluid, the susceptibility averaged over all configurations can be written as a scalar times the idemfactor **I**, i.e., $\langle \hat{\mathbf{g}}(q,\omega) \rangle_q = \langle \hat{g}(q,\omega) \rangle_q \mathbf{I}$. The scalar quantity can be equated to the macroscopic susceptibility $\hat{g}(\omega)$ and, on the basis of the continuum model, can be written as [see Eq. (10)]

$$\hat{g}(\omega) = \{[2\hat{\varepsilon}(\omega) - 2]/[2\hat{\varepsilon}(\omega) + 1]\}(1/a^3) \tag{32}$$

where $\hat{\varepsilon}(\omega) = \varepsilon'(\omega) - i\varepsilon''(\omega)$, which gives

$$g'(\omega) = a^{-3} \frac{[2\varepsilon'(\omega) - 2][2\varepsilon'(\omega) + 1] + 4[\varepsilon''(\omega)]^2}{[2\varepsilon'(\omega) + 1]^2 + 4[\varepsilon''(\omega)]^2} \tag{33a}$$

and

$$g''(\omega) = a^{-3} \frac{6\varepsilon''(\omega)}{[2\varepsilon'(\omega) + 1]^2 + 4[\varepsilon''(\omega)]^2} \tag{33b}$$

C. Molecular Description

In this section, we develop $\hat{\mathbf{g}}(q,\omega)$ as a series expansion in terms of molecular susceptibilities.[27,28] First, we consider the case of a static moment. We picture the reaction field to arise as follows. Let $\mathbf{m}_i$ be the moment of particle i. This moment will produce a dipolar field which extends over all space. The electric field at the site of a neighboring molecule k will be

$$\mathbf{E}_k = -\mathbf{T}_{ki} \cdot \mathbf{m}_i \tag{34}$$

where $\mathbf{T}_{ik}$ is a tensor of dyadic form

$$\mathbf{T}_{ik} = \frac{1}{r_{ik}^3} \left[\mathbf{I} - \frac{3\mathbf{r}_{ik}\mathbf{r}_{ik}}{r_{ik}^2} \right] \tag{35}$$

and $\mathbf{r}_{ik} = \mathbf{r}_i - \mathbf{r}_k$. The field $\mathbf{E}_k$ induces a moment $\mathbf{m}_k = \chi_k \mathbf{E}_k$ in k, which in turn produces a field $(\mathbf{E}_i)_k$ at i:

$$(\mathbf{E}_i)_k = -\mathbf{T}_{ik} \cdot \mathbf{m}_k = \chi_k \mathbf{T}_{ik} \cdot \mathbf{T}_{ki} \cdot \mathbf{m}_i \tag{36}$$

where χ_k is the susceptibility of the isolated molecule k, associated with all electrical displacements, electronic as well as rotational and is, for simplicity, assumed to be isotropic. The field $(\mathbf{E}_i)_k$ is part of the reaction field.

Now suppose i has two neighbors, k and l. The field produced at i will then consist of two terms similar to the ones above, namely, $(\mathbf{E}_i)_k$ and $(\mathbf{E}_i)_l$ but, in addition, new terms will arise, of the form

$$(\mathbf{E}_i)_{k,l} = -\chi_k\chi_l\mathbf{T}_{ik}\cdot\mathbf{T}_{kl}\cdot\mathbf{T}_{li}\cdot\mathbf{m}_i \tag{37}$$

The latter is the field produced at i by l which results from the polarization of l by k, which in turn was polarized by i. The two neighbors k and l give rise also to a field characterized by the symbol $(\mathbf{E}_i)_{l,k}$. The reaction field is the sum total of all the field strengths $(\mathbf{E}_i)_k$, $(\mathbf{E}_i)_{k,l}$, $(\mathbf{E}_i)_{l,k}$, etc. (The manner in which the various reaction-field components arise is depicted schematically in Figures 1*a*–1*d*.) This process must be

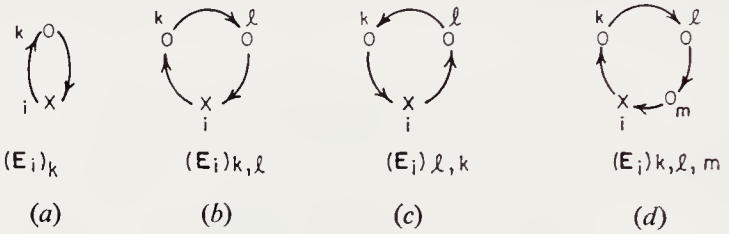

(*a*) (*b*) (*c*) (*d*)

Fig. 1. Diagrams corresponding to the reaction-field terms (*a*) $(\mathbf{E}_i)_k$; (*b*) $(\mathbf{E}_i)_{k,l}$; (*c*) $(\mathbf{E}_i)_{l,k}$; (*d*) $(\mathbf{E}_i)_{k,l,m}$.

continued so as to include all $N-1$ neighbors of i. Since each of these is a tensor times $\mathbf{m}_i$, the reaction field is also established as the product of a tensor and $\mathbf{m}_i$, i.e.,

$$\mathbf{R}_i(q) = \left[\sum_{\substack{k=1\\k\neq i}}^{N-1}\mathbf{T}^2_{ik}\chi_k - \sum_{\substack{k=1\\k\neq i,l\neq i\\k\neq l}}^{N-1}\sum_{l=1}^{N-2}\mathbf{T}^3_{ikl}\chi_k\chi_l + \cdots\right]\cdot\mathbf{m}_i = \mathbf{g}(q)\cdot\mathbf{m}_i \tag{38}$$

where $\mathbf{T}^2_{ik}$, $\mathbf{T}^3_{ikl}$, etc. are short notations for $\mathbf{T}_{ik}\cdot\mathbf{T}_{ki}$, $\mathbf{T}_{ik}\cdot\mathbf{T}_{kl}\cdot\mathbf{T}_{li}$, etc., respectively, and the q has been reintroduced to emphasize that the results pertain to a particular molecular configuraion.

We now turn to time-dependent fields. In first approximation, the Fourier components of $\mathbf{R}_i(q,t)$ and $\mathbf{m}_i(t)$ bear the following relation to each other

$$\mathbf{R}_{i,\omega}(q) = \left[\sum_k \mathbf{T}^2_{ik}\hat{\chi}_k(\omega) - \sum_k\sum_l \mathbf{T}^3_{ikl}\hat{\chi}_k(\omega)\hat{\chi}_l(\omega) + \cdots\right]\cdot\mathbf{m}_{i,\omega} = \hat{\mathbf{g}}(q,\omega)\cdot\mathbf{m}_{i,\omega} \tag{39}$$

where the bracketed expression defines $\hat{\mathbf{g}}(q,\omega)$ and where the $\hat{\chi}_k(\omega)$,

$\hat{\chi}_l(\omega)$ etc. are the frequency-dependent susceptibilities of the isolated molecules. To see this, we consider the time evolution of $\mathbf{m}_i(t)$ which gives

$$\mathbf{R}_i(q,t) = \sum_k \mathbf{T}_{ik}^2 \int_{-\infty}^{t} dt' K_k(t-t') \cdot \mathbf{m}_i(t') - \sum_{k,l} \mathbf{T}_{ikl}^3 \int_{-\infty}^{t} dt' K_k(t-t') \int_{-\infty}^{t'} dt'' K_l(t'-t'') \cdot \mathbf{m}_i(t'') + \cdots \quad (40)$$

where $K_k(t-t')$ and $K_l(t'-t'')$, etc. are the response functions of k and l, respectively, and the times are so arranged that the later time is always to the left, i.e., $t > t' > t'' \ldots$ The summands correspond to the reaction-field parts $(\mathbf{E}_i)_k$, $(\mathbf{E}_i)_{kl}$, etc. and the time ordering establishes the particular polarization sequence. (For example, the summand under the double summation sign, as written, indicates that $\mathbf{m}_i$ polarizes l which then polarizes k.) Fourier decomposition of Eq. (40) gives

$$\int_{-\infty}^{\infty} \mathbf{R}_{i,\omega}(q) e^{i\omega t} d\omega = \int_{-\infty}^{\infty} d\omega \left[\sum_k \mathbf{T}_{ik}^2 \int_{-\infty}^{t} dt' K_k(t-t') e^{-i\omega(t-t')} - \sum_{k,l} \mathbf{T}_{ikl}^3 \int_{-\infty}^{t} dt' K_k(t-t') e^{-i\omega(t-t')} \times \int_{-\infty}^{t'} dt'' K_l(t'-t'') e^{-i\omega(t'-t'')} + \cdots \right] \cdot \mathbf{m}_{i,\omega} e^{i\omega t} \quad (41)$$

which establishes Eq. (39) on replacing all time integrals by their corresponding susceptibilities, e.g.,

$$\int_{-\infty}^{t'} dt'' K_l(t'-t'') e^{-i(t'-t'')\omega} = \int_0^{\infty} K_l(\tau) e^{-i\omega\tau} d\tau \equiv \hat{\chi}_l(\omega) \quad (42)$$

The form for $\mathbf{R}_{i,\omega}(q)$ as given by Eq. (39) does not take retardation effects into consideration. Although a detailed discussion of the retarded potential is beyond the scope of the present presentation, retardation effects can formally be included within the framework of the reaction field technique by using a more general expression for $\mathbf{T}_{ik}$ than given by Eq. (35), namely,

$$\mathbf{T}_{ik}(\omega) = -(\nabla\nabla + (\omega^2/c^2)\mathbf{I}) e^{-i\omega r_{ik}/c}/r_{ik} \quad (43)$$

where c is the velocity of light. This expression can be obtained by

considering the field at k due to a radiating dipole $\mathbf{m}_i$, which is[48]

$$\mathbf{E}_k(t) = \text{grad div} \frac{\mathbf{m}_i(t')}{r_{ik}} - \frac{1}{c^2} \frac{\ddot{\mathbf{m}}_i(t')}{r_{ik}} \tag{44a}$$

where $t' = t - (r_{ik}/c)$. Decomposition of this expression gives

$$\int_{-\infty}^{\infty} (\mathbf{E}_{k,\omega}) e^{i\omega t} d\omega = \int_{-\infty}^{\infty} \left[\text{grad div} \frac{e^{-i\omega r_{ik}/c}}{r_{ik}} + \frac{\omega^2}{c^2} \frac{e^{-i\omega r_{ik}/c}}{r_{ik}} \right] \mathbf{m}_{i,\omega} e^{i\omega t} d\omega \tag{44b}$$

which implies

$$\mathbf{E}_{k,\omega} = -\mathbf{T}_{ik}(\omega) \cdot \mathbf{m}_{i,\omega}$$

where $\mathbf{T}_{ik}(\omega)$ is defined by Eq. (43). For zero frequency, $\mathbf{T}_{ik} = -\nabla\nabla r_{ik}^{-1}$, which is the same as Eq. (35).

The prediction of Eq. (39) that the reaction-field function $\hat{\mathbf{g}}(q,\omega)$ can be characterized by a single frequency, even though the system has multiple scattering centers, requires some comments. This is in harmony with the original assumption that $\mathbf{R}_i(t)$ and $\mathbf{m}_i(t)$ are linearly dependent—an approximation which greatly simplifies the subsequent derivation of the many-body potential, as will be shown in the following section. This simplification is achieved by excluding from the summation those reaction-field components which correspond to multiple excitations, such as the ones depicted diagrammatically in Figure 2. These diagrams

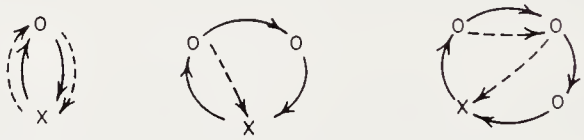

Fig. 2. Diagrams corresponding to reaction-field terms which involve multiple-frequency transitions.

give rise to nonlinear field terms, which are not rigorously expressible in terms of the ordinary susceptibilities but involve susceptibilities of mixed frequencies. These nonlinear terms may also be regarded as arising from the distortions of the molecules. In this regard, it may be pointed out that the formulation based on the static approach of Section II-B

takes account of the nonlinear terms as can be seen by expanding the extended reaction field in which case

$$\bar{\mathbf{R}}' = \boldsymbol{\mu}[g/(1 - \alpha g)] = \boldsymbol{\mu} g(1 + \alpha g + \alpha^2 g^2 + \cdots) \tag{45}$$

In this case, the dipolar distortions are expressed in terms of the polarizability. A more general theory which is based on time-varying fields and which also accounts for changes in polarizability, leads to great mathematical difficulties[49] and has not been fully developed. The contribution of the nonlinear terms to dispersion energy is of secondary importance; for example, the first nonvanishing correction to the interaction between two spherically symmetrical molecules would correspond to a term which is part of the fourth-order perturbation energy. The subsequent discussion will be based only on the linear reaction field.

IV. GENERALIZED POTENTIAL

In this section, we derive a general expression for the mutual potential of interaction between a given molecule i and all its neighbors. The treatment will be based on the general symmetry properties of the reaction-field response function and not on its specific form. In the next section, we apply the results to particular types of interactions.

We first calculate the work required to polarize the surroundings (to be denoted S) by the electrical fluctuations in i. In terms of the time varying reaction field, this is

$$w_{i\to S}(q) = -\frac{1}{2}\langle \mathbf{R}_i(q,t) \cdot \mathbf{m}_i(t)\rangle \tag{46}$$

where the brackets denote an averaging process. This expression has the nature of a correlation function as can be seen by substituting the value given in Eq. (28a) for $\mathbf{R}_i(q,t)$ which yields

$$w_{i\to S}(q) = -\frac{1}{2}\int_0^\infty \mathbf{G}(q,\tau) \cdot \langle \mathbf{m}_i(t-\tau) \cdot \mathbf{m}_i(t)\rangle d\tau \tag{47}$$

where the brackets denote an ensemble average over all values that the product can take at a given time t (for a given τ). This statistical averaging should be equivalent to a time averaging and $w_{i\to S}$ is independent of t. To proceed, we express $\mathbf{m}_i(t)$ and $\mathbf{m}_i(t-\tau)$ in terms of their respective Fourier components of frequencies ω' and ω and obtain

$$w_{i\to S}(q) = -\frac{1}{2}\int_0^\infty d\tau \int_{-\infty}^\infty d\omega' \int_{-\infty}^\infty d\omega \langle \mathbf{m}_{\omega'} e^{i\omega' t} \cdot \mathbf{G}(q,\tau) \cdot \mathbf{m}_\omega e^{i\omega(t-\tau)} \rangle$$

$$= -\frac{1}{2}\int_{-\infty}^\infty d\omega' \int_{-\infty}^\infty d\omega e^{i(\omega+\omega')t} \langle \mathbf{m}_\omega \cdot \mathbf{m}_{\omega'} \rangle \cdot \int_0^\infty \mathbf{G}(q,\tau) e^{-i\omega\tau} d\tau$$

$$= -\frac{1}{2}\int_{-\infty}^\infty d\omega' \int_{-\infty}^\infty d\omega e^{i(\omega+\omega')t} \langle \mathbf{m}_\omega \mathbf{m}_{\omega'} \rangle : \hat{\mathbf{g}}(q,\omega) \quad (48)$$

(For simplicity, the i subscript on $\mathbf{m}$ has been dropped.) In reducing this expression, use has been made of the property that if $\mathbf{A}$ and $\mathbf{B}$ are vectors, and $\mathbf{Q}$ is a tensor, then $\mathbf{A}\cdot\mathbf{Q}\cdot\mathbf{B} = \mathbf{BA} : \mathbf{Q}$. Since i is taken to be isotropic, there can be no preferred orientation in space of its moment and so the xx, yy, and zz components of the symmetric tensor $\mathbf{m}_\omega \mathbf{m}_{\omega'}$ (assumed to have been diagonalized) contribute equally. Hence, we can replace this tensor by a scalar times the idemfactor, i.e., $\langle \mathbf{m}_\omega \mathbf{m}_{\omega'} \rangle = \langle (m_\omega)_z (m_\omega)_z \rangle \mathbf{I}$, where $(m_\omega)_z$ is the z component of the vector $\mathbf{m}_\omega$; Eq. (48) then reduces to

$$w_{i\to S}(q) = -\frac{1}{2}\int_{-\infty}^\infty d\omega' \int_{-\infty}^\infty d\omega e^{i(\omega+\omega')t} \langle (m_\omega)_z (m_{\omega'})_z \operatorname{tr} \hat{\mathbf{g}}(q,\omega) \rangle \quad (49)$$

upon replacing $\mathbf{I} : \hat{\mathbf{g}}(q,\omega)$ by trace $\hat{\mathbf{g}}(q,\omega)$.

If $w_{i\to S}$ is to be time independent, then frequencies ω and ω' must be equal and of opposite sign or, more precisely, the integrand must contain a δ function of the type $\delta(\omega + \omega')$.[50] If, following Landau and Lifshitz,[50] we define $(m_\omega^2)_z$ by the relation

$$\langle (m_\omega)_z (m_{\omega'})_z \rangle = (m_\omega^2)_z \delta(\omega + \omega')$$

we get, on integrating out the ω' in Eq. (49),

$$w_{i\to S}(q) = -\frac{1}{2}\int_{-\infty}^\infty (m_\omega^2)_z \operatorname{tr} \hat{\mathbf{g}}(q,\omega) d\omega \quad (50)$$

In Section V, we derive an expression for $(m_\omega^2)_z$ in terms of molecular parameters; here, we merely note that $(m_\omega^2)_z$ is an even function of ω. Since the imaginary part of $\hat{\mathbf{g}}(q,\omega)$ is an odd function of ω, it contributes nothing to the integral and so Eq. (50) becomes

$$w_{i\to S}(q) = -\int_0^\infty (m_\omega^2)_z \operatorname{tr} \mathbf{g}'(q,\omega) d\omega \quad (51)$$

upon changing the limits of integration from $(-\infty, \infty)$ to $(0, \infty)$.

The quantity $(m_\omega^2)_z$ is the spectral density of the mean square fluctuation, i.e., $\langle m_z^2 \rangle = \int_{-\infty}^{\infty} (m_\omega^2)_z d\omega$, and is related to the imaginary part of the susceptibility by the Callen and Welton formula[51]

$$(m_\omega^2)_z = (\hbar/2\pi)\chi''(\omega) \coth (\hbar\omega/2kT) \tag{52}$$

The complex susceptibility, here, is the susceptibility of the ith molecule and is associated with the total charge fluctuation, that is, rotational as well as oscillatory. On substituting Eq. (52) into Eq. (51), we get

$$w_{i\to S}(q) = -\frac{\hbar}{2\pi} \int_0^\infty \chi_i''(\omega) \operatorname{tr} \mathbf{g}'(q,\omega) \coth \frac{\hbar\omega}{2kT} d\omega \tag{53}$$

For an isotropic fluid $\mathbf{g}'(q,\omega) = g'(q,\omega)\mathbf{I}$ and Eq. (53) reduces to

$$w_{i\to S}(q) = -\frac{3\hbar}{2\pi} \int_0^\infty \chi_i''(\omega) g'(q,\omega) \coth \frac{\hbar\omega}{2kT} d\omega \tag{54}$$

The results obtained so far are quite general and apply to systems obeying classical- as well as quantum mechanics. In the case of quantal behavior, the quantities $\mathbf{R}_i(q,t)$ and $\mathbf{m}_i(t)$ are to be interpreted to mean operators and the brackets $\langle\ \rangle$ are quantum-statistical averages over the unperturbed states. Since time-dependent operators do not, in general, commute, the derivation must be slightly modified; instead of Eq. (47) we now have

$$w_{i\to S}(q) = -\frac{1}{4} \int_0^\infty d\tau \mathbf{G}(q,\tau) \langle \mathbf{m}_i(t-\tau) \cdot \mathbf{m}_i(t) + \mathbf{m}_i(t) \cdot \mathbf{m}_i(t-\tau) \rangle \tag{55}$$

The subsequent expressions retain their general form provided $\langle \mathbf{m}_\omega \mathbf{m}_{\omega'} \rangle$ is replaced by $\frac{1}{2}\langle \mathbf{m}_\omega \mathbf{m}_{\omega'} + \mathbf{m}_{\omega'} \mathbf{m}_\omega \rangle$ and the spectral density is defined by the relation

$$\frac{1}{2} \langle (\mathbf{m}_\omega)_z (\mathbf{m}_{\omega'})_z + (\mathbf{m}_{\omega'})_z (\mathbf{m}_\omega)_z \rangle = (m_\omega^2)_z \delta(\omega + \omega')$$

We now return to the general expression for $w_{i\to S}(q)$ as given by Eq. (53). As stated before, this represents the interaction of i with the surroundings, brought about by the electrical fluctuation in i. A similar expression, with the prime and double prime interchanged, gives the polarization free energy resulting from fluctuations which originate in the surroundings. The mutual work of polarization, $w_{i\to S}(q) + w_{S\to i}(q)$,

constitutes the potential of interaction between i and the entire surrounding and this will be denoted also as $\phi_{i;S}(q)$; thus

$$\phi_{i;S}(q) = -\frac{\hbar}{2\pi}\int_0^\infty [\chi_i''(\omega)\,\mathrm{tr}\,\mathbf{g}'(q,\omega) + \chi_i'(\omega)\,\mathrm{tr}\,\mathbf{g}''(q,\omega)]\coth\frac{\hbar\omega}{2kT}\,d\omega \tag{56}$$

which can be written more compactly as

$$\phi_{i;S}(q) = -\frac{\hbar}{2\pi}\,Re\int_0^\infty \hat{\chi}_i(\omega)\,\mathrm{tr}\,\hat{\mathbf{g}}(q,\omega)\coth\frac{\hbar\omega}{2kT}\,id\omega \tag{57}$$

We shall refer to $\phi_{i;S}(q)$ as the generalized potential.

Up to this point, we have considered the frequencies ω to be real. It is sometimes advantageous to extend the definition of the susceptibilities to functions of complex argument. This can be accomplished in two ways: by regarding ω as the real axis of some complex plane or by regarding it as the imaginary axis of a plane. We prefer the latter approach and take as definition of the molecular susceptibility

$$\hat{\chi}^{(p)}(p) = \int_0^\infty K(\tau)e^{-p\tau}d\tau \tag{58}$$

where $p = \sigma + i\omega$ (σ and ω real) and as definition of $\hat{\mathbf{g}}^{(p)}(q,p)$ a similar expression. When $\sigma = 0$ this definition reduces to the previous one [Eq. (42)]; thus $\hat{\chi}^{(p)}(i\omega) \equiv \hat{\chi}(\omega) \equiv \chi'(\omega) - i\chi''(\omega)$. Of special interest is the susceptibility along the σ axis.

$$\chi^p(\sigma) = \int_0^\infty K(\tau)e^{-\sigma\tau}d\tau \tag{59}$$

which is the Laplace transform of $K(\tau)$ and is necessarily real. (The function is defined only for positive values of σ; for negative values, it diverges and has no physical meaning.) The same considerations apply to the reaction-field susceptibility $\hat{\mathbf{g}}^{(p)}(q,p)$.

Equation (57) has been written in a form that makes extension of the integrand into the interior of the p plane obvious. In terms of the p variable,

$$\phi_{i;S}(q) = -\frac{\hbar}{2\pi}\,Re\int_c \hat{\chi}_i^{(p)}(p)\,\mathrm{tr}\,\hat{\mathbf{g}}^{(p)}(q,p)\coth\frac{\hbar p}{2ikT}\,dp \tag{60}$$

where the path of integration can be any path in the first quadrant of

the complex p plane having zero and infinity as extremities. A particularly convenient path is the σ axis where the susceptibilities are real. When $T = 0$, the hyperbolic cotangent function is eliminated and Eq. (60) reduces to

$$\phi_{i;S}(q) = -\frac{\hbar}{2\pi}\int_0^\infty \chi_i^{(p)}(\sigma)\,\mathrm{tr}\,\mathbf{g}^{(p)}(q,\sigma)d\sigma \qquad T = 0 \tag{61}$$

When T is not zero the hyperbolic cotangent function has an infinite number of singularities along the σ axis at the points

$$\sigma_r = (2kT\pi/\hbar)r \qquad r = 0,1,2\ldots \tag{62}$$

with residues equal to $2ikT/\hbar$. In carrying out the integration, these poles have to be avoided by going around them in clockwise direction by a quarter-circle indentation of the first point $\sigma_0 = 0$ and half-circle indentations of all other points. The segments along the σ axis between the points need not be considered since they are pure imaginary and drop out when the real part is taken. The contour is closed by a quarter circle of infinite radius which, however, does not contribute to the integral since the integral drops off faster than p^{-1} as $p \to \infty$. From the residues at the poles we obtain

$$\begin{aligned}\phi_{i;S}(q) = &-\frac{\hbar}{2\pi}(-2\pi i)\left(\frac{2ikT}{\hbar}\right)\\ &\times\left[\frac{1}{4}\chi_i(0)\,\mathrm{tr}\,\mathbf{g}(q,0) + \frac{1}{2}\sum_{r=1}^{\infty}\chi_i^{(p)}(\sigma_r)\,\mathrm{tr}\,\mathbf{g}^{(p)}(q,\sigma_r)\right]\\ &= -kT\sum_{r=0}^{\infty}{}'\,\chi_i^{(p)}(\sigma_r)\,\mathrm{tr}\,\mathbf{g}^{(p)}(q,\sigma_r)\end{aligned} \tag{63}$$

where the prime on the summation sign denotes that the leading term is to be multiplied by $\frac{1}{2}$. [Note that $\chi^{(p)}(0) \equiv \chi(0)$.]

We consider two limiting cases: $T \to \infty$ (the classical limit) and $T \to 0$ (the quantal limit). In Section V-B it is shown that $\chi^{(p)}(\sigma_r)$ and therefore also that $\mathbf{g}^{(p)}(q,\sigma_r)$ are decreasing functions of T. Hence, for $T \to \infty$, all the terms in Eq. (63) beyond the leading one can be neglected and

$$\phi_{i;S}(q) = -(kT/2)\chi_i(0)\,\mathrm{tr}\,\mathbf{g}(q,0) \qquad \text{(classical)} \tag{64}$$

When $T \to 0$, the spacing between the poles tends to zero and the summation can then be replaced by an integration, i.e.,

$$\sum_{r=0}^{\infty}{}' \rightarrow \int_0^\infty dr = \frac{\hbar}{2\pi kT}\int_0^\infty d\sigma$$

The resulting expression is then identical with Eq. (61). This potential can be reduced further by making use of the transformation[52]

$$\hat{\mathfrak{Q}}^{(p)}(p) = \frac{2}{\pi}\int_0^\infty \frac{y\mathfrak{Q}''(y)}{y^2+p^2}\,dy \tag{65}$$

which is a generalization of the Kramers-Kronig transform[52]

$$\mathfrak{Q}'(\omega) = \frac{2}{\pi}\mathscr{P}\int_0^\infty \frac{y\mathfrak{Q}''(y)}{y^2-\omega^2}\,dy \tag{66}$$

where $\hat{\mathfrak{Q}}^{(p)}(p)$ is a general susceptibility, and $\mathfrak{Q}'(\omega)$ and $\mathfrak{Q}''(\omega)$ are its real and imaginary parts along the $i\omega$ axis, i.e., $\hat{\mathfrak{Q}}^{(p)}(i\omega) = \mathfrak{Q}'(\omega) - i\mathfrak{Q}''(\omega) \equiv \hat{\mathfrak{Q}}(\omega)$; the symbol $\mathscr{P}$ denotes that the integral is the principal value. On substituting Eq. (65) into Eq. (61), we get the quantal expression

$$\phi_{i;S}(q) = -\frac{2\hbar}{\pi^3}\int_0^\infty\int_0^\infty\int_0^\infty \frac{\chi_i''(\omega_i)\,\mathrm{tr}\,\mathbf{g}''(q,\omega_s)\omega_i\omega_s}{(\omega_i^2+\sigma^2)(\omega_s^2+\sigma^2)}\,d\omega_i d\omega_s d\sigma \tag{67}$$

which reduces to

$$\phi_{i;S}(q) = -\frac{\hbar}{\pi^2}\int_0^\infty\int_0^\infty \frac{\chi_i''(\omega_i)\,\mathrm{tr}\,\mathbf{g}''(q,\omega_s)}{\omega_i+\omega_s}\,d\omega_i d\omega_s \tag{68}$$

In an isotropic fluid the classical and quantal limits become, respectively,

$$\phi_{i;S}(q) = -\frac{3}{2}kT\chi_i(0)g(q,0) \qquad \text{(classical)} \tag{69}$$

$$\phi_{i;S}(q) = -\frac{3\hbar}{\pi^2}\int_0^\infty\int_0^\infty \frac{\chi_i''(\omega_i)g''(q,\omega)}{\omega_i+\omega_s}\,d\omega_i d\omega_s \qquad \text{(quantal)} \tag{70}$$

If it is assumed that the local reaction-field susceptibility deviates little from the average or macroscopic one (as in the continuum model), then

$$\phi_{i;S} = -\frac{3}{2}kT\chi_i(0)g(0)$$

and thus $\phi_{i;S}$ is independent of q. Recall that $\phi_{i;S}$ represents the mutual polarization of center molecule and surroundings; in Section II, this

was denoted as w. It is shown in Section V-B that the rotational susceptibility $\chi^{\text{rot}}(0) \to \mu^2/3kT$ in the classical limit. Thus, if we confine ourselves to rotational interaction, we can replace Eq. (69) by

$$w = -\frac{1}{2}\mu^2 g$$

which is identical with the result obtained on the basis of the static reaction field. A similar expression for the dispersion interaction in terms of the static susceptibility cannot rigorously be obtained even on the basis of the continuum model except in case of harmonic oscillators and even then, one has to assume that the surrounding is characterized by one single frequency ω_s.

V. ADDITIVE AND NONADDITIVE VAN DER WAALS POTENTIALS

In this section, we write the generalized potential as a series expansion of molecular susceptibilities and extract from this general forms for the two-body-, three-body-, and higher-order potentials. The results are then specialized to dispersion—orientation—and induction potentials.

By expressing the virial form for $\mathbf{g}(q,\omega)$ [see Eq. (39)] as a function of σ_r and substituting it into Eq. (63), we obtain

$$\begin{aligned}\phi_{i;S}(q) = -kT \sum_{r=0}^{\infty}{}' \Bigg[& \sum_{k=1}^{N-1} \chi_i^{(p)}(\sigma_r)\chi_k^{(p)}(\sigma_r) \operatorname{tr} \mathbf{T}_{ik}^{2(p)}(\sigma_r) \\ & - \sum_{k=1}^{N-1} \sum_{l=1}^{N-2} \chi_i^{(p)}(\sigma_r)\chi_k^{(p)}(\sigma_r)\chi_l^{(p)}(\sigma_r) \operatorname{tr} \mathbf{T}_{ikl}^{3(p)}(\sigma_r) \\ & + \sum_{k=1}^{N-3} \sum_{l=1}^{N-2} \sum_{m=1}^{N-1} \chi_i^{(p)}(\sigma_r)\chi_k^{(p)}(\sigma_r)\chi_l^{(p)}(\sigma_r)\chi_m^{(p)}(\sigma_r) \operatorname{tr} \mathbf{T}_{iklm}^{4(p)}(\sigma_r) + \cdots \Bigg]\end{aligned} \tag{71}$$

This expression takes account of retardation; the $\mathbf{T}^n$ tensors are the frequency-dependent tensors based on Eq. (43), which, along the σ axis, take the form

$$\mathbf{T}_{ik}^{(p)}(\sigma) = -\left(\nabla\nabla - \frac{\sigma^2}{c^2}\mathbf{I}\right)\frac{e^{-\sigma r_{ik}/c}}{r_{ik}} \tag{72}$$

The χ's are the molecular susceptibilities defined by Eq. (59).

The various sums in Eq. (71) represent contributions from two-body, three-body, etc. interactions. These can be expressed also in terms of the pair potentials, the (nonadditive) triple potentials, etc. To generate these we first assume that i has only one neighbor, k. The potential is then the pair potential, $\phi^{(2)}(ik)$, and is given by

$$\phi^{(2)}(ik) = -kT \sum_{r=0}^{\infty}{}' \chi_i^{(p)}(\sigma_r)\chi_k^{(p)}(\sigma_r) \operatorname{tr} \mathbf{T}_{ik}^{2(p)}(\sigma_r) \tag{73}$$

Next suppose i has two neighbors, k and l. The resulting potential consists of two terms as in Eq. (73) and a nonadditive contribution:

$$\phi^{(3)}(ikl) = 2kT \sum_{r=0}^{\infty}{}' \chi_i^{(p)}(\sigma_r)\chi_k^{(p)}(\sigma_r)\chi_l^{(p)}(\sigma_r) \operatorname{tr} \mathbf{T}_{ikl}^{3(p)}(\sigma_r) \tag{74}$$

By continuing this process, we find that the nonadditive n-tuple potential is

$$\phi^{(n)}(ik \ldots t) = -kT(-1)^n(n-1)! \sum_{r=0}^{\infty}{}' \chi_i^{(p)}(\sigma_r) \ldots \chi_t^{(p)}(\sigma_r) \operatorname{tr} \mathbf{T}_{ik\ldots t}^{(p)}(\sigma_r) \tag{75}$$

Accordingly, Eq. (71) can also be written as

$$\phi_{i;S}(q) = \sum_k \phi^{(2)}(ik) + \sum_{k<l} \phi^{(3)}(ikl) + \ldots \sum_{k<l<\ldots t} \phi^{(n)}(ik \ldots t) \tag{76}$$

Note that in this representation, the summations are restricted.

A. Pair and Triple Potentials

We now examine the pair and triple potentials in more detail. By replacing $\sum_{r=0}^{\infty}{}'$ with $\frac{\hbar}{2\pi kT}\int_0^\infty d\sigma$, we obtain the low-temperature (quantal) limits

$$\phi^{(2)}(ik) = -\frac{\hbar}{2\pi}\int_0^\infty \chi_i^{(p)}(\sigma)\chi_k^{(p)}(\sigma) \operatorname{tr} \mathbf{T}_{ik}^{2(p)}(\sigma)d\sigma \qquad \text{(quantal)} \tag{77}$$

and

$$\phi^{(3)}(ikl) = \frac{\hbar}{\pi}\int_0^\infty \chi_i^{(p)}(\sigma)\chi_k^{(p)}(\sigma)\chi_l^{(p)}(\sigma) \operatorname{tr} \mathbf{T}_{ikl}^{3(p)}(\sigma)d\sigma \quad \text{(quantal)} \tag{78}$$

In the absence of retardation, the tensor $\mathbf{T}_{ik}(\sigma)$ reduces to the expression given by Eq. (35), which readily yields[8]

$$\operatorname{tr} \mathbf{T}_{ik}^2 = 6/r_{ik}^6 \tag{79}$$

$$\text{tr } \mathbf{T}_{ikl}^3 = 3(1 + 3\cos\theta_i \cos\theta_k \cos\theta_l)/r_{ik}^3 r_{kl}^3 r_{li}^3 \tag{80}$$

In the last expression, r_{ik}, r_{kl}, and r_{li} are the sides and θ_i, θ_k, and θ_l the inner angles of the triangle formed by i, k, and l, respectively. On using Eq. (79) and the transformation given by Eq. (65), the potentials become

$$\phi^{(2)}(ik) = -\frac{12\hbar}{\pi^3 r_{ik}^6} \int_0^\infty \int_0^\infty \int_0^\infty \frac{\omega_i \omega_k \chi_i''(\omega_i)\chi_k''(\omega_k)}{(\omega_i^2 + \sigma^2)(\omega_k^2 + \sigma^2)} d\omega_i d\omega_k d\sigma$$

$$= -\frac{6\hbar}{\pi^2 r_{ik}^6} \int_0^\infty \int_0^\infty \frac{\chi_i''(\omega_i)\chi_k''(\omega)}{\omega_i + \omega_k} d\omega_i d\omega_k \qquad \text{(quantal)} \tag{81}$$

and

$$\phi^{(3)}(ikl) = \frac{4\hbar}{\pi^3} \text{tr } \mathbf{T}_{ikl}^3$$

$$\times \int_0^\infty \int_0^\infty \int_0^\infty \frac{(\omega_i + \omega_k + \omega_l)\chi_i''(\omega_i)\chi_k''(\omega_k)\chi_l''(\omega_l)}{(\omega_i + \omega_k)(\omega_k + \omega_l)(\omega_l + \omega_i)} d\omega_i d\omega_k d\omega_l$$

(quantal) (82)

The high-temperature (classical) forms for these potentials are just the leading ($\sigma_r = 0$) terms of $\phi^{(2)}$ and $\phi^{(3)}$, as given, respectively, by Eqs. (73) and (74); i.e.,

$$\phi^{(2)}(ik) = -(3kT/r_{ik}^6)\chi_i(0)\chi_k(0) \qquad \text{(classical)} \tag{83}$$

and

$$\phi^{(3)}(ikl) = kT\chi_i(0)\chi_k(0)\chi_l(0) \text{ tr } \mathbf{T}_{ikl}^3 \qquad \text{(classical)} \tag{84}$$

Note that the classical potentials are always independent of frequency and, therefore, are independent of retardation effects.[53]

B. Molecular Susceptibilities

All the potentials of the preceding section can be calculated from a knowledge of the frequency dependence of the molecular susceptibilities. In principle, these could be determined experimentally or calculated theoretically. In this section we develop general formulas for $\chi'(\omega)$, $\chi''(\omega)$ and $\chi^{(p)}(\sigma_r)$, and explicit expressions for the rigid rotor and harmonic oscillator.

Let us first consider the functional form of the spectral density

$(m_\omega^2)_z$. This is the Fourier transform of the zz component of the anti-commutator $\frac{1}{2}\langle[\mathbf{m}(\tau),\mathbf{m}]_+\rangle^0$, where the brackets denote an average over the unperturbed states of the equilibrium ensemble.[54,55] To verify this, we write

$$\frac{1}{2}\langle[\mathbf{m}(t-\tau),\mathbf{m}(t)]_+\rangle^0 = \frac{1}{2}\langle[\mathbf{m}(t),\mathbf{m}(t+\tau)]_+\rangle^0$$

$$= \int_{-\infty}^{\infty}\int_{-\infty}^{\infty}\frac{1}{2}\langle\mathbf{m}_\omega\mathbf{m}_{\omega'} + \mathbf{m}_{\omega'}\mathbf{m}_\omega\rangle^0 e^{i(\omega+\omega')t}e^{i\omega\tau}d\omega d\omega'$$

$$= \int_{-\infty}^{\infty}\mathbf{m}_\omega^2 e^{i\omega\tau}d\omega \tag{85}$$

which shows that

$$\mathbf{m}_\omega^2 = \frac{1}{2\pi}\int_{-\infty}^{\infty}\frac{1}{2}\langle[\mathbf{m}(\tau),\mathbf{m}]_+\rangle^0 e^{-i\omega\tau}d\tau \tag{86}$$

In order to obtain $(m_\omega^2)_z$ we take the zz component of the anticommutator i.e., $\frac{1}{2}\langle[ez(\tau),ez]_+\rangle^0$. The latter can be written as

$$\frac{1}{2}\langle[ez(\tau),ez]_+\rangle^0 = \frac{1}{2}\operatorname{tr}\rho_0[ez(\tau),ez]_+ \tag{87}$$

where ρ_0 is the equilibrium density matrix of the unperturbed system, i.e.,

$$\rho_0 = e^{-\mathscr{H}_0/kT}/\operatorname{tr}e^{-\mathscr{H}_0/kT} = e^{-\mathscr{H}_0/kT}/Q \tag{88}$$

in which $\mathscr{H}_0$ is the unperturbed Hamiltonian of the molecule and Q is its partition function. By writing out the operators in the Heisenberg representation, we get

$$\frac{1}{2}\langle[ez(\tau),ez]_+\rangle^0 = \frac{e^2}{2Q}\operatorname{tr}[e^{-\mathscr{H}_0/kT}(e^{i\tau\mathscr{H}_0/\hbar}ze^{-i\tau\mathscr{H}_0/\hbar}z + ze^{i\tau\mathscr{H}_0/\hbar}ze^{-i\tau\mathscr{H}_0/\hbar})]$$

$$= \frac{e^2}{2Q}\sum_p\sum_q e^{-Eq/kT}(e^{i\tau Eq/\hbar}z_{qp}e^{-i\tau Ep/\hbar}z_{pq}$$

$$+ z_{qp}e^{i\tau Ep/\hbar}z_{pq}e^{-i\tau Eq/\hbar})$$

$$= \frac{1}{2Q}\sum_p\sum_q e^{-Eq/kT}(e^{-i\tau\omega_{pq}} + e^{-i\tau\omega_{qp}})|ez_{pq}|^2 \tag{89}$$

where $\omega_{pq} = (E_p - E_q)/\hbar$ and E_p and E_q are states of the unperturbed system. On taking the Fourier transform we get

$$(m_\omega^2)_z = \frac{1}{2Q} \sum_p \sum_q e^{-Eq/kT} |ez_{pq}|^2 [\delta(\omega + \omega_{pq}) + \delta(\omega + \omega_{qp})] \quad (90a)$$

which can also be written as

$$(m_\omega^2)_z = \frac{1}{2Q} \sum_p \sum_q (e^{-Ep/kT} + e^{-Eq/kT}) |ez_{pq}|^2 \delta(\omega + \omega_{pq}) \quad (90b)$$

Equation (90b) is obtained from Eq. (90a) by interchanging the indices q and p of the terms pertaining to $\delta(\omega + \omega_{qp})$.

We now proceed to evaluate $\chi''(\omega)$, $\chi'(\omega)$, and $\chi^{(p)}(\sigma_r)$. On combining Eqs. (90) with the Callen and Welton formula [Eq. (52)], we get

$$\chi''(\omega) = \frac{\pi}{hQ} \tanh \frac{\hbar\omega}{2kT} \sum_p \sum_q (e^{-Ep/kT} + e^{-Eq/kT}) |ez_{pq}|^2 \delta(\omega + \omega_{pq}) \quad (91)$$

and by bringing $\tanh h\omega/2kT = (1 - e^{-\hbar\omega/kT})/(1 + e^{-\hbar\omega/kT})$ inside the summand (which requires replacing of ω by ω_{qp}), we get

$$\chi''(\omega) = \frac{\pi}{hQ} \sum_p \sum_q (e^{-Ep/kT} - e^{-Eq/kT}) |ez_{pq}|^2 \delta(\omega + \omega_{pq}) \quad (92)$$

This expression does not include damping, but it is otherwise quite general. The states p and q are discrete, although they can be degenerate. (In case of continuous spectra, the δ function must be replaced by an energy density of states function and the summations must be replaced by integrations.) In practice, it is more convenient to work with energy levels rather than energy states. Let us assume that a given level is characterized by the set of quantum numbers n, n', n'' ... and that the energy is dependent only on the nth quantum number.[30] Transition to another level with quantum numbers m, m', m'' ... is possible only if $n \neq m$. Hence, if we characterize the transition moment by $|ez_{nn'n''...;mm'm''...}|^2$, we can write

$$x''(\omega) = \frac{\pi}{hQ} \sum_{n,n',n''...} \sum_{m,m',m''...} (e^{-En/kT} - e^{-Em/kT}) |ez_{nn'n''...;mm'm''...}|^2$$

$$\times \delta(\omega + \omega_{nm}) = \frac{\pi}{\hbar Q} \sum_n \sum_m (e^{-En/kT} - e^{-Em/kT}) |ez_{n;m}|^2 \delta(\omega + \omega_{nm}) \quad (93)$$

where

$$|ez_{n;m}|^2 = \sum_{n'n''\ldots} \sum_{m'm''\ldots} |ez_{nn'n''\ldots;mm'm''\ldots}|^2 \tag{94}$$

Equation (93) is an odd function of ω; it is positive when $\omega_{nm} < 0$ (or when $n < m$) and negative when $\omega_{nm} > 0$ (or when $n > m$).

The real part of the susceptibility can be obtained at once by application of the Kramers-Konig relation [Eq. (66)] and gives

$$x'(\omega) = \frac{2}{\hbar Q} \mathscr{P} \sum_{\substack{n \\ n<m}} \sum_{m} (e^{-En/kT} - e^{-Em/kT}) \frac{\omega_{mn}|ez_{n;m}|^2}{\omega_{mn}^2 - \omega^2} \tag{95}$$

where $\mathscr{P}$ stands for the principal value when $\omega_{mn} = \omega$. Note that in this expression, the summation is restricted to values of $n < m$. It is sometimes convenient to remove this restriction and this can be accomplished by writing

$$x'(\omega) = \frac{1}{\hbar Q} \mathscr{P} \sum_{n} \sum_{m} (e^{-En/kT} - e^{-Em/kT}) \frac{|ez_{n;m}|^2}{\omega_{mn} - \omega} \tag{96}$$

which is based on the Hilbert transform

$$x'(\omega) = \frac{1}{\pi} \mathscr{P} \int_{-\infty}^{\infty} \frac{x''(y)}{y - \omega} \, dy \tag{97}$$

of which the Kramers-Kronig relation is a special case.

To obtain $\chi^{(p)}(\sigma_r)$ we replace $-\omega^2$ in Eq. (95) by σ_r^2 and substitute the value given by Eq. (62) for σ_r. The result is

$$x^{(p)}(\sigma_r) = \frac{2}{\hbar Q} \sum_{\substack{n \\ n<m}} \sum_{m} (e^{-En/kT} - e^{-Em/kT}) \frac{\omega_{mn}|ez_{n;m}|^2}{\omega_{mn}^2 + (2\pi kT\hbar^{-1}r)^2} \tag{98}$$

This expression must be restricted to positive values of ω_{mn} inasmuch as $\chi^{(p)}(\sigma_r)$ is not defined for negative σ and the Hilbert transform does not apply.

From these expressions one can, in principle, calculate all forms of van der Waals interactions, including the nonadditive potentials. The dispersion potentials are the most difficult to evaluate, inasmuch as detailed knowledge of the electronic states is required and no explicit formula can be given for the susceptibilities associated with electronic transitions. Expressions for the harmonic oscillator susceptibilities can

readily be obtained which (lacking more convenient formulas) could then be used to approximate the dispersion potentials. The susceptibilities associated with rotational motion can be obtained with relative ease, particularly when they are based on a rigid rotor model, and these should describe the electrostatic interaction reasonably well. In the following, we give general expressions for the harmonic oscillator and rigid-rotor susceptibilities.

1. *Harmonic Oscillator*[30,31]

The zeroth-order wave functions for the linear harmonic oscillator are

$$\psi_n^{(0)}(\xi) = C_n e^{-1/2\xi^2} H_n(\xi) \tag{99}$$

where the $H_n(\xi)$ are the Hermite polynomials, $\xi = (\mu_e\omega^0/\hbar)^{(1/2)}z$ in which μ_e is the reduced mass and ω^0 the circular frequency, and

$$C_n = (\mu_e\omega^0/\hbar\pi)^{1/4}(2^n n!)^{-1/2} \qquad n = 0,1 \ldots$$

The matrix elements are

$$z_{n,m} = \sqrt{n\hbar/2\mu_e\omega^0} \qquad \text{if } m = n-1 \text{ and } n \neq 0 \tag{100a}$$

$$= \sqrt{(n+1)\hbar/2\mu_e\omega^0} \qquad \text{if } m = n+1 \tag{100b}$$

$$= 0 \qquad \text{(otherwise)} \tag{100c}$$

and the susceptibilities are

$$x''(\omega) = (\pi e^2/2\mu_e\omega^0)[\delta(\omega-\omega^0) - \delta(\omega+\omega^0)] \tag{101a}$$

$$x'(\omega) = (e^2/\mu_e)\mathcal{P}\{1/[(\omega^0)^2 - \omega^2]\} \tag{101b}$$

$$x^{(p)}(\sigma_r) = (e^2/\mu_e)[(\omega^0)^2 + (2\pi kT\hbar^{-1}r)^2] \tag{101c}$$

2. *Rigid Rotor*[29,30]

The zeroth-order wave functions for the linear rigid rotor are

$$\psi_{jm}^{(0)} = [(2j+1)(j-m)!/4\pi(j+m)!]^{1/2}P_j^{(m)}(\cos\theta)e^{im\phi} \tag{102}$$

where the $P_j^{(m)}(\cos\theta)$ are the associated Legendre functions and m can take on any integral value between $-j$ and j. The matrix elements are

$$z_{jm;j'm'} = [r_0/(2j+3)^{1/2}][(j+1-m)(j+1+m)/(2j+1)]^{1/2}$$
$$\text{if } j' = j+1 \text{ and } m' = m$$
$$= [r_0/(2j-1)^{1/2}][(j-m)(j+m)/(2j+1)]^{1/2}$$
$$\text{if } j' = j-1 \text{ and } m' = m$$
$$= 0 \qquad \text{otherwise} \tag{103}$$

where r_0 is the length of the rotor. These produce the transition moments

$$|ez_{j,j+1}|^2 = \sum_{m=-j}^{j} |ez_{jm;j+1,m}|^2 = \frac{1}{3}\mu^2(j+1) \tag{104}$$

and

$$|ez_{j,j-1}|^2 = \sum_{m=-j}^{j} |ez_{jm;j-1,m}|^2 = \frac{1}{3}\mu^2 j$$

where μ is the dipole moment, $\mu = er_0$. To obtain these results, use is made of the relation

$$\sum_{m=-j}^{j} m^2 = \frac{1}{3}(2j+1)j(j+1) \tag{105}$$

The rigid rotor susceptibilities are

$$x''(\omega) = \frac{\pi\mu^2}{3\hbar Q}\left[\sum_{j=0}^{\infty}(e^{-j(j+1)\hbar\omega^0/kT} - e^{-(j+1)(j+2)\hbar\omega^0/kT}) \times (j+1)\delta(\omega+\omega_{j,j+1}) + \sum_{j=1}^{\infty}(e^{-j(j+1)\hbar\omega^0/kT} - e^{-(j-1)j\hbar\omega^0/kT})j\delta(\omega+\omega_{j,j-1})\right]$$

$$x'(\omega) = \frac{2\mu^2}{3\hbar Q}\mathscr{P}\sum_{j=0}^{\infty}\frac{2(j+1)^2\omega^0(e^{-j(j+1)\hbar\omega^0/kT} - e^{-(j+1)(j+2)\hbar\omega^0/kT})}{[2(j+1)\omega^0]^2 - \omega^2} \tag{106}$$

$$x^{(p)}(\sigma_r) = \frac{2\mu^2}{3\hbar Q}\sum_{j=0}^{\infty}\frac{2(j+1)^2\omega^0(e^{-j(j+1)\hbar\omega^0/kT} - e^{-(j+1)(j+2)\hbar\omega^0/kT})}{[2(j+1)\omega^0]^2 + (2\pi kT\hbar^{-1}r)^2}$$

where $\omega^0 = \hbar/2I$ in which I is the moment of inertia, $\omega_{j,j+1} = -2(j+1)\omega^0$, $\omega_{j,j-1} = 2j\omega^0$, and $Q = \sum_{j=0}^{\infty}(2j+1)e^{-j(j+1)\hbar\omega^0/kT}$. The transition frequency $\omega_{j,j-1}$ is not defined for $j = 0$, since $j = 0$ is the

lowest quantum state, and terms involving $\omega_{j,j-1}$ must be deleted from the summation.

It may be noted that for zero frequency, $\chi(0) = (2\mu^2/3\hbar Q)(2\omega^0)^{-1}$, the classical (high temperature) limit of which is the Debye-Langevin expression

$$\chi(0) = \mu^2/3kT \tag{107}$$

C. Dispersion-, Orientation-, and Induction Forces

In deriving the generalized potentials $\phi^{(2)}$, $\phi^{(3)}$, etc. in Section V-A, we were noncommittal as to the nature of the electrical fluctuations which gave rise to these potentials. It is clear from the discussion in the preceding section that, in general, all types of van der Waals interactions are temperature-dependent. By making reasonable assumptions regarding the nature of the fluctuations, we can greatly simplify the problem and obtain a set of potential functions which, although not exact, are adequate for most ordinary temperatures.

In first approximation, we may consider only two types of fluctuations —those associated with the oscillatory motion of the electrons about the nuclei and those associated with rotational motion of the molecule as a whole. As a rule, the maximum absorption frequencies associated with these motions, peak in vastly different regions of the spectrum. In fact, for most ordinary molecules, the maximum absorption frequency associated with electronic motion is so large compared to kT (i.e., $\hbar\omega \gg kT$) that ordinary room temperature can be regarded as zero temperature; the rotational frequencies, on the other hand, are so low (i.e., $\hbar\omega \ll kT$) that the classical limiting values for the susceptibilities are applicable. Accordingly, we split the susceptibilities into two components,

$$\hat{\chi} = \hat{\alpha} + \hat{\beta} \tag{108}$$

where the α's and β's are, respectively, the high- and low-frequency susceptibilities. (In first approximation, we may take the rigid rotor susceptibilities to represent the β's.) From these we can obtain the three constituents of the van der Waals interactions.

1. *Pair Potentials*

On substituting Eq. (108) into Eq. (73) we get

$$\phi^{(2)}(ik) = -kT \sum_{r=0}^{\infty}{}' \left[\alpha_i^{(p)}(\sigma_r)\alpha_k^{(p)}(\sigma_r) + \alpha_i^{(p)}(\sigma_r)\beta_k^{(p)}(\sigma_r) + \beta_i^{(p)}(\sigma_r)\alpha_k^{(p)}(\sigma_r) + \beta_i^{(p)}(\sigma_r)\beta_k^{(p)}(\sigma_r)\right] \operatorname{tr} \mathbf{T}_{ik}^{2(p)}(\sigma_r) \tag{109}$$

By taking the classical limit for $\beta(\sigma_r)$, i.e., $\beta(\sigma_r) \to \beta(0) = \mu^2/3kT$, we obtain

$$\phi^{(2)}(ik) = \phi^{(2)}_{\text{dis}}(ik) + \phi^{(2)}_{\text{or}}(ik) + \phi^{(2)}_{\text{ind}}(r_{ik})$$

where

$$\phi^{(2)}_{\text{dis}}(ik) = -kT \sum_{r=0}^{\infty}{}' \alpha_i^{(p)}(\sigma_r)\alpha_k^{(p)}(\sigma_r) \operatorname{tr} \mathbf{T}^{2(p)}_{ik}(\sigma_r) \tag{110}$$

and, if retardation is neglected,

$$\phi^{(2)}_{\text{dis}}(ik) = -\frac{6\hbar}{\pi^2 r_{ik}^6} \int_0^\infty \int_0^\infty \frac{\alpha_i''(\omega_i)\alpha_k''(\omega_k)}{\omega_i + \omega_k} d\omega_i d\omega_k \tag{111}$$

$$\begin{aligned} \phi^{(2)}_{\text{or}}(ik) &= -\frac{1}{2} kT\beta_i(0)\beta_k(0) \operatorname{tr} \mathbf{T}^2_{ik} \\ &= -\frac{\mu_i^2\mu_k^2}{3kTr_{ik}^6} \end{aligned} \tag{112}$$

and

$$\begin{aligned} \phi^{(2)}_{\text{ind}}(ik) &= -\frac{1}{2} kT\{\alpha_i(0)\beta_k(0) + \beta_i(0)\alpha_k(0)\} \operatorname{tr} \mathbf{T}^2_{ik} \\ &= -\frac{\alpha_i(0)\mu_k^2 + \alpha_k(0)\mu_i^2}{r_{ik}^6} \end{aligned} \tag{113}$$

Equations (111), (112), and (113) are equivalent to the dispersion-, orientation-, and induction potentials of London,[3] Keesom,[1] and Falkenhagen,[2] respectively. We wish to emphasize that the potentials given here are free energies of interaction and not energies (in the statistical sense, i.e., the interaction Hamiltonian averaged over all electronic and rotational coordinates for fixed internuclear separations). The interaction energies can be obtained by differentiating the functions (ϕ/T), in accordance with the Gibbs-Helmholtz equation,

$$\varepsilon(T) = \frac{\partial(\phi/T)}{\partial(1/T)}$$

Accordingly,

$$\varepsilon(T) = -2\mu_i^2\mu_k^2/3kTr_{ik}^6 \tag{114}$$

which is often taken as the definition of the Keesom potential. The distinction between energy and free energy does not arise when the potentials are temperature independent.

Equation (111) can be written also as a sum over discrete states. According to Eq. (93), the polarizability of spherical molecules in the ground state at zero degrees is

$$\alpha''(\omega) = (\pi/3\hbar)|\mu_{om}|^2\delta(\omega + \omega_{om}) \tag{115}$$

where $|\mu_{om}|^2 = 3|ez_{om}|^2$. On substituting this expression into Eq. (111), and after integrating out the δ functions, we get

$$\phi^{(2)}_{\text{dis}}(ik) = -\frac{2}{3\hbar r_{ik}^6} \sum_{n} \sum_{\substack{m \\ \neq 0}} \frac{|\mu^{(i)}_{om}|^2 |\mu^{(k)}_{on}|^2}{\omega^{(i)}_{mo} + \omega^{(k)}_{no}} \tag{116}$$

For harmonic oscillators [see Eq. (101)], the ground-state transition moment is

$$|\mu_{01}|^2 = \frac{3}{2}\frac{e^2\hbar}{\mu_e\omega^0} = \frac{3}{2}\hbar\omega^0\alpha(0),$$

whence

$$\phi^{(2)}_{\text{dis}}(ik) = -\frac{3}{2}\frac{\hbar}{r_{ik}^6}\frac{\omega_i^0\omega_k^0}{\omega_i^0 + \omega_k^0}\alpha_i(0)\alpha_k(0) \tag{117}$$

where ω_i^0 and ω_k^0 are the natural frequencies of i and k, respectively.

2. *Triple Potentials*

Decomposition of the general triple potential [Eq. (74)] proceeds in exactly the same fashion and yields[27]

$$\phi^{(3)}(ikl) = \phi^{(3)}_{\text{dis}}(ikl) + \phi^{(3)}_{\text{or}}(ikl) + \phi^{(3)}_{\text{ind}}(ikl)$$

where (neglecting retardation)

$$\phi^{(3)}_{\text{dis}}(ikl) = \frac{4\hbar}{\pi^3}\,\text{tr}\,\mathbf{T}^3_{ikl}\int_0^\infty\int_0^\infty\int_0^\infty \frac{(\omega_i + \omega_k + \omega_l)\alpha_i''(\omega_i)\alpha_k''(\omega_k)\alpha_l''(\omega_l)}{(\omega_i + \omega_k)(\omega_k + \omega_l)(\omega_l + \omega_i)} \times d\omega_i d\omega_k d\omega_l \tag{118}$$

$$\phi^{(3)}_{\text{or}}(ikl) = \frac{1}{3}[\mu_i^2\mu_k^2\mu_l^2/(3kT)^2]\,\text{tr}\,\mathbf{T}^3_{ikl} \tag{119}$$

and

$$\phi^{(3)}_{\text{ind}}(ikl) = \frac{1}{3}\,\text{tr}\,\mathbf{T}^3_{ikl}[\alpha_i(0)\alpha_k(0)\mu_l^2 + \alpha_i(0)\alpha_l(0)\mu_k^2 + \alpha_k(0)\alpha_l(0)\mu_i^2 + (3kT)^{-1}(\alpha_i(0)\mu_k^2\mu_l^2 + \alpha_k(0)\mu_i^2\mu_k^2 + \alpha_l(0)\mu_i^2\mu_k^2)] \quad (120)$$

The dispersion potential can be put in the form

$$\phi^{(3)}_{\text{dis}}(ikl) = \frac{4}{27\hbar^2}\,\text{tr}\,\mathbf{T}^3_{ikl}\sum_n \sum_{\substack{m \\ \neq 0}} \sum_l \frac{(\omega^{(i)}_{no} + \omega^{(k)}_{mo} + \omega^{(l)}_{po})|\mu^{(i)}_{on}|^2|\mu^{(k)}_{om}|^2|\mu^{(l)}_{op}|^2}{(\omega^{(i)}_{no} + \omega^{(k)}_{mo})(\omega^{(k)}_{mo} + \omega^{(l)}_{po})(\omega^{(l)}_{po} + \omega^{(i)}_{no})} \quad (121)$$

by substitution of Eq. (115). A particularly simple expression is obtained for harmonic oscillators,

$$\phi^{(3)}_{\text{dis}}(ikl) = \frac{\hbar}{2}\,\text{tr}\,\mathbf{T}^3_{ikl}\,\frac{(\omega_i^0 + \omega_k^0 + \omega_l^0)\omega_i^0\omega_k^0\omega_l^0\alpha_i(0)\alpha_k(0)\alpha_l(0)}{(\omega_i^0 + \omega_k^0)(\omega_k^0 + \omega_l^0)(\omega_l^0 + \omega_i^0)} \quad (122)$$

which, for identical particles, reduces to the well-known expression of Axilrod and Teller[6], upon substitution of Eq. (80); i.e.,

$$\phi^{(3)}_{\text{dis}}(ikl) = \frac{9}{16}[\hbar\omega^0\alpha(0)^3(1 + 3\cos\theta_i\cos\theta_k\cos\theta_l)/r^3_{ik}r^3_{kl}r^3_{li}] \quad (123)$$

VI. FORCES IN DENSE MEDIA

From the molecular formulation of the preceding section one could, in principle, develop distribution functions and thus obtain the bulk properties of the macroscopic system by standard statistical mechanical procedure. The mathematical complexities are so great, however, that this approach is not feasible except in very simple cases. This is true even if the potentials can be determined accurately either from experimental data or theoretically. The main difficulty comes about in computing the average values of the T" tensors. The same types of averages also appear in the virial expansion of the dielectric constant and it is natural to seek a formulation in terms of the macroscopic dielectric constant in the hope of circumventing some of these computational difficulties. The continuum-model treatment accomplishes this in an approximate way, but there are serious objections to this model—especially when applied to ordinary fluids where statistical fluctuations are prominent. In Section A we present a general outline based on the molecular

approach. In Section B-I, we discuss the thermodynamic properties on the basis of the continuum model with special reference to systems involving very large dissolved molecules. In Section B-2, we present a statistical formulation of the average reaction-field response function for a simplified model and define a cavity radius which, in an approximate way, incorporates the effects of statistical fluctuations.

A. Molecular Formulation

The potential functions considered so far represent only the long-range part of interaction and are not valid at close distances where there is appreciable overlap. Before we can relate the potential functions to the thermodynamic properties, we must specify their range of validity and, for the purpose of the present discussion, we shall assume that for distances less than d_0 ($\sim$the molecular diameter), the potentials are infinitely repulsive; for distances greater than d_0, the formulas developed in the preceding sections are assumed to hold.

Up to this point, we have considered only potential functions at fixed internuclear separations. In order to proceed, we must average over all configurations. The fact that the potentials $\phi^{(2)}$, $\phi^{(3)}$, etc. arise from preliminary averaging over the electronic and rotational coordinates, causes some complications when additional averaging over the q coordinates is imposed. However, by limiting our discussion to the quantal forms of the dispersion interaction and the classical forms of the electrostatic interaction, we can largely avoid these difficulties, which are of a formal nature.

We first consider the dispersion forces. Let $U_{\text{dis}}(\mathbf{r}_1 \ldots \mathbf{r}_N)$ denote the overall dispersion potential of all N molecules combined, i.e.,

$$U_{\text{dis}}(\mathbf{r}_1 \cdots \mathbf{r}_N) = \sum_{i<k} \sum_{k} \phi^{(2)}_{\text{dis}}(ik) + \sum_{i<k} \sum_{k<l} \sum_{l} \phi^{(3)}_{\text{dis}}(ikl) + \cdots \quad (124)$$

where $\phi^{(2)}_{\text{dis}}(ik)$, $\phi^{(3)}_{\text{dis}}(ikl)$, etc. are the $T = 0$ limiting forms of the dispersion potentials given by Eqs. (111) and (118). It is convenient to write

$$U_{\text{dis}}(\mathbf{r}_1 \cdots \mathbf{r}_N) = \phi^{\text{dis}}_{i;S}(q) + \gamma(q) \quad (125)$$

where $\phi_{i;S}$ is the interaction potential of i with all other molecules (the generalized potential!), i.e.,

$$\phi^{\text{dis}}_{i;S}(q) = \sum_{k} \phi^{(2)}_{\text{dis}}(ik) + \sum_{k<l} \phi^{(3)}_{\text{dis}}(ikl) + \cdots \quad (126)$$

and γ is the remainder, i.e.,

$$\gamma(q) = \sum_{\substack{k<l \\ \neq i}} \phi^{(2)}_{\text{dis}}(kl) + \sum_{\substack{k<l<m \\ \neq i}} \phi^{(3)}_{\text{dis}}(klm) + \cdots \tag{127}$$

Recall that in Section II, the chemical potential was obtained by integrating the expression $\Phi^{(R)}(|e_i'|)d|e_i'|$ where $\Phi^{(R)}(|e_i'|)$ was the reaction potential at i for the fractional dipolar charge $|e_i'|$. [We shall henceforth suppress the bars on $|e_i'|$ and denote the reaction potential simply as $\Phi^{(R)}(e_i')$]. As stated before and as shown in the following, the proper value of $\Phi^{(R)}(e_i')$, which is mentioned in the discussion of the chemical potential, is one which has been averaged over all configurations. This is automatically satisfied in the continuum model which is expressed in terms of the macroscopic dielectric constant (and thus implies preliminary averaging); but for an arbitrary distribution, **R** and therefore $\Phi^{(R)}$ are q-dependent, and $\Phi^{(R)}$ has to be averaged first over the q coordinates. Denoting the average value of the reaction potential at i as $\langle \Phi_i^{(R)}(e_i') \rangle_q$, we have in general

$$\mu_{i;\text{ex}} = \int_0^{e_i} \langle \Phi_i^{(R)}(e_i') \rangle_q de_i' \tag{128}$$

where $\mu_{i;\text{ex}}$ is the excess chemical potential of i.

In order to obtain an explicit expression for $\langle \Phi_i^{(R)}(e_i') \rangle_q$, we suppose that the ith molecule has the fractional charge e_i' and that all other molecules have their full dipolar charges e_k, e_l, etc. Thus, if we write

$$U_{\text{dis}}(\mathbf{r}_1 \cdots \mathbf{r}_N; e_i') = \phi^{\text{dis}}_{i;S}(q; e_i') + \gamma(q) \tag{129}$$

as a variable function of e_i' (with all other e_k, e_l, etc. being fixed), we can construct the partition function

$$Z(e_i') = \int \cdots \int \exp[-U_{\text{dis}}(\mathbf{r}_1 \cdots \mathbf{r}_N; e_i')/kT] d\mathbf{r}_1 \cdots d\mathbf{r}_N \tag{130}$$

and calculate

$$\left\langle \frac{\partial U_{\text{dis}}(e_i')}{\partial e_i'} \right\rangle_q = \frac{\int \cdots \int \dfrac{\partial U_{\text{dis}}(e_i')}{\partial e_i'} e^{-U_{\text{dis}}(e_i')/kT} d\mathbf{r}_1 \cdots d\mathbf{r}_N}{Z(e_i')} \tag{131}$$

This expression represents the increase in the interaction energy (averaged over all configurations) of the system per unit increase in dipolar charge

at the location of i and this defines the reaction potential at i. We therefore write

$$\langle \Phi^{(R)}_{i;\mathrm{dis}}(e_i') \rangle_q = \left\langle \frac{\partial U_{\mathrm{dis}}(e_i')}{\partial e_i'} \right\rangle_q \tag{132}$$

which, by virtue of Eq. (129), reduces to

$$\langle \Phi^{(R)}_{i;\mathrm{dis}}(e_i') \rangle_q = \left\langle \frac{\partial \phi^{\mathrm{dis}}_{i;S}(e_i')}{\partial e_i'} \right\rangle_q \tag{133}$$

The chemical potential associated with the dispersion forces is then

$$\mu_{i;\mathrm{dis}} = \int_0^{e_i} \langle \Phi^{(R)}_{i;\mathrm{dis}}(e_i') \rangle_q de_i'$$

$$= \int_0^{e_i} de_i' \frac{\int \cdots \int \dfrac{\partial \phi^{\mathrm{dis}}_{i;S}(e_i')}{\partial e_i'} e^{-U_{\mathrm{dis}}(e_i')/kT} d\mathbf{r}_1 \cdots d\mathbf{r}_N}{Z(e_i')} \tag{134}$$

This expression can be put in a more familiar form. It may be noted that all the potentials $\phi^{(2)}(e_i')$, $\phi^{(3)}(e_i')$, etc. vary as $e_i'^2$. Hence, if we introduce the variable $\xi_i = e_i'^2/e_i^2$, where e_i is the true charge of i, we can write $\phi^{\mathrm{dis}}_{i;S}(e_i') = \xi_i \phi^{\mathrm{dis}}_{i;S}$ where $\phi^{\mathrm{dis}}_{i;S}$ is independent of any variable charging parameter. Instead of Eq. (129), we then have

$$U_{\mathrm{dis}}(\mathbf{r}_1 \cdots \mathbf{r}_N;\xi_i) = \xi_i \phi^{\mathrm{dis}}_{i;S}(q) + \gamma(q) \tag{135}$$

and Eq. (134) reduces to

$$\mu_{i;\mathrm{dis}} = \int_0^1 d\xi_i \frac{\int \cdots \int \phi^{\mathrm{dis}}_{i;S}(q) \exp[-U_{\mathrm{dis}}(\mathbf{r}_1 \cdots \mathbf{r}_N;\xi_i)/kT] d\mathbf{r}_1 \cdots d\mathbf{r}_N}{\int \cdots \int \exp[-U_{\mathrm{dis}}(\mathbf{r}_1 \cdots \mathbf{r}_N;\xi_i)/kT] d\mathbf{r}_1 \cdots d\mathbf{r}_N} \tag{136}$$

This is the standard form for the chemical potential and can be derived on the basis of coupling parameters without recourse to any (reaction or other) potential.[56] Equation (136) also contains the nonadditive potentials which are usually ignored.

We now introduce the set of distribution functions $\rho^{(n)}_{\mathrm{dis}}(\mathbf{r}_1 \cdots \mathbf{r}_n;\xi_i)$ defined by

$$\rho^{(n)}_{\mathrm{dis}}(\mathbf{r}_1 \cdots \mathbf{r}_n;\xi_i) = \exp[-\psi(\mathbf{r}_1 \cdots \mathbf{r}_n;\xi_i)/kT]$$

$$= \frac{V^n \int \cdots \int \exp[-U_{\mathrm{dis}}(\mathbf{r}_1 \cdots \mathbf{r}_N;\xi_i)/kT] d\mathbf{r}_{n+1} \cdots d\mathbf{r}_N}{\int \cdots \int \exp[-U_{\mathrm{dis}}(\mathbf{r}_1 \cdots \mathbf{r}_N;\xi_i)/kT] d\mathbf{r}_1 \cdots d\mathbf{r}_N} \tag{137}$$

where $\psi(\mathbf{r}_1 \cdots \mathbf{r}_n;\xi_i)$ is the potential of mean force acting on the group

of n molecules and V is the volume of the system. The distribution functions depend on the vector distances between the particles but for fluids, they depend only on the scalar magnitudes r_{il}, r_{ik}, r_{kl}, etc. Hence, if we take all coordinates relative to the ith coordinate and assume, for simplicity, that all particles are identical, we have

$$\mu_{\text{dis}} = \int_0^1 d\xi_i \left[\frac{N}{V} \int \phi_{\text{dis}}^{(2)}(r_{ik}) \rho_{\text{dis}}^{(2)}(r_{ik};\xi_i) d\mathbf{r}_{ki} + \frac{N^2}{2V^2} \iint \phi_{\text{dis}}^{(3)}(r_{ik}, r_{kl}, r_{li}) \rho_{\text{dis}}^{(3)}(r_{ik}, r_{kl}, r_{li};\xi_i) d\mathbf{r}_{ki} d\mathbf{r}_{li} + \cdots \right] \quad (138)$$

For a uniform distribution (as in the continuum model), the weighting functions drop out (that is, all $\rho^{(n)} = 1$ for $r_{ik} \geq d_0$) and $\mu_{\text{dis}} = \langle \phi_{i;S}^{\text{dis}}(q) \rangle_q^0$ where $\langle \phi_{i;S}^{\text{dis}}(q) \rangle_q^0$ is the nonweighted average of the generalized dispersion potential.

We now turn to the electrostatic interaction. In principle, the chemical potential is obtained in the same manner, namely, by integrating the average reaction potential over the fractional charge or coupling parameter of the ith molecule. Because of the extreme rapidity of the motion of the electrons in comparison with rotational and translational motion of the molecule as a whole, the dispersion force field is established instantaneously and is also the predominant factor in weighting the average distances r_{ik}, r_{kl}, etc. in the electrostatic potentials. Accordingly, in a first approximation

$$\mu_{\text{el}} = \frac{N}{V} \int \phi_{\text{el}}^{(2)}(r_{ik}) \rho_{\text{dis}}^{(2)}(r_{ik}) d\mathbf{r}_{ki} + \frac{N^2}{2V^2} \iint \phi_{\text{el}}^{(3)}(r_{ik}, r_{kl}, r_{li}) \rho_{\text{dis}}^{(3)}(r_{ik}, r_{kl}, r_{li}) d\mathbf{r}_{ki} d\mathbf{r}_{li} \quad (139)$$

where $\phi_{\text{el}}^{(n)} = \phi_{\text{or}}^{(n)} + \phi_{\text{ind}}^{(n)}$ and the distribution functions are defined for fully coupled values of ξ_i, i.e., $\xi_i = 1$.

To elaborate further on this point, let us consider the following specific example whereby the dispersion force field (fully established) is augmented by the orientation interaction. A quantum mechanical treatment leads to unnecessary complications and we shall confine our discussion to a classical calculation. Let $\mathscr{H}'_{\text{rot}}(ik)$ represent the interaction Hamiltonian between two permanent dipoles. For example, if r_{ik} is along the Z axis, then

$$\mathscr{H}'_{\text{rot}}(ik) = -(\mu_i \mu_k / r_{ik}^3)[2 \cos\theta_i \cos\theta_k - \sin\theta_i \sin\theta_k \cos(\phi_k - \phi_i)]$$

To obtain the orientation part of the chemical potential, $\mu_{i;\text{or}}$, we let the charge of the ith permanent moment, e'_i, increase from 0 to its full value, e_i, while holding all other charges fixed—or, equivalently—we take $\mathscr{H}'_{\text{rot}}(il;e'_i) = \eta_i \mathscr{H}'_{\text{rot}}(il)$, where $\mathscr{H}'_{\text{rot}}(il)$ is the fully coupled value of the interaction Hamiltonian and $\eta_i = e'_i/e_i$. (Note that the dipole moment μ_i is linearly dependent on the charge.) We next introduce the quantity

$$\Upsilon_{\text{rot}}(\eta_i) = \eta_i \sum_{l=1} \mathscr{H}'_{\text{rot}}(il) + \sum_{\substack{l<k \\ \neq i}} \sum \mathscr{H}'_{\text{rot}}(lk) \tag{140}$$

and, using the same arguments which led to the formulation of $\mu_{i;\text{dis}}$, we find that

$$\mu_{i;\text{or}} = \int_0^1 d\eta_i \times \frac{\int \cdots \int \sum_{l=1} \mathscr{H}'_{\text{rot}}(il) \exp[-U_{\text{dis}}/kT] \exp[-\Upsilon_{\text{rot}}(\eta_i)/kT] d\Omega d\mathbf{r}_1 \cdots d\mathbf{r}_N}{\int \cdots \int \exp[-U_{\text{dis}}/kT] \exp[-\Upsilon_{\text{rot}}(\eta_i)/kT] d\Omega d\mathbf{r}_1 \cdots d\mathbf{r}_N} \tag{141}$$

where U_{dis} is the total dispersion energy for fully coupled values of ξ_i, i.e., $\xi_i = 1$, and Ω denotes the angular coordinates of the dipole moments. If we expand $\exp[-\Upsilon_{\text{rot}}(\eta_i)/kT]$ and keep only the linear terms, we get

$$\mu_{i;\text{or}} = \int_0^1 d\eta_i \times \frac{\int \cdots \int \sum_{l=1} \mathscr{H}'_{\text{rot}}(il) \exp[-U_{\text{dis}}/kT](1 - \Upsilon_{\text{rot}}(\eta_i)/kT) d\Omega d\mathbf{r}_1 \cdots d\mathbf{r}_N}{\int \cdots \int \exp[-U_{\text{dis}}/kT](1 - \Upsilon_{\text{rot}}(\eta_i)/kT) d\Omega d\mathbf{r}_1 \cdots d\mathbf{r}_N} \tag{142}$$

It is easy to see that $\mathscr{H}'_{\text{rot}}(il)$ when averaged over the angular coordinates is zero, whence Eq. (142) gives, in first approximation,

$$\mu_{i;\text{or}} = -\frac{1}{2kT} \frac{\int \cdots \int \exp[-U_{\text{dis}}/kT] \sum_{l=1} \langle \mathscr{H}'^2_{\text{rot}}(il) \rangle_{\text{ang}} d\mathbf{r}_1 \ldots d\mathbf{r}_N}{\int \cdots \int \exp[-U_{\text{dis}}/kT] d\mathbf{r}_1 \cdots d\mathbf{r}_N} \tag{143}$$

where $\langle \mathscr{H}'^2_{\text{rot}}(il)\rangle_{\text{ang}}$ is the square of the interaction Hamiltonian averaged over the angular coordinates. It can be shown[57] that

$$-\frac{\langle \mathscr{H}'^2_{\text{rot}}(il)\rangle_{\text{ang}}}{2kT} = -\frac{\mu_i^2\mu_l^2}{3kTr_{il}^6} \tag{144}$$

which is just $\phi^{(2)}_{\text{or}}(il)$. Accordingly, for identical particles Eq. (143) yields

$$\mu_{\text{or}} = \frac{N}{V}\int \phi^{(2)}_{\text{or}}(il)\rho^{(2)}_{\text{dis}}(r_{il})d\mathbf{r}_{li} \tag{145}$$

in harmony with Eq. (139).

B. Dielectric Formulation

1. *The Continuum Model*

In this section, we treat the forces of interaction on the basis of the continuum model. To be explicit, we shall assume that the dissolved molecule is so large that translational fluctuations are of minor importance and that it is permissible to replace the surrounding dielectric by the macroscopic dielectric constant. Accordingly, the potential $\phi_{i;S}$ is independent of the configuration q and on the basis of Eq. (63), we have for an isotropic fluid

$$\phi_{i;S} = -3kT\sum_{r=0}^{\infty}{}' \chi_i^{(p)}(\sigma_r)g^{(p)}(\sigma_r) \tag{146}$$

If we assume, as before, that both susceptibilities, χ_i and g, exhibit two widely separated regions of strong absorption, namely, $\hat{\chi}_i(\omega) = \hat{\alpha}_i(\omega) + \hat{\beta}_i(\omega)$ and $\hat{g}(\omega) = \hat{g}_\alpha(\omega) + \hat{g}_\beta(\omega)$ where the α components are the high-frequency ($\hbar\omega > kT$) and the β components the low-frequency ($\hbar\omega \ll kT$) components associated with electronic and rotational motion, respectively, we get the following simplification,

$$\phi_{i;S} = -\frac{3}{2}kT[\beta_i(0)g_\beta(0) + \alpha_i(0)g_\beta(0) + \beta_i(0)g_\alpha(0)] - \frac{3\hbar}{2\pi}\int_0^\infty \alpha_i^{(p)}(\sigma)g_\alpha^{(p)}(\sigma)d\sigma \tag{147}$$

The first term represents the orientation interaction; the two middle

terms are the induction potentials; the last term is the dispersion potential, which generally includes retardation effects.

To achieve further simplification, we shall take $\beta_i(0) = \mu_i^2/3kT$ and replace the high-frequency dielectric constant appearing in g_α by the refractive index of the medium, i.e.,

$$\hat{g}_\alpha(\omega) = \frac{2\hat{n}^2(\omega) - 2}{2\hat{n}^2(\omega) + 1} \frac{1}{a^3} \tag{148a}$$

and

$$\hat{g}_\beta(\omega) = \frac{1}{a^3}\left[\frac{2\hat{\varepsilon}(\omega) - 2}{2\hat{\varepsilon}(\omega) + 1} - \frac{2\hat{n}^2(\omega) - 2}{2\hat{n}^2(\omega) + 1}\right] \tag{148b}$$

Equation (147) then reduces to

$$\phi_{i;S} = -\frac{\mu_i^2}{2}\frac{2\varepsilon(0) - 2}{2\varepsilon(0) + 1}\frac{1}{a^3} - 9\frac{kT\alpha_i(0)}{a^3}\frac{\varepsilon(0) - n_\infty^2}{(2\varepsilon(0) + 1)(2n_\infty^2 + 1)} - \frac{3\hbar}{2\pi}\int_0^\infty \alpha_i^{(p)}(\sigma)\frac{2n^{2(p)}(\sigma) - 2}{2n^{2(p)}(\sigma) + 1}\frac{1}{a^3}\,d\sigma \tag{149}$$

where $\varepsilon(0)$ is the static dielectric constant and n_∞ is the refractive index extrapolated to infinite wavelength; $n^{(p)}(\sigma)$ is the refractive index along the σ axis. Note that the first term is identical with the work function obtained on the basis of the static reaction field. Evidently, this term includes the rotational interaction and part of the induction interaction, namely, the polarization of the medium by the permanent moment of i. The middle term, which is also part of the electrostatic interaction, is the interaction which results from the induction of i by the permanent moments in the surroundings.

The last term—the dispersion term—can be further simplified to yield

$$\phi_{i;S}^{\text{dis}} = -\frac{3\hbar}{\pi^2}\int_0^\infty \int_0^\infty \frac{\alpha_i''(\omega)g_\alpha''(\omega_s)}{\omega_i + \omega_s}\,d\omega_i d\omega_s \tag{150}$$

If we further assume that α_i'' and g_α'' are strongly peaked only at the effective frequencies ω_i^0 and ω_s^0, respectively—a poor assumption in general, particularly, in a many-body system—we obtain

$$\phi_{i;S}^{\text{dis}} = -\frac{3}{4}\hbar[\omega_i^0\omega_s^0/(\omega_i^0 + \omega_s^0)]\alpha_i(0)g_\alpha(0) \tag{151a}$$

which, for identical absorption frequencies, $\omega_i^0 = \omega_s^0 = \omega^0$, reduces to

$$\phi_{i;S}^{\text{dis}} = -\frac{3}{8}\hbar\omega^0\alpha_i(0)[(2n_\infty^2 - 2)/(2n_\infty^2 + 1)](1/a^3) \qquad (151b)$$

It may be noted that for the continuum model (uniform distribution) $\phi_{i;S}^{\text{dis}} = \mu_{\text{dis}}$. Accordingly, for a system of like particles, the molar free energy associated with the dispersion force field is

$$\tilde{F}_{\text{dis}} = \int_0^{N_0} \mu_{\text{dis}} dN = -\frac{3}{8}\hbar\omega^0\alpha(0)\int_0^{N_0} g_\alpha(0)dN \qquad (152a)$$

where N_0 is Avogadro's number. The susceptibility $g_\alpha(0)$ is in first approximation linearly dependent on the density and, therefore, also on N. Hence, if we write g_α as a function of N, i, g, $g_\alpha(0;N)$, we obtain

$$\tilde{F}_{\text{dis}} \approx -\frac{3}{16} N_0\hbar\omega^0\alpha(0)g_\alpha(0;N_0) \qquad (152b)$$

or

$$\tilde{F}_{\text{dis}} \approx -\frac{1}{8} N_0\langle m^2\rangle g_\alpha(0;N_0) \qquad (152c)$$

where $\langle m^2\rangle$ is the mean square fluctuation of the electronic oscillations in a molecule,[32,33] i.e., $\langle m^2\rangle = \frac{3}{2}\hbar\omega^0\alpha(0)$.

2. *The Cavity Concept*

In Section VI-A, we discussed a general scheme for evaluating the thermodynamic functions from the generalized potentials $\phi_{i;S}(q)$. To a good approximation, this function, averaged over all configuration space, is given by

$$\langle\phi_{i;S}(q)\rangle_q = -\frac{\hbar}{2\pi} Re\int_0^\infty \hat{\chi}_i(\omega)\,\text{tr}\,\langle\hat{\mathbf{g}}(q,\omega)\rangle_q \coth\frac{\hbar\omega}{2kT}\, id\omega \qquad (153)$$

which entails averaging over the $\mathbf{T}^n$ tensors. The evaluation of tr $\hat{\mathbf{g}}$ (ω,q) presents a major obstacle in obtaining the thermodynamic properties from first principles. However, the same types of averages also appear in the statistical formulation of the dielectric constant and it is natural to seek a formulation in terms of the dielectric properties of the medium in the hope of circumventing some of the computational difficulties.

The continuum-model treatment aims to accomplish this in an approximate way. In this section, we examine the statistical formulation of the dielectric constant in some detail and define a cavity radius in terms of more fundamental concepts. It is shown that by properly choosing a^3, it is possible to obtain a reaction field within the framework of the continuum model which is in reasonably good agreement with statistically calculated fields. The theory has been worked out only for nonpolar substances in a dc field,[59] although the extension to more complicated situations is apparent from the general discussion.

In the Onsager theory of polarization,[40] the local field $\mathbf{F}$ acting on a molecule i is formally decomposed into two components: the cavity field, $\mathbf{G}$, which is the homogeneous field inside the empty cavity in the presence of an external field, and the reaction field, $\mathbf{R}$, which is the field due to the polarization of the surroundings by the moment, $\mathbf{p}_i$. The cavity and reaction fields are, respectively,

$$\mathbf{G} = [3\varepsilon/(2\varepsilon + 1)]\mathbf{E} \equiv f\mathbf{E} \tag{154}$$

$$\mathbf{R} = [(2\varepsilon - 2)/(2\varepsilon + 1)](\mathbf{p}_i/a^3) \equiv g\mathbf{p}_i \tag{155}$$

and the local-field vector is

$$\mathbf{F} = \mathbf{R} + \mathbf{G} \tag{156}$$

In the present context, $\mathbf{p}_i$ is the moment induced by the applied field $\mathbf{E}$ and, in fact, can be related to the local field

$$\mathbf{p}_i = \alpha\mathbf{F} = \alpha(\mathbf{G} + \mathbf{R}) = \alpha f\mathbf{E}/(1 - \alpha g) \tag{157}$$

If this result is combined with the basic relations

$$\mathbf{P} = \sum \mathbf{p}_i/V = [N\alpha f/(1 - \alpha g)]\mathbf{E}/V \tag{158}$$

and

$$(\varepsilon - 1)/4\pi = P/E \tag{159}$$

the Böttcher-Onsager formula is obtained

$$\frac{(\varepsilon - 1)(2\varepsilon + 1)}{9\varepsilon} = \frac{(4\pi/3)(N\alpha/V)}{1 - (\alpha/a^3)[(2\varepsilon - 2)/(2\varepsilon + 1)]} \tag{160}$$

This expression reduces to the Clausiuss-Mossotti formula,

$$(\varepsilon - 1)/(\varepsilon + 2) = (4\pi/3)(N\alpha/V) \tag{161}$$

on setting $(4\pi/3)Na^3$ equal to V (the Onsager approximation).

The foregoing field equations are based on macroscopic theory and will be referred to as the dielectric formulation of the field quantities. We now proceed to develop expressions for their statistical analogs. Following Kirkwood,[58] we consider a dielectric slab placed between two parallel condenser plates. The local field acting as the ith molecule is

$$\mathbf{F}_i(q) = \left[\mathbf{I} - \alpha \sum_k \mathbf{T}_{ik} + \alpha^2 \sum_k \mathbf{T}_{ik} \cdot \mathbf{T}_{ki} + \alpha^2 \sum_k \sum_{\substack{l \\ \neq i}} \mathbf{T}_{ik} \cdot \mathbf{T}_{kl} + \cdots\right] \cdot \mathbf{D} \tag{162}$$

where $\mathbf{D}$ is the displacement vector. The reaction field acting on i is taken to be

$$\begin{aligned} \mathbf{R}_i(q) &= \left[\alpha \sum_k \mathbf{T}_{ik} \cdot \mathbf{T}_{ki} - \alpha^2 \sum_{k,l} \mathbf{T}_{ik} \cdot \mathbf{T}_{kl} \cdot \mathbf{T}_{li} + \cdots\right] \cdot \mathbf{p}_i \\ &= \mathbf{g}(q) \cdot \mathbf{p}_i \end{aligned} \tag{163}$$

This expression is identical in form with Eq. (38) except that $\mathbf{p}_i$ here is the moment of i in the presence of the applied field, $\mathbf{E}$. The cavity field is obtained by subtracting $\mathbf{R}_i(q)$ from $\mathbf{F}_i(q)$, i.e., $\mathbf{G}_i(q) = \mathbf{F}_i(q) - \mathbf{g}(q) \cdot \mathbf{p}_i$.

The field vectors discussed so far pertain to a particular configuration, q. Before we can relate the response functions to the dielectric constants, we must average over all configurations and express the cavity field as a function of $\mathbf{E}$ rather than $\mathbf{D}$. Thus, if we let $\langle\ \rangle_q$ denote the average over all configuration space, we obtain

$$\langle \mathbf{F}(q) \rangle_q = [\mathbf{I} - \alpha N \langle \mathbf{T}_{ik} \rangle + \alpha^2 N \langle \mathbf{T}_{ik} \cdot \mathbf{T}_{ki} \rangle + \alpha^2 N^2 \langle \mathbf{T}_{ik} \cdot \mathbf{T}_{kl} \rangle + \cdots] \cdot \mathbf{D} \tag{164}$$

We next introduce the dimensionless quantity

$$\theta = (4\pi/3)(N\alpha/V) \tag{165}$$

and rewrite the basic relations

$$\mathbf{D} = \mathbf{E} + 4\pi\mathbf{P}$$

and

$$\mathbf{P}V = N\langle \mathbf{p} \rangle = N\alpha \langle \mathbf{F}(q) \rangle_q \tag{166}$$

in the form

$$\mathbf{D} = \mathbf{E} \Big/ \left(1 - 3\theta \frac{|\langle \mathbf{F}(q) \rangle_q|}{|\mathbf{D}|}\right)$$

(It should be pointed out that $\langle \mathbf{F}(q) \rangle_q$ and $\mathbf{D}$ have the same direction.[59]) Accordingly, Eq. (164) can be written as (see ref. 59)

$$\langle \mathbf{F}(q) \rangle_q = \langle \mathbf{G}(q) \rangle_q + \langle \mathbf{R}(q) \rangle_q$$

where

$$\langle \mathbf{G}(q) \rangle_q = [\mathbf{I} - \alpha N \langle \mathbf{T}_{ik} \rangle + 3\theta \mathbf{I} - 6\alpha N \theta \langle \mathbf{T}_{ik} \rangle + \alpha^2 N^2 \langle \mathbf{T}_{ik} \cdot \mathbf{T}_{kl} \rangle + 9\theta^2 \mathbf{I} + O(\alpha^3)] \cdot \mathbf{E} \quad (167)$$

and

$$\langle \mathbf{R}(q) \rangle_q = [\alpha N \langle \mathbf{T}_{ik} \cdot \mathbf{T}_{ki} \rangle - \alpha^2 N^2 \langle \mathbf{T}_{ik} \cdot \mathbf{T}_{kl} \cdot \mathbf{T}_{li} \rangle] \cdot \langle \mathbf{p} \rangle = \langle \mathbf{g}(q) \rangle_q \cdot \langle \mathbf{p} \rangle \quad (168)$$

The latter expression is not exact, for it neglects the correlation between $(\mathbf{g}q)$ and $\mathbf{p}$, which is also q dependent. It is easy to see that this correlation does not affect the first term in Eq. (168). This term varies as V^{-1}, the next term as V^{-2}, etc. corresponding to second, third, etc. virial terms in the dielectric expansion. The correlation affects only the third- and higher-order virial terms which are small to begin with.

To proceed, we must evaluate the tensor averages $\langle \mathbf{T}^n \rangle$. The cyclic tensor $\langle \mathbf{T}_{ik} \cdot \mathbf{T}_{ki} \rangle$ can readily be reduced to give[58,59]

$$\begin{aligned} \langle \mathbf{T}_{ik} \cdot \mathbf{T}_{ki} \rangle &= \frac{1}{V} \int_0^\infty \frac{1}{r_{ik}^6} \left(\mathbf{I} + \frac{3\mathbf{r}_{ik}\mathbf{r}_{ik}}{r_{ik}^2} \right) e^{-\psi(r_{ik})/kT} d\mathbf{r}_{ki} \\ &= \frac{2\mathbf{I}}{V} \int_0^\infty \frac{4\pi r^2 e^{-\psi(r)/kT}}{r^6} dr \\ &= \frac{8\pi \mathbf{I}}{3V} \int_0^\infty \frac{3\rho^{(2)}(r)}{r^4} dr \\ &= \frac{8\pi \mathbf{I}}{3V} \kappa \end{aligned} \quad (169)$$

where $\rho^{(2)}(r)$ is the radial distribution function, i.e., $\rho^{(2)}(r) = \rho^{(2)}(r_{ik})$; $\psi(r)$ is the potential of mean force and

$$\kappa = \int_0^\infty \frac{3\rho^{(2)}(r)}{r^4} dr \quad (170)$$

For a dilute gas of hard spheres of diameter d_0

$$\begin{aligned} \rho^{(2)}(r) &= 0 \quad \text{when} \quad r < d_0 \\ &= 1 \quad \text{when} \quad r \geq d_0 \end{aligned} \tag{171}$$

and

$$\mathbf{T}_{ik} \cdot \mathbf{T}_{ki} = (8\pi^2/3V)(\mathbf{I}/d_0^3) \tag{172}$$

The reduction of the cyclic triple-tensor product $\mathbf{T}_{ik} \cdot \mathbf{T}_{kl} \cdot \mathbf{T}_{li}$ is considerably more involved and has been attempted only for hard-sphere averaging. It can be shown to reduce to[59]

$$\langle \mathbf{T}_{ik} \cdot \mathbf{T}_{kl} \cdot \mathbf{T}_{li} \rangle = \frac{24\pi^2}{V^2} \mathbf{I} \int_{d_0}^{\infty}\int\int\int \frac{(1 + 3\cos\theta_i \cos\theta_k \cos\theta_l)}{r_{ik}^3 r_{kl}^3 r_{li}^3} r_{ik} r_{kl} r_{li} dr_{ik} dr_{kl} dr_{il} \tag{173}$$

where the integral has to be taken over all values of r_{il}, r_{kl}, and r_{ik} which are greater than d_0 and for which $r_{ik} \geq r_{kl}$ and $r_{ik} \geq r_{li}$. The result of this integration is

$$\langle \mathbf{T}_{ik} \cdot \mathbf{T}_{kl} \cdot \mathbf{T}_{li} \rangle = \left[(4\pi/3V)^2 \frac{15}{16} (\mathbf{I}/d_0^3) \right]^* \tag{174}$$

The quantity on the right is the value obtained on the basis of hard-sphere averaging; the asterisk denotes that this expression must be modified if temperature-dependent weighting functions are used in averaging the tensor.

On substituting the tensors $\langle \mathbf{T}_{ik} \cdot \mathbf{T}_{ki} \rangle$ and $\langle \mathbf{T}_{ik} \cdot \mathbf{T}_{kl} \cdot \mathbf{T}_{li} \rangle$ into Eq. (168), we obtain

$$\langle \mathbf{R}(q) \rangle_q = \left[\frac{8\pi}{3V} N\alpha\kappa - \left(\frac{4\pi}{3V} \right)^2 \frac{15}{16} \frac{N^2\alpha^2}{d_0^3} + \cdots \right] \mathbf{I} \cdot \langle \mathbf{p} \rangle \tag{175}$$

which defines

$$\begin{aligned} \langle \mathbf{g}(q) \rangle_q &= \left[2\theta\kappa - \left(\frac{15}{16} \theta^2/d_0^3 \right)^* + O(\alpha^3) \right] \mathbf{I} \\ &= \langle g(q) \rangle_q \mathbf{I} \end{aligned} \tag{176}$$

To define a^3, we equate the statistical and dielectric values of reaction-field susceptibilities; that is, we set g equal to $\langle g(q) \rangle_q$. The dielectric

constant can be shown to reduce to[59]

$$(\varepsilon - 1)/3 = \theta\left[1 + \theta + 2\theta\alpha\kappa + \theta^2 - \left(\frac{15}{16}\theta^2\right)^* + O(\alpha^3)\right] \quad (177)$$

where the asterisk again denotes that $(\frac{15}{16}\theta^2)^*$ is the limiting value in the absence of intermolecular forces. Accordingly

$$g = (2\varepsilon - 2)/(2\varepsilon + 1)(1/a^3) = (2\theta/a^3) \times \left[1 - \theta + 2\alpha\kappa\theta + \theta^2 - \left(\frac{15}{16}\theta^2\right)^* + O(\alpha^3)\right] \quad (178)$$

By combining Eq. (178) with Eq. (176), we get

$$a^{-3} = \kappa\left[1 + \theta - \left(\frac{15}{16}\theta^2/d_0^3\right)^*(2\theta\kappa)^{-1} - 2\alpha\theta\kappa - \left(\frac{15}{16}\theta^2/d_0^3\right)^*(2\kappa)^{-1} + \left(\frac{15}{16}\theta^2\right)^* + \cdots\right] \quad (179)$$

which shows that a^3 is a complicated function of molecular parameters, temperature, and density. For a gas, the terms beyond the first one are negligibly small, due to the fact that $\theta \ll 1$. But even for a liquid, they contribute little. To get some idea of their magnitude, we compute these for temperature-independent weighting factors (that is, omit the asterisks and replace κ by $1/d_0^3$). For such liquids as argon, krypton, and xenon at the triple point,[60] θ ranges from 0.145 to 0.236 and α/d_0^3 is about one-third the value of θ. If we take $\theta = 1/5$ and omit the temperature-dependent weighting factors, the quantity within brackets differs from unity by about 10 %. It is unlikely that an exact calculation would alter this value by an order of magnitude. Thus, in a first approximation, we may take

$$a^{-3} \approx \kappa = \int_0^\infty \frac{3\rho^{(2)}(r)}{r^4}\, dr \quad (180)$$

as a reasonable estimate of a^3.

The value a^3 has been computed for liquid Xe on the basis of Eq. (180) using the experimental data for $\rho^{(2)}(r)$ obtained by Campbell and Hildebrand[61] for Xe at -110°C and 1 atm from x-ray scattering data. This calculation gave a value $a^{-3} = 0.28 \times 10^{23}$ cm^{-3} which corresponds to a molar volume $(4\pi/3)a^3N$ of 89 cm^3. The latter is nearly equal to

the van der Waals constant $b = (2\pi/3)Nd_0^3 = 85$ cm^3 based on $d_0 = 4$Å, the latter being the distance of closest approach in the Lennard-Jones potential obtained from the second virial coefficient of gaseous Xe.[62]

Another method for estimating a^3, which should be used with circumspection, is to determine a^3 from dielectric data, itself. The cavity radius appears, for example, in the Böttcher-Onsager equation which can be rearranged to give

$$\frac{4\pi}{3} Na^3 = V\theta \frac{2\varepsilon - 2}{2\varepsilon + 1} \Big/ \left[1 - \frac{9\theta\varepsilon}{(\varepsilon - 1)(2\varepsilon + 1)}\right] \tag{181}$$

On the basis of this expression,[63] the cavity volume $(4\pi/3)Na^3$ is 82.7 cm^3 for liquid Xe—in good agreement with the value obtained from x-ray data. The agreement may, however, be fortuitous, for in the foregoing analysis, the effects of density on the polarizability were not taken into consideration. It has been well established that the presence of neighboring molecules can affect the polarizability of a given molecule in two ways: overlap forces cause a decrease,[64] attractive forces an increase.[65,66] While these effects are small (of the order of a few per cent), their neglect can nevertheless give rise to large errors in the computed a^3 value, which entails taking a small difference between two large numbers. (This criticism applies to the method of obtaining a^3 from the dielectric formula and not from the radial distribution function.)

Assuming that a "proper" a^3 can be found, then one can replace $\mathrm{tr}\langle\hat{\mathbf{g}}(q,\omega)\rangle_q$ in Eq. (153) by $3\langle\hat{g}(q,\omega)\rangle_q$ and the latter by $3\hat{g}(\omega)$, where $\hat{g}(\omega)$ is the dielectric expression given by Eq. (32). The resulting formula for $\phi_{i;S}$ will then be formally identical with the continuum-model expression discussed in Section B-1, but will include the effect of statistical fluctuations.

The method employed here for defining a^3 can readily be extended to more complicated situations. In particular, if the distribution functions which are needed are function of ξ_i, as in the calculation of μ_{dis}, then Eq. (180) must be modified to read

$$a^{-3}(\xi_i) = \int_0^\infty \frac{3\rho^{(2)}(r;\xi_i)}{r^4}\, dr \tag{182}$$

where $\rho^{(2)}(r;\xi_i)$ is defined by Eq. (137).*

* In an earlier paper [B. Linder, *J. Chem. Phys.*, **35**, 371 (1961)], the cohesive energy

VII. TWO-TEMPERATURE POTENTIALS

The method for obtaining the pair potential can at once be generalized to two-temperature potentials. Unlike the ordinary van der Waals pair potentials, which are always attractive, the two-temperature potentials can be attractive as well as repulsive. The two-temperature Keesom potential has been discussed in connection with beam experiments involving dipolar molecules, in which the scattering gas and beam molecules have different temperatures.[34,35] Implied in the derivation of the Keesom potential is the assumption that the period of rotation is very much smaller than the collision time and that the fast rotations can preaverage the potential. There is some question as to whether potentials which have been preaveraged are applicable to scattering phenomena[67] and this subject needs to be studied further.

As a working model for obtaining two-temperature potentials, we imagine the interacting molecules to be located in separate heat baths: electrical energy can be transferred but not heat. According to the reaction-field technique, the overall interaction is regarded as arising from two separate events, namely, the polarization of molecule *1* by the electrical fluctuations of molecule *2* and vice versa. The mechanism for generalizing the single-temperature potential to two temperatures is thus present from the start. Assuming that molecule *1* has the temperature T_1 and molecule *2* the temperature T_2, we get at once

$$\phi^{(2)}(q;T_1,T_2) = -\frac{3\hbar}{\pi r_{12}^6}\left[\int_0^\infty (\chi_1'(\omega)\chi_2''(\omega)\coth\frac{\hbar\omega}{2kT_2} + \chi_2'(\omega)\chi_1''(\omega)\coth\frac{\hbar\omega}{2kT_1}\right]d\omega \quad (183)$$

---

was computed from the free energy [Eq. (152)] by the Gibbs-Helmholtz equation. A constant value was assumed for a^3. This is consistent with the continuum model but inconsistent with a model in which translational fluctuations are present. In the latter case the chemical potential and, therefore, also the molar free energy are dependent on ξ. If it is assumed that g_a is temperature dependent only through the temperature dependence of a^3 (i.e., the molecular polarizabilities are temperature independent), then the free energy can be obtained directly by substitution of a^3 as defined by Eq. (182) into Eq. (152) and the energy can be obtained by substitution of a^3 as defined by Eq. (180). In both cases, however, a^3 must be temperature dependent.

Because the two hyperbolic cotangent functions have different temperatures, the two terms cannot be added to yield an expression which can be continued inside the complex plane and integrated in the same way as the single-temperature potential. Equation (183), however, is a perfectly workable formula and, with the aid of the expressions for $\chi''(\omega)$ and $\chi'(\omega)$ derived in Section V-B, it can be further reduced and expressed in terms of the state properties of the molecules. The general features are such that the potential can be attractive as well as repulsive.[29,30]

A detailed analysis of the double-temperature potential has been carried out for two rotating dipolar systems[29] and also, analysis has been made of the interaction between model molecules which are assumed to have the low-frequency characteristics of rigid rotors and the high-frequency characteristics of the harmonic oscillators.[31] For such a system, the induction potential is always attractive; the orientation potential can be attractive as well as repulsive depending on the temperatures and moments of inertia, and will always be repulsive, when the temperature difference is large; the dispersion potential becomes repulsive when the temperature difference is large, provided the hotter system has the higher natural frequency.

To underscore the quantum-statistical implications underlying the double-temperature potential, we start with the fundamental expression based on Eq. (50) and write

$$\phi^{(2)}(q;T_1,T_2) = -\frac{3}{r_{12}^6}\int_{-\infty}^{\infty}[(\hat{\chi}_1(\omega)(m_{2,\omega}^2)_z + \hat{\chi}_2(\omega)(m_{1,\omega}^2)_z]d\omega \quad (184)$$

The $\hat{\chi}$'s in this expression include both the real and imaginary parts but, as indicated before, the imaginary parts make no contribution to the integral. Remembering that

$$\lim_{\delta\to 0}\frac{1}{\omega_{qp}-\omega+i\delta} = \frac{\mathscr{P}}{\omega_{qp}-\omega} - i\pi\delta(\omega+\omega_{pq}) \quad (185)$$

we can express $\hat{\chi}(\omega)$ in terms of the matrix elements as follows [see Eqs. (92) and (96)].

$$\hat{\chi}(\omega) = \frac{1}{hQ}\sum_p\sum_q \frac{(e^{-Ep/kT} - e^{-Eq/kT})|ez_{pq}|^2}{\omega_{qp}-\omega+i\delta} \quad (186)$$

Combining this with Eq. (90b) gives

$$\phi^{(2)}(q;T_1,T_2) = -\frac{3}{\hbar r_{12}^6 Q_1 Q_2}\sum_m\sum_n\sum_s\sum_t |ez_{n;m}^{(1)}|^2|ez_{t;s}^{(2)}|^2$$
$$\times\left\{\frac{(e^{-E_n^{(1)}/kT_1}-e^{-E_m^{(1)}/kT_1})(e^{-E_t^{(2)}/kT_2}+e^{-E_s^{(2)}/kT_2})}{\omega_{mn}^{(1)}-\omega_{st}^{(2)}+i\delta}\right.$$
$$\left.+\frac{(e^{-E_n^{(1)}/kT_1}+e^{-E_m^{(1)}/kT_1})(e^{-E_t^{(2)}/kT_2}-e^{-E_s^{(2)}/kT_2})}{\omega_{st}^{(2)}-\omega_{mn}^{(1)}+i\delta}\right\} \tag{187}$$

where the indices n, m and the superscript *1* denote particle *1*; the indices s, t, and the superscript *2* denote particle *2*. This expression can be reduced to

$$\phi^{(2)}(q;T_2,T_2) = -\frac{3}{\hbar r_{12}^6 Q_1 Q_2}\sum_m\sum_n\sum_s\sum_t |ez_{n;m}^{(1)}|^2|ez_{t;s}^{(2)}|^2$$
$$\times\frac{(\omega_{mn}^{(1)}-\omega_{st}^{(2)})[e^{-E_n^{(1)}/kT_1}e^{-E_s^{(2)}/kT_2}-e^{-E_m^{(1)}/kT_1}e^{-E_t^{(2)}/kT_2}]}{(\omega_{mn}^{(1)}-\omega_{st}^{(2)})^2+\delta^2} \tag{188}$$

For the purpose of interpreting this expression, we shall delete the δ^2; the resulting summation is then to be taken as a principle value in the sense that $\omega_{mn}^{(1)}$ can come arbitrarily close to $\omega_{st}^{(2)}$ but cannot be identical to it. (If the summation were to be replaced by an integration, the resulting integral would be the principal value.) We next introduce the notation λ to represent a state of the *combined system* of the two particles such that particle *1* is in state n and particle *2* in state s; similarly ν represents a state of the *combined system* such that particle *1* is in state m and particle *2* in state t. We further note that $\exp[-E_n^{(1)}/kT_1]/Q_1$, to be denoted as $\mathscr{P}_n^{(1)}$, represents the probability that particle *1* is in state n and that $\exp[-E_s^{(2)}/kT_2]/Q_2 = \mathscr{P}_s^{(2)}$ is the probability that particle *2* is in state s. The product $\mathscr{P}_n^{(1)}\mathscr{P}_s^{(2)}$ is the probability that the combined system is in the state λ and this will be denoted as $\mathscr{P}_\lambda$, i.e., $\mathscr{P}_\lambda = \mathscr{P}_n^{(1)}\mathscr{P}_s^{(2)}$. Similarly, we write $\mathscr{P}_\nu = \mathscr{P}_m^{(1)}\mathscr{P}_t^{(2)}$. Also, since $|z_{n;m}|^2$ is invariant of the axis of quantization, we can write

$$\frac{6}{r_{12}^6}|ez_{n;m}^{(1)}|^2|ez_{t;s}^{(3)}|^2 = \frac{e^4}{r_{12}^6}[|x_{n;m}^{(1)}|^2|x_{t;s}^{(2)}|^2 + |y_{n;m}^{(1)}|^2|y_{t;s}^{(2)}|^2$$
$$+ 4|z_{n;m}^{(1)}|^2|z_{t;s}^{(2)}|^2] = |\mathscr{H}'_{\lambda\nu}|^2 \tag{189}$$

where $\mathscr{H}'$ is the interaction Hamiltonian, expressed in cartesian coordinates as $\mathscr{H}' = (e^2/r_{12}^3)(x_1x_2 + y_1y_2 - 2z_1z_2)$. In this notation, Eq. (188) takes the form

$$\phi^{(2)}(q;T_1,T_2) = -\frac{1}{2}\sum_{\lambda}\sum_{\nu}\frac{(\mathscr{P}_\lambda - \mathscr{P}_\nu)|\mathscr{H}'_{\lambda\nu}|^2}{E_\nu - E_\lambda} \tag{190}$$

We may interpret this expression by regarding the interaction to arise from the virtual transitions between the states of the combined systems. It is seen that every transition from a given state ν to another state λ is accompanied by a transition in the opposite direction and if it were not for the fact that the states are not equally populated, the potential would be zero. In the normal course of events, that is, when the two temperatures are equal, the energy difference $E_\nu - E_\lambda$ and the probability difference $\mathscr{P}_\lambda - \mathscr{P}_\nu$ always have the same sign and the potential is attractive. This is a direct consequence of the fact that the more densely populated states have the lower energies and vice versa. Thus, for example, if $E_\nu < E_\lambda$ then, for equal temperatures,

$$\mathscr{P}_\lambda = \frac{\exp\left[-(E_n^{(1)} + E_s^{(2)})/kT\right]}{Q_1Q_2} < \mathscr{P}_\nu = \frac{\exp\left[-(E_m^{(1)} + E_t^{(2)})/kT\right]}{Q_1Q_2}$$

and this is true regardless of how the energy is partitioned among the individual particle states. The net result is that transitions from lower to higher energy states predominate and thereby mix in states with more polar character, resulting in a lowering of free energy. On the other hand, when the temperatures are different, $E_\nu - E_\lambda$ and $\mathscr{P}_\lambda - \mathscr{P}_\nu$ do not necessarily have the same sign and the probabilities $\mathscr{P}_\nu$ and $\mathscr{P}_\lambda$ depend not only on the energies E_ν and E_λ but also on the manner in which the energy is partitioned among the particle states. It is, then, possible to have a situation where the lower energy states have lower probabilities than the higher energy states and vice versa. If such states predominate, there will be a net transition from high- to low-energy states causing a depolarization of the system as a whole. The net result is an increase in free energy.

It would be of interest to compare the predictions based on the reaction-field technique with results obtained on the basis of quantum-statistical theory. An *a priori* statistical derivation of the two temperature potential has not yet been advanced and no direct comparison can be made. In case of the single-temperature potential with no resonance

interaction, the two approaches can be analyzed in detail and there the results are the same.

VIII. CONCLUDING REMARKS

In the preceding, we have traced the reaction-field approach to intermolecular forces from its early inception in electrostatic theory to its present development in fluctuation theory. Of prime importance is the generalized potential $\phi_{i;S}$, which represents the potential of interaction between i and all the neighboring molecules. The surrounding molecules can be treated on an individual basis or collectively as a dielectric. From the molecular picture, one can abstract the pair and nonadditive potentials. These potentials can be further decomposed to produce the dispersion- (retarded as well as nonretarded), orientation- and induction potentials. The potential $\phi_{i;S}$ is also intimately related to the chemical potential (associated with the establishment of the intermolecular force field) and thus provides a link between the molecular and thermodynamic description of the many-body system.

The present development is based on a linear response-function theory. This approximation has the effect of deleting certain interaction diagrams from the reaction potential, namely, those involving multiple-frequency transitions. The latter are corrections to the higher-order (nonadditive) potentials and, although they are of secondary importance, they ought to be included in a general formulation of the many-body problem. In problems dealing explicitly with the distortions of the molecules, such as polarizability changes with density, NMR shifts, etc., they may be of prime importance.

The present formalism treats only the interactions associated with the electrical motion by fluctuation theory. To obtain the thermodynamic properties, it is necessary to include the effects of translational and other types of fluctuations. In the molecular description of the reaction-field formulation, these are brought in statistically; in the dielectric formulation, they can be accounted for by the "proper" choice of a cavity radius. (The continuum model avoids this problem by assuming that the macroscopic dielectric constant is the same as the local one.) An obvious extension of the present formalism is the development of a general theory which treats both the electrical and molecular fluctuations in a unified manner. To be of any use, however, such a theory must be reducible to measurable quantities and must not be of a merely

formal nature. We must wait to see how this program can be pursued.

Finally, we wish to point out that the method based on the fluctuating reaction field is concerned only with one aspect of intermolecular forces, namely, those due to dipolar interactions. Short-range repulsive forces and forces associated with higher-order multipole moments, for example, are not included. To include the repulsive forces in a meaningful way would probably require the full complexity of quantum mechanics. The forces due to the higher-order multipole moments can be incorporated within the framework of the present theory by a suitable generalization of the reaction-field response function.

Acknowledgments

I am greatly indebted to Professor Robert A. Kromhout for his many valuable discussions, and helpful suggestions and criticisms, and to Herschel Cohen for reading of the manuscript.

References

1. W. H. Keesom, *Physik Z.*, **22**, 129 (1921).
2. H. Falkenhagen, *Physik Z.*, **23**, 87 (1922).
3. F. London, *Z. Physik*, **63**, 245 (1930); *Z. Physik Chem.*, **B11**, 222 (1930); *Trans. Faraday Soc.*, **33**, 8 (1937); R. Eisenshitz and F. London, *Z. Physik*, **60**, 491 (1930).
4. H. Margenau, *Rev. Mod. Phys.*, **11**, 1 (1939).
5. K. S. Pitzer, *Advan. Chem. Phys.*, **2**, 59 (1959).
6. B. M. Axilrod and E. Teller, *J. Chem. Phys.*, **11**, 299 (1943); B. M. Axilrod, *J. Chem. Phys.*, **19**, 724 (1951).
7. Y. Muto, *Proc. Phys. Math. Soc. Japan*, **17**, 629 (1943).
8. T. Kihara, *Advan. Chem. Phys.*, **1**, 267 (1958).
9. W. L. Bade and J. G. Kirkwood, *J. Chem. Phys.*, **27**, 1284 (1957).
10. W. L. Bade, *J. Chem. Phys.*, **27**, 1280 (1957); **28**, 282 (1958).
11. N. R. Kestner and O. Sinanoğlu, *J. Chem. Phys.*, **38**, 1730 (1963).
12. H. B. G. Casimir and D. Polder, *Phys. Rev.*, **73**, 360 (1948).
13. E. M. Lifshitz, *Soviet Phys. JETP* (*English Trans.*), **2**, 73 (1956); *Zh. Eksperim. Teor. Fiz.*, **29**, 94 (1955).
14. I. E. Dzyaloshinski, E. M. Lifshitz, and L. P. Pitaeevski, *Advan. Phys.*, **10**, 165 (1961).
15. E. A. Power and S. Zienau, *Nuovo Cimiento*, **6**, 7 (1957); M. R. Aub, E. A. Power, and S. Zienau, *Phil. Mag.*, **2**, 571 (1957).
16. C. Mavroyannis and M. J. Stephen, *Mol. Phys.*, **5**, 629 (1962).
17. A. D. McLachlan, *Proc. Roy. Soc.* (*London*), **A271**, 387 (1963).
18. W. J. Meath and J. O. Hirschfelder, *J. Chem. Phys.*, **44**, 3210 (1966).
19. E. A. Power, in *Intermolecular Forces* (*Advances in Chemical Physics*, Vol. 12), J. O. Hirschfelder, Ed., Interscience, New York, 1967, Chap. 4.
20. A. D. McLachlan, *Proc. Roy. Soc.* (*London*), **A274**, 80 (1963).

21. A. A. Abrikosov, L. P. Gorkov, and I. E. Dzyaloshinski, *Methods of Quantum Field Theory in Statistical Mechanics*, Prentice-Hall, Englewood Cliffs, New Jersey, 1963, Chap. 6.
22. J. Linderberg, *Arkiv Fysik*, **26**, 323 (1964); S. Lundquist and A. Sjölander, *Arkiv Fysik*, **26**, 17 (1964); S. Doniach, *Phil. Mag.*, **8**, 129 (1963).
23. A. D. McLachlan, *Mol. Phys.*, **6**, 423 (1963).
24. H. Jehle, J. M. Yos, and W. L. Bade, *Phys. Rev.*, **110**, 793 (1957); J. M. Yos, *Phys. Rev.*, **110**, 800 (1958); H. Jehle, W. C. Parke, and A. Salyers, *Electronic Aspects of Biochemistry*, B. Pullman, Ed., Academic Press, New York, 1964, p. 313; H. Jehle, *Proc. Natl. Acad. Sci. U.S.*, **49**, 516 (1963).
25. J. O. Hirschfelder, *Molecular Biophysics*, B. Pullman and M. Weissbluth, Eds., Academic Press, New York, 1965, p. 325.
26. Among these are investigations on (a) Stability of DNA in Solvents [O. Sinanoğlu and S. Abdulnur, *Federation Proc.*, **24**, S-12 (1965) and *Photochemistry and Photobiology*, **3**, 333 (1964)]; (b) Spectral Shifts [A. D. Buckingham, T. Schaefer, and W. G. Schneider, *J. Chem. Phys.*, **32**, 1227 (1960); A. D. Buckingham, *Can. J. Chem.*, **38**, 300 (1960); B. B. Howard, B. Linder, and M.T. Emerson *J. Chem. Phys.*, **36**, 485 (1962); E. G. McRae, *J. Phys. Chem.*, **61**, 562 (1957); M. E. Baur and M. Nicol, *J. Chem. Phys.*, **44**, 3337 (1966); S. Basu, *Advances in Quantum Chemistry*, Vol. I, P. O. Löwdin, Ed., Academic Press, New York, 1964, p. 145; W. Liptay, *Modern Quantum Chemistry*, Part II, O. Sinanoğlu, Ed., Academic Press, New York, 1965, p. 173 and references therein]; (c) Band Intensities [O. E. Weigang, Jr., *J. Chem. Phys.*, **41**, 1435 (1964) and G. Wills-Johnson, Ph.D. Dissertation, University of Western Australia, 1966]; (d) Dielectric Theory [W. F. Brown, Jr., *Handbuch der Physik*, Vol. 17, p. 1; S. Flugge, Ed., Springer-Verlag, Berlin, 1956; H. Frölich, *Theory of Dielectrics*, Oxford University Press, New York, 1949; see also ref. 44].
27. B. Linder, *J. Chem. Phys.*, **40**, 2003 (1964).
28. B. Linder and D. Hoernschemeyer, *J. Chem. Phys.*, **40**, 622 (1964).
29. B. Linder, *J. Chem. Phys.*, **44**, 265 (1966).
30. B. Linder, *Discussions Faraday Soc.*, **40**, 164 (1965).
31. J. P. Rosenkrans, B. Linder, and R. Kromhout, to be published.
32. B. Linder, *J. Chem. Phys.*, **33**, 668 (1960); **35**, 371 (1961).
33. B. Linder, *J. Chem. Phys.*, **37**, 963 (1962).
34. (a) E. W. Rothe and R. B. Bernstein, *J. Chem. Phys.*, **31**, 1619 (1959); (b) H. Schumacher, R. B. Bernstein, and E. W. Rothe, *J. Chem. Phys.*, **33**, 584 (1960).
35. (a) R. J. Cross, Jr. and R. G. Gordon, *J. Chem. Phys.*, **45**, 3571 (1966); (b) R. J. Cross, Jr., E. A. Gislason, and D. R. Herschbach, *J. Chem. Phys.*, **45**, 3582 (1966).
36. P. Debye and E. Hückel, *Physik Z.*, **24**, 185, 305 (1923).
37. A. R. Martin, *Phil. Mag.*, **8**, 550 (1929); *Trans. Faraday Soc.*, **33**, 191 (1937).
38. R. P. Bell, *Trans. Faraday Soc.*, **27**, 797 (1931); *ibid*, **31**, 1557 (1935); *J. Chem. Soc.*, **139**, 1371 (1931).
39. J. G. Kirkwood, *J. Chem. Phys.*, **2**, 351 (1934).
40. L. Onsager, *J. Am. Chem. Soc.*, **58**, 1486 (1936).
41. A. Wada, *J. Chem. Phys.*, **22**, 198 (1954).

42. W. B. Bonnor, *Trans. Faraday Soc.*, **47**, 1143 (1951).
43. J. H. Van Vleck, *J. Chem. Phys.*, **5**, 320 (1937).
44. C. J. F. Böttcher, *Theory of Electric Polarization*, Elsevier, New York, 1952.
45. L. Onsager, *Chem. Rev.*, **13**, 73 (1933).
46. R. H. Fowler, *Statistical Mechanics*, Cambridge, University Press, 2nd ed., pp. 267–269.
47. Th. G. Scholte, *Physica*, **15**, 437 (1949).
48. L. D. Landau and E. M. Lifshitz, *The Classical Theory of Fields*, Addison-Wesley, Reading, Mass., 1951, Chap. 9, Sect. 6.
49. R. Kromhout and B. Linder, to be published.
50. L. D. Landau and E. M. Lifshitz, *Statistical Physics*, Pergamon Press, London, 1958, Chap. XII, Sec. 118.
51. H. B. Callen and T. A. Welton, *Phys. Rev.*, **83**, 34 (1951).
52. J. R. MacDonald and M. K. Brachman, *Rev. Mod. Phys.*, **28**, 393 (1956).
53. This may have some bearing on the relative importance of the electrostatic energies versus the dispersion energies in systems involving very large molecules [J. O. Hirschfelder and B. Linder (to be published)].
54. H. B. Callen, in *Fluctuation, Relaxation and Resonance in Magnetic Systems*, D. ter Haar, Ed., Oliver and Boyd, London, 1962, p. 15; W. Bernard and H. B. Callen, *Rev. Mod. Phys.*, **31**, 1017 (1959).
55. R. Kubo, *J. Phys. Soc. (Japan)*, **12**, 570 (1957).
56. J. G. Kirkwood, *J. Chem. Phys.*, **3**, 300 (1935).
57. M. J. Sparnaay, *Physica*, **25**, 217, 444 (1959).
58. J. G. Kirkwood, *J. Chem. Phys.*, **4**, 592 (1936).
59. B. Linder and D. Hoernschemeyer, *J. Chem. Phys.*, **46**, 784 (1967).
60. Molecular polarizabilities taken from A. A. Maryott and F. G. Buckley, *Natl. Bur. Std. (U.S.) Circ.*, No. 537 (1953); Molar volumes and molecular diameter taken from G. Boato and G. Casanova, *Physica*, **27**, 571 (1961).
61. J. A. Campbell and J. H. Hildebrand, *J. Chem. Phys.*, **11**, 334 (1943).
62. J. O. Hirschfelder, C. F. Curtiss, and R. B. Bird, *Molecular Theory of Gases and Liquids*, Wiley, New York, 1954, p. 110.
63. The dielectric data was taken from R. L. Amey and R. H. Cole, *J. Chem. Phys.*, **40**, 146 (1964).
64. A. Michels, J. de Boer, and A. Bijl, *Physica*, **4**, 981 (1937); S. R. De Groot and C. A. ten Seldam, *Physica*, **13**, 47 (1947); **18**, 905, 910 (1952).
65. L. Jansen and P. Mazur, *Physica*, **21**, 193208 (1955); L. Jansen and A. D. Solem, *Phys. Rev.*, **104**, 1291 (1956); L. Jansen, *Phys. Rev.*, **112**, 434 (1958).
66. R. Yaris and B. Kirtman, *J. Chem. Phys.*, **37**, 1775 (1962).
67. R. F. Cross, Jr., *J. Chem. Phys.*, **46**, 609 (1967).

6. Intermolecular Forces in Liquids

OKTAY SINANOĞLU

Center for Theoretical Studies
University of Miami, Coral Gables, Florida
and
Sterling Chemistry Laboratory
Yale University, New Haven, Connecticut

CONTENTS

I. Introduction 283
II. Effective Pair Potentials 284
III. The Two-Body Potential in the Gas Phase 289
IV. N-Body Potentials 292
V. Effective Nonpolar Pair Potentials in Liquids 298
A. Evaluation of L_{AB} 299
B. Evaluation of L_{AB} for $R < R_A + R_B + 4R_C$ and the Role of the Structure of the Liquid 306
1. Region 1 309
2. Region 2 310
3. Region 3—$R_A + R_B + 2\kappa R_C > R \geqslant R_A + R_B$ 311
4. Region 4—$R_A + R_B > R > 0$ 311
VI. Summary of the Effective Pair Potential $V_{AB}^{eff}(R, R_A/R_C, R_B/R_C, \rho_1)$ in the Liquid 315
A. The Lennard-Jones Case ($l = 0$) 315
B. The Kihara Case ($l \neq 0$) 316
VII. The Effective Potential in Other Density Ranges and Phases 319
VIII. Examples of Potentials in Some Nonpolar Liquids 319
References 326

I. INTRODUCTION

In the statistical mechanics of liquids and solutions, it is convenient to work with pairwise additive potentials, $V = \sum_{i>j} v_{ij}$. The pair potential is usually a semiempirical function such as a Lennard-Jones or a Kihara potential, the parameters of which are determined from dilute gas properties such as the second virial coefficient $B(T)$, gas viscosity, etc.

This article is concerned with (*a*) how the nonpolar parts of gas phase two-body potentials are modified due to the nonpolar effects of a liquid medium, and (*b*) what happens to pairwise additivity in such liquids. It is possible to incorporate the medium effects arising from 3,4 ... *n*-body forces into effective pair potentials dependent on liquid structure, retaining some of the usual statistical mechanical formalism.

Effective interactions in liquids are also needed for use in a theory of solvent effects on association reactions of the type

$$A + B \rightarrow (AB)$$

(AB) may be a physical association affected by solvent, or a chemical reaction in which chemical bonds are formed between A and B. The (AB) may also be an "activated complex" in which case one would be treating the solvent effects on reaction rates where the rates are not diffusion controlled.

The presentation in this chapter will be restricted to nonpolar parts of the interactions. When the liquid and/or the solute molecules are polar, additional terms—some of them well known—are added to the equations presented here.

II. EFFECTIVE PAIR POTENTIALS

Consider a system of N identical molecules whose total potential energy function $V(\mathbf{r}_1,\mathbf{r}_2, \ldots \mathbf{r}_N)$ may be expanded as a sum of two, three, ... *n*-body potentials,

$$V = \frac{1}{2!}\sum_{\substack{i\geq 1\\ i\neq j}}^{N}\sum_{j\geq 1}^{N} v_{ij} + \frac{1}{3!}\sum_{i\geq 1}^{N}\sum_{\substack{j\geq 1\\ i\neq j\neq k}}^{N}\sum_{k\geq 1}^{N} V_{ijk} + \cdots + \frac{1}{n!}\sum_{i}^{N}{}'\sum_{j}^{N}{}'\cdots\sum_{n'}^{N}{}' V_{ijk\ldots n'} + \cdots \quad (1)$$

where, e.g., $v_{ij} \equiv v_{12}(\mathbf{r}_i,\mathbf{r}_j)$; $V_{ijk} \equiv V_{123}(\mathbf{r}_i,\mathbf{r}_j,\mathbf{r}_k)$ and so on. Much statistical mechanical theory would still be applicable at least in certain density ranges if

$$V \equiv \frac{1}{2!}\sum_{\substack{i\geq 1\\ i\neq j}}^{N}\sum_{j\geq 1}^{N} v_{ij}^{\text{eff}} \quad (2)$$

and if v_{ij}^{eff} were related to the "bare" two-body potentials in simple ways.

In Eq. (1), carrying out the i,j summations last, one has

$$V = \frac{1}{2!} \sum_{\substack{i \geq 1 \\ i \neq j}}^{N} \sum_{j \geq 1}^{N} \left\{ v_{ij} + \frac{2!}{3!} \sum_{\substack{k \geq 1 \\ k \neq i,j}}^{N} V_{ijk} + \cdots + \frac{2!}{n!} \sum_{\substack{k \\ k \neq n' \neq i,j}}^{N} \sum_{n'}^{N} V_{ijk \cdots n'} + \cdots \right\} \quad (3)$$

Thus*

$$v_{ij}^{\text{eff}} = v_{ij} \left\{ 1 + \frac{1}{3} \sum_{k \neq i,j}^{N} (V_{ijk}/v_{ij}) + \cdots \right\} \quad (4a)$$

For a given configuration $(\mathbf{r}_1, \mathbf{r}_2, \ldots \mathbf{r}_N)$, a static distribution of the N-molecules, the factor multiplying the bare two-body potential v_{ij}, will depend, in addition to $\mathbf{r}_i$ and $\mathbf{r}_j$, on all the other $(N-2)$, $\mathbf{r}_k$. For a crystal, the k summation $\sum_{k \neq i,j}^{N} V_{ijk}$ is carried over all lattice points except the chosen pair i,j. If we neglect the vibrations, this defines a

$$v_{ij}^{\text{eff}} = v_{ij}^{\text{eff}}(\mathbf{r}_i, \mathbf{r}_j; \{\mu\})$$

where $\{\mu\}$ symbolizes dependence on some bulk properties of the solid.

For a liquid, one may obtain a v_{ij}^{eff} by averaging the sum over all $(\mathbf{r}_1, \mathbf{r}_2, \ldots \mathbf{r}_N)$ while keeping the $\mathbf{r}_i, \mathbf{r}_j$ fixed. In this case

$$v_{ij}^{\text{eff}} = v_{ij} + \frac{1}{3} \left\langle \sum_{k \neq i,j}^{N} V_{ijk} \right\rangle_k + \cdots \quad (4b)$$

will depend on the density ρ of the fluid as well as on $\mathbf{r}_{ij} = \mathbf{r}_i - \mathbf{r}_j$ or for spherical molecules on $r_{ij} \equiv |\mathbf{r}_i - \mathbf{r}_j|$. The $\langle \ \rangle_k$ denotes statistical averaging over k. One thus obtains a *density-dependent pair potential*

$$v_{ij}^{\text{eff}} = v_{ij}^{\text{eff}}(r_{ij}; \rho) \quad (5)$$

The correction factor in Eq. (4) would become particularly convenient, were it a simple function of r_{ij}.

In a solution, with n_a solvent molecules a, and n_b solute molecules b, distribution of the nonpairwise potentials into effective pairs depends on the type of pairing (aa,ab,bb) and on context. Care is needed to avoid counting some of the interactions more than once while still defining physically meaningful effective potentials. For an arbitrary

* For the interactions considered in this article $\sum_k V_{ijk} \to 0$ before the point where $v_{ij} = 0$, so there is no difficulty in defining the factor $v_{ij}^{\text{eff}}/v_{ij}$. For other cases, one could also define a correction factor multiplying only a part of v_{ij}, e.g., $v_{ij}^a + v_{ij}^b(1 + \cdots)$.

distribution of the n_a and n_b molecules

$$V = \frac{1}{2!}\sum_{\substack{i\geq 1\\ i\neq j}}^{n_a}\sum_{j\geq 1}^{n_a} v_{ij}^{aa} + \frac{1}{2!}\sum_{\substack{m\geq 1\\ m\neq n}}^{n_b}\sum_{n\geq 1}^{n_b} v_{mn}^{bb} + \sum_{i\geq 1}^{n_a}\sum_{m\geq 1}^{n_b} v_{im}^{ab}$$
$$+ \frac{1}{3!}\sum_{\substack{i\\ i\neq j\neq k}}^{n_a}\sum_{j}^{n_a}\sum_{k}^{n_a} V_{ijk}^{aaa} + \frac{1}{3!}\sum_{\substack{m\\ m\neq n\neq o}}^{n_b}\sum_{n}^{n_b}\sum_{o}^{n_b} V_{mno}^{bbb}$$
$$+ \frac{1}{2!}\sum_{\substack{m\\ i\neq j}}^{n_b}\sum_{i}^{n_a}\sum_{j}^{n_a} V_{ijm}^{aab} + \frac{1}{2!}\sum_{\substack{i\\ m\neq n}}^{n_a}\sum_{m}^{n_b}\sum_{n}^{n_b} V_{imn}^{abb}$$
$$+ \{4 \text{ and higher-body terms}\} \quad (6)$$

Again we may wish to define

$$V \equiv \frac{1}{2!}\sum_{\substack{i\\ i\neq j}}^{n_a}\sum_{j}^{n_b} \overline{v_{ij}^{aa}}^{\text{eff}} + \frac{1}{2!}\sum_{\substack{m\\ m\neq n}}^{n_b}\sum_{n}^{n_b} \overline{v_{mn}^{bb}}^{\text{eff}} + \sum_{i}^{n_a}\sum_{m}^{n_b} \overline{v_{im}^{ab}}^{\text{eff}} \quad (7)$$

Definition of the effective pair potentials is now ambiguous. The environment of a given pair contains some a and some b molecules. It would be desirable to define the $\bar{v}^{\text{eff}}$ as the effective potential of a pair immersed in a medium of given bulk composition $[x_a + x_b = 1;\ x_a = n_a/(n_a + n_b)]$. This may be possible if a and b are quite similar and if there are no local concentration effects. One would then obtain

$$\overline{v_{kl}^{\alpha\beta}}^{\text{eff}} = \overline{v_{kl}^{\alpha\beta}}^{\text{eff}}(r_{kl};\rho,x_a) \quad (8)$$

a *composition- as well as density-dependent potential* after suitable statistical averaging. However, there still remains the problem of how many V_{ijm}^{aab} terms are attributable to $\overline{v_{ij}^{aa}}^{\text{eff}}$ and how many to $\overline{v_{im}^{ab}}^{\text{eff}}$.

In a dilute solution of b in a the situation is again simplified. The environment of the bb pair is essentially all a. The same is true for an ab or an aa pair. Consistent with this picture, all the V_{ijm}^{aab} terms are assigned to the v_{im}^{ab} pair, the V_{imn}^{abb} terms to v_{mn}^{bb}, and so on. Thus, Eq. (6) is rewritten as

$$V = \frac{1}{2!}\sum_{\substack{i\\ i\neq j}}^{n_a}\sum_{j}^{n_a}\left\{v_{ij}^{aa} + \frac{2!}{3!}\sum_{k\neq i,j}^{n_a} V_{ijk}^{aaa} + \cdots\right\}$$
$$+ \sum_{i}^{n_a}\sum_{m}^{n_b}\left\{v_{im}^{ab} + \frac{1}{2!}\sum_{j\neq i}^{n_a} V_{imj}^{aba} + \cdots\right\}$$
$$+ \frac{1}{2!}\sum_{\substack{m\\ m\neq n}}^{n_b}\sum_{n}^{n_b}\left\{v_{mn}^{bb} + \sum_{i}^{n_a} V_{mni}^{bba} + \frac{2!}{3!}\sum_{o\neq m,n}^{n_b} V_{mno}^{bbb} + \cdots\right\} \quad (9)$$

In dilute solution, the V^{bbb} term on v_{mn}^{bb} is negligible.

The dilute-solution effective pair potentials become:

1. Between two solvent molecules:

$$\overline{v_{ij\,(\text{soln})}^{aa\,\text{eff}}} \equiv v_{ij}^{aa} B_{(aa)a}(r_{ij};\rho_a) \tag{10a}$$

$$B_{(aa)a}(r_{ij};\rho_a) = 1 + \frac{1}{3}\left\langle \sum_{\substack{k \\ \text{soln}}}^{n_a} V_{ijk}^{aaa}/v_{ij}^{aa} \right\rangle_k + \cdots \tag{10b}$$

2. Between one solvent and one solute molecule:

$$\overline{v_{im\,(\text{soln})}^{ab\,\text{eff}}} = v_{im}^{ab} B_{(ab)a}(r_{im};\rho_a) \tag{11a}$$

$$B_{(ab)a}(r_{im};\rho_a) = 1 + \frac{1}{2}\left\langle \sum_{\substack{j \\ \text{soln}}}^{n_a} V_{imj}^{aba}/v_{im}^{ab} \right\rangle_j + \cdots \tag{11b}$$

3. Between two solute molecules:

$$\overline{v_{mn\,(\text{soln})}^{bb\,\text{eff}}} = v_{mn}^{bb} B_{(bb)a}(r_{mn};\rho_a) \tag{12a}$$

$$B_{(bb)a} = 1 + \left\langle \sum_{\substack{i \\ \text{soln}}}^{n_a} V_{mni}^{bba}/v_{mn}^{bb} \right\rangle_i + \cdots \tag{12b}$$

The following points about these equations may be noted:

All the B factors which put in the effect of the medium depend on the solvent density ρ_a. The terms in parentheses following each B will be nearly the same if a and b are similar molecules, or for certain interactions (see below); however these terms are multiplied by $\frac{1}{3}$ for aa, $\frac{1}{2}$ for ab and 1 for bb. There will be similarly different factors multiplying the higher n-body terms. The effect of the medium on a given gas-phase pair potential is most pronounced for two solute molecules immersed in a solvent.

The sums in Eqs. (10b), (11b), and (12b) are over n_a of the molecules found in a given volume, whereas the similar sum in Eq. (4) for a pure liquid covers all the N molecules which exhaust the volume. In a dilute solution, in the relatively small region that contributes to the sums, only a molecules will be found. In this case, the difference between $\sum^{n_a}$ and $\sum^{N}$ is negligible (except when b is a much larger molecule than a) making the B's composition independent. Also in dilute solution

$$\overline{v_{ij\,(\text{soln})}^{aa\,\text{eff}}} \cong \overline{v_{ij\,(\text{pure liquid})}^{aa\,\text{eff}}} \tag{13}$$

except when i and j are near a b molecule.*

Equations (1)–(4) above apply to any dense medium or assembly with finite or infinite N. For a liquid, it is also convenient to express the effective potentials in terms of distribution functions.[1]

For a pure fluid of number density ρ and $N \to \infty$, Eq. (4b) becomes:

$$v_{aa}^{\text{eff}}(r_{ij},\rho) = v_{aa}(r_{ij}) + \frac{1}{3}\int_{\text{liq}} V_{aaa}(\mathbf{r}_i,\mathbf{r}_j,\mathbf{r}_k) \times g^{[3]}(\mathbf{r}_i,\mathbf{r}_j,\mathbf{r}_k)\rho d^3\mathbf{r}_k \qquad (14)$$

The

$$\rho^{[3]}(\mathbf{r}_i,\mathbf{r}_j,\mathbf{r}_k) = \rho g^{[3]}(\mathbf{r}_i,\mathbf{r}_j,\mathbf{r}_k)$$

is the "unsymmetric distribution function" giving the probability density for finding *any* one molecule at $\mathbf{r}_k$, while two definite molecules are kept fixed at $\mathbf{r}_i$ and $\mathbf{r}_j$.

This effective potential is defined to reproduce the total *average energy* of the fluid correctly. One has for the thermodynamic energy

$$E = \tfrac{3}{2}NkT + \langle V(\mathbf{r}_1,\mathbf{r}_2,\ldots\mathbf{r}_N)\rangle$$

$$\langle V\rangle = \frac{1}{2!}\rho^2\mathscr{V}\int_0^\infty v_{aa}(r_{12})g^{(2)}(r_{12})4\pi r_{12}^2\,dr_{12}$$

$$+ \frac{1}{3!}\rho^3\iiint_{\mathscr{V}} V_{aaa}(\mathbf{r}_1,\mathbf{r}_2,\mathbf{r}_3)g^{(3)}(\mathbf{r}_1,\mathbf{r}_2,\mathbf{r}_3)\,d^3\mathbf{r}_1\,d^3\mathbf{r}_2\,d^3\mathbf{r}_3 + \cdots$$

Thus

$$\langle V\rangle = \frac{1}{2!}\rho^2\mathscr{V}\int_0^\infty v_{aa}^{\text{eff}}(r_{12})g^{(2)}(r_{12})4\pi r_{12}^2\,dr_{12}$$

since the symmetrical correlation factor, $g^{(3)}$, equals

$$g^{(3)}(\mathbf{r}_1,\mathbf{r}_2,\mathbf{r}_3) = g^{(2)}(r_{12})g^{[3]}(\mathbf{r}_1,\mathbf{r}_2,\mathbf{r}_3)$$

The $\mathscr{V}$ is the total volume of the liquid.

Care must be exercised in calculating other thermodynamic properties with an effective potential, however. The v_{ij}^{eff} in part has the character

* When the solubility of a b molecule is treated in terms of first creating a cavity in the pure solvent and then by placing a b molecule in this cavity and letting it interact with its environment, the discrepancy between $\overline{v_{ij}^{aa\text{eff}}}_{(\text{soln})}$ and $\overline{v_{ij}^{aa\text{eff}}}_{(\text{pure liq})}$ around b appears in the microscopic surface-tension term.

of a free energy. Thus, even where the fluctuations

$$\left\{V(\mathbf{r}_1,\mathbf{r}_2, \ldots \mathbf{r}_N) - \sum_{i>j}^{N} V_{ij}^{\text{eff}}(r_{ij},\rho)\right\}$$

are negligible, there will still be entropy effects* arising from the density dependence of the potential replacing the V in the configuration integral

$$Z = \int \cdots \int \exp\{V(\mathbf{r}_1,\mathbf{r}_2, \ldots \mathbf{r}_N)/kT\}\, d^3\mathbf{r}_1 \cdots d^3\mathbf{r}_N$$

For a dilute solution of b in a, equations similar to Eq. (13) apply with $\frac{1}{3}$ replaced by $\frac{1}{2}$ or 1 as in Eqs. (11) and (12).

Before evaluating specific effective potentials as a function of distance and liquid structure, we first discuss certain relevant aspects of dilute gas, i.e., "bare" two-body and n-body potentials.

III. THE TWO-BODY POTENTIAL IN THE GAS PHASE

Consider the potential energy (PE) curve of two closed-shell nonreacting molecules. This curve may be derived continuously from the long-range dispersion limit to the short-range steep repulsion region (which also covers the region around the minimum). A quantum theory of such a curve that does not require separate approaches for the long-range and short-range regions has been discussed in references 2 and 3. The basic aspect of such a theory is that it starts with the Hartree-Fock theory of molecular orbitals† (H-F MO) of the composite system of two interacting molecules A and B. One then writes the exact energy at each intermolecular distance, R, as a sum H-F ($E_{\text{H-F}}$) and electronic correlation energies (E_{CORR}). The two-atom picture is recovered by unitary transformations to localized (distorted atom) orbitals at each R which leaves the exact energy unchanged.

Thus, for the *composite* (A ... B) system

$$E(\text{AB}) = E_{\text{H-F}}(\text{AB}) + E_{\text{CORR}}(\text{AB})$$

* See also Linder (Chapter 5 of this volume) on potentials which have partially free-energy character.

† For (AB), and A, and B all having closed shells, MO theory gives dissociation to the appropriate atomic states. The MO wave functions are single determinants at each R.

and hence for the PE curve

$$V(R) = \Delta E = \Delta E_{\text{H-F}}(R) + \Delta E_{\text{CORR}}(R) \tag{15}$$

where for example:

$$\Delta E_{\text{H-F}}(R) = E_{\text{H-F}}(\text{AB};R) - E_{\text{H-F}}(\text{A}) - E_{\text{H-F}}(\text{B})$$

The $\Delta E_{\text{H-F}}(R)$ part of the curve contains the exchange repulsions, and for asymmetrical molecules, the electrostatic (dipole–dipole, etc.), and the dipole–induced-dipole interactions, as well as the analogous higher multipole effects. $\Delta E_{\text{CORR}}(R)$ is mainly responsible for the nonpolar attractions. For large R, distortions in A and B are negligible; in this limit, also upon retaining only the dipole–dipole terms in the expansion of electron–electron repulsions, $\Delta E_{\text{CORR}}(R)$ reduces to the well-known London formula

$$\Delta E_{\text{CORR}}(R) \xrightarrow[\text{large } R]{} E^{(2)}_{\text{dispersion}} \cong -\frac{3}{2}\left[\frac{\delta_{\text{A}}\delta_{\text{B}}}{\delta_{\text{A}} + \delta_{\text{B}}}\right]\frac{\alpha_{\text{A}}\alpha_{\text{B}}}{R^6} \equiv -\frac{C}{R^6} \tag{16}$$

where, e.g., α_{A} is the average polarizability of molecule A and δ_{A} is a multiple of its ionization potential I_{A},

$$\delta_{\text{A}} \equiv \mu_{\text{A}} I_{\text{A}} \tag{17}$$

The μ_{A} is a constant originally taken as 1.0 by London, but empirically

$$2 \gtrsim \mu_{\text{A}} \gtrsim 1 \tag{18}$$

for small molecules.[4]

Though more quantum mechanical PE curves may become available with the advent of computing methods, at present, semiempirical potentials are very useful. The well-known Lennard-Jones (6–12) potential is obtained if in addition to the calculated C or Eq. (16), a reasonable value of σ_{AB} (i.e., the distance of closest approach at zero initial relative kinetic energy), can be guessed at where the parameters are not available from a fit to an empirical gas property [$B(T)$, viscosity, etc.]. However, this potential

$$V_{\text{L-J}}(R) = C[(\sigma^6/R^{12}) - (1/R^6)] \tag{19}$$

is known not to be sufficiently typical of even the rare gases. Since the size of a molecule is very important in determining properties such as the hard spherelike packing in a liquid, radial distribution function, and reduced equations of state,[5] the Kihara potential[6] is much more

applicable. It considers the size as well as the shape of a molecule through a "core" parameter l.

$$V_K(\rho) = C[(\sigma^6/\rho^{12}) - (1/\rho^6)] \tag{20}$$

where ρ is the shortest distance* between A and B in fixed orientations with centers R apart:

$$\rho_{AB} = R_{AB} - (l_A/2)F_A(\theta_A,\psi_A, \ldots) - (l_B/2)F_B(\theta_B,\psi_B, \ldots) \tag{21}$$

F_A, F_B are functions of angles orienting A and B depending on core shape; l_A, l_B are core diameters or lengths. The C in Eq. (20) is still given by Eq. (16) in terms of the averaged polarizabilities of A and B, since for large R, V_K also reduces to $-C/R_{AB}^6$.

Equations (19) and (20) are often written in terms of the minimum point (lowest minimum for V_K) parameters ε and R_0 or ρ_0. In terms of these parameters,

$$R_0 = 2^{1/6}\sigma \quad \text{(L-J)} \tag{22a}$$

$$\rho_0 = 2^{1/6}\sigma \quad \text{(K)} \tag{22b}$$

$$C = 4\varepsilon_{(L\text{-}J)}\sigma_{(L\text{-}J)}^6 \quad \text{(L-J)} \tag{23a}$$

$$C = 4\varepsilon_{(K)}\sigma_{(K)}^6 \quad \text{(K)} \tag{23b}$$

It may be noted that, if an ε and a σ are obtained by fitting, for example, the second virial coefficient $B(T)$ of a gas, the (ε,σ) so obtained from a Lennard-Jones fit need not bear any relationship to the (ε,σ) of a Kihara fit. Rossi and Danon[7] have recently shown that the C's obtained from the Kihara potential for Ar, Kr, Xe, ... are in much closer agreement with calculated C's[8] than the Lennard-Jones fitted [Eq. (23a)] C's. The new C's compared with Eqs. (16) and (17) yield for the heavier rare gases

$$\delta \cong 1.35I \tag{24}$$

For the liquids below, the quasi-spherical approximation will be used with ρ of Eq. (21) averaged over all orientations;

$$\overline{\rho_{AB}} = (R_{AB} - l_{AB}) \tag{25}$$

with

$$l_{AB} \approx (l_A + l_B)/2 \tag{26}$$

* The writer apologizes for the notation ρ_i for density, ρ, for the shortest distance between cores in the Kihara potential. Context and subscript will prevent confusion of the two symbols.

and l_i average core diameters. Plotted against R_{AB}, the minimum of V_K [Eq. (20)] occurs at

$$R^0_{AB} = 2^{1/6}\sigma_{AB} + l_{AB} \tag{27}$$

Danon and Pitzer[7b] relate the R^0 to the l of the Kihara potential semiempirically. For like (A = B) and quasi-spherical molecules:

$$3l_A/(R^0_{AA} - l_A) = 7\varpi + 0.24 \tag{28}$$

where ϖ is the acentric factor[5] ($\varpi = -\log P_r - 1$ and P_r = reduced vapor pressure of the liquid at $(T/T_c) = 0.7$). The correlation, Eq. (28), has been obtained from a dilute gas property, the second virial coefficient.

In Section V, the V_{Kihara}, [Eq. (20)] of the dilute gas will be modified when A and B are in a liquid.

IV. N-BODY POTENTIALS

A system of closed-shell N-molecules with fixed locations $\mathbf{R}_A,\mathbf{R}_B,\mathbf{R}_C \ldots \mathbf{R}_N$, may again be viewed as a composite system with its "supramolecular" H-F orbitals running over all N molecules. It then has the energy

$$E(\mathbf{R}_A,\mathbf{R}_B, \ldots \mathbf{R}_N) = E_{H\text{-}F}(\mathbf{R}_A,\mathbf{R}_B, \ldots \mathbf{R}_N) + E_{CORR}(\mathbf{R}_A,\mathbf{R}_B, \ldots \mathbf{R}_N)$$

E_{CORR} is again in terms of correlations between the various overall H-F orbitals. Taking out the individual H-F and correlation energies of separated molecules, one obtains in principle a $3N$-dimensional potential energy surface

$$V(\mathbf{R}_A,\mathbf{R}_B, \ldots \mathbf{R}_N) = V^{H\text{-}F} + V^{CORR} = \Delta E_{H\text{-}F}(\mathbf{R}_A,\mathbf{R}_B, \ldots \mathbf{R}_N) + \Delta E_{CORR}(\mathbf{R}_A,\mathbf{R}_B, \ldots \mathbf{R}_N) \tag{29}$$

e.g.,

$$V^{CORR} \equiv \Delta E_{CORR}(\mathbf{R}_A,\mathbf{R}_B, \ldots \mathbf{R}_N) \equiv E_{CORR}(\mathbf{R}_A,\mathbf{R}_B, \ldots \mathbf{R}_N) - E_{CORR}(A) - E_{CORR}(B) \ldots - E_{CORR}(N) \tag{30}$$

For an unsymmetrical arrangement of $\mathbf{R}_A,\mathbf{R}_B \ldots \mathbf{R}_N$, a unitary transformation of the supra-H-F MO's to orbitals localized on A,B, ... N is difficult but possible by the methods of Ruedenberg and coworkers.[9] Expansion of these LO's in terms of the various overlap

integrals $S_{K_iL_j}(R_{KL})$, and the corresponding transformations and expansions in $E_{\text{CORR}}(\text{AB} \ldots N)$ would then lead to*

$$V^{\text{H-F}} = \frac{1}{2!} \sum_{\substack{i,j \\ i \neq j}}^{N} V_{ij}^{\text{H-F}} + \frac{1}{3!} \sum_{\substack{i,j,k \\ i \neq j \neq k}}^{N} V_{ijk}^{\text{H-F}} + \cdots \tag{31}$$

and

$$V^{\text{CORR}} = \frac{1}{2!} \sum_{\substack{i,j \\ i \neq j}}^{N} V_{ij}^{\text{CORR}} + \frac{1}{3!} \sum_{\substack{i,j,k \\ i \neq j \neq k}}^{N} V_{ijk}^{\text{CORR}} + \cdots \tag{32}$$

with the sum Eq. (1) and e.g.,

$$V_{ijk}^{\text{CORR}} = V_{(123)}^{\text{CORR}}(\mathbf{R}_i, \mathbf{R}_j, \mathbf{R}_k)$$

For a system of closed-shell molecules like Ar, CCl_4, or even benzene, $V^{\text{H-F}}$ is expected to converge much faster than V^{CORR} since it is a series in the powers and products of overlap integrals $S(R_{kl})$ which drop off roughly exponentially with R_{kl}. Such multiple overlap and exchange effects are essential, especially for spherical molecules, in determining the small energy differences between different ways of packing the molecules into a crystal.[10] The average distance between molecules is larger in most liquids due to volume expansion on melting. There, the multiple overlap and exchange effects would be expected to diminish and average out, although an investigation of these effects for such distances and orientations and a comparison with the other effects below would be desirable.

We shall assume that in liquids, only the longer range n-body potentials remain. Then, the "molecular size" type parameters σ and l in the semiempirical potentials [Eqs. (19)–(21) and (25)] may be taken unchanged from the gas-phase values. Further, in nonpolar liquids with nearly spherical molecules,

$$\underbrace{V_{ijk\ldots}^{\text{H-F}}}_{n} \approx 0 \quad \text{where} \quad n \geq 3 \tag{33a}$$

In a perturbation expansion of V_{ijk}^{CORR}, V_{ijkl}^{CORR}, ... in inverse powers of the R's, one has (as $R^{-1} \to 0$) 3,4, ... n-body dispersion energies. It is consistent with Eqs. (19)–(26) to retain only these terms in Eq. (32),

* The methodology is available and would be analogous to that in refs. 2 and 3, but such a theory apparently has not been completely worked out for all of Eq. (29).

unless it is desirable to give up the simple but very useful semiempirical potentials like $V_{\text{Kihara}}(R)$ and aim for more detailed potential curves in the gas as well as liquid phases. Thus for nonpolar nearly spherical molecules of one kind

$$V(\mathbf{R}_A,\mathbf{R}_B,\ldots\mathbf{R}_N) \approx \frac{1}{2!}\sum_{i,j}^{N}(v_{ij}^{\text{H-F}} + v_{ij}^{\text{CORR}}) + \frac{1}{3!}\sum_{i,j,k}^{N}{}' V_{ijk}^{(\text{disp})} + \frac{1}{4!}\sum_{i,j,k,l}{}' V_{ijkl}^{(\text{disp})} + \cdots \quad (33b)$$

and

$$(v_{ij}^{\text{H-F}} + v_{ij}^{\text{CORR}}) \approx V_{\text{Kihara}}(\rho_{ij})_{(\text{from dilute gas})} \quad (34)$$

The three-body dispersion potential[11] may be written for large distances as:

$$V_{ABC}^{(\text{disp})} \Rightarrow \left[\frac{3}{2}\left(\frac{\delta_A\delta_B}{\delta_A+\delta_B}\right)\frac{\alpha_A\alpha_B}{R_{AB}^6}\right](\Delta'\alpha_c)\left(\frac{R_{AB}^3}{R_{BC}^3R_{AC}^3}\right) \times (1 + 3\cos\theta_A\cos\theta_B\cos\theta_C) \quad (35a)$$

(for large R_{AB}, R_{BC}, R_{AC}). θ_i is the angle with vertex at molecule i, and

$$\Delta' = \frac{\delta_C(\delta_A+\delta_B+\delta_C)}{(\delta_A+\delta_C)(\delta_B+\delta_C)} = \frac{3}{4}\left[1 - \frac{1}{6}(\varepsilon_{AC}-\varepsilon_{BC}) + O\{\varepsilon^2\}\right] \quad (36a)$$

where

$$\varepsilon_{PC} \equiv \frac{\delta_P - \delta_C}{\delta_C} \qquad (P = \text{A or B})$$

The mean excitation energies δ_i that come from the summations in the third-order energy have been assumed to be the same as those from the second order [Eq. (16)].

For like molecules

$$\Delta' = \tfrac{3}{4} \qquad (\text{A} = \text{B} = \text{C}) \quad (36b)$$

For most molecules, the ionization potentials I are around 9–12 eV, so that often Δ' will differ from $\frac{3}{4}$ only within 10%. It may also be noted that Δ' is independent of the μ_i of Eq. (17) even for $\text{A} \neq \text{B} \neq \text{C}$ if μ_i is nearly a constant; then

$$\varepsilon_{PC} \cong (I_P - I_C)/I_C \quad (36c)$$

The higher-order, $n = 4,5,\ldots$ terms may be estimated from Bade and Kirkwood's Drude model formulas[12] and these terms diminish roughly as

$$|V^{(n+1)}/V^{(n)}| \sim (\alpha_i/R^3) \tag{37}$$

where R may be taken as the shortest R_{ij} for an overestimate of the corrections.

Equation (35a) applies at large distances between A,B, and C, i.e., for

$$R_{AB} \gg l_{AB} \qquad R_{BC} \gg l_{BC} \qquad R_{AC} \gg l_{AC}$$

For shorter distances, this interaction is expected to become inadequate in the same ways as the $-C_{AB}/R_{AB}^6$ term. The Kihara potential replaces the R_{AB} by $R_{AB} - l_{AB}$ mainly because between two molecules like CCl_4, the interaction between the peripheral atoms is felt before the center-to-center R_{AB}^6 effect. Because of the 6th power, the nearest atoms contribute most to the overall interaction; hence the $R_{AB} \to \rho_{AB} \approx R_{AB} - l_{AB}$. A similar effect could be taken into account for the three-body forces by summing the primary three-atom dispersion energy over all the triplets of atoms A_i, B_j, C_k between two polyatomic molecules. In such a summation, the angles $\bar{\theta}_{Ai},\ldots$ will change, but in the "quasi-spherical" approximation, they will remain around the central angles $\bar{\theta}_A$, $\bar{\theta}_B$, and $\bar{\theta}_C$. Moreover, the nearest atoms of A, B, C should contribute most to the sum

$$V'^{(\mathrm{disp})}_{ABC} \approx \sum_{i,j,k}^{A,B,C\,\prime} V^{(\mathrm{disp})}_{A_iB_jC_k}$$

Thus it is reasonable to extend the $V^{(\mathrm{disp})}_{ABC}$, Eq. (35a) for molecules with finite cores, such that

$$V'^{(\mathrm{disp})}_{ABC} \approx \frac{C_{AB}}{(R_{AB} - l_{AB})^6}(\Delta'\alpha_c)\frac{(R_{AB} - l_{AB})^3(1 + 3\bar{\Theta})}{(R_{BC} - l_{BC})^3(R_{AC} - l_{AC})^3} \tag{35b}$$

where C_{AB} is still the same as the coefficient in Eqs. (35a) and (16) since for large R's, we must have $V'^{(\mathrm{disp})}_{ABC} \to V^{(\mathrm{disp})}_{ABC}$. Also,

$$\bar{\Theta} = \langle \cos\theta_{Ai} \cos\theta_{Bj} \cos\theta_{Ck} \rangle_{i,j,k}$$
$$\approx \cos\bar{\theta}_A \cos\bar{\theta}_B \cos\bar{\theta}_C$$

with the average, "central" angles. The approximation is shown in Figure 1.

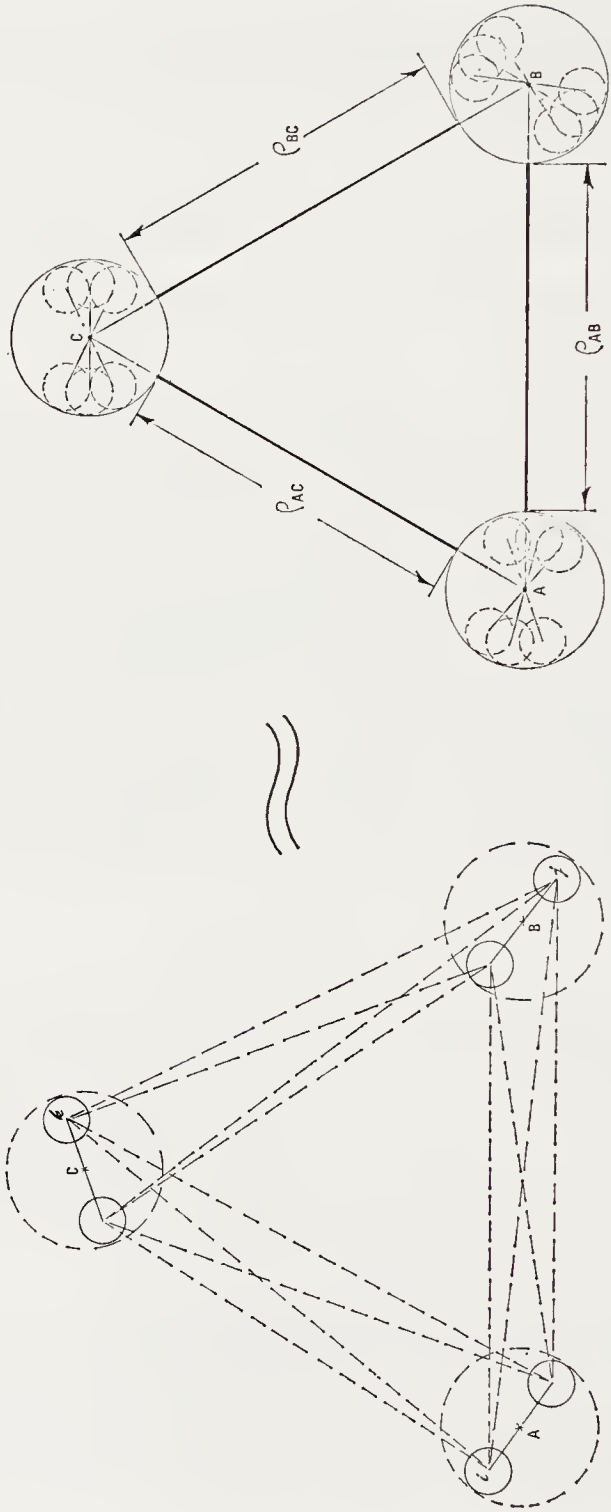

Fig. 1. Approximate three-body potential for polyatomic molecules.

For polar or nonspherical molecules, multipole and induced multipole interactions augment both the pair and the n-body potentials in Eq. (31). In the Stockmayer potential[13] dipole–dipole (μ–μ) terms are added to the dilute gas $V_{\text{L-J}}(R)$. Danon and Pitzer[7b] have added the quadrupole (Q–Q) term to the gas-phase Kihara potential of N_2 and CO_2, examining the effect on the Kihara parameters ε_K and ρ_0 (see also Pople[14]). Such electrostatic effects (as well as multipole-induced multipole effects) arise from the $v_{ij}^{\text{H-F}}$. Thus, comparing this with Eq. (34), we may take the dilute gas-pair potential as

$$(v_{ij}^{\text{H-F}} + v_{ij}^{\text{CORR}}) \cong \{V_{\text{Kihara}}(\rho_{ij}) + V[\mu_i,\mu_j,Q_i,Q_j,\ldots;R_{ij},(\theta,\phi,\ldots)]\}_{(\text{from dilute gas})} \quad (38)$$

for polar and/or nonspherical molecules.

For such molecules, one also has

$$\underbrace{V_{ijk\ldots}^{\text{H-F}}}_{n} \neq 0 \qquad n \geq 3 \quad (39)$$

Well-known n-body effects, such as μ_i inducing a dipole in j (with polarizability α_j) which in turn interacts with a net dipole $\mu_k(\mu_i \to \alpha_j \to \mu_k)$, or a μ_i-induced dipole in j which induces another in k which interacts back with $\mu_i(\mu_i \to \alpha_j \to \alpha_k \to \mu_i)$, are included mainly in Eq. (39).*

In liquids, such effects are usually accounted for by using the macroscopic static dielectric constant $\varepsilon(0)$ or its microscopic modifications. For example, for the sum of $\mu_i \to \alpha_j \to \mu_k$ terms over j's close to i and k, the microscopic $\varepsilon(0)$'s of Kirkwood and Westheimer[15] may be used. Similarly, effects such as $(\mu_i \to \alpha_j \to \alpha_k \to \mu_i)$ come in through the Onsager reaction field[16] which gives the interaction of μ_i with the liquid environment.

For such effects of liquids on the electrostatic parts of intermolecular potentials, one may consult these and other references. The following

* The $V_{ijk\ldots n}^{\text{H-F}}$ are terms in the expansion of the *overall* $V^{\text{H-F}}(\mathbf{R}_A,\mathbf{R}_B,\ldots,\mathbf{R}_N)$ of N molecules. A process like $(\mu_A \to \alpha_B)$ will be included in this term in the sense of the "perturbed individual-molecule Hartree-Fock" method for calculating molecular polarizability. This method gives most of the polarizability although it still omits some of the electron correlation changes in the "perturbed" polarized molecule. A rigorous treatment of multiple polarizations and the relation of these to Eqs. (31) and (32) is not intended in the above discussion.

section evaluates the effect of a liquid medium on the nonpolar interactions starting in Eqs. (33)–(37).

V. EFFECTIVE NONPOLAR PAIR POTENTIALS IN LIQUIDS

For nonpolar interactions and quasi-spherical molecules, the main part of the effective potential in a pure liquid or dilute solution is given by the following equation,

$$v_{AB}^{eff}(R_{AB},\rho_1) \cong v_{AB}(R_{AB}) + \frac{1}{n}\left\langle \sum_{\substack{C\neq A,B \\ liq}} V_{ABC}^{\prime(disp)} \right\rangle_C + \cdots \tag{40}$$

with $n = 3.2$ or 1 depending on whether i,j are solute or solvent molecules. From Eqs. (35) and (40) we have (with finite), cores

$$\left\langle \sum_C V_{ABC}^{\prime(disp)} \right\rangle_C \equiv \frac{C_{AB}}{(R_{AB} - \bar{l}_{AB})}\mathscr{F}' \tag{41a}$$

$$\mathscr{F}' \equiv \Delta' D_1 L'_{AB} \tag{41b}$$

where C_{AB} is the theoretical dispersion coefficient as in Eqs. (19) and (20) and $\Delta' \approx \frac{3}{4}$ is given by Eq. (36a). D_1 is the Clausius-Mosotti expression for the solvent ① with the refractive index n_1,

$$D_1 = \alpha_C/R_C^3 = (n_1^2 - 1)/(n_1^2 + 2) \tag{42}$$

with R_C as the radius of a sphere containing, on the average, one solvent molecule C; i.e.,

$$R_C = (3/4\pi\rho_1)^{1/3} \tag{43}$$

L'_{AB} is defined from Eqs. (35) and (40) as a dimensionless factor that is dependent on the relative sizes of the fixed molecules A,B with radii R_A,R_B and solvent molecules C, and on R_{AB}.

$$L'_{AB} = \left\langle \sum_C \frac{(R_{AB} - \bar{l}_{AB})^3 R_C^3 (1 + 3\bar{\Theta})}{(R_{AC} - \bar{l}_{AC})^3 (R_{BC} - \bar{l}_{BC})^3} \right\rangle_C \tag{44a}$$

$$\bar{\Theta} \equiv \cos\bar{\theta}_A \cos\bar{\theta}_B \cos\bar{\theta}_C \tag{44b}$$

Even when the effect of a third molecule on the potential between A and B [given by Eq. (35)] is quite small, the effect of the liquid on a given V_{AB} may be large [about 15% on two solutes in argon (l), 33% on solutes in CCl_4(l)[17]]. Secondly, it may be noted that because $V_{ABC}^{(3)}$

[Eq. (35)] is a very sensitive function of the (ABC) geometry [attractive for A–B–C linear; repulsive for (ABC) equilateral], the effect will depend sensitively on the local structure of the liquid around A and B. This structure comes in through the $g^{[3]}$ in Eq. (14) and is determined to a large extent by how spheres of radius R_C can be packed around the fixed R_A and R_B spheres a given distance apart.

Equations (35) and (41) are for third-order three-body forces. In higher orders, Bade's estimates[12] indicate that the corrections are still mainly the three-body parts of the 4th and 5th-order energies (see also discussion in ref. 17). From Eqs. (37) and (42) and if one assumes that L'_{AB} is not greatly affected, the resulting higher-order corrections are of such a form that they modify the D_1 in Eq. (41b),

$$\mathscr{F}' \Rightarrow \mathscr{F}^{(3)} + \mathscr{F}^{(4)} + \cdots \cong \Delta' L'_{AB} D'_1 \tag{45a}$$

$$D'_1 = D_1(1 - a_1 D_1 + a_2 D_1^2 - \cdots) \tag{45b}$$

$$D'_1 \approx D_1/(1 + aD_1) \qquad (0 < a < 1) \tag{45c}$$

where $a_1, a_2 \ldots$ are constants $\lesssim 1 [a_1 \approx (4.2 \times 2)/8 \approx 1$, $a_2 \lesssim \approx \frac{1}{8}$ for the Eq. (21) in reference 17 where $R_0 \approx 2R_C$; note also the extra factor of 2 for this case, from $n = 2$ in Eq. (40)] and (D'_1/D_1) an alternating series. Since $D_1 \approx 0.2$ for most liquids, the correction is usually less than 20% and in any case is brought in for the most part through Eq. (45).

A. Evaluation of L_{AB}

For a fluid, the L'_{AB} [Eq. (44)] may be conveniently evaluated in terms of "bicentric" coordinates (see e.g., ref. 1, p. 203). This coordinate system is shown in Figure 2. We have set the fixed distance

$$R_{AB} \equiv R$$

also

$$R_{AC} \equiv s \tag{46}$$

and

$$R_{BC} \equiv r$$

specifying (along with an angle around the R_{AB} axis) a point $\mathbf{r}_c$ in the liquid. The system is cylindrically symmetric around the R axis. The volume element $d^3\mathbf{r}_c$ becomes

$$d^3\mathbf{r}_c = (sr/R)\, dsdrd\phi \tag{47}$$

where ϕ is the azimuthal angle around the AB axis.

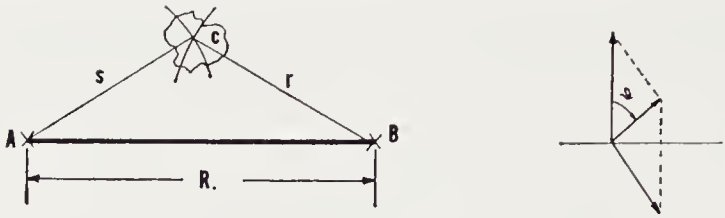

Fig. 2. Bicentric coordinates.

The case L_{AB}, i.e., the L'_{AB} in Eq. (44a) with l_{AB},l_{BC},l_{AC} set equal to zero, corresponds to the use of Lennard-Jones, instead of Kihara potential for the gas-phase pair potential. We shall derive this case below in detail. The resulting B_{ABC}, medium effect, may be applied to Lennard-Jones potential directly. The evaluation of the general case L_{AB} with $l_{AB},l_{BC},l_{AC} \neq 0$ becomes considerably more involved, but will be treated approximately. The three-body potential $V'^{(disp)}_{ABC}$ Eq. (35b) itself is more approximate than Eq. (35a).

For the general case, using the Eqs. (14), (4b), (41), and (44) and $\rho_1 = 3/4\pi R_c^3$ for the number density of the liquid (solvent $\equiv$ *1*), one obtains

$$L'_{AB} = \frac{3}{2}\int_0^\infty \int_0^\infty \frac{(R - l_{AB})^3}{R}\, g^{[3]}(R,s,r)\, \frac{(1 + 3\overline{\Theta})sr\, ds dr}{(s - l_{AB})^3 (r - l_{BC})^3} \tag{48a}$$

Also using the cosine theorem on the three cosines in $\overline{\Theta}$, Eq. (44b),

$$\overline{\Theta} = \frac{(s^2 - r^2 + R^2)(r^2 - s^2 + R^2)(r^2 + s^2 - R^2)}{8r^2 s^2 R^2} \tag{49}$$

For the $l_{AB},l_{BC},l_{AC} = 0$ case, Eq. (48a) reduces to

$$L_{AB} = \frac{3}{2}\int_0^\infty \int_0^\infty \frac{R^2(1 + 3\Theta)}{r^2 s^2}\, g^{[3]}(R,s,r)\, ds\, dr \tag{48b}$$

which will now be evaluated.

The part of the integrand in Eq. (48b) multiplying $g^{[3]}$, is singular at $r = 0$, $s = 0$. However, $g^{[3]} = 0$ at $r = 0$ or $s = 0$ because of the hard sphere-like exclusion of solvent molecules from A and B. The continuum approximation corresponds to setting

$$\begin{aligned} g^{[3]}(R,s,r) &= 1 \quad \text{for} \quad s > s_0 \qquad r > r_0 \\ &= 0 \quad \text{for} \quad s \leq s_0 \quad \text{or} \quad r \leq r_0 \end{aligned} \tag{50}$$

where s_0 and r_0 are the radii of spheres containing the molecules A and B. Then the integration may be carried out by dividing the region outside r_0,s_0 into three parts as shown in Figure 3.

$$L_{AB(contin.)} = (I) + (II) + (III) \tag{51}$$

$$(I) = \frac{3}{2}\int_{s_0}^{1-r_0} ds \int_{1-s}^{1+s} dr\, F(r,s) \tag{52}$$

$$(II) = \frac{3}{2}\int_{1-r_0}^{1+r_0} ds \int_{r_0}^{1+s} dr\, F(r,s) \tag{53}$$

$$(III) = \frac{3}{2}\int_{1+r_0}^{\infty} ds \int_{s-1}^{1+s} dr\, F(r,s) \tag{54}$$

where, in

$$F(r,s) \equiv (1 + 3\Theta)/r^2 s^2 \tag{55}$$

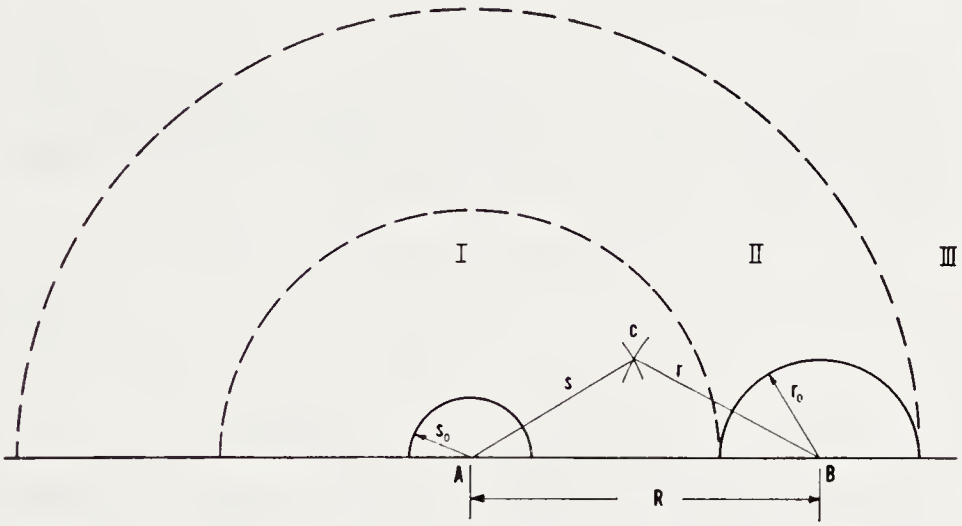

Fig. 3. Three regions of continuum integration outside of excluded regions.

and Eq. (49), we have set $R \equiv 1$, i.e., all distances are measured in units of R so that $r \Rightarrow r/R$, and $s \Rightarrow s/R$.

The indefinite integral over r equals

$$K(a,s) \equiv \int^a F(r,s)\, dr = \frac{1}{8s^4}\left\{\frac{(1+s^2)(1-s^2)^2}{a^3} - \frac{8s^2 + 3(1-s^2)^2}{a} - a^3 + 3(1+s^2)a\right\} \tag{56}$$

This equation gives

$$K[1 + s, s] = 0 \tag{57}$$

$$K[\pm(1 - s), s] = 0 \tag{58}$$

so that one has immediately,

$$\begin{aligned} (\mathrm{I}) &= 0 \\ (\mathrm{III}) &= 0 \end{aligned} \tag{59}$$

for Eqs. (52) and (54). By the equivalence of the choice of the centers of s and r, this result indicates that the remaining part of L_{AB}, i.e., (II) must come out independent of r_0,s_0 and R so long as $R > r_0 + s_0$ in Figure 3. Integrating over s in Eq. (53), after using Eqs. (56) and (57), one obtains

$$L_{AB(\text{contin.})} = -\frac{3}{2}\int_{1-r_0}^{1+r_0} ds\, K(r_0,s) = 2 \quad \text{for} \quad 1 \geq \frac{r_0 + s_0}{R} \tag{60}$$

Down to which values of R the actual L_{AB} in Eq. (48b) will equal that in Eq. (60) will depend not only on the molecular radii R_A and R_B, but also on the solute size. (Note that these considerations apply regardless of l_{AB},l_{AC}, and l_{BC}.) As $R \to \infty$ one must have,

$$\begin{aligned} g^{[3]}(R,s,r) &\to g^{(2)}(s) \quad \text{near A} \\ &\to g^{(2)}(r) \quad \text{near B} \end{aligned} \tag{61}$$

and

$$g^{[3]}(R,s,r) \to 1 \quad \text{for} \quad \begin{cases} s \gg R_A \\ r \gg R_B \end{cases}$$

The minimum R at which L_{AB} still $\cong 2$ may be found in the following way:

The radial distribution function $g^{(2)}(s)$ around a single fixed molecule A displays maxima at radial distances corresponding to the first, second, ... solvation layers as shown in Figure 4. The peaks are roughly at $R_A + R_C$, $R_A + 3R_C$, ... but in a liquid, in general, only the first peak is most pronounced. Beyond this first solvation layer, for our purposes, we already have a nearly random distribution with $g^{(2)}(s) \approx 1$ and $\rho^{(2)}(s) \approx \rho$. If we retain only these first peaks around A and around B, we have

$$L_{AB} = 2 \quad \text{for} \quad R \gtrsim R_A + R_B + 4R_C \tag{62}$$

The reason for this is illustrated in Figure 5 and the proof is as follows:
Let

$$s_0 = R_A + 2R_C$$
$$r_0 = R_B + 2R_C \tag{63}$$

and

$$g_A^{(2)}(s) \cong 1 \quad \text{when} \quad s > s_0$$
$$g_B^{(2)}(r) \cong 1 \quad \text{when} \quad r > r_0 \tag{64}$$

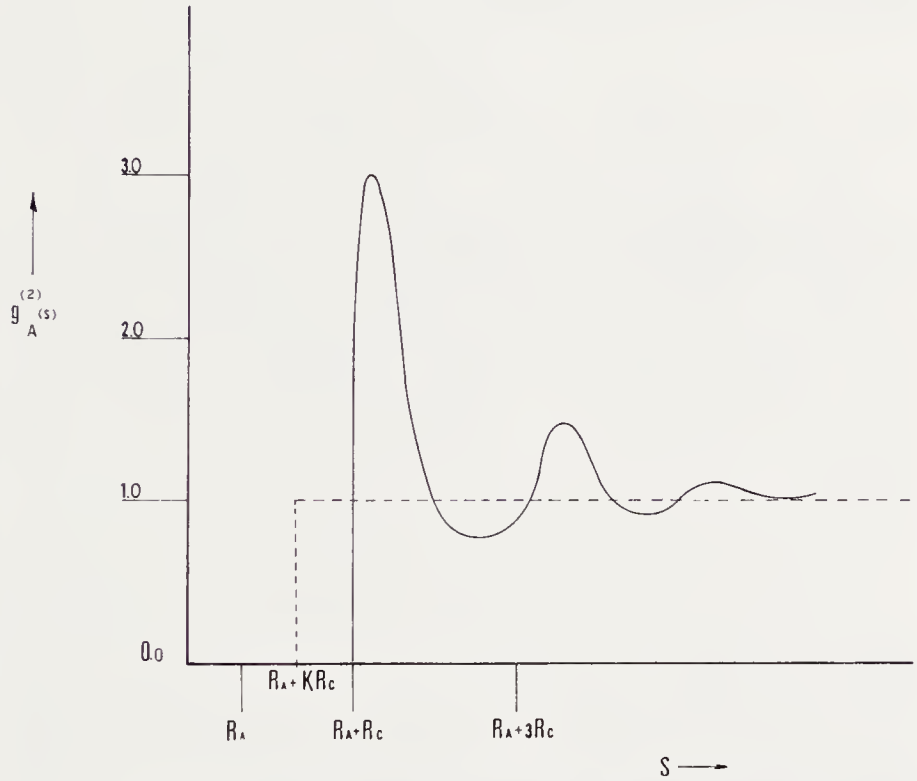

Fig. 4. Radial distribution function and solvation layers.

This implies

$$g^{[3]}(R,s,r) \cong g_A^{(2)}(s) \cdot 1 \quad \text{for} \quad R_A < s < s_0 \quad \text{when} \quad r > r_0$$
$$\cong 1 \cdot g_B^{(2)}(r) \quad \text{for} \quad r_0 > r > R_B \quad \text{when} \quad s > s_0 \tag{65}$$

We have

$$L_{AB}(R \cong R_A + R_B + 4R_C) \cong L_{AB}^{(\text{outer})}(R,r_0,s_0) + L_{AB}^{(\text{inner};s_0)} + L_{AB}^{(\text{inner};r_0)} \tag{66}$$

For the region outside r_0,s_0, from Eqs. (64) and (60),

$$L_{AB}^{(outer)} = 2 \tag{67}$$

So long as the solvation layers around A and B are uncorrelated and still individually spherically symmetric, they do not contribute to L_{AB}. One has (Fig. 5) from Eqs. (65) and (48b),

$$L_{AB}^{(inner;s_0)} = \frac{3}{2}\int_0^{s_0} ds\, g_A^{(2)}(s) \int_{1-s}^{1+s} dr\, F(r,s) \tag{68}$$

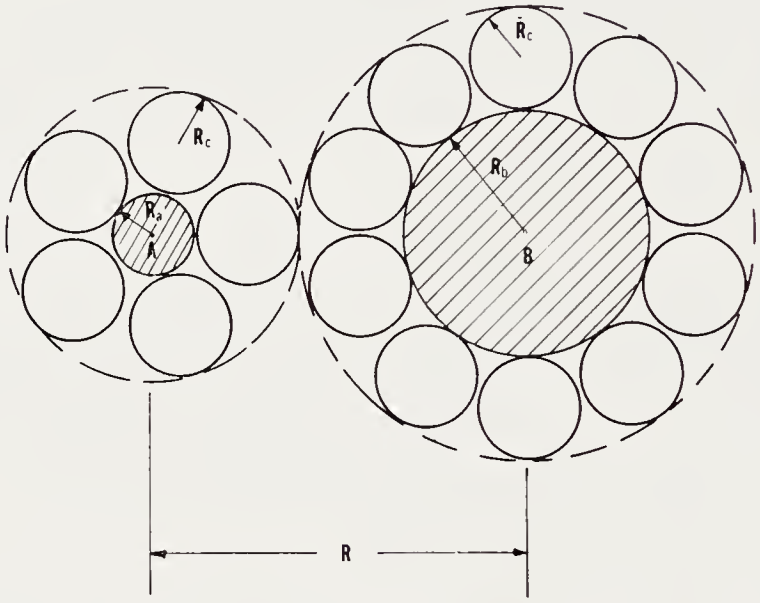

Fig. 5. The distance $R \approx R_A + R_B + 4R_C$ at which L_{AB} begins to deviate appreciably from the constant value 2.

Therefore $L_{AB}^{(inner;s_0)} = 0$ by Eqs. (55)–(58), and similarly for $L_{AB}^{(inner;r_0)}$. We have again used the reduced distances with $R \equiv 1$.

Thus

$$L_{AB}(R \cong R_A + R_B + 4R_C) = 2 \qquad \text{Q.E.D.} \tag{62'}$$

The above argument could have been given of course for a larger "minimum R" if higher accuracy on L_{AB} were desired, by including more of the smaller peaks in $g^{(2)}(r)$ and choosing larger s_0,r_0 in Eq. (64).

Even though there will still be some small fluctuations around the value $L_{AB} = 2$ for somewhat larger R's corresponding to, say, the second and third solvation peaks in $g^{(2)}(r)$, Figure 4, only below

$R \approx R_A + R_B + 4R_C$, are severe deviations from the "continuum value" expected [Eq. (62)].

In previous work[17] the continuum case (also for $l = 0$) was treated by taking the two "cavities" to correspond to the bare molecular volumes ($\mathscr{V}_A = 4\pi R_A^3/3, \mathscr{V}_B = 4\pi R_B^3/3$). An approximate result was obtained using cylindrical coordinates and replacing the A and B spheres with cylindrical cavities of height = base diameter = $2R_A$ and for the case $R_A = R_B$. The dimensionless integral L_{AB} (related to the function $K_{\text{contin.}}$ of ref. 17 by $L_{AB} = (3/4\pi)K_{\text{contin.}}$) was evaluated in part numerically and with this geometry contained some elliptic-type integrals. For large R, its limit is

$$\underset{R\to\infty}{L_{AB(\text{cylindrical cavities})}} = 3/4\pi \times [8\pi(1/\sqrt{2} - 1/3)] = 3\sqrt{2} - 2 = 2.24$$

For shorter R, and with the same R_A, R_B cylindrical cavities, the $K_{\text{contin.}}$ decreased slightly. This decrease seems to be an artifact of the cylindrical model. For the spherical case, the $L_{AB(\text{continuum})} = 2$ [Eqs. (60) and (62)] is a constant, independent of R, r_0, s_0 so long as $R \geq r_0 + s_0$.

For large R, the continuum case has also been treated by several authors from the macroscopic point of view using frequency dependent dielectric constants[18-21] [see also ref. 17, pp. 1731 and 1733–1734 for a discussion of many-body dispersion forces and dielectric constants, $\varepsilon(\nu)$]. This approach has the advantage that it includes the higher-order corrections more accurately than in Eqs. (45b) and (45c), but the disadvantage of requiring a knowledge of the frequency dependence of $\alpha(\nu)$ or $\varepsilon(\nu)$ and the difficulty of taking the solvation structure into account, hence of applying to molecular dimensions. At R's of the order of several solute molecule diameters, solvation structures around A and B begin to overlap and distort each other strongly, requiring a complicated $g^{[3]}(R,s,r,) \neq g^{(2)}(r)g^{[2]}(s)$. An opposite extreme to the continuum approximation is provided for $g^{[3]}$ at small R's, and the case $R_A = R_B = R_C$, by replacing the "local short-range order" around A and B with a closed packed lattice (e.g., fcc). The lattice is taken to extend several solute diameters beyond which again a continuum integration is performed.[17] The $L_{AA}(R_A = R_B = R_C)$, $(L = (3/4\pi)K)$ exhibits sharp peaks and dips at $R/2R_C = 1,2, \ldots$. We shall refer to the results of this "discrete model" more quantitatively below. Clearly in the actual liquid, the maxima, minima will be less sharp and damp out much faster. The packing of solvent molecules around A and B

will result in structural features, oscillations in V_{AB}^{eff} versus R. In the next section, these variations in the L_{AB} depending on R_C/R_A, R_C/R_B and R are evaluated.

B. Evaluation of L_{AB} for $R < R_A + R_B + 4R_C$ and the Role of the Structure of the Liquid

So long as $R > R_A + R_B + 4R_C$ and so long as solvent structure beyond the layers shown in Figure 5 is neglected, solvent shells around A and B remain spherically symmetric and contribute zero to L_{AB}. R can now decrease at first only if some B-shell solvent molecules get in between A-shell molecules as in Figure 6*a*. At this point, the A shell loses its spherical averaging property, it is locked in position although one of the shells, the B shell in the figure, may still be taken as being about the same as the free B shell.

Further decreases in R will be possible only if either the A or the B shells begin to lose some solvent molecules, the remaining molecules taking up the slack. It is convenient to think of this decrease as happening in stages, first A losing solvent molecules as in Figure 6*b*, until there is, on the average, one layer left between A and B as in Figure 6*c*. The B shell then starts loosing solvent molecules making smaller R's possible (Fig. 7*a*). The B-shell loss continues, until the R_A,R_B spheres are in contact (Fig. 7*b*).

The L_{AB} for these $R < R_A + R_B + 4R_C$ situations can be obtained as

$$L_{AB} = L_{AB}^{(inner)}(R,s_0,r_0) + L_{AB}^{(outer)}(R,s_0,r_0) \tag{69}$$

Again we have

$$\begin{aligned} s_0 &\cong R_A + 2R_C \\ r_0 &\cong R_B + 2R_C \end{aligned} \tag{70}$$

however the s_0,r_0 spheres now intersect, since $R < r_0 + s_0$. The $L_{AB}^{(inner)}$ is contributed by those solvent molecules that can be packed into the two intersecting spheres, i.e.,

$$L_{AB}^{(inner)}(R,s_0,r_0) = \left\langle \sum_{C \neq A,B}^{(inner)} \frac{R^3 R_C^3}{R_{AC}^3 R_{BC}^3} (1 + 3\Theta_C) \right\rangle_C \tag{71}$$

This sum can be carried out on the computer by placing an R_C sphere (the "origin") within the r_0,s_0 spheres at a definite location, generating the locations of neighboring spheres by close-packing and summing. When the "origin" molecule is changed in the next run, a slightly different sum results. The average of such values yield Eq. (71).

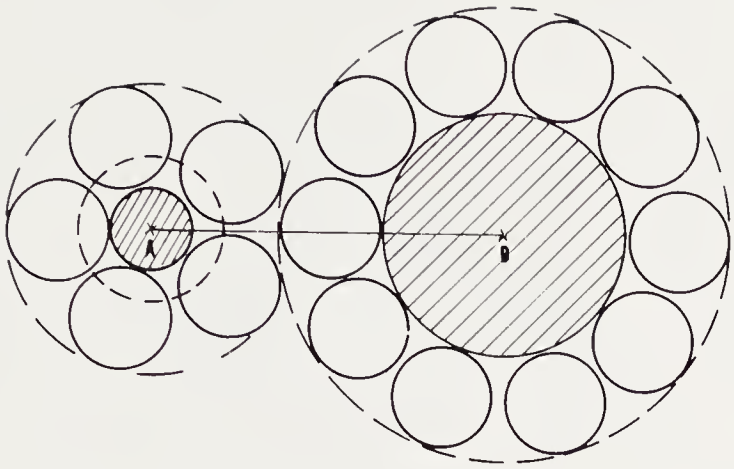

(*a*)

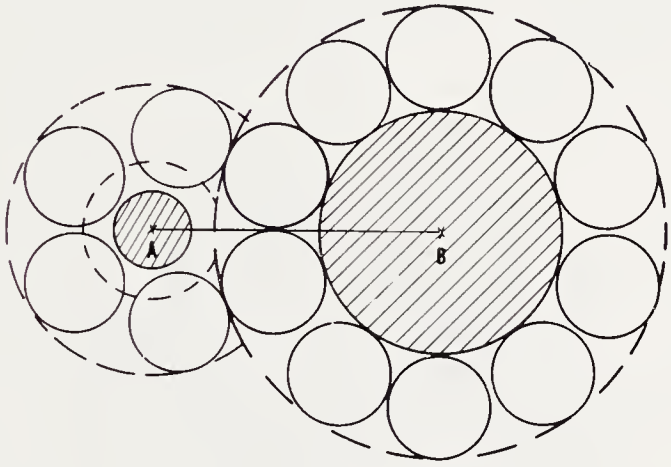

(*b*)

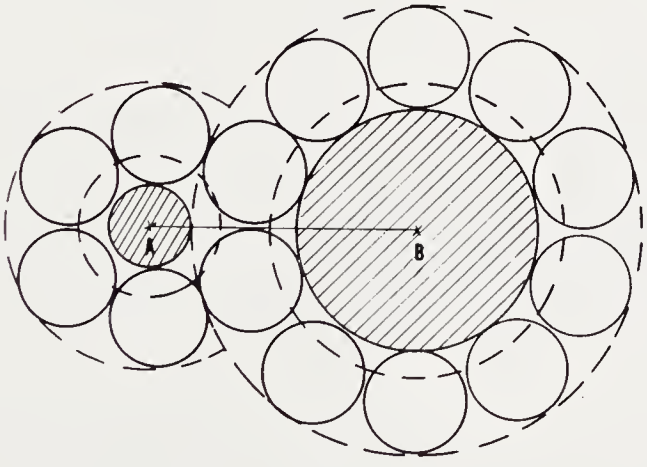

(*c*)

Fig. 6. (*a*) The start of the penetration of the B shell into the A shell. (*b*) Partial A shell intersecting a B shell. (*c*) Distance R at which on the average one solvent layer is found between A and B.

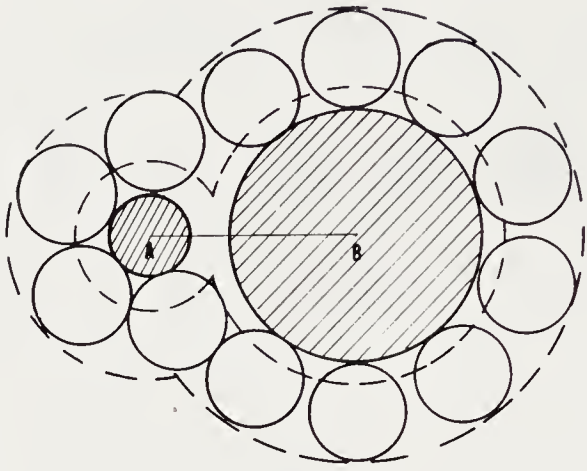

(*a*)

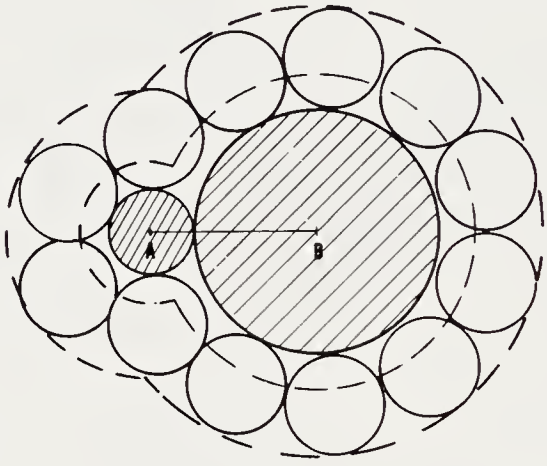

(*b*)

Fig. 7. (*a*) A distance R at which both the A and the B shells are incomplete. (*b*) $R = R_A + R_B$.

The outer region, assuming $g^{[3]} \approx 1$ outside of r_0,s_0, is now given by the following integral (see Fig. 8):

$$L_{AB}^{(\text{outer})}\left(R \equiv 1,\, s_0 \equiv \frac{s_0}{R},\, r_0 \equiv \frac{r_0}{R}\right) = \frac{3}{2}\int_{s_0}^{1+r_0} ds \int_{r_0}^{1+s} dr\, F(r,s)$$

$$= -\frac{3}{2}\int_{s_0}^{1+r_0} ds\, K(r_0,s) \quad (72)$$

$F(r,s)$ is given by Eq. (55) and in the last step, Eqs. (56) and (57) have

been used. A straightforward integration yields

$$L_{AB}^{outer}(R,s_0,r_0) = 1 - \frac{1}{16}\left(\frac{R^2 - s_0^2 - r_0^2}{s_0 r_0}\right)^3 + \frac{3}{4}\left(\frac{R^2 - s_0^2 - r_0^2}{s_0 r_0}\right) \quad (73)$$

$$(|s_0 - r_0| \leq R \leq s_0 + r_0)$$

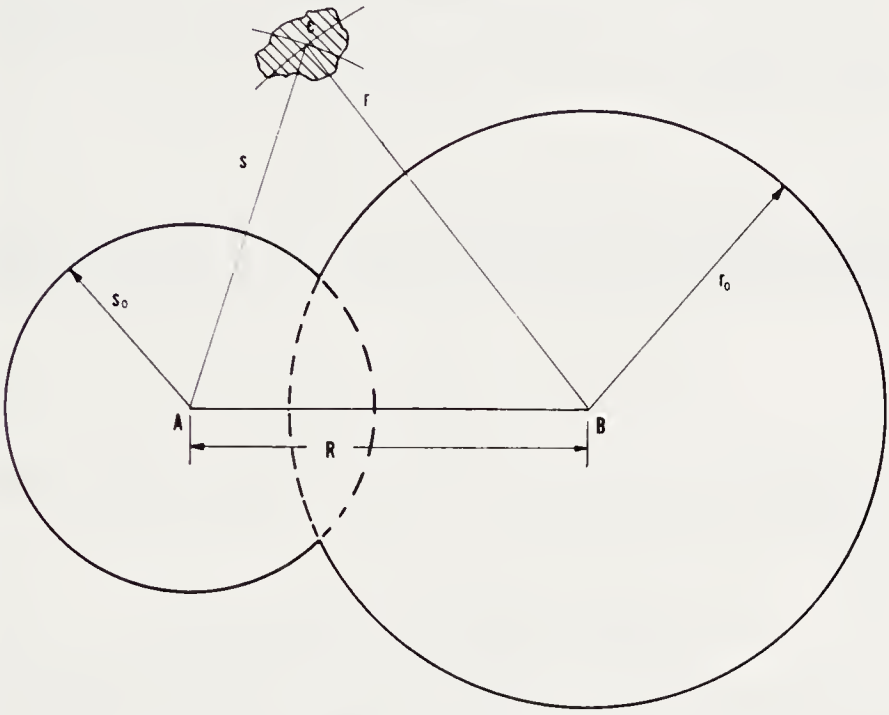

Fig. 8. Evaluation of $L_{AB}^{(\text{outer region})}(R,s_0,r_0)$ for $|s_0 - r_0| \leq R \leq s_0 + r_0$.

For $R = s_0 + r_0$, this reduces to $L_{AB} = 2$, and it approaches zero as $R \to 0$ if $s_0 = r_0$.

We shall evaluate the sum $L_{AB}^{(inner)}(R,s_0,r_0)$ by a method more approximate than the computer summation. This evaluation, nevertheless, yields the basic features of L_{AB} which exhibit oscillations depending on how many solvation layers remain on the average between A and B at any R (Figs. 6–7). Several regions of R are treated separately.

1. *Region 1*

In Figures 6*a* and 6*b*, the solvation shell of A is incomplete; it is intersected by the full shell of B. We have

$$L_{AB}^{(inner)}(R,s_0,r_0) = L_{AB}^{(inner;s_0)} + L_{AB}^{(inner,r_0)} \quad (74)$$

and

$$\begin{aligned} L_{AB}^{(inner,ro)} &\approx 0 \\ L_{AB}^{(inner,so)} &\neq 0 \end{aligned} \tag{75}$$

To obtain $L_{AB}^{(inner,so)}$, we approximate what is left of the solvation layer around A in $g^{(2)}(s)$, Figure 4, by also disregarding the first bump, but compensating for it by starting the integrations from a shorter radius; i.e., replace

$$s_0 \Rightarrow s_p = R_A + \kappa R_C \tag{76}$$

while keeping $r_0 \Rightarrow r_0$, where $0 < \kappa < 1$, a constant for all quasi-spherical solvents. As shown by dotted lines in Figure 4, for A, alone, this would mean

$$\begin{aligned} g_A^{(2)}(s) &= 0 \qquad 0 \leq s < R_A + \kappa R_C \\ &\approx 1 \qquad s \geq R_A + \kappa R_C \end{aligned} \tag{77}$$

This extends the $L_{AB} \approx 2$ region down to $R \geq R_A + R_B + (2 + \kappa)R_C$, though more approximately.

For

$$R_A + R_B + (2 + \kappa)R_C > R > R_A + R_B + \kappa R_C \tag{78}$$

the $s_p = R_A + \kappa R_C$ sphere intersects the $r_0 = R_A + 2R_C$ sphere. As Figures 6*a*–6*c* indicate, the centers of forces of molecules solvating A are now included in $L_{AB}^{(outer)}(R,s_p,r_0)$. Hence, from Eqs. (69) and (73)–(77), one has

$$L_{AB}(R) \approx 1 - \tfrac{1}{16}F^3 + \tfrac{3}{4}F \tag{79}$$

$$F = \frac{R^2 - (R_A + \kappa R_C)^2 - (R_B + 2R_C)^2}{(R_A + \kappa R_C)(R_B + 2R_C)}$$

for

$$R_A + R_B + 2R_C < R \leq R_A + R_B + (2 + \kappa)R_C$$

2. *Region 2*

Just below $R \cong R_A + R_B + 2R_C$, Figure 6*c*, the R_A sphere begins to intersect the B shell. Due to the fact that its spherical symmetry is

destroyed as the average number of B solvent molecules diminishes, it no longer gives $L_{AB}^{(inner,r_0)} = 0$ as it did in the case in Eq. (75). This new contribution is taken into account by now switching the r_0 sphere as well, into the $r_p = R_B + \kappa R_C$ sphere. There is no such actual discontinuity in L_{AB} of course; nevertheless, L_{AB} may be expected to increase in the region

$$R_A + R_B + 2R_C \geq R \geq R_A + R_B + 2\kappa R_C \tag{80}$$

possibly to 2. The model gives $L_{AB} \approx 2$.

3. *Region 3*—$R_A + R_B + 2\kappa R_C > R \geq R_A + R_B$

Here, as shown in Figure 7*a* and 7*b*, the centers of the remaining molecules solvating A and B are taken into account with no inner region left, by choosing

$$\begin{aligned} s_q &= R_A + \kappa R_C \\ r_q &= R_B + \kappa R_C \end{aligned} \tag{81a}$$

Thus, from Eqs. (73) and (81),

$$\begin{aligned} L_{AB}(R) &\approx 1 - \tfrac{1}{16}Q^3 + \tfrac{3}{4}Q \\ Q &= \frac{R^2 - (R_A + \kappa R_C)^2 - (R_B + \kappa R_C)^2}{(R_A + \kappa R_C)(R_B + \kappa R_C)} \end{aligned} \tag{81b}$$

for

$$R_A + R_B + 2\kappa R_C > R \geq R_A + R_B$$

For $R < R_A + R_B$, we may take $L_{AB} = 0$; however, the molecules are not hard spheres. The R_A, R_B, R_C are simply radii for average molecular volumes at a given density. Hence we have another region, $R_A + R_B > R > 0$.

4. *Region 4*—$R_A + R_B > R > 0$

In calculations we choose the average radii R_A, R_B, R_C as follows: R_C is given by Eq. (43) using the density of the pure solvent at the given $T,P;\rho(T,P)$. To make the average radii for individual solutes compatible with the average potential seen in the solvent environment, we take

$$\begin{aligned} R_A &= \{[3/4\pi\rho_A(T_r)]\}^{1/3} \\ R_B &= \{[3/4\pi\rho_B(T_r)]\}^{1/3} \end{aligned} \tag{82}$$

where ρ_A is the number density of *pure* A(l) at the same reduced temperature T_r as the given solvent, and a similar process may be applied for B.

$$T_r = \frac{T(\text{solution})}{T_C(\text{solvent})} = \frac{T_A}{T_C(A)} = \frac{T_B}{T_C(B)} \tag{83}$$

T_C(solvent) is the critical temperature of the pure solvent; T_A,T_B are the actual temperatures at which ρ_A,ρ_B are obtained.

The s_q,r_q used in region 3, Eq. (81), are average solute–solvent distances at T,P. If A and B are placed and fixed at some $R < R_A + R_B$, the distance of each of them from the solvent molecules will still be the average distance $R_A + \kappa R_C$, $R_B + \kappa R_C$. (The $g^{[3]}(R,s,r)$ is the "unsymmetric correlation function" where only the solvent molecules are averaged over.) Thus, it is reasonable in the region

$$|R_A - R_B| = |s_q - r_q| \leq R \leq R_A + R_B \tag{84}$$

to retain the same cavity radii s_q,r_q of Eq. (81) and simply decrease the arbitrarily fixed R. We take $L_{AB}(R)$ equal to Eq. (81b) for $R_A + R_B + 2\kappa R_C > R \geq |R_A - R_B|$ and $L_{AB}(R) = 0$ for $|R_A - R_B| > R > 0$.

The total $L_{AB}(R,R_A,R_B,R_C)$ is summarized in Table I. Figures 9–13 show the function for several values of (R_A/R_C) and (R_B/R_C), and for $\kappa = 0.5$.

TABLE I

The Dimensionless Function $L_{AB}(R,R_A,R_B,R_C)$ Related to the Reduction of A–B Intermolecular Potential in a Liquid
(R_C is radius of average volume per solvent molecule; $\kappa \approx 0.5$)

R	L_{AB}
$\infty > R \gtrsim R_A + R_B + 4R_C$	2
$R_A + R_B + 4R_C > R \gtrsim R_A + R_B + (2+\kappa)R_C$	≈ 2
$R_A + R_B + (2+\kappa)R_C \geq R > R_A + R_B + 2R_C$	$L_{AB} = 1 - \frac{1}{16}F^3 + \frac{3}{4}F$, $F = \dfrac{R^2 - (R_A + 2R_C)^2 - (R_B + \kappa R_C)^2}{(R_A + 2R_C)(R_B + \kappa R_C)}$
$R_A + R_B + 2R_C \geq R \geq R_A + R_B + 2\kappa R_C$	≈ 2
$R_A + R_B + 2\kappa R_C > R \geq \|R_A - R_B\|$	$L_{AB} = 1 - \frac{1}{16}Q^3 + \frac{3}{4}Q$, $Q = \dfrac{R^2 - (R_A + \kappa R_C)^2 - (R_B + \kappa R_C)^2}{(R_A + \kappa R_C)(R_B + \kappa R_C)}$
$0 < R < \|R_A - R_B\|$	0

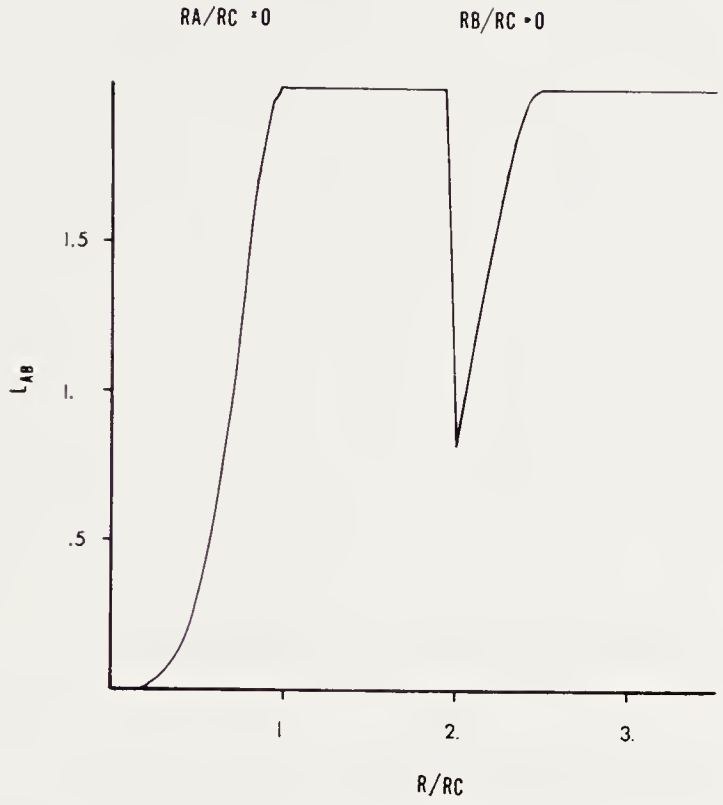

Fig. 9. The dimensionless function $L_{AB}(R/R_C;R_A/R_C,R_B/R_C)$ for $R_A/R_C = 0$, $R_B/R_C = 0$.

The actual curves should look like the dotted free-hand ones rather than the solid lines with the discontinuities. Further minima with decreasing depths could have been obtained by extending the above treatment to second and third solvation shells as well. The dips are most pronounced for $R_A \ll R_C$. They come towards smaller R's and also decrease in size as R_A,R_B are made larger than R_C. Already for $R_A = R_B = R_C$, the first dip is only about 20% below $L_{AB} = 2$. The continuum result applies of course for $R_A,R_B \gg R_C$. Already for $(R_A/R_C) = (R_B/R_C) = 5.0$ (Fig. 12), the continuum result ($L_{AB} = 2$) is sufficient for $R \gtrsim R_A + R_B$.

Timur Halıcıoğlu of the author's laboratory has carried out additional "discrete model" calculations as in reference 17, for the $R_A = R_B = R_C$ case, packing nine layers of solvents in each direction in a simple cubic pattern, in one case placing solvent molecule centers on the R_{AB} line, in another case not. The contribution beyond these layers is negligible for $R \lesssim 8R_C$. In these nonaveraged cases, the depths vary with type of packing, but the minima occur at roughly $R \approx 2R_C,4R_C,6R_C,8R_C, \ldots,$

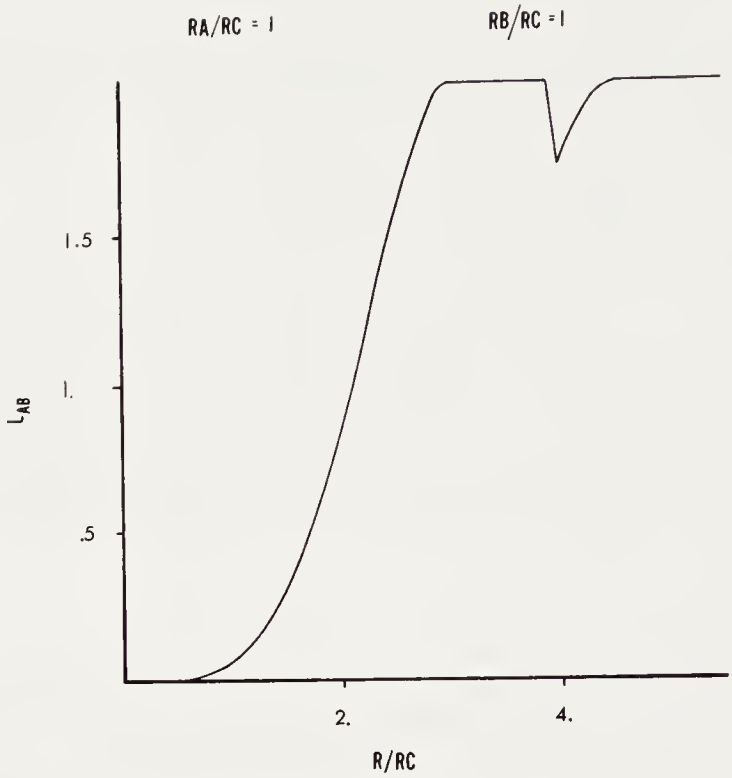

Fig. 10. $L_{AB}(R/R_C;R_A/R_C,R_B/R_C)$ for $R_A/R_C = R_B/R_C = 1$.

the maxima at $\approx 3R_C,5R_C,7R_C, \ldots$. The minima damp out for larger R; the maxima have values of about $L_{AB} \approx 2$. These observations are consistent with the "semicontinuum" result in Figure 10. The discrete $g^{[3]}$ "lattice" model calculations of reference 17 also give for $R_A = R_B = R_C$, with maxima at $R \approx 3R_C,5R_C$ and dips at $R \approx 2R_C,4R_C$ for the fcc packing.* The "$K_{lattice}$" values, too, are consistent with $(4\pi/3)L_{AA}$, once they are defined on the same basis as $K_{contin.} = (4\pi/3)L_{AA}$.† For the choice $\kappa = 0.5$ in Table I and Figure 10, the

* All the "discrete" calculations quoted are for R's corresponding to distances between various two lattice points.

† The $K_{contin.}$ in reference 17 was defined as $\Delta'\alpha_C/\mathscr{V}_C K_{contin.}$ or since $\alpha_C/\mathscr{V}_C^3 = D_1$ and $\Delta' D_1[(3/4\pi)K_{contin.}] \equiv \Delta' D_1 L_{AB}$. For a simple cubic lattice, average molecular volume $\mathscr{V}_C$ is d^3 where d is the nearest neighbor distance. On the other hand for nearly close packing, $\mathscr{V}_C \approx (\pi d^3/6)$. Equation (13) and Table I in reference 17 define "$K_{lattice}$" as the product of $\Delta'\alpha/d^3$ and "$K_{lattice}$." Since liquid corresponds to nearly close packing, this "$K_{lattice}$" will not correspond to $K_{contin.}$, but to $\approx[(6/\pi)K_{contin.}]$. Thus multiplying the values of "$K_{lattice}$" in Table I of reference 17 by $\pi/6$ we get at $R/2R_C$, 3.46 ($L_{AA} = 0.83$), at $R/2 \times 1.41$, 8.85 ($L_{AA} = 2.11$) and so on. Again the maximum value is close to the $K_{contin.}$($L_{AA} = 2$).

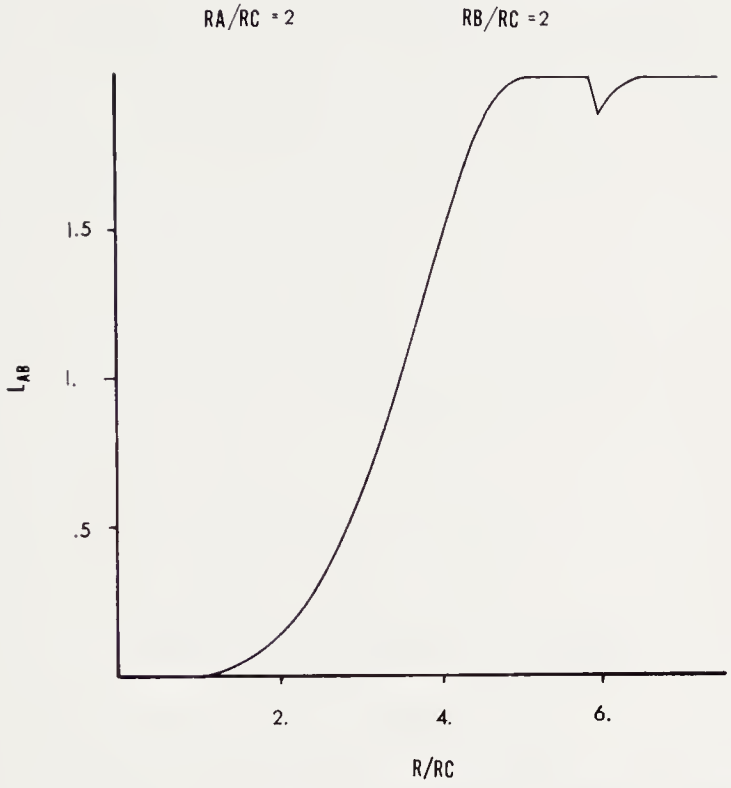

Fig. 11. $L_{AB}(R/R_C;R_A/R_C,R_B/R_C)$ for $R_A/R_C = R_B/R_C = 2$.

"semicontinuum" L_{AB} at $R = 2R_C$ and $R_A = R_B = R_C$ is nearly equal to the discrete fcc model ($L_{AB} \cong 0.83$) value.

VI. SUMMARY OF THE EFFECTIVE PAIR POTENTIAL $V_{AB}^{eff}(R,R_A/R_C,R_B/R_C,\rho_1)$ IN THE LIQUID

A. The Lennard-Jones Case ($l = 0$)

If, for the gas phase, a Lennard-Jones potential [Eq. (19)] has been used, for the modification in the liquid, Eq. (35a), Eq. (40) on, and Table I apply if all the "core" parameters, l_{AB},l_{BC},l_{AC}, are taken as zero also in the liquid.

In this case,

$$V_{AB}^{eff}\left(R;\frac{R_A}{R_C},\frac{R_B}{R_C},\rho_1\right) = C_{AB}\left\{\frac{\sigma_{AB}^6}{R^{12}} - \frac{1}{R^6}\left[1 - \frac{1}{n}\Delta' D_1' L_{AB}\right]\right\} \quad (85)$$

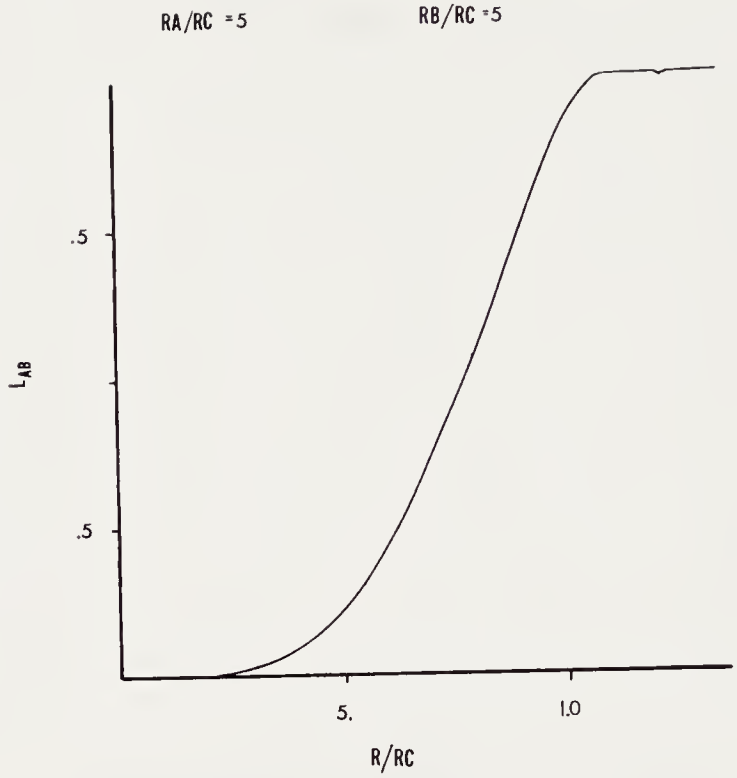

Fig. 12. $L_{AB}(R/R_C;R_A/R_C,R_B/R_C)$ for $R_A/R_C = R_B/R_C = 5$.

or

$$V_{AB}^{eff} = V_{AB}^{L\text{-}J}(R)B_{ABC}$$

$$B_{ABC} = 1 - \frac{1}{n}\frac{\Delta' D_1' L_{AB}}{1-(\sigma_{AB}/R)^6} \qquad \begin{cases} l_{AB} = 0 \\ l_{AC} = 0 \\ l_{BC} = 0 \end{cases} \tag{86}$$

ρ_1 is the number density of the pure solvent and $n = 3$, 2, or 1 depending on whether A and/or B are the same as a solvent molecule C [Eqs. (10)–(12)].

The $L_{AB} = L_{AB}(R;R_A/R_C,R_B/R_C)$ dimensionless function is given in Table I and Figures 9–13. In general, the L_{AB} function will become zero for R's slightly less than the R_{AB}^0 of the potential minimum. Thus, for the repulsive region of the $V(R)$ curve, one has $B_{ABC} \approx 1$ (cf. Sec. IV).

B. The Kihara Case ($\bar{l} \neq 0$)

If for the "bare" two-body potentials between individual solute or solvent molecules, the Kihara potential [Eqs. (20) and (25)–(28)] is

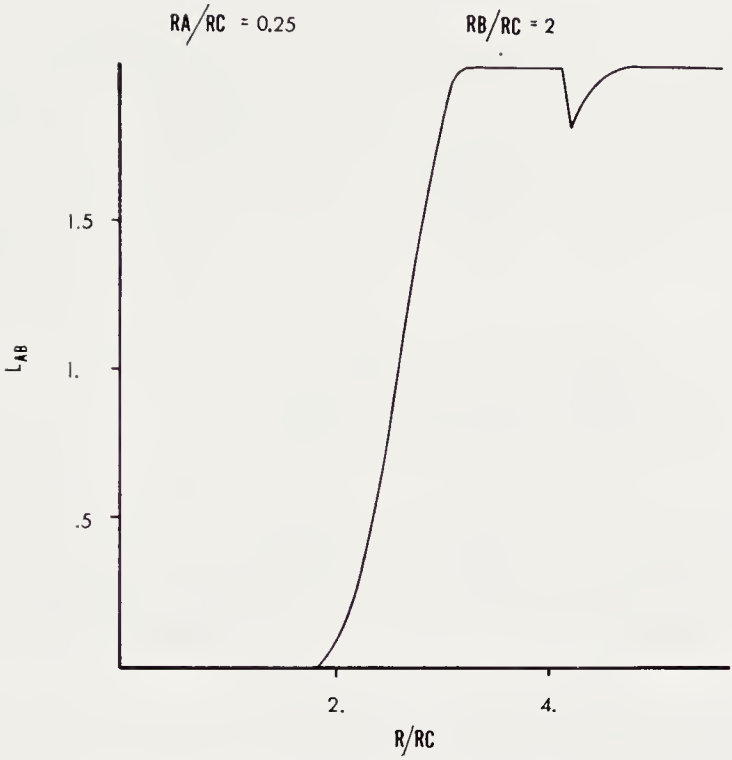

Fig. 13. $L_{AB}(R/R_C;R_A/R_C,R_B/R_C)$ for $R_A/R_C = 0.25$, $R_B/R_C = 2$.

appropriate, in the liquid, the modified form will become

$$V_{AB}^{eff} = C_{AB}\left\{\frac{\sigma_{AB}^6}{\bar{\rho}_{AB}^{12}} - \frac{1}{\bar{\rho}_{AB}^6}\left[1 - \frac{1}{n}\Delta' D_1' L_{AB}'\right]\right\} \tag{87}$$

or

$$\begin{aligned} V_{AB}^{eff} &= V_{AB}^{K}(R) B_{ABC}' \\ B_{ABC}' &= 1 - \frac{1}{n}\frac{\Delta' D_1' L_{AB}'}{1 - [\sigma_{AB}/(R - l_{AB})]^6} \end{aligned} \tag{88}$$

The function L_{AB}' is now given not by Eq. (48b) and Table I, but by Eq. (48a). The overall behavior, the regions and structural features however are expected to be very nearly the same in L_{AB}' as in the $l_{AB} = l_{AC} = l_{BC} = 0$ derivations, L_{AB}' (Table I). These aspects are determined by $g^{[3]}(R,s,r)$ and the sphere-packing models used above apply equally well to L_{AB}' and to L_{AB}. In any given region, the values of L_{AB}' and L_{AB} will differ somewhat.

TABLE II

Effective Intermolecular Nonpolar Interaction in Liquids

$$V_{AB}^{eff}[R,\rho_1,(\rho_A/\rho_1)_r,(\rho_B/\rho_1)_r] = [V_{AB}(R)]_{\substack{\text{dilute gas}\\ \text{(nonpolar part}\\ \text{of potential)}}} \times B'_{ABC}[R,\rho_1,(\rho_A/\rho_1)_r,(\rho_B/\rho_1)_r]$$

For Ar, CCl_4, C_6H_6, ...

$$V_{AB}(R) \cong V_{AB}^{K}(R) \cong C_{AB}\left[\frac{\sigma_{AB}^6}{(R-l_{AB})^{12}} - \frac{1}{(R-l_{AB})^6}\right]$$

$$B'_{ABC} = 1 - \frac{1}{n}\cdot\frac{\Delta' D_1' L'_{AB}(R,(R_A/R_C),(R_B/R_C);l_{AB},l_{BC};l_{AC})}{1-[\sigma_{AB}/(R-l_{AB})]^6}$$

$\Delta' = \frac{3}{4}[1 - \frac{1}{6}(\varepsilon_{AC}+\varepsilon_{BC}) + O\{\varepsilon^2\}]$ or Eqs. (36a) and (24)

$\varepsilon_{PC} = (I_P - I_C)/I_C$; ($P$ = A or B, C = solvent molecule)

$D_1' = D_1/(1+aD_1)$; $D_1 = (n_1^2-1)/(n_1^2+2)$; n_1 = refractive index of solvent at number density $\rho_1(T,P)$
$0 < a < 1$

$L'_{AB}(R;R_A/R_C,R_B/R_C;l_{AB}l_{BC}l_{AC}) \approx L_{AB}(R;R_A/R_C,R_B/R_C)$

$L_{AB}(R,R_A/R_C,R_B/R_C)$ in Table I and Figures 9–13

$R_A/R_C = (\rho_1/\rho_A)_r^{1/3}$; $R_B/R_C = (\rho_1/\rho_B)_r^{1/3}$; ρ_A,ρ_B = no. densities of pure liquid A, pure liquid B at the same reduced temperature as solvent

$$C_{AB} = \frac{3}{2}\frac{\alpha_A\alpha_B\delta_A\delta_B}{\delta_A+\delta_B}; \qquad \delta_i = \mu I_i$$

$$\sigma_{AB} \approx \frac{\sigma_A+\sigma_B}{2}$$

$$l_{AB} \approx \frac{l_A+l_B}{2}$$

C, σ, l gas phase quasi-spherical Kihara parameters

$$R_{AB}^0 = 2^{1/6}\sigma_{AB} + l_{AB};\ \text{empirically}\ R_A + R_B = \frac{1}{2}\left(\frac{3}{4\pi}\right)^{1/3}\left[\frac{1}{\rho_A^{1/3}}+\frac{1}{\rho_B^{1/3}}\right] \equiv \beta R_{AB}^0$$

For Ar,CH_4,CCl_4,C_6H_6,CS_2, ... $\beta \approx 1.15$

$$n = \begin{cases} 3 \text{ for A = B = C; pure liquid or solvent–solvent molecule interaction} \\ 2 \text{ for A} \neq \text{B = C; solute–solvent molecule interaction} \\ 1 \text{ for A = B} \neq \text{C or A} \neq \text{B} \neq \text{C; solute–solute interaction in solvent} \end{cases}$$

Comparing Eqs. (48a) and (48b), we have

$$L'_{AB} \approx \left(\frac{R - l_{AB}}{R}\right)^3 \left(\frac{\bar{s}}{\bar{s} - l_{AC}}\right)^3 \left(\frac{\bar{r}}{\bar{r} - l_{BC}}\right)^3 L_{AB} \tag{89}$$

where $\bar{s}$ and $\bar{r}$ are some average R'_{AC} and R_{BC} distances for the regions of the integrand in L'_{AB}, Eq. (48a) that contribute. It appears that $L'_{AB} \gtrapprox L_{AB}$, and one may take

$$\begin{aligned} L'_{AB} &= L_{AB}(R;R_A/R_C,R_B/R_C,\rho_1) \\ &\quad + L^{(1)}_{AB}(R,R_A/R_C,R_B/R_C,\rho_1;l_{AB},l_{BC},l_{AC}) + \cdots \\ &\approx L_{AB} \end{aligned} \tag{90}$$

The equations needed in calculating the effective pair potential in a dense medium are summarized in Table II.

VII. THE EFFECTIVE POTENTIAL IN OTHER DENSITY RANGES AND PHASES

Equation (87) applies also to molecular crystals with L_{AB} calculated by lattice summations with A,B on various lattice points ($R \to \mathbf{R}_A,\mathbf{R}_B$). The maxima, minima in L_{AB} will now be much sharper and continue over a larger range.

The equation is also applicable over a wider range of densities from the liquid to the gaseous phase [still using e.g., $\langle R_C \rangle = (3/4\pi\rho_1)^{1/3}$]. As density decreases, the structural dips in L_{AB} disappear while L_{AB} itself rapidly drops to zero. Also, $D'_1 \to 0$ for $\rho_1 \to 0$, so that $B_{ABC} \to 1$.

An interesting question is what happens to the theorem of corresponding states with such a density-dependent potential. Over a narrow density range, a slightly modified version would hold, but what form it would take over the entire range (especially in the two-phase region) seems to require investigation.

VIII. EXAMPLES OF POTENTIALS IN SOME NONPOLAR LIQUIDS

Properties needed in the effective potential are listed in Tables IIIa and b for a number of nonpolar liquids. Table IIIa gives the parameters related to the $v_{AA}(R)$ Kihara potential. One may note the comparison of Kihara parameters ρ^0 reported in the literature [mostly from

TABLE IIIa

Molecular Properties

	Ionization Potential (eV)[d]	Polarizability $\alpha(Å^3)$[g]	Acentric factor ($\bar{\omega}$)	Gas phase Kihara potential minimum at ρ^0(Å)	$\sigma^0 = \rho^0 2^{-1/6}$	Quasi-spherical Kihara core diameter, l(Å)	$C_L = \frac{3}{4}\alpha^2 I$ (erg-cm$^6 \times 10^{-60}$) $C = \mu C_L$
N_2	15.70	1.703	0.04[e]	3.3, 3.4, 3.47, 3.6[a]	3.49[h]	3.11[h]	0.604[h]	54.7
Argon	15.75	1.653	−0.002[e]	3.48, 3.45[b]	3.63	3.23	0.273	51.7
Krypton	13.99	2.45	−0.002[e]	3.73[b]	3.87	3.45	0.291	101.0
Xenon	12.16	4.01	+0.002[e]	4.08[b]	4.10	3.66	0.347	233.5
CH_4	12.99	2.567	0.013[e]	3.15, 3.75[a], 3.81[c]	3.78	3.37	0.416	102.8

Benzene	9.25	10.39	0.215[e]	3.0 / 3.4 [a]	3.6	3.21	2.103	1199.0
CCl_4	11.46	10.49	0.255[f]		3.51	3.13	2.370	1517.0
CS_2	10.08	8.44	0.115[f]		3.72	3.31	1.294	863.0
n-Hexane	10.40	11.81	0.309[f]		3.57	3.18	2.860	1743.0
Cyclo-hexane	9.50	10.99	0.262[f]		3.60	3.21	2.489	1377.0

[a] F. Danon and K. Pitzer, *J. Chem. Phys.*, **36**, 425 (1962).
[b] J. C. Rossi and F. Danon, *Discussions Faraday Soc.*, **40**, 97 (1965).
[c] V. McKoy and O. Sinanoğlu, *J. Chem. Phys.*, **38**, 2946 (1963).
[d] D. W. Kiser, *Tables of Ionization Potentials*, Kansas State University, 1960.
[e] K. Pitzer, D. Z. Lippmann, R. F. Curl, C. M. Huggins, and D. E. Petersen, *J. Am. Chem. Soc.*, **77**, 3433 (1955).
[f] Calculated from the equation $\bar{\omega} = -\log P'_r - 1.0$, using reduced vapor pressure data for $T'_r = 0.7$.
[g] From Clausius-Mosotti relation and Table IIIb.
[h] The values in this column are those calculated from Eqs. (28) and (91), as indicated in the text.

$B(T)$ or geometric] and those estimated from Eqs. (27) and (28) and the liquid number density ρ_1 using

$$2R_C = 2(3/4\pi\rho_1)^{1/3} = \beta R^0 \tag{91}$$

and

$$\beta \cong 1.15$$

where

$$R^0 = 2^{1/6}\sigma^0 + l = \rho^0 + l$$

In the last column of Table IIIb, the maximum reduction ($L_{AB} = 2$; $a = 0$; $n = 1$; $\Delta' \approx \frac{3}{4}$) each liquid would cause on some pair of solutes

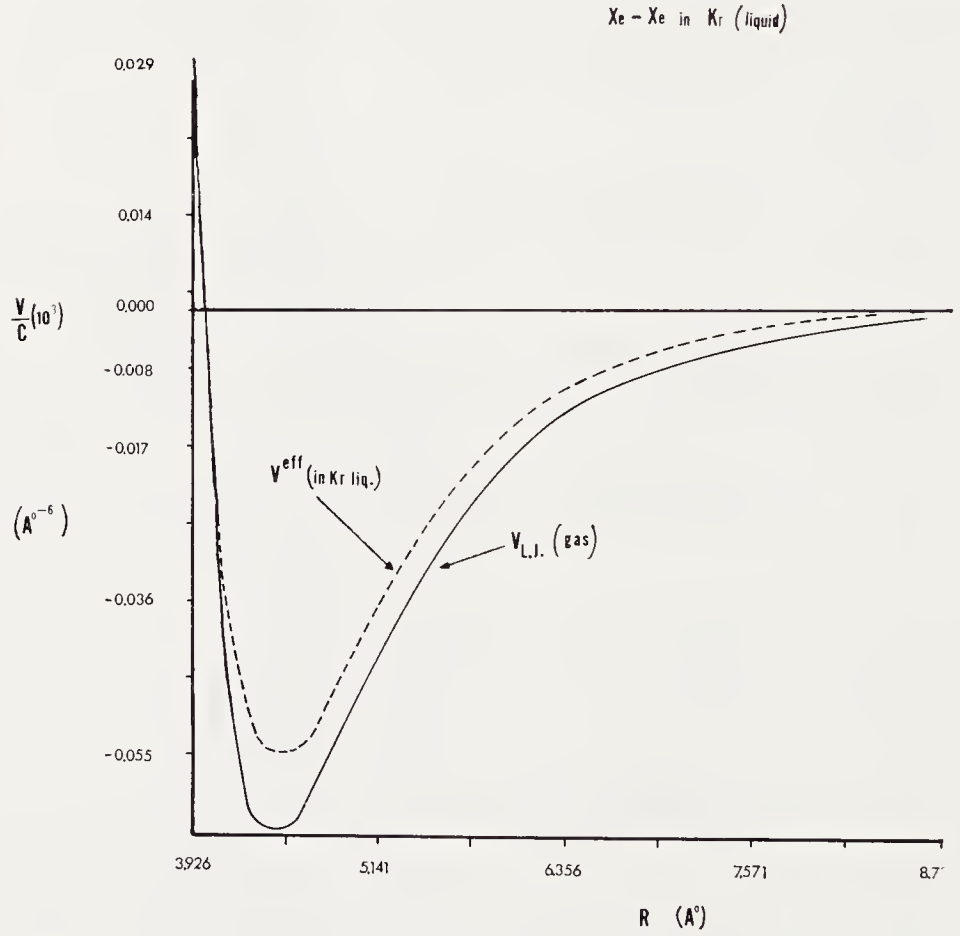

Fig. 14. The effective potential between two xenon molecules in krypton liquid. (l's = 0; $n = 1$, $a = 1$). The Xe–Xe gas phase Lennard-Jones (6-12) potential is also shown (solid line).

immersed in it, is shown. This amounts to, e.g., 22% in Ar (solvent), and 44% in C_6H_6 (solvent). Per pair of pure liquid molecules the amounts are one third as much ($n = 3$).

Examples of effective potential energy curves, $V_{AB}^{eff}(R)$ are shown in Figure 14–16 along with the respective gas phase $V_{AB}(R)$. The equations of Table II and the data in Tables IIIa and b have been used.

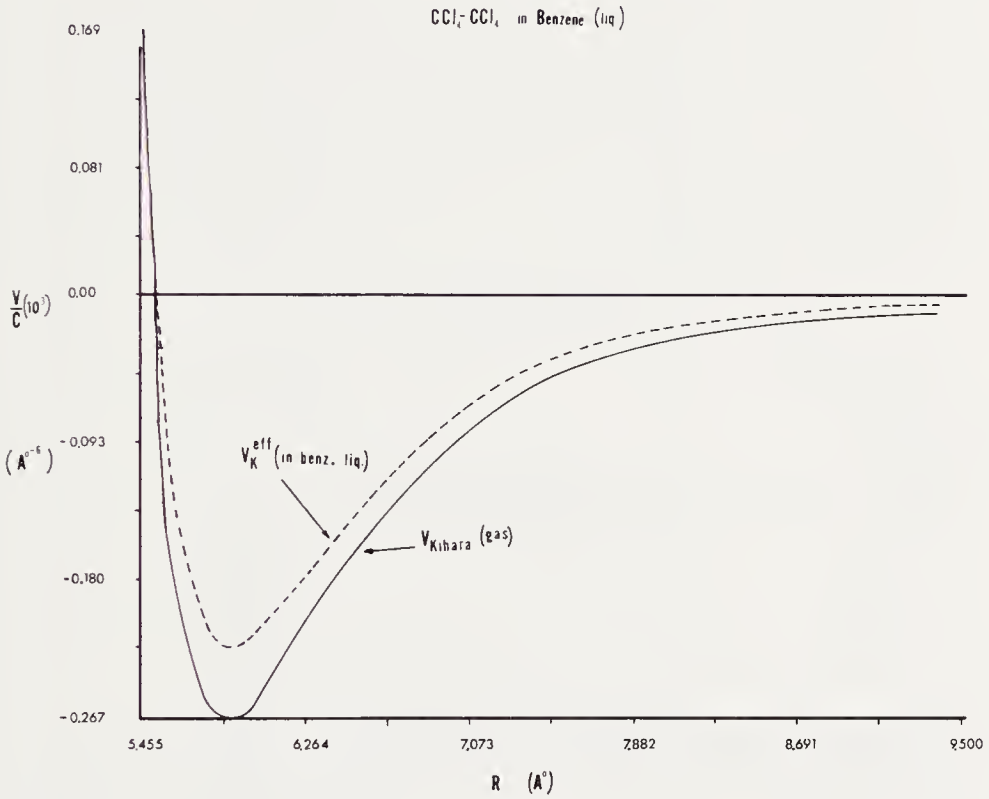

Fig. 15. The effective potential between two CCl_4 molecules in benzene liquid (l's $\neq 0$; $n = 1$, $a = 1$). The CCl_4–CCl_4 gas phase Kihara potential is also shown (solid line).

Figure 14 is for Lennard-Jones-type potentials for the solute as well as solvent molecules: two Xe molecules interacting in Kr (l) [Eq. (86)]. Equations (91) with $l = 0$ have been used for consistency. They give the Xe and Kr Lennard-Jones R^0 parameters quite closely [$R_0(\text{Xe}) = 4.56$ Å; $R_0(\text{Kr}) = 4.14$ Å].[7a]

Figure 15 shows the Kihara-type potentials for two CCl_4 molecules in benzene (l), and Figure 16 shows a CCl_4–benzene interaction in

TABLE IIIb

Properties Needed in the Effective Potentials of Some Liquids

Solvent ①	$T(°K) = 0.534T_C$	Refractive index[a] n_1	$D_1 = \frac{n_1^2 - 1}{n_1^2 + 2}$	Density[a] at T (g/cm³)	$R_A = (3/4\pi\rho_1)^{1/3}$ (Å)	$(\Delta_1' D_1 L_{AB}^{max} = \frac{3}{4} \times D_1 \times 2 = \frac{3}{2} D_1)$ $(a = 0;\ D_1' = D_1)$ $(n = 1;\ A, B \neq C)$
Ne	67	1.20500	0.1309	0.854	2.35	0.196
Argon	81	1.23300	0.1478	1.415	2.24	0.222
Krypton	112	1.28800	0.1801	2.44	2.39	0.270
Xenon	155	1.37100	0.2267	3.09	2.56	0.340
CH_4	102	1.29200	0.1824	0.452	2.41	0.274
Benzene	300	1.49635	0.2923	0.871	3.29	0.438
CCl_4	297	1.45759	0.2727	1.585	3.38	0.409
CS_2	291	1.62704	0.3545	1.267	2.88	0.532
n-Hexane	271	1.38460	0.2341	0.667	3.70	0.351
Cyclohexane	296	1.42470	0.25555	0.776	3.50	0.383

[a] Data for densities and refractive indices (at $\lambda = 5893$Å) from *Landolt-Börnstein, Zahlenwerte und Funktionen*, (6. Auflage); *International Critical Tables*; and *Physical Chemical Constants of Pure Organic Compounds* (Vols. 1, 2).

In some cases, value extrapolated for desired temperature.

benzene (l). In the latter case, one has $n = 2$. The "bare", $V_{AB}^{K}(R)$, Kihara parameters $\sigma,\bar{l},C$ are those calculated from Eqs. (28) and (91). In D_1', Eq. (45), $a = 1$ has been chosen to put in higher order corrections; i.e., $D_1' \cong D_1/1 + aD_1 \approx D_1/1 + D_1$.

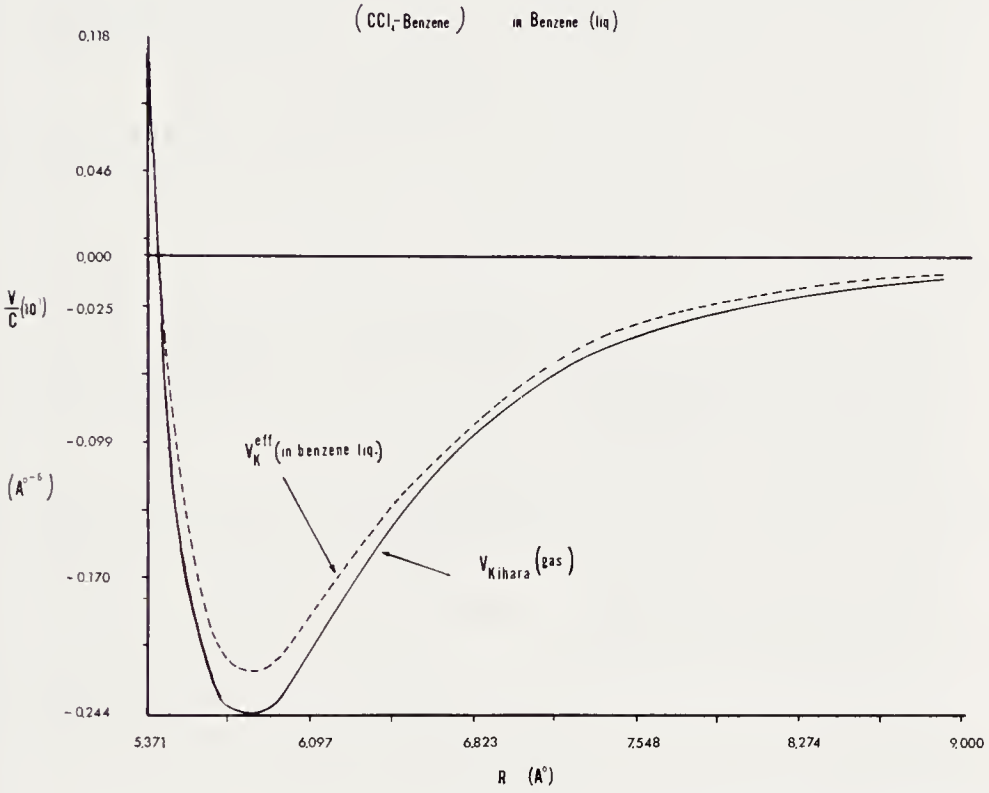

Fig. 16. The effective potential between CCl_4 and a benzene molecule, both in liquid benzene. ($\bar{l}$'s $\neq 0$; $n = 2$; $a = 1$). The CCl_4–benzene two-body gas phase Kihara potential is also shown (solid line).

Acknowledgments

The support of this work in parts by a grant from the National Science Foundation, by an Alfred P. Sloan Foundation Fellowship, and by the Center for Theoretical Studies, Coral Gables, Florida is gratefully acknowledged. It is a pleasure to thank Professor Lars Onsager and Mr. Timur Halıcıoğlu for very helpful discussions, Professor J. O. Hirschfelder for encouraging this work, Professor Behram Kursunoğlu and other members of the Center for Theoretical Studies for their hospitality, and Mrs. Rosa Salom of the University of Miami Computer Center for her help in computations.

References

1. See for example, T. L. Hill, *Statistical Mechanics*, McGraw-Hill, New York, 1956, 179 ff.
2. O. Sinanoğlu, *Interactions* (*Modern Quantum Chemistry*, Vol. 2), Academic Press, New York, 1965, pp. 223–231.
3. N. R. Kestner and O. Sinanoğlu, *J. Chem. Phys.*, **94**, 194 (1966). This article contains an evaluation of the various contributions to the He...He potential curve as a function of the He...He distance, *R*.
4. K. S. Pitzer, *Quantum Chemistry*, Prentice Hall, New York, 1953.
5. K. S. Pitzer, *J. Am. Chem. Soc.*, **77**, 3427 (1955); subsequent series of paper gives equations of state reduced in addition to T_c, P_c with an "acentric factor" ϖ related to molecular size [see Eq. (28)].
6. T. Kihara, *Rev. Mod. Phys.*, **25**, 831 (1953); *Advances in Chemical Physics*, Vol. 5, I. Prigogine, Ed., Interscience, New York, 1963, p. 147.
7. (a). J. C. Rossi and F. Danon, *Discussions Faraday Soc.*, **40**, 104 (1965); (b). F. Danon and K. S. Pitzer, *J. Chem. Phys.*, **36**, 425 (1962).
8. A. Dalgarno and O. Kingston, *Proc. Phys. Soc.*, **78**, 607 (1961); and O. Kingston, *Phys. Rev.*, **135**, 1018A (1964).
9. K. Ruedenberg, *Orbitals* (*Modern Quantum Chemistry*, Vol. 1), Academic Press, New York, 1965, pp. 85–100.
10. L. Jansen and E. Lombardi, unpublished work.
11. (a) B. M. Axilrod and E. Teller, *J. Chem. Phys.*, **11**, 299 (1943); (b) Y. Muto, *Proc. Phys. Math. Soc. Japan*, **17**, 629 (1943); (c) Y. Midzuno and T. Kihara, *J. Chem. Phys.*, **11**, 1045 (1956).
12. W. L. Bade, *J. Chem. Phys.*, **27**, 1280 (1957); W. L. Bade and J. G. Kirkwood, *J. Chem. Phys.*, **27**, 1284 (1957).
13. W. Stockmayer, *J. Chem. Phys.*, **9**, 398 (1941). (Or see J. O. Hirschfelder, C. F. Curtiss, and R. B. Bird, *Molecular Theory of Gases and Liquids*, Wiley, New York, 1954).
14. J. A. Pople, *Proc. Roy. Soc.* (*London*), **A221**, 498 (1954).
15. J. G. Kirkwood and F. H. Westheimer, *J. Chem. Phys.*, **6**, 506 (1938).
16. L. Onsager, *J. Am. Chem. Soc.*, **58**, 1486 (1936).
17. N. R. Kestner and O. Sinanoğlu, *J. Chem. Phys.*, **38**, 1730 (1963).
18. L. P. Pitaevskii, *J. Exptl. Theoret. Phys. USSR*, **37**, 577 (1959); *Soviet Phys. JETP* (*English Trans.*), **10**, 408 (1960).
19. S. Doniach, *Phil. Mag.*, **8**, 129 (1963).
20. A. D. McLachlan, *Discussions Faraday Soc.*, **40**, 239 (1965); *Proc. Roy. Soc.* (*London*), **A274**, 80 (1963).
21. B. Linder, *Discussions Faraday Soc.*, **40**, 164 (1965); *J. Chem. Phys.*, **40**, 2003 (1964).

PART II

EXPERIMENTAL DETERMINATIONS

7. Methods for the Determination of Intermolecular Forces*

E. A. MASON†

Institute for Molecular Physics, University of Maryland
College Park, Maryland

and

L. MONCHICK

Applied Physics Laboratory, The Johns Hopkins University
Silver Spring, Maryland

CONTENTS

I. Introduction 330
II. Quantal Calculations 331
A. *Ab Initio* Calculations 332
B. Semiempirical Calculations 333
1. Long-Range Forces 334
2. Short-Range Forces 338
3. Intermediate-Range Forces 345
C. Model Calculations 346
D. Survey of Accuracy 350
III. Spectroscopic Observations 350
A. Vibration–Rotation Bands 351
B. Predissociation 354
C. Intensity Distribution 355
D. Pressure Effects 357
IV. Beam Scattering 358
A. General Remarks 358
B. High-Energy Beams 361
C. Thermal-Energy Beams 364
1. Rainbows and Haloes 364
2. Shadows 367
3. Glories and Glorified Shadows 369

* This work was supported in part by the National Aeronautics and Space Administration (Grant NsG-5-59), and in part by the Bureau of Naval Weapons, Department of the Navy, under Contract NOw 62-0604-c.

† Present address: Brown University, Providence, Rhode Island.

V. Bulk Properties 370
A. Virial Coefficients 370
B. Transport Coefficients 372
C. Condensed Phases 375
VI. Relaxation Methods 377
VII. Final Remarks 379
References 379

I. INTRODUCTION

Although the concept of intermolecular forces is fundamental to the understanding of a great variety of phenomena, the information which we have on them is surprisingly meager. What information we have comes from rather diverse sources, and ranges from the accurate to the crude. Our purpose is to survey the methods used for the determination of intermolecular forces. Clearly, we cannot go into any one topic in great detail—that is done in other chapters of this volume; we try only to give enough detail to make each method understandable, to give key references, and to discuss the merits and limitations of each method. Because of these limitations, we rely more heavily than usual on arguments of the intuitive or "hand-waving" variety, feeling that it is easier for a reader to add mathematical details himself once the physical basis is clear, instead of vice versa.

It should be noted that no direct way of measuring intermolecular forces is known. What is generally available are measurements of some macroscopically observable quantity having some functional dependence on intermolecular forces. The problem, then, is to extract information about these forces by analysis of the measurements. The degree of success will depend on the accuracy of both the measurements and the theory connecting the forces to macroscopic properties, and on the sensitivity of this connection (i.e., on how deeply the forces are "buried" in the theory). In almost all cases, the intermolecular potential cannot be reconstructed uniquely from the measured property, even in principle. The intermolecular potential may be regarded as having been mapped onto some macroscopic property. Since the mapping may not have a one-to-one correspondence to the property, the inversion of experimental data need not yield a unique potential. Indeed, in several instances, a rigorous proof can be devised showing that a unique potential is not obtained. Therefore, it is generally convenient to assume some mathematical form for the potential, and then to determine the parameters of

the model by comparison of calculated macroscopic properties with experiment. The advent of modern computers is making it possible to consider models which are increasingly intricate, and to attempt the simultaneous fit of a number of different properties over wide ranges. A major danger here is that, as the number of adjustable parameters increases, the ability to determine them unambiguously can easily be surpassed. The procedure then degenerates into complicated curve fitting of little physical significance.

One antidote for this malady is a liberal dose of theoretical guidance in the choice of a mathematical model for the potential, i.e., a judicious mixing of theory and empiricism is sometimes very fruitful. The bottleneck at the moment seems to be that theory is not supplying as many hints as we would like to have in the choice of a model. Most of the good results obtained recently are for one system and are given in the form of numerical tables, and thus are not easily generalized. We will probably have to wait for many more such calculations before a general pattern begins to emerge.

II. QUANTAL CALCULATIONS

In principle, intermolecular forces can be calculated starting from a knowledge of the fundamental constants and the Schrödinger equation. Unfortunately, this program rapidly bogs down in mathematical difficulties (of complexity, rather than of technique); even for systems with just a few electrons, we are forced to make compromises and approximations. In quantal calculations of intermolecular forces, three levels of activity may be distinguished: *ab initio*, semiempirical, and model calculations, each of which is discussed briefly in this section.

It is also often convenient to classify an intermolecular interaction arbitrarily as a long-range, a short-range, or an intermediate-range force; this classification results largely from the different mathematical techniques required in the various regions of molecular forces. This distinction is used universally in qualitative discussions, often with the exact meaning left somewhat ambiguous. For the sake of definiteness, we shall use the classification in the following, somewhat arbitrary, sense. In the long-range region, the electronic charge clouds have negligible overlap; in the short-range region, the charge clouds overlap in varying degree and strongly perturb each other; in the intermediate-range, the charge clouds overlap slightly and perturb each other weakly.

A. *Ab Initio* Calculations

These calculations use only the values of e, m_e, and h, and assume the validity of the Born-Oppenheimer separation of electronic and nuclear motions. For very refined work, spin–orbit coupling and the diagonal elements of the electronic–nuclear coupling have also been included. Without these refinements, exact solutions are possible for one-electron systems and accurate values have been obtained for H_2^+ and HeH^{2+}.[1,2] For two or more electrons, only approximations are available. Much computational effort has been expended on the interaction of two H atoms, largely because of chemical interest, and rather accurate results have been obtained,[3–7] but the situation is much less satisfactory for other atoms. The interaction of two He atoms is probably the most complicated case for which substantial bodies of both experimental data and accurate *ab initio* calculations exist; this case merits some detailed comments because it is the prototype for quantal calculations of intermolecular forces.

At separation distances of about 2 Å or less, the most accurate *ab initio* calculations are probably those of Phillipson,[8] who included up to 64 configurations. For separations greater than 1 Å, these agree reasonably well with the values obtained by Amdur and co-workers from molecular beam scattering experiments. For some time, a large and unexplained discrepancy existed between the calculated and experimental potential energies in the range of separations from 0.5 to 1 Å, but this has now been resolved in favor of Phillipson's values, as discussed in Section IV. For separations greater than 2 Å, however, the situation is less satisfactory. Phillipson's method (molecular orbitals plus configuration interaction) becomes inaccurate for larger intermolecular separations. Although an energy minimum is predicted by the calculations, it is only a few per cent of that deduced from experiment.

At very large separations, the potential varies as $-c/r^6$. The best *ab initio* value of c is probably 1.4586 a.u. as computed by Davison,[9] using a variational procedure and very refined wave functions. This is a lower bound, and is in error by probably less than 1%. Davison also computed the coefficient of the next term, which varies as $-c'/r^8$. An upper limit of $c = 1.540$ a.u. has been obtained by Kestner and Sinanoğlu[10] using *ab initio* many-electron theory.

For intermediate separations, only a few *ab initio* calculations have been reported. Moore[11] and Kim[12] have used wave functions of the

Hirschfelder-Linnett[6] type in a straightforward variational calculation. Their energy minima are only about half that given by experiment, and it seems that, using their methods, a substantial increase in computational effort would be required to improve their results near the minimum. More recently, Kestner and Sinanoğlu[13] have applied *ab initio* many-electron theory to the calculation of the potential energy of two He atoms. Their numerical results are not significantly better than those of Moore and Kim, but their methods may be more easily adapted to computational refinements.

In short, we still lack a sufficiently accurate calculation *ab initio* of the interaction energy of two He atoms over all ranges of nuclear separation.[14] The best estimates of the He–He potential therefore are still based, to a large extent, on experimental measurements of various types. For *ab initio* calculations for more complicated atoms, the situation is much worse and seems likely to remain so for some time. Indeed, a skeptic might question whether such investigations are worth the trouble, seeing that so much computing effort is required to produce a result competitive in accuracy with that obtainable from a good semiempirical method plus experimental data. There is some truth to this, but *ab initio* calculations are still desirable. They form the standard against which approximation schemes and semiempirical calculations are judged; to see this more clearly, we need only recall how much our ideas about chemical bonding and molecular physics have been influenced over the years by the *ab initio* calculations on hydrogen and helium. Moreover, in some situations *ab initio* calculations are the only reliable source of information available, and furnish a valuable guide to experimentation.

B. Semiempirical Calculations

Although completely *ab initio* calculations are extremely difficult, very good results are often obtained, with only a modest amount of effort, by judiciously mixing in some extra experimental information. Sometimes some of the terms occurring in the theoretical expressions for the energy can be related to other experimental quantities. Often these are more easily and accurately determined by experiment than from a calculated wave function. Examples are polarizabilities, oscillator strengths, ionization potentials, and dipole moments. Another approach is to introduce approximations to obtain a simplified theory which, though not quantitatively accurate, is still qualitatively correct and

which indicates the general form of the interaction energy. That is, quantum theory is used only to indicate the probable form of the intermolecular potential, and then experiment is used to evaluate the adjustable constants in an (assumed) force-law model having the proper qualitative behavior. This contribution of theory may seem slight, but actually is absolutely essential.

It is worthwhile to point out that even if computing machines were capable of turning out accurate intermolecular forces by *ab initio* calculations, the useful output would be purely numerical and every new system would have to be treated as a completely new problem. In addition, *ab initio* theories are sometimes so complex as to be unsurveyable. On the other hand, an approximate calculation, even if very crude, often reveals trends and relationships which are usually obscured in an accurate but complex calculation. Physical insight is often obtained from a simple theory, but lost in an elaborate theory.

1. Long-Range Forces

The best examples of highly accurate semiempirical calculations occur in the theory of long-range forces. There is a plausible physical reason for this: when two molecules are far apart, the mutual distortion of their charge clouds is small; it is not surprising, then, that the long-range force can be correlated with the isolated atom (or molecule) properties which are often measurable experimentally. The simplest example of this is the long-range interaction between molecules with nonzero multipole moments (dipoles, quadrupoles, etc.). The dependence of the interaction energy on separation distance and molecular orientation is fairly simple and is, externally, the same in classical and quantum mechanics, the difference lying solely in the determination of the multipole moments which enter the expression. An *ab initio* quantal calculation of the multipole moments is possible in principle once the Schrödinger equation has been solved for the electronic charge distribution, but a completely classical treatment cannot account for the multipole moments at all (or for the stability of an atom, for that matter), and must take them as empirical quantities. In fact, a quantal calculation of dipole and quadrupole moments requires extremely accurate wave functions and so, in practice, it is usually much easier and more precise to take them from experiment. Long-range interactions are thus most accurately obtained by a semiempirical theory using experimental values of the multipole moments.

Long-range electrostatic interactions admittedly are an optimum example of a semiempirical approach. These interactions do not involve any mutual distortion of the electronic charge clouds, and thus are already present in a first-order perturbation calculation of the energy. Since they involve the first-order perturbation to the wave-function, second-order perturbations allow for some distortion, and may be expected to be more difficult to evaluate in terms of the isolated atom and molecule properties only. The simplest long-range second-order force is caused by the induction of a multipole in one molecule by the permanent multipoles of some other molecule. The induced multipoles can then interact with the permanent multipole. Two important interactions of this sort are the dipole–induced dipole interaction (varying as r^{-6}) and the dipole–induced quadrupole interaction (varying as r^{-8}). These interactions are all described by the polarizabilities of the isolated molecules. Once again, it is usually found that, although the polarizability may be calculated from quantum theory but not from classical theory, the easiest and most accurate procedure is to obtain polarizabilities from experiment.

The most important long-range second-order forces are usually the London dispersion forces. These depend in a more subtle way on the distortion of the electronic charge clouds and are more difficult to calculate accurately than the induction forces just discussed. A simple semiclassical description (not to be taken too literally) of the origin of the dispersion forces attributes them to the interaction between the instantaneous dipole moment of a fluctuating dipole in one molecule and the dipole it induees in another. These dipoles are always in phase, producing a net attraction even though the average dipole moment, averaged over all fluctuations, vanishes. An accurate second-order perturbation calculation, due to London, yields as the fundamental formula for the interaction energy $\varphi_{12}(r)$ between atoms 1 and 2,

$$\varphi_{12}(\text{dispersion}) = -\frac{3}{2r^6}\frac{e^4\hbar^4}{m_e^2} \times \sum_{i,j\neq 0} \frac{f_{1i}f_{2j}}{(E_{10}-E_{1i})(E_{20}-E_{2j})(E_{10}+E_{20}-E_{1i}-E_{2j})} \quad (1)$$

where E_{ki} is the energy of the ith electronic state of the kth atom and f_{ki} is the corresponding dipole oscillator strength of the transition from the ground state to the ith electronic state. This is only the leading

term of a series in which the higher terms correspond to quadrupole–induced dipole and higher-order effects, as follows:

$$\varphi_{12}(\text{dispersion}) = -(c_{12}/r^6) - (c'_{12}/r^8) - (c''_{12}/r^{10}) + \cdots \qquad (2)$$

The formulas for the coefficients c'_{12} and c''_{12} have been worked out and are considerably more complicated than Eq. (1).

An *ab initio* calculation would obtain the E's and the f's from solutions of the Schrödinger equation; a semiempirical equation would take them from experiment. The energy levels, E_{ki}, are generally known with great accuracy from spectra; values of f_{ki} are somewhat more difficult to obtain. However, oscillator strengths enter into similar theoretical expressions for experimentally accessible single atom (or molecule) properties such as refractive indices, polarizabilities, Verdet constants, and photoionization cross sections. Moreover, the oscillator strengths must also satisfy certain "sum rules," which are essentially conservation laws. The most widely used rule is based on a type of sum

$$S(k) = \sum_{i \neq 0} f_i (E_i - E_0)^k \qquad (3)$$

with theoretical conditions holding for certain $S(k)$ values; for instance, $S(0)$ must equal the number of electrons in an atom. Other values of $S(k)$ are obtainable from experimental data, such as refractive indices. If enough $S(k)$ values are available, it is possible to synthesize plausible sets of f values from them, and then calculate accurate London constants by direct summation of Eq. (1). Using this procedure, Margenau,[15,16] a number of years ago, calculated the dispersion energy of a pair of He atoms with considerable accuracy. This procedure has since been elaborated and extended to obtain accurate values of c for a number of other pairs of atoms.[17–20] More recently, Bell[21] has shown how c can be written directly in terms of $S(k)$ if the sum in Eq. (1) is approximated in a certain way.

When there are not sufficient data to obtain the necessary E and f values, useful semiempirical results can still be obtained from Eq. (1) with the aid of some simplifying assumptions. The denominator is replaced by a mean energy value and taken outside the summation (the Unsöld closure approximation), or only the leading term of the summation is taken. The energies and oscillator strengths then may be approximately expressed in terms of experimental quantities such as ionization potentials, polarizabilities, diamagnetic susceptibilities, or

the number of valence electrons. Using the closure approximation and polarizabilities, London[22] obtained the formula

$$c_{12} = \tfrac{3}{2}\alpha_1\alpha_2[\bar{E}_1\bar{E}_2/(\bar{E}_1 + \bar{E}_2)] \tag{4}$$

and suggested that the mean energies $\bar{E}_1$ and $\bar{E}_2$ could be approximated by the ionization potentials. Slater and Kirkwood[23] used a variation method, which was later proved to be equivalent to the perturbation method,[24] and they obtained

$$c_{12} = \frac{3}{2}\frac{e^2\hbar^2}{m_e}\frac{\alpha_1\alpha_2}{(\alpha_1/N_1)^{1/2} + (\alpha_2/N_2)^{1/2}} \tag{5}$$

where N_1 and N_2 are the numbers of electrons in the valence or outer subshells of the atoms. Finally, the Kirkwood-Müller formula is[25,26]

$$c_{12} = (6m_e c_{\text{light}}^2)\alpha_1\alpha_2/[(\alpha_1/\chi_1) + (\alpha_2/\chi_2)] \tag{6}$$

where χ_1 and χ_2 are the atomic diamagnetic susceptibilities. Extensions and refinements of such simple closed formulas have been discussed by Salem.[27]

Comparison of the foregoing results with accurate values of c_{12} obtained by direct summation of Eq. (1) shows that the London formula [Eq. (4)] gives results that are somewhat low, the Kirkwood-Müller formula [Eq. (6)] gives results that are much too high (probably because of its neglect of correlation[27]), and the Slater-Kirkwood formula [Eq. (5)] gives results which are remarkably accurate.[20]

Even when formulas like Eqs. (4)–(6) are not very accurate on an absolute basis, they suggest useful relationships which may be more accurate. For instance, if c_{11} and c_{22} are known, the value of c_{12} may be predicted from Eq. (4) as

$$c_{12} = (c_{11}c_{22})^{1/2}[(\bar{E}_1\bar{E}_2)^{1/2}/\tfrac{1}{2}(\bar{E}_1 + \bar{E}_2)] \approx (c_{11}c_{22})^{1/2} \tag{7}$$

the last step following because $\bar{E}$ often does not vary much from molecule to molecule. Results from Eq. (7) agree quite well with the accurate values of c_{12} that Dalgarno and Kingston obtained by direct summation of Eq. (1).[28] Even more accurate results can be obtained from the Slater-Kirkwood equation [Eq. (5)] by taking N_1 and N_2 as adjustable constants calculated from known values of c_{11}, c_{22}, α_1, and α_2.[29]

The semiempirical theory has also been applied to cylindrical molecules,[27] and although the prediction of the absolute value of c_{12}

(averaged over all angles) is poor, the dependence of c_{12} on the relative orientation of the two molecules is predicted with satisfactory accuracy. This appears to be a useful approximation if $\bar{c}_{12}$ is taken as an adjustable parameter. Only recently has the orientation dependence of c_{12} been calculated on an *ab initio* basis.[30]

Finally, second-order perturbation theory predicts that the London dispersion energies are pairwise additive, nonadditive effects not appearing until the third order. This suggests that dispersion energies between polyatomic molecules might be built up by summation over pairs of constituent atoms, groups of atoms, or bonds. Such semiempirical procedures lead to good correlations among measured properties of paraffin hydrocarbons[31,32] and fluoromethanes,[33] for example. Pitzer[34] has given a good review of correlation procedures based on semiempirical dispersion energies. This procedure also works for the prediction of second virial coefficients.[35] The validity of the central assumption—local additivity of the different pieces of large molecules—has been investigated theoretically by Longuet-Higgins and Salem.[36]

2. *Short-Range Forces*

In contrast to long-range forces, relatively little general theoretical information is available on short-range forces. The physical origin of short-range forces is clear enough, but detailed calculations usually have been either inaccurate or too complicated to be generally helpful. Nevertheless, a good deal of useful information can be pieced together from rough semiempirical calculations plus judicious use of experimental data. A simple physical picture can be given in terms of the Hellmann-Feynman electrostatic theorem and the Pauli exclusion principle. According to the electrostatic theorem, which holds for the exact solution of the clamped-nuclei Schrödinger equation, the force acting on any one nucleus is just the classical Coulomb interaction between it and the other nuclei and the electronic charge distribution. At distances short enough for an appreciable overlap of the charge cloud, large distortions in these distributions are required by the Pauli exclusion principle. (Some distortion also results from the Coulomb repulsion among the electrons, but this appears to be a secondary effect.) In the interaction of two atoms with closed electronic shells, the net effect is that the electronic clouds of the two atoms tend to avoid each other. This leads to a decrease of charge density in the region between the atoms and a reduction of the screening of the nuclear charges by the

electrons, and the net effect is a repulsion between the atoms. In the case of the interaction of atoms with incomplete shells, on the other hand, there can also be an enhancement of the electron distribution in the region between nuclei, leading to the formation of a chemical bond. Thus, short-range atomic and molecular repulsions have the same origin as do chemical bonds. It may be expected, therefore, that information on one effect may be applied to the other. Short-range forces are often called overlap or valence forces, and sometimes exchange forces. The last term results from the particular mathematical way in which approximate wave functions are constructed to satisfy the Pauli principle.

Short-range forces appear in a first-order perturbation calculation. Unfortunately, when one sets up an approximate wave function which satisfies the Pauli principle, most of the electrons have to be treated individually and the calculations become very complex. For atoms with closed shells, all that can be seen in a general way are sums of terms like $P(r)e^{-ar}$ where $P(r)$ is a relatively slowly varying function of r (such as a polynomial). The simplest function which might reasonably be expected to mimic this behavior is a single exponential, and therefore the first-order exchange energy is often written as

$$\varphi(\text{exchange}) \approx Ae^{-ar} \tag{8}$$

where A and a are constants. *Ab initio* calculations of φ(exchange) may often be represented accurately over remarkably long ranges of r by Eq. (8). In most approximate calculations, the parameters appearing in the exponents are the so-called effective nuclear charges or orbital exponents. The scattering experiments of Berry, cited later, correspond almost exactly to an exponential law. Examination of the formulas suggests a combination rule connecting the effective nuclear charges for the 1–2 interaction to the values for the 1–1 and 2–2 interactions,[37]

$$a_{12} = \tfrac{1}{2}(a_{11} + a_{22}) \tag{9}$$

More recently,* the theoretical problem has been approached from a different point of view. Working outward from the united atom at $r = 0$,

$$\varphi(\text{exchange}) \approx (Z_1Z_2/r)P(r)e^{-ar} \tag{10}$$

where Z_1 and Z_2 are the nuclear charges and $P(r)$ is again a relatively

* For a review of the united atom expansion, see reference 38.

slowly varying function of r. It was once thought that $P(r)$ could be represented as a polynomial but subsequent work has shown the presence of a nonanalytic term of the form $r^6 \ln r$.[38] In any case, Eq. (10) suggests as another useful combination rule,

$$A_{12} = (A_{11}A_{22})^{1/2} \tag{11}$$

The combination rules given by Eqs. (7), (9), and (11) seem remarkably successful,[39] even though the semiempirical theories suggesting them are too crude to give the absolute values of the constants with any accuracy. Moreover, Eqs. (9) and (11) may be combined into the single empirical rule, which may be considered separately from the assumption of the forms postulated by Eq. (8) or (10),

$$\varphi_{12}(\text{exchange}) = [\varphi_{11}(\text{exchange})\varphi_{22}(\text{exchange})]^{1/2} \tag{12}$$

This has been verified experimentally in several cases by the scattering of fast atomic beams in gases.[40,41]

In short, quantum theory is used largely to predict relations among short-range intermolecular forces, rather than to make absolute calculations. Such relations become especially valuable when interactions between atoms with incomplete electron shells are considered, for here one may be concerned with many potential energy curves, corresponding to all the possible molecular states involved.[42] In the best known examples, for instance, two ground-state hydrogen atoms can interact in either of two ways corresponding to the $^1\Sigma_g^+$ and $^3\Sigma_u^+$ states of H_2, and two ground-state N atoms in any of four ways corresponding to the $^1\Sigma_g^+$, $^3\Sigma_u^+$, $^5\Sigma_g^+$, and $^7\Sigma_u^+$ states of N_2. Information about such multiple interactions is needed for such problems as the calculation of transport properties of dissociated and ionized gases, theories of flames, shocks and detonations, and some upper atmosphere and astrophysical phenomena. The procedure used to obtain useful relations begins in the same way as before, i.e., with the writing of a fairly simple approximate wave function, and the obtaining of the energy as a series of integrals involving the wave function and the individual electron and nuclear interactions. Now instead of evaluating all the integrals, one notices that when the procedure is repeated for all other possible molecular states, the same few integrals usually occur in the energy expression for each state. If several of the energy curves are already known experimentally, enough relations may be available to

estimate the integrals. Using these, one may construct the remaining potential energy curves.

To take a specific example, the interaction energy of two ^{2}S H atoms is given by simple Heitler-London valence-bond theory as[43]

$$\varphi(\text{exchange}) = (Q \pm J)/(1 \pm S^2) \tag{13}$$

where Q has come to be known as the coulombic integral, J the exchange integral, and S the overlap integral. The positive signs correspond to the $^1\Sigma_g^+$ state and the negative signs to the $^3\Sigma_u^+$ state (the numerical value of J is negative). Neglecting S^2, since it is usually small except at very small separations, Q and J may be determined in terms of the potentials, which are known:

$$Q = \tfrac{1}{2}[\varphi(^1\Sigma_g) + \varphi(^3\Sigma_u)] \tag{14}$$

$$J = \tfrac{1}{2}[\varphi(^1\Sigma_g) - \varphi(^3\Sigma_u)] \tag{15}$$

These formulas can be given an improved theoretical basis by suitable redefinition of Q and J,[44a] but this refinement need not concern us here. As a rough first approximation we might also neglect Q, since this is usually much smaller than $|J|$ at the internuclear separations of interest. This predicts that the two potential curves are mirror images of each other across the r axis. This is in fact approximately true, at least for distances greater than the equilibrium separation of the bound state $^1\Sigma_g^+$. An improved estimate, to cover small r as well, would fit $\varphi(^1\Sigma)$ to a two-term expression of the form

$$\varphi(^1\Sigma) = f(r) - g(r) \tag{16}$$

Identifying $f(r)$ with Q and $g(r)$ with $-J$, we would then predict $\varphi(^3\Sigma)$ to be

$$\varphi(^3\Sigma) = f(r) + g(r) \tag{17}$$

There is, of course, no unique way of making the decomposition in Eq. (16) and the success of the method depends on the judgment of the investigator. This sort of approximation has been used by Keyes[44b] to predict potential energy curves for excited states of diatomic molecules from known ground-state curves. Keyes used Morse functions in which $f(r)$ and $g(r)$ were exponential functions of r, with the exponential of $f(r)$ twice that of $g(r)$. Many other empirical potential functions[45] are available for this procedure; several different ones have been used to

predict short-range intermolecular forces in Li + H gas mixtures for use in estimating transport coefficients at high temperatures.[46]

To continue the example to larger r, an improved estimate would include the dispersion energy, as follows:

$$\varphi(r) \approx \pm J + \varphi(\text{dispersion}) \tag{18}$$

Q and S dying off rapidly at large r. Although this expression joins the long-range formula more or less smoothly, it is not quite consistent, as is pointed out in the next section. Nevertheless, it may be used to infer the relation,

$$\varphi(\text{dispersion}) = \tfrac{1}{2}[\varphi(^1\Sigma_g) + \varphi(^3\Sigma_u)] \tag{19}$$

which possibly has a greater range of validity. Kolos and Wolniewicz,[4] using their accurate *ab initio* calculations on H_2, have shown that φ(dispersion) estimated from Eq. (19) agrees well with φ(dispersion) calculated by Eq. (2). Thus, in the interaction of all hydrogenlike atoms, e.g., the alkali metals, one could estimate $\varphi(^3\Sigma)$ from a knowledge of $\varphi(^1\Sigma)$:

$$\varphi(^3\Sigma) \approx -\varphi(^1\Sigma) + 2\varphi(\text{dispersion}) \tag{20}$$

where φ(dispersion) is calculated by the methods already discussed. This will yield accurate results in regions where Q and S may be safely neglected.

The idea of using experimental information to evaluate coulombic and exchange integrals, as in Eqs. (14) and (15), is not new. It was first used over 30 years ago by Polanyi and Eyring to calculate the potential energy surface for the H + H_2 reaction.[47] They first obtained Q and J from a Morse curve representation of the energy of the ground state of H_2, and then synthesized the potential for the linear H_3 complex by means of the London formula,[47]

$$\varphi_{123} = (Q_{12} + Q_{23} + Q_{31}) \pm 2^{-1/2}[(J_{12} - J_{23})^2 + (J_{23} - J_{31})^2 + (J_{31} - J_{21})^2]^{1/2} \tag{21}$$

in which overlap and multiple-exchange integrals have been neglected. In this approximation, φ_{123} involves only the integrals for all possible atom pairs. The earliest results obtained by this method were not very accurate, probably because of the use of Morse curves, but with more accurate data becoming available to evaluate Q and J, the method has

been revived recently. The best estimate of the $H + H_2$ potential energy surface probably is still the one given by this semiempirical method. (See ref. 48 for the most recent work in this area.) In another development, more elaborate formulas than Eq. (21) have been proposed.[49] These ideas have also been applied by Eyring[50] to interatomic interactions within a single molecule in his discussion of hindered rotation in ethane.

The application of these ideas to the calculation of interatomic forces is much more recent, however,[51] the impetus coming from the need for knowledge of gas properties at very high temperatures, where interactions between molecular fragments are important. Equation (13) for the interaction of two H atoms is just a particular case of a more general approximation occurring in simple valence-bond theory. According to this approximation, called the perfect-pairing approximation, the interaction between the two atoms is[43,50]

$$\varphi(r) = \sum_{\substack{\text{orbitals with} \\ \text{paired spins}}} J_{ij} - \sum_{\substack{\text{orbitals with} \\ \text{parallel spins}}} J_{ij} - \frac{1}{2} \sum_{\substack{\text{orbitals with} \\ \text{nonpaired spins}}} J_{ij} \tag{22}$$

in which coulombic, overlap, and multiple-exchange integrals have been neglected. The coulombic and overlap integrals can easily be put back if required. As an example, consider the interaction between two ground-state N atoms, and suppose that the interaction is due entirely to the three unpaired $2p$ electrons on each atom. There are then four possible electronic states, giving rise to four potential energies,

$$\varphi(^1\Sigma) = J_\sigma + 2J_\pi \tag{23a}$$

$$\varphi(^3\Sigma) = J_\sigma \tag{23b}$$

$$\varphi(^5\Sigma) = J_\sigma - 2J_\pi \tag{23c}$$

$$\varphi(^7\Sigma) = -J_\sigma - 2J_\pi \tag{23d}$$

where J_σ is the exchange integral for the p orbitals along the internuclear axis (the σ orbital), and J_π that for the p orbitals perpendicular to the nuclear axis (the π orbitals). Thus, if the energies of two of the states are known experimentally (e.g., from spectroscopic data), the other two potential curves may be inferred. For N_2 it so happened that more data were available than the bare minimum necessary, so that checks for internal consistency were possible. The agreement with the predictions of Eq. (23) was quite good.[52] For molecules like O_2 and NO, with a

number of unpaired electrons, one can set up extensions of Eq. (23) which also work well.[53]

All gradations are possible between the simple perfect-pairing approximation and a highly accurate *ab initio* calculation, and a number of gradations have been used. For instance, Meador[54] has suggested a number of refinements for O–O and N–O interactions. More elaborate formulations than Eq. (22) have been used for Li + H and O + H gas mixtures[46] and for N^+–N and O^+–O collisions,[55,56] and Ellison[57] has developed a rather elaborate atoms-in-molecules calculation. The most elaborate semiempirical procedure would be to make a complete *ab initio* calculation of low or moderate accuracy, which could then be adjusted to an accurate result on the basis of a few experimental facts. A simple example would be the addition of a constant energy correction to the calculated potential curve; that is, the electron correlation energy would be assumed to be almost independent of internuclear separation.[58] Unfortunately, most *ab initio* calculations would require more elaborate corrections than that. At the other extreme, a strongly empirical approach would be to look for some scaling procedure, suggested perhaps by theory, that would reduce a whole series of potential energy curves to one curve.[59] Jenč and Plíva[60] developed a rather simple scheme of this sort which works well for first-row diatomic molecules and which has been extended to include all the alkali metals.[61] In all such semiempirical work, a major consideration must be to avoid introducing as many parameters as there are pieces of data to fit.

Much the same semiempirical procedure may be used to calculate atom–molecule and molecule–molecule interactions. The calculation of the $H–H_2$ potential energy surface, given previously in Eq. (21), is an example of such a procedure. The perfect-pairing approximation, Eq. (22), gives an even simpler result, illustrated by the N_2–N_2 interaction. It is predicted by Eq. (22) that the molecular interaction energy is just the sum of the interactions between the atoms of the two molecules. The orientational dependence of the N_2–N_2 energy is then given implicitly by the dependence of the atom–atom distances on the relative orientation of the molecular axes, the distances between the molecular centers of mass remaining fixed. Furthermore, the interaction energy of a nitrogen atom in one molecule and a nitrogen atom in another is approximately

$$\varphi(\mathrm{N}\cdots\mathrm{N}) \approx -\tfrac{1}{2}J_\sigma - J_\pi = \tfrac{1}{2}\varphi(^7\Sigma) = -\tfrac{1}{2}\varphi(^1\Sigma) \qquad (24)$$

When only the orientation-averaged potential is concerned, interactions calculated in this way seem to be in reasonable agreement with experiment.[52–54,62,63] Regarding the orientation dependence, the situation is less clear. A general theoretical analysis by Salem[64] indicates that in many cases molecular interactions can be approximately represented as the sum of atom–atom interactions, although the specific form of Eq. (24) might be oversimplified (this is the dumbbell or peripheral-force approximation). But detailed *ab initio* calculations on $He–H_2$ indicate a weaker orientational dependence than can be accounted for on this basis.[65,66]

3. Intermediate-Range Forces

The long-range forces first appear in a second-order perturbation with unsymmetrized wave functions (exchange does not seem to be important at large separations), whereas short-range forces appear in a first-order calculation with symmetrized wave functions. At some intermediate separations, the two calculated energies will be comparable, but it would be a dubious procedure simply to add them, inasmuch as they have been obtained by mutually inconsistent approximations.[16] A consistent calculation would use a properly symmetrized wave function and proceed at least as far as a second-order perturbation calculation. This will give rise to a new set of energy terms, usually called second-order exchange terms, which are not important at small separations (except for three-body effects) because the first-order effects are so much larger. At large separations they die off fast enough to be neglected compared to the dispersion energy, but at intermediate separations they are not negligible. The existence of these terms was first pointed out by Eisenschitz and London,[67] and further considered by Margenau,[15,16] who also recognized that the main reason for the failure of the dispersion energy series, Eq. (2), at intermediate separations was the neglect of symmetry in the trial wave function. If the second-order exchange terms are kept separate, they are frequently approximated by a single exponential, in similar fashion to Eq. (8) for the first-order terms.[12,15] Another reason that the dispersion energy series fails at intermediate separations is the breakdown of the multipole expansion of the electrostatic part of the interaction Hamiltonian.

A painful remedy for these difficulties is an *ab initio* calculation. A less drastic procedure is the replacement of the multipole expansion of the Hamiltonian by a "monopole" approximation,[68,69] but the difficulty

in obtaining the exchange terms still remains. A very accurate semiempirical calculation scheme has been devised by Dalgarno and Lynn,[70,71] using second-order perturbation theory and symmetrized unperturbed wave functions. The semiempirical step comes in the use of the Unsöld closure approximation and in the assignment of the value of the mean energy $\bar{E}$. If $\bar{E}$ is chosen to reproduce the correct asymptotic value of the London coefficient (as known from a semiempirical oscillator strength calculation, for instance), then the resulting values of φ seem to be accurate at both intermediate and long range. If $\bar{E}$ is allowed to be a weak function of r,

$$\bar{E}(r) = \bar{E}(\infty) + C[1 - \Delta(r)] \tag{25}$$

where C is a constant and $\Delta(r)$ a suitable overlap integral, the short-range region can also be accurately covered, provided one value of φ is known at small separations in order to determine the parameter C. Unfortunately, even this semiempirical method involves taking explicit account of all the electrons, and so such calculations have never been carried beyond two He atoms because of the complicated algebra. Generally, since good theoretical procedures are lacking for intermediate-range forces, one is often forced to add the short-range forces to the long-range forces, and hope for the best.

C. Model Calculations

The methods discussed so far began with the correct Hamiltonian and then proceeded to approximate the wave functions or the integrals containing them. An even simpler procedure is to approximate the Hamiltonian; that is, to replace the original physical problem with one that is more tractable mathematically. In other words, a model is selected. Hopefully, the model accurately mimics all the interesting features of the original problem, and discards only the useless complications. Anyone who devises such a model is said to have great physical insight, and physical insight, like common sense, is rather an uncommon quality.

One very simple model, devised long ago, represents each atom or molecule as a harmonic oscillator of frequency ν. London[22,67,68,72] was the first to apply the oscillator model to the quantal calculation of long-range forces. The result is the same as Eq. (4), with $h\nu$ replacing $\bar{E}$. The advantage of this model is that it can be used for cases in which other approximations would be extremely cumbersome. For instance,

London[68] used the model to derive the orientation dependence of the coefficient c_{12} for cylindrical molecules; a more formal derivation by quantum theory of the same result was given much later.[27] Margenau[15,73] generalized the model slightly to the case where each oscillator contains f charges, all vibrating with the same frequency, and derived the coefficients c' and c'' as well;

$$c = \tfrac{3}{4}\alpha^2 h\nu \tag{26a}$$

$$c' = \tfrac{15}{4}[\alpha^3(h\nu)^2/fe^2] \tag{26b}$$

$$c'' = \tfrac{315}{32}[\alpha^4(h\nu)^3/(fe^2)^2] \tag{26c}$$

f is sometimes considered an oscillator strength and is taken from index-of-refraction measurements; $h\nu$ is often taken to be equal to the ionization energy. The oscillator model itself can be used to estimate f if ν and α are known:

$$f = \alpha m_e \nu / h \tag{27}$$

Eliminating ν we find[15,73]

$$c = \tfrac{3}{4}(e^2\hbar^2\alpha^3 f/m_e)^{1/2} \tag{28a}$$

$$c' = \tfrac{15}{4}(\hbar^2\alpha^2/m_e) \tag{28b}$$

$$c'' = \tfrac{315}{32}(\hbar^3\alpha^2/em_e)(\alpha/fm_e)^{1/2} \tag{28c}$$

If f is identified with N, Eq. (28a) is identical with Eq. (5), the Slater-Kirkwood formula. Since this has been found to be very accurate,[20] c' and c'' obtained from Eqs. (28) are likely to be fairly accurate also. The extension to unlike molecules has been given by Hornig and Hirschfelder.[74]

The oscillator model, also called the Drude model, is most valuable in application to problems that are too difficult for rigorous calculations. Accordingly, it has enjoyed considerable use in calculations of interactions among many molecules (nonadditivity effects),[75,76] or of interactions between molecules composed of saturated chains[77] or other clusters of atoms.

Another model, useful for calculating long-range interactions, is the free-electron model, in which the electrons are free to wander over large parts of a molecule instead of being constrained to the vicinity of one nucleus, as in the oscillator model. Long-chain conjugated polyenes seem to behave as if the π-electrons were free to move from one side of

the conjugated system to the other. London's monopole approximation has been applied to this model,[69] as have the methods of many-body theory,[78] with somewhat contradictory results. These methods all assume that the motions of the free charges are strongly correlated. Sparnaay[79] considered the opposite assumption, in which charges move at random inside a spherical volume, and showed that this model can be made to mimic the long-range electrostatic and dispersion forces.

Models for short-range intermolecular forces have been fewer and less successful. If we recall the discussion presented earlier on the Hellmann-Feynman theorem and the physical origin of intermolecular forces, this is not unexpected. The electronic charge distribution controlling short-range forces is determined by the Pauli exclusion principle, which is rather difficult to replace by a simple model. The most successful model for short-range forces is, in fact, one which is applicable at such high energies that the detailed electronic structure of the atoms is unimportant, namely a screened Coulomb function. Bohr[80] suggested an exponential screening function and Firsov[81] suggested a screening function derived from a statistical model of the electrons. Such models have found frequent use in investigations of radiation damage.[82] The ion–atom scattering experiments of Lane and Everhart[83] at kilovolt energies give reasonable agreement with these models, which, however, are not useful at the usual energies involved in discussions of intermolecular forces.

Electronic structure problems connected with the Pauli principle can be bypassed by considering only closed shell atoms or ions. Then statistical models or effective one-electron models may be useful. Abrahamson[84] has devised a model using a Thomas-Fermi-Dirac statistical treatment for the electron distribution. The calculated φ(exch) agrees with other methods within a factor of two for separations ranging from very small to $\approx$3–4 Å, and is generally better than the Bohr or Firsov model results. Somewhat surprisingly, the geometric mean rule of Eq. (11) is followed to within a few per cent. Gáspár[85] also uses a statistical treatment (Thomas-Fermi) to describe short-range forces between rare gas atoms. He does not calculate absolute values of φ(exch), but, instead, uses his theory as a basis for correlation and interpolation formulas which may then be applied to empirical potentials.

In a one-electron model discussed at greater length in another

chapter of this book, Jansen and co-workers[86] calculate the three-body interaction relative to the two-body interaction. The mathematical problem is similar to the interaction of hydrogen atoms with parallel electron spins, except that the atomic charge distributions are assumed to be Gaussian rather than exponential. These results can be mimicked by another model in which the Pauli distortion of each atom is described by an electric dipole.[87] The magnitudes and relative phase angles of the distortion dipoles are calibrated with known results for two-body interactions. The basic idea of this model is similar to that of the Drude model for dispersion forces.

Hirschfelder and Eliason[88] have considered the use of Slater electronic orbitals for rough estimates of intermolecular forces on the basis of the degree of overlap of the orbitals of the interacting atoms. A rather similar idea has been proposed by Hindmarsh.[89]

When the details of electronic structure cannot be ignored, one is faced with the problem of devising a model which will encompass nearly all of chemical binding theory. Only a few rough attempts have been made in this direction. In the delta-function model, the Coulomb wells at the nuclei are replaced by square wells which are eventually allowed to degenerate to delta functions. Electron–electron interactions are ignored, and a one-dimensional treatment is followed. This model was used by Frost[90] to describe hydrogenlike atoms and simple diatomic molecules, and with some empirical modifications, was adapted by Lippincott[91] to describe some properties of bonds in more complicated molecules. The extension to short-range intermolecular forces is easy; Mason and Vanderslice[92] used it in conjunction with a one-electron approximation to calculate forces between rare gas atoms. Remarkably good results are obtained despite the fact that the only parameters needed are the atomic number, the first ionization potential, and a very rough value for the average radius of the largest electronic orbit. Weber[93] has applied the model to the interaction of two-electron atoms and ions, and Olander[94] has modified the Mason-Vanderslice procedure to estimate O^{-2} interactions in uranium dioxide crystals.

An even simpler model has been suggested by Jefimenko.[95] This model represents an atom as a point nucleus whose surrounding electron cloud is just a thin, uniformly charged, spherical shell. The effective charge and radius of the shell are adjustable constants and the energy is completely electrostatic. The electrostatic self-energy of the

shell replaces the electronic kinetic energy. Although the potential curves derived from this model have kinks and cusps, the calculated potentials are surprisingly good.

In summary, available models are rather good for long-range forces; for short-range forces they are, at best, fair (and even then only for closed-shell atoms), and models are practically nonexistent for intermediate-range forces.

D. Survey of Accuracy

It is hard to summarize the status of quantal and semiempirical calculations in a few words, but we feel obliged to make the attempt, nevertheless. At the present time, *ab initio* calculations seem out of the question for atoms more complex than helium; one is almost always forced to use semiempirical calculations. In the most favorable case—a complete calculation of dispersion energy using experimental oscillator strengths—the accuracy is a few per cent. The reliability of a dispersion energy calculation decreases as the available experimental information decreases, but accuracy within a factor of two should almost always be available. The situation is less favorable in the area of short-range forces, and again depends on the availability of experimental data. With accurate data and a fairly accurate quantal calculation serving as a guide, accuracies in φ(exch) of about 25% may be possible. With scanty data and a rough quantal calculation, one may be doing very well to get φ(exch) within a factor of two. For intermediate-range forces, available information is too scarce for any reliable judgment at present. The scanty theoretical and empirical evidence indicates that it may not be a bad approximation simply to add together the long-range and short-range forces. This region has been neglected because of the mathematical difficulties involved, but, as we shall see in the next sections, there are effects (such as crystal stability) which may be determined by the details of intermediate-range forces.

III. SPECTROSCOPIC OBSERVATIONS

The forces between atoms with open electronic shells correspond to the energies of the various possible electronic states of the diatomic molecule, which are often available experimentally. Vibration–rotation spectroscopic bands give information on bound states, predissociation indicates the energies at which different potential curves cross, and intensity distributions in continua give information on repulsive curves.

A. Vibration–Rotation Bands

The basic idea is that the vibration–rotation bands locate the vibrational–rotational energy levels of a diatomic molecule. The structure of these levels is determined by the shape of the electronic potential energy curve, and so yields information on the energy of interaction of the atoms composing the molecule.

For small quantum numbers, the vibrational and rotational motion of a diatomic molecule are nearly separable, but their coupling increases with the energy. Empirically, the vibrational–rotational energy levels for a given electronic state may be represented as a polynomial in $(v + \frac{1}{2})$ and $J(J + 1)$, where v and J are the vibrational and rotational quantum numbers,[42]

$$E = \sum_{i,j} Y_{ij}(v + \tfrac{1}{2})^i[J(J + 1)]^j \tag{29}$$

The simplest procedure, one that is still used quite often, limits Eq. (29) to the first few terms and then matches coefficients with the corresponding series for some soluble potential model, such as the Morse potential,[42,96]

$$\varphi(r) = D_e[e^{-2a(r-r_e)} - 2e^{-a(r-r_e)}] \tag{30}$$

This potential has the right qualitative form and is useful for a semiquantitative discussion of vibrational and rotational motion. But it is not accurate enough for many purposes: for instance, the long-range part near the top of the potential well may be badly in error,[97] as may the dissociation energy,[98] and the axis of the well may be canted at the wrong angle.[99] A large number of models similar to the Morse potential, but containing more adjustable parameters, have been proposed,[100,101] but all suffer drawbacks of one sort or another.

A much better procedure is to use the Rydberg-Klein-Rees (RKR) method, in which no special assumptions about the mathematical form of the potential are made. Instead, the experimentally known energy levels are used to calculate points on the potential curve corresponding to the classical turning points of the nuclear motion. This determines very accurately pairs of points on the potential curve up to the highest vibrational energy level known experimentally. The method was devised by Rydberg[102] and Klein[103] on the basis of the Bohr-Sommerfeld quantization of the phase integral for the vibrational motion; the

method is thus a first-order WKB approximation. Rees[104] in 1947 developed analytical modifications to Rydberg and Klein's graphical methods and showed how the method could be applied rapidly and accurately to the analysis of spectroscopic data. For some reason, this work made little impression until 1959, when Vanderslice et al.[105] revived it in order to obtain accurate short-range intermolecular forces for high-temperature gas transport properties.[52,53] The general availability of electronic computers has stimulated the development of rapid methods of analysis,[99,106–111] and by now the RKR method has been adopted by a host of workers too numerous to enumerate here. Higher-order WKB approximations have been studied, and it has been shown that the first-order result is remarkably accurate.[112]

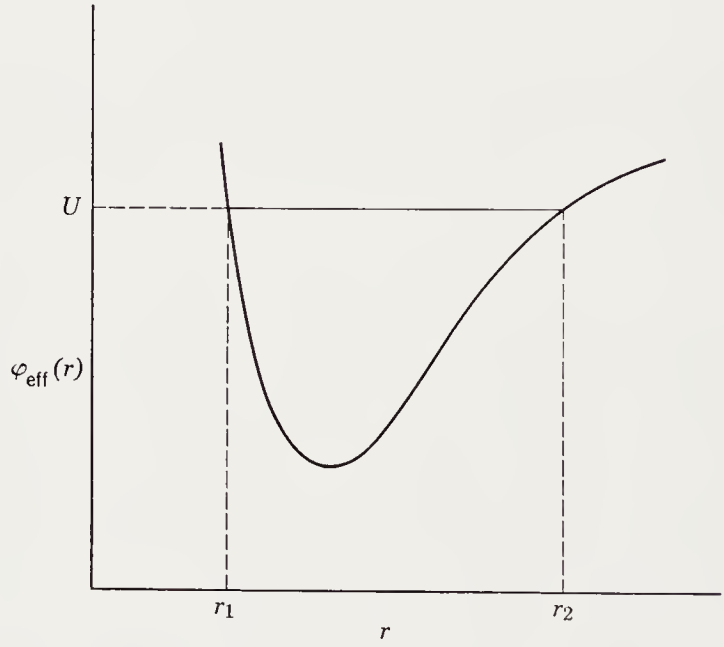

Fig. 1. Schematic diagram for the physical interpretation of the RKR method.

The RKR method has a simple physical interpretation.[105,113] The two quantum conditions required to evaluate the classical turning points r_1 and r_2 of the vibrational motion at a given energy U may be represented in terms of the area enclosed by a line of constant energy and the effective potential energy curve, $\varphi_{\text{eff}}(r)$. From Figure 1 it can

be seen that the area A is given by

$$A = \int_{r_1}^{r_2} (U - \varphi_{\text{eff}})\, dr \tag{31}$$

where

$$\varphi_{\text{eff}} = \varphi(r) + K/r^2 \tag{32}$$

in which K/r^2 is the centrifugal energy. It follows that

$$\left(\frac{\partial A}{\partial U}\right)_K = \int_{r_1}^{r_2} dr = r_2 - r_1 \tag{33}$$

$$-\left(\frac{\partial A}{\partial K}\right)_U = -\int_{r_1}^{r_2} \frac{dr}{r^2} = \frac{1}{r_1} - \frac{1}{r_2} \tag{34}$$

Since U and K are clearly related to the vibrational and rotational energies, A need only be expressible in terms of the experimental energy levels to solve the problem. The area integral can be transformed into a double integral by the use of the following Eulerian integral of the first kind:

$$U - \varphi_{\text{eff}} = \frac{2}{\pi} \int_{\varphi_{\text{eff}}}^{U} \left(\frac{U - E}{E - \varphi_{\text{eff}}}\right)^{1/2} dE \tag{35}$$

The area expression then reduces to

$$A = \frac{2}{\pi} \int_{r_1}^{r_2} dr \int_{\varphi}^{U} \left(\frac{U - E}{E - \varphi_{\text{eff}}}\right)^{1/2} dE$$

$$A = \frac{1}{\pi} \int_{U_0}^{U} (U - E)^{1/2} \oint \frac{dr}{(E - \varphi_{\text{eff}})^{1/2}} \tag{36}$$

where U_0 is the energy at the minimum of φ_{eff}. From the phase integral

$$I = \int p\, dq$$

we have

$$\frac{dI}{dE} = \frac{\mu^{1/2}}{2} \oint \frac{dr}{(E - \varphi_{\text{eff}})^{1/2}} \tag{37}$$

where μ is the reduced mass of the pair of atoms, so that the expression for A finally becomes

$$A = \left(\frac{2}{\mu\pi^2}\right)^{1/2} \int_{U_0}^{U} (U - E)^{1/2} \frac{dI}{dE}\, dE \tag{38a}$$

or

$$A = \left(\frac{2}{\mu\pi^2}\right)^{1/2} \int_{0}^{I'} (U - E)^{1/2}\, dI \tag{38b}$$

where I' is the value of I for which $E(I,K) = U$. The Bohr-Sommerfeld quantum rules identify I with $(v + \frac{1}{2})$ and K with $J(J + 1)$. Since E is normally given as a power series in I and K by Eqs. (29), the preferred form for the numerical calculation of A is usually Eq. (38b).

Thus the area A is calculated from the observed levels, and its variation as the upper limit U is changed gives the difference in the turning points, whereas its variation as φ_{eff} is shifted (by varying K) gives the difference in the reciprocals of the turning points. It should also be mentioned that the series-expansion methods of Dunham,[114] Sandeman,[115] and Jarmain[99] can also be used. These have been shown to be equivalent to the RKR method.[113]

The high accuracy of the RKR method, in spite of its being a first-order WKB approximation, can be rationalized. Near the minimum, it is known that the first-order WKB energy levels are exact. Near the dissociation limit, the motion becomes more clearly classical and first-order WKB results should also be accurate. The RKR method stands alone among those discussed in this chapter as far as ease and accuracy of reconstructing a potential curve are concerned. From the standpoint of a mathematician, it is also the most satisfying because the reconstruction is almost unique.

B. Predissociation

In some cases the rotational structure of a vibration–rotation band may be diffuse in absorption, or broken off in emission. This phenomenon of predissociation[42] is usually caused by another potential curve crossing the potential curve for one of the states producing the band system; radiationless transitions into the predissociating state reduce the lifetime of the radiating state to the order of magnitude of the period of rotation of the molecule, and this broadens or washes out the rotational band structure. The vibrational band structure is usually unaffected.

Thus, it is sometimes possible to obtain one or two points on an unknown curve, by using predissociation data to locate the points where it crosses accurately known curves.

The precise nature of the information that can be extracted from predissociation data depends on the nature of the curves and the details of the manner in which they cross.[42,116] Clearly, the amount of information available will be rather limited, since only a few curve crossings will occur, but predissociation results are valuable in conjunction with other methods. Much of our knowledge of the $^5\Sigma^+$ state resulting from the collision of two ground-state N atoms comes from predissociation data.[52,117]

Another cause of predissociation is the rotational motion of the molecule itself.[42] The addition of the centrifugal energy K/r^2 to the potential $\varphi(r)$ in Eq. (32) produces another curve, φ_{eff}, with a shallower minimum and a potential hill at large r. The energy levels near the top of the hill are unstable due to quantum-mechanical tunneling, resulting in broadened rotational lines (usually, but not invariably); eventually, the band system breaks off because of dissociation caused by the centrifugal motion. If something is known or assumed *a priori* about the shape of the potential hill, such rotational predissociation data may permit numerical values of parameters to be determined. For instance, if the potential hill occurs at such large r that the main component of $\varphi(r)$ is the dispersion energy, $-c/r^6$, then the constant c may be determined and the index 6 of the power law verified. Although information on the potential hill has long been obtained from rotational predissociation data, it is only recently that Bernstein[118] has emphasized the special simplicity of interpretation possible when just the long-range portion of $\varphi(r)$ is important.

C. Intensity Distribution

The intensity of electronic absorption depends on the overlap of the vibrational wave functions for the two electronic states involved at the same internuclear separation. The situation is sketched in Figure 2 for the case where the lower state is bound and the upper state is repulsive, a situation which gives rise to continuum absorption. The maximum absorption occurs approximately at the frequency corresponding to the vertical transition shown in the figure (Franck-Condon principle[42]). If the absorption is measured as a function of frequency and the wavefunction of the lower state is known, then it is possible to infer some of

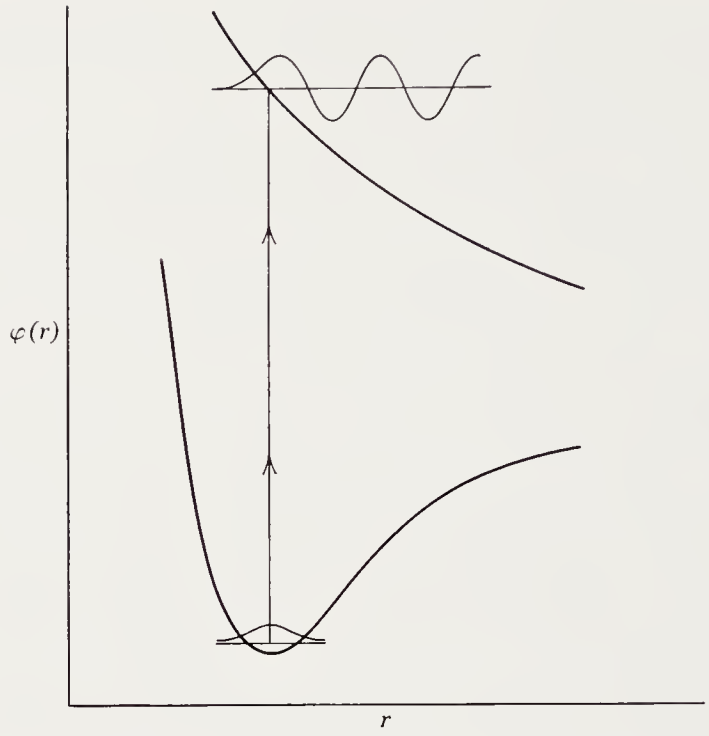

Fig. 2. Schematic energy level diagram for continuum absorption.

the properties of the upper-state wavefunction and hence something about the shape of the upper-state potential curve. The simplest treatment[119] assumes that the lower state is a harmonic oscillator and the upper state potential a straight line. The frequency of the absorption thus gives the height of the upper potential curve above the ground state, and the shape of the absorption curve versus frequency gives the slope of the potential curve near this point. Various mathematical improvements can be made,[120–124] such as using an anharmonic lower potential and an exponential upper potential. The best present procedure would probably be to use an RKR potential for the lower state and an exponential for the upper state.

Very few repulsive potential curves have been obtained by this method. A recent study[124] of the mathematical approximations available indicates that the method can be made to yield potentials that are quite accurate with a minimum of computational labor, and is thus definitely worth fuller exploitation. Moreover, there is no fundamental necessity for the upper curve to be purely repulsive in order to use the method.

D. Pressure Effects

The absorption of radiation by a molecule may be affected by the presence of other molecules nearby, and some information on intermolecular forces may thereby be obtained. In other words, the measured absorption may depend on the pressure of the absorbing gas (or gas mixture), and such pressure effects depend on intermolecular forces. Absorption lines (or bands) may be broadened and/or shifted, or new absorption bands may appear. This type of measurement has so far yielded only sporadic information on intermolecular forces, but should be capable of much greater development. We do not attempt here to give complete references to this rather vast subject, but only to cite a few recent key references.

The pressure broadening of spectral lines has been studied for a long time,[125] and continues to attract attention.[126,127] Most of the information, as applied to the study of intermolecular forces, has come from the microwave region. This subject is reviewed in detail by Birnbaum in Chapter 9 of this volume, and need not be discussed here. The broadening of resonant absorption lines as well as nonresonant absorption and collision-induced absorption, gives information on the long-range forces. In practice, this has been a major source of information on molecular quadrupole moments.[128]

In the infrared region, both the shifts of absorption lines due to foreign gases and pressure-induced absorption have been studied. The shifts of rotational lines in the vibration–rotation bands of HCl by addition of noble gases have been given considerable experimental attention. Margenau and Jacobson[129] have shown that both long-range attraction and short-range repulsion are needed to account for the experimental features, but the problem has not yet been inverted in order to apply it as a tool for the study of intermolecular forces. At present, pressure-induced infrared absorption spectra supply the most information. Their use in determining molecular quadrupole moments has been established for some time.[128,130,131] More recently, Welsh and co-workers[132,133] in Toronto have observed features in the spectrum which could be ascribed to the presence of weakly bound molecular dimers. Gordon and Cashion[134] have undertaken a detailed theoretical analysis of this work in order to determine intermolecular forces, and their results appear quite promising.

Satellite bands have been observed in the spectra of alkali atoms mixed

with inert gases, which have been interpreted to be caused by the presence of a collision complex of the alkali atom and the gas molecule.[135] This suggests that information on the potential curves might be obtained from such satellite bands; the results have been interpreted in terms of Jefimenko's electrostatic shell model of atomic interactions.[95]

IV. BEAM SCATTERING

In principle, one of the most direct ways of studying interactions experimentally is to investigate the scattering of a beam of particles by a collection of other particles. It is convenient, although arbitrary, to divide the discussion of atomic and molecular scattering according to whether the beams have high energy (greater than a few electron volts) or thermal energy (less than 0.1 eV, for example). The experimental techniques and theoretical analyses are rather different in practice for the two cases. The intermediate energy range from about 0.1 eV to several eV is experimentally extremely difficult. The best prospects for this important region at the moment appear to lie with supersonic nozzle beams. Since the techniques are still under development, we will not discuss these nozzle beams further. Two good general reviews have recently appeared.[136,137]

A number of reviews of molecular beam scattering have appeared in the past few years, and we refer the reader to them for various details. The recent books by Hasted[138] and McDaniel[139] contain much material on molecular beams and intermolecular forces, and Volume 10 of the present series is devoted entirely to molecular beams.[140] General reviews have been given by Pauly,[141] Fite and Datz,[142] and Leonas.[143] The high-energy scattering work was reviewed a few years ago by Mason and Vanderslice,[144] and more recently by Amdur and Jordan.[145] Muschlitz[146] has discussed the special subject of collisions involving electronically excited atoms and molecules. Excellent reviews of thermal-energy scattering have been prepared by Pauly and Toennies,[147] by Bernstein,[148] and by Greene, Moursund, and Ross[149]; most recently it has been reviewed by Bernstein and Muckerman in Chapter 8 of this volume.

A. General Remarks

All central-field elastic scattering is described from a fundamental point of view as wave scattering, for which the differential cross section $I(\theta,v)$ is[150–152]

$$I(\theta,v) = |f(\theta,v)|^2 \tag{39}$$

$$f(\theta,v) = (2ik)^{-1} \sum_{l=0}^{\infty} (2l+1)[\exp(2i\delta_l) - 1]P_l(\cos\theta) \tag{40}$$

where $f(\theta,v)$ is the scattering amplitude, $k = \mu v/\hbar$ is the wave number of relative motion, δ_l is the lth phase shift, and P_l the lth Legendre polynomial of argument cos θ. That is, a wave packet describing the angular distribution of scattered particle can be decomposed into a weighted sum of spherical waves corresponding to different quantized values of relative angular momentum $l\hbar$. Due to the energy interaction, the phase of each spherical wave will be shifted by an amount δ_l, corresponding to a retardation or acceleration Δt_l:

$$\Delta t_l = 2\hbar \frac{\partial \delta_l}{\partial E} \qquad E = \tfrac{1}{2}\mu v^2 \tag{41}$$

In principle, the phase shifts are to be obtained by solution of the radial wave equation, but for molecular scattering they are often approximated by the first-order JWKB formula (with the Langer modification),[150]

$$\delta_l \approx \tfrac{1}{2}\pi(l+\tfrac{1}{2}) - kr_0 - \int_{r_0}^{\infty} (k_r - k)\, dr \tag{42}$$

$$k_r = \{(2\mu/\hbar^2)(E-\varphi) - [(l+\tfrac{1}{2})^2/r^2]\}^{1/2} \tag{43}$$

where r_0 is the outermost zero of k_r. The quantity r_0 corresponds to the classical distance of closest approach, and the classical impact parameter b corresponds to

$$kb = l + \tfrac{1}{2} \tag{44}$$

Alternate forms of Eqs. (42) and (43) are[150]

$$\delta_l \approx k \int_{r_0}^{\infty} [1 - (b/r)^2 - (\varphi/E)]^{1/2}\, dr - \int_{b}^{\infty} [1 - (b/r)^2]^{1/2}\, dr \tag{45}$$

and[153]

$$\delta_l \approx \frac{k}{2} \int_{r_0}^{\infty} [1 - (b/r)^2 - (\varphi/E)]^{1/2} \frac{r(d\varphi/dr)}{(E-\varphi)}\, dr \tag{46}$$

Although the JWKB approximation is very useful, there are always values of b and E for which it fails in practice.[154,155] This failure can be

partly alleviated by making corrections for tunneling through the centrifugal barrier,[156] but for light particles at low energies, the JWKB approximation may be essentially useless for some purposes.

A very elegant body of theory, developed primarily for nuclear scattering, has grown up[151] for methods of abstracting δ_l from $I(\theta,v)$ and of subsequently reconstructing the potential. If the energies and eigenfunctions of the bound states are known, this potential may even be determined unambiguously. These methods do not seem to have been applied to atomic and molecular scattering, except in the classical limit. One reason for this is the very large number of phase shifts that contribute appreciably to $I(\theta,v)$ in atomic and molecular scattering; another reason is that extensive experimental data on cross sections as functions of energy and scattering angle have only recently become available.

When many partial waves contribute to the observed scattering, several mathematical approximations become permissible, which lead to the so-called semiclassical description of scattering. Under certain limiting conditions, the semiclassical description of wave scattering becomes identical to the classical description of particle scattering. Since the mathematical description of wave scattering is the same whether photons, electrons, atoms, or baseballs are being considered, there are many analogies between particle scattering and optical phenomena, some of which were first pointed out by Ford and Wheeler.[154] The classical limit of particle scattering corresponds to the ray tracing of geometric optics; a classical description is therefore inadequate whenever diffraction or interference effects are important. There are three distinct parts to the semiclassical approximation for scattering.[154] The first is the use of the JWKB approximation for the δ_l. The second is the replacement of summations over l, as in Eq. (40), by integrations, and the replacement of differences by derivatives, as

$$\delta_{l+1} - \delta_l \approx \frac{d\delta_l}{dl} \qquad \delta_{l+2} - \delta_l \approx 2\frac{d\delta_l}{dl} \cdots \tag{47}$$

The third is the use of asymptotic formulas for $P_l(\cos\theta)$. A fourth approximation sometimes used is the evaluation of integrals over l by the method of stationary phase.

Differentiation of the JWKB expression for δ_l demonstrates a relation between the classical deflection angle and the phase shift,

$$\frac{d\delta_l}{dl} = \frac{\pi}{2} - b\int_{r_0}^{\infty} [1 - (b/r)^2 - (\varphi/E)]^{-1/2} \frac{dr}{r^2} \tag{48}$$

or

$$\theta(b) = 2\frac{d\delta_l}{dl} \tag{49}$$

The asymptotic expressions for $P_l(\cos\theta)$ are

$$P_l(\cos\theta) \approx J_0[(l + \tfrac{1}{2})\theta] \quad \text{for } \sin\theta \leq 1/l \tag{50a}$$

$$P_l(\cos\theta) \approx [\tfrac{1}{2}\pi(l + \tfrac{1}{2})\sin\theta]^{-1/2} \sin[(l + \tfrac{1}{2})\theta + \tfrac{1}{4}\pi] \quad \text{for } \sin\theta \geq 1/l \tag{50b}$$

where J_0 is the Bessel function of order zero. If Eq. (50b) is substituted into Eq. (40) for $f(\theta,v)$, the summation replaced by integration, and the integral evaluated by the lowest-order stationary-phase approximation, the classical results are obtained, namely Eq. (49) and

$$I_{cl}(\theta,v) = b/(|d\theta/db| \sin\theta) \tag{51}$$

This result fails in three cases important in the study of intermolecular forces. The first is small-angle scattering, in which case Eq. (50a) must be used instead of (50b). The second occurs when $d\theta/db$ is zero but b is not zero; Eq. (51) then diverges. The third occurs when more than one molecular state contributes to the scattering; it is the amplitudes $f(\theta)$ for the different states which add together rather than the intensities $I(\theta)$, and interference phenomena result. Actually, both the second and third cases are really subcases of a general interference effect which can occur whenever there are two or more distinct contributions to the total $f(\theta)$.

B. High-Energy Beams

The usual method here is not to measure $I(\theta,v)$, but to measure all the scattering beyond some angle θ_0, which depends on the apparatus geometry,

$$S(\theta_0,v) = 2\pi\int_{\theta_0}^{\pi} I(\theta,v)\sin\theta\, d\theta \tag{52}$$

Measurements of the "total" cross section $S(\theta_0,v)$ as a function of beam energy then supply the information needed to study $\varphi(r)$. The angle θ_0 is

usually large enough for an accurate classical description of the scattering,[157,158] but small enough so that the interaction energy between beam and scattering particles need be only a small fraction of their relative kinetic energy. Thus, high kinetic energies of the beam can be used with attendant ease of experimentation. But a price is paid, in that a small value of θ_0 makes the results strongly dependent on experimental details such as the relative size of the beam and the detector. The apparent disagreement between theory and experiment for the short-range interaction between He atoms has finally been traced to an unexpected peculiarity in the correction for such experimental effects.[159]

Most of our experimental knowledge of short-range forces between simple atoms and molecules has come from the neutral beam measurements of Amdur and co-workers. This has been reviewed recently,[144,145] but several subsequent papers have appeared,[159–161] of which one is particularly notable for resolving the discrepancy noted above.[159] This scattering work is internally consistent and is now in agreement with the few available quantum-mechanical calculations on He–He[8] and H–He.[162–164] Leonas and co-workers of Moscow have recently reported on high-energy beam scattering,[41,63,165,166] which is in encouraging agreement with the M.I.T. data. Thus, there is little doubt of the essential correctness of these results.

More information on $\varphi(r)$ is obtainable with fewer assumptions if $I(\theta,v)$ is measured rather than $S(\theta_0,v)$, but the measurements are more difficult. If a classical description is adequate, then $\varphi(r)$ can be obtained from $I(\theta,v)$ with no assumptions other than that $\varphi(r)$ is monotonic.[167–169] Analysis of $S(\theta_0,v)$ measurements, in contrast, requires the assumption of a specific mathematical form for $\varphi(r)$. An early attempt to obtain $\varphi(r)$ directly from $I(\theta,v)$ was made by Berry[170] for neutral beams but, by far, the most successful analysis of this type has been carried out by Lane and Everhart[83] for the scattering of kilovolt ions by neutral atoms. These collisions are energetic enough for the interaction to be described by a single potential which turns out to be nearly a screened Coulomb potential.

In the classical description of scattering, it is not possible to unambiguously disentangle the scattering pattern if more than one state or more than one branch of $\varphi(r)$ contributes to the observed $I(\theta,v)$. Some *a priori* assumptions about the potential must first be made. However, the situation is more favorable when such separate contributions to the scattering produce quantum-mechanical interference effects.[154] At first

it seems surprising that any such effects could be observed in high-energy beam scattering, but they are quite strong when resonant charge exchange is possible; i.e., in systems like H^+–H, He^+–He, Ne^+–Ne, etc. The differential cross sections for charge exchange show remarkable oscillations as a function of energy and angle, which are nothing more than the interference pattern from the superposition of scattering amplitudes from two or more states. These were first observed by Ziemba and Everhart[171] for He^+–He collisions, and studied in further detail by Everhart and co-workers,[172–175] and by others.[176–180] The basic theoretical description was given long ago by Massey and Smith,[181] but recent experimental work has given rise to considerably more detailed theoretical discussion.[182–186] The theoretical analyses have thus far concentrated on the simplest systems, H^+–H and He^+–He, in order to be sure that the basic physical mechanisms were identified, including such detailed effects as nuclear symmetry and perturbations induced by curve-crossing. Although quantum interference phenomena are involved, it is still possible to give a good description on a semiclassical basis, using adiabatic potential curves for the different molecular states.[182–186] Now that the theoretical preliminaries seem settled, we may expect that the increasingly detailed experimental differential cross sections will be analyzed to give reliable estimates of the potential energy curves involved. As an example of the present experimental capability, Jones and his students[178] have recently been able to resolve the two superposed interference patterns for Ne^+–Ne charge-exchange scattering, which is a four-state system.

Oscillations also occur in the total charge-exchange cross section as a function of energy,[187] but these are a quite different sort of interference phenomenon[188] analogous to the "glorified shadows" discussed in connection with thermal-energy beams below.

A remarkable new method of studying interatomic potentials with high-energy beams has been discovered in connection with a channeling effect in the scattering of ion beams of meV energies by single crystals.[189] In single crystals, almost open "channels" between crystallographic planes exist, through which a beam of fast particles can pass with very small attenuation, the beam being kept in focus by glancing collisions with the channel walls. This is analogous to the propagation of light between two parallel mirrors. Depending on the glancing angle, the beam particle penetrates more or less deeply into the electronic structure of the atoms lining the channel, and consequently suffers energy losses.

The emerging beam consists of only those particles for which the entrance and exit angles to the channel are equal, and these come through in distinct energy groups, one for each angle which can be transmitted. Each energy group thus corresponds to a different average distance of closest approach of the beam ion to the crystal atoms. The method appears quite promising, and should lead to important new information about the effective potentials in crystals.

C. Thermal-Energy Beams

The general approach here is really the same as for high-energy beam scattering, but the measured cross sections at thermal energies usually show different features than those at high energies, because of the different de Broglie wavelengths and because the depth of the potential well is usually comparable to thermal energies. One result is that true total scattering cross sections can be measured because the aperture angle θ_0 can easily be made small compared to the width of the forward scattering peak, which is comparatively broad at thermal energies. Another result is that interference phenomena and other optical analogies are more commonly observed. Since the subject of low-energy beam scattering is well covered elsewhere in this volume, we will confine ourselves here to qualitative remarks about some of the optical analogies in particle scattering.

The mathematical theory of most of the interesting optical analogies in particle scattering has been given by Ford and Wheeler.[154] These analogies correspond to the semiclassical limit of the quantal theory of particle scattering, in which many partial waves must be considered. The reason for this is that the relevant optical phenomena (i.e., photon scattering) occur in situations where the wavelength is much smaller than the size of the scattering or refracting objects. In particle scattering, this corresponds to the fact that the de Broglie wavelength is much smaller than distances over which the potential changes appreciably—a condition necessary for the validity of the semiclassical approximation.

We wish to discuss here three optical analogies which are of current interest in beam scattering studies: rainbows and haloes, shadows (total cross sections), and glories and glorified shadows.

1. Rainbows and Haloes

The simple physical reason for the formation of an optical rainbow is often lost amid a welter of complicated geometry in elementary

textbooks. The rainbow depends on the fact that there is an angle of minimum deviation for light rays refracted by a water droplet. The intensity "piles up" at the "turning-around" angle of the minimum; that is, the rays which enter the drop near the minimum-deviated ray all emerge at nearly the same angle. Hence, there is a bright band of light. If the wavelength is of the order of the drop diameter, there is interference among different refracted light waves emerging at the same angle and a diffraction pattern develops. That is, a set of bright bands of light are observed at angles inside the main band. These are called supernumerary rainbows.[190] The rainbow angle θ_r, which is about 42° for optical rainbows, depends on the refractive index of the raindrops. The spacing of the supernumerary rainbows depends on the drop size.

The scattering of molecules can also be represented by classical trajectories analogous to light rays, if we remember that wave interference may take place between trajectories with nearly the same deflection angle θ, but different impact parameters b. If θ versus b (or l) has a minimum, a molecular rainbow will occur. A minimum in θ versus b is usually (but not necessarily) an indication of both attractive and repulsive components in the intermolecular potential. By the optical analogy, the value of θ_r will depend primarily on the depth of the potential energy well and the initial kinetic energy. The well depth ε thus plays the role of the index of refraction in the optical case, and the kinetic energy plays the role of the frequency or wavelength. In addition, the spacing of the supernumeraries may be expected to be a function of the range of the potential, σ. Detailed calculations on the 12-6 potential by Munn and Smith[191] illustrate these expectations quantitatively, and also show that the rainbow effect depends principally on the potential beyond the minimum of the well. The rainbow angle, of course, depends to some extent on the detailed shape of the potential; semiempirical studies by Schlier and Düren[192] on several model potentials indicate that θ_r correlates well with $r_i(d\varphi/dr)_{r_i}$, where r_i is the inflection point of the potential just beyond the minimum.

The first molecular rainbow was probably seen, but not recognized, by Knauer.[193] Since there was no velocity selection and the angular resolution was low, it corresponded to what would be seen in the optical case by a color-blind, nearsighted man. There is a barely perceptible bump in his curve of scattered intensity approximately at the angle expected for the most probable kinetic energy of the beam molecules. This apparently went unrecognized for over 20 years, until the "ray-

tracing" or classical-mechanical explanation was given.[194] The optical analogy was pointed out shortly afterwards.[154] Recently, the scattering of thermal beams of molecules has again been undertaken experimentally, and many primary rainbows have been seen, and used to give information on potential well depths.[147–149,185,186] In two of these early investigations,[195a,196b] a small bump appeared corresponding to the first supernumerary rainbow. A detailed numerical calculation[197] showed that these were indeed supernumeraries; very well-resolved supernumeraries were experimentally observed by Hundhausen and Pauly[198] at about the same time. Even higher resolution was achieved shortly thereafter,[199–201] and the results showed further "high-frequency" oscillations caused by interference between waves scattered through the same observed (absolute) angle by close collisions and distant collisions.[154]

The two pieces of information on ε and σ given by the positions of the primary and supernumerary rainbows are almost independent, which is a considerable advantage over information obtained from virial coefficients and other bulk properties, where ε and σ are usually closely coupled together. The detailed shape of the edge of the primary bow can also be used to determine σ,[195a] but requires better intensity measurements than does the supernumerary spacing. The angular spacing of the "high-frequency" oscillations gives a measure of the inner repulsive core of the potential. Incidentally, the existence of both the supernumerary rainbows and the high-frequency oscillations are pure quantum effects. The observation of these interference phenomena gives very detailed information on the potential, but requires a full phase-shift calculation for a quantitative analysis of the results. The traditional theory of rainbows involving the Airy integral,[154] although easy to use,[202,203] has limited applicability.[191,200]

As the de Broglie wavelength of the colliding particles becomes larger, the separation of the rainbow and the high-frequency interference patterns becomes more indistinct, and eventually the two merge. This has been investigated in some detail by Bernstein and coworkers, both theoretically[204] and experimentally with Li beams.[205] As with any interference pattern, the spacing of the maxima and minima gives information on some "size" or range-of-force parameter.

Strictly speaking, the analogy between optical and molecular rainbows has one small defect—optical rainbows involve backward scattering, but all molecular rainbows so far reported involve forward scattering. In

this respect, the analogy is closer to optical haloes,[190] but there is no harm in keeping the slight misnomer.

2. *Shadows*

Shadows are simply total cross sections. According to classical ray-tracing theory, if parallel light illuminates a polished sphere, the scattered light has the same intensity at every angle and the shadow cast by the sphere is completely dark. The wave theory predicts that diffraction at the edge of the sphere produces a narrow cone of light in the center of the shadow; the shorter the wavelength, the narrower the cone and the greater the light intensity in the cone.

Molecules would behave similarly if they interacted like rigid elastic spheres, as was shown by Massey and Mohr.[150,206] But they do not; the force fields extend out to infinity (nominally), finally decaying as some inverse power of the distance. The optical analogy is a refracting sphere that nominally extends to infinity, but whose refractive index weakens as the distance of the light ray from the center increases. This type of scattering is infinitely strong in the forward direction and has an infinitely large cross section according to ray-tracing optics and its particle equivalent, classical mechanics. But the wave theory shows, in both cases, that the weakly refracted rays or trajectories interfere just enough to disturb the refraction and make both the forward scattering and the total shadow finite instead of infinite. Thus, quantum mechanics predicts that both $I(0)$ and the total cross section $S(0)$ are finite. The fact that $S(0)$ is finite was demonstrated in some classic experiments of Rosin and Rabi,[207] and more recently a number of other groups have not only shown $S(0)$ to be finite but have measured it as a function of velocity (as discussed in more detail in the following subsection). Good observations of the shadow effect in $I(\theta,v)$ have been more recent, although the early measurements of Knauer[193] can be shown to indicate the effect.[194] Pauly[208] and Helbing and Pauly[109] have reported some excellent measurements of $I(\theta,v)$ at small θ which show that $I(\theta,v)$ becomes constant as θ approaches zero, instead of rising towards infinity as predicted classically. Detailed quantal calculations have been made of the shape of $I(\theta)$ at small angles,[155,157,208,209] which appear to be in good agreement with experiment.

The shadow phenomena are all small-angle phenomena, and hence are dominated by large values of l, the angular-momentum quantum number. At low energies, this corresponds to large impact parameters

and measures the longest-ranged component of the intermolecular potential, usually the $-c/r^6$ London dispersion energy. The ways in which information on the potential can be extracted from various kinds of shadow phenomena are easily illustrated with a potential of the form $\varphi(r) = K/r^s$. One way is to measure the total cross section $S(0)$ as a function of beam velocity. Since $S(0)$ varies as $v^{-2/(s-1)}$, the value of s can be found from the slope of a suitable logarithmic plot, and K from the intercept (which requires absolute intensity measurements, although the slope requires only relative measurements). A number of experimental scattering measurements have confirmed that $s = 6$, but, until recently, there was a factor-of-two discrepancy in the values of c obtained by scattering and by other means. The discrepancy, it has been discovered, was caused by a pressure-measurement error in the scattering work.[210,211]

At angles larger than about $\theta_c \approx \pi/kr_0$, the behavior of $I(\theta)$ is essentially classical[155,157,158,206]; and $I(\theta)$ varies as $\theta^{-2-(2/s)}$; the value of s can therefore be found from the slope of a suitable logarithmic plot, and K from the intercept, if the absolute value of $I(\theta)$ is shown. A number of measurements[208,209] confirm the value of $s = 6$. An analogous result holds for the velocity dependence of the "total" cross section $S(\theta_0,v)$ if $\theta_0 > \theta_c$, since $S(\theta_0,v)$ varies as $v^{-4/s}$. Superposed on the classical angular dependence of $I(\theta)$ is an oscillation whose "wavelength" is roughly equal to[158]

$$\Delta\theta \approx 2\pi/kb \tag{53}$$

These have not been resolved experimentally, but in principle are capable of giving information on K from only relative measurements of $I(\theta)$.

For $\theta < \theta_c$, the behavior of $I(\theta)$ is as $\exp(-\alpha\theta^2)$, with α proportional to the total cross section $S(0)$.[157,208,209] The value of α could be determined with only *relative* measurements of $I(\theta)$, but would yield an *absolute* value of $S(0)$ and hence a value of K. This determination of an absolute cross section from relative intensity measurements looks attractive, but gives insufficient accuracy at the present stage of experimental development.[209]

Thus, the rainbow and shadow scattering phenomena give complementary information; the shadow effects are controlled by the long-range part of the potential, whereas the rainbow effects are controlled by the intermediate-range part.

3. Glories and Glorified Shadows

The optical glory is an intense scattering of light at $\theta = 0, \pi, 2\pi$, etc. A backward glory ($\theta = \pi$) can be seen on looking into a dense bank of mist or cloud with a bright light behind the observer. A bright light appears around the observer's shadow, giving a sort of corona effect (hence the name, "glory"). A related optical phenomenon is the heiligenschein.[190] Similar effects should also be seen in particle scattering; Ford and Wheeler[154] discuss backward glories in some detail. The classical explanation of a glory is readily seen from Eq. (51); $\sin\theta$ in the denominator vanishes and $I(\theta)$ becomes infinite. No glories have been seen with atoms or molecules, although they might be found by suitable crossed-beam techniques. They would be uninteresting from a classical point of view because they are a geometrical effect, not a molecular one. The quantal description of glory scattering softens the classical singularity to a finite contribution whose magnitude gives the slope of the θ versus b curve at the glory angle. Interference among the waves following trajectories on either side of the glory angle would, in principle, give some extra information on the size or range of the potential, but these effects would probably be difficult to measure accurately. The forward glory scattering is usually much smaller in magnitude than the shadow scattering.

The most important effects of glory scattering are indirect, and come about from the interference between the waves from the forward glory and the waves from the shadow scattering, all of which are near $\theta = 0$. This interference gives rise to oscillations in $S(0)$ versus v around a smooth curve, or to oscillations in $I(0)$ versus v (which is essentially the same thing, according to the optical theorem). If one wishes to be facetious, this might be termed a "glorified shadow" and it would correspond in the optical case to a pulsation in shadow size as a function of the wavelength of the light. Many experimental observations and theoretical analyses have been made of glorified shadows; these are ably reviewed in detail in Chapter 8 by Bernstein and Muckerman, as well as elsewhere.[147,148,212] Our only object here has been to give a brief qualitative discussion of the phenomenon in order to place it in the context of previous remarks.

The fact that the glorified-shadow phenomenon depends on forward glory scattering means that information is obtained about the θ versus b curve around $\theta = 0$, which corresponds to the intermediate-range

part of the potential. The mean value of the shadow, however, gives information on the long-range part of the potential, and so the two phenomena give complementary information.

V. BULK PROPERTIES

In principle, any macroscopic property influenced by intermolecular forces might be used to determine the forces. In practice, only a few macroscopic properties are suitable, since two very restrictive conditions must be met. These are (*1*) an accurate statistical-mechanical theory connecting the intermolecular forces and the macroscopic property must be available, and (*2*) the forces must not be buried under too many layers of theory or sensitivity is lost. A third condition is perhaps obvious—the macroscopic property must be measurable with sufficient accuracy. The most useful properties for the study of intermolecular forces have been the equation of state, the transport coefficients of low-density gases, and a few crystal properties such as lattice spacing and heat of sublimation. The discussion in this section is devoted primarily to these properties.

The calculational procedure is necessarily somewhat indirect, since all that is available are certain weighted averages of functions of the potential as in virial coefficients or some function of the deflections suffered by colliding molecules averaged over all possible trajectories, as in transport coefficients. Mathematically, one may regard the detailed form of the potential as having been mapped onto some macroscopic property. In practice, the potential cannot be reconstructed uniquely from that property alone; in many cases such a reconstruction is impossible even in principle. Only a very few definite statements about the potential can be made solely on the basis of the behavior of bulk properties,[213] and one must resort to mathematical models of the potential. Despite these limitations, analysis of bulk properties is still our best source of information on intermolecular forces.

A. Virial Coefficients

The second virial coefficient takes into account only binary interactions. For central potentials, the classical statistical-mechanical expression is

$$B(T) = 2\pi N_0 \int_0^\infty [1 - e^{-\varphi(r)/kT}] r^2 \, dr \tag{54}$$

where N_0 is Avogadro's number so that $B(T)$ is in molar units. An analogous expression holds for noncentral potentials. Investigations[214,215] of the mathematical problem of inverting this integral to find $\varphi(r)$ have shown that only the positive, single-valued part of $\varphi(r)$ is determined uniquely. The potential well is only partly determined, in that its width can be found as a function of its depth. This provides an understanding of the empirical observation[216] that the second virial coefficients of a number of simple molecules can all be fitted fairly well by a number of potentials of quite different shape, having in common only equal areas of the potential well. The closest attempt at a direct inversion of Eq. (54) has been carried out by Jonah and Rowlinson[217] for He at high temperatures; even this is not unique, because corrections for the small potential well and for quantum effects must first be made, and then it must be assumed that an analytical form fits the corrected values of $B(T)$. The result agrees well with Phillipson's quantal calculations.[8]

The crucial point in the use of potential models is the guidance furnished by theory in the selection of a model in the first place. Without some theoretical foundation for a model, the number of reasonable possibilities is distressingly large. The amount of sheer groping necessary is not likely to encourage an attack along purely empirical lines. A short account of the history of this groping period in intermolecular forces has been given by Margenau,[15] with interesting comments on a parallel development of a theory of nuclear forces. Extensive work on virial coefficients did not start until the development of a fundamental theory of intermolecular forces.

The approximate theories discussed in Section II form the basis for models of intermolecular forces. Usually investigators have represented the potential as a sum of several simple functions suggested by theory. One simple example is the (exp-6) potential, an r^{-6} attractive term plus an exponential repulsive term. The large body of literature on this subject is ably summarized in the treatise of Hirschfelder, Curtiss, and Bird[216]; little more needs to be said here, except to offer a few general comments and to call attention to some of the more recent work. Perhaps the most important comment to be made is that all sins of omission and commission made in choosing the model have to be absorbed into the numerical values of the adjustable constants. Caution is therefore necessary in giving any absolute interpretation to such numerical values. For instance, the coefficient of the r^{-6} term of a

Lennard-Jones (12-6) potential, as determined from $B(T)$, is certainly not the true value of the London coefficient. In fact, it is too large by a factor of about two.[34,216] The use of a more flexible model shows that this discrepancy is not real,[218] but is only a symptom of over-simplification in the model.

The general availability of high-speed computers has recently encouraged a much more systematic approach to models and curve-fitting than was previously feasible. Transport coefficients are now often routinely analyzed simultaneously with virial coefficients. Recent work which should be mentioned includes that of Sherwood and Prausnitz[219] on the 12-6, exp-6, square-well, Sutherland, and Kihara core models applied to $B(T)$; the work of Konowalow and Carrá[220] on the Morse potential applied to viscosity as well as $B(T)$; the work of Munn and Smith on a generalized potential of Boys and Shavitt applied to both $B(T)$[221] and viscosity[222]; of Barker, Fock, and Smith[223] on the Kihara core and Guggenheim-McGlashan potentials applied to $B(T)$ and viscosity; of Dymond, Rigby, and Smith[224] on some new potential functions applied to virial and transport coefficients; of Hanley[225] on the 12-6, exp-6, and Kihara core potentials applied to viscosity; of Tee, Gotoh, and Stewart[226] on the 12-6 and Kihara core potentials applied to $B(T)$ and viscosity; and of Klein[227] on the 12-6 potential applied to several equation-of-state and transport coefficients. This work will be discussed further in connection with the transport coefficients, in Section V-B which follows.

At one time it was hoped that the third virial coefficient could be used to supply further information on the pair potential, but it now appears that three-body forces have an important effect. The first studies of the pairwise nonadditivity of intermolecular forces showed that the third virial coefficient was appreciably affected by the nonadditivity of the long-range dispersion forces.[228–230] More recent work indicates that nonadditivity of the short-range forces is also important.[87,231] The corrections to $C(T)$ from the various nonadditivities are such that considerable cancellation occurs, and the net correction is very sensitive to the models chosen. At present, it seems that advances in our knowledge of three-body forces will depend fundamentally on improvement of our knowledge of two-body forces.

B. Transport Coefficients

The transport coefficients of dilute gases depend only on binary interactions and are discussed in detail by Hirschfelder, Curtiss, and

Bird.[216] They are similar to the second virial coefficient as far as the study of intermolecular forces is concerned, although the integrations involved are rather different. For instance, the kinetic theory expressions for the viscosity and diffusion coefficients of monatomic gases are, respectively,

$$\eta = \tfrac{5}{16}(mkT/\pi)^{1/2}[f_\eta/\sigma^2\Omega^{(2,2)*}] \tag{55}$$

$$D_{12} = (3/8n)(kT/2\pi\mu_{12})^{1/2}[f_D/\sigma_{12}^2\Omega_{12}^{(1,1)*}] \tag{56}$$

where m is the mass of a single molecule, μ_{12} is the reduced mass of a pair of colliding molecules of masses m_1 and m_2, n is the number density, f_η and f_D are slowly varying functions of temperature which are usually close to unity, σ is a distance or size parameter, and the $\Omega_{ij}^{(l,s)*}$ are reduced collision integrals wherein the effects of intermolecular forces appear. The reduced collision integrals $\Omega^{(l,s)*}$ are ratios of collision integrals $\Omega^{(l,s)}$ evaluated for the actual potential to collision integrals $\Omega^{(l,s)}$ evaluated for rigid spheres of diameter σ, and the $\Omega^{(l,s)}$ are Boltzmann-like averages of transport cross sections,

$$\Omega_{ij}^{(l,s)} = \left(\frac{kT}{2\pi\mu_{ij}}\right)^{1/2} \int_0^\infty S^{(l)} e^{-\gamma^2} \gamma^{2s+3}\, d\gamma \tag{57}$$

$$\gamma^2 = \tfrac{1}{2}\mu_{ij} v^2/kT$$

The transport cross section $S^{(l)}(v)$ are

$$S^{(l)}(v) = 2\pi \int_0^\pi (1 - \cos^l\theta) I(\theta,v) \sin\theta\, d\theta \tag{58}$$

The angular weighting functions $(1 - \cos^l\theta)$ suppress the small-angle contribution to $I(\theta,v)$ which dominates the ordinary scattering cross section. A classical approximation is therefore valid, except for light gases at low temperatures, and the cross sections can be calculated from the formulas

$$S^{(l)}(v) = 2\pi \int_0^\infty (1 - \cos^l\theta) b\, db \tag{59}$$

$$\theta = \pi - 2b \int_{r_0}^\infty [1 - (b/r)^2 - (\varphi/E)]^{-1/2} r^{-2}\, dr \tag{60}$$

From these formulas, it might appear that the transport coefficients are less sensitive to the potential than is the second virial coefficient, since they are buried under three layers of integration rather than only one layer. This is not necessarily so, for the following reason. Most of the contribution to θ in Eq. (60) comes from separations near the

distance of closest approach, r_0, and much of the contribution to $S^{(l)}$ in Eq. (59) comes from angles near some most effective angle ($\theta = \pi$ for $l = 1$ and $\theta = \pi/2$ for $l = 2$). Thus, the integrations of Eqs. (59) and (60) do not suppress as much information as might at first be expected.

Recent work on intermolecular forces and transport coefficients has already been mentioned in connection with virial coefficients. Several fairly general conclusions can be drawn from all this work. First, it has been demonstrated at some length that these properties differ in their abilities to act as probes of the potential function, and that these abilities depend on the temperature ranges involved. For example, at very low temperatures the viscosity gives information concerning the tail of the potential curve, and the second virial coefficient gives information on the potential curve around the bottom of the potential well. Thus, fairly reliable values of the r^{-6} London coefficient c can be obtained by extrapolation of the apparent value from viscosity to the limit of 0°K.[213,232,233] However, if c is determined by fitting a potential model to viscosity and second virial coefficient data in the region of the Boyle temperature, the value obtained will depend on the model used and will not be very close to the true value (relative values of c from the ∞-6, 12-6, and 9-6 models are 0.390, 1.118, and 1.820, respectively).[234] Although these differences are recognized to exist, there is no general agreement yet about the relative sensitivities of different properties at arbitrary temperatures.[226,227]

A second conclusion is that no potential function yet proposed is able to describe both the transport and second virial coefficients of even the inert gases within estimated experimental errors, even when several adjustable constants are available. This suggests that better theoretical guidance is needed on the choice of the form of the potential function.

A third conclusion is that even simple potentials like the n-6 or exp-6 do remarkably well, although not perfectly, in representing a variety of data over rather wide temperature ranges.

All the recent work thus affirms the old conclusion that transport and virial coefficients cannot by themselves determine potentials, but can act as important tests for the acceptance or rejection of proposed potentials.

In many ways, thermal diffusion stands apart from the other transport properties. It was not predicted by Maxwell's pioneering analysis or by the elementary mean-free-path theories, seemingly because it is a secondary effect. That is, the existence of the other transport coefficients

depends primarily on the fact that molecular interactions take place, but the existence of a thermal diffusion effect depends more on the nature of the intermolecular force. This increased sensitivity to the nature of molecular interactions has brought attention to the use of thermal diffusion as a probe of intermolecular forces. The subject of thermal diffusion in gases has recently been reviewed in detail,[235] and so we do not discuss it further here.

In the remaining part of this section, we offer a few summarizing remarks about the effects of nonspherical potentials and of inelastic collisions on transport coefficients. Dalgarno and Henry[236] have considered such phenomena in terms of their effects on the $S^{(l)}(v)$ of Eq. (58); this is inadequate because the cross-section formulas are changed in essential ways by inelastic collisions, and it is necessary to reconsider the kinetic-theory description from the beginning.[237] The internal degrees of freedom do affect the thermal conductivity strongly.[238,239] but probably affect the viscosity only weakly. The effects of angular-dependent forces are more difficult to describe quantitatively. These can act in two ways; by inducing transitions in the internal states, and by their effect on the total elastic scattering cross section. An approximate calculation scheme, applied by Monchick and Mason[240] to polar molecules, fixed the relative orientation of the molecular axes during the course of a collision. Cross and Herschbach[241] made some detailed scattering calculations for a 12-6 potential with an angular-dependent part, and found that perhaps a more suitable model would be to assume that the rotational motion of the molecules stayed fixed during collision (flywheel approximation). This model seems to be the classical analog of the distorted-wave approximation in the quantum theory of scattering. Rigorous calculations are now in progress to evaluate the effects of internal degrees of freedom, but these proceed from special models such as rough spheres,[242,243] loaded spheres,[244] or spherocylinders.[245] The effects of inelastic collisions on thermal diffusion have also recently been estimated.[246] They prove not to be overwhelming (generally less than 15%), but they must be taken into account in any accurate work. Fortunately, extensive work on intermolecular forces based on thermal diffusion has usually been restricted to the rare gases.

C. Condensed Phases

The study of intermolecular forces through the properties of solids and liquids is plagued by the problem of many-body forces. The

pioneering work of Born and Mayer, Lennard-Jones, and others showed that the assumption of pairwise additive potentials gave at least a semiquantitative account of many crystal properties. Corner[247] showed that the 12-6 and exp-6-8 potentials could be used to obtain highly consistent results for the binding energy of simple crystals and the Joule-Thomson and second virial coefficients of gases, and this work was extended to include other gas properties and other simple potential models.[248,249] Many other crystal properties can also be used to characterize the intermolecular potential, such as entropy, specific heat, molar volume, vapor pressure, sound velocity, etc., *provided* that one believes in pairwise additivity. For instance, Guggenheim and McGlashan[250] based their piecewise-constructed potential heavily on crystal data.

Unfortunately, there are both theoretical and experimental grounds for believing that three-body interactions (at least) are not negligible.[251,252] When these are included, they destroy the previous good agreement. But it has become increasingly evident that potentials such as the 12-6, exp-6, Kihara core, etc., are only good semiquantitative models that must not be taken too literally. A more accurate determination[221,222] using gas-phase properties that depend only on pair interactions results in a potential that differs slightly from the 12-6 potential for the rare gases. Although the differences are slight, they are significant when crystal properties are calculated. When the lattice energy is summed with this new two-body potential, the result differs from experiment by 10–15%. If just the triple-dipole dispersion energy is included, it accounts nicely for this discrepancy[253]; however, it leaves open the question of the contribution from other many-body terms. Indeed, various correlations suggest that the *net* nonadditivity may be quite small.[247–249,254]

We believe it is a fair statement to say that a good *effective* pair potential may be fitted to crystal data, but that it is not a good direct measure of two-body forces if a precise determination is desired. Unfortunately, there is, as yet, no agreement on the signs and magnitudes of the various many-body contributions to the crystal properties. It is quite conceivable that the total many-body contribution may be small, although various terms may be individually large. One approach would be to obtain a very accurate two-body potential from sources uncontaminated by many-body effects (e.g., scattering cross sections, transport coefficients, etc.), and then determine many-body effects in

crystals as the difference between experimental and calculated two-body properties. It would appear very risky to base conclusions about effects of many-body forces on calculations involving approximate two-body potentials.

One of the motivations for important theoretical work on three-body exchange forces, carried out by Jansen and co-workers,[252] has been to account for the stability of crystal lattices for molecular and ionic crystals. In general, this has met with fair success. However, in the case of argon, Alder and Paulson[255] have shown that a slight change in the attractive rim of the potential well also accounts for the correct stable lattice. The change required is qualitatively similar to that required by the new potential of Munn and Smith[222] or by a potential derived from x-ray scattering in the gas phase.[256]

Liquids and dense gases are even more difficult to use than solids for the determination of intermolecular forces; not only do the questions of many-body forces still exist, but the basic statistical-mechanical theory of liquids is still in a rudimentary state. One fairly direct approach is the inversion of the experimental pair distribution function for liquids and dense gases as determined from x-ray scattering,[257,258] but the many-body problem still exists. Rowlinson and co-workers have also discussed other liquid properties suitable for the determination of intermolecular forces, such as the isotopic separation factor in vapor–liquid equilibrium. This work has recently been reviewed by Rowlinson.[213]

VI. RELAXATION METHODS

By relaxation methods, we mean the studies of inelastic molecular collisions in which vibrational or rotational energy is interchanged with translational energy. Such effects are usually studied experimentally by relaxation methods, such as absorption or dispersion of sound, or shock front thicknesses. Relaxation times are more sensitive functions of the asymmetry of molecular forces than are elastic scattering cross sections or transport coefficients. In order to excite or suppress vibration, one part of a molecule must interact with a colliding particle more strongly than the rest; to excite or suppress rotation, a torque must be applied which cannot exist for spherically symmetric fields. Moreover, relaxation times may be more sensitive to collision energy than are most bulk processes. For example, vibrational relaxation in gases at ordinary

temperatures is specifically sensitive to the energetic collisions occurring, and thus "looks at" a different portion of the intermolecular potential than does the viscosity of the gas at the same temperature.

The first theory to give a qualitatively accurate description of vibrational relaxation time as a function of temperature is the quantal calculation of Schwartz, Slawsky, and Herzfeld (SSH theory) and is reviewed by Herzfeld and Litovitz.[259] It can very easily be inverted and used to determine short-range intermolecular forces from experimental measurements of the temperature dependence of the vibrational relaxation time.[52,260,261] However, almost all the major assumptions of the SSH theory have recently been questioned and found to be only qualitatively valid, at best. Recent work by Widom[262] and Shin[263] indicates that the transition probability is sensitive to the shape of the potential. The SSH assumption that the attractive well of the potential can be accounted for by increasing the effective relative kinetic energy therefore seems to be questionable. The work of Widom and of Shin also indicates a questionable element in the "modified-wave number" approximation, in which the centrifugal energy is replaced by a constant equal to its value at the distance of closest approach. In some very elegant studies, Mies[264] found that anharmonicities affect the transition probabilities greatly. That is, the shift of the translational wave function is small in magnitude, but for high kinetic energies is sufficient to shift the outgoing wave out of phase with the incoming wave. Finally, the commonly adopted approximation of a steepest-descent evaluation of the average over kinetic energies involves several compensating errors and thus is fairly good.[265] When the SSH theory is used to determine potentials,[52,260,261] the potential determined is often steeper than expected from beam scattering experiments.

Recent calculations indicate that classical and semiclassical calculations are sufficient to describe vibrational relaxation.[262,266,267] Parker's classical theory,[268] in particular, has some interesting features. The field of a diatomic molecule is assumed to arise from the superposition of two centers of force that need not coincide with the nuclei. Empirically, they are shifted toward the center of the molecule. This agrees with the observation from x-ray scattering and from theory that the centers of electron distributions of bonded H atoms do not coincide with the nucleus.[269] The predicted smaller nonsphericity of diatomic molecules is also in qualitative agreement with the theoretical calculations of Roberts[65] and of Krauss and Mies.[66] The values of the poten-

tial steepness derived from Parker's theory are more in line with scattering results than are those from the SSH theory.

In general, rotational relaxation involves transitions among many states and is, therefore, too complicated for present quantum theory to handle. Hydrogen is an exception because of its small moment of inertia. The first-order distorted-wave approximation is applicable to hydrogen and indicates[270] that the transition probability is proportional to the square of the parameter describing the nonsphericity of the interaction. Empirically, the value of this parameter is twice the theoretical values. For other molecules, a classical calculation of rotational relaxation should be valid. Parker's classical theory[268] predicts an unexpected temperature dependence for the rotational relaxation time, which seems to be confirmed by thermal conductivity measurements.[238]

In short, vibrational and rotational relaxation measurements are potentially valuable sources of information on intermolecular forces, but the basic theory needs refinement.

VII. FINAL REMARKS

If this rather long account of methods of determining intermolecular forces has any moral, it is that theory and experiment must go hand-in-hand, and that one should not take models over-seriously. Analysis of experimental data depends heavily on theory to suggest the form of the potential model; theoretical calculations of intermolecular forces almost always rely on experiment to furnish a few crucial numbers. At present, work on intermolecular forces tends to be strongly polarized in either an experimental or a theoretical direction; more work in the middle ground should prove fruitful. We seem to be on the verge of accurate determinations of "true" potential energy curves for simple atoms, and this would be fundamental to a number of advances in other fields.

References

1. D. R. Bates, K. Ledsham, and A. L. Stewart, *Phil. Trans. Roy. Soc.* (*London*), **A246**, 215 (1953).
2. D. R. Bates and T. R. Carson, *Proc. Roy. Soc.* (*London*), **A234**, 207 (1956).
3. H. M. James and A. S. Coolidge, *J. Chem. Phys.*, **1**, 825 (1933); **6**, 730 (1938); H. M. James, A. S. Coolidge, and R. D. Present, *ibid.*, **4**, 187 (1936).
4. W. Kolos and C. C. J. Roothan, *Rev. Mod. Phys.*, **32**, 219 (1960); W. Kolos and L. Wolniewicz, *J. Chem. Phys.*, **41**, 3663 (1964); **43**, 2429 (1965).
5. L. Pauling and J. Y. Beach, *Phys. Rev.*, **47**, 686 (1935).
6. J. O. Hirschfelder and J. W. Linnett, *J. Chem. Phys.*, **18**, 130 (1950).

7. A. Dalgarno and N. Lynn, *Proc. Roy. Soc.* (*London*), **A69**, 821 (1956).
8. P. E. Phillipson, *Phys. Rev.*, **125**, 1981 (1962). The accuracy of these calculations at very small separations has recently been confirmed and improved by G. M. Matsumoto, C. F. Bender, and E. R. Davidson, *J. Chem. Phys.*, **46**, 402 (1967).
9. W. D. Davison, *Proc. Phys. Soc.* (*London*), **87**, 133 (1966).
10. Reported by O. Sinanoğlu and D. F. Tuan, *Ann. Rev. Phys. Chem.*, **15**, 251 (1964).
11. N. Moore, *J. Chem. Phys.*, **33**, 471 (1960).
12. D. Y. Kim, *Z. Physik*, **166**, 359 (1962).
13. N. R. Kestner and O. Sinanoğlu, *J. Chem. Phys.* **45**, 194 (1966). See also N. R. Kestner, *ibid*, **45**, 208, 213 (1966).
14. See the comments by J. O. Hirschfelder, *J. Chem. Phys.*, **43**, S199 (1965).
15. H. Margenau, *Rev. Mod. Phys.*, **11**, 1 (1939).
16. H. Margenau, *Phys. Rev.*, **56**, 1000 (1939).
17. A. Dalgarno and N. Lynn, *Proc. Phys. Soc.* (*London*), **A70**, 802 (1957).
18. A. Dalgarno and A. E. Kingston, *Proc. Phys. Soc.* (*London*), **72**, 1053 (1958); **73**, 455 (1959); **78**, 607 (1961).
19. A. E. Kingston, *Phys. Rev.*, **135**, A108 (1964).
20. J. A. Barker and P. J. Leonard, *Phys. Letters*, **13**, 127 (1964).
21. R. J. Bell, *Proc. Phys. Soc.* (*London*), **86**, 17 (1965).
22. F. London, *Z. Physik. Chem.*, **B11**, 222 (1930).
23. J. C. Slater and J. G. Kirkwood, *Phys. Rev.*, **37**, 682 (1931).
24. A. Dalgarno and J. T. Lewis, *Proc. Phys. Soc.* (*London*), **A69**, 628 (1956).
25. J. G. Kirkwood, *Phys. Z.*, **33**, 57 (1932).
26. A. Müller, *Proc. Roy. Soc.* (*London*), **A154**, 624 (1936).
27. L. Salem, *Mol. Phys.*, **3**, 441 (1960).
28. J. A. Barker, *Ann. Rev. Phys. Chem.*, **14**, 229 (1963).
29. J. N. Wilson, *J. Chem. Phys.*, **43**, 2564 (1965).
30. M. Karplus and H. J. Kolker, *J. Chem. Phys.*, **41**, 3955 (1964).
31. K. S. Pitzer and E. Catalano, *J. Am. Chem. Soc.*, **78**, 4844 (1956).
32. L. Salem, *J. Chem. Phys.*, **37**, 2100 (1962). This paper contains references to many earlier related papers.
33. D. E. Petersen and K. S. Pitzer, *J. Phys. Chem.*, **61**, 1252 (1957).
34. K. S. Pitzer, in *Advances in Chemical Physics*, Vol. 2, I. Prigogine, Ed., Interscience, New York, 1959, p. 59.
35. M. D. McKinley and T. M. Reed III, *J. Chem. Phys.*, **42**, 3891 (1965), and references contained therein.
36. H. C. Longuet-Higgins and L. Salem, *Proc. Roy. Soc.* (*London*), **A259**, 433 (1961).
37. C. Zener, *Phys. Rev.*, **37**, 556 (1931).
38. W. Byers Brown, *Discussions Faraday Soc.* **40**, 140 (1965); W. Byers Brown and E. Steiner, *J. Chem. Phys.*, **44**, 3934 (1966).
39. E. A Mason, *J. Chem. Phys.*, **23**, 49 (1955); S. Weissman, S. C. Saxena, and E. A. Mason, *Phys. Fluids*, **3**, 510 (1960); E. A. Mason, M. Islam, and S. Weissman, *Phys. Fluids*, **7**, 1011 (1964).
40. I. Amdur, E. A. Mason, and A. L. Harkness, *J. Chem. Phys.*, **22**, 1071 (1954); I. Amdur and E. A. Mason, *ibid.* **25**, 632 (1965).

41. A. B. Kamnev and V. B. Leonas, *Soviet Phys. Doklady* (*Engl. Trans.*), **10**, 1202 (1966) [*Dokl. Akad. Nauk SSSR*, **165**, 1273 (1965)].
42. G. Herzberg, *Spectra of Diatomic Molecules*, Van Nostrand, Princeton, New Jersey, 1950.
43. C. A. Coulson, *Valence*, Oxford University Press, London, 1952.
44. (a) P. O. Löwdin, *Rev. Mod. Phys.*, **34**, 80 (1962); (b) R. W. Keyes, *J. Chem. Phys.*, **29**, 523 (1958); *Nature*, **182**, 1071 (1958).
45. Y. P. Varshni, *Rev. Mod. Phys.*, **29**, 664 (1957); D. Steele, E. R. Lippincott, and J. T. Vanderslice, *ibid.*, **34**, 239 (1962).
46. P. H. Krupenie, E. A. Mason, and J. T. Vanderslice, *J. Chem. Phys.*, **39**, 2399 (1963).
47. S. Glasstone, K. J. Laidler, and H. Eyring, *The Theory of Rate Processes*, McGraw-Hill, New York, 1941.
48. J. K. Cashion and D. R. Herschbach, *J. Chem. Phys.*, **40**, 2358 (1964); **41**, 2199 (1964).
49. F. O. Ellison, *J. Chem. Phys.*, **41**, 2198 (1964), and references therein.
50. H. Eyring, *J. Am. Chem. Soc.*, **54**, 3191 (1932); see also ref. 43, pp. 166–171.
51. J. T. Vanderslice and E. A. Mason, *Rev. Mod. Phys.*, **62**, 417 (1960); *Advances in Molecular Spectroscopy*, Pergamon Press, New York, 1962, pp. 323–330.
52. J. T. Vanderslice, E. A. Mason, and E. R. Lippincott, *J. Chem. Phys.*, **30**, 129 (1959); **33**, 614 (1960).
53. J. T. Vanderslice, E. A. Mason, and W. G. Maisch, *J. Chem. Phys.*, **31**, 738 (1959); **32**, 515 (1960); **33**, 614 (1960).
54. W. E. Meador, Jr., *Natl. Aeron. Space Admin. Tech. Rept.* NASA-TR-R-68 (1960).
55. H. Knof, E. A. Mason, and J. T. Vanderslice, *J. Chem. Phys.*, **40**, 3548 (1964).
56. J. M. Yos, Avco Corporation Tech. Rept. RAD-TR-65-7, May 1965.
57. F. O. Ellison, *J. Chem. Phys.*, **43**, 3654 (1965).
58. R. J. Fallon, J. T. Vanderslice, and E. A. Mason, *J. Chem. Phys.*, **32**, 1453 (1960); **33**, 944 (1960).
59. F. Jenč, *Collection Czech. Chem. Commun.*, **28**, 2052 (1963).
60. F. Jenč and J. Plíva, *Collection Czech. Chem. Commun.*, **28**, 1449 (1963).
61. R. H. Davies, E. A. Mason, and R. J. Munn, *Phys. Fluids*, **8**, 444 (1965).
62. I. Amdur, E. A. Mason, and J. E. Jordan, *J. Chem. Phys.*, **27**, 527 (1957); I. Amdur, M. S. Longmire, and E. A. Mason, *ibid.*, **35**, 895 (1961); E. A. Mason and I. Amdur, *ibid.*, **41**, 2695 (1964).
63. Yu. N. Belyaev and V. B. Leonas, *Soviet Phys. Tech. Phys.* (*Engl. Trans.*), **11**, 257 (1966) [*Zh. Tekh. Fiz. SSSR*, **36**, 353 (1966)].
64. L. Salem, *Proc. Roy. Soc.* (*London*), **A264**, 379 (1961).
65. C. S. Roberts, *Phys. Rev.*, **131**, 203 (1963).
66. M. Krauss and F. H. Mies, *J. Chem. Phys.*, **42**, 2703 (1965).
67. R. Eisenschitz and F. London, *Z. Physik*, **60**, 491 (1930).
68. F. London, *J. Phys. Chem.*, **46**, 305 (1942).
69. E. F. Haugh and J. O. Hirschfelder, *J. Chem. Phys.*, **23**, 1778 (1955).
70. A. Dalgarno and N. Lynn, *Proc. Phys. Soc.* (*London*), **A69**, 821 (1956).
71. N. Lynn, *Proc. Phys. Soc.* (*London*), **72**, 201 (1958).
72. F. London, *Trans. Faraday Soc.*, **33**, 8 (1937).

73. H. Margenau, *J. Chem. Phys.*, **9**, 896 (1938).
74. J. H. Hornig and J. O. Hirschfelder, *J. Chem. Phys.*, **20**, 1812 (1952).
75. W. L. Bade, *J. Chem. Phys.*, **27**, 1280 (1957); **28**, 282 (1958); W. L. Bade and J. G. Kirkwood, *ibid.*, **27**, 1284 (1957). References to many other papers are contained in these.
76. M. J. Sparnaay, *Physica*, **25**, 217 (1959).
77. R. Zwanzig, *J. Chem. Phys.*, **39**, 2251 (1963).
78. H. Sternlicht, *J. Chem. Phys.*, **40**, 1175 (1964).
79. M. J. Sparnaay, *Physica*, **25**, 444 (1959).
80. N. Bohr, *Kgl. Danske Videnskab. Selskab, Mat. Fys. Medd.*, **18**, 8 (1948).
81. O. B. Firsov, *Soviet Phys. JETP (Engl. Trans.)*, **6**, 534 (1958) [*Zh. Eksperim. Teor. Fiz.*, **33**, 696 (1957)].
82. F. Seitz, *Discussions Faraday Soc.*, **5**, 271 (1949); L. Monchick, K. Funabashi, and J. L. Magee, *J. Chem. Phys.*, **27**, 734 (1957).
83. G. M. Lane and E. Everhart, *Phys. Rev.*, **120**, 2064 (1960).
84. A. A. Abrahamson, R. D. Hatcher, and G. H. Vineyard, *Phys. Rev.*, **121**, 159 (1961); A. A. Abrahamson, *ibid.*, **130**, 693 (1963); **133**, A990 (1964).
85. R. Gáspár, *Acta Phys. Acad. Sci. Hung.*, **11**, 71 (1960); **16**, 187 (1963).
86. L. Jansen, *Phys. Rev.*, **125**, 1798 (1962); **135**, A1292 (1964); L. Jansen and S. Zimering, *Phys. Letters*, **4**, 91, 95 (1963).
87. A. E. Sherwood, A. G. DeRocco, and E. A. Mason, *J. Chem. Phys.*, **44**, 2984 (1966).
88. J. O. Hirschfelder and M. A. Eliason, *Ann. N. Y. Acad. Sci.*, **67**, 451 (1957).
89. W. R. Hindmarsh, *Phys. Letters*, **7**, 115 (1963).
90. A. A. Frost, *J. Chem. Phys.*, **25**, 1150 (1956).
91. E. R. Lippincott, *J. Chem. Phys.*, **26**, 1678 (1957); and succeeding papers.
92. E. A. Mason and J. T. Vanderslice, *J. Chem. Phys.*, **28**, 432 (1958).
93. G. G. Weber, *J. Chem. Phys.*, **40**, 1762 (1964).
94. D. R. Olander, *J. Chem. Phys.*, **43**, 779 (1965).
95. O. Jefimenko, *J. Chem. Phys.*, **37**, 2125 (1962); **42**, 205 (1965).
96. P. M. Morse, *Phys. Rev.*, **34**, 57 (1929).
97. A. S. Coolidge, H. M. James, and E. L. Vernon, *Phys. Rev.*, **54**, 726 (1938).
98. E. R. Lippincott, *J. Chem. Phys.*, **23**, 603 (1955); E. R. Lippincott and R. Schroeder, *ibid.*, **23**, 1131 (1955).
99. W. R. Jarmain, *Can. J. Phys.*, **38**, 217 (1960).
100. Y. P. Varshni, *Rev. Mod. Phys.*, **29**, 684 (1957).
101. D. Steele, E. R. Lippincott, and J. T. Vanderslice, *Rev. Mod. Phys.*, **34**, 239 (1962).
102. R. Rydberg, *Z. Physik*, **73**, 376 (1931); **80**, 514 (1933).
103. O. Klein, *Z. Physik*, **76**, 226 (1932).
104. A. L. G. Rees, *Proc. Phys. Soc. (London)*, **59**, 998 (1947).
105. J. T. Vanderslice, E. A. Mason, W. G. Maisch, and E. R. Lippincott, *J. Mol. Spectry.*, **3**, 17 (1959); **5**, 83 (1960).
106. S. Weissman, J. T. Vanderslice, and R. Battino, *J. Chem. Phys.*, **39**, 2226 (1963).
107. W. G. Richards and R. F. Barrow, *Trans. Faraday Soc.*, **60**, 797 (1964); *Proc. Phys. Soc. (London)*, **83**, 1045 (1964).
108. R. N. Zare, *J. Chem. Phys.*, **40**, 1934 (1964).

109. F. R. Gilmore, *J. Quant. Spectry. Radiative Transfer*, **5**, 369 (1965).
110. F. J. Zeleznik, *J. Chem. Phys.*, **42**, 2836 (1965).
111. M. L. Ginter and R. Battino, *J. Chem. Phys.*, **42**, 3222 (1965).
112. J. T. Vanderslice, R. Davies, and S. Weissman, *J. Chem. Phys.*, **43**, 1075 (1965); R. H. Davies and J. T. Vanderslice, *ibid.*, **45**, 95 (1966).
113. R. H. Davies and J. T. Vanderslice, *Can. J. Phys.*, **44**, 219 (1966).
114. J. L. Dunham, *Phys. Rev.*, **41**, 721 (1932).
115. I. Sandeman, *Proc. Roy. Soc.* (*Edinburgh*), **60**, 210 (1940).
116. R. S. Mulliken, *J. Chem. Phys.*, **33**, 247 (1960).
117. P. K. Carroll, *J. Chem. Phys.*, **37**, 805 (1962).
118. R. B. Bernstein, *Phys. Rev. Letters*, **16**, 385 (1966).
119. E. C. G. Stueckelberg, *Phys. Rev.*, **42**, 522 (1932).
120. G. E. Gibson, O. K. Rice, and N. S. Bayliss, *Phys. Rev.*, **44**, 193 (1933).
121. N. S. Bayliss, *Proc. Roy. Soc.* (*London*), **A158**, 551 (1937).
122. L. Mathieson and A. L. G. Rees, *J. Chem. Phys.*, **24**, 753 (1956).
123. A. L. G. Rees, *J. Chem. Phys.*, **26**, 1567 (1957).
124. S. K. Luke, M.S. thesis, University of Maryland, 1964. S. K. Luke, S. Weissman, and J. T. Vanderslice, in preparation.
125. R. G. Breene, Jr., *The Shift and Shape of Spectral Lines*, Pergamon Press, New York, 1961.
126. U. Fano, *Phys. Rev.*, **131**, 259 (1963).
127. G. P. Reck, H. Takebe, and C. A. Mead, *Phys. Rev.*, **137**, A683 (1965).
128. A. D. Buckingham, *Quart. Rev.* (*London*), **13**, 183 (1959).
129. H. Margenau and H. C. Jacobson, *J. Chem. Phys.*, **38**, 1259 (1963); *J. Quant. Spectry. Radiative Transfer*, **3**, 35 (1963).
130. J. D. Poll, *Phys. Letters*, **7**, 32 (1963).
131. J. A. A. Ketelaar and R. P. H. Rettschnick, *Mol. Phys.*, **7**, 191 (1964).
132. A. Watanabe and H. L. Welsh, *Phys. Rev. Letters*, **13**, 810 (1964); *Can. J. Phys.*, **43**, 818 (1965).
133. A. Kudian, H. L. Welsh, and A. Watanabe, *J. Chem. Phys.*, **43**, 3397 (1965).
134. R. G. Gordon and J. K. Cashion, *J. Chem. Phys.*, **44**, 1190 (1966); J. K. Cashion, *ibid.*, **45**, 1656 (1966).
135. O. Jefimenko and R. J. Exton, *J. Chem. Phys.*, **39**, 229 (1963); O. Jefiimenko, *ibid.*, **39**, 2457 (1963); O. Jefimenko and G. M. Williams, *ibid.*, **42**, 207 (1965).
136. J. B. Anderson, R. P. Andres, and J. B. Fenn, *Advan. At. Mol. Phys.*, **1**, 345 (1965).
137. J. B. Anderson, R. P. Andres, and J. B. Fenn, in *Molecular Beams* (*Advances in Chemical Physics*, Vol. 10), J. Ross, Ed., Interscience, New York, 1966, p. 275.
138. J. B. Hasted, *Physics of Atomic Collisions*, Butterworths, Washington, D.C., 1964.
139. E. W. McDaniel, *Collision Phenomena in Ionized Gases*, Wiley, New York, 1964.
140. J. Ross, Ed., *Molecular Beams* (*Advances in Chemical Physics*, Vol. 10), Interscience, New York, 1966.
141. H. Pauly, *Fortsch. Physik*, 9, 613 (1961).
142. W. L. Fite and S. Datz, *Ann. Rev. Phys. Chem.*, **14**, 61 (1963).

143. V. B. Leonas, *Soviet Phys. Usp.* (*Engl. Trans.*), **7**, 121 (1964) [*Usp. Fiz. Nauk*, **82**, 287 (1964)].
144. E. A. Mason and J. T. Vanderslice, in *Atomic and Molecular Processes*, D. R. Bates, Ed. Academic Press, New York, 1962, Chap. 17.
145. I. Amdur and J. E. Jordan, in *Molecular Beams* (*Advances in Chemical Physics*, Vol. 10), J. Ross, Ed., Interscience, New York, 1966, p. 29.
146. E. E. Muschlitz, Jr., in *Molecular Beams* (*Advances in Chemical Physics*, Vol. 10), J. Ross, Ed., Interscience, New York, 1966, p. 171.
147. H. Pauly and J. P. Toennies, *Advan. At. Mol. Phys.*, **1**, 201 (1965).
148. R. B. Bernstein, in *Molecular Beams* (*Advances in Chemical Physics*, Vol. 10), J. Ross, Ed., Interscience, New York, 1966, p. 75.
149. E. F. Greene, A. L. Moursund, and J. Ross, in *Molecular Beams*, (*Advances in Chemical Physics*, Vol. 10), J. Ross, Ed., New York, 1966, p. 135.
150. N. F. Mott and H. S. W. Massey, *The Theory of Atomic Collisions*, Oxford University Press, London, 3rd ed., 1965.
151. T.-Y. Wu and T. Ohmura, *Quantum Theory of Scattering*, Prentice-Hall, Englewood Cliffs, New Jersey, 1962.
152. M. L. Goldberger and K. M. Watson, *Collision Theory*, Wiley, New York, 1964.
153. F. T. Smith, *J. Chem. Phys.*, **42**, 2419 (1965).
154. K. W. Ford and J. A. Wheeler, *Ann. Phys.* (*N.Y.*), **7**, 259, 287 (1959).
155. R. J. Munn, E. A. Mason, and F. J. Smith, *J. Chem. Phys.*, **41**, 3978 (1964).
156. P. M. Livingston, *J. Chem. Phys.*, **45**, 601 (1966).
157. E. A. Mason, J. T. Vanderslice, and C. J. G. Raw, *J. Chem. Phys.*, **40**, 2153 (1964).
158. F. J. Smith, E. A. Mason, and J. T. Vanderslice, *J. Chem. Phys.*, **42**, 3257 (1965).
159. J. E. Jordan and I. Amdur, *J. Chem. Phys.*, **46**, 165 (1967).
160. I. Amdur, *Progress in International Research on Thermodynamics and Transport Properties*, American Society of Mechanical Engineers, New York, 1962, pp. 369–377.
161. E. A. Mason and I. Amdur, *J. Chem. Phys.*, **41**, 2695 (1964).
162. E. A. Mason, J. Ross, and P. N. Schatz, *J. Chem. Phys.*, **25**, 626 (1956).
163. H. S. Taylor and F. E. Harris, *Mol. Phys.*, **7**, 287 (1964).
164. A. K. Barua and S. Chatterjee, *Mol. Phys.*, **7**, 443 (1964).
165. A. B. Kamnev and V. B. Leonas, *Soviet Phys. Doklady* (*Engl. Trans.*), **10**, 529 (1965) [*Dokl. Akad. Nauk SSSR*, **162**, 798 (1965)].
166. A. B. Kamnev and V. B. Leonas, *High Temp.* (*Engl. Trans.*), **3**, 744 (1965) [*Tepl. Vys. Temp.*, **3**, 804 (1965)].
167. F. C. Hoyt, *Phys. Rev.*, **55**, 664 (1939).
168. O. B. Firsov, *Zh. Eksperim. Teor. Fiz.*, **24**, 279 (1953).
169. J. B. Keller, I. Kay, and J. Shmoys, *Phys. Rev.*, **102**, 557 (1956).
170. H. W. Berry, *Phys. Rev.*, **75**, 913 (1949); **99**, 553 (1955).
171. F. P. Ziemba and E. Everhart, *Phys. Rev. Letters*, **2**, 299 (1959).
172. G. J. Lockwood and E. Everhart, *Phys. Rev.*, **125**, 567 (1962).
173. G. J. Lockwood, H. F. Helbig, and E. Everhart, *Phys. Rev.*, **132**, 2078 (1963).
174. E. Everhart, *Phys. Rev.*, **132**, 2083 (1963).
175. H. F. Helbig and E. Everhart, *Phys. Rev.*, **140**, A715 (1965).

176. P. R. Jones, P. Costigan, and G. Van Dyk, *Phys. Rev.*, **129**, 211 (1963).
177. P. R. Jones, N. W. Eddy, H. P. Gilman, A. K. Jhaveri, and G. Van Dyk, *Phys. Rev.*, **147**, 76 (1966).
178. P. R. Jones, T. L. Batra, and H. A. Ranga, *Phys. Rev. Letters*, **17**, 281 (1966).
179. D. C. Lorents and W. Aberth, *Phys. Rev.*, **139**, A1017 (1965).
180. W. Aberth and D. C. Lorents, *Phys. Rev.*, **144**, 109 (1966).
181. H. S. W. Massey and R. A. Smith, *Proc. Roy. Soc.* (*London*), **A142**, 142 (1933).
182. W. L. Lichten, *Phys. Rev.*, **131**, 229 (1963).
183. F. J. Smith, *Phys. Letters*, **10**, 290 (1964); *Proc. Phys. Soc.* (*London*), **84**, 889 (1964).
184. W. Aberth, D. C. Lorents, R. P. Marchi, and F. T. Smith, *Phys. Rev. Letters*, **14**, 776 (1965).
185. R. P. Marchi and F. T. Smith, *Phys. Rev.*, **139**, A1025 (1965).
186. F. T. Smith, D. C. Lorents, W. Aberth, and R. P. Marchi, *Phys. Rev. Letters*, **15**, 742 (1965).
187. J. Perel, R. H. Vernon, and H. L. Daley, *Phys. Rev.*, **138**, A937 (1965).
188. F. J. Smith, *Phys. Letters*, **20**, 503 (1966).
189. H. O. Lutz, S. Datz, C. D. Moak, and T. S. Noggle, *Phys. Rev. Letters*, **17**, 285 (1966).
190. M. Minnaert, *Light and Colour in the Open Air*, Dover, New York, 1954.
191. R. J. Munn and F. J. Smith, *Mol. Phys.*, **10**, 163 (1966).
192. C. Schlier and R. Düren, *Discussions Faraday Soc.* **40**, 56 (1965).
193. F. Knauer, *Naturwiss.*, **21**, 366 (1933); *Z. Physik*, **90**, 599 (1934).
194. E. A. Mason, *J. Chem. Phys.*, **26**, 667 (1957).
195. (a) D. Beck, *J. Chem. Phys.*, **37**, 2884 (1962); (b) D. Beck, E. F. Greene, and J. Ross, *ibid.*, **37**, 2895 (1962).
196. (a) F. A. Morse, R. B. Bernstein, and H. U. Hostettler, *J. Chem. Phys.*, **36**, 1997 (1962); (b) F. A. Morse and R. B. Bernstein, *ibid.*, **37**, 2019 (1962).
197. E. A. Mason and L. Monchick, *J. Chem. Phys.*, **41**, 2221 (1964).
198. E. Hundhausen and H. Pauly, *Z. Naturforsch.*, **19a**, 810 (1964).
199. E. Hundhausen and H. Pauly, *Z. Physik*, **187**, 305 (1965).
200. D. Beck, H. Dummel, and U. Henkel, *Z. Physik*, **185**, 19 (1965).
201. P. Barwig, U. Buck, E. Hundhausen, and H. Pauly, *Z. Physik*, **196**, 343 (1966).
202. Ch. Schlier, *Z. Physik*, **173**, 352 (1963).
203. E. A. Mason, R. J. Munn, and F. J. Smith, *J. Chem. Phys.*, **44**, 1967 (1966).
204. R. B. Bernstein, *J. Chem. Phys.*, **33**, 795 (1960); **34**, 361 (1961).
205. H. U. Hostettler and R. B. Bernstein, *Phys. Rev. Letters*, **5**, 318 (1960); P. J. Groblicki and R. B. Bernstein, *J. Chem. Phys.*, **42**, 2295 (1965).
206. H. S. W. Massey and C. B. O. Mohr, *Proc. Roy. Soc.* (*London*), **A141**, 434 (1933).
207. S. Rosin and I. I. Rabi, *Phys. Rev.*, **48**, 373 (1935).
208. H. Pauly, *Z. Physik*, **157**, 54 (1959).
209. R. Helbing and H. Pauly, *Z. Physik*, **179**, 16 (1964).
210. H. G. Bennewitz and H. D. Dohrmann, *Z. Physik*, **182**, 524 (1965).
211. E. W. Rothe and R. H. Neynaber, *J. Chem. Phys.*, **42**, 3306 (1965); **43**, 4177 (1965).
212. R. B. Bernstein and T. J. P. O'Brien, *Discussions Faraday Soc.*, **40**, 35 (1965).

213. J. S. Rowlinson, *Discussions Faraday Soc.*, **40**, 19 (1965).
214. J. B. Keller and B. Zumino. *J. Chem. Phys.* **30**, 1351 (1959).
215. H. L. Frisch and E. Helfand, *J. Chem. Phys.*, **32**, 269 (1960).
216. J. O. Hirschfelder, C. F. Curtiss, and R. B. Bird, *Molecular Theory of Gases and Liquids*, Wiley, New York, 1964.
217. D. A. Jonah and J. S. Rowlinson, *Trans. Faraday Soc.*, **62**, 1067 (1966)
218. A. E. Kingston, *J. Chem. Phys.*, **42**, 719 (1965).
219. A. E. Sherwood and J. M. Prausnitz, *J. Chem. Phys.*, **41**, 429 (1964).
220. D. D. Konowalow and S. Carrá, *Phys. Fluids*, **8**, 1585 (1965); D. D. Konowalow, *ibid.*, 9, 23 (1966).
221. R. J. Munn, *J. Chem. Phys.*, **40**, 1439 (1964).
222. R. J. Munn and F. J. Smith, *J. Chem. Phys.*, **43**, 3998 (1965).
223. J. A. Barker, W. Fock, and F. Smith, *Phys. Fluids*, **7**, 897 (1964).
224. J. H. Dymond, M. Rigby, and E. B. Smith, *J. Chem. Phys.*, **42**, 2801 (1965); *Phys. Fluids*, **9**, 1222 (1966).
225. H. J. M. Hanley, *J. Chem. Phys.*, **44**, 4219 (1966).
226. L. S. Tee, S. Gotoh, and W. E. Stewart, *Ind. Eng. Chem. Fundamentals*, **5**, 356, 363 (1966).
227. M. Klein, *J. Res. Natl. Bur. Stds.*, **70A**, 259 (1966).
228. T. Kihara, in *Advances in Chemical Physics*, Vol. 1, I. Prigogine, Ed., Interscience, New York, 1958, p. 267.
229. H. W. Graben and R. D. Present, *Phys. Rev. Letters*, **9**, 247 (1962).
230. A. E. Sherwood and J. M. Prausnitz, *J. Chem. Phys.*, **41**, 413 (1964).
231. H. W. Graben, R. D. Present, and R. D. McCulloch, *Phys. Rev.*, **144**, 140 (1966).
232. R. J. Munn, *J. Chem. Phys.*, **42**, 3032 (1965).
233. E. A. Mason, R. J. Munn, and F. J. Smith, *Discussions Faraday Soc.*, **40**, 27 (1965).
234. F. J. Smith, E. A. Mason, and R. J. Munn, *J. Chem. Phys.*, **42**, 1334 (1965).
235. E. A. Mason, R. J. Munn, and F. J. Smith, *Advan. At. Mol. Phys.*, **2**, 33 (1966).
236. A. Dalgarno and R. J. W. Henry, in *Atomic Collision Processes*, M. R. C. McDowell, Ed., North-Holland, Amsterdam, 1964, pp. 914–920.
237. C. S. Wang Chang, G. E. Uhlenbeck, and J. de Boer, in *Studies in Statistical Mechanics*, Vol. 2, J. de Boer and G. E. Uhlenbeck, Eds., Wiley, New York, 1964, 243 ff.
238. E. A. Mason and L. Monchick, *J. Chem. Phys.*, **36**, 1622 (1962).
239. L. Monchick, A. N. G. Pereira, and E. A. Mason, *J. Chem. Phys.*, **42**, 3241 (1965).
240. L. Monchick and E. A. Mason, *J. Chem. Phys.*, **35**, 1676 (1961).
241. R. J. Cross, Jr., and D. R. Herschbach, *J. Chem. Phys.*, **43**, 3530 (1965).
242. L. Waldmann, *Z. Naturforsch.*, **18**a, 1033 (1963).
243. D. W. Condiff, W. K. Lu, and J. S. Dahler, *J. Chem. Phys.*, **42**, 3445 (1965).
244. S. I. Sandler and J. S. Dahler, *J. Chem. Phys.*, **43**, 1750 (1965).
245. S. I. Sandler and J. S. Dahler, *J. Chem. Phys.*, **44**, 1229 (1966).
246. L. Monchick, R. J. Munn, and E. A. Mason, *J. Chem. Phys.*, **45**, 3051 (1966).
247. J. Corner, *Trans. Faraday Soc.*, **35**, 711 (1939); **44**, 914 (1948).
248. E. A. Mason and W. E. Rice, *J. Chem. Phys.*, **22**, 843 (1954).

249. E. Whalley and W. G. Schneider, *J. Chem. Phys.*, **23**, 1644 (1955).
250. E. A. Guggenheim and M. L. McGlashan, *Proc. Roy. Soc.* (*London*), **A255**, 456 (1960); *Mol. Phys.*, **3**, 563, 571 (1960).
251. B. M. Axilrod, *J. Chem. Phys.*, **19**, 724 (1951).
252. L. Jansen and E. Lombardi, *Discussions Faraday Soc.*, **40**, 78 (1965), and earlier papers.
253. M. L. Klein and R. J. Munn, private communication.
254. J. Walkley, *J. Chem. Phys.*, **44**, 2417 (1966).
255. B. J. Alder and R. H. Paulson, *J. Chem. Phys.*, **43**, 4172 (1965).
256. P. G. Mikolaj and C. J. Pings, *Phys. Rev. Letters*, **16**, 4 (1965).
257. M. D. Johnson, P. Hutchinson, and N. H. March, *Proc. Roy. Soc.* (*London*), **A282**, 283 (1964).
258. P. G. Mikolaj and C. J. Pings, *Phys. Rev. Letters*, **15**, 849 (1965).
259. K. F. Herzfeld and T. A. Litovitz, *Absorption and Dispersion of Ultrasonic Waves*, Academic Press, New York, 1959.
260. P. G. Dickens and A. Ripamonti, *Trans. Faraday Soc.*, **57**, 735 (1961).
261. N. A. Generalov and S. A. Losev, *Soviet Phys. Doklady* (*Engl. Trans.*), **8**, 60 (1963) [*Dokl. Akad. Nauk SSSR*, **148**, 552 (1963)].
262. B. Widom, *Discussions Faraday Soc.*, **33**, 37 (1962).
263. H. K. Shin, *J. Chem. Phys.*, **41**, 2864 (1964); **42**, 59 (1965).
264. F. H. Mies, *J. Chem. Phys.*, **40**, 523 (1964); **41**, 903 (1964); **42**, 2709 (1965).
265. J. T. Vanderslice and S. Weissman, *J. Chem. Phys.*, **37**, 2247 (1962).
266. T. L. Cottrell and J. C. McCoubrey, *Molecular Energy Transfer in Gases*, Butterworths, London, 1961.
267. D. Rapp, *J. Chem. Phys.*, **40**, 2813 (1964).
268. J. G. Parker, *Phys. Fluids*, **2**, 449 (1959); *J. Chem. Phys.*, **41**, 1600 (1964).
269. D. E. Williams, *J. Chem. Phys.*, **43**, 4427 (1965).
270. C. S. Roberts, *Phys. Rev.*, **131**, 209 (1961).

8. Determination of Intermolecular Forces via Low-Energy Molecular Beam Scattering*

R. B. BERNSTEIN and J. T. MUCKERMAN

Theoretical Chemistry Institute and Chemistry Department
University of Wisconsin, Madison, Wisconsin

CONTENTS

I. Introduction 390
II. General Remarks 391
A. Short-Range Repulsive Forces 392
B. Intermediate- and Long-Range Attractive Forces 393
III. Description of the Measurements 397
A. Arrangement of the Experiments 397
B. Measured Quantities 398
IV. Description and Illustration of the Phenomena 401
A. General Angular Dependence of Scattering 402
1. Quantum Mechanical Preliminaries 402
2. Quantum Interferences. 405
3. Low-Angle Classical Behavior 408
4. Rainbow Scattering 409
B. Velocity Dependence of Total Cross Sections 413
1. General Dependence 413
2. Determination of C_6 Constants 414
3. Glory Extrema in $Q(v)$. 414
V. Requirements for Suitability of Systems 418
A. Theoretical Requirements 419
B. Experimental Requirements 420
VI. Inventory of Scattering Measurements 424
A. Systems Studied 424
B. Types of Measurements 424
C. Annotated Bibliography 445

* This work received financial support from the National Aeronautics and Space Administration (Grant NsG-275-62) and the U.S. Atomic Energy Commission, Division of Research.

VII. Summary and Appraisal of the More Reliable Determinations . . . 459
A. Semiempirical Aids to Correlation of Data 460
B. "Best" Potential Parameters for Systems of Atoms and/or Diatomics 464
C. Regularities and Systematics 465
VIII. Concluding Remarks: Scope of the Method 479
References 484

I. INTRODUCTION

Since the early 1930's[1] there has been a continuing effort to extract information on intermolecular forces from molecular beam scattering measurements. However, it is only recently that the full potentiality of the method is beginning to be realized in practice. During the past decade, particularly, there has been a considerable upsurge of activity in elastic (as well as inelastic and reactive) scattering of molecular beams,[2] due to substantial improvements in experimental techniques and advances in the theoretical understanding of molecular scattering phenomena.

It was recognized from the outset, of course, that the elastic scattering behavior of atoms and molecules is completely determined by their interaction potential, not only from classical considerations but also according to the quantum treatment of scattering.[3] Yet, the problem of rigorous "inversion" of experimental cross-section data to yield the potential still remains to be solved, even for a spherically symmetrical (or orientation-averaged) potential referring to a single ground electronic state of the system. Part of the problem (and of the solution) is associated with the fact that many important features of the scattering behavior cannot be accounted for on the basis of classical mechanics alone, but require wave-mechanical analysis.[4] However, since certain of the observations are strongly influenced by the interaction over certain ranges of inter-particle separation, it is usually possible to build up, by parts, an overall picture of the potential for a given system.

We may conveniently divide the elastic scattering studies (on the basis of experimental as well as theoretical techniques) into two parts: (*1*) the evaluation of the short-range, repulsive part of the potential by means of high-energy beam scattering measurements, and (*2*) the determination of the attractive well and long-range "tail" of the potential from scattering observations at thermal and epithermal energies. These will be dealt with separately below.

The goals as well as the methods of molecular beam scattering have already been discussed extensively in the literature,[2] the most authorita-

tive and complete presentation being the recent review by Pauly and Toennies.[2f] In addition, the preceding chapter by Mason and Monchick has given an admirable description of the broad aspects of molecular beam scattering, emphasizing the main effects, the underlying physical principles, and their implications regarding determination of intermolecular forces.

The main purpose of the present chapter, therefore, is to summarize (and appraise) the *practical* results obtained to date.

Most of the significant experimental results which comprise the bulk of this chapter are derived from the recent activities of a relatively small number of the existing molecular beam laboratories, namely those which happen to be concerned with the study of *elastic* scattering of neutral particles. With apologies for the inevitable omissions, the following is a list of the principal currently active laboratories which are contributing data to the literature on experimental intermolecular potentials, including the names of the senior investigator(s) responsible for the current program of elastic molecular beam scattering.

1. Bonn, University of (Germany); H. G. Bennewitz, H. Pauly, J. P. Toennies.

2. Brown University (Providence, R.I.); E. F. Greene.

3. Convair/General Dynamics (San Diego, Cal.); R. H. Neynaber, E. W. Rothe.

4. Freiburg, University of (Germany); D. Beck, Ch. Schlier.

5. Harvard University (Cambridge, Mass.); D. R. Herschbach.

6. Massachusetts Institute of Technology (Cambridge, Mass.); I. Amdur, J. Ross.

7. New York University (New York, N.Y.); B. Bederson.

8. Oak Ridge National Laboratory (Oak Ridge, Tenn.); S. Datz.

9. Purdue University (Lafayette, Ind.); C. R. Mueller.

10. Wisconsin, University of (Madison, Wis.); R. B. Bernstein.

The authors acknowledge the kind cooperation of these investigators, their collaborators, and others who have, in many instances, made their results available prior to publication in order to facilitate their inclusion in the present review.

II. GENERAL REMARKS

A fairly large number of papers on elastic molecular scattering have now been published. A considerable body of conclusive, though fragmentary, information on intermolecular potentials has been acquired—

some of it available from no other experimental source. Unfortunately, as will be seen in Section VII, very few unambiguous and complete potential curves have emerged to date. In retrospect, it appears that the principal contribution of most of these studies has been to spur the development of the experimental technique and to advance the methodology of data analysis. Nevertheless, it seems appropriate at the present time to review the existing results and assess the status of the method.

A. Short-Range Repulsive Forces

This part of the problem has been thoroughly investigated since 1940 by Amdur and co-workers[5] and, with only slight reservation, it appears to have been fairly well solved. It is possible to make a one-to-one connection between the classical impact parameter, b, and the angle of deflection, θ, so that from experimental data on the energy (E) dependence of the "classical" or low-resolution total cross section, one can obtain the deflection function $\theta(b,E)$ uniquely and thus obtain the potential function in the repulsive region (in which it is monotonic).

The experiments have yielded reliable values of the short-range forces between rare gas atoms, simple molecules, etc. Potential energy curves are usually obtained in the form of inverse power repulsions, e.g., $V(r) = ar^{-n}$ over limited ranges of r; however, over a wider range of separations the exponential form of repulsion, $V(r) = Ae^{-Br}$, is a better representation of the potential. The recent experimental results from Amdur's laboratory appear to be accurate to within about 10 % in $V(r)$ over the experimentally accessible range, based upon consideration of systematic errors in the measurements and upon comparisons with potentials inferred from high-temperature equilibrium and transport data. In addition, there is good agreement with recent, quite reliable, theoretical computations of the short-range forces between rare gas atoms. Since this work has been recently reviewed,[5] it will not be discussed in the present chapter, with the following exception.

In the very important case of the He–He system, the most recent experimental study, by Jordan and Amdur,[6] has effectively removed the much-discussed discrepancy between the experimentally derived $V(r)$ and the accurate (configuration-interaction) computations over the range $0.5 < r < 1.0$ Å. Figure 1 shows the present status of the He–He potential in the repulsive region, comparing the beam-derived results with potentials from high-temperature measurements of thermal conductivity,[7] viscosity, and virial coefficient data,[8] as well as the theoretically

determined[9,10] $V(r)$. It may be concluded that there are no important discrepancies remaining, and that the He–He repulsive potential may be considered fairly well established in the range from 0.5 to 2.3 Å. Within

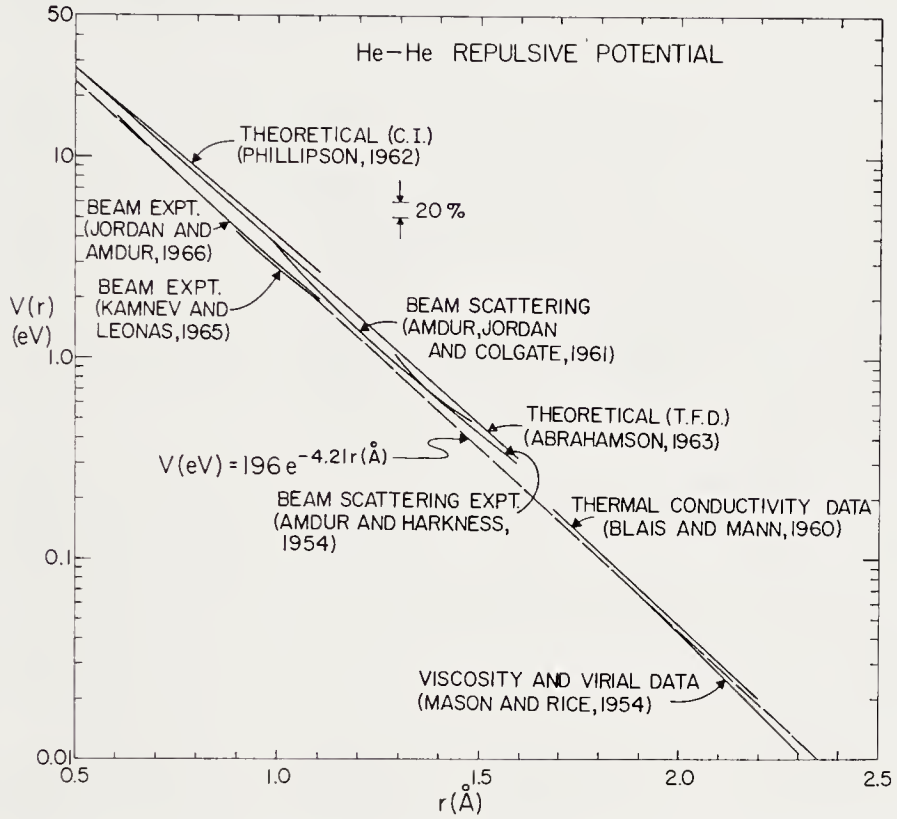

Fig. 1. He–He repulsive potential [5–10]: comparison of beam-derived results with theoretical calculations and with empirical potentials (based on high-temperature thermal conductivity data and on viscosity and virial coefficient data). The dashed line (– – –) is Amdur's equation: $V(eV) = 196 \exp [-4.21\, r(\text{Å})]$, which represents all the data within about 20 %.

about 20 % the results may be represented by Amdur's empirical equation $V(eV) = 196 \exp [-4.21r\ (\text{Å})]$.

B. Intermediate- and Long-Range Attractive Forces

The second part of the problem, dealing with the attractive part of the potential, is somewhat more difficult (and in certain ways more interesting). Since the macroscopic properties of the bulk fluid at ordinary temperatures are strongly influenced by the potential well, it

is an important area of investigation, which is accordingly receiving ever-increasing attention.

The principal reason for the difficulty in carrying out a proper inversion of the beam scattering data is the fact that the nonmonotonic potential function gives rise to a deflection function $\theta(b)$ with a minimum, i.e., the $b(\theta)$ relationship is multivalued.[11]

Thus, classically, the scattered intensity at a given angle may arise from more than one impact parameter. The difficulty caused by the problem of "resolving" the separate contributions or branches of the deflection function (and thus of the potential) leads to a lack of uniqueness, i.e., an ambiguity in the inferred potential. On the other hand, this classical disadvantage is turned by quantum mechanics into a modest advantage, through the existence of oscillatory "interferences" in the scattering from the different branches. By suitable analysis of these and other so-called "quantum effects,"[12] the potential in the region of the well may (in principle) be elucidated in detail.

As yet it has not been possible to deduce the intermolecular potential $V(r)$ in an explicit analytical or even "pointwise" form from scattering data. Normally, one of several semiempirical potential functions is assumed and the attempt is made to determine the parameters by successive approximations. This kind of parameter-fitting operation is, of course, very much reminiscent of that done with the more conventional measurements such as virial coefficients or transport properties.

Listed below are the equations for a number of the most frequently used empirical or semiempirical intermolecular potential functions, expressed in "reduced" notation. Here $V^* \equiv V/\varepsilon$ and $z \equiv r/r_m$, where ε is the well depth and r_m the position of the minimum.

Lennard-Jones $(n,6)$:

$$V^* = \frac{6}{n-6} z^{-n} - \frac{n}{n-6} z^{-6} \tag{1}$$

(typically $n \cong 12$, usually ranging from 8 to 20)

Buckingham Exp $(\alpha,6)$

$$V^* = \frac{6}{\alpha-6} e^{-\alpha(z-1)} - \frac{\alpha}{\alpha-6} z^{-6} \tag{2}$$

(typically $\alpha \cong 12$; similar range as for n)

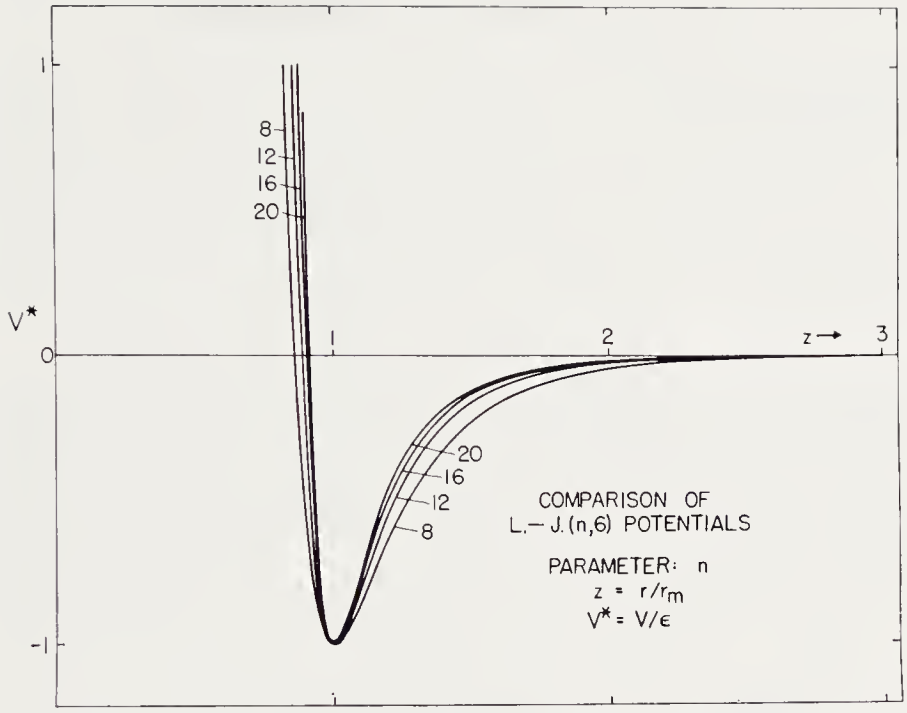

Fig. 2. Family of Lennard-Jones (n,6) potentials for $n = 8$, 12, 16, and 20. $V^* \equiv V/\varepsilon$ plotted vs. $z = r/r_m$.

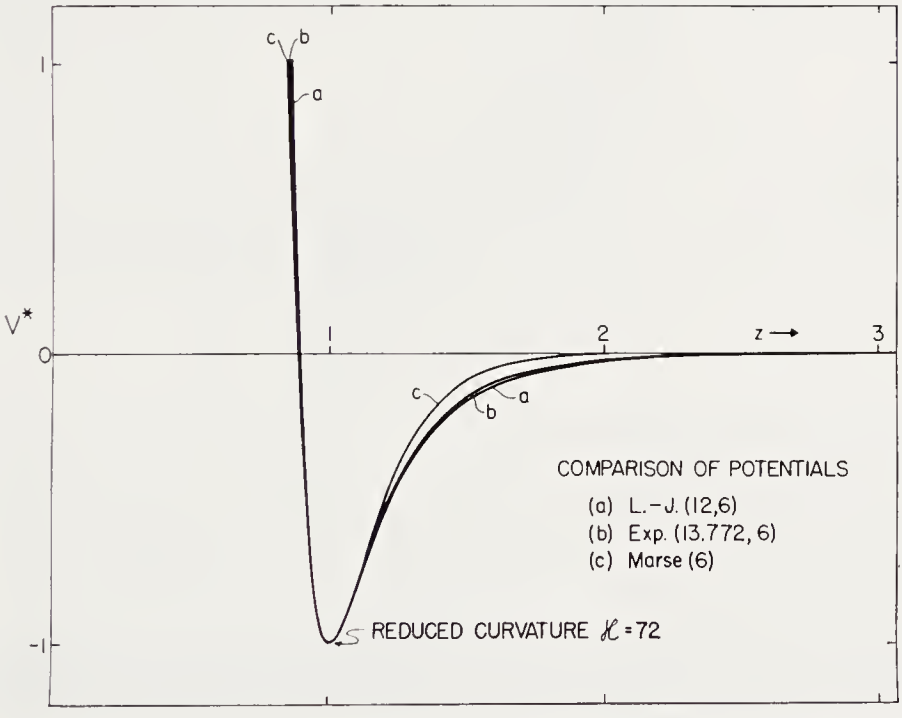

Fig. 3. Comparison of L.-J. (12,6), exp (13.772,6) and Morse (6) potentials, all of which have the same value of the reduced curvature ($\kappa \equiv d^2V^*/dz^2 = 72$) at the minimum.

Kihara (γ,12,6):

$$V^* = \left(\frac{1-\gamma}{z-\gamma}\right)^{12} - 2\left(\frac{1-\gamma}{z-\gamma}\right)^{6} \tag{3}$$

(typically $\gamma \cong 0$, usually ranging from -0.2 to 0.4)

Morse (a):

$$V^* = e^{-2a(z-1)} - 2e^{-a(z-1)} \tag{4}$$

(typically $a \cong 6$, usually ranging from 4 to 8)

Some of these commonly used potentials are shown in Figures 2 and 3. Figure 4 shows deflection functions calculated[11] for a L.-J. (12,6) potential function. The angles of deflection are plotted versus the reduced impact parameter $b^* \equiv \beta \equiv b/\sigma$ as a function of the reduced kinetic

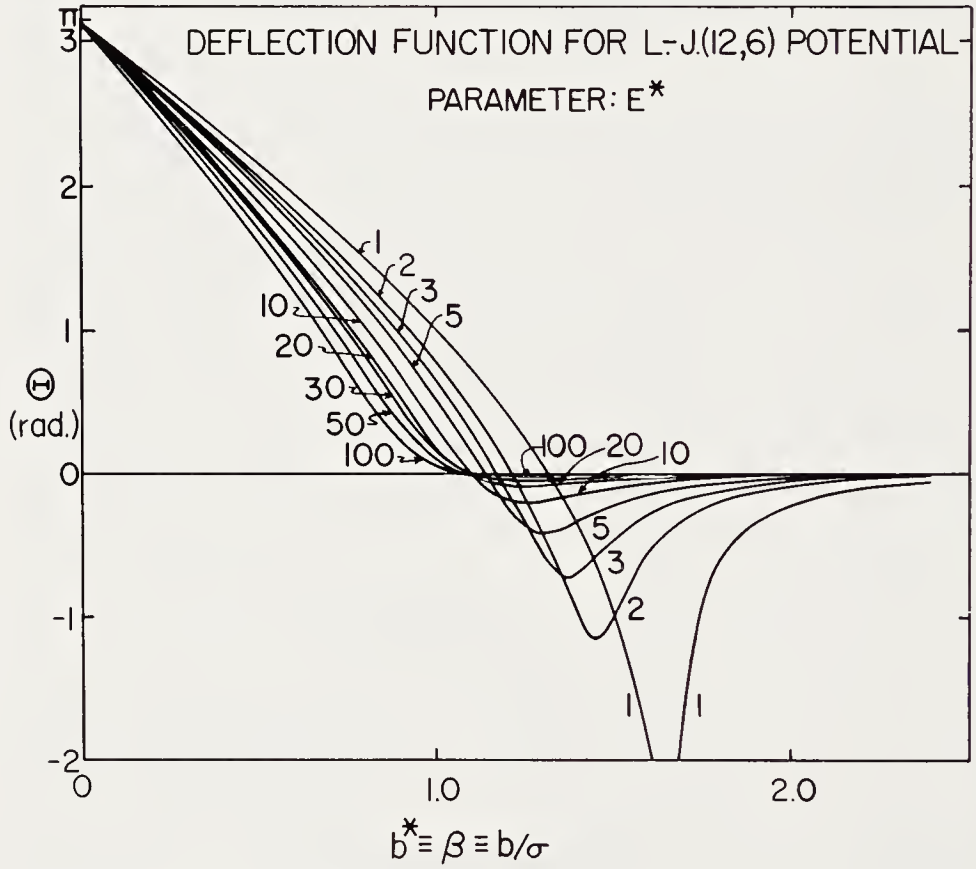

Fig. 4. Deflection functions $\Theta(b^*,E^*)$ calculated for the L.-J. (12,6) potential. Note the decrease of the magnitude of the minimum angle (denoted as the "rainbow angle," θ_r) with increasing energy.

energy $E^* \equiv K \equiv E/\varepsilon$. As usual, σ is the zero of the potential, the "collision diameter." Since this potential function is the only realistic *two*-parameter potential (ε, r_m, or ε, σ), it has been widely used. However, as more refined data become available, the need for a more flexible potential with one or more additional parameters (such as n, α, γ, or a, in the equations listed above) is becoming apparent.

III. DESCRIPTION OF THE MEASUREMENTS

As mentioned earlier, the experimental aspects of molecular beam scattering have been amply reviewed[2] so that it will be unnecessary to elaborate on the technical details of the experiments here. However, it is important to establish the kinds of phenomena, the nature of the measurements, and the method of their analysis in order to assess the interpretation of the results in terms of intermolecular potentials.

A. Arrangement of the Experiments

There are many superficial differences in the experimental arrangements which have been adopted in the various laboratories where elastic scattering studies of molecular beams are carried out. However, it is possible to classify most of the arrangements into a few principal categories as follows:

(a) Primary beam
(1) Thermal velocity distribution [T_1]
(2) Velocity-selected [v_1]
(3) State-selected [i_1].
(b) Secondary (target)
(1) thermal scattering gas [$T_2 - g$]
(2) thermal beam [$T_2 - b$]
(3) velocity-selected beam [v_2]

The symbols in brackets have their obvious significance; they characterize the arrangement, and will be used later. Other more sophisticated arrangements have been suggested but have not been widely used. Figure 5 is a composite of commonly used arrangements for the measurement of total elastic scattering cross sections and their velocity dependence—and also for the measurement of the angular distribution of the scattering.[2e] The symbols used in the legends for the various cross sections are defined in the following subsection.

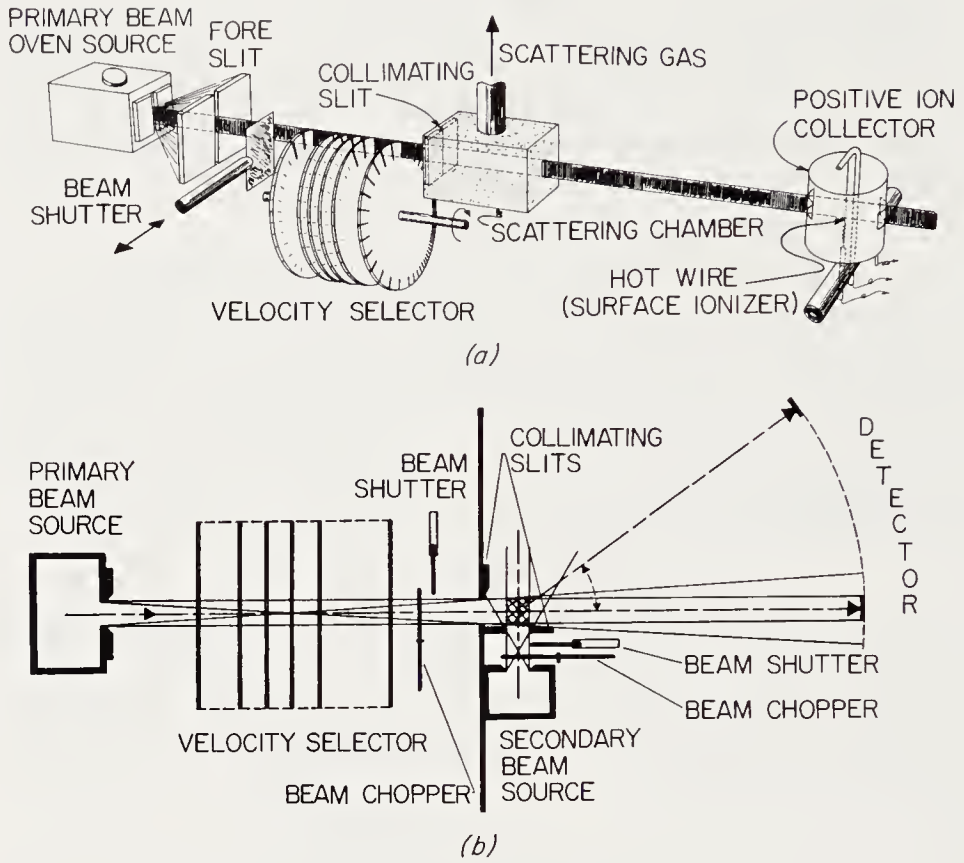

Fig. 5. (*a*) Diagram of simple apparatus for measurement of $Q_{\text{eff}}[v_1,T_2-g](v_1)$; the Langmuir-Taylor detector limits the studies to easily ionizable primary beams, e.g., alkalis, alkali halides, etc. (*b*) Schematic diagram of a more general composite apparatus for the measurement of total elastic scattering cross sections and the angular distribution of the scattering as a function of velocity, i.e., $Q_{\text{eff}}[v_1,T_2-b](v_1)$ yielding $Q(v)$ and $I_{\text{app}}[v_1,T_2-b](\theta_{\text{lab}},v_1)$ yielding $I(\theta,v)$.

B. Measured Quantities

Ideally, it would be desirable to measure the differential elastic scattering cross section, $I(\theta)$, over the complete angular range (0–180° in the center-of-mass system) as a function of the relative velocity, v (or collision energy, E) and the integral or total cross section, Q, independently (by primary beam attenuation data) over a wide energy regime. In practice, experimental difficulties severely limit the accessible range of the independent variables as well as the "quality" of the measured cross section.

There are three principal problems which set limitations on the quality of reported total cross sections, of which the first two are also applicable to differential cross sections. They are (*a*) the difficulty of determining the total number or density of target particles, required for a knowledge of the absolute value of a cross section,[13] (*b*) the necessity of proper correction for the influence upon the apparent cross section of velocity distributions in both the primary beam and the target molecules,[14] and (*c*) the problem of imperfect angular resolution (low "resolving power") and its strong detrimental effect upon the apparent total cross section.[15]

These points have been fully clarified only recently, but they are thoroughly discussed in the review by Pauly and Toennies[2f] and will not be pursued further here. However, it is of interest to point out the magnitudes of the errors associated with these difficulties: improper density measurements have caused (systematic) errors from 5–30 % in cross sections, usually giving rise to spuriously large values; improper velocity-distribution corrections have introduced discrepancies of $\pm$5–10 %; imperfect angular resolution has yielded apparent total cross sections low by 5–50 %. It is probably safe to say that *absolute* values of cross sections reported prior to 1965 must be regarded with extreme caution. However, for a great many reported experiments the *relative* values of cross sections are quite precise, and, by comparison with a reference or "standard" value measured under known, similar conditions, these have provided considerable useful information.

Particularly attractive to the experimentalist interested in the determination, by scattering, of intermolecular forces have been methods which do *not* require high absolute accuracy of cross sections, rather only observations of certain "critical" angles or velocities, i.e., "quantum effects" such as interferences in the angular distribution, "semiclassical effects" such as the rainbow effect in $I(\theta)$ and glory extrema in $Q(v)$. These have proven to be of great value in the elucidation of the interaction potentials via the low-energy molecular beam scattering technique. These phenomena are discussed in Section IV.

In order to classify (and clarify) the particular measurements which will be referred to later, certain arbitrary symbols are now introduced and adopted to specify in a simple way the restrictions and the variables of the experiments. The qualifications or restrictions appear as subscripts or in brackets, while the independent variable(s) studied follow in parentheses. Anticipating the problem of summarizing the

observations (Sec. VI and VII), the phenomena under study are stated next, in an obvious (abbreviated) notation.

Examples of the *kinds* of measurements made are as follows, listed in a hierarchy according to increasing "quality."

$Q_{app}[\theta_0,T_1,T_2-g]$ "apparent" total cross section, inadequate angular resolution (i.e., θ_0), thermal primary beam, and secondary gas; of qualitative significance only.

$Q_{app}[T_1,T_2-g]$ "apparent" total cross section, "adequate" resolution, thermal primary beam and secondary gas. See Figure 6 for typical data.[16]

$Q_{app}[T_1,T_2-b]$ "apparent" total cross section, as above, but with secondary beam.

$Q_{app}[T_1,T_2-g](T_2)$ "apparent" total cross section, thermal beam, scattering gas; measurements as function of scattering gas temperature.

$Q_{eff}[T_1,T_2-g]$ "effective" total cross section, measured under conditions suitable for correction by Berkling et al.[14] method to yield $Q(v)$ for $v=\alpha_1=(2kT_1/m_1)^{1/2}$.

$Q_{eff}[T_1,T_2-b]$ similar, but with secondary beam instead of gas.

$Q_{eff}[v_1,T_2](v_1)$ "effective" total cross section, measurements as a function of primary beam velocity, to yield the $Q(v)$ functionality.

$Q_{eff}^{abs}\left[v_1,T_2-\begin{Bmatrix}g\\b\end{Bmatrix}\right](v_1)$ similar, but special attention to accuracy of absolute values.

$I_{app}[T_1,T_2-g](\theta_{lab})$ apparent angular distribution of scattering intensity, lab coordinates, thermal beam, and scattering gas.

$I_{app}[T_1,T_2-b](\theta_{lab})$ similar, but with secondary beam.

$I\left[T_1,T_2-\begin{Bmatrix}g\\b\end{Bmatrix}\right](\theta)$ angular distribution, corrected to center-of-mass system; secondary gas or beam, as designated.

$I\left[v_1,T_2-\begin{Bmatrix}g\\b\end{Bmatrix}\right](\theta,v_1)$ angular distribution, similar, but measurements as function of primary beam velocity to yield the $I(\theta,v)$ functionality.

$I^{abs}[T_1,T_2-g](\theta)$ special attention to absolute values, thus "differential scattering cross section."

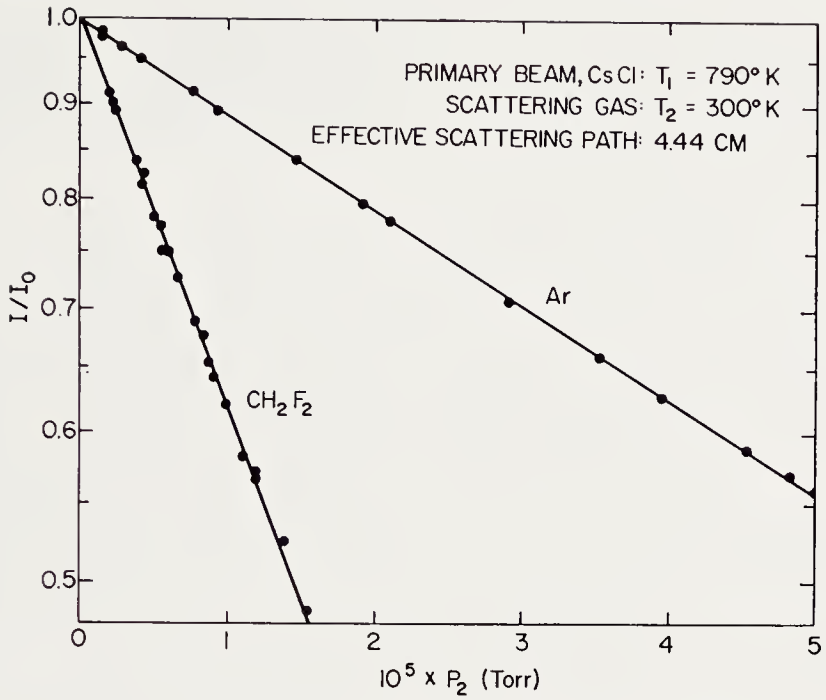

Fig. 6. Typical attenuation plots[16] used to determine $Q_{app}[T_1,T_2-g]$. Here the primary beam is CsCl, scattered by a reference gas (Ar) and by a polar molecule (CH_2F_2). Experiments at different scattering gas temperatures, i.e., $Q_{app}[T_1,T_2-g](T_2)$, yielded information on dipole–dipole interactions.

Obviously, the above list is incomplete, but it should suffice to illustrate the symbols employed in the sections on data analysis and results.

IV. DESCRIPTION AND ILLUSTRATION OF THE PHENOMENA

It has been possible to interpret most of the existing experiments on elastic scattering of molecular beams using the well-known theory of scattering of structureless particles interacting according to a central potential. However, it is found that a purely classical treatment is unsatisfactory and that at least a semiclassical (and preferably a full, quantal) treatment is required.[12]

Classically, the differential solid-angle scattering cross section (in the center-of-mass system) is given by

$$\frac{d\sigma}{d\Omega} = \sum_{i=1}^{N} b_i/\sin\theta \left|\frac{d\Theta}{db_i}\right| \tag{5}$$

where the sum is over the N "branches" of the deflection function $\Theta(b)$ which may contribute to the scattering at an angle $\theta = |\Theta(b)|$. The deflection function is, in turn, dependent upon the potential $V(r)$ by the following relationship.

$$\Theta(b) = \pi - 2b \int_{r_0}^{\infty} dr/r^2[1 - b^2/r^2 - V(r)/E]^{1/2} \tag{6}$$

For realistic intermolecular potentials $b(\Theta)$ is a multivalued function (see Fig. 4), so that at any value of the collision energy E there is an angle θ_r (the so-called "rainbow angle"[17]) below which more than one value of b contributes to the scattering at a given θ. Classically, the differential cross section [Eq. (5)] should exhibit an infinity (and a discontinuity) at the rainbow angle and a "forward infinity" at $\theta = 0$; quantum mechanically, these defects are repaired and a number of new features appear, which are in accordance with experiment. For this reason, it is necessary to make use of the quantal treatment in deriving interaction potentials from low-energy beam scattering data.

The reader is referred to the preceding chapter by Mason and Monchick for a lucid, general discussion of the physical basis and structure of the various phenomena and their optical analogs, i.e., rainbows, glories, shadows, and glorified shadows.

A. General Angular Dependence of Scattering

1. *Quantum Mechanical Preliminaries*

The differential cross section or intensity, $I(\theta)$, is the absolute square of the amplitude, $f(\theta)$, which is, in turn, a sum over all orbital angular momentum quantum numbers, l, of a function of the partial-wave phase shifts η_l:

$$f(\theta) = \frac{1}{2ik} \sum_{l=0}^{\infty} (2l + 1)(e^{2i\eta_l} - 1)P_l(\cos\theta) \tag{7}$$

The phase shifts are determined by the potential function via the radial Schrödinger equation:

$$\left[\frac{d^2}{dr^2} + k^2 - \frac{2\mu}{\hbar^2} V(r) - \frac{l(l+1)}{r^2}\right] G_l(r) = 0 \tag{8}$$

with $G_l(0) = 0$ and $G_l(r) \sim \sin(kr - l\pi/2 + \eta_l)$ asymptotically. One compares the radial function with a spherical Bessel function of the

same order and obtains the asymptotic phase shift at a specified wave number $k = \mu v/\hbar$ (where μ is the reduced mass and v is the relative velocity; here the collision energy $E = \frac{1}{2}\mu v^2$). Figure 7 shows typical

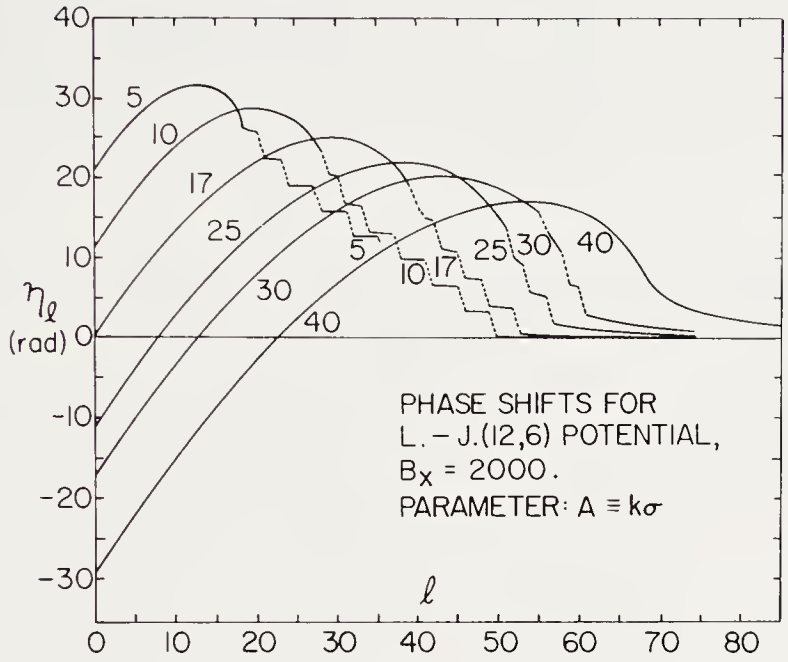

Fig. 7. Typical behavior of phase shifts η_l for a L.-J. (12,6) potential calculated[33b] as a function of the wavenumber parameter $A_x = k\sigma$; here the well "capacity parameter" $B_x \equiv 2\mu\varepsilon\sigma^2/\hbar^2 = 2000$.

curves of the dependence of the phase shift upon the angular momentum quantum number. (According to the semiclassical theory, the equivalence relation between the classical impact parameter and the orbital quantum number l is $b = (l + \frac{1}{2})/k$; in addition, one has $\Theta = 2d\eta_l/dl$.) Note that at low angular momentum, the phase shifts are negative (dominated by the repulsion) while at high angular momentum they are positive (attraction predominates). The maximum in η_l leads to the phenomenon known as "glory scattering," to be discussed later.

For a monotonic phase-shift curve, it can be shown by the method of stationary phase that the main contribution to the sum in Eq. (7) at any angle, θ, is from the few partial waves for which $l \cong kb(\theta)$. For the case when there are three branches of the deflection function, there are

three classical contributions to the differential cross section, Eq. (5):

$$\left[\frac{d\sigma(\theta)}{d\Omega}\right]_{\mathrm{Cl}} \equiv [I(\theta)]_{\mathrm{Cl}} = I_a(\theta) + I_b(\theta) + I_c(\theta) \tag{9}$$

where a, b, and c represent the three impact parameters associated with the given θ (a being the largest one, influenced largely by the long-range attractive part of the potential). For this case, the quantum mechanical analog, in terms of the amplitude, is:

$$f(\theta) \cong f_a(\theta) + f_b(\theta) + f_c(\theta) \tag{10}$$

so that

$$[I(\theta)]_{\mathrm{Qu}} = |f_a(\theta)|^2 + |f_b(\theta)|^2 + |f_c(\theta)|^2 + \text{interference terms} \tag{11}$$

i.e.,

$$[I(\theta)]_{\mathrm{Qu}} = [I(\theta)]_{\mathrm{Cl}} + \Delta I(\theta) \tag{12}$$

where $\Delta I(\theta)$ is an oscillatory "interference contribution."

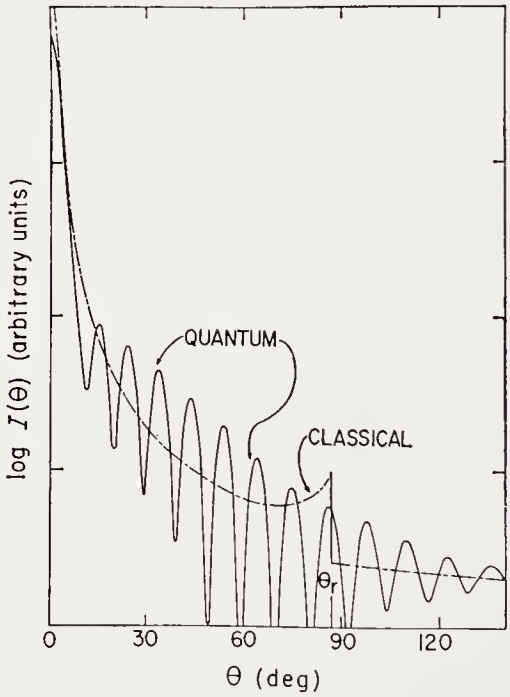

Fig. 8. Comparison of quantum with classically calculated[4b] angular distribution of scattering: log $I(\theta)$ for a L.-J. (12,6) potential, $B_x = 125$, $A_x = 14.1$ (corresponding to $E^* = 1.6$). Note the classical "rainbow angle," θ_r, at 87°.

2. *Quantum Interferences*

Figure 8 shows an early calculation[4b] comparing classical and quantum angular distributions of intensity for a physical situation in which the de Broglie wavelength $\lambda = h/\mu v$ is comparable with the characteristic distance σ, the "collision diameter" of the system, a measure of the "range" of the interaction. For angles smaller than the rainbow angle θ_r, the amplitude of the interferences is appreciable under all circumstances, while for $\theta > \theta_r$, the amplitude decreases with angle and with increasing wavenumber k.

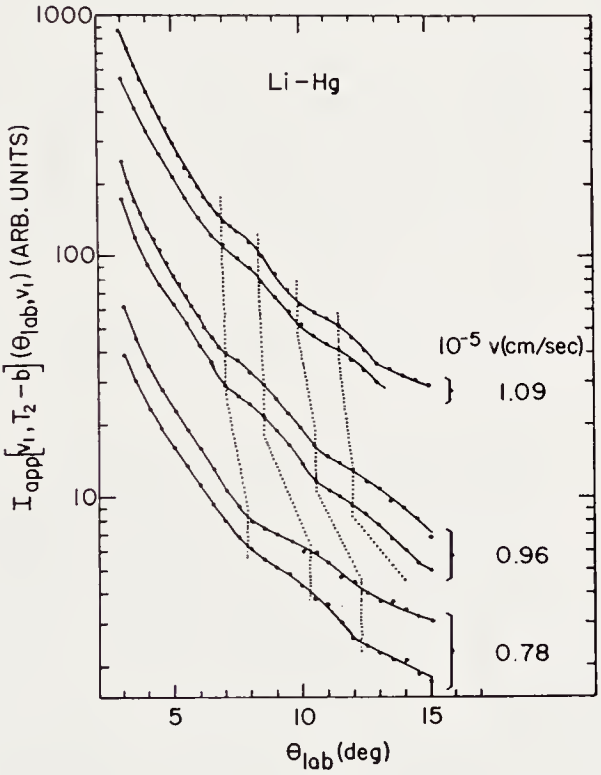

Fig. 9. Early observations[18a] of quantum interferences in the angular distribution of the scattering of Li by Hg. Plotted, for three "duplicate" pairs of experiments, is log $I_{app}[v_1, T_2 - b](\theta_{lab}, v_1)$.

First to be considered are the fine interference effects in the differential cross section at angles below the rainbow angle. Figure 9 shows the first such observations[18a] (for the Li–Hg system). Figure 10 shows more refined and recent measurements[18b] with the oscillations fully resolved.

The velocity dependence of the scattering pattern is in the expected direction. Figure 11 summarizes the entire set of data for ^{6}Li- and ^{7}Li–Hg.[18b] Figures 12 and 13 show some recent high-resolution measurements[19] on Na–Xe. The experimental data accord better with calculations based on a L.-J. (8,6) potential rather than a L.-J. (12,6) function.

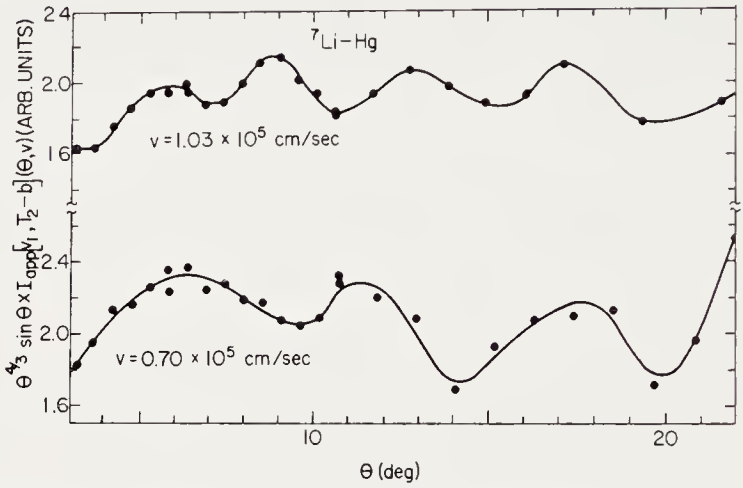

Fig. 10. Later, better-resolved observations[18b] of the quantum interferences in the angular distribution of the scattering of ^{7}Li by Hg at two velocities.[2e]

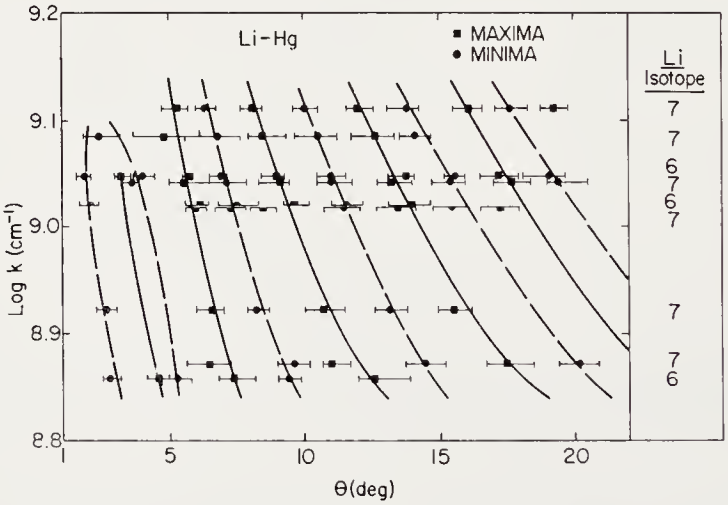

Fig. 11. Summary of observed scattering patterns[18b] for the Li–Hg system. The angular positions of the maxima and minima are plotted as a function of the collision wavenumber k(cm^{-1}), for experiments with ^{6}Li–Hg and ^{7}Li–Hg.

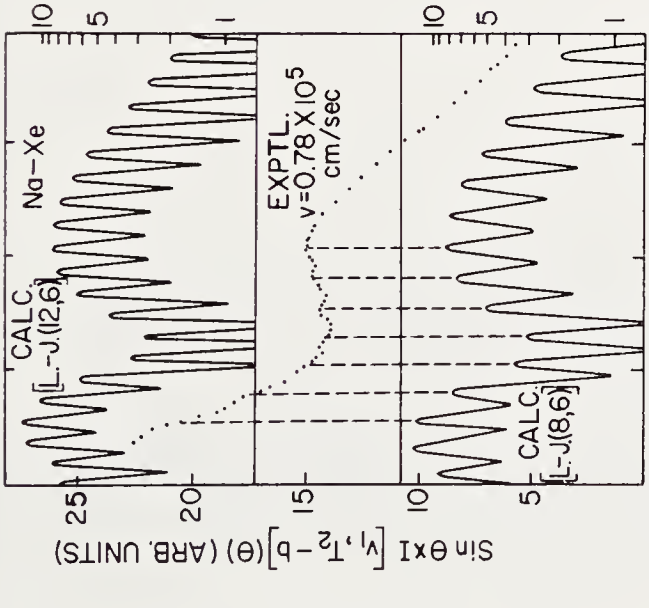

Fig. 12. Well-resolved angular distribution[19a] for the scattering of Na by Xe. The observed quantum oscillations accord well with the positions calculated assuming a L.-J. (8,6) potential, with optimized parameters. (Calculations at the single, specified relative velocity.)

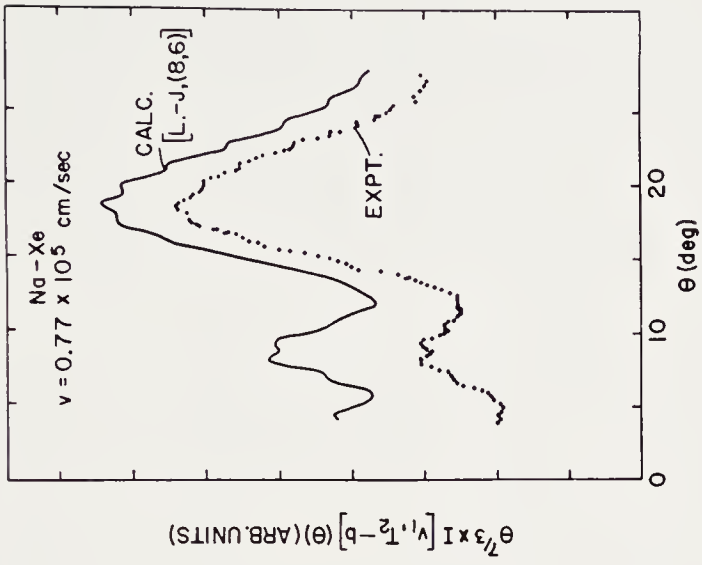

Fig. 13. Well-resolved angular distribution[19b] for the scattering of Na by Xe. The calculated curve, based on a L.-J. (8,6) potential with optimized parameters, has been appropriately velocity-averaged.

3. *Low-Angle "Classical" Behavior*

Figure 14 shows a log–log plot of the low-resolution or "classical" differential cross section for the K–Hg system.[20] For a long-range r^{-6} potential, one expects at low angles

$$I(\theta) \propto \theta^{-4/3} csc\, \theta \cong \theta^{-7/3} \tag{13}$$

as observed. Note the implication, Eq. (13), of a classical divergence

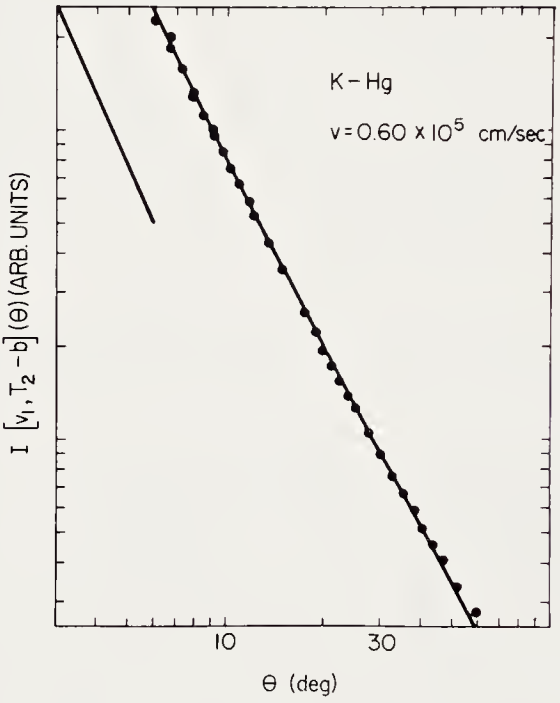

Fig. 14. Log–log plot of the low-resolution angular distribution[20] of the scattering of K by Hg. The classical limiting low-angle slope of $-7/3$ is shown by the short line segment at the upper left.

at $\theta = 0$ (the "forward infinity") associated with the infinite range of the potential, i.e., $d\Theta/db \to 0$ as $b \to \infty$, leading to an infinite total (integral) scattering cross section (see Eq. (5)]. This is removed by the quantum treatment (as discussed below).

4. *Rainbow Scattering*

The previously-mentioned classical "rainbow infinity" at $\theta = \theta_r$ (shown in the classically calculated curve in Fig. 8) disappears in the quantum or semiclassical treatment. The semiclassical treatment[17a] predicts a smooth "bump" in the low-resolution angular distribution near θ_r. Figure 15 shows an early experiment[20] in which the semiclassical rainbow peak is clearly resolved. The observations yield only the mean of

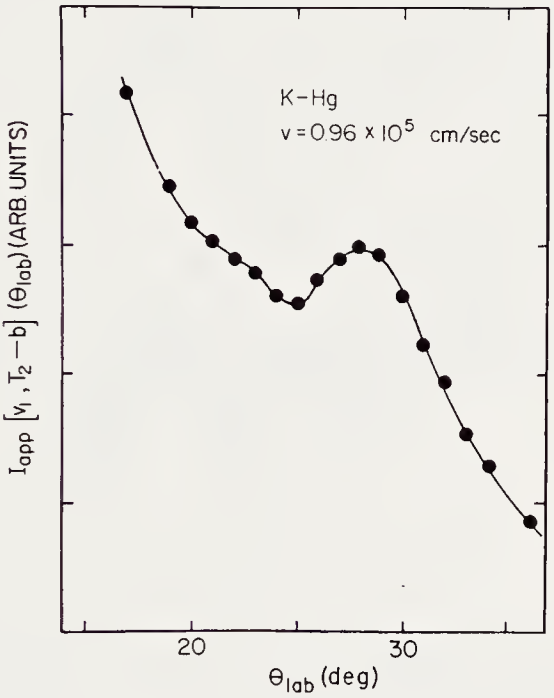

Fig. 15. Early observation[20] of the rainbow effect in the scattering of K by Hg. The possibility of auxiliary or "supernumerary" rainbows[21] at smaller angles than θ_r was not yet known at the time of these experiments.

the rapid oscillations which bunch together in the angular region near θ_r. The rainbow maximum is accompanied by subsidiary maxima, designated "supernumerary rainbows"[21] at lower angles. These are illustrated in Figure 16 for the Na–Hg system[19]; the experimental points are compared to the calculated curves based on L.-J. (12,6) and (8,6) potentials.

Figure 17 shows the energy dependence of the primary and supernumerary rainbow angles for the K–Hg system[22]; the experimental points are to be compared with the behavior calculated for a L.-J. (8,6) potential. In the high-energy limit $\theta_r \propto 1/K$, where $K = E/\varepsilon$ is the reduced collision energy. From such data the well depth, ε, and with

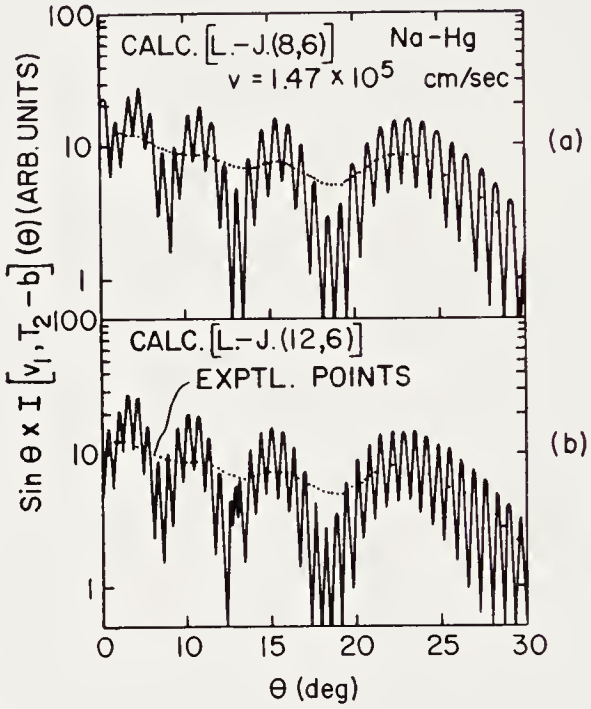

Fig. 16. Rainbow scattering for the Na–Hg system:[19a] the observations are compared with calculations based on (*a*) a L.-J. (8,6) and (*b*) a L.-J. (12,6) potential (each with optimized parameters); calculations at the single, specified relative velocity.

lesser accuracy, the position of the potential minimum, r_m, may be estimated. However, it must be noted that the derived potential parameters are somewhat dependent on the functional form assumed for the potential. Typically, this introduces an uncertainty of about ± 10 % in the derived ε values. Recently, it has been shown[23] that, independent of the form of the potential, the rainbow angle is well correlated with the product $r_i V_i'$, i.e., $\theta_r K$ is a nearly linear function of $r_i V_i'$, where r_i is the position of the *inflection* point in $V(r)$, and V_i' is $(dV/dr)_{r_i}$.

Next to be considered is the fate of the classical "forward infinity." The quantum mechanical treatment yields[24] a very well-behaved angular

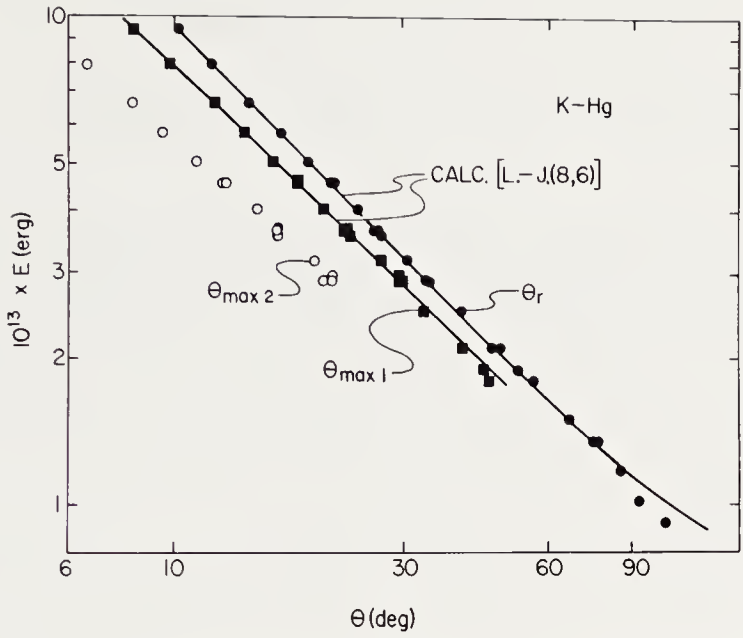

Fig. 17. Energy dependence of the rainbow angles for the K–Hg system.[22] The values designated θ_r refer to the so-called "classical" rainbow angle (located nearly at the outer inflection point following the experimental rainbow bump); $\theta_{max\ 1}$ is the angular position of the maximum in the primary rainbow peak, $\theta_{max\ 2}$ that of the secondary (supernumerary) rainbow. The solid lines are calculated assuming a L.-J. (8,6) potential, with fitted parameters.

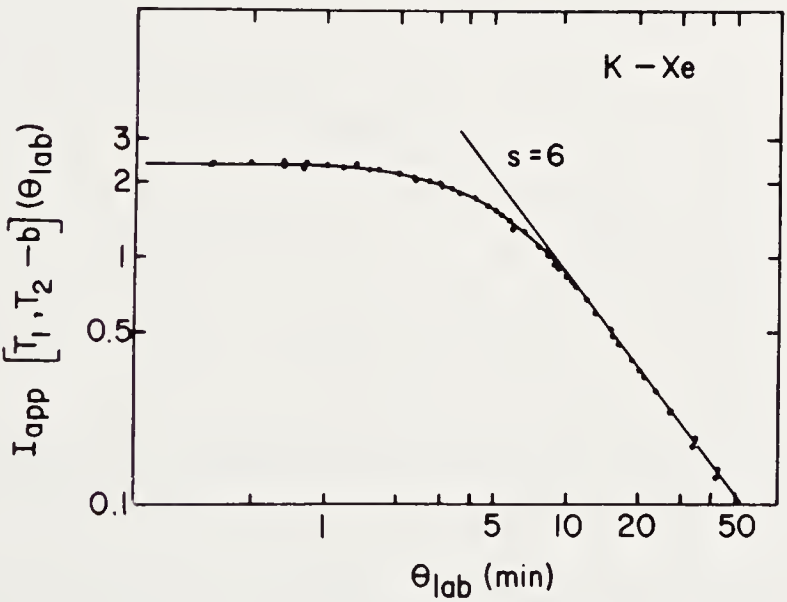

Fig. 18. Log–log plot of the laboratory angular distribution[24b] of the scattering of K by Xe at very low angles. The line designated $s=6$ represents the classical low-angle dependence while the curve, seen to approach a limiting value at very low angles, is that calculated by the quantum treatment.

distribution for an inverse sixth-power long-range potential:

$$I(\theta) \propto e^{-c\theta^2} \tag{14}$$

where c is a combination of angular-independent terms. Figure 18 illustrates experimental results for the K–Xe system[24b]; the solid curve is a calculated fit assuming an r^{-6} long-range potential. These and other measurements of low-angle scattering (and of the influence of angular resolution in total cross section measurements) have not only verified the expected functionality of the long-range part of the potential but have justified the very existence of a total or integral elastic scattering cross section:

$$Q = 2\pi \int_0^{\pi} I(\theta) \sin\theta \, d\theta \tag{15}$$

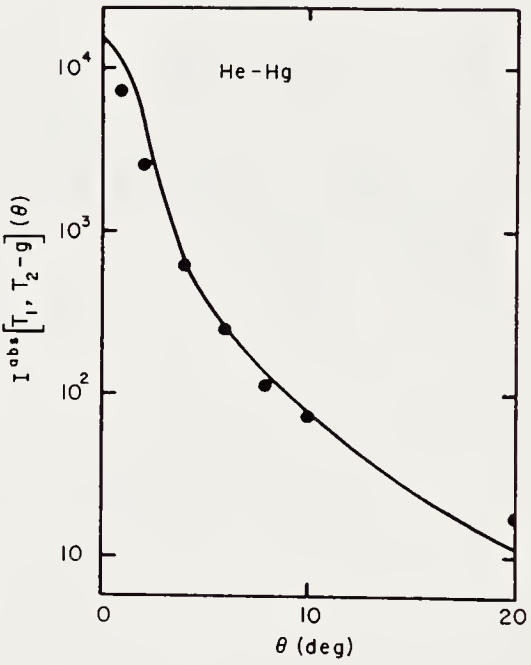

Fig. 19. Semilog plot[25] of early data[26] on the differential cross section for the scattering of He by Hg compared with a velocity-averaged, computed angular distribution from a fitted potential.[25]

Figure 19 shows a recent computational fit[25] to the very early, low-resolution angular distribution measurements of Knauer[26] using an empirically modified L.-J. (12,6) potential, with full averaging over velocity distributions to simulate the experimental situation.

B. Velocity Dependence of Total Cross Sections

1. *General Dependence*

Since most total cross-section measurements are now carried out with angular resolution such that $I(\theta)$ is well in the parabolic region (i.e., Eq. (14), in the low angle limit), they are termed "quantum" total cross sections. Using Eq. (15), the quantum cross section is given by the expression:

$$Q = \frac{4\pi}{k^2} \sum_{l=0}^{\infty} (2l + 1) \sin^2 \eta_l \tag{16}$$

The simple random-phase approximation of Massey and Mohr[27] predicts the following velocity dependence of the quantum cross section for a potential $V(r) \sim -C_s/r^s$,

$$Q = p(s)[C_s/\hbar v]^{2/(s-1)} \tag{17}$$

where $p(s)$ is a known function[28] of s. For a large number of systems, the dependence corresponding to $s = 6$ has been verified experimentally. Figure 20 shows the first such data for the K–N_2 system[29]; the line

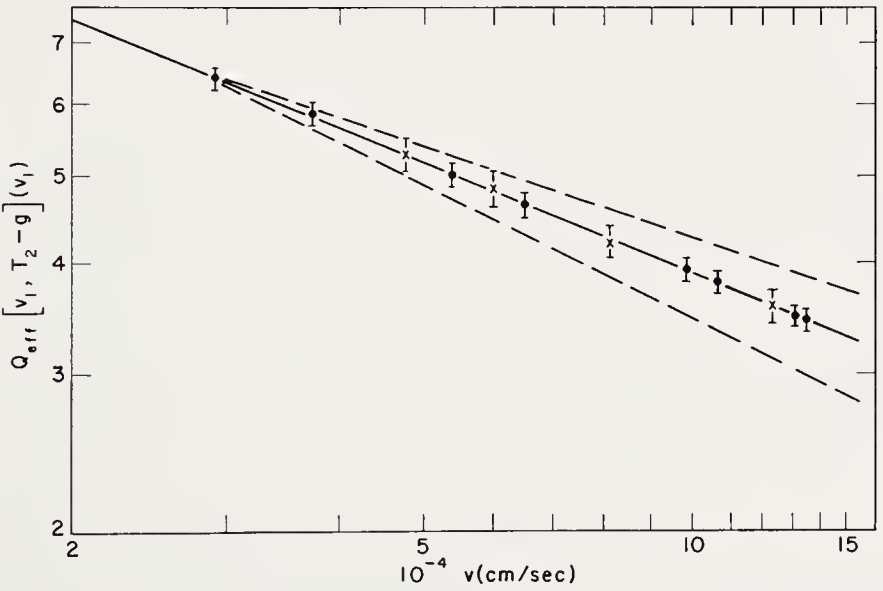

Fig. 20. Log–log plot of $Q(v)$ for the scattering of K by N_2.[29] The solid line has a slope of $-2/5$, corresponding to $s=6$; the dashed lines have slopes corresponding to $s=5$ and 7, respectively.

through the experimental points has a slope of $-2/5$, corresponding to $s = 6$, while the other lines have slopes appropriate to $s = 5$ and 7.

2. *Determination of C_6 Constants*

From absolute values of integral or total elastic cross sections (termed "shadows" by Mason and Monchick, Chapter 7) in the thermal energy range, the C_6 constants may be derived[28] from Eq. (17):

$$C_6(\text{erg cm}^6) = 5.676 \times 10^{-30} v(\text{cm sec}^{-1}) Q(\text{cm}^2)^{5/2} \tag{18}$$

Unfortunately, until quite recently, accurate absolute cross sections have rarely been obtained; however, relative values have been known quite precisely and are well correlated with theory. For example, in a study[30] of the scattering of alkali beams by a large number of species of atoms and simple molecules, it was found that the calculated C_6 constants (by the simple Slater-Kirkwood formula from the polarizabilities of the interacting species, with an added Debye induction term where appropriate) reproduced the experimental relative C_6 values to within about ± 20 %. Moreover, excluding those scattering gases for which the influence of the short-range forces is known to invalidate the use of the simple Eq. (18), the discrepancy between experimental and "theoretical" relative C_6 values for the remaining 82 different interacting pairs is reduced to an average deviation of ± 10 %, which is well within the uncertainty of the Slater-Kirkwood approximation.

During the past few years, it has become possible to measure total cross sections with an absolute accuracy[31] of 5–10 %, so that the C_6 constants are now known within 15–20 %. For a number of systems, accurate theoretical calculations of these constants are now available[32] (e.g., by Dalgarno, Kingston, Barker, and others) and the accord between theory and experiment is now within the mutual limits of uncertainty.[32] Thus, part of the "inversion" problem, namely, to obtain the long-range part of the potential from the total cross section, has been fairly well solved.

3. *Glory Extrema in $Q(v)$*

A valuable new source of information about the shape of the potential well has become available via high-precision measurements of the velocity dependence of the total cross section. The glory-extrema effect is reviewed in references 2f and 12. By considering phase shift curves such as Figure 7, it is apparent that the region near the maximum

phase will contribute a nonnegligible increment ΔQ to the cross section of Eq. (17) (based on the random-phase approximation). Starting at high energies, where the maximum phase is small (i.e., $< \pi/2$), and then reducing the energy, the maximum phase passes successively through $\pi/2$, π, $3\pi/2$, etc., yielding alternate positive and negative glory extrema, $\pm\Delta Q$ superimposed on the random phase-approximated cross section Q of Eq. (17). It has been found convenient to index the various extrema. The index $N = 1$ designates the maximum at highest velocity, due to a maximum phase near $\pi/2$; other integer indices designate successive maxima at lower velocities (half-integers denote minima). According to the simple theory[33a,b,e] the intercept of a plot of N versus $1/v$ should be 3/8 and the limiting (high-velocity) slope yields the product $\varepsilon\sigma$ or εr_m, subject to the assumption of a given functionality for the interaction potential. Typically, the latter introduces an uncertainty of about $\pm 10\,\%$ in the derived εr_m values.

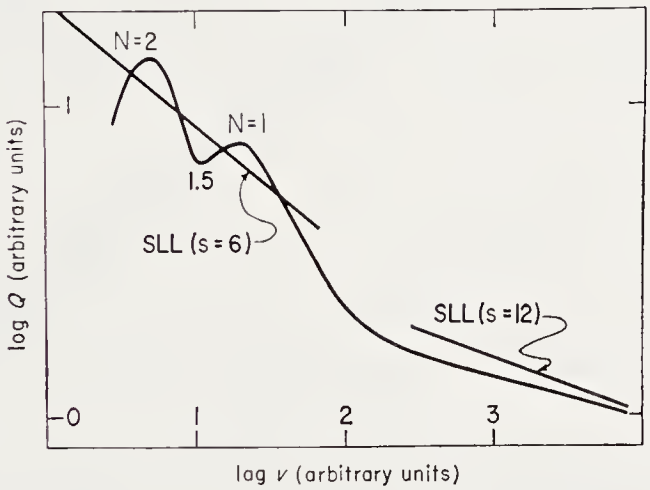

Fig. 21. Log–log plot of $Q(v)$, calculated[12] for a L.-J. (12,6) potential with $B_x = 125$. The low-velocity cross section undulates about the random-phase-approximated (SLL[28]) line given by Eq. (17), based on an attractive potential with $s = 6$, gradually approaching the limiting high velocity behavior[33h] corresponding to the repulsive ($s = 12$) potential.

Figure 21 shows a calculated curve,[12] $\log Q$ versus $\log v$, for a L.-J. (12,6) potential with specified parameters. The two straight lines show the random-phase cross sections for a pure inverse sixth power attraction, and for an inverse twelfth-power repulsion. The transition

from "low-" to "high-velocity" behavior takes place over a broad region of velocity around $v \cong \varepsilon r_m/\hbar$.

Figure 22 shows the first experimental observations[34] of glory-extrema, for the Li–Xe system. The plot displays the extrema in the

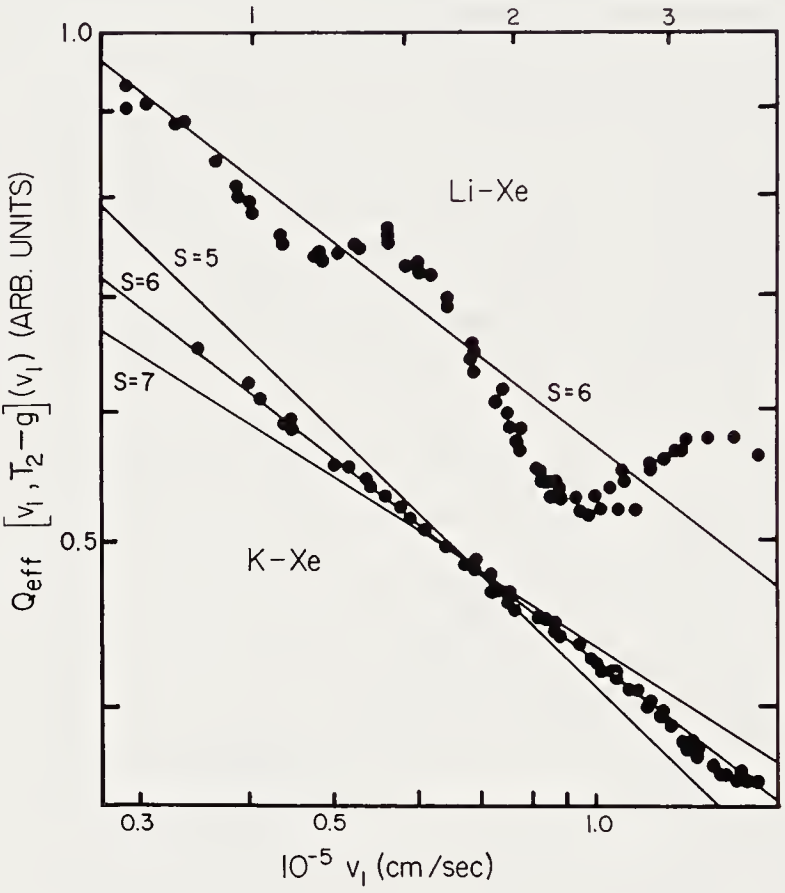

Fig. 22. Log–log plot of early experimental data[34a] on $Q_{\text{eff}}(v_1)$ for the Li–Xe and K–Xe systems; the glory extrema for Li–Xe are clearly resolved. The straight lines have their usual significance. Later observations[35b,c] show extrema for K–Xe as well.

velocity dependence of the total cross section, superimposed on the $s = 6$ behavior of Eq. (17). Figure 23 shows a plot[2e] of the results versus reciprocal velocity, with the extrema indexed. Figure 24 summarizes extrema data from three different laboratories,[35a,b,c] for the K–Kr system.

Further analysis[33f,g] of the glory-extrema effect shows that one may

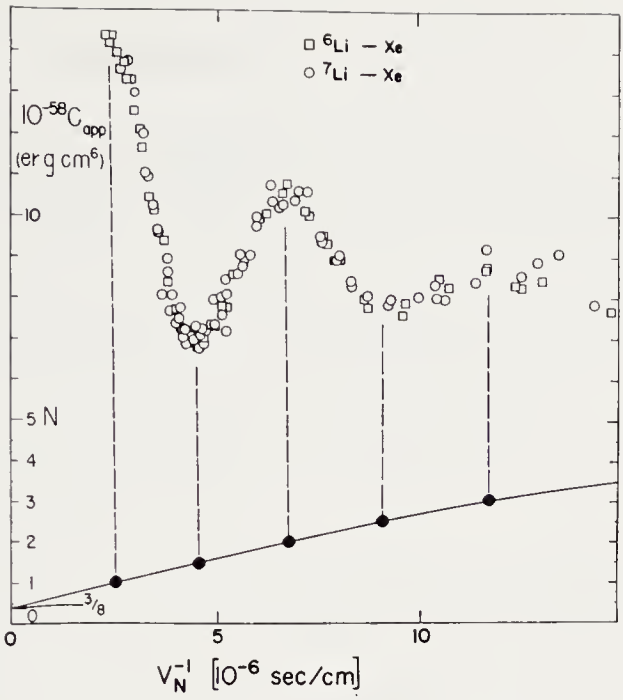

Fig. 23. Plot[2e] of an elastic atom–atom impact spectrum for the ^{6}Li–Xe and ^{7}Li–Xe systems.[34b]

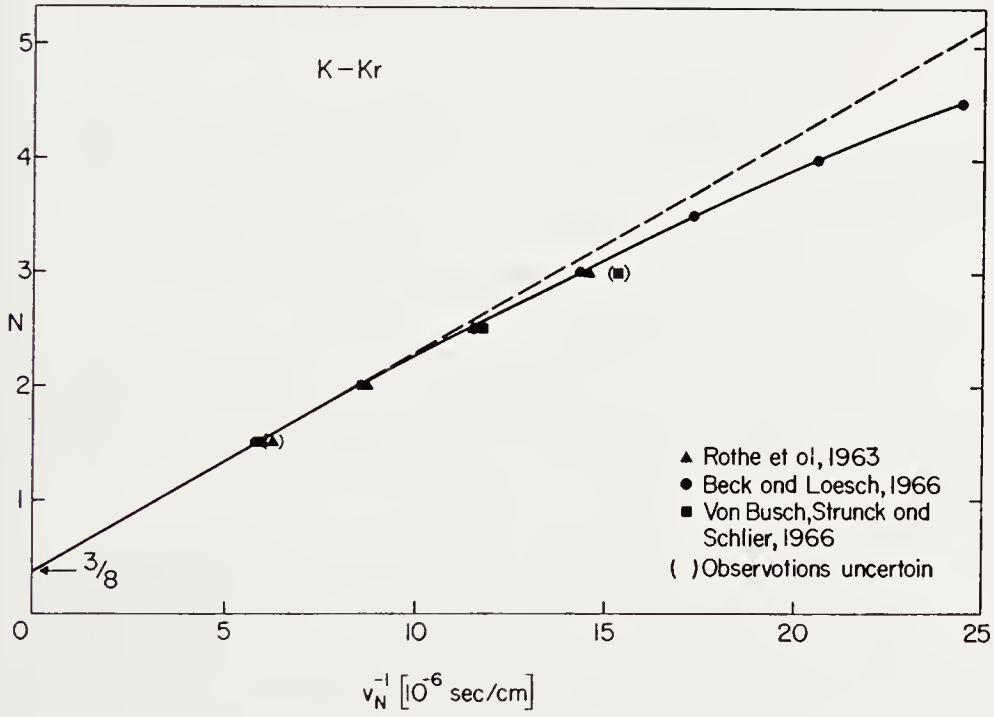

Fig. 24. Glory extrema indexing plot for the K–Kr system, comparing results of experiments carried out in three laboratories.[35a,b,c]

obtain the quantity $\varepsilon^2 r_m$ with good accuracy, nearly independent of the assumed functional form of the potential. In addition, one may estimate the curvature of the potential well at its minimum (i.e., the force constant of the diatom).

Figure 25 shows some recent data[36] for H_2–Xe and D_2–Xe. The solid curves through the experimental points are calculated for an

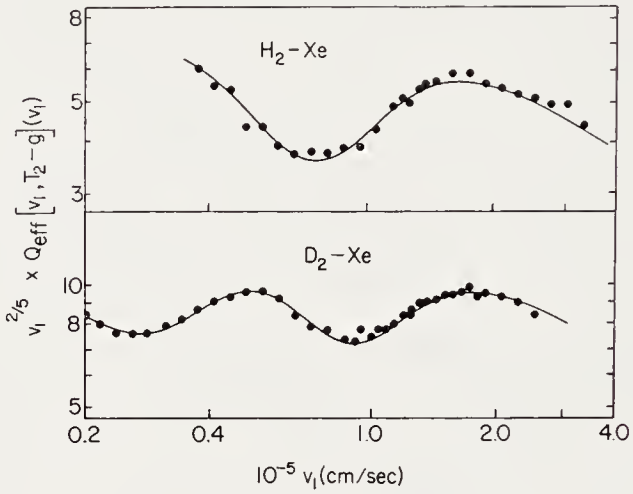

Fig. 25. Log-log plot of glory extrema for the H_2–Xe and D_2–Xe systems:[36a,b] $v_1^{2/5} \times Q_{\text{eff}}[v_1, T_2 - g](v_1)$. The solid curves are calculated[36b] assuming a L.-J. (12,6) potential with $\varepsilon = 1.19 \times 10^{-14}$ erg, $r_m = 3.90 \times 10^{-8}$ cm, the same for both (isotopic) systems.

L.-J. (12,6) potential with optimized parameters, as indicated, the same for both (isotopic) systems.

To summarize, the glory extrema in the total cross section ("glorified shadows") help in the characterization of the potential well. Combined with data on rainbow scattering, the parameters ε, r_m, and even the curvature of the well may be obtained. Thus, there is further limited progress in the direction of "inversion."[37]

V. REQUIREMENTS FOR SUITABILITY OF SYSTEMS

There are certain limitations upon the kinds of systems which may be effectively studied by the low-energy molecular beam scattering technique. Some of these are imposed by theoretical considerations while others are associated primarily with experimental factors. They are discussed briefly below.

A. Theoretical Requirements

1. *Existence of a Single Ground Electronic State for the Molecular System*

It is important that one or both of the scattering partners be a "closed-shell" species so that they interact according to a single potential curve. This is especially true in the conventional studies of atomic or molecular beam scattering with unselected states. For the collision of like atoms, this implies that they belong to group II (or VIII) of the periodic table, i.e.,

$$2\ \mathrm{II}(^1S_0) \rightarrow \mathrm{II}\ \mathrm{II}(^1\Sigma_g^+)$$

For unlike atoms (in their ground states), only the following cases apply (where VIII may be substituted for II throughout):

$$\mathrm{I}(^2S_{1/2}) + \mathrm{II}(^1S_0) \rightarrow \mathrm{I}\ \mathrm{II}(^2\Sigma^+)$$

$$\mathrm{II}(^1S_0) + \mathrm{II}'(^1S_0) \rightarrow \mathrm{II}\ \mathrm{II}'(^1\Sigma^+)$$

$$\mathrm{II}(^1S_0) + \mathrm{VA}(^4S_{3/2}) \rightarrow \mathrm{II}\ \mathrm{VA}(^4\Sigma^-)$$

A few experiments have been carried out for cases in which more than one electronic state is involved, of the type:

$$2\ \mathrm{I}(^2S_{1/2}) \rightarrow \mathrm{I}\ \mathrm{I}(^1\Sigma^+);\ \mathrm{I}\ \mathrm{I}(^3\Sigma_u^+)$$

$$\mathrm{I}(^2S_{1/2}) + \mathrm{I}'(^2S_{1/2}) \rightarrow \mathrm{I}\ \mathrm{I}'(^1\Sigma^+);\ \mathrm{I}\ \mathrm{I}'(^3\Sigma^+)$$

Experiments have also been done with Zeeman state-selected atoms:

$$\mathrm{III}(^2P_{3/2}) + \mathrm{VIII}(^1S_0) \rightarrow \mathrm{III}\ \mathrm{VIII}(^2\Sigma^+);\ \mathrm{III}\ \mathrm{VIII}(^2\Pi)$$

and for spin-selected, metastable atoms

$$\mathrm{II}(^3S_1) + \mathrm{VIII}(^1S_0) \rightarrow \mathrm{I}\ \mathrm{I}\ \mathrm{VIII}(^3\Sigma^+)$$

For further details see references 33b and 2f.

2. *Absence of Concurrent Inelastic Processes*

The ordinarily used interpretation of molecular beam scattering observations assumes only single-channel elastic scattering and does not take cognizance of other channels corresponding to internal excitation or chemical reaction. This point is discussed in reference 12.

3. *Spherically Symmetrical Potential*

The interpretation of the scattering data is straightforward for a central interaction potential of the form $V(r)$, such that the differential

cross section is a function only of the polar angle θ (in the barycentric system). For an anisotropic potential $V(\mathbf{r})$, the treatment is more complicated and the cross section involves an additional dependence upon the azimuthal angle ϕ. With the use of polarized beams, it is possible to learn something of the anisotropy,[38,39] but in the conventional experiments, spatial averaging reduces the information content of the data and the observations bear only upon the orientation-averaged potential. For atom–molecule and molecule–molecule scattering, the appropriate potentials are often strongly angle-dependent and the interpretation is accordingly more difficult.

4. *Low Reduced Mass and Relative Velocities, i.e., Long de Broglie Wavelengths*

Much of the "detail" in the scattering is associated with the quantum interference effects whose ease of resolution is related[12] to the ratio of the de Broglie wavelength, λ, to the characteristic distance, say r_m, of the potential. With improvements in experimental techniques, of course, this limitation is becoming progressively less important.

B. Experimental Requirements

1. *Beams of Relatively Stable Atomic and Molecular Species*

Since the "transit time" for the beam across ordinary apparatus dimensions is typically in the range 10^{-5} to 10^{-2} sec, relatively long-lived species are required. Most of the beam experiments have therefore involved ground state atoms or molecules, or metastable states with free lifetimes of at least a millisecond. Excited states with allowed (dipole) transitions to the ground state are not suitable, nor are excited molecular states (or radicals) which can undergo rapid rearrangement to a more stable species.

2. *Efficient Production and Detection of Beams*

Due to stringent requirements of angular and velocity resolution for both differential and total cross section measurements, it is important that the detected intensity (more properly, the signal-to-noise ratio) be as large as possible in the original (unscattered) primary beam, to allow for all the attrition which is to follow. With the advent[2f] of supersonic nozzle beams and efficient so-called "universal" detectors, this limi-

tation is being overcome. Nevertheless, the experiments to date have been limited to a great extent by intensity and detectability problems. The ease of formation and detection of alkali atom beams with low background densities has been responsible for the preponderance of scattering studies with alkali systems.

3. *Unambiguity in Species*

It is important that the beam species be known and uniform in composition, i.e., that the extent of association or dissociation be either minimized or determined (and the interpretation suitably corrected). Although the molecular beam technique has made a historically important contribution[1] in connection with related thermodynamically interesting problems, from the viewpoint of scattering experiments it is preferable to have a single atomic or molecular species constituting the beam or target particles. Of course, with selective detectors it is no longer rigorously necessary to work with "pure" beams, but it is still desirable.

4. *Secondary (Target) Particles of Heavy Mass*

Up until very recently, the secondary beam (or gas) has usually been thermal, with a near-Maxwellian velocity distribution. When using a velocity-selected primary beam, in order to reduce the spread of relative velocities due to this velocity distribution of the secondary beam or gas, it has been helpful to use "heavy" secondary particles, often at low temperatures, such that their most probable speed $\alpha_2 \ll v_1$. Then the distribution in $\mathbf{v} = \mathbf{v}_1 - \mathbf{v}_2$ will be only slightly broadened over that of $\mathbf{v}_1$ by the distribution in $\mathbf{v}_2$. Of course, this is a purely technical consideration, sure to become obsolete with the advancement of the experimental techniques of beam scattering.

5. *General Comments*

All of the aforementioned considerations have resulted in a rather disproportionate emphasis in the experimental scattering literature upon the interaction of ground state atoms (mainly alkalis) with rare gases, mercury, and simple diatomics. (This will become evident in the next section, Table I, presenting the status of systems studied.) This situation is rapidly improving, however, so that it is expected that the scope of scattering studies will be vastly expanded within the next 5–10 years.

TABLE I

Status of Systems Studied (Atoms and Diatomic Molecules)[a]

	Beam																												
Target	H	D	Li	Na	K	Rb	Cs	Ga	Ga[i]	He	He*	Ne	Ne*	Ar	Kr	Xe	Ag	H_2	D_2	Li_2	K_2	N_2	O_2	I_2	KCl	KBr*	CsF	CsCl	CsBr	TlF	TlF[i]
Na				⊗[b]	⊗	⊗	⊗																	X[c]		X					
K				⊗	⊗	⊗	⊗																								
Rb				⊗	⊗	⊗	⊗																								
Cs				⊗	⊗	⊗	⊗																								
He	X		●[d]	⊗	⊗	X	⊗	⊗	⊗	●	⊗	⊗	⊗	⊗	⊗			X	⊗	X	X							⊗		⊗	⊗
Ne	H[e]		●	X	⊗	X	⊗	⊗	⊗	●	⊗	H	⊗	⊗	⊗			●	●									⊗		⊗	⊗
Ar	H		●	⊗	●	X	●	⊗	⊗	●	●	⊗	⊗	⊗	⊗	⊗		●	●	X	X				⊗		X	⊗		⊗	⊗
Kr			●	●	●	⊗	●	⊗		●	●	⊗		⊗	⊗			●	●						⊗			⊗		⊗	⊗
Xe			●	●	●		●	⊗	⊗	●						⊗		●	●						⊗			⊗	⊗	⊗	⊗
Zn					X																										
Cd					X																										
Hg			●	●	●	●	●			●								●						X							
H_2	⊗	X	X	X	⊗	X	⊗			⊗				⊗				⊗			X							⊗		X	
D_2	X	H	X	X	X	X	⊗			H											X							⊗			

| | | |

VI. INVENTORY OF SCATTERING MEASUREMENTS

This section summarizes the kinds of data available on systems studied by molecular beam scattering. It is intended that the inventory be essentially complete through October, 1966. Experimental results *per se* are presented in Section VII.

A. Systems Studied

Table I gives a "bird's-eye view" of the present status of systems studied, restricting attention to combinations involving ***atoms*** and ***diatomic molecules***. For simplicity, only four symbols are employed in the table. H denotes "high energy" only, i.e., that Amdur-type scattering studies are available, yielding the repulsive potential. No review of these measurements will be presented. The other three symbols refer to low-energy beam scattering measurements. (See table footnotes.)

The table distinguishes between beam and target and is thus not diagonally symmetric. Of course, reliable measurements of barycentric differential cross sections and total cross sections should be invariant to the experimental beam configuration. This invariance is often used as a criterion of quality of data for a given interacting pair.

B. Types of Measurements

Table II is a catalog of the kinds of measurements and types of results obtained on the various systems which have been studied by low-energy molecular beam scattering. The ordering of the systems is based on the "complexity" of the scattering partners, starting with rare gases and ending with the complicated organic compounds. For a given system, the successive entries are chronological. The columns are as follows: the first lists the system, the second the references (in abbreviated form, corresponding to the annotated bibliography on pp. 445–459); the third the kinds of measurements made (indicated by the symbols defined in Section III-B); and the fourth the types of potential data obtained.

Additional symbols used in Table II are as follows:

1. NESD is an abbreviation for "no elastic scattering data."

2. gl'y extr represents "glory extrema" in the total cross sections.

3. r'bow$^{(1)}$ and r'bow$^{(N)}$ refer to "primary rainbow" and "supernumerary rainbows," respectively, in angular distributions.

4. qu osc represents "quantum oscillations" or interferences in the angular distribution.

5. $I(\theta_c)$ indicates an intensity measurement at one angle only.

TABLE II

Catalog of Systems Studied, Kinds of Measurements, and References

System	Reference	Measurement	Potential characteristics deduced
H–He[a]	HAR–62b	$Q_{eff}[T_1,T_2-g](T_1)$	
$H–H_2$	HAR–62a	NESD	
	HAR–62b	$Q_{eff}[T_1,T_2-g](T_1)$	
$H–D_2$	HAR–62a	NESD	
	FIT–64	$I_{app}[T_1,T_2-b](\theta_{lab})$	
	FIT–65	$I_{app}[T_1,T_2-b](\theta_{lab})$	
$D–H_2$	DAT–62	NESD	
	HAR–62a	NESD	
	DAT–63	NESD	
Li–He	ROS–35	$Q_{app}[\theta_0,T_1,T_2-g]$	
	ROS–40	$Q_{app}[\theta_0,T_1,T_2-g]$	
	ROL–62	$Q_{eff}[v_1,T_2-g](v_1)$ for ^{7}Li	
	ROT–63b	Data of ROL–62	ε, σ
	ROT–64	$Q_{eff}[v_1,T_2-g](v_1)$ for ^{6}Li	ε, σ
Li–Ne	ROS–35	$Q_{app}[\theta_0,T_1,T_2-g]$	
	ROL–62	$Q_{eff}[v_1,T_2-g](v_1)$ for ^{7}Li	
	ROT–63b	Data of ROL–62	ε, σ
Li–Ar	ROS-35	$Q_{app}[\theta_0,T_1,T_2-g]$	
	ROS–40	$Q_{app}[\theta_0,T_1,T_2-g]$	
	ROL–62	$Q_{eff}[v_1,T_2-g](v_1)$, gl'y extr for ^{7}Li	
	ROT–63b	Data of ROL–62	C_6, ε, σ
	ROT–65b	Data of ROL–62	C_6
	ROT–66b	Data of ROT-63b	C_6, ε, σ
Li–Kr	ROL–62	$Q_{eff}[v_1,T_2-g](v_1)$, gl'y extr for ^{7}Li	
	ROT–63b	Data of ROL–62	C_6, ε, σ
	DÜR–64	Data of ROT–63c	α, ε, r_m
	ROT–65b	Data of ROL–62	C_6
	ROT–66b	Data of ROT–63b	C_6, ε, σ
Li–Xe	BER–62b	Data of ROT–62b	ε, σ
	ROL–62	$Q_{eff}[v_1,T_2-g](v_1)$, gl'y extr for ^{6,7}Li	
	ROT–62b	$Q_{eff}[v_1,T_2-g](v_1)$, gl'y extr	
	ROT–63b	Data of ROL–62 and ROT–62b	C_6, ε, σ
	FLO–64	$Q_{eff}[v_1,T_2-g]$	C_6
	ROT–66b	Data of ROT–63b	C_6, ε, σ
Li–Hg	HOS–60	$Q_{eff}[v_1,T_2-b](v_1)$, $I_{app}[v_1,T_2-b](\theta_{lab},v_1)$, qu osc	
	GRO–63	$Q_{eff}[v_1,T_2-b](v_1)$, gl'y extr, $I[v_1,T_2-b](\theta)$, qu osc for ^{6,7}Li	ε, σ

(*continued*)

TABLE II (*continued*)

System	Reference	Measurement	Potential characteristics deduced
Li–Hg (*cont.*)	GRO–65a	$Q_{\text{eff}}[v_1,T_2-b](v_1)$, gl'y extr, $I[v_1,T_2-b](\theta)$, qu osc for ^{6,7}Li	ε, σ
	ROT–67	$Q_{\text{eff}}[v_1,T_2-b](v_1)$, gl'y extr for ^{6}Li	ε, r_m
$Li–H_2$	ROS–35	$Q_{\text{app}}[\theta_0,T_1,T_2-g]$	
$Li–D_2$	ROS–35	$Q_{\text{app}}[\theta_0,T_1,T_2-g]$	
Na–Na	BUC–65	$Q_{\text{eff}}[T_1,T_2-g]$	C_6
	SMI–66	Comments on BUC–65	C_6
Na–K	BUC–65	$Q_{\text{eff}}[T_1,T_2-g]$	C_6
	SMI–66	Comments on BUC–65	C_6
Na–Rb	BUC–65	$Q_{\text{eff}}[T_1,T_2-g]$	C_6
	SMI–66	Comments on BUC–65	C_6
Na–Cs	BUC–65	$Q_{\text{eff}}[T_1,T_2-g]$	C_6
	SMI–66	Comments on BUC–65	C_6
Na–He	ROS–35	$Q_{\text{app}}[\theta_0,T_1,T_2-g]$	
	KOD–61	$Q_{\text{app}}[\theta_0,T_1,T_2-g]$	
	TOS–61	$Q_{\text{eff}}[v_1,T_2-g]$	
	BER–62a	$Q_{\text{eff}}[v_1,T_2-g]$	
Na–Ne	ROS–35	$Q_{\text{app}}[\theta_0,T_1,T_2-g]$	
	KOD–61	$Q_{\text{app}}[\theta_0,T_1,T_2-g]$	
Na–Ar	ROS–35	$Q_{\text{app}}[\theta_0,T_1,T_2-g]$	
	KOD–58	$Q_{\text{app}}[\theta_0,T_1,T_2-g]$	
	KOD–61	$Q_{\text{app}}[\theta_0,T_1,T_2-g]$	
	TOS–61	$Q_{\text{eff}}[v_1,T_2-g]$	
	BER–62a	$Q_{\text{eff}}[v_1,T_2-g]$	
	VON–67	$Q_{\text{eff}}[v_1,T_2-g](v_1)$, gl'y extr	εr_m
Na–Kr	BAR–66	$I[v_1,T_2-b](\theta,v_1)$, r'bow$^{(N)}$, qu osc	n, ε, r_m
	VON–67	$Q_{\text{eff}}[v_1,T_2-g](v_1)$, gl'y extr	εr_m
Na–Xe	FLO–64	$Q_{\text{eff}}[v_1,T_2-g](v_1)$, gl'y extr	ε, r_m
	HUN–65a	$I[v_1,T_2-b](\theta,v_1)$, r'bow$^{(N)}$, qu osc	ε, r_m
	BAR–66	$I[v_1,T_2-b](\theta,v_1)$, r'bow$^{(N)}$, qu osc	n, ε, r_m
	HOL–66	$Q_{\text{eff}}[v_1,T_2-g](v_1)$, gl'y extr, $Q_{\text{eff}}[T_1,T_2-g]$	ε, r_m
	HOL–67	$Q_{\text{eff}}[v_1,T_2-g](v_1)$	εr_m
	VON–67	$Q_{\text{eff}}[v_1,T_2-g](v_1)$, gl'y extr	εr_m
Na–Hg	BRO–33	$Q_{\text{app}}[\theta_0,T_1,T_2-b](\theta_0)$	
	PAU–57	$Q_{\text{app}}[T_1,T_2-b]$	C_6
	PAU–59	$Q_{\text{app}}[\theta_0,T_1,T_2-b](\theta_0)$	
	HUN–64	$I[v_1,T_2-b](\theta,v_1)$, r'bow$^{(N)}$	ε, r_m
	HUN–65a	$I[v_1,T_2-b](\theta,v_1)$, r'bow$^{(N)}$, qu osc	ε, r_m
	HUN–65b	$I_{\text{app}}[v_1,T_2-b](\theta_{\text{lab}})$, r'bow$^{(1)}$	
	NEU–66	$Q_{\text{eff}}[v_1,T_2-b](v_1)$, gl'y extr	εr_m

(*continued*)

TABLE II (*continued*)

System	Reference	Measurement	Potential characteristics deduced
Na–H_2	ROS–35	$Q_{app}[\theta_0,T_1,T_2-g]$	
	KOD–61	$Q_{app}[\theta_0,T_1,T_2-g]$	
Na–D_2	ROS–35	$Q_{app}[\theta_0,T_1,T_2-g]$	
Na–N_2	SAS–36c	$Q_{app}[\theta_0,T_1,T_2-g]$	
	PAU–57	$Q_{eff}[T_1,T_2-b]$	C_6
	KOD–61	$Q_{app}[\theta_0,T_1,T_2-g]$	
	TOS–61	$Q_{eff}[v_1,T_2-g]$	
	BER–62a	$Q_{eff}[v_1,T_2-g]$	
Na–O_2	SAS–36c	$Q_{app}[\theta_0,T_1,T_2-g]$	
	KOD–61	$Q_{app}[\theta_0,T_1,T_2-g]$	
	TOS–61	$Q_{eff}[v_1,T_2-g]$	
	BER–62a	$Q_{eff}[v_1,T_2-g]$	
Na–Cl_2	SAS–36b	NESD	
Na–Br_2	GIS–67	$Q_{eff}[v_1,T_2-g](v_1)$	
Na–HBr	HUN–65a	$I[v_1,T_2-b](\theta,v_1)$, r'bow$^{(1)}$	ε, r_m
Na–CO	KOD–61	$Q_{app}[\theta_0,T_1,T_2-g]$	
Na–NO	KOD–61	$Q_{app}[\theta_0,T_1,T_2-g]$	
Na–CO_2	KOD–61	$Q_{app}[\theta_0,T_1,T_2-g]$	
Na–CH_4	TOS–61	$Q_{eff}[v_1,T_2-g]$	
	BER–62a	$Q_{eff}[v_1,T_2-g]$	
Na–CH_3I	WIL–62	NESD	
	HUN–65a	$I[v_1,T_2-b](\theta,v_1)$, r'bow$^{(N)}$	ε, r_m
	GIS–67	$Q_{eff}[v_1,T_2-g](v_1)$	
Na–CCl_4	GIS–67	$Q_{eff}[v_1,T_2-g](v_1)$	
Na–CBr_4	GIS–67	$Q_{eff}[v_1,T_2-g](v_1)$	
Na–$SiCl_4$	GIS–67	$Q_{eff}[v_1,T_2-g](v_1)$	
Na–$SnCl_4$	GIS–67	$Q_{eff}[v_1,T_2-g](v_1)$	
Na–SF_6	GIS–67	$Q_{eff}[v_1,T_2-g](v_1)$, gl'y extr	ε, r_m
Na–$(CH_2Br)_2$	HUN–65a	$I[v_1,T_2-b](\theta,v_1)$, r'bow$^{(N)}$	ε, r_m
Na–*trans*-CHI=CHI	FRA–33	$I_{app}[T_1,T_2-b](\theta_{lab})$, structure	
K–Na	BUC–65	$Q_{eff}[T_1,T_2-g]$	C_6
	SMI–66	Comments on BUC–65	C_6
K–K	BUC–65	$Q_{eff}[T_1,T_2-g]$	C_6
	SMI–66	Comments on BUC–65	C_6
K–Rb	BUC–65	$Q_{eff}[T_1,T_2-g]$	C_6
	SMI–66	Comments on BUC–65	C_6
K–Cs	BUC–65	$Q_{eff}[T_1,T_2-g]$	C_6
	SMI–66	Comments on BUC–65	C_6
K–He	MAI–33	$I_{app}[T_1,T_2-g](\theta_{lab},T_1)$	
	MAI–34	$Q_{app}[\theta_0,T_1,T_2-g]$	

(*continued*)

TABLE II (*continued*)

System	Reference	Measurement	Potential characteristics deduced
K–He	ROS–35	$Q_{app}[\theta_0,T_1,T_2-g]$	
(*cont.*)	ROS–39	$Q_{app}[\theta_0,T_1,T_2-g]$	
	ROT–59a	$Q_{app}[T_1,T_2-g]$	C_6
	ROT–59b	$Q_{app}[T_1,T_2-g]$	C_6
	PAU–60a	$Q_{eff}[\theta_0,T_1,T_2-b](\theta_0)$	
	HEL–61	$I_{app}[T_1,T_2-b](\theta_{lab})$, $Q_{eff}[\theta_0,T_1,T_2-b](\theta_0)$	C_6
	BLY–64	$I[v_1,T_2-b](\theta_c)$	
	HEL–64	$I_{app}[T_1,T_2-b](\theta_{lab})$, $Q_{eff}[\theta_0,T_1,T_2-b](\theta_0)$	C_6
	LUL–64	$Q_{eff}[v_1,T_2-g](v_1,T_2)$	
	VON–65c	$Q_{eff}[v_1,T_2-g](v_1)$	εr_m
	VON–67	$Q_{eff}[v_1,T_2-g](v_1)$	
K–Ne	MAI–34	$Q_{app}[\theta_0,T_1,T_2-g]$	
	ROS–35	$Q_{app}[\theta_0,T_1,T_2-g]$	
	ROT–59a	$Q_{app}[T_1,T_2-g]$	C_6
	ROT–59b	$Q_{app}[T_1,T_2-g]$	C_6
	BRO–64a	$Q_{eff}[v_1,T_2-g](v_1,T_2)$	
	BRO–64b	$Q_{eff}[T_1,T_2-g]$, $Q_{eff}[\theta_0,T_1,T_2-g](\theta_0)$	
	LUL–64	$Q_{eff}[v_1,T_2-g](v_1,T_2)$	
	BRO–65	$Q_{eff}[T_1,T_2-g]$	C_6
	VON–65c	$Q_{eff}[v_1,T_2-g](v_1)$	εr_m
	VON–67	$Q_{eff}[v_1,T_2-g](v_1)$	
K–Ar	MAI–34	$Q_{app}[\theta_0,T_1,T_2-g]$	
	ROS–35	$Q_{app}[\theta_0,T_1,T_2-g]$	
	ROS–39	$Q_{app}[\theta_0,T_1,T_2-g]$	
	SAS–41	$Q_{app}[\theta_0,T_1,T_2-g](T_1)$	
	KOD–44	$Q_{app}[\theta_0,T_1,T_2-g]$	
	KOD–45	$Q_{app}[\theta_0,T_1,T_2-g]$	
	SAS–49	$Q_{app}[\theta_0,T_1,T_2-g]$	
	ROT–59a	$Q_{app}[T_1,T_2-g]$	C_6
	ROT–59b	$Q_{app}[T_1,T_2-g]$	C_6
	PAU–60a	$Q_{eff}[\theta_0,T_1,T_2-g](\theta_0)$	
	HEL–61	$I_{app}[T_1,T_2-b](\theta_{lab})$, $Q_{eff}[\theta_0,T_1,T_2-b](\theta_0)$	C_6
	KRA–62	$Q_{eff}[v_1,T_2-g]$	
	TOS–62	Data of other workers	
	BRO–64a	$Q_{eff}[v_1,T_2-g](v_1,T_2)$	
	BRO–64b	$Q_{eff}[T_1,T_2-g]$, $Q_{eff}[\theta_0,T_1,T_2-g](\theta_0)$	
	FLO–64	$Q_{eff}[v_1,T_2-g]$	C_6

(*continued*)

TABLE II (*continued*)

System	Reference	Measurement	Potential characteristics deduced
K–Ar (*cont.*)	HEL–64	$I_{app}[T_1,T_2-b](\theta_{lab})$, $Q_{eff}[\theta_0,T_1,T_2-b](\theta_0)$	C_6
	LUL–64	$Q_{eff}[v_1,T_2-g](v_1,T_2)$, gl'y extr	C_6
	STR–64	$Q_{eff}[v_1,T_2-g](v_1)$, gl'y extr, $Q_{eff}[T_1,T_2-g]$	C_6, ε, σ
	BEN–65	Data of earlier workers	C_6
	BRO–65	$Q_{eff}[T_1,T_2-g]$	C_6
	ROT–65a	$Q_{eff}^{abs}[T_1,T_2-g]$	C_6
	ROT–65d	$Q_{eff}^{abs}[T_1,T_2-g]$	C_6
	VON–65a	$Q_{eff}[v_1,T_2-g](v_1,T_2)$, gl'y extr	
	VON-65b	$Q_{eff}[v_1,T_2-g](v_1,T_2)$, gl'y extr	
	VON–65c	$Q_{eff}[v_1,T_2-g](v_1,T_2)$, gl'y extr	ε, r_m
	BEC–66a	$Q_{eff}[v_1,T_2-b](v_1)$, gl'y extr	ε, r_m
	HOL–66	$Q_{eff}[v_1,T_2-g](v_1)$, gl'y extr, $Q_{eff}[T_1,T_2-g]$	ε, r_m
	HOL–67	$Q_{eff}[v_1,T_2-g](v_1)$	εr_m
	VON–67	$Q_{eff}[v_1,T_2-g](v_1)$, gl'y extr	εr_m
K–Kr	ROT–59a	$Q_{app}[T_1,T_2-g]$	C_6
	ROT–59b	$Q_{app}[T_1,T_2-g]$	C_6
	BEC–61a	$I[v_1,T_2-b](\theta)$	
	BEC–62a	$I[v_1,T_2-b](\theta,v_1)$, r'bow[1]	ε, r_m
	ROT–63a	$Q_{eff}[v_1,T_2-g](v_1)$, gl'y extr	ε, σ
	CRO–65	$Q_{eff}[v_1,T_2-g](v_1)$	C_6
	ROT–65b	Data of ROT–63a	C_6
	VON–65a	$Q_{eff}[v_1,T_2-g](v_1)$, gl'y extr	
	VON–65b	$Q_{eff}[v_1,T_2-g](v_1)$, gl'y extr	
	BEC–66a	$Q_{eff}[v_1,T_2-b](v_1)$, gl'y extr	ε, r_m
	CRO–66	$Q_{eff}[v_1,T_2-g](v_1)$	C_6
	HOL–66	$Q_{eff}[v_1,T_2-g](v_1)$, gl'y extr, $Q_{eff}[T_1,T_2-g]$	ε, r_m
	ROT–66b	Data of ROT–63a	C_6, ε, σ
	HOL–67	$Q_{eff}[v_1,T_2-g](v_1)$	εr_m
	VON–67	$Q_{eff}[v_1,T_2-g](v_1)$, gl'y extr	εr_m
K–Xe	ROT–59a	$Q_{app}[T_1,T_2-g]$	C_6
	ROT–59b	$Q_{app}[T_1,T_2-g]$	C_6
	HEL–61	$I_{app}[T_1,T_2-b](\theta_{lab})$, $Q_{eff}[\theta_0,T_1,T_2-b](\theta_0)$	C_6
	BER–62b	Data of ROT–62b	$\varepsilon\sigma$
	ROT–62b	$Q_{eff}[v_1,T_2-g](v_1)$, gl'y extr	
	BRO–64a	$Q_{eff}[v_1,T_2-g](v_1,T_2)$, gl'y extr	
	FLO–64	$Q_{eff}[v_1,T_2-g]$	C_6

(*continued*)

TABLE II (*continued*)

System	Reference	Measurement	Potential characteristics deduced
K–Xe (*cont.*)	HEL–64	$I_{app}[T_1,T_2-b](\theta_{lab})$, $Q_{eff}[\theta_0,T_1,T_2-b](\theta_0)$	C_6
	LUL–64	$Q_{eff}[v_1,T_2-g](v_1,T_2)$, gl'y extr	C_6
	CRO–65	$Q_{eff}[v_1,T_2-g](v_1)$	C_6
	HUN–65a	$I[v_1,T_2-b](\theta,v_1)$, r'bow$^{(N)}$	ε, r_m
	VON–65a	$Q_{eff}[v_1,T_2-g](v_1)$, gl'y extr	
	VON–65b	$Q_{eff}[v_1,T_2-g](v_1)$, gl'y extr	
	VON–65c	$Q_{eff}[v_1,T_2-g](v_1)$, gl'y extr	ε, r_m
	BEC–66a	$Q_{eff}[v_1,T_2-b](v_1)$, gl'y extr	ε, r_m
	CRO–66	$Q_{eff}[v_1T_2-g](v_1)$	C_6
	HOL–66	$Q_{eff}[v_1,T_2-g](v_1)$, gl'y extr, $Q_{eff}[T_1,T_2-g]$	ε, r_m
	MIN–66	$I[v_1,T_2-b](\theta)$, r'bow$^{(1)}$	ε
	HOL–67	$Q_{eff}[v_1,T_2-g](v_1)$	εr_m
	VON–67	$Q_{eff}[v_1,T_2-g](v_1)$, gl'y extr	εr_m
K–Zn	JAW–55	$Q_{app}[\theta_0,T_1,T_2-b](\theta_0,T_1)$	
K–Cd	JAW–55	$Q_{app}[\theta_0,T_1,T_2-b](\theta_0,T_1)$	
K–Hg	BRO–33	$Q_{app}[\theta_0,T_1,T_2-b](\theta_0)$	
	JAW–52	$Q_{app}[\theta_0,T_1,T_2-b](\theta_0,T_1,T_2)$	
	JAW–55	$Q_{app}[\theta_0,T_1,T_2-b](\theta_0,T_1)$	
	PAU–57	$Q_{app}[T_1,T_2-b]$	C_6
	GER–59	$I[T_1,T_2-b](\theta)$	
	PAU–59	$Q_{app}[\theta_0,T_1,T_2-b](\theta_0)$	
	HOS–60	$Q_{eff}[v_1,T_2-b](v_1)$, $I[v_1,T_2-b](\theta)$	
	PAU–60a	$I[T_1,T_2-b](\theta)$, $Q_{eff}[T_1,T_2-g]$	ε, σ
	MOR–62a	$I[v_1,T_2-b](\theta,v_1)$, r'bow$^{(1)}$	ε, r_m
	MOR–62b	$I[v_1,T_2-b](\theta)$, r'bow$^{(1)}$	ε
	MOR–62c	$I[v_1,T_2-b](\theta,v_1)$, r'bow$^{(1)}$	ε, r_m
	GER–63	$I[T_1,T_2-b](\theta,T_1)$	ε, r_m
	MUE–63	Data of MOR–62b	ε, σ
	HUN–64	$I[v_1,T_2-b](\theta)$, r'bow$^{(N)}$	ε, r_m
	BEC–65	$I[v_1,T_2-b](\theta,v_1)$, r'bow$^{(N)}$, qu osc	
	HUN–65a	$I[v_1,T_2-b](\theta,v_1)$,r'bow$^{(N)}$	ε, r_m
	BEC–66a	$Q_{eff}[v_1,T_2-b](v_1)$, gl'y extr	ε, r_m
	BEC–66b	$Q_{eff}[v_1,T_2-b](v_1)$, gl'y extr, $I[v_1,T_2-b](\theta_0)$, r'bow$^{(N)}$, qu osc	n, ε, r_m
	NEU–66	$Q_{eff}[v_1,T_2-b](v_1)$, gl'y extr	εr_m
K–H_2	MAI–33	$I_{app}[T_1,T_2-g](\theta_{lab},T_1)$	
	MAI–34	$Q_{app}[\theta_0,T_1,T_2-g]$	
	ROS–35	$Q_{app}[\theta_0,T_1,T_2-g]$	
	ROS–39	$Q_{app}[\theta_0,T_1,T_2-g]$	
	SAS–41	$Q_{app}[\theta_0,T_1,T_2-g](T_1)$	

(*continued*)

TABLE II (*continued*)

System	Reference	Measurement	Potential characteristics deduced
$K-H_2$ (*cont.*)	KOD–44	$Q_{app}[\theta_0,T_1,T_2-g]$	
	KOD–45	$Q_{app}[\theta_0,T_1,T_2-g]$	
	SAS–49	$Q_{app}[\theta_0,T_1,T_2-g]$	
	ROT–59a	$Q_{app}[T_1,T_2-g]$	C_6
	ROT–59b	$Q_{app}[T_1,T_2-g]$	C_6
	LUL–64	$Q_{eff}[v_1,T_2-g](v_1,T_2)$	C_6
$K-D_2$	ROS–35	$Q_{app}[\theta_0,T_1,T_2-g]$	
	ROS–39	$Q_{app}[\theta_0,T_1,T_2-g]$	
	ROT–59a	$Q_{app}[T_1,T_2-g]$	C_6
	ROT–59b	$Q_{app}[T_1,T_2-g]$	C_6
	BLY–64	$I[v_1,T_2-b](\theta_c)$	
$K-N_2$	MAI–33	$I_{app}[T_1,T_2-g](\theta_{lab},T_1)$	
	MAI–34	$Q_{app}[\theta_0,T_1,T_2-g]$	
	ROS–39	$Q_{app}[\theta_0,T_1,T_2-g]$	
	SAS–41	$Q_{app}[\theta_0,T_1,T_2-g]$	
	KOD–44	$Q_{app}[\theta_0,T_1,T_2-g]$	
	KOD–45	$Q_{app}[\theta_0,T_1,T_2-g]$	
	SAS–49	$Q_{app}[\theta_0,T_1,T_2-g]$	
	PAU–57	$Q_{app}[T_1,T_2-b]$	C_6
	ROT–59a	$Q_{app}[T_1,T_2-g]$	C_6
	ROT–59b	$Q_{app}[T_1,T_2-g]$	C_6
	PAU–60a	$Q_{app}[\theta_0,T_1,T_2-b](\theta_0)$, $Q_{eff}[v_1,T_2-b](v_1)$	
	PAU–60b	$Q_{eff}[v_1,T_2-g](v_1)$	s in $V\sim -C/r^s$
	HEL–61	$I_{app}[T_1,T_2-b](\theta_{lab})$, $Q_{eff}[\theta_0,T_1,T_2-b](\theta_0)$	C_6
	SCH–61	$Q_{eff}[v_1,T_2-g](v_1)$, $Q_{eff}[T_1,T_2-g]$	s
	HEL–64	$I_{app}[T_1,T_2-b](\theta_{lab})$, $Q_{eff}[\theta_0,T_1,T_2-b](\theta_0)$	C_6
	HES–65a	$Q_{eff}[v_1,T_2-g](v_1)$	s
	HES–65b	$Q_{eff}[v_1,T_2-g](v_1)$	s
$K-O_2$	SAS–41	$Q_{app}[\theta_0,T_1,T_2-g](T_1)$	
	KOD–44	$Q_{app}[\theta_0,T_1,T_2-g]$	
	KOD–45	$Q_{app}[\theta_0,T_1,T_2-g]$	
	SAS–49	$Q_{app}[\theta_0,T_1,T_2-g]$	
	ROT–59a	$Q_{app}[T_1,T_2-g]$	C_6
	ROT–59b	$Q_{app}[T_1,T_2-g]$	C_6
$K-Cl_2$	SAS–49	$Q_{app}[\theta_0,T_1,T_2-g]$	
	GIE–59	$Q_{app}[T_1,T_2-b]$	
	GIE–61	$Q_{app}[T_1,T_2-b]$	
$K-Br_2$	GRE–58	NESD	

(*continued*)

TABLE II (*continued*)

System	Reference	Measurement	Potential characteristics deduced
$K-Br_2$ (*cont.*)	ROB–59	$Q_{eff}[v_1,T_2-b](v_1)$, $Q_{eff}[v_1,T_2-g]$	
	HEL–61	$I_{app}[T_1,T_2-b](\theta_{lab})$, $Q_{eff}[\theta_0,T_1,T_2-b](\theta_0)$	C_6
	HEL–64	$I_{app}[T_1,T_2-b](\theta_{lab})$, $Q_{eff}[\theta_0,T_1,T_2-b](\theta_0)$	C_6
	HER–64	NESD	
	WIL–64b	NESD	
	BIR–65	NESD	
	DAT–65	NESD	
	GRO–65c	$I_{app}[v_1,T_2-b](v_1,\theta_{lab})$	
	GRO–65d	$I_{app}[v_1,T_2-b](v_1,\theta_{lab})$	
	HER–65	NESD	
	BIR–66	$I_{app}[T_1,T_2-b,v_a](\theta_{lab},v_a)$	
	MIN–66	$I[v_1,T_2-b](\theta)$	
	MOU–66	NESD	
$K-I_2$	WIL–64	NESD	
	DAT–65	NESD	
	MIN-66	NESD	
K–HCl	ROT–59a	$Q_{app}[T_1,T_2-g]$	C_6
	ROT–59b	$Q_{app}[T_1,T_2-g]$	C_6
	ACK–64	$I[v_1,T_2-b](\theta,v_1)$	ε, r_m
	MOU–64	$I[v_1,T_2-b](\theta,v_1)$, r'bow[1]	ε, r_m
K–HBr	TAY–55	$Q_{app}[\theta_0,T_1,T_2-g](T_1)$	
	ROT–59a	$Q_{app}[T_1,T_2-g]$	C_6
	ROT–59b	$Q_{app}[T_1,T_2-g]$	C_6
	GRE–60	$I[\theta_0,v_1,T_2-b]$	
	HER–60	Data of GRE–60	
	BEC–61a	$I[v_1,T_2-b](\theta)$	
	BEC–61b	NESD	
	DAT–61	Data of TAY–55	
	BEC–62a	$I[v_1,T_2-b](\theta,v_1)$, r'bow[1]	ε, r_m
	BEC–62b	Data of BEC–62a	r_m
	MIN–62	NESD	
	CRO–65	$Q_{eff}[v_1,T_2-g](v_1)$	C_6
	GRO–65b	$I_{app}[v_1,T_2-b](v_1,\theta_{lab})$	
	GRO–65d	$I_{app}[v_1,T_2-b](v_1,\theta_{lab})$	
	HUN–65a	$I[v_1,T_2-b](\theta,v_1)$, r'bow[1]	ε, r_m
	CRO–66	$Q_{eff}[v_1,T_2-g](v_1)$	C_6
	AIR–67b	$I[v_1,T_2-b](\theta)$, r'bow[1]	ε, r_m
K–HI	GIE–61	$Q_{app}[T_1,T_2-b]$	
	ACK–64	$I[v_1,T_2-b](\theta,v_1)$	ε, r_m
	MOU–64	$I[v_1,T_2-b](\theta,v_1)$, r'bow[1]	ε, r_m

(*continued*)

TABLE II (*continued*)

System	Reference	Measurement	Potential characteristics deduced
K–DBr	AIR–67b	$I[v_1,T_2-b](\theta)$, r'bow[1]	ε, r_m
K–CO	ROT–59a	$Q_{app}[T_1,T_2-g]$	C_6
	ROT–59b	$Q_{app}[T_1,T_2-g]$	C_6
K–NO	ROT–59a	$Q_{app}[T_1,T_2-g]$	C_6
	ROT–59b	$Q_{app}[T_1,T_2-g]$	C_6
K–ICl	HER–64	NESD	
	WIL–64	NESD	
K–IBr	WIL–64	NESD	
K–H_2O	ROT–59a	$Q_{app}[T_1,T_2-g]$	C_6
	ROT–59b	$Q_{app}[T_1,T_2-g]$	C_6
K–H_2S	ROT–59a	$Q_{app}[T_1,T_2-g]$	C_6
	ROT–59b	$Q_{app}[T_1,T_2-g]$	C_6
K–CO_2	MAI–33	$I_{app}[T_1,T_2-g](\theta_{lab},T_1)$	
	MAI–34	$Q_{app}[\theta_0,T_1,T_2-g]$	
	ROT–59a	$Q_{app}[T_1,T_2-g]$	C_6
	ROT–59b	$Q_{app}[T_1,T_2-g]$	C_6
K–CS_2	ROT–59a	$Q_{app}[T_1,T_2-g]$	C_6
	ROT–59b	$Q_{app}[T_1,T_2-g]$	C_6
K–N_2O	ROT–59a	$Q_{app}[T_1,T_2-g]$	C_6
	ROT–59b	$Q_{app}[T_1,T_2-g]$	C_6
K–SO_2	ROT–59a	$Q_{app}[T_1,T_2-g]$	C_6
	ROT–59b	$Q_{app}[T_1,T_2-g]$	C_6
K–$HgCl_2$	GER–63	$I[T_1,T_2-b](\theta,T_1)$	
K–HgI_2	GER–63	$I[T_1,T_2-g](\theta,T_1)$	
	HEL–64	$I_{app}[T_1,T_2-b](\theta_{lab})$, $Q_{eff}[\theta_0,T_1,T_2-b](\theta_0)$	C_6
For systems K–H_2CO, K–NH_3, K–CH_4, K–CH_3F, and K–CH_3Cl, see ROT–59			
K–CH_3Br	ROT–59a	$Q_{app}[T_1,T_2-g]$	C_6
	ROT–59b	$Q_{app}[T_1,T_2-g]$	C_6
	ACK–63	$I[v_1,T_2-b](\theta,v_1)$, r'bow[1]	ε
	MOU–64	$I[v_1,T_2-b](\theta,v_1)$, r'bow[1]	ε
K–CH_3I	ROT–59a	$Q_{app}[T_1,T_2-g]$	C_6
	ROT–59b	$Q_{app}[T_1,T_2-g]$	C_6
	KWE–60	$I[T_1,T_2-b](\theta)$	
	HER–61	$I_{app}[T_1,T_2-b](\theta_{lab})$	
	KWE–61	$I[T_1,T_2-b](\theta)$	
	HER–62	$I_{app}[T_1,T_2-b](\theta_{lab})$	
	BRO–64b	$Q_{eff}[T_1,T_2-g]$, $Q_{eff}[\theta_0,T_1,T_2-g](\theta_0)$	
	HER–64	NESD	
	CRO–65	$Q_{eff}[v_1,T_2-g](v_1)$	C_6
	HUN–65a	$I[v_1,T_2-b](\theta,v_1)$, r'bow[1]	ε, r_m
	BRO–66	$I[T_1,T_2-b,i_2](i_2,\theta_c)$	

(*continued*)

TABLE II (*continued*)

System	Reference	Measurement	Potential characteristics deduced
K–CH_3I	CRO–66	$Q_{eff}[v_1,T_2-g](v_1)$	C_6
(*cont.*)	AIR–67a	$I[v_1,T_2-b](\theta)$, r'bow[1]	ε, r_m
For systems K–CH_2F_2, K–CH_2FCl, K–CH_2Cl_2, K–CH_2ClBr, K–CHF_3, K–CHF_2Cl, K–$CHFCl_2$, K–CHFClBr, and K–$CHCl_3$, see ROT–59			
K–$CHBr_3$	HEL–61	$I_{app}[T_1,T_2-b](\theta_{lab})$, $Q_{eff}[\theta_0,T_1,T_2-b](\theta_0)$	C_6
	HEL–64	$I_{app}[T_1,T_2-b](\theta_{lab})$, $Q_{eff}[\theta_0,T_1,T_2-b](\theta_0)$	C_6
For systems K–CF_4, K–$CClF_3$, K–$CBrF_3$, and K–CF_2Cl_2, see ROT–59			
K–CCl_4	ROT–59a	$Q_{app}[T_1,T_2-g]$	C_6
	ROT–59b	$Q_{app}[T_1,T_2-g]$	C_6
	HEL–61	$I_{app}[T_1,T_2-b](\theta_{lab})$, $Q_{eff}[\theta_0,T_1,T_2-b](\theta_0)$	C_6
	HEL–64	$I_{app}[T_1,T_2-b](\theta_{lab})$, $Q_{eff}[\theta_0,T_1,T_2-b](\theta_0)$	C_6
	AIR–67a	$I[v_1,T_2-b](\theta)$, r'bow[1]	ε, r_m
K–CBr_4	GRE–66	$I[v_1,T_2-b](\theta,v_1)$	ε
K–SiF_4	ROT–59a	$Q_{app}[T_1,T_2-g]$	C_6
	ROT–59b	$Q_{app}[T_1,T_2-g]$	C_6
K–$SiCl_4$	ROT–59a	$Q_{app}[T_1,T_2-g]$	C_6
	ROT–59b	$Q_{app}[T_1,T_2-g]$	C_6
	AIR–67a	$I[v_1,T_2-b](\theta)$, r'bow[1]	ε, r_m
K–$SnCl_4$	ROT–59a	$Q_{app}[T_1,T_2-g]$	C_6
	ROT–59b	$Q_{app}[T_1,T_2-g]$	C_6
	AIR–67a	$I[v_1,T_2-b](\theta)$	ε, r_m
K–SnI_4	GER–63	$I[T_1,T_2-b](\theta,T_1)$	
	HEL–64	$I_{app}[T_1,T_2-b](\theta_{lab})$, $Q_{eff}[\theta_0,T_1,T_2-b](\theta_0)$	C_6
	HUN–65a	$I[v_1,T_2-b](\theta,v_1)$, r'bow[N]	ε, r_m
For systems K–C_2H_4 and K–CH_3OH, see ROT–59			
K–*trans*-CHI=CHI	FRA–33	$I_{app}[T_1,T_2-b](\theta_{lab})$	
For systems K–C_2HCl_3, K–C_2Cl_4, and K–CH_3NH_2, see ROT–59			
K–SF_6	ROT–59a	$Q_{app}[T_1,T_2-g]$	C_6
	ROT–59b	$Q_{app}[T_1,T_2-g]$	C_6
	AIR–67a	$I[v_1,T_2-b](\theta)$, r'bow[1]	ε, r_m
For systems K–C_2H_6, K–C_2H_5Cl, and K–C_2H_5Br, see ROT–59			
K–C_2H_5I	KWE–60	$I[T_1,T_2-b](\theta)$	
	HEL–61	$I_{app}[T_1,T_2-b](\theta_{lab})$, $Q_{eff}[\theta_0,T_1,T_2-b](\theta_0)$	C_6
	HER–61	$I_{app}[T_1,T_2-b](\theta_{lab})$	

(*continued*)

TABLE II (*continued*)

System	Reference	Measurement	Potential characteristics deduced
K–C_2H_5I (*cont.*)	HEL–64	$I_{app}[T_1,T_2-b](\theta_{lab})$, $Q_{eff}[\theta_0,T_1,T_2-b](\theta)$	C_6
For systems K–1,1-$C_2H_4Cl_2$ and K–1,2-$C_2H_4Cl_2$, see ROT–59			
K–1,2-$C_2H_4Br_2$	HEL–61	$I_{app}[T_1,T_2-b](\theta_{lab})$, $Q_{eff}[\theta_0,T_1,T_2-b](\theta_0)$	C_6
	HEL–64	$I_{app}[T_1,T_2-b](\theta_{lab})$, $Q_{eff}[\theta_0,T_1,T_2-b](\theta_0)$	C_6
For systems K–1,1,1-$C_2H_3Cl_3$, K–1,1,2-$C_2H_3Cl_3$, and K–*s*-$C_2H_2Cl_4$, see ROT–59			
K–$S_{(x)}$	JAW–55	$Q_{app}[\theta_0,T_1,T_2-b](\theta_0,T_1)$	
For systems K–C_3H_6, K–C_3H_5Cl, K–$(CH_3)_2CO$, K–C_3H_8, K–*n*-C_3H_7Br, K–C_4H_8-1, K–*cis*-C_4H_8-2, K–*trans*-C_4H_8-2, and K–*i*-C_4H_8, see ROT–59			
K–C_6H_6	ROT–59a	$Q_{app}[T_1,T_2-g]$	C_6
	ROT–59b	$Q_{app}[T_1,T_2-g]$	C_6
	AIR–67a	$I[v_1,T_2-b](\theta)$, r'bow[1]	ε, r_m
For systems K–C_6H_5Br, K–*n*-C_4H_{10}, K–*i*-C_4H_{10}, K–*n*-C_4H_9Br, K–cyclopentane (C_5H_{10}), K–$C_6H_5CH_3$, and K–*n*-C_5H_{12}, see ROT–59			
K–$C(CH_3)_4$	GRE–66	$I[v_1,T_2-b](\theta,v_1)$, r'bow[1]	ε, r_m
	AIR–67a	$I[v_1,T_2-b](\theta)$, r'bow[1]	ε, r_m
K–pyrene ($C_{16}H_{10}$)	GER–63	$I[T_1,T_2-b](\theta,T_1)$	ε, r_m
	HEL–64	$I_{app}[T_1,T_2-b](\theta_{lab})$, $Q_{eff}[\theta,T_1,T_2-b](\theta_0)$	C_6
K–*n*-$C_8H_{17}Br$	ROT–59a	$Q_{app}[T_1,T_2-g]$	C_6
	ROT–59b	$Q_{app}[T_1,T_2-g]$	C_6
K–Apiezon oil F	JAW–52	$Q_{app}[\theta_0,T_1,T_2-b](\theta,T_1,T_2)$	
	JAW–55	$Q_{app}[\theta_0,T_1,T_2-b](\theta_0,T_1)$	
K–Silicone oil DC 703	JAW–52	$Q_{app}[\theta_0,T_1,T_2-b](\theta_0,T_1,T_2)$	
	JAW–55	$Q_{app}[\theta_0,T_1,T_2-b](\theta_0,T_1)$	
K–cyclohexane (C_6H_{12})	ROT–59a	$Q_{app}[T_1,T_2-g]$	C_6
	ROT–59b	$Q_{app}[T_1,T_2-g]$	C_6
	HER–65	$I_{app}[T_1,T_2-b](\theta_{c,lab})$	
	AIR–67a	$I[v_1,T_2-b](\theta)$, r'bow[1]	ε, r_m
K–$C_2(CH_3)_4$	AIR–67a	$I[v_1,T_2-b](\theta)$, r'bow[1]	ε, r_m
For systems *K*–*n*-C_6H_{14} and K–*n*-$C_6H_{13}Br$, see ROT–59			
K–anthracene ($C_{14}H_{10}$)	GER–63	$I[T_1,T_2-b](\theta,T_1)$	ε, r_m
Rb–Na	BUC–65	$Q_{eff}[T_1,T_2-g]$	C_6
	SMI–66	Comments on BUC–65	C_6
Rb–K	BUC–65	$Q_{eff}[T_1,T_2-g]$	C_6
	SMI–66	Comments on BUC–65	C_6
Rb–Rb	BUC–65	$Q_{eff}[T_1,T_2-g]$	C_6

(*continued*)

TABLE II (*continued*)

System	Reference	Measurement	Potential characteristics deduced
Rb–Rb (*cont.*)	SMI–66	Comments on BUC–65	C_6
Rb–Cs	BUC–65	$Q_{\text{eff}}[T_1,T_2-g]$	C_6
	SMI–66	Comments on BUC–65	C_6
Rb–He	ROS–35	$Q_{\text{app}}[\theta_0,T_1,T_2-g]$	
Rb–Ne	ROS–35	$Q_{\text{app}}[\theta_0,T_1,T_2-g]$	
Rb–Ar	ROS–35	$Q_{\text{app}}[\theta_0,T_1,T_2-g]$	
Rb–Kr	VON–67	$Q_{\text{eff}}[v_1,T_2-g](v_1)$, gl'y extr	εr_m
Rb–Hg	PAU–57	$Q_{\text{app}}[T_1,T_2-b]$	C_6
	HUN–64	$I[v_1,T_2-b](\theta)$, r'bow$^{(N)}$	ε
	HUN–65a	$I[v_1,T_2-b](\theta,v_1)$, r'bow$^{(1)}$	ε, r_m
Rb–H_2	ROS–35	$Q_{\text{app}}[\theta_0,T_1,T_2-g]$	
Rb–D_2	ROS–35	$Q_{\text{app}}[\theta_0,T_1,T_2-g]$	
Rb–N_2	PAU–57	$Q_{\text{app}}[T_1,T_2-b]$	C_6
Rb–Br_2	WIL–64	NESD	
Rb–I_2	WIL–64	NESD	
Rb–ICl	WIL–64	NESD	
Rb–IBr	DAT–65	NESD	
	MIN–66	NESD	
Rb–HBr	MIN–62	NESD	
Rb–SCl_2	BIR–64	NESD	
Rb–CH_3I	KIN–61	NESD	
	KWE–61	$I_{\text{app}}[T_1,T_2-b](\theta_{\text{lab}})$	
	HER–62	$I_{\text{app}}[T_1,T_2-b](\theta_{\text{lab}})$	
	BEU–66	$I[T_1,T_2-b,i_2](i_2,\theta_c)$	
Cs–Na	BUC–65	$Q_{\text{eff}}[T_1,T_2-g]$	C_6
	SMI–66	Comments on BUC–65	C_6
Cs–K	BUC–65	$Q_{\text{eff}}[T_1,T_2-g]$	C_6
	SMI–66	Comments on BUC–65	C_6
Cs–Rb	BUC–65	$Q_{\text{eff}}[T_1,T_2-g]$	C_6
	SMI–66	Comments on BUC–65	C_6
Cs–Cs	EST–47	$Q_{\text{app}}[\theta_0,v_1,T_2-g]$	
	BUC–65	$Q_{\text{eff}}[T_1,T_2-g]$	C_6
	SHE–65	$Q_{\text{eff}}[\theta_0,T_1,T_2-g](\theta_0)$	C_6
	SMI–66	Comments on BUC–65	C_6
Cs–He	ROS–35	$Q_{\text{app}}[\theta_0,T_1,T_2-g]$	
	EST–47	$Q_{\text{app}}[\theta_0,v_1,T_2-g]$	
	ROT–59a	$Q_{\text{app}}[T_1,T_2-g]$	C_6
	ROT–59b	$Q_{\text{app}}[T_1,T_2-g]$	C_6
	HEL–61	$I_{\text{app}}[T_1,T_2-b](\theta_{\text{lab}})$, $Q_{\text{eff}}[\theta_0,T_1,T_2-b](\theta_0)$	C_6

(*continued*)

TABLE II (*continued*)

System	Reference	Measurement	Potential characteristics deduced
Cs–He (*cont.*)	HEL–64	$I_{app}[T_1,T_2-b](\theta_{lab})$, $Q_{eff}[\theta_0,T_1,T_2-b](\theta_0)$	C_6
Cs–Ne	ROS–35	$Q_{app}[\theta_0,T_1,T_2-g]$	
	ROT–59a	$Q_{app}[T_1,T_2-g]$	C_6
	ROT–59b	$Q_{app}[T_1,T_2-g]$	C_6
Cs–Ar	ROS–35	$Q_{app}[\theta_0,T_1,T_2-g]$	
	ROT–59a	$Q_{app}[T_1,T_2-g]$	C_6
	ROT–59b	$Q_{app}[T_1,T_2-g]$	C_6
	HEL–61	$I_{app}[T_1,T_2-b](\theta_{lab})$, $Q_{eff}[\theta_0,T_1,T_2-b](\theta_0)$	C_6
	HEL–64	$I_{app}[T_1,T_2-b](\theta_{lab})$, $Q_{eff}[\theta_0,T_1,T_2-b](\theta_0)$	C_6
	HOL–66	$Q_{eff}[v_1,T_2-g](v_1)$, $Q_{eff}[T_1,T_2-g]$	ε, r_m
	HOL–67	$Q_{eff}[v_1,T_2-g](v_1)$	εr_m
Cs–Kr	ROT–59a	$Q_{app}[T_1,T_2-g]$	C_6
	ROT–59b	$Q_{app}[T_1,T_2-g]$	C_6
	HOL–66	$Q_{eff}[v_1,T_2-g](v_1)$, $Q_{eff}[T_1,T_2-g]$	ε, r_m
	HOL–67	$Q_{eff}[v_1,T_2-g](v_1)$	εr_m
	VON–67	$Q_{eff}[v_1,T_2-g](v_1)$, gl'y extr	εr_m
Cs–Xe	ROT–59a	$Q_{app}[T_1,T_2-g]$	C_6
	ROT–59b	$Q_{app}[T_1,T_2-g]$	C_6
	HOL–66	$Q_{eff}[v_1,T_2-g](v_1)$, gl'y extr, $Q_{eff}[T_1,T_2-g]$	ε, r_m
	HOL–67	$Q_{eff}[v_1,T_2-g](v_1)$, gl'y extr	εr_m
Cs–Hg	PAU–57	$Q_{app}[T_1,T_2-b]$	C_6
	MOR–62a	$I[v_1,T_2-b](\theta,v_1)$, r'bow[1]	ε, r_m
	MOR–62b	$I[v_1,T_2-b](\theta)$, r'bow[1]	ε
	MOR–62c	$I[v_1,T_2-b](\theta,v_1)$, r'bow[1]	ε, r_m
	BEC–66a	$Q_{eff}[v_1,T_2-b](v_1)$	ε, r_m
	NEU–66	$Q_{eff}[v_1,T_2-b](v_1)$, gl'y extr	εr_m
Cs–H_2	ROS–35	$Q_{app}[\theta_0,T_1,T_2-g]$	
	ROT–59a	$Q_{app}[T_1,T_2-g]$	C_6
	ROT–59b	$Q_{app}[T_1,T_2-g]$	C_6
Cs–D_2	ROS–35	$Q_{app}[\theta_0,T_1,T_2-g]$	
	ROT–59a	$Q_{app}[T_1,T_2-g]$	C_6
	ROT–59b	$Q_{app}[T_1,T_2-g]$	C_6
Cs–N_2	EST–47	$Q_{app}[\theta_0,v_1,T_2-g]$	
	PAU–57	$Q_{app}[T_1,T_2-b]$	C_6
	ROT–59a	$Q_{app}[T_1,T_2-g]$	
	ROT–59b	$Q_{app}[T_1,T_2-g]$	
	HEL–61	$I_{app}[T_1,T_2-b](\theta_{lab})$, $Q_{eff}[\theta_0,T_1,T_2-b](\theta_0)$	

(*continued*)

TABLE II (*continued*)

System	Reference	Measurement	Potential characteristics deduced
Cs–N_2 (*cont.*)	HEL–64	$I_{app}[T_1,T_2-b](\theta_{lab})$, $Q_{eff}[\theta_0,T_1,T_2-b](\theta_0)$	C_6
Cs–Br_2	DAT–64	$I[v_1,T_2-b](\theta)$	
	WIL–64b	NESD	
	DAT–65	NESD	
	MIN–66	NESD	
Cs–I_2	WIL–64b	NESD	
Cs–HBr	HER–65	NESD	
Cs–ICl	WIL–64b	NESD	
Cs–IBr	WIL–64b	NESD	
For systems Cs–H_2O, Cs–CO_2, Cs–H_2CO, and Cs–CH_4, see ROT–59			
Cs–CH_3I	KWE–61	$I[T_1,T_2-b](\theta)$	
	HER–62	$I_{app}[T_1,T_2-b](\theta_{lab})$	
For systems Cs–CF_4, Cs–$SiCl_4$, and Cs–SF_6, see ROT–59			
Cs–$(CH_3)_2CO$	ROT–59a	$Q_{app}[T_1,T_2-g]$	C_6
	ROT–59b	$Q_{app}[T_1,T_2-g]$	C_6
	HEL–61	$I_{app}[T_1,T_2-b](\theta_{lab})$, $Q_{eff}[\theta_0,T_1,T_2-b](\theta_0)$	
	HEL–64	$I_{app}[T_1,T_2-b](\theta_{lab})$, $Q_{eff}[\theta_0,T_1,T_2-b)(\theta_0)$	C_6
He–He	KNA–33a	$I^{abs}[T_1,T_2-g](\theta_{lab})$	
	ZAB–33b	$I[T_1,T_2-g](\theta_{lab})$, structure	
	HAR–62b	$Q_{eff}[T_1,T_2-g](T_1)$	
	ROT–62a	$Q_{eff}[T_1,T_2-g]$	C_6
	ROT–65a	Data of ROT–62a	
	ROT–65d	$Q^{abs}_{eff}[T_1,T_2-g]$	
	BEI–66a	$Q_{eff}[T_1,T_2-g](T_1)$	ε,σ
	BEI–66b	$Q_{eff}[T_1,T_2-g](T_1)$	ε,σ
	MOO–67	$Q_{eff}[T_1,T_2-g](T_1)$for ^{4}He	
He–Ne	DÜR–65a	$Q_{eff}[T_1,T_2-g](T_1)$	C_6
	DÜR–65b	$Q_{eff}[T_1,T_2-g](T_1)$	C_6
	DÜR–65c	$Q_{eff}[v_1,T_2-g[(v_1)$	ε, r_m
	BEI–66a	$Q_{eff}[T_1,T_2-g](T_1)$	ε,σ
	BEI–66b	$Q_{eff}[T_1,T_2-g](T_1)$	ε,σ
He–Ar	ROT–61b	$Q_{app}[T_1,T_2-g]$	
	ROT–62a	$Q_{eff}[T_1,T_2-g]$	C_6
	BEI–65	$Q_{eff}[T_1,T_2-g](T_1)$, gl'y extr	ε,σ
	DÜR–65a	$Q_{eff}[T_1,T_2-g](T_1)$	C_6
	DÜR–65b	$Q_{eff}[T_1,T_2-g](T_1)$	C_6
	DÜR–65c	$Q_{eff}[v_1,T_2-g](v_1)$, gl'y extr	ε, r_m
	ROT–65a	Data of ROT–62a	

(*continued*)

TABLE II (*continued*)

System	Reference	Measurement	Potential characteristics deduced
He–Ar	BEI–66a	$Q_{\text{eff}}[T_1,T_2-g](T_1)$, gl'y extr	ε, σ
(*cont.*)	BEI–66b	$Q_{\text{eff}}[T_1,T_2-g](T_1)$, gl'y extr	ε, σ
	LAN–66a	$Q_{\text{eff}}[T_1,T_2-b]$	
	LAN–66b	$Q_{\text{eff}}[T_1,T_2-b]$	
He–Kr	BEI–65	$Q_{\text{eff}}[T_1,T_2-g](T_1)$, gl'y extr	ε, σ
	DÜR–65a	$Q_{\text{eff}}[T_1,T_2-g](T_1)$	C_6
	DÜR–65b	$Q_{\text{eff}}[T_1,T_2-g](T_1)$	C_6
	DÜR–65c	$Q_{\text{eff}}[v_1,T_2-g](v_1)$, gl'y extr	ε, r_m
	BEI–66a	$Q_{\text{eff}}[T_1,T_2-g](T_1)$, gl'y extr	ε, σ
	BEI–66b	$Q_{\text{eff}}[T_1,T_2-g](T_1)$, gl'y extr	ε, σ
He–Xe	BEI–65	$Q_{\text{eff}}[T_1,T_2-g](T_1)$, gl'y extr	ε, σ
	DÜR–65a	$Q_{\text{eff}}[T_1,T_2-g](T_1)$	C_6
	DÜR–65b	$Q_{\text{eff}}[T_1,T_2-g](T_1)$	C_6
	DÜR–65c	$Q_{\text{eff}}[v_1,T_2-g](v_1)$, gl'y extr	ε, r_m
	BEI–66a	$Q_{\text{eff}}[T_1,T_2-g](T_1)$, gl'y extr	ε, σ
	BEI–66b	$Q_{\text{eff}}[T_1,T_2-g](T_1)$, gl'y extr	ε, σ
He–Hg	KNA–33a	$I^{\text{abs}}[T_1,T_2-g](\theta_{\text{lab}})$	σ
	KNA–33b	Data of KNA–33a	
	ZAB–33a	$I_{\text{app}}[T_1,T_2-g](\theta_{\text{lab}})$	
	KNA–34	$I^{\text{abs}}[T_1,T_2-g](T_1,\theta_{\text{lab}})$, structure, $Q_{\text{app}}[T_1,T_2-g]$	
	ZAB–34	$I^{\text{abs}}[T_1,T_2-g](\theta_{\text{lab}})$	
	MUE–63	Data of KNA–34	ε, σ
$He–H_2$	HAR–62b	$Q_{\text{eff}}[T_1,T_2-g](T_1)$	
He*–He	DOR–39	$Q_{\text{app}}[\theta_0,T_1,T_2-g]$	
	STE–57	$Q_{\text{app}}[\theta_0,T_1,i_1,T_2-g]$	
	HAS–58	$Q_{\text{app}}[\theta_0,T_1,i_1,T_2-g]$	
	HAS–59	$Q_{\text{app}}[\theta_0,T_1,i_1,T_2-g]$	
	SMI–60	$Q_{\text{app}}[\theta_0,T_1,i_1,T_2-g](i_1)$	
	ROT–61a	Data of STE–57 and HAS–58, 59	
	RIC–64	$Q_{\text{app}}[\theta_0,T_1,i_1,T_2-g](\theta_0,i_1)$	
	ROT–65b	$Q_{\text{eff}}[v_1,i_1,T_2-g]$	
	ROT–65c	$Q_{\text{eff}}[v_1,i_1,T_2-g](v_1)$	
He*–Ne	STE–57	$Q_{\text{app}}[\theta_0,T_1,i_1,T_2-g]$	
	HAS–58	$Q_{\text{app}}[\theta_0,T_1,i_1,T_2-g]$	
	HAS–59	$Q_{\text{app}}[\theta_0,T_1,i_1,T_2-g]$	
	SMI–60	$Q_{\text{app}}[\theta_0,T_1,i_1,T_2-g](i_1)$	
	ROT–61a	Data of STE–57 and HAS–58, 59	
	RIC–64	$Q_{\text{app}}[\theta_0,T_1,i_1,T_2-g](\theta_0,i_1)$	
	ROT–65b	$Q_{\text{eff}}[v_1,i_1,T_2-g]$	
He*–Ar	STE–57	$Q_{\text{app}}[\theta_0,T_1,i_1T_2-g]$	

(*continued*)

TABLE II (*continued*)

System	Reference	Measurement	Potential characteristics deduced
He*–Ar	HAS–58	$Q_{app}[\theta_0,T_1,i_1,T_2-g]$	
(*cont.*)	HAS–59	$Q_{app}[\theta_0,T_1,i_1,T_2-g]$	
	SMI–60	$Q_{app}[\theta_0,T_1,i_1,T_2-g](i_1)$	
	ROT–61a	Data of STE–57 and HAS–58, 59	
	ROT–65b	$Q_{eff}[v_1,i_1,T_2-g]$	C_6
	ROT–65c	$Q_{eff}[v_1,i_1,T_2-g](v_1)$, gl'y extr	ε, σ
He*–Kr	STE–57	$Q_{app}[\theta_0,T_1,i_1,T_2-g]$	
	ROT–61a	Data of STE–57	
	ROT–65b	$Q_{eff}[v_1,i_1,T_2-g]$	C_6
	ROT–65c	$Q_{eff}[v_1,i_1,T_2-g](v_1)$, gl'y extr	ε, σ
Ne–He	CAL–58	$Q_{app}[T_1,T_2-g]$	C_6
Ne–Ar	CAL–58	$Q_{app}[T_1,T_2-g]$	C_6
	ROT–62a	$Q_{eff}[T_1,T_2-g]$	C_6
	ROT–65a	Reinterpretation of ROT–62a	
Ne–Kr	CAL–58	$Q_{app}[T_1,T_2-g]$	C_6
Ne*–He	HAS–58	$Q_{app}[\theta_0,T_1,i_1,T_2-g]$	
	HAS–59	$Q_{app}[\theta_0,T_1,i_1,T_2-g]$	
	ROT–61a	Data of HAS–58, 59	
	ROT–65b	$Q_{eff}[v_1,i_1,T_2-g]$	
Ne*–Ne	HAS–58	$Q_{app}[\theta_0,T_1,i_1,T_2-g]$	
	HAS–59	$Q_{app}[\theta_0,T_1,i_1,T_2-g]$	
	ROT–61a	Data of HAS–58, 59	
	ROT–65b	$Q_{eff}[v_1,i_1,T_2-g]$	
Ne*–Ar	HAS–58	$Q_{app}[\theta_0,T_1,i_1,T_2-g]$	
	HAS–59	$Q_{app}[\theta_0,T_1,i_1,T_2-g]$	
	ROT–61a	Data of HAS–58, 59	
	ROT–65b	$Q_{eff}[v_1,i_1,T_2-g]$	C_6
Ar–He	CAL–58	$Q_{app}[T_1,T_2-g]$	C_6
	LAN–66a	$Q_{eff}[T_1,T_2-b]$	
	LAN–66b	$Q_{eff}[T_1,T_2-b]$	
Ar–Ne	CAL–58	$Q_{app}[T_1,T_2-g]$	C_6
	LAN–66a	$Q_{eff}[T_1,T_2-b]$	
	LAN–66b	$Q_{eff}[T_1,T_2-b]$	
Ar–Ar	ROT–61b	$Q_{app}[T_1,T_2-g]$	
	ROT–62a	$Q_{app}[T_1,T_2-g]$	C_6
	ROT–65a	Reinterpretation of ROT–62a	
	ROT–65d	$Q^{abs}_{eff}[T_1,T_2-g]$	C_6
Ar–Kr	ROT–65d	$Q^{abs}_{eff}[T_1,T_2-g]$	C_6
Ar–H_2	LAN–66a	$Q_{eff}[T_1,T_2-b]$	
	LAN–66b	$Q_{eff}[T_1,T_2-b]$	
Ar–N_2	LAN–66a	$Q_{eff}[T_1,T_2-b]$	

(*continued*)

TABLE II (*continued*)

System	Reference	Measurement	Potential characteristics deduced
$Ar–N_2$ (*cont.*)	LAN–66b	$Q_{eff}[T_1,T_2-b]$	
Kr–He	CAL–58	$Q_{app}[T_1,T_2-g]$	C_6
Kr–Ne	CAL–58	$Q_{app}[T_1,T_2-g]$	C_6
Kr–Ar	ROT–61b	$Q_{app}[T_1,T_2-g]$	
	ROT–62a	$Q_{app}[T_1,T_2-g]$	C_6
	ROT–65a	Reinterpretation of ROT–62a	
	ROT–65d	$Q_{eff}^{abs}[T_1,T_2-g]$	C_6
Kr–Kr	ROT–65d	$Q_{eff}^{abs}[T_1,T_2-g]$	C_6
Xe–Ar	ROT–61b	$Q_{app}[T_1,T_2-g]$	
	ROT–62a	$Q_{app}[T_1,T_2-g]$	C_6
	ROT–65a	Reinterpretation of ROT–62a	
Xe–Xe	BRO–64b	$Q_{eff}[T_1,T_2-g]$	
$Xe–CH_3I$	BRO–64b	$Q_{eff}[T_1,T_2-g]$	
$O^*–NO_2$	NUT–61	NESD	
$I–COCl_2$	MAR–52b	NESD	
Ga–He	BER–60	$Q_{eff}[v_1,i_1,T_2-g](i)$	
	BER–61b	$Q_{eff}[v_1,i_1,T_2-g](i_1)$	C_6
	TOS–61	$Q_{eff}[v_1,i_1,T_2-g](i_1)$, $Q_{eff}[v_1,T_2-g]$	
	BER–62a	$Q_{eff}[v_1,i_1,T_2-g](i_1)$, $Q_{eff}[v_1,T_2-g]$	
	TOS–65	Data of TOS–61	
Ga–Ne	BER–62a	$Q_{eff}[v_1,T_2-g]$	
	TOS–65	$Q_{eff}[v_1,i_1,T_2-g](i_1)$	
Ga–Ar	BER–60	$Q_{eff}[v_1,i_1,T_2-g](i_1)$	
	BER–61b	$Q_{eff}[v_1,i_1,T_2-g](i_1)$	C_6
	TOS–61	$Q_{eff}[v_1,i_1,T_2-g](i_1)$, $Q_{eff}[v_1,T_2-g]$	
	BER–62a	$Q_{eff}[v_1,i_1,T_2-g](i_1)$, $Q_{eff}[v_1,T_2-g]$	
	TOS–65	Data of TOS–61	
Ga–Kr	BER–62a	$Q_{eff}[v_1,T_2-g]$	
Ga–Xe	BER–60	$Q_{eff}[v_1,i_1,T_2-g](i_1)$	
	PAU–60a	$Q_{eff}[v_1,i_1,T_2-g](i_1)$	
	BER–61a	$Q_{eff}[v_1,i_1,T_2-g](i_1)$	
	BER–61b	$Q_{eff}[v_1,i_1,T_2-g](i_1)$	C_6
	TOS–61	$Q_{eff}[v_1,i_1,T_2-g](i_1)$, $Q_{eff}[v_1,T_2-g]$	
	BER–62a	$Q_{eff}[v_1,i_1,T_2-g](i_1)$, $Q_{eff}[v_1,T_2-g]$	
	TOS–65	Data of TOS–61	
$Ag–N_2$	BIE–25	$Q_{app}[\theta_0,T_1,T_2-g]$	
Ag–air	BOR–20	$Q_{app}[\theta_0,T_1,T_2-g]$	
H_2–He	HAR–62b	$Q_{eff}[T_1,T_2-g](T_1)$	
	VAN–65	$Q_{eff}[T_1,T_2-g]$	
	MOO–67	$Q_{eff}[T_1,T_2-g](T_1)$ for $^{3,4}He$	
H_2–Ne	HEL–66	$Q_{eff}[v_1,T_2-g](v_1)$, gl'y extr	ε, r_m

(*continued*)

TABLE II (*continued*)

System	Reference	Measurement	Potential characteristics deduced
H_2–Ar	FEL–66	$Q_{eff}[v_1,T_2-g](v_1)$, gl'y extr	ε, r_m
	HEL–66	$Q_{eff}[v_1,T_2-g](v_1)$, gl'y extr	ε, r_m
	LAN–66a	$Q_{eff}[T_1,T_2-b]$	
	LAN–66b	$Q_{eff}[T_1,T_2-b]$	
H_2–Kr	DÜR–65c	$Q_{eff}[v_1,T_2-g](v_1)$, gl'y extr	
	FEL–66	$Q_{eff}[v_1,T_2-g](v_1)$, gl'y extr	ε, r_m
	HEL–66	$Q_{eff}[v_1,T_2-g](v_1)$, gl'y extr	ε, r_m
H_2–Xe	FEL–66	$Q_{eff}[v_1,T_2-g](v_1)$, gl'y extr	ε, r_m
	HEL–66	$Q_{eff}[v_1,T_2-g](v_1)$, gl'y extr	ε, r_m
H_2–H_2	KNA–29	$Q_{app}[\theta_0,T_1,T_2-g]$	
	ELL–31	$Q_{app}[\theta_0,T_1,T_2-g]$	
	KNA–33a	$I^{abs}[T_1,T_2-g](\theta_{lab})$	
	ZAB–33b	$I_{app}[T_1,T_2-g](\theta_{lab})$, structure	
	MIN–58	$Q_{app}[T_1,T_2-g]$	C_6
	HAR–62a	NESD	
	HAR–62b	$Q_{eff}[T_1,T_2-g](T_1)$	
H_2–N_2	MIN–58	$Q_{app}[T_1,T_2-g]$	C_6
H_2–air	ELL–31	$Q_{app}[\theta_0,T_1,T_2-g]$	
H_2–Hg	KNA–33a	$I^{abs}[T_1,T_2-g](\theta_{lab})$	σ
	KNA–33b	Data of KNA–33a	
	ZAB–33a	$I_{app}[T_1,T_2-g](\theta_{lab})$	
	KNA–34	$I^{abs}[T_1,T_2-g](T_1,\theta_{lab})$, structure, $Q_{eff}[\theta_0,T_1,T_2-g]$	
	ZAB–34	$I^{abs}[T_1,T_2-g](\theta_{lab})$	
	MAS–57	Data of KNA-34	ε, r_m
	HOS–59	Data of KNA–34	ε, r_m
	MUE–63	Data of KNA–34	ε, σ
D_2–He	MOO–67	$Q_{eff}[T_1,T_2-g](T_1)$ for ^{3}He	
D_2–Ne	HEL–66	$Q_{eff}[v_1,T_2-g](v_1)$, gl'y extr	ε, r_m
D_2–Ar	FEL–66	$Q_{eff}[v_1,T_2-g](v_1)$, gl'y extr	ε, r_m
	HEL–66	$Q_{eff}[v_1,T_2-g](v_1)$, gl'y extr	ε, r_m
D_2–Kr	DÜR–65c	$Q_{eff}[v_1,T_2-g](v_1)$, gl'y extr	
	FEL–66	$Q_{eff}[v_1,T_2-g](v_1)$, gl'y extr	
	HEL–66	$Q_{eff}[v_1,T_2-g](v_1)$, gl'y extr	ε, r_m
D_2–Xe	FEL–66	$Q_{eff}[v_1,T_2-g](v_1)$, gl'y extr	ε, r_m
	HEL–66	$Q_{eff}[v_1,T_2-g](v_1)$, gl'y extr	ε, r_m
Li_2–He	ROS–40	$Q_{app}[\theta_0,T_1,T_2-g]$	
Li_2–Ar	ROS–40	$Q_{app}[\theta_0,T_1,T_2-g]$	
For systems K_2–He, K_2–Ar, K_2–H_2, K_2–D_2, and K_2–N_2, see ROS–39			
O_2–O_2	KNA–33a	$I^{abs}[T_1,T_2-g](\theta_{lab})$	
I_2–Na	NIS–36	NESD	
I_2–Hg	SAS–36a	$Q_{app}[\theta_0,T_1,T_2-g]$	

(*continued*)

TABLE II (*continued*)

System	Reference	Measurement	Potential characteristics deduced
I_2–Hg (*cont.*)	NIS–37	$Q_{app}[\theta_0,T_1,T_2-g]$	
I_2–ClO_2	MAR–52a	NESD	
	MAR–52b	NESD	
I_2^*–Hg	SAS–36a	$Q_{app}[\theta_0,T_1,T_2-g]$	
	NIS–37	$Q_{app}[\theta_0,T_1,T_2-g]$	
KCl–Ar	HES–65a	$Q_{eff}[v_1,T_2-g](v_1,T_2)$	s
	HES–65b	$Q_{eff}[v_1,T_2-g](v_1,T_2)$	s
KCl–Kr	CRO–65	$Q_{eff}[v_1,T_2-g](v_1)$	C_6
	CRO–66	$Q_{eff}[v_1,T_2-g](v_1)$	C_6
KCl–Xe	CRO–65	$Q_{eff}[v_1,T_2-g](v_1)$	C_6
	CRO–66	$Q_{eff}[v_1,T_2-g](v_1)$	C_6
KCl–N_2	SCH–61	$Q_{eff}[v_1,T_2-g](v_1)$, $Q_{eff}[T_1,T_2-g]$	s
	HES–65a	$Q_{eff}[v_1,T_2-g](v_1,T_2)$	s
	HES–65b	$Q_{eff}[v_1,T_2-g](v_1,T_2)$	
KCl–HBr	CRO–65	$Q_{eff}[v_1,T_2-g](v_1)$	
	CRO–66	$Q_{eff}[v_1,T_2-g](v_1)$	
KCl–CH_3I	CRO–65	$Q_{eff}[v_1,T_2-g](v_1)$	
	CRO–66	$Q_{eff}[v_1,T_2-g](v_1)$	
KBr*–Na	MOU–66	NESD	
CsF–Ar	WIL–64a	NESD	
For systems CsCl–He and CsCl–Ne see ROT–59b and SCH–60			
CsCl–Ar	ROT–59b	$Q_{app}[T_1,T_2-g]$	C_6
	SCH–60	$Q_{app}[T_1,T_2-g](T_2)$	s,C_6
CsCl–Kr	ROT–59b	$Q_{app}[T_1,T_2-g]$	C_6
	SCH–60	$Q_{app}[T_1,T_2-g]$	C_6
	CRO–65	$Q_{eff}[v_1,T_2-g](v_1)$	C_6
	CRO–66	$Q_{eff}[v_1,T_2-g](v_1)$	C_6
CsCl–Xe	ROT–59b	$Q_{app}[T_1,T_2-g]$	C_6
	SCH–60	$Q_{app}[T_1,T_2-g]$	C_6
	CRO–65	$Q_{eff}[v_1,T_2-g](v_1)$	C_6
	CRO–66	$Q_{eff}[v_1,T_2-g](v_1)$	C_6
For systems CsCl–H_2 and CsCl–D_2, see ROT–59b and SCH–60			
CsCl–HBr	CRO–65	$Q_{eff}[v_1,T_2-g](v_1)$	
	CRO–66	$Q_{eff}[v_1,T_2-g](v_1)$	
CsCl–NO	SCH–60	$Q_{app}[T_1,T_2-g](T_1)$	C_6
CsCl–H_2O	ROT–59b	$Q_{app}[T_1,T_2-g]$	C_6
CsCl–H_2S	SCH–60	$Q_{app}[T_1,T_2-g](T_1)$	C_6
CsCl–H_2CO	ROT–59b	$Q_{app}[T_1,T_2-g]$	C_6
CsCl–NH_3	SCH–60	$Q_{app}[T_1,T_2-g](T_1)$	C_6
CsCl–$SbCl_3$	HEL–64	$I_{app}[T_1,T_2-b](\theta_{lab})$, $Q_{eff}[\theta_0,T_1,T_2-g](\theta_0)$	C_6

(*continued*)

TABLE II (*continued*)

System	Reference	Measurement	Potential characteristics deduced
$CsCl–CH_4$	ROT–59b	$Q_{app}[T_1,T_2-g]$	C_6
	SCH–60	$Q_{app}[T_1,T_2-g](T_2)$	s,C_6
$CsCl–CH_3I$	CRO–65	$Q_{eff}[v_1,T_2-g](v_1,T_2)$	
	CRO–66	$Q_{eff}[v_1,T_2-g](v_1,T_2)$	
$CsCl–CH_2F_2$	ROT–59b	$Q_{app}[T_1,T_2-g]$	C_6
	SCH–60	$Q_{app}[T_1,T_2-g](T_2)$	C_6
$CsCl–CHF_3$	SCH–60	$Q_{app}[T_1,T_2-g](T_2)$	C_6
$CsCl–CF_4$	ROT–59b	$Q_{app}[T_1,T_2-g]$	C_6
	SCH–60	$Q_{app}[T_1,T_2-g](T_2)$	s,C_6
For systems CsCl–$SiCl_4$, CsCl–*trans*-$C_2H_2Cl_2$, CsCl–*cis*-$C_2H_2Cl_2$, and CsCl–SF_6, see ROT–59b and SCH–60			
$CsCl–(CH_3)_2CO$	ROT–59b	$Q_{app}[T_1,T_2-g]$	C_6
CsBr–Xe	CRO–65	$Q_{eff}[v_1,T_2-g](v_1)$	C_6
	CRO–66	$Q_{eff}[v_1,T_2-g](v_1)$	C_6
$CsBr–CH_3I$	CRO–65	$Q_{eff}[v_1,T_2-g](v_1)$	
	CRO–66	$Q_{eff}[v_1,T_2-g](v_1)$	
TlF–He	KRA–62	$Q_{eff}[T_1,i_1,T_2-b](i_1)$ $Q_{eff}[v_1,T_2-g]$	
	TOE–62	NESD	
	BEN–64	$Q_{eff}[T_1,i_1,T_2-b](i_1)$	Anisotropic C_6
	TOE–64	NESD	
	TOE–65	$Q_{eff}[\theta_0,T_1,T_2-g]$	
TlF–Ne	KRA–62	$Q_{eff}[T_1,i_1,T_2-b](i_1)$ $Q_{eff}[v_1,T_2-g]$	
	TOE–62	NESD	
	BEN–64	$Q_{eff}[T_1,i_1,T_2-b](i_1)$	Anisotropic C_6
	TOE–64	NESD	
	TOE–65	$Q_{eff}[\theta_0,T_1,T_2-g]$	
TlF–Ar	BEN–61	$Q_{app}[T_1,i_1,T_2-b](i_1)$	
	KRA–62	$Q_{eff}[T_1,i_1,T_2-b](i_1)$ $Q_{eff}[v_1,T_2-g]$	
	TOE–62	NESD	
	BEN–64	$Q_{eff}[T_1,i_1,T_2-b](i_1)$	Anisotropic C_6
	GEN–64	$Q_{eff}[T_1,i_1,T_2-b](i_1)$	Anisotropic C_6
	TOE–64	NESD	
	TOE–65	$Q_{eff}[\theta_0,T_1,T_2-g]$	
TlF–Kr	KRA–62	$Q_{eff}[T_1,i_1,T_2-b](i_1)$ $Q_{eff}[v_1,T_2-g]$	
	TOE–62	NESD	

(*continued*)

TABLE II (*continued*)

System	Reference	Measurement	Potential characteristics deduced
TlF–Kr (*cont.*)	BEN–64	$Q_{\text{eff}}[T_1,i_1,T_2-b](i_1)$	Anisotropic C_6
	TOE–64	NESD	
	TOE–65	$Q_{\text{eff}}[\theta_0,T_1,T_2-g]$	
TlF–Xe	GEN–64	$Q_{\text{eff}}[T_1,i_1,T_2-b](i_1)$	Anisotropic C_6
For systems TlF–H_2, TlF–O_2, TlF–H_2O, TlF–N_2O, TlF–NH_3, TlF–ND_3, TlF–CH_4, TlF–CF_2Cl_2, TlF–SF_6, and TlF–air, see TOE–65			
H_2O–H_2O	KNA–33a	$I^{\text{abs}}[T_1,T_2-g](\theta_{\text{lab}})$	
	KYD–62	$Q_{\text{app}}[T_1,T_2-g](T_1)$	
NH_3–H_2O	KYD–62	$Q_{\text{app}}[T_1,T_2-g](T_1)$	
For systems CH_3I–CH_3I, CH_3I–i-C_3H_7I, and CH_3I–n-C_3H_7I, see BRO–64b			
CCl_4–Cs	BUL–64	NESD	
$CF_2ClCFCl_2$	MAR–52a	NESD	
–ClO_2	MAR–52b	NESD	
For systems i-C_3H_7I–CH_3I, i-C_3H_7I–i-C_3H_7I, i-C_3H_7I–n-C_3H_7I, n-C_3H_7I–CH_3I, n-C_3H_7I–i-C_3H_7I, and n-C_3H_7I–n-C_3H_7I, see BRO–64b			

C. Annotated Bibliography

This bibliography is limited to references quoted in Table II, consisting of articles which contain experimental results or present data analysis.

ACK–63 M. Ackerman, E. F. Greene, A. L. Moursund, and J. Ross, "A study of the Reaction of Potassium with CH_3Br in Crossed Molecular Beams," *Ninth International Symposium on Combustion*, Academic Press, New York, 1963, p. 669.

ACK–64 M. Ackerman, E. F. Greene, A. L. Moursund, and J. Ross, "Elastic and Reactive Scattering of K by HCl and HI in Crossed Molecular Beams," *J. Chem. Phys.*, **41**, 1183 (1964).

AIR–67a J. R. Airey, E. F. Greene, G. P. Reck, and J. Ross, "Scattering of Potassium by a Series of Reactive and Non-Reactive Compounds in Molecular Beams," *J. Chem. Phys.*, **46**, 3295 (1967). K–$C(CH_3)_4$, K–C_6H_6, K–C_6H_{12}, K–$C_2(CH_3)_4$, K–CH_3I, K–CCl_4, K–$SiCl_4$, K–$SnCl_4$, K–SF_6.

AIR–67b J. R. Airey, E. F. Greene, K. Kodera, G. P. Reck, and J. Ross, "Non-Reactive Scattering of K by HBr and DBr in Crossed Molecular Beams," *J. Chem. Phys.*, **46**, 3287 (1967).

BAR–66 P. Barwig, U. Buck, E. Hundhausen, and H. Pauly, "Interferenzen bei atomaren Stossprozessen. Die Systeme Na–Kr und Na–Xe," *Z. Physik.*, **196**, 343 (1966).

BEC–61a D. Beck, "Elastic Scattering in Molecular Beams. The Scattering of a Velocity Selected Potassium Beam by Krypton and HBr," *2nd International Conference on the Physics of Electronic and Atomic Collisions*, abstracts of papers, Benjamin, New York, 1961, p. 93. No data quoted.

BEC–61b D. Beck, E. F. Greene, and J. Ross, "The Reactive Scattering of Velocity Selected K Atoms by HBr," *2nd International Conference on the Physics of Electronic and Atomic Collisions*, abstracts of papers, Benjamin, New York, 1961, p. 94.

BEC–62a D. Beck, "Wide-Angle Scattering in Molecular Beams. The Rainbow Effect," *J. Chem. Phys.*, **37**, 2884 (1962). K–Kr, K–HBr.

BEC–62b D. Beck, E. F. Greene, and J. Ross, "A Study of the Reaction of K with HBr in Crossed Molecular Beams," *J. Chem. Phys.*, **37**, 2895 (1962).

BEC–65 D. Beck, H. Dummel, and U. Henkel, "Regenbogenstreuung an Kalium-Quecksilber," *Z. Physik.*, **185**, 19 (1965). K–Hg.

BEC–66a D. Beck and H. J. Loesch, "Atom-Atom-Streuexperimente: Geschwindigkeitsabhängigkeit einiger totaler Streuquerschnitte," *Z. Physik.*, **195**, 444 (1966). K–Ar, K–Kr, K–Xe, K–Hg, Cs–Hg.

BEC–66b D. Beck and H. J. Loesch, "Interatomares Potential aus Streuexperimenten: K–Hg," *Z. Physik.*, **196**, 66 (1966).

BEI–65 H. J. Beier, "Observation of Undulations of the Total Elastic Scattering Cross Section for the Scattering of Helium Atomic Beams in Xe, Kr, and Ar," *Phys. Letters*, **18**, 285 (1965).

BEI–66a H. J. Beier, "Messung totaler elastischer Streuquerschnitte für Streuung von Helium-Atomstrahlen in Edelgasen," Dissertation, University of Berlin, 1966. He–He, He–Ne, He–Ar, He–Kr, He–Xe.

BEI–66b H. J. Beier, "Streuung von Helium Atomstrahlen in Edelgasen," *Z. Physik.*, **196**, 185 (1966). He–He, He–Ne, He–Ar, He–Kr, He–Xe.

BEN–61 H. G. Bennewitz, K. H. Kramer, and J. P. Toennies, "Ratio of the Collision Cross-Sections of Oriented TlF Molecules in the (1,0) and (1,1) Rotational States," *2nd International Conference on the Physics of Electronic and Atomic Collisions*, abstracts of papers, Benjamin, New York, 1961, p. 113. TlF–Ar.

BEN–64 H. G. Bennewitz, K. H. Kramer, W. Paul, and J. P. Toennies, "Messung der Anisotropie des van der Waals-Potentials durch Streuung von Molekülen in definiertem Quantenzustand," *Z. Physik.*, **177**, 84 (1964). TlF in (1,0) and (1,1) rotational states vs. He, Ne, Ar, and Kr.

BEN–65 H. G. Bennewitz and H. D. Dohmann, "Bemerkung zur Bestimmung der van der Waals-Konstanten aus Streuquerschnitten," *Z. Physik.*, **182**, 524 (1965). K–Ar.

BER–60 K. Berkling, Ch. Schlier, and P. Toschek, "Streuung von Galliumatomen in verschiedenen Zeeman-Zuständen," *Z. Naturforsch.*, **15a**, 838 (1960). Ga in $^2P_{3/2,3/2}$ and $^2P_{3/2,1/2}$ Zeeman states vs. He, Ar, and Xe.

BER–61a K. Berkling, "Streuversuche an Galliumatomen in bestimmten Zeemanzuständen. Streuung an Xenon," Dissertation, University of Bonn, 1961. Ga in $^2P_{3/2,3/2}$ and $^2P_{3/2,1/2}$ Zeeman states vs. Xe.

BER–61b K. Berkling, Ch. Schlier, and P. Toschek, "Scattering of Gallium Atoms in Selected Zeeman States," *2nd International Conference on the Physics of Electronic and Atomic Collisions*, abstracts of papers, Benjamin, New York, 1961, p. 111. Ga in $^2P_{3/2,3/2}$ and $^2P_{3/2,1/2}$ Zeeman states vs. He, Ar, and Xe.

BER–62a K. Berkling, Ch. Schlier, and P. Toschek, "Messung der Anisotropie der van der Waals-Kraft," *Z. Physik.*, **168**, 81 (1962). Ga in $^2P_{3/2,3/2}$ and $^2P_{3/2,1/2}$ Zeeman states vs. He, Ar, and Xe. Also Ga–He, Ga–Ne, Ga–Ar, Ga–Kr, Ga–Xe, Na–He, Na–Ar, Na–N_2, Na–O_2, Na–CH_4.

BER–62b R. B. Bernstein, "Extrema in Velocity Dependence of Total Elastic Cross Sections for Atomic Beam Scattering: Relation to Di-Atom Bound States," *J. Chem. Phys.*, **37**, 1880 (1962). Li–Xe, K–Xe.

BEU–66 R. J. Beuhler, Jr., R. B. Bernstein, and K. H. Kramer, "Observation of the Reactive Asymmetry of Methyl Iodide. Crossed Beam Study of the Reaction of Rubidium with Oriented Methyl Iodide Molecules," *J. Am. Chem. Soc.*, **88**, 5331 (1966).

BIE–25 F. Bielz, "Versuche zur direkten Messung der mittleren freien Weglänge von ungeladenen Silberatomen in Stickstoff," *Z. Physik.*, **32**, 81 (1925). Ag–N_2.

BIR–64 J. H. Birely, R. R. Herm, K. R. Wilson, and D. R. Herschbach, "Reactive Scattering in Crossed Molecular Beams: Rb Atoms with SCl_2," *Bull. Am. Phys. Soc.*, 9, 709 (1964).

BIR–65 J. H. Birely and D. R. Herschbach, "Velocity Analysis of KBr Formed in Reactive Scattering of K and Br_2 Molecular Beams," *Bull. Am. Phys. Soc.*, **10**, 634 (1965).

BIR–66 J. H. Birely and D. R. Herschbach, "Reactive Scattering in Molecular Beams: Velocity Analysis of KBr Formed in the K + Br_2 Reaction," *J. Chem. Phys.*, **44**, 1690 (1966).

BLY–64 A. R. Blythe, A. E. Grosser, and R. B. Bernstein, "Observation of Rotational De-Excitation of D_2 Using Crossed Molecular Beams," *J. Chem. Phys.*, **41**, 1917 (1964). K–D_2, K–He.

BOR–20 M. Born, "Eine direkte Messung der freien Weglänge neutraler Atome," *Phys. Z.*, **21**, 578 (1920). Ag–air.

BRO–33 L.F. Broadway, "Experiments on Molecular Scattering in Gases. II. The Collision of Sodium and Potassium Atoms with Mercury," *Proc. Roy. Soc. (London)*, **A141**, 634 (1933).

BRO–64a H. H. Brown, Jr., K. Lulla, and B. Bederson, "Scattering of a Velocity-Selected Potassium Beam by Neon, Argon, and Xenon Gases at Different Temperatures," *Atomic Collision Processes*, M. R. C. McDowell, Ed., North-Holland, Amsterdam, 1964, p. 921.

BRO–64b P. R. Brooks, "Molecular Scattering at Thermal Energies," Ph.D. Thesis, University of California, 1964. Also University Microfilms Order No. 64–8993. $Q_{\text{eff}}[T_1,T_2-g]$ for Xe–Xe, Xe–CH_3I. Also for

CH_3I, i-C_3H_7I, and n-C_3H_7I each scattered by CH_3I, i-C_3H_7I, and n-C_3H_7I. $Q_{eff}[T_1,T_2-g]$ and $Q_{eff}[\theta_0,T_1,T_2-g](\theta_0)$ for K–Ne, K–Ar, K–CH_3I.

BRO–65 P. R. Brooks, "Thermal-Collision Cross Sections for K–Ar and K–Ne," *Bull. Am. Phys. Soc.*, **10**, 382 (1965).

BRO–66 P. R. Brooks and E. M. Jones, "Reactive Scattering of K Atoms from Oriented CH_3I Molecules," *J. Chem. Phys.*, **45**, 3449 (1966).

BUC–65 U. Buck and H. Pauly, "Messungen des van der Waals-Potentials zwischen Alkaliatomen," *Z. Physik.*, **185**, 155 (1965). Na, K, Rb, and Cs each scattered by Na, K, Rb, and Cs. See SMI-66.

BUL–54 T. H. Bull and P. B. Moon, "A Mechanical Method for the Activation of Fast Reactions," *Discussions Faraday Soc.*, **17**, 54 (1954). CCl_4–Cs.

CAL–58 N. Calderon, Diplom Thesis, University of Bonn, 1958, as quoted in reference 2f. Ne–He, Ne–Ar, Ne–Kr. Ar–He, Ar–Ne. Kr–He, Kr–Ne.

CRO–65 R. J. Cross, Jr., "Rotational Effects in Molecular Scattering," Ph.D. Thesis, Harvard University (1965). K–Kr, K–Xe, K–HBr, K–CH_3I, KCl–Kr, KCl–Xe, KCl–HBr, KCl–CH_3I, CsCl–Kr, CsCl–Xe, CsCl–HBr, CsCl–CH_3I, CsBr–Xe, CsBr–CH_3I.

CRO–66 R. J. Cross, Jr., E. A. Gislason, and D. R. Herschbach, "Dipole–Dipole Scattering in Molecular Beams. Variation of Total Cross Section with Velocity and Rotational Overlap," *J. Chem. Phys.*, 45, 3582 (1966). Same systems as CRO–65.

DAT–61 S. Datz, D. R. Herschbach, and E. H. Taylor, "Collision Mechanics in Crossed Maxwellian Molecular Beams," *J. Chem. Phys.*, **35**, 1549 (1961). K–HBr.

DAT–62 S. Datz, G. E. Moore, and E. H. Taylor, "Molecular Beam Studies: Reaction of D with H_2," Oak Ridge National Laboratory Rept. 3320, 1962, p. 122.

DAT–63 S. Datz and E. H. Taylor, "Atom–Molecule Reaction of Hydrogen Studied by Molecular Beams," *J. Chem. Phys.*, **39**, 1896 (1963). D–H_2.

DAT–64 S. Datz and R. E. Minturn, "Study of the Reaction of Cs with Br_2 in Crossed Molecular Beams," *J. Chem. Phys.*, **41**, 1153 (1964).

DAT–65 S. Datz and R. E. Minturn, "Molecular-Beam Studies of the Alkali–Halogen Reactions: The Spectator Stripping Model," *4th International Conference on the Physics of Electronic and Atomic Collisions*, abstracts of papers, Science Bookcrafters, New York, 1965, p. 177. Cs–Br_2, K–I_2, K–Br_2, Rb–IBr.

DOR–38 R. Dorrestein and J. A. Smit, "Determination of the Cross Section of Metastable Helium Atoms with the Aid of their Photoelectric Effect," *Proc. Acad. Sci. Amsterdam*, **41**, 725 (1938). He*–He.

DÜR–64 R. Düren and H. Pauly, "Numerische Berechnungen zum Resonanzverhalten der Streuquerschnitte bei atomaren Stössen. II," *Z. Physik.*, **177**, 146 (1964). Li–Kr.

DÜR–65a R. Düren, "Untersuchungen zur Bestimmung des Wechselwirkungspotentials zwischen Edelgasatomen". Diplom Thesis, University of Bonn, 1965. He–Ne, He–Ar, He–Kr, He–Xe.

DÜR–65b R. Düren, R. Helbing, and H. Pauly, "Messungen der van der Waals–Wechselwirkung zwischen Edelgasatomen," *Z. Physik.*, **188**, 468 (1965). He–Ne, He–Ar, He–Kr, He–Xe.

DÜR–65c R. Düren, R. Feltgen, W. Gaide, R. Helbing, and H. Pauly, "Messungen der Geschwindigkeitsabhängigkeit des totalen Streuquerschnittes für die Streuung von He, H_2 und D_2—Molekularstrahlen an Edelgasen". *Phys. Letters*, **18**, 282 (1965). He–Ne, He–Ar, He–Kr, He–Xe, H_2–Kr, D_2–Kr.

ELL–31 A. Ellett and R. M. Zabel, "Measuring the Intensity of Molecular Beams," *Phys. Rev.*, **37**, 1112 (1931). H_2–H_2, H_2–air.

EST–47 I. Estermann, S. N. Foner, and O. Stern, "The Mean Free Paths of Cesium Atoms in Helium, Nitrogen, and Cesium Vapor," *Phys. Rev.*, **71**, 250 (1947).

FEL–66 R. Feltgen, W. Gaide, R. Helbing, and H. Pauly, "Weitere Messungen der Geschwindigkeitsabhängigkeit des totalen Streuquerschnittes für die Streuung von H_2– und D_2–Molekularstrahlen an Edelgasen," *Phys. Letters*, **20**, 501 (1966). H_2–Ar, H_2–Kr, H_2–Xe, D_2–Ar, D_2–Kr, D_2–Xe.

FIT–64 W. L. Fite and R. T. Brackmann, "Scattering of Hydrogen Atoms by Deuterium Molecules," *Atomic Collision Processes*, M. R. C. McDowell, Ed., North-Holland, Amsterdam, 1964, p. 955.

FIT–65 W. L. Fite and R. T. Brackmann, "Scattering of H Atoms by D_2 Molecules," *J. Chem. Phys.*, **42**, 4057 (1965).

FLO–64 H. Florin, Diplom Thesis, University of Bonn, 1964, as quoted in reference 2f and HOL–66. Li–Xe, K–Ar, K–Xe, Na–Xe.

FRA–33 R. G. J. Fraser and L. F. Broadway, "Experiments on Molecular Scattering in Gases. I. The Method of Crossed Molecular Beams," *Proc. Roy. Soc.* (*London*), **A141**, 626 (1933). Na and K vs. *trans*-CHI=CHI.

GEN–64 R. Gengenbach, Diplom Thesis, University of Bonn, 1964, as quoted in reference 2f. TlF in (1,0) and (1,1) rotational states vs. Ar and Xe.

GER–59 E. Gersing, R. Jaeckel, and H. Pauly, "Die Winkelverteilung bei Streuversuchen an Molekularstrahlen," *Z. Naturforsch.*, **14a**, 1083 (1959). K–Hg.

GER–63 E. Gersing, E. Hundhausen, and H. Pauly, "Differentielle Streuquerschnitte bei der Wechselwirkung neutraler Moleküle," *Z. Physik.*, **171**, 349 (1963). K–Hg, K–pyrene ($C_{16}H_{10}$), K–anthracene ($C_{14}H_{10}$), K–$HgCl_2$, K–HgI_2, K–SnI_4.

GIE–59 H. Gienapp, "Der Gesamtwirkungsquerschnitt des Stossprozesses zwischen Kaliumatomen und Chlormolekülen," *Z. Naturforsch.*, **14a**, 1084 (1959). K–Cl_2.

GIE–61 H. Gienapp, "Die Wirkungsquerschnitte der Stossprozesse Kalium-Chlor und Kalium-Jodwasserstoff," *Z. Elektrochem.*, **65**, 417 (1961). K–Cl_2, K–HI.

GIS–67 E. A. Gislason and G. H. Kwei, "Quenching of Glory Undulations in Scattering of Na Atoms from Polyhalide Molecules," *J. Chem. Phys.*, **46**, 2838 (1967). Na scattered by CBr_4, Br_2, $SnCl_4$, CCl_4, CH_3I, SF_6, and $SiCl_4$.

GRE–58 E. F. Greene, R. W. Roberts, and J. Ross, "A Study of Chemical Kinetics with Monoenergetic Molecular Beams," *134th Meeting, American Chemical Society*, abstracts of papers, 1958, p. 52S. K–Br_2.

GRE–60 E. F. Greene, R. W. Roberts, and J. Ross, "Variation of a Chemical Reaction Cross Section with Energy," *J. Chem. Phys.*, **32**, 940 (1960). K–HBr.

GRE–66 E. F. Greene, A. L. Moursund, and J. Ross, "Elastic Scattering in Chemically Reactive Systems," in *Molecular Beams* (*Advances in Chemical Physics*, Vol. 10), J. Ross, Ed., Interscience, New York, 1966, p. 135. Review. New data for K–$C(CH_3)_4$ and K–CBr_4.

GRO–63 P. J. Groblicki, "Atomic Beam Scattering Studies on the Li-Hg System: Velocity Dependence of Total and Differential Cross Sections as a Route to the Interaction Potential," Ph.D. Thesis, University of Michigan, 1963. Also University Microfilms Order No. 64-8167. ^{6,7}Li–Hg.

GRO–65a P. J. Groblicki and R. B. Bernstein, "Atomic-Beam Scattering Studies on the Li-Hg System: Quantum Effects and Velocity Dependence of the Cross Sections," *J. Chem. Phys.*, **42**, 2295 (1965). ^{6,7}Li–Hg.

GRO–65b A. E. Grosser, A. R. Blythe, and R. B. Bernstein, "Internal Energy of Reaction Products by Velocity Analysis. I. Scattered KBr* from the Crossed Molecular Beam Reaction K + HBr," *J. Chem. Phys.*, **42**, 1268 (1965).

GRO–65c A. E. Grosser and R. B. Bernstein, "Internal Energy of Reaction Products by Velocity Analysis. II. Scattered KBr* from the Crossed Molecular Beam Reaction K + Br_2," *J. Chem. Phys.*, **43**, 1140 (1965).

GRO–65d A. E. Grosser and R. B. Bernstein, "Velocity Analysis of Reactive Scattering in Crossed Molecular Beams: Internal Energy and Center-of-Mass Angular Distribution of Products," *4th International Conference on the Physics of Electronic and Atomic Collisions*, abstract of papers, Science Bookcrafters, New York, 1965, p. 180. K–HBr, K–Br_2.

HAR–62a H. Harrison and W. L. Fite, "Chemical Reactions Using Modulated Free Radical Beams," Final Report, contract AF 49(638)-301, 1962. H–D_2, H–H_2, H_2–H_2. Also summary of other preliminary studies.

HAR–62b H. Harrison, "Total Collision Cross Sections for Scattering of Thermal Beams of Hydrogen, Hydrogen Atoms, and Helium by Hydrogen and Helium," *J. Chem. Phys.*, **37**, 1164 (1962).

HAS–58 J. B. Hasted and P. Mahadevan, "Reactions of Metastable Atoms and Resonance Photons," *Proc. Roy. Soc.* (*London*), **A249**, 42 (1958). He(2^3S) and Ne($^3P_{2,0}$) each scattered by He, Ne, and Ar.

HAS–59 J. B. Hasted, "Collisions of Metastable Atoms," *J. Appl. Phys.*, **30**, 22 (1959). He(2^3S) and Ne(^{3}P) each scattered by He, Ne, and Ar.

HEL–61 R. Helbing, "Untersuchungen zur Kleinwinkelstreuung bei Streuversuchen an Molekularstrahlen," Diplom Thesis, University of Bonn, 1961. K–He, K–Ar, K–Xe, K–N_2, K–Br_2, K–$CHBr_3$, K–CCl_4, K–C_2H_5I, K–$(CH_2Br)_2$, Cs–He, Cs–Ar, Cs–N_2, Cs–$(CH_3)_2CO$.

HEL–64 R. Helbing and H. Pauly, "Differentielle Streuquerschnitte bei der Wechselwirkung neutraler Moleküle. Messungen der Kleinwinkel-

streuung," *Z. Physik.*, **179**, 16 (1964). K–He, K–Ar, K–Xe, K–N_2, K–Br_2, K–HgI_2, K–$CHBr_3$, K–CCl_4, K–SnI_4, K–C_2H_5I, K–$(CH_2Br)_2$, K–$C_{16}H_{10}$, Cs–He, Cs–Ar, Cs–N_2, Cs–$(CH_3)_2CO$, CsCl–$SbCl_3$.

HEL–66 R. Helbing, "Messungen und quantenmechanische Berechnungen der Energieabhängigkeit des totalen Stossquerschnittes für die Streuung von H_2– und D_2–Molekularstrahlen an Edelgasen," Dissertation, University of Bonn, 1966. H_2 and D_2 each scattered by Ne, Ar, Kr, and Xe.

HER–60 D. R. Herschbach, "Analysis of Reactive Scattering in Crossed Molecular Beams," *J. Chem. Phys.*, **33**, 1870 (1960). K–HBr.

HER–61 D. R. Herschbach, G. H. Kwei, and J. A. Norris, "Reactive Scattering in Crossed Molecular Beams. K Atoms with CH_3I and C_2H_5I," *J. Chem. Phys.*, **34**, 1842 (1961).

HER–62 D. R. Herschbach, "Reactive Collisions in Crossed Molecular Beams," *Discussions Faraday Soc.*, **33**, 149 (1962). K, Rb, and Cs each scattered by CH_3I and other alkyl iodides.

HER–64 R. R. Herm, R. Gordon, and D. R. Herschbach, "Magnetic Analysis of Elastic and Reactive Scattering in Crossed Molecular Beams of K Atoms with CH_3I, Br_2, and ICl," *J. Chem. Phys.*, **41**, 2218 (1964). K–CH_3I, K–Br_2, K–ICl, K–cyclohexane.

HER–65 R. R. Herm and D. R. Herschbach, "Reactive Scattering in Molecular Beams: Electric-Deflection Analysis of Rotational Excitation of Products," *J. Chem. Phys.*, **43**, 2139 (1965). Cs–HBr, K–Br_2, K–cyclohexane.

HES–65a M. M. Hessel and P. Kusch, "Deviation from the $1/r^6$ Potential in Scattering of a Polar Molecule by Non-Polar Gases," *J. Chem. Phys.*, **43**, 305 (1965). K–N_2, KCl–Ar, KCl–N_2.

HES–65b M. M. Hessel, "The Velocity Dependence of the Total Collision Cross Sections in the Scattering of a Thermal Energy Polar Molecule by Nonpolar Gases," Ph.D. Thesis, Columbia University, 1965. K–Ar, K–N_2, KCl–Ar, KCl–N_2.

HOL–66 M. Hollstein, "Messungen zur Geschwindigkeitsabhängigkeit des totalen Streuquerschnittes beim Stoss von Alkaliatomen mit Energien von 6 eV– 1000 eV gegen thermische Edelgase," Dissertation, University of Bonn, 1966. Na–Xe, K–Ar, K–Kr, K–Xe, Cs–Ar, Cs–Kr, Cs–Xe.

HOL–67 M. Hollstein and H. Pauly, "Messungen der Geschwindigkeitsabhängigkeit totaler Streuquerschnitte für Atom–Atom Stösse im Energiebereich zwischen 6 und 1000 eV, "*Z. Physik.*, **201**, 10 (1967). K and Cs each scattered by Ar, Kr, and Xe. Also Na–Xe.

HOS–59 H. U. Hostettler and R. B. Bernstein, "Comparison of Exp–6, L.-J. (12,6), and Sutherland Potential Functions Applied to the Calculation of Differential Scattering Cross Sections," *J. Chem. Phys.*, **31**, 1422 (1959). H_2–Hg.

HOS–60 H. U. Hostettler and R. B. Bernstein, "Observation of Quantum Effects in the Scattering of a Monoenergetic Li Beam by a Crossed Hg Beam," *Phys. Rev. Letters*, **5**, 318 (1960). Li–Hg, K–Hg.

HUN–64 E. Hundhausen and H. Pauly, "Untersuchungen des Wechselwirkungspotentials von van der Waals–Molekülen mit Hilfe der Regenbogenstreuung," *Z. Naturforsch.*, **19a**, 810 (1964). Na, K, and Rb each scattered by Hg.

HUN–65a E. Hundhausen and H. Pauly, "Der Regenbogeneffekt und Interferenzerscheinungen bei molekularen Stössen," *Z. Physik.*, **187**, 305 (1965). Na–Xe, Na–Hg, Na–HBr, Na–CH_3I, Na–$(CH_2Br)_2$, K–Xe, K–Hg, K–HBr, K–CH_3I, K–SnI_4, Rb–Hg.

HUN–65b E. Hundhausen and H. Pauly, "Die Erzeugung intensiver Molekularstrahlen mit Hilfe von Laval-Düsen und ihre Anwendung auf Streuexperimente," *Z. Naturforsch.*, **20**a, 625 (1965). Na–Hg.

JAW–52 W. Jawtusch, "Streuversuche mit gekreuzten Molekularstrahlen," *Z. Physik.*, **133**, 541 (1952). K–Hg, K–Apiezon oil F, K–Silicone oil DC 703.

JAW–55 W. Jawtusch, G. Schuster and R. Jaeckel, "Grosse Wirkungsquerschnitte bei Stössen zwischen neutralen Atomen," *Z. Physik.*, **141**, 146 (1955). K–Zn, K–Cd, K–Hg, K–S_x, K–Apiezon oil F, K–Silicone oil DC 703.

KIN–61 J. L. Kinsey, G. H. Kwei, and D. R. Herschbach, "Reactive Scattering in Crossed Molecular Beams. Rubidium Atoms with Methyl Iodide," *Bull. Am. Phys. Soc.*, **6**, 152 (1961).

KNA–29 F. Knauer and O. Stern, "Intensitätsmessungen an Molekularstrahlen von Gasen," *Z. Physik.*, **53**, 766 (1929). H_2–H_2.

KNA–33a F. Knauer, "Über die Streuung von Molekularstrahlen in Gasen. I," *Z. Physik.*, **80**, 80 (1933). He–He, He–Hg, H_2–H_2, H_2–Hg, O_2–O_2, H_2O–H_2O.

KNA–33b F. Knauer, "Der Nachweis der Wellennatur von Molekularstrahlen bei der Streuung in Quecksilberdampf," *Naturwiss.*, **21**, 366 (1933). He–Hg, H_2–Hg.

KNA–34 F. Knauer, "Uber die Streuung von Molekularstrahlen in Gasen. II," *Z. Physik.*, **90**, 559 (1934). He–Hg, H_2–Hg.

KOD–44 K. Kodera, "Chemical Studies by Means of Molecular Rays. IX. Direct Determination of the Effective Collision Radii between Material Corpuscles: Potassium versus Hydrogen, Nitrogen, Oxygen, and Argon," *J. Chem. Soc.* (*Japan*), **65**, 645 (1944).

KOD–45 K. Kodera, "Chemical Studies by Means of Molecular Rays. X," *J. Chem. Soc.* (*Japan*), **66**, 52 (1945). K–H_2, K–N_2, K–O_2, K–Ar.

KOD–58 K. Kodera and T. Tamura, "The Scattering of Beams of Alkali Atoms in Various Gases. I. Sodium and Argon," *Bull. Chem. Soc.* (*Japan*), **31**, 206 (1958).

KOD–61 K. Kodera and T. Tamura, "The Scattering of Beams of Alkali Atoms in Various Gases. II. Sodium Atom Beam in Non-Reactive and Reactive Gases." *Bull. Chem. Soc.* (*Japan*), **34**, 566 (1961). Na–He, Na–Ne, Na–Ar, Na–H_2, Na–N_2, Na–CO, Na–NO, Na–O_2, Na–CO_2.

KRA–62 K. H. Kramer, "Streuung von TlF-Molekülen in ausgewählten Rotationszuständen an Edelgasen," Dissertation, University of Bonn, 1962.

TlF in selected rotational states scattered by He, Ne, Ar, Kr. Also K–Ar. Unselected TlF scattered by He, Ar, Kr.

KWE–60 G. H. Kwei, J. A. Norris, and D. R. Herschbach, "Reactive Scattering in Crossed Molecular Beams," *Bull. Am. Phys. Soc.*, **5**, 503 (1960). K–CH_3I, K–C_2H_5I.

KWE–61 G. H. Kwei, J. A. Norris, J. L. Kinsey, and D. R. Herschbach, "Reactive Scattering in Crossed Molecular Beams," *2nd International Conference on the Physics of Electronic and Atomic Collisions*, abstract of papers, Benjamin, New York, 1961, p. 98. K, Rb, and Cs each scattered by CH_3I.

KYD–62 P. H. Kydd, "Total Scattering Cross Sections for H_2O and NH_3," *J. Chem. Phys.*, **37**, 931 (1962). H_2O–H_2O, NH_3–H_2O.

LAN–66a R. W. Landorf and C. R. Mueller, "Total Collision Cross Sections of Argon with Light Gases by Crossed Molecular Beams," *Phys. Letters*, **19**, 658 (1966). He–Ar, H_2–Ar, Ar–He, Ar–Ne, Ar–H_2, Ar–N_2.

LAN–66b R. W. Landorf and C. R. Mueller, "Crossed Molecular Beam Measurements of the Total Cross Sections of Ar–N_2, Ar–Ne, Ar–He, and Ar–H_2 at Thermal Energies," *J. Chem. Phys.*, **45**, 240 (1966). Also He–Ar, H_2–Ar.

LUL–64 K. Lulla, H. H. Brown, and B. Bederson, "Total Cross Sections for the Scattering of Potassium by He, Ne, Ar, Xe, and H_2 in the Thermal Energy Range," *Phys. Rev.*, **136**, A1233 (1964).

MAI–33 W. H. Mais and I. I. Rabi, "Direct Measurement of the Scattering of Potassium Atoms by Other Atoms and Molecules," *Phys. Rev.*, **43**, 378 (1933). K–H_2, K–He, K–N_2, K–CO_2.

MAI–34 W. H. Mais, "The Scattering of a Beam of Potassium Atoms in Various Gases," *Phys. Rev.*, **45**, 773 (1934). K–H_2, K–He, K–Ne, K–N_2, K–Ar, K–CO_2.

MAR–52a H. Martin and H. J. Meyer, "Anregung chemischer Elementarprozesse durch Molekularstrahlen," *Naturwiss.*, **39**, 85 (1952). I_2 and $CF_2ClCFCl_2$ each scattered by ClO_2.

MAR–52b H. Martin and H. J. Meyer, "Anregung chemischer Elementarprozesse durch Molekularstrahlen," *Z. Elektrochem.*, **56**, 740 (1952). ClO_2–$CF_2ClCFCl_2$, I_2–ClO_2, I–$COCl_2$.

MAR–56 H. Martin and H. Diskowski, "Der Vorgang $H + Cl_2 \rightarrow HCl + Cl$ al Molekularstrahlreaktion," *Z. Elektrochem.*, **60**, 964 (1956).

MAS–57 E. A. Mason, "Scattering of Low Velocity Molecular Beams in Gases," *J. Chem. Phys.*, **26**, 667 (1957). H_2–Hg.

MIN–58 A. Minten and O. Osberghaus, "Die Erzeugung von intensiven Molekularstrahlen nicht kondensierender Gase. Wirkungsquerschnitte für den Stoss H_2–H_2 und H_2–N_2," *Z. Physik.*, **150**, 74 (1958).

MIN–62 R. E. Minturn, S. Datz, and E. H. Taylor, "Molecular Beam Studies: Reactions of Alkali Metals," Oak Ridge National Laboratory Rept. 3320, p. 124 (1962). K–HBr, Rb–HBr.

MIN–66 R. E. Minturn, S. Datz, and R. L. Becker, "Alkali-Atom–Halogen-Molecule Reactions in Molecular Beams; the Spectator Stripping

Model," *J. Chem. Phys.*, **44**, 1149 (1966). K–Xe, K–Br_2, K–I_2, Cs–Br_2, Rb–IBr.

MOO–67 G. E. Moore, S. Datz, and F. van der Valk, "Total Scattering Cross Sections for Hydrogen and Deuterium by Helium," *J. Chem. Phys.*, **46**, 2012 (1967). H_2–^{3}He, H_2–^{4}He, D_2–^{3}He, ^{4}He–^{4}He.

MOR–62a F. A. Morse, "Velocity Dependence of the Differential Cross Sections, and Potential Well Depths from Atomic Beam Scattering Measurements: K–Hg and Cs–Hg Systems," Ph.D. Thesis, University of Michigan, 1962. Also University Microfilms Order No. 63–412.

MOR–62b F. A. Morse, R. B. Bernstein, and H. U. Hostettler, "Evaluation of the Intermolecular Potential Well Depth from Observations of Rainbow Scattering: Cs–Hg and K–Hg," *J. Chem. Phys.*, **36**, 1947 (1962).

MOR–62c F. A. Morse and R. B. Bernstein, "Velocity Dependence of the Differential Cross Sections for the Scattering of Atomic Beams of K and Cs by Hg," *J. Chem. Phys.*, **37**, 2019 (1962).

MOU–64 A. L. Moursund, "The Elastic and Reactive Scattering of K by HCl, CH_3Br, and HI in Crossed Molecular Beams," Ph.D. Thesis, Brown University, 1964. Also University Microfilms Order No. 65–13,673.

MOU–66 M. C. Moulton and D. R. Hershbach, "Chemiluminescence in Molecular Beams. Electronic Excitation of Alkali Atoms in Exchange Reactions of Vibrationally Excited Alkali Halides," *J. Chem. Phys.*, **44**, 3010 (1966). KBr*, formed by reactive scattering of K and Br_2, inelastically scattered by Na.

MUE–63 C. R. Mueller and R. P. Marchi, "WKB Analysis of Molecular Beam Scattering and the Lennard-Jones Potential," *J. Chem. Phys.*, **38**, 745 (1963). He–Hg, H_2–Hg, K–Hg.

NEU–66 W. Neumann and H. Pauly, "The Velocity Dependence of Atom–Atom Total Scattering Cross Sections in the 7–500 eV Energy Range," *Phys. Letters*, **22**, 291 (1966). Na–Hg, K–Hg, Cs–Hg.

NIS–36 E. Nishibori, "Chemical Studies by Means of Molecular Beams. III. Iodine Molecule and Sodium Atom," *J. Chem. Soc. (Japan)*, **57**, 1291 (1936).

NIS–37 E. Nishibori, "V. Direct Determination of the Effective Radius of Collision of the Vibrationally Excited Iodine Molecule with the Mercury Atom," *J. Chem. Soc. (Japan)*, **58**, 14 (1937). I_2–Hg, I_2^*–Hg.

NUT–61 C. W. Nutt and A. J. Biddlestone, "A Molecular Beam Reactor for Examining the Rate, and Primary Products, of Reactive Bimolecular Collisions," *Nature*, **191**, 798 (1961). O*–NO_2.

PAU–57 H. Pauly, "Weitere Wirkungsquerschnitte bei Zusammenstössen zwischen neutralen Atomen," *Z. Angew. Phys.*, **9**, 600 (1957). Na–Hg, Na–N_2, K–Hg, K–N_2, Rb–Hg, Rb–N_2, Cs–Hg, Cs–N_2.

PAU–59 H. Pauly, "Die Kleinwinkelstreuung bei Stössen zwischen neutralen Atomen," *Z. Physik.*, **157**, 54 (1959). K–Hg, Na–Hg.

PAU–60a H. Pauly, "Recent Scattering Experiments at Bonn University," *Proc. Atomic and Molecular Beams Conference*, University of Denver,

Colorado, June, 1960, p. 49. K–Hg (with Gersing and Jaeckel). K–He, K–Ar, K–N_2 (with Helbing). Ga in (1,0) and (1,1) Zeeman states vs. Xe (Berkling, Schlier, and Toschek).

PAU–60b H. Pauly, "Streuversuche an Molekularstrahlen bei verschiedenen Strahlgeschwindigkeiten," *Z. Naturforsch.*, **15a**, 277 (1960). K–N_2.

RIC–64 H. L. Richards and E. E. Muschlitz, Jr., "Angular Dependence of the Scattering of Metastable He Atoms in He and Ne," *J. Chem. Phys.*, **41**, 559 (1964). He(2^1S) and He(2^3S) each scattered by He and Ne.

ROB–59 R. W. Roberts, "The Scattering of a Potassium Atomic Beam by a Crossed Beam of Bromine Molecules," Ph.D. Thesis, Brown University, 1959. Also University Microfilms Order No. 62–5758.

ROL–62 P. K. Rol and E. W. Rothe, "Velocity Dependence of the Total Cross Section for Atom–Atom Scattering at Thermal Energies," *Phys. Rev. Letters*, **9**, 494 (1962). ^{7}Li–He, ^{7}Li–Ne, ^{7}Li–Ar, ^{7}Li–Kr, ^{7}Li–Xe, ^{6}Li–Xe.

ROS–35 S. Rosin and I. I. Rabi, "Effective Collision Cross Sections of the Alkali Atoms in Various Gases," *Phys. Rev.*, **48**, 373 (1935). Li, Na, K, Rb, Cs each scattered by H_2, D_2, He, Ne, Ar.

ROS–39 P. Rosenberg, "Collision Cross-Sections of K Atoms and K_2 Molecules in Gases," *Phys. Rev.*, **55**, 1267 (1939). K and K_2 each scattered by H_2, D_2, He, Ar, N_2.

ROS–40 P. Rosenberg, "Collision Cross Sections of Li Atoms and Li_2 Molecules Scattered in He and Ar," *Phys. Rev.*, **57**, 561 (1940).

ROT–59a E. W. Rothe and R. B. Bernstein, "Total Collision Cross Sections for the Interaction of Atomic Beams of Alkali Metals with Gases," *J. Chem. Phys.*, **31**, 1619 (1959). $Q_{app}[T_1,T_2 - g]$ for K vs. 77 atoms and molecules, and Cs vs. 16 atoms and molecules. C_6 determined in each case.

ROT–59b E. W. Rothe, "Total Collision Cross-Sections for the Interaction of Molecular Beams with Gases," Ph.D. Thesis, University of Michigan, 1959. Also University Microfilms Order No. 59-4980. $Q_{app}[T_1,T_2 - g]$ for K vs. 77 atoms and molecules, Cs vs. 16 atoms and molecules, and CsCl vs. 17 atoms and molecules.

ROT–61a E. W. Rothe and J. B. Hasted, as quoted by E. E. Muschlitz, Jr., in *Molecular Beams*, (*Advances in Chemical Physics*, Vol. 10), J. Ross, Ed., Interscience, New York, 1966, p. 180. He*–He, He*–Ne, He*–Ar, He*–Kr, Ne*–He, Ne*–Ne, Ne*–Ar.

ROT–61b E. W. Rothe, L. L. Marino, R. H. Neynaber, and S. M. Trujillo, "Scattering of Thermal Rare Gas Beams by Argon," *2nd International Conference on the Physics of Electronic and Atomic Collisions*, abstracts of papers, Benjamin, New York, 1961, p. 103. Ar–He, Ar–Ne, Ar–Ar, Ar–Kr, Ar–Xe.

ROT–62a E. W. Rothe, L. L. Marino, R. H. Neynaber, P. K. Rol, and S. M. Trujillo, "Scattering of Thermal Rare Gas Beams by Argon. Influence of the Long-Range Dispersion Forces," *Phys. Rev.*, **126**, 598 (1962). Ar–He, Ar–Ne, Ar–Ar, Ar–Kr, Ar–Xe, He–He.

ROT–62b E. W. Rothe, P. K. Rol, S. M. Trujillo, and R. H. Neynaber, "Velocity Dependence of the Total Cross Section for the Scattering of Li and K by Xe," *Phys. Rev.*, **128**, 659 (1962).

ROT–63a E. W. Rothe, R. H. Neynaber, B. W. Scott, S. M. Trujillo, and P. K. Rol, "Substantiation of a Method for Obtaining Interatomic Potential Energy Parameters," *J. Chem. Phys.*, **39**, 493 (1963). K–Kr.

ROT–63b E. W, Rothe, P. K. Rol, and R. B. Bernstein, "Interaction Potentials from the Velocity Dependence of Total Atom–Atom Scattering Cross Sections," *Phys. Rev.*, **130**, 2333 (1963). ^{7}Li–He, ^{7}Li–Ne, ^{7}Li–Ar, ^{7}Li–Kr, ^{7}Li–Xe, ^{6}Li–Xe.

ROT–64 E. W. Rothe, P. K. Rol, R. H. Neynaber, and S. M. Trujillo, "Interaction Potentials from the Velocity Dependence of Total Atom–Atom Scattering Cross Sections," *Atomic Collision Processes*, M. R. C. McDowell, Ed., North-Holland, Amsterdam, 1964, p. 927. ^{6}Li–He.

ROT–65a E. W. Rothe and R. H. Neynaber, "Measurements of Total Cross Sections for Rare Gas Collisions," *4th International Conference on the Physics of Electronic and Atomic Collisions*, abstracts of papers, Science Bookcrafters, New York, 1965, p. 162. He, Ar–He, Ar–Ne, Ar–Ar, Ar–Kr, Ar–Xe He–He. No numbers quoted.

ROT–65b E. W. Rothe and R. H. Neynaber, "Atomic-Beam Measurements of van der Waals Forces," *J. Chem. Phys.*, **42**, 3306 (1965). He*($^3S_1$)–He, He*–Ne, He*–Ar, He*–Kr; Ne*($^3P_2$)–He, Ne*–Ne, Ne*–Ar. Also corrected C_6 values for Li–Ar, Li–Kr, K–Kr.

ROT–65c E. W. Rothe, R. H. Neynaber, and S. M. Trujillo, "Velocity Dependence of the Total Cross Section for the Scattering of Metastable He($^3S_1$) by Helium, Argon, and Krypton," *J. Chem. Phys.*, **42**, 3310 (1965).

ROT–65d E. W. Rothe and R. H. Neynaber, "Measurements of Absolute Total Cross Sections for Rare-Gas Scattering," *J. Chem. Phys.*, **43**, 4177 (1965). He–He, Ar–Ar, Ar–Kr, Kr–Ar, Kr–Kr, K–Ar.

ROT–66a E. W. Rothe and R. H. Neynaber, "Absolute Measurement of Total Atom–Atom Scattering Cross Section," *Bull. Am. Phys. Soc.*, **11**, 70 (1966). K–Ar.

ROT–66b E. W. Rothe, private communication (1966). Results of ROT–63a and ROT–63b corrected.

ROT–67 E. W. Rothe and L. H. Veneklasen, "Glory Extrema in Total Cross Sections: Li–Hg," *J. Chem. Phys.*, **46**, 1209 (1967). ^{6}Li–Hg.

SAS–36a N. Sasaki and E. Nishibori, "Eine unmittelbare Bestimmung des Wirkungsradius der stark schwingenden Moleküle mit Hilfe der Molekularstrahlmethode," *Proc. Imp. Acad.* (*Tokyo*), **12**, 10 (1936). I_2–Hg, I_2^*–Hg.

SAS–36b N. Sasaki, E. Nishibori, and H. Uchida, "Chemical Studies by Means of Molecular Beams. Direct Determination of the Radii of Spheres of Action between Particles which can Combine with Each Other. I. Chlorine Molecule and Sodium Atom," *J. Chem. Soc.* (*Japan*), **57**, 1277 (1936).

SAS–36c N. Sasaki, E. Nishibori, G. Kondo, and K. Kodera. "II Sodium Atom and Oxygen Molecule," *J. Chem. Soc.* (*Japan*), **57**, 1284 (1936). Also Na–N_2.

SAS–41 N. Sasaki and K. Kodera, "On the Measurement of the Effective Collision Radii of the Potassium Atom in Various Gases," *Proc. Imp. Acad.* (*Tokyo*), **17**, 70 (1941). K–H_2, K–N_2, K–O_2, K–Ar.

SAS–49 N. Sasaki and K. Kodera, "On the Direct Measurement of the Effective Collision Radii of Potassium with Chlorine and Other Gases," *Mem. Coll. Sci. Univ. Kyoto*, **A25**, 83 (1949). K–Cl_2, K–H_2, K–N_2, K–O_2, K–Ar.

SCH–60 H. Schumacher, R. B. Bernstein, and E. W. Rothe, "Total Collision Cross Sections for the Interaction of Molecular Beams of CsCl with Gases. Influence of the Dipole–Dipole Force upon the Scattering," *J. Chem. Phys.*, **33**, 584 (1960). $Q_{app}[T_1,T_2 - g]$ for CsCl vs. He, Ne, Ar, Kr, Xe, H_2, D_2, CH_4, CF_4, $SiCl_4$, *trans*-$C_2H_2Cl_2$, SF_6. $Q_{app}[T_1,T_2 - g](T_2)$ for CsCl vs. Ar, NO, H_2S, NH_3, CH_4, CH_2F_2, CHF_3, CF_4, *cis*-$C_2H_2Cl_2$, *trans*-$C_2H_2Cl_2$. s in $V \sim -C/r^s$ for CsCl–Ar, CsCl–CH_4, CsCl–CF_4, CsCl–*trans*–$C_2H_2Cl_2$.

SCH–61 R. C. Schoonmaker, "Long Range Attractive Potentials from Molecular Beam Studies on the Systems K, N_2(g), and KCl, N_2(g)," *J. Phys. Chem.*, **65**, 892 (1961). See HES–65.

SHE–65 J. W. Sheldon and E. J. Manista, "Atomic Beam Determination of Cesium–Cesium Total Scattering Cross Section," Report NASA–TN–D–3160 (1965).

SMI–60 G. M. Smith and E. E. Muschlitz, Jr., "Scattering of Metastable Helium Atoms in Helium, Neon, and Argon," *J. Chem. Phys.*, **33**, 1819 (1960). He(2^3S) and He(2^1S) each scattered by He, Ne, Ar.

SMI–66 F. J. Smith, "Total Collision Cross Sections between Alkali Atoms at Thermal Energies." *Mol. Phys.*, **10**, 283 (1966). Comments on BUC–65.

STE–57 R. F. Stebbings, "Gaseous and Surface Reactions Involving Helium Metastable Atoms and Resonance Photons," *Proc. Roy. Soc.* (*London*), **A241**, 270 (1957). He(2^3S)–He, He*–Ne, He*–Ar, He–Kr.

STR–64 H. J. Strunck, "Messung der Geschwindigkeitsabhängigkeit des Streuquerschnitts von Kalium-Argon bei thermischen Energien," Diplom Thesis, University of Bonn, 1964. K–Ar.

TAY–55 E. H. Taylor and S. Datz, "Study of Chemical Reaction Mechanisms with Molecular Beams. The Reaction of K with HBr," *J. Chem. Phys.*, **23**, 1711 (1955).

TOE–62 J. P. Toennies, "Molecular Beam Measurements of Inelastic Cross Sections for the Excitation of the Rotational Transition TlF(2,0) → (3,0) in Collisions with Atoms," *Discussions Faraday Soc.*, **33**, 96 (1962). Cross sections for transitions to the (3,0) rotational state from the (2,0) and (1,0) states of TlF for collisions with He, Ne, Ar, Kr.

TOE–64 J. P. Toennies, "Molecular Beam Measurements of Inelastic Cross Sections for the Excitation of the Rotational Transition TlF(2,0) → (3,0) in Collisions with Atoms," *Atomic Collision Processes*, M. R. C. McDowell, Ed., North-Holland, Amsterdam, 1964, p. 1113. See TOE–62.

TOE–65 J. P. Toennies, "Molekularstrahlmessungen von Stossquerschnitten für Übergänge zwischen definierten Rotationszuständen," *Z. Physik.*, **182**, 257 (1965). Cross sections for transitions to the (J', M') rotational state from the (J,M) state of TlF for various (J,M) and $(J'M')$ in collisions with He, Ne, Ar, Kr, CH_4, SF_6, H_2, O_2, air, N_2O, CF_2Cl_2, NH_3, ND_3. Also $Q_{\text{eff}}[\theta_0, T_1, T_2 - g]$ measured for TlF vs. each scattering gas.

TOS–61 P. Toschek, "Streuung von Gallium-Atomen in definierten Zeeman-Zuständen an Argon und Helium," Dissertation, University of Bonn, 1961. Ga($^2P_{3/2,3/2}$) and Ga($^2P_{3/2,1/2}$) Zeeman states each scattered by He, Ar, Xe. Also unselected Ga–He, Ga–Ar, Ga–Xe, Na–He, Na–Ar, Na–N_2, Na–O_2, Na–CH_4.

TOS–62 P. Toschek, "Ein Bezugsquerschnitt für die Streuung neutraler Moleküle," *Z. Naturforsch.*, **17a**, 356 (1962). K–Ar.

TOS–65 P. Toschek, "Anomale Anisotropie der zwischenmolekularen Kraft," *Z. Physik.*, **187**, 52 (1965). Ga($^2P_{3/2,3/2}$) and Ga($^2P_{3/2,1/2}$) Zeeman states each scattered by Ne. Results correlated with previous results obtained with He, Ar.

VAN–65 F. van der Valk, G. E. Moore, and S. Datz, "Elastic Scattering in Hydrogen–Helium Systems: Measurement of the 'Knock-On' Cross Section," *4th International Conference on the Physics of Electronic and Atomic Collisions*, abstracts of papers, Science Bookcrafters, New York, 1965, p. 164. Mixed gas (H_2 and D_2) scattered by He.

VON–65a F. von Busch, H. J. Strunck, and Ch. Schlier, "The Velocity Dependence of the Total Scattering Cross Section of K on Rare Gases," *4th International Conference on the Physics of Electronic and Atomic Collisions*, abstracts of papers, Science Bookcrafters, New York, 1965, p. 167. K–Ar, K–Kr, K–Xe.

VON–65b F. von Busch, H. J. Strunck, and Ch. Schlier, "The Velocity Dependence of the Total Scattering Cross Section of K on Rare Gases," *Phys. Letters*, **16**, 268 (1965). K–Ar, K–Kr, K–Xe.

VON–65c F. von Busch, "Eine Präzisionsmessung der Geschwindigkeitsabhängigkeit atomarer Streuquerschnitte im thermischen Energiebereich," Dissertation, University of Bonn, 1965. K–He, K–Ne, K–Ar, K–Kr, K–Xe.

VON–67 F. von Busch, H. J. Strunck, and Ch. Schlier, "Die Geschwindigkeitsabhängigkeit totaler Streuquerschnitte von Alkalien an Edelgasen." *Z. Physik.*, **199**, 518 (1967). Na–Ar, Na–Kr, Na–Xe, K–He, K–Ne, K–Ar, K–Kr, K–Xe, Rb–Kr, Cs–Kr.

WIL–62 K. R. Wilson and D. R. Herschbach, "Reactive Scattering in Crossed Molecular Beams," *Bull. Am. Phys. Soc.*, **7**, 497 (1962). Na–CH_3I.

WIL–64a C. H. Williams, "The Dissociation of a Cesium Fluoride Molecule by Impact with a Fast Argon Atom," Ph.D. Thesis, Brown University, 1964. Also University Microfilms Order No. 65-13,702.

WIL–64b K. R. Wilson, G. H. Kwei, J. A. Norris, R. R. Herm, J. H. Birely, and D. R. Herschbach, "Reactive Scattering in Molecular Beams: Evidence for a Stripping Mechanism in Reactions of Alkali Atoms with Halogens," *J. Chem. Phys.*, **41**, 1154 (1964). K, Rb, Cs each scattered

by Br_2, I_2, ICl, IBr. Data shown only for K–Br_2 and Cs–Br_2, Cs–ICl, Cs–IBr, Cs–I_2.

ZAB–33a R. M. Zabel, "Scattering of Molecular Rays in Gases," *Bull. Am. Phys. Soc.*, **8**, 10 (1933). He–Hg, H_2–Hg.

ZAB–33b R. M. Zabel, "Scattering of Molecular Rays in Gases," *Phys. Rev.*, **44**, 53 (1933). He–He and H_2–H_2.

ZAB–34 R. M. Zabel, "The Scattering of Hydrogen and Helium Beams in Mercury Vapor." *Phys. Rev.*, **46**, 411 (1934). He–Hg, H_2–Hg.

VII. SUMMARY AND APPRAISAL OF THE MORE RELIABLE DETERMINATIONS

The main purpose of this section is to summarize the best-determined potentials derived from low-energy molecular beam scattering measurements. For the great majority of systems studied (see Table II) only a single potential parameter, namely the C_6 constant, has been evaluated. As mentioned in Section IV-B-2, the agreement between the experimental and theoretical determination of the long-range C_6 coefficient is usually within the mutual limits of uncertainties, at least for the simpler systems for which the theoretical calculations are feasible. The recent, extensive review of van der Waals interactions by Dalgarno and Davison,[32] which includes a survey of most of the experimental results, makes it unnecessary to summarize or discuss in detail the C_6 determinations; of course, results are readily available through Table II and the annotated bibliography.

In this Section, attention will be restricted, therefore, to a consideration of those systems of ***atoms*** and/or ***diatomics*** for which sufficient data are available to evaluate a two- (or more) parameter potential.

In principle, it should be possible to take the experimenter's reported values of, say, ε and r_m, together with his assumed functional form for $V(r)$, and construct a summary table of "experimental potentials." Unfortunately, inconsistencies would arise because of the previously noted nonnegligible dependence of the derived "potential parameters" upon the assumed functionality of the potential, the different sensitivity of the various measurements to different parts of the potential, and the wide variation in the parameter values reported for the same system, depending upon the type of measurement used and the experimenter's preference for a particular method of data analysis and curve fitting of results.

Because of these ambiguities, it does not seem worthwhile merely to list the several "competing" sets of derived potential constants; these

are accessible in any case via Table II and the annotated bibliography. Rather, an attempt has been made to estimate (after considering all the factors involved) a "best" set of parameters characterizing the potential well. Obviously, these estimates will soon become obsolete, as further research results become available. Nevertheless, even at the present stage of imperfection, they may be of some value to the limited group of "consumers" of intermolecular potentials, for whom they are intended.

In Section VII-A certain semiempirical aids to the correlation of different kinds of scattering measurements are presented. The results, i.e., "best" potential parameters, are tabulated in Section VII-B. Finally, in Section VII-C, the regularities and systematics among the potentials are discussed.

A. Semiempirical Aids to Correlation of Data

In view of the difficulty in directly establishing the functional form of the potential from the scattering measurements, most authors have selected one or another of the conventional 3-parameter functionalities [such as the L.-J. (n,6), the Buckingham Exp (α,6), the Kihara (γ,12,6), or the Morse (a) equations, Eqs. (1)–(4)], fixed the free parameter (n,α,γ or a) somewhat arbitrarily, and determined ε and r_m values compatible with this choice. With any assumed value of the "third parameter,"[40] the resulting ε, r_m values are often very precisely evaluated; yet, since they depend markedly upon this choice, they *appear* superficially to be quite poorly determined. Differences in parameters derived for a given system by different investigators most often originate not in experimental discrepancies but rather in data analysis. For these reasons it seems desirable that, in the future, authors report their primary data (or abstracted "key" data) in addition to their "interpreted" results (in terms of potential constants).

For example, consider the interpretation of absolute total or integral cross sections Q in terms of the long-range C_6 constant via the well-documented Massey-Mohr (MM) or Schiff-Landau-Lifshitz (SLL) approximations [Eq. (18)]. At least three effects are known to weaken or destroy the relationship between Q and C_6. (*1*) The energies of the experiments may be too high, so that the measurements belong to the "transition" or "high-velocity" region,[33h] (i.e., $v \gtrsim \varepsilon r_m/\hbar$), where the Q's are mainly sensitive to the repulsive interactions. As an example, all the studies to date involving He scattering belong in this class. (*2*) The

energy range may include a region in which the collisions probe the attractive potential well at intermediate distances where higher-order terms such as the induced dipole–induced quadrupole ($C_8 r^{-8}$) term becomes significant compared to the $C_6 r^{-6}$ contribution. This effect[41] has apparently been seen experimentally[35c] for a number of systems involving alkalis and has been used to estimate the C_8 contribution. (*3*) For molecular scattering, concurrent inelastic processes such as rotational excitation,[42] and chemical reaction[43] may be very important, as for a large class of systems studied (e.g., K–HBr, etc.). The distinction between a "total" cross section and an integral *elastic* cross section must be maintained.

Thus, the (fully corrected, if possible) *observed* quantity is the desideratum for preservation. Also, since the connection between the long-range C_6 constant and the ε, r_m parameters is essentially an artifice of the assumed form of the potential [e.g., for a L.-J. (n,6) potential, $C_6 = [n/(n-6)]\varepsilon r_m^6$], it seems preferable not to impose this constraint on the properties of the well (i.e., ε, r_m and κ), but rather consider the derived C_6 as a "fourth" characterization parameter of the potential.

As has been discussed previously, thermal-energy beam scattering studies give most information about the attractive potential well, especially for weakly bound (van der Waals) molecules. In analogy with the interpretation of spectroscopic measurements for stable diatomic molecules, the well may be characterized by the three quantities ε (same as D_e), r_m (same as r_e), and the reduced curvature[40] κ (related to the force constant $k \equiv \kappa\varepsilon/r_m^2$). Thus one may best correlate results obtained for different assumed functional forms of the potential if the third parameter (e.g., n,α,γ,a) is replaced by the reduced curvature, via the equivalence relations:

$$\kappa = 6n = 6\alpha(\alpha - 7)/(\alpha - 6) = 72/(1-\gamma)^2 = 12a \tag{19}$$

As already seen in Figure 3, the four empirical potential functions with the same curvature κ are nearly identical in the important range $-\varepsilon \gtrsim V(r) \gtrsim -\varepsilon/2$ over which the glory-extrema and rainbow effects serve as probes of the potential well.[23,40] Thus, *if* such experiments have sufficient information content to yield a "greater-than-2"-parameter potential, the natural third parameter would appear to be κ.[40] In the absence of such detailed data, it has been customary to employ the simple 2-parameter L.-J. (12,6) potential ($\kappa = 72$); this is at least a reasonable starting point for a subsequent iterative procedure. Thus,

it is convenient to define a curvature ratio $c \equiv \kappa/72$, which is assumed to be unity unless the experimental results suggest or (better) establish a need for a third parameter in fitting the data. In these cases the appropriate value [from Eq. (19)] of the curvature ratio c will be listed as the third parameter in Table III of the following subsection, i.e., ε, r_m, and c.

In order to allow for future changes in the interpretation of glory-extrema and rainbow-effect data based on improved potential functions, and to preserve the observational aspects, the following minimal procedures are recommended.

The limiting (high energy) behavior of the glory-extrema velocities v_N may be represented by the limiting slope of a graph of N versus $1/v_N$. Thus an "observed" quantity I is obtained

$$I \equiv \lim_{1/v_N \to 0} [dN/d(1/v_N)] \qquad (\text{cm sec}^{-1}) \tag{20}$$

(Alternatively, I is the intercept of a plot[33g,36e] of $(N\text{-}3/8)v_N$ versus $1/E_N$.)

Similarly, the limiting (high energy) behavior of the rainbow angles θ_r may be expressed in terms of the limiting slope of a curve of θ_r versus $1/E$; an "observed" quantity J is obtained:

$$J \equiv \lim_{1/E \to 0} [d\theta_r/d(1/E)] = \lim_{E \to \infty} [\theta_r E] \qquad (\text{erg}) \tag{21}$$

The quantities I and J are the natural "invariants" to be recorded, which then lead to potential parameters subject to the assumed functional form of $V(r)$, as follows. From the known[2f,33] high-energy behavior of the maximum phase shift, one evaluates εr_m from I by the relation

$$\varepsilon r_m/\hbar = G_i I \tag{22}$$

where G_i is a dimensionless "glory constant," which can be computed for any assumed potential function labeled i. For a L.-J. (12,6) potential, the "reference" potential, $i = 0$ and $G_0 = 3.7261$. Based on computations for several of the commonly used potentials, it is found[40] that G_i is primarily dependent upon the reduced curvature κ, and only secondarily a function of the particular potential functionality i. For the purpose of facile correlation among the common potentials, it is convenient to express this dependence in terms of the curvature ratio c. A "glory constant ratio" $G \equiv G_i/G_0$ is defined; thus $G = 1$ for the L.-J. (12,6) "reference" potential.

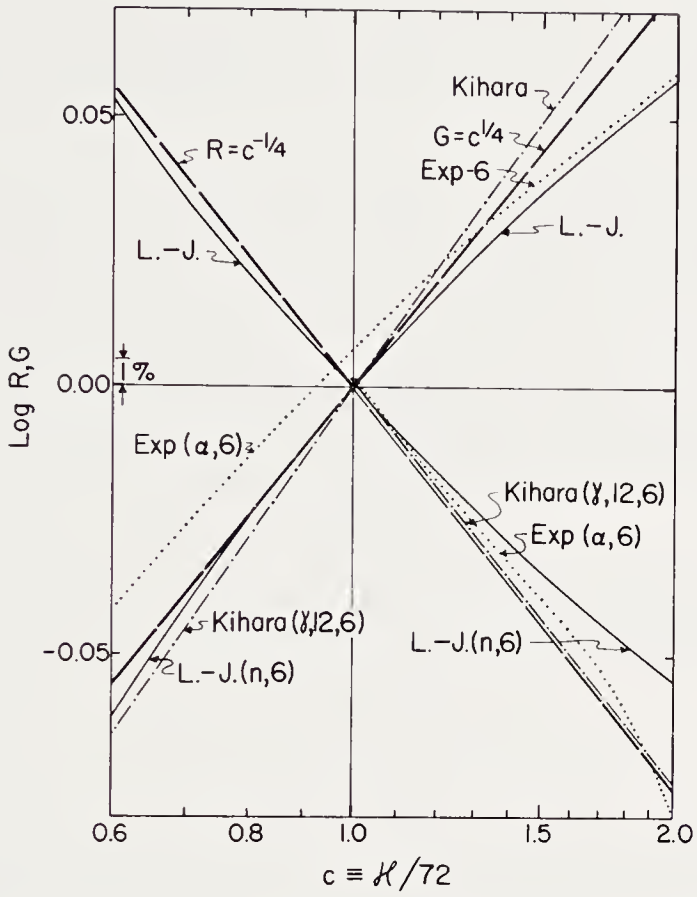

Fig. 26. Log–log correlation of rainbow (R) and glory extrema (G) "ratio-coefficients" with the curvature ratio $c \equiv \kappa/72$ for various potential functions. The straight lines represent the simple correlation equations $G = c^{\pm 1/4}$.

Figure 26 shows a (log–log) plot of $G(c)$ for various potentials (based on the calculations of reference 40), together with a line corresponding to a simple empirical relation

$$G = c^{1/4} \tag{23}$$

which appears to be adequate over the range shown. Thus the glory-extrema constant of Eq. (22) may be approximated by

$$G_i \cong 3.73c^{1/4} \tag{24}$$

so that

$$(\varepsilon r_m)_c = (\varepsilon r_m)_1 c^{1/4} \tag{25}$$

A similar treatment may be carried out for the rainbow effect. From the known[2f,23,44] high-energy behavior of the deflection function near its minimum one may evaluate ε from the measured J by the relation

$$\varepsilon = R_i J \tag{26}$$

where R_i is a dimensionless "rainbow constant," which can be considered known for any assumed potential. For the L.-J. (12,6) reference potential, $R_i \equiv R_0 = 0.49019$. A "rainbow constant ratio" may be defined, $R \equiv R_i/R_0$ which may then be correlated with curvature. (Note that there is a close correspondence between the curvature and the quantity $r_i V_i'$ employed in reference 23 for correlation purposes.) In Figure 26, $R(c)$ is plotted (based on the calculations of reference 44 and 17b), together with a line corresponding to an empirical equation

$$R = c^{-1/4} \tag{27}$$

which best expresses the overall correlation over the range shown. Thus the rainbow constant of Eq. (26) may be approximated by

$$R_i \cong 0.490 c^{-1/4} \tag{28}$$

so that

$$(\varepsilon)_c = (\varepsilon)_1 \, c^{-1/4} \tag{29}$$

For the frequent situations in which r_m is obtained as the ratio of the εr_m derived from glory extrema and the ε from rainbow data, one has

$$(r_m)_c = (r_m)_1 \, c^{1/2} \tag{30}$$

implying a rather strong sensitivity to curvature.

In the next subsection, use will be made of Eqs. (24, 25) and Eqs. (28–30) in the correlation of data from various sources.

B. "Best" Potential Parameters for Systems of Atoms and/or Diatomics

Based on the considerations of the preceding subsection, the available experimental results for ***atom–atom***, ***atom–diatomic*** systems have been analyzed, and Table III constructed of "best" parameters of the potential well. The references listed are the "prime" sources; however, the chosen parameters may differ slightly from those of the original authors. Due to the previously discussed experimental uncertainties, the parameters are rounded to 2 (occasionally 3) significant figures.

C. Regularities and Systematics

All of the discussion which follows makes use of the "best estimates" of potential well parameters from Table III of Section VII-B. Thus, the correlations must be regarded as provisional ones, subject to revision as improved determinations of the potentials become available. Even at this stage, however, it is of interest to examine the overall consistency of the results. Occasional striking deviations or irregularities are themselves suggestive and point to particular systems which may need further attention.

Figure 27*a* shows the potential wells for He–He, He–Ne, He–Ar, He–Kr, and He–Xe; Figure 27*b* displays the rccent semiempirical He–He potential of reference 45, which may be more reliable than the L.-J. (12,6) function plotted in the family of curves.

Figure 28 is a comparison of the potentials for Li–Ar, Li–Kr, and Li–Xe; Figures 29 and 30 are the analogs for the Na and K systems. Figure 31 compares the potential wells for the more tightly bound alkali–Hg systems. Figure 32 shows the wells for the alkali–Ar systems; Figures 33 and 34 are the analogs for Kr and Xe.

Results for several atom–diatomic systems are also available. Figure 35 shows the orientation-averaged potentials for H_2–rare gas systems. The potentials for D_2–Ar, D_2–Kr, and D_2–Xe are essentially identical to the H_2 systems. Figure 36 presents the wells for several K–HX systems (X = Cl, Br, and I). The analysis of the experimental scattering data is, of course, less reliable due to (*a*) the anisotropy of the potential and (*b*) the concomitant inelastic and reactive scattering; but the results are of sufficient interest to warrant inclusion in this summary.

It is of interest to investigate the relationship between the potential well characteristics and the nature of the interacting atoms. The most obvious approach is to explore the applicability of Badger's rule,[46a] which has had remarkable success in correlating force constants of stable diatomic molecules with their equilibrium internuclear separations as a function of the periodic row positions of the atoms.

Johnston[46b] has extended this relation to include the rare gas van der Waals diatoms. In the process he revised Badger's rule constants slightly, making use of the rare gas L.-J. (12,6) parameters from reference 11. In the notation of the present chapter, the Badger-Johnston equations may be expressed as follows:

$$\log_{10}(10^{14}\varepsilon c) = 1.143 + 2\log_{10}(r_m) - (r_m - a_{ij})/b_{ij} \qquad (31)$$

TABLE III

"Best Estimates" of Potential Well Characterization Parameters Derived from Molecular Beam Scattering Data. (Values in Parentheses Are Less Reliable).

System	$10^{-5}I$, cm sec^{-1}	$10^{14}J$, erg	c	$10^{14}\varepsilon$, erg	$10^{8}r_m$, cm	$10^{58}C_6$(erg cm^6)[a] Expt.	Theor.
1. Atom–atom[b]							
(*a*) He–He	—	—	(1)	(0.14)	(3.0)	(0.02_0)	0.014
(*b*) He–Ne	—	—	(1)	(0.23)	(3.0)	(0.03_7)	0.028
(*c*) He–Ar	0.3_1	—	1	0.35	3.4	0.12	0.087
(*d*) He–Kr	0.3_5	—	1	0.37	3.7	0.20	0.13
(*e*) He–Xe	0.4_0	—	1	0.39	4.0	0.34	0.17
(*f*) He–Hg	—	—	<1	(1.5)	($2._7$)	(0.1)	(0.1_4)
(*g*) Li–Ne	—	—	(1)	(0.1_9)	($4._6$)	(0.4)	0.40
(*h*) Li–Ar	1.1_0	—	2/3	0.9_2	4.2	$2._0$	1.6
			(1)	(0.9)	(4.7)	($2._0$)	
(*i*) Li–Kr	1.7_5	—	2/3	1.5	4.0	$2._6$	2.4
			(1)	(1.5)	(4.5)	($2._6$)	
(*j*) Li–Xe	2.7_0	—	2/3	2.4	4.1	$4._5$	3.8
			(1)	(2.3)	(4.6)	($4._1$)	
(*k*) Li–Hg	$16._7$	—	1	13.	4.9	($3_5.$)	($4._5$)
			(2/3)	(15.)	(4.0)	($1_2.$)	
(*l*) Na–Ar	1.1_5	—	(2/3)	($1._0$)	($4._1$)	(theor.)	1.8
(*m*) Na–Kr	1.8_0	2.6	2/3	1.4	5.0	(8.)	2.7
			2/3	(1.5)	(4.1)	(theor.)	
(*n*) Na–Xe	2.7_5	3.9	2/3	2.1	4.9	($1_2.$)	4.3
			2/3	(2.4)	(4.1)	(theor.)	
(*o*) Na–Hg	—	17.	2/3	9.2	4.1	($1_8.$)	($4._5$)
(*p*) K–Ne	—	—	(1)	(0.1_4)	($5._3$)	(theor.)	0.63
(*q*) K–Ar	1.1_5	—	2/3	1.0	4.3	3.0	2.6
			(1)	(1.1)	(4.1)	($1._0$)	
(*r*) K–Kr	1.9_5	2.5_5	2/3	1.4	5.1	(9.)	3.8
			(1)	(1.5)	(5.1)	$5._5$	
(*s*) K–Xe	3.0_0	3.4	2/3	1.8	5.8	7.4	6.0
			(1)	(2.5)	(4.8)	($6._1$)	
(*t*) K–Hg	$11._7$	$16._5$	3/4	8.7	4.8	($3_2.$)	($6._3$)
			(1)	(7.7)	(5.3)	($3_4.$)	
(*u*) Rb–Kr	2.0_0	—	(2/3)	($1._6$)	($4._4$)	(theor.)	4.1
(*v*) Rb–Hg	—	15.	2/3	8.1	4.4	($2_3.$)	($6._4$)
			(1)	(7.1)	(5.5)	($4_0.$)	
(*w*) Cs–Ar	—	—	(<1)	(0.8)	($5._8$)	$3._2$	3.3
(*x*) Cs–Kr	2.1_0	—	(2/3)	(1.7)	(4.4)	$4._8$	5.0
			(<1)	($1._4$)	($5._2$)	—	
(*y*) Cs–Xe	—	—	(<1)	$1._9$	$5._6$	$7._4$	7.9

(*continued*)

TABLE III (*continued*)

System	$10^{-5}I$, cm sec^{-1}	$10^{14}J$, erg	c	$10^{14}\varepsilon$, erg	$10^{8}r_m$, cm	$10^{58}C_6$(erg cm^6)[a] Expt.	Theor.
(*z*) Cs–Hg	—	17.	(3/4)	9.0	5.$_7$	(9$_0$.)	(7.$_5$)
			(1)	(8.$_0$)	(6.$_0$)	(7$_5$.)	
(*c'*)He(2^3S)–Ar	1.0$_0$	—	1	0.7$_7$	5.1	2.$_6$	(2.$_6$)
(*d'*)He(2^3S)–Kr	1.5$_5$	—	1	1.2	5.0	3.$_8$	(3.$_9$)
2. Atom–diatomic[c]							
(*A*) Ne–H_2(D_2)	—	—	(1)	(0.6)	(3.1)	(0.1$_1$)	(0.1$_1$)
(*B*) Ar–H_2(D_2)	0.84	—	1	1.0	3.3	(0.2$_7$)	(0.3$_1$)
(*C*) Kr–H_2(D_2)	1.0$_0$	—	1	1.1	3.7	(0.5$_1$)	(0.4$_2$)
(*D*) Xe–H_2(D_2)	1.2$_0$	—	1	1.2	3.9	(0.8$_4$)	(0.6$_1$)
(*E*) Hg–H_2	—	—	(1)	2.$_9$	3.$_2$	(0.$_6$)	(0.4$_6$)
(*F*) Na–HBr	—	5.8	2/3	3.1	(5.$_6$)	(4$_0$.)	(3.$_6$)
(*G*) K–HCl	—	6.2	(5/6)	3.2	3.$_3$	4.9	(3.$_6$)
(*H*) K–HBr(DBr)	—	7.6	(5/6)	3.9	4.$_4$	5.9	(4.$_8$)
(*I*) K–HI	—	9.1	(5/6)	4.7	3.$_9$	(3.$_3$)	(7.$_3$)

[a] All theoretical C_6 values from Dalgarno and Davison,[32] with the exception of the parenthesized values which have been calculated via the Slater-Kirkwood equation using experimental polarizabilities.

[b] *Atom–atom* systems:

(*a*) He–He. All experiments in "high-velocity" region, insensitive to shape of well. BEI–66a; MOO–67; ROT–65d. Results consistent, however, with parenthesized parameters based on transport and virial data. Cf. recent semi-empirical potential of Bruch and McGee[45]: $10^{14}\varepsilon$(erg) = 0.17$_3$, $10^{8}r_m$(cm) = 2.98, c = 1.11, with C_6 taken to be the theoretical value.

(*b*) He–Ne. Experiments in "high-v" region, as for (*a*). DÜR–65b,c; BEI–66a; HEL–66. Parameters doubtful.

(*c*) He–Ar. DÜR–65b,c; BEI–65, 66a,b; HEL–66. A lower (but less precise) value of C_6 is that of ROT–62a, quoted in reference 32.

(*d*) He–Kr. Same references as for (*c*). Significant discrepancy in ε between BEI–65, 66 and other references. Latter results preferred, since velocity selection employed.

(*e*) He–Xe. Same references and comments as for (*d*).

(*f*) He–Hg. KNA–34, analyzed by MUE–63. See also reference 25. Very early data; parameters doubtful.

(*g*) Li–Ne. Experiments in "high-v" region, as for (*b*). ROT–66b, 63b. Parameters doubtful. Additional high-v experiments on Li–He (not included in Table III); parameters very doubtful.

(*footnotes continued*)

(TABLE III footnotes *continued*)

(*h*) Li–Ar. ROT–66b, 63b. Parenthesized set of parameters are corrected results assuming $c = 1$. First (best) set are reanalyzed results using $c = 2/3$, thought better for alkali–rare gases (cf. VON–67, HUN–65a). As discussed in text, I (and J) values are independent of assumed c.

(*i*) Li–Kr. Same references and comments as for (*h*).

(*j*) Li–Xe. Same references and comments as for (*h*).

(*k*) Li–Hg. ROT–67. Parenthesized "experimental C_6" value obtained by calculation from indicated parameters. Second (parenthesized) set of parameters, with $c = 2/3$, for comparison with other alkali–Hg results. Resulting calculated C_6 in better agreement with estimated theoretical value (via S.-K. equation). Independent of c, however, $10^{34}\varepsilon^2 r_m(\text{erg}^2\text{cm}) = 8.8$ ($\pm 5\%$).

(*l*) Na–Ar. VON–67. Parenthesized values of ε, r_m estimated from the theoretical C_6 using the observed I and stated c.

(*m*) Na–Kr. BAR–66; VON–67. "Best" set ε, r_m were precisely determined, but the resulting C_6 calculated from the parameters seems high. Second (parenthesized) set estimated from the theoretical C_6, as for (*l*).

(*n*) Na–Xe. Same references and comments as for (*m*). However, cf. HUN–65a, FLO–64.

(*o*) Na–Hg. HUN–65a. As for (*k*)–(*n*), "experimental C_6" is calculated from the given parameters. As for Li–Hg (*k*), the C_6 is high relative to the S.-K. estimate.

(*p*) K–Ne. Experiments in "high-v" region, as for (*g*). VON–67. As for Na–Ar (*l*), parenthesized parameters estimated from the theoretical C_6. Additional high-v experiments on K–He (not included in Table III); parameters very doubtful.

(*q*) K–Ar. BEC–66a, VON–67. "Best" values from reanalysis with $c = 2/3$, using the theoretical C_6. However, the C_6 listed is experimental, from ROT–65d, in good agreement with FLO–64.

(*r*) K–Kr. BEC–66a, 62a; VON–67; ROT–66b, 63b. "Best" values from reanalysis with $c = 2/3$, making use of both I and J: for $c = 2/3$, $r_m = 6.53 \times 10^{27}\, I/J$. The preferred value of C_6, listed in second set, is experimental from ROT–66b, 63b (in fair agreement with a more direct measurement of 4.9 by comparison with K–Ar; ROT–59).

(*s*) K–Xe. HUN–65a, BEC–66a, VON–67, FLO–64. Same comments as for (*r*). The listed, preferred value of C_6 is experimental, from FLO–64 (in fair agreement with a measurement of 6.8 by comparison with K–Ar; ROT–59). That calculated from the "best" set of parameters is ca. fourfold greater than the theoretical C_6.

(*t*) K–Hg. BEC–66a,b, HUN–65a. Slight reanalysis of data. Discounting the high-velocity observations of NEU–66, parameters fairly reliable. Parenthesized "experimental C_6" values calculated from parameters. Discrepancy with more direct measurement by PAU–57 (corrected data) yielding 8_3. As for Li–Hg and Na–Hg, the experimental C_6 values are high relative to the S.-K. estimate. Independent of c, $10^{-34}\varepsilon^2 r_m(\text{erg}^2\text{cm}) = 3.7_5(\pm 5\%)$.

(TABLE III footnotes *continued*)

(*u*) Rb–Kr. VON–67. Parenthesized parameters estimated from the theoretical C_6, as in (*l*).

(*v*) Rb–Hg. HUN–65a. Parenthesized "experimental C_6" values calculated from parameters, as in (*t*); doubtful. As for K–Hg, these are high relative to the S.-K. estimate.

(*w*) Cs–Ar. HOL–66. Experiments in "high-v" region. Parenthesized parameters doubtful. The experimental C_6 is that of ROT–59, corrected, quoted in reference 32.

(*x*) Cs–Kr. VON–67. First set of parenthesized parameters calculated from theoretical C_6, as in (*u*). Second set from high-v experiments of HOL–66. The experimental C_6 is that of ROT–59, corrected, quoted in reference 32.

(*y*) Cs–Xe. Same references and comments as for (*w*).

(*z*) Cs–Hg. MOR–62c. Reanalyzed using ratio of results relative to K–Hg (*t*). Experiments give precise ratio $J(\text{Cs–Hg})/J(\text{K–Hg}) = 1.03$; however, r_m ratio 1.2($\pm$10%). Thus ε fairly reliable, r_m doubtful. Parenthesized "experimental C_6" values calculated from parameters, as in (*v*); doubtful. As for other alkali–Hg systems, experimental C_6 values high relative to S.-K. estimate.

(*c'*) He(2^3S)–Ar. ROT–65b,c. Additional experiments on He*–He, He*–Ne in high-v region (not included in Table III); parameters very doubtful.

(*d'*) He(2^3S)–Kr. Same references and comments as for (*c'*).

[c] *Atom–diatomic systems:*

(*A*) Ne–H_2(D_2). HEL–66. Experiments in high-v region. Parenthesized parameters doubtful. "Experimental C_6" calculated from parameters. Discordant ε for Ne–H_2 disregarded.

(*B*) Ar–H_2(D_2). FEL–66, HEL–66. "Experimental C_6" calculated from parameters. Good agreement between H_2 and D_2 parameters.

(*C*) Kr–H_2(D_2). Same references and comments as for (*B*).

(*D*) Xe–H_2(D_2). Same references and comments as for (*B*) and (*C*).

(*E*) Hg–H_2. KNA–34, analyzed by MUE–63. Parameters very doubtful, as for (*f*). Parenthesized "experimental C_6" calculated from parameters; doubtful.

(*F*) Na–HBr. HUN–65a. Parenthesized "experimental C_6", calculated from parameters, very high relative to the S.-K. estimate; doubtful in view of high value also reported for K–HBr by HUN–65a.

(*G*) K–HCl. ACK–64, reanalyzed by Greene *et al.* in reference 2g. The experimental C_6 is from ROT–59; cf. the value calculated from parameters, 0.8. Thus r_m seems low.

(*H*) K–HBr(DBr). AIR–67b, BEC–62a, HUN–65a. The experimental C_6 is from ROT–59; cf. the value calculated from parameters, 5.7 (good agreement). Precise comparison of HBr with DBr shows same ε but suggests smaller r_m value for K–DBr: 3.9 Å. Slight discrepancy in J from data of HUN–65a.

(*I*) K–HI. Same references as for (*G*). Parenthesized "experimental C_6" calculated from parameters.

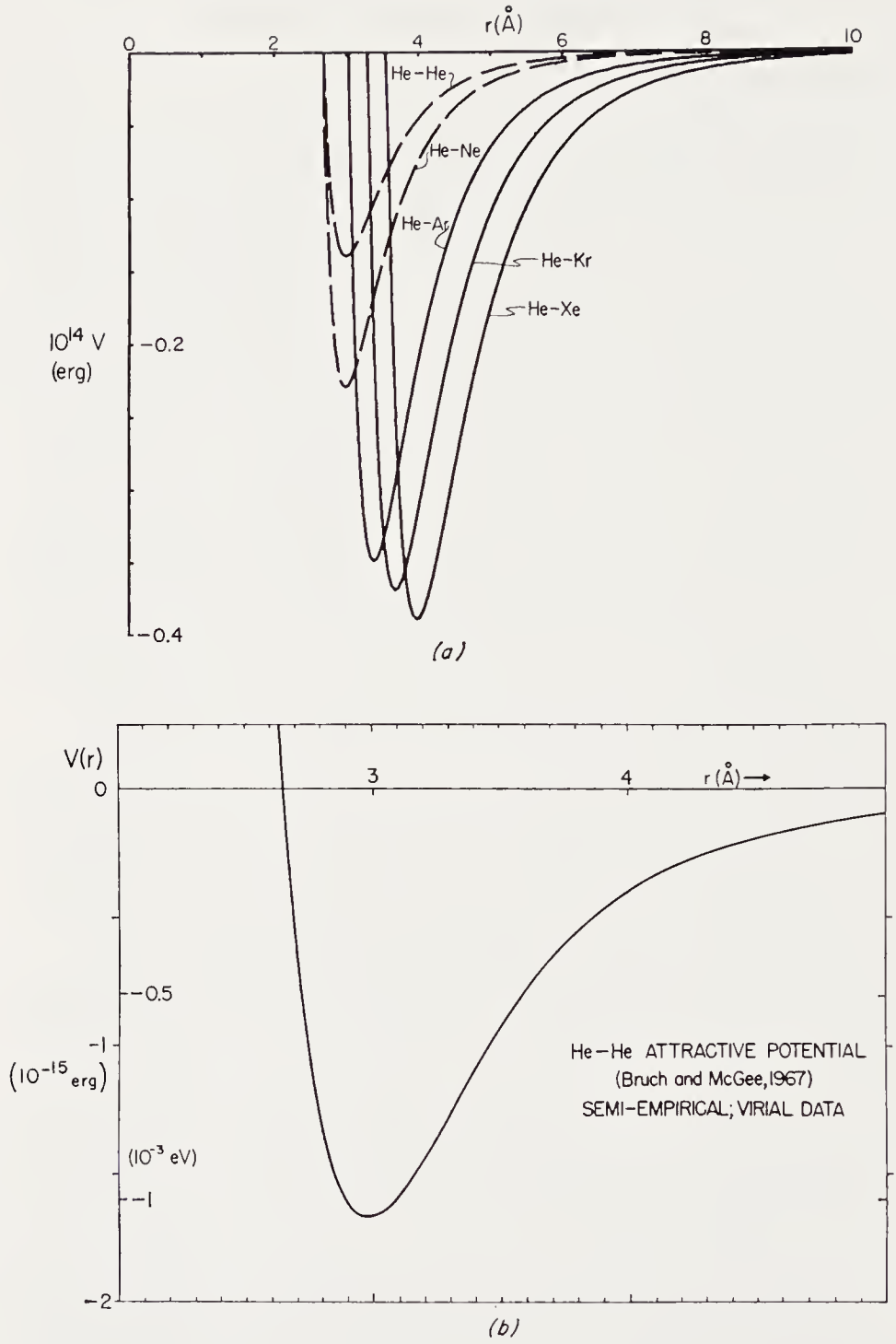

Fig. 27. (*a*) Potential wells for He–rare gas systems. (*b*) Semiempirical He–He potential of reference 45.

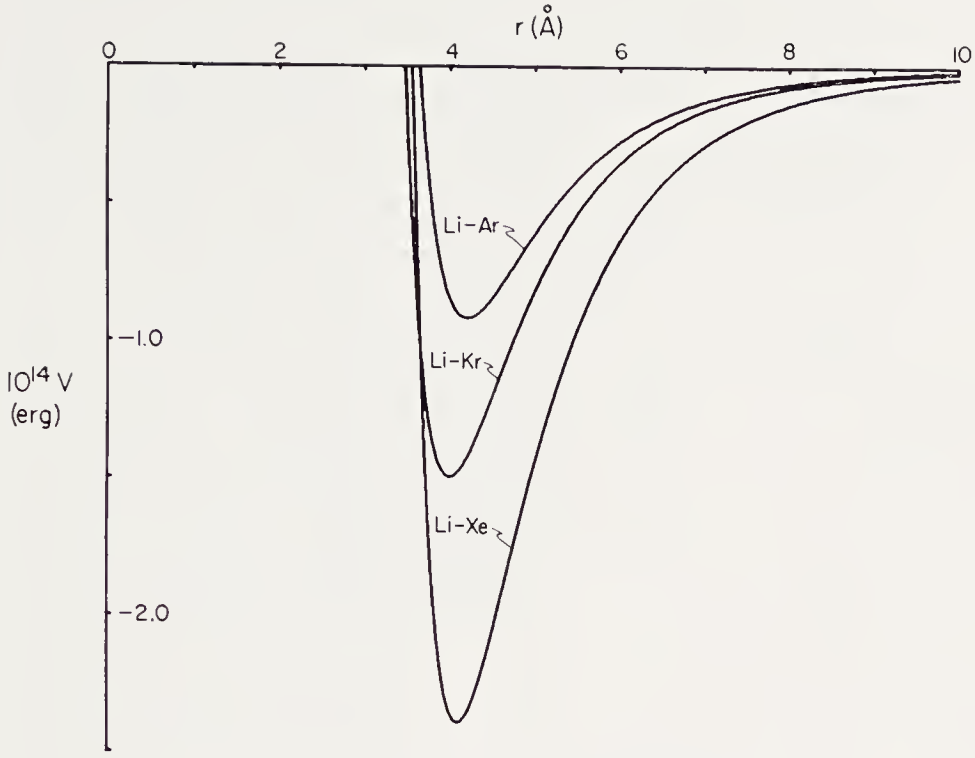

Fig. 28. Potential wells for Li–rare gas systems.

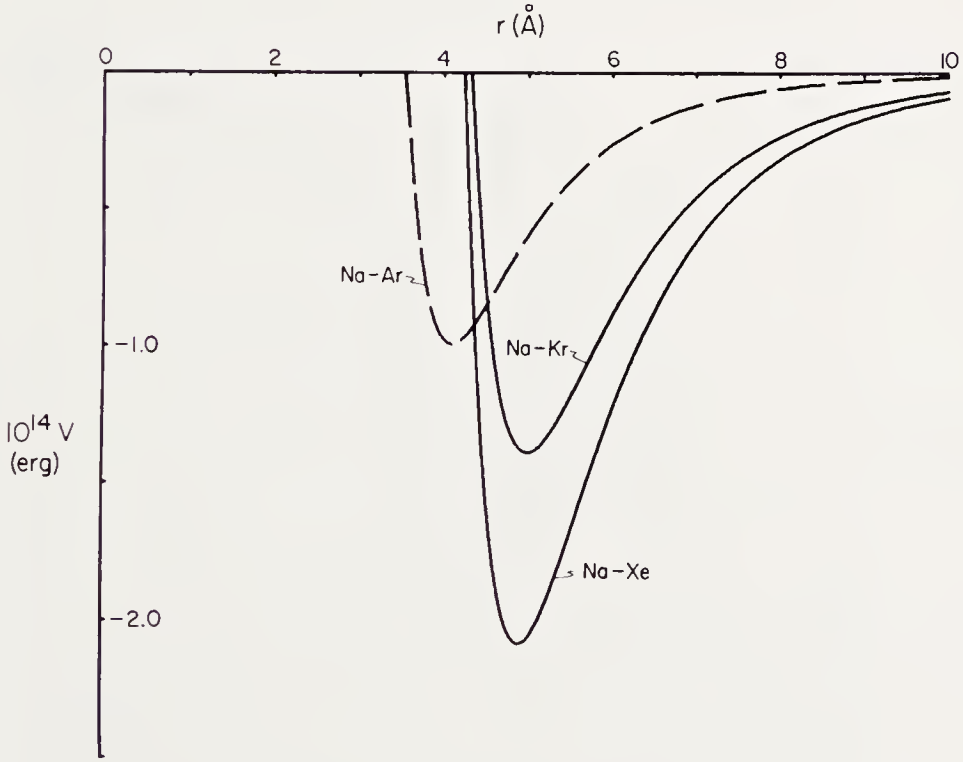

Fig. 29. Potential wells for Na–rare gas systems.

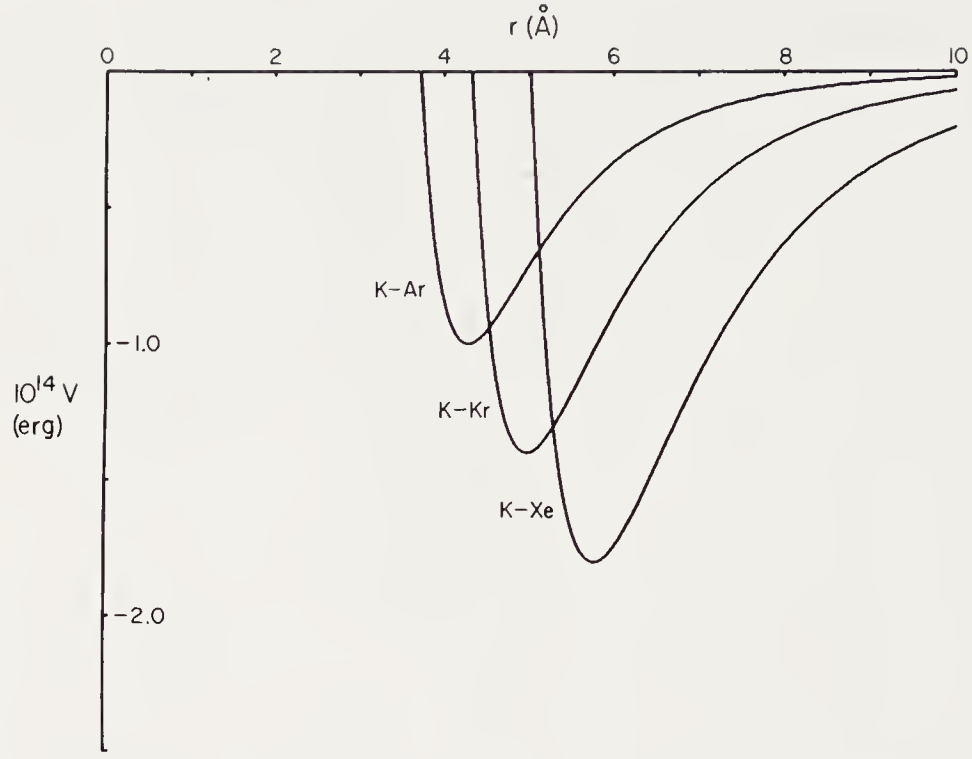

Fig. 30. Potential wells for K–rare gas systems.

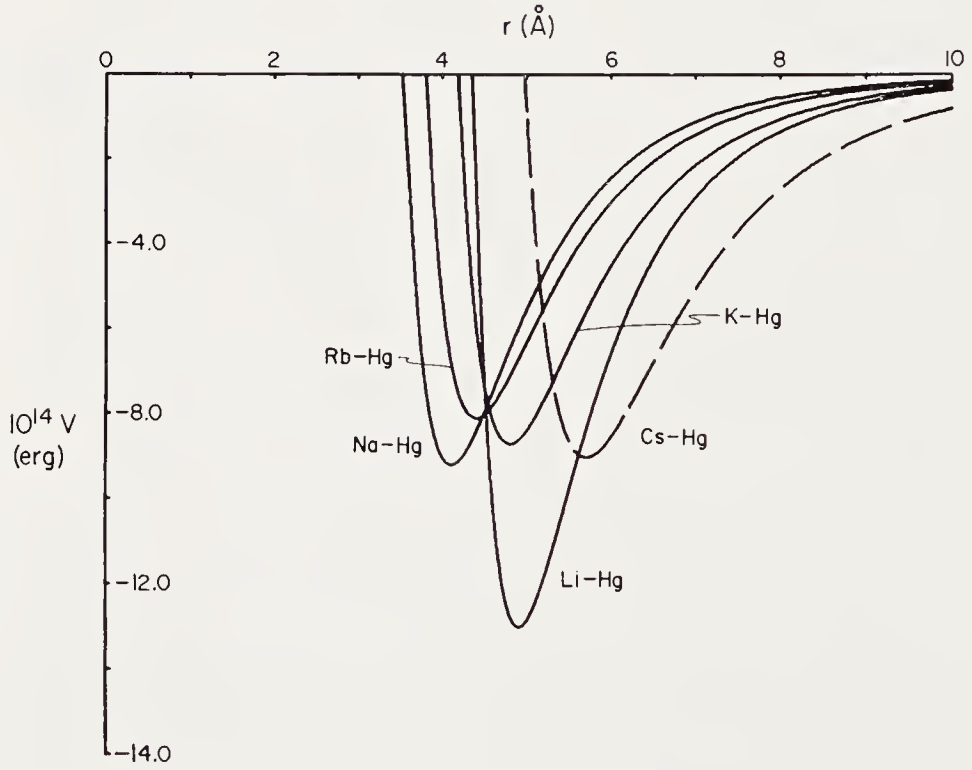

Fig. 31. Potential wells for alkali–Hg systems.

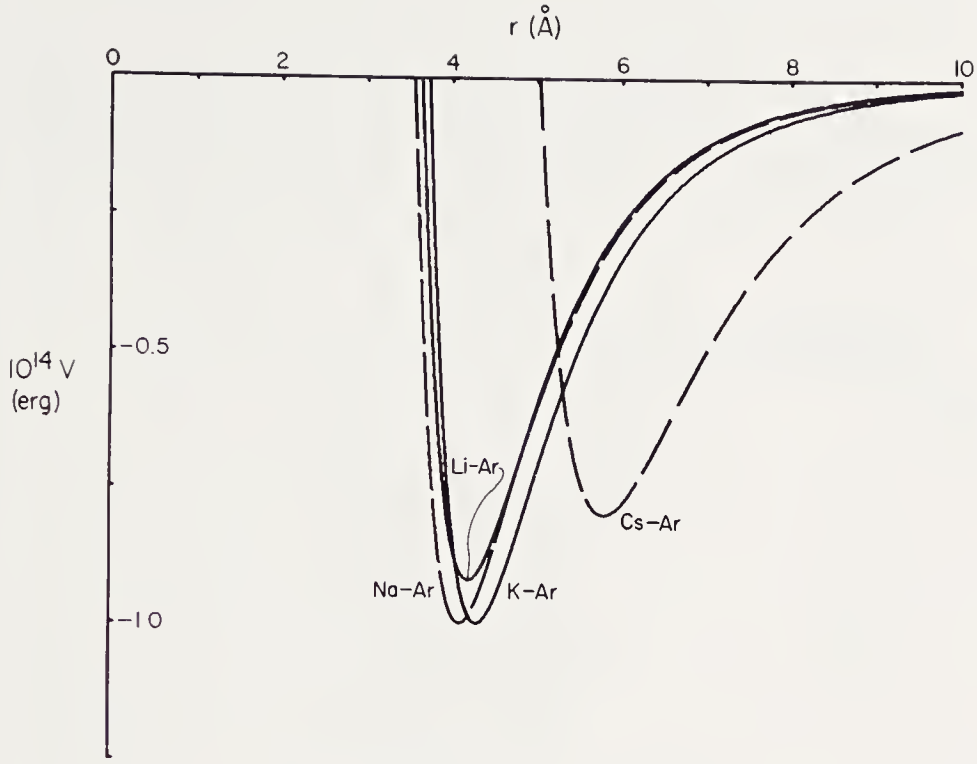

Fig. 32. Potential wells for alkali–Ar systems.

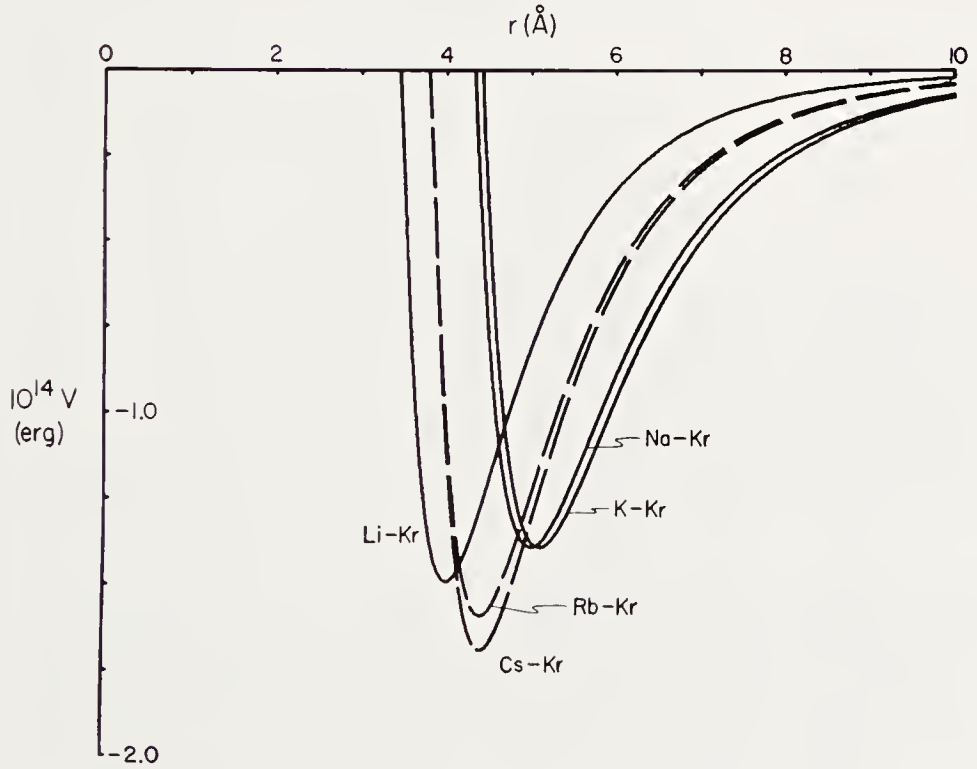

Fig. 33. Potential wells for alkali–Kr systems.

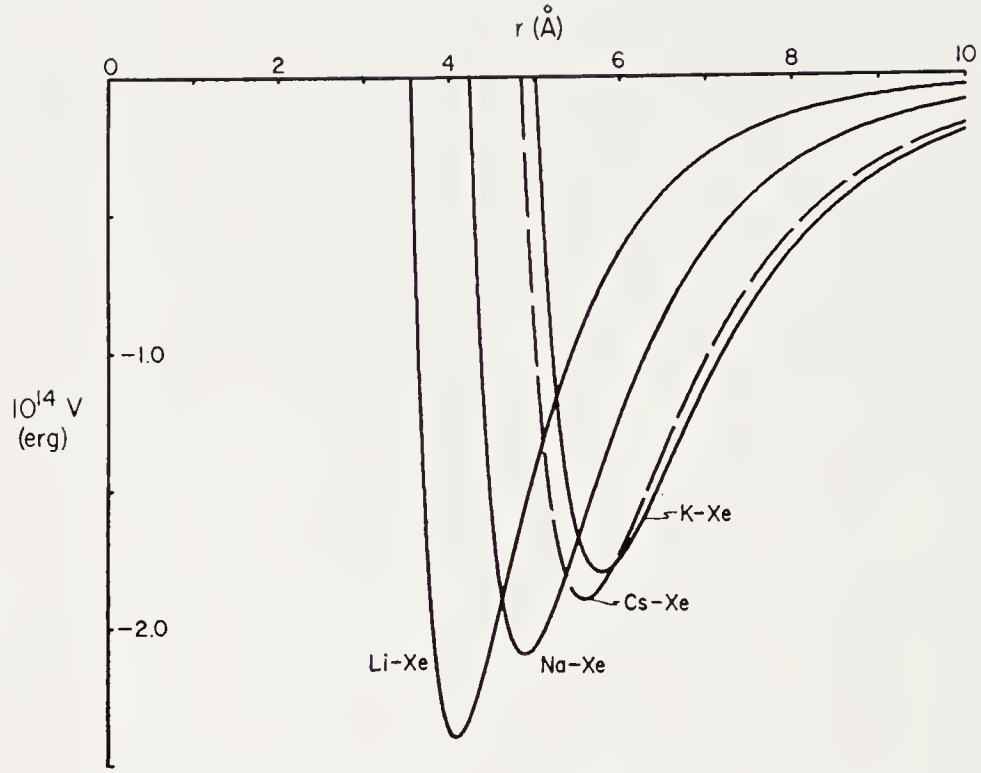

Fig. 34. Potential wells for alkali–Xe systems.

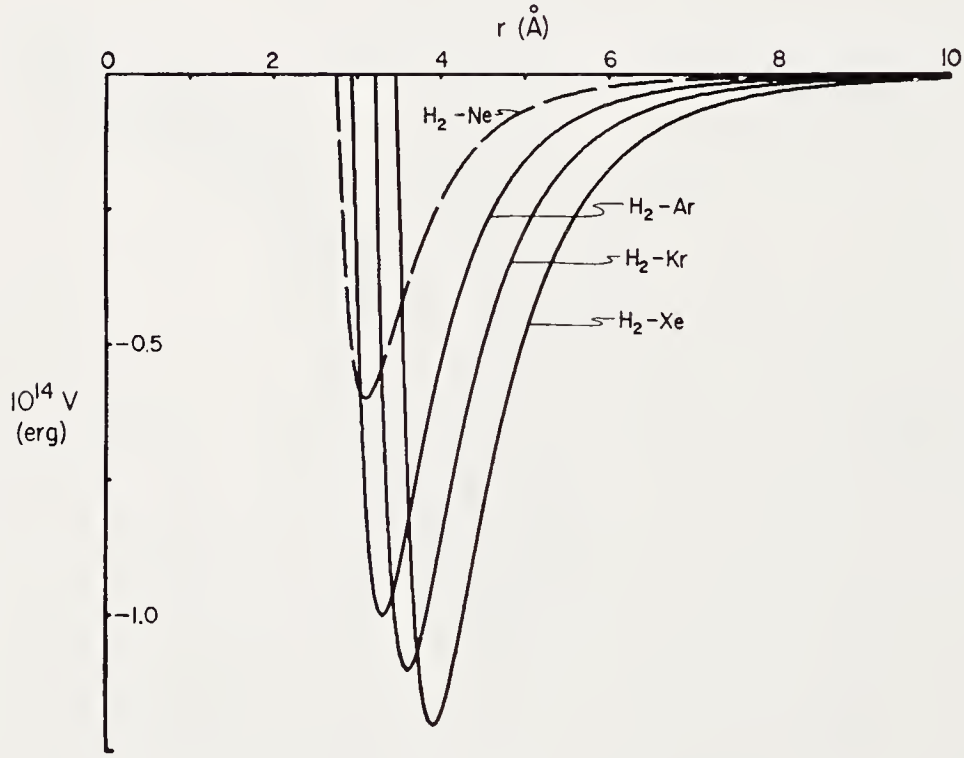

Fig. 35. Orientation-averaged potentials for H_2–rare gas systems.

where r_m is in Å, ε in ergs, and c is the dimensionless "curvature ratio." Here a_{ij} and b_{ij} are the empirical constants characteristic of the rows in the periodic table occupied by the pair of atoms i, j which comprise the molecule; $a_{ij} = a_{ji}$, $b_{ij} = b_{ji}$.

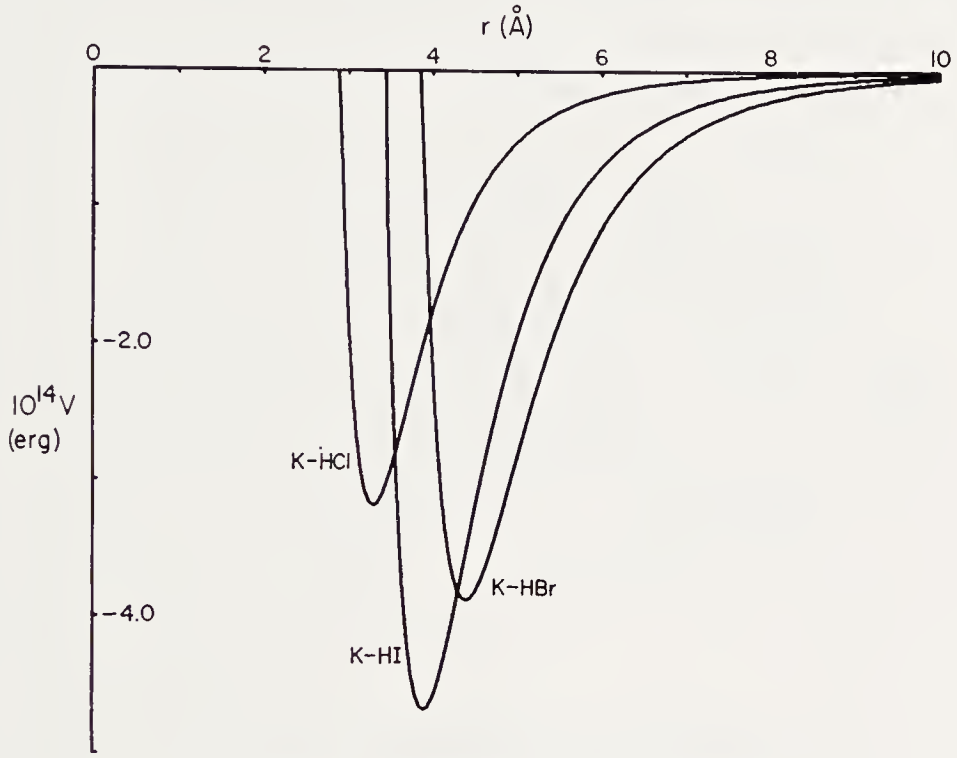

Fig. 36. "Effective two-body potentials" for K–HX systems.

Making use of Johnston's constants, Eq. (31) has been calculated and the results displayed graphically in Figures 37 and 38: a series of semilog curves (nearly linear and fairly regularly spaced) of r_m versus $10^{14}\varepsilon c$ for $i, j = 0, 1, \ldots, 4$. A few lines corresponding to a short extrapolation to $j = 5$ have also been included. For the sake of definiteness the following examples are indicative of the conventions on i. For $i = 0$: H, He; $i = 1$: Li, ..., Ne; $i = 2$: Na, ..., Ar; $i = 3$: K, ..., Kr; $i = 4$: Rb, ..., Xe; $i = 5$: Cs, ..., Hg, ..., Rn.

Superimposed on the calculated curves are the experimental points taken from Table III. The open circles denote the less reliable determinations (parenthesized in the table). The only omissions are for nonground-state atoms. For the atom–diatomic systems (part 2 of Table III), the

following assignments of i for the diatomics have been made: $i_{HCl} = i_{Ar} = 2$; $i_{HBr} = i_{Kr} = 3$; $i_{HI} = i_{Xe} = 4$; $i_{H_2} = 1$. The point plotted for H_2–H_2 is based upon the L.-J. (12,6) parameters of reference 11 (extracted from virial data); this is the only nonbeam-derived data point displayed in the figures.

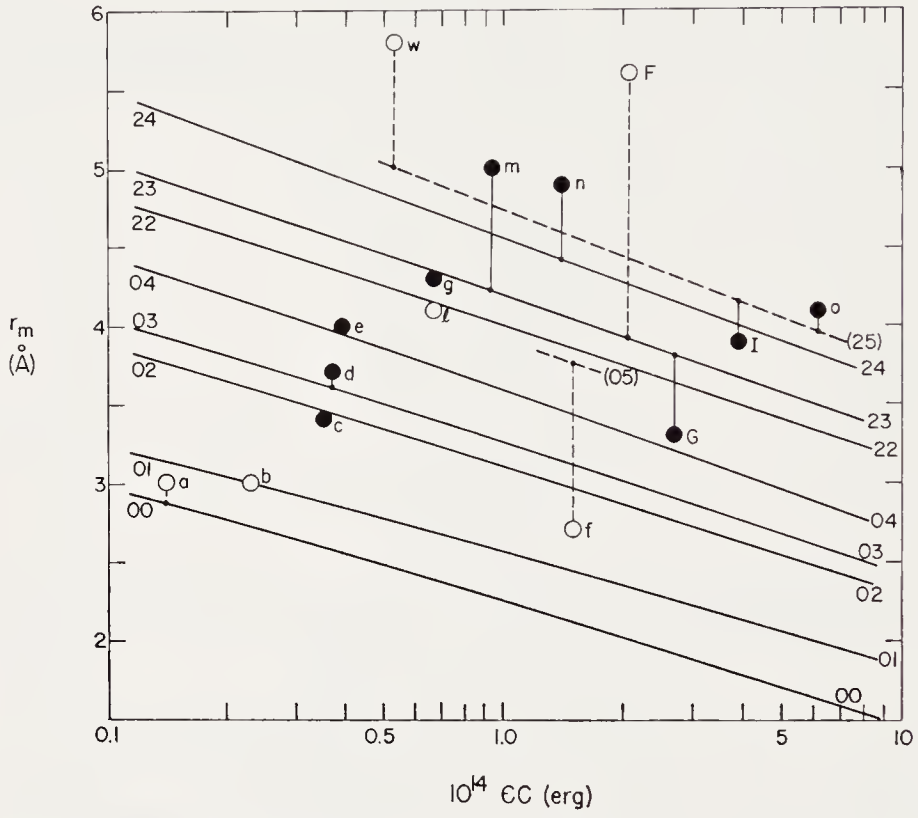

Fig. 37. Badger-Johnston relation applied to the beam-derived potential well data (from Table III). Solid lines (—) are calculated using Johnston's[46b] empirical constants for the designated (ij) type (pair) of interacting atoms. Shown are lines for $i = 0$ and 2. Dashed lines (– – –) are estimated, for $j = 5$. Solid circles (●) denote "reliable" experimental results, open circles (○) "less reliable" (parenthesized values in Table III). The letters adjacent to the circles designate the system according to the index of Table III.

Inspection of Figures 37 and 38 indicates that the Badger-Johnston equations are quite satisfactory in correlating the rare gas–rare gas and rare gas–H_2 systems but less so for the alkali systems, where, for the most part, the predicted r_m values are low by some 0.5 Å. In a few cases, the deviations are sufficiently great to suggest an error in the experiment

itself or analysis of the scattering data. In this sense, this type of empirical correlation scheme has some value, albeit limited.*

In view of the uncertainties, however, both in the accuracy of the present data and in the Johnston constants, it seems unwarranted to use the full, detailed set of Badger-Johnston equations with their many

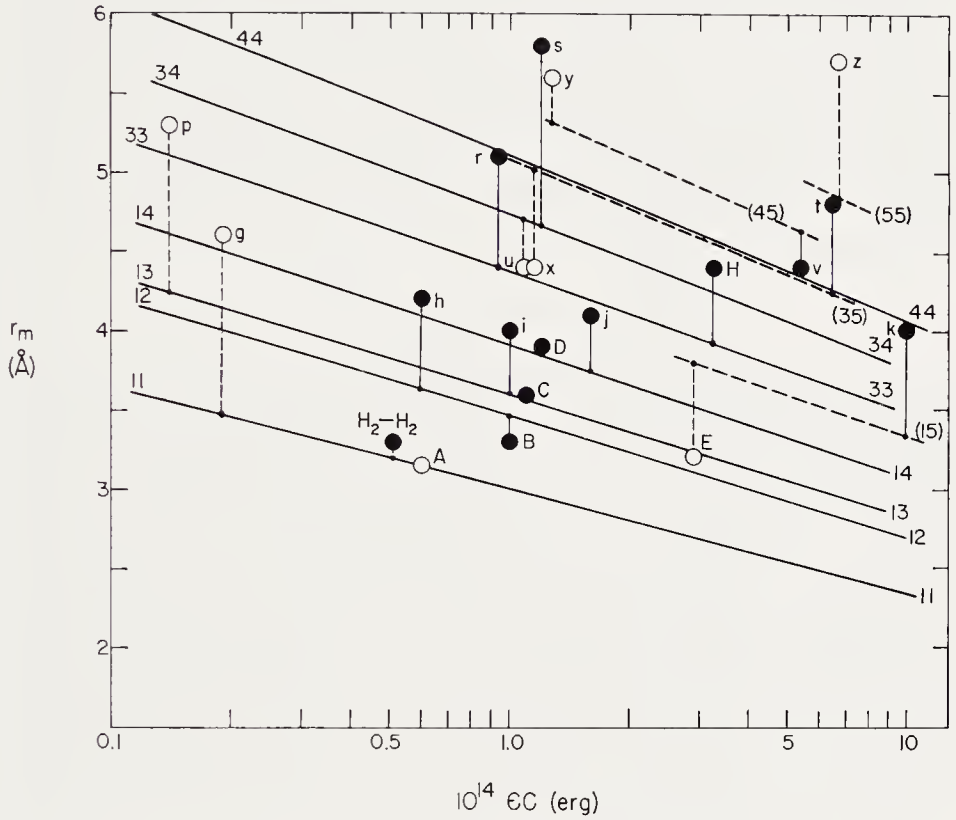

Fig. 38. Same as Figure 37, for $i = 1$, 3, 4, and 5.

empirical parameters; rather, in view of the near-regularity of the plots in Figures 37 and 38, a simplified, single "rule-of-thumb" equation was developed[47b] (which did not involve any revision of the Johnston constants), as follows.

Rule-of-thumb (A):

$$r_m = 2.28 + 0.36(i + j) - 0.81 \log_{10}(10^{14}\varepsilon c) \qquad (32)$$

* A recent study of H atom scattering (in the "high velocity" region) by rare gases, H_2, and hydrocarbons has been carried out, including a detailed correlation of the resulting parameters.[47a]

where r_m is in Å and ε is in ergs. Equation (32) reproduces the family of curves of Figures 37 and 38 over the range shown within an average deviation of ca., ± 0.1 Å, more than adequate for the present purposes. Of course, the rule-of-thumb estimates, on the average, are no better than the Badger-Johnston equations in correlating the experimental results; the only advantage is simplicity.

The general problem of prediction, estimation, or correlation of the equilibrium separations of diatomic molecules has received much attention for the past half century, with important names such as Bragg, Fajans, Goldschmidt, Pauling, and Slater figuring significantly in the history. More recently, Hirschfelder and Eliason[48] have considered the question of estimation of "collision diameters" for nonbonding atoms, and suggested the empirical rule,

$$\sigma_{ab} = \bar{r}_a + \bar{r}_b + 1.8 \quad (\text{Å}) \tag{33}$$

where σ_{ab} is the usual L.-J. (12,6) parameter (the zero of the potential) and $\bar{r}_a$ and $\bar{r}_b$ are the respective "Slater screening constant mean radii," which are very nearly equal to the covalent binding radii of the atoms.[48] For the present purposes, a slight modification of this relation has been adopted,[47b] and a more recent, improved approach to the orbital radii has been employed, namely, that of Waber and Cromer.[49] These authors computed radii of the principal maxima in the radial distribution functions for all ground-state atoms, following Slater's procedures using relativistic wavefunctions. The radii of the outermost shells agreed "remarkably well"[50] with Slater's empirical atomic radii[50] based on crystal-and molecular-structure data for cases in which comparisons were possible.

Thus an approximation for r_m is taken to be

Rule-of-thumb (B):

$$r_m = r_i + r_j + 2.0 \quad (\text{Å}) \tag{34}$$

where r_i and r_j are the orbital radii of the atoms (i,j) taken from the calculations of reference 49.

Table IV lists selected values of orbital radii for atoms of interest in the present survey, rounded to the nearest 0.05 Å, comparing the mean (Slater-screened) orbital radii of reference 48 with the empirical "atomic radii" of reference 50 and the "orbital radii" of reference 49. The latter

values, as rounded, were used in connection with Eq. (34) to estimate r_m values for the systems of Table III (part 1).

Table V summarizes the results. The systems are listed following the indexing of Table III. The "best experimental" values of r_m are compared with the estimates based on *rule-of-thumb* (*A*) [Eq. (32) for correlation with εc] and *rule-of-thumb* (*B*) [Eq. (34) for direct estimation from orbital radii.]

TABLE IV

Selected Values of "Orbital Radii" (Å)
(Rounded to the Nearest 0.05 Å)

Atom	Method of ref. 48		Values from ref. 50	Preferred values, from ref. 49
	r	r_{max}		
He	0.45	0.30		0.30
Ne	0.45	0.35		0.35
Ar	0.80	0.70		0.65
Kr	1.00	0.90		0.80
Xe	1.15	1.05		1.00
Li			1.45	1.60
Na			1.80	1.70
K			2.20	2.15
Rb			2.35	2.30
Cs			2.60	2.50
Hg			1.50	1.10

Inspection of the results indicates that much remains to be desired. Nevertheless, the experimental data appear to be correlated within an average deviation of ca. $\pm$ 0.5 Å, so that the obviously deviant systems can be identified and considered worthy of reexamination in the future.

VIII. CONCLUDING REMARKS: SCOPE OF THE METHOD

At the present stage of its development, the molecular beam scattering method for the determination of attractive intermolecular forces is beginning to yield useful "numbers," albeit of relatively low accuracy.

TABLE V

Experimental versus Estimated r_m Values
(Entries in Å)

System	Experimental (from Table III)	Rule-of thumb	
		(*A*) Eq. 32	(*B*) Eq. 34
(*a*) He–He	(3.0)	3.1	2.6
(*b*) He–Ne	(3.0)	3.2	2.6_5
(*c*) He–Ar	3.4	3.4	2.9_5
(*d*) He–Kr	3.7	3.8	3.1
(*e*) He–Xe	4.0	4.1	3.3
(*f*) He–Hg	$(2._7)$	3.9	3.4
(*g*) Li–Ne	$(4._6)$	3.8	3.9_5
(*h*) Li–Ar	4.2	3.5	4.2_5
(*i*) Li–Kr	4.0	3.7	4.4
(*j*) Li–Xe	4.1	3.9	4.6
(*k*) Li–Hg	4.9	3.5	4.7
(*l*) Na–Ar	$(4._1)$	3.9	4.3_5
(*m*) Na–Kr	5.0	4.1	4.5
(*n*) Na–Xe	4.9	4.3	4.7
(*o*) Na–Hg	4.1	4.2	4.8
(*p*) K–Ne	$(5._3)$	4.5	4.5
(*q*) K–Ar	4.3	4.2	4.8
(*r*) K–Kr	5.1	4.5	4.9_5
(*s*) K–Xe	5.8	4.7	5.1_5
(*t*) K–Hg	4.8	4.5	5.2_5
(*u*) Rb–Kr	(4.4)	4.8	5.1
(*v*) Rb–Hg	4.4	4.9	5.4
(*w*) Cs–Ar	$(5._8)$	5.0	5.1_5
(*x*) Cs–Kr	(4.4)	5.1	5.3
(*y*) Cs–Xe	$(5._6)$	5.4	5.5
(*z*) Cs–Hg	$(5._7)$	5.2	5.6
(*A*) Ne–H_2	(3.1)	3.2	—
(*B*) Ar–H_2	3.3	3.4	—
(*C*) Kr–H_2	3.7	3.7	—
(*D*) Xe–H_2	3.9	4.0	—
(*E*) Hg–H_2	$(3._2)$	4.1	—
(*F*) Na–HBr	$5._6$	3.8	—
(*G*) K–HCl	$3._3$	3.7	—
(*H*) K–HBr	$4._4$	4.0	—
(*I*) K–HI	$3._9$	4.3	—

Surely within the next decade, such elastic scattering measurements will provide a substantial body of reliable data on intermolecular potential wells to serve as a meaningful exprimental reference against which to compare *ab initio* theoretical computations.

Before projecting into the future, however, it seems appropriate to summarize the main phenomena which *have* been observed and the conclusions which can be drawn from the measurements made to date. The following paragraphs are intended to serve as such a survey.

1. High-energy beam scattering measurements of "classical" total cross sections (by Amdur and collaborators) have yielded reliable values of the short-range repulsive forces for rare gas and simple molecule systems. Potential energy curves, which may usually be approximated by a simple exponential form $V(r) = A \exp(-Br)$ over the range of the observations, are obtained with an accuracy of ca. 10 %. The experimental results are in good accord both with theoretical calculations and with potentials deduced empirically from high-temperature transport and virial coefficients.

2. Thermal-energy measurements of "quantum" total cross sections Q have been made in a number of laboratories (e.g., the early work of Rabi; later several groups including Bederson, Bernstein, Kusch, Mueller, Pauly, Rothe, and their respective co-workers) for a large number of systems involving rare gases, alkali atoms, etc., with an accuracy of the order of some 10 %, yielding the long-range attractive constant C_6 (for appropriate systems) within ca. 25 %. For the most part, the results are consistent with recent theoretical calculations (e.g., by Dalgarno and co-workers) within the mutual uncertainties.

3. Angular distributions of elastic scattering at thermal energies have been measured by several groups (including those of Beck, Bernstein, Datz, Greene, Herschbach, Pauly, Ross, and their collaborators) studying a variety of nonreactive (as well as reactive) collision partners. The following features have been observed.

a. At very small angles, the differential cross section $I(0)$ becomes nearly constant (Pauly et al.) in accord with quantum predictions, thus justifying the concept of an absolute total cross section Q.

b. At moderately small angles, for heavy-particle systems, the "smoothed" $I(0)$ is found to vary as $\theta^{-7/3}$ (Bernstein, Pauly, and their respective co-workers), in accord with classical low-angle scattering theory, assuming a potential asymptotically of the form $-C_6/r^6$.

c. So-called "rainbow maxima" are observed (Beck, Bernstein, Greene, Pauly, Ross, and respective co-workers) and are explainable by semiclassical theory. The energy dependence of the primary and supernumerary "rainbow angles" yields the depth of the well, ε, within about 10% (subject to the constraint of an assumed functional form for the potential) and the position of the minimum, r_m, within about 20%.

d. With high angular and velocity resolution, the differential cross section shows an oscillatory interference pattern, for angles smaller than the primary rainbow angle (Beck, Bernstein, Pauly, and their respective co-workers). From an analysis of the pattern and its "shrinkage" with increasing relative velocity, the value of r_m is determined within ca. 10%. Very accurate recent measurements (by Pauly et al.) have made it possible to discriminate among various potential functions, i.e., to estimate the "third parameter."

4. Extrema in the velocity dependence of the total cross section, $Q(v_r)$, (glory extrema) have been extensively investigated (Beck, Beier, Bernstein, Neynaber, Pauly, Rol, Rothe, Schlier, and their respective co-workers). From the extrema velocities (and extrema amplitudes), the product εr_m can be estimated within ca. 10% (again subject to the assumption of a functionality for the potential). With a sufficient range and accuracy in the extrema pattern, the combination $\varepsilon^2 r_m$ may be determined within ca. 5%, nearly independent of the functional form of the potential.

The "smoothed" or mean $Q(v_r)$ is found to vary as $v_r^{-2/5}$ at low velocities, in accord with expectation for an r^{-6} long-range potential[51] and to approach a limiting high-velocity form in which Q is a very slowly decreasing function of v_r, governed mainly by the repulsive interaction (Bederson, Bernstein, Datz, Herschbach, Neynaber, Pauly, Rothe, and respective co-workers).

5. Small differences in the total cross sections for scattering of atoms in selected Zeeman states and of diatomic molecules in specified rotational states have been measured (Bennewitz, Kramer, Paul, Schlier, Toennies, and respective co-workers). The results have been interpreted to yield information on the anisotropy of the potential functions, both at long- and short-range.

6. Dipole–dipole interactions have been observed (Bernstein, Herschbach, Rothe, Toennies, and respective co-workers) and interpreted in terms of elastic plus inelastic contributions.

Next, it is perhaps appropriate to project slightly and point out a few imminent developments which may soon provide new information on intermolecular potential wells.

1. Resonances in atom–atom scattering cross sections (associated with the quasi-bound states) have been predicted[52] for a number of light-atom systems. The results should be directly correlated with predissociation data on the diatom[52b,e] and serve as a sensitive probe of the long-range attractive potential.

2. Spin-exchange cross sections, at present obtainable only indirectly via optical pumping techniques, should soon be directly measureable with atomic beam methods (Beck, Schlier, and respective co-workers). Results, e.g., on alkali atoms would give information on both singlet and triplet potentials.

A few closely related techniques undergoing refinement may soon yield relevant experimental data on interatomic forces. They may be mentioned here, although peripheral to the main subject of this chapter.

1. Measurements of atomic line shapes and satellite band positions may be used to deduce differences in potentials between a ground and excited state, e.g., for alkali–rare gas systems, currently of astrophysical interest. This technique has already yielded results for the Cs–Xe system.[53]

2. Direct absorption spectrophotometric measurements, i.e., study of intensities of satellite bands as a function of pressure and temperature have been used to estimate equilibrium constants and dissociation energies for alkali dimers; encouraging results have recently been obtained for certain Cs–rare gas pairs as well.[54] Such "thermodynamic" measurements of bond dissociation energies for van der Waals diatoms would serve as a welcome complement to the beam-derived data on potential well depths.

Returning again to the molecular beam scattering approach to the determination of intermolecular forces, future developments in the field will depend largely upon technical advances, e.g., more sensitive, universal detectors and more intense and monochromatic beam sources. The fragmentary studies to date, which have been summarized in the present chapter, must be considered merely as prototype investigations which have served principally to sharpen the tools of the trade. The field is now approaching maturity and, hopefully, should soon be producing reliable experimental interaction potentials for a large number of systems involving ground-state and metastable atoms, molecules, and radicals.

References

1. The very early pioneering work of O. Stern, F. Knauer, I. I. Rabi, and others is reviewed in *Recent Research in Molecular Beams*, I. Estermann, Ed., Academic Press, New York, 1959; N. F. Ramsey, *Molecular Beams*, Oxford University Press, London, 1956; K. F. Smith, *Molecular Beams*, Methuen, London, 1955.
2. For reviews see:
   (a) H. Pauly, *Fortschr. Physik*, **9**, 613 (1961); (b) W. Fite and S. Datz, *Ann. Rev. Phys. Chem.*, **14**, 61 (1963); (c) R. B. Bernstein, in *Atomic Collision Processes*, M. R. C. McDowell, Ed., North-Holland, Amsterdam, 1964; (d) V. B. Leonas, Uspekhi, **7**, 121 (1964); (e) R. B. Bernstein, *Science*, **144**, 141 (1964); (f) H. Pauly and J. P. Toennies, in *Advances in Atomic and Molecular Physics*, Vol. 1, D. R. Bates and I. Estermann, Eds., Academic Press, New York, 1965; (g) J. Ross, Ed., *Molecular Beams* (*Advances in Chemical Physics*, Vol. 10), Interscience, New York, 1966.
3. (a) H. S. W. Massey and C. B. O. Mohr, *Proc. Roy. Soc.* (*London*), **A144**, 188 (1934); (b) H. S. W. Massey and R. A. Buckingham, *Nature*, **138**, 77 (1936).
4. See, for example, (a) K. W. Ford and J. A. Wheeler, *Ann. Phys.* (*N. Y.*), **7**, 259, 287 (1959); (b) R. B. Bernstein, *J. Chem. Phys.*, **33**, 795 (1960).
5. See review by I. Amdur and J. E. Jordan, in *Molecular Beams* (*Advances in Chemical Physics*, Vol. 10), J. Ross, Ed., Interscience, New York, 1966, Chap. 2.
6. J. E. Jordan and I. Amdur, *J. Chem. Phys.*, **46**, 165 (1967).
7. N. E. Blais and J. B. Mann, *J. Chem. Phys.*, **32**, 1459 (1960).
8. E. A. Mason and W. E. Rice, *J. Chem. Phys.*, **22**, 522 (1954).
9. P. E. Phillipson, *Phys. Rev.*, **125**, 1981 (1962).
10. A. A. Abrahamson, *Phys. Rev.*, **130**, 693 (1963).
11. J. O. Hirschfelder, C. F. Curtiss, and R. B. Bird, *Molecular Theory of Gases and Liquids*, Wiley, New York, 1964.
12. See review by R. B. Bernstein, in *Molecular Beams* (*Advances in Chemical Physics*, Vol. 10), J. Ross, Ed., Interscience, New York, 1966, Chap. 3; see also ref. 2f.
13. See, for example, H. G. Bennewitz and H. D. Dohmann, *Z. Physik.*, **182**, 524 (1965).
14. K. Berkling, R. Helbing, K. Kramer, H. Pauly, Ch. Schlier, and P. Toschek, *Z. Physik.*, **166**, 406 (1962).
15. F. von Busch, *Z. Physik.*, **193**, 412 (1966).
16. H. Schumacher, R. B. Bernstein, and E. W. Rothe, *J. Chem. Phys.*, **33**, 584 (1960).
17. (a) K. W. Ford and J. A. Wheeler, ref. 4a; (b) E. A. Mason, *J. Chem. Phys.*, **26**, 667 (1957); (c) O. B. Firsov, *Soviet Phys. JETP* (*Engl. Trans.*), **24**, 279 (1953).
18. (a) H. U. Hostettler and R. B. Bernstein, *Phys. Rev. Letters*, **5**, 318 (1960); (b) P. J. Groblicki and R. B. Bernstein, *J. Chem. Phys.*, **42**, 2295 (1965).
19. (a) E. Hundhausen and H. Pauly, *Z. Physik.*, **187**, 305 (1965); (b) P. Barwig, U. Buck, E. Hundhausen, and H. Pauly, *Z. Physik.*, **196**, 343 (1966).
20. F. A. Morse and R. B. Bernstein, *J. Chem. Phys.*, **37**, 2019 (1962).
21. E. A. Mason and L. Monchick, *J. Chem. Phys.*, **41**, 2221 (1964).
22. D. Beck and H. J. Loesch, *Z. Physik.*, **196**, 66 (1966).
23. R. Düren and Ch. Schlier, *Discussions Faraday Soc.*, **40**, 56 (1965).

24. (a) E. A. Mason, J. T. Vanderslice, and C. J. Raw, *J. Chem. Phys.*, **40**, 2153 (1964); (b) R. Helbing and H. Pauly, *Z. Physik.*, **179**, 16 (1964).
25. J. Luoma and C. R. Mueller, *Discussions Faraday Soc.*, **40**, 45 (1965).
26. F. Knauer, *Z. Physik.*, **90**, 559 (1934).
27. H. W. Massey and C. B. O. Mohr, ref. 3a.
28. For a discussion of this point, see R. B. Bernstein and K. H. Kramer, *J. Chem. Phys.*, **38**, 2507 (1963). The preferred value of $p(s)$ is from the Schiff-Landau-Lifshitz (SLL) approximation.
29. H. Pauly, *Z. Naturforsch.*, **15a**, 277 (1960).
30. E. W. Rothe and R. B. Bernstein, *J. Chem. Phys.*, **31**, 1619 (1959).
31. (a) E. W. Rothe and R. H. Neynaber, *J. Chem. Phys.*, **43**, 4177 (1965); (b) H. G. Bennewitz and H. D. Dohmann, ref. 13.
32. For review, see A. Dalgarno and W. D. Davison, in *Advances in Atomic and Molecular Physics*, Vol. 2, D. R. Bates and I. Estermann, Eds., Academic Press, New York, 1966. See also A. Dalgarno, I. H. Morrison, and R. M. Pengelly, *Intl. J. Quantum Chem.*, **1**, 161 (1967).
33. E.g.,(a) R. B. Bernstein, *J. Chem. Phys.*, **37**, 1880 (1962); (b) R. B. Bernstein, *J. Chem. Phys.*, **38**, 2599 (1963); (c) R. Düren and H. Pauly, *Z. Physik.*, **175**, 227 (1963); (d) R. Düren and H. Pauly, *Z. Physik.*, **177**, 146 (1964); (e) E. W. Rothe, P. K. Rol, and R. B. Bernstein, *Phys. Rev.*, **130**, 2333 (1963); (f) R. B. Bernstein and T. J. P. O'Brien, *Discussions Faraday Soc.*, **40**, 35 (1965); (g) R. B. Bernstein and T. J. P. O'Brien, *J. Chem. Phys.*, **46**, 1208 (1967); (h) R. B. Bernstein, *J. Chem. Phys.*, **38**, 515 (1963).
34. (a) E. W. Rothe, P. K. Rol., S. M. Trujillo, and R. H. Neynaber, *Phys. Rev.*, **128**, 659 (1962); (b) P. K. Rol and E. W. Rothe, *Phys. Rev. Letters*, **9**, 494 (1962).
35. (a) E. W. Rothe, R. H. Neynaber, B. W. Scott, S. M. Trujillo, and P. K. Rol, *J. Chem. Phys.*, **39**, 493 (1963). (b) F. von Busch, H. J. Strunck, and Ch. Schlier, *Phys. Letters*, **16**, 268 (1965); *Z. Physik.*, **199**, 518 (1967). (c) D. Beck and H. J. Loesch, *Z. Physik.*, **195**, 444 (1966).
36. (a) R. Feltgen, W. Gaide, R. Helbing, and H. Pauly, *Phys. Letters*, **20**, 501 (1966); (b) R. Helbing, Dissertation, Univ. of Bonn, 1966; (c) R. Düren and Ch. Schlier, ref. 23; (d) R. Düren, R. Feltgen, W. Gaide, R. Helbing, and H. Pauly, *Phys. Letters*, **18**, 282 (1965); (e) E. W. Rothe and L. H. Veneklasen, *J. Chem. Phys.*, **46**, 1209 (1967).
37. Some progress in the problem of a practical inversion scheme has been reported by Mueller and co-workers. See R. E. Olson and C. R. Mueller, *J. Chem. Phys.*, **45**, 2519 (1966) and refs. cited therein.
38. K. Berkling, Ch. Schlier, and P. Toschek, *Z. Physik.*, **168**, 81 (1962).
39. H. G. Bennewitz, K. H. Kramer, W. Paul, and J. P. Toennies, *Z. Physik.*, **177**, 84 (1964).
40. R. B. Bernstein and T. J. P. O'Brien, refs. 33f and g.
41. P. R. Fontana and R. B. Bernstein, *J. Chem. Phys.*, **41**, 1431 (1964).
42. See, e.g., R. B. Bernstein, A. Dalgarno, H. S. W. Massey, and I. C. Percival, *Proc. Roy. Soc.* (*London*), **A274**, 427 (1963).
43. See, e.g., D. R. Herschbach, in *Molecular Beams* (*Advances in Chemical Physics*, Vol. 10), J. Ross, Ed., Interscience, New York, 1966, Chap. 9.
44. Ch. Schlier, *Z. Physik.*, **173**, 352 (1963).

45. L. W. Bruch and I. J. McGee, *J. Chem. Phys.*, **46**, 2959 (1967).
46. (a) R. M. Badger, *J. Chem. Phys.*, **2**, 128 (1934). (b). H. S. Johnston, *J. Am. Chem. Soc.*, **86**, 1643 (1964). See also D. R. Herschbach and V. W. Laurie, *J. Chem. Phys.*, **35**, 458 (1961).
47. (a) M. A. Fluendy, R. M. Martin, E. E. Muschlitz, Jr., and D. R. Herschbach, *J. Chem. Phys.*, **46**, 2172 (1967). (b) R. B. Bernstein, *Bull. Am. Phys. Soc.*, **12**, 402 (1967).
48. J. O. Hirschfelder and M. A. Eliason, *Ann. N.Y. Acad. Sci.*, **67**, 451 (1957).
49. J. T. Waber and D. T. Cromer, *J. Chem. Phys.*, **42**, 4116 (1965).
50. J. C. Slater, *J. Chem. Phys.*, **41**, 3199 (1964).
51. An unexplained questionable deviation for KCl scattering was reported by M. M. Hessel and P. Kusch, *J. Chem. Phys.*, **43**, 305 (1965). Also, the influence of the $C_8 r^{-8}$ term in the potential upon the velocity dependence of the total cross section has been observed by D. Beck and H. J. Loesch, ref. 35c, as predicted in ref. 41.
52. (a) R. Düren, R. Helbing, and H. Pauly, *Z. Physik.*, **188**, 468 (1965); (b) R. B. Bernstein, *Phys. Rev. Letters*, **16**, 385 (1966); (c) R. B. Bernstein, C. F. Curtiss, S. Imam-Rahajoe, and H. T. Wood, *J. Chem. Phys.*, **44**, 4072 (1966); (d) R. Helbing, ref. 36b; (e) T. G. Waech and R. B. Bernstein, *J. Chem. Phys.*, **46**, 4905 (1967).
53. R. Herman and L. Herman, *J. Quant. Spectry. Radiative Transfer*, **4**, 487 (1964). See also related work by S. Y. Ch'en and co-workers; R. Granier et al.; O. Jefimenko; and W. R. Hindmarsh.
54. (a) See, for example, the method of M. Lapp and L. P. Harris, *J. Quant. Spectry. Radiative Transfer*, **6**, 169 (1966); (b) M. Lapp, private communication.

9. Microwave Pressure Broadening and Its Application to Intermolecular Forces

GEORGE BIRNBAUM

North American Aviation Science Center
Thousand Oaks, California

CONTENTS

I. Introduction 488
A. Scope of this Review 488
B. Historical Survey of Theories of Spectral Line Shape and Width .. 489
C. The Impact Approximation 491
II. Widths of Resonant Lines 493
A. Anderson's Theory of Pressure-Broadened Lines 493
1. Appendix. Intermolecular Potentials 505
B. Simplifications of Anderson's Theory 509
C. Gordon's Theory of Pressure-Broadened Lines 513
III. Comparison of Theoretical and Experimental Line Widths 515
A. Introduction 515
B. Linear Molecules 516
1. OCS 516
2. HCl 523
3. BrCN 525
4. N_2O 525
5. O_2 526
C. Symmetric Top Molecules. Rotational Lines 527
D. Asymmetric Top Molecules 527
1. H_2O 527
2. SO_2 528
E. Inversion Spectrum of NH_3 529
1. Self-Broadening 529
2. Foreign-Gas Broadening 531
F. Summary 533
IV. Molecular Quadrupole Moments 535
V. Nonresonant Absorption and Relaxation 539
A. Introduction 539
B. Theory 540
C. Comparison of Theory and Experiment 543
VI. Conclusions 545
References 545

I. INTRODUCTION

A. Scope of this Review

Because of the availability of coherent sources of radiation in the microwave region, it is possible to make accurate measurements of the width and shape of spectral lines. Consequently, considerable attention has been devoted to the study of line shape and width for a wide variety of gases over extended ranges of pressure and temperature. Early developments in microwave line-width studies were reviewed by Gordy et al.[1] and Hirschfelder et al.[2] A detailed account of the status of the subject as of 1955 was presented by Townes and Schawlow.[3] They also gave simplified treatments of the Van Vleck-Weisskopf theory of microwave line shape[4] and Anderson's theory of the width of pressure-broadened lines[5]—theories which play central roles in the interpretation of microwave line widths and shapes. These and numerous other theories of line shape and width have been reviewed in considerable detail by Breene.[6,7]

It is the object of this review to bring the subject of pressure broadening in the microwave region and its application to intermolecular forces up to date. We are concerned with the critical evaluation of Anderson's theory of pressure broadening and comparison of this theory with experiment, and not with theoretical developments *per se* or with experimental techniques. Although the major interest in microwave pressure broadening has been with the study of sharp lines in gases at low pressures, i.e., below 1 mm Hg, a growing body work has been concerned with the very broad nonresonant spectra which certain gases exhibit at atmospheric pressure in the microwave region.* The study of pressure broadening in nonresonant spectra can, in principle, give valuable information regarding anisotropic intermolecular forces. However, since the calculations required to interpret nonresonant line widths in terms of specific intermolecular forces have not yet been made, this subject is discussed rather briefly.

Experiments on the microwave hyperfine transitions of optically pumped alkali metal vapors in the presence of rare gases have produced an interesting body of information on pressure-dependent line widths and shifts.[8,9] However, this work is outside the scope of this review and

* A brief assessment of progress in this area was presented by Birnbaum and Maryott[8] in 1961.

is not included. Closely related to the work reviewed here is pressure broadening in the infrared and far infrared regions, and some of these results are discussed.

B. Historical Survey of Theories of Spectral Line Shape and Width

The sources of spectral line broadening are: pressure broadening; collisions between molecules and the walls of the gas cell; saturation broadening; Doppler broadening; and radiation damping. The most important source of broadening in most microwave experiments is pressure broadening arising from inelastic bimolecular collisions which interrupt the radiation process. Broadening by collisions with walls or by the Doppler effect is ordinarily much less important than pressure broadening in the microwave region, but may be observed at sufficiently low pressures. Orders of magnitude smaller than these sources of broadening and, in fact, completely negligible for microwave molecular transitions in the ground electronic state, is radiation damping. The effect of saturation, the broadening of a spectral line when the radiation intensity is sufficiently high, is observable at low pressure where the lines are very narrow. It is not uncommon for saturation to set a lower limit on the width of microwave lines.

The pressure broadening of spectral lines is an effect which can be regarded physically in two different ways, and these two different aspects have given rise to two different theories: the statistical theory of Kuhn[10] and Margenau,[11] and the impact theory of Lorentz,[12] Weisskopf,[13] and Lenz.[14] The statistical theory treats the idealized physical situation in which all the molecules around the radiating one are at rest and cause a static but random perturbation in the energy levels of the radiating atom. The impact theory considers the incoherency in the emitted radiation caused by molecular collisions during the radiation process. Each theory can be regarded as a limiting case of the actual situation. Spitzer[15] and Holstein[16] have indicated the limits of validity of the two types of theory: at low pressures (where bimolecular collisions predominate), the statistical theory is valid in the wings of the line, while the impact theory is valid in the line center. A unified treatment of these two theories has been developed by Anderson,[17] and Anderson and Talman.[18]

The classical impact theory was developed by Lorentz[12] who considered that the broadening was due to the interruption by collisions of

a wave train that is otherwise unperturbed. These interruptions were assumed to completely destroy the coherence of the radiation. Weisskopf[13] developed an impact theory in which the collisions were assumed to cause broadening by changing the phase of the emitted radiation. This theory suffered, however, from the *ad hoc* assumption that only phase changes greater than a phase shift of the order unity were an important source of broadening. Improvement of the phase-shift theory followed as a result of the classical treatment of Lindholm[19] and the quantum formulation of Foley[20] who gave formulas for the width and shift of spectral lines with the general perturbation $C/R^n(t)$. Mizushima[21] later adapted a theory of this type to the calculation of microwave line widths. These theories, however, neglected the effect of transitions induced by collisions (nonadiabatic effects*), which are very important in the microwave region. Anderson[5] took the important step of developing a theory which includes nonadiabatic effects and is applicable for molecules with degenerate initial and final states.

Anderson's theory in its most general form relates the line width to a quantum mechanically calculated rate of change in phase of the molecular radiation due to bimolecular interactions. It includes as limiting cases both the situation where neither the radiating nor the colliding molecule undergoes changes in the internal quantum numbers governing its unperturbed energy (adiabatic case), and the situation where either one or both of the molecules do change such quantum numbers (nonadiabatic case). The nonadiabatic case includes the possibilities of exact resonance (most commonly in self-broadening when the net energy change in the two colliding molecules is zero) or near resonance.

In Anderson's theory,[5] the effect of collisions on the internal coordinates of the molecules is treated quantum mechanically, whereas the translational motion of the molecules is treated in the classical path approximation, i.e., the molecules move as classical particles. Leslie[22] and Baranger,[23–25] for example, have extended this work by treating the translational coordinates as well as the internal coordinates quantum mechanically. Additional steps in the development of the theory were the extension to coupled spectral lines by Baranger[23–25] and by Kolb and Griem,[26] and the introduction by Fano[27] of statistical mechanical methods to present pressure broadening as a relaxation process, and to include non-Markoffian effects of the collisions. DiGiacomo[28] has

* Townes and Schawlow[3] have introduced the term diabatic rather than nonadiabatic to describe the case where the internal energy of a molecule is changed in collisions.

obtained results very similar to that of Baranger except that effects of the identity of molecules, and correlations between successive collisions of a molecule are taken into account. Ohno[29] has considered the effect of higher-order collisions on the line width. Gordon[30] has treated the problem of pressure broadening semiclassically rather than quantum mechanically, and has calculated a number of line widths on this basis. This work is discussed in Section II-C.

Thus far, we have been discussing theoretical developments in the pressure broadening of microwave resonant lines. However, certain types of molecules, the most important of which are symmetric tops, have diagonal dipole matrix elements which give rise to zero frequency or nonresonant absorption. Pressure broadening in nonresonant and resonant microwave spectra of gases as well as the transition from resonant to nonresonant absorption with increasing pressure have been treated in a unified way in the impact approximation by Ben-Reuven.[31,32] His work is based on the theories of Baranger,[23–25] Kolb and Griem,[26] and Fano.[27] Starting from a different point of view, Birnbaum[33] has developed a theory of nonresonant absorption and relaxation in gases which gives results similar to that of Ben-Reuven. The theory of nonresonant absorption and its relation to experiment is briefly discussed in Section V.

To round out this outline of theoretical developments in spectral line broadening, reference may be made to the work of Van Kranendonk and Fiutak[34–36] who have extended the impact nonadiabatic theory to Raman spectral lines, and to Galatry[37] and von Roos[38] who have treated the simultaneous effect of Doppler and collision broadening. The considerable advances in the quantum theory of pressure broadened lines in plasmas have been reviewed by Margenau and Lewis.[39]

C. The Impact Approximation

Impact theories of pressure broadening are a generalization of Lorentz's classical theory which assumes that the sufficiently close collisions interrupt the radiation process completely, while the more distant collisions do not influence the radiation process at all. The emitted (or absorbed) radiation then consists of monochromatic wave trains of finite duration. This situation is schematically represented in Figure 1*a*, where the radiation is interrupted at precisely the instant that two molecules, represented by spheres, collide. In Figure 1*b*, the molecules are represented more realistically by an inner hard sphere, representing the region of the repulsive forces, and an outer sphere representing the

region of the molecular forces responsible for the interruption of the radiation. The duration of collision τ_c is the time that the outer spheres are interpenetrating and the molecular interactions are extremely

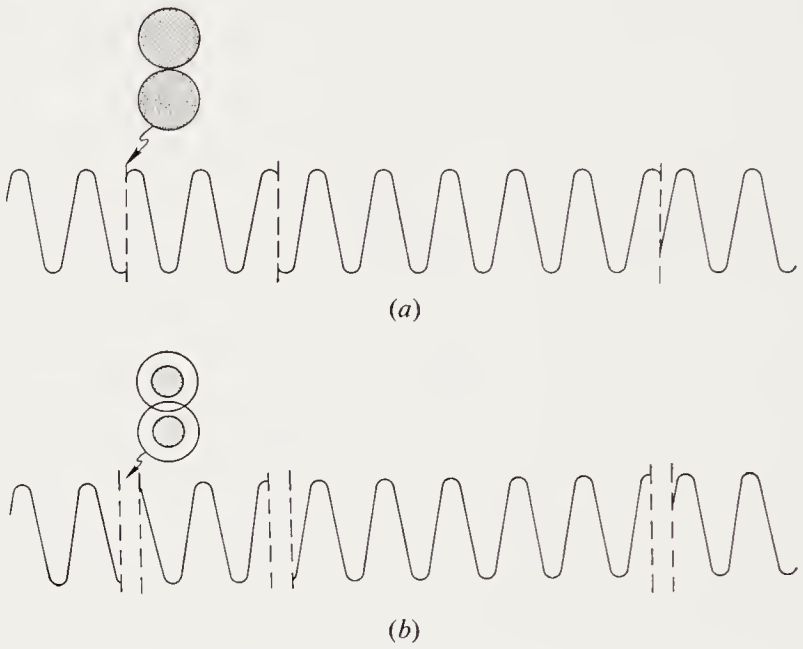

Fig. 1. Radiation from a molecule interrupted by collisions. Molecule represented by (*a*) a sphere with the optical diameter, and (*b*) an inner hard-sphere and an outer sphere with the optical diameter.

strong. Fortunately, it is legitimate to neglect the direct influence of the very complex happenings during the collision on the absorption spectrum if the duration of collision is small compared with the average time, τ, between collisions. This will be true for relatively small values of the density, where only binary collisions are of importance.

The assumptions of binary collisions and $\tau_c \ll \tau$, made universally in all impact theories of pressure broadening, are known as the impact approximation. Only the final changes produced by the collisions are taken into account, while the direct influence of the happenings during collision on the spectrum is entirely neglected. Pressure-induced absorption is thus excluded in impact theories.

Treatments of line shape from the correlation function approach start with the equation for the spectral intensity,

$$I(\omega) = \int_{-\infty}^{\infty} dt\varphi(t) \exp\left[it(\omega_{if} - \omega)\right] \tag{1}$$

where $\varphi(t)$ is the correlation function and ω_{if} is the frequency of the transition $i \rightarrow f$. The impact approximation, based on the requirement that $t \gg \tau_c$, leads to a correlation function of the form

$$\varphi(t) = \gamma e^{-Nv\sigma t} \tag{2}$$

N is the number of dipoles per cc, v is the mean relative velocity, and σ is the optical cross section which, in general, is complex. It is easy to see on substituting Eq. (2) into Eq. (1), that a Lorentz line shape is obtained with a width and shift expressed in terms of cross sections.

II. WIDTHS OF RESONANT LINES

A. Anderson's Theory of Pressure Broadened Lines

Anderson's theory of pressure broadening[5] has been discussed in considerable detail and extended by Tsao and Curnutte.[40] It has also been discussed by Townes and Schawlow,[3] Ch'en and Takeo,[41] and Breene.[6,7] This treatment follows the work of Tsao and Curnutte and emphasizes the basic assumptions in the theory and the simplifications introduced to make the calculations more tractable.

These assumptions are as follows:

1. In the commonly used impact approximation, it is assumed that (*a*) the duration of collision is small compared with the time between collisions, and (*b*) the collisions are binary and, hence, the resulting perturbation is proportional to gas pressure.

2. The translational motions of the molecules are not treated quantum mechanically, but are taken to follow classical prescribed paths. Since the range of the intermolecular force is several times larger than the wave packet (de Broglie waves) associated with a moving molecule —except for very light molecules—the wave packet may be considered as a point without large error. In very close collisions this is a poor assumption, but the errors introduced are unimportant when the interaction completely interrupts the radiation. On the other hand, collisions near the limit of the effective collision radius must be treated accurately; however, the wave packet for each molecule, in almost all cases, may be considered sufficiently small compared with the collision radius to make the classical path a good approximation.

3. The spectral lines are well resolved. This makes the theory inapplicable to overlapping spectral lines coupled by collisions and to

nonresonant absorption which may be regarded as arising from coupled lines at zero frequency.

On the basis of these assumptions and the use of a suitably generalized Fourier integral theory, Anderson[5] computed the spectrum of radiation emitted from molecules interrupted by quantum transitions and modulated by phase shifts produced by molecular interactions. He obtained a correlation function of the form of Eq. (2) which gives the Lorentz line shape,

$$\alpha = \frac{8\pi^2 N_1 \rho_i}{3ckT} |\mu_{fi}|^2 v^2 \frac{\Delta v}{(v - v_{fi} - \Delta v_s)^2 + \Delta v^2} \tag{3}$$

where

N_1 = number of absorbing molecules per cubic centimeter in the absorption cell,

ρ_i = fraction of these molecules in the lower of the two states involved in the transition,

$|\mu_{fi}|^2$ = square of the dipole moment matrix element for the transition summed over all directions in space,

v = frequency in Hz,

Δv = the line half-width at half amplitude,

Δv_s = the shift in resonance frequency, v_{fi},

c = velocity of light,

k = Boltzmann's constant,

T = absolute temperature.

The line width and shift are given by

$$2\pi\Delta v = N_1 v_{11} \sigma'_{11} + N_2 v_{12} \sigma'_{12} \tag{4}$$

$$2\pi\Delta v_s = N_1 v_{11} \sigma''_{11} + N_2 v_{12} \sigma''_{12} \tag{5}$$

where σ' and σ'' are, respectively, the real and imaginary parts of the optical cross section, and the subscripts 1 and 2 refer, respectively, to the absorber and perturber.* Since it is assumed that all molecules of a given type have the same velocity, v is the mean relative velocity. Microwave measurements have demonstrated that at low pressures and in the vicinity of the resonance frequency, the line shape is accurately represented by Eq. (3), and that Δv is proportional to pressure over a wide range of low pressures.[3]

The cross section is computed from

$$\sigma = \int_0^\infty 2\pi b \, db S(b) \tag{6}$$

* For self-broadening, $N_2 = 0$.

where

$$S(b) = 1 - \sum_{d} \sum_{J'_2} \frac{C(J_f 1 J_i; M_f M M_i) C(J_f 1 J_i; M'_f M M'_i)}{(2J_i + 1)(2J_2 + 1)}$$
$$\times \langle J_f M_f J_2 M_2 | \, T^{-1}(b) \, | J_f M'_f J'_2 M'_2 \rangle \langle J_i M'_i J'_2 M'_2 | \, T(b) \, | J_i M_i J_2 M_2 \rangle \tag{7}$$

and d signifies all the degenerate quantum numbers, M_i, M'_i, M_f, M'_f, M_2, M'_2, M. The initial and final states of the radiating molecule* are designated, respectively, by subscripts i and f, and the initial state of the perturbing molecule is designated by subscript 2. States connected to the initial states by the intermolecular potential are designated by a prime. J and M are, respectively, the rotational and degenerate quantum numbers; $C(\ )$ is a Clebsch-Gordan coefficient. The collision operators $T(b)$ and $T^{-1}(b)$ for the internal states of the molecules are defined by the equations of motion

$$i\hbar \dot{T} = H'_c(t) T \tag{8}$$

$$i\hbar \dot{T}^{-1} = -T^{-1} H'_c(t) \tag{9}$$

where

$$H'_c = U(t)^{-1} H_c U(t) \tag{10}$$

H_c is the intermolecular potential, and $U(t)$ is defined by

$$U(t) = \exp\left[-(i/\hbar)(H_1 + H_2)t\right]$$

where $H_1 + H_2$ is the unperturbed Hamiltonian containing only the internal coordinates of molecules 1 and 2.

To see the meaning of $S(b)$, let us consider the special case of no intermolecular potential, $H_c = 0$, in which case Eqs. (8) and (9) give $T_0 = T_0^{-1} = 1$. Then it is readily found that $S_0(b) = 0$, and consequently $\sigma = 0$. On the other hand, from the unitarity of the collision operator S(b), it follows that $|S(b)|$ can never exceed unity. $|S(b_0)| = 1$ means that a collision with impact parameter b_0 interrupts the radiation process completely. Thus $S(b)$ may be regarded as a weight factor which indicates whether or not a collision is effective in disturbing the molecular radiation. The probability of a collision with impact parameter b is proportional to $2\pi b \, db$.

* Molecule 1 is referred to as either the radiating or absorbing molecule.

If $H_c(t)$ commutes with $H_1 + H_2$, then Eq. (8) is solved by

$$T(b) = \exp\left[-(i/\hbar)\int_{t_0}^{t} H_c'(t')\,dt'\right] \tag{11}$$

The commutivity requirement demands for all levels that $E_\beta - E_\alpha = 0$, where

$$\begin{aligned} E_\beta &= E_1' + E_2' \\ E_\alpha &= E_1 + E_2 \end{aligned} \tag{12}$$

However, it has been argued that for the particular levels considered, it is only necessary that[5,42]

$$|E_\beta - E_\alpha| \ll \hbar v/b \tag{13}$$

This inequality may be written as

$$k = |\omega_\beta - \omega_\alpha|\,(b/v) \ll 1 \tag{14}$$

which is roughly the ratio of the time b/v required for the collision to be completed to the time $1/|\omega_\beta - \omega_\alpha|$ for the molecular wave functions to change phase. For microwave transitions, k is much less than unity, signifying fast collisions with negligible change in phase.

A series expansion of $T(b)$ and $T^{-1}(b)$ to the second order, and the substitution of these results in Eq. (7) give for the first-order terms

$$S_1(b) = i\left[\sum_{M_i,M_2} \frac{\langle J_i M_i J_2 M_2|\ P\ |J_i M_i J_2 M_2\rangle}{(2J_i+1)(2J_2+1)} - \sum_{M_f,M_2} \frac{\langle J_f M_f J_2 M_2|\ P\ |J_f M_f J_2 M_2\rangle}{(2J_f+1)(2J_2+1)}\right] \tag{15}$$

The second-order terms in the expansion of $T(b)$ and $T^{-1}(b)$ give

$$S_2(b)_0 = \frac{1}{2}\left[\sum_{\substack{M_i,M_2\\ M_i',M_2'}} \sum_{J_i'J_2'} \frac{|\langle J_i' M_i' J_2' M_2'|\ P\ |J_i M_i J_2 M_2\rangle|^2}{(2J_i+1)(2J_2+1)} + \sum_{\substack{M_f M_2\\ M_f' M_2'}} \sum_{J_f'J_2'} \frac{|\langle J_f' M_f' J_2' M_2'|\ P\ |J_f M_f J_2 M_2\rangle|^2}{(2J_f+1)(2J_2+1)}\right] \tag{16}$$

$$S_2(b)_m = -\sum_d \sum_{J_2'} \frac{C(J_f 1 J_i; M_f M M_i) C(J_f 1 J_i; M_f' M M_i')}{(2J_i+1)(2J_2+1)} \times \langle J_f M_f J_2 M_2|\ P\ |J_f M_f' J_2' M_2'\rangle \langle J_i M_i' J_2' M_2'|\ P\ |J_i M_i J_2 M_2\rangle \tag{17}$$

The operator P is given by

$$P = \hbar^{-1} \int_{-\infty}^{\infty} H_c'(t)\, dt \tag{18}$$

where $H_c'(t)$ is defined by Eq. (10). Because of the impact approximation, the time integration of the interaction $H_c(t)$ can be taken between the limits $\pm\infty$ since dt can contain, at most, a single collision.

The first-order term, $S_1(b)$, is imaginary and consequently contributes to the frequency shift, but not to the line width. Although frequency shifts are frequently observed in infrared and optical spectra, only some results of frequency shifts in the microwave 3,3 inversion line of NH_3 due to self-broadening and foreign-gas broadening have been reported.[43] These shifts, of the order $10^{-2}\,\Delta\nu$, are about one to two orders of magnitude smaller than in infrared spectra. This is to be expected because adiabatic collisions, i.e., those which do not change the state of the molecule, are of little importance in the microwave region where the molecular state is changed in practically all collisions. Matrix elements governing the change of state are found in $S_2(b)$ which is real and contributes to the line width.

In the most general formulation of the problem of the interaction between the radiating molecule 1 and the colliding molecule 2, the Hamiltonian of the complete interaction may be expanded into a series of multipoles of differing polarity, strength, and range.[2,44] The three terms of longest range are dipole–dipole, $\mu_1\mu_2R^{-3}$, dipole–quadrupole, $\mu_1Q_2R^{-4}$, and quadrupole–quadrupole, $Q_1Q_2R^{-5}$. The forces of the next shorter range R^{-6} are of several types and include higher-order terms arising from the fact that the multipoles are not point multipoles as well as the induction force, $\mu_1^2\alpha_2R^{-6}$, and the dispersion force. Only the anisotropic part of the dispersion force makes a contribution to $S_2(b)$. Numerous other poles of shorter range than R^{-6} will also be present. Only one has been found to be significant in microwave pressure broadening thus far, $\mu_1Q_1\alpha_2/R^7$, the interaction of Q_1 with the dipole induced in molecule 2 by μ_1, and the interaction of μ_1 with the dipole induced by Q_1. Shorter-range interactions such as those due to repulsive forces have also been considered.[44] Expressions for the potentials mentioned here are given in the appendix to this section.

The sums in $S_2(b)$ can be evaluated with some generality for a variety of intermolecular potentials for symmetric top and linear molecules by expanding the interaction operator H_c as a sum of spherical harmonics

of the internal coordinates of the molecules,

$$H_c = \sum_{\substack{k_1 k_2 \\ l_1 l_2}} \frac{C_{l_1 l_2}^{k_1 k_2}}{R^s} Y_{l_1}^{k_1}(1) Y_{l_2}^{k_2}(2) \tag{19}$$

where $C_{l_1 l_2}^{k_1 k_2}$ is a constant independent of R and angular coordinates and depends on the type of the interaction. The time dependence of $H_c[R(t)]$ is due to the translational motion of the molecules (classical path assumption), and the time integration in Eqs. (16) and (17) can be taken independently of the matrix elements. For each type of intermolecular interaction p with potential $H_c^{(p)}(t)$, $S_2^{(p)}(b)$ may be obtained from Eqs. (16) and (17) in the form,[40]

$$\begin{aligned} S_2^{(p)}(b) = {} & \frac{C_p}{b^n} \sum_{J_i'}{}' \sum_{J_2'} C(J_i k_i J_i'; K_i 0 K_i)^2 C(J_2 k_2 J_2'; K_2 0 K_2)^2 f_p(k) + (i \to f) \\ & + \left\{ \frac{C_p}{b^n} C(J_i k_i J_i; K_i 0 K_i)^2 \sum_{J_2'} C(J_2 k_2 J_2'; K_2 0 K_2)^2 f_p(k) \right. \\ & \left. + (i \to f) + S_2^{(p)}(b)_m \right\} \end{aligned} \tag{20}$$

where

$$\begin{aligned} S_2^{(p)}(b)_m = {} & \frac{2 C_p \phi_p}{b^n} (2J_i + 1)^{1/2} (2J_f + 1)^{1/2} C(J_i k_i J_i; K_i 0 K_i) \\ & \times C(J_f k_f J_f; K_f 0 K_f) W(J_i J_f J_i J_f; 1 k_i) \\ & \times \sum_{J_2'} C(J_2 k_2 J_2'; K_2 0 K_2)^2 f_p(k) \end{aligned} \tag{21}$$

and $(i \to f)$ designates a term to be obtained from the preceding one by replacing the subscript i by f. The prime on the J_i' sum signifies that the $J_i \to J_i$ term is to be omitted. The functions C and W are, respectively, Clebsch-Gordan and Racah coefficients.[45] The quantities C_p and ϕ_p are defined for a variety of intermolecular potentials in Table I. The functions $f_p(k)$,* where k is defined by Eq. (14), depend on the degree to which the internal energy of the absorbing and perturbing molecules is conserved in the collision. As shown in Figure 2*a*, these functions equal unity for $k = 0$ (internal energy conserved), and approach zero when k becomes much greater than unity.

* These functions (see Table I for notation) are tabulated in ref. 45a.

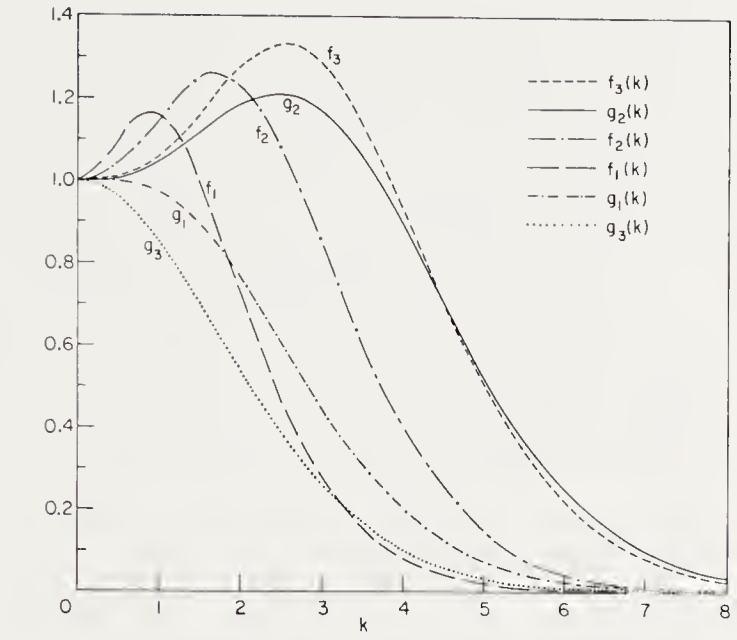

(*a*)

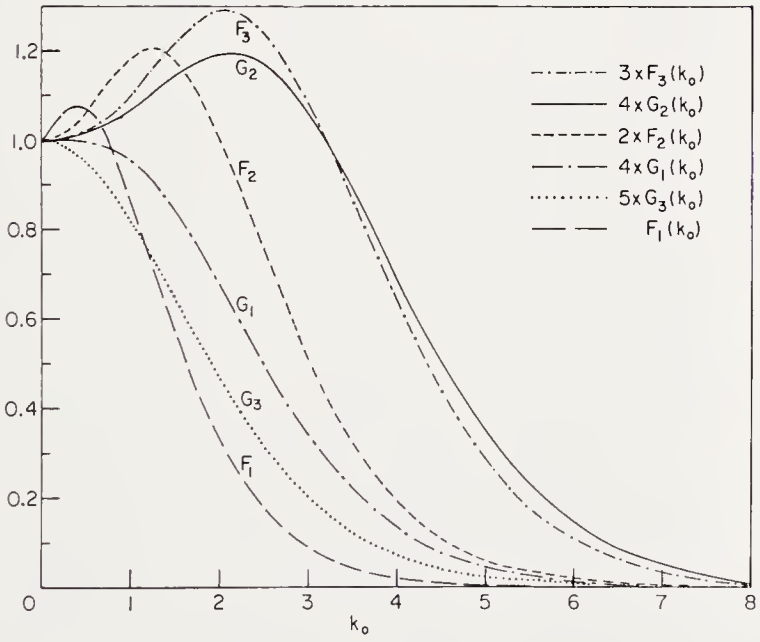

(*b*)

Fig. 2. (*a*) Off-resonance functions $f(k)$ and $g(k)$ as a function of k. Table I shows the intermolecular interactions for which these functions apply. k is defined by Eq. (24). (*b*) Off-resonance functions $F(k_0)$ and $G(k_0)$ as a function of k_0. Note that the curves plotted are $F_1(k_0)$, $2F_2(k_0)$, $3F_3(k_0)$, $4G_1(k_0)$, $4G_2(k_0)$, and $5G_3(k_0)$.

TABLE I

Quantities in Eqs. (20) and (21) for Various Intermolecular Potentials[a]

Type of interaction							
p	$H_c^{(p)}$[b]	n	k_1	k_2	C_p[c]	$f_p(k)$[d]	Ref.
1	Dipole–dipole	4	1	1	$\frac{4}{9}\left(\frac{\mu_1\mu_2}{\hbar v}\right)^2$	$f_1(k)$	40
2	Dipole–quadrupole	6	1	2	$\frac{16}{45}\left(\frac{\mu_1 Q_2}{\hbar v}\right)^2$	$f_2(k)$	40
3	Quadrupole–dipole	6	2	1	$\frac{16}{45}\left(\frac{Q_1\mu_2}{\hbar v}\right)^2$	$f_2(k)$	—
4	Quadrupole–quadrupole	8	2	2	$\frac{16}{25}\left(\frac{Q_1 Q_2}{\hbar v}\right)^2$	$f_3(k)$	40
5	Dipole–induced-dipole	10	2	0	$\frac{21\pi^2}{640}\left(\frac{\mu_1^2\alpha_2}{\hbar v}\right)^2$	$g_1(k)$	40

6	Dispersion	*a.*	10	2	0	$\frac{21\pi^2}{10{,}240}\left[\frac{I_1 I_2}{I_1+I_2}\frac{(\alpha_1''-\alpha_1')\alpha_2}{\hbar v}\right]^2$	$g_1(k)$	46
		b.	10	2	2	$\frac{559\pi^2}{1229\times 10^3}\left[\frac{I_1 I_2}{I_1+I_2}\frac{(\alpha_1''-\alpha_1')(\alpha_2''-\alpha_2')}{\hbar v}\right]^2$	$g_2(k)$	46
7	Quadrupole–induced-dipole[e]		12	1	0	$\frac{27\pi^2}{32}\left(\frac{\mu_1 Q_1 \alpha_2}{\hbar v}\right)^2$	$g_3(k)$	47
				3	0	$\frac{153\pi^2}{1792}\left(\frac{\mu_1 Q_1 \alpha_2}{\hbar v}\right)^2$	$g_4(k)$	47

[a] $\phi_{1,2}=(-1)^{J_i+J_f+1}$, $\phi_{3,4,5,6,7}=(-1)^{J_i+J_f}$. The product of ϕ and the phase factor of the Racah coefficient, see Eq. (21), is always negative.

[b] The effect of the repulsive interaction on line broadening is considered in Sections III-B-2 and III-B-5.

[c] μ is the dipole moment, Q is the quadrupole moment, α is the isotropic or mean polarizability, α'' and α' are the two components of polarizability in a molecule with axial symmetry, I is the ionization energy, and v is the mean relative velocity.

[d] This column gives the notation for the functions $f_p(k)$ that are commonly in use.

[e] The contribution of the $k_1=3$ term to the collision cross section will not be greater than 10%.[47]

It is useful to write Eqs. (20) and (21) in the form

$$S_2^{(p)}(b) = (1/b^n)[A_{p,i}f_{p,i}(k) + A_{p,f}f_{p,f}(k) + A_{p,m}f_{p,m}(k)] = A_p/b^n \quad (22)$$

When more than one type of interaction is involved, as is usually the case, the contributions from the various interactions simply add and

$$S_2(b) = \sum_p S_2^{(p)}(b) \quad (23)$$

This follows from the fact that there are no interference terms among the various orders of the spherical harmonics for the same molecule.

The resonance factor k is defined by

$$k = (b/v\hbar)(E_\beta - E_\alpha) \quad (24)$$

where $E_\beta - E_\alpha$ is the total change in the rotational energy of the radiating and colliding molecules. Since it is sufficiently accurate for our purpose to assume that the molecules are rigid and that there is no frequency perturbation due to centrifugal distortion, the expression for k for linear and symmetric top molecules becomes

$$k = (2\pi b/v)\{B_1[J_i'(J_i' + 1) - J_i(J_i + 1)] + B_2[J_2'(J_2' + 1) - J_2(J_2 + 1)]\} \quad (25)$$

where B is the rotational constant in Hz. The expression for k when molecule 1 is in state f is Eq. (25) with i and i' replaced by f and f'. If the perturber is spherically symmetric, J_2 and J_2' must be set equal to zero. Although k may be positive or negative, only its magnitude is important in $f_p(k)$. The expressions for $f_p(k)$ are given in the references listed in Table I. It will be seen later that a great simplification in the theory occurs when it is possible to replace $f(k)$ by unity.

The expressions for $S_2(b)$, (20) and (21), are applicable for linear and symmetric top molecules. To extend these formulas to asymmetric rotors for dipole–dipole, dipole–quadrupole, and the most important part of the quadrupole–induced-dipole interactions, i.e., interactions involving dipole transitions of the asymmetric top, it is only necessary to replace the dipole terms, $C(J1J';K0K)^2$, by the line strength for type B transitions, tabulated in references 48 and 49, divided by $(2J + 1)$.[50] Since there are no diagonal dipole matrix elements of asymmetric rotors, $S_2(b)_m = 0$. The energy of the rotational levels of asymmetric rotors can be calculated from the equations and tables given in reference 50a. Knowing the rotational energies, one can compute k

from Eq. (24). The special case of the inversion spectrum of NH_3 will be discussed in Section III-E.

The first two terms in Eq. (20) may be interpreted as the contributions to the cross section from interruption of the radiation process by inelastic collisions, i.e., collisions which change the initial and final rotational states of the radiating molecule. The terms in the curly braces may be interpreted as the contributions from elastic collisions which leave the initial and final rotational states of the radiating molecule unchanged except for M transitions, e.g., $J_i M_i\rangle \rightarrow J_i M_i'\rangle$. Such collisions between components of the same level do not interrupt the radiation process, but produce phase shifts and amplitude modulation of the radiation (see Sec. II-C). The so-called mixed term, $S_2(b)_m$, is negative and occurs for all collisions which are elastic for the radiating molecule. The interference or correlation effects represented by $S_2(b)_m$ are responsible for the fact that the phase shifts and amplitude modulation produced in the initial and final states do not contribute independently to the resulting effect on the radiation. It has been shown that except for the first few J_1 states, the effect on the line width of the terms in Eq. (20) in the curly braces is negligible.[51]

Once $S_2(b)$ is known, the cross section is evaluated from Eq. (6). However, the requirement imposed by perturbation theory that $S_2(b) \ll 1$ breaks down even for distant collisions when the interaction is strong. The widely used interpolation scheme adopted by Anderson[5] for this case gives*

$$\sigma = \pi b_0^2 + \int_{b_0}^{\infty} 2\pi b S_2(b)\, db \tag{26}$$

where b_0 is determined by the condition

$$S_2(b_0) = 1 \tag{27}$$

and $S_2(b)$ is taken to be unity from $b = 0$ to $b = b_0$. With $S_2(b)$ given by Eq. (22), Eq. (26) becomes

$$\sigma = \pi b_0^2 \left\{ 1 + \frac{1}{b_0^4} \sum_{\kappa} A_{1,\kappa} F_{1,\kappa}(k_0) + \frac{1}{b_0^6} \sum_{\kappa} A_{2,\kappa} F_{2,\kappa} k_0 + \cdots \right\} \tag{28}$$

where $\kappa = i, f, m$. The factor k_0 is given by Eq. (25) with b replaced by

* Unless otherwise noted, all calculations of line width discussed in this paper use Eqs. (26) and (27).

b_0, and the $F(k_0)$ functions[4,5a] are defined in the references listed in Table I. These functions are plotted in Figure 2*b*. If at the distance at which repulsive forces set in, say b_k, $S(b_k) < 1$, then instead of Eq. (28), we have

$$\sigma = \pi b_k^2 S_2(b_k) + 2\pi \int_{b_k}^{\infty} S_2(b) b \, db \tag{29}$$

The partial cross section given by Eq. (28) or Eq. (29), actually $\sigma_{J_1K_1,J_2K_2}$, must be averaged over all states of molecule 2 and the degenerate K states of molecule 1, namely,

$$\sigma_{J_1} = \sum_{K_1 J_2 K_2} \rho_{K_1} \rho_{J_2 K_2} \sigma_{J_1 K_1, J_2 K_2} \tag{30}$$

where ρ is the fractional number of molecules in the indicated states. σ_{J_1}, or $\sigma_{J_1K_1}$ when the K degeneracy is removed by centrifugal distortion, is the cross section associated with the spectral line $J \to J+1$, $K \to K$. The optical collision diameter is defined by

$$\sigma_{J_1} = \pi b_{J_1}^2 \tag{31}$$

Before completing this discussion of Anderson's theory, we summarize the approximations that have been introduced to make the numerical calculations tractable. (Basic assumptions in the theory are discussed at the beginning of this section.)

1. All molecules assumed to have the same velocity—the mean velocity. When $k = \omega_{\alpha\beta} b/v \approx 0$, the line width will depend on the mean relative velocity as $\Delta\nu \sim v^{(n-1)/n}$, and the only difference between using $\langle v \rangle$ in this expression and taking the average $\langle \Delta\nu \rangle$ is the small difference between $\langle v \rangle^{(n-1)/n}$ and $\langle v^{(n-1)/n} \rangle$. The error is small even if $k \neq 0$.

2. Approximations used in the coupling of $S_2(b)$ for small and large values of b. Anderson[5] gave three ways of coupling $S_2(b) \ll 1$ to $S_2(b) = 1$ which are illustrated in Figure 3. Approximation *1* is

$$S_2(b)_1 = 1 - \cos\left[2S_2(b)\right]^{1/2} \tag{32}$$

and approximation *3* is

$$S_2(b)_3 = 1 - \exp\left[-2S_2(b)\right] \tag{33}$$

Approximation *2* is given by Eqs. (26) and (27). However, he suggested that the true curve for $S(b)$ might resemble either of the curves labeled

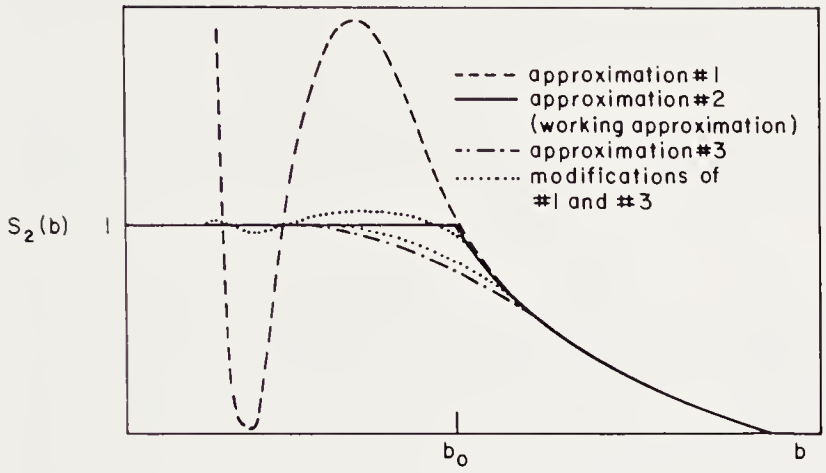

Fig. 3. Different approximations used in the coupling of $S_2(b)$ for small and large values of b (after Anderson[5]).

"modification" in Figure 3. For the simple case of self-broadening of the inversion spectrum of NH_3, Anderson found that the widths obtained with approximations *1* and *3* were about 12% higher and lower, respectively, than the width obtained with approximation *2*.

3. Choice of the minimum value of b. For weak interactions where $S(b) < 1$, b must have some lower limit. A reasonable value that is frequently used is the kinetic diameter of the colliding molecules. However, this value really has no precise significance but must be considered a catchall for all the shorter-range interactions, attractive as well as repulsive. However, when most of the collisions are so strong that $S(b_0) = 1$ when $b_0 > b_k$, then clearly the exact value of b_k hardly has any effect on the computed cross section.

4. Straight-line trajectory. Taking the collision trajectory to be a straight line is satisfactory for collisions with large impact parameters, i.e., $b > b_k$. Although such collisions are capable of inducing transitions, the energy of microwave transitions is so small compared with the thermal energy that the reaction on the translatory motion is negligible. For close-in collisions, however, the trajectory will certainly be modified by the spherical part of the intermolecular potential, and a straight-line path will not be a good approximation to the actual trajectory.

Appendix. Intermolecular Potentials[51a]

a. Electrostatic Contributions. The electrostatic contributions to the intermolecular potential energy result from the interactions of various

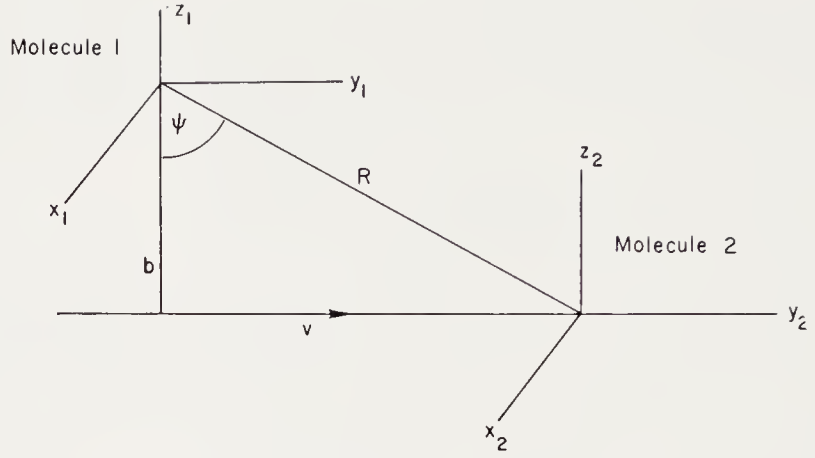

Fig. 4. Coordinate axes for the radiating molecule, 1, and perturbing molecule, 2.

multipole moments. A set of coordinates as shown in Figure 4 is used for the two molecules. In the straight-line path approximation, R, the intermolecular distance is related to b, the distance of closest approach, by

$$R = (b^2 + v^2t^2)^{1/2} \tag{A1}$$

The angle Ψ is given by

$$\begin{aligned} \sin \Psi &= vt/R \\ \cos \Psi &= b/R \end{aligned} \tag{A2}$$

(1) *Dipole–Dipole Interaction.*[40] The interaction between two polar molecules is given by

$$H_c^{(1)}(t) = (\mu_1\mu_2/R^3)[\mathbf{e}_1 \cdot \mathbf{e}_2 - 3(\mathbf{e}_1 \cdot \mathbf{R}_0)(\mathbf{e}_2 \cdot \mathbf{R}_0)] \tag{A3}$$

where μ_1 and μ_2 are the magnitudes of the dipole moments, $\mathbf{e}_1$ and $\mathbf{e}_2$ are, respectively, the unit vectors along the direction of $\boldsymbol{\mu}_1$ and $\boldsymbol{\mu}_2$, and $\mathbf{R}_0$ is the unit vector along R. In terms of the coordinates shown in Figure 4, $\mathbf{e} \cdot \mathbf{R}_0$ is given by

$$\mathbf{e} \cdot \mathbf{R}_0 = \sin \theta \sin \phi \sin \Psi - \cos \theta \cos \Psi \tag{A4}$$

(2) *Dipole–Quadrupole Interaction.*[40] Several different definitions of quadrupole moment are in use, unfortunately, so that care is needed in interpreting results in the literature. Buckingham[51b] defines the molecular quadrupole moment, Q, for molecules whose charge distribution is axially symmetric about any axis, say the z axis, as

$$Q = Q_{zz} = -2Q_{xx} = -2Q_{yy} \tag{A5}$$

$$Q = \tfrac{1}{2}\sum_i e_i(3z_i^2 - r_i^2) \tag{A6}$$

This is the definition used here. Hirschfelder et al.[51a] define quadrupole moment instead by

$$Q' = \sum_i e_i(3z_i^2 - r_i^2) \tag{A7}$$

where $Q' = 2Q$. To complicate matters further, some of the values of the quadrupole moments in the literature are for rotating molecules. These values are average values of the quadrupole moment in a space-fixed coordinate system. They depend upon the exact rotational state of the molecule, but usually they are about half the value for the non-rotating molecule, i.e., $Q'_R = Q'/2$ and $Q_R = Q/2$.

The dipole–quadrupole interaction is given by

$$H_c^{(2)} = \tfrac{3}{2}(\mu_1 Q_2/R^4)[-(\mathbf{R}_0 \cdot \mathbf{e}_1) - 2(\mathbf{e}_1 \cdot \mathbf{e}_2)(\mathbf{R}_0 \cdot \mathbf{e}_2) + 5(\mathbf{R}_0 \cdot \mathbf{e}_2)^2] \tag{A8}$$

where $\mathbf{e}_1$, $\mathbf{e}_2$ are, respectively, the unit vectors along the direction of $\boldsymbol{\mu}_1$ and the quadrupole moment of molecule 2. The sense of $\mathbf{e}_2$ is obviously immaterial.

(3) *Quadrupole–Quadrupole Interaction.*[40] The next term in the multipolar expansion arises from the interaction between the dipole moment of one molecule and the octupole moment of the other, or between the quadrupole moments of both molecules. The interaction Hamiltonian of the latter is given by

$$H_c^{(4)}(t) = \tfrac{3}{4}(Q_1 Q_2/R^5)[1 - 5(\mathbf{R}_0 \cdot \mathbf{e}_1)^2 - 5(\mathbf{R}_0 \cdot \mathbf{e}_2)^2 + 2(\mathbf{e}_1 \cdot \mathbf{e}_2)^2 - 20(\mathbf{R}_0 \cdot \mathbf{e}_1)(\mathbf{R}_0 \cdot \mathbf{e}_2)(\mathbf{e}_1 \cdot \mathbf{e}_2) + 35(\mathbf{R}_0 \cdot \mathbf{e}_1)^2(\mathbf{R}_0 \cdot \mathbf{e}_2)^2] \tag{A9}$$

The effect of the dipole–octupole interaction on microwave line widths has not been studied.

b. Induction Contributions. A molecule with some multipole moment interacting with a molecule which is spherically symmetric induces in the latter a dipole moment.

(1) *Dipole–Induced-Dipole.*[40] The permanent dipole of molecule 1 interacts with the dipole induced in molecule 2 by molecule 1 according to

$$H_c^{(5)}(t) = -(\alpha_2 \mu_1^2/R^6)[1 + 3(\mathbf{e}_1 \cdot \mathbf{R}_0)^2] \tag{A10}$$

where α_2 is the isotropic polarizability.

(2) *Quadrupole–Induced-Dipole.*[47] The interaction Hamiltonian of two molecules when Q_1 interacts with $\alpha_2\mu_1$, the dipole induced in 2 by μ_1, and μ_1 interacts with $\alpha_2 Q_1$, the dipole induced in 2 by Q_1, is given by

$$H_c^{(7)}(t) = -(6\mu_1 Q_1 \alpha_2 / R^7)(\mathbf{e}_1 \cdot \mathbf{R}_0)^3 \tag{A11}$$

c. Dispersion Contributions. In the quantum mechanical calculation of the energy of interaction between two nonpolar molecules, the London dispersion force appears in the second-order perturbation terms. In classical language, at any instant the electrons in a molecule have a definite configuration so that the molecule has an instantaneous dipole moment, even if it possesses no permanent electric moment. This instantaneous dipole in molecule 1 induces a dipole in molecule 2, and vice versa. This interaction between two molecules with axial symmetry can be written in terms of polarizability anisotropies and ionization energies, I_1 and I_2, as[47]

$$H_c^{(6)}(t) = -\frac{1}{4R^6}\frac{I_1 I_2}{I_1 + I_2}\{(\alpha_1'' - \alpha_1')(\alpha_2'' - \alpha_2')[\mathbf{e}_1 \cdot \mathbf{e}_2 - 3(\mathbf{e}_1 \cdot \mathbf{R}_0) \times (\mathbf{e}_2 \cdot \mathbf{R}_0)]^2 + 3(\alpha_1'' - \alpha_1')\alpha_2'(\mathbf{e}_1 \cdot \mathbf{R}_0)^2 + 3\alpha_1'(\alpha_2'' - \alpha_2') \times (\mathbf{e}_2 \cdot \mathbf{R}_0)^2 + 3(\alpha_1\alpha_2' + \alpha_1'\alpha_2)\} \tag{A12}$$

provided the oscillator frequencies ν' and ν'' are approximately equal. The quantities $\mathbf{e}_1$ and $\mathbf{e}_2$ are the unit vectors along the polarizability ellipsoids of molecules 1 and 2, α'' and α' are the parallel and perpendicular components of the polarizability, and α is the mean polarizability.

The isotropic portion of this interaction is of no significance in line broadening since this interaction cannot induce transitions. However, Herman[52] has shown that when the center of dispersion force is displaced from the center of mass through a distance d, a new term of the form $-6(d/R')R'^{-6}P_1(\cos\theta')$ appears where R' and θ' are measured in the center-of-mass coordinates.

Buckingham[52a] has found a higher-order dispersion interaction varying as $\cos^3\theta/R^7$, which may make a significant contribution to pressure broadening in some cases.

d. Exchange Interaction. Equations which have been used to represent this interaction in pressure-broadening calculations are given in Sections III-B-2 and III-B-5.

B. Simplifications of Anderson's Theory

The computation of cross sections from Eq. (28) is complicated not only by the large number of terms that are involved, especially when several types of molecular interactions must be considered, but also because the functions $f_p(k)$ involve the impact parameter b making it necessary to solve Eq. (27) by iteration. This process must be carried out for each value of J_2 and K_2, since no algebraic expression for σ_{J_2,K_2} is available when $k \neq 0$. However, a great simplification in the calculation occurs when $k \simeq 0$ and $f_r(k) \simeq 1$, since there is then a simple analytic expression for the cross section.

For the purpose of examining the contribution of various types of transitions to the cross section, we write Eq. (20) in the form[36]

$$S_2(b) = S_{\text{el}} + S_{\text{inel}} + S'_{\text{inel}} + S''_{\text{inel}} \tag{34}$$

where for simplicity the superscript p has been omitted. S_{el} contains the elastic transition $\Delta J_{i,f} = 0$, $\Delta J_2 = 0$; and S_{inel}, S'_{inel}, and S''_{inel} contain terms involving rotational transitions for one or both molecules as shown in Table II. It may be noted that the bracketed term in Eq. (20) equals S_{el} plus S'_{inel} ($\Delta J_{i,f} = 0$, $\Delta J_2 = \pm k_2$), where k_2 is the order of the spherical harmonic in Eq. (19).* The S_{inel} term includes the case of exact resonance, i.e., $\Delta E_1 = \Delta E_2$.

For the rotational states of the perturbing molecule that are well populated, ΔE_2 is so great that $k \gg 1$, and we take $f(k) = 0$ for all inelastic transitions of molecule 2, except for exact resonance. Although in this case $k = 0$, the probability of such collisions is usually too small to be significant. With this in mind, we see from Table II that the terms S_{inel}, $S'_{\text{inel}}(\Delta J_{i,f} = \pm 0, \Delta J_2 = \pm k_2)$, and S''_{inel} may be neglected. The remaining terms, provided ΔE_i and ΔE_f are small as is true for microwave lines, result from collisions elastic in J_2, i.e., S_{el}, and $S'_{\text{inel}}(\Delta J_{i,f} = \pm k_1, \Delta J_2 = 0)$. Then, keeping only these terms, we obtain from Eq. (20)

$$\begin{aligned} S_2^{(p)}(b) = (2C_p/b^n)&C(J_2 k_2 J_2; K_2 0 K_2)^2 \\ &\times [1 + \phi_p(2J_i + 1)^{1/2}(2J_f + 1)^{1/2} C(J_i k_i J_i, K_i 0 K_i) \\ &\times C(J_f k_f J_f; K_f 0 K_f) W(J_i J_f J_i J_f; 1 k_i)] \end{aligned} \tag{35}$$

* When molecule 2 is a symmetric top and $k_2 = 2$, for example, there are $\Delta J_2 = \pm 1$ transitions as well as the $\Delta J_2 = \pm 2$ transitions.

where we have used the fact that $\sum_{J_i} C(J_i k_i J_i'; K_i 0 K_i)^2 = 1$. It should be emphasized that Eq. (35) contains all the transitions for those interactions where the perturber is spherically symmetric.

TABLE II

Collision Factors and Types of Transitions

Collision factor	Transition[a]	Internal energy change
S_{el}	$\Delta J_i = 0, \Delta J_2 = 0$	0
S_{inel}	$\Delta J_i = k_i, \Delta J_2 = -k_2$	$\Delta E_i - \Delta E_2$
	$\Delta J_i = -k_i, \Delta J_2 = k_2$	$-\Delta E_i + \Delta E_2$
S'_{inel}	$\Delta J_i = k_i, \Delta J_2 = 0$	ΔE_i
	$\Delta J_i = -k_i, \Delta J_2 = 0$	$-\Delta E_i$
	$\Delta J_i = 0, \Delta J_2 = k_2$	ΔE_2
	$\Delta J_i = 0, \Delta J_2 = -k_2$	$-\Delta E_2$
S''_{inel}	$\Delta J_i = k_i, \Delta J_2 = k_2$	$\Delta E_i + \Delta E_2$
	$\Delta J_i = -k_i, \Delta J_2 = -k_2$	$-\Delta E_i - \Delta E_2$

[a] Also, the transitions obtained by replacing i by f; k is the order of the spherical harmonic involved in the intermolecular potential [Eq. (19)].

The results for $S_2^{(p)}(b)$ for a variety of interactions are summarized below,[51] where

$$Q(J_2, K_2) = \frac{[3K_2^2 - J_2(J_2+1)]^2}{(2J_2-1)J_2(J_2+1)(2J_2+3)} \tag{36}$$

$$Q_m(J_1, K_1) = \frac{3K_1^2 - J_1(J_1+1)}{(J_1+1)(2J_1+1)} \frac{3K_1^2 - (J_1+1)(J_1+2)}{(J_1+1)(2J_1+3)} \tag{37}$$

Dipole-dipole

$$S_2^{(1)}(b) = \frac{2C_1}{b^4} \frac{K_2^2}{J_2(J_2+1)} \left[1 - \frac{K_1^2}{(J_1+1)^2}\right] \tag{38}$$

Dipole–quadrupole

$$S_2^{(2)}(b) = \frac{2C_2}{b^6} Q(J_2,K_2)\left[1 - \frac{K_1^2}{(J_1+1)^2}\right] \tag{39}$$

Quadrupole–dipole

$$S_2^{(3)}(b) = \frac{2C_3}{b^6} \frac{K_2^2}{J_2(J_2+1)} [1 - Q_m(J_1,K_1)] \tag{40}$$

Quadrupole–quadrupole

$$S_2^{(4)}(b) = \frac{2C_4}{b^8} Q(J_2,K_2)[1 - Q_m(J_1,K_1)] \tag{41}$$

Dipole–induced-dipole

$$S_2^{(5)}(b) = \frac{2C_5}{b^{10}} [1 - Q_m(J_1,K_1)] \tag{42}$$

Dispersion

$$S_2^{(6)}(b) = \frac{2}{b^{10}} [1 - Q_m(J_1,K_1)][C_{6a} + C_{6b}Q(J_2,K_2)] \tag{43}$$

Quadrupole–induced-dipole

$$S_2^{(7)}(b) = \frac{2C_7}{b^{12}}\left[1 - \frac{K_1^2}{(J_1+1)^2}\right] \tag{44}$$

A small contribution (less than 10%) of a higher-order term is neglected in Eq. (44).

If the perturber is a linear molecule, $K_2 = 0$. With $K_1 = 0$, Eqs. (38)–(44) apply for microwave rotational lines of linear molecules. The simple formulas given here can be easily applied to determine the relative importance of various interactions responsible for the pressure broadening of a given line, and to obtain a preliminary value for an interaction parameter such as the quadrupole moment.

From Eqs. (26) and (27) we obtain, for the cross section due to a particular interaction,

$$\sigma = \pi[n/(n-2)]A_p^{2/n} \tag{45}$$

where

$$S_2^{(p)}(b) = A_p/b^n \tag{46}$$

The line width due to a particular interaction is given by

$$\Delta\nu = (N\bar{v}/2)[n/(n-2)]A_p^{2/n} \tag{47}$$

Equations (45) and (47) can easily be averaged over the states of molecule 2. However, when the perturbing molecule is linear and $K_2 = 0$, it is sufficiently accurate to replace $Q(J_2)$ by $\frac{1}{4}$.

It is easy to obtain the temperature dependence of the line width from Eq. (47) namely

$$\Delta\nu \propto T^{-(n+4)/2n} \tag{48}$$

by noting that $A_p \propto v^{4/n}$, $N \propto T^{-1}$, and $\bar{v} \propto T^{1/2}$.

Equation (45), obtained on the basis that $S(b_0) = 1$ when $b_0 > b_k$, shows that as the range of the interaction decreases, the cross section becomes quite insensitive to the exact value of A_p and hence to the intermolecular-force parameters. On the other hand, the cross section obtained from Eq. (29) when $S(b_k) < 1$,

$$\sigma = \pi[(n)/(n-2)]A_p/b_k^{n-2}$$

gives a much stronger dependence of the cross section on intermolecular-force parameters, and is now a sensitive function of the kinetic diameter, b_k.

The dipole–dipole broadening of microwave lines of the symmetric top molecules CH_3F, CHF_3, and PF_3 has been calculated from Eqs. (38) and (47), and from the complete equation for $S_2(b)$. The discrepancy between the line widths calculated from the complete and approximate expressions varies from 0–17%.[51] Calculations of the microwave broadening of foreign gas mixtures of CHF_3, OCS, and N_2O due to a variety of interactions using the approximate expressions for $S_2^{(p)}(b)$ to obtain $\sum_p S_2^{(p)}(b)$ differ from calculations based on the complete theory by 1–12% for $k < 0.2$.

A number of previous attempts have been made to simplify Anderson's theory by assuming that all collisions are resonant, i.e., $f_p = 1$.[53–56†] These authors start with $S_2(b)_0$ in the form given by Eq. (16), neglect $S_2(b)_m$ (justifiable only when $J_1 \gg 1$), and take a classical average of the coordinates of the perturbing molecule. This averaging procedure is not the

* Unpublished work by A. Rosenberg and G. Birnbaum.

† According to a private communication by Dr. Kiefer, the expressions for the cross section in ref. 54 are to be disregarded in favor of those given in ref. 53.

same as the procedure followed here, i.e., the results of the complete quantum treatment are used and only the terms involving $\Delta J_2 = 0$ transitions are kept.

Kiefer and Bushkovitch[53] have compared the collision diameters given by their simplified theory with experimental values for the dipolar self-broadening of linear molecules. The discrepancy between these values are large, in most cases by factors of 1.5–5. A large discrepancy is to be expected in this case since there is no term diagonal in J_2 and, consequently, the approximation $f_1(k) \simeq 1$ fails. They estimated the error* in their simplified formulas for the cross sections for the μQ, QQ, $\mu^2\alpha$, and dispersion interactions. These errors are much less than that for the $\mu\mu$ interaction, namely 30% for the μQ interaction decreasing to 10% for the dispersion interaction. De Wijn[57] has attempted to improve matters for the $\mu\mu$ interaction between linear molecules by taking a Boltzmann average of $S_2(b)$ over J_2 and then solving Eq. (27) for an average b_0. Although reasonable agreement with experimental values was obtained for molecules with dipole moments less than 10^{-18} esu, the agreement was poor for molecules with dipole moments greater than 10^{-18} esu.

C. Gordon's Theory of Pressure-Broadened Lines

Gordon[30] has developed a semiclassical theory of line width and line shift in gases which does not make the approximations of perturbation theory and a straight-line trajectory upon which Anderson's work is based. Gordon's result for the line width is

$$\Delta\nu = N\langle v \int_0^\infty [1 - P_{el} \cos\eta \cos^2(\tfrac{1}{2}\alpha)]b \, db\rangle \tag{49}$$

and for the line shift,

$$\Delta\nu_s = N\langle v \int_0^\infty P_{el} \sin\eta \cos^2(\tfrac{1}{2}\alpha) b \, db\rangle \tag{50}$$

The reorientation angle α is determined simply as the angle between the initial and final angular momentum vectors as shown in Figure 5. The rotational phase shift η is determined by comparing the direction of the dipole, at some time after the collision, with the reference direction which would have been reached at that time if the dipole had rotated freely in the initial plane up to intersection **i**, and then freely for the

* For $k \leq 0.5$.

rest of the time in the final plane. The probability of an elastic collision, P_{el}, may be estimated by assigning initial and final values of J, the classical angular momentum, to the nearest integer and assuming that

$$P_{el} = \begin{cases} 1 - |\Delta J|\,\hbar & \text{for } |\Delta J| \leq 1 \\ 0 & \text{for } |\Delta J| \geq 1 \end{cases} \tag{51}$$

This assumption is equivalent to Anderson's result that a change in J constitutes a complete interruption of the radiation process

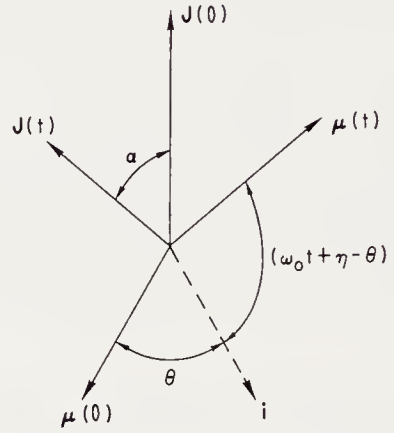

Fig. 5. Geometry of angles specifying a collision. μ is the dipole moment and J is the total angular momentum.

In order to evaluate the expressions for line widths and shifts, one must follow classical trajectories of molecular collisions, and then average over all types of collisions having a thermal distribution of initial conditions. It is clear that unless one choose highly idealized intermolecular potentials, these calculations must be done by machine. A comparison of this theory with some experimental results is given in Section III-B-1.

By expanding Eq. (49) to second order, Gordon[30] obtains

$$\Delta\nu = N\langle v \int_0^\infty [(1 - P_{el}) + \tfrac{1}{2}\eta^2 + \tfrac{1}{2}(1 - \cos\alpha)]2\pi b\, db\rangle \tag{52}$$

The first term $(1 - P_{el})$ gives the average probability of an inelastic collision and corresponds to the first two terms in Eq. (20). The second term, $\frac{1}{2}\eta^2$, gives the mean-square phase shift (perturbation within a J manifold), and the third term, $\frac{1}{2}(1 - \cos\alpha)$, arises from amplitude

modulation of the radiation produced by reorientation of the angular momentum by angle α. The sum of these two terms corresponds to the term in braces in Eq. (20).

III. COMPARISON OF THEORETICAL AND EXPERIMENTAL LINE WIDTHS

A. Introduction

In this section, we present comparisons of experimental line widths and those calculated by Anderson's theory. Unless otherwise indicated, the calculations are based on the use of Eq. (20) rather than the approximate expressions, although for many cases, the results obtained by the exact and approximate expressions should be in satisfactory agreement. In the theory, the dipole moments, quadrupole moments, and other such quantities appear as parameters. If these are known from other sources, then there are no variables except for higher-order interaction parameters. In this case, a comparison between theory and experiment has the purpose of establishing the validity of the theory and estimating the error due to neglected terms. If, on the other hand, an interaction parameter is unknown, for example, the quadrupole moment, this parameter can be evaluated by fitting the theory to the experimental width. In the discussion that follows, the comparison of experiment and theory is considered from both points of view.

Although a discussion of experimental details is outside the scope of this review, we should mention that most of the experimental line widths discussed here are the result of careful work. The line width parameters, $\Delta\nu/p$, have been obtained from the slope of the line width versus pressure curves rather than from dividing the line width obtained at a single pressure by that pressure. Line-width parameters obtained by the latter procedure are subject to large error when there are sources of line broadening other than collisions. Many of the measured line widths have been corrected for a small amount of broadening due to modulation of the source of microwaves. In addition, a correction due to the length of the absorption cell has been applied for intense lines. In some cases, a correction has been applied for the small amount of Doppler broadening that appears at very low pressures.

The experimental and theoretical line widths discussed in this section are given in Tables III–VIII). Tables III and IV give the interactions used in the calculation of line width, and the microwave and kinetic

diameters.* The reference column gives the source of the calculation; however, in many cases the same investigators made the measurements and calculations. Authors have presented their results in a variety of ways: line widths, cross sections, and collision diameters. To present these results in a uniform way, the relation

$$\Delta\nu/p = 0.406(b_{\text{opt}}^2/M^{1/2})(300/T)^{1/2}$$

between $\Delta\nu/p$ in MHz/mm Hg and the optical diameter b_{opt} in Å was used with $T = 300°\text{K}$, since the measurements were made at approximately this temperature.

B. Linear Molecules

1. OCS

Anderson[58] has made an extensive series of measurements on the self-broadening of OCS rotational transitions in the ground vibrational state from $J = 3 \rightarrow 4$ to $J = 15 \rightarrow 16$ at Dry Ice and room temperatures. His results are shown in Figure 6, where the curves were computed from the essentially empirical formula

$$\Delta\nu/p = 1815/T + 0.00312T^{1/2}(J+1)^2 \exp[-hBJ(J+1)/kT] \quad (53)$$

where $\Delta\nu/p$ is in MHz/mm Hg. Crosses are calculations made by Smith et al.[59] on the basis of the dipole–dipole interaction and are seen to be in very good agreement with experiment.

Berendts[62] has carefully remeasured the width of the OCS($J = 1 \rightarrow 2$) line and obtained the value 6.44 ± 0.18 MHz/mm Hg—in good agreement with previous values.[58,64–68] The results of his calculations of line width† as a function of assumed value of quadrupole moment for different interactions are shown in Figure 7. By using only the $\mu_1\mu_1$ interaction, he obtained for $\Delta\nu/p$ the value 5.8 MHz/mm Hg (black dot on abscissa).

Curve *1* was obtained from calculations in which $\mu_1 Q_1$ and $Q_1\mu_1$

* Unless otherwise indicated, the kinetic diameters are those obtained from viscosity measurements and tabulated by J. O. Hirschfelder, C. F. Curtiss, and R. B. Bird, *Molecular Theory of Gases and Liquids*, Wiley, New York, 1964, pp. 1110–1112, 1200. The kinetic diameters for mixtures are obtained from the usual combination rule, $b = (b_1 + b_2)/2$.

† According to Berendts,[62] the calculations of Krishnaji et al.[60,61] on the self-broadening of the OCS $J = 1 \rightarrow 2$ line are in error because one of the dipolar transitions of the absorbing molecule was missed.

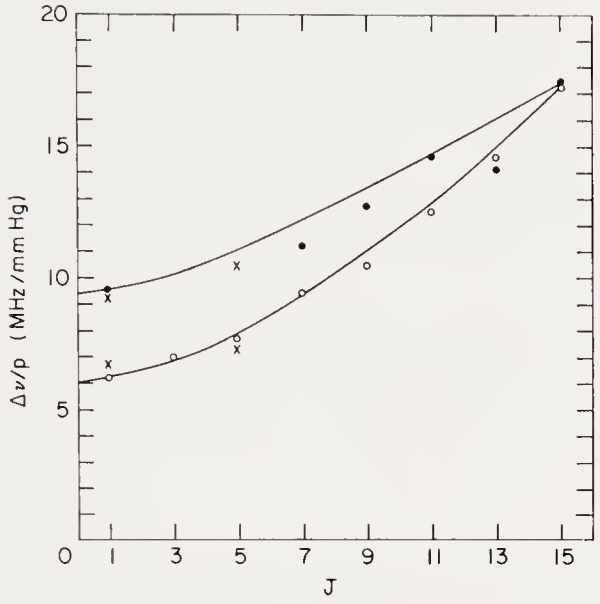

Fig. 6. Line width of OCS as a function of rotational state and temperature (Anderson[58]): (●) data at 195°K; (○) data at 300°K; and (×) calculated values by Smith et al.[59]

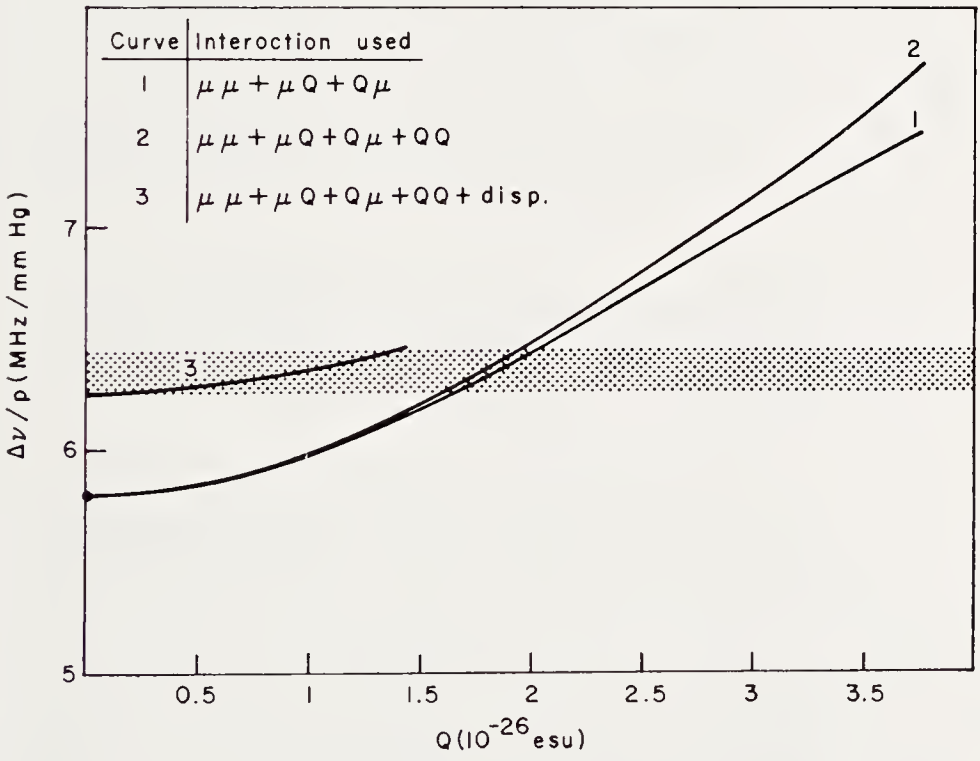

Fig. 7. Calculation of the line width of OCS($J = 1 \rightarrow 2$) as a function of quadrupole moment for various interactions (adapted from Berendts[62]).

TABLE III

Quadrupole Moments Calculated from Microwave Line Widths (Measured at Approximately 300°K)

Molecule (transition)	Perturber	Measured $\Delta\nu/p$, MHz/mm Hg	Interactions	Q $\times 10^{-26}$ esu	Measured b_{opt} Å	Kinetic diam., Å	Ref.
OCS($J=0\rightarrow1$)	OCS	6.44 ± 0.18	$\mu_1\mu_1+\mu_1Q_1+Q_1\mu_1$	1.0	9.33	4.13	62
	H_2	6.10	$\mu_1Q_2+Q_1Q_2+$disp.	2.45	4.59	3.55	62
	HD	6.10	$\mu_1Q_2+Q_1Q_2+$disp.	3.25	5.05	3.54	62
	D_2	5.57	$\mu_1Q_2+Q_1Q_2+$disp.	3.1	5.16	3.54	62
	N_2	4.41	$\mu_1Q_2+Q_1Q_2+$disp.	3.05	6.89	3.91	62
	CO_2	5.13	$\mu_1Q_2+Q_1Q_2+$disp.	3.95	7.99	4.07	62
	NO	4.15	$\mu_1\mu_2+\mu_1Q_2+Q_1\mu_2+Q_1Q_2$	2.9	6.78	3.80	62
BrCN($J=2\rightarrow3$)	BrCN	22.0	$\mu_1\mu_1+\mu_1Q_1+Q_1\mu_1+Q_1Q_1$	6.8	19.8	—	71
$^{15}N_2O$($J=1\rightarrow2$)	$^{15}N_2O$	5.22	$\mu_1\mu_1+\mu_1Q_1+Q_1\mu_1+Q_1Q_1$	3.9	7.85	3.88	62
	H_2	5.15	$\mu_1Q_2+Q_1Q_2+$disp.	1.23	4.19	3.43	62
	D_2	4.20	$\mu_1Q_2+Q_1Q_2+$disp.	1.33	4.46	3.42	62
	N_2	3.89	$\mu_1Q_2+Q_1Q_2+$disp.	2.11	6.32	3.78	62
	NO	3.65	$\mu_1\mu_2+\mu_1Q_2+Q_1\mu_2+Q_1Q_2$	1.89	6.22	3.68	62
	CO_2	4.12	$\mu_1Q_2+Q_1Q_2+$disp.	2.24	6.95	3.94	62

$CHF_3(J=0\rightarrow 1)$	H_2	4.9	$\mu_1 Q_2$	0.82	4.11	3.65	62
	D_2	4.3	$\mu_1 Q_2$	1.02	4.55	3.64	62
	N_2	4.1	$\mu_1 Q_2$	1.35	6.73	4.01	62
	CO_2	6.65	$\mu_1 Q_2$	2.81	9.24	4.17	62
	NO	3.55	$\mu_1\mu_2+\mu_1 Q_2$	0.93	6.45	3.90	62
$NH_3(3,3)$	H_2	3.28 ± 0.14	$\mu_1 Q_2$	0.71	3.30	3.06	91
	N_2	3.91 ± 0.05	$\mu_1 Q_2$	1.49	5.66	3.42	91
	O_2	2.79 ± 0.28	$\mu_1 Q_2$	0.65	4.79	3.29	91
	CO_2	6.48 ± 0.48	$\mu_1 Q_2$	3.19	7.49	3.58	91
$H_2O(5_{-1}\rightarrow 6_{-5})$	N_2	3.51[a]	$\mu_1 Q_2$	1.23	5.43	3.05	50
$SO_2(9_{1,9}\rightarrow 8_{2,6})$	N_2	4.19	$\mu_1 Q_2$	1.4	6.75	3.86	81
	CO_2	7.22	$\mu_1 Q_2$	2.79	9.54	4.02	82

[a] $T=318°K$.

TABLE IV

Calculated and Measured Values of Line Width. Line Widths Measured at Approximately 300°K

Molecule (transition)	Perturber	Interactions	Measured $\Delta\nu/p$, MHz/mm Hg	Computed $\Delta\nu/p$, MHz/mm Hg	Measured b_{opt}, Å	Kinetic diam., Å	Refs.
$OCS(J=1\rightarrow 2)$	He	disp.	2.20	2.05	3.03[63]	3.35	46
	He	disp.	2.20	2.67	3.03[63]	3.35	30
	A	disp.	3.29	2.45	6.30[55]	3.78	46
	A	disp.	3.29	3.86	6.30[55]	3.78	30
	CHF_3	$\mu_1\mu_2$	16.2	19.7	15.1	4.23	62
$CH_3F(J=0\rightarrow 1)$	CH_3F	$\mu_1\mu_1$	20[73]	27.5	14.2	4.0[a]	51
	CH_3F	$\mu_1\mu_1$	20[73]	22.1	14.2	4.0[a]	116
$(J=2\rightarrow 3)$							
$K=0$	CH_3F	$\mu_1\mu_1$	17.2	21.2	13.2	4.0	72
$K=1$	CH_3F	$\mu_1\mu_1$	17.2	20.4	13.2	4.0	72
$K=2$	CH_3F	$\mu_1\mu_1$	17.2 ± 0.6	17.5	13.2	4.0	72
$CHF_3(J=0\rightarrow 1)$	CHF_3	$\mu_1\mu_1$	35.1 ± 0.5[68]	44.0	23.8	4.33[b]	51
	CHF^3	$\mu_1\mu_1$	35.1 ± 0.5[68]	35.3	23.8	4.33[b]	116
$(J=1\rightarrow 2)$[c]	CHF_3	$\mu_1\mu_1$	18[73]	36.1	16.2	4.33	51
$(J=6\rightarrow 7)$							
$K=3$	CHF_3	$\mu_1\mu_1$	9.0	17.0	11.5	4.33	72
$K=4$	CHF_3	$\mu_1\mu_1$	9.0	16.3	11.5	4.33	72
$K=5$	CHF_3	$\mu_1\mu_1$	9.0	15.0	11.5	4.33	72
$K=6$	CHF_3	$\mu_1\mu_1$	9.0 ± 0.5	12.7	11.5	4.33	72

$PF_3(J = 0 \rightarrow 1)$	PF_3	$\mu_1\mu_1$	15.9 ± 1[68]	15.1	17.2	—	116
$PF_3(J = 1 \rightarrow 2)$[c]	PF_3	$\mu_1\mu_1$	13.4 ± 0.4[68]	16.4	16.2		51
	PF_3	$\mu_1\mu_1$	13.4 ± 0.4[68]	12.8	16.2	—	116
$H_2O(2_2 \rightarrow 3_{-2})$	H_2O	$\mu_1\mu_1$	19.1	19.5	11.9	2.52	75
	N_2	μ_1Q_2	3.76	3.75	5.54	3.10	75
$(1_1 \rightarrow 2_1)$	H_2O	$\mu_1\mu_1$	31.6	20.8	15.3	2.52	76
	N_2	μ_1Q_2	7.19	4.04	7.65	3.10	76
$(3_1 \rightarrow 4_1)$	H_2O	$\mu_1\mu_1$	28.7	18.7	14.5	2.52	76
	N_2	μ_1Q_2	4.82	3.43	6.27	3.10	76
$(4_0 \rightarrow 5_0)$	H_2O	$\mu_1\mu_1$	23.3	18.7	13.1	2.52	76
	N_2	μ_1Q_2	5.10	3.52	6.45	3.10	76
$SO_2(9_{1,9} \rightarrow 8_{2,6})$	CH_3Br	$\mu_1\mu_2$	13.64	22.4	14.4	4.03	80

[a] G. T. Fogg, P. A. Hanks, and J. D. Lambert, *Proc. Roy. Soc.* (*London*), **A219**, 497 (1953).
[b] G. A. Miller and R. B. Bernstein, *J. Chem. Phys.*, **63**, 710 (1959).
[c] The K degeneracy is not resolved in these measurements.

interactions were also considered. The effect of introducing the Q_1Q_1 interaction (curve *2*) was negligible at small values of Q—becoming more important for larger Q. Curve *3* was obtained when, in addition to the $\mu_1\mu_1$, μ_1Q_1, $Q_1\mu_1$, and Q_1Q_1 interactions, the dispersion interaction was added. Since the dispersion interaction gives a contribution to the line broadening for $Q = 0$, this curve intersects the vertical axis at a higher value of the line width. The shaded area in Figure 7 gives the error range of the value $\Delta\nu/p = 6.35 \pm 0.10$ MHz/mm Hg averaged from the results of different authors.[58,64—68] It is clear that a relatively small error in $\Delta\nu/p$ results in a great uncertainty in the calculated value of Q. This situation occurs because most of the contribution to $\Delta\nu/p$ comes from the $\mu_1\mu_1$ interaction, and hence the value of $\Delta\nu/p$ is rather insensitive to Q. From Figure 7, Berendts concludes that the best value of Q_{OCS} is 1.0×10^{-26} esu.

Values of $\Delta\nu/p$ for the foreign-gas broadening of OCS ($J = 1 \rightarrow 2$) measured by Berendts[62] and the value of quadrupole moment he calculated by using $Q_{OCS} = 1.0 \times 10^{-26}$ are shown in Table III. No dispersion interaction could be used in the case of NO because the required molecular constants are unknown. For each molecule, curves of the type plotted in Figure 6 were drawn, and the intersection of the calculated curve with a line parallel to the Q axis for the measured line width parameter gave Q. This determination is more sensitive to Q than in OCS self-broadening because of the absence of the $\mu_1\mu_1$ interaction in the foreign-gas broadening.

Krishnaji and Srivastava[46] have considered the widths of the OCS ($J = 1 \rightarrow 2$) line broadened by helium and argon, which are nonpolar and isotropic. The interactions they considered in this case are the dipole–induced-dipole and London dispersion ($k_1 = 2, k_2 = 0$). However, they found that the dipole–induced-dipole interaction contributes less than 0.2% to $S_2(b)$. The values of the calculated and experimental line widths for OCS–He and OCS–A are given in Table IV. Agreement between theory and experiment is good for OCS–He but rather unsatisfactory for OCS–A. However, the calculated value of $\Delta\nu/p$ for OCS–He is in doubt because Krishnaji and Srivastava[46] used Eqs. (25) and (26) in their calculations although $b_0 < k_k$, where b_k is the kinetic diameter.

Gordon[30] has calculated the line width for OCS–He and OCS–A collisions by assuming that the dominant angle-determinant interaction is the anisotropic dispersion force. Using the polarizabilities of OCS, A, and He and the usual combining rules, he estimated the potential,

$$V(r, \theta) = 4\varepsilon\{(\sigma/r)^{12} - (\sigma/r)^6[1 + 0.28P_2(\cos\theta)]\} \quad (54)$$

with $\varepsilon = 63°K$ and $\sigma = 3.5$ Å for OCS–He, and $\varepsilon = 220°K$ and $\sigma = 4$ Å for OCS–A. The line widths calculated with these potentials are in satisfactory agreement with experiment (see Table IV).

2. *HCl*

Pressure broadening in the rotational–vibrational spectrum of HCl occurring in the infrared region has been extensively studied. In this spectrum the line widths and shifts are due to collisions which not only change and modulate the rotational states, but also modulate the vibrational states involved in the radiative transitions. However, since we are primarily concerned with pressure broadening in the microwave region where vibrational transitions are not involved, we consider either rotation–vibration spectra in which the vibrational phase shifts are small, or pure rotational spectra. In particular, we discuss the broadening of HCl by He which has been studied in the pure rotation and rotation–vibration spectra, in which we infer that the effect of vibrational phase shifts on the line width will be small from the very small magnitude of the line shifts.[69]

The most detailed treatment of impact broadening in HCl–rare gas collisions is that of Herman[52] who considered line widths and shifts in the 0–1 and 0–2 rotational–vibrational bands. His theory is fundamentally that of Anderson, except that by using adiabatic eigenstates, he was able to take into account the contribution to the width and shift arising from the rotation of the collision axis. He used the intermolecular potential

$$H_c = -C(v)/R'^6[1 + 6(d/R')(1 + \delta)P_1(\cos\theta')] \quad (55)$$

where δ represents the contribution from the μ' Q, α_2 interaction and has a value of roughly 0.1. The first term represents chiefly the isotropic portion of the London dispersion force and is shown as a function of the vibrational quantum number v. The second term arises because of an eccentricity in heteronuclear diatomic molecules, i.e., the center of dispersion force is displaced from the dynamical center by a distance d. Estimating a value of $d = 0.49$ Å and a value of $C_0(v)$ deduced from the measured line shifts, Herman obtained the line widths shown in Table V, which are from two to three times greater than the rotational–vibrational widths measured by Rank et al., or the pure rotational widths measured by Gebbie and Stone. However, his theory gives widths for

HCl–A and HCl–Xe collisions in better agreement with experiment and accounts for the observed line shifts.

Krishnaji and Srivastava[69a] have treated HCl–rare gas broadening in the pure rotational spectrum within the framework of the Anderson–Tsao and Curnutte theory by using a potential which includes the $\mu_1^2\,\alpha_2$, $\mu_1 Q_1 \alpha_2$ dispersion, and exchange interactions. However, they did not include the contribution due to the eccentricity of HCl, which is predominant in interrupting the molecular radiation process in close-in collisions. In their calculations for HCl–He collisions (Table V), they obtained good agreement with experiment for the $J = 0 \rightarrow 1$ line but a value much smaller than the experimental value for the $J = 4 \rightarrow 5$ line. Their widths for HCl–A and HCl–Xe collisions are much smaller than the experimental values for lines higher than $J = 1 \rightarrow 2$.

TABLE V

Calculated and Measured Values of Line Width for HCl–He Collisions

	Measured $\Delta\nu/p$, MHz/mm Hg		Computed $\Delta\nu/p$, MHz/mm Hg		
Transition	Rot. line[a]	Rot.–vib. line[b]	Ref. 69a	Ref. 52	Ref. 30
$J = 0 \rightarrow 1$	0.91	1.12	1.1	2.8	1.31
$J = 4 \rightarrow 5$	0.55	0.87	0.012	2.0	1.08
$J = 9 \rightarrow 10$	—	0.67	—	—	0.77

[a] Ref. 70.
[b] Ref. 70a.

Gordon[30] has calculated the line width for HCl–He collisions for several transitions (Table V). He adopted the potential

$$H_c = [\varepsilon/(\alpha - 6)]\{[1 + 0.36\cos\theta + 0.1P_2(\cos\theta)]\exp[\alpha(1 - R/R_m)] - [1 + 0.18(R_m/R)\cos\theta + 0.1P_2(\cos\theta)]\alpha(R_m/R)^6\} \quad (56)$$

where $\varepsilon = 60°\text{K}$, $R_m = 3.3$ Å, and $\alpha = 12$. This potential includes not only the dispersion and exchange interactions, but also a term in $\cos\theta$ in both interactions due to the displacement between the center of mass and center of dispersion force. The line widths calculated using this potential and neglecting vibrational phase shifts are in reasonable

agreement with the experiment of Rank et al.[70] on the rotation vibration bands of HCl.

Since Gordon[30] has used a different potential function from that of Herman[52] and Krishnaji and Srivastava,[69a] it is not possible to say whether Gordon achieved better agreement with experiment because of a more accurate potential function, a theory which does not make use of a perturbation expansion and the straight-line path approximation, or both. To settle this question, it would be valuable to have further tests of Gordon's theory.

The widths of the hydrogen halides in self- and foreign-gas broadening have been calculated by Benedict and Herman[70b] using Anderson's theory.

3. *BrCN*

The quadrupole moment of the BrCN molecule has been calculated by Srivastava and Prakash[71] from the self-broadened width of the $J = 2 \rightarrow 3$ transition, using the $\mu_1\mu_1$, $\mu_1 Q_1$, $Q_1\mu_1$, and $Q_1 Q_1$ interactions. For values of $J_2 < 20$, the $\mu_1\mu_1$ interaction is mainly responsible for the broadening. For the higher J_2 values, the $\mu_1 Q_1$ and $Q_1\mu_1$ interactions can never be neglected, whereas the $Q_1 Q_1$ interaction contributes only 5% to $S_2(b)$. The variation of $\Delta\nu/p$ with Q was calculated for two temperatures, 228 and 373°K, which gave the values $Q_{\mathrm{BrCN}}(228°\mathrm{K}) = 10.8 \times 10^{-26}$ esu and $Q_{\mathrm{BrCN}}(373°\mathrm{K}) = 2.8 \times 10^{-26}$ esu. Thus, no single value of the quadrupole moment could explain the temperature dependence of $\Delta\nu/p$. However, one may take the quadrupole moment to be $6.75 \pm 4.0 \times 10^{-26}$ esu for which the experimental line widths are within $\pm 16\%$ of the calculated values. As has been emphasized for OCS, small errors in the line width cause large errors in Q when there is substantial $\mu_1\mu_1$ interaction. Smith et al.[59] earlier tried to explain the width and temperature dependence of the BrCN($J = 2 \rightarrow 3$) line by considering the $\mu_1\mu_1$ interaction as responsible for the broadening for $J_2 < 20$ and considering only the $\mu_1 Q_1$ interaction for $J_2 > 20$. They obtained the value $Q_{\mathrm{BrCN}} = 10.1 \times 10^{-26}$ esu which apparently fit the data for the two temperatures 228 and 373°K.

4. N_2O

Berendts[62] has measured the self-broadening of the $^{15}N_2O$ ($J = 1 \rightarrow 2$) line and its broadening with various foreign gases (Table IV). The

isotope ^{15}N was chosen since N has a nuclear spin of $\frac{1}{2}$ and no quadrupole hyperfine structure is present. From the $\mu_1\mu_1$ interaction, a value of $\Delta\nu/p = 1.3$ MHz/mm Hg was obtained, which is much less than the measured value 5.22 MHz/mm Hg. A very large quadrupole moment ($\sim 12.5 \times 10^{-26}$ esu) must be assumed to obtain a line width equal to the measured width when only $\mu_1 Q_1$ and $Q_1\mu_1$ interactions were added. But the addition of the Q_1Q_1 interaction in the calculation gave $Q = 3.9 \times 10^{-26}$ esu, which is a more reasonable value. The dispersion interaction had no influence on the values of Q. The results of calculations of Q for broadening of N_2O by foreign gases are given in Table III.

5. O_2

Oxygen differs from all other absorbing molecules discussed in this report in that it interacts with the radiation field via a magnetic dipole rather than an electric dipole. In the ground electronic state of O_2 ($^3\Sigma_g^-$), the electron spins pair to give a net spin of unity. This electronic spin is compounded vectorially with the rotational quantum number exclusive of spin, N, to yield a resultant rotational quantum number J for the molecule which can take on the values $N-1$, N, $N+1$. The radiative selection rules connecting these states, $\Delta J = \pm 1$, $\Delta N = 0$, permit transitions which lie in the 5 mm wavelength region, with the exception of a single line near 2.5 mm. A fairly constant value of 1.94 MHz/mm Hg has been found for the width of the 5-mm lines, independent of the rotational state of the molecule.[92] Using Anderson's theory, Artman and Gordon[92] calculated the line widths for O_2–O_2 collisions on the basis of dispersion and exchange forces. Electric dipole–dipole forces are absent and quadrupole and magnetic dipole forces were found to be too weak to be effective. The interaction was taken to be

$$H_{\text{exch}} = \frac{3}{3+\gamma}\frac{4}{\pi} kT(1+\gamma\cos^2\theta)\exp\left[(R-b_k)/a\right]$$

where $\gamma = (\alpha'' - \alpha')/\alpha$ and b_k is the kinetic diameter. With the values of these parameters fixed, i.e., $b_k = 3.60$ Å, $\gamma = 0.85$, and $T = 300°$K, the range of the exchange force was chosen to be $a = 0.42$ Å to match theoretical and experimental widths. The theoretical widths, like the experimental values, were found to be fairly independent of rotational state. However, the theoretical variation of line width with temperature did not agree with experiment.

C. Symmetric Top Molecules. Rotational Lines

It is an interesting fact that until very recently, essentially no reliable data were available on collision-broadened line widths of pure rotational transitions of symmetric top molecules.[62,68,72]

Experimental and theoretical values for the microwave line widths of symmetric top molecules resulting from dipolar broadening are listed in Table IV. For $CHF_3(J = 0 \rightarrow 1)$, $CHF_3(J = 0 \rightarrow 1)$, and $PF_3(J = 1 \rightarrow 2)$, the theoretical widths are from 20 to 30% larger than the experimental values.[51]* The theoretical width for $CH_3F(J = 1 \rightarrow 2)$ is twice as large as the experimental value, which is not well established. However, the discrepancy between theory and experiment persists in the millimeter region where the accuracy of the recently obtained data is very good.[72] Except for the CH_3F $(J = 2, K = 2)$ line where agreement between theory and experiment is good, the theoretical widths are again larger than the experimental values. In addition, the theoretically predicted variation of line width with quantum number K was not observed.

The results of a study of the broadening of the CHF_3 $(J = 0 \rightarrow 1)$ line by foreign gases[62] are summarized in Table III. The quadrupole moments were calculated with only the $\mu_1 Q_2$ interaction, except for NO for which the $\mu_1\mu_2$ interaction was added.

D. Asymmetric Top Molecules

1. H_2O

Benedict and Kaplan[50,74] have made a detailed application of Anderson's theory in their calculation of the breadth of lines in the pure rotational spectrum of H_2O in H_2O–H_2O, H_2O–O_2, and H_2O–air collisions. They calculated the cross section from Eq. (28) where b_0 is the value of b for which $S(b_0) = 1$, or b_k—whichever is greater. This procedure assumes that all collisions at the distance of closest approach, b_k, completely interrupt the radiation process. Consider the results for H_2O–H_2O collisions shown in Table IV. Except for the excellent agreement of their calculated line width with Rusk's experimental value of the millimeter $2_2 \rightarrow 2_{-2}$ line,[75] all the other experimental results,[76,77] do not confirm their calculations. These results include the $5_{-1} \rightarrow 6_{-5}$ line at 0.78 cm^{-1}, and lines in the far infrared region at 92 cm^{-1}, 170 cm^{-1}, and 188 cm^{-1}.

* Note added in proof. The theory of Murphy and Boggs[115] gives widths in good agreement with experiment for these lines[116] (see Table IV).

In calculating the widths of the rotational lines of H_2O for H_2O–N_2 collisions, Benedict and Kaplan[50] assumed that only the dipole–quadrupole interaction is significant, and adopted the parameters $Q_{N_2} = 1.23 \times 10^{-26}$ and $b_k = 3.2$ Å which give an exact fit of the observed width of the microwave $5_{-1} \rightarrow 6_{-5}$ line.[78]* This quadrupole moment is less than that obtained from NH_3–N_2 broadening,[55] 1.6×10^{-26}, and that obtained from the intensity of the absorption induced by H_2–N_2 collisions in the H_2 vibration–rotation band,[79] 1.64×10^{-26}. They chose the value $b_k = 3.20$ Å somewhat higher than the kinetic theory value of 3.05 Å inasmuch as b_k has no precise significance, but represents the effect of all short-range forces—attractive as well as repulsive. However, the exact value of b_k is significant only for those collisions where $b \leq b_k$. We see from Table IV that their calculated values are in very good agreement with observations for the $2_2 \rightarrow 3_{-2}$ line at 6.1 cm^{-1},[75] but in poor agreement with the $1_1 \rightarrow 2_1$ (92 cm^{-1}), $3_1 \rightarrow 4_1$ (170 cm^{-1}), and $4_0 \rightarrow 5_0$ (188 cm^{-1}) lines.[76]

2. SO_2

The line width of the $9_{1,9} \rightarrow 8_{2,6}$ transition of SO_2 broadened by collisions with CH_3Br has been measured and calculated by Krishnaji and Chandra[80] using the dipole–dipole interaction. Their results given in Table IV show that the calculated value is almost twice the measured value. To reduce the labor of the computations, they took an average over all possible values of K in the $S_2(b)$ function rather than in the expression for the cross section. However, this approximation was checked and found to introduce errors no more than $\pm 5\%$.

Krishnaji and Chandra have measured the line widths due to SO_2–N_2[81] and So_2–CO_2[82] collisions and have calculated the quadrupole moments of N_2 and CO_2 assuming that only a dipole–quadrupole interaction to be responsible for the width (Table III). The quadrupole moments of N_2 and CO_2 obtained from this calculation, however, are probably too great because they failed to include the Q_1Q_2 interaction, which should be significant because of the large value of $Q_{SO_2} = 4.4 \times 10^{-26}$ esu.[56]

The temperature dependence of the line width for SO_2–N_2 collisions calculated on the basis of the $\mu_1 Q_2$ interaction was found to be in

* Inasmuch as the measurements of microwave pressure broadening were made in air rather than pure N_2, these calculations should apply to H_2O–air collisions rather than H_2O–N_2 collisions. However, the difference in line width between these cases should be small.

agreement with the following experimental results: $\Delta\nu \propto T^{-0.86}$ from 195 to 340°K, $\Delta\nu \propto T^{-0.78}$ from 340 to 600°K.[81] From Eq. (48) we obtain, for $n = 6$, $\Delta\nu \propto T^{-0.82}$, a result midway between the high- and low-temperature results calculated from expressions where the approximation $f_p(k) = 1$ is not made.[81]

E. Inversion Spectrum of NH_3

1. Self-Broadening

The states of the ammonia molecule, exclusive of vibrational and electronic quantum numbers, are specified by the symmetric top quantum numbers J, K, M, and by $\pm$, denoting the symmetry of the wave function with respect to inversion. For such wave functions, all matrix elements vanish between states which are both + or both −, while the $\langle + | \mu | - \rangle$ elements are precisely those of the ordinary symmetric top for states of the correct J, K, and M. The matrix elements for a molecule undergoing inversion are then those for a symmetric top, provided that these elements are to be understood to be always off-diagonal in the index $\pm$.

There are two kinds of dipole matrix elements of the interaction matrix which do not vanish: (*a*) those corresponding to $\Delta J = 0$, and (*b*) those corresponding to rotational resonance involving $J_2 = J_1 \pm 1$. All other matrix elements are negligible by comparison because of the large energy changes involved in rotational transitions, of the order 10 cm^{-1}. It is not necessary to have resonance as far as the inversion transition is concerned, since for a total energy change of 1.6 cm^{-1} for collisions of + molecules with + molecules or − molecules with − molecules, k will not be greater than about 0.5. Approximating such a value of k by 0 and $f_p(k)$ by unity may lead to an error of only a few per cent. Then for dipolar broadening, $S_2(b)$ is given by

$$S_2(b) = \frac{8}{9}\left(\frac{\mu^2}{b^4 v^2 \hbar^2}\right)\left\{\frac{K_1^2}{J_1(J_1+1)}\frac{K_2^2}{J_2(J_2+1)} + \frac{[(J_1+1)^2 - K_1^2][(J_1+1)^2 - K_2^2]}{(J_1+1)^2(2J_1+1)(2J_1+3)} + \frac{(J_1^2 - K_1^2)(J_1^2 - K_2^2)}{J_1^2(2J_1+1)(2J_1-1)}\right\} \quad (57)$$

where the first term on the right side is due to $\Delta J_1 = \Delta J_2 = 0$ transitions,

and the second and third terms arise from rotational resonance. The contribution of the rotational resonance terms to the line width is quite small. No $S_2(b)_m$ sums enter into this problem because the matrix elements of $\boldsymbol{\mu}$ are off-diagonal in the nondegenerate index $\pm$.

Lin and co-workers[83] have recently conducted a careful and systematic experimental investigation of line widths in the inversion spectrum of ammonia for self- and foreign-gas broadening. Corrections for various effects such as source modulation, cell-length broadening, and even for Doppler broadening at the lowest pressures, were applied to the experimental data. Their experimental results for self-broadening, about 20% lower than the earlier results of Bleaney and Penrose,[84] are shown in Table VI. The estimated accuracy of the experimental data in this

TABLE VI

Inversion Line-Width Parameters of NH_3 Due to Self-Broadening[83]

Lines (J,K)	$\Delta\nu/p$, MHz/mm Hg		Lines (J,K)	$\Delta\nu/p$, MHz/mm Hg	
	Obs.	Calc.[a]		Obs.	Calc.[a]
(2,2)	22.3	22.6	(4,3)	22.1	20.1
(3,3)	24.0	23.9	(4,2)	16.1	14.5
(4,4)	24.4	(24.4)	(4,1)	13.4	10.3
(5,5)	24.6	24.7	(6,5)	22.0	22.0
(6,6)	24.0	24.9	(6,4)	19.6	18.4
(7,7)	24.6	25.0	(6,3)	16.6	14.9
(8,8)	24.7	25.1	(6,2)	13.8	11.5
(9,9)	24.6	25.2	(8,7)	21.9	22.5
(10,10)	23.8	25.3	(8,6)	19.8	19.5
(3,2)	17.6	17.6	(8,5)	17.5	16.7

[a] These are relative values normalized to the (4,4) line.

table is about 1% for the $J = K$ lines and about 2.5% for the other lines. The theoretical values, computed by using Eq. (57) were all multiplied by an adjustable constant to fit the (4,4) line exactly.

The rotational resonance terms becomes very small for the lines with $J = K$—their contribution to the total cross section being less than 0.6% for the (7,7) line, for example. For these lines, the expression for line width according to Eq. (47) takes the form

$$\Delta\nu_{J_1=K_1} \propto [K_1^2/J_1(J_1+1)]^{2/n} \tag{58}$$

For dipole–dipole interaction, $n = 4$ and Eq. (58) becomes

$$\Delta\nu_{J_1=K_1} \propto K_1[J_1(J_1+1)]^{-1/2} = [J_1/(J_1+1)]^{1/2} \tag{59}$$

From the (2,2) to (5,5) lines, the agreement with Eq. (59) is excellent, but a distinct trend of deviation is found for the higher lines. The deviation of the theoretical widths from the experimental values becomes more pronounced as $(J–K)$ increases.* For the $J = 6$ series, the percentage difference is 3.5% for the (6,6) line and 15% for the (6,2) line. Similar trends are found for the other series.

In an effort to improve the agreement between theory and experiment, Lin et al.[83] formulated a theory for NH_3 along the following lines. They assumed, in essence, that there are just two energy states, i.e., channels, of the two-molecule system. With the assumption that these energies are equal, the Schroedinger equation for this system can be solved exactly. Since the interaction operator connects a given sublevel M of the initial state $\pm$ to the M and $M \pm 1$ sublevels of the final state $\mp$, the problem is in fact a multichannel one. However, this problem is reduced to a two-channel one by summing the interaction matrix over final M states and averaging over initial M states. A transition probability is obtained on this basis which never exceeds unity for any value of the impact parameter. The resulting expression for the cross section of the NH_3 inversion lines is identical with Anderson's approximation *2*† except for a multiplicative factor of 0.785. This result points up the uncertainty of the Anderson interpolation procedure but does not resolve the discrepancies in the line-width dependence on J,K discussed in the preceding paragraph.

2. Foreign-Gas Broadening

More detailed studies of the line-width dependence on quantum numbers have been made for the broadening of NH_3 inversion lines by CH_3Cl and CO_2. The quantum-number dependence of the line width is given by Eq. (58) where $n = 4$ for the dipole–dipole and $n = 6$ for dipole–quadrupole interactions. Experimental widths along with the widths computed by using Eq. (58) and normalized to the (4.4) line[83] are given in Tables VII and VIII. For CH_3Cl, the difference between

* As may be seen in Table IV, such a trend also occurs in the rotational lines of CH_3F and CHF_3.

† Obtained by substituting Eq. (57) in Eq. (26).

experimental and theoretical widths appears to increase with $(J-K)$. Considerable deviations of the theoretical widths from the experimental values are also found for the $J \neq K$ lines in the CO_2 broadening. These deviations may be due to the fact that Eq. (58) does not include the effect of rotational transitions.

TABLE VII

Inversion Line-Width Parameters of NH_3 Due to Broadening by CH_3Cl[83]

Lines (J,K)	$\Delta\nu/p$, MHz/mm Hg		Lines (J,K)	$\Delta\nu/p$, MHz/mm Hg	
	Obs.	Calc.[a]		Obs.	Calc.[a]
(3,3)	16.7	15.8	(5,3)	12.2	10.1
(4,4)	16.3	(16.3)	(6,3)	10.5	8.5
(6,6)	17.0	16.9	(7,6)	15.0	14.7
(4,3)	14.1	12.3	(8,6)	14.6	12.9
			(9,6)	13.7	11.6

[a] These are relative values normalized to the (4,4) line.

TABLE VIII

Inversion Line Width Parameters of NH_3 Due to Broadening by CO_2[83]

Lines (J,K)	$\Delta\nu/p$, MHz/mm Hg		Lines (J,K)	$\Delta\nu/p$, MHz/mm Hg	
	Obs.	Calc.[a]		Obs.	Calc.[a]
(2,2)	6.58	5.98	(6,6)	6.44	6.52
(3,3)	6.35	6.23	(6,4)	5.93	4.98
(4,4)	6.37	(6.37)	(6,2)	4.18	3.12

[a] These are relative values normalized to the (4,4) line.

We consider next the broadening of inversion lines due to collisions with spherically symmetric perturbers. The anisotropic part of the interaction between a polar molecule and a polarizable atom according to Eq. (A10) depends on $\cos^2\theta$ where θ is the angle between the dipole and the intermolecular distance. In the case of inversion transitions, since $\cos\theta$ has matrix elements of the form $\langle +|\cos\theta|-\rangle$, $\cos^2\theta$ can

have diagonal matrix elements only of the form $\langle + | \cos^2 \theta | + \rangle$, and, consequently, the $\cos^2 \theta$ interaction cannot cause inversion transitions.[85] This interaction can cause rotational transitions and transitions among the spatially degenerate states of different M. However, because of the wide spacing of the NH_3 levels $k \gg 1$, and the probability of J transitions is very small. Furthermore, it has been shown that the cross sections arising from solely M transitions is greatly reduced from those produced by nondegenerate quantum transitions.[55] In this circumstance, the most important interaction is likely to be of the $\mu_1 Q_1 \alpha_2$ form. Anderson[85] has computed $S_2(b)$ for this interaction for a molecule undergoing inversion with the following result:

$$S_2(b) = \left(\frac{5\pi}{128 b^6}\right)^2 \left(\frac{6\alpha_2 \mu_1 Q_1}{\hbar v}\right)^2 \frac{3}{4} \frac{K^2}{J(J+1)} \times \left[1 + \frac{22}{5} \frac{K^2}{J(J+1)} + \frac{121}{21} \frac{K^4}{J^2(J+1)^2} - \frac{K^2}{3J^2(J+1)^2} \times \left(\frac{22}{5} + \frac{121}{7} \frac{K^2}{J(J+1)}\right) + \frac{K^4}{J^4(J+1)^4} \frac{121}{63}\right] \quad (60)$$

The application of Eq. (60) to calculations of the cross section for collisions of NH_3 with He, H_2, and A has given results in general agreement with experiment.[85]

The variation of line width with quantum number for the $\mu_1 Q_1 \alpha_2$ interaction has been examined by Legan et al.[83] for the NH_3 (3,3), (4,4), and (6,6) lines broadened by He and A. According to the line width obtained from Eqs. (47) and (60), the theoretical ratio of the widths for these lines is 1:1032:1.067. Instead, the experimental ratio decreased somewhat rather than increased. Since this data is accurate to about 5%, part of the disagreement here may be attributed to experimental error.

F. Summary

There is little doubt that Anderson's theory of pressure broadening is useful in identifying the major types of intermolecular forces responsible for the broadening. In a number of cases where the molecular constants are known, the quantitative agreement between theory and experiment is good, but in other cases which are summarized below, the agreement is poor (see Tables IV–VIII).

1. When the perturbing molecule has a large diagonal dipole moment interacting with a sizeable dipole in the radiating molecule, the interaction is so strong that higher-order interactions need not be considered. Furthermore, the collision diameter is so large that the straight line-path approximation should be particularly good. Nevertheless, calculated widths due to SO_2–CH_3Br and CHF_3–CHF_3 collisions ($J = 1 \rightarrow 2$, and $J = 6 \rightarrow 7^*$ lines) are about twice as great as the experimental values. In other cases of the self-broadening of symmetric top molecules† and linear molecules with large dipole moments, and the foreign-gas broadening of OCS by CHF_3, and NH_3 by CHF_3, [51] calculated values of $\Delta\nu$ are 25–35% greater than the experimental values. When the calculated width is smaller than the measured value, it may be argued that inclusion of higher-order interactions could be a reasonable explanation. In opposite cases such as those cited here, this is obviously not possible.

2. Values of the quadrupole moment of a given perturber calculated from measured widths obtained with different absorbing molecules give different values of the quadrupole moment (see Table III).

3. The method of interpolating the collision interruption function, $S_2(b)$, from values of b where $S_2(b) \ll 1$ and $S_2(b)$ can be accurately calculated by perturbation theory, to values of b where $S_2(b) \sim 1$ introduces an error of about 25%[5,83] in the line widths of the inversion spectrum of NH_3. An alternative formulation of line broadening in the inversion spectrum of NH_3 based upon treating the radiating molecule as a two-level system and obtaining an exact solution for the transition matrix gives widths about 20% lower than Anderson's approximation 2. This result suggests that the discrepancies noted in *1* could be due to the method of interpolating the collision interruption function.*

4. The straight-line path and perturbation approximations in Anderson's theory were tested by a calculation in which these approximations were not made.[30] Although better agreement with experiment was obtained with this theory as compared with Anderson's theory (Table V), such results are not yet sufficiently extensive to draw definitive conclusions regarding the errors introduced by the approximations in question.

5. The final point, but certainly not least in importance, is the failure of Anderson's theory to account for the variation of line width with

* $K = 3$.

† See notes on pages 527 and 548.

quantum number. In this type of comparison, the importance of systematic experimental errors or approximations in the theory and calculations are minimized.

It is clear that progress in the quantitative application of pressure-broadening theory to the study of intermolecular forces requires that the discrepancies in question be resolved.

IV. MOLECULAR QUADRUPOLE MOMENTS

The first to suggest that molecular quadrupole moments could be obtained from line-width measurements were Smith and Howard.[86] The main mechanism responsible for the line broadening of NH_3 in collisions with nonpolar nonspherically symmetric molecules was considered to be between the dipole moment of NH_3 and the quadrupole moment of the foreign molecule. Smith and co-workers,[56,86,87] using a simplified version of Anderson's theory, obtained the quadrupole moment of about 20 molecules. The self-broadening of OCS and of BrCN was also measured by the same group of investigators[65,88] and was interpreted by including $\mu_1\mu_1$ and $\mu_1 Q_1$ interactions in the theory of Anderson.[55,59] Smith[55] compared OCS and NH_3 for their usefulness as absorbing molecules for quadrupole-moment determinations and concluded that NH_3 would be preferable because when it is used, fewer interactions are important. Subsequent work on the determination of molecular quadrupole moments from microwave pressure broadening is discussed in Section III.

The evaluation of molecular quadrupole moments from microwave line widths has been reviewed by Berendts[62]; the evaluation of molecular quadrupole moments from all methods has been reviewed by Buckingham,[51b] Krishnaji and Prakash,[44] and Stogryn and Stogryn.[89] The spectral line-broadening method, which gives only the magnitude of the quadrupole moment, has been applied only to axially symmetric molecules. The difficulty with asymmetric molecules is that the quadrupole transition probabilities are still not known.

Some confusion has arisen because several definitions of quadrupole moment are in use (see Appendix II-A-1), and errors occur in the calculation. The calculation of quadrupole moments from the foreign gas broadening of NH_3 by Smith and Howard[56] contains an error which was corrected later by Smith.[55] Thus, the values of Smith and Howard, which were also tabulated by Gordy et al.[90] and Townes and Schawlow,[3]

should be multiplied by 2.40/2.09 and interpreted according to the definition of quadrupole moment given by Eq. (A7). In their tabulation of quadrupole moments, Berendts,[62] Krishnaji and Prakash,[44] and Stogryn and Stogryn[89] have multiplied the results of Smith and Howard[56] by the factor $\frac{1}{2}(2.40/2.09)$ in order to obtain values of quadrupole moment in accordance with the definition given by Eq. (A6), the definition used here.

Unfortunately, this is not the end of the matter. Struck by the fact that quadrupole moments obtained from measurements with NH_3 as the absorber are always much smaller than those obtained with other absorbers, we compared the calculations of Smith[55] with that obtained from the theory presented here. According to Smith, the cross section for dipole–quadrupole broadening of NH_3 is given by

$$\sigma_S = 1.19\pi\left[0.309\left(\frac{\mu_1 Q_S'}{\hbar v}\right)^2 \frac{K_1^2}{J_1(J_1+1)}\right]^{1/3} \tag{61}$$

where Q' is defined by Eq. (A7), and the subscript S means Q' as determined by Eq. (61). We obtain from Eq. (20) [with $S_2(b)_m = 0$ and $f(k) = 1$] and Eq. (26)

$$\sigma = 1.5\pi\left[\frac{2}{45}\left(\frac{\mu_1(2Q)}{\hbar v}\right)^2 \frac{K_1^2}{J_1(J_1+1)}\right]^{1/3} \tag{62}$$

where Q is defined by Eq. (A6). In both calculations, use is made of the fact that the important matrix elements of the interaction are diagonal in J_2. In the calculation of Q from measured cross sections, σ_S and σ are given experimentally and therefore are equal. Thus Eqs. (61) and (62) give

$$2Q = 1.862Q_S' \tag{63}$$

Since $2Q = Q'$, we see that for the same definition of quadrupole moment, Smith's analysis gives a value too small by the factor 1.862. As was discussed earlier, Q_S' is related to Q_{S-H} by

$$Q_S' = (2.40/2.09)\, Q_{S-H}' \tag{64}$$

where Q_{S-H}' is obtained from the work of Smith and Howard.[56] Combining Eqs. (63) and (64), we have

$$Q = 1.07Q_{S-H}' \tag{65}$$

For the purpose of comparing quadrupole moments evaluated from the microwave line widths of different absorbing molecules, we have assembled the results shown in Table IX. The most reliable determination

TABLE IX

Quadrupole Moments of Various Perturbing Molecules Evaluated from Microwave Pressure-Broadened Lines

	Absorbing molecule					
Perturber	NH_3[a]	OCS	CHF_3	N_2O	H_2O	SO_2
H_2	0.71[91]	2.45[62]	0.82[62]	1.23[62]		
D_2		3.1[62]	1.02[62]	1.33[62]		
N_2	1.49[91]	3.05[62]	1.35[62]	2.11[62]	1.23[50]	1.4[81]
O_2	0.65[91]				0.41[74]	
CO_2	3.19[91]	3.95[62]	2.81[62]	2.24[62]		2.7[82]
OCS	2.74[56]	1.0[62]				
NO	1.50[87]	2.9[62]	0.93[62]	1.89[62]		

[a] These values have been corrected according to Eq. (62).

should be the one with NH_3 as an absorber, since the only important interaction is that between the dipole of NH_3 and the quadrupole of the perturber. The Q_1Q_2, $\mu_1^2\alpha_2$, and dispersion interactions are of the $\cos^2\theta$ type and, as discussed in Section III-E-2, are negligibly small. The only other interaction that need be considered is of the $\mu_1 Q_1 \alpha_2$ type, but this is negligible compared with the $\mu_1 Q_2$ interaction. One would expect other absorbers with large dipole moments such as CHF_3, H_2O, and SO_2 to give reliable results for the quadrupole moment since the $\mu_1 Q_2$ interaction should be predominant.

Quadrupole moments deduced from foreign-gas broadening of molecules with small dipole moments such as OCS and N_2O are expected to be of poorer accuracy than the cases cited previously, since now the Q_1Q_2 interaction is important and the accuracy with which Q_2 can be determined depends on how well Q_1 is known. In the case of OCS, Berendts[62] used the value $Q_{OCS} = 1.0 \times 10^{-26}$ esu, which is 1/2.7 times the value obtained from NH_3–OCS broadening. Smaller values of Q_2 would be obtained if the larger value of Q_{OCS} were used. However, it

TABLE X

Selected List of Quadrupole Moments Evaluated by Various Methods

Method of determination	H_2	N_2	CO_2	O_2	CO	NO	C_2H_4
Microwave pressure broadening	0.71[91] 0.82[62]	1.49[91] 1.35[62]	3.19[91] 2.81[62]	0.65[91]	1.71[87]	1.50[87] 0.93[62]	2.57[87]
Collision-induced absorption	0.6[93]	1.64[79]	4.4[95]	—	—	—	2.6[96]
Second dielectric virial coefficient	0.52[97]	1.90[97]	4.59[97]	—	2.81[97]	—	3.92[97]
Nuclear magnetic resonance	0.60[98]	1.70[98]	4.85[98]	0.92[98]	2.0[98]	2.05[98]	—
Viscosity and second virial coefficient	—	2.05[99]	4.1[99]	1.48[99]	2.43[99]	2.2–2.4[99]	3.85[99]
Miscellaneous	0.63[a 100]	—1.221[b 94]	4.1[c 101]	—	2.0[d 69]	—	—

[a] Molecular beam
[b] Molecular orbital calculation
[c] Induced optical anisotropy
[d] Infrared line broadening

would require $Q_{OCS} = 8.5 \times 10^{-26}$ esu to give $Q_{N_2} = 1.4 \times 10^{-26}$ esu and $Q_{H_2} = 0.8 \times 10^{-26}$ esu, for example.

Even with the use of favorable absorbers, it may not be possible to obtain accurate values of the quadrupole moment from Anderson's theory because of approximations and simplifications.

Table X gives a selected list of quadrupole moments evaluated by various methods: microwave pressure broadening, collision-induced absorption,[79,93,95,96] second dielectric virial coefficient,[97] nuclear magnetic resonance,[98] viscosity and second virial coefficients,[99] molecular-beam measurements,[100] induced optical anisotropy,[101] infrared pressure broadening,[69] and molecular-orbital calculations.[94,192] Considering the diversity of methods with different accuracies, and the difficulties inherent in quadrupole-moment determinations, the overall agreement is encouraging. Except for H_2, the quadrupole moments deduced from microwave pressure broadening are for the most part smaller than those obtained by other methods. We believe that this may be due to inaccuracy in the Anderson-Tsao and Curnutte theory.

Deducing quadrupole moments from pressure-broadened infrared lines is in no better situation than their deduction from microwave lines. The work of Benedict and Kaplan[50] on H_2O–N_2 collisions has already been discussed in Section III-D-1. In addition, James and Thibault[103] attempted to obtain Q_{HCl} and Q_{DCl} from the widths of the rotational–vibrational transitions of HCl broadened by DCl and DCl broadened by HCl. They hoped that by studying several isotopes where the values of μ, Q, etc. are presumed to be the same, they could obtain a reliable determination of Q. They found that Anderson's theory gave results in general agreement with experiment provided that $Q_{DCl} < Q_{HCl}$.

V. NONRESONANT ABSORPTION AND RELAXATION

A. Introduction

In early measurements of the microwave absorption in gases by Walter and Hershberger[104] and by Bleaney and Loubser,[105] it was noted that the methyl halides exhibit, in addition to the ordinary rotational spectrum, a nonresonant or relaxation spectrum of the Debye type. Such absorption occurs quite generally in dipolar gases with a symmetric-top structure,[106] and in diatomic molecules such as O_2 [107] * and NO[108]

* Nonresonant absorption in O_2 is due to the transition $\Delta J = 0$, $\Delta N = 0$ (see p. 526).

which are not in the $^1\Sigma$ electronic ground state. Dipole radiative selection rules for symmetric-top molecules are $\Delta J = 0, \pm 1$, and $\Delta K = 0$, where J and K are the quantum numbers designating, respectively, the total angular momentum and the angular momentum about the symmetry axis. In addition, there is the inversion selection rule $+ \leftrightarrow -$, where $+$ and $-$ represent, respectively, the symmetric and antisymmetric combination of the rotational wave functions $|J,K\rangle$ and $|J,-K\rangle$.

In certain cases, e.g., NH_3 and ND_3, the barrier to inversion is comparatively low and the transition $\Delta J = 0, + \leftrightarrow -$, are resonant transitions between the inversion levels whose degeneracy is split by the low-potential barrier. With compression* however, the resonant inversion spectrum of NH_3 and ND_3 disappears and the spectrum assumes the Debye shape.[105,109] The more typical symmetric tops, however, have very high inversion barriers and the inversion levels are degenerate. The inversion dipole matrix element may then be regarded classically as a component of the dipole moment along the axis of total angular momentum, $\boldsymbol{\mu}K/[J(J+1)]^{1/2}$ (see Fig. 8), which in the absence of collisions is stationary in space. This dipole component gives rise to a nonresonant absorption with a relaxation rate that is governed by bimolecular collisions at moderate pressures.

Although the literature on nonresonant absorption in gases has been increasing,[8] and theoretical interest in this type of absorption has been growing,[32,33,110] the relation between the relaxation time and intermolecular forces has not yet been elucidated. For this reason, our discussion of nonresonant absorption in gases is rather brief although, in principle, this type of absorption is capable of yielding valuable information on anisotropic intermolecular forces.

B. Theory

The stationary or diagonal component of the dipole moment of a symmetric top molecule in the direction of an applied electric field is given by

$$\mu_{JKM} = \mu\langle J,K,M|\cos\theta|J,K,M\rangle = \mu KM/J(J+1) \qquad (66)$$

* The pressures involved, however, are sufficiently low so that the collisions are still bimolecular.

If, as is assumed here, the frequency of the applied field is not resonant with any pair of rotational levels, the applied field cannot induce rotational transitions. In addition, it is clear that the applied field cannot exert a torque and, therefore, reorient the molecule. However, the transitions $M \rightarrow M'$, $J \rightarrow J'$, and $M,J \rightarrow M',J'$ can occur because of molecular collisions. In terms of Eq. (66), these transitions signify,

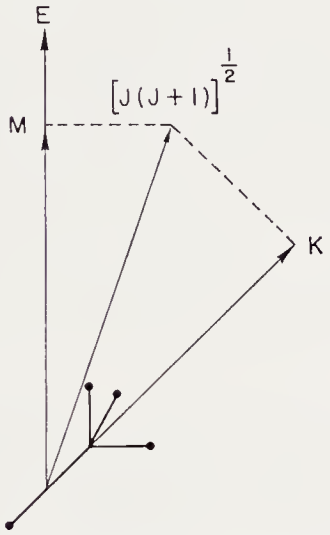

Fig. 8. Vector diagram of the angular momenta for a symmetric top molecule The permanent dipole is along the symmetry axis. The molecule represented is, for example, CH_3F.

respectively, a reorientation of the stationary component of the dipole moment, a change in its magnitude, and both. Detailed balancing in the presence of the applied field preferentially weights those transitions which increase the dipole moment in the direction of the field and, consequently, the gas becomes polarized. A theoretical treatment of nonresonant absorption along these lines has been developed by Birnbaum.[33] Ben-Reuven,[32] regarding nonresonant absorption as a result of the contribution of many lines at zero frequency which are coupled by collisions, has developed a theory giving results similar to those obtained by Birnbaum. Anderson's theory of pressure broadening,[5] applicable for isolated lines and, moreover, developed in a perturbation approximation, does not correctly describe nonresonant relaxation.

On the basis of very general considerations, it is found that the

complex dielectric constant $\varepsilon' - i\varepsilon'' = \varepsilon$ is given by* [33]

$$\varepsilon - \varepsilon_\infty = \frac{4\pi}{3kT} \sum_{JK} N_{JK} \mu_{JK}^2 \frac{\Delta\omega_{JK}}{\Delta\omega_{JK} + i\omega} \tag{67}$$

where N_{JK} is the number of dipoles in state J,K, $\Delta\omega_{JK}$ is a relaxation parameter, and μ_{JK}^2 is given by†

$$\mu_{JK}^2 = \mu^2[K^2/J(J+1)] \tag{68}$$

Equation (67) has the form of a sum by Debye shapes and, consequently, represents the case where there is a distribution of relaxation frequencies. The major restriction on the validity of Eq. (67) is that the departure from the simple Debye shape must be rather small—in other words, $\Delta\omega_{JK}$ must not be too strong a function of J and K. The relaxation parameter is given by

$$\Delta\omega_{JK} = \sum_{J'M'} A_{J'M'JM}(1 - \mu_{J'M'}/\mu_{JM}) \tag{69}$$

where $A_{J'M'JM}$ is the collision-induced rate of transition from initial state JM to final state $J'M'$. For simplicity, the quantum number K is suppressed in the quantities on the right side of Eq. (69).‡ In the impact approximation, the transition rate becomes

$$A_{J'M',JM} = v \sum_{J_2 J_2'} N_{J_2} \int_0^\infty 2\pi b \, db \langle |T_{J_2'J'M';J_2JM}|^2 \rangle \tag{70}$$

where v is the mean relative velocity, and T is the collision operator defined by Eq. (11). The quantity $|T|^2$ has been averaged over all degenerate states of the perturbing molecule, and the angular brackets signify an average over all direction of collisions. According to Eq. (70), the relaxation parameter is directly proportional to density.

The factor $(1 - \mu_{J'M'}/\mu_{JM})$ weights the transition rates so that transitions where $\mu_{J'M'} \simeq \mu_{JM}$ make a negligible contribution to the relaxation frequency. Such transitions are controlled by selection rules such as $\Delta J = 0, \pm 1, \pm 2$, $\Delta M = 0, \pm 1, \pm 2$, obtained by a perturbation expansion of the collision operator T. These selection rules allow only small change in μ_{JM} for the states which are well occupied, i.e.,

* The absorption coefficient α is related to ε'' for $\varepsilon'' \ll 1$ by $\alpha = 2\pi\varepsilon''/\lambda$, where λ is the frequency of the radiation.

† Equations (67), (69), (70) are generally applicable to nonresonant absorption in gases, although the nomenclature is specialized for symmetric top molecules.

‡ In most of the transitions of interest, the selection rule $\Delta K = 0$ applies.

$J = 20$–30 for many symmetric top molecules. Consider now collisions so strong that all final orientations of the dipole are equally likely. In this case, the transition rate will be independent of the orientation quantum number and $\sum_{J'M'} A_{J'M',JM}(\mu_{J'M'}/\mu_{JM}) = 0$ since $\sum_{M'} \mu_{J'M'} = 0$. Then, instead of Eq. (69), we have

$$\Delta\omega_J = \sum_{J'} A^{(S)}_{J'J} \tag{71}$$

where $A^S_{J'J}$ is the transition rate for strong collisions. It has been shown that for strong collisions, the complex dielectric constant is given by Eq. (67) without the restriction that the departure from the simple Debye shape be small.[33]

C. Comparison of Theory and Experiment

Since nonresonant spectra in gases nearly have the Debye shape,[106] it is sufficiently accurate to represent the dielectric loss in the vicinity of the maximum by

$$\varepsilon'' = \frac{4\pi}{3kT}\gamma\left(\sum_{JK} N_{JK}\mu^2_{JK}\right)\frac{\langle\Delta\omega_{JK}\rangle\omega}{\langle\Delta\omega_{JK}\rangle^2 + \omega^2} \tag{72}$$

where $\langle\Delta\omega_{JK}\rangle$ is the intensity-weighted average of $\Delta\omega_J$, namely,

$$\langle\Delta\omega_{JK}\rangle = \sum_{JK} N_{JK}\mu^2_{JK}\Delta\omega_{JK}/\sum_{JK} N_{JK}\mu^2_{JK} \tag{73}$$

and γ is a correction factor, slightly less than unity, which accounts for the depression of the maximum because of the distribution of relaxation frequencies. We see from Eq. (72) that the maximum value of the dielectric loss is obtained when $\omega = \langle\Delta\omega_{JK}\rangle$. Since for many symmetric top gases at atmospheric pressure $\langle\Delta\omega_{JK}\rangle \sim 10^{10}$ Hz, absorption can be conveniently studied in the microwave region. To avoid overlapping the pure rotational spectra, $\langle\Delta\omega_{JK}\rangle$ and, hence, the gas pressure must be kept sufficiently low, usually atmospheric pressure or lower.

The nonresonant collision diameter for self- and foreign-gas broadening, as well as the rotational and kinetic collision diameters for some symmetric top molecules are collected in Table XI. Also included are the resonant and nonresonant collision diameters for O_2 and NH_3. The nonresonant diameter for NH_3 is determined in the pressure region where the resonant inversion lines disappear and the absorption becomes the nonresonant type. In all cases, the nonresonant diameter is distinctly smaller than the resonant diameter for a given absorber and perturber. Theory shows that collisions causing transitions to

nondegenerate states, for example, the rotational transitions $\Delta J = \pm 1$, are strong in that they completely interrupt the radiation process.[5] The effect of such collisions on the nonresonant relaxation rate has been

TABLE XI

Collision Diameters Obtained from Nonresonant Absorption and Rotational Lines

Molecule	Perturber	Nonres. diam.	Rotat. diam.[a]	Transition	Kinetic diam.
CH_3F	CH_3F	6.5[106]	14.2	$0 \rightarrow 1$	4.0
			13.2	$2 \rightarrow 3$	4.0
CHF_3	CHF_3	5.3[113]	23.8	$0 \rightarrow 1$	4.33
			16.2	$1 \rightarrow 2$	4.33
	H_2	0.82[113]	4.13	$0 \rightarrow 1$	3.65
	D_2	1.14[113]	4.57	$0 \rightarrow 1$	3.65
	N_2	2.84[113]	6.74	$0 \rightarrow 1$	4.01
	CO_2	4.23[113]	9.25	$0 \rightarrow 1$	4.17
O_2	O_2	2.64[107]	4.4[92]	Spin reorient.[b]	3.43
NH_3	NH_3	7.7[105]	13.8[114]	3,3 line[c]	3.15

[a] See Tables III and IV.

[b] Transitions between spin fine-structure components of the ground state ($^3\Sigma_g$) rotational levels. The widths of these lines are about the same, 1.94 MHz/mm Hg.

[c] The 3,3 inversion line.

computed for the case of dipole–dipole interaction and found to make a negligible contribution.[33] It seems clear that the collisions making the important contributions to the relaxation rate are those producing large reorientations, i.e., $\Delta M \sim \pm J$. It is thought that transitions producing large changes in J are not nearly as likely because of energy conservation considerations.

Several attempts have been made to correlate the nonresonant width of symmetric top molecules with molecular parameters both for self-[111] and foreign-gas broadening.[112,113] An interesting development along these lines relates the nonresonant cross section to the effective viscosity cross section, the ratio of total internal to orbital angular momentum, and the shape (prolateness or oblateness) of the top.[113] However, to obtain specific information regarding anisotropic intermolecular forces from pressure broadening in nonresonant spectra, calculations using Eqs. (69) and (70), where $|T|^2$ is solved exactly rather than by perturbation methods, are required.

VI. CONCLUSIONS

The study of pressure broadening in the microwave region has been fruitful in its application to the investigation of intermolecular forces. However, it has not been possible to make quantitative studies with any great degree of accuracy because of deficiencies in the theories that have been applied to interpret the experimental data on resonant line widths. The study of nonresonant absorption can, in principle, give valuable information regarding anisotropic intermolecular forces; however, the relevant calculations have not been made. It is clear then that further progress in the application of microwave pressure broadening to intermolecular forces is dependent on advances in the theory. It appears, however, that such advances are in progress.

Note added in proof. A theory of pressure broadening,[115] which neglects the effect of phase shifts on line width, gives for the collision interruption function $\{1 - \exp[-\Gamma_i(b)]\} + \{1 - \exp[-\Gamma_f(b)]\}$ where Γ_i of b and Γ_f of b are, respectively, twice the first and second terms in Eq. (20). This theory is expected to be good for linear and symmetric top molecules but not for NH_3 and asymmetric molecules having few closely spaced energy levels.[115]

Acknowledgments

The author thanks Dr. A. A. Maryott and Dr. D. A. McQuarrie for helpful suggestions regarding the manuscript.

References

1. W. Gordy, W. V. Smith, and R. F. Trambarulo, *Microwave Spectroscopy*, Wiley, New York, 1953, pp. 185–199.
2. J. O. Hirschfelder, C. F. Curtiss, and R. B. Bird, *Molecular Theory of Gases and Liquids*, Wiley, New York, 1964, pp. 1020–1029.
3. C. H. Townes and A. L. Schawlow, *Microwave Spectroscopy*, McGraw-Hill, New York, 1944, Chap. 13.
4. J. H. Van Vleck and V. F. Weisskopf, *Rev. Mod. Phys.*, **17**, 227 (1945).
5. P. W. Anderson, *Phys. Rev.*, **76**, 647 (1949).
6. R. G. Breene, Jr., *Rev. Mod. Phys.*, **29**, 94 (1957).
7. R. G. Breene, Jr., *The Shift and Shape of Spectral Lines*, Pergamon Press, New York, 1961.
8. G. Birnbaum and A. A. Maryott, *Line Shapes, Widths, and Shifts in Microwave Spectra of Gases*, Hughes Research Lab. Rept No. 228, December, 1961.
9. G. V. Skrotskii and T. G. Izyumova, *Soviet Phys. Usp.* (*Engl. Trans.*) **4**, 177 (1961).
10. H. Kuhn, *Phil. Mag.*, **18**, 987 (1934).
11. H. Margenau, *Phys. Rev.*, **48**, 755 (1935).
12. H. A. Lorentz, *Proc. Amsterdam Acad.*, **8**, 591 (1906).

13. V. Weisskopf, *Physik. Z.*, **34**, 1 (1933).
14. W. Lenz, *Z. Physik.*, **80**, 423 (1934).
15. L. Spitzer, *Phys. Rev.*, **58**, 348 (1940).
16. T. Holstein, *Phys. Rev.*, **79**, 744 (1950).
17. P. W. Anderson, *Phys. Rev.*, **86**, 809 (1952).
18. P. W. Anderson and J. D. Talman, *Proceedings of Conference on Broadening of Spectral Lines*, University of Pittsburgh, Pittsburgh, 1956, Bell Telephone System Monograph 3117.
19. E. Lindholm, Dissertation, University of Uppsala, Sweden, 1942.
20. H. M. Foley, *Phys. Rev.*, **69**, 616 (1946).
21. M. Mizushima, *Phys. Rev.*, **83**, 94 (1951); *Physica*, 17, 453A (1951); *Phys. Rev.* (Errata), **84**, 363 (1961).
22. D. C. M. Leslie, *Phil. Mag.*, **42**, 37 (1951).
23. M. Baranger, *Phys. Rev.*, **111**, 494 (1958).
24. M. Baranger, *Phys. Rev.*, **112**, 855 (1958).
25. M. Baranger, *Phys. Rev.*, **111**, 481 (1958).
26. A. C. Kolb and H. Griem, *Phys. Rev.*, **111**, 514 (1958).
27. U. Fano, *Phys. Rev.*, **131**, 259 (1963).
28. A. DiGiacomo, *Nuovo Cimento*, **34**, 473 (1964).
29. A. Ohno, *J. Phys. Soc. Japan*, **16**, 2402 (1961).
30. R. G. Gordon, *J. Chem. Phys.*, **44**, 3083 (1966).
31. A. Ben-Reuven, *Phys. Rev. Letters*, **14**, 349 (1965).
32. A. Ben-Reuven, *Phys. Rev.*, **145**, 7 (1966).
33. G. Birnbaum, *Phys. Rev.*, **150**, 101 (1966).
34. J. Van Kranendonk, *Can. J. Phys.*, **41**, 433 (1963).
35. J. Fiutak and J. Van Kranendonk, *Can. J. Phys.*, **40**, 1085 (1962).
36. J. Fiutak and J. Van Kranendonk, *Can. J. Phys.*, **41**, 21 (1963).
37. L. Galatry, *Phys. Rev.*, **122**, 1218 (1961).
38. O. von Roos, *Proceedings of the Vth International Conference on Ionization Phenomena in Gases*, Munich, 1961, p. 913; Jet Propulsion Laboratory Tech. Rept. No. 32–100, April 1961.
39. H. Margenau and M. Lewis, *Rev. Mod. Phys.*, **31**, 569 (1959).
40. C. J. Tsao and B. Curnutte, *J. Quart. Spectry. Radiative Transfer*, **2**, 41 (1962).
41. S. Ch'en and M. Takeo, *Rev. Mod. Phys.*, **29**, 20 (1957).
42. R. B. Bernstein and K. H. Kramer, *J. Chem. Phys.*, **44**, 4473 (1966).
43. K. Matsuura, Y. Sugiura, and G. M. Hatoyama, *J. Phys. Soc. Japan*, **12**, 835 (1957).
44. Krishnaji and V. Prakash, *Rev. Mod. Phys.*, **38**, 690 (1966).
45. M. E. Rose, *Elementary Theory of Angular Momentum*, Wiley, New York, 1957.
45a. Krishnaji, Research Rept. No. 3, Physics Department, University of Allahabad, Allahabad, India, December, 1964.
46. Krishnaji and S. L. Srivastava, *J. Chem. Phys.*, **41**, 2266 (1964).
47. Krishnaji and S. L. Srivastava, *J. Chem. Phys.*, **42**, 1546 (1965).
48. R. H. Schwendeman and V. W. Laurie, *Tables of Line Strengths*, Pergamon Press, New York, 1958.
49. P. C. Cross, R. M. Hannier, and G. W. King, *J. Chem. Phys.*, **12**, 210 (1944).

50. W. S. Benedict and L. D. Kaplan, *J. Chem. Phys.*, **30**, 388 (1959).
50a. C. H. Townes and A. L. Schawlow, *Microwave Spectroscopy*, McGraw-Hill, 1955, Chapter 4.
51. G. Birnbaum, *J. Chem. Phys.*, **42**, 2455 (1967).
51a. J. O. Hirschfelder, C. F. Curtiss, and R. B. Bird, *Molecular Theory of Gases and Liquids*, Wiley, New York, 1964, pp. 25–30, 835–846, 954–974.
51b. A. D. Buckingham, *Quart. Rev. (London)*, **13**, 183 (1959).
52. R. M. Herman, *Phys. Rev.*, **132**, 262 (1963); *J. Quant. Spectry. Radiative Transfer*, **3**, 449 (1963); *J. Chem. Phys.*, **4**, 1346 (1966).
52a. A. D. Buckingham, *Discussions Faraday Soc.*, **40**, 232 (1965).
53. L. J. Kiefer and A. V. Bushkovitch, *J. Mol. Spectry.*, **2**, 558 (1958).
54. K. L. Perkins, A. V. Bushkovitch, and L. J. Kiefer, *J. Chem. Phys.*, **26**, 779 (1957).
55. W. V. Smith, *J. Chem. Phys.*, **25**, 510 (1956).
56. W. V. Smith and R. Howard, *Phys. Rev.*, **79**, 132 (1950).
57. H. W. De Wijn, *Physica*, **31**, 1215 (1965).
58. R. S. Anderson, *Phys. Rev.*, **97**, 1654 (1955).
59. W. V. Smith, H. A. Lackner, and A. B. Volkov, *J. Chem. Phys.*, **23**, 389 (1955); **23**, 1559 (1955).
60. Krishnaji, S. Chandra, and S. L. Srivastava, *J. Chem. Phys.*, **41**, 409 (1964).
61. Krishnaji and S. L. Srivastava, *J. Chem. Phys.*, **41**, 2201 (1964).
62. B. Th. Berendts, Thesis, Catholic University of Nijmegen, Netherlands, 1966.
63. F. A. Liuima, A. V. Bushkovitch, and A. G. Rouse, *Phys. Rev.*, **96**, 434 (1954).
64. C. M. Johnson and D. M. Slager, *Phys. Rev.*, **87**, 677 (1952).
65. H. Feeny, H. Lackner, P. Moser, and W. V. Smith, *J. Chem. Phys.*, **22**, 79 (1954).
66. A. Dymanus, H. A. Dijkerman, and G. R. D. Zijderveld, *J. Chem. Phys.*, **32**, 717 (1960).
67. H. A. Dijkerman, thesis, University of Utrecht, The Netherlands, 1966.
68. C. O. Britt and J. E. Boggs, *J. Chem. Phys.*, **45**, 3877 (1966).
69. A. Ben-Reuven, H. Friedman, and J. H. Jaffe, *J. Chem. Phys.*, **38**, 3021 (1963).
69a. Krishnaji and S. L. Srivastava, *J. Chem. Phys.*, **43**, 1345 (1965).
70. D. H. Rank, D. P. Eastman, B. S. Rao, and T. A. Wiggins, *J. Mol. Spectry.*, **10**, 34 (1963).
70a. H. A. Gebbie and N. W. B. Stone, *Proc. Phys. Soc. (London)*, **82**, 309 (1963).
70b. W. S. Benedict and R. Herman, *J. Quant. Spectry. Radiative Transfer*, **3**, 265 (1963).
71. S. L. Srivastava and V. Prakash, *J. Chem. Phys.*, **42**, 3738 (1965).
72. G. Birnbaum, E. R. Cohen, and J. R. Rusk, to be published.
73. O. R. Gilliam, H. D. Edwards, and W. Gordy, *Phys. Rev.*, **75**, 1014 (1949).
74. W. S. Benedict and L. D. Kaplan, *J. Quant. Spectry. Radiative Transfer*, **4**, 453 (1964).
75. J. R. Rusk, *J. Chem. Phys.*, **42**, 493 (1965).
76. R. B. Sanderson and N. Ginsburg, *J. Quant. Spectry. Radiative Transfer*, **3**, 435 (1963).
77. C. H. Townes and F. R. Merritt, *Phys. Rev.*, **70**, 558L (1946).

78. G. E. Becker and S. H. Autler, *Phys. Rev.*, **70**, 300 (1945).
79. J. Van Kranendonk, *Physica*, **24**, 347 (1958).
80. Krishnaji and S. L. Chandra, *J. Chem. Phys.*, **38**, 2690 (1963).
81. Krishnaji and S. L. Chandra, *J. Chem. Phys.*, **38**, 232 (1963).
82. Krishnaji and S. L. Chandra, *J. Chem. Phys.*, **38**, 1019 (1963).
83. R. L. Legan, J. A. Roberts, E. A. Rinehart, and C. Lin, *J. Chem. Phys.*, **43**, 4337 (1965).
84. B. Bleaney and R. P. Penrose, *Proc. Roy. Soc.* (*London*), **A189**, 358 (1947).
85. P. W. Anderson, *Phys. Rev.*, **80**, 511 (1950).
86. W. V. Smith and R. R. Howard, *Phys. Rev.*, 79, 128 (1950).
87. R. M. Hill and W. V. Smith, *Phys. Rev.*, **82**, 451 (1951).
88. R. Trambarulo, H. Lackner, P. Moser, and H. Feeny, *Phys. Rev.*, **95**, 622 (1954).
89. D. E. Stogryn and A. P. Stogryn, *Mol. Phys.*, **11**, 371 (1966).
90. W. Gordy, W. V. Smith, and R. F. Trambarulo, *Microwave Spectroscopy*, Wiley, New York, 1953, p. 345.
91. H. Feeny, W. Madigorsky, and B. Winters, *J. Chem. Phys.*, **27** (1957).
92. J. O. Artman and J. P. Gordon, *Phys. Rev.*, **96**, 1237 (1954).
93. J. P. Colpa and J. A. A. Ketelaar, *Mol. Phys.*, **1**, 343 (1958).
94. R. K. Nesbet, *J. Chem. Phys.*, **40**, 3619 (1964).
95. A. A. Maryott and S. J. Kryder, *J. Chem. Phys.*, **41**, 1580 (1964).
96. G. Birnbaum and A. A. Maryott, *J. Chem. Phys.*, **36**, 2032 (1962).
97. R. H. Orcutt, *J. Chem. Phys.*, 39, 605 (1963).
98. M. Bloom, I. Oppenheim, M. Lipsicas, C. G. Wade, and C. F. Yarnell, *J. Chem. Phys.*, **43**, 1036 (1965).
99. T. H. Spurling and E. A. Mason, *J. Chem. Phys.*, **46**, 322 (1967).
100. N. J. Harrick and N. F. Ramsey, *Phys. Rev.*, **88**, 228 (1952).
101. A. D. Buckingham and R. L. Disch, *Proc. Roy. Soc.* (*London*), **A273**, 275 (1963).
102. W. Kolos and C. C. J. Roothaan, *Rev. Mod. Phys.*, **32**, 219 (1960).
103. T. C. James and R. J. Thibault, *J. Chem. Phys.*, **40**, 534 (1964).
104. J. E. Walter and W. D. Hershberger, *J. Appl. Phys.*, **17**, 814 (1946).
105. B. Bleaney and J. H. N. Loubser, *Proc. Roy. Soc.* (*London*), **A63**, 483 (1950).
106. G. Birnbaum, *J. Chem. Phys.*, **27**, 360 (1957).
107. A. A. Maryott and G. Birnbaum, *J. Chem. Phys.*, **33**, 686 (1960).
108. A. A. Maryott and S. J. Kryder, *J. Chem. Phys.*, **31**, 617 (1959).
109. G. Birnbaum and A. A. Maryott, *Phys. Rev.*, **92**, 270 (1953).
110. R. G. Gordon, *J. Chem. Phys.*, **45**, 1635 (1966).
111. G. Birnbaum and A. A. Maryott, *J. Chem. Phys.*, **29**, 1422 (1958).
112. A. A. Maryott and G. Birnbaum, *J. Chem. Phys.*, **41**, 154 (1964).
113. L. Frenkel, S. J. Kryder and A. A. Maryott, *J. Chem. Phys.*, **44**, 2610 (1966).
114. B. Bleaney and R. P. Penrose, *Proc. Phys. Soc.* (*London*), **60**, 540 (1948).
115. J. S. Murphy and J. E. Boggs, *J. Chem. Phys.*, **47**, 691 (1967).
116. J. S. Murphy and J. E. Boggs, to be published.

10. Intermolecular Forces Determined by Nuclear Magnetic Resonance

MYER BLOOM*

Department of Physics, University of British Columbia, Vancouver, British Columbia, Canada

and

IRWIN OPPENHEIM†

Department of Chemistry, Massachusetts Institute of Technology, Cambridge, Massachusetts, and Department of Chemistry and Institute for Radiation Physics and Aerodynamics, University of California, San Diego, La Jolla, California

CONTENTS

I. Introduction 550
A. Macroscopic Measurements 550
B. Physical Significance of the Relaxation Time Measurements . . . 553
II. Theory of Nuclear Spin Relaxation in Dilute Hydrogen Gas 555
A. Intramolecular Correlation Functions 556
B. The Number of Distinct Correlation Functions 559
C. Exact Correlation Function in the Low-Density Region 561
D. Relationship of the Correlation Function to the Master Equation 562
1. Weak-Collision Approximation 564
III. Application of the Theory to Some Special Cases 567
A. Infrequent Transitions Between States of Different J 567
B. The Two-Level System 568
IV. Correlation Functions of Anisotropic Intermolecular Potentials . . . 572

* Research supported by National Research Council of Canada.

† This research was supported in part by the Advanced Research Projects Agency (Project DEFENDER) and was monitored by the U.S. Army Research Office, Durham under Contract DA-31-124-ARO-D-257; and the National Science Foundation.

V. Calculation of the Intermolecular Correlation Functions 578
A. High-Temperature Approximation to the Intermolecular Correlation Functions 579
B. The Constant Acceleration Approximation (CAA) 581
VI. Interpretation of Some Experiments Using the CAA 585
A. Infrequent Transitions Between States of Different J 585
B. Application to Pure H_2 Gas 587
C. Effect of Transitions Between Rotational States in H_2 591
D. Quadrupole–Quadrupole Interactions Between H_2 and Diatomic Molecules Having Large Moments of Inertia 592
VII. Miscellaneous Topics 594
A. Other Theoretical Work 594
B. Spin Diffusion Constant in H_2 596
C. Nuclear Spin Relaxation in HD and D_2 596
D. Nuclear Spin Relaxation in Polyatomic Molecules 597
References 598

I. INTRODUCTION

Ever since the first nuclear magnetic resonance (NMR) experiments were performed,[1,2] the technique has been a powerful tool in the study of the properties of solids and liquids. More recently, the usefulness of NMR measurements in gases has also been recognized.[3–13] These measurements can be interpreted to yield quite precise information about intermolecular interactions, especially the anisotropic interactions responsible for molecular reorientation. In this article we shall review in some detail the available experimental NMR data in gases and the theoretical interpretation of these data. Our comments on the experimental NMR techniques used in the study of gases shall be brief since these techniques are adequately described in the literature.[14]

A. Macroscopic Measurements

All the experimental measurements which we shall discuss can be interpreted in terms of the phenomenological Bloch equations[2,14] for the macroscopic magnetization $\mathbf{M}$ of a nuclear spin system

$$\frac{d\mathbf{M}}{dt} = \gamma \mathbf{M} \times \mathbf{H} - \frac{M_x}{T_2}\,\mathbf{i} - \frac{M_y}{T_2}\,\mathbf{j} + \frac{M_0 - M_z}{T_1}\,\mathbf{k} \tag{1}$$

where the external field $\mathbf{H}$ is taken to be of the form

$$\mathbf{H} = H_0\mathbf{k} + 2H_1(t)\cos\omega t\mathbf{i} \qquad H_1 \ll H_0 \tag{2}$$

In Eq. (1), γ is the nuclear gyromagnetic ratio, **i**, **j**, and **k** are unit vectors in the x, y, and z directions, respectively, T_1 and T_2 are the longitudinal and transverse spin relaxation times, respectively, and M_0 is the equilibrium magnetization in the constant field H_0. The time variation of $H_1(t)$ for different experiments will be discussed below.

Using nuclear magnetic resonance techniques, we can measure the dependence on time of **M** for an applied rf field of amplitude $H_1(t)$. This time dependence can be analyzed to yield T_1 and T_2 and it is mainly the relationship of these relaxation times to the molecular interactions which is of interest to us here. For molecular gases which are not too dense, the spin–spin interactions between nuclei on different molecules are completely negligible and the spin-dependent interactions responsible for nuclear spin relaxation are those which couple the nuclear spins to the rotational degrees of freedom of the molecule. These *intra*molecular spin-dependent interactions are modulated by the rotation of the molecule and by those collisions between molecules which cause molecular reorientation, i.e., by definition, those collisions which cause transitions between molecular states having different rotational quantum numbers. The relaxation times T_1 and T_2 depend on the Larmor frequency $\omega_0 = -\gamma H_0$, the correlation time τ_c for molecular reorientation, and the strength of the *intra*molecular spin-dependent interactions. For $\omega_0\tau_c \ll 1$, $T_1 \approx T_2 \propto \tau_c^{-1} \propto$ the number of molecules per unit volume ρ, providing that ρ is not so large that three-body effects are important. T_2 is a monotonic function of ρ even for $\omega_0\tau_c \geq 1$, but the T_1 versus ρ curve goes through a characteristic minimum when $\omega_0\tau_c \approx 1$. For $\omega_0\tau_c \gg 1$, $T_1 \propto \rho^{-1}$. The minimum value of T_1 depends on the strength of the intermolecular interactions. For H_2 at 77°K, $(T_1)_{\min}$ has been measured to be 235 μsecs[15] while for other molecules, $(T_1)_{\min}$ is expected to range from a few microseconds to seconds.

Steady-state[5] and transient[4] NMR techniques have both been used to study NMR in gases. In steady-state experiments, H_1 is independent of time and the frequency ω is very slowly varied through the resonance which is centered at ω_0. The magnetization is driven at the frequency ω and one can measure the component of $\mathbf{M}(t)$ which is in phase with the rf field (dispersion) or out of phase with it (absorption). For sufficiently small H_1, $\gamma^2 H_1^2 T_1 T_2 \ll 1$, the induced rf magnetization is proportional to H_1 and the line shape of the absorption versus ω curve is Lorentzian[14] with a half-width at half-maximum of $1/T_2$. Thus, it is possible to measure T_2 using the relatively simple apparatus necessary to do NMR

absorption measurements. A severe limitation to the use of steady-state techniques is that the inhomogeneity of the magnet used has to be sufficiently small to enable a measurement of the natural line width. For $T_2 = 1$ sec for photons, the field must vary by less than about 40×10^{-6} gauss over the sample. T_1 may also be measured using steady-state techniques by studying the absorption in high rf fields, $\gamma^2 H_1^2 T_1 T_2 \geq 1$, but such measurements are as a rule less accurate and much more tedious than measurements using transient methods.

The two most common transient methods used to study T_1 and T_2 in fluids are the method of "adiabatic rapid passage"[14] and the pulse

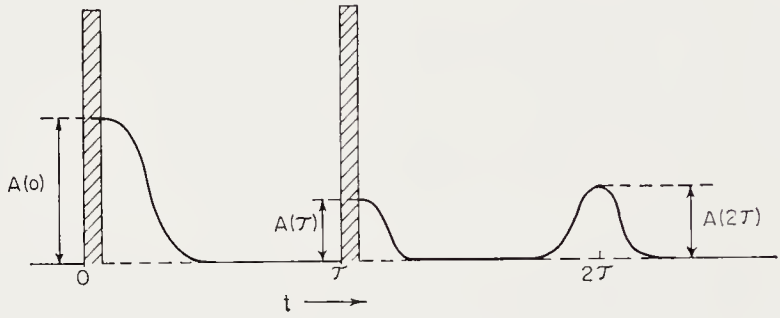

Fig. 1. Schematic display of the signals observed in a spin-echo experiment. Radio frequency pulses are applied at $t = 0$ and τ. The amplitudes of the free induction signals following the two pulses are indicated by $A(0)$ and $A(\tau)$, respectively, while the height of the echo at $t = 2\tau$ is given by $A(2\tau)$.

or "spin-echo" technique.[14,16] Of these, the spin-echo technique is more versatile for the study of fluids because one can also use it to measure directly the spin diffusion constant D. We illustrate the spin-echo technique in Figure 1. Two rf pulses of length t_w such that $\gamma H_1 t_w = \pi/2$ are applied at times $t = 0$ and τ, respectively. These pulses each rotate the nuclear magnetization by 90°. It is assumed that the time-independent magnetic field is inhomogeneous with a gradient G which is constant over the volume of the sample. This condition is not too difficult to satisfy experimentally. The gradient G is assumed to be sufficiently large that the induced components of magnetization decay in a time short compared with τ. Free induction signals of maximum amplitude $A(0)$ and $A(\tau)$ are observed after the pulses at $t = 0$ and τ, respectively. In addition, a characteristic echo of maximum amplitude $A(2\tau)$ appears at $t = 2\tau$. It may be shown by solving Eqs. (1) and (2) for this sequence

of rf pulses that

$$A(0) - A(\tau) = A(0) \exp(-\tau/T_1) \tag{3}$$

Furthermore, if the spatial motion of the molecules in the inhomogeneous field is adequately described by the solution to the diffusion equation, the echo amplitude is given by[17,18]

$$A(2\tau) \propto \exp\left[-\frac{2\tau}{T_2} - \frac{2}{3}\gamma^2 G^2 D\tau^3\right] \tag{4}$$

B. Physical Significance of the Relaxation Time Measurements

We illustrate by means of a simple model the information which measurements of T_1 and T_2 can yield. Suppose that in the absence of the rf field ($H_1 = 0$) the nuclei having angular momentum $\mathbf{I}\hbar$ interact only with the dc field $\mathbf{H}_0$ and with a fluctuating internal field $\mathbf{H}(t)$ as described by the Hamiltonian

$$\mathscr{H} = \hbar\omega_0 I_z - \gamma\hbar\mathbf{I} \cdot \mathbf{H}(t) \tag{5}$$

The time dependence of $\mathbf{H}(t)$ is assumed to be governed by the "lattice," the term "lattice" being used here to denote the equilibrium heat reservoir with temperature T associated with all degrees of freedom of the system other than those associated with the nuclear spins. The effect of $\mathbf{H}(t)$ is to cause nuclear spin transitions governed by the selection rule $\Delta m = \pm 1$, where m is an eigenvalue of I_z. If time-dependent perturbation theory is applicable and if the Zeeman splitting is small, i.e., $\hbar\omega_0 \ll kT$, then the transition probability for a $\Delta m = \pm 1$ transition is proportional to the Fourier transform of the "correlation function" of $H_x(t) \pm iH_y(t)$. If H_0 is not too large, the lattice is not polarized appreciably by the external field and we may set $\langle \mathbf{H} \rangle = 0$, where the symbol $\langle\ \rangle$ implies an average over the equilibrium ensemble for lattice degrees of freedom. Since equilibrium gases are isotropic for small H_0, we may set

$$\langle H_x^2 \rangle = \langle H_y^2 \rangle = \langle H_z^2 \rangle = \frac{1}{3}\langle |\mathbf{H}|^2 \rangle \tag{6}$$

and the general theory of spin relaxation[14] gives the results

$$\frac{1}{T_1} = \frac{1}{3}\gamma^2 \langle |\mathbf{H}|^2 \rangle J(\omega_0) \tag{7}$$

$$\frac{1}{T_2} = \frac{1}{6}\gamma^2\langle|\mathbf{H}|^2\rangle[J(0) + J(\omega_0)] \tag{8}$$

where the correlation function of $\mathbf{H}(t)$ is written

$$\langle\mathbf{H}(t)\cdot\mathbf{H}(t+\tau)\rangle = \langle|\mathbf{H}|^2\rangle g(\tau) \tag{9}$$

and

$$J(\omega) = \int_{-\infty}^{\infty} g(\tau)e^{-i\omega\tau}d\tau \tag{10}$$

$g(\tau)$ is the "reduced correlation function" of $\mathbf{H}(t)$.

In order to specify T_1, one needs two parameters, the *magnitude* of the field which couples the nuclear spins to the lattice and the Fourier component of the reduced correlation function evaluated at the Larmor frequency. To obtain T_2 one needs, in addition, the zero-frequency Fourier component of $g(\tau)$. This is a manifestation of the fact that it is possible for M_x and M_y to change without any spin-energy exchange with the lattice while a change of M_z necessarily requires that energy be exchanged.

It is often assumed that $g(\tau)$ decays exponentially, i.e.,

$$g(\tau) = e^{-\tau/\tau_c} \tag{11}$$

Then, Eqs. (7) and (8) become

$$\frac{1}{T_1} = \frac{2}{3}\gamma^2\langle|\mathbf{H}|^2\rangle\tau_c/(1+\omega_0^2\tau_c^2) \tag{12}$$

$$\frac{1}{T_2} = \frac{1}{3}\gamma^2\langle|\mathbf{H}|^2\rangle[\tau_c + \tau_c/(1+\omega_0^2\tau_c^2)] \tag{13}$$

For this case, the plot of T_1 versus τ_c goes through a characteristic minimum at $\omega_0\tau_c = 1$ while for $\omega_0\tau_c \gg 1$, $T_1 \propto \tau_c$. If this model is applied to a dilute gas* in which the time between changes in $\mathbf{H}(t)$ is associated with the time between certain types of molecular collisions, $\tau_c \propto \rho^{-1}$. Then in the region $\omega_0\tau_c \gg 1$, T_1 decreases as the frequency of collisions increases, but in the region $\omega_0\tau_c \ll 1$ the opposite behavior (pressure narrowing) is obtained.

As we shall show later, the experimental dependence of T_1 on ρ in

* We are neglecting the effects of free rotation. These effects will be discussed in Section II.

H_2 gas indicates that at low temperatures, where all the *ortho*-H_2 molecules are in their ground rotational state ($J = 1$), the correlation functions of the internal magnetic fields are indeed exponential.[15] At higher temperatures, where more rotational states are excited, this is not so.

The property of primary importance to us is that the temperature dependence of T_1 (and T_2) at constant density is very sensitive to the detailed form of the anisotropic intermolecular interaction responsible for molecular reorientation, and hence for fluctuations in $\mathbf{H}(t)$.

In order to obtain molecular information from measurements of T_1 and T_2, it is necessary first to consider the actual *intra*molecular spin-dependent interactions. As we shall see in the next section, the general theory of nuclear spin relaxation can be applied to the case of molecules such as H_2 to yield quite rigorous expressions for T_1 and T_2, which are analogous to Eqs. (7) and (8). In these expressions, it is necessary to evaluate correlation functions of the rotational angular momentum operator $\mathbf{J}(t)$ of a single molecule and of the spherical harmonics $Y_{2m}[\Omega(t)]$ of the orientation $\Omega(t)$ of the molecule relative to a space-fixed coordinate system. When the collisions between molecules are "weak" in the sense that transitions between single molecule states of different rotational quantum numbers J, M can be calculated using first-order time-dependent perturbation theory, it proves possible to relate the above-mentioned correlation functions explicitly to the *inter*molecular anisotropic interactions.

II. THEORY OF NUCLEAR SPIN RELAXATION IN DILUTE HYDROGEN GAS

Molecular hydrogen is an excellent system in which to test the theory of nuclear spin relaxation in molecular gases and to illustrate the type of molecular information obtainable from T_1 measurements. This system has two modifications, *ortho*-H_2, which has total nuclear spin $I = 1$ and odd rotational states $J = 1, 3, \ldots$, and *para*-H_2 which has $I = 0$ and $J = 0, 2, \ldots$. Only the protons of *ortho*-H_2 contribute to the NMR signal. The probability of a collision between two H_2 molecules inducing a transition between an *ortho* and a *para* state is very small because it corresponds to a highly forbidden transition from a triplet to a singlet state of the nuclear spins. The half-life for this process at 0°C at 1 atm pressure is of the order of three years in the absence of

impurities. Since the equilibrium concentration of *ortho*-H_2 at high temperatures is 75% and it is easy to produce almost 100% *para*-H_2 at low temperatures using catalysts, it is easy to study gaseous mixtures of *ortho*-H_2 and *para*-H_2 whose *ortho*-H_2 concentration ranges from 0 to 75% at any temperature. As we shall show later, it is very important to be able to vary the concentration of *ortho*-H_2 to obtain precise molecular information from T_1 measurements in H_2 gas.

A. Intramolecular Correlation Functions

For the *dilute* gas, the contribution of the dipolar interactions between nuclear spins on *different* molecules to spin relaxation is very small and may be neglected. The coupling between the nuclear spins and the "lattice" is due to the *intra*molecular spin–rotation and dipolar interactions. Thus, the Hamiltonian for a dilute gas of NH_2 molecules in a magnetic field H_0 applied along the z axis can be written

$$\mathcal{H} = \mathcal{H}_z^I + \mathcal{H}_z^J + \mathcal{H}_J + \mathcal{H}_L + \mathcal{H}' \tag{14}$$

where the spin Zeeman Hamiltonian $\mathcal{H}_z^I$ is

$$\mathcal{H}_z^I = \hbar\omega_I \sum_{i=1}^{N} I_{iz} \tag{15}$$

where I_{iz} is the z component of nuclear spin of the ith molecule; the molecular Zeeman Hamiltonian $\mathcal{H}_z^J$ is

$$\mathcal{H}_z^J = \hbar\omega_J \sum_{i=1}^{N} J_{iz} \tag{16}$$

the molecular rotational Hamiltonian $\mathcal{H}_J$ is

$$\mathcal{H}_J = \sum_{i=1}^{N} \frac{\hbar^2 J_i^2}{2I_0} \tag{17}$$

where I_0 is the moment of inertia of an H_2 molecule; the lattice Hamiltonian $\mathcal{H}_L$

$$\mathcal{H}_L = \sum_{i=1}^{N} \frac{p_i^2}{2m} + V(R^N\Omega^N) \tag{18}$$

contains the kinetic energy of the centers of mass of the various molecules and the *inter*molecular potential energy V; and the spin–lattice interaction Hamiltonian $\mathcal{H}'$ is a sum of single molecule terms[14]

$$\mathcal{H}' = \sum_{i=1}^{N} \left\{ \frac{\gamma\hbar H'}{2} \sum_m L^i_{1m} S^i_{1-m} + \left(\frac{6\pi}{5}\right)^{1/2} \gamma\hbar H'' \sum_m L^i_{2m} S^i_{2-m} \right\} \quad (19)$$

In the following we delete the index i when referring to one-particle operators. In these expressions, ω_I and ω_J are the Larmor frequencies in the field of H_0 of **I** and **J**, respectively, $\gamma = 2.69 \times 10^4$ sec^{-1}gauss^{-1} is the proton gyromagnetic ratio and $H' = 26.752 \pm 0.007$ gauss and $H'' = 33.862 \pm 0.015$ gauss are the coupling constants associated with the *intra*molecular spin–rotation and dipolar interactions, respectively. The quantities S_{lm} and L_{lm} are components of irreducible tensors associated with nuclear spin operators and molecular rotation operators, respectively, and are defined by

$$S_{10} = (2)^{1/2} I_z, \; S_{1\pm1} = I_\pm \equiv I_x \pm iI_y \quad (20)$$

$$S_{20} = \left(\frac{2}{3}\right)^{1/2} [3I_z^2 - I(I+1)], \; S_{2\pm1} = I_z I_\pm + I_\pm I_z, \; S_{2\pm2} = I_\pm^2 \quad (21)$$

$$L_{10} = (2)^{1/2} J_z, \; L_{1\pm1} = J_\pm \equiv J_x \pm iJ_y \quad (22)$$

$$L_{2m} = Y_{2m}(\Omega) \quad (23)$$

where $Y_{2m}(\Omega)$ is the spherical harmonic of order 2 of the orientation Ω of the molecular axis.

The effect of collisions between molecules is to produce transitions between states of different J and M because of the anisotropic *inter*molecular interactions. The resulting changes in L_{lm} produce changes in the nuclear magnetization. Thus, using a perturbation expansion in the small coupling term $\mathcal{H}'$, the nuclear spin relaxation times T_1 and T_2 can be calculated in terms of the Fourier transform of the correlation functions of $L_{lm}(t)$[14,19]

$$\frac{1}{T_1} = (\gamma^2 H'^2/2) J_{11}(\omega_I) + (12\pi/5)\gamma^2 H''^2 [J_{21}(\omega_I) + 4J_{22}(2\omega_I)] \quad (24)$$

$$\frac{1}{T_2} = (\gamma^2 H'^2/4)[J_{11}(\omega_I) + J_{10}(0)] + (12\pi/5)\gamma^2 H''^2 \times \left[\frac{3}{2} J_{20}(0) + \frac{5}{2} J_{21}(\omega_I) + J_{22}(2\omega_I)\right] \quad (25)$$

where

$$J_{lm}(\omega) = \int_{-\infty}^{\infty} e^{-i\omega t} G_{lm}(t)\, dt \quad (26)$$

and the correlation function $G_{lm}(t)$ is given by

$$G_{lm}(t) = \frac{1}{2}\{\langle L_{lm}(t)L^{+}_{lm}(0)\rangle + \langle L_{lm}(0)L^{+}_{lm}(t)\rangle\} \tag{27}$$

where

$$L_{lm}(t) = \exp\left[i/\hbar(\mathscr{H}^{J}_{z} + \mathscr{H}_{J} + \mathscr{H}_{L})t\right]L_{lm}\exp\left[-i/\hbar(\mathscr{H}^{J}_{z} + \mathscr{H}_{J} + \mathscr{H}_{L})t\right] \tag{28}$$

L_{lm} is a single-particle operator, and the average $\langle\ \rangle$ involves the trace of the quantity in the brackets with the density matrix

$$\rho = \frac{\exp\left[-\beta(\mathscr{H}^{J}_{z} + \mathscr{H}_{J} + \mathscr{H}_{L})\right]}{Tr\{\exp\left[-\beta(\mathscr{H}^{J}_{z} + \mathscr{H}_{J} + \mathscr{H}_{L})\right]\}} \tag{29}$$

with everything assumed to be in equilibrium except for the ratio of *ortho* to *para* molecules.

It is instructive to examine the *correlation function for free molecules*, in which case $V(\mathbf{R}^N) = 0$

$$[G_{lm}(t)]_{\text{free}} = \sum_{J_0,M_0}\sum_{J,M} P_{J_0M_0}\,|(J_0M_0\,|\,L_{lm}\,|\,JM)|^2 \cos\left[(E_J - E_{J_0} + m\hbar\omega_J)t/\hbar\right] \tag{30}$$

where the term $m\hbar\omega_J$ arises from the fact that the only nonzero matrix elements of L_{lm} are those for which $M_0 - M = m$ and

$$P_{J_0M_0} = \frac{1}{2J_0 + 1}\,P_{J_0} = \frac{\exp\left[-E_{J_0}/kT\right]}{\sum_{J}(2J+1)\exp\left[-E_J/kT\right]} \tag{31}$$

is the probability that a molecule is in the state J_0, M_0 with energy E_{J_0} for a system at a temperature T if $J_0\hbar\omega_J \ll kT$. In Eq. (31), P_{J_0} is the probability that a molecule has the rotational energy E_{J_0}.

The operator L_{1m} has nonzero matrix elements only for states $J = J_0$, while the operator L_{2m} has matrix elements for states $J = J_0$ and $J = J_0 \pm 2$. The latter terms oscillate for the free molecule at the angular frequency $[(E_{J_0\pm 2} - E_{J_0})/\hbar + m\omega_J]$. This quantity is always greater than 10^{12}sec^{-1} for *ortho*-H_2. The Fourier transform or "spectral density" of the free molecule correlation function is a series of δ functions at the frequencies $\pm m\omega_J$ and $\pm[(E_{J_0\pm 2} - E_{J_0})/\hbar + m\omega_J]$. The effect of the *inter*molecular interaction term $V(\mathbf{R}^N)$ is to spread the spectral density associated with each δ function over a range of frequen-

cies of the order of the collision frequency. The collision frequency in H_2 gas, even at pressures as high as several hundred atmospheres, is never greater than 10^{12} sec^{-1}. We wish to calculate $J_{lm}(\omega)$ at frequencies $\omega = 0$, ω_I, and $2\omega_I$, where ω_I, which is about five times as large as ω_J for H_2, is always smaller than about 10^9 sec^{-1} for the magnetic fields available to the experimentalist. Therefore, as first pointed out by Needler and Opechowski,[12] we may safely neglect the matrix elements of L_{2m} between states of different J for H_2.

B. The Number of Distinct Correlation Functions

To proceed further, the form of the correlation functions $G_{lm}(t)$ must be determined. We have seen in Eqs. (24) and (25) that five such functions are required to specify the relaxation times for H_2. In order to reduce the number of variables, various assumptions have been made in the past. We describe them briefly in order of increasing sophistication following closely the arguments of Hardy.[15]

In the original theory developed by Schwinger,[1,14] the assumption is made that the correlation functions $G_{lm}(t)$ all decay exponentially with the same time constant τ_c, i.e.,

$$\langle L_{lm}(t)L_{lm}^{+}(0)\rangle = \langle L_{lm}(0)L_{lm}^{+}(0)\rangle e^{-t/\tau_c} \tag{32}$$

It was first suggested by Needler and Opechowski[12] that a more correct expression is

$$\langle L_{lm}(t)L_{lm}^{+}(0)\rangle = \langle L_{lm}(0)L_{lm}^{+}(0)\rangle e^{im\omega_J t}e^{-t/\tau_c} \tag{33}$$

and a similar expression was given by Abragam.[14] The quantity ω_J is the Larmor frequency of the molecular magnetic moment and the term $e^{im\omega_J t}$ represents the free precession of J between collisions. It is easily seen from Eq. (30) that in the absence of collisions, the time dependence of $G_{lm}(t)$ is given exactly by cos $(m\omega_J t)$ if the matrix elements of L_{lm} between states of different J are neglected.

Johnson and Waugh[5] have pointed out that if the rate of effective collisions (i.e., collisions effective in reorienting **J**) is much higher than ω_J, then only two of the five possible correlation functions are distinct: one for L_{1m} and one for L_{2m}. Although this condition has been well satisfied in most experimental work thus far, at the lowest densities encountered in Hardy's work[15] the reorientation rate was only slightly larger than ω_J. Fortunately, however, Hardy has been able to make a

convincing argument that there are only two distinct correlation functions under much less restrictive conditions than proposed originally by Johnson and Waugh.

First note that if the magnetic field is zero, then the correlation functions of the L_{lm} are independent of m for a given l. This follows from the fact that the L_{lm} transform in the same way under coordinate rotations as the spherical harmonics $Y_{lm}(\Omega)$. For $H_0 = 0$ there is complete spatial isotropy and the result follows. This is just a limiting case of the argument by Johnson and Waugh for weak H_0. Next we note that even for magnetic fields up to several hundred kilogauss, the time of a single collision is much shorter than the molecular Larmor period $2\pi/\omega_J$. Therefore, spatial isotropy can be claimed during a molecular collision. Any effect of H_0 must therefore be due to the free precession of the molecular angular momentum between collisions. Let us assume no net molecular polarization ($\hbar\omega_J \ll kT$) and also that in zero magnetic field there is no correlation between **J** and the molecular momentum **p**. Since the magneic field cannot create a correlation between **J** and **p** after a collision and since H_0 has no effect during a collision, we must conclude that immediately before, during, and immediately after a collision, all directions are equivalent. Except for the precession of **J** between collisions, the correlation functions of the L_{lm} must be independent of m. Hence we can write

$$\langle L_{lm}(t)L_{lm}^{+}(0)\rangle = \langle L_{lm}(0)L_{lm}^{+}(0)\rangle e^{im\omega_J t}g_l(t) \tag{34}$$

independently of the relative magnitude of $1/\omega_J$ and the correlation times associated with the $g_l(t)$.

The critical assumption in the above discussion is the one concerning the correlation between **J** and **p**. There is no *à priori* reason for believing it is zero and, in fact, such a correlation has been demonstrated experimentally for a number of diatomic gases.[20—22] It is observed that the viscosity and thermal conductivity decrease slightly in a magnetic field. These effects can be understood in terms of a collision-induced correlation between **p** and **J**. The precession of **J** in an applied magnetic field can partially destroy this correlation between collisions and, since the molecules are nonspherical, this leads to a change in the collision cross section. As a result, the mean free path depends on the direction of **J** with respect to $\mathbf{H}_0$. For hydrogen, however, one expects the correlation to be very small inasmuch as the molecule is nearly spherical. From a slightly different point of view, one can say that since many collisions

are required to change m_J for an H_2 molecule, the correlation is necessarily small; obviously, **J** cannot remain simultaneously correlated to **p** and also to some other fixed direction for the duration of many collisions. Furthermore, the change in viscosity of H_2 with magnetic field has been measured recently and found to be exceedingly small—of the order of a few parts in 10,000. It is expected, then, that Eq. (34) can be assumed with some confidence. Corrections to this result can be computed using the techniques of Waldmann,[23] Snider,[24] and Andersen.[25]

C. Exact Correlation Function in the Low-Density Region

It is quite easy to obtain a rigorous low-density expression for $J_{l0}(\omega)$ and therefore for T_1 and T_2. We shall present a brief discussion of this result because of its usefulness in determining the low-density form of the time dependence of $G_l(t)$. The details of the calculation will be published in an article by one of the authors (I.O.) and J. Wang. We rewrite Eqs. (26) and (27) as

$$J_{l0}(\omega) = Rl \lim_{\varepsilon \to 0} \int_0^\infty e^{-\varepsilon t} e^{-i\omega t} \{ \langle e^{i\mathscr{L}t} L_{l0}(0) L_{l0}^{+}(0) + L_{l0}(0) e^{-i\mathscr{L}t} L_{l0}^{+}(0) \rangle \} \, dt \quad (35)$$

where Rl denotes the real part of the integral and $\mathscr{L}$ is an N-particle tetradic operator which is defined such that

$$L_{l0}(t) = e^{i\mathscr{L}t} L_{l0}(0) \quad (36)$$

[see Eq. (28)]. The integration over time in Eq. (35) can be performed explicitly to yield

$$J_{l0}(\omega) = Rl \lim_{\varepsilon \to 0} \left\{ \left\langle \left[\frac{1}{\varepsilon + i\omega - i\mathscr{L}} L_{l0}(0) \right] L_{l0}^{+}(0) + L_{l0}(0) \frac{1}{\varepsilon + i\omega + \mathscr{L} i} L_{l0}^{+}(0) \right\rangle \right\} \quad (37)$$

By making use of the binary collision expansion and the techniques developed by Zwanzig[26] and Kawasaki and Oppenheim,[27] one can obtain in the low-density limit.

$$J_{l0}(\omega) = \left\langle L_{l0}(0) \frac{\rho \overline{\mathscr{L}}}{\omega^2 + (\rho \overline{\mathscr{L}})^2} L_{l0}^{+}(0) \right\rangle_0 \quad (38)$$

where $\overline{\mathscr{L}}$ is a two-particle scattering operator which contains the *exact* dynamics of a binary collision. The subscript 0 on the average implies that the density matrix to be used is that given by Eq. (29) setting $V(\mathbf{R}^N)$ equal to zero. For very low densities $\rho\overline{\mathscr{L}} \ll \omega$ and $J_{l0} \propto \rho$; for higher densities such that $\rho\overline{\mathscr{L}} \gg \omega$, $J_{l0} \propto \rho^{-1}$. The behavior of $J_{l0}(\omega)$ for densities such that $\rho\overline{\mathscr{L}} \sim \omega$ cannot be analyzed completely without detailed calculation. However, if $L_{l0}(0)$ is expanded in the orthonormal eigenfunctions of $\overline{\mathscr{L}}$, i.e.,

$$L_{l0}(0) = \sum_{\alpha} a_\alpha \chi_\alpha \tag{39}$$

where

$$\overline{\mathscr{L}}\chi_\alpha = \lambda_\alpha \chi_\alpha \tag{40}$$

and a_α and γ_α are numbers, Eq. (38) can be written

$$J_{l0}(\omega) = \sum_{\alpha} \frac{|a_\alpha|^2 \rho\lambda_\alpha}{\omega^2 + (\rho\lambda_\alpha)^2} \tag{41}$$

This form for $J_{l0}(\omega)$ implies that $G_{l0}(t)$ has the form

$$G_{l0}(t) = \sum_{\alpha} |a_\alpha|^2 e^{-\lambda_\alpha t} \tag{42}$$

The analysis above is similar to the Chapman Enskog analysis of the ordinary transport coefficients. If $L_{l0}(0)$ is approximately an eigenfunction of $\overline{\mathscr{L}}$, then Eq. (41) becomes

$$J_{l0}(\omega) = \frac{|a|^2 \rho\lambda}{\omega^2 + (\rho\lambda)^2} \tag{43}$$

This result is consistent with Hardy's low-temperature measurements of T_1 in the region of its minimum[15] which will be discussed later.

D. Relationship of the Correlation Function to the Master Equation

From the discussion of Section II-B, we see that there are only two independent correlation functions to be considered for H_2, namely G_{10} and G_{20}. Since all matrix elements of L_{l0} between states of different J can be neglected, the only remaining nonzero matrix elements are

$$(JM|L_{l0}|JM) = [f_l(J)]^{1/2} C(Jl J; M0) \tag{44}$$

where $C(Jl J; M0)$ is a Clebsch-Gordon coefficient as defined by Rose[28]

and

$$f_1(J) = 2J(J+1) \tag{45}$$

$$f_2(J) = 5/4\pi[J(J+1)/(2J-1)(2J+3)] \tag{46}$$

Thus, the correlation function of $L_{l0}(t)$ may be written

$$\begin{aligned} G_{l0}(t) &= \sum_{J_0M_0} P_{J_0M_0}(J_0M_0\,|L_{l0}|\,J_0M_0) \sum_{JM} w(JM;t/J_0M_0;0)(JM\,|L_{l0}|\,JM) \\ &= \sum_{J_0M_0} P_{J_0M_0}[f_1(J_0)]^{1/2} C(J_0lJ_0;M_00) \sum_{JM} w(JM;t/J_0M_0;0) \\ &\qquad \times [f_1(J)]^{1/2} C(JlJ;M0) \end{aligned} \tag{47}$$

where the conditional probability $w(JM;t/J_0M_0;0)$ is the probability that the molecule is in the rotational state J,M at time t given that it is in the state J_0, M_0 at $t=0$, and $P_{J_0M_0}$ is defined by Eq. (31). We assume that $w(JM;t/J_0M_0;0)$ satisfies the temporally homogeneous master equation

$$\frac{\partial w}{\partial t} = \dot{w}(JM;t/J_0M_0;0) = \sum_{J'M'} A(JM;J'M')w(J'M';t/J_0M_0;0) \tag{48}$$

where $A(JM;J'M')$, $J,M \neq J',M'$, is the transition rate for the transition $J',M' \to J,M$. For $J=J'$, $M=M'$,

$$A(J'M';J'M') = -\sum_{J\neq J'} \sum_{M} A(JM;J'M') - \sum_{M\neq M'} A(J'M;J'M') \tag{49}$$

Since there is no upper boundary to J, there is an infinite number of coupled equations [Eq. (48)]. In practice, however, those rotational states which have an extremely small population contribute very little to G_{l0} so that the hierarchy may be truncated. The number of equations required depends on the temperature and on the accuracy with which it is necessary to calculate T_1 in order to obtain a meaningful comparison of theory with experiment.

We shall find it useful to define the tensor polarization of order l in the state J for molecules initially in the state J_0, M_0 as

$$m^l_{JJ_0M_0}(t) = \sum_{M} C(JlJ;M0)w(JM;t/J_0M_0;0) \tag{50}$$

Using Eq. (48), we see that m satisfies the differential equation

$$\dot{m}^l_{JJ_0M_0}(t) = \sum_{J'M'} w(J'M';t/J_0M_0;0) \sum_{M} C(JlJ;M0)A(JMJ;'M') \tag{51}$$

1. Weak-Collision Approximation

We now assume that the intermolecular interactions V between the molecules consist of an isotropic part $V_0(R^N)$ and an anisotropic part V_A which is "weak" in the sense that first-order perturbation theory may be used to calculate the transition rates $A(JM;J'M')$. Suppose that each term in the anisotropic interaction Hamiltonian V_A is a product of a "lattice" operator and a rotational operator $Y_{\lambda\mu}(\Omega)$, where $Y_{\lambda\mu}$ is a spherical harmonic of order λ. The matrix element of $Y_{\lambda\mu}$ between states J,M and J',M' is given by[28]

$$(JM\,|Y_{\lambda\mu}|\,J'M') = \delta_{M,M'+\mu}\left[\frac{(2J'+1)(2\lambda+1)}{4\pi(2J+1)}\right]^{1/2} \times C(J'\lambda J;M'\mu)C(J'\lambda J;00) \quad (52)$$

where $C(\,)$ is a Clebsch-Gordon coefficient. Since the transition rate is proportional to the square of the matrix element of V_A between the initial and final states, the contribution of this term to the transition probability is

$$A_\lambda(JM;J'M') = Q_\lambda(J,J')[C(J'\lambda J;M',\mu]^2\delta_{M,M'+\mu} \quad (53)$$

where the only dependence of the transition rate on M and M' is given explicitly by the Clebsch-Gordon coefficient and the Kronecker δ.

The functions $Q_\lambda(J,J')$ will be evaluated later when the anisotropic intermolecular interactions appropriate to H_2 are considered in more detail.

Using Eq. (53) and Eqs. (6.23a) and (6.24) of Rose[28] it can be shown that

$$\sum_M C(JlJ;M0)A_\lambda(JM;J'M') = C(J'lJ';M'0)B_{l\lambda}(J,J') \quad (54)$$

where

$$[(2J'+1)/(2J+1)]B_{l\lambda}(J,J') = Q_\lambda(J,J')(-1)^{\lambda+l-J-J'}[(2J+1)(2J'+1)]^{1/2}W(J,J',J,J';\lambda l) - \delta_{JJ'}\sum_{J''}\left(\frac{2J''+1}{2J'+1}\right)Q_\lambda(J'',J') \quad (55)$$

where $W(JJ'JJ';\lambda l)$ is a Racah coefficient.[28] Using Eqs. (51), (54), and (55), it is easily shown that the tensor polarization satisfies the following

equation in the weak-collision approximation.

$$\dot{m}^l_{JJ_0M_0}(t) = \sum_{J'} B_l(J,J')m^l_{J'J_0M_0}(t) \tag{56}$$

where

$$B_l(J,J') = \sum_{\lambda} B_{l\lambda}(J,J') \tag{57}$$

Equation (56) must be solved with the initial conditions

$$m^l_{JJ_0M_0}(0) = C(J_0lJ_0;M_00)\delta_{JJ_0} \tag{58}$$

which follow from Eq. (50) and the fact that $w(JM;0/J_0M_0;0) = \delta_{JJ_0}\,\delta_{MM_0}$. The solutions are of the form

$$m^l_{JJ_0M_0}(t) = \sum_{\alpha} a^{l\alpha}_{JJ_0M_0}e^{-\Lambda_{l\alpha}t} \tag{59}$$

where the a's are independent of time and depend on the initial condition [Eq. (58)] and the eigenfunctions of the matrix $\tilde{B}_l$ with elements $B_l(J,J')$ and the $-\Lambda_{l\alpha}$ are the eigenvalues of the $\tilde{B}_l$. The number of terms in the sum is equal to the number of Eqs. (56) which depends on the number of Eqs. (48). Since

$$A(JM;J'M')P_{J'M'} = A(J'M';JM)P_{JM} \tag{60}$$

i.e., the $A(JM;J'M')$ all obey detailed balance, the $\Lambda_{l\alpha}$ are greater than or equal to zero.[29] From the initial conditions and the fact that $B_l(J,J')$ is independent of M_0, it follows that

$$a^{l\alpha}_{JJ_0M_0} = b^{l\alpha}_{JJ_0}C(J_0lJ_0;M_00) \tag{61}$$

where the $b^{l\alpha}_{JJ_0}$ are independent of time.

The correlation function $G_{l0}(t)$ defined by Eq. (47) can now be written using Eqs. (50), (59), and (61) as follows

$$G_{l0}(t) = \sum_{J_0}[f_l(J_0)]^{1/2}\sum_{M_0}P_{J_0M_0}[C(J_0lJ_0;M_00)]^2\sum_{\alpha}e^{-\Lambda_{l\alpha}t} \times \sum_{J}[f_l(J)]^{1/2}b^{l\alpha}_{JJ_0} \tag{62}$$

Finally, by using Eq. (31), noting that

$$\frac{1}{2J_0+1}\sum_{M_0}[C(J_0lJ_0;M_00)]^2 = \frac{1}{2l+1} \tag{63}$$

and defining $C_{J_0}^{l\alpha}$ by

$$C_{J_0}^{l\alpha} = \left[\frac{1}{f_l(J_0)}\right]^{1/2} \sum_J [f_l(J)]^{1/2} b_{JJ_0}^{l\alpha} \tag{64}$$

we can write the correlation function as

$$G_{l0}(t) = \frac{1}{2l+1} \sum_{J_0} P_{J_0} f_l(J_0) \sum_\alpha C_{J_0}^{l\alpha} e^{-\Lambda_{l\alpha} t} \tag{65}$$

Equation (65) is the expression for $G_{l0}(t)$ for $t \geq 0$. For $t < 0$, we use the symmetry condition $G_{l0}(t) = G_{l0}(-t)$.

It is noteworthy that in the weak-collision approximation, the correlation function can always be written as a sum of exponential functions of time. Of course, the time dependence of $G_{l0}(t)$ depends on the spectrum of eigenvalue $\Lambda_{l\alpha}$. We are interested in the Fourier transform of the correlation function which is given, for the general case, by

$$J_{l0}(\omega) = \frac{2}{2l+1} \sum_{J_0} P_{J_0} f_l(J_0) \sum_\alpha \frac{C_{J_0}^{l\alpha} \Lambda_{l\alpha}}{\Lambda_{l\alpha}^2 + \omega^2} \tag{66}$$

Since it follows from Eq. (34) that

$$J_{lm}(\omega) = J_{l0}(\omega - m\omega_J) \tag{67}$$

we can write T_1^{-1}, Eq. (24) in the form

$$\frac{1}{T_1} = \sum_{J_0} P_{J_0} \left(\frac{1}{T_1}\right)_{J_0} \tag{68}$$

where, using Eqs. (45) and (46)

$$\begin{aligned}\left(\frac{1}{T_1}\right)_{J_0} = {} & \frac{2}{3} \gamma^2 H'^2 J_0(J_0+1) \sum_\alpha \frac{C_{J_0}^{1\alpha} \Lambda_{1\alpha}}{\Lambda_{1\alpha}^2 + (\omega_I - \omega_J)^2} \\ & + \frac{6}{5} \gamma^2 H''^2 \frac{J_0(J_0+1)}{(2J_0-1)(2J_0+3)} \sum_\alpha C_{J_0}^{2\alpha} \left[\frac{\Lambda_{2\alpha}}{\Lambda_{2\alpha}^2 + (\omega_I - \omega_J)^2} \right. \\ & \left. + \frac{4\Lambda_{2\alpha}}{\Lambda_{2\alpha}^2 + 4(\omega_I - \omega_J)^2}\right]\end{aligned} \tag{69}$$

The quantity $(1/T_1)_{J_0}$ is the relaxation rate for an ensemble of molecules which are all initially in the state J_0. Following the same procedure, expressions analogous to Eqs. (68) and (69) may be written for $1/T_2$.

Although the explicit results for T_1 and T_2 given here apply only to H_2, the results for the Fourier transforms of the correlation functions derived here can be applied to any gas of diatomic molecules.

III. APPLICATION OF THE THEORY TO SOME SPECIAL CASES

A. Infrequent Transitions Between States of Different J

In order to compare the general result for weak collisions with previous calculations, we consider the special case in which it is assumed that transitions between states of different J occur much less frequently than between states of different M within a J manifold. This implies that

$$Q_\lambda(J,J') \ll Q_\lambda(J,J) \qquad J \neq J' \tag{70}$$

Equations (55), (57), and (70) imply that we can approximate the elements of the $\tilde{B}_l$ by

$$B_l(J,J') = B_l(J,J)\delta_{JJ'} \tag{71}$$

Equation (56) then reduces to

$$\dot{m}^l_{JJ_0M_0} = B_l(J,J)m^l_{JJ_0M_0} \tag{72}$$

which can be solved to yield

$$m^l_{JJ_0M_0}(t) = m^l_{JJ_0M_0}(0)e^{B_l(J,J)t} \tag{73}$$

Under these conditions, Eq. (66) reduces to

$$J_{l0}(\omega) = \frac{2}{2l+1}\sum_{J_0} P_{J_0} f_l(J_0)\,\frac{\Lambda_{lJ_0}}{\Lambda^2_{lJ_0} + \omega^2} \tag{74}$$

where*

$$\Lambda_{lJ_0} = -B_l(J_0, J_0) = +\,|\,B_l(J_0, J_0)\,| \tag{75}$$

This result is in agreement with previous calculations[7,9] for this special case, which obtain for H_2 at temperatures below about 150°K, since at this temperature all but 0.8% of the *ortho*-H_2 molecules are

* In general, if transitions between different J states are not much less frequent than between states of different M, for a given J, one cannot identify the $\Lambda_{l\alpha}$ with any specific rotational states.

in the $J = 1$ state. In using Eq. (68) to compute $1/T_1$, we implicitly assume that many transitions between states of different J occur during a time T_1.

A critical test of the theory for this case has been made by Hardy[15] who has studied T_1 and T_2 as a function of the density ρ for normal-H_2 in the vicinity of the T_1 minimum at 78°K. His data for T_1 and T_2 are shown in Figures 2 and 3, respectively. Since H' and H'' are of comparable magnitudes and since $\Lambda_{l1} \propto \rho$ for both $l = 1$ and 2, the value of $(T_1)_{\text{min}}$ and the shape of the T_1 and T_2 versus ρ curves are sensitive to the ratio $\Lambda_{21}/\Lambda_{11}$. Hardy concludes from a detailed analysis of his data that

$$0.6 \leq \Lambda_{21}/\Lambda_{11} \leq 1.0 \tag{76}$$

The theory for the special case given above predicts the following result using Eqs. (55) and (75) and assuming that only one value of λ contributes to the sum in Eq. (57)

$$\frac{\Lambda_{2J}}{\Lambda_{1J}} = \frac{B_{2\lambda}(J,J)}{B_{1\lambda}(J,J)} = \frac{3[4J(J+1) - \lambda(\lambda+1) - 1]}{(2J-1)(2J+3)} \tag{77}$$

For the case of H_2 in the $J = 1$ state, the only allowed value of λ is $\lambda = 2$. Terms for $\lambda = 0$ give no transitions, $\lambda = 1$ is excluded by the reflection symmetry of H_2 and terms for $\lambda > 2$ can give no transitions within a $J = 1$ manifold. Therefore the result of Eq. (77) is $\Lambda_{21}/\Lambda_{11} = 0.6$, in agreement with experiment. Furthermore, Hardy has been able to conclude that within experimental error $\Lambda_{l1} \propto \rho$ and that the correlation functions is exponential. This is an important experiment in that it checks the basic approximations made in the theory. It would be of interest to extend Hardy's measurements to lower densities in order to narrow the limits on the inequalities of Eq. (76).

B. The Two-Level System

We shall present here the general results for the case in which only two levels characterized by J_1 and J_2, respectively, are appreciably populated so that only two of the equations [Eq. (56)] are required to give an accurate representation of T_1 and T_2. For the case of *ortho*-H_2, these two levels correspond to $J_1 = 1$ and $J_2 = 3$. To illustrate the range of temperature over which these results will be applicable with reasonable precision, we note that the fractional population of the $J = 5$ state is

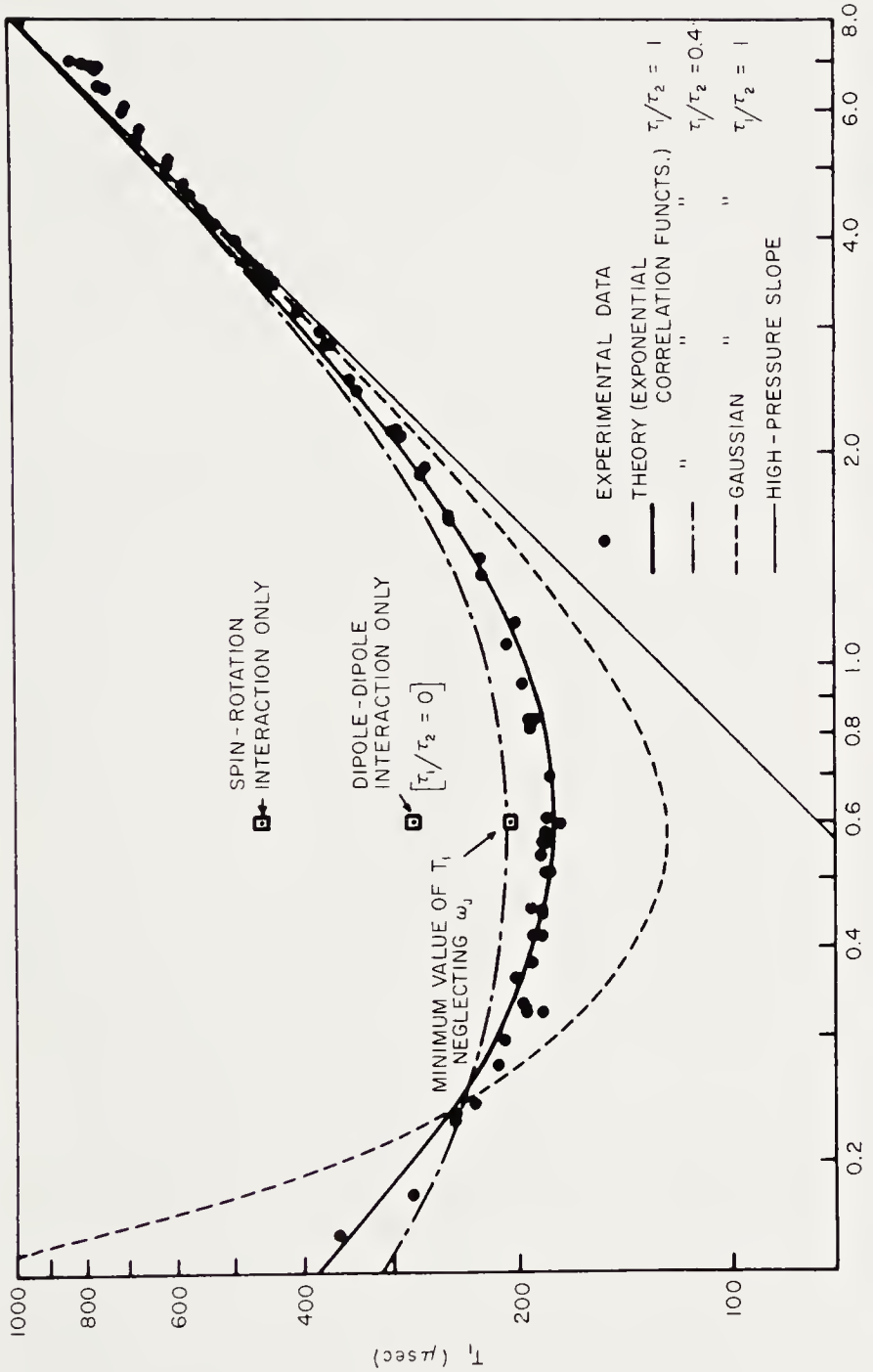

Fig. 2. Plot of T_1 versus density in H_2 gas at 77.5°K (ref. 15).

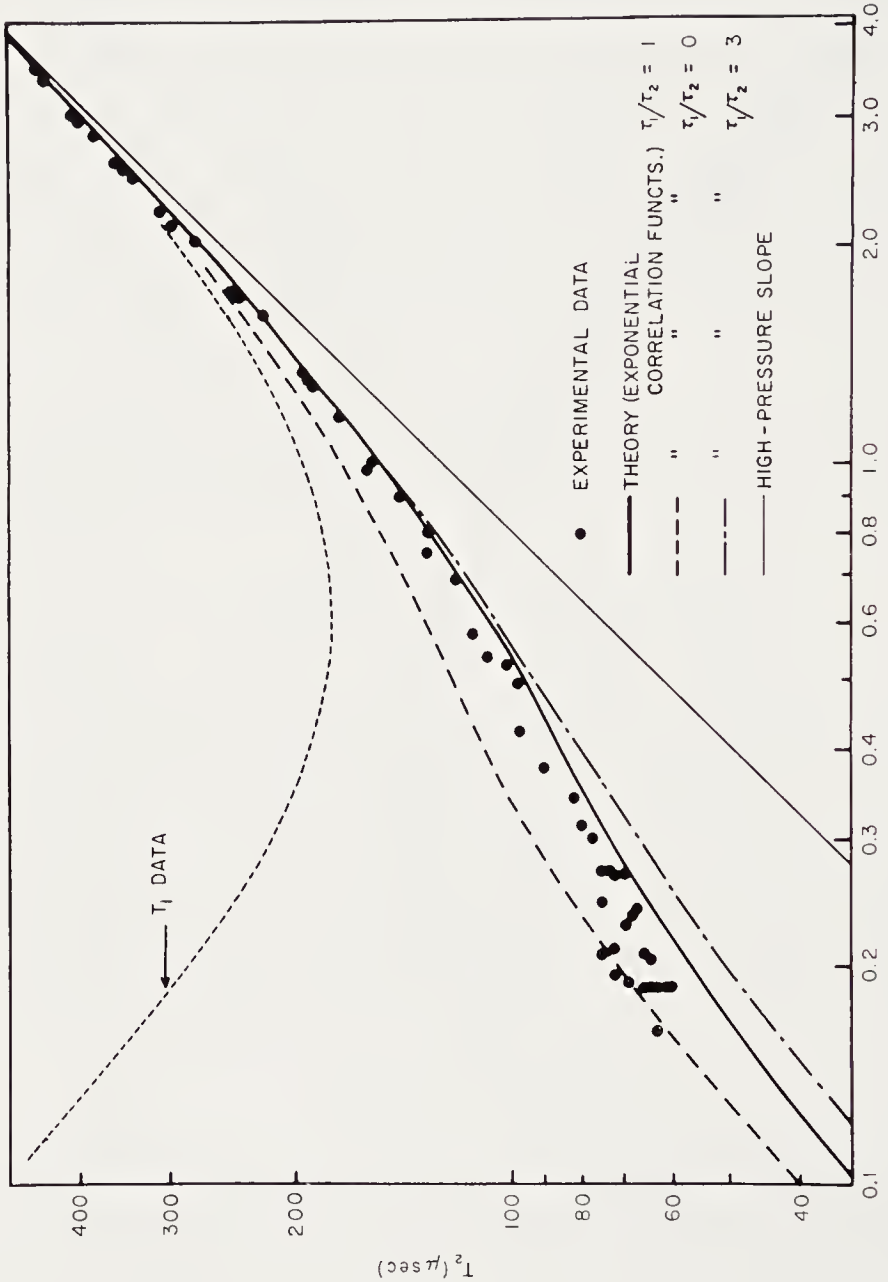

Fig. 3. Plot of T_2 versus density in H_2 gas at 77.5°K (ref. 15).

$P_5 = 0.01$ at a temperature $T = 425°\text{K}$ and $P_5 = 0.03$ at $T = 550°\text{K}$. Note, however, that the fractional contribution to T_1^{-1} and T_2^{-1} by the $J = 5$ state could be either appreciably greater or smaller than its fractional population. In order to make a more precise prediction of the importance of the neglected terms when the set of equations [Eq. (56)] is truncated, it is necessary to know the $B_l(J,J')$. These coefficients can be calculated for specified anisotropic *inter*molecular potentials as will be discussed in the next section.

The equations to be solved for the two-level system are

$$\begin{aligned} \dot{m}^l_{J_1 J_0 M_0} &= B_l(J_1,J_1)m^l_{J_1 J_0 M_0} + B_l(J_1,J_2)m^l_{J_2 J_0 M_0} \\ \dot{m}^l_{J_2 J_0 M_0} &= B_l(J_2,J_1)m^l_{J_1 J_0 M_0} + B_l(J_2,J_2)m^l_{J_2 J_0 M_0} \end{aligned} \tag{78}$$

where J_0 can take on the values J_1 and J_2. The solution of these equations is straightforward and yields the rate constants $\Lambda_{l\alpha}$ and the coefficients $C^{l\alpha}_{J_0}$, where $\alpha = 1,2$ and $J_0 = J_1,J_2$ as

$$\Lambda_{l\alpha} = -\frac{1}{2}[B_l(J_1,J_1) + B_l(J_2,J_2) + (-1)^{\alpha+1}\{[B_l(J_1,J_1) - B_l(J_2,J_2)]^2 + 4B_l(J_1,J_2)B_l(J_2,J_1)\}^{1/2}] \tag{79}$$

$$\begin{aligned} C^{l1}_{J_1} &= \frac{\Lambda_{l2} + B_l(J_1,J_1)}{\Lambda_{l2} - \Lambda_{l1}} + \left[\frac{f_l(J_2)}{f_l(J_1)}\right]^{1/2} \frac{B_l(J_2,J_1)}{\Lambda_{l2} - \Lambda_{l1}} \\ C^{l2}_{J_1} &= -\frac{\Lambda_{l1} + B_l(J_1,J_1)}{\Lambda_{l2} - \Lambda_{l1}} - \left[\frac{f_l(J_2)}{f_l(J_1)}\right]^{1/2} \frac{B_l(J_2,J_1)}{\Lambda_{l2} - \Lambda_{l1}} \end{aligned} \tag{80}$$

and $C^{l2}_{J_2}$ and $C^{l1}_{J_2}$ are obtained from $C^{l1}_{J_1}$ and $C^{l2}_{J_1}$, respectively, by permuting 1 and 2.

By substituting Eqs. (79) and (80) into Eqs. (68) and (69), one obtains T_1 for this case in terms of the $B_l(J,J')$.

The results presented above can also be applied to other diatomic molecules in which only two of the rotational levels contributing to the tensor polarization are appreciably populated. For example, for HD, the criterion for the two-level formula being applicable is that P_3 be small since the $J = 0$ state does not contribute to the tensor polarization. For HD, $P_3 = 0.03$ for $T = 180°\text{K}$. The fact that the HD molecule can occupy the $J = 0$ state does play a role, however, since terms $Q_\lambda(0,J)$ or $Q_\lambda(J,0)$ may be nonzero as a result of the molecule performing transitions between the $J = 0$ and other rotational states. It may be seen

from Eq. (55) that these terms contribute to the $B_l(J,J)$. Their effect is to decrease the lifetime of the molecule in the state J.

para-D_2 ($I = 1$) has only odd rotational states and $P_5 = 0.03$ for $T = 275°K$. *ortho*-D_2 ($I = 0,2$) on the other hand has only even rotational states and here it is of interest to see that $P_6 = 0.03$ for $T = 400°K$.

It does not seem that the two-level results are applicable to any other gaseous system than molecular hydrogen and its isotopic modifications. For any other molecule, the equilibrium vapor pressure at temperatures sufficiently low that only two or three rotational levels are appreciably populated is too low to permit the NMR measurements to be made.

IV. CORRELATION FUNCTIONS OF ANISOTROPIC INTERMOLECULAR POTENTIALS

In this chapter we obtain expressions for $Q(J,J')$ [Eq. (53)], and therefore of $A(JM;J'M')$ for some special forms of the anisotropic intermolecular potential, $V_A(\mathbf{R}^N,\Omega^N)$. We assume that V_A can be written as a sum of two particle terms

$$V_A = \sum_{i<j} v_A(\mathbf{R}_{ij}, \Omega_i, \Omega_j) \tag{81}$$

where $\mathbf{R}_{ij}$ is the vector distance between the centers of mass of molecules i and j and $\Omega_i(\Omega_j)$ specifies the orientation of molecule $i(j)$ with respect to a space-fixed coordinate system in which the magnetic field $\mathbf{H}_0$ is along the z axis.

We shall assume that the anisotropic *inter*molecular potential v_A between two molecules labeled 1 and 2, respectively, consists of two terms

$$v_A = v_A^{(1)} + v_A^{(2)} \tag{82}$$

where

$$v_A^{(1)} = b^{(1)}(R)P_2(\cos\theta_1') \tag{83}$$

and

$$v_A^{(2)} = b^{(2)}(R) \sum_{q=-2}^{+2} a_q Y_{2q}(\Omega_1') Y_{2q}^*(\Omega_2') \tag{84}$$

where $b^{(1)}(R)$ and $b^{(2)}(R)$ are functions of the separation of the centers of mass of 1 and 2, $P_2(\cos\theta_1')$ is the Legendre polynomial of order 2 of the angle θ_1' which the molecular axis of molecule 1 makes with $\mathbf{R}$, which is the vector distance between the centers of mass, while $Y_{2q}(\Omega_1')$

and $Y_{2q}(\Omega_2')$ are spherical harmonics of order 2 and Ω_1' and Ω_2', are, respectively, the orientations of the symmetry axes of molecules 1 and 2 with respect to **R**. The a_q are constants.

The above interaction potential is the most general one possible if both 1 and 2 are *ortho*-H_2 molecules in the ground ($J = 1$) rotational state, providing that no transitions between states of different J are allowed. If molecule 1 is an *ortho*-H_2 molecule restricted to the $J = 1$ state and molecule 2 has no rotational degree of freedom, such as He, A, etc. or *para*-H_2 restricted to its ground ($J = 0$) rotational state, then the most general potential is $v_A^{(1)}$. In our discussion we shall not restrict ourselves to sufficiently low temperatures for these conditions to hold. Therefore, $v_A^{(1)}$ and $v_A^{(2)}$ are to be considered as two important terms in the anisotropic *inter*molecular potential. The number of terms required to specify the most general form of v_A depends on the state of largest J which contributes appreciably to the relaxation rate.

Both $v_A^{(1)}$ and $v_A^{(2)}$ have the index $\lambda = 2$ as given in Eqs. (52) and (53). The distinction between $v_A^{(1)}$ and $v_A^{(2)}$ is that $v_A^{(1)}$ involves rotational operators for molecule 1 only, while $v_A^{(2)}$ involves rotational operators for both molecules 1 and 2. For this reason, when we calculate $Q_2(J,J')$ from the transition rate for molecule 1 going from state J',M' to J,M, the contributions of the two terms are additive, i.e., there are no interference terms and we may write

$$Q_2(J,J') = Q_2^{(1)}(J,J') + Q_2^{(2)}(J,J') \tag{85}$$

The transition rates $A(JM;J'M')$ to be evaluated are those associated with molecule 1. We shall denote the rotational states of molecule 1 by J and J' and those of the second molecule by J'' and J'''. In calculating $Q_2(J,J')$ we shall average over an equilibrium ensemble of molecule 2, the average being taken over all position, momentum, and angular momentum states of molecule 2.

Using the standard formula for the transition probability per unit time as given by perturbation theory[14]

$$A^{(1)}(J,M;J'M') = \frac{1}{\hbar^2}\int_{-\infty}^{\infty} e^{+i\omega_{JJ'}t} \times \langle (J'M' \mid V_A^{(1)}(0) \mid JM)(JM \mid V_A^{(1)}(t) \mid J'M') \rangle dt \tag{86}$$

where

$$\hbar\omega_{JJ'} = E_J - E_{J'} \tag{87}$$

is the energy difference between the rotational states J and J',

$$\langle (J'M' \mid V_A^{(1)}(0) \mid JM)(JM \mid V_A^{(1)}(t) \mid J'M') \rangle$$

is the correlation function of the matrix element of $V_A^{(1)}$ between states J,M and J',M' where the average is performed with the density matrix $e^{-\beta \mathscr{H}_L{}^0}/\mathrm{Tr}\{e^{-\beta \mathscr{H}_L{}^0}\}$ and

$$V_A^{(1)}(t) = e^{i/\hbar \mathscr{H}_L{}^0 t} V_A^{(1)}(0) e^{-i/\hbar \mathscr{H}_L{}^0 t} \tag{88}$$

where

$$\mathscr{H}_L^0 = \mathscr{H}_L - V_A \tag{89}$$

is that part of the lattice Hamiltonian which contains the kinetic energy of the centers of mass of the molecules and the *isotropic inter*molecular potential.

In order to calculate the matrix elements of $V_A^{(1)}$ we make the transformation to the laboratory reference frame

$$P_2(\cos\theta') = \frac{4\pi}{5} \sum_{\mu=-2}^{+2} Y_{2\mu}(\Omega_1) Y_{2\mu}^*(\Omega) \tag{90}$$

where Ω_1 and Ω are the orientations of molecule 1 and the vector $\mathbf{R}$, respectively, in the space-fixed coordinate system in which the z axis is along $\mathbf{H}_0$.

Substituting Eq. (90) into (86) and using Eqs. (43), (52), and (86), we obtain

$$Q_2^{(1)}(J,J') = \frac{4\pi}{5} \left(\frac{2J'+1}{2J+1}\right) [C(J'2J;00)]^2 j^{(1)}(\omega_{JJ'}) \tag{91}$$

where

$$j^{(1)}(\omega_{JJ'}) = \frac{1}{\hbar^2} \int_{-\infty}^{\infty} e^{+i\omega_{JJ'}t} k^{(1)}(t)\,dt \tag{92}$$

and, for a dilute gas,

$$k^{(1)}(t) = (N-1)\langle b^{(1)}[R(0)]\, Y_{2-\mu}[\Omega(0)]\, b^{(1)}[R(t)]\, Y_{2\mu}[\Omega(t)] \rangle \tag{93}$$

is the correlation function of $b^{(1)}(R)\, Y_{2-\mu}(\Omega)$ which is independent of μ for a gas. The correlation function $k^{(1)}(t)$ decays in a time of the order of the average time of a single collision τ_{coll} between a pair of molecules

in a dilute gas, i.e.,

$$\tau_{\text{coll}} \approx a/(3kT/\mu)^{1/2} = a/v_0 \tag{94}$$

where a is the approximate range of the intermolecular interactions, μ is the reduced mass of molecules 1 and 2, and v_0 is the rms value of their relative velocity.

We can easily distinguish between the limiting case of those transitions in which very little energy is exchanged between the rotational and translational degrees of freedom ($\omega_{JJ'}\tau_{\text{coll}} \ll 1$) and the opposite limiting case ($\omega_{JJ'}\tau_{\text{coll}} \gg 1$), since

$$\begin{aligned} j^{(1)}(\omega_{JJ'}) &\approx j^{(1)}(0) \qquad & \omega_{JJ'}\tau_{\text{coll}} &\ll 1 \\ j^{(1)}(\omega_{JJ'}) &\ll j^{(1)}(0) \qquad & \omega_{JJ'}\tau_{\text{coll}} &\gg 1 \end{aligned} \tag{95}$$

The nonzero values of $Q_A^{(1)}(J,J')$ correspond to $J' = J$ and $J' = J \pm 2$. For the H_2 molecule, it is quite clear that

$$Q_2^{(1)}(J,J \pm 2) \ll Q_2^{(1)}(J,J) \tag{96}$$

Since, for $T = 300°\text{K}$ and $a = 2.93 \times 10^{-8}$ cm, $\omega_{31}\tau_{\text{coll}} \approx 12$.

Evaluating the Racah coefficients in Eq. (55), the contribution of $V_A^{(1)}$ to the $B_l(J,J)$ coefficients is found to be

$$B_1^{(1)}(J,J) = -[3/J(J+1)]Q_2^{(1)}(J,J) \tag{97}$$

The value of $B_2^{(1)}(J,J)$ is obtained from Eqs. (77), (91), and (97).

We now turn to the evaluation of the contribution of $V_A^{(2)}$ to the $B_l(J'J,)$ coefficients. To do this we shall restrict ourselves to quadrupole–quadrupole interactions for which $a_0 = 6$, $a_1 = a_{-1} = -4$, $a_2 = a_{-2} = 1$ and

$$b^{(2)}(R) = 4\pi Q_1 Q_2 / R^5 \tag{98}$$

Making the transformation to the laboratory reference frame, we find that

$$v_A^{(2)} = \left(\frac{56\pi}{45}\right)^{1/2} b^{(2)}(R) \sum_{\substack{mm' \\ \mu}} (-1)^{\mu} C(224;m,m',\mu) Y_{2m}(\Omega_1) Y_{2m'}(\Omega_2) Y_{4-\mu}(\Omega) \tag{99}$$

The effect of $v_A^{(2)}$ is to produce transitions of molecule 1 from the state J',M' to the state J,M while a molecule 2 simultaneously undergoes a

transition from state J''',M''' to state J'',M''. Denoting the transition rate for this process by $A[(JM;J'M')(J''M'';J'''M''')]$, we have

$$A^{(2)}(JM;J'M') = \sum_{J''}\sum_{J'''}\sum_{M''}\sum_{M'''} A[(JM;J'M')(J''M'';J'''M''')] \quad (100)$$

where

$$A[(JM;J'M')(J''M'';J'''M''')] = \sum_{m,m'}\left(\frac{56\pi}{45}\right) j^{(2)}(\omega_{JJ';J''J'''})[C(224;m,m')]^2$$

$$\times \frac{P_{J'''}}{2J''' + 1} |(JM \mid Y_{2m}(\Omega_1) \mid J'M')|^2 |(J''M'' \mid Y_{2m'}(\Omega_2) \mid J'''M''')|^2 \quad (101)$$

where

$$\hbar\omega_{JJ';J''J'''} = (E_J - E_{J'}) + (E_{J''} - E_{J'''}) \quad (102)$$

and $j^{(2)}(\omega)$ is the Fourier transform of $k^{(2)}(t)$ which is given by

$$k^{(2)}(t) = (N-1)\langle b^{(2)}[R(0)]Y_{4-\mu}[\Omega(0)]b^{(2)}[R(t)]Y_{4\mu}[\Omega(t)]\rangle \quad (103)$$

Using Eq. (52) to obtain the matrix elements in Eq. (101), evaluating the sums over m,m', M'', and M''' in Eqs. (100) and (101) by standard methods[28] and using Eq. (53) to define $Q^{(2)}(J,J')$, we obtain

$$Q^{(2)}(J,J') = \frac{7}{10\pi}[C(J2J';00)]^2 \sum_{J'',J'''} P_{J'''}[C(J'''2J'';00)]^2 j^{(2)}(\omega_{JJ';J''J'''}) \quad (104)$$

Again, $k^{(2)}(t)$ decays in a time of order τ_{coll} so that we can write

$$j^{(2)}(\omega) \approx j^{(2)}(0) \qquad \omega\tau_{\text{coll}} \ll 1$$

$$j^{(2)}(\omega) \ll j^{(2)}(0) \qquad \omega\tau_{\text{coll}} \gg 1 \quad (105)$$

The nonzero contributions to $Q^{(2)}(J,J')$ arise from $J' = J$ and $J' = J \pm 2$; and $J''' = J''$ and $J''' = J'' \pm 2$. For low-temperature H_2, we need consider only the $J = 1$ and 3 states for *ortho*-H_2 and the $J = 0$, 2, and 4 states for *para*-H_2. For *ortho–ortho* interactions, the following transitions $(J',J''' \leftrightarrow J,J'')$ give appreciable contributions to $Q^{(2)}(J,J')$: $(J,J'' \leftrightarrow JJ'')$, $(1,3 \leftrightarrow 3,1)$. For these transitions $\omega_{JJ';J''J'''} = 0$. For all other transitions $\omega_{JJ';J''J'''}\tau_{\text{coll}} \geq 12$ at room temperature. For *ortho–para* interactions, only $(J,J'' \leftrightarrow J,J'')$ gives $\omega_{JJ';J''J'''} = 0$. The transitions

$(1,2 \leftrightarrow 3,0)$ and $(1,4 \leftrightarrow 3,2)$ may have to be considered since $\omega_{JJ';J''J'''}\tau_{\text{coll}} \approx 4.7$ for them at room temperature. According to van Kranendonk's calculation[30] of $j(\omega)$ versus ω for a quadrupole–quadrupole interaction, $j(\omega)$ is large for $\omega\tau_{\text{coll}} \leq 5$ and decreases rapidly for higher ω. Thus, the other transitions are probably negligible.

In order to illustrate the care that must be taken in reducing the quantum lattice correlation functions, Eqs. (93) and (103), to their classical counterparts we consider a system in which the transition rate is given by Eq. (86). It follows from Eqs. (53), (91), and (60) that

$$A^{(1)}(J,M;J',M')/A^{(1)}(J',M';J,M) = j^{(1)}(\omega_{JJ'})/j^{(1)}(-\omega_{JJ'}) = e^{-\beta\hbar\omega_{JJ'}} \tag{106}$$

where the last equality follows from the condition of detailed balance. On the other hand, if $k^{(1)}(t)$ is computed by replacing the operator $b^{(1)}[(R(0)]\,Y_{20}[\Omega(0)]\;\; b^{(1)}[R(t)]\,Y_{20}[\Omega(t)]$ by the classical quantity $b^{(1)}[R(0)]\,Y_{20}[\Omega(0)]\; b^{(1)}[R_{cl}(t)]\,Y_{20}[\Omega_{cl}(t)]$,

$$k^{(1)}(t) = k^{(1)}(-t) \tag{107}$$

and therefore

$$j^{(1)}(\omega) = j^{(1)}(-\omega) \tag{108}$$

and the Boltzmann factor in Eq. (106) is lost. The difficulty met here is the fact that the operator appearing in Eq. (93) is not Hermitian and, therefore, its classical counterpart is not apparent.

On the other hand, we consider the expression

$$\frac{k^{(1)}(t) + k^{(1)}(-t)}{2} = \frac{1}{2}\langle b^{(1)}[R(0)]\,Y_{20}[\Omega(0)]b^{(1)}[R(t)]\,Y_{20}[\Omega(t)] + b^{(1)}[R(t)]\,Y_{20}[\Omega(t)]b^{(1)}[R(0)]\,Y_{20}[\Omega(0)]\rangle \tag{109}$$

where we have used the fact that the time operators commute with the density matrix. The operator in brackets in Eq. (109) is Hermitian and thus we would expect that the classical counterpart to Eq. (109) would be

$$\left(\frac{k^{(1)}(t) + k^{(1)}(-t)}{2}\right)_{cl} = \langle b^{(1)}[R_{cl}(t)]\,Y_{20}[\Omega_{cl}(t)]b^{(1)}[R(0)]\,Y_{20}[\Omega(0)]\rangle \tag{110}$$

Thus, the classical correspondence of

$$\left(\frac{j^{(1)}(\omega_{JJ'}) + j^{(1)}(\omega_{J'J})}{2}\right) = \frac{1}{\hbar^2}\int_{-\infty}^{\infty} e^{i\omega_{JJ'}t}\left(\frac{k^{(1)}(t) + k^{(1)}(-t)}{2}\right)dt \tag{111}$$

is easily obtained. This result together with the condition

$$j_{cl}^{(1)}(\omega_{JJ'}) = e^{-\beta\hbar\omega_{JJ'}} j_{cl}^{(1)}(\omega_{J'J}) \tag{112}$$

enables us to compute classical correlation functions and transition rates which preserve detailed balance. An application of these results will be discussed in Section VI.

V. CALCULATION OF THE INTERMOLECULAR CORRELATION FUNCTIONS

In this section we consider some approximate techniques for obtaining explicit expressions for the intermolecular correlation functions $k^{(1)}(t)$ [Eq. (93)] and $k^{(2)}(t)$ [Eq. (103)]. We shall then use these expressions to obtain $j^{(1)}(0)$ [Eq. 92)] and $j^{(2)}(0)$ from which we can obtain $Q^{(1)}$ and $Q^{(2)}$ and eventually T_1 and T_2. Since we restrict our attention to zero frequency $j^{(1)}$ and $j^{(2)}$ we need not be concerned with the detailed balance problem described at the end of Section IV. We first present the results of approximating the quantum correlation functions by classical correlations plus first quantum corrections. Then we introduce the constant acceleration approximation (CAA) which simplifies the correlation function calculation immensely.

Although neither of these approximations is necessary to carry out the dilute gas calculations which are of most interest here, they are essential if we wish to compute T_1 for dense fluids. We have derived the rigorous low-density expression for T_1 in Section II-C and, in principle, numerical results could be obtained from this expression since it involves only two-particle dynamics. If the weak coupling approximation of Section II-D is made, i.e., V_A small, then the calculations are simplified; some numerical results have been obtained by Riehl et al.[31] These results will be discussed and compared with the present calculations in Section VII. Again we emphasize the relative simplicity of the calculations described here and their applicability to dense systems.

A. High-Temperature Approximation to the Intermolecular Correlation Functions

We consider the high-temperature approximation to the correlation function

$$\langle I_{op}(t)I_{op}\rangle = \mathrm{Tr}[\rho I_{op}(t)I_{op}] \tag{113}$$

where $I_{op} \equiv I_{op}(0)$ is an arbitrary dynamical variable

$$I_{op}(t) = e^{i/\hbar\mathscr{H}t}I_{op}e^{-i/\hbar\mathscr{H}t} \tag{114}$$

$$\rho = e^{-\beta\mathscr{H}}/\mathrm{Tr}(e^{-\beta\mathscr{H}}) \tag{115}$$

and $\mathscr{H}$ is the Hamiltonian operator. Quantum mechanics enters into the calculation of Eq. (113) in two ways; one in the calculation of the statistical average with the density matrix ρ and the other in the calculation of the time dependence of $I_{op}(t)$. In a previous paper,[6] we considered the quantum effects due to the averaging procedure but we did not, at that time, compute the quantum effects on the time dependence of $I(t)$. We have now obtained expressions for these quantum effects as well. Their derivation and application to a number of correlation-function calculations will be presented in a paper by one of the authors (I.O.) and J. Wang.

The result is

$$\langle I_{op}(t)I_{op}\rangle = \langle I(t)I\rangle_{cl} + \hbar^2\{\langle I(t)I(\phi - \langle\phi\rangle_{cl})\rangle_{cl} + \langle I(0)I_1(t)\rangle_{cl} + \langle I(t)I_2(0)\rangle_{cl}\} + O(\hbar^4) \tag{116}$$

where we have neglected the effects of quantum statistics, i.e., Bose-Einstein or Fermi-Dirac statistics. The quantity $I \equiv I(\mathbf{R}^N,\mathbf{P}^N)$ is the classical dynamical variable which corresponds to I_{op}; it is a function of $\mathbf{R}^N$ and $\mathbf{P}^N$, the position and momenta of the centers of mass of the N particles in the system.

The quantity $I(t) \equiv I[\mathbf{R}^N(t),\mathbf{P}^N(t)]$ where $\mathbf{R}^N(t)$ and $\mathbf{P}^N(t)$ are solutions to the classical equations of motion with initial conditions $R^N(0) = R^N$ and $\mathbf{P}^N(0) = \mathbf{P}^N$. The subscript cl on the brackets implies that the average is taken over a classical ensemble with distribution function

$$f^N(\mathbf{R}^N,\mathbf{P}^N) = e^{-\beta H(\mathbf{R}^N,\mathbf{P}^N)} \Big/ \int e^{-\beta H} d\mathbf{R}^N d\mathbf{P}^N \tag{117}$$

where H is the classical Hamiltonian. Thus

$$\langle I(t)I\rangle_{cl} = \int f^N(\mathbf{R}^N,\mathbf{P}^N)I(\mathbf{R}^N,\mathbf{P}^N)I[\mathbf{R}^N(t),\mathbf{P}^N(t)]d\mathbf{R}^N d\mathbf{P}^N \tag{118}$$

The quantity $\phi(\mathbf{R}^N,\mathbf{P}^N)$ is given by

$$\phi(\mathbf{R}^N,\mathbf{P}^N) = -\frac{1}{8m}\left\{\beta^2\nabla^2_{\mathbf{R}^N}V_0(\mathbf{R}^N) - \frac{\beta^3}{3}\left[(\nabla_{\mathbf{R}^N}V_0(\mathbf{R}^N))^2 + \nabla_{\mathbf{R}^N}\nabla_{\mathbf{R}^N}V_0(\mathbf{R}^N) : \frac{\mathbf{P}^N\mathbf{P}^N}{m}\right]\right\} \tag{119}$$

The terms containing ϕ in Eq. (116) are corrections to the classical correlation function arising from the quantum averaging procedure. The quantity $I_1(t)$ contains the integral

$$\frac{1}{24}\int_0^t d\tau e^{i\mathscr{L}_{cl}\tau}(\nabla_{\mathbf{R}^N}\cdot\nabla_{\mathbf{P}^N})^3 V_0(\mathbf{R}^N)e^{i\mathscr{L}_{cl}(t-\tau)}I(\mathbf{R}^N,\mathbf{P}^N) \tag{120}$$

where $\mathscr{L}_{cl}$ is the classical Liouville operator and the derivatives with respect to $\mathbf{R}^N$ act only on $V_0(\mathbf{R}^N)$. The terms containing $I_1(t)$ and $I_2(0)$ are corrections due to the difference between the quantum and classical time dependence of $I(t)$. The expansion parameter in Eq. (116) is $(\Lambda_D/a)^2$ where

$$\Lambda_D = h/(mkT)^{1/2} \tag{121}$$

is the mean de Broglie wavelength and a is the range of the intermolecular potential.

We wish to compute

$$k^{(1)}(t) = (N-1)\langle I^{(1)}_{op}(0)I^{(1)}_{op}(t)\rangle \tag{122}$$

and

$$k^{(2)}(t) = (N-1)\langle I^{(2)}_{op}(0)I^{(2)}_{op}(t)\rangle \tag{123}$$

where [Eq. (93)]

$$I^{(1)} = b^{(1)}(R)Y_{20}(\Omega) \tag{124}$$

and [Eq. (103)]

$$I^{(2)} = b^{(2)}(R)Y_{40}(\Omega) \tag{125}$$

The quantities $b^{(1)}$ and $b^{(2)}$ which describe the R dependence of the

anisotropic intermolecular potentials $v_A^{(1)}$ and $v_A^{(2)}$, respectively, are short-range functions of R. As we shall see in Section VI, the experimental data for H_2 gas can be fit by assuming that $b^{(1)}(R) \propto R^{-n}$, $n > 15$, and $b^{(2)}(R) \propto R^{-5}$. If $b(R) \propto R^{-n}$, then it is easy to see that $I_1(t) \propto n^3$. We expect from comparison with experiments and with other calculations,[31] that the correction involving $I_1(t)$ is small for quadrupole–quadrupole interactions but appreciable for the short-range interaction $b^{(1)}(R)$. The computation of this correction is in progress at the moment.

B. The Constant-Acceleration Approximation (CAA)

In this section we describe the calculation of the classical correlation functions, $k_{cl}^{(q)}(t)(q = 1,2)$ using the CAA. The computation of the quantum correction terms involving ϕ is described in references 6 and 9 and will not be presented here. From this point on, we shall omit the subscript *cl* for the classical quantities.

In a classical system, $k^{(q)}(t)$ may be written as:

$$k^{(q)}(t) = (N-1)\int f^N(\mathbf{R}^N,\mathbf{P}^N)b^{(q)}(R_{12})b^{(q)}[R_{12}(t)]Y^{(q)}(\Omega_{12}) \times Y^{(q)}[\Omega_{12}(t)]d\mathbf{R}^N d\mathbf{P}^N \quad (126)$$

where $Y^{(1)} = Y_{2-\mu}$ and $Y^{(2)} = Y_{4-\mu}$

$$f^N(\mathbf{R}^N,\mathbf{P}^N) = \frac{1}{Z}\left(\frac{\beta}{2\pi m}\right)^{3N/2}\exp\left\{-\beta\left[\frac{\mathbf{P}^N\cdot\mathbf{P}^N}{2m} + V_0(\mathbf{R}^N)\right]\right\} \quad (127)$$

$$Z = \int d\mathbf{R}^N e^{-\beta V_0(\mathbf{R}^N)} \quad (128)$$

and

$$\mathbf{R}_i(t) = \mathbf{R}_i(\mathbf{R}^N,\mathbf{P}^N,t) \quad (129)$$

which indicates that the position of a particular particle at time t is a function, through the classical equations of motion, of the time and the initial positions, $\mathbf{R}^N$, and the initial momenta, $\mathbf{P}^N$, of all the particle. If one defines the time-dependent pair distribution function (TDPDF) as:

$$h(\mathbf{R}^2,\mathbf{R}'^2,t) = N(N-1)\int f^N(\mathbf{R}^N,\mathbf{P}^N)\delta[\mathbf{R}'^2 - \mathbf{R}^2(t)]d\mathbf{R}^{N-2}d\mathbf{P}^N \quad (130)$$

$k^{(q)}(t)$ may be rewritten as:

$$k^{(q)}(t) = \frac{1}{N} \int h(\mathbf{R}^2,\mathbf{R}'^2,t) b^{(q)}(R_{12}) b^{(q)}(R'_{12}) Y^{(q)}(\Omega_{12}) Y^{*(q)}(\Omega'_{12}) d\mathbf{R}^2 d\mathbf{R}'^2 \tag{131}$$

The problem of calculating $k^{(q)}(t)$ is reduced to a calculation of the TDPDF.

In reference 6, the CAA expression for the TDPDF was obtained. A more concise technique for obtaining this expression has been developed by Nijboer.[32] The procedure begins by considering the equations of motion for a particular particle i. These are:

$$\mathbf{R}_i(t) = \mathbf{R}_i + 1/m \int_0^t \mathbf{P}_i(\tau) d\tau \tag{132}$$

$$\mathbf{P}_i(\tau) = \mathbf{P}_i - \int_0^\tau \nabla_{\mathbf{R}_i(\tau')} V_0[\mathbf{R}^N(\tau')] d\tau' \tag{133}$$

The CAA assumes that the initial force on the particle does not change with time, i.e.,

$$\nabla_{R_i(\tau)} V_0[\mathbf{R}^N(\tau)] = \nabla_{\mathbf{R}_i} V_0(\mathbf{R}^N) \tag{134}$$

This results in the following approximate equations of motion:

$$\mathbf{P}_i(\tau) = \mathbf{P}_i - \tau \nabla_{\mathbf{R}_i} V_0(\mathbf{R}^N) \tag{135}$$

$$\mathbf{R}_i(t) = \mathbf{R}_i + (t/m)\mathbf{P}_i - (t^2/2m)\nabla_{\mathbf{R}_i} V_0(\mathbf{R}^N) \tag{136}$$

These approximate equations of motion are substituted in each of the two 3-dimensional delta functions in Eq. (130) to yield

$$\delta[\mathbf{R}'_i - \mathbf{R}_i(t)] = \delta[\mathbf{R}'_i - \mathbf{R}_i + (t^2/2m)\nabla_{\mathbf{R}_i} V_0(\mathbf{R}^N) - (t/m)\mathbf{P}_i] \tag{137}$$

Using this approximate form, and the definition of f^N, the integrations over the momenta may be carried out to yield

$$\begin{aligned} h(\mathbf{R}^2,\mathbf{R}'^2,t) = \left(\frac{\beta m}{2\pi t^2}\right)^3 \frac{N(N-1)}{Z} \int d\mathbf{R}^{N-2} \Big\{ & \exp[-\beta V_0(\mathbf{R}^N)] \\ & \times \exp\left[-\frac{\beta m}{2t^2} \left(\mathbf{R}'_1 + \mathbf{R}_1 + \frac{t^2}{2m} \nabla_{R_1} V_0(\mathbf{R}^N) \right)^2 \right] \\ & \times \exp -\frac{\beta m}{2t^2} [\mathbf{R}'_2 + \mathbf{R}_2 + t^2/2m \nabla_{\mathbf{R}_2} V_0(\mathbf{R}^N)]^2 \Big\} \end{aligned} \tag{138}$$

The terms in the exponent are squared and, consistent with the CAA, orders of t^2 are dropped to obtain

$$h(\mathbf{R}^2,\mathbf{R}'^2,t) = \frac{N(N-1)}{Z}\left(\frac{\beta m}{2\pi t^2}\right)^3 \exp\left[-\frac{\beta m}{2t^2}(\mathbf{R}_1' - \mathbf{R}_1)^2\right]$$
$$\times \exp\left[-\frac{\beta m}{2t^2}(\mathbf{R}_2' - \mathbf{R}_2)^2\right] \int d\mathbf{R}^{N-2}$$
$$\times \left[\exp[-\beta V_0(\mathbf{R}^N)] \exp[-\beta/2(\mathbf{R}_1' - \mathbf{R}_1)\cdot \nabla_{\mathbf{R}_1} V_0(\mathbf{R}^N)]\right.$$
$$\left.\times \exp[-\beta/2(\mathbf{R}_2' - \mathbf{R}_2)\cdot \nabla_{\mathbf{R}_2} V_0(\mathbf{R}^N)]\right] \quad (139)$$

Now consider the quantity:

$$V_0 = V_0[(\mathbf{R}_1' + \mathbf{R}_1)/2, (\mathbf{R}_2' + \mathbf{R}_2)/2, \mathbf{R}_3, \ldots, \mathbf{R}_N] \quad (140)$$

A Taylor series expansion around $\mathbf{R}_1' = \mathbf{R}_1$ and $\mathbf{R}_2' = \mathbf{R}_2$ demonstrates that, consistent with the CAA, the exponent of the integrand of Eq. (139) may be rewritten to yield

$$h(\mathbf{R}^2,\mathbf{R}'^2,t) = \left(\frac{\beta m}{2\pi t^2}\right)^3 \frac{N(N-1)}{Z} \exp\left[-\frac{\beta m}{2t^2}(\mathbf{R}_1' - \mathbf{R}_1)^2\right]$$
$$\times \exp\left[-\frac{\beta m}{2t^2}(\mathbf{R}_2' - \mathbf{R}_2)^2\right] \int d\mathbf{R}^{N-2}$$
$$\times \exp\left\{-\beta\left[V_0\left(\frac{\mathbf{R}_1' + \mathbf{R}_1}{2}, \frac{\mathbf{R}_2' + \mathbf{R}_2}{2}, \mathbf{R}_3, \ldots, \mathbf{R}_N\right)\right]\right\} \quad (141)$$

Using the definition of the equilibrium radial distribution function,

$$g(\mathbf{R}^2) = g^{(2)}(\mathbf{R}^2) \qquad \rho^n g^{(n)}(\mathbf{R}^n) = f^{(n)}(\mathbf{R}^n) = \frac{N!}{(N-n)!}\int d\mathbf{R}^{N-n} f^N \quad (142)$$

where $\rho = N/V$ is the number density, we find

$$h(\mathbf{R}^2,\mathbf{R}'^2,t) = \left(\frac{\beta m}{2\pi t^2}\right)^3 \exp\left[-\frac{\beta m}{2t^2}(\mathbf{R}_1' - \mathbf{R}_1)^2\right] \exp\left[-\frac{\beta m}{2t^2}(\mathbf{R}_2' - \mathbf{R}_2)^2\right]$$
$$\times g\left(\frac{\mathbf{R}_1' + \mathbf{R}_1}{2}, \frac{\mathbf{R}_2' + \mathbf{R}_2}{2}\right) \quad (143)$$

If one expands to orders consistent with the CAA one may verify the identity:

$$g\left(\frac{\mathbf{R}_1' + \mathbf{R}_1}{2}, \frac{\mathbf{R}_2' + \mathbf{R}_2}{2}\right) = [g(\mathbf{R}'^2)g(\mathbf{R}^2)]^{1/2} + 0(\nabla_R V_0)^2 \quad (144)$$

Thus one obtains by Nijboer's procedure the TDPDF:

$$h(\mathbf{R}^2,\mathbf{R}'^2,t) = \rho^2\left(\frac{\beta m}{2\pi t^2}\right)^3 \exp\left[-\frac{\beta m}{2t^2}(\mathbf{R}_1' - \mathbf{R}_1)^2\right]$$

$$\times \exp\left[-\frac{\beta m}{2t^2}(\mathbf{R}_2' - \mathbf{R}_2)^2\right][g(\mathbf{R}^2)g(\mathbf{R}'^2)]^{1/2} \quad (145)$$

Equation (145) is valid for all densities. From Eq. (145) and Eq. (131) it is possible to obtain an explicit form for $k^{(q)}(t)$. In order to obtain this explicit form it is convenient to write the TDPDF in terms of center of mass and relative coordinates, since $g(R)$ depends only upon the relative positions of the particles. This permits the integration of Eq. (131) over the center of mass coordinates to yield

$$k^{(q)}(t) = \rho\left(\frac{z}{\pi}\right)^{3/2} \int d\mathbf{R}_{12} d\mathbf{R}_{12}' \exp[-z(\mathbf{R}_{12}' - \mathbf{R}_{12})^2][g(R_{12})g(R_{12}')]^{1/2}$$

$$\times [Y^{(q)}(\Omega_{12})Y^{*(q)}(\Omega_{12}')b^{(q)}(R_{12})b^{(q)}(R_{12}')] \quad (146)$$

where $z = \beta m/4t^2$.

The integrations involved in Eq. (146) may be simplified by use of the following two identities:

$$e^{-z|\mathbf{R}'-\mathbf{R}|^2} = 1/(4\pi z)^{3/2} \int d\mathbf{u} e^{-u^2/4z} e^{i\mathbf{u}\cdot(\mathbf{R}'-\mathbf{R})} \quad (147)$$

and

$$e^{\pm i\mathbf{u}\cdot\mathbf{R}} = 4\pi\left(\frac{\pi}{2uR}\right)^{1/2} \sum_{l=0}^{\infty} \sum_{m=-l}^{+l} (\pm i)^l J_{l+1/2}(uR) Y_{lm}(\Omega_u) Y_{lm}^*(\Omega_R) \quad (148)$$

When these two identities are used in Eq. (146) one obtains:

$$k^{(q)}(t) = \rho \int_0^{\infty} u F^{(q)}(u) e^{-u^2/4z} du \quad (149)$$

where

$$F^{(q)}(u) = \left[\int_0^\infty dR J^{(q)}(uR) g(R)^{1/2} b^{(q)}(R) R^{3/2}\right]^2 \tag{150}$$

where $J^{(1)} = J_{5/2}$ and $J^{(2)} = J_{9/2}$ are Bessel functions. The time integral of the correlation function is:

$$j^{(q)}(0) = \frac{2}{\hbar^2}\int_0^\infty k^{(q)}(t)dt = \frac{\rho}{\hbar^2}\sqrt{\pi\beta m}\int_0^\infty F^{(q)}(u)du \tag{151}$$

The rationalizations for the use of the CAA have been presented in a number of articles.[6-9,19] In the final analysis, its use is justified by the agreement of its predictions with experiment and with the results of more exact calculations.

VI. INTERPRETATION OF SOME EXPERIMENTS USING THE CAA

We are now in a position to interpret T_1 and T_2 measurements in H_2 gas in terms of the anisotropic *inter*molecular potentials. In order to complete the program, however, there remains the job of evaluating $j^{(q)}(\omega)$, $q = 1,2$ for $\omega\tau_{coll} \geq 1$. For very small rotational energy changes $\omega\tau_{coll} \ll 1$ or very large rotational energy changes $\omega\tau_{coll} \gg 1$, the inequalities of Eqs. (95) and (105) may be used with assurance and it is felt that the CAA enables one to estimate $j^{(q)}(0)$ with adequate precision. In the following paragraphs, we shall review the steps that have already been taken to analyze the experimental data using the approach described here. We shall also explicitly indicate extensions in the theory and the experimental data which are likely to lead to an improvement in our description of the intermolecular potentials.

A. Infrequent Transitions between States of Different J

The formulas required to relate T_1 and T_2 to the coefficients $B_l(J,J)$ for the case where transitions between states of different J can be neglected have already been developed in Section III-A. For this model, we can write

$$j^{(1)}(\omega_{JJ'}) = j^{(1)}(0)\delta_{JJ'} \tag{152}$$

$$j^{(2)}(\omega_{JJ';J''J'''}) = j^{(2)}(0)\delta_{JJ'}\delta_{J''J'''} \tag{153}$$

The terms $j^{(q)}(0)$ have been evaluated using the CAA and are given

by Eq. (151). It is convenient to rewrite Eq. (151) in terms of the dimensionless variables x and y defined by

$$x = R/a \qquad y = ua \tag{154}$$

The quantity a is a length parameter which is a measure of the range of the isotropic *inter*molecular potential. In the following analysis we shall *assume* that the isotropic part of the *inter*molecular potential is given by the Lennard-Jones potential

$$v_0(x) = 4\varepsilon(x^{-12} - x^{-6}) \tag{155}$$

in which ε and a are the Lennard-Jones energy and length parameters, respectively. Equation (151) can now be written as

$$j^{(q)}(0) = \rho a^4 \hbar^{-2}(2\pi\beta\mu)^{1/2} I^{(q)}(p) \tag{156}$$

where

$$I^{(q)}(p) = \int_0^\infty dy \left[\int_0^\infty x^{3/2}[g(x)]^{1/2} b^{(q)}(ax) J_{p+1/2}(xy) dx \right]^2 \tag{157}$$

Substituting Eqs. (152) and (156) into Eq. (91), we obtain

$$Q_2^{(1)}(J,J) = \left(\frac{4\pi}{5\hbar^2}\right) \rho a^4 (2\pi\beta\mu)^{1/2} I^{(1)}(2) \left[\frac{J(J+1)}{(2J-1)(2J+3)} \right] \tag{158}$$

and substituting Eqs. (153) and (156) into Eq. (104) ,we obtain

$$Q_2^{(2)}(J,J) = \left(\frac{7}{25\pi\hbar^2}\right) \rho a^4 (2\pi\beta\mu)^{1/2} I^{(2)}(4) \left[\frac{J(J+1)}{(2J-1)(2J+3)} \right] C \tag{159}$$

where

$$C = \frac{5}{2} \sum_{J''} P_{J''} \frac{J''(J''+1)}{(2J''-1)(2J''+3)} = \frac{5}{2} \left\langle \frac{J(J+1)}{(2J-1)(2J+3)} \right\rangle' \tag{160}$$

and the prime indicates that the average is taken over the rotational states of all of the molecules 2 which collide with the *ortho*-H_2 molecule 1. Using Eqs. (85), (97), (158), and (159), we obtain the result[9] that

$$B_1(J,J) = \frac{-12\pi}{5\hbar^2} \frac{\rho a^4 (2\pi\beta\mu)^{1/2}}{(2J-1)(2J+3)} \left[I^{(1)}(2) + \frac{7}{20\pi^2} C I^{(2)}(4) \right] \tag{161}$$

while Eq. (77) gives, for $\lambda = 2$,

$$B_2(J,J) = [3(4J^2 + 4J - 7)/(2J-1)(2J+3)] B_1(J,J) \tag{162}$$

B. Application to Pure H_2 Gas

The above results may be applied to H_2 gas at temperatures sufficiently low that the $J = 3$ state is not appreciably populated. As mentioned earlier, the fraction of H_2 molecules $\rho_o/\rho = x_o$ which are *ortho*-H_2 may be easily varied between 0 and 0.75. Denoting by C_o, the value of C for *ortho*-H_2, i.e., taking the average in Eq. (160) over *odd* rotational states only, and denoting the value of C for *para*-H_2 by C_p, i.e., averaging over even rotational states, we find

$$C = x_o C_o + (1 - x_o) C_p \tag{163}$$

Equations (68), (69), (71), (75), and (161)–(163) predict that, in the *short correlation time limit*, i.e., $\Lambda_{1J_o} \gg \omega_I - \omega_J$,

$$T_1/\rho = (0.98 \times 10^{-13}/D)\rho a^4 (2\pi\beta\mu)^{1/2}[k_0 + Ck_1]$$

$$= x_o (T_1/\rho)^{op} + (1 - x_o)(T_1/\rho)^{op} \tag{164}$$

where

$$D = \langle D(J) \rangle_{ortho\text{-}H_2} = \sum_{J\ \text{odd}} P_J D(J) \tag{165}$$

$$D(J) = \frac{J(J+1)(2J-1)(2J+3)}{57.4}\left\{1 + \frac{4.74}{4J^2 + 4J - 7}\right\} \tag{166}$$

$$k_0 = (6\pi/5\hbar^2) I^{(1)}(2) \tag{167}$$

$$k_1 = (21/50\pi\hbar^2) I^{(2)}(4) \tag{168}$$

The numerical values of γ, H', and H'' for H_2 have been used in Eq. (69) in order to obtain the numerical factor in Eq. (164). The quantities $(T_1/\rho)^{oo}$ and $(T_1/\rho)^{op}$ are the values of T_1/ρ in the limits of 100% *ortho*-H_2 ($x_o = 1$) and 100% *para*-H_2 ($x_o = 0$), respectively. Lipsicas and Hartland[33] have shown that the predicted linear dependence of T_1/ρ on x_o holds within experimental errors up to room temperature. A plot of T_1/ρ versus *ortho*-H_2 concentration is shown in Figure 4. From such data, they have constructed the dependence of $(T_1/\rho)^{oo}$ and $(T_1/\rho)^{op}$ on temperature as shown in Figure 5.

The experimental temperature dependence of $I^{(1)}(2)$ and $I^{(2)}(4)$ may be obtained from the temperature dependence of $(T_1/\rho)^{oo}$ and $(T_1/\rho)^{op}$ since, using Eqs. (164) and (163),

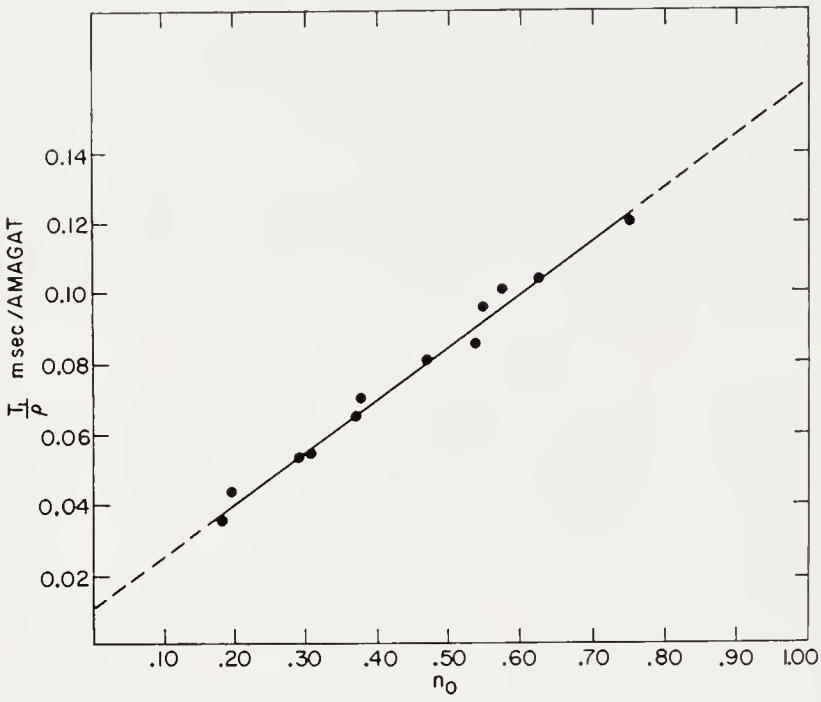

Fig. 4. Plot of T_1/ρ in H_2 gas at 77.5°K as a function of the concentration of *ortho*-H_2 (ref. 33).

$$k_0 = \frac{1.02 \times 10^{13} D}{a^4 (2\pi\beta\mu)^{1/2}} \left[C_o \left(\frac{T_1}{\rho} \right)^{op}_{\text{exptl}} - C_p \left(\frac{T_1}{\rho} \right)^{oo}_{\text{exptl}} \right] (C_o - C_p)^{-1} \tag{169}$$

$$k_1 = \frac{1.02 \times 10^{13} D}{a^4 (2\pi\beta\mu)^{1/2}} \left[\left(\frac{T_1}{\rho} \right)^{oo}_{\text{exptl}} - \left(\frac{T_1}{\rho} \right)^{op}_{\text{exptl}} \right] (C_o - C_p)^{-1} \tag{170}$$

The resulting experimental temperature dependence of k_0 and k_1 is shown in Figure 6. As has been shown elsewhere,[9] the fact that k_0 increases rapidly with increasing T indicates that there must be an important contribution to $b^{(1)}(R)$ which is of very short range. Attempts were made to fit k_0 using $b^{(1)}(ax)$ of the form[9]

$$b^{(1)}(ax) = \hbar\omega_n^{(1)}/x^n + \hbar\omega_6^{(1)}/x^6 \tag{171}$$

where it was possible from other considerations to estimate the van der Waals term to be $\omega_6^{(1)} = -1.85 \times 10^{12}$ sec^{-1}. Values of n up to $n = 19$ were tried and the best fit was obtained for $n = 19$. We shall not discuss the specific form of $b^{(1)}(ax)$ any further here for the following reasons:

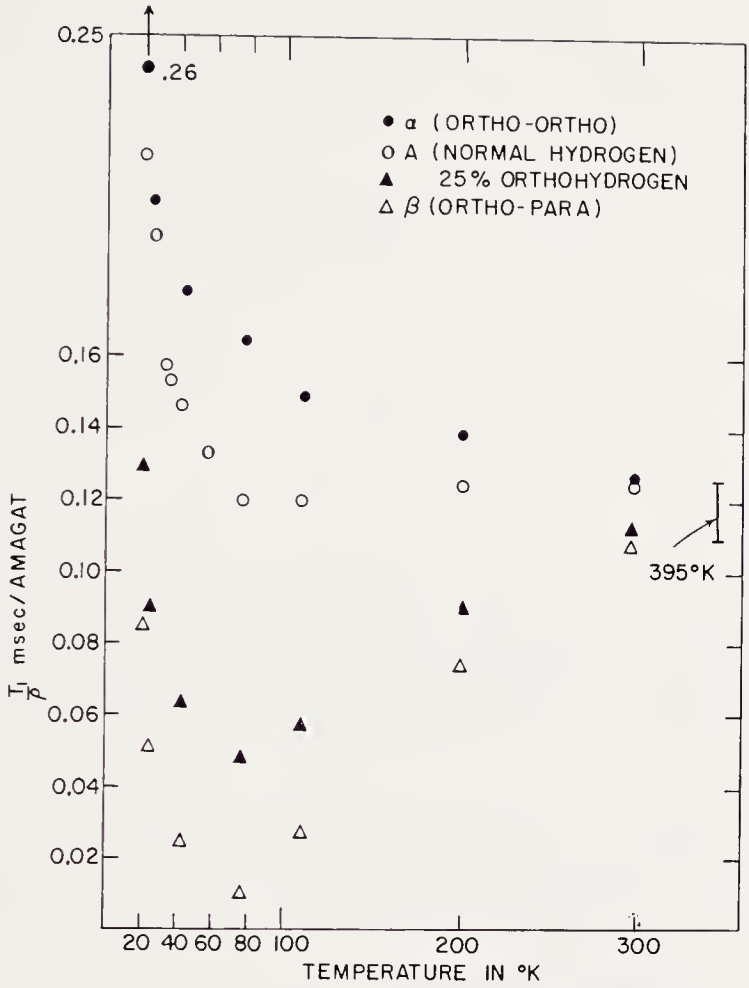

Fig. 5. Temperature dependence of T_1/ρ for dilute H_2 gas for different *ortho*-H_2 concentration. The points α in the figure correspond to $(T_1/\rho)^{oo}$ in the text while the points β correspond to $(T_1/\rho)^{op}$ (ref. 33).

(*a*) A detailed analysis of $I^{(1)}(2)$ requires a more accurate representation of the short-range behavior of the isotropic part of the *inter*molecular potential than is given by the Lennard-Jones potential originally used to calculate $I^{(1)}(2)$ for different forms of $b^{(1)}(ax)$. (*b*) Quantum corrections to $I^{(1)}(2)$ are important for very short-range interactions as has been discussed in Section IV, but not all of these corrections have been calculated numerically.

The same remarks hold for the analysis of the H_2–He data.[9] Riehl et al.[31] have carried out an analysis of the H_2–He system using a more

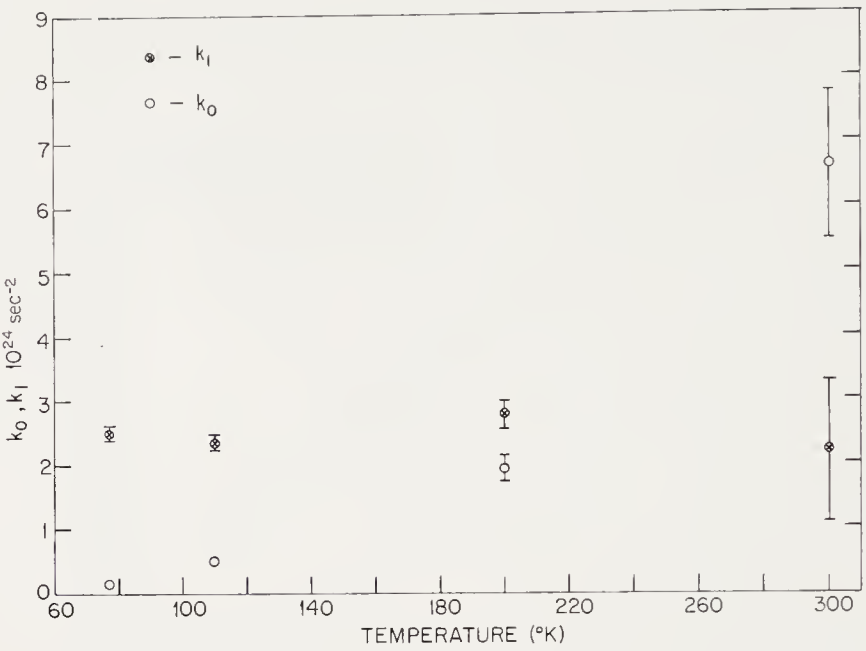

Fig. 6. Temperature dependence of k_0 and k_1 for H_2 derived from Eqs. (169) and (170), respectively, using the experimental values of $(T_1/\rho)^{OO}$ and $(T_1/\rho)^{Op}$ of Lipsicas and Hartland shown in Figure 5 (ref. 9).

realistic potential and taking into account quantum effects. We shall comment on their work in the next section.

If $b^{(2)}(R)$ is given by Eq. (98), the above comments do not apply[31] to $I^{(2)}(4)$. We rewrite Eq. (168) as

$$k_1(T) = (21/50\pi)(4\pi Q^2/a^5\hbar)^2 I(4,5) \tag{172}$$

where Q is the quadrupole moment of the H_2 molecule and the integrals

$$I(p,n) = \int_0^\infty dy \left\{ \int_0^\infty [g(x)]^{1/2} x^{(3/2)-n} J_{p+1/2}(xy) dx \right\}^2 \tag{173}$$

have been tabulated elsewhere[9] assuming that $V_0(x)$ is given by Eq. (155). In Figure 7, the temperature dependence of k_1 is compared to that of $I(4,n)$ for $n = 3,5,7$, and 13. Of these, $I(4,5)$ gives the best fit. The experimental value of $k_1(T)$ at $T = 200°K$ has been used to calculate Q for H_2 using $a = 2.93 \times 10^{-8}$ cm and the theoretical value of $I(4,5)$. The result is $Q = 0.60 \times 10^{-26}$ esu. This compares well with the theoretical value $Q = 0.65 \times 10^{-26}$ esu[34] and the molecular beam measurement[35] $Q = 0.63 \times 10^{-26}$ esu.

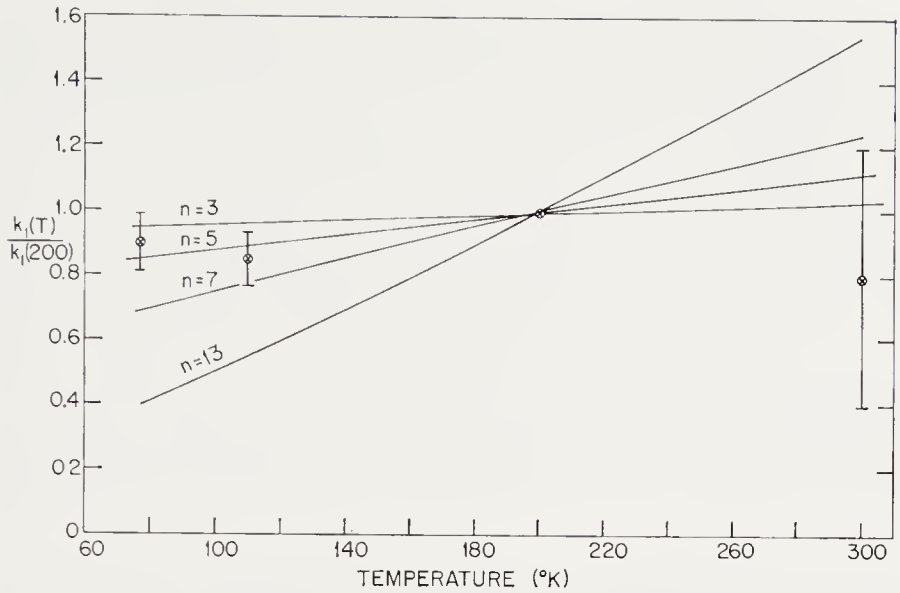

Fig. 7. Comparison of experimental values of $k_1(T)/k_1(200)$ for H_2 with theoretical values of this quantity using Eq. (168) and the numerical values of $I(4,n)$ tabulated in reference 9. The points are the experimental values and the lines are the theoretical results.

C. Effect of Transitions between Rotational States in H_2

When the analysis described in the previous section was first carried out,[9] it was felt that the effect of transitions of the *ortho*-H_2 molecules between different rotational states could be neglected to a good approximation, at least up to 200°K. At that temperature $P_3 \approx 0.03$ so that collisions which conserve rotational energy $(1,3) \leftrightarrow (3.1)$ discussed in Section IV [see below Eq. (105)] were thought to be quite infrequent. The influence of these terms may be taken into account below room temperature using the CAA and the formulas developed in Section III-B for a two-level system. These calculations have now been carried out by Lalita.[36] She finds that the effect of such collisions is much larger than that indicated by the small value of P_3. At 200°K, inclusion of these terms in the analysis of the dependence of T_1/ρ on x_o leads to a value of k_1 which differs from the value obtained by the analysis described in the previous section by almost a factor of two. Also, the temperature dependence of k_1 then obtained from the experimental data does not agree with the results of the CAA. Lalita then investigated the contributions of the transitions $(1,2) \leftrightarrow (3,0)$ and $(1,4) \leftrightarrow (3,2)$, associated with

ortho–para interactions, to $Q^{(2)}(1,3)$ and $Q^{(2)}(3,1)$. These terms were first treated by replacing $j^{(2)}(\omega_{13;20})$, $j^{(2)}(\omega_{31;02})$, etc. by $j^{(2)}(0)$. The *ad hoc* justification for this procedure is that van Kranendonk's calculation of collision cross sections[30] in H_2 indicates that these transitions are "quasi-resonant." Then $j^{(2)}(\omega)$ and $j^{(2)}(-\omega)$ were calculated from $j^{(2)}(0)$ using equations similar to Eqs. (111) and (112) to ensure the maintenance of a detailed balance. When these results were applied to the analysis of the experimental values of T_1/ρ as a function of T and x_o, it was found that the experimental temperature dependence of k_1 now agreed within experimental and theoretical error with the values obtained using Eq. (172). We conclude that the results obtained in Section VI-B for k_1 are valid because of the cancellation of two large resonant collision terms. The numerical results for k_0 are, however, affected.

As a final comment, we remark that the experimental results of Lipsicas and Hartland[33] for T_1/ρ in normal $H_2(x_o = 0.75)$ at room temperature are approximately 20% higher than those obtained more recently. The more recent experiments[31,36] were done at lower densities than those of Lipsicas and Hartland[33] and it is tentatively suggested that the 20% discrepancy is due to three-body effects. Remeasurement of the temperature dependences of $(T_1/\rho)^{oo}$ and $(T_1/\rho)^{op}$ would be of great value because of their importance in the determination of the H_2–H_2 intermolecular potential.

D. Quadrupole–Quadrupole Interactions between H_2 and Diatomic Molecules Having Large Moments of Inertia

When H_2 is mixed with a gas composed of molecules X, the $Q(J,J')$ of the *ortho*-H_2 molecules are influenced by H_2–X interactions. Because of this, T_1/ρ for the protons on the *ortho*-H_2 molecules is a function of ρ_x, where $\rho = \rho_{H_2} + \rho_x$, and ρ_x and ρ_{H_2} are the number densities of the X and H_2 molecules, respectively. By extrapolating the experimental plot of T_1/ρ versus ρ_x/ρ to $\rho_x/\rho = 1$, one can define an experimental $(T_1/\rho)^{ox}$, which is the value of (T_1/ρ) for an ensemble of H_2 molecules each of which interacts only with X molecules. We shall now consider molecules X which have large quadrupole moments so that the dominant anisotropic *inter*molecular interaction term is the quadrupole–quadrupole interaction [Eq. (99)] with R dependence

$$b^{(2)}(R) = 4\pi Q_{H_2} Q_X / R^5 \tag{174}$$

The term $Q^{(2)}(J,J')$ can now be calculated using Eq. (104). If the molecules X have a large moment of inertia so that many rotational states are populated at the temperature T of the gas, the average value of J for the X molecules, $\langle J \rangle$, generally satisfies the condition that $\omega_{JJ;\langle J\rangle;\langle J\rangle\pm 2}\tau_{\text{coll}} \leq 5$. Therefore, the terms $j^{(2)}(\omega_{JJ';J''J'''})$ in Eq. (104) can be divided into two groups. Those for which $J \neq J'$ have $\omega\tau_{\text{coll}} \gg 1$ and may be dropped, while most of those for which $J = J'$ have $\omega\tau \leq 5$ so that $j^{(2)}(\omega)$ can be replaced by $j^{(2)}(0)$. If this is done, the sums over J'' and J''' in Eq. (104) can be carried out. The final result is

$$Q^{(2)}(J,J') \approx (7/10\pi)j^{(2)}(0)[J(J+1)/(2J-1)(2J+3)]\delta_{JJ'} \qquad (175)$$

so that the model of Section VI-A can be used to calculate $(T_1/\rho)^{ox}$. The result is

$$\left(\frac{T_1}{\rho}\right)^{ox} = \frac{2.45 \times 10^{-13}}{D} \rho_x a_{ox}^4 (2\pi\beta\mu)^{1/2} \left(\frac{4\pi Q_{H_2} Q_X}{a_{ox}^5 \hbar}\right)^2 I(4,5) \qquad (176)$$

We assume that the isotropic intermolecular potential is a Lennard-Jones potential with parameters a_{ox} and ε_{ox} which are related to the parameters of interaction for the pure species by the usual relations

$$a_{ox} = \frac{1}{2}(a_{oo} + a_{xx}) \qquad (177)$$

$$\varepsilon_{ox} = (\varepsilon_{oo}\varepsilon_{xx})^{1/2} \qquad (178)$$

Most of the data for $(T_1/\rho)^{ox}$ were obtained at room temperature by Johnson and Waugh.[5] Mixtures of H_2–N_2 were also studied by Williams.[37] For H_2–N_2 and H_2–CO_2, the dependence of $(T_1/\rho)^{ox}$ on temperature has been analyzed[9] to yield the experimental temperature dependence of $I(4,5)$. The results obtained are in agreement with the CAA. In addition the absolute values of $(T_1/\rho)^{ox}$ at room temperature[5] for a number of molecules have been used in conjunction with Eq. (176) to yield values of Q_X for these molecules. The results are presented in Table I where they are compared with other determinations. The present results agree quite well with some of the more reliable previous determinations. Some aspects of the analysis presented here are discussed in more detail in reference 9.

VII. MISCELLANEOUS TOPICS

A. Other Theoretical Work

Gordon[13] has developed a classical kinetic theory technique for computing $J(0)$ [Eq. (26)]. His results are equivalent to the first Chapman-Enskog like approximation to Eq. (38) for $\omega = 0$ in which the translational and rotational degrees of freedom are treated classically. Gordon[38]

TABLE I

Comparison of Molecular Quadrupole Moments Obtained From the Interpretation of Nuclear Spin Relaxation Measurements with those Obtained by Other Methods. The Quadrupole Moment Is Defined in Terms of the Molecular Charge Distribution by $Q = 1/2 \sum_i q_i(3z_i^2 - r_i^2)$. All of the Values of Q Given by Nuclear Spin Relaxation are Understood to be Upper Limits. The Units Used Are 10^{-26} esu.

Molecule	Spin-relaxation experiment	Other experiments
H_2	0.60	0.63[a]; <1.0[b]; —[h]
O_2	0.92	h
N_2	1.70	1.64[c]; 1.48[d]; 1.5[e]; 1.9[f]; 1.0[b]; —[h]
CO	2.0	2.8[f]; 2.0[i]; —[h]
NO	2.05	—[h]
N_2O	4.25	—[h]
CO_2	4.85	4.1[g]; 4.6[e]; 5.9[b]; —[h]

[a] J. Harrick and N. F. Ramsey, *Phys. Rev.*, **88**, 228 (1952), by molecular-beam techniques. The number given is for the ground vibrational state.

[b] G. Birnbaum and A. A. Maryott, *J. Chem. Phys.*, **36**, 2032 (1962), from collision-induced microwave absorption.

[c] J. van Kranendonk, *Physica*, **24**, 347 (1954), from collision-induced vibrational spectrum of H_2–N_2 mixtures.

[d] J. D. Poll, *Phys. Letters*, **7**, 32 (1963), from induced absorption in the far infrared.

[e] J. A. A. Ketelaar and R. P. H. Rettschnick, *Mol. Phys.*, **7**, 191 (1963), from the pressure-induced rotational spectrum of N_2.

[f] R. H. Orcutt, *J. Chem. Phys.*, **39**, 605 (1963), from second virial coefficients.

[g] A. D. Buckingham and R. L. Disch, *Proc. Roy. Soc. (London)*, **A273**, 275 (1963), from birefringence induced by an inhomogeneous electric field. The value of Q is in doubt to within $\pm 20\%$ because of lack of knowledge of the anisotropic polarizability of CO_2.

[h] Values of quadrupole moments for these molecules have been obtained from pressure-broadening experiments. The quadrupole moments determined by this technique are smaller by a factor of 2 than those obtained by other methods.

[i] W. S. Benedict and R. Herman, *J. Quant. Spectry. Radiative Transfer*, **3**, 265 (1963).

has also discussed the close relationship between the correlation functions that appear in the theory of nuclear spin relaxation and Raman spectroscopy.

Freed[11] has considered the relationship between T_1 and T_2 and the rotational relaxation times within and between J manifolds. He considers two models in detail: (*1*) Each collision completely randomizes M but does not affect J; (*2*) each collision completely randomizes M and J. He also makes some remarks on situations intermediate between *1* and *2*. He does not, however, relate the rotational relaxation times to molecular quantities. Model *1* does not occur in nature when more than one J state is populated; model *2* is a special case of the considerations of Section III.

Torrey[39] has considered the spin relaxation in xenon gas using a classical kinetic theory approach. The relaxation mechanism is a spin–rotation coupling between Xe atoms when they are close together. He assumes that the isotropic potential is that for hard sphere interactions. His results agree very well (within 13%) with the more approximate CAA calculation for the same system.[8]

The fact that the dipole–dipole interaction between nuclear spins on different Xe atoms gives a much smaller contribution to nuclear spin relaxation than the momentum-dependent interaction postulated by Torrey was first indicated by the experiments of Carr et al.[40,41] There is good agreement between the experimental and theoretical[8] temperature and density dependence of T_1.

Riehl et al.[42] have carried out a dilute gas kinetic theory calculation for a case in which quantum effects were expected to be important: H_2 gas ($J = 1$) infinitely dilute in He.[31] The cross sections were obtained by a quantum mechanical scattering calculation using the distorted wave approximation (DWA). The approximations inherent in the DWA were justified by a close-coupling calculation. Correlation functions were evaluated using a master equation. The transition probabilities connecting the various molecular magnetic sublevels of H_2 were taken as $W_{m_j m_j'} = \rho\langle v\delta(m_j m_j';v)\rangle$, where ρ is the total number density and v is the relative speed. The brackets indicate an average over a Maxwellian distribution. They found that for cases where $v_A(R)$ is relatively long ranged [e.g., $v_A(R) \propto R^{-5}$], their value of T_1 agreed with the predictions of Section VI-B to within 5–10% over a temperature range 75–225°K.

For potentials whose asymmetric component also contains a steep

short-range part, however, there are substantial differences between their results[42] and those of reference 9. For $v_A(R) \propto R^{-15}$, the results of reference 9 for T_1 were four times as large as those of Riehl et al. We ascribe this difference to the neglect of the quantum correction $I_1(t)$ [see Eq. (120)] in reference 9.

B. Spin Diffusion Constant in Gaseous H_2

The spin-echo method can be used to measure the spin diffusion constant D by studying the decay of the echo in an inhomogeneous magnetic field as indicated by Eq. (4). Although many measurements of D using spin echoes have been made in liquids, surprisingly few measurements have been made in gases. The only measurements in dilute gases of which we are aware are those on He^3 and H_2 gases by Luszczynski et al.[43] and Lipsicas and Hartland,[44] respectively.

The measurements in H_2 have been made between 20 and 90°K at densities below 850 Amagats as a function of *ortho*-H_2 concentration. The values of D at any density and temperature were found to be independent of *ortho*-H_2 concentration and systematically greater than the values of the self-diffusion constant D_0 calculated from the Chapman-Enskog theory of transport processes. These results have been explained by the theory of Emery.[45] In principle, these measurements can be interpreted to give information on intermolecular potentials.

C. Nuclear Spin Relaxation in HD and D_2

The relaxation time T_1 has been measured for the protons and deuterons in HD gas and for the deuterons in D_2 by Hardy[46] at temperatures below room temperature and at densities such that T_1/ρ is independent of density at constant temperature. Measurements of the proton T_1 in HD gas between 15 and 20°K have also been carried out.[3] The T_1 data in D_2 have already been discussed briefly[9] but the analysis given neglects the effects of transitions between states of different J, which are probably important for this case. The results of Section III-B should be useful in interpreting the data for HD and D_2.

The special feature of HD which merits some comment is that, unlike H_2, there is no statistical restriction on the rotational states accessible to the molecule. Therefore, at very low temperatures, almost all of the molecules are in the $J = 0$ state in which $f_l(J) = 0$ [see Eqs. (45) and (46)]. For the *intra*molecular interactions to produce spin relaxation, the molecule must be promoted to excited rotational states. It

is easy to see from Eqs. (68) and (69) that at low temperatures, $T^{-1} \propto P_1$. Hardy[46] has found that below 100°K, $T^{-1} \propto \exp(-E_1/kT)$ for both protons and deuterons where the value of E_1 which he obtains is equal to the energy of the $J = 1$ state of HD.

In the case of D_2, Hardy has observed that the approach to equilibrium of M_z is not exponential but can be represented within experimental error as the sum of two exponentials. The shorter of the two relaxation times is associated with *para*-D_2 ($I = 1$) for which the ground rotational state is $J = 1$. The longer relaxation time is associated with *ortho*-D_2 for which the rotational states $J = 0, 2, \ldots$ are allowed. The relaxation rate associated with *ortho*-D_2 is proportional to $\exp(-E_2/kT)$, where E_2 is the energy of the $J = 2$ state of D_2.

D. Nuclear Spin Relaxation in Polyatomic Molecules

The first measurements on polyatomic gases were by Johnson and Waugh[47] who studied CH_4 and CH_4–O_2 mixtures between 200 and 300°K and Bloom, Lipsicas, and Muller[48] who also studied CH_4 over the same range and, in addition, C_2H_4 and C_2H_6 near room temperature. More recently, Bridges[49] has studied the proton and deuteron relaxation times in CH_4, CH_3D, CH_2D_2, CHD_3, and CD_4 between 100 and 300°K at densities between 0.1 and 8 Amagats. The proton relaxation times in the first four of these isotopic modifications of methane have also been studied as a function of temperature at fixed density (near 75 Amagats) by Trappeniers et al.[50] Lalita[36] has extended the CH_4 measurements and, in addition, has also studied CH_4–He mixtures, up to 700°K.

The values of T_1 for the protons in $CH_{4-n}D_n$ obey (approximately) the temperature dependence $T_1/\rho \propto T^{-1.5}$ and do not depend strongly on n. This result has been interpreted[47,49] to indicate that the intramolecular interactions responsible for proton spin relaxation are the spin–rotation interactions. In this approach, the dependence of temperature associated with the form of the anisotropic *inter*molecular interactions was neglected. More precisely, it was implicitly assumed that the isotropic interactions were those described by a hard sphere potential. Lalita found that for CH_4 infinitely diluted in helium, $T_1/\rho \propto T^{-0.8}$ indicating that the temperature dependence of T_1/ρ is sensitive to the nature of the anisotropic interactions. It is likely that the CAA can be applied to this problem, but that the treatment of the rotational transition rates using first-order perturbation theory, which we have given

in Section II-D, is not applicable to a system like CH_4 in which most of the molecules have high values of J. A semiclassical treatment of the rotational transitions[13] would seem to be more appropriate for this case.

The values of T_1 for the deuterons in $CH_{4-n}D_n$ depend strongly on n. The *intra*molecular quadrupolar interaction is responsible for spin relaxation in this case. The variation of T_1 with n in $CH_{4-n}D_n$ is due to a geometrical effect, i.e., the effective magnitude of the electric field gradient at a nuclear site depends on the orientation of the C–D axis relative to the molecular axes. Geometrical effects such as this are important when the frequencies associated with the energy splitting between states of different rotational quantum numbers (e.g., J, K for a symmetric top molecule) are much greater than the collision frequency.

Acknowledgment

We wish to thank Miss K. Lalita for making some important corrections of the manuscript.

References

1. N. Bloembergen, E. M. Purcell, and R. V. Pound, *Phys. Rev.*, **73**, 679 (1948).
2. F. Bloch, *Phys. Rev.*, **70**, 460 (1946).
3. M. Bloom, *Physica*, **23**, 237, 378 (1957).
4. M. Lipsicas and M. Bloom, *Can. J. Phys.*, **39**, 881 (1961).
5. C. S. Johnson, Jr., and J. S. Waugh, *J. Chem. Phys.*, **36**, 2266 (1962).
6. I. Oppenheim and M. Bloom, *Can. J. Phys.*, **39**, 845 (1961).
7. M. Bloom and I. Oppenheim, *Can. J. Phys.*, **41**, 1580 (1963).
8. I. Oppenheim, M. Bloom, and H. C. Torrey, *Can. J. Phys.*, **42**, 70 (1964).
9. M. Bloom, I. Oppenheim, M. Lipsicas, C. G. Wade, and C. F. Yarnell, *J. Chem. Phys.*, **43**, 1036 (1965).
10. J. M. Deutch and I. Oppenheim, *J. Chem. Phys.*, **44**, 2843 (1966).
11. J. H. Freed, *J. Chem. Phys.*, **41**, 7 (1964).
12. G. T. Needler and W. Opechowski, *Can. J. Phys.*, **39**, 870 (1961).
13. R. G. Gordon, *J. Chem. Phys.*, **44**, 228 (1966).
14. A. Abragam, *The Principles of Nuclear Magnetism*, Oxford University Press, London, 1961.
15. W. N. Hardy, *Can. J. Phys.*, **44**, 265 (1966).
16. E. L. Hahn, *Phys. Rev.*, **80**, 580 (1950).
17. H. C. Torrey, *Phys. Rev.*, **104**, 563 (1956).
18. B. Muller and M. Bloom, *Can. J. Phys.*, **38**, 1318 (1960).
19. J. M. Deutch and I. Oppenheim, *Advances in Magnetic Resonance*, Vol. 2, J. S. Waugh, Ed., Academic Press, New York, 1967.
20. H. Senftleben, *Z. Physik.*, **31**, 961 (1930).
21. J. J. M. Beenakker, H. Hulsman, H. F. P. Knaap, J. Korving, and G. Scoles, *Advances in Thermo-Physical Properties at Extreme Temperatures and Pressures*, S. Gratch, Ed., ASME, Purdue University, Lafayette, Indiana, 1965, page 216.

22. L. L. Gorelik, J. N. Redkobody, and V. V. Sinitsyn, *Soviet Phys. JETP, Engl. Translation*, **19**, 272 (1964).
23. L. Waldmann, *Z. Naturforsch.*, **12a**, 660 (1967); **13**a; 609 (1958).
24. R. F. Snider, *J. Chem. Phys.*, **32**, 1051 (1960).
25. H. C. Andersen, Ph.D. Thesis, Massachusetts Institute of Technology, 1966.
26. R. Zwanzig, *Phys. Rev.*, **129**, 486 (1963).
27. K. Kawasaki and I. Oppenheim, *Phys. Rev.*, **136**, A1519 (1964).
28. M. E. Rose, *Elementary Theory of Angular Momentum*, Wiley, New York, 1957.
29. K. E. Shuler, *Phys. Fluids*, **2**, 442 (1959).
30. J. Van Kranendonk, *Can. J. Phys.*, **41**, 433 (1963).
31. J. W. Riehl, J. L. Kinsey, J. S. Waugh, and J. R. Rugheimer, to be published. J. W. Riehl, Ph.D. Thesis, Massachusetts Institute of Technology, 1966.
32. B. R. A. Nijboer, private communication.
33. M. Lipsicas and A. Hartland, *Phys. Rev.*, **131**, 1187 (1963).
34. W. Kolos and C. C. J. Roothaan, *Rev. Mod. Phys.*, **32**, 219 (1960).
35. N. J. Harrick and N. F. Ramsey, *Phys. Rev.*, **88**, 228 (1952).
36. K. Lalita, Ph.D. Thesis, University of British Columbia, 1967. K. Lalita and M. Bloom, to be published.
37. D. Ll. Williams, *Can. J. Phys.*, **40**, 1027 (1962).
38. R. G. Gordon, *J. Chem. Phys.*, **42**, 3658 (1965).
39. H. C. Torrey, *Phys. Rev.*, **130**, 2306 (1963).
40. R. L. Streever and H. Y. Carr, *Phys. Rev.*, **121**, 20 (1961).
41. E. R. Hunt and H. Y. Carr, *Phys. Rev.*, **130**, 2302 (1963).
42. J. W. Riehl, J. L. Kinsey, and J. S. Waugh, *J. Chem. Phys.*, **46**, 4546 (1967).
43. K. Luszczynski, R. E. Norberg, and J. E. Opfer, *Phys. Rev.*, **128**, 186 (1962).
44. M. Lipsicas and A. Hartland, *Phys. Rev.*, **133**, A665 (1964).
45. V. J. Emery, *Phys. Rev.*, **133**, A661 (1964).
46. W. N. Hardy, Ph.D. Thesis, University of British Columbia, 1965.
47. C. S. Johnson, Jr., and J. S. Waugh, *J. Chem. Phys.*, **35**, 1128, 2020 (1961).
48. M. Bloom, M. Lipsicas, and B. H. Muller, *Can. J. Phys.*, **39**, 1093 (1961).
49. F. Bridges, M.S. Thesis, University of British Columbia, 1964. F. Bridges, M. Bloom, and W. N. Hardy, to be published.
50. N. J. Trappeniers, C. J. Gerritsma, and P. H. Oosting, *Physica*, **31**, 202 (1965).

AUTHOR INDEX

Numbers in parentheses are reference numbers and indicate that the author's work is referred to although his name is not mentioned in the text. Numbers in *italics* show the pages on which the complete references are listed.

A

Abdulnar, S., 227(26), *281*
Aberth, W., 363(179,180,184,186), 366 (186), *385*
Abragam, A., 550–553(14), 556(14), 557 (14), 559, 573(14), *598*
Abrahamson, A. A., 348, *382*, 393, *484*
Abramowitz, M., 181(28), *223*
Abrikosov, A. A., 227(21), *281*
Abrikosova, I. I., 186(43), *223*
Ackerman, M., 445
Adamov, M. N., 150(21), *165*
Adler, F. T., 14, *99*
Adrian, F., 163(55), *166*
Airey, J. R., 445
Akhiezer, A. I., 215, *224*
Alder, B. J., 139(49), *142*, 377, *387*
Alexander, M. H., 66, *103*
Amdur, I., 340(40), 345(62), 358, 362, *380*, *381*, *384*, 392, 393, *484*
Amey, R. L., 274(63), *282*
Amos, A. T., 72(182), 73(182a), 75 (182), 92(182), *104*
Andersen, H. C., 561, *599*
Anderson, J. B., 358(136,137), *383*
Anderson, P. W., 133, *141*, 488–490, 493, 494, 496(5), 503–505, 533, 534 (5), 541, 544(5), *545*, *546*, *548*
Anderson, R. S., 516, 517, 522(58), *547*
Andres, R. P., 358(136,137), *383*
Aono, S., 50, *102*
Artman, J. O., 526, 544(92), *548*
Ashkin, M., 66(166), *103*
Aub, M. R., 79(201), 80(201), 82(201), *105*, 145(4), 161(4), *164*, 179(27), 182 (31), 187, 193(27), *223*, 227(15), *280*
Autler, S. H., 528(78), *548*
Avery, J. S., 75(196), 87(196), *105*, 187 (53,54), *223*
Axilrod, B. M., 187, *223*, 226, *280*, 294(11), *326*, 376(251), *387*

B

Bade, W. L., 226, 227(24), *280*, *281*, 295, 299, *326*, 347(75), *382*
Bader, R. F. W., 55(139), *103*
Badger, R. M., 469, *486*
Baranger, M., 490, 491, *546*
Barker, J. A., 151(25), *165*, 336(20), 337 (20,28), 347(20), 372, *380*, *386*
Barnett, M. P., 26(56,57), *100*
Barrow, R. F., 352(107), *382*
Barua, A. K., 362(164), *384*
Barwig, P., 366(201), *385*, 406(19), 407 (19b), 409(19,) 410(19), 445, *484*
Basu, S., 227(26), *281*
Bates, D. R., 16(33), 17, *99*, 332(1,2), *379*
Batra, T. L., 363(178), *385*
Battino, R., 352(106,111), *382*, *383*
Baur, M. E., 227(26), *281*
Bay, Z., 187(53), *223*
Bayliss, N. S., 356(120,121), *383*
Beach, J. Y., 127(23), *141*, 147, *164*, 332(5), *379*
Beams, J. W., 135, *141*

Beck, D., 366(195a,200), *385*, 410(22), 411(22), 416(35c), 417, 446, 461, *484*, *485*
Becker, G. E., 528(78), *548*
Becker, R. L., 453
Bederson, B., 447, 453
Beenakker, J. J. M., 560(12), *598*
Beier, H. J., 446
Bell, R. J., 27(159,160), 65, *103*, 151, 152, 161, 162, *165*, 336, *380*
Bell, R. P., 229(38), *281*
Belyaev, Yu. N., 345(63), 362(63), *381*
Bender, C. F., 69, 70, *106*, 332(8), 362 (8), *380*
Bender, P. L., 72(183), 92(183d), 97 183, *104*
Benedict, W. S., 502(50), 519(50), 525, 527, 528, 537(50,74), 538(74), 539, *547*, 594
Bennewitz, H. G., 368(210), *385*, 399 (13), 414(31), 420(39), 446, *484*, *485*
Ben-Reuven, A., 491, 540(32), 541, *546*
Benston, M. L., 52(130,131), 55(130), *102*
Berencz, F., 38(92), *101*
Berendts, B. T., 516, 517, 518–520(62), 522, 527(62), 535–537, 538(62), *547*
Beresketskii, V. B., 215, *224*
Berkling, K., 399(14), 400, 420(38), 446, 447, *484*, *485*
Berlin, T., 51, 68(125), *102*
Bernard, W., 252(54), *282*
Bernstein, R. B., 10(26), 18(26), 20, 22 (26), 23(26b), 85, *99*, *100*, *105*, 228 (34), 275(34), *281*, 355, 358, 366, 369, *383–385*, 389, 390(2,4), 394(12), 397 (2), 401(12,16), 403(33b), 404(4b), 405(4b,18a,18b), 406(18b), 408(20), 409(20), 413(28), 414(12,28,30), 415 (12,28,33a,33b,33e,33h), 416(2e,33f, 33g), 417(2e), 419(12,33b), 420(12), 447, 450, 451, 454–457, 460(33b,40), 461 (40–42), 462(33,40), 477(47b), 478 (47b), 483(52), *484–486*, 496(42), 521, *546*
Berry, H. W., 362, *384*
Bethe, H. A., 72, 73, 74(179), 92(179), *104*, 174, 201(12), 210, 216(12), *222*
Beuhler, R. J., Jr., 447
Bhagavantam, S., 112, *140*
Biddlestone, A. J., 454
Bielz, F., 447
Bijl, A., 274(64), *282*
Bingel, W. A. 66(164) *103*
Bird, R. B., 8, 18(1), 31(1), 32(1), 36–38(1), 42(1), *98*, 127(25), *141*, 170(5), 209(5), *222*, 274(62), *282*, 297(13), *326*, 371, 373, *386*, 394(11), 396(11), 469(11), *484*, 488(2), 497(2), 507 (51a), 516, *545*, *547*
Birely, J. H., 447, 458
Birnbaum, G., 41, 487, 488, 491, 503 (51), 512, 520(51,72), 521(51), 527(51, 72), 534(51), 538(96), 539(96), 540 (8,33,109), 541, 542(33), 543(33,106), 544(33,106,107,111,112), *545–548*, 594
Black, W., 139(47), 140(47), *142*, 186 (45), *223*
Blais, N. E., 392(7), 393, *484*
Bleaney, B., 530, 539, 540(105), 544 (105,114), *548*
Bloch, F., 550, *598*
Bloembergen, N., 550(1), 559(1), *598*
Bloom, M., 538(98), 539(98), *548*, 549, 550(3,4,6–9), 551(4), 553(18), 567(7, 9),579(6), 585(6–9), 586(9), 588–590 (9), 591(9,36), 592(36), 593(9), 595(8), 596(9), 597, *598*, *599*
Blythe, A. R., 447, 450
Boato, G., 273(60), *282*
Boer, J. de, 274(64), *282*, 375(237), *386*
Böttcher, C. J. F., 229(44), 234(44), 235 (44), *282*
Boggs, J. E., 516(68), 522(68), 527(68), *547*
Bohr, N., 348, *382*
Bonnor, W. B., 229(42), 234(42), 235 (42), *282*
Born, M., 8, *98*, 120(15,) *141*, 179, *223*, 447
Boyle, L. L., 137(36), *141*
Boys, S. F., 26, *100*

Brachman, M. K., 248(52), *282*
Brackmann, R. T., 449
Brattsev, V. F., 13, *99*
Breene, R. G., Jr., 357(125), *383*, 488, 493, *545*
Breit, G., 71, *104*, 174, 209(11,77,78), *222*, *224*
Bridge, N. J., 137(39), *141*
Bridges, F., 597, *599*
Brillouin, L., 46(111), 47, *102*
Britt, C. O., 516(68), 522(68), 527(68), *547*
Broadway, L. F., 447, 449
Brooks, P. R., 447, 448
Brown, G. E., 213, *224*
Brown, H. H. Jr., 447, 453
Brown, W. B., 146(7), 147(7), 155, 156 (7), *164*
Brown, W. F., Jr., 227(26), *281*
Browne, J. C., 150(21), *165*
Bruch, L. W., 465, 470(45), *485*
Brueckner, K. A., 160, *166*, 188(63), *224*
Buck, U., 366(201), *385*, 406(19), 407 (19b), 409(19), 410(19), 445, 448, *484*
Buckingham, R. A., 5, 69, 70, *104*, 107, 112, 119(14), 123(20,21), 127(20), 131 (21), 136(32,34), 137(36,39,40), 138 (43,44), 139(50), *140–142*, 227(26), *281*, 357(128), *383*, 390(3), *484*, 505 (51b), 506, 508, 535, 539(101), *547*, *548*, 594
Buckley, F. G., 273(60), *282*
Buehler, R. J., 31(76), *101*
Bull, T. H., 448
Burke, P. G., 144(2), *164*
Busch, F. v., 399(15), 416(35b), 417, 458, *484*, *485*
Bushkovitch, A. V., 512(53,54), 513, *547*
Byers Brown, W., 29(71), 38(71), 45 (71), 51, 58(71b), 86(71b), *100*, *102*, 188(64), *224*, 339(38), 340(38), *380*
Byrne, M. A., 21, *106*

C

Calderon Diplom, N., 448
Callen, H. B., 74(189), *105*, 245, 252 (54), *282*
Campbell, J. A., 273, *282*
Carlson, B. C., 31(76), *101*, 170(6), *222*
Carr, H. Y., 595, *599*
Carr, W. J., Jr., 66(166), *103*
Carrá, S., 372, *386*
Carroll, P. K., 355(117), *383*
Carson, T. R., 332(2), *379*
Casanova, G., 273(60), *282*
Cashion, J. K., 16, 18(29), 23(29a), *99*, 343(48), 357, *381*, *383*
Casimir, H. B. G., 7, 78, 79, 82, 85, *105*, 139, *142*, 168, 176, 177, 186, *222*, 226, *280*
Catalano, E., 338(31), *380*
Chan, Y. M., 27(158), 65(158), 83, *103*, 145(5), 146, 147(12), 148(12,18), 149 (12), 161(50), 162, *164–166*
Chandra, S., 516(60), 519(81,82), 521 (80), 528, 529(81), 537(81,82), *547*, *548*
Chang, T. Y., 32–34(78), 36, 42(78), 44, 86, 91, *101*
Chatterjee, S., 362(164), *384*
Ch'en, S., 483(53), *486*, 493, *546*
Chiu, L. C., 75(194), *105*
Christoffersen, R. E., 74(189), 75(193), *105*
Clementi, E., 26, 73(187), 74(187), 75, *100*, *104*
Cohen, E. R., 520(72), 527(72), *547*
Cohen, H. D., *165*
Cole, R. H., 274(63), *282*
Colgate, 393
Colpa, J. P., 538(93), 539(93), *548*
Condiff, D. W., 86, *105*, 375(243), *386*
Condon, E. U., 43(88), *101*, 114(6), 119 (12), *140*, *141*
Coolidge, A. S., 332(3), 351(97), *379*, *382*
Corner, J., 376, *386*
Costigan, P., 363(176), *385*

Cottrell, T. L., 62(147), *103*, 378(266), *387*
Coulson, C. A., 8(10), 16(10), 17, 26 (56), 51(10), 57(127), 61, 62(144), 67, *98*, *100*, *102–104*, 138(44), *142*, 341 (43), 343(43), *381*
Craig, D. P., 186, *233*
Cromer, D. T., 478, 479(49), *486*
Cross, P. C., 502(49), *546*
Cross, R. J., Jr., 228(35), 275(35,67), *281*, *282*, 375, *386*, 448
Curl, R. F., 321
Curnutte, B., 493, 498(40), 500(40), 506 (40), 507(40), *546*
Curtiss, C. F., 8, 14, 18(1), 19(41), 31 (1), 32(1), 36–38(1), 42(1), *98*, *99*, 127 (25), *141*, 170(5), 209(5), *222*, 274 (62), *282*, 297(13), *326*, 371, 372, *386*, 394(11), 396(11), 469(11), 483(52), *484*, *486*, 488(2), 497(2), 507(51a), 516, *545*, *547*
Cusachs, L. C., 33(80), *101*

D

Dahler, J. S., 10(17), 31(73), 33(73), 34 (73), 39(73), 41(73), 65(73), 86(73), *98*, *100*, 375(243–245), *386*
Daley, H. L., 363(187), *385*
Dalgarno, A., 10(14), 12(14), 16, 27, 29 (71), 30(71a), 33(80), 38, 45(71), 48, 49, 65(158), 72(183), 83, 97(183), *98*, *100–104*, 119(13), 127(13), *141*, 143, 144(1,2), 145(1,5), 146, 147(1,12), 148 (12,17,18), 149(12), 150–152, 154(32), 155, 156(38,39), 157(37,42), 159(39), 161(28,37,50), 162, 163(56), *164–166*, 291(8), *326*, 332(7), 336(17,18), 337, 346, 375, *380*, *381*, *386*, 414(32), 459, 461(42), 465, 467(32), *485*
Danon, F., 291, 292, 297, 321, 323(7a), *326*
Darwin, C. G., 72(184), *104*, 175, *222*
Das, G., 29(69), *100*
Datz, S., 358, 363(189), *383*, *385*, 390 (2), 397(2), 448, 453, 454, 457, 458, *484*
Davidson, E. R., 5, 25, 69, 70, *100*, *104*, *106*, 332(8), 362(8), *380*
Davies, R. H., 344(61), 352(112,113), *381*, *383*
Davis, D. R., 26, *100*
Davison, W. D., 38(97), 65(97), *101*, 144(1), 145(1), 147, 149, 151(1), 155, *164–166*, 332, *380*, 414(32), 459, 465, 467(32), *485*
Deal, W. J., Jr., 39(98), *101*, 154, 155, 157, *165*
Debye, P., 37(90), *101*, 134, *141*, 229, *281*
De Groot, S. R., 274(64), *282*
De Jongh, J. G. V., 186(45), *223*
DeRocco, A. G., 349(87), 372(87), *382*
Deryagin, B. V., 177, 186, *223*
Deutch, J. M., 550(10), 557(19), 585 (19), *598*
De Wijn, H. W., 513, *547*
Dicke, R. H., 90, 92(227), *105*, *106*, 205, *224*
Dickens, P. G., 378(260), *387*
Diehl, H., 14(37), *99*
DiGiacomo, A., 491, *546*
Dijkerman, H. A., 516(66,67), 522(66, 67), *547*
Dirac, P. A. M., 65(157), *103*, 167, 188 (1), *222*
Disch, R. L., 137(36,40), *141*, *142*, 539 (101), *548*, 594
Discowski, H., 453
Dissado, L., 186, *223*
Dohmann, H. D., 368(210), *385*, 399 (13), 414(31), 446, *484*, *485*
Doniach, S., 227(22), *281*, 305(19), *326*
Dorrestein, R., 448
Dousmanis, G. C., 134(30), *141*
Düren, R., 365, *385*, 410(23), 418(36), 448, 449, 461(23), 462(33), 468(23), 483(52), *484–486*
Dummel, D., 366(200), *385*
Dummel, H., 446

Dunham, J. L., 354, *383*
Dunmur, D. A., 137(36,37), 138(37), *141*
Duparc, D. M., 69, 70, *104*
Dymanus, A., 516(66), 522(66), *547*
Dymond, J. H., 372, *386*
Dzyaloshinskii, I. E., 79(201), 80(201), 82(201), *105*, 182, 186, 195, *223*, 227 (14,21), *280*, *281*

E

Eastman, D. P., 524(70), 525(70), *547*
Eddy, N. W., 363(177), *385*
Edwards, H. D., *547*
Eisenshitz, R., 169, *222*, 226(3), 258(3), *280*, 345, 346(67), *381*
Eliason, M. A., 55(143), 58, 59, 60(143), *103*, 349, *382*, 478, 479(48), *486*
Ellett, A., 449
Ellison, F. O., 34(74), 65(74), *101*, 343 (49), 344, *381*
Emerson, M. T., 227(26), *281*
Emery, V. J., 596, *599*
Epstein, S. T., 13, 29(71), 38(71), 45 (71), 46(104–106), 52(126,132), 58 (71b), 62, 83, 86(71b), *99*, *100*, *102*, *103*, *105*, 146(7), 147(7,14), 148(14), 155, 156(7), 157(41), *164–166*, 188 (64), *224*
Estermann, I., 390(1), 421(1), 449, *484*
Evarestov, R. A., 150(21), *165*
Everhart, E., 348, 362, 363, *382*, *384*
Exton, R. J., 358(135), *383*
Eyring, H., 10, 47(114), 66(114), *99*, *102*, 116(7), *141*, 342, 343, *381*

F

Falkenhagen, H., 37(89), *101*, 226, 258, *280*
Fallon, R. J., 344(58), *381*
Fano, U., 357(126), *383*, 490, 491, *516*
Feeny, H., 516(65), 519(91), 522(65), 535(65,88), 537(91), 538(91), *547*, *548*
Feinberg, G., 79(201), 80(201), 82(201), *105*, 198, *224*
Feltgen, R., 418(36), 449, *485*
Fenn, J. B., 358(136,137), *383*
Fermi, E., 187(52), 201(52), *223*
Feynman, R. P., 51, 52(124), 54(124), 60, *102*, 173(8), 177, 197(66), *222*, *224*
Firsov, O. B., 348, 362(168), *382*, 384, 402(17), *484*
Fischer, I., 67, *104*
Fite, W., 358, *383*, 390(2), 397(2), 449, 450, *484*
Fiutak, J., 117(10), *141*, 491, 509(36), *546*
Flicker, M., 7(165c), 65, 66(165), *103*
Florin, H., 449
Flügge, S., 14(37), *99*
Fluendy, M. A., 477(47a), *486*
Fock, V., 61(145), *103*
Fock, W., 372, *386*
Förster, T., 87(214,215), *105*, 201(69), *224*
Fogg, G. T., 521
Foley, H. M., 490, *546*
Foner, S. N., 449
Fontana, P. R., 15(36), 32(77), 34(77c), 38, 39(77b), 41, 42(77c), 43(77c), 45, 73(185), 75(36,185), 85, *99*, *101*, *104*, *105*, 144(3), *164*, 461(41), *485*
Ford, K. W., 359(154), 360, 364, 366 (154), 369, *384*, 390(4), 402(17), 409 (17a), *484*
Foster, J. M., 26, *100*
Fowler, R. H., 232(46), *282*
Fraga, S., 29(68), *100*
Fraser, R. G. J., 449
Freed, J. H., 550(11), 595, *598*
Frenkel, L., 544(113), 545(113), *548*
Frisch, H. L., 371(215), *386*
Fröhlich, H., 140(51), *142*, 227(26), *281*
Fröman, A., 10, 14(37), *98*, *99*
Frost, A. A., 55(140), 59, 60(140), *103*, 349, *382*
Funabashi, K., 348(82), *382*

G

Gaide, W., 418(36), 449, *485*
Galatry, L., 491, *546*
Garcia, J. D., 74, *105*
Gáspár, R., 348, *382*
Gavrila, M., 147(13), *165*
Gebbie, H. A., 523, 524(70a), *547*
Generalov, N. A., 378(261), *387*
Gengenbach, R., 449
Gerhauser, J., 25, *100*
Gerritsma, C. J., 597(50), *599*
Gersing, E., 449
Ghirardi, G. C., 46(105), *102*
Gibson, G. E., 356(120), *383*
Gienapp, H., 449
Gilliam, O. R., *547*
Gilman, H. P., 363(177), *385*
Gilmore, F. R., 352(109), *383*
Ginsburg, N., 521(76), 527(76), 528 (76), *547*
Ginter, M. L., 352(111), *383*
Gislason, E. A., 228(35), 275(35), *281*, 448, 449
Glassgold, A. E., 72(183), 97(183), *104*
Glasstone, S., 342(47), *381*
Goeppert-Meyer, M., 117(9), *141*
Goldberger, M. L., 358(152), *384*
Goldstone, J., 160, *166*
Gomberoff, L., 75(195), 86(195), 88 (195), 90, *105*, 187(55,57,60), 195(60), 201(55), 207(57), 209, 222(79), *223*, *224*
Gordon, J. P., 526, 544(92), *548*
Gordon, R. G., 228(35), 275(35), *281*, 357, *383*, 451, 491, 513, 514, 520(30), 522, 524, 525, 534(30), 540(110), *546*, *548*, 550(13), 594, 598(13), *598*, *599*
Gordy, W., 488, 535, *545*, *547*, *548*
Gorelik, L. L., 560(22), *599*
Gorkov L. P. 65, 66(162), *103*, 227 (21), *281*
Gotch, S., 372, 374(226), *386*
Graben, H. W., 372(229,231), *386*
Granier, R., 483(53), *486*
Greene, E. F., 358, 366(149), *384*, *385*, 445, 446, 450
Griem, H., 490, 491, *546*
Groblicki, P. J., 366(205), *385*, 405 (18b), 406(18b), 450, *484*
Grosser, A. E., 447, 450
Guggenheim, E. A., 376, *387*

H

Hahn, E. L., 552(16), *598*
Hall, G. G., 53, 62, 72(182), 73(182a), 75(182,193), 92(182), *103*, *104*
Hameka, H. F., 16(32), 75(32,192), 90, *99*, *105*, 205, *224*
Hanks, P. A., 521
Hanley, H. J. M., 372, *386*
Hardy, W. N., 551(15), 555(15), 559, 562, 568, 569(15), 570(15), 596, 597, *598*, *599*
Harkness, A. L., 340(40), *380*, 393
Harrick, N. J., 538(100), 539(100), *548*, 590(35), 594, *599*
Harrier, R. M., 502(49), *546*
Harriman, J. E., 7(225), 91(225), 92–95, 97(225), *106*
Harris, F. E., 70(176), *104*, 139(49), *142*, 362(163), *384*
Harris, L. P., 483(54), *486*
Harrison, H., 450
Hartland, A., 587, 588(33), 589(33), 590, 592, 596, *599*
Hartman, H., 73(187), 74(187), 75, *104*
Hassé, H. R., 65(142), *103*
Hasted, J. B., 358, *383*, 450, 455
Hatcher, R. D., 348(84), *382*
Hatoyama, G. M., 497(43), *546*
Haugh, E. F., 345(69), 348(69), *381*
Heisenberg, W., 119, *141*, 177, *223*
Heitler, W., 66, *103*, 120(17), *141*, 188 (62), *224*
Helbig, H. F., 363(173,175), *384*, 367, 368(209), *385*, 399(14), 400(14), 410 (24), 411(24b), 412(24b), 418(36), 449–451, 483(52), *484–486*

Helfand, E., 371(215), *386*
Hellmann, H., 51, 54(123), *102*
Henkel, U., 366(200), *385*, 446
Henry, R. J. W., 375, *386*
Herm, R. R., 447, 451, 458
Herman, L., 483(53), *486*
Herman, R. M., 72(183), 97(183), *104*, 134, *141*, 163(54), *166*, 483(53), *486*, 508, 523, 525, *547*, 594
Herring, C., 7(165c), 65, 66(165), *103*
Herschbach, D. R., 228(35), 275(35), *281*, 343(48), 375, *381*, *386*, 447, 448, 451–454, 458, 461(43), 469(46b), 476 (46b), 477(47a), *485*, *486*
Hershberger, W. D., 539, *548*
Herzberg, G., 6(50), 8, 15(36), 22(50), 23(50), 43(36a), 75(36), *98–100*, 340(42), 351(42), 354(42), 355(42), *381*
Herzfeld, K. F., 117(9), *141*, 378, *387*
Hessel, M. M., 451, 482(51), *486*
Hildebrand, J. H., 273, *282*
Hill, R. M., 535(87), 537(87), 538(87), *548*
Hill, T. L., 288(1), *326*
Hindmarsh, W. R., 349, *382*, 483(58), *486*
Hirschfeld, M. A., 523(69), 538(69), 539 (69), *547*
Hirschfelder, J. O., 3, 7(225), 8, 10, 14, 16, 18(1), 19(42), 20(43), 27, 29(71), 31(1,73,76), 32(1,72a), 33(72b,73,79), 34(72.73), 36(1), 37(1), 38(1,71,93), 39(73), 41, 42(1), 45(71,101,102), 46 (111), 52(126), 55(143), 58, 59, 60(143), 61, 62, 64, 65(66,73), 67(168), 68(141), 73(72), 75(72a), 76, 78(72a), 79(72a, 72b), 80–86, 90(221), 91(225), 92–95, 96(221), 97(225), 98(226), *98–104*, *106*, 127(24,25), *141*, 146(7), 147, 155, 156 (7), *164*, *165*, 170(5), 176, 182, 187(61), 188(64), 201(61), 202, 209(5), *222–224*, 227(18,25), 251(53), 274(62), *280–282*, 297(13), *326*, 332(6), 333, 345(69), 347, 348(69), 349, 371, 372, *379–382*, *386*, 394(11), 396(11), 469(11), 478, 479(48), *484*, *486*, 488, 497(2), 507(51a), 516, *545*, *547*
Hoernschemeyer, D., 145(4), 161(4), *164*, 227(28), 239(28), 269(59), 271–273(59), *281*, *282*
Hollstein, M., 451
Holstein, T., 489, *546*
Hornig, J. F., 38(93), *101*, 347, *382*
Horsely, J. A., 21, *106*
Hostettler, H. U., 366(205), *385*, 405 (18a), 451, 454, *484*
Howard, B. B., 227(26), *281*
Howard, R., 512(56), 528(56), 535, 536, 537(56), *547*, *548*
Hoyt, F. C., 362(167), *384*
Huang, K., 8(8), *98*, 120(15), *141*
Hückel, E., 229, *281*
Huggins, C. M., 321
Hulsman, H., 560(21), *598*
Hundhausen, E., 366, *385*, 406(19), 407 (19a,19b), 409(19),410(19), 445, 449, 452, *484*
Hunt, E. R., 595(41), *599*
Hunter, G., 10(26), 13(26a), 16, 18(26), 22(26), 23, *99*
Hurley, A. C., 52(127,129), 53, 61, 62, *102*, *103*
Hurst, R. P., 153(33), *165*
Hutchinson, D. A., 90, *105*, 205, *224*
Hutchinson, P., 377(257), *387*
Huzinaga, S., 69(174), *104*

I

Imam-Rahajoe, S., 483(52), *486*
Inokuti, M., 82(202), *105*
Islam, M., 340(39), *380*
Itoh, T., 72, *104*, 216(82), 220, *224*
Izyumova, T. G., 488(9), *545*

J

Jacobson, H. C., 357, *383*
Jaeckel, R., 449, 452

Jaffe, J. H., 523(69), 538(69), 539(69), *547*
Jahn, H. A., 112, *140*
James, H. M., 332(3), 351(97), *379*, *382*
James, T. C., 539, *548*
Jansen, L., 113(5), *140*, 274(65), *282*, 293(10), *326*, 349, 376(252), 377, *382*, *387*
Jarmain, W. R., 351(99), 352(99), 354, *382*
Jawtusch, W., 452
Jefimenko, O., 349, 358(95,135), *382*, *383*, 483(53), *486*
Jehle, H., 227(24), *281*
Jenč, F., 344, *381*
Jepson, D. W., 10, 16, *98*, *99*
Jhaveri, A. K., 363(177), *385*
Johnson, C. M., 516(64), 522(64), *547*
Johnson, C. S., Jr., 550(5), 551(5), 559, 560, 593, 597, *598*, *599*
Johnson, M. D., 377(257), *387*
Johnson, R. E., 83, *105*
Johnston, H. S., 469, 476, *486*
Jonah, D. A., 371, *386*
Jones, E. M., 448
Jones, L. L., 5, 69, *104*
Jones, M. N., 139(48), 140(48), *142*
Jones, P. R., 363, *385*
Jones, W. J., 87(216), *105*
Jongh, J. G. V. de, 139(47), 140(47), *142*
Jordan, J. E., 345(62), 358, 362(145, 159), *381*, *384*, 392, 393, *484*

K

Kamnev, A. B., 340(41), 362(41,165, 166), *381*, *384*, 393
Kaplan, L. D., 502(50), 519(50), 527, 528, 537(50,74), 538(74), 539, *547*
Karl, G., 18(29), 23(29b), *99*
Karl, J. H., 46(106), *102*
Karplus, M., 26, 83, *100*, *105*, 147(11, 14), 148(14), 150(21), 152, 153(33), 154, *165*, 338(30), *380*
Kasha, M., 16(32), 75(32), *99*
Kauzmann, W., 120(16), *141*
Kawasaki, K., 561, *599*
Kay, I., 362(169), *384*
Keesom, W. H., 139(45), *142*, 226, 258, *280*
Keller, J. B., 362(169), 371(214), *384*, *386*
Kelly, H. P., 160(48), *166*
Kern, C. W., 26, *100*
Kestner, N. R., 8, 38(95,96), 39(98,99), 49, *98*, *101*, 154, 155, 157–160, *165*, *166*, 226, *280*, 289(3), 293(3), 298(17), 299(17), 305(17), 313(17), 314(17), *326*, 332, 333, *380*
Ketelaar, J. A. A., 357(131), *383*, 538 (93), 539(93), *548*, 594
Keyes, R. W., 341, *381*
Kiefer, L. J., 512, 513, *547*
Kihara, T., 226, *280*, 290, 294(11), *326*, 372(228), *386*
Kikuchi, R., 26, *100*
Kim, D. Y., 332, 345(12), *380*
Kim, H. J., 33(79), 41, 62, 86, *101*, *103*
Kim, K. Y., 73, *104*
Kim, S. K., 20(44), *100*
Kimball, G. E., 47(114), 66(114), *102*, 116(7), *141*
Kimel, S., 523(69), 538(69), 539(69), *547*
Kincaid, J. F., 62, *103*
King, G. W., 41(84), *101*, 502(49), *546*
Kingston, A. E., 151(23,25,27), 161(27), 162, *165*, 336(18,19), 337, 372(218), *380*, *386*
Kingston, O., 291(8), *326*
Kinsey, J. L., 14(37), *99*, 452, 453, 578 (31), 589(31), 590(31), 592(31), 595 (42), *599*
Kirkwood, J. G., 21, *100*, 128, *141*, 226, 229, 263(56), 270, 271(58), *280–282*, 295, 297, 299(12), *326*, 337, 347(75), *380*, *382*
Kirtman, B., 52(130), 55(130), *102*, 274 (66), *282*
Kiser, D. W., 321

Kitchener, J. A., 186(44), *223*
Klein, M., 372, 374(227), 376(253), *386 387*
Klein, O., 351, *382*
Knapp, H. F. P., 560(21), *598*
Knauer, F., 365, 367, *385*, 412, 452, *485*
Knipp, J. K., 34(81), 36, 42(81), 43, *101*, 144(2), *164*
Knof, H., 344(55), *381*
Kodera, K., 445, 452, 457
Koide, S., 16(32), 75(32), *99*
Kolb, A., C., 490, 491, *546*
Kolker, H. J., 83, *105*, 147(11,14), 148 (14,16), 152, 154, *165*, 338(30), *380*
Kolos, W., 6, 10(15), 11, 13, 14, 16, 21 (49), 22–28, 34(49), 40(67), 58, 65–68, 74, *98–100*, 332(4), 342, *379*, 539 (102), *548*, 590(34), *599*
Kondo, G., 457
Konowalow, D. D., 372, *386*
Korving, J., 560(21), *598*
Kramer, K. H., 399(14), 400(14), 413–415(28), 420(39), 446, 447, 452, *484*, *485*, 496(42), *546*
Kramers, H. A., 15(36), 75(36), *99*, 119, *141*, 173(7), *222*
Krauss, M., 26(64), *100*, 345(66), 378, *381*
Krishnaji, (C. S.), 497(44), 498(45a), 501(46,47), 504(45a), 508(47), 516, 519(81,82), 520(46), 521(80), 522, 524, 525, 528, 529(81), 535, 536, 537(81, 82), *546–548*
Kromhout, R., 227(31), 243(49), 255 (31), *281*, *282*
Krupenie, P. H., 342(46), 344(46), *381*
Kryder, S. J., 538(95), 539(93), 544 (113), 545(113), *548*
Kubo, R., 252(55), *282*
Kudian, A., 357(133), *383*
Kuhn, H., 489, *545*
Kuhn, H. G., 41(86), *101*
Kusch, P., 451, 482(51), *486*
Kwei, G. H., 449, 451–453, 458
Kydd, P. H., 453

L

Lackner, H. A., 516(59,65), 517(59), 522(65), 525(59), 535(59,65,88), *547*, *548*
Ladik, J., 74, *105*
Lahiri, J., *165*
Laidler, K. J., 342(47), *381*
Lalita, K., 591, 592(36), 597, *599*
Lambert, J. D., 521
Landau, L. D., 16(34), 17, 51(34), *99*, 185(36), 186, *223*, 242(48), 244, *282*
Landorf, R. W., 453
Lane, G. M., 348, 362, *382*
Langhoff, P. W., 153(33), *165*
Lansit, V. W., 502(48), *546*
Lapp, M., 483(54), *486*
Laue, H., 16(75), *101*
Laurie, V. W., 469(46b), 476(46b), *486*
Lebedeff, P. N., 173, *222*
Ledsham, K., 332(1), *379*
Leech, J., 182(30), *223*
Le Fèvre, C. G., 136(33), *141*
Le Fèvre, R. J. W., 134(29), 136(33), *141*
Legan, R. L., 530–532(83), 533, 534 (83), *548*
Lennard-Jones, J. E., 46(111), 47(111), *102*
Lenz, W., 489, *546*
Leonard, P. J., 151(25), *165*, 336(20), 337(20), 347(20), *380*
Leonas, V. B., 340(41), 345(63), 358, 362, *381*, *384*, 390(2), 393, 397(2), *484*
Leslie, D. C. M., 490, *546*
Levine, H. B., 160(49), *166*
Lewis, J. T., 33(80), *101*, 138(44), *142*, 162, *166*, 337(24), *380*
Lewis, M., 491, *546*
Lichten, W. L., 363(182), *385*
Lifshitz, E. M., 185(36), 186, *223*, 227, 242(48), 244, *280*, *282*
Lin, C., 530–532, 533(83), 534(83), *548*
Linder, B., 5, 63, 145(4), 161(4), *164*, 225, 227(26–33), 239(27,28), 243(49),

251(53), 253(30), 255(29–31), 268(32, 33), 269(59), 271–273(59), 274, 276 (29,30), *281*, *282*, 289, 305(21), *326*
Linderberg, J., 227(22), *281*
Lindholm, E., 490, *546*
Linnett, J. W., 59, 64, 68(141), *103*, 332(6), 332, *379*
Lippincott, E. R., 341(45), 343(52), 345 (52), 349, 351(98,101), 352(52,105), 378(52), *381*, *382*
Lippmann, D. Z., 321
Lipsicas, M., 538(98), 539(98), *548*, 550 (4,9), 551(4), 567(9), 585(9), 586(9), 587, 588(9,33), 589(9,33), 590, 591 (9), 592, 593(9), 596, 597, *598*, *599*
Liptay, W., 227(26), *281*
Litovitz, T. A., 378, *387*
Liuima, F. A., *547*
Livingston, P. M., 360(156), *384*
Lockwood, G. J., 363(172,173), *384*
Loesch, H. J., 410(22), 411(22), 416 (35c), 417, 446, 461, *484*, *485*
Löwdin, P. O., 26(58), 27, 46, 58, 62, 65(66,156), *100*, *102*, *103*, 127(24), *141*, 147, *165*, 341(44a), *381*
Lombardi, E., 293(10), *326*, 376(252), 377(252), *387*
London, F., 38, 66, *101*, *103*, 108, 126, *140*, 168, 169, *222*, 226, 258, *280*, 337, 345–348, *380*, *381*
Longmire, M. S., 345(62), *381*
Longstaff, J. V. L., 26(64), *100*
Longuet-Higgins, H. C., 9(35), *99*, 122 (19), *141*, 338, *380*
Lorents, D. C., 363(179,180,184,186), 366(186), *385*
Lorentz, H. A., 489, *545*
Losev, S. A., 378(261), *387*
Loubser, J. H. N., 539, 540(105), 544 (105), *548*
Lu, W. K., 375(243), *386*
Luke, S. K., 356(124), *383*
Lulla, K., 447, 453
Lundquist, S., 227(22), *281*
Luoma, J., 412(25), 465(25), *485*
Luszczynski, K., 596, *599*
Lutz, H. O., 363(189), *385*
Lynn, N., 48, 49, *102*, 151, *165*, 332(7) 336(17), 346, *380*, *381*
Lyon, W. D., 45(101,102), *101*
Lyons, J. D., *165*

M

McCarroll, R., 10(14), 12(14), 16, 27, *98*
McClure, D. S., 16(32), 75(32), *99*
McCoubrey, J. C., 378(266), *387*
McCulloch, R. D., 372(231), *386*
McDaniel, E. W., 358, *383*
MacDonald, J. R., 248(52), *282*
McGee, I. J., 465, 470(45), *485*
McGlashan, M. L., 376, *387*
McIntyre, H. A., *165*
McKinley, M. D., 338(35), *380*
McKoy, V., 321
McLachlan, A. D., 79(201), 80(201), 82 (201), 86(213), *105*, 145(4), 161(4), *164*, 185–187, *223*, 227(17,20,23), *280*, *281*, 305(20), *326*
McLone, R. R., 85, 86(211), 87, 88 (211), *105*, 175(14), 176(21), 179(21), 187(57), 193(21), 202(14), 207(21,57), *222*, *223*
McRae, E. G., 227(26), *281*
McWeeny, R., 72(182), 75(182), 92 (182), *104*
Madigorsky, W., 519(91), 537(91), 538 (91), *548*
Magee, J. L., 50(119), *102*, 348(82), *382*
Mahadevan, P., 450
Mais, W. H., 453
Maisch, W. G., 344(53), 345(53), 352 (53,105), *381*, *382*
Maker, P. D., 136(35), *141*
Manista, E. J., 457
Mann, J. B., 392(7), 393, *484*
March, N. H., 377(257), *387*
Marchi, R. P., 363(184–186), 366(185, 186), *385*, 454
Margenau, H., 5(4), 8, 38, 39(4), 48, 49, 86(4), 90(4), *98*, *101*, *102*, 122(18), 127

(18), *141*, 150(22), 163(54), *165*, *166*, 226, *280*, 336, 345, 347, 357, 371, *380*, *382*, *383*, 489, 491, *545*, *546*
Marino, L. L., 455
Martin, A. R., 229(37), *281*
Martin, H., 453
Martin, R. M., 477(47a), *486*
Maryott, A. A., 41, 273(60), *282*, 488, 538(95,96), 539(95,96), 540(8,109), 544(107,111–113), 545(113), *545*, *548*, 594
Mason, E. A., 329, 340(39,40), 342(46), 343(51,52), 344(46,53,55,58,61), 345 (52,53,62), 349, 352(52,53,105), 358, 359(155), 362(144,157,158,161,162), 366(194,197,203), 367(155,157,194), 368(155,157,158), 372(87), 374(233, 234), 375, 376(248), 378(52), 379(238), *380–382*, *384–386*, 391, 392(8), 393, 402, 409(21), 410(24), 414, 453, *484*, *485*, 538(99), 539(99), *548*
Massey, H. S. W., 358(150), 359(150), 362, 367, 368(206), *384*, *385*, 390(3), 461(42), *484*, *485*
Matcha, R. L., 45, *101*
Mathieson, L., 356(122), *383*
Matsumoto, G. M., 69, 70, *106*, 332(8), 362(8), *380*
Matsuura, K., 497(43), *546*
Mavroyannis, C., 79(201), 80(201), 82 (201), 83, 85, 86(201d), *105*, 145(4), 147(11), 161(4), *164*, *165*, 184(34), *223*, 227(16), *280*
Mazur, P., 274(65), *282*
Mead, C. A., 357(127), *383*
Meador, W. E., Jr., 344, 345(54), *381*
Meath, W. J., 3, 32(72a), 33(72b), 34 (72), 45(101), 62(150), 73(72,185), 75 (72a,185), 76, 78(72a), 79(72a,72b), 80–85, 86(210), 87(217), 88, 90(210, 217, 221), 96(221), *100*, *101*, *103–106*, 175 (15), 176, 182, 187(61), 201(61), 202, 206, 209(76), *222–224*, 227(18), *280*
Merritt, F. R., 527(77), *547*
Meyer, H. J., 453
Michels, A., 274(64), *282*
Michels, H. H., 147(11), 148(16), *165*
Midzuno, Y., 294(11), *326*
Mies, F. H., 345(66), 378, *381*, *387*
Mikolaj, P. G., 377(256,258), *387*
Miller, G. A., 521
Miller, R. V., 69, 70, *104*
Milleur, M. B., 7(225), 91(225), 92–95, 97(225), *106*
Minnaert, M., 365(190), 367(190), 369 (190), *385*
Minten, A., 453
Minturn, R. E., 448, 453
Mizushima, M., 16(32), 75(32), *99*, 490, *546*
Moak, C. D., 363(189), *385*
Mohr, C. B. O., 367, 368(206), *385*, 390 (3), *484*
Monchick, L., 329, 348(82), 366(197), 375, 379(238), *382*, *385*, *386*, 391, 402, 409(21), 414, *484*
Monfils, A., 6(50), 22(50), 23(50), *100*
Moon, P. B., 448
Moore, G. E., 448, 454, 458
Moore, N., 64(155), *103*, 332, *380*
Morrison, I. H., 151(28), 152, 161(28), 162, *165*
Morse, F. A., 366(196b), *385*, 408(20), 409(20), 454, *484*
Morse, P. M., 351(96), *382*
Moser, C., 71, *104*
Moser, P., 516(65), 522(65), 535(65,88), *547*, *548*
Mott, N. F., 358(150), 359(150), 367 (150), *384*
Moulton, M. C., 454
Moursund, A. L., 358, 366(149), *384*, 445, 450, 454
Muckerman, J. T., 85, 358, 369, 389
Müller, A., 337, *380*
Mueller, C. R., 412(25), 418(37), 453, 454, 465(25), *485*
Mukherji, A., *165*
Muller, B., 553(18), 597, *598*, *599*
Mulliken, R. S., 8, 39(5c), 40, 41(5c), 43(5a,5b), 50(119), *98*, *101*, *102*, 355 (116), *383*

Munn, R. J., 344(61), 359(155), 365, 366(191,203), 367(155), 368(155), 372, 374(232–234), 375(235,246), 376(221, 222,253),377, *381*, *384–386*
Murrell. J. N., 29(70), 46(70,107), 47, *100*, *102*
Muschlitz, E. E., Jr., 358, *384*, 455, 457, 477(47a), *486*
Musher, J. I., 46(109), *102*
Musulin, B., 155, 157(41), *166*
Muto, Y., 226, *280*, 294(11), *326*
Mysels, K. J., 139(48), 140(48), *142*

N

Namioka, T., 24, *100*
Needler, G. T., 550(12), 559, *598*
Nes, K. van, 78(198), *105*
Nesbet, R. K., 67, *103*, 538(94), 539 (94), *548*
Neumann, W., 454
Neynaber, R. H., 368(211), *385*, 414 (31), 416(34,35a), 417(35a), 455, 456, *485*
Nicol, M., 227(26), *281*
Nijboer, B. R. A., 582, *599*
Nishibori, E., 454, 456, 457
Noggle, T. S., 363(189), *385*
Norberg, R. E., 596(43), *599*
Norris, J. A., 451, 453, 458
Nutt, C. W., 454

O

O'Brien, T. J. P., 369(212), *385*, 416(33f, 33g), 460(40), 461(40), 462(33,40), *485*
Ohmura, T., 358(151), 360(151), *384*
Ohno, A., 491, *546*
Olander, D. R., 349, *382*
Olson, R. E., 418(37), *485*
Onsager, L., 229, 232(45), 269, *281*, *282*, 297, *326*
Oosterhoff, L. J., 16(32), 75(32), *99*
Oosting P. H., 597(50), *599*
Opechowski, W., 550(12), 559, *598*
Opfer, J. E., 596(43), *599*
Oppenheim, I., 538(98), 539(98), *548*, 549, 550(6–10), 557(19), 561, 567(7, 9), 579, 585(6–9,19), 586(9), 588–591 (9), 593(9), 595(8), 596(9), *598*, *599*
Oppenheimer, J. R., 8, *98*
Orcutt, R. H., 538(97), 539(97), *548*, 594
Orr, B. J., 136(34), *141*
Osberghaus, O., 453
Overbeek, J. T. G., 78(198), *105*, 139 (47), 140(47), *142*, 176, 177, 186(45), *223*

P

Pack, R. T., 6(16), 10, 14, 15(16), 18, 27, 72(16), *98*
Pariseau, M., 138(43), *142*
Parke, W. C., 227(24), *281*
Parker, J. G., 378, 379, *387*
Parr, R. G., 62, *103*
Paterson, S., 62(147), *103*
Paul, W., 420(39), 446, *485*
Pauling, L., 69(171), *104*, 127(23), *141*, 147, *164*, 332(5), *379*
Paulson, R. H., 377, *387*
Pauly, H., 358, 366, 367, 368(208, 209), 369(147), *383–385*, 390(2), 391, 397(2), 399(14), 400(14), 406(19), 407 (19a,19b), 409(19), 410(19,24), 411 (24b), 412(24b), 413(29), 414(2f), 418 (36), 419(2f), 420(2f), 445, 448–452, 454, 455, 462(2f,33), 468(2f), 483(52), *484–486*
Penfield, R. H., 78(200), 79, *105*, 175 (16), *222*
Pengelly, R. M., 151(28), 152, 161(28), 162, *165*
Penrose, R. P., 530, 544(114), *548*
Percival, I. C., 461(42), *485*
Pereira, A. N. G., 375(239), *386*
Perel, J., 363(187), *385*

Perkins, K. L., 512(54), *547*
Petersen, D. E., 321, 338(33), *380*
Phillipson, P., 52(128), 70, *102*, *104*, 332, 362(8), *380*, 393, *484*
Philpott, M. R., 85, *105*, 186, 187, 193 (50), *223*
Pings, C. J., 377(256,258), *387*
Pitaevskii, L. P., 65, 66(162), *103*, 186, *223*, 227(14), *280*, 305(18), *326*
Pitzer, K. S., 226, *280*, 290(4,5), 291(7), 292, 297, 321, *326*, 338, 372(34), *380*
Plíva, J., 344, *381*
Polanyi, M., 10, *99*, 342
Polder, D., 7, 78, 79, 82, 85, *105*, 139, *142*, 168, 176(2), 177, *222*, 226, *280*
Poll, J. D., 18(29), 23(29b), *99*, 357 (130), *383*, 594
Pople, J. A., 136(32), *141*, 297, *326*
Pound, R. V., 550(1), 559(1), *598*
Power, E. A., 34, 73, 75(195), 78(186), 79, 80(186,201), 82(186,201), 85, 86 (195,211), 87, 88(195,211), 90, 96 (221), *104–106*, 167, 173(9), 175, 176 (21), 179(21), 182(31), 183(33), 184, 187(55,57,60,61), 188(33), 192(46), 193(21), 195(60), 201(55,61), 202(14), 205, 207(21,57), 209, *222–224*, 227 (15,19), *280*
Prakash, V., 497(44), 518(71), 525, 535, 536, *546*, *547*
Prausnitz, J. M., 372, *386*
Present, R. D., 69, 70, *104*, 332(3), 372 (229,231), *379*, *386*
Preuss, H., 26(64), 66(164), *100*, *103*
Prichard, H. O., 10(26), 18(26), 22(26), *99*
Primas, H., 45(229), *106*
Prosser, A. P., 186(44), *223*
Purcell, E. M., 550(1), 559(1), *598*

R

Rabi, I. I., 367, *385*, 453, 455
Ramsey, N. F., 390(1), 421(1), *484*, 538 (100), 539(100), *548*, 590(35), 594, *599*
Randić, M., 29(70), 46(70), 47, *100*
Ranga, H. A., 363(178), *385*
Rank, D. H., 523, 524(70), 525, *547*
Ransil, B. J., 29(68), *100*
Rao, B. S., 524(70), 525(70), *547*
Rapp, D. 378(267), *387*
Raw, C. J., 362(157), 367(157), 368 (157), *384*, 410(24), *485*
Reck, G. P., 357(127), *383*, 445
Redkobody, J. N., 560(22), *599*
Reed, T. M., III, 338(35), *380*
Rees, A. L. G., 352, 356(122,123), *382*, *383*
Rettschnick, R. P. H., 357(131), *383*, 594
Rice, O. K., 356(120), *383*
Rice, S. A., 186, *223*
Rice, W. E., 376(248), *386*, 392(8), 393, *484*
Richards, H. L., 455
Richards, W. G., 21, *106*, 352(107), *382*
Riehl, J. W., 578, 589, 590(31), 592(31), 595, *599*
Rigby, M., 372, *386*
Rimini, A., 46(105), *102*
Rinehart, E. A., 530–534(83), *548*
Ripamonti, A., 378(260), *387*
Roberts, C. S., 345(65), 378, 379(270), *381*, *387*
Roberts, J. A., 530–534(83), *548*
Roberts, R. W., 450, 455
Rodberg, L. S., 197(67), *224*
Rol, P. K., 415(33e), 416(34,35a), 417 (34b,35a), 455, 456, 462(33), *485*
Roos, O, v., 72(183), 97(183), *104*, 491, *546*
Roothaan, C. C. J., 14(37), 25, *99*, *100*, *165*, 332(4), *379*, 539(102), *548*, 590 (34), *599*
Rose, M. E., 31(76), *101*, 498(45), *546*, 564, 576(28), *599*
Rosenberg, A., 512
Rosenberg, P., 455
Rosenkrans, J. P., 227(31), 255(31), *281*
Rosin, S., 367, *385*, 455
Ross, J., 20(44), *100*, 358, 362(162), 366 (149), *383–385*, 390(2), 397(2), 445, 446, 450, 467(2g), *484*

Rossi, J. C., 291, 321, 323(7a), *326*
Rothe, E. W., 228(34), 275(34), *281*, 368(211), *385*, 401(16), 414(30,31), 415 (33e), 416(34,35a), 417, 418(36), *455–457*, 462(33,36e), *484*, *485*
Rouse, A. G., *547*
Rowlinson, J. S., 370(213), 371, 374 (213), 377, *386*
Rudge, M. R. H., 72(183), 97(183), *104*
Ruedenberg, K., 292, *326*
Rugheimer, J. R., 578(31), 589(31), 590 (31), 592(31), *599*
Rushbrooke, G. S., 31(76), *101*, 170(6), *222*
Rusk, J. R., 520(72), 521(75), 527, *547*
Rydberg, R., 351, *382*

S

Sack, R. A., 14(37), *99*
Salem, L., 46(108,109), 53(135), 55(135), 66, *102*, *103*, 337, 338, 345, 347(27), *380*, *381*
Salpeter, E. E., 72, 73, 74(179), 92(179), *104*, 174, 201(12), 210, 216(12), *222*
Salyers, A., 227(24), *281*
Sandeman, I., 354, *383*
Sanders, W. A., 45(101), *101*
Sanderson, R. B., 521(76), 527(76), 528 (76), *547*
Sandler, S. I., 375(244,245), *386*
Sasaki, N., 456, 457
Savage, C. M., 136(35), *141*
Saxena, S. C., 340(39), *380*
Schaefer, T., 227(26), *281*
Schatz, P. N., 362(162), *384*
Schawlow, A. L., 488, 490, 493, 494(3), 502(50a), 535, *545*, *547*
Schiff, L. I., 116(8), *141*
Schlier, C., 365, 366(202), *385*, 399(14), 400(14), 410(33), 416(35b), 417, 418 (36), 420(38), 446, 447, 458, 461(23), 468(23,44), *484*, *485*
Schmidtke, H. H., 66(164), *103*
Schneider, W. G., 87(216), *105*, 227(26), *281*, 376(249), *387*
Scholte, T. G., 234(47), *282*
Schoonmaker, R. C., 457
Schroeder, R., 351(98), *382*
Schröder, U., 14(37), *99*
Schumacher, H., 228(34), 275(34), *281*, 401(16), 457, *484*
Schuster, G., 452
Schwarz, R. F., 134(30), *141*
Schweber, S. S., 196(65), *224*
Schwendeman, R. H., 502(48), *546*
Scoles, G., 560(21), *598*
Scott, B. W., 416(35a), 417(35a), 456, *485*
Seitz, F., 348(82), *382*
Seldam, C. A. ten, 274(64), *282*
Senftleben, H., 560(20), *598*
Series, G. W., 201(70), *224*
Sewell, G. L., 137(38), *141*
Shavitt, I., 26, *100*
Shaw, G., 29(70), 46(70,107), 47(70), *100*, *102*
Sheldon, J. W., 457
Sherwood, A. E., 349(87), 372, *382*, *386*
Shin, H. K., 378, *387*
Shmoys, J., 362(169), *384*
Shortley, G. H., 43(88), *101*, 114(6), *140*
Shuler, K. E., 565(29), *599*
Shumaker, J. B., 128, *141*
Siebrand, W., 87(216), *105*
Silbey, R., 46(110), *102*
Simpson, W. T., 86(212), *105*, 186, *223*
Sinanoğlu, O., 5, 38(96), 49, *101*, *102*, 158, 159, *166*, 182(29), *223*, 226, 227 (26), *280*, *281*, 283, 289(2,3), 293(2,3), 298(17), 299(17), 305(17), 313(17), 314(17), 321, *326*, 332, 333, *380*
Singer, K., 26(64), *100*
Singh, S., 87(216), *105*
Sinitsyn, V. V., 560(22), *599*
Sjölander, A., 227(22), *281*
Skrotskii, G. V., 488(9), *545*
Slager, D. M., 516(64), 522(64), *547*

Slater, J. C., 21, 61(145), 72(180), *100*, *103*, *104*, 337, *380*, 478, 479(50), *486*
Slichter, C. P., 72(182), 75(182), 92(182), *104*
Smit, J. A., 448
Smith, E. B., 372, *386*
Smith, F. J., 359(155), 362(158), 363 (183,188), 356, 366(191,203), 367 (155), 368(155,158), 372, 374(233, 234), 375(235), 376(222), 377, *384–386*, 457
Smith, F. T., 359(153), 363(184–186), 366(185,186), *384*, *385*
Smith, G. M., 457
Smith, K. F., 390(1), 421(1), *484*
Smith, R. A., 363, *385*
Smith, W. V., 488(1), 512(55,56), 516, 517, 522(65), 525, 528(55,56), 533 (55), 535, 536, 537(56,57), 538(87), *545*, *547*, *548*
Snider, R. F., 561, *599*
Solem, A. D., 274(65), *282*
Sommerfeld, A., 204(71), *224*
Sparnaay, M. J., 139(47), 140(47), *142*, 186(45), *223*, 266(57), *282*, 347(76), 348, *382*
Spitzer, L., 489, *546*
Spurling, T. H., 538(99), 539(99), *548*
Srivastava, S. L., 501(46,47), 508(47), 516(60,61), 518(71), 520(46), 522, 524, 525, *546*, *547*
Stacey, G. M., 150, *165*
Stebbings, R. F., 457
Steele, D., 341(45), 351(101), *381*, *382*
Stegun, I. A., 181(28), *223*
Steiner, E., 51, *102*, 339(38), 340(38), *380*
Stephen, M. J., 79(201), 80(201), 82 (201), 83, 85, 86(201d,208), 87, 88 (208), 90, *105*, 112, *140*, 145(4), 147 (11), 161(4), *164*, *165*, 175(13), 184 (34), 195(13), 200, 204(13), 205, 206, *222*, *223*, 227(16), *280*
Stephens, P. J., 119(14), *141*
Stern, O., 449, 452
Sternlicht, H., 348(78), *382*
Stewart, A. L., 155, 156(38,39,42), 159 (39), 163(56), *166*, 332(1), *379*
Stewart, W. E., 372, 374(226), *386*
Stockmayer, W., 297, *326*
Stogryn, A. P., 35(100), *101*, 138(42), *142*, 535, 536, *548*
Stogryn, D. E., 20(43), 35(100), *100*, *101*, 138(42), *142*, 535, 536, *548*
Stoicheff, B. P., 87(216), *105*
Stone, N. W. B., 523, 524(70a), *547*
Streever, R. L., 595(40), *599*
Strunck, H. J., 416(35b), 417, 457, 458, *485*
Stueckelberg, E. C. G., 16(34), 17, *99*, 356(119), *383*
Sucher, J., 79(201), 80(201), 82(201), *105*, 198, *224*
Sugiura, Y., 497(43), *546*
Suryanarayana, D., 112, *140*
Szent-Györgyi, A., 187(53), *223*

T

Tait, J. H., 144(2), *164*
Takebe, H., 357(127), *383*
Takeo, M., 493, *546*
Talman, J. D., 489, *546*
Tamura, T., 452
Taylor, E. H., 448, 453, 457
Taylor, H. S., 25, 70(176), *100*, *104*, 160(48,49), *166*, 362(163), *384*
Tee, L. S., 372, 374(226), *386*
Teller, E., 187, *223*, 226, *280*, 294(11), *326*
Terhune, R. W., 136(35), *141*
Thibault, R. J., 539, *548*
Toennies, J. P., 358, 366(147), 369(147), *384*, 390(2), 391, 397(2), 414(2f), 419 (2f), 420(2f,39), 446, 457, 458, 462 (2f), 468(2f), *484*, *485*
Torrey, H. C., 550(8), 553(17), 585(8), 595, *598*, *599*
Toschek, P., 399(14), 400(14), 420(38), 446, 447, 458, *484*, *485*

Townes, C. H., 134(30), *141*, 488, 490, 493, 494(3), 502(50a), 527(77), 535, *545*, *547*
Trambarulo, R., 488(1), 535(88), *545*, *548*
Trappeniers, N. J., 597, *599*
Trujillo, S. M., 416(34,35a), 417(35a), 455, 456, *485*
Tsao, C. J., 493, 498(40), 500(40), 506 (40), 507(40), *546*
Tuan, D. F., 332(10), *380*
Twerdochlib, M., 7(225), 91(225), 92–95, 97(225), *106*

U

Uchida, H., 456
Ufford, C. W., 74(189), *105*
Uhlenbeck, G. E., 375(237), *386*
Unsöld, A., 48, *102*, 126, *141*

V

Valk, F. van der, 454, 458
Vanderslice, J. T., 341(45), 342(46), 343 (51,52), 344(46,53,55,58,) 345 (52, 53), 349, 351(101), 352, 356(124), 358, 362(144,157,158), 367(157), 368(157, 158), 378(52,265), *381–384*, *387*, 410 (24), *485*
Van Dyk, G., 363(176,177), *385*
Van Kranendonk, J., 491, 509(36), 528 (79), 538(79), 539(79), *546*, *548*, 577, 592, 594, *599*
Van Vleck, J. H., 16, 41(84), 65(157), *99*, *101*, *103*, 229(43), *282*, 488, *545*
Varshni, Y. P., 341(45), 351(100), *381*, *382*
Vaughn, J. M., 41(86), *101*
Veillard, A., 26
Veneklasen, L. H., 418(36), 456, 462 (36e), *485*
Vernon, E. L., 351(97), *382*
Vernon, R. H., 363(187), *385*
Verwey, E. J. W., 78(198), *105*, 177, *223*
Victor, G. A., 148(17), 149, 150(21), 152, 154, 157(37), 161(37), 162(51), *165*, *166*
Vineyard, G. H., 348(84), *382*
Völkel, A., 14(37), *99*
Volkov, A. B., 516(59), 517(59), 525 (59), 535(59), *547*

W

Waber, J. T., 478, 479(49), *486*
Wada, A., 229(41), *281*
Wade, C. G., 538(98), 539(98), *548*, 550 (9), 567(9), 585(9), 586(9), 588–591 (9), 593(9), 596(9), *598*
Waech, T. G., 10(26), 18(26), 22(26), 23 (26b), *99*, 483(52), *486*
Wahl, A. C., 29(69), 67(168), 68, *100*, *104*
Waldmann, L., 375(242), *386*, 561, *599*
Walkley, J., 376(254), *387*
Walsh, J. P., 186
Walter, J., 47(114), 66(114), *102*, 116 (7), *141*, 539, *548*
Wang, J., 561, 579
Wang Chang, C. S., 375(237), *386*
Watanabe, A., 357(132,133), *383*
Watson, K. M., 358(152), *384*
Waugh, J. S., 550(5), 551(5), 559, 560, 578(31), 589(31), 590(31), 592(31), 593, 595(42), 597, *598*, *599*
Weber, G. G., 349, *382*
Weigang, O. E., Jr., 227(26), *281*
Weiguny, A., 14(37), *99*
Weiss, A., 150, *165*
Weisskopf, V. F., 488–490, *545*, *546*
Weissman, S., 340(39), 352(106,112), 356(124), 378(265), *380*, *382*, *383*, *387*
Welsh, H. L., 357, *383*
Welton, T. A., 245, *282*

Westheimer, F. H., 297, *326*
Whalley, E., 376(249), *387*
Wheeler, J. A., 176, *222*, 359(154), 360, 364, 366(154), 369, *384*, 390(4), 402 (17), 409(17a), *484*
White, R. L., 134(30), *141*
Widom, B., 378, *387*
Wiggins, T. A., 524(70), 525(70), *547*
Wigner, E., 10, 14, 40(83), 46(111), 47 (111), *99*, *101*, *102*
Williams, C. H., 458
Williams, D. A., 151(25), *165*
Williams, D. E., 378(269), *387*
Williams, D. L., 593, *599*
Williams, D. R., 29(70), 46(70), 47, *100*
Williams, G. M., 358(135), *383*
Wills-Johnson, G., 227(26), *281*
Wilson, E. B., Jr., 53(135), 55(135), 69 (171), *102*, *104*
Wilson, J. N., 337(29), *380*
Wilson, K. R., 447, 458
Winters, B., 519(91), 537(91), 538(91), *548*
Witmer, E. E., 40(83), *101*
Wittke, J. P., 92(227), *106*
Wolniewicz, L., 6, 10(15), 11, 13, 14, 16, 18(24), 21(49), 22–24, 26, 34(49), 65–68, 74, *98–100*, 138(41), *142*, 332(4), 342, *379*
Wood, H. T., 19(41), *99*, 483(52), *486*
Wu, T.-Y., 358(151), 360(151), *384*
Wyatt, R. E., 62, *103*

Y

Yaris, R., 53(133), 54, 55(133), 61(133), *102*, 147(15), *165*, 274(66), *282*
Yarnell, C. F., 538(98), 539(98), *548*, 550(9), 567(9), 585(9), 586(9), 588–591(9), 593(9), 596(9), *598*
Yos, J. M., 227(24), *281*, 344(56), *381*
Yoshamine, M., *165*

Z

Zabel, R. M., 449, 459
Zalewski, K., 8(10), 16(10), 17, 51(10), *98*
Zare, R. N., 352(108), *382*
Zatzkis, H., 78(200), 79, *105*, 175(16), *222*
Zeleznik, F. J., 352(110), *383*
Zener, C., 16(34), 17, 51(34), *99*, 339 (37), *380*
Ziemba, F. P., 363, *384*
Zienau, S., 73, 78(186), 79, 80(186,201), 82(186,201), *104*, *105*, 145(4), 161(4), *164*, 173(9), 175, 182(31), 183(33), 184, 187, 188(33), *222*, *223*, 227(15), *280*
Zijderveld, G. R. D., 516(66), 522(66), *547*
Zimering, S., 349(86), *382*
Zumino, B., 371(214), *386*
Zwanzig, R., 347(77), *382*, 561, *599*

SUBJECT INDEX

A

Ab initio calculations, 332
Absorption coefficient, 121
Absorption of radiation, 119
Acentric factor, 292
Activated complex, 284
Adiabatic approximation, 9, 12, 13, 16, 24
  application to $B^1\Sigma_u^+$ H_2, 24
  ground-state D_2, 22
  ground-state H_2, 22
  ground-state HD, 22
Ammonia inversion microwave spectrum, 133
Amplitude, scattered, 402
Anderson's theory, approximations, 504
  assumptions, 493
  dipole–dipole broadening, 512, 516, 525–529, 531, 534
  frequency shift, 497
  impact theory, 493
  phase shift, 496, 503
  simplifications of, 509
Anderson's theory of pressure broadening, comparison with experiment, summary, 533
Angular distribution of scattering intensity, 400
Angular distributions, 481
  quantum interferences in, 389
Angular resolutions, in molecular beam measurements, 399
Anisotropic intermolecular interactions, 555, 557, 564, 571, 572, 581, 585, 597
Anomalous heat conductivity for NO_2, 20
Atomic hydrogen, 146–148
Attraction between macroscopic bodies, 227
Attractive potential well, 461
Average energy, 288

B

B_2 ground state, quadrupole–quadrupole interaction energy in various coupling schemes, 44
Beam scattering, 358
Beam scattering experiments, 85
Bibliography, annotated, of beam scattering data, 445
Bicentric coordinates, 299
Bloch equations, 550
Bond polarizabilities, 136
Born-Oppenheimer approximation, 6, 8, 12, 24
  accuracy of, 16, 23
  application to $B^1\Sigma_u^+$ H_2, 24
  corrections to, 9, 15
  coupling of electronic and nuclear motions, 9
  diagonal corrections, 9
  ground-state D_2, 22
  ground-state H_2, 22
  ground-state HD, 22
  mass polarization correction, 6, 11, 27
  nondiagonal corrections, 9
Breit Hamiltonian, 174, 210, 219
Breit-Pauli Hamiltonian, generalization to a molecular system, 72
  limitations of, 72, 73
  significance of the terms in, 72
Breit-Pauli relativistic correction term, 6
Breit operator, 209, 213
  exchange potential for, 215
Brillouin perturbation theory, application to intermediate-range force problem, 46

convergence of, 47
Bulk dielectric constants, 139
Bulk properties, 370

C

C_6 constants, determination of, 389, 414, 459, 481
Slater-Kirkwood approximation, 414
Casimir and Polder interaction energies, 82
Cavity field, 270
Cavity field, **G**, 269
Cavity radius, 279
Cd_2, *S–P* dipole resonance interaction energy, potential energy curve maximum, 41
Center of charge, 110
Center of dipole, 110
Center of dispersion forces, 134
Centrifugal potential, 18
Charge transfer interactions, 47, 49, 68
Chemical potential, 229, 232, 263, 264
associated with dispersion forces, 263
electrical part of, 232
excess chemical potential, 262
orientation part of, 265
Chemical shifts, 75
Circular dichroism, 122
Clausius-Mosotti expression, 298
Close packing, 314
Closed-shell molecules, 293
CO, fine structure effects on long-range energy, 45
Collision energy, reduced, 410
Combination rule, 339
Complex susceptibility, 245
Condensed phases, 375
Conditional probability, 563
Configuration integral, 289
Constant acceleration approximation, 581, 591
Continuum approximation, 300
Core parameter, 291
Correlation effects in dispersion energies, 38
Correlation energies, 289, 292
Correlation function, 553, 554, 557–559, 563, 565, 566, 574, 578, 579, 595
Fourier transform, 566, 567, 576
Coulomb energy, definition for H_2, 65
Coupling of the electronic and nuclear angular momenta, Hund's case, 15
Λ-doubling, 15
Ω-coupling, 15
Coupling between the electronic and rotational angular momenta, 14
Coupling parameter, 263, 265
Cross sections, absolute values, 399
integral or total, 398
quantum, 481
random-phase-approximated, 415
velocity dependence, 414
Cross sections, absolute, 414
random-phase approximation, 413, 415
resonances in atom–atom scattering, 483
Cu_2, O_g^+ state, long-range magnetic interaction energy of, 91

D

D_2 ground state, adiabatic approximation, 23
Born-Oppenheimer approximation, 23
dissociation energies, 22
nonadiabatic approximation, 23
relativistic corrections, 22
Debye line shape, 542, 543
Deflection function, 402
classical, 394
Delta-function model, 349
Detailed balance, 565, 577
DF, dispersion energy of, 21
Diamagnetic susceptibilities, aromatic compounds, 75

Differential elastic scattering cross section, 398, 400, 481
Dipolar linear molecules, 132
Dipole–dipole interaction, 145, 150, 154
Dipole moment, 230
Dipole moments, 109
Dipole–quadrupole induction energy, 133
Dipole resonance interaction energies, S–P and P–D, 41
Discrete model, 305, 314
Dispersion energy, 108, 124, 125
  dipole–dipole, 6
  dipole–octopole, 6
  dipole–octopole interactions, 38
  dipole–quadrupole, 6
  dipole–quadrupole interactions, 38
  intraatomic correlation effects, 38
  quadrupole–quadrupole, 6
  quadrupole–quadrupole interactions, 38
  third-order dipole–quadrupole–dipole, 6
Dispersion force, 168
  Casimir–Polder potential, 176, 177, 181, 187, 192
Distorted atom, 289
Distortion dipoles, 349
Distribution functions, 263, 288
  radial distribution function, 271
  unsymmetric distribution function, 288
Double perturbation theory, 154, 155, 157, 158
  interchange theorems, 155, 156, 159
Drude model, 347
Dunham method, 354
Dynamic susceptibilities, 227

E

Effective potential, 17
  determination of long-range forces from, 20
  hump in, 18
Effect of the medium, 287
Electric field, 123, 125
Electrical fluctuations, 227, 243
  oscillations of the electrons about their equilibrium positions, 237
  polarization of molecule by, 275
  rotational motion of the permanent dipole moment, 237
Electrochemical potential, 235
Electron correlations, in–out to the left–right types, 51
Electron correlations in intermolecular forces, explanation of London dispersion energy, 63
  for H_2, 68
  for H_2, N_2, 67
  hydrogen molecule, 69
  in–out correlations, 69, 70
  interaction of two ground-state helium atoms, 69
  intermediate separations, 67
  large separations, 63
  left–right electron, 69
  small separations, 69
Electrostatic effects, 297
Electrostatic energy, 107, 124
Electrostatic Hellmann-Feynman theorem, 54, 55, 60
  application to the long-range interaction of two hydrogen atoms, 55
  validity of, 60
Electrostatic multipole interactions, 32
Electrostatic perturbation calculations of the interaction energy, 29
Electrostatic shell model, 349
Electrostatic variational calculations of the interaction energy, 21
Emission (stimulated) of radiation, 119
Exchange energies, 34
  at large separations, 31
Exchange energy, 92
  asymptotic formula for H_2, 65
  definition for H_2, 65
  of H_2, 96

Heitler-London exchange energy, 66
for H_2, 66
intermediate separations, 45
Exchange forces, 339

F

Faraday effect, 119
Field gradient, 123, 125
Fine structure, rotational energy levels, 75
Fine structure effects in intermolecular forces, intermediate coupling, 43
(J_a,J_b) coupling, 43
(Λ,S) coupling, 43
resonance interactions, 45
Fine structure energy splittings, 91
"Floating" wave functions, 53
Forbidden transitions, probability of, 16
Forces, intermediate-range, 389, 393
long-range attractive, 389, 393
short-range repulsive, 389, 392, 481
Free-electron model, 347
Free energy, 289
Frequency-dependent susceptibilities, 236

G

Generalized Hellmann-Feynman theorem, 52
cartesian coordinates with laboratory-fixed origin, 60
confocal elliptic coordinates, 61
electronic coordinates relative to the associated nucleus, 60
electrostatic Hellmann-Feynman theorem, 55
Rayleigh-Schrödinger perturbation theory of, 53
virial theorem, 61
Generalized potential, 228, 243, 246, 249, 268, 279
Glorified shadows, 369
Glories, 369, 402
Glory extrema, 389, 399, 414, 424, 482
Glory scattering, 403

H

H_2, $b\ ^3\Sigma_g^+$ state, 26
$b\ ^3\Sigma_u^+$ state, 26
$B\ ^1\Sigma_u^+$ state, adiabatic approximation, 24
Born-Oppenheimer approximation, 24
dissociation energy of, 24
$E\ ^1\Sigma_g^+$ state, a double minimum problem, 25
ground state, adiabatic approximation, 23
Born-Oppenheimer approximation, 23
coulombic energy, 65
dispersion energies, 26
dissociation energy of, 13, 22, 74
electron correlations in, 67, 69
exchange energy, 65, 92
Hellmann-Feynman calculation of long-range forces in, 55
hyperfine interaction effects, 92
nonadiabatic approximation, 23
ortho hydrogen, 97
para hydrogen, 97
polarization correction to energy, 16
radiative corrections, 74
relativistic corrections, 22
through $O(\alpha^2)$, 74
rotational quantum numbers of the hyperfine states, 97
interactions of, 1*s*, 2*s*, or 2*p* atoms, dispersion energies, 27
resonance energies, 27
S–*P* dipole resonance interaction energy, 41
fine-structure splitting, 45
potential energy curve maximum, 41

H_2–He interaction, 589, 595
Haloes, 364
Hartree-Fock and related methods, 28
Hartree-Fock theories, 172
  coupled, 152, 157
  uncoupled, 152, 154, 159
Hartree-Fock theory, 157, 160
  coupled, 154, 155, 162
  uncoupled, 160, 162
HD, ground state, adiabatic approximation, 23
    Born-Oppenheimer approximation, 23
    dissociation energies, 22
    nonadiabatic approximation, 23
    open-shell wave function, 69
    relativistic corrections, 22
  S–P and *P–D* dipole resonance interaction energy, 41
Heitler-London energy, 47
Helium, 148
He_2, dispersion energy of, 49
H_2, ground state, electron correlations in, 69
  interaction energies, "large" and "small" R expansions of, 84
  Hellmann-Feynman theorem, validity of, 51
HF, dispersion energy of, 21
Hg_2, *S–P* dipole resonance interaction energy, potential energy curve maximum, 41
HgD, $X^2\,\Sigma^+$ state, dispersion energy of, 20
HgH, $X^2\,\Sigma^+$ state, dispersion energy of, 20
High-energy beams, 361
High-frequency dielectric constants, 139
Hund's cases, 15
Hydrogen, 560, 562, 568
  D_2, 572, 596
  HD, 571, 596
  ortho, 555, 558, 567, 568, 573, 576, 587, 591, 596
  para, 555, 573, 576
Hydrogen 1*s* atoms, interaction of, 5
Hyperfine interactions, 7
Hyperfine splitting constant of H_2, 96,
Hyperfine splittings, 91
Hyperfine structural states, *a priori* probability for H_2, 96
Hyperfine structure effects in intermolecular forces H_2, ground state, 92
Hyperfine structure effects in intermolecular forces, rotational quantum numbers of the hyperfine states 97
Hyperpolarizabilities, 110, 136, 137
Hypervirial relations, 62

I

Impact parameter, 394
  classical, 403
Induction energy, 107, 124
  ion–molecule interaction, 37
  polar–nonpolar interaction, 37
  quadrupole molecule induced-dipole interaction, 37
In–out correlations, 69
Integral Hellmann-Feynman theorem, 62
Intensity distribution, 355
Interference contribution to the differential cross section, 404, 424, 482
Interference patterns, 363
Intermediate-range forces, 345
Intermolecular forces from molecular beam scattering, 390
Intermolecular potential, concept of, 8
Intramolecular spin-dependent interactions, 551, 555–557, 597
Ionization potential, 290, 294
Isotropic interactions, 597
Isotropic intermolecular interactions, 564
Isotropic intermolecular potential, 574, 586, 593

J

Jahn-Teller effects, 9
JWKB approximation, 359

K

K_2, S–P dipole resonance interaction energy, potential energy curve maximum, 41
Kerr effect, 135
Kihara potential, 290, 295

L

Larmor frequencies, 557
Lennard-Jones potential, 589, 593
Lennard-Jones (6-12) potential, 290
Li_2, S–P dipole resonance interaction energy, potential energy curve maximum, 41
Line broadening, causes of, 489
Line width, BrCN, 525
  CH_3F, 527
  CHF_3, 527
  H_2O, 527
  HCl, 523
  N_2O, 525, 526
  NH_3, 529–531, 533, 535, 536
  O_2, 526
  OCS, 516, 522, 535
  PF_3, 527
  SO_2, 528
  temperature dependence, 512, 516, 528
Lithium, 149
Local field, 270
Local field **F**, 269
London dispersion energy, 38, 78
London dispersion forces, 335
London formula, 290
London–van der Waals interaction, 171
  relativistic corrections, 210
Long-range dipolar interactions, 138
Long-range effects, hyperfine structure, 162
Long-range forces, 334
Long-range interactions, 146, 162
  H–H, 162
  H–He, 149
  He–He, 147, 148, 151, 154, 155, 160
  Li–H, 150
  Li–He, 150
  Li–Li, 150
  Li^+–Li^+, 158
  recommended values, 163
  third-order energy, 162
Lorentz line shape, 493, 494

M

Magnetic dipole interactions, 85
Magnetic intermolecular forces, 71
Magnetic moment, 116
Magnetic multipole interactions, 76
Magnetic susceptibility, 118
Many-body perturbation theory, 160
Many-electron theory of atoms and molecules, application to He–He interaction, 49
Mass polarization, 6, 11
  long-range corrections for two-electron atoms, 27
  polarization corrections to long range energy terms, 16
Master equation, 563, 595
Maxwell's equations, 116
Mean excitation energies, 294
Medium effect, 284
Metastable diatomic molecules, 18
Metastable vibrational energy states, 18
Models, 346
Molecular beam scattering, elastic, 391
  experimental arrangements of, 397
    secondary (target), 397
    secondary beam (or gas), 421
  investigators, 391
  laboratories, 391

low-energy, 389
primary beam, 397, 420, 421
Molecular hydrogen, 150
Molecular polarizabilities, 109
Molecular quadrupole moments, 137
Molecular reorientation, 551, 555
Molecular scattering phenomena, elastic, 390, 424
Molecular susceptibilities, 239, 251, 255
harmonic oscillator susceptibilities, 254
rigid rotor susceptibilities, 256
susceptibilities associated with rotational motion, 255
Multipole effects, 290
Multipole moments, 112, 124, 129
maximum number of constants, 112
Multipole polarizabilities, 145, 146

N

N-body potentials, 292
n-body potentials, 297
N_2, $C^3\Pi_u$ state, dispersion energy of, 21
ground state, electron correlations in, 67
Na_2, *S*–*P* dipole resonance interaction energy, potential energy curve maximum, 41
Nonadiabatic approximation, 9
direct calculation of the electronic–vibrational–rotational wave function, 14
ground-state D_2, 22
ground-state H_2, 22
ground-state HD, 22
Nondispersive forces in the long-range limit, 209
Nonpolar attractions, 290
Nonpolar interactions, 284, 298
Nonresonant absorption, 539
CH_3F, 544
CHF_3, 544
NH_3, 540, 544
NO, 539
O_2, 539, 544
theory of, 491, 540
Nonresonant intermolecular forces, first-order, 34
dipole–dipole interactions, 36
fine structure effects, 44
quadrupole–quadrupole interactions, 36, 43
Nonresonant intermolecular forces, second-order, 36
dispersion energy, 37
induction energy, 37
Nonretarded first-order interaction energies, permanent electrostatic dipole–dipole interaction, 90
permanent magnetic dipole–dipole interaction, 90
Nonspherical molecules, 297
Nuclear motion, equations for, 11

O

O_2, O_g^+ state, long-range magnetic interaction energy of, 91
One-electron models, 348
Onsager reaction field, 297
Optical activity, 119
Optical rotation, 122
Orbiting, 18
Ortho hydrogen, 97, 138
Oscillator model, 347

P

Pair potential, 283
bare two-body potentials, 284, 285, 316
composition-dependent potentials, 286
density-dependent pair potentials, 285
density-dependent potentials, 286, 319
effective pair potentials, 284, 319
nonpairwise potentials, 285

Para hydrogen, 97, 138
Perturbation calculation of the interaction energy, application to H_2, 46
  Brillouin theory, 46
  difficulties of, 45
  intermediate separations, 45
  large separations, 31, 32
    electrostatic dipole–dipole interaction, 32
    validity of the calculations, 32
  multipole expansion of the interaction potential, 31
  Sternheimer techniques, 45
  united atom expansion, 51
  very small separations, 51
Perturbation theory, 179, 188
Phase shifts, 402, 403
Polarizabilities of excited states, 128
Polarizability tensors, 135
  number of independent constants for axial symmetry, 112
Polar molecules, 297
Polyatomic molecules, 597
Potential, He–He repulsive, 393
Potential characteristics, deduced from beam scattering, 425
Potential energy curves, 289
  effective potential energy curves, 323
Potential functions, Buckingham Exp (α,6), 394
  ϵ, well depth of, 394, 482
  empirical or semiempirical, 394
  experimental interaction, 483
  Kihara (γ,12,6), 396
  Lennard-Jones (n,6), 394
  Morse (α), 396
  r_m, position of minimum in, 394, 482
  σ, zero of, or collision diameter, 397
Potential parameters, best values from scattering, 390, 460, 464
  orbital radii, 478, 479
  regularities and systematics, 390, 465
  rule-of-thumb equations for, 477–480
  atom–atom systems, 466, 467
  atom–diatomic systems, 467, 469
Potential well, curvature at minimum, 418
Potential well characterization parameters, 466
  curvature of, 461
Predissociation, 354
Pressure broadening, adiabatic, 490
  Anderson's theory, B-3, 493; B-4, 496; B-5, 497; B-7, 503; B-8, 504; B-9, 509; B-10, 512, B-12, 516; (2)B-16, 525, 526; (2)B-17, 527, 528; (2)B-18, 529, 531; B-19, 534
  diabatic, 490
  impact theory, 489, 491, 492
  intermolecular potentials, 497, 505, 522, 524, 526
  nonadiabatic, 490
  phase shift, 490
  semiclassical theory, 513
  theories of, 489
Probability density, 288

Q

Quadrupolar ground-state atoms, 42
Quadrupole moments, 109, 516, 522, 525, 526, 528, 535, 537
  quantum effect, 138
Quadrupole–quadrupole interactions, 577, 581, 592
Quantum effects in scattering, 399
Quantum electrodynamics, 167, 176, 195
Quantum interference phenomena, 363
Quantum interferences, 405
Quantum oscillations, 424
Quasi-spherical approximation, 291, 295

R

Radial distribution function, 583
Radiation, absorption of, 119
  stimulated emission of, 119
Rainbow angle, 402

Rainbow effect, 399
Rainbow maxima, 481
Rainbows, 364, 402
  primary, 424
  supernumerary, 424
Rainbow scattering, 409
  primary, 410
  rainbow maximum, 409
  supernumerary, 409, 410
Random distribution, 302
Rayleigh-Schrödinger perturbation theory, 29
  application to long-range interactions, 31
  differential equations, 29
  generalized Hellmann-Feynman theorem, 53
  perturbed wave functions, 30
Rb_2, S–P dipole resonance interaction energy, potential energy curve maximum, 41
Reaction field, 227–229, 234, 239, 270
  arbitrary system of charges, 233
  cavity concept, 268
  cavity radius, 269
  complex susceptibility, 238
  continuous dielectric, 227
  continuous medium, 227, 233
  continuum model, 228, 229, 235, 239, 260, 261, 264, 266, 268, 269, 279
  dipole moment, 234
  fluctuating moment, 228, 237
  higher-order moments, 234
  medium of arbitrary distribution, 237
  molecular description, 228
  molecules of the medium treated individually, 227
  nonpolarizable dipole, 229
  polarizable charge distribution, 233
  radius of the cavity, 236
  reaction-field response function, 229, 261
  reaction potential, 231, 233, 234, 263, 279
  response function of the medium, 238
  spherical cavity, 229
  static moment, 227, 228
  static reaction, 267
  uniform medium of dielectric constant ϵ, 229
Reaction field concept, 229
Reaction field formulation, 279
Reaction field of a molecule, 237
Reaction field, **R**, 269
Reaction-field technique, 241
Refractive index, 119, 121, 122, 135, 136
Relative coordinates, 10
  diatomic molecules, 10, 11
  triatomic and polyatomic molecular systems, 10
Relativistic dispersion energies, 78
Relativistic first-order energies, nonretarded first-order interaction energies, 90
  retarded first-order interaction energies, 86
Relativistic intermolecular forces, 71
  calculation of the interaction energy, 75
  H_2, radiative corrections, 74
  H_2, through $O(\alpha^2)$, 74
  large separations, 75
  magnetic dipole interactions, 85
  multipole expansion of the Breit-Pauli Hamiltonian, 75
  retarded dispersion energy for the interaction of two ground-state atoms, 78
  small and intermediate separations, 74
Relaxation methods, 377
Renner effects, 9
Resonance energies, 127
Resonance interaction, 171, 199, 202
Resonance interaction forces between like atoms, first-order dipole resonance, 40
  first-order quadrupole resonance, 41
  second-order energy, 41
Resonance intermolecular forces within one molecule, $2s$ or $2p$ H atom colliding with a proton, 42

Response functions, 236
Retardation effects, 75
  magnetic dipole interactions, 85
  nonresonant interactions, 85
  retarded dispersion energy for the interaction of two ground-state atoms, 78
Retarded dipole–dipole interaction energy, large R expansion of, 82
  small R expansion of, 80
Retarded dipole resonance energy, expansion of, 88
Retarded dispersion energies, 8
Retarded first-order energies, fine structure splittings in, 89
  natural line width of interaction energy, 89
  ^1S–^1P interaction, 86
  ^2S–^2P interaction, 89
Retarded intermolecular forces, 139, 170
  covariant calculations, 182, 195
  noncovariant calculation, 187
  nondispersive forces in the long-range limit, 209
  retarded dipole–dipole potential, 175
  retarded off-resonance energy, 176
  with spin, 221
Rotational magnetic moment, 134
Rydberg-Klein-Rees (RKR) method, 351
Rydberg-Klein-Rees potential, 21

S

Scattering, angular dependence, 389
  low-angle classical behavior, 389, 408, 481
  quantum effects in, 394
Scattering data, inversion of, yielding potentials, 390, 418
Scattering measurements, annotated bibliography, 389
  dipole–dipole interactions, 482
  inventory of, 389, 424
  systems studied, 389, 424
  types of measurements, 389, 424
Scattering results, appraisal of more reliable determinations, 390, 459
Se_2, first-order quadrupole–quadrupole energy of, 21
Second-order exchange terms, 345
Semiclassical scattering, 360
Semiclassical theory of scattering, 403
Semiempirical calculations, 333
  Smiempirical correlation of potentials from scattering, 390, 460
Semiempirical potentials, 293
Senftleben effect, 560
Separation of the center of mass, 10
Separation of the rotational motion of a molecular system, 14
Shadows, 367
  glorified, 402
Short-range forces, 338
Sign of the dipole moment, 134
Solvation layers, 302
Solvent effects, 284
Solvent structure, 306
Spectral density, 251
  of the mean square fluctuation, 245
Sphere-packing models, 317
Spin diffusion constant, 596
Spin-echo, 596
Spin-echo technique, 552
Spin-exchange scattering, alkali atoms, 97
Spin–spin interactions, 7
Spin–spin magnetic dipole interaction, for H_2, 96
  line broadening of the hyperfine structure, of atomic hydrogen, 97
  line (21-cm) in radio astronomy, 97
  optical pumping in a hydrogen maser, 97
  polarization in electron spin resonance, 97
  for small separations, 96
  for very large separations, 96
"Stable" wave functions, 53

Stark splittings, 134
Static dielectric constant, 297
Statistical fluctuations, 228, 236, 260
  concentration fluctuations, 236
  density fluctuations, 236
  translational fluctuations, 228, 237
Statistical models, 348
Steady-state NMR techniques, 551
Sternheimer potential, 45
Stockmayer potential, 297
Sum rules, 150
Supernumerary rainbows, 365
Systems for scattering studies, experimental requirements, 420
  suitability of, 389, 418
  theoretical requirements, 419

T

T_2 ground state, dissociation energies, 22
  relativistic corrections, 22
Tensor polarization, 563, 564
Tetrahedral molecules, 130
Theorem of corresponding states, 319
Thermal-energy beams, 364
Thomas-Fermi-Dirac treatment, 348
Three-body forces, 160, 295, 299
Three-body potential, 294, 300
Time-dependent pair distribution function, 581
Total cross sections, 367, 400, 424
  velocity dependence, 389, 413
Transition probabilities, forbidden, 75
Transport coefficients, 372

U

Unsöld's approximation, 48

V

van der Waals constant, 274
van der Waals forces, 226
  dispersion forces, 257
    retardation effects, 226, 227, 241, 249, 267
  dispersion interaction, 226
    overall dispersion, 261
  dispersion potentials, 228, 249, 258, 267, 276
    nonretarded, 279
    retarded, 279
  double-temperature potential, 276
  electrostatic forces, 226, 228
  electrostatic interaction, 229, 232, 264, 267
  higher-order potentials, 228, 249
    nonadditive, 279
  induction forces, 257
  induction interaction, 226, 267
  induction potentials, 228, 249, 258, 267, 276, 279
  nonadditive, 249
  nonadditive corrections, 226
  nonadditive potentials, 254, 279
  nonadditive triple potentials, 250
  orientation forces, 257
  orientation interaction, 226, 267
  orientation potentials, 228, 249, 258, 276, 279
  pair potentials, 228, 250, 257, 279
  rotational interaction, 267
  single-temperature potential, 278
  three-body interactions, 250
  three-body potentials, 249
  triple potentials, 228, 250, 259
  two-body interactions, 250
  two-body potentials, 249
  two-temperature Keesom potential, 275
  two-temperature potentials, 228, 275, 278
van der Waals interactions, 254, 257
van der Waals minimum, H_2, $b\ ^3\Sigma_g^+$ state, 26
van der Waals potentials, additive, 249
Variational calculations of the interaction energy, difficulties of, 25

ground state of the hydrogen molecule, 22
H_2, first excited state, 26
ground state, 26
large separations, 25
small and intermediate separations, 22
Velocity-dependent forces, 12
Velocity distribution, in molecular beam measurements, 399
Vibration–rotation bands, 351
Virial coefficients, 370
Virial theorem, 55, 61

W

Weak-collision approximation, 565, 566

CUMULATIVE INDEX TO VOLUMES 1–13

Authors of Articles

Numerals in **bold** type are volume numbers.

Allnatt, A. R., **11**, 1
Amdur, I., **10**, 29
Anderson, J. B., **10**, 275
Andres, R. P., **10**, 275
Aroeste, H., **6**, 1

Bak, T. A., **3**, 33
Ball, J. G., **13**, 267
Barriol, J., **8**, 5
Bastiansen, O., **3**, 323
Bearman, R. J., **1**, 1
Bederson, B., **10**, 1
Bellemans, A., **6**, 85; **11**, 117
Bernstein, R. B., **10**, 75;**12**, 389
Bigeleisen, J., **1**, 15
Birnbaum, G., **12**, 487
Blander, M., **11**, 83
Bloom, M., **12**, 549
Braterman, P. S., **7**, 359
Braams, R., **7**, 259
Brocas, J., **11**, 317
Brouckère, L. de, **1**, 77
Buckingham, A. D., **12**, 107

Careri, G., **1**, 119
Chanu, J., **13**, 349
Collins, F. C., **1**, 135
Craig, D. P., **8**, 27
Curtiss, C. F., **3**, 59

Dalgarno, A., **12**, 143
Das, T. P., **4**, 303
Daudel, R., **1**, 165
Davies, R. C., **7**, 359
Dewar, M. J. S., **8**, 65
Douzon, P., **7**, 339
Drickhamer, H. G., **4**, 161
Duchesne, J., **2**, 187

Ehrenberg, A., **7**, 602
Eley, D. D., **7**, 238
Elving, P. J., **3**, 1
Englman, R., **8**, 13
Eriksson, J. C., **6**, 145
Eschenroeder, A. Q., **13**, 19
Eyring, H., **4**, 1

Fenn, J. B., **10**, 275
Fernández-Alonso, J. I., **7**, 3
Ferreira, R., **13**, 55
Fixman, M., **1**, 1; **6**, 175
Friedmann, H., **4**, 225
Frisch, H. L., **6**, 229

Giese, C. F., **10**, 247
Goodman, G. L., **9**, 169
Greene, E. F., **10**, 135

Halperin, B. I., **13**, 123
Harasima, A., **1**, 203
Harris, F. E., **13**, 205
Hartmann, H., **5**, 1
Hasselle-Schuermans, N., **11**, 159
Herschbach, D. R., **10**, 319
Himmelblau, D. M., **13**, 267
Hirschfelder, J. O., **3**, 59; **12**, 3
Hoarau, J., **3**, 171
Hoffman, T. A., **7**, 84

Imelik, B., **8**, 141

Jagger, J., **7**, 584
Jardetzky, O., **7**, 499
Johnston, H. S., **3**, 131

Jordan, J. E., **10**, 29
Jørgensen, C. K., **5**, 33; **8**, 47

Kearns, D. R., **7**, 282
Keck, J. C., **13**, 85
Kende, A., **8**, 133
Kihara, T., **1**, 267; **5**, 147
Kirkwood, J. G., **1**, 1
Koide, S., **5**, 189
Kotani, M., **7**, 159
Koutecký, J., **9**, 85
Kyoguku, Y., **7**, 435

Labhart, H., **13**, 179
Ladik, J., **7**, 84
Laforgue, A., **8**, 141
Lamm, O., **6**, 291
Lecomte, J., **7**, 408
Leener, M. de, **6**, 85
Leslie, R. B., **7**, 238
Lichten, W., **13**, 41
Liehr, A. D., **5**, 241
Linder, B., **12**, 225
Longuet-Higgins, H. C., **1**, 239
Löwdin, P.-O., **2**, 207; **8**, 3, 177

McLennan, J. A., Jr., **5**, 261
Mandel, M., **1**, 77
Marchand, A., **3**, 171
Mason, E. A., **12**, 329
Mathot, V., **11**, 117
Mazur, P., **1**, 309
Meath, W. J., **12**, 3
Michels, H. H., **13**, 205
Monchick, L., **12**, 329
Montroll, E. W., **1**, 361
Moscowitz, A., **4**, 67
Moursund, A. L., **10**, 135
Muckerman, J. T., **12**, 389
Muschlitz, E. E., Jr., **10**, 171

Nesbet, R. K., **9**, 321
Nicolau, C. S., **7**, 628
Nicolis, G., **13**, 299

Oguchi, T., **5**, 189
Ono, S., **3**, 267
Oppenheim, I., **12**, 549
Oriani, R. A., **2**, 119

Pacault, A., **3**, 171
Philippot, J., **11**, 289
Pitzer, K. S., **2**, 59
Platteeuw, J. C., **2**, 1
Pollard, E. C., **7**, 201
Power, E. A., **12**, 167
Prager, S., **4**, 201
Pullman, B., **3**, 1; **8**, 163

Raffel, H., **1**, 135
Ree, F. H., **4**, 1
Ree, T., **4**, 1
Ree, T. S., **4**, 1
Regnier, J., **8**, 5
Reiss, H., **9**, 1
Résibois, P., **11**, 159
Richardson, M. J., **2**, 85
Robinson, E. J., **10**, 1
Ross, J., **10**, 135
Rousseau, Mme. J., **8**, 141
Rowlinson, J. S., **2**, 85

Sadron, C., **7**, 339
Schoffa, G., **7**, 182
Scrocco, E., **5**, 319
Shimanouchi, T., **7**, 435
Shuler, K. E., **1**, 361
Simon, M., **11**, 117
Sinanoğlu, O., **6**, 315; **12**, 283
Skanche, P. N., **3**, 323
Smaller, B., **7**, 532
Stebbings, R. F., **10**, 195
Stecki, J., **6**, 413
Szwarc, M., **2**, 147

Tinoco, I., Jr., **4**, 113
Tomassi, W., **3**, 239
Tsuboi, M., **7**, 435

Ubbelohde, A. R. J. P., **6**, 459

Van Herpen, G., **7**, 259

Waals, J. H. van der, **2**, 1
Walter, C., **7**, 645
Weinstock, B., **9**, 169
Weiss, G. H., **13**, 1
Wentorf, R. H., Jr., **9**, 365
Widom, B., **5**, 353
Williams, R. J. P., **7**, 359
Wilson, E. B., Jr., **2**, 367
Wolfsberg, M., **1**, 15

Yoshizumi, H., **2**, 323

Zahner, J. C., **4**, 161

Titles of Articles

	Vol.	Page
Absorptions, Optical, and Charge Transfer States (Englman)	**8**	13
Adsorption of Water on Solid Proteins with Special Reference to Haemoglobin (Eley & Leslie)	**7**	238
Aging, Heredity, Mutations, and Tumours in View of the Quantum Theory of the DNA Molecule (Löwdin)	**8**	177
Ammonia-Metal Solutions, Structure and Properties of (Das)	**4**	303
Analytic Theory of Chemical Reactions, [Approach to] an (Aroeste)	**6**	1
Application of the Theory of Stochastic Processes to Chemical Kinetics (Montroll and Shuler)	**1**	361
Application of Ligand-Field Theory to Complexes (Jørgensen)	**8**	47
Applications of Spectroscopic Methods [in Biology]	**7**	408
Aspects Récents du Diamagnétisme (Pacault, Hoarau, & Marchand)	**3**	171
Atomic Polarizabilities, Beam Measurements of (Bederson & Robinson)	**10**	1
Atoms and Molecules, Electronic Correlation in (Nesbet)	**9**	321
Atoms and Molecules, Electronically Excited, Collisions of (Muschlitz)	**10**	171
Atoms and Molecules, Many-Electron Theory of (Sinanoğlu)	**6**	315
Average Potential Method [in the] Statistical Mechanics of Mixtures (Bellemans)	**11**	117
Beam Measurements of Atomic Polarizabilities (Bederson & Robinson)	**10**	1
Beams, High-Energy, Elastic Scattering of (Amdur & Jordan)	**10**	29
Beams, Molecular, Reactive Scattering in (Herschbach)	**10**	319
Beams, Supersonic Nozzle (Anderson, Andres, & Fenn)	**10**	275
Biochemical and Chemical Activity	**8**	65
Biological Systems, Physio-chemical Mechanisms in	**7**	584
Biology, Use of Infrared Spectroscopy in (Lecomte)	**7**	408
Boltzmann Equations, Comparison between two Generalized (Brocas)	**11**	317

	Vol.	Page
Calculation of Transition Energies from the Geometry of the System (Barriol & Regnier)	8	5
Carbonyl Base Strength, S.C.F.M.O. Treatment of (Kende)	8	133
Carcinogenesis by Aromatic Hydrocarbons (Daudel)	1	165
Carcinogens, Polycyclic Aromatic (Pullman)	8	163
Charge Transfer (Stebbings)	10	195
Charge Transfer States and Optical Absorptions (Englman)	8	13
Chemical and Biochemical Activity	8	65
Chemical Bond and Magnetic Susceptibilities in Hemoproteins (Schoffa)	7	182
Chemical Reactions, [Approach to] an Analytic Theory of (Aroeste)	6	1
Chemical Reactivity (Dewar)	8	65
Chemisorption of Ethylene on Metals and Catalytic Hydrogenation (Laforgue, Rousseau, & Imelik)	8	141
Clathrate Solutions (van der Waals & Platteeuw)	2	1
Collision Theory of Chemical Reaction Rates (Widom)	5	353
Collisions of Electronically Excited Atoms and Molecules (Muschlitz)	10	171
Comparison between Two Generalized Boltzmann Equations (Brocas)	11	317
Complexes, Applications of Ligand-Field Theory to (Jørgensen)	8	47
Complexes, Metal-Porphyrin, Properties of (Braterman, Davies, & Williams)	7	359
Complexes, Transition-Group, Spectroscopy of (Jørgensen)	5	33
Conduction, Electronic, in Organic Molecular Solids (Kearns)	7	282
Convex Molecules in Gaseous and Crystalline States (Kihara)	5	147
Correlation, Electronic, in Atoms and Molecules (Nesbet)	9	321
Correlation Problem in Many-Electron Quantum Mechanics. I. Review of Different Approaches and Discussion of Some Current Ideas (Löwdin)	2	207
Correlation Problem in Many-Electron Quantum Mechanics. II. Bibliographical Survey of the Historical Developments with Comments (Yoshizumi)	2	323
Correlation Problem [in regard to] the Quantum Theory of Many-Electron Systems (Löwdin)	8	3
Critical Region (Fixman)	6	175
Crystal Surfaces, Quantum Chemistry of (Koutecký)	9	85
Crystals, Irradiated, Nuclear Quadrupole Resonance in (Duchesne)	2	187
Crystals, Melting Mechanisms of (Ubbelohde)	6	459
Deoxyribonucleic Acid, Electronic Properties of (Douzouz & Sadron)	7	339
Detonations, and Propagation of Flames (Hirschfelder & Curtiss)	3	59
Diamagnétisme, Aspects Récents de (Pacault, Hoaran, & Marchand)	3	171
Diamond Synthesis (Wentorf)	9	365

	Vol.	Page
Dielectric Properties of Dilute Polymer Solutions (de Brouckère & Mandel)	1	77
Diffusion, Isothermal, Kinematics of (Lamm)	6	291
Diffusion, Multicomponent Fluid, Macrodynamical Theory of (Lamm)	6	291
Diffusion, Thermal, of Halides in Aqueous Solution (Chanu)	13	349
Dimensional Methods in the Statistical Mechanics of Ionic Systems (Blander)	11	83
Distribution Function, Quantum-Mechanical, of Molecular Systems: Translational and Rotational Motions (Friedmann)	4	225
DNA, Quantum-Mechanical Considerations for Some Properties of (Hoffmann and Ladik)	7	84
DNA, Quantum Theory of, [in relation to] Heredity, Mutations, Aging, and Tumours (Löwdin)	8	177
Effects of Ionizing Radiations on Some Fibrous Proteins (Braams & Van Herpen)	7	259
Effect of Pressure on Electronic Structure (Drickamer & Zahner)	4	161
Elastic Molecular Scattering, Quantum Scattering in (Bernstein)	10	75
Elastic Scattering in Chemically Reactive Systems (Greene, Moursund, & Ross)	10	135
Elastic Scattering of High-Energy Beams: Repulsive Forces (Amdur & Jordan)	10	29
Electrical and Magnetic Properties of Organic Molecular Solids, Proteins, and Nucleic Acids	7	282
Electrochromism (Labhart)	13	179
Electrode Reactions, Organic, Mechanism of (Elving & Pullman)	3	1
Electrodes, Power, and Their Application (Tomassi)	3	239
Electrolytes, Microscopic Approach to Equilibrium and Non-Equilibrium Properties of (Résibois and Hasselle-Schuermans)	11	159
Electromagnetic Properties of Matter, and Statistical Mechanics (Mazur)	1	309
Electron Diffraction in Gases and Molecular Structure (Bastiansen & Skancke)	3	323
Electronegativity, and Chemical Bonding (Ferreira)	13	55
Electron Gas in a Lattice of Positive Charges (Bellemans & de Leener)	6	85
π-Electron Systems, New Developments in the One-Electron Theory of (Hartmann)	5	1
Electronic Conduction in Organic Molecular Solids (Kearns)	7	282
Electronic Correlation in Atoms and Molecules (Nesbet)	9	321
Electronic Properties of Deoxyribonucleic Acid (Douzou & Sadron)	7	339
Electronic Structure and Magnetic Properties of Hemoproteins, Particularly of Hemoglobins (Kotani)	7	159
Electronic Structure and Spectra	8	3

	Vol.	Page
Electronic Structure of Proteins and Nucleic Acids	7	3
Electronic Structures in Quantum Biochemistry (Fernández-Alouso)	7	3
Electronically Excited Atoms and Molecules, Collisions of (Muschlitz)	10	171
EPR Spectroscopy, Recent Advances in (Smaller)	7	532
Equation of State and Intermolecular Forces of Gases (Kihara)	1	267
Equation of State of the Classical Hard Sphere Fluid (Frisch)	6	229
Equilibrium and Non-Equilibrium Properties of Electrolytes, Microscopic Approach to (Résibois and Hasselle-Schuermans)	11	159
ESR Investigations on Different Plant Systems (Nicolau)	7	628
Ethylene, Chemisorption on Metals; and Catalytic Hydrogenation (Laforgue, Rousseau, & Imelik)	8	141
Flames, Propagation of (Hirschfelder & Curtiss)	3	59
Fluid, Classical Hard Sphere, Equation of State of (Frisch)	6	229
Fluids, Scaled Particle Methods in Statistical Thermodynamics of (Reiss)	9	1
Forbidden Transitions in Organic and Inorganic Systems (Liehr)	5	241
Formal Statistical Theory of Transport Processes (McLennan)	5	261
Gaseous Chemical Kinetics, Some Physical Aspects of (Careri)	1	119
Gases, Compressed, Solubility of Solids in (Rowlinson and Richardson)	2	85
Gases, Electron Diffraction in, and Molecular Structure (Bastiansen & Skancke)	3	323
Gases, Intermolecular Forces and Equation of State of (Kihara)	1	267
Hard Sphere Fluid, Classical, Equation of State of (Frisch)	6	229
Heat of Transport in Binary Liquid Systems (Bearman, Kirkwood, & Fixman)	1	1
Hemoglobin, Solid, Adsorption of Water on (Eley & Leslie)	7	238
Hemoglobins, Electronic Structure and Magnetic Properties of (Kotani)	7	159
Hemoproteins, Electronic Structure and Magnetic Properties of (Kotani)	7	159
Hemoproteins, Magnetic Susceptibilities and Chemical Bond in (Schoffa)	7	182
Heredity, Mutations, Aging, and Tumours in View of the Quantum Theory of the DNA Molecule (Löwdin)	8	177
Hexafluoride Molecules, Vibrational Properties of (Weinstock & Goodman)	9	169
Hydrocarbons, Aromatic, Relation between Structure and Chemical Reactivity, with Particular Reference to Carcinogenic Properties (Daudel)	1	165

	Vol.	Page
Hydrogenation, Catalytic, and Chemisorption of Ethylene on Metals (Laforgue, Rousseau, Imelik)	8	141
Influence of Physical Agents on Proteins and Nucleic Acids	7	201
Infrared Spectra of Nucleic Acids and Related Compounds (Shimanouchi, Tsuboi, and Kyogoku)	7	435
Infrared Spectroscopy in Biology (Lecomte)	7	408
Intermolecular Forces, Determination of, via Low-Energy Molecular Beam Scattering (Bernstein & Muckerman)	12	389
Intermolecular Forces, Determined by Nuclear Magnetic Resonance (Bloom & Oppenheim)	12	549
Intermolecular Forces, and Equation of State of Gases (Kihara)	1	267
Intermolecular Forces, in Liquids (Sinanoğlu)	12	283
Intermolecular Forces, Methods for the Determination of (Mason & Monchick)	12	329
Intermolecular Forces, Long Range, New Methods for Calculating (Dalgarno)	12	143
Intermolecular Forces, Nature of (Hirschfelder & Meath)	12	3
Intermolecular Forces, Very Long Range [Retardation Effect] (Power)	12	167
Inter- and Intra-molecular Forces and Molecular Polarizability (Pitzer)	2	59
Internal Rotation in Molecules, Barriers to (Wilson)	2	367
Ionic Solvation (Stecki)	6	413
Ionic Systems, Dimensional Methods in the Statistical Mechanics of (Blander)	11	83
Ion-Neutral Reactions (Giese)	10	247
Irradiated Crystals, Nuclear Quadrupole Resonance in (Duchesne)	2	187
Irreversible Processes, Non-Linear Problems in Thermodynamics of (Bak)	3	33
Irreversible Processes, Variation Principles in Thermodynamics and Statistical Mechanics of (Ono)	3	267
Isothermal Diffusion, Kinematics of. A Macrodynamical Theory of Multicomponent Fluid Diffusion (Lamm)	6	291
Isotope Effects in Chemical Kinetics, Theoretical and Experimental Aspects of (Bigeleisen & Wolfsberg)	1	15
Kinematics of Isothermal Diffusion. A Macrodynamical Theory of Multicomponent Fluid Diffusion (Lamm)	6	291
Kinetic Methods, Including Product Inhibition, Used in the Study of the Mechanism of Enzyme Actions (Walter)	7	645
Kinetics, Chemical, Application of the Theory of Stochastic Processes to (Montroll & Shuler)	1	361
Kinetics, Chemical, Theoretical and Experimental Aspects of (Bigeleisen & Wolfsberg)	1	15

	Vol.	Page
Kinetics, Gaseous Chemical, Some Physical Aspects of (Careri)	1	119
Large Tunnelling Corrections in Chemical Reaction Rates (Johnston)	3	131
Ligand Theory, Applied to Complexes (Jørgensen)	8	47
Liquids, Transport Processes in (Collins & Raffel)	1	135
Liquid Systems, Binary, Heat of Transport in (Bearman, Kirkwood, & Fixman)	1	1
Local Potential Applied to Instability Problems (Ball & Himmelblau)	13	267
Local Potential Methods in the Study of Kinetic Equations (Nicolis)	13	299
Magnetic and Electrical Properties of Organic Molecular Solids, Proteins, and Nucleic Acids	7	282
Magnetic Properties and Electronic Structure of Hemoproteins, Particularly of Hemoglobins (Kotani)	7	159
Magnetic Properties of Compounds, Theories on (Koide and Oguchi)	5	189
Magnetic Susceptibilities and the Chemical Bond in Hemoproteins (Schoffa)	7	182
Many-Electron Quantum Mechanics, Correlation Problem in I (Löwdin), II (Yoshizumi)	2	207, 323
Many-Electron Systems, Recent Developments in the Quantum Theory of (Löwdin)	8	3
Many-Electron Theory of Atoms, Molecules, and their Interactions (Sinanoğlu)	6	315
Mechanisms of Enzyme Action, Use of Product Inhibition and Other Kinetic Methods in the Study of (Walter)	7	645
Mechanisms of Organic Electrode Reactions (Elving & Pullman)	3	1
Melting Mechanisms of Crystals (Ubbelohde)	6	459
Metal-Ammonia Systems, Structure and Properties of (Das)	4	303
Metal-Porphyrin and Similar Complexes, Properties of (Braterman, Davies, & Williams)	7	359
Metallic Solutions, Thermodynamics of (Oriani)	2	119
Microscopic Approach to Equilibrium and Non-Equilibrium Properties of Electrolytes (Résibois & Hasselle-Schuermans)	11	159
Microwave Pressure Broadening, and Its Application to Intermolecular Forces (Birnbaum)	12	487
Mixed-Crystal Spectra, Model Calculations in the Theory of (Craig)	8	27
Mixtures, Statistical Mechanics of—The Average Potential Model (Bellemans, Mathot, & Simon)	11	117
Model Calculations in the Theory of Mixed-Crystal Spectra (Craig)	8	27
Molecular Beam Research, Selected References in (Herschbach)	10	359
Molecular Beams, Reactive Scattering in (Herschbach)	10	319
Molecular Integrals for Slater-type Orbitals, Evaluation of (Harris & Michels)	13	205

	Vol.	Page
Molecular Moments, and Long-Range Intermolecular Forces, Permanent and Induced (Buckingham)	12	107
Molecular Orbital Theory, Recent Developments in (Longuet-Higgins)	1	239
Molecular Polarizability and Inter- and Intra-molecular Forces (Pitzer)	2	59
Molecular Theory of Surface Tension (Harasima)	1	203
Molecules, Barriers to Internal Rotation in (Wilson)	2	367
Molecules, Convex, in Gaseous and Crystalline States (Kihara)	5	147
Molecules and Atoms, Electronic Correlation in (Nesbet)	9	321
Molecules and Atoms, Electronically Excited, Collisions of (Muschlitz)	10	171
Molecules and Atoms, Many-Electron Theory of (Sinanoğlu)	6	315
Mutations, Heredity, Aging, and Tumours in view of the Quantum Theory of the DNA Molecule (Löwdin)	8	163
New Developments in the One-Electron Theory of π-Electron Systems (Hartmann)	5	1
Non-Equilibrium and Equilibrium Properties of Electrolytes, Microscopic Approach to (Résibois and Hasselle-Schuermans)	11	159
Non-linear Problems in Thermodynamics of Irreversible Processes (Bak)	3	33
Nozzle Beams, Supersonic (Anderson, Andres, & Fenn)	10	275
Nuclear Magnetic Relaxation Methods for the Study of Specific Molecular Interactions (Jardetzky)	7	499
Nuclear Paramagnetic (Spin-Spin) Relaxation in Solids (Philippott)	11	289
Nuclear Quadrupole Coupling Data, Quantum-Mechanical Interpretation of (Scrocco)	5	319
Nuclear Quadrupole Resonance in Irradiated Crystals (Duchesne)	2	187
Nucleic Acid, Protein, and Viruses, Thermal Effects on (Pollard)	7	201
Nucleic Acids, Electrical and Magnetic Properties of	7	282
Nucleic Acids and Proteins, Electronic Structure	7	3
Nucleic Acids and Proteins, Influence of Physical Agents on	7	201
Nucleic Acids and Related Compounds, Infrared Spectra of (Shimanouchi, Tsuboi, & Kyogoku)	7	435
One-Dimensional Plasma (Prager)	4	201
One-Electron Theory of π-Electron Systems, New Developments in (Hartmann)	5	1
Optical Absorptions and Charge Transfer States (Englman)	8	13
Optical Activity, Theoretical Aspects of. I. Small Molecules (Moscowitz). II. Polymers (Tinoco)	4	67, 113
Organic Electrode Reactions, Mechanisms of (Elving & Pullman)	3	1

	Vol.	Page
Paramagnetic Species of Biological Interest (Ehrenberg)	7	602
Particle, Properties of, in a One-Dimensional Random Potential (Bertram & Halperin)	13	123
Photoprotection from Far Ultraviolet Effect in Cells (Jagger)	7	584
Physio-chemical Mechanisms in Biological Systems	7	584
Plant Systems, ESR Investigations of (Nicolau)	7	628
Plasma, One-Dimensional (Prager)	4	201
Point Interactions in Solids, Statistical Mechanics of (Allnatt)	11	1
Polarizabilities, Atomic, Beam Measurements of (Bederson & Robinson)	10	1
Polarizability, Molecular, and Inter- and Intra-molecular Forces (Pitzer)	2	39
Polymer Chemistry, Recent Advances in (Szwarc)	2	147
Polymer Solutions, Dilute, Dielectric Properties of (de Brouckère & Mandel)	1	77
Polymers, Theoretical Aspects of Optical Activity [in] (Tinoco)	4	113
Porphyrin-Metal and Similar Complexes, Properties of (Braterman, Davies, & Williams)	7	359
Power Electrodes and Their Application (Tomassi)	3	239
Pressure, Effect on Electronic Structure (Drickamer & Zahner)	4	161
Problem of Barriers to Internal Rotation in Molecules (Wilson)	2	367
Propagation of Flames and Detonations (Hirschfelder & Curtiss)	3	59
Properties of Metal-Porphyrin and Similar Complexes (Braterman, Davies, & Williams)	7	359
Prospects for the Use of Infrared Spectroscopy in Biology (Lecomte)	7	408
Protein, Nucleic Acid, and Viruses, Thermal Effects on (Pollard)	7	201
Proteins, Electrical and Magnetic Properties of	7	282
Proteins, Fibrous, Effects of Ionizing Radiations on (Braams and Van Herpen)	7	259
Proteins, Solid, Adsorption of Water on (Eley & Leslie)	7	238
Proteins and Nucleic Acids, Electronic Structure	7	3
Proteins and Nucleic Acids, Influence of Physical Agents on	7	201
Purine-Pyrimidine Pairs, Steroids, and Polycyclic Aromatic Carcinogens (Pullman)	8	163
Quantum Biochemistry, Electronic Structures in (Fernández-Alonzo)	7	3
Quantum Chemistry of Crystal Surfaces (Koutecký)	9	85
Quantum Effects in Elastic Molecular Scattering (Bernstein)	10	75
Quantum Theory of DNA [in relation to] Heredity, Mutations, Aging, and Tumours (Löwdin)	8	177
Quantum Theory of Many-Electron Systems and the Correlation Problem (Löwdin)	8	3

	Vol.	Page
Quantum-Mechanical Considerations for Some Properties of DNA (Hoffman & Ladik)	7	84
Quantum-Mechanical Distribution Function of Molecular Systems: Translational and Rotational Motions (Friedmann)	4	225
Quantum-Mechanical Interpretation of Nuclear Quadrupole Coupling Data (Scrocco)	5	319
Radiations, Ionizing, Effects on Some Fibrous Proteins (Braams & Van Herpen)	7	259
Random Walk and Related Physical Problems (Ree, Ree, & Eyring)	4	1
Reaction-Field Techniques, and Their Applications to Intermolecular Forces (Linder)	12	225
Reaction Kinetics in Hypersonic Flows (Eschenroeder)	13	19
Reaction Rates, Chemical, Collision Theory of (Widom)	5	353
Reaction Rates, Chemical, Large Tunnelling Corrections in (Johnston)	3	131
Reactions, Ion-Neutral (Giese)	10	247
Reactive Scattering in Molecular Beams (Herschbach)	10	319
Reactivity, Chemical (Dewar)	8	65
Recent Advances in EPR Spectroscopy (Smaller)	7	532
Recent Advances in Polymer Chemistry (Szwarc)	2	147
Recent Developments in Molecular Orbital Theory (Louguet-Higgins)	1	239
Relation between Structure and Chemical Activity of Aromatic Hydrocarbons with Particular Reference to Carcinogenic Properties (Daudel)	1	165
Relaxation, Nuclear Paramagnetic (Spin–Spin), in Solids (Philippott)	11	289
Relaxation Methods, Nuclear Magnetic, in the Study of Specific Molecular Interactions (Jardetzky)	7	499
Repulsive Forces [in] Elastic Scattering of High-Energy Beams (Amdur & Jordan)	10	29
Resonant Charge Exchange in Atomic Collisions (Lichten)	13	41
Rotational and Translational Motions [in] Molecular Systems (Friedmann)	4	225
Scaled Particle Methods in the Statistical Thermodynamics of Fluids (Reiss)	9	1
Scattering, Elastic, in Chemically Reactive Systems (Greene, Moursund, & Ross)	10	135
Scattering, Elastic, of High-Energy Beams: Repulsive Forces (Amdur & Jordan)	10	29
Scattering, Elastic Molecular, Quantum Effects in (Bernstein)	10	75
Scattering, Reactive, in Molecular Beams (Herschbach)	10	319
Self-Consistent Field Molecular-Orbital Treatment of Carbonyl Base Strength (Kende)	8	133

	Vol.	Page
Small Molecules, Theoretical Aspects of Optical Activity [in] (Moscowitz)	4	67
Solids, Nuclear Paramagnetic (Spin–Spin) Relaxation in (Philippott)	11	289
Solids, Statistical Mechanics of Point Interactions in (Allnatt)	11	1
Solubility of Solids in Compressed Gases (Rowlinson and Richardson)	2	85
Solvation, Ionic (Stecki)	6	413
Some Aspects of the Biological Problems of Heredity, Mutations, Aging, and Tumours in View of the Quantum Theory of the DNA Molecule (Löwdin)	8	177
Some Physical Aspects of Gaseous Chemical Kinetics (Careri)	1	119
Some Recent Developments in the Quantum Theory of Many-electron Systems and the Correlation Problem (Löwdin)	8	3
Some Recent Developments in the Study of Paramagnetic Species of Biological Interest (Ehrenberg)	7	602
Spectra, Infrared, of Nucleic Acids and Related Compounds (Shimanouchi, Tsuboi, and Kyogoku)	7	435
Spectra, Mixed-Crystal, Model Calculations in the Theory of (Craig)	8	27
Spectra and Electronic Structure	8	3
Spectroscopic Methods, [Biological] Applications of	7	408
Spectroscopy, EPR, Recent Advances in (Smaller)	7	532
Spectroscopy, Infrared, Use in Biology (Lecomte)	7	408
Spectroscopy of Transition-Group Complexes (Jørgensen)	5	33
Statistical-Mechanical Theory of Transport Processses. X. The Heat of Transport in Binary Liquid Systems (Bearman, Kirkwood, & Fixman)	1	1
Statistical Mechanics and Electromagnetic Properties of Matter (Mazur)	1	309
Statistical Mechanics and Thermodynamics of Irreversible Processes, Variational Principles in (Ono)	3	267
Statistical Mechanics of Ionic Systems, Dimensional Methods in (Blander)	11	83
Statistical Mechanics of Mixtures—The Average Potential Model (Bellemans, Mathot, and Simon)	11	117
Statistical Mechanics of Point Interactions in Solids (Allnatt)	11	1
Statistical Thermodynamics of Fluids, Scaled Particle Methods in (Reiss)	9	1
Steroids, Purine-Pyrimidine Pairs, and Polycyclic Aromatic Carcinogens (Pullman)	8	163
Stochastic Processes, Theory of, Applied to Chemical Kinetics (Montroll & Shuler)	1	361
Structure, Electronic, Effect of Pressure on (Drickamer & Zahner)	4	161
Structure and Properties of Metal-Ammonia Systems (Das)	4	303
Studies in the Kinematics of Isothermal Diffusion. A Macrodynamical Theory of Multicomponent Fluid Diffusion (Lamm)	6	291

	Vol.	Page
Study of Specific Molecular Interactions by Nuclear Magnetic Relaxation Methods (Jardetzky)	7	499
Supersonic Nozzle Beams (Anderson, Andres, & Fenn)	10	275
Surface Systems, Thermodynamics of (Eriksson)	6	145
Surface Tension, Molecular Theory of (Harasima)	1	203
Theoretical and Experimental Aspects of Isotope Effects in Chemical Kinetics (Bigeleisen & Wolfsberg)	1	15
Theoretical Aspects of Optical Activity. I. Small Molecules (Moscowitz). II. Polymers (Tinoco)	4	67, 113
Theories on the Magnetic Properties of Compounds (Koide & Oguchi)	5	189
Thermal Effects on Protein, Nucleic Acid, and Viruses (Pollard)	7	201
Thermodynamics and Statistical Mechanics of Irreversible Processes, Variational Principles in (Ono)	3	267
Thermodynamics of Irreversible Processes, Non-linear Problems in (Bak)	3	33
Thermodynamics of Metallic Solutions (Oriani)	2	119
Thermodynamics of Surface Systems (Eriksson)	6	145
Time Problems, First Passage, in Chemical Physics (Weiss)	13	1
Towards an Analytic Theory of Chemical Reactions (Aroeste)	6	1
Transition Energies; Calculation [thereof] from the Geometry of the System (Barriol & Regnier)	8	5
Transition-Group Complexes, Spectroscopy of (Jørgensen)	5	33
Transitions, Forbidden, in Organic and Inorganic Systems (Liehr)	5	241
Translational and Rotational Motions [in] Molecular Systems (Friedmann)	4	225
Transport Process, Statistical-Mechanical Theory of. X (Bearman, Kirkwood, & Fixman)	1	1
Transport Processes, Formal Statistical Theory of (McLennan)	5	261
Transport Processes in Liquids (Collins & Raffel)	1	135
Tumours, Heredity, Mutations, and Aging in View of the Quantum Theory of the DNA Molecule (Löwdin)	8	177
Tunnelling Corrections, Large, in Chemical Reaction Rates (Johnston)	3	131
Ultraviolet (Far) Effect in Cells, Photoprotection from (Jagger)	7	584
Use of Product Inhibition and Other Kinetic Methods in the Determination of Mechanisms of Enzyme Action (Walter)	7	645
Variational Theory of Reaction Rates (Keck)	13	85
Variation Principles in Thermodynamics and Statistical Mechanics of Irreversible Processes (Ono)	3	267
Vibrational Properties of Hexafluoride Molecules (Weinstock & Goodman)	9	169
Viruses, Protein, and Nucleic Acid, Thermal Effects on (Pollard)	7	201

Date Due

MAR 07 2007

bd

CAT. NO. 23 233 PRINTED IN U.S.A.

TRENT UNIVERSITY
0 1164 0085772 2

QD453 .A27 v. 12 1967

Advances in chemical physics.

DATE	ISSUED TO 98471

98471

40067